UNITED STATES DEPARTMENT OF THE INTERIOR

GEOLOGICAL SURVEY

NATIONAL EARTHQUAKE HAZARDS REDUCTION PROGRAM, SUMMARIES OF TECHNICAL REPORTS VOLUME XXIII

Prepared by Participants in

NATIONAL EARTHQUAKE HAZARDS REDUCTION PROGRAM

October 1986

OPEN-FILE REPORT 87-63

Menlo Park, California

1986

UNITED STATES
DEPARTMENT OF THE INTERIOR
GEOLOGICAL SURVEY

NATIONAL EARTHQUAKE HAZARDS REDUCTION PROGRAM, SUMMARIES OF TECHNICAL REPORTS VOLUME XXIII

Prepared by Participants in

NATIONAL EARTHQUAKE HAZARDS REDUCTION PROGRAM

Compiled by

Muriel L. Jacobson

Thelma R. Rodriguez

The research results described in the following summaries were submitted by the investigators on May 16, 1986 and cover the 6-months period from May 1, 1986 through October 31, 1986. These reports include both work performed under contracts administered by the Geological Survey and work by members of the Geological Survey. The report summaries are grouped into the three major elements of the National Earthquake Hazards Reduction Program.

Open File Report No. 87-63

The data and interpretations in these progress reports may be reevaluated by the investigators upon completion of the research. Readers who wish to cite findings described herein should confirm their accuracy with the author.

CONTENTS

Earthquake Hazards Reduction Program

Page

Objective (II-1): Prediction Methodology and Evaluation

Develop methods to provide a rational basis for estimates of increased earthquake potential. Evaluate the relevance of various geophysical, geochemical, and hydrological data for earthquake prediction.

1. Develop, operate and evaluate instrumentation for monitoring potential earthquake precursors.

2. Analyze and evaluate seismicity data collected prior to medium and large earthquakes.

3. Obtain and analyze data from seismically active regions of foreign countries through cooperative projects with the host countries.

4. Systematically evaluate data and develop statistics that relate observations of specific phenomena to earthquake occurrence.

5. Develop, study and test prediction methods that can be used to proceed from estimates of long-range earthquake potential to specific short-term predictions..... 183

Objective (II-2): Earthquake Prediction Experiments

Conduct data collection and analysis experiments in areas of California capable of great earthquakes, where large populations are at risk. The experiments will emphasize improved coordination of data collection, data reporting, review and analysis according to set schedules and standards.

1. Collect and analyze data for an earthquake prediction experiment in southern California, concentrating on the southern San Andreas fault from Parkfield, California to the Salton Sea.

2. Collect and analyze data for an earthquake prediction experiment in central California, concentrating on the San Andreas fault north of Parkfield, California..... 290

Objective (II-3): Theoretical, Laboratory and Fault Zone Studies

Improve our understanding of the physics of earthquake processes through theoretical and laboratory studies to guide and test earthquake prediction observations and data analysis. Measure physical properties of those zones selected for earthquake experiments, including stress, temperature, elastic and anelastic characteristics, pore pressure, and material properties.

Southern California Seismic Arrays

Cooperative Agreement No. 14-08-0001-A0257

Clarence R. Allen and Robert W. Clayton
Seismological Laboratory, California Institute of Technology
Pasadena, California 91125 (818-356-6912)

Investigations

This semi-annual Technical Report Summary covers the six-month period from 1 April 1986 to 30 September 1986. The Cooperative Agreement's purpose is the partial support of the joint USGS-Caltech Southern California Seismographic Network, which is also supported by other groups, as well as by direct USGS funding to its own employees at Caltech. According to the Agreement, the primary visible product will be a joint Caltech-USGS catalog of earthquakes in the southern California region; quarterly epicenter maps and preliminary catalogs have been submitted as due during the Agreement period. About 250 preliminary catalogs are routinely distributed to interested parties.

Results

Figure 1 shows the epicenters of all cataloged shocks that were located during the six-month recording period, although, because of the unusually high activity during the period, many smaller shocks still remain to be processed. Some of the seismic highlights of this period were:

Number of earthquakes fully or partially processed: 5917
Number of earthquakes of M = 3.0 and greater: 445
Number of earthquakes of M = 4.0 and greater: 57
Number of earthquakes of M = 5.0 and greater: 9
Largest event within network area: M = 5.6 (8 July, North Palm Springs)
Number of earthquakes reported felt: 60
Number of earthquakes for which systematic telephone notification to emergency-response agencies was made: 12

This was an unusually active period in southern California seismicity. Not only was the North Palm Springs earthquake of 8 July (M_L = 5.6) a widely felt and locally damaging event, but the offshore Oceanside earthquake (M_L = 5.3) 5 days later, on 13 July, was also felt over a surprisingly wide area of southern California. Seven days following that event, the Chalfant Valley earthquake (M_L = 6.2) occurred north of Bishop, California, and although it was technically outside of our area of network responsibility, it caused even further public interest and concern. Each of these three earthquakes has had numerous felt aftershocks which continue to this writing.

Studies of the North Palm Springs earthquake (Jones et al., in press) indicate that it probably occurred on the Banning fault , which is an east-trending, north-dipping thrust fault in the San Gorgonio Pass area but steepens in dip as it changes to a southeasterly trend toward the southeast into the Coachella Valley-Salton Sea area. The North Palm Springs earthquake occurred in this transition zone, at a depth of 11.3 km (Fig. 2). The focal

mechanism of the main shock indeed indicates a northerly fault dip of about 45°, but, surprisingly, the displacement was almost pure strike slip. Aftershock locations support the concept of a north-dipping rupture zone. Relocation of the 1948 Desert Hot Springs earthquake (M_L = 6.5), formerly thought to have occurred on the Mission Creek fault, suggest that it, too, occurred on the Banning fault, in the segment abutting that of the North Palm Springs earthquake to the southeast (Nicholson et al., in press).

The offshore Oceanside earthquake of 13 July occurred about 45 km southwest of Oceanside, California, in the vicinity of a number of northwest-trending faults in the San Diego trough (Fig. 1). The short-period focal mechanism indicates right-lateral displacement on a fault of somewhat more northerly strike. The earthquake was widely felt in both the San Diego and Los Angeles metropolitan areas, and the epicentral area has been one of continuing moderate seismic activity during the history of seismographic recording in southern California.

Publications

Jones, L. M., Hutton, L. K., Given, D. D., and Allen, C. R., in press, The North Palm Springs earthquake sequence of July 1986: Seismol. Soc. America Bull.

Nicholson, C., Wesson, R. L., Given, D., Boatwright, J., and Allen, C. R., in press, Aftershocks of the 1986 North Palm Springs earthquake and relocation of the 1948 Desert Hot Springs earthquake sequence [abstract]: Am. Geophys. Union 1986 Fall meeting, San Francisco.

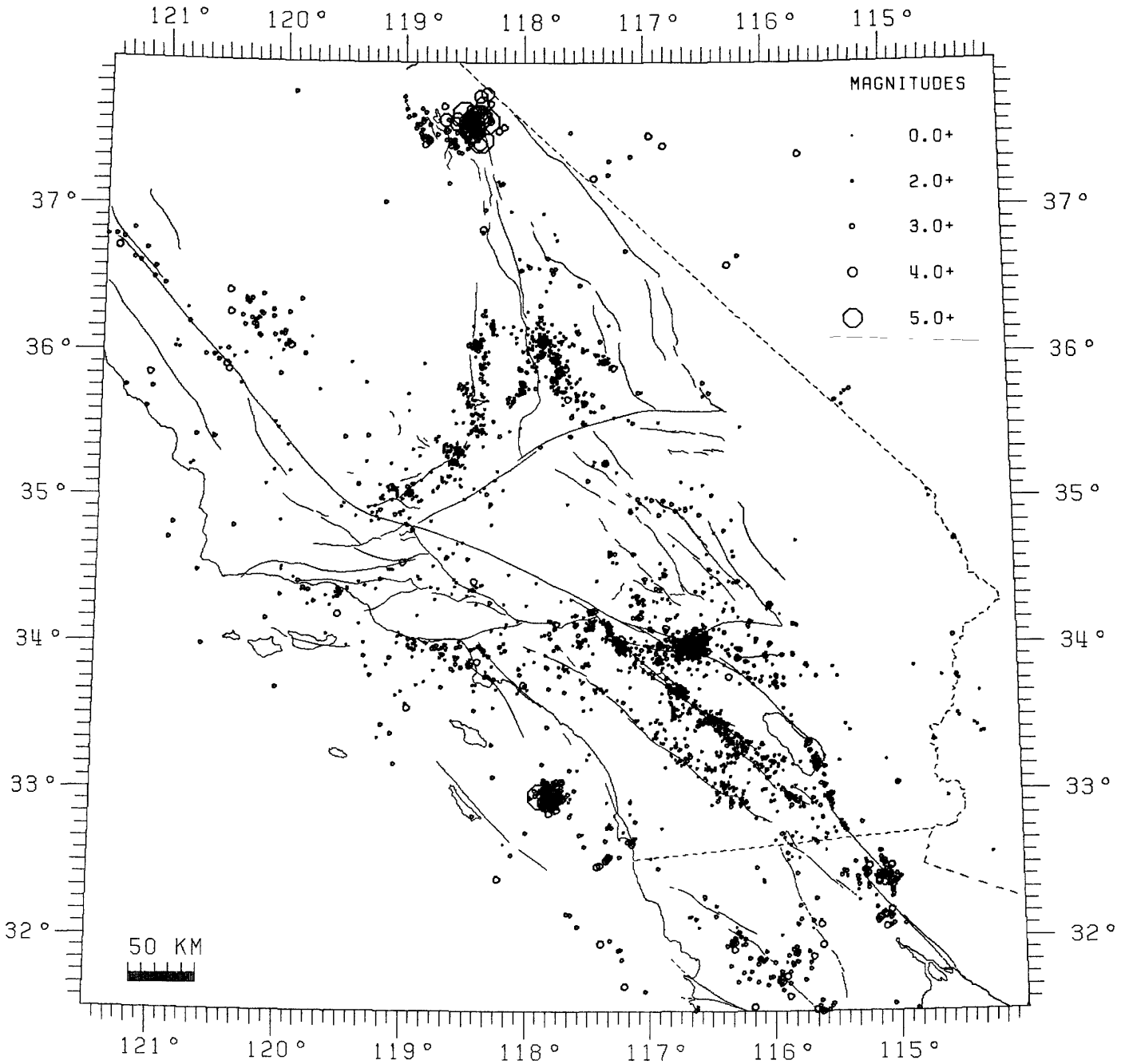

Fig. 1.--Epicenters of larger earthquakes in the southern California region, 1 April to 30 September 1986.

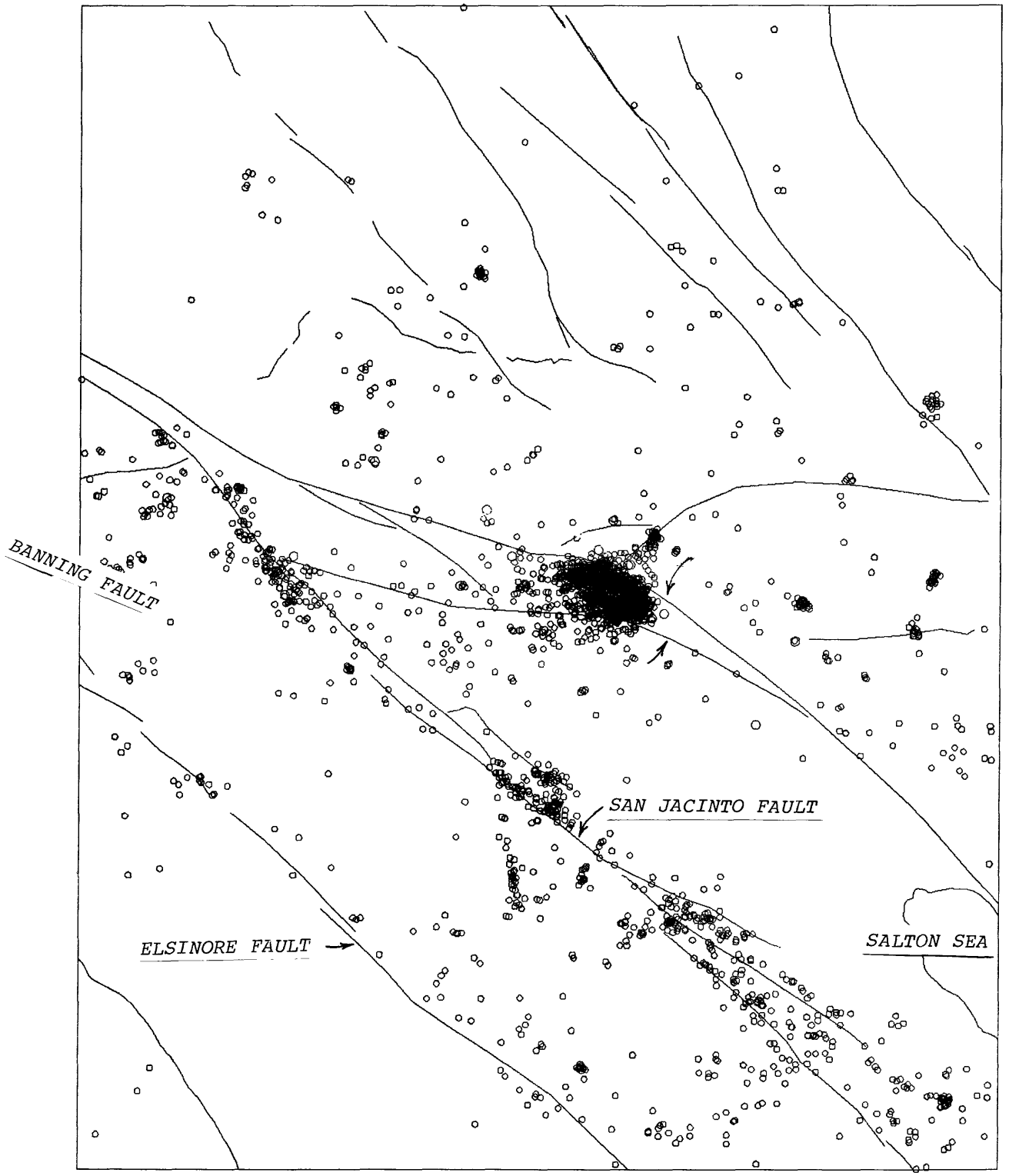

Fig. 2.--Epicenters of the North Palm Springs earthquake sequence (center), sandwiched between the traces of the Banning fault to the south and the Mission Creek fault to the north.

Regional Seismic Monitoring Along the Wasatch Front Urban Corridor and Adjacent Intermountain Seismic Belt

14-08-0001-A0265

W. J. Arabasz, R.B. Smith, J.C. Pechmann, and E.D. Brown
Department of Geology and Geophysics
University of Utah
Salt Lake City, Utah 84112
(801)581-6274

Investigations

This cooperative agreement supports "network operations" (including a computerized central recording laboratory) associated with the University of Utah 80-station regional seismic telemetry network. USGS support focuses on the seismically hazardous Wasatch Front urban corridor of north-central Utah but also encompasses neighboring areas of the Intermountain seismic belt between Yellowstone Park and southernmost Utah. The State of Utah, the U.S. Bureau of Reclamation, the National Park Service, and the U.S. Geological Survey Volcanic Hazards Program also contributed support to operation of the University of Utah network during the report period.

Primary products of this USGS cooperative agreement are quarterly earthquake catalogs and a semi-annual data submission, in magnetic-tape form, to the USGS Data Archive.

Results

1. Network Seismicity

Figure 1 shows the epicenters of 207 earthquakes ($M \leq 4.1$) located in part of the University of Utah study area designated the "Utah region" (lat. 36.75°-42.5°N, long. 108.75°-114.25°W) during the six-month period April 1 to September 30, 1986. The seismicity includes six shocks of magnitude 3.0 or greater, several areas of spatial clustering, and two felt events.

The largest earthquake during the report period, M4.1, occurred on August 22, and was located 32 km southeast of Bullfrog Basin in southeastern Utah at $37^{\circ}27.2$N, $110^{\circ}31.5$W. This earthquake occurred in a sparsely populated area and was not reported felt. An earthquake of M3.5 on September 19, located roughly 30 km south of Logan, Utah, was felt in the southern Cache Valley. The second felt earthquake was a shock of M3.2 on August 29, felt in Preston, Idaho, just north of the Utah border; the shock was located 16 km east of Preston at $42^{\circ}6.4$N, $111^{\circ}39.2$W.

The epicenters shown in Figure 1, including several spatial clusters, reflect typical earthquake activity scattered throughout Utah's main seismic region. A cluster 20 km east of Ogden is associated with an M3.6 event which occurred on June 5. Clustered epicenters located 50 km southwest of Richfield, Utah, are close to the Roosevelt geothermal field, which has exhibited episodic swarm activity in the past.

2. Network Upgrading

During the report period, extensive field-construction efforts were made as part of a project to upgrade six single-component stations of the University of Utah seismic network to high-quality four-component stations. Vandal-proof vaults at all of these stations have been designed to house a vertical-component Geotech S-13 seismometer recording on both high- and low-gain channels, plus two matching horizontal-component S-13 seismometers. A seventh station, DUG, was upgraded to a matching six-component station (3 high-gain and 3 low-gain) in August 1985. Vaults are in place for 5 of the 6 four-component stations, and multicomponent digital recording is in effect for two of the stations—plus that for station DUG. The selected stations are spaced roughly 75-150 km apart and were chosen on the basis of site quality and location. Three are located in abandoned mine tunnels and the other four are buried in concrete enclosures.

The multicomponent scheme was designed to provide on-scale digital recordings at several stations throughout the Wasatch Front area for earthquakes of M3.0 or less, and at least two on-scale digital records at distances less than 100 km for earthquakes of M4.0 or less. The scheme is a relatively inexpensive one for addressing the low-dynamic-range problem of short-period telemetry networks and allows straightforward recording with our PDP-11/34 event-detection algorithm.

Reports and Publications

Brown, E.D., 1986, Utah earthquake activity: Wasatch Front Forum, U.S. Geological Survey, v. 2, no. 3, p. 7.

Brown, E.D., 1986, Utah earthquake activity: Survey Notes, Utah Geological and Mineral Survey, v. 19, no. 4, p. 6 (October-December 1985); v. 20, no. 2, p. 8 (January-March 1986); v. 20, no. 2, p. 10 (April-June 1986).

Brown, E.D., Arabasz, W.J., Pechmann, J.C., McPherson, E., Hall, L.L., Oehmich, P.J., and Hathaway, G.M., 1986, Earthquake Data for the Utah Region, January 1, 1984 to December 31, 1985: Special publication, University of Utah Seismograph Stations, Salt Lake City, 83 p.

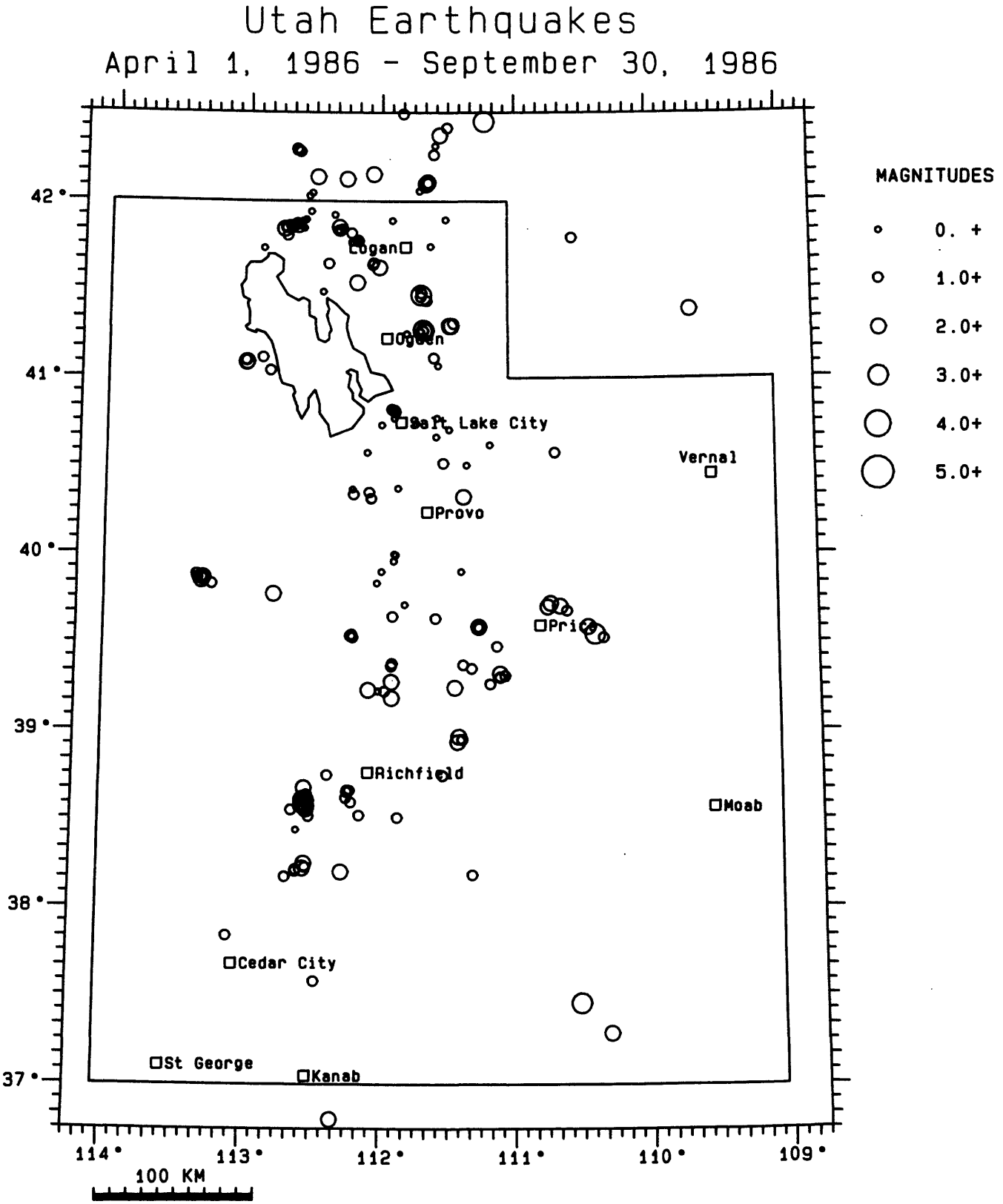
Utah Earthquakes
April 1, 1986 - September 30, 1986
MAGNITUDES
0. +
1.0+
2.0+
3.0+
4.0+
5.0+
Logan
Ogden
Salt Lake City
Vernal
Provo
Price
Richfield
Moab
Cedar City
St George
Kanab
42°
41°
40°
39°
38°
37°
114°
113°
112°
111°
110°
109°
100 KM

Figure 1

Seismological Data Processing

9930-03954

Barbara Bekins and Thomas Jackson

Branch of Seismology
U.S. Geological Survey
345 Middlefield Rd. MS 977
Menlo Park, California, 94025
(415) 323-8111 ext. 2965

Investigations

Computer data processing is now an integral part of seismological research. The purpose of this project is to provide for general purpose and specialized computer data processing systems to meet the research computing needs of scientists in the earthquake prediction program and monitor earthquakes in northern California. This goal includes providing for transfer of data and programs between computers over data networks and facilitating sharing of data and programs with USGS external contractors.

To meet the stated project goals, this project has responsibility for maintaining and enhancing existing computer systems and planning and purchasing new systems. Existing systems include a PDP 11/70 UNIX system, a VAX 750 VMS system, two Data General Eclipse systems, a Motorola 68020 UNIX system, a VAX 785 VMS system, and two PDP 11/44 RSX systems. These systems presently perform a variety of functions such as digitizing of analog tapes, real-time monitoring of Northern and Central California seismicity, and general purpose research computing. All of these systems are connected via various networking schemes including Ethernet, phone links to other sites, and dedicated direct connections. This project is also responsible for assessing the need for new network connections, selecting appropriate hardware, and adding and maintaining connections.

Recent work has been focused on four main efforts. The first is enhancing performance of the VAX 750 system to handle increased waveform data anticipated as a result of the Parkfield Prediction Experiment. The second is migrating users and real-time monitoring functions from the PDP 11/70 UNIX system to the new Integrated Solutions Motorola 68020 UNIX system. The third is networking the VMS VAX systems and the UNIX systems on ethernet. The fourth is planning for uninterrupted data processing and real-time monitoring while asbestos is removed from the beams in the building.

Results

Enhancing the performance of the VAX 750 VMS system involved first monitoring the system to determine the best way to improve user response time. From the results of this monitoring a decision was made to purchase more memory, new terminal port boards, and additional disk drives. The new memory has been installed and resulted in a marked performance increase. The system now has the maximum allowed amount of eight million bytes of memory. The new terminal ports have been delivered and will be installed shortly. These ports are expected to provide a five percent performance increase. New disk space totaling 1.2 billion bytes is also planned for the system. This added space will facilitate research using digital seismic data. Finally the ability to read in digital seismic data from an analog-to-digital converter has recently been implemented on the system. This will provide for research using seismic traces currently stored on analog tape.

The migration of users and programs from the PDP 11/70 UNIX system to the Integrated Solutions system is continuing. At this point about 50 percent of the users and programs have been moved. The system is still performing very well under this load with an average of three to four simultaneous users. Eventually the system must accommodate six simultaneous users. Some questions remain about the difference between the IEEE floating point standard and the DEC floating point format. Various floating point test and evaluation routines have been investigated. Future plans for the system include installing the IMSL subroutine package, the Maxima system for simplifying and expanding mathematical expressions, and a laser printer.

The networking of the VMS VAX systems and the UNIX systems is nearly complete. From the VAX 785, VAX 750, and the Integrated Solutions UNIX system, users may request a connection and login via Ethernet to the other systems. File transfers may also be requested to or from a remote machine. Future plans include adding this capability to an IBM PC-AT and implementing an electronic mail facility which will forward mail sent on any system to the recipient's preferred computer system via the Ethernet.

Planning for asbestos removal in the building has moved to high priority. Starting in February, 1987, three public terminal rooms will be established using existing terminals. Existing and new laser printers will be used for printer output. The computer equipment will remain running at all times with restricted access to the computer room. Operators will be trained to mount tapes and operate the existing lineprinters. Altogether Seismology Branch will require standby computing facilities for six months.

Earthquake Prediction Experiments

In the Anza-Coyote Canyon Seismic Gap

14-08-0001-A0258

Jonathan Berger and James N. Brune
Institute of Geophysics and Planetary Physics
Scripps Institution of Oceanography
University of California, San Diego
La Jolla, CA 92093

1. Investigations

This report covers the progress of the research investigating the Anza-Coyote Canyon seismic gap for the period of the first half of 1986. The objectives of this research are: 1) To study the mechanisms and seismic characteristics of small and moderate earthquakes, and 2) To determine if there are premonitory changes in seismic observables preceeding small and moderate earthquakes. This work is carried out in cooperation with Tom Hanks, Joe Fletcher and Linda Haar, of the U.S. Geological Survey, Menlo Park.

2. Network Status

During the period of this report, ten stations of the Anza Seismic Network were telemetering three component data. The network was set at a low gain for most of the time of this report to try to record earthquakes up to magnitude 4 occurring inside the array.

There were no significant modifications to the data acquisition equipment.

3. Seismicity

In the six months of winter and spring, the Anza network recorded over 50 events which were large enough to locate and determine source parameters. These events had moments ranging from 1×10^{18} to 1.4×10^{21} dyne-cm, and stress drops ranging from about 1 to 100 bars (Brune model). The seismicity pattern seems unchanged from what has been observed before (Figure 1). The seismicity does not appear to be associated with the main trace of the San Jacinto fault on the north-west end of the array. These events in this area tend to be between the Hot Springs fault and the San Jacinto fault at depths of 12 to 19 km. The events on the south-east end of the array near the trifurcation of the San Jacinto fault also do not have any obvious associations with the identified fault traces. These earthquakes are occurring at depths between 8 and 12 km. The shallowest events are still occurring in the Cahuilla area.

4. Data Analysis

4.1. Studies of the 30 Hz Energy of Earthquakes

During the period of this report we made observations of 30 Hz spectra of P-waves from numerous earthquakes, covering a range of locations and magnitudes and compared these observations with various theoretical predictions, including the Archambeau (1968, 1972) stress relaxation model, which has been used in a recent article by Evernden *et al.* (1986) proposing a method for discriminating underground nuclear explosions from earthquakes.

One of the factors of crucial importance in the Evernden *et al.* proposal is the shape of the P-wave spectrum beyond the corner frequency, which is the focus of our studies. The Archambeau (1968, 1972) model predicts a high-frequency fall-off, beynd the corner frequency, proportional to ω^{-3}. For simplicity in this paper we will refer to the model as the W3P model (ω^{-3} fall-off for P-waves). This kind of a fall-off has a paradoxical result that for a given stress drop very large earthquakes do not radiate any more high-frequency energy than small earthquakes ($m_b \approx 1.8$), a consequence of the fact that the low-frequency spectral level is proportional to the cube of the source dimension, this being exactly cancelled out by the ω^{-3} fall-off from the corner frequency (which decreasees linearly with the source dimension). In the Evernden *et al.* earthquake model the ω^{-3} fall-off of the P-wave spectrum for earthquakes, being different from an ω^{-2} fall-off for explosionss, is proposed as acting to enhance the discrimination achievable from the differences in P-wave corner frequencies between comparable earthquakes and explosions (comparable in that they have the same low-frequency P-wave amplitudes).

The primary sources of data used in this study include events recorded on the Anza array and events from the Mammoth Lakes swarm (Archuleta *et al.*, 1982; Priestley *et al.*, 1986; Priestley and Brune, 1986). Because the Anza array sites are on solid rock we expect little distortion due to attenuation and site effects. We also have strong motion data for two earthquakes, a $M \approx 5.0$ and a $M \approx 4.7$, which occurred prior to the installation of the Anza array.

Additional data include some events recorded at Anza but occurring outside the array with hypocentral distances of about 30-100 km, where at least four station recordings were available to average. These off-array events were corrected for attenuation, using a Q of 500.

Our results are summarized in Figure 1, a plot of observations of spectral density at 30 Hz, corrected to a distance of 10 km (hypocentral distances) and plotted as a function of moment. The results show the $\Omega(30)$ spectrum increasing linearly with moment up to about 10^{19} dyne-cm. This is expected for any source model, since for moments lower than 10^{19} dyne-cm the source dimensions are small compared to the wavelength for 30 Hz P-wave energy (approximately 200 meters). These small events have corner frequencies higher than 30 Hz, so $\Omega(30)$ scales with moment. For moments above about 10^{20} dyne-cm, the W3P model predicts the spectral values will remain constant, whereas the data show a clear continuing increase with moment, approximately proportional to $M_0^{1/3}$, as would be expected from a constant stress drop W2P model (high-frequency fall-off for P-waves beyond the corner frequency proportional to ω^{-2}). Thus the data clearly indicate that large earthquakes ($M_0 > 10^{21}$ dyne-cm) radiate much more 30-Hz energy than small earthquakes ($M_0 \approx 10^{20}$ dyne-cm).

REFERENCES

Archambeau, C.B. 1968. General theory of elastodynamic source fields. *Rev. Geophys.* **6**, 241-288.

Archambeau, C.B. 1972. The theory of stress wave radiation from explosions in prestressed media. *Geophys. J.* **29**, 329-366.

Archuleta, R.J., E. Cranswick, C. Mueller, and P. Spudich. 1982. Source parameters of the 1980 Mammoth Lakes, California earthquake sequence. *J. Geophys. Res.* **87**, 4559-4585.

Evernden, J.F., C.B. Archambeau, and E. Cranswick. 1986. An evaluation of seismic decoupling and underground nuclear test monitoring using high frequency seismic data. *Rev. Geophys.* **24**, 143-216.

Priestley, K.F., J.N. Brune, and J.G. Anderson. 1985. Surface wave excitation and source mechanism of Mammoth Lakes, California earthquakes. *J. Geophys. Res.* **90:B13**, 11,177-11,185.

Priestley, K.F., and J.N. Brune. 1986. Spectral scaling for the Mammoth Lakes, California earthquakes. (Submitted to *Geophys. J. R. Astr. Soc.*)

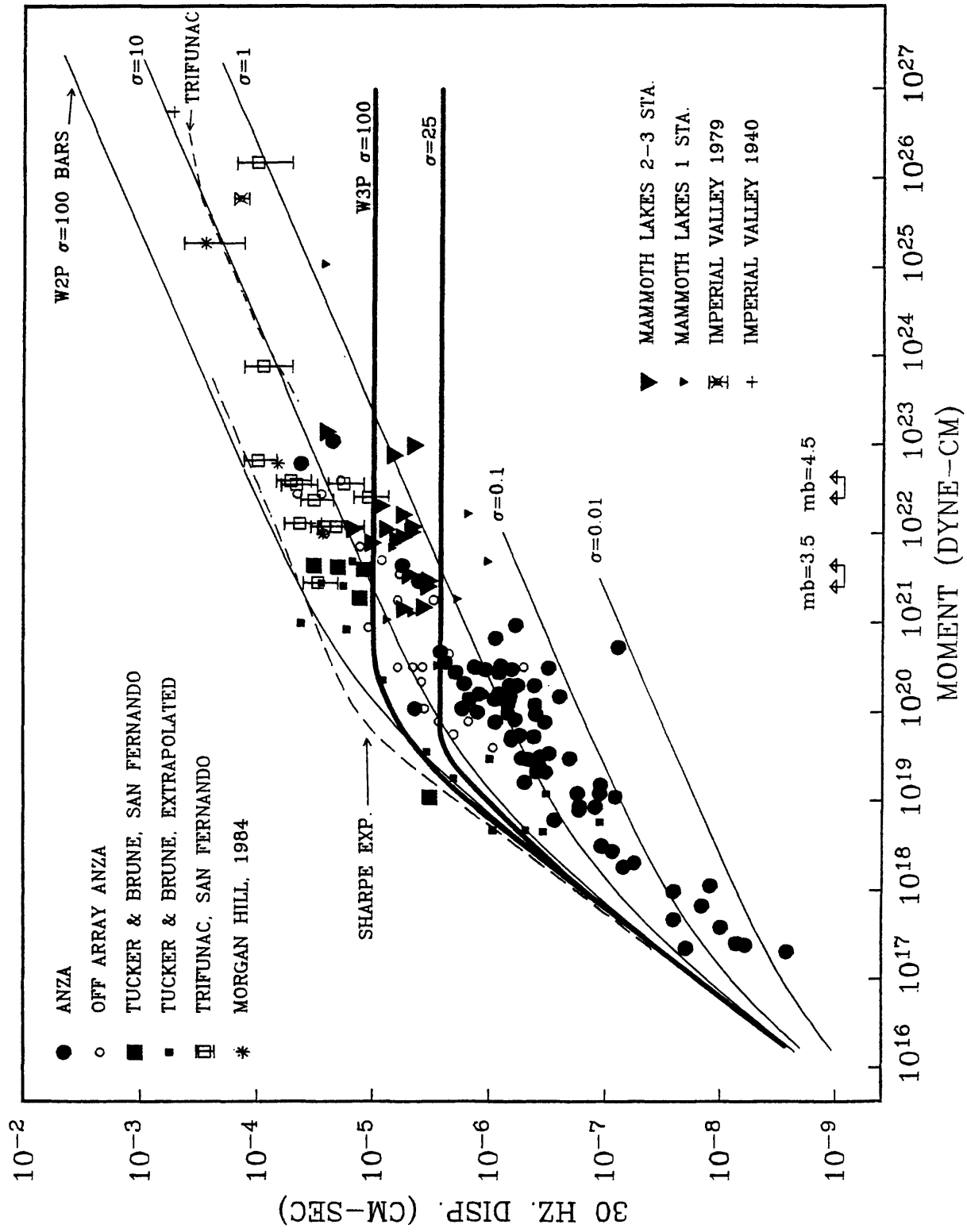
W2P σ=100 BARS
σ=10
TRIFUNAC
σ=1
W3P σ=100
σ=25
SHARPE EXP.
σ=0.1
σ=0.01
ANZA
OFF ARRAY ANZA
TUCKER & BRUNE, SAN FERNANDO
TUCKER & BRUNE, EXTRAPOLATED
TRIFUNAC, SAN FERNANDO
MORGAN HILL, 1984
MAMMOTH LAKES 2-3 STA.
MAMMOTH LAKES 1 STA.
IMPERIAL VALLEY 1979
IMPERIAL VALLEY 1940
mb=3.5 mb=4.5
30 HZ. DISP. (CM-SEC)
MOMENT (DYNE-CM)
10^-2
10^-3
10^-4
10^-5
10^-6
10^-7
10^-8
10^-9
10^16 10^17 10^18 10^19 10^20 10^21 10^22 10^23 10^24 10^25 10^26 10^27

FIGURE 1.

Central Aleutian Islands Seismic Network

Agreement No. 14-08-0001-A0259

Selena Billington and Carl Kisslinger
Cooperative Institute for Research in Environmental Sciences
Campus Box 449, University of Colorado
Boulder, Colorado 80309

(303) 492-6042

Brief Description of Instrumentation and Data Reduction Methods

The Adak seismic network consists of 13 high-gain, high-frequency, two-component seismic systems and one six-component system (ADK) located at the Adak Naval Base. Station ADK has been in operation since the mid-1960s; nine of the additional stations were installed in 1974, three in 1975, and one each in 1976 and 1977.

Data from the stations are FM-telemetered to recording sites near the Naval Base, and are then transferred by cable to the Observatory on the Base. Data were originally recorded by Develocorder on 16 mm film; since 1980 the film recordings are back-up and the primary form of data recording has been on analog magnetic tape. The tapes are mailed to CIRES once a week.

At CIRES the analog tapes are played back at four-times the speed at which they were recorded into a computer which digitizes the data, automatically detects events, and writes an initial digital event tape. This tape is edited to eliminate spurious triggers, and a demultiplexed tape containing only seismic events is created. All subsequent processing is done on this tape. Times of arrival and wave amplitudes are read from an interactive graphics display terminal. The earthquakes are located using a program developed for this project by E. R. Engdahl, which uses corrections to the arrival times which are a function of the station and the source region of the earthquake.

Data Annotations

A major earthquake (M_S 7.6) occurred immediately to the east of the network coverage area on May 7, 1986 (at 22:47). A discussion of the prediction of that earthquake and subsequent investigations to date is published under the report for Grant No. 14-08-0001-G1099 (Kisslinger) elsewhere in this issue. Hundreds of aftershocks of that earthquake occurred within the network coverage area. At the time of this writing, the local catalog of hypocenters is still incomplete for the immediate time period following the mainshock. However, several hundred hypocenters have been located so far in the area of network coverage during the first 24 hours after the mainshock. This report will cover the time period of January through May 8, 1986, although we are still in the process of locating aftershocks which occurred on May 8.

The network was serviced from mid-July through September, 1986. Because of major logistic problems, two of the westernmost stations could not be reached at that time, and we were also unable to make a needed return trip to one other far-west station. Of the 28 short-period vertical and horizontal components, 21 were operating for most of the period of January through May 8, 1986. Near the end of the time period being reported, AD3 and AD5 were intermittent. By the end of the 1986 summer field trip to Adak, 23 of the 28 components were operating (AK2z, AK5h, AD3 and AD5 having been brought back up).

Current Observations

372 earthquakes have been located so far with data from the network during the time period from January through May 8, 1986. Of these, 157 occurred between January 1 and the time (20:43) of the M_S 6.0 foreshock of the May 7 mainshock, and 215 are the aftershocks to these two events located to date. Epicenters of all these events are shown in Figure 1 and a vertical cross-section is given in Figure 2. So far, 19 of the events located with data from the Adak network in this time period were large enough to be located teleseismically (USGS PDEs), of which 16 occurred on May 7 and May 8 and are foreshocks and aftershocks to the May 7 earthquake. A number of other teleseismically located aftershocks within the network region are difficult for us to locate due to their arrivals being masked by the codas of other aftershocks. Work on locating these and other earthquakes on May 8 continues. No attempt is being made to locate aftershocks with duration magnitudes (m_d) of less than 2.3.

More detailed information about the network status and a catalog of the hypocenters determined for the time period reported here are included in our semi-annual data report to the U.S.G.S. Recent research using these data is reported in the Technical Summary for U.S.G.S. Grant No. 14-08-0001-G1099.

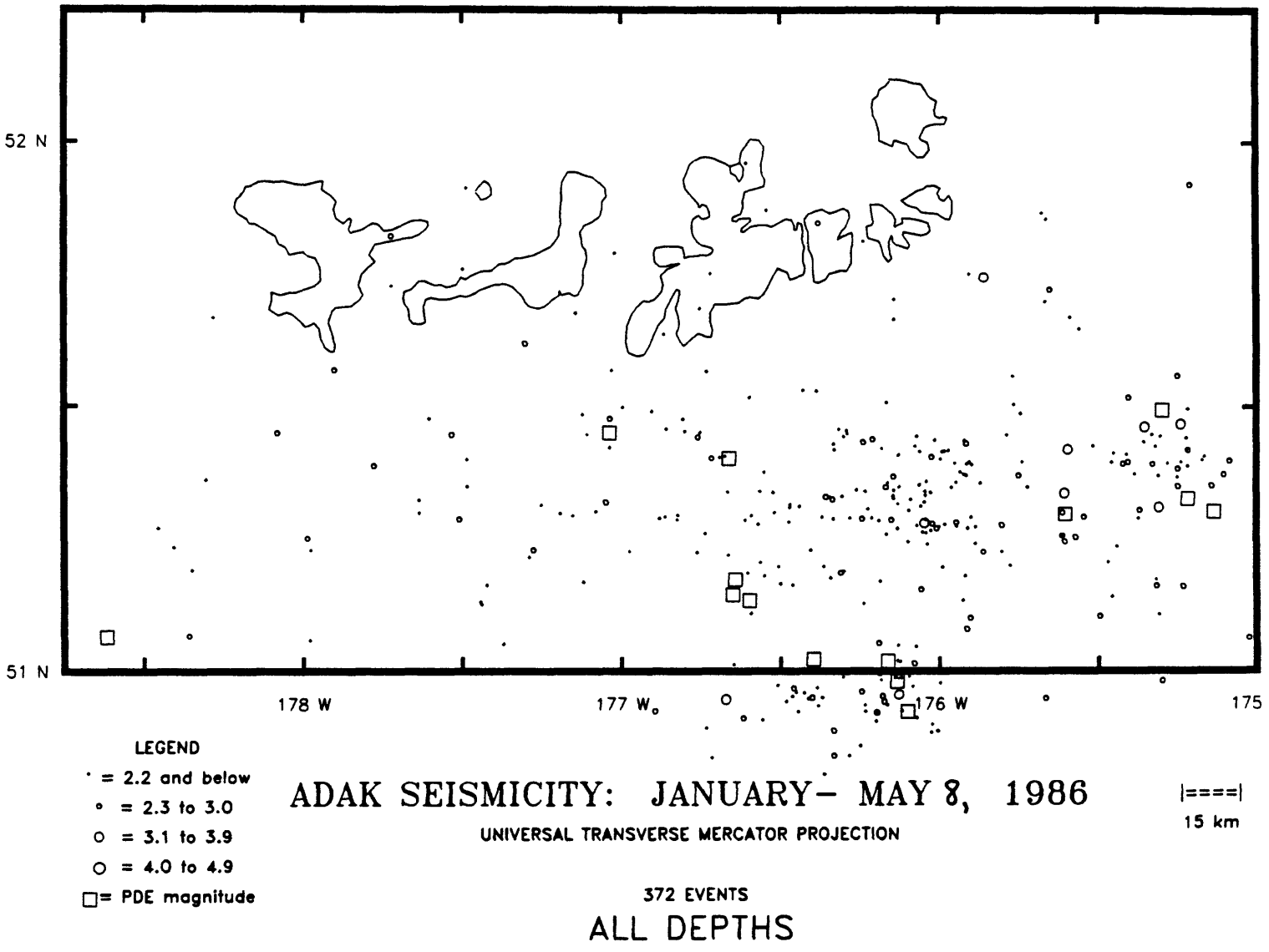

Figure 1: Map of seismicity which occurred from January 1 through May 8, 1986. All epicenters were determined from Adak network data. Events marked with squares are those for which a teleseismic body-wave magnitude has been determined by the USGS; all other events are shown by symbols which indicate the duration magnitude determined from Adak network data. The islands mapped (from Tanaga on the west to Great Sitkin on the east) indicate the geographic extent of the Adak seismic network.

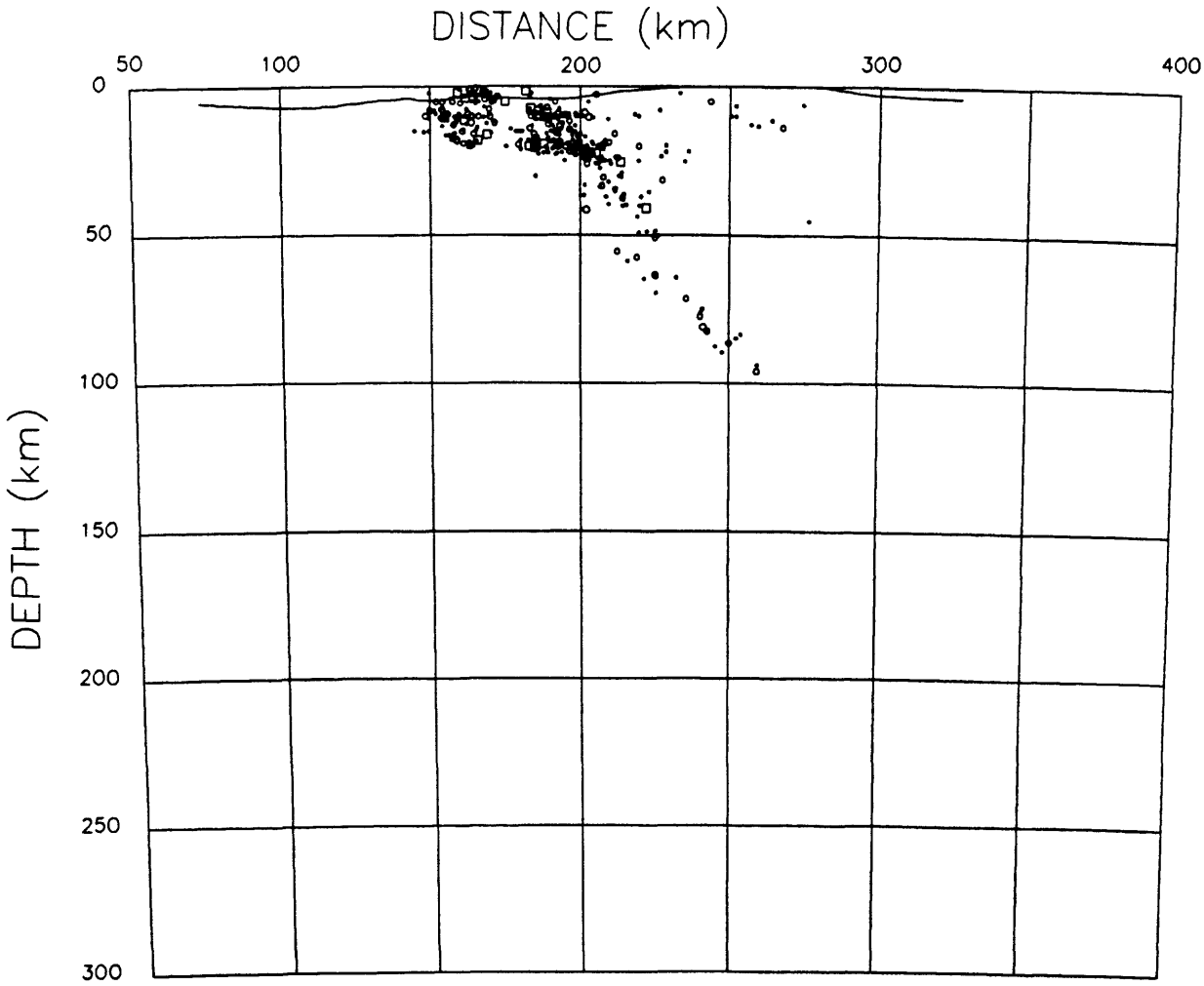

ADAK SEISMICITY: JANUARY– MAY 8, 1986

Figure 2: Vertical cross section of seismicity which occurred from January 1 through May 8, 1986. Events are projected according to their depth (corresponding roughly to vertical on the plot) and distance from the pole of the Aleutian volcanic line. The zero-point for the distance scale marked on the roughly-horizontal axis of the plot is arbitrary. Events marked with squares are those for which a teleseismic body-wave magnitude has been determined by the USGS; all other events are shown by symbols which indicate the duration magnitude determined from Adak network data. The irregular curve near the top of the section is bathymetry.

Regional Seismic Monitoring in Western Washington

14-08-0001-A0266

R.S. Crosson and S.D. Malone
Geophysics Program
University of Washington
Seattle, WA 98195
(202) 543-8020

Investigations

Operation of the western Washington regional seismograph network and routine preliminary analysis of earthquakes in western Washington are carried out under this contract. Quarterly catalogs of seismic activity in Washington and Northern Oregon are available for 1984, 1985, and the first two quarters of 1986. These catalogs are funded jointly by this contract and others. The University of Washington operates approximately 80 stations west of 120.5 ° W. Twenty eight are funded under this contract including a new station, CMW (Cultus Mountains), installed in the Skagit Valley in June 1986.

Data are provided for USGS contract 14-08-0001-G1080 and other research programs. Efforts under this contract are closely related to and overlap objectives under contract G1080, also summarized in this volume. Publications are listed in the G1080 summary. This summary covers a six month period from April 1, 1986 through September 30, 1986. During this period the U.W. seismic network located 738 events west of 120.5 ° W. Only 415 events were located during the preceding six months. This increase was due to seismicity associated with the extrusion of a new lobe at Mt. St. Helens in May. Excluding Mt. St. Helens, 315 earthquakes were located west of 120.5 ° W, compared to 309 in the preceding six months. The dome building eruption took place between May 3 and May 20. During the six months covered by this summary, the largest earthquake located in western Washington was a M_C 3.5, which occurred on July 8, at 60 km depth, about 20 km south of Anacortes near the Saratoga Passage. This earthquake had a focal mechanism indicating normal faulting; it was also the deepest earthquake located in Washington during the summary period.

Central California Network Operations

9930-01891

Wes Hall
Branch of Seismology
U.S. Geological Survey
345 Middlefield Road, Mail Stop 977
Menlo Park, California 94025
(415) 323-8111, Ext. 2509

Investigations

Maintenance and recording of 324 seismograph stations (393 components) located in Northern and Central California. Also recording 71 components from other agencies. The area covered is from the Oregon border south to Santa Maria.

Results

1. Modified and installed one hundred-nine (208) VCO/AMPS for greater frequency stability; temperature stability; and dynamic range.
   114 ea J302M to J302ML
   1 ea J402 to J402ML
   80 ea J402 to J402H
   13 ea J502

2. Installed two way microwave data channel to Department of Water Resources (DWR) via Corps of Engineers Microwave System.

3. Established two way microwave voice channel to Hog Canyon (PHO) and Car Hill (PCH). This aids communication between USGS personnel in the Parkfield area and Menlo Park.

4. Install base for new microwave tower at Mt. Tamalpais.

5. Install 3-component FBA units at PMM, PHO, PCH.

6. Reduce number of develocorders from five(5) to three(3).

7. Compile data base consisting of the following items.

   a) discriminator number
   b) station ID
   c) VCO freq and type
   d) radio info
   e) signal pair
   f) CUSP
   g) RTP/PRO
   h) tape channel
   i) discriminator type

This data base is sorted by items a, b, e, f, g, and h.

8. Compile data base of Telco drop locations.

9. Ordered parts for 250 ea., J502A VCO/AMPS.

ALASKA SEISMIC STUDIES

9930-01162

John C. Lahr, Christopher D. Stephens, Robert A. Page
Branch of Seismology
U. S. Geological Survey
345 Middlefield Road, MS 977
Menlo Park, California 94025
(415) 323-8111, Ext. 2510

Investigations

1) Continued collection and analysis of data from the high-gain, short-period seismograph network extending across southern Alaska from the volcanic arc west of Cook Inlet to Yakutat Bay, and inland across the Chugach mountains.

2) Continued monitoring in the region of the proposed Bradley Lake hydroelectric project on the southern Kenai Peninsula, a cooperative effort with the Alaska Power Authority.

3) Cooperated with the Branch of Engineering Seismology and Geology in operating 19 strong-motion accelerographs in southern Alaska, including 13 between Icy Bay and Cordova in the area of the Yakataga seismic gap.

Results

1) During the past six months preliminary hypocenters have been determined for 1353 earthquakes that occurred between February and July, 1986 (Figure 1). This total is nearly 400 lower than for the previous six month period, but this decrease most likely results from two systematic changes: a higher detection threshold in the eastern part of the network due to reduced telemetry capacity and to telemetry failures, and, beginning in May, relaxation of criteria to preferentially include small (duration magnitude, $M_D < 2$) shocks occurring along the Castle Mountain fault and beneath western Prince William Sound. Fifteen shocks have magnitudes of at least 4.0 m_b, and the largest has a magnitude of 4.9 m_b. All but one of these larger shocks occurred at depths of 50 km or greater within the Wadati-Benioff zone of the subducted Pacific plate beneath the Cook Inlet area. The other larger event has a magnitude of 4.7 m_b and was located at shallow depth (above 30 km) within the aftershock zone of the 1979 St. Elias earthquake near the U.S.-Canada border northeast of Icy Bay.

Earthquakes located shallower than 30 km (Figure 2) along the volcanic arc west of Cook Inlet, along and north of the Castle Mountain fault system, beneath northern Cook Inlet, along the Denali fault system, and beneath the Wrangell volcanoes clearly represent crustal activity within the overthrust North American plate. Two unusual swarms of crustal seismicity occurred in June and July at nearly identical locations about 10 km south of Talkeetna near 62.25°N, 150.25°W. For the June sequence, seven shocks of at least 1.9 M_D were located, the largest being 3.0 M_D. In July, seven shocks ranging in magnitude from 2.0 to 3.2 M_D were located. The four largest shocks from these swarms were also felt at Talkeetna. From August 28 to September 10, four event-triggered seismic recorders (ELOG's) were deployed in the epicentral area of the Talkeetna seismicity in an effort to obtain better

hypocenter control for any continuing activity. The records obtained from this experiment are currently being analyzed, but at least six nearby earthquakes triggered three or more stations.

Relatively few earthquakes associated with the March 27 and later eruptions of Augustine volcano in southern Cook Inlet (Figure 2) were detected by stations of the USGS seismograph network. Only one event near Augustine, a magnitude 2 M_D shock that occurred on March 26, was large enough to be located by the regional network. This is in marked contrast to the 1976 eruptive episode in which the initial eruption was accompanied by an energetic earthquake swarm including over 250 events with magnitudes between 2.0 and 2.5 (Reeder and Lahr, in press). The epicenter for the one located event from 1986 determined using only regional stations was about 10 km southwest of the volcano, but the addition of readings from seismographs operated by the Geophysical Institute of the University of Alaska on the volcano moved the location to a few kilometers below the volcano. Tremor from major eruptive episodes of the volcano was detected at the closest regional stations.

Beneath Prince William Sound and in adjacent areas extending eastward to Yakutat Bay most of the shallow earthquakes probably occur either within the subducted Pacific plate or along the thrust interface between the Pacific and North American plates. The area between eastern Prince William Sound and Icy Bay includes the Yakataga seismic gap. Although the distribution of shallow seismicity across the network is highly non-uniform, principal features in the spatial pattern have remained remarkably stable for at least the past seven years and no unusual deviations from this pattern were observed during the past six-month period.

2) Velocity models derived from TACT (Trans-Alaska Crustal Transect) seismic-refraction profiles in southern Alaska are being used in the relocation of earthquakes recorded by the southern Alaska regional seismograph network. Redetermined hypocenters of 14 well-recorded earthquakes ($0.8 \leq M_D \leq 2.5$) occurring beneath the Chugach Mountains along the Richardson Highway near 61.25°N, 145.25°W fall into two groups. Three of the shocks are shallower than 10 km and lie within the thin accreted Chugach terrane. The remaining events range in depth from 29 to 44 km and belong to the regional NNE-dipping Wadati-Benioff zone associated with the Wrangell Mountains. Modeling of seismic-refraction data indicates the presence of four north-dipping paired layers of low and high ($\geq$ 7.6 km/sec) seismic velocities beneath the Chugach terrane. These paired layers, or duplexes, possibly correspond to sections of subducted oceanic crust and upper mantle. The deeper group of shocks lies within the deepest of the four pairs, or duplexes. This observation suggests that the deepest duplex was subducted most recently and that the three overlying duplexes were emplaced earlier.

Single-event and composite focal-mechanism solutions for the Wadati-Benioff zone shocks indicate a diversity of fault types and orientations; however, strike-slip faulting, often with a component of thrusting, seems to dominate. This faulting is characterized by horizontal north-south P axes and subhorizontal-to-moderately-eastward-dipping T axes.

3) An improved model for the velocity structure of the crust beneath the southern Kenai Peninsula was developed using P- and S- phases recorded from regional crustal and Wadati-Benioff zone earthquakes and from quarry explosions. Wadati diagrams of S- versus P-arrival times indicate that the

Vp/Vs ratio in the upper crust is about 1.73, significantly lower than the previously assumed value of 1.78. Interval velocities of P-waves across the Bradley Lake sub-array were used to infer a velocity of close to 6.0 km/sec in upper crust, although data from quarry blasts indicate a velocity of about 4.5 km/sec in the upper few kilometers below the surface. Pronounced S-to-P converted phases from Wadati-Benioff zone earthquakes below 35 km depth and from crustal events at about 20 to 25 km depth suggest the presence of a major velocity discontinuity at about 15 km depth. Additional evidence for this feature comes from apparent P- and S-wave reflections observed from quarry blasts and from shallow earthquake sources above the inferred discontinuity. It is interesting to note that Fisher and others (1983) also identified a pronounced reflector at about 15 km depth from marine seismic reflection profiling southwest of the southern Kenai Peninsula along strike of the regional tectonic trends. There is as yet insufficent evidence to determine if the same or similar structures are responsible for the seismic signals observed from the two areas, but Byrne (1986) interprets the marine reflection data as possible evidence for the presence of an underplated Eocene sedimentary sequence that may extend from at least Kodiak Island to the Kenai Peninsula. Hypocenters of crustal earthquakes determined using the revised velocity model are more tightly clustered than when the standard model is used, and the average RMS residual for the events is decreased from about 0.33 to 0.15 sec. Most of the crustal activity is located at depths shallower than about 15 km, although in a few areas well-recorded crustal events are located as deep as 25 km. The distribution of revised hypocenter locations still shows no strong correlation with mapped fault traces.

4) In addition to the routine maintenance of the seismic network, several improvements were made to the instrumentation. These changes include the installation of solar panels at two additional sites, the addition of high-dynamic range (90 dB) gain-ranging amplifier cards to the A1VCO amplifier/oscillator unit (Rogers, 1986) at twelve more sites, and the addition of a charging circuit to another SMA-1 strong-motion accelerograph co-located with a high-gain seismograph station. None of the strong-motion recorders was triggered by an earthquake during the past year.

References

Byrne, Tim, 1986, Eocene underplating along the Kodiak Shelf, Alaska: implications and regional correlations, Tectonics, v. 5, p. 403-421.

Fisher, M. A., von Huene, Roland, Smith, G. I., and Bruns, T. R., 1983, Possible seismic reflections from the downgoing Pacific plate, 275 km arcward from the eastern Aleutian Trench, Journal of Geophysical Research, v. 88, p. 5835-5849.

Reports

Lahr, J. C., Page, R. A., Stephens, C. D., and Fogleman, K. A., 1986, Sutton, Alaska earthquake of 1984: evidence for activity on the Talkeetna segment of the Castle Mountain fault system, Bulletin of the Seismological Society of America, v. 76, p. 967-983.

Lahr, J. C., Stephens, C. D., and Page, R. A., 1986, Regional seismic monitoring in southern Alaska: application to earthquake hazards assessment, in, Hays, W., ed., Workshop on evaluation of regional and urban earthquake hazards and risk in Alaska, U. S. Geological Survey Open-File Report 86-79, p. 64-75.

Page, R. A., 1986, Comments on "Earthquake frequency and prediction" by Liu Z.-R., Bulletin of the Seismological Society of America, v. 76, p. 1491-1496.

Page, R. A., Fuis, G. S., Ambos, E. L. and Stephens, C. D., 1986, Relocated earthquakes along the TALI corridor in the Chugach mountains, southern Alaska, (abs), EOS, Transactions of the American Geophysical Union, vol. 67, no. 44, p. 1197-1198.

Reeder, J. W. and Lahr, J. C., Seismological aspects of the 1976 eruption of Augustine volcano, Alaska, U.S. Geological Survey Bulletin 1768, in press.

Rogers, J. A., 1986, Increasing dynamic range in analog seismic data systems used in Alaska, U. S. Geological Survey Open-File Report 86-78, 17 p.

Rogers, J. A., and Lahr, J. C., 1986, An on-site seismic data recording system, U. S. Geological Survey Open-File Report 86-251, 47 p.

Stephens, C. D., Fogleman, K. A., Lahr, J. C., and Page, R. A., 1986, Seismicity in southern Alaska, October 1984 - September 1985, in Bartsch-Winkler, Susan, and Reed, K. M., eds., The United States Geological Survey in Alaska -- Accomplishments during 1985, U. S. Geological Survey Circular 978, p. 81-85.

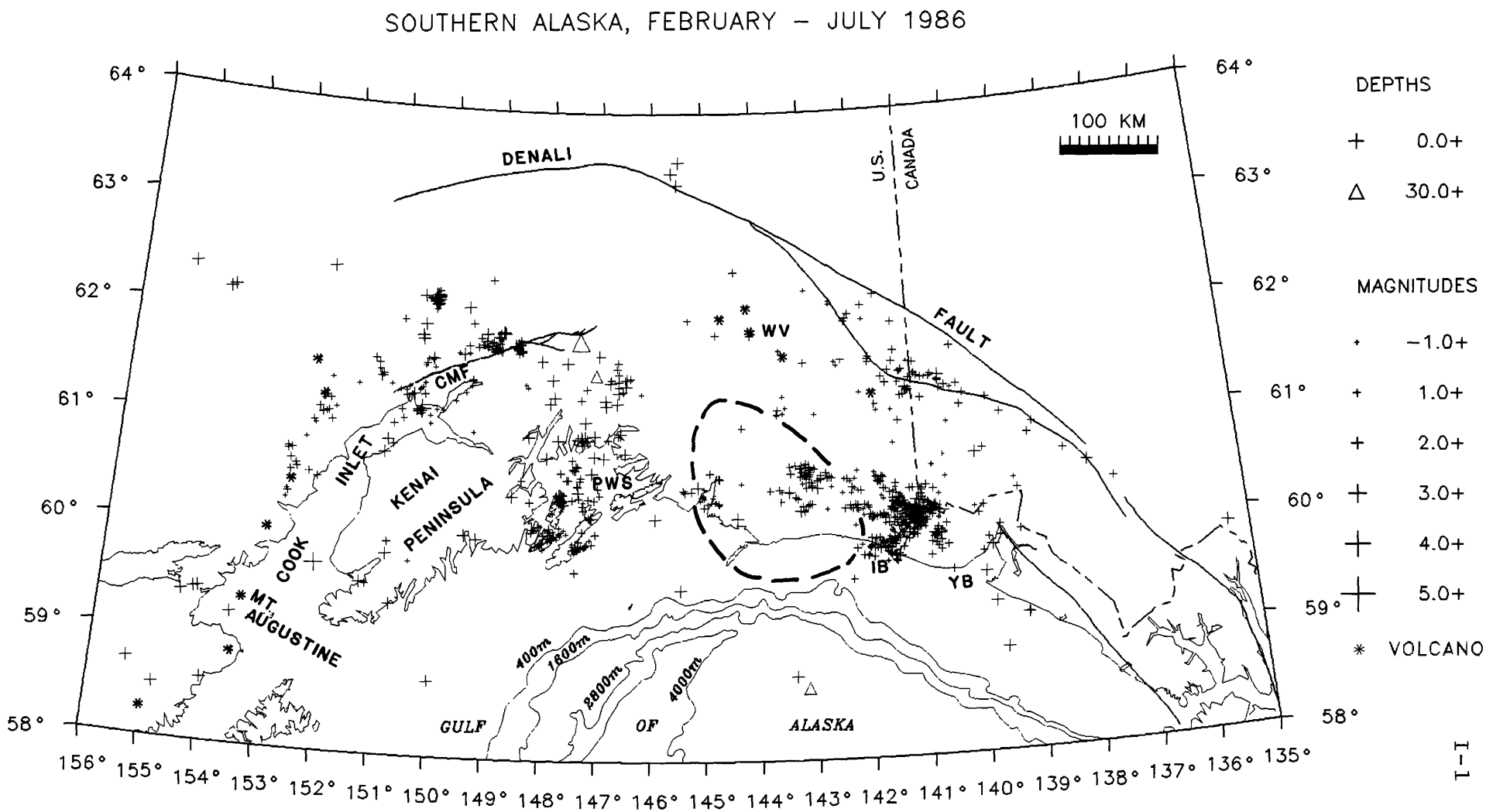

Figure 2. Epicenters of earthquakes from Figure 1 which were located at depths of 30 km or less. Heavy dashed contour indicates inferred extent of Yakataga seismic gap. Abbreviations are: CMF - Castle Mountain fault, IB - Icy Bay, PWS - Prince William Sound, WV - Wrangell volcanoes, YB - Yakutat Bay.

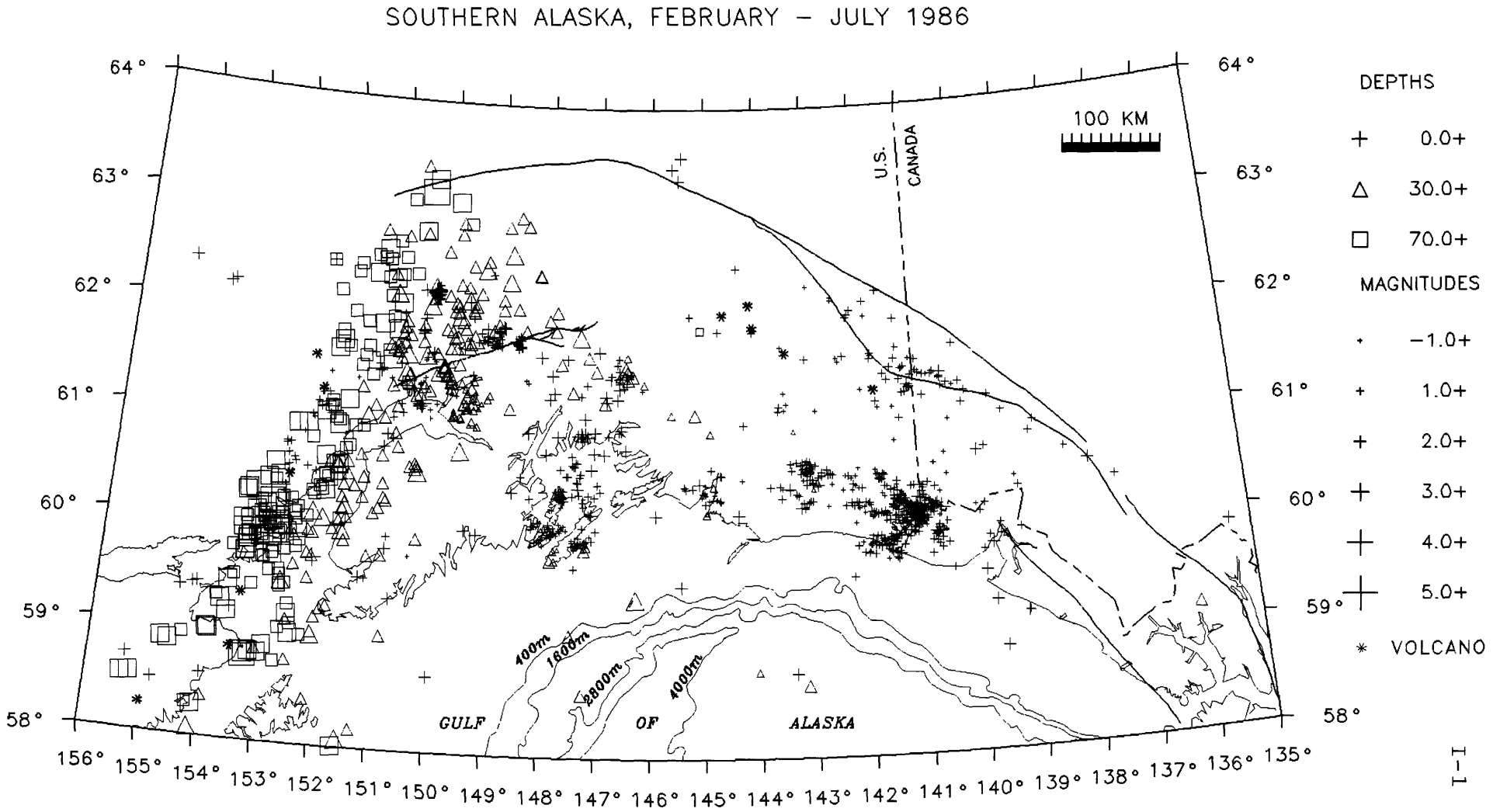

Figure 1. Epicenters located by the USGS southern Alaska seismograph network during February - July, 1986. Epicenters of 1353 earthquakes are plotted. Magnitudes are determined from coda-duration or maximum amplitude, and events of magnitude 3 and larger can be as much as one unit smaller than the teleseismic m_b magnitude. The lowest level to which data is processed varies across the mapped are due to uneven station spacing and to criteria used to select earthquakes for processing. See Figure 2 for identification of map features.

Seismic Data Library

9930-01501

W. H. K. Lee
U.S. Geological Survey
Branch of Seismology
345 Middlefield Road, Mail Stop 977
Menlo Park, California 94025
(415) 323-8111, Ext. 2630

This is a non-researech project and its main objective is to provide access of seismic data to the seismological community. This Seismic Data Library was started by Jack Pfluke at the Earthquake Mechanism Laboratory before it was merged with the Geological Survey. Over the past ten years, we have built up one of the world's largest collections of seismograms (almost all of them on microfilm) and related materials. Our collection includes approximately 4.5 million WWNSS seismograms (1962 - present), 1 million USGS local earthquake seismograms (1966-1979), 0.5 million historical seismograms (1900-1962), and 20,000 earthquake bulletins, reports and reprints.

Early this year, we recieved about 3,500 magnetic tapes containing a complete set of digital waveform data of the Global Digital Seismic Network. These are the so called "Date Tapes". With support from Professor Robert Kovach of Stanford University, these tapes were labelled and set up for any one who wishes to borrow them.

Northern and Central California Seismic Network Processing

9930-01160

Fredrick W. Lester
Branch of Seismology
U.S. Geological Survey
345 Middlefield Road M/S 977
Menlo Park, California 94025
(415) 323-8111, ext. 2149

Investigations

1. In 1966 a seismographic network was established by the USGS to monitor earthquakes in central California. In the following years the network was expanded to monitor earthquakes in most of northern and central California, particularly along the San Andreas Fault, from the Oregon border to Santa Maria. In its present configuration there are over 350 single and multiple component stations in the network. There is a similar network in southern California. From about 1969 to 1984 the primary responsibility of this project was to manually monitor, process, analyze, and catalog the data recorded from this network. In 1984 a more efficient and automatic computer-based monitoring and processing system (CUSP) began online operation, gradually replacing most of the manual operations previously performed by this project. For a more complete description of the CUSP system see the project description "Consolidated Digital Recording and Analysis" by S. W. Stewart.

   Since the introduction of the CUSP system the responsibilities of this project have changed considerably. The main focus of the project now is that of finalizing and publishing preliminary network data from the years 1978 through 1984. We also continue to manually scan network seismograms as back-up event detection for the CUSP system and supplement the CUSP data base with data from the back-up magnetic tapes that were detected only visually or by the other automatic detection system (RTP). Project personnel also act as back-up for the processing staff in the CUSP project. As time permits some research projects are underway on some of the more interesting or unusual events or sequences of earthquakes that have occurred within the network.

   This project continues to maintain a data base for the years 1969 - present on both a computer and magnetic tapes for those interested in research on the network seismic data. As soon as the older data are finalized they are exchanged for the preliminary data existing in the data base.

Results

1. Figure 1 illustrates the more than 13000 earthquakes located by this office for northern and central California during the time period April through September 1986. The largest earthquake during that time

was a magnitude 6.5 shock that occurred on July 21. This earthquake was located approximately 20 km north of Bishop, California in Chalfant Valley. It was accompanied by a M6.0 foreshock on July 20 and many hundreds of aftershocks, three of which were magnitude 5 or larger.

2. Final processing of data for the second half of the calendar year 1982 is complete and those data are ready for publication. Work is currently underway on the final processing of data for the areas around Lake Shasta, Mt. Shasta, and Lassen Volcanic National Park. Some of these data are very preliminary and need extensive reprocessing and analysis, but it is expected that this work will be completed by late 1986 or early 1987. Final processing of the second half of 1978 and all of 1983 is progressing and will be complete in 1987. (see item 3)

3. Since this summer this project has been involved in a combined effort with personnel from many different projects. The first purpose of this group endeavor is to collect all available seismic data pertaining to the more than 150,000 earthquakes that the USGS has located in northern and central California, mainly from 1969 to the present. Those data will then be combined, checked for errors and omissions, reprocessed as necessary, and finalized for publication. It is estimated that this job will take at least one year, which is much less time that would be necessary for this project alone. Personnel in this project will be responsible for coordinating much of this group effort.

4. For the time period April 1986 - September 1986 there were an average of 4 to 6 events per day missed by the CUSP automatic detection system. These were added to the existing CUSP data base from the back-up magnetic tape and processed using standard CUSP processing techniques. Most of the earthquakes that were missed occurred in northern California, north of latitude 39 degrees. This is a particular problem in the north because of telemetry noise that exists on those circuits. To avoid producing an abnormally large number of false triggers in the detection system the trigger thresholds are often set higher than normal and therefore some of the real events are missed.

5. Steve Walter is currently investigating some unusual low frequency events that he has detected in Lassen Volcanic National Park over the last four years. Most of these are deep events, focal depths between 15 and 20 kilometers, and most are concentrated west of Lassen Peak. These events are of interest because they resemble events seen in other volcanic regions, particularly Hawaii, that have been associated with magma transport. Results of this investigation will be presented at the Fall AGU meeting in San Francisco.

6. Quarterly reports were prepared on seismic activity around Warm Springs Dam, the Auburn Dam site and, New Melones Dam for the appropriate funding agencies. Quarterly reports on seismic activity in the Mount Shasta area and in Lassen Volcanic National Park were also prepared and distributed to interested agencies and individuals.

Reports

Walter, S. R., 1986, Long period earthquakes at Lassen Peak - evidence for magma movement, (abs.), submitted the AGU FAll meeting.

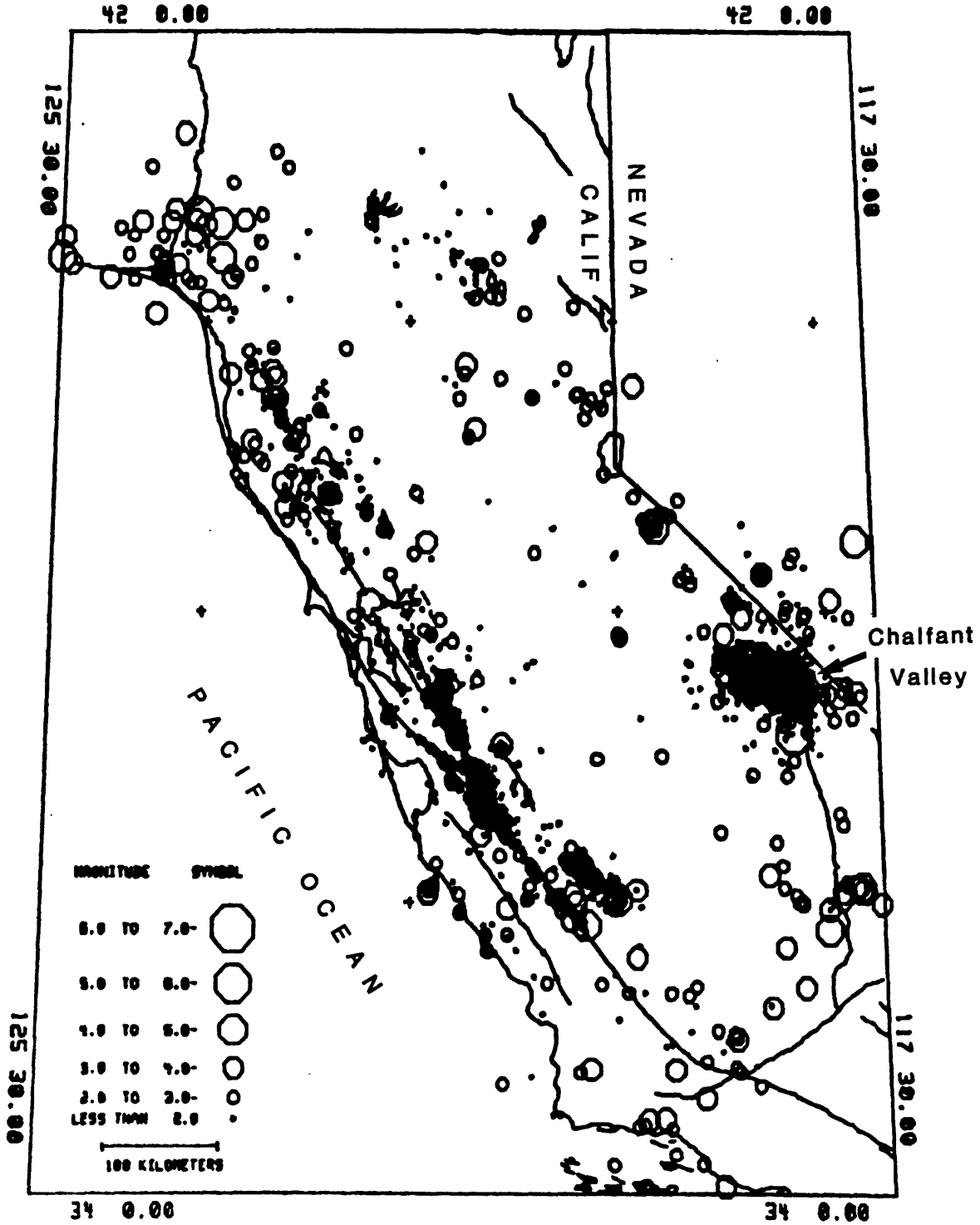

Figure 1. Northern and central California seismicity April - September 1986

Regional Microearthquake Network in the Central Mississippi Valley

14-08-0001-A0263

William V. Stauder and Robert B. Herrmann
Department of Earth and Atmospheric Sciences
Saint Louis University
P.O. Box 8099 Laclede Station
St. Louis, MO 63156
(314) 658-3131

Investigations

The purpose of the network is to monitor seismic activity in the Central Mississippi Valley Seismic zone, in which the large 1811-1812 New Madrid earthquakes occurred. The following section gives a summary of network observations during the first six months of the year 1986.

Results

In the first six months of 1986, 107 earthquakes were located and 29 other nonlocatable earthquakes were detected by the 42 station regional telemetered microearthquake network operated by Saint Louis University for the U. S. Geological Survey and the Nuclear Regulatory Commission. Figure 1 shows 74 earthquakes located within a 4° x 5° region centered on 36.5 °N and 89.5 °W. Seismograph stations are denoted by triangles and are labeled by the station code. The magnitudes are indicated by the size of the open symbols. Figure 2 shows the locations and magnitudes of 58 earthquakes located within a 1.5° x 1.5° region centered at 36.25 °N and 89.75 °W. Figures 3 and 4 are similar to Figures 1 and 2, but the epicenter symbols (squares) are scaled to focal depth.

In the first six months of 1986, 106 teleseisms were recorded by the PDP 11/34 microcomputer. Epicentral coordinates were determined by assuming a plane wave front propagating across the network and using travel-time curves to determine back azimuth and slowness, and by assuming a focal depth of 15 kilometers using spherical geometry. Arrival-time information for teleseismic P and PkP phases has been published in the quarterly earthquake bulletin.

The significant earthquakes occurring in the first six months of 1986 include the following:

1. 31 January 1986, UTC 1646, 41.41 °N, 81.25 °W: large enough to warrant an aftershock study by network personnel. Four MEQ 800 recorders were deployed within 12 hours after the main shock and remained in operation for 60 hours. Felt (VI) in Painesville-Mentor, Ohio area. Felt throughout most of Ohio and parts of Illinois, Indiana, Kentucky, Michigan, New York, Pennsylvania, West Virginia, and Ontario, Canada. Some additional states with only a few felt reports included Delaware, Maryland, New Jersey, Virginia, Wisconsin, and the District of Columbia. m_{Lg}(10Hz) = 4.9(SLM), m_b = 5.0(NEIS).

2. 13 February 1986, UTC 1135, 34.81 °N, 82.94 °W: felt (IV) at Liberty, Six Mile, and West Union, North Carolina. Felt (IV) at Lavonia, Georgia. Felt (III) at Highlands, Hendersonville, North Carolina and Franklin Springs, Georgia. m_{Lg}(10Hz) = 3.0(SLM), m_{bLg} = 3.5(NEIS), m_D = 3.5(TEIC).

3. 24 May 1986, UTC 0815, 35.22 ° N, 92.22 ° W: felt (V) at Enola, Arkansas. m_{Lg}(10Hz) = 3.2(SLM), m_{Lg}(3Hz) = 3.2<FVMZ>, m_D = 3.2(TEIC).

4. 24 May 1986, UTC 1248, 36.58 ° N, 89.88 ° W: felt (IV) at Bernie, Broseley, Campbell, Malden, Parma, Portageville, and Risco, Missouri. Felt (III) at Canalou, Catron, Dudley, Kewanee, New Madrid, Steele, and Tallapoosa. Also felt (III) at Pollard, Arkansas and Tiptonville, Tennessee. m_{Lg}(10Hz) = 3.4(SLM), m_{Lg}(3Hz) = 3.4<FVMZ>, m_D = 3.5(TEIC), m_{bLg} = 3.4(NEIS).

Acknowledgements

The cooperation of the Tennessee Earthquake Information Center, National Earthquake Information Service, and the University of Kentucky is gratefully acknowledged for providing station readings, magnitude data, and felt information. The results reported were supported by the Department of the Interior, U. S. Geological Survey, under Contract 14-08-0001-A0263 and the U.S. Nuclear Regulatory Commission under Contract NRC-04-81-195-03.

References

Central Mississippi Valley Earthquake Bulletin, Department of Earth and Atmospheric Sciences, Saint Louis University. 1986 No. 47

PDE Preliminary Determination of Epicenters, Monthly Listings, U.S. Geological Survey, 1986

TEIC Quarterly Seismological Bulletin, Tennessee Earthquake Information Center, Memphis State University. 1986, Vol. 7, No. 1.

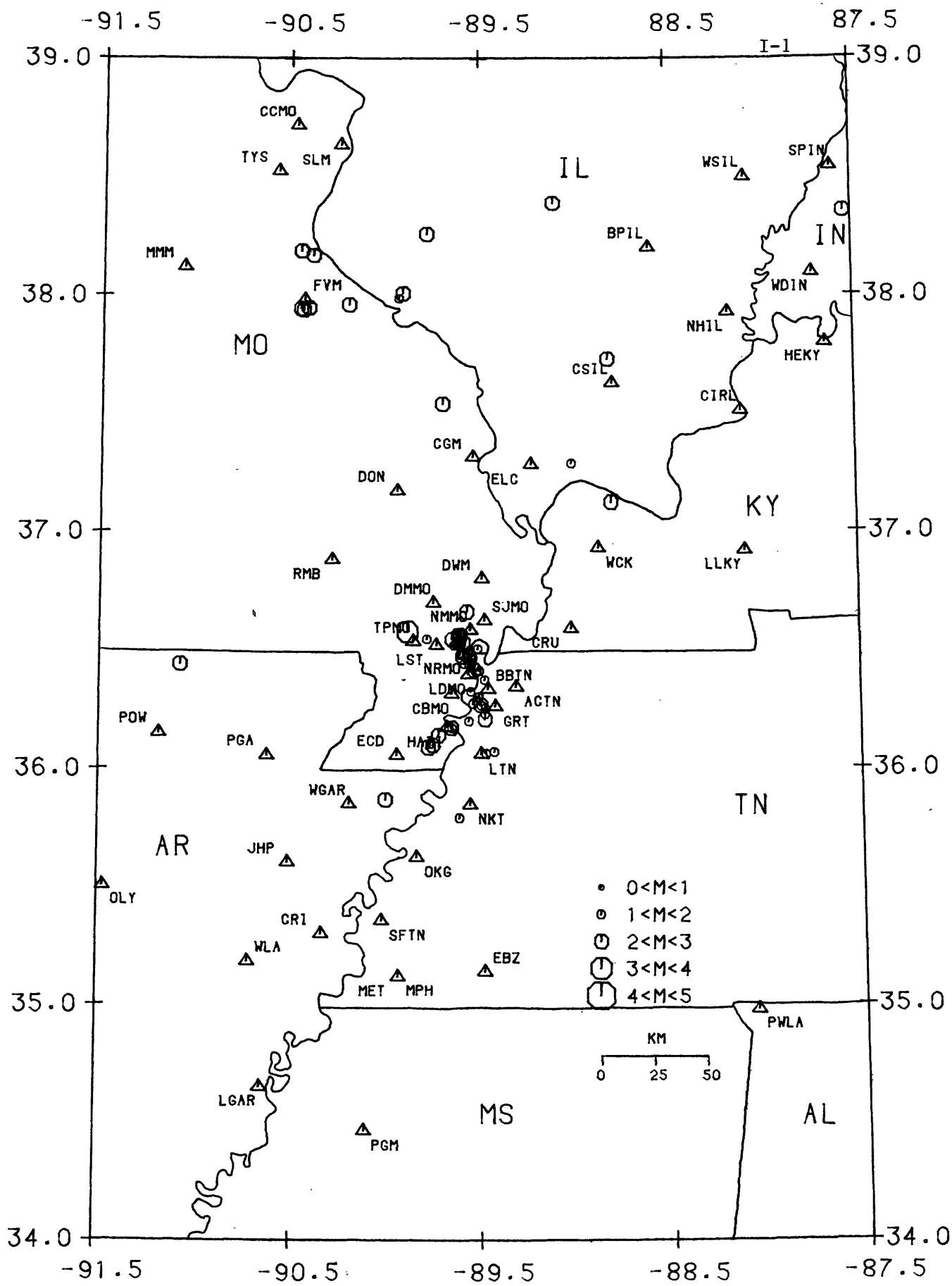

FIGURE 1

CUMULATIVE EVENTS 01 JAN 1986 TO 30 JUNE 1986

LEGEND . △ STATION ⊙ EPICENTER

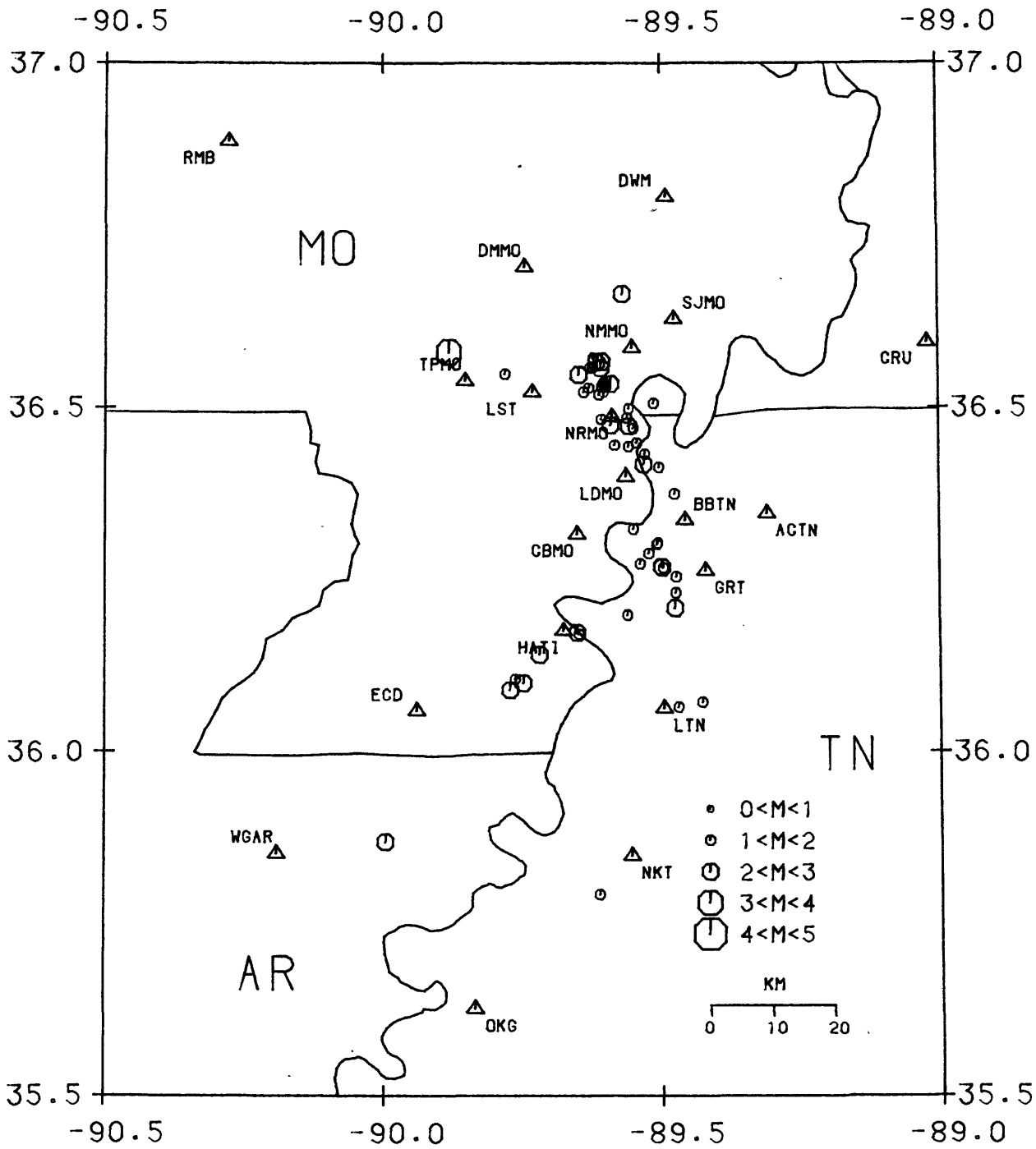

FIGURE 2

CUMULATIVE EVENTS 01 JAN 1986 TO 30 JUNE 1986

LEGEND . ▲ STATION ⊙ EPICENTER

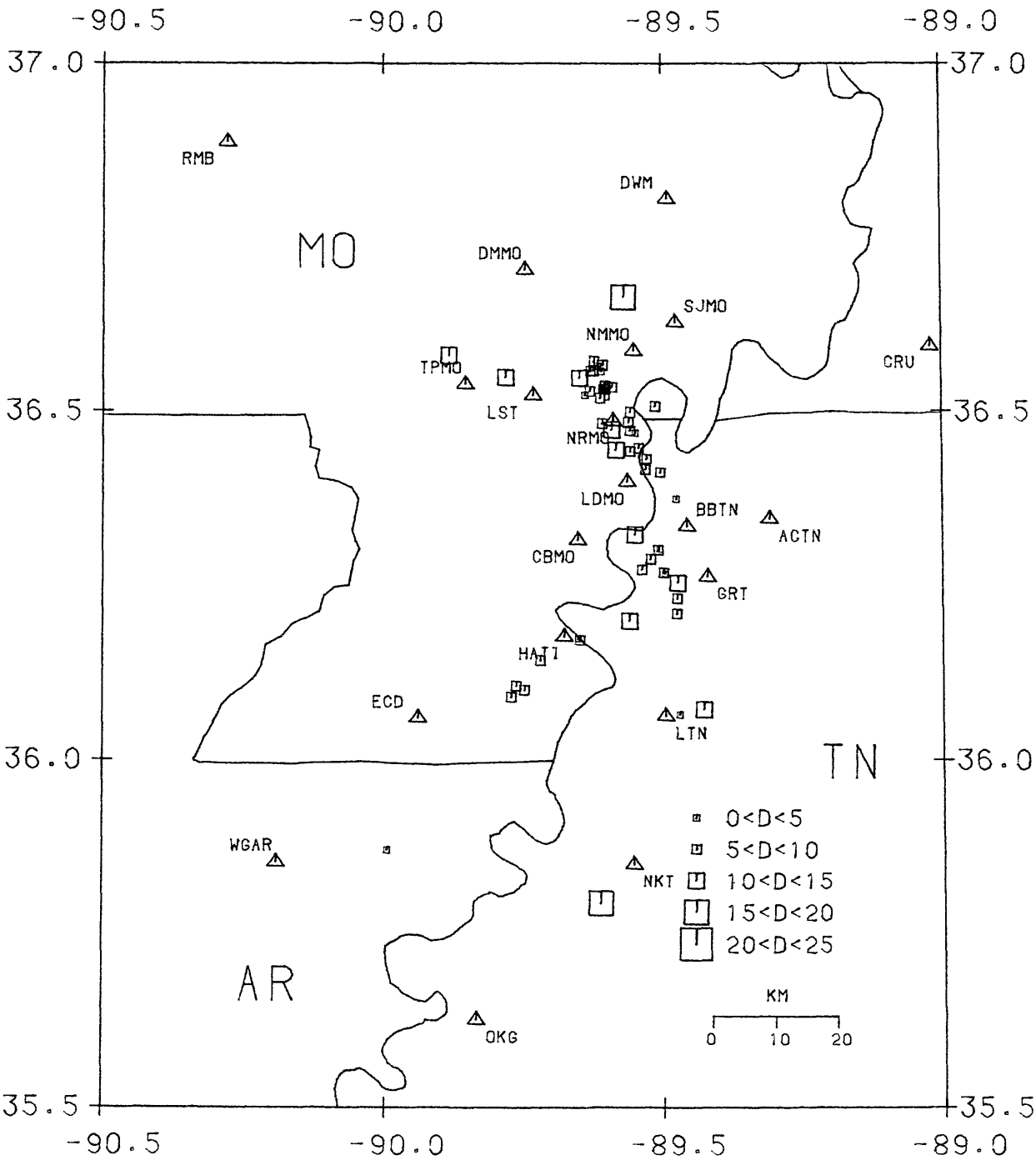

FIGURE 4

CUMULATIVE EVENTS 01 JAN 1986 TO 30 JUNE 1986

LEGEND . △ STATION ⊡ EPICENTER

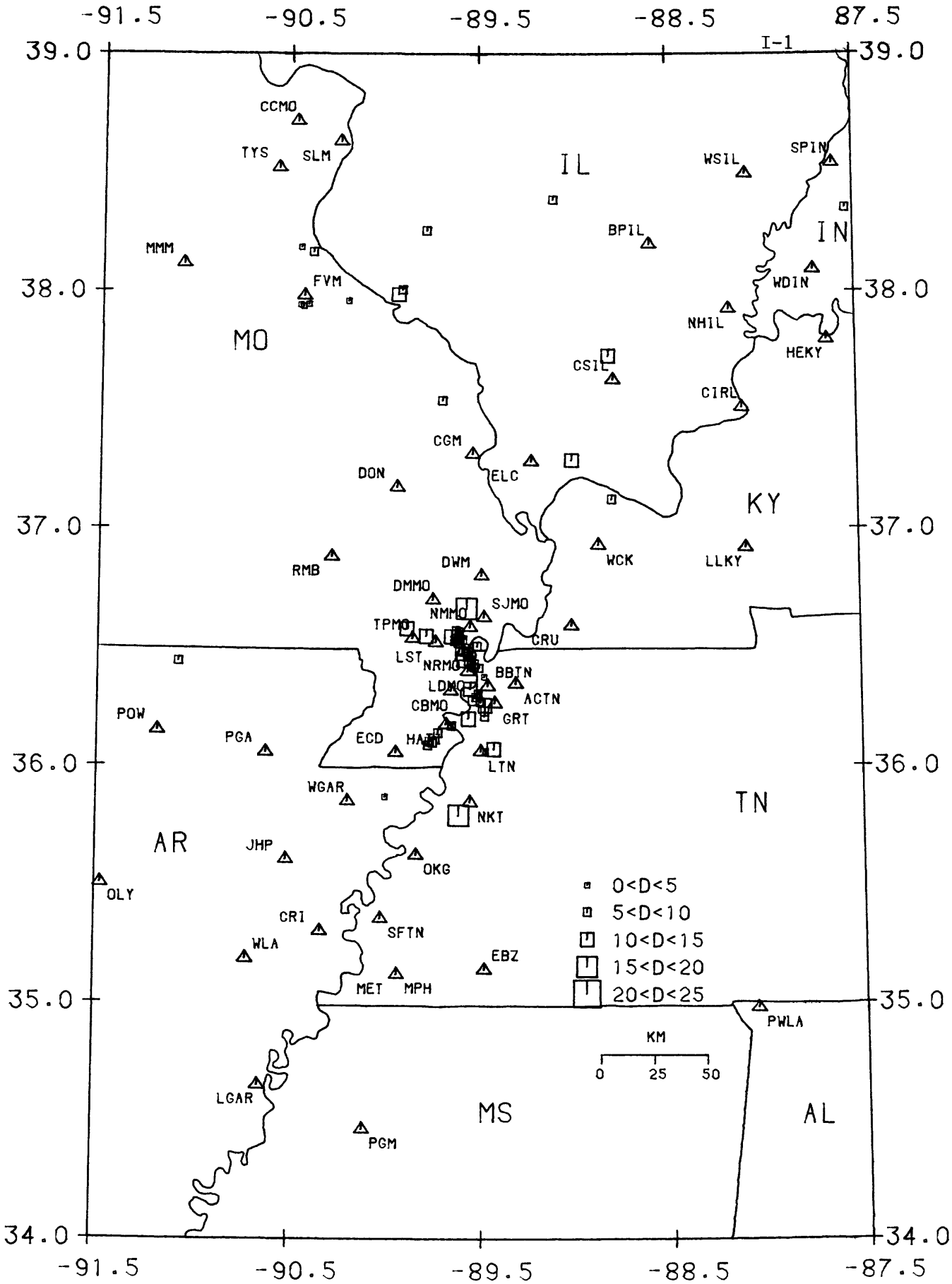

FIGURE 3

CUMULATIVE EVENTS 01 JAN 1986 TO 30 JUNE 1986

LEGEND . △ STATION ⊡ EPICENTER

Consolidated Digital Recording and Analysis

9930-03412

Sam W. Stewart
Branch of Seismology
U.S. Geological Survey
345 Middlefield Road - M/S 977
Menlo Park, California 94025
(415) 323-8111 Ext. 2577

Investigations

The goal is to operate, on a routine and reliable basis, a computer-automated system that will detect and process earthquakes occurring within the USGS Central California Earthquake Network (also known as CALNET). Presently, the output from more than 460 short-period seismic stations is telemetered to a central recording point in Menlo Park, California. Two DEC PDP11/44 computers, and a VAX/750, are used on this project. The 11/44A is dedicated to the task on online, realtime detection of earthquakes and storing the waveforms for later analysis. The 11/44B is used for offline processing and archiving of earthquakes. Both computers have a 512 channel analog-to-digital converter, so the 11/44B can serve as backup to the online system whenever necessary. (One of the a/d converters can be connected to the VAX/750 computer as well, to be used both for Calnet realtime monitoring experiments, and for offline digitizing from analog magentic tapes.) The two 11/44 computers communicate with each other via a simple digital-bit I/O "semaphore" system, and transfer large amounts of data via a dual-ported disk subsystem or a dual-ported magnetic tape subsystem.

The VAX/750 is a general purpose computer used by the Branch of Seismology. We use it as the primary "research" computer for the CUSP system. It holds the primary data base of earthquake summary data and phase card data, which is available for research purposes. We update and maintain the CALNET data on this computer.

Both 11/44 computers use the RSX11M-PLUS (v2.1) operating system. The VAX/750 uses the DEC VMS operating system. Software has been developed largely by Carl Johnson in Pasadena, but with considerable modification by Peter Johnson, Bob Dollar and Sam Stewart, to meet Menlo Park's specific needs. Our applications are all written in Fortran-77, but with heavy use of system functions unique to the RSX or VMS operating systems.

Results

1. During the period April 1986 thru September 1986 approximately 13200 events were processed through the CUSP system. This includes 11600 events that were classified as 'LOCAL' events, i.e., they occurred within or near

enough to the network that hypocenters were calculated and the data entered into the catalogs. The remaining 1600 events were either regional or teleseismic events, or unprocessed copies of local events that were too small (magnitude less than 1.0) to be timed.

In addition, a few thousand non-seismic noise events detected by the online 11/44A computer had to be examined and deleted. Considering only the seismic events, this projects to an annual rate of processing about 26400 events per year.

The magnitude 6.5 Chalfant Valley, California earthquake of July 20, 1986 produced an enormous number of online detections of aftershocks. We estimate about 1250 detections remain to be processed. Because each detection may contain several timeable aftershocks, there may be 2500 or more events remaining to be timed and located.

2. The VAX/750 system is now able to do all the CUSP offline timing and processing that formerly was done only on the 11/44B system. This is significant in that (1) the VAX can serve as a backup CUSP processor to the routine Calnet processing done on the 11/44B; (2) very long online detections can be processed directly on the VAX/750, eliminating the need for special, time-consuming treatment of these long detections on the 11/44B; (3) other researchers can retrieve archived waveform data and carry out special studies in a CUSP environment, using the superior facilities of the VAX/VMS system; (4) other networks (e.g. Alaska) can begin processing their event data using the CUSP system (5) other VAX/VMS systems (e.g. microvax-II) can use the CUSP system with little or no modification.

3. The VAX/VMS system is not able to do digitizing from analog magnetic tapes, working in a CUSP environment. The interfacing and digitizing software was done largely by Bob Dollar, with help from Peter Johnson and Tom Jackson. Currently the digitizing system works with either daily telemetry tapes or our dubbed event tapes. Forty channels are digitized at a tape rate of 100 samples/second. Because the tape is being played back at 16x realtime, this corresponds to a real digitizing rate of 64000 samples/second. By camparison, the realtime 11/44A system runs at about 50000 samples/second. This digitizing system replaces the ECLIPSE system, which served well for many years.

Reports

none

Seismic Monitoring of the Shumagin Seismic Gap, Alaska

USGS 14-08-0001- 21919

John Taber
Lamont-Doherty Geological Observatory of Columbia University
Palisades, New York 10964
(914) 359-2900

Investigations

Seismic data from the Shumagin seismic network were processed to obtain origin times, hypocenters, and magnitudes for local and regional events. The processing resulted in files of hypocenter solutions and phase data, and archive tapes of digital data. These files are used for the analysis of possible earthquake precursors, seismic hazard evaluation, and studies of regional tectonics and volcanicity (see Analysis Report, this volume). A yearly bulletin is available for 1984 and 1985 data.

Results

The Shumagin network was used to locate 344 earthquakes in the first half of 1986. The seismicity of the Shumagin Islands region for this time period is shown in map view and cross section in figure 1. The largest event in this period had a magnitude of 4.5 and was located over the main thrust zone at a depth of 4.5 km. A magnitude 4.1 earthquake occurred at a depth of 201 km. This was the first deep event larger than magnitude 4 since 1981. Otherwise the overall pattern over this time period is similar to the long term seismicity. Concentrations of events occur at the base of the main thrust zone and in the shallow crust directly above it. The continuation of the thrust zone towards the trench is poorly defined. West of the network (which ends at 163°) the seismicity is more diffuse in map view. Below the base of the main thrust zone (~45 km) the dip of the Benioff zone steepens. Part of the double plane of the lower Benioff zone is evident near 100 km depth.

The yearly network servicing was successfully completed in July and August. The network is capable of digitally recording and locating events as small as Ml = 0.4 with uniform coverage at the 2.0 level. Onscale recording is possible to ~Ms=6.5 on a telemetered 3 component force-balance accelerometer. Larger events are recorded by one digitally recording accelerometer and on photographic film by 12 strong-motion accelerometers.

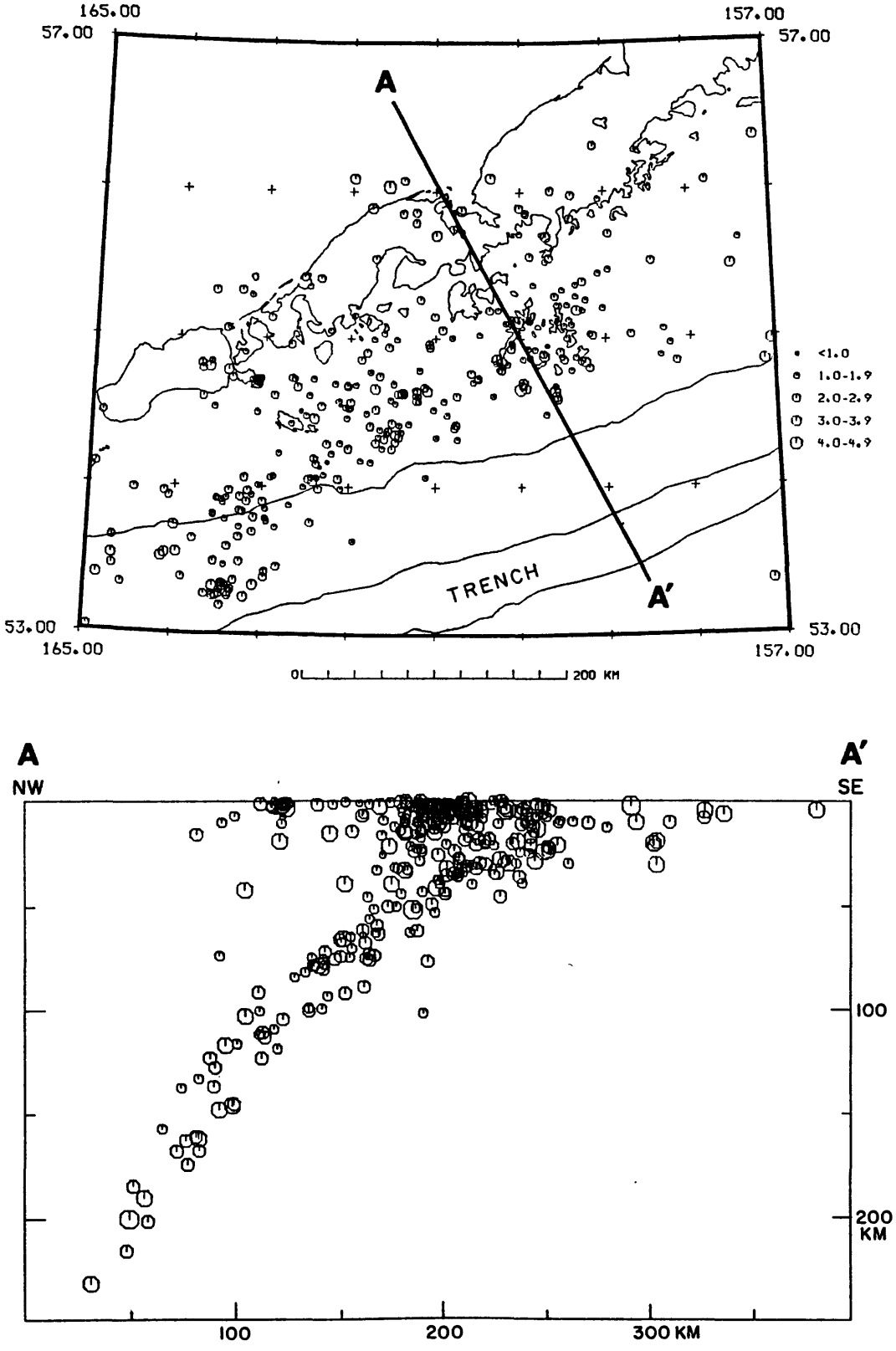

Figure 1. Top: Seismicity recorded by the Shumagin seismic network from January 1 to June 30, 1986. Bottom: Cross section of seismicity projected along the line A-A' in the upper figure.

Earthquake Hazard Research in the Greater Los Angeles Basin and Its Offshore Area

#14-08-0001-A0264

Ta-liang Teng
Thomas L. Henyey
Egill Hauksson

Center for Earth Sciences
University of Southern California
Los Angeles, CA 90089-0741
(213) 743-6124

INVESTIGATIONS

(1) Monitor earthquake activity in the Los Angeles Basin and the adjacent offshore area.

(2) Upgrade remote field stations. One new field station has been installed in the eastern Los Angeles basin. The microprocessor-based Optimal Telemetry System has been deployed for field testing at three seismic stations.

RESULTS

(1) The earthquake activity that occurred in the Los Angeles basin and the southern California coastal zone during January-September 1986 is shown in Figure 1. The seismicity rate is similar to the rate that was recorded during the previous three years. The earthquake activity in the Los Angeles basin is characterized by single shocks that are scattered throughout the region. Several spatial clusters are observed in the monitoring region. Clusters of seismicity are observed at the northern segments of both the Newport-Inglewood fault as well as the Palos Verdes fault during January-September 1986. The adjacent offshore area in Santa Monica Bay is also characterized by a moderate level of seismic activity. A cluster of earthquakes is observed on the Palos Verdes fault in the City of Torrence. The largest earthquake to occur within the Los Angeles basin had a magnitude of 3.7 and was located in Santa Ana, just east of the City of Long Beach. In summary, although the January-September 1986 seismicity in the southern California coastal zone and the Los Angeles basin is characterized by several spatial clusters of seismicity, the overall level of activity is moderate to low as compared with other regions of southern California.

(2) A mainshock of M_L=5.4 occurred 45km southwest of Oceanside on July 13th 13h 47m (U.T.C.). The mainshock was followed by an extensive aftershock sequence (Figure 2). The epicenters of the mainshock and aftershocks are located near the northern end of the San Diego Trough, just to the east of the Thirtymile Bank. Although the epicentral locations are still preliminary, this sequence appears to be associated with the East Santa

Cruz Basin fault system rather than the Newport-Inglewood-Coronado Bank fault system. The preliminary single event, lower hemisphere local mechanisms shown in Figure 3 indicate that the faulting associated with this sequence is either strike slip or thrust or possibly a mixture of both. Teleseismic data show a thrust mechanism for the mainshock (similar to the mechanism in Figure 3C) (J. Nabelek, pers. comm. 1986). The difference between the short period first motion mechanism and the teleseismic mechanism can possibly be resolved by adding first notions from stations located in southern Baja in Mexico. If the teleseismic mechanism is correct this sequence will provide important new constraints on the velocity structure of the California Continental Borderland. Oceanside aftershocks are still occurring (in October, 1986) thought at a decreasing rate (see Figure 3D).

(3) A new seismograph station (FLA) was installed in a 1400ft deep borehole in the City of Fullerton in Orange County. The station that began operating in September 1986 is located adjacent to the Norwalk fault and fills an important gap in the station distribution in the eastern Los Angeles basin.

A second generation of the optimal telemetry system (OTS) is currently being designed and built. The front-end anti-aliasing filters have been upgraded to 7 poles. To minimize electronic noise the microprocessor has been placed on a separate circuit board. The design goals are to achieve a background noise level of 1 mV or less. Field testing of the new OTS is planned to begin in December 1986.

REPORTS

Hauksson, E., T. L. Teng, T. L. Henyey, J. K. McRaney, L. Hsu, M. Robertson and G. Saldivar, Earthquake Hazard Research in the Los Angeles Basin and Its Offshore Area, U.S.C. Technical Report #86-1, February 1986.

Teng, T. L. and M. Hsu, A Seismic Telemetry System of Large Dynamic Range, Bull. Seism. Soc. Amer., 76, 1461-1471, 1986.

Hauksson, E. and G. Saldivar, The 1930 Santa Monica and the 1979 Malibu, California, Earthquakes, to appear in BSSA, December 1986.

Hauksson, E., Seismotectonics of the Newport-Inglewood fault zone in the Los Angeles Basin, Southern California, in press BSSA, 1987.

Hauksson, E., T. L. Teng and T. L. Henyey, Near-Surface Attenuation of Waveforms of Local Earthquakes: Results from a 1500 m Deep Downhole Seismometer Array, submitted to fall AGU meeting 1986.

Saldivar, G. V., E. Hauksson and T. L. Teng, Seismotectonics of the Santa Monica and Palos Verdes Fault Systems in the Santa Monica Bay, Southern California, submitted to fall AGU meeting 1986.

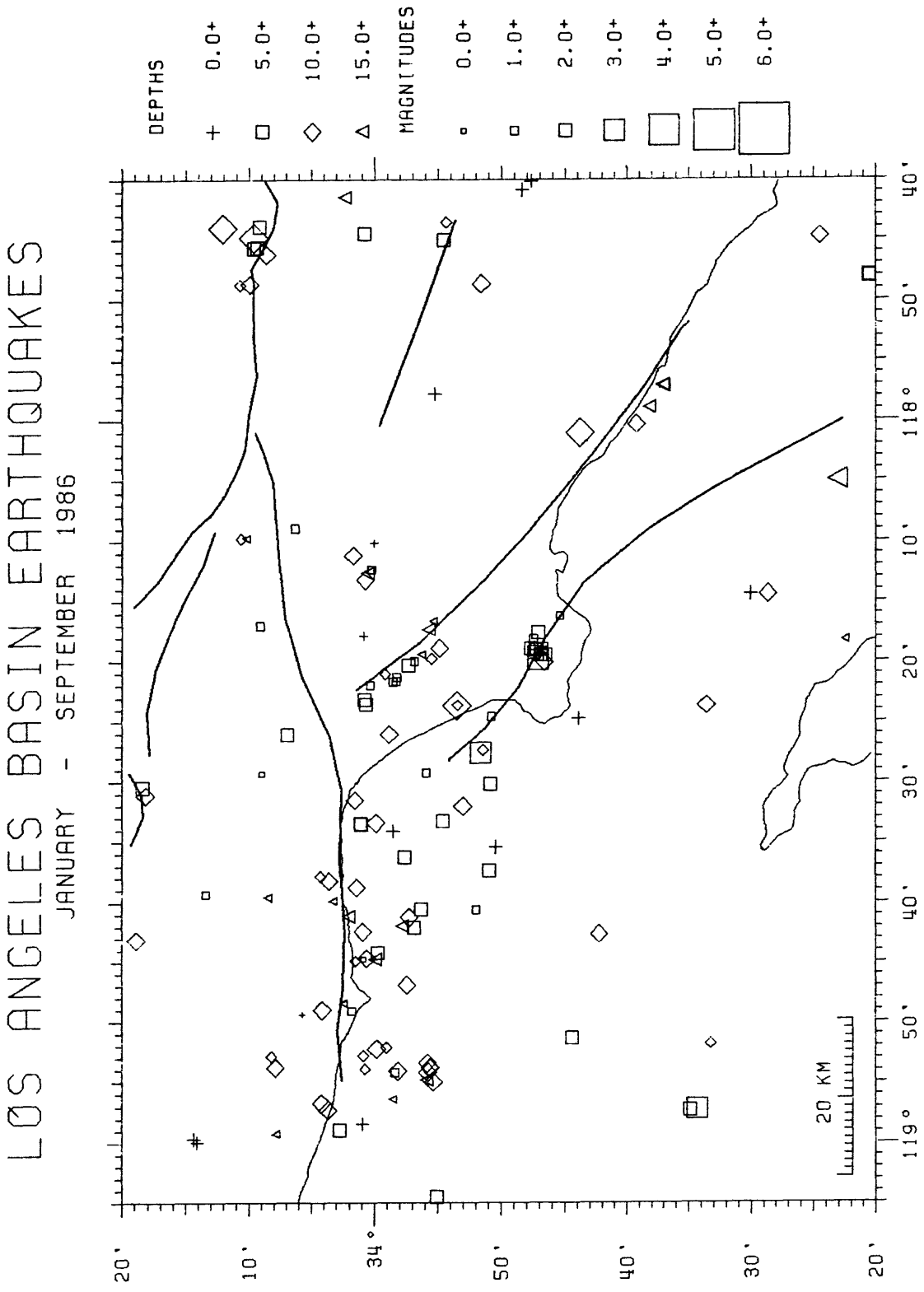

Figure 1. Seismicity in the Los Angeles basin, January-September, 1986.

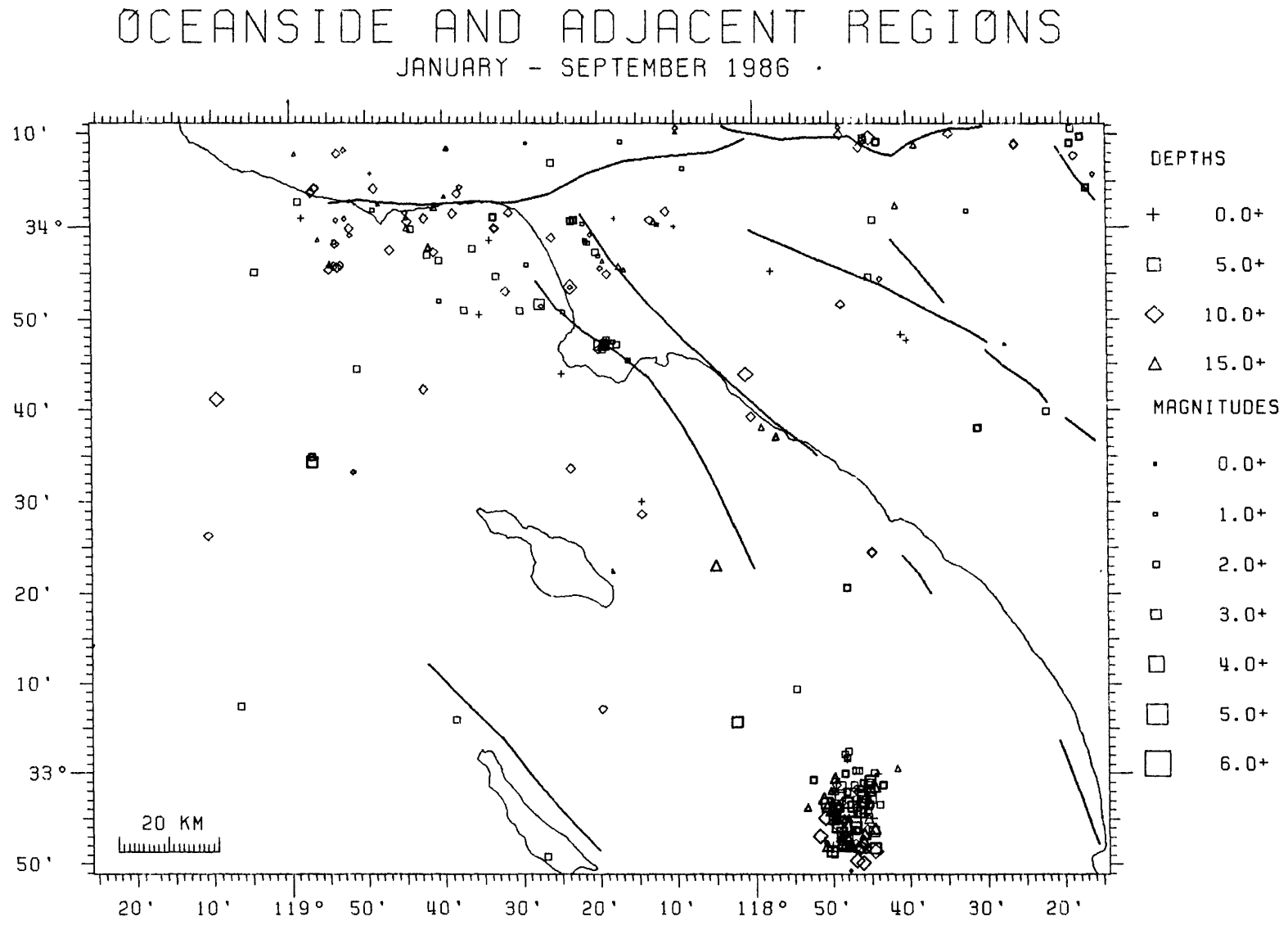

Figure 2. Seismicity in the offshore region, including the Oceanside (July 13, 1986) mainshock-aftershock sequence.

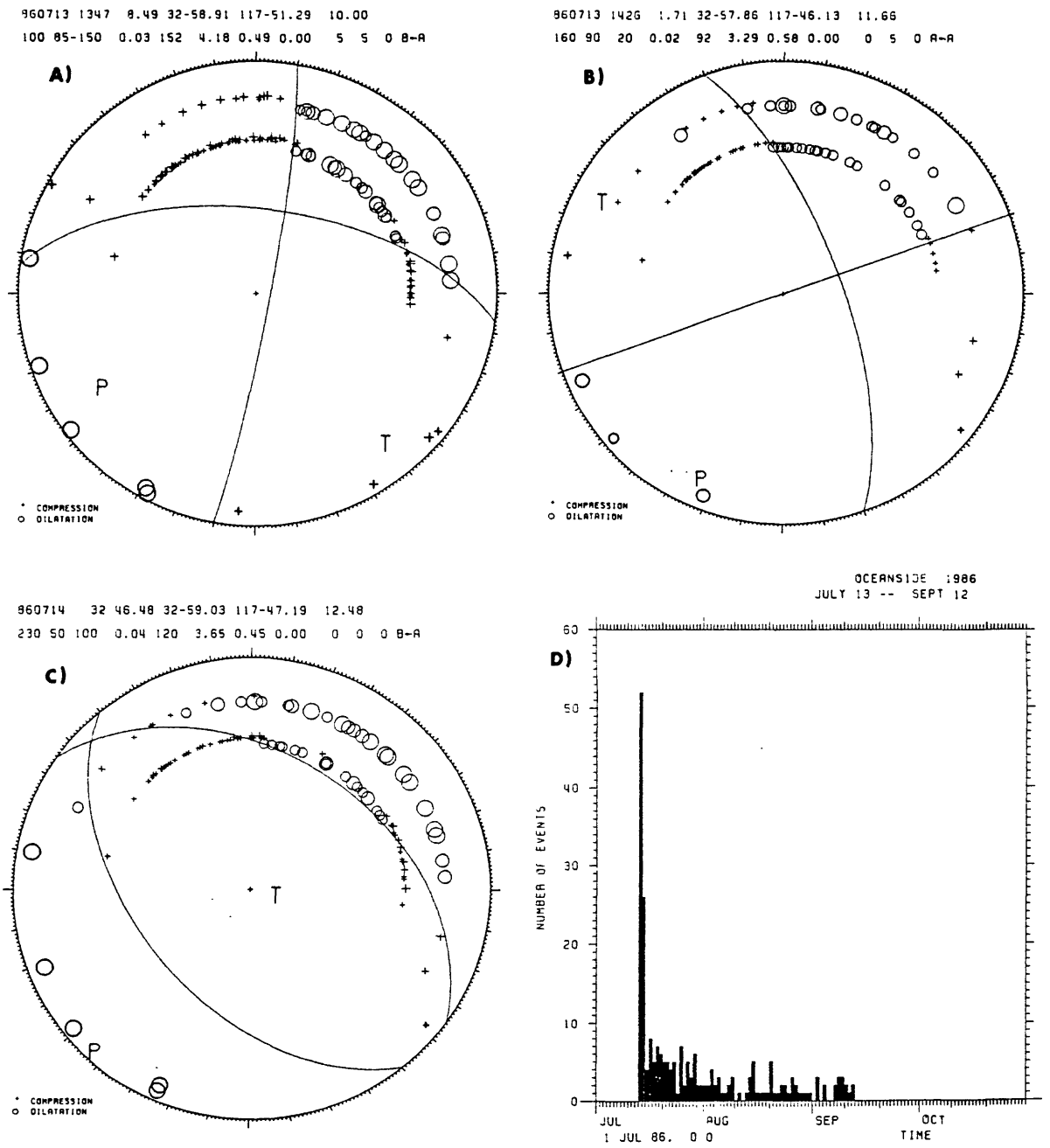

Figure 3. A) Focal mechanism of the Oceanside (July 13) mainshock (M=5.4).
B) Focal mechanism of an aftershock (M=3.6) at 14h 26m.
C) Focal mechanism of an aftershock (M=4.0) at 0h 32m. July 14
D) Histogram showing rate of aftershock activity of ($M \geq 2.9$) at Oceanside.

Data Processing Center Operations

9930-01499

John Van Schaack
Branch of Seismology
U. S. Geological Survey
345 Middlefield Road- Mail Stop 977
Menlo Park, California 94025
(415) 323-8111, Ext. 2584

Investigations

This project has the general housekeeping, maintenance and management authority over the Earthquake Prediction Data Processing Center. Its specific responsibilities include:

1. Day to day operation and performance quality assurance of 5 network magnetic tape recorders.
2. Day to day management, operation, maintenance, and performance quality assurance of 2 analog tape playback stations.
3. Day to day management, operation, maintenance and performance quality assurance of the U.S.G.S. telemetered seismic network event library tape dubbing facility (for California, Alaska, and Hawaii).
4. Projection of usage of critical supplies, replacement parts, etc., maintenance of accurate inventories of supplies and parts on hand, uninterrupted operation of the Data Processing Center.

Results

Procedures and staff for fulfilling assigned responsibilities have been developed and the Data Processing Center is operating smoothly and serving a large variety of scientific user projects.

Field Experiment Operations

9930-01170

John Van Schaack
Branch of Seismology
U. S. Geological Survey
345 Middlefield Road MS-977
Menlo Park, California 94025
(415) 323-8111, ext. 2584

Investigations

This project performs a broad range of management, maintenance, field operation, and record keeping tasks in support of seismology and tectonophysics networks and field experiments. Seismic field systems that it maintains in a state of readiness and deploiys and operates in the field (in cooperation with user projects) include:

a. 5-day recorder portable seismic systems.
b. "Cassette" seismic refraction systems.
c. Portable digital event recorders.
d. Smoked paper recorder portable seismic systems

This project is responsible for obtaining the required permits from private landowners and public agencies for installation and operation of network sensors and for the conduct of a variety of field experiments including seismic refraction profiling, aftershock recording, teleseism P-delay studies, volcano monitoring, etc.

This project also has the responsibility for managing all radio telemetry frequency authorizations for the Office of Earthquakes, Volcanoes, and Engineering and its contractors.

Results

Seismic Refraction

One hundred twenty seismic cassette recorders were used in the PASSCAL experiment in Central Nevada in July 1986.. This experiment was conducted in cooperation with a number of Universities and the U. S. Air Force. Two profiles were shot. One profile extended from Winnemucca to Fallon and the other from Gerlach to Austin.

Telemetry Networks

The telemetry networks have remained constant for the last 6 months except for the Parkfield area. We have installed 4 telemetered Force Balance Accelerometers near Parkfield with sensitivities ranging from .02G full scale to 2.0G full scale. We are presently in the process of installing 6 more FBAs in the same general area. All of these sensors will be monitored by the CUSP and RTP automatic earthquake detection systems in Menlo Park.

Portable Networks

Six 5-Day recorders were deployed near Palm Springs CA to record aftershocks of the M 5.9 earthquake there this Spring. These recorders were then immediately deployed North of Bishop to record aftershocks of the Chalfant Valley earthquake of July 1986. At the same time 3 seismic telemetry stations were installed North of Bishop and the data telemetered to Menlo Park, CA.

Characteristics of Active Faults

9950-03870

R. C. Bucknam
Branch of Geologic Risk Assessment
U.S. Geological Survey
Box 25046, MS966, Denver Federal Center
Denver, CO 80225
(303) 236-1604

Investigations

Fault-scarp degradation studies--Lost River Range, Idaho

Results

As part of a general study to associate variations in the rate of modification of the free face of fault scarps with lithologic and other site-specific variables, I have begun photogrammetric documentation of the modification of scarps formed by the 1983 Borak Peak, Idaho, earthquake. Three sets of approximately horizontal close-range photographs have been taken at a site on the fault scarp. The photographs were taken in October 1985, May 1986, and September 1986 with a calibrated mapping camera at a distance of about 5 m from the scarp. Coordinates of series of targets distributed across the scarp face, determined by triangulation with a theodolite from a stable, permanent baseline, provide controls for the photogrammetric models. Using an analytical stereo plotter, photogrammetric compilation has been done by Frank Schafer (Branch of Astrogeology, Flagstaff) in collaboration with Sherman Wu. Residuals determined with the stereo plotter for the coordinates of the control targets after absolute orientation of the model are generally several millimeters; thus, resolution of changes in scarp morphology is probably considerably better than 1 cm.

Profiles of the scarp, spaced at 20-cm intervals, were drawn directly from the photogrammetric models along a 5-m-long interval of scarp for each of the three sets of photographs. Two representative profiles are shown on figure 1. The solid line shows the profile of the scarp at the time of the first photographs in October 1985. The dashed line shows the profile of the scarp at the times of the May 1986 photographs and the September 1986 photographs. Changes in the scarp profile between May and September are typically less than 2 mm (about the width of the line in the figure) and are too small to show at this scale. The average retreat of the scarp face between 17 October 1985 and 23 September 1986 was 4.5 cm (Profile 4) and 3.0 cm (Profile 11). Nearly all of the observed scarp retreat occurred between 17 October 1985 and 5 May 1986. These observations suggest possible seasonal control of scarp degradation with the most rapid retreat occurring during a period with freeze-thaw cycles and of presumably relatively high ground moisture.

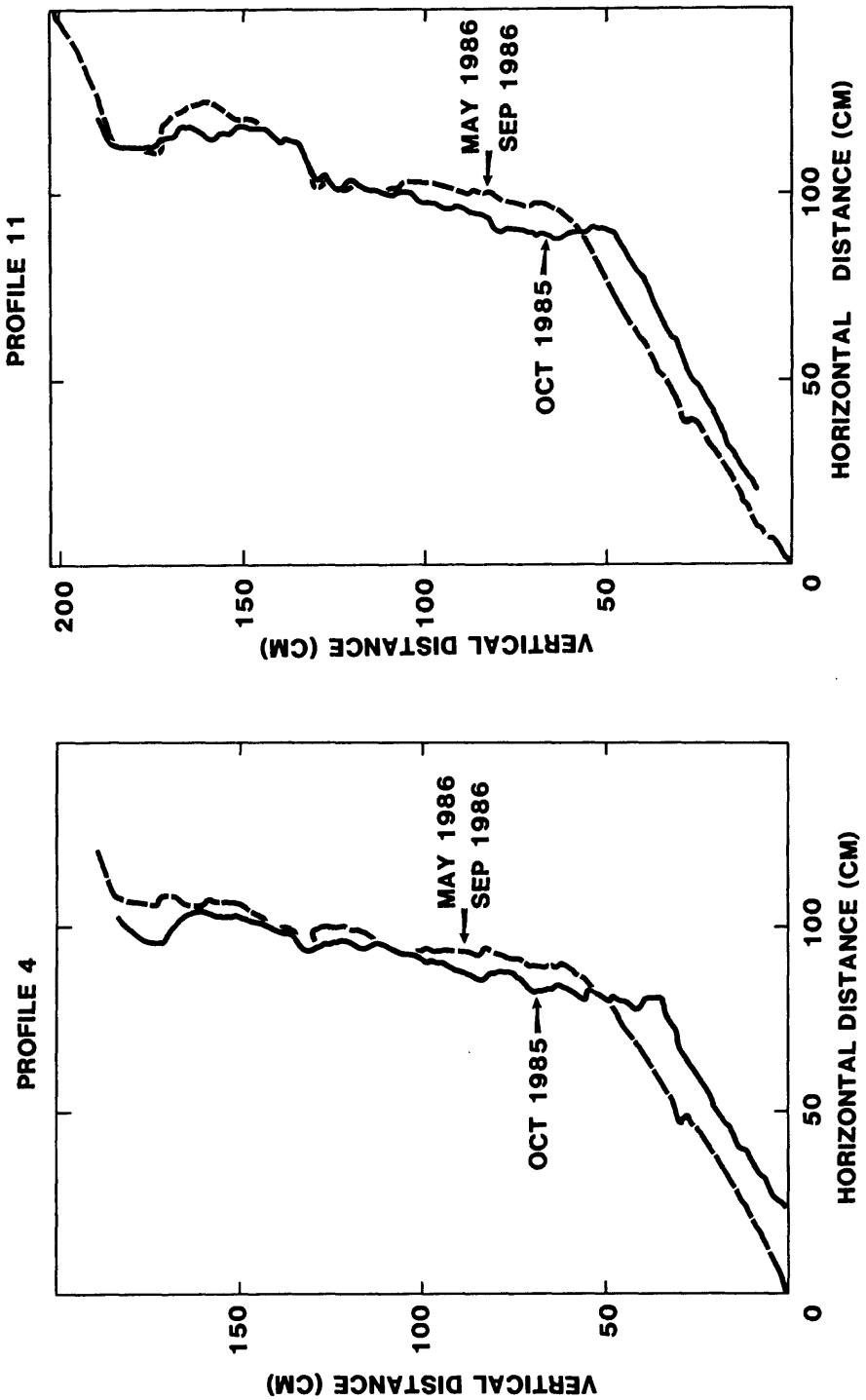

FIGURE 1.--Profiles across the Borah Peak fault scarp compiled from photographs taken at the dates indicated. The two profiles are separated by 1.4 m. The sloping surface at the uppermost part of each profile is the face of the early to middle Holocene fault scarp that was reactivated by the 1983 earthquake.

Comparative Earthquake and Tsunami Potential for Zones in the Circum-Pacific Region

9600-98700

George L. Choy
Stuart P. Nishenko
William Spence
Branch of Global Seismology and Geomagnetism
U.S. Geological Survey
Denver Federal Center
Box 25046, Mail Stop 967
Denver, Colorado 80225
(303) 236-1506

Investigations

1. Prepare detailed maps and text of comparative earthquake potential for west coasts of Mexico, Central America, and South America.

2. Conduct investigations of the historic repeat-time data for great earthquakes in the North Pacific Ocean margin.

3. Develop a working model for the interaction between forces that drive plate motions and the occurrence of great subduction zone earthquakes.

4. Develop a rapid method for the estimation of the source properties of significant earthquakes.

Results

1. The probabilistic work for northern Mexico has been completed (Nishenko and Singh, 1986). Two regions have the highest probabilities for recurrence of large earthquakes within the next two decades: the central Oaxaca gap and the Acapulco-Marcos gap. With the occurrence of the catastrophic earthquake of September 19, 1985, the Michoacan seismic gap now has a very low probability for recurrence of a great earthquake within 20 years. However, plate motions related to this earthquake could cause stress to transfer to the seismic gap at Acapulco and trigger a great earthquake there within the next few years. A study of aftershocks of the greater 1979 Columbia earthquake has been submitted for publication (Mendoza, 1986). This study of this event in the context of the great earthquakes of 1906 and 1958 will help the probabilistic assessment for the recurrence of great earthquakes in this region.

2. Data on the occurrence of great earthquakes and tsunamis from the Queen Charlotte Islands to the Aleutian Islands have been collected and the evaluation of probabilistic recurrence is being conducted by Drs. Nishenko and Jacob.

3. An evaluation of the ridge-push and slab-pull forces in the context of stresses that lead to great subduction zone earthquakes has been completed (Spence, 1986). An important conclusion is that specific parts of a subducting plate may be monitored for precursors to seismic gap-filling earthquakes.

4. We are developing computer packages that will permit the rapid estimation of source properties of significant earthquakes on a routine basis. We are routinely using broadband data to obtain depth phases for all earthquakes over m_b 5.8. We are nearly finished with an algorithm that will permit semi-automated on-line computation of radiated energy, moment and apparent stress for all earth quakes over m_b 5.8.

Reports

Boatwright, J., and Choy, G.L., 1986, Teleseismic estimates of the energy radiated by shallow earthquakes: Journal of Geophyscial Research, v. 91, p. 2095-2112.

Choy, George L., and Cormier, V.F., 1986, Direct measurement of the mantle attenuation operator from broadband P and S waveforms: Journal of Geophysical Research, v. 91, p. 7326-7342.

Choy, George L., and Engdahl, E.R., 1986, Analysis of broadband seismograms from selected IASPEI events: Physics of the Earth and Planetary Interiors, in press.

Mendoza, C., 1986, Aftershock source properties using digital surface wave data--The 1979 Colombia sequence: Bulletin of the Seismological Society of America, in press.

Nishenko, S.P., and Buland, R.P., 1986, A generic recurrence interval distribution for earthquake forecasting: Bulletin of the Seismological Society of America, submitted.

Nishenko, S.P., and Singh, S.K., 1986, Conditional probabilities for the recurrence of large and great interplate earthquakes along the Mexican subduction zone--1986-2006: Journal of Geophysical Research, submitted.

Spence, W., 1986, The 1977 Sumba earthquake series--Evidence for slab pull force acting at a subduction zone: Journal of Geophysical Research, v. 91, p. 7225-7239.

_____1986, Slab pull and the earthquake cycle: Reviews of Geophysics, in press.

Earthquake Hazard Investigations in the Pacific Northwest

14-08-0001-G1080

R.S. Crosson
Geophysics Program
University of Washington
Seattle, WA 98195
(202) 543-8020

Investigations

The objectives of this research are to provide fundamental data and interpretations for earthquake hazard investigations. Currently, we are focusing on seismicity, structure, and tectonic questions related to the possibility of a major subduction earthquake on the Juan de Fuca - North American plate boundary. Specific tasks which we have worked on in this contract period are:

1. Tomographic inversion of travel times to determine three-dimensional earth structure.

2. Locations, focal mechanisms and occurrence characteristics of crustal and subcrustal earthquakes beneath western Washington and their relationship to subduction processes.

3. Development of new network analysis programs.

4. Investigation of offshore earthquakes.

Results

1. A study of crustal velocity in western Washington is being done using tomographic techniques. The study area is divided into a grid of blocks, and travel times from the U. W. network data base are compared to travel-times computed from a starting velocity model. We are applying direct conjugate gradient techniques to the model inversion, and initial tests have been made using successive layers with 2-D inversion in each layer. Extension to full 3-D structure is planned as a final step.

2. A data base of focal mechanisms is being established. The objective is to determine the most probable regional tectonic stress in western Washington. Focal mechanisms have been determined for about 275 earthquakes in western Washington. All western Washington earthquakes which had ten or more polarities read in routine processing from 1982 through 1985 were examined. Since the suite of events deeper than 30 km is of particular interest, a special effort was made to include all possible deep events. Trace data were examined for all earthquakes from 1980 through 1985 which were deeper than 30 km and had ten or more P arrivals read. For earthquakes with valid focal mechanisms, software was developed to check orthogonality of P and T axes, to select events by focal mechanism type, and to make stereographic plots of nodal planes and stress axes, singly or in composite. We are working on a grading scheme to indicate quality of the focal mechanism solution by considering the possible range of focal mechanisms, the degree of constraint imposed by the polarity information, and inconsistent or ambiguous arrivals.

Examination of 121 focal mechanisms in the Puget Sound area indicates that systematic differences exist between shallow and deep earthquakes in the Puget Sound region. About half of both shallow and deep earthquakes have strike slip mechanisms, but many more normal

mechanisms occur in the deep suite than in the shallow; while thrust events are more common in the shallow suite. The table below shows how the three types of focal mechanisms are distributed in the shallow and deep suites.

The shallow and deep suites also show significantly different distributions of P and T axes. P axes for shallow events are clustered around the North-South direction, while P axes for deep earthquakes scatter in a broad girdle roughly about the E-W equatorial plane.

Distribution of Focal Mechanism Type by Depth Range

	Total	Strike-slip	Normal	Thrust
		P plunge $\leq 45°$ T plunge $\leq 45°$	P plunge $> 45°$ T plunge $\leq 45°$	P plunge $\leq 45°$ T plunge $> 45°$
Shallow ≤ 30 km	71	39 (55%)	6 (8%)	26 (37%)
Deep > 30 km	50	23 (46%)	19 (38%)	8 (16%)

3. Updated software which combines automatic picking of arrival times with interactive seismic processing has been developed to run on a Ridge 32C computer. Current network data collection and analysis are being carried out on a PDP 11/34 and a PDP 11/70, which need to be replaced within a few years. Software now being developed may by used in the next generation of network processing, and could be transferred to many 32 bit machines. Combining automated picking with interactive pick editing also enhances development and refinement of phase picking, polarity picking, and location routines, by making the data more immediately accessible for research use. Programs for picking, displaying and editing the regional network data are a part of this effort. Special utilities to handle local, regional and teleseismic data have been constructed and tested.

4. We have initiated a study of earthquakes occurring off the coast of Washington and Oregon. In the past digital data for these events were kept, but the events were not located. Since these events are both sizable and fairly frequent, we are exploring this data source. These earthquakes are generally shallow, and most of them are located on the Blanco Fracture Zone.

Articles

Zervas, C.E., and R.S. Crosson, 1986, P_n Observations and Interpretations in Washington, BSSA Vol. 76, no. 2, pp. 521-546

Ludwin, R.S., S.D. Malone, R.S. Crosson, 1986 (in press), Washington Earthquakes, 1983, National Earthquake Information Service

Ludwin, R.S., S.D. Malone, R.S. Crosson, 1986 (in press), Washington Earthquakes, 1984, National Earthquake Information Service

Reports

Univ. of Wash. Geophysics Program, 1986, Quarterly Network Report 86-A on Seismicity of Washington and Northern Oregon

Univ. of Wash. Geophysics Program, 1986, Quarterly Network Report 86-B on Seismicity of

Washington and Northern Oregon

Earthquake Hazard Research in the Pacific Northwest, 1986, Contract 14-08-0001-22007 Final Technical Report 1985.

Univ. of Wash. Geophysics Program,1986 (in press), Compilation of Earthquake Hypocenters in Washington, 1980.

Univ. of Wash. Geophysics Program,1986 (in preparation), Compilation of Earthquake Hypocenters in Washington, 1981.

Univ. of Wash. Geophysics Program,1986 (in preparation), Compilation of Earthquake Hypocenters in Washington, 1982.

Abstracts

Ma, Li, and R.S. Ludwin, 1986, Can Focal Mechanisms be used to Separate Subduction Zone from Intra-plate Earthquakes in Western Washington, Pacific Northwest AGU 1986

Lees, J.,1986, Tomographic Inversion for Lateral Velocity Variations in Western Washington, Pacific Northwest AGU 1986

Ludwin, R.S., L.L. Noson, A.I. Qamar, R.S. Crosson, C.S. Weaver, S.D. Malone, W.C. Grant, T.S. Yelin, Seismicity in the Northwestern U.S., submitted for AGU Fall 1986.

Crosson, R.S., and E.L. Crosson, 1986, Preliminary Analysis of Juan de Fuca Plate Seismicity using the Washington Regional Seismograph Network, submitted for AGU Fall 1986.

Investigations of Intraplate Seismic-Source Zones

9950-01504

W. H. Diment
Branch of Geologic Risk Assessment
U.S. Geological Survey
Box 25046, MS 966, Denver Federal Center
Denver, CO 80225
(303) 236-1574

Investigations

1. Reprocessing and interpretation of seismic-reflection data in upper Mississippi Embayment to investigate deep structure.

2. Quantitative geomorphic study of stream profiles in the southeastern part of the Ozark Mountains.

3. Interpretation of seismic-reflection data recorded on the Mississippi River.

4. Analysis of level line data in the upper Mississippi Embayment and environs.

5. Geologic investigation of Meers fault in Comanche County, Okla.

6. Publication of a report on a trench excavated near Blytheville, Ark.

7. Analysis of high-resolution reflection data obtained across the Meers fault.

8. Effects of earthquakes on high temperature wells in the Long Valley caldera, Mono County, Calif.

9. Analyses of seismological data from China.

10. Regional studies.

11. Analysis of stream profile data in an area of active faulting immediately west of Pierre, South Dakota.

Results

1. Reprocessing of field tape records of seismic-reflection profiles to 11 s two-way traveltime has been completed on four profiles (Dwyer, 1985). Two abstracts have been publised (Dwyer and Harding, 1985; Harding, 1985). The manuscript on the seismic reflection lines near Caurthersville, Missouri is being modified and a manuscript on the reflection lines on the east side of the Reel Foot rift is in preparation.

2. A draft report entitled "Analysis of stream-profile data and Inferred Tectonic Activity Eastern Ozark Mountains region," by F. A. McKeown, M. J. Cecil, B. L. Askew, and M. B. McGrath, has been returned to BCTR after making editorial corrections. Publication as a USGS Bulletin has been requested.

3. The interpretation of part of the seismic-reflection data recorded on the Mississippi River has been completed (Crone and others, 1986). First cut processing of the data collected along the Mississippi is complete; sections for interpretation and possible further processing are being chosen.

4. Compilation and analysis of level-line data for the upper Mississippi Embayment and vicinity was completed by Richard Dart and an open-file report is nearly ready for technical review. Completion of this report has been delayed temporarily by other activities (Dart, 1985 and 1986; Zoback and others, 1985; Dart and Zoback, 1986).

5. Geologic relationships in several backhoe excavations strongly suggest a large component of left-lateral slip on the Meers fault in southwestern Oklahoma. Two excavations on either side of a 1.07-m-high scarp formed in limestone suggest hat the channel of a small gulley has been displaced at least 0.65 m vertically and about 5 m left-laterally. Radiocarbon dating of the deposits in the channel will constrain the time of movement on the fault.

   In another nearby excavation, the rakes of striae in limestone on the upthrown side of the scarp are nearly horizontal indicating mainly lateral slip on the fault. The preservations of delicate striae in soluble limestone in a near-surface environment suggest that these striae record the slip direction during a late Quaternary faulting event.

6. The report describing the trench, excavated across a prominent linear feature in the Blytheville, Ark., area of the New Madrid seismic zone has been published (Haller and Crone, 1986).

7. A short, high-resolution seismic-reflection line was conducted across the Meers fault in Oklahoma. This data has been processed and shows a fault at approximately 271 m in depth which can be connected to the surface faulting. This fault has a displacement of about 30 m (Harding, 1985).

8. Temperature logs obtained in Chance No. 1 (south moat of the Long Valley caldera, Mono County, Calif.) in 1976, 1982, 1983, 1985 and 1986 show a progressive cooling in the uncased part of the hole. Examination of the rate of change suggests that the cooling began to accelerate about the time of the strong earthquakes of May 1980 (Diment and Urban, 1985). Temperature logs from Mammoth No. 1 (near Casa Diablo Hot Springs, 3 km west of Chance No. 1) obtained in 1979, 1982, and 1983 are also being processed and examined for seismically induced phenomena (Urban and Diment, 1984; 1985).

More recently, precision temperature logs and gamma-ray logs were also obtained in two other hot wells (PLV-1 and RDO-8) in the south moat 6-11 days before and 3-4 days, and 61-64 days after the Chalfant (50 Km ESE of wells) earthquake (M_S = 6.2 PDE, M_L = 6.4 BRK) of July 21, 1986. The work in RDO-8 was partially supported by participants in the Continental Scientific Drilling Program.

9. Under the Chinese-American Cooperative Earth Sciences Program, K. M. Shedlock and her colleagues from MIT and The Peoples Republic of China have conducted extensive studies of the structure and tectonics of the North China Basin (Shedlock and Roecker, 1985; Shedlock and others, 1986). These studies are applicable to the better understanding of similar regimes in the United States.

10. L.C. Pakiser and W.D. Mooney perceived the need for the summary/review volume: "Geophysical framework of the Continental United States." A conference was held in Golden between March 17 and 20, 1986 and 24 papers were presented. GSA has agreed to publish the product in their Memoir series. Most manuscripts have been received and are now being reviewed.

    Pakiser (1985) completed a review of seismic exploration of the crust and upper mantle in the Basin and Range Province.

11. At the request of T.C. Nichols and D.S. Collins (Project 02478, Rock deformation induced by subsurface excavation and use) Meridee Cecil digitized 24 streams within about 50 km west of Pierre, S. D., and made an analysis of several fluvial parameters. Known Holocene faults are readily detected as sharp changes in slope and stream gradient index.

    Other sharp changes in slope and stream gradient index are evident on a number of profiles, but have not yet been field checked. Anomalous logarithmic slope-stream length plots and low concavity to convex stream profiles are characteristic of the entire area studied to date. The cause of the faulting and presumably other deformation is not know but may be related to glacial rebound.

Reports

Crone, A.J., Harding, S.T., Russ, D.P., and Shedlock, K.M., 1986, Seismic-reflection profiles of the New Madrid seismic zone--Data along the Mississippi River near Caruthersville, Missouri: U.S. Geological Survey Miscellaneous Field Studies Map MF-1863, 4 oversized sheets with text.

Crone, A.J., and Luza, K.V. 1986, Holocene deformation associated with the Meers fault, southwestern Oklahoma: Geological Society of America Field Trip Guidebook Article, Annual Meeting, San Antonio, Texas [in press].

Crone, A.J. and Luza, K.V., 1986, Characteristics of late Quaternary surface faulting on the Meers fault, Commanche County, Oklahoma [abs.]: Transactions of the American Geophysical Union [EOS], v. 67, p. 1188.

Dart, Richard L., 1985, Horizontal stress directions in the Denver and Illinois Basins from the orientation of borehole breakouts: U. S. Geological Survey Open-File Report 85-733, 44 p.

Dart, Richard L., 1986, Well-bore breakouts and horizontal stress in the Denver and Illinois Basins: Geological Society of America, Abstracts with Programs, v. 18, p. 350.

Dart, Richard L., and Zoback, Mary Lou, 1986, Principal stress directions on the Atlantic Continental shelf inferred from the orientations of borehole elongations: U.S. Geological Survey Open-File Report 86-, 40 p. (Branch review).

Diment, W.H., and Urban, T.C., 1985, Temperature variations with time in a perennially boiling well in the Long Valley caldera, Mono County, California: Observations in Change No. 1 (1976-83): Geothermal Resources Council Transactions, v. 9, part 1, p. 417-422.

Dwyer, Ruth-Ann, 1985, Seismic-reflection investigation of the New Madrid rift zone near Caruthersville, Missouri: Golden, Colo., Colorado School of Mines, Master's Thesis T-3159, 108 p.

Dwyer, R.A., and Harding, S.T., 1985, Mid-crustal seismic reflections from part of the New Madrid seismic zone: Earthquake Notes, v. 56, p. 26.

_____1985, Midcrustal fault in the New Madrid seismic zone as interpreted from seismic-reflection data: Earthquake Notes, v. 56, p. 72.

Haller, K.M., and Crone, A.J., 1986, Log of an exploratory trench in the New Madrid seismic zone near Blytheville, Arkansas: U.S. Geological Survey Miscellaneous Field Studies Map MF-1858, 1 oversized sheet with text.

Harding, S.T., 1985, Preliminary results of a high-resolution reflection survey across the Meers Fault, Comanche County, Oklahoma: Earthquake Notes, v. 56, p. 2.

Harding, S.T., 1985, The use of seismic-reflection data to interpret the earthquake history associated with intracratonic earthquakes: Society of Exploration Geophysicists, Expanded Abstracts, 55th Annual International Meeting, p. 188.

Hellinger, S.Z., Shedlock, K.M., Sclater, J.G., and Ye, Hong, 1985, The Cenozoic evolution of the North Shina Basin: Tectonics, v. 4, p. 343-358.

Madole, R.F., and Rubin, Meyer, 1985, Holocene movement on the Meers fault, southwest Oklahoma: Earthquake Notes, v. 56, p. 1.

Pakiser, L.C., 1985, Seismic exploration of the crust and upper mantle of the Basin and Range province: Geological Society of America, Centennial Special Volume 1, p. 453-469.

Shedlock, K.M., Baranowski, J., Xizo, W., and Hu, X., The Tangshan aftershock sequence, accepted by JGR, Sept. 1986.

Shedlock, K.M., Roecker, S.W., and Jin Anshu, 1985, Crust and upper mantle of the Bohai, China region: Transactions of the American Geophysical Union [EOS], v. 66, p. 987.

Urban, T.C., and Diment, W.H., 1984, Precision temperature measurements in a deep geothermal well in the Long Valley caldera, Mono County, California: Transactions of theAmerican Geophysical Union [EOS], v. 65, p. 1084-1085.

Urban, T.C., and Diment, W.H., 1985, Convection in boreholes: limits on interpretation of temperature logs and methods for determining anomalous fluid flow, in Proceedings National Water Well Association Conference on surface and borehole geophysical methods in ground-water investigations: National Water Well Association, Worthington, Ohio, p. 399-414.

Zoback, Mary Lou, Zoback, M.D., and Dart, R.L., 1985, Reassessment of the state of stress in the Atlantic Coast region: Geological Society of America, Abstracts with Programs, v. 17, p. 759.

Preliminary Seismological Investigations of the North-Central Alaska Earthquake Sequences of February and March, 1985

G1109

Larry Gedney and John N. Davies*
Geophysical Institute
University of Alaska
Fairbanks, Alaska 99775-0800
(907) 474-7320

*also of Division of Geological and Geophysical Surveys, State of Alaska

INVESTIGATION

On 14 February, 1985, a magnitude (Mb) 5.4 earthquake near the trans-Alaska pipeline 30 km north of the Yukon River crossing signalled the beginning of a three-month-long sequence of earthquakes which were the largest ever to have been recorded this far north in Alaska. This study concentrated on determining the source mechanism and relationship of this earthquake series to intraplate tectonics in this part of the state.

RESULTS

During the three months following the initial large shock on 14 February, at least four other earthquakes exceeding magnitude 5.0, and at least forty others exceeding magnitude 4.0 occurred in the same area. The largest shock was a magnitude 6.0 event on 9 March. The area is not known to have a previous history of significant seismicity, and these shocks are the strongest ever to have been recorded this far north in the state. The opportunity was thus afforded to gain an insight into the mode of ongoing tectonic deformation in this little-studied area.

Because of the relative accesibility of the site (by Alaskan standards), it was possible to install three remote seismographic stations around the epicentral area, despite the blizzard conditions of the season. The signals from these stations were telemetered directly back to the seismological laboratory at the Geophysical Institute, and over 1,400 events were located, utilizing the temporary network in conjunction with stations of the permanent regional University of Alaska network.

Aside from the pipeline itself, and the accompanying pump stations, there are no manmade structures in the immediate epicentral area (which was named for a mining camp deserted in 1901), but the effects of the earthquakes included numerous stream overflows and rejuvenated springs. No fault offsets were observed during several helicopter overflights.

The three temporary telemetered seismographic installations around the epicentral area which could be emplaced by helicopter and snow machine before the sequence died away permitted the relatively accurate determination of focal depths and crustal velocities. A Vp/Vs ratio of 1.68 ± 0.03 was established. Focal depths were nearly all shallower than 15 km. Distinctive Pn and crustal layer phases made it possible to quantify a crustal layer model which includes an upper layer 24 km thick with a P-wave velocity of 6.0 km/sec, and a lower crustal layer 10 km thick with a P-wave velocity of 7.2 km/sec. The Pn velocity between the epicentral region and Fairbanks, 180 km to the SSE, was found to be 7.91 km/sec.

The focal mechanism solutions for the two largest events indicate either left-lateral faulting on a NNE-SSW oriented plane, or right-lateral faulting perpendicular to that. The former solution is preferred, largely because it is similar to the solution obtained for a magnitude 6.8 earthquake occurring 100 km to the south in 1968 (Huang & Biswas, 1983). The Dall City earthquakes appear to be an extension of the aftershock zone of the earlier Rampart earthquake to the north.

The findings to date are in accord with a regional stress pattern in Interior Alaska that is dominated by an azimuth of horizontal compressive stress in a NW-SE direction (Gedney et al., 1980; Gedney, 1985).

References

Gedney, L., S. Estes and N. Biswas, Earthquake migration in the Fairbanks, Alaska seismic zone, Bull. Seis.Soc. Am., 70, 223-241-, 1980.

Gedney, L., Stress trajectories across the northeast Alaska Range, Bull. Seism. Soc. Am., 75, 1125-1134, 1985.

Huang, P. and N. Biswas, Rampart seismic zone of central Alaska, Bull. Seism. Soc. Am. , 73, 813-829, 1983.

Reports

Estabrook, C., J. Davies, L. Gedney and S. Estes, Strong Alaskan Earthquake sequence, EOS, V. 66, 685, Oct. 1, 1985.

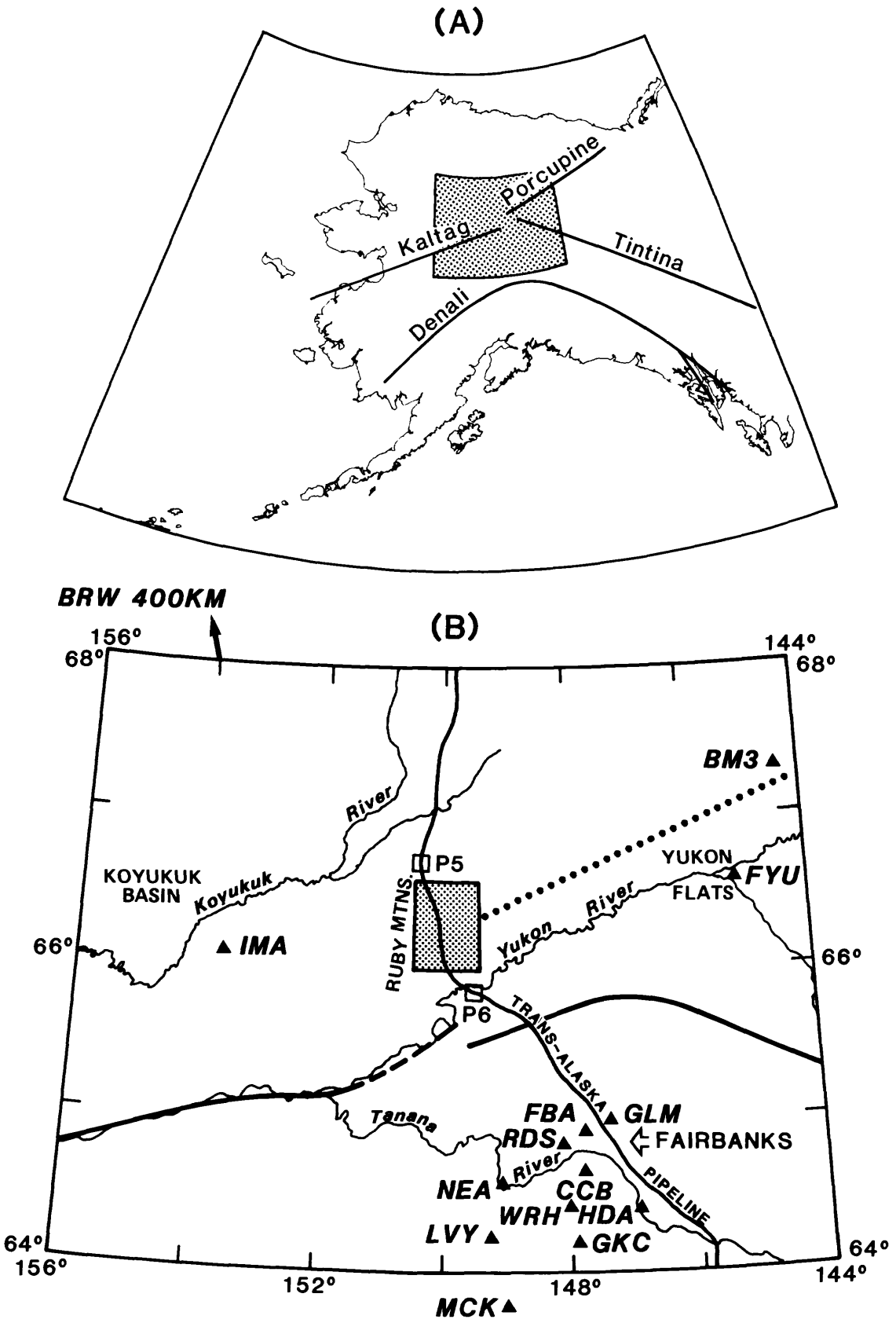

Figure 1. (A) General location map showing major faults and lineaments in study area. Stippled area is that shown enlarged in 1(B). (B) Local map showing locations of seismographic stations used in study. Stippled area is that shown enlarged in Figures 2(A)-(D). P5 and P6 are pump stations.

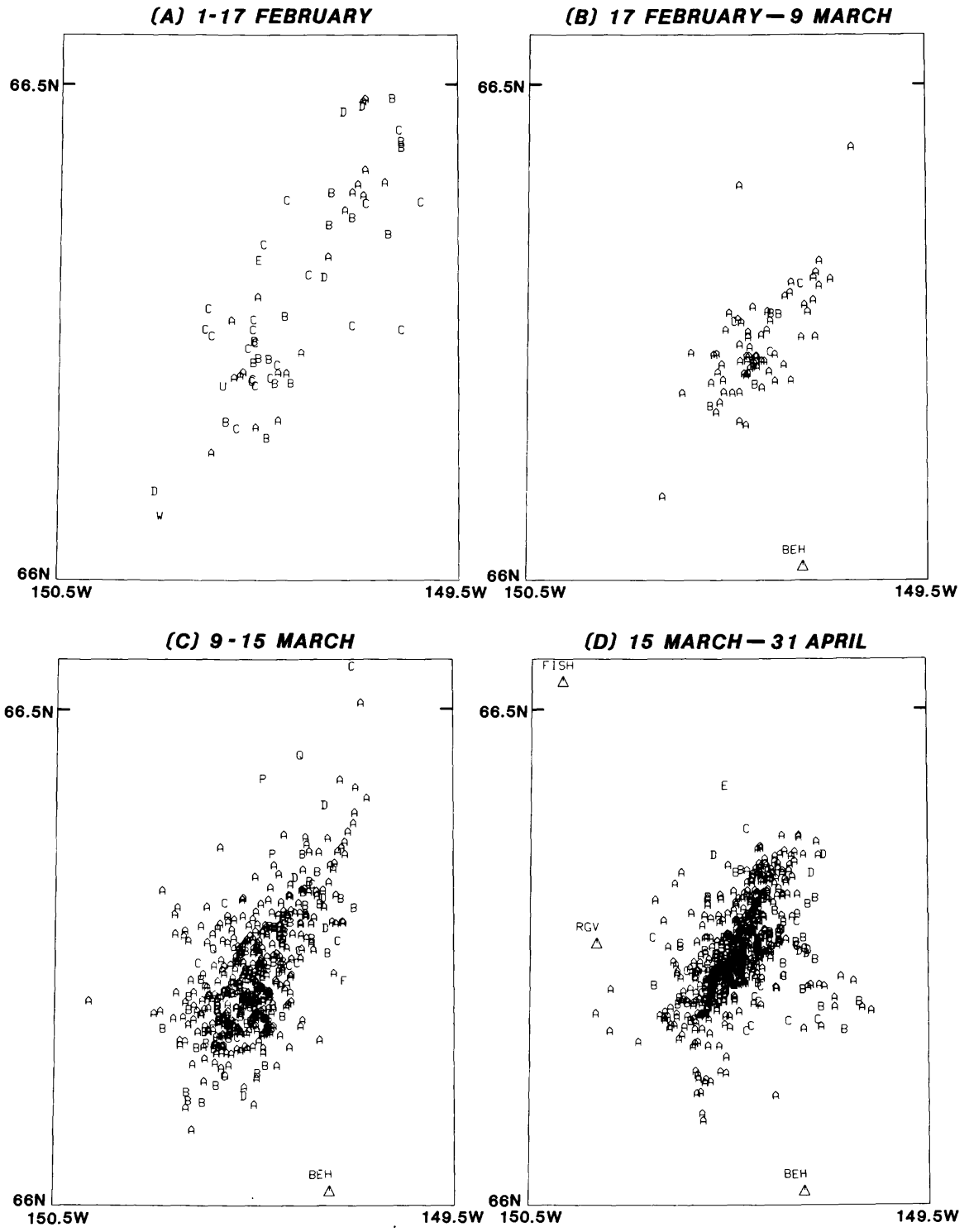

Figure 2. Epicentral distributions for various time periods during earthquake sequence. FISH, RGV and BEH are local recording stations installed after first earthquakes. Epicentral letter designators represent focal depths in 10-km increments, i.e., A=0-10 km, B=10-20 km, etc.

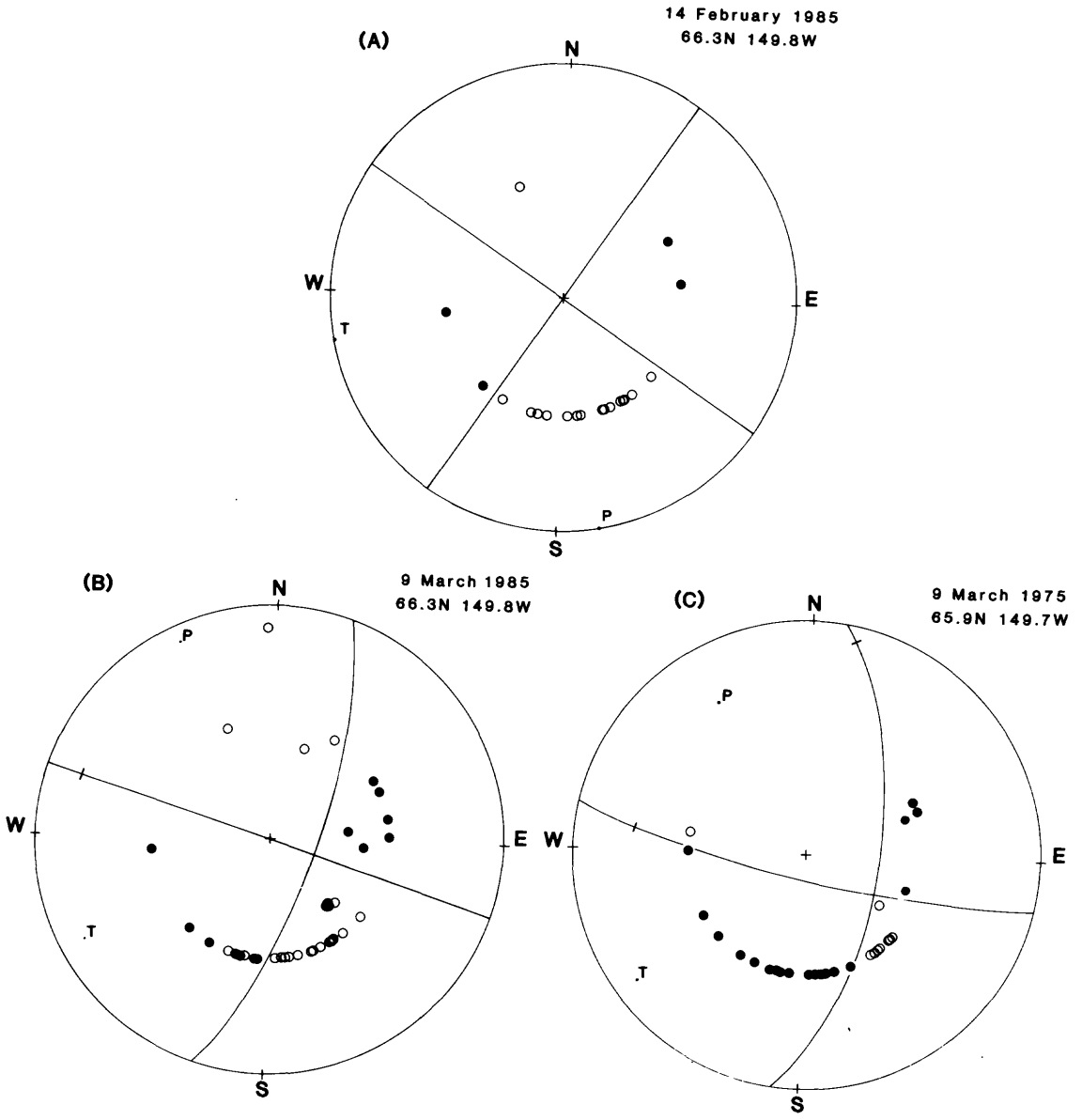

Figure 4. Focal mechanism solutions of two earthquakes of the present sequence (A) and (B) compared with that of an earthquake which occurred in nearly the same area 10 years earlier (the earlier location solution is probably not as reliable due to a sparcity of recording stations at the time). The preferred mechanism is left-lateral faulting on the NNE-SSW trending plane.

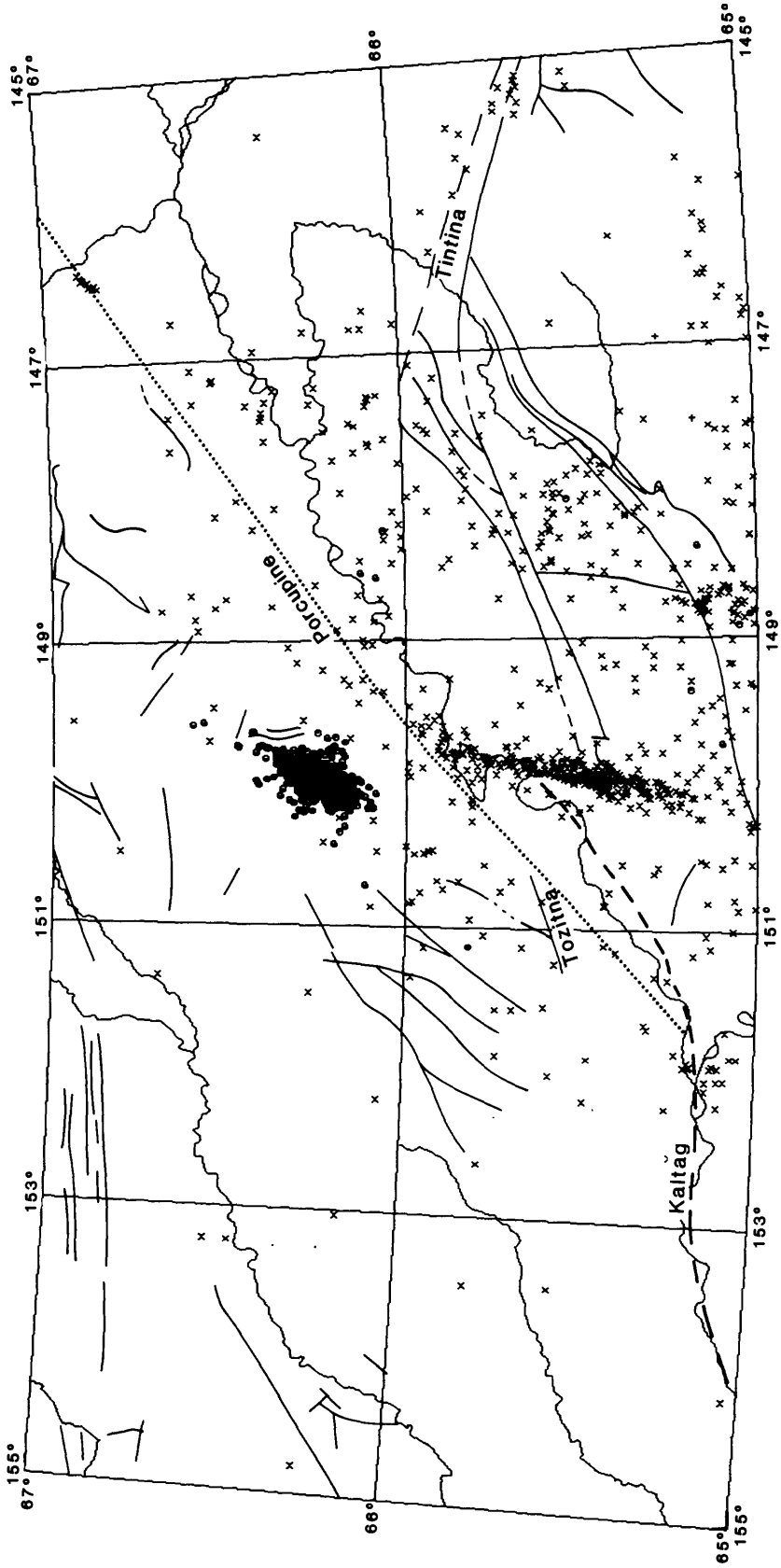

Figure 3. Map showing the location of the present earthquake sequence (which has been called the Dall City sequence after a deserted mining camp) at the upper center relative to the lineal aftershock zone which followed a magnitude 6.5 earthquake near Rampart to the south in 1968.

Investigation of Seismic-Wave Propagation for Determination of Crustal Structure

9950-01896

Samuel T. Harding
Branch of Geologic Risk Assessment
U.S. Geological Survey, MS 966
Denver Federal Center, Box 25046
Denver, CO 80225
(303) 236-1572

Investigations

1. Investigating and processing high-resolution seismic-reflection lines for the following:

   a. During June, high-resolution seismic-reflection lines were run to complete the surveys of the Becks Hot Springs area in Salt Lake City, Utah. The surveys were conducted for 3 miles along Redwood Drive. Lines were tied along 1700 Ave. and State road 249, and a line was run between 1700 Ave and 2100 North Ave. along Cuddy Lane. A third line was run north of the Bonneville Supply canal through the Chevron Refinery.

   b. Two surveys were conducted across fault scarps south of Toole, Utah, in Edwards and Bell Canyons.

   c. During September 1986, six shallow reflection profiles were run across the southern San Andreas fault using the Mini-Sosie system. Profiles transverse the fault in Whitewater Canyon, Old Twentynine Palms Highway, Palm Avenue, Thousand Palms Canyon Road, and an unnamed road near Mortmar.

Results

1. Processing of high-resolution seismic-reflection lines:

   a. The data from Becks Hot Springs have been processed to a brute stack and work is being done to complete this study.

   b. The processing of this data is still in progress.

   c. The data collected across the San Andreas fault present a number of problems. The geology was considerably more complex than first anticipated. The profiles indicate a very complex reflection-return pattern and may necessitate wave-equation modeling to unravel the reflection patterns seen on these cross sections.

Reports

Harding, S.T., Wesson, R.L., Nicholson, Craig, and Morton, P., 1986, Shallow reflection profiling across the base of the southern San Andreas fault [abs.]: Transactions of the American Geophysical Union [EOS], v. 67, p. 1200.

Whitney, J.W., Shrobs, R.R., Simonds, F.W., and Harding, S.T., Recurrent Quaternary movement of the Windy Wash fault, Nye County, Nevada [abs.]: Geolgoical Society of America Abstracts with Programs, v. 18, p. 787.

Seismic Source Characteristics of Western States Earthquakes

Contract No. 14-08-0001-G1183

Dr. Donald V. Helmberger

Seismological Laboratory
California Institute of Technology
Pasadena, California 91125
(818) 356-6998

Summary Report

Investigation and Results

A program of continuing work on the characteristics of pre-and--post 1962 U.S. earthquakes is in progress. It is based primarily on some recent advances in wave-propagational codes for laterally varying Earth models. Structures with arbitrary variations in two dimensions can now be handled with distributed double-couple excitations. More precise Green's functions lead directly to a clearer picture of detailed source properties as well as to provide am exploration of complex strong motion patterns. For example, finite-difference seismograms calculated for the 1971 San Fernando earthquake show strong effects due to lateral variation in sediment thickness in the San Fernando valley and the Los Angeles basin. Using known basin structure and teleseismically determined source parameters, two-dimensional SH and P-SV finite difference calculations can reproduce the amplitude and duration of the strong motion velocities recorded across the basins in Los Angeles in the period range from 1 to 10 seconds. The edges of basins nearest the seismic source show ground motion amplification up to a factor of three, and tend to convert direct shear waves into Love and Rayleigh waves that travel within the basins. The computed motions are sensitive to the mechanism and location of earthquakes. A strike-slip earthquake on the Newport-Inglewood fault zone, for example, would show different patterns of peak velocity and duration of shaking across the San Fernando and Los Angeles basins, see Vidale and Helmberger (1986). (Elastic finite-difference modeling of the 1971 San Fernando, California Earthquake, submitted to BSSA).

The major task of collecting and analyzing the WWSSN and LRSM recording of United States earthquakes (m>5) has taken considerably more effort than anticipated. Some preliminary results on source parameter inversion for representative events were discussed in the USGS Open-File Report 86-31. Essentially, the depth estimates come from modeling the short period depth phases pP and sP while the moment and orientation are established by modeling the long period body waves

and Pl regional waveforms. The intensity of the short period signals relative to the long periods signals is used primarily to set the stress level. When events occur in regions of good local array coverage we generally find quite good fault parameter comparisons with our results, source depth, etc. Out of the 20 or so events studied to date, we find that Walker Pass (1962), source depth, h=16 km, and Homestead Valley, h=4, have high stress drops while some of the lowest stress drops occur in Imperial Valley. The aftershocks of Coalinga occurring at various depths, likewise, do not show any clear pattern. In short, we have not found much evidence for a correlation between stress drop and depth. Apparently, complex geology and recurrence relationships are probably playing a more important role than depth.

Analysis of Earthquake Data from the Greater Los Angeles Basin and Adjacent Offshore Area, Southern California

#14-08-0001-G-1158

Egill Hauksson
Ta-liang Teng
Geoffrey Saldivar
Center for Earth Sciences
University of Southern California
Los Angeles, CA 90089-0741
(213) 743-7007

INVESTIGATIONS

Analyze earthquake data recorded by the USC and CIT/USGS networks during the last 12 years in the Los Angeles basin to improve earthquake locations including depth and to determine the detailed patterns of faulting in the study region. A study of the seismotectonics of the Newport-Inglewood fault has been completed.

RESULTS

The Newport-Inglewood fault zone (NIF) strikes northwest along the western margin of the Los Angeles basin in southern California. The seismicity (1973-1985) of $M_L \geq 2.5$ that occurred within a 20 km wide rectangle centered on the NIF extending from the Santa Monica fault in the north to Newport Beach in the south is analyzed. A simultaneous full inversion scheme (VELEST) is used to invert for hypocentral parameters, two velocity models and a set of station delays. Arrival time data from three quarry blasts are included to stabilize the inversion. The first velocity model applies to stations located along the rim and outside the Los Angeles basin and is well resolved. It is almost identical to the starting model, which is the model routinely used by the CIT/USGS southern California seismic network for locating local earthquakes. The second velocity model applies to stations located within the Los Angeles basin. It shows significantly lower velocities down to depths of 12-16 km, which is consistent with basement of Catalina Schist below the sediments in the western Los Angeles basin. The distribution of relocated hypocenters shows an improved correspondence to mapped surface traces of late Quaternary fault segments of the NIF (Figure 1). A diffuse trend of seismicity is observed along the Inglewood fault from the Dominguez Hills, across the Baldwin Hills to the Santa Monica fault in the north. The seismicity adjacent to Long Beach, however, is offset 4-5 km to the east, near the trace of the subsurface Los Alamitos fault. The depth distribution of earthquakes along the NIF shows clustering from 6 km to 11 km depth, which is similar to average seismogenic depths in southern California. Thirty-nine single-event focal mechanisms of small earthquakes (1977-1985) show mostly strike-slip faulting with some reverse faulting along the north segment (north of Dominguez Hills) and some normal faulting along the south segment (south of

Dominguez Hills to Newport Beach). The results of an inversion of the focal mechanism data for orientations of the principal stress axes and their relative magnitudes indicate that the minimum principal stress is vertical along the north segment while the intermediate stress is vertical along the south segment (Figure 2). The maximum principal stress axis is oriented 10-25° east of north. Reverse faulting along the north segment indicates that a transition zone of mostly compressive deformation exists between the Los Angeles block and the Central Transverse Ranges.

REPORTS

Hauksson, E., T. L. Teng and G. Saldivar, Analysis of Earthquake Data from the Greater Los Angeles Basin and Adjacent Offshore Area, Southern California, U.S.C. Annual Technical Report #86-5, prepared for the U.S.G.S., 31 pp., 1986.

Hauksson, E. and G. Saldivar, The 1930 Santa Monica and the 1979 Malibu, California, Earthquakes, to appear in BSSA, December 1986.

Hauksson, E., Seismotectonics of the Newport-Inglewood fault zone in the Los Angeles Basin, Southern California, in press BSSA, 1987.

Hauksson, E., T. L. Teng and T. L. Henyey, Near-Surface Attenuation of Waveforms of Local Earthquakes: Results from a 1500 m Deep Downhole Seismometer Array, submitted to fall AGU meeting 1986.

Saldivar, G. V., E. Hauksson and T. L. Teng, Seismotectonics of the Santa Monica and Palos Verdes Fault Systems in the Santa Monica Bay, Southern California, submitted to fall AGU meeting 1986.

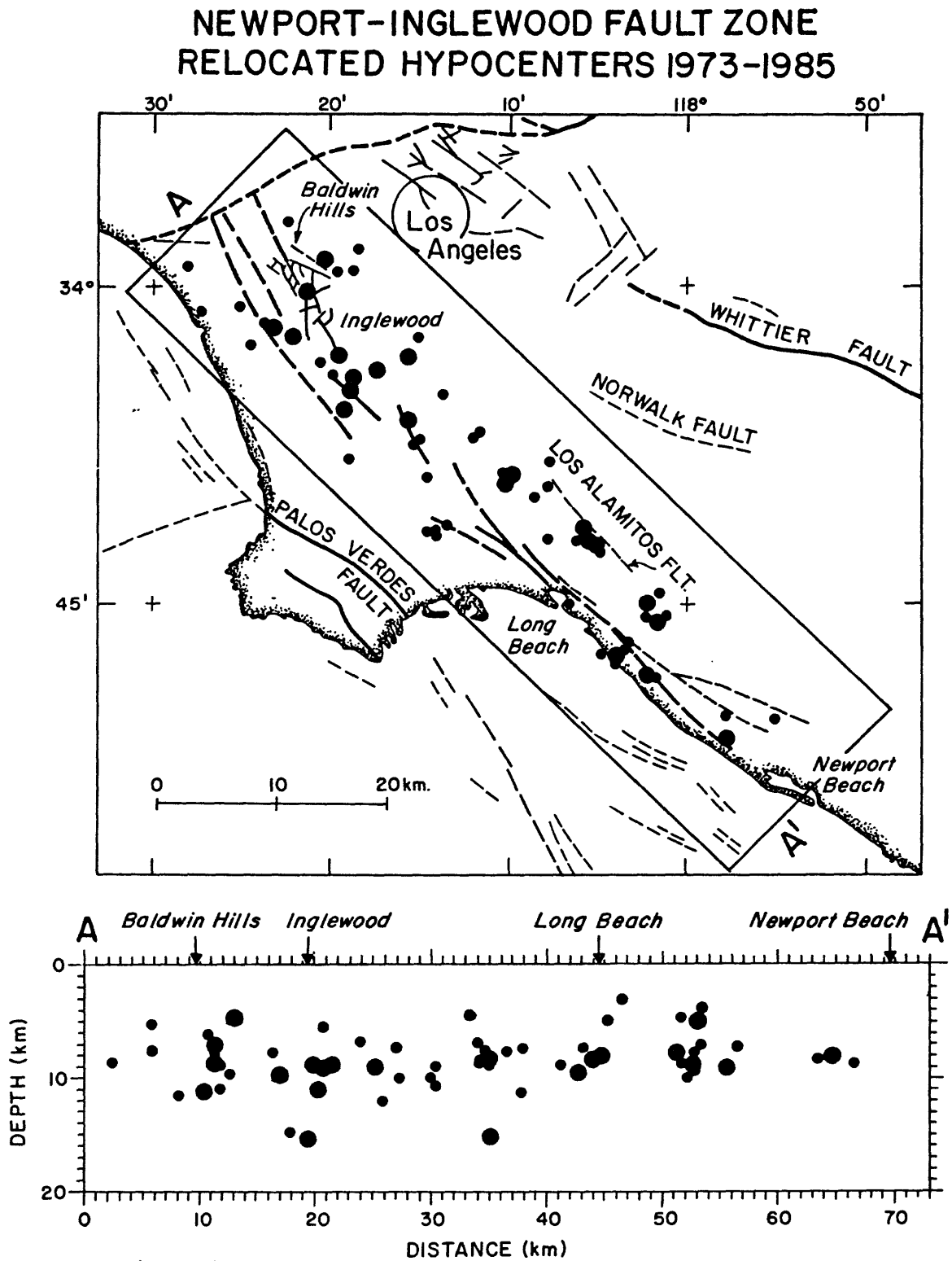

Figure 1. (Above) Map of the Los Angeles basin and the Newport-Inglewood fault zone showing relocated hypocenters determined with two velocity models and a corresponding set of station delays. (Below) Depth section (A-A') showing the relocated hypocenters along the Newport-Inglewood fault zone.

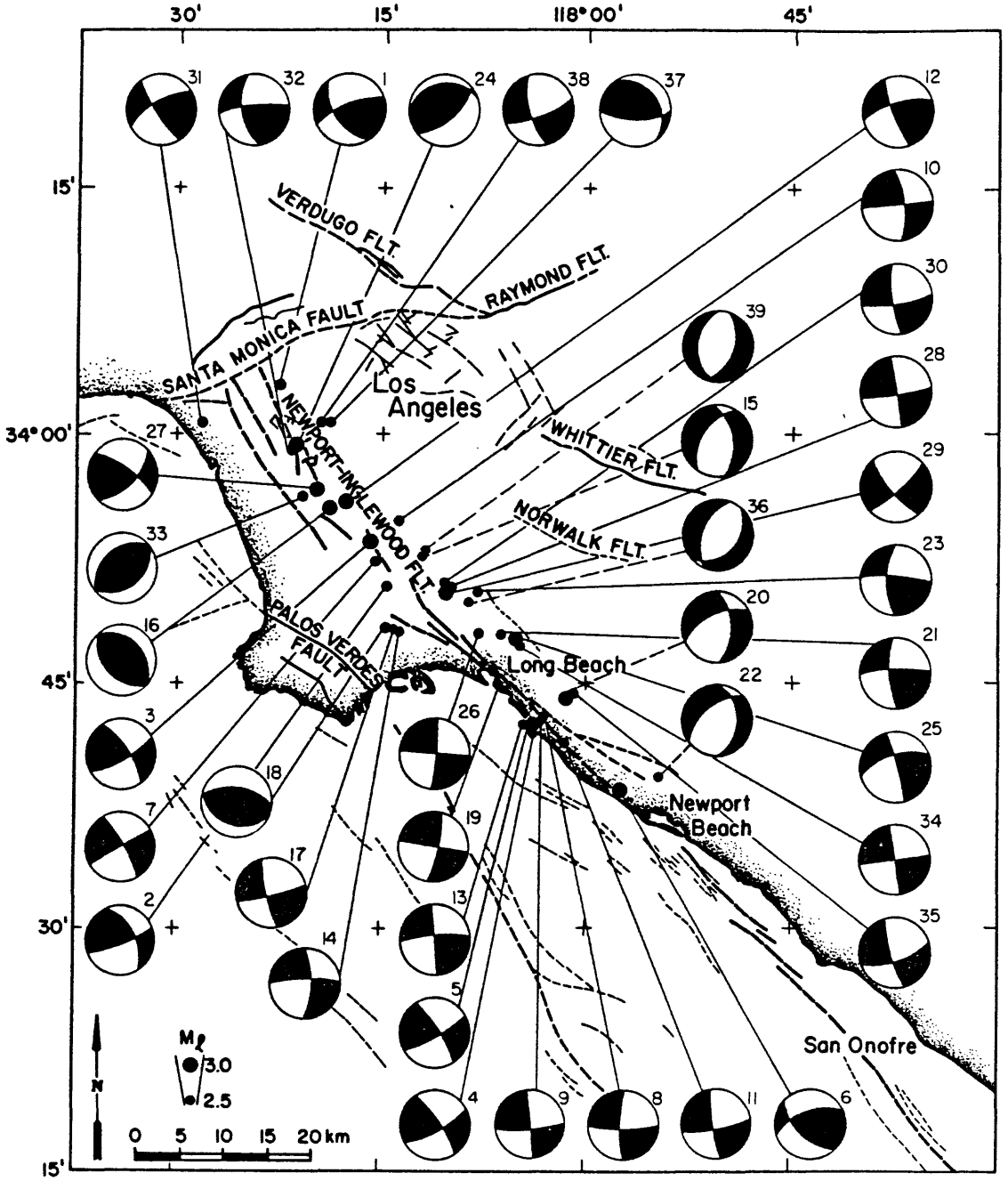

Figure 2. Lower hemisphere (single event) focal mechanisms of earthquakes ($M_L \geq 2.5$) near the Newport-Inglewood fault zone (1973-1985).

Earthquake Hazard Research in the Central United States

14-08-0001-G1090

Robert B. Herrmann
Department of Earth and Atmospheric Sciences
Saint Louis University
P.O. Box 8099 Laclede Station
St. Louis, MO 63156
(314) 658-3131

Goals

1. Perform research on the earthquake process in the New Madrid Seismic Zone to delineate the active tectonic processes.

2. Perform more general research relating to the problems of the eastern U. S. earthquake process and of the nature of eastern U. S. earthquakes compared to western U. S. earthquakes.

Investigations

1. A reinvestigation of spectral scaling of earthquakes in the Central Mississippi Valley Seismic zone is proceeding. Spectral data from 5 magnetic tapes of digitized LRSM data provided by EPRI have been processed. In addition, data from digitized old seismograms, pre 1941, have been obtained from R. Street, University of Kentucky, for reanalysis.

There is a problem in determining the corner frequency from the Lg-wave for large historical events. When the corner period is on the order of 10 seconds, the Lg wave is composed of only one or two higher modes, and the ability of the superposition of higher mode surface waves to scale as a simple body wave spectrum fails due to the small number of modes. In addition, the Lg on horizontal components becomes contaminated by the fundamental mode Love wave. The lack of a sharp corner frequency leads to an ambiguous relation between corner frequency and seismic moment that can only be resolved by using independent seismic moment data. However, the spectral excitation at 1 Hz is very stable.

2. Surface waves of the January 31, 1986 Cleveland, Ohio earthquake are being studied. Preliminary results are as follow:

The focal mechanism of the magnitude 5, Perry, Ohio earthquake determined using long period surface waves is one that strikes 115°, dips 70° to the south and which has a slip angle of 10°. The focal depth is shallow, in the range of 3 - 8 km, and the seismic moment is approximately 1.0 10^{23} dyne-cm.

This earthquake triggered a strong motion accelerograph 16 km north of the epicenter. Attempts are made to model this accelerogram. The focal mechanism with a focal depth of 6 km fits the gross properties of the accelerogram well, e.g., the polarity of the SH pulse, the relative amplitudes of the radial and transverse traces. The vertical amplitudes are underestimated by a factor of 2 - 4. There is a tradeoff between detailed shallow velocity structure (20 meters) and the seismic moment estimate. The modeling does resolve the surface wave ambiguity of a 180° rotation of the nodal planes.

In order to fit high frequency waveforms, or to estimate source properties from such data, it is essential that high frequency data acquisition experiments also make efforts to define earth structure. Recording surfaces waves from nearby blasts can provide sufficient detail.

Results

A paper entitled "Focal Mechanisms Studies of the January 31, 1986 Perry, Ohio Earthquake" has been presented at the Eastern Section, Seismological Society of America meeting in October.

Tectonics of Central and Northern California

9910-01290

William P. Irwin
Branch of Engineering Seismology and Geology
U. S. Geological Survey
345 Middlefield Road, MS 977
Menlo Park, CA 94025
(415) 323-8111, ext. 2065

Investigations

1. Extensional tectonics of northern California, in collaboration with R.A. Schweickert. Field investigation was done on both the NW and SE sides of the Trinity ultramafic sheet, a structure that may be the equivalent of a metamorphic core complex.

2. Distribution of radiolarian cherts in the central and southern Coast Ranges, in collaboration with C.D. Blome and M.J. Rymer.

3. Paleomagnetic study of accreted terranes of the Klamath Mouontains and adjacent regions, in collaboration with E.A. Mankinen and C.S. Gromme.

4. Preparing a chapter titled "Geology and Plate Tectonic Development" for a multi-authored report on the San Andreas fault.

Results

1. A detachment surface, similar to those associated with core complexes, was seen only at the La Grange mine. There the detachment surface is remarkably well exposed for several hundred feet along highway 299 and consists of a gently SE-dipping layer of mylonite with well developed mullion structures that are oriented downdip. The boundary between the the Trinity sheet and the adjacent Paleozoic strata of the Redding section is aligned with the La Grange fault for nearly 80 km to the NE, and although it probably is a continuation of the detachment fault seen at the La Grange mine, no exposures of the contact could be found during the field work.

2. Samples were taken of the principal known exposures of Franciscan radiolarian chert on both the eastern and western sides of the Salinian block in the central and southern Coast Ranges. Particular attention was given to the chert that was thought likely to be Lower Jurassic and that was seen to lie depositionally on the mafic volcanic rocks. Study of the distribution and faunal differences of the radiolarian cherts may yield important data relating to large lateral dislocation of the Franciscan to either side of the Salinian block. Laboratory work on the chert samples is not yet complete.

3. Additional core drilling was done on the Pit River stock (Triassic) at Shasta Lake, northern California, during the report period. A comprehensive report on our paleomagnetic study of northern California is now being prepared.

4. A first draft of the chapter has been completed.

Reports

Schweickert, R.A., and Irwin, W.P., 1986, Tertiary detachment faulting in the Klamath Mountains, California: *Geological Society of America, Abstracts with Programs*, v. 18, no. 6, p. 742.

Lanphere, M.A., and Irwin, W. P., 1986, In search of the Abrams Post Office: *California Geology*, (in press).

Investigation of Prediction Methods for Subduction-Zone Earthquakes

Grant Number 14-08-0001-G-1099

Carl Kisslinger
Cooperative Institute for Research in Environmental Sciences
Campus Box 449, University of Colorado
Boulder, Colorado 80309
(303) 492-6089

Prediction of the May 7, 1986 Andreanof Islands Earthquake.

Prediction research in the Adak seismic zone, central Aleutian Islands, underway since 1974 and supported by the NEHRP since 1977, reached a milestone with the occurrence of the M_S 7.7 earthquake on May 7, 1986. The USGS preliminary fixed depth epicenter is south of Atka Island, in the easternmost section of the part of the seismic zone that is monitored by the Central Aleutian Seismic Network. The rupture plane defined by the distribution of PDE-located aftershocks for the first 24 hours was about 220 km long, extending mostly to the southwest through the eastern and central part of the region of coverage of the local network. Rupture terminated near the eastern margin of Adak Canyon. An M_S 6.0 foreshock occurred two hours before the main shock and four aftershocks with magnitudes greater than 6 have followed. The USGS has located 270 aftershocks through August 21, 105 days after the main shock. The many hundreds of aftershocks recorded by the local network have saturated the data analysis system and several months will be required before all of these are located, even though a lower magnitude cutoff of 2.3 has been imposed. The data set contains much information about the rupture zone, and studies of such characteristics as changes in stresses associated with the events and the distribution of Q within and on the margin of the rupture zone have been started, but cannot move forward until the massive location effort is completed.

This event appears to fulfill our prediction for a major earthquake, even though the specification of each of the parameters was in error to some extent. The prediction was formulated and made public more than two years before the event. In the post-event evaluation, the prediction is being treated as consisting of two parts, the general statement that an event greater than magnitude 7 would occur near Adak at about this time, and the specific statements as to magnitude, place, and time. We recognized and acknowledged from the beginning that the attempt to be specific, considered essential if prediction research is to make progress, was based on limited knowledge of fundamental processes and limited experience.

The prediction was based on the observation of a clear quiescence in locally determined seismicity over the part of the seismic zone that ultimately proved to be the major portion of the rupture plane. The quiescence is also seen in the events with body wave magnitudes of 4.5 and greater, as reported in the PDE, but because the total number of events in small sections of the zone is small for these data, the observation is perhaps not as convincing as in the local data. The quiescence observed in the local data lasted 3 years and 10 months, which seems in reasonable agreement with the 3 year teleseismic quiescence found by Habermann for the 1971 Adak Canyon earthquake. This single case was the basis for our time prediction of the recent

event.

We are now analyzing the reasons for the errors in the specifications and beginning to draw some of the lessons from this experience that are important for further prediction research. With the actual characteristics of the event known, we have found the form of presentation of the seismicity data that would have been most revealing as to what was to come. The error in recurrence time was clearly the result of lack of enough prior cases to permit an assessment of the uncertainties. The underestimation of magnitude by about 0.5 was due to the influence of general recurrence concepts, which suggested that it was rather soon after the great 1957 event for another as large as that which actually happened. If the judgement had been based solely on the size of the area over which quiescence occurred, an event close to 8 would have been called for. The epicenter error, about 150 km too far west, and the location of the rupture plane, proposed as across Adak Canyon rather than to the east of it, were due in part to a misinterpretation of the significance of the SW2 asperity (it turned out to be the stopping place rather than the nucleation point), and the observed deficiency of moderate earthquake activity under Adak Canyon since 1971. Also, human bias in over-emphasizing what was happening within the area well-monitored by our network and ignoring equally important behavior just outside of it played a role.

The occurrence supports strongly the hypothesis that pronounced and prolonged quiescence is a precursor to a major earthquake. More cases based on data acquired with local networks, providing the high resolution needed, are required to provide a basis for establishing the reliability of this precursor in terms of false alarms and failures to predict. A paper summarizing the prediction has been submitted to Geophysical Research Letters.

The Aftershocks of the May 7 Earthquake.

An analysis of the temporal distribution of the aftershock sequence based on the PDE list has been undertaken in a search for quiescence that might have occurred before the largest aftershocks, as suggested recently by by Matsu'ura. No indications of such quiescence have been found, but a remarkable, if subtle, change in the properties of the time sequence at day 3.5 after the main shock has been discovered. The corresponds to the beginning of expansion of the aftershock zone to the northeast, but the effect seems to involve the whole aftershock zone. At about the same time a marked change in b-value, from 0.89 to 1.2 occurred. A relation between the rate of decrease of aftershock occurrence and b-value has been suggested by Utsu, but no firm conclusions have been reached yet.

Distribution of Q within and on the Margin of the Rupture Zone

The amplitude decay rate of high-frequency coda from small local earthquakes can be used to derive an apparent Q value which is a statistical indicator of the heterogeneity and anelasticity of the earth medium in the vicinity of the source-receiver region. Precursory coda-Q changes have been reported for some moderate to large earthquakes. The May 7 Andreanof Islands earthquake provides a good opportunity to test the possibility of precursory coda-Q changes for subduction zone earthquakes.

One goal of our study is to find if there is any difference in the coda Q between the eastern part of the network area (which became part of the rupture zone of the May 7 earthquake) and the seismically less active west regions. The data from 1985 through April 1986 have been processed and analyzed. The scatter of the resulting Q values is reasonable (standard deviation about 20% of the mean) and can be improved slightly by culling the original data. No spatial

difference in Q can be claimed between the eastern and western regions of the Adak network coverage area. The resulting data are being searched for any precursory changes.

When data become available for times after the May 7 earthquake, Q values will be determined for a comparison of the values before and after this large earthquake. This should provide insight as to how temporal variations in the stress field affect the coda Q in this subduction zone.

Stress Distributions

In response to our prediction several years ago of a major earthquake in the Adak region, an examination of the stress distribution in vicinity of the predicted epicenter was started. With the occurrence of the May 7 earthquake, the focus of the study has been shifted both to the east of the original study area, well within the rupture zone, and to the west of it, where the region under Adak Canyon still has not broken. So far values of stress drop and apparent stress have been determined for about 60 earthquakes in the eastern part of the network from November, 1985, through May 8, 1986, and for about 25 events in the Adak Canyon region for 1986 through May 8, but no patterns of variation of stress drop or apparent stress as a function of time or space has yet been recognized in the resulting data.

Seismological Field Investigations

9950-01539

C. J. Langer
Branch of Geologic Risk Assessment
U.S. Geological Survey
Box 25046, MS 966, Denver Federal Center
Denver, CO 80225
(303) 236-1593

Investigations

1. Guinea, West Africa, postearthquake study--local investigation of aftershocks resulting from M_S = 6.2 earthquake of 22 December 1983.

2. North Yemen postearthquake study--local investigation of aftershocks resulting from m_b = 6.0 earthquake of 13 December 1982.

3. Western Argentina postearthquake study--local investigation of aftershocks resulting from M_S = 7.3 earthquake of 23 November 1977.

Results

1. The recently completed study (Langer and others, 198__) reports on results of geologic and seismologic field studies conducted following the rare occurrence of a moderate-sized west African earthquake (m_b = 6.4) with associated ground breakage. The epicentral area of the northwestern Guinea earthquake of December 22, 1983, is a coastal margin, intraplate locale with a very low level of historical seismicity. The principal results include observations that the seismic faulting occurred on a preexisting fault system and the achievement of good agreement between the surface faulting, the spatial distribution of the aftershock hypocenters, and the composite focal mechanism solutions. We are not able, however, to shed any light on the reason(s) for the unexpected occurrence of this intraplate earthquake. Thus, the significance of this study is its contribution to the observational datum for such earthquakes and for the seismicity of west Africa.

   The main shock was associated with at least 9 km of surface fault-rupture. Trending east-southeast to east-west, measured fault displacements up to ~13 cm were predominantly right-lateral strike slip and were accompanied by an additional component (5-7 cm) of vertical movement, southwest side down. The surface faulting occurred on a preexisting fault whose field characteristics suggest a low slip rate with very infrequent earthquakes. There were extensive rockfalls and minor liquefaction effects at distances less than 10 km from the surface faulting and main-shock epicenter. Main shock focal mechanism solutions derived from teleseismic data by other workers show a strong component of normal faulting motion that was not observed in the ground ruptures.

   A 15-day period of aftershock monitoring, commencing 22 days after the main shock, was conducted. Eleven portable, analog short-period vertical seismographs were deployed in a network with an aperture of 25 km and an

average station spacing of 7 km. More than 200 aftershocks, with duration magnitudes of about 1.5 or greater, were recorded; analysis of a selected subset (95) of those events define a tabular aftershock volume (26 km long by 14 km wide by 4 km thick) trending east-southeast and dipping steeply (~60°) to the south-southwest. Composite focal mechanisms for groups of events distributed throughout the aftershock volume, exhibit right-lateral, strike-slip motion on sub-vertical planes that strike almost due east. Thus, the general agreement between the field geologic and seismologic results is good, however, our preferred interpretation is for three en-echelon faults striking almost due east-west.

2. The North Yemen epicentral locale in the southwestern part of the Arabian Peninsula is 200-300 km landward from the active rifting of the Red Sea and Sea of Aden. The magnitude 6.0 (M_S and m_b) main shock of December 13, 1982, caused considerable death, injury, and damage locally and was followed by an extensive aftershock sequence. A 12-day study employing a 10-station portable seismograph network was conducted between December 9, 1982, and January 9, 1983.

   Hypocentral locations were determined for 230 shocks selected from the thousands of recorded events (duration magnitudes between 1.8 and 4.6). These aftershocks define a source volume that is roughly 20X20X10 km. From that volume, about half (~110) of only the best constrained hypocenters with depths greater than 3 km were selected for detailed analysis. The 110 aftershock data set was divided into subsets according to geographic position (northern and southern) and temporal sequencing (a distinct aftershock sequence late in the monitoring period). A series of composite focal mechanism solutions (CFMS) show the aftershocks are dip-slip faulting (normal) on planes with north-northwest to northwest strikes and dips that were variable in amount (~30° to ~80°) and in direction (southwest and northeast).

   The strike and extensional nature of these CFMS are in good agreement with the main shock focal mechanisms, the surficial and bedrock geology in the epicentral area and the linear surface cracks observed in the field there following the December mainshock. We interpret the spatial distribution of our results to describe conjugate faulting episodes associated with a north-northwest striking fault.

3. An aftershock survey, using a network of eight portable and two permanent seismographs, was conducted for the western Argentina (Caucete) earthquake (M_S = 7.3) of November 23, 1977. The monitoring began on December 6, almost 2 weeks after the main shock and continued for a period of 11 days. A data set of 185 aftershock hypocenters in the depth range from near surface to 30+ km was obtained. The spatial distribution of those events occupied a volume of about 100X40X30 km (length X width X thickness, respectively). The volumnar nature of the aftershock distribution is principally a result of a bimodal distribution of foci that define east- and west- dipping planar zones. Efforts to select which of those zones was associated with the causal faulting include special attention to the determination of the mainshock focal depth and dislocation theory modeling of the coseismic surface deformation in the epicentral locale. Our focal depth (25-30 km, rather than a previous estimate of 17 km) and modeling studies lead us to prefer the east-

dipping plane as causal. Previous interpretations by Kadinsky-Cade and others (1985) that used the shallower focal depth and similar modeling calculations had selected the west-dipping plane. Our selection has the advantage of having fault initiation at the base of the crustal seismogenic layer (rather than in the middle of that layer) and fault propagation updip (rather than downdip).

The ten stations included in our temporary seismograph network for locating aftershocks were sited where the underlying sedimentary rock columns had thicknesses ranging from 0 to 6 km (up to 1.5-sec variation in vertical one-way travel times for the P-waves). Such rapid changes in the velocity structure cause considerable difficulty in obtaining accurate hypocenter locations. Fortunately, velocity data were available in the form of 26 refraction profiles for the near surface (0-6+ km). Those profiles gave the velocities for the sedimentary column and the underlying Precambrian basement in the network area. An estimate of the regional crustal velocity structure for this geologically complex area had also been determined previously by analysis of data from a well-located nearby earthquake. Unpublished surface-wave studies extend the model to the upper mantle. This study describes the use of the available data to refine the velocity estimates for the uppermost layers of the regional crustal velocity model and the method used to calculate P-wave travel time corrections for each station. The resulting model and station corrections were used, with good results, to locate 185 aftershocks. Average HYPO71 error measures for the aftershock hypocenters were: RMS=0.12 sec, ERH=±0.7 km, ERZ=±1.3 km.

References:

Kadinsky-Cade, Katherine, Reilinger, Robert, Isacks, B.L., 1985, Surface deformation associated with the November 23, 1977, Caucete, Argentina earthquake sequence: Journal of Geophysical Research, v. 90, p. 12691-12700.

Langer, C.J., Bonilla, M.G., Bollinger, G.A., 198__, Aftershocks and surface faulting associated with the intraplate Guinea, West Africa, earthquake of 22 December 1983: (Submitted to BSSA, November 1986).

Reports:

Bollinger, G.A., and Langer, C.J., 198__, Development of a velocity model for locating aftershocks in the Sierra Pie de Palo region of western Argentina: (Submitted for publication as U. S. Geological Survey Bulletin, received Director's approval August 1986).

Bollinger, G.A., and Langer, C.J., 1987, A note on the geometric configuration of seismogenic zones: (Accepted for publication in Seismological Research Letters, 1987).

Goter, S.K., Richans, W.D., and Langer, C.J., 1986, Aftershocks of the Borah Peak, Idaho, earthquake of 28 October 1983: Catalog of locations and single-event focal mechanisms: U.S. Geological Survey Open-File Report 86-277, 392 p.

Langer, C.J., Bonilla, M.G., Bollinger, G.A., 198__, Aftershocks and surface faulting associated with the intraplate, West Africa, earthquake of 22 December 1983: (submitted to BSSA, November 1986).

Langer, C.J., Bollinger, G.A., and Merghelani, H.M., 198__, Aftershocks of the December 13, 1982, North Yemen earthquake: Conjugate normal faulting in an extensional setting: (submitted to BSSA, November 1986).

Langer, C.J., and Bollinger, G.A., 198__, The western Argentina (Caucete) earthquake of November 23, 1977--spatial distribution and some tectonic implications of the aftershock sequence: in U.S. Geological Survey Open-File Report _____, edited by S. T. Algermissen.

Nicholson, C., Langer, C.J., and Valdez, C., 1986, Aftershock locations and focal mechanism solutions: in Studies of the January 31, 1986, northeastern Ohio earthquake: U.S. Geological Survey Open-File Report 86-331, p. 10-12.

Richins, W.D., Pechmann, J.C., Smith, R.B., Langer, C.J., Goter, S.K., Zollweg, J.E., and King, J.J., 198__, The 1983 Borah Peak, Idaho, earthquake and its aftershocks: (submitted to BSSA for publication, October 1986)

PALEOLIQUEFACTION STUDIES NEAR CHARLESTON, SOUTH CAROLINA

9950-03868

Stephen F. Obermeier and Gregory Gohn
Branch of Geologic Risk Assessment
U.S. Geological Survey
MS 922, National Center
Reston, Virginia 22092
(703) 648-6791 or (703) 648-6900

Investigations

Field searches were made for paleoliquefaction sites in coastal South Carolina, near Beaufort. In addition, sand blow sites previously discovered, such as the site at Hollywood, were re-examined for the purpose of further developing criteria that can be used to interpret an earthquake origin to liquefaction features.

Results

Liquefaction-induced features were discovered near Beaufort (at Bluffton); the features at Bluffton have most of the same sedimentological relations and ground disruption characteristics as the sand blows at Hollywood, and thus are believed to be probably earthquake in origin. The final conclusion of origin must be based on an on-going (FY87) study of mechanical properties of source sands at depth, and a study of the local ground-water setting.

A draft report has been completed, discussing geologic criteria for interpreting an earthquake origin to liquefaction features in coastal South Carolina and the New Madrid seismic zones. These criteria are based on the nature of the surficial ground disruption, in combination with study of the local ground-water setting. The report makes it clear that geologic criteria may not be sufficient for determining origin at some sites. The report also points out that engineering studies on source sands at depth can probably determine origin at some sites, and discusses types of mechanical property relationships that can be used to interpret origin.

References

(P) Obermeier, S. F., Jacobson, R. B., Powars, D. S., Weems, R. E., Hallbick, D. C., Gohn, G. S., and Markewich, H. W., 1986, Holocene and late Pleistocene(?) earthquake-induced sand blows in coastal South Carolina: Proceedings of Third U.S. National Conference on Earthquake Engineering, Charleston, S.C., August 1986, v. 1, pp. 197-208.

(a) Obermeier, S. F., Jacobson, R. B., Weems, R. E., and Gohn, G. S., 1986, Holocene and late Pleistocene(?) earthquake-induced sandblows in coastal South Carolina: Seismological Society of America, Earthquake Notes, v. 57, no. 1, p. 17.

(a) Schaefer, J. P., Obermeier, S. F., and Stone, J. R., 1987, on the origin of wedge structures in southern New England: GSA Abstract.

(P) Weems, R. E., Obermeier, S. F., Pavich, M. J., Gohn, G. S., Rubin, M., Phipps, R. L., and Jacobson, R. B., 1986, Evidence for three moderate to large prehistoric Holocene earthquakes near Charleston, S.C.: Proceedings of Third U.S. National Conference on Earthquake Engineering, Charleston, S.C., August 1986, v. 1, pp. 3-13.

Charleston Project -- Geologic and Engineering Studies

9950-03868

Stephen F. Obermeier
Br. of Geologic Risk Assessment
U.S. Geological Survey
National Center, MS 926
Reston, VA 22092
(703) 648-6791

9510-01343

Gregory S. Gohn
Br. of Eastern Regional Geology
U.S. Geological Survey
National Center, MS 926
Reston, VA 22092
(703) 648-6901

Investigations

1. An extensive search for 1886 and pre-1886 liquefaction features was continued in the 30-mile-wide belt along the coast of South Carolina. This coastal belt has now been searched in reconnaissance fashion from the North Carolina border to the Georgia border.

2. The ages of numerous sand blows at the Hollywood, Charleston County, locality have been determined within limits set by the radiocarbon ages of associated organic materials. Radiocarbon ages have been determined for organic soils disrupted by sand blows, wood within filled sand blow craters, roots cut by sand blows, and roots growing into sand blow craters.

3. Organic materials associated with sand blows at numerous sites in the coastal area of South Carolina have been sampled for radiocarbon analysis.

Results

1. Multiple late Pleistocene to Holocene sand blows have been discovered at several sites throughout the coastal area of South Carolina. The fact that pre-1886 sand blows have a much wider geographic distribution than do the 1886 sand blows suggests that either multiple seismic source zones capable of generating liquefaction-producing earthquakes exist in South Carolina or that a pre-1886 earthquake larger than the 1886 earthquake has occurred in the 1886 source zone.

2. Analysis of the radiocarbon ages for organic materials associated with sand blows at the Hollywood locality indicates that liquefaction-producing earthquakes occurred in that area: at about 1230 y.b.p., between about 1670 and about 3700 y.b.p., and between about 4200 and about 7100 y.b.p.

3. The Pleistocene beach sands of coastal South Carolina are much more susceptible to liquefaction than standard sands used for engineering analysis (for a given relative density). This very high susceptibility explains in part the commonplace occurrence of liquefaction features in the 1886.

Reports

Gohn, G. S., 1986, Geologic studies of the Charleston, South Carolina, earthquake zone by the U.S. Geological Survey, 1975-1986: Earthquake Notes, v. 57, no. 1, p. 16.

Gohn, G. S., and Weems, R. E., 1986, Drill-hole investigations of proposed faults near Summerville, South Carolina: Earthquake Notes, v. 57, no. 1, p. 17.

Obermeier, S. F., Jacobson, R. B., Powars, D. S., Weems, R. E., Hallibick, D. C., Gohn, G. S., and Markewich, H. W., 1986, Holocene and late Pleistocene(?) earthquake-induced sand blows in coastal South Carolina, in Earthquake Engineering Research Institute, Proceedings of the Third U.S. National Conference on Earthquake Engineering, v. I, p. 197-208.

Obermeier, S. F., Jacobson, R. B., Weems, R. E., and Gohn, G. S., 1986, Holocene and late Pleistocene(?) earthquake-induced sandblows in coastal South Carolina: Earthquake Notes, v. 57, no. 1, p. 17.

Weems, R. E., Obermeier, S. F., Pavich, M. J., Gohn, G. S., Rubin, M., Phipps, R. L., and Jacobson, R. B., 1986, Evidence for three moderate to large prehistoric Holocene earthquakes near Charleston, S.C., in Earthquake Engineering Research Institute, Proceedings of the Third U.S. National Conference on Earthquake Engineering, v. I, p. 3-13.

Array Studies of Seismicity

7-9930-02106

David H. Oppenheimer
Branch of Seismology
United States Geological Survey
345 Middlefield Road - MS 977
Menlo Park, California 94025
415-323-8111 X2791

Investigations

1. Analyze fault-plane solutions of aftershocks of the M6.2 Morgan Hill earthquake which occurred on April 24, 1984 to gain understanding of regional stress field.

2. Begin consolidation and clean-up phase data of central California Seismic Network (CALNET) from 1969 through 1984.

3. Analysis of P- and S-velocity structure at Coalinga, California.

4. Begin investigation of characteristic earthquake sets (M>4.0) in Stone Canyon/Bear Valley region of the San Andreas fault.

Results

1. We computed 315 fault-plane solutions for aftershocks (M > 1.5) of the Morgan Hill earthquake on the Calaveras fault. The distribution of polarity discrepancies with respect to the position of observing stations is strongly non-uniform. Sixty-three percent of the discrepancies occur at only 10 stations, all but one of which are located along the trace of the Calaveras fault. The fact that most of the discrepancies occur at stations close to the fault suggests that these errors stem from either unmodeled lateral refractions across the fault or errors in epicentral determination.

   Most of the aftershock focal mechanisms for earthquakes locating on the Calaveras fault are similar to mechanisms reported for the mainshock, but the dip of the assumed slip plane tends to dip 50-70° NE as opposed to 84° SW of the mainshock or the 85° NE alignment of aftershocks. We believe that this discrepancy arises because the computation procedure attempts to accomodate the discrepant polarities of nearby stations affected by the problem of unmodeled lateral refraction.

   Focal mechanisms for shallow aftershocks of north-south seismicity trends northwest of the Calaveras fault zone indicate right-lateral slip on vertically oriented faults parallel to the seismicity trends. The orientation of these aftershocks suggests that the latter represents frictional failure on prexisting faults rather than failure of intact rock.

Fault plane solutions for aftershocks in the vicinity of the Anderson Reservoir exhibit pure reverse motion along fault planes parallel to the north-dipping, reverse Silver Creek and Coyote Creek faults. The following causes for generating pure reverse slip on these fault orientations can be rejected:

a) The motion is inconsistent with estimates of the orientation of the regional stress field. From the orientation of the stress field inferred from geodetic measurements and specification of the relative magnitudes of the principal stresses, slip would be predicted as oblique, right-lateral reverse (phi=0) through pure right-lateral to oblique, right-lateral normal slip (phi=1); pure reverse slip is not predicted.

b) Stress perturbations due to the mainshock have not appreciably altered the regional stress field in this region. Because fault plane solutions for earthquakes occurring in the vicinity of the Anderson Reservoir prior to the mainshock also exhibit pure reverse motion, the stress field responsible for these earthquakes is a long-term feature of this region.

c) The stress field arising from repeated rupture along this characteristic segment of the Calaveras fault does not give rise to reverse faulting. Preliminary attempts to model the resulting stress field assuming a linear, elastic half-space for rectangular dislocations deduced from strong ground motion studies (Hartzell and Heaton, 1986) predicts normal faulting instead of reverse.

These mechanisms indicate that the stress field is nonuniform in this region. This local stress field may represent a component of regional contraction normal to the orientation of the Calaveras fault, as indicated in geodetic measurements at Parkfield (Segall and Harris, 1986), and reverse faulting and folding throughout central California. Alternatively, the stress field may represent attempts to accomodate the bifurcation of the Calaveras and Hayward faults to the north, or Calaveras and San Andreas faults to the south. A manuscript describing these results is in preparation.

2. The large volume of seismic data recorded by the CALNET since 1969 has frequently overwhelmed our capacity to process the data. The result has been inconsistent data archiving, uncorrected data errors, and undocumented procedures. In an effort to correct this situation, all the available CALNET P-wave phase data have been assimilated, chronologically sorted, and corrected for gross data errors. These data will be relocated with appropriate regional velocity models, and the hypocenters will be examined for obvious data errors. Disjointed data sets will then be merged together and magnitudes will be recalculated, incorporating known systematic biases through time. The resulting data will be stored in a permanent data base that will be available to the general research community. Accompanying documentation will describe the data quality, location procedures, and network history.

3. Existing computer programs which simultaneously invert local earthquake traveltime data for the 3-dimensional velocity structure and hypocentral parameters have been extensively modified. The inversion now solves for both S- and P-velocity through an improved ray-tracing method, and the velocity at designated nodes may be fixed. More stations, arrival times, and velocity nodes are also permited in the new code.

   Inversion of traveltime data recorded in the vicinity of Coalinga, California for 3-dimensional velocity structure reveals that the axes of the Joaquin Ridge and Coalinga Anticline are expressed as high velocity features. Lower velocities are observed in the San Joaquin and Pleasant Valleys. The basement appears to dip at a moderately steep angle beneath the Coalinga Anticline. There are several locales that exhibit lower velocity than is predicted from the existing knowledge of geologic structure, and several other locales exhibit velocity reversals. The latter may be interpreted as overpressured zones analagous to results derived in laboratory settings in which reduced P- and S-velocities were observed under high pore pressure conditions.

4. Seismograms written on the Wood-Anderson seismograph at Mount Hamilton were collected for all M > 4.0 earthquakes in the Stone Canyon/Bear Valley region of the San Andreas for the time period of 1/34 through 6/86. This instrument has been continuous operation at its present location since 1928; therefore the general character of the records should not be significantly altered by changes in instrumentation or site. A systematic comparison of the seismograms has revealed a dozen characteristic sets, each containing 2 to 5 events displaying highly repeatable waveforms. Phase data was also assembled for those events occurring between 1/69 and 6/86. Joint hypocenter determinations for those characteristic pairs falling within this time range show a separation of only a few hundred meters in each case. Present efforts are directed toward high precision scaling of the S-wave and coda wave amplitudes to determine the temporal stability of the coda waves. Preliminary results show that the ratio of the S-wave amplitude to the coda wave amplitude varies by as much as 50 percent between 1934 and 1986. A manuscript detailing the results of this study is in preparation.

   A more detailed study of one characteristic set at Stone Canyon is in progress. This set contains three events, August 6, 1951, September 4, 1972, and May 31, 1986 having catalogue magnitudes of 4.7, 4.6 and 4.5 respectively. Moment ratios determined by the amplitude scaling between seismograms for 1951:1972:1986 of 2:2:1 are not in simple agreement with either the time or slip predictable models. A joint hypocenter determination between 1972 and 1986 using 18 common Calnet stations reveals that the two events nucleated within 100 m (or less) of each other. The 1972 and 1986 events were preceded by a similar foreshock sequence; however, records from Mt. Hamilton suggest that there was no foreshock activity in 1951. Aftershock activity, although more vigorous in 1972, followed virtually the same spatial and temporal patterns in 1972 and 1986.

Reports

Eberhart-Phillips, D., 1986, Three-dimensional P- and S-velocity structure at Coalinga, California: possible evidence for high pore pressure in the hypocentral zone, EOS, Tran. Am. Geophys. Union, in press.

Eberhart-Phillips, D., 1986, Three-dimensional velocity structure in northern California Coast Ranges from inversion of local earthquake arrival times, Bull. Seis. Soc. Am., 1025-1052.

Oppenheimer, D. H., 1986, Extensional tectonics at The Geysers geothermal area, California, J. Geophys. Res., 91, 11463-11476.

Spudich, P. and D. Oppenheimer, 1986, Dense seismograph array observations of earthquake rupture dynamics, in Earthquake Source Mechanics, Maurice Ewing Series, vol.6, edited by S. Das, J. Sims, and C. H. Scholz, 285-296, AGU, Washington, D.C.

Dietz, L. D. and W. L. Ellsworth, 1986, A characteristic earthquake source at Stone Canyon, California, EOS, Tran. Am. Geophys. Union, in press.

Mountain Run Fault Zone of Virginia

9510-03680

Louis Pavlides
Branch of Eastern Regional Geology
U.S. Geological Survey
National Center, MS 928
Reston, Virginia 22092
(703) 648-6925

Investigations

The Mountain Run fault zone (MRFZ) is a regional feature about 75 km in length, as presently known from mapping and interpretation of published reports. It is best defined as a physiographic feature in the Unionville Quadrangle. There it contains a linear fault-line scarp that transects the quadrangle in a northeast direction. At its north end, the MRFZ forms part of the southeast boundary of the early Mesozoic Culpeper basin. The scarp is held up by phyllonite, and such phyllonite extends over a width at least 2.5 km to the southeast of the scarp. An alluvium-filled valley lies on the northwest side of the scarp and to the northwest of this valley is a narrow zone of faulted and sheared rocks that form the northwest boundary of the MRFZ. Mapping has followed the MRFZ from about the Mesozoic Culpeper basin near the Rappahannock River southwestward to near Charlottesville, Va.

The MRFZ separates a thrust faulted early Paleozoic (pre-440 m.y.) melange terrane on its southeast side (which is considered to be the remnants of a back-arc basin) from a phyllite, slate, and limestone unit that unconformably overlies the Precambrian Catoctin Greenstone and which together are considered as part of ancestral (pre-440 m.y.) North America. Therefore, the MRFZ is considered as a suture that juxtaposed a Cambrian island arc (Central Virginia volcanic-plutonic belt) and its associated fault-imbricated back-arc basin (melange terrane) onto or against ancestral North America in pre-440 m.y. time. Part of the MRFZ was reactivated in early Mesozoic time to define, in part, the southeast boundary of the Triassic-Jurassic Culpeper basin. The discovery recently of a thrust fault within the MRFZ that offsets gravels of probably post-Pliocene age, indicates additional local reactivation within the MRFZ during late Cenozoic time.

Results

A recent project result has been the development of the hypothesis that some of the topographic scarps in the central Virginia Piedmont are the result of neotectonic effects rather than due entirely to lithologic control. Specifically, the long Mountain Run scarp (MRS) within the MRFZ in the Unionville quadrangle and the shorter Kelleys Ford scarp (KFS) along a strand of the MRFZ in the northeast part of Germanna Bridge quadrangle, apparently have tectonically controlled the eastward flow of the major rivers in this region starting in the Tertiary and continuing up to the present. Both scarps

are underlain by quartz-veined phyllonite. This lithology is continuous in a belt along strike between two en echelon scarps. However, the intervening phyllonitic terrane lacks scarps and both the Rappahannock and Rapidan Rivers flow eastward across this scarpless phyllonitic terrane and continue across the Piedmont and eventually (Rappahannock River) onto the Coastal Plain. The Rappahannock in particular is deflected by the KFS and only crosses the phyllonitic terrane at the south end of this scarp. In the Unionville quadrangle, the northeast flowing Mountain Run first starts flowing eastward across the phyllonite terrane at the northeast end of the MRS.

These drainage-controlling scarps are believed to have formed as discontinuous en echelon fault segments along and within the MRFZ. These faults are believed to be steep to vertical in attitude with the southeast side upthrown. They are now buried beneath alluvium close to the foot of the northwest facing scarps. The bold relief of these scarps supports the hypothesis that uplift has been continuous along their controlling faults since the Tertiary and into fairly recent time, otherwise they would not have escaped the obliterating effects of weathering and erosion that produce the generally subdued land forms found within the Piedmont. The scarpless, phyllonite-floored terrane intervening between the MRS and KFS is characterized by a generally gentle, northwest-sloping surface that gradually grades into the Culpeper basin immediately to the northwest.

A geologic study supplemented by geophysical and isotopic studies along the MRFZ to the southwest of its present study area and involving the mapping, in their entirety, of quadrangles traversed by the MRFZ should enable (1) a better understanding of the nature and movement history of the MRFZ as it relates to accretion along the Paleozoic North American continental margin, and (2) evaluation of neotectonics, with the possibility of recognizing additional young faults along the strike length of the MRFZ. Also, reconnaissance to the southwest has encountered slates and phyllites on the northwest side of the MRFZ that locally bear a resemblance to the Ijamsville Phyllite of the western Maryland Piedmont. Through the proposed study, it may be possible therefore to better understand the tectonic relationships between these two terranes in Virginia and Maryland. A high-resolution reflection survey run across the MRS and KFS would help to determine whether these scarps are indeed fault controlled.

Seismotectonics of the Central Calaveras Fault

14-08-0001-G1084

Gary L. Pavlis
Department of Geology
Indiana University
Bloomington, Indiana 47405
(812) 335-5141

Atilla Aydin
Department of Geosciences
Purdue University
West Lafayette, Indiana 47907

Objective: To improve our understanding of the nature of the faulting process leading to moderate size, strike slip earthquakes in California through combined geologic and seismological investigations.

Investigation: This is a cooperative effort between groups at Indiana University and Purdue University. The present work has focused on analysis of data from the source region of the 1984 Morgan Hill earthquake. Work at Indiana University is focused on analysis of seismic data. The Purdue group has focused on field mapping of fault structures in the rupture zone of the Morgan Hill earthquake. Details of current progress follow. By the conclusion of the project we hope to combine our data to better understand the processes shaping both the seismic and geologic data.

Results from work at Indiana University: Our work has progressed in two different directions. The greatest progress has been made through the work of Mariana Eneva. In this study we apply statistical analysis based on pairs of earthquakes to study the spatial and temporal patterns of seismicity in the region of the Calaveras fault zone defined by aftershocks of the Morgan Hill earthquake. We examined 15 years of preshock and 21 months of aftershock data using two major statistical tools: (1) frequency distributions of all possible combinations of earthquake pairs, and (2) the theory of runs. The first is used to examine nonuniformities in the spatial and temporal distribution of the seismicity by comparison with average expected distributions calculated by computer simulations. The significance of departures from the expected distributions are appraised by a novel method using tolerance limits that account for deviations in the distribution resulting from the finiteness of the sample. We find the spatial distribution is nonuniform in two major ways. (1) Short distance clustering (distances < 5 km) occur in both the preshock and aftershock sequence. (2) A long distance nonuniformity caused by concentrations of activity in two active areas separated by a gap leads to a relative excess of events separated by 11-19 km. This feature is present in the preshock and early aftershock sequence, but disappears in the late aftershock sequence. This suggests a return to a more

homogeneous stress field. Time interval distributions for the preshock data imply a marginally significant difference from a Poissonian distribution. The aftershock activity is dominated by the classic power law decay in time. However, comparison with a statistical model derived from the power law shows significant systematic departures. Finally, application of the theory of runs reveals a long term pattern in earthquake occurrence related to alternation of "along strike" and "across strike" subsequences. We are currently in the final stages of submitting a paper describing this work.

The second direction that we have pursued in examining the seismic data is presently incomplete. We are in the process of relocating all the earthquakes for which we have data from this sequence using technique recently developed by Pavlis and Hokanson (1985). This technique will combine information obtained using Thurber's (1983) local earthquake, 3-D inversion program with a specialized multiple event location program to provide very precise hypocenter locations. These will be combined at the end of the project with Aydin's fault maps at which point we will attempt to correlate the two data sets.

Results from work at Purdue University: The central portion of the Calaveras fault between the Calaveras Reservior in the northwest and Coyote Lake in the southeast has been studied by using aerial photographs and field mapping. A preliminary strip map of 1/24000 scale is prepared. The strip map shows a fault zone marked by a valley about 4 km wide from one watershed line to the other. Within the fault valley are numerous fault strands which are determined with various degrees of confidence. Some major fault strands are defined geologically by juxtaposition of the Franciscan and the Late Mesozoic/Tertiary formations (Crittenden, 1951; Dibble, 1972-1980) and in one case by an offset alluvial fan. Others are recognized by their geomorphic expression in the form of fault scarps, distribed drainage systems and conspicuous linear features such as valleys, ridges, gullies, saddles, benches and notches. These expressions appear to be more decisive along deeply incised margins of the valley bottom. it is found that these portions of major strands were basically mapped by Herd (1978, 1982). Major fault strands lie in general slightly oblique to the axis of the valley so that while a part of a major fault strand follows the deeply incised margin the extension of the same strand goes into the slopes on either side of the valley. Landslides of various sizes are common on both sides of the valley with a less conspicuous signature. Consequently, probable genetic relationships between landslides and active faults are obscured by the former.

Major fault strands are arranged en echelon and step aside primarily in a right-handed sense and overlap by various amounts. One exception occurs in a relatively narrow zone northeast of Anderson Lake, where the sense of stepping is left-handed. Fault strands with two trends different than that of the fault zone are recognized in the zone and surroundings. These trends are about north-south and east-west and appear to be related to interaction among verious fault strands and the Calaveras and neighboring faults.

EARTHQUAKE RESEARCH IN THE WESTERN GREAT BASIN

Contract 14-08-0001-G1193

W.A. Peppin, E.J. Corbett, and U.R. Vetter
Seismological Laboratory
University of Nevada
Reno, NV 89557
(702)784-4975

Investigations

This program supports continuing studies with research focussed on: (1) seismotectonics of the White Mountains gap; (2) magmatic processes in Long Valley caldera; (3) the UNR experimental digital network; (4) attenuation changes in earthquake regions connected with volcanism; (5) relocations of Mammoth Lakes earthquakes; (6) analysis of wideband digital waveforms; and (7) digitization of field tapes for a more direct analysis of the 1978 Wheeler Crest earthquakes. Progress has been made in each of these areas, and in this report we summarize those of greatest interest.

Results

The 1986 Chalfant Valley sequence

For the second time in 18 months, a major earthquake sequence has occurred in the middle of a seismic network deployed in connection with our work on Mammoth Lakes and the White Mountains seismic gap. As for the Round Valley earthquake of November 1984, station coverage was complete and dense. Seismicity is summarized in **Figure 1.** This sequence was the largest since May of 1980, with two events above magnitude 6 and two others nearly as large, plus about 8,000 aftershocks. The sequence continued the pattern that has been going on since October 1978, in which this region experiences a seismic event near or above magnitude 6 each 18 months (the 1986 sequence would be the sixth such episode). Because of our long-standing concern about the White Mountains region as the possible locus of the next major Basin and Range earthquake (Wallace, 1978; Ryall and Ryall, 1983), this sequence caused the U.S.G.S. to issue a public warning that the probability of a major earthquake should be considered significantly higher for the moment. In response to the sequence, both UNR and the U.S.G.S. mounted field experiments to record the aftershocks. UNR placed three wideband digital event recorders in mine adits east and west of the aftershock zone, to compliment the placement of 5-day recorders directly over the aftershock zone by the U.S.G.S. New permanent short-period stations were placed in the field, with both UNR and the U.S.G.S. now sharing all data channels.

Figure 1 shows a complex aftershock pattern as have all of the preceding events except that of 4 October 1978. Again there appears to be no obvious correlation of the trends of the aftershocks with such features as the 3-km-high,

west-facing scarp of the White Mountains. Cross sections bring this out more clearly (**Figure 2**). Not only that, but again the first-motion data show mechanisms with dominantly strike-slip motion on trends not revealed in the surface geology, i.e., virtually no component of normal faulting (Figure 1). Thus we are faced with the same problem over and over again: *why do earthquakes which occur along the Sierra Nevada front, topographically the most spectacular normal-faulting feature of the Great Basin, show essentially no component of normal faulting?* This question is really quite important to answer from the viewpoint of earthquake hazard in this region. The two most obvious possibilities (with rather different implications for the hazard problem) are that (1) strike-slip (i.e., San Andreas style) faulting now dominates the Sierra Nevada eastern border region, so that normal faulting events are not expected here (and indeed the great earthquake of 1872 was dominantly strike-slip), or (2) only the larger earthquakes produce significant components of normal faulting, so that the relatively moderate strike-slip earthquakes we are now experiencing provide no information at all about the major earthquake to come in this region.

Work by Vetter (1986) has made a contribution toward unravelling this major seismotectonic problem. In **Figure 3** are presented rose diagrams for the frequency of occurrence of P- and T-axes in earthquakes occurring between September 1984 and December 1985 *west* and *east* of the Round Valley fault, which are compared with the 1986 earthquakes still further east. The T-axes are the ones trending generally EW in Figure 3. Note that the dominant trend of the T-axes is rotated ever more clockwise as we move from west to east: the earthquakes characteristic of the mountain block south of Long Valley caldera show the characteristic "Mammoth" ENE direction of extension; the July 1986 events show T-axes clustering around EW; the earthquakes between these two groups show an intermediate trend of T-axes. Furthermore, note that just about all of the earthquakes considered here are strike-slip mechanisms, with the normal-faulting events fewer in number and all of relatively small magnitude. These observations led Vetter (1986) to suggest that the Round Valley fault marks the boundary of a transitional tectonic region, extending eastward to perhaps the NW-trending Tertiary strike-slip zone known as the Walker Lane. If this is correct, then we expect EW, i.e., San Andreas style horizontal tectonics, to be important, perhaps dominant, in the region between Round Valley and the Walker Lane (which, as mentioned above, is surprising because of the presence of recent, spectacular normal fault scarps in this region). This concept more or less fits the pattern of 1986 seismicity and the sense of motion along the Owens Valley fault in 1872 (whose northward extension trends into the 1986 aftershock zone). The implication is that, should a major earthquake occur in the White Mountains gap, we would expect it to have strike slip motion as its major component. Furthermore, analysis of the 1986 seismicity would appear of critical importance to assessing the nature and timing of future major seismicity extending northward into the White Mountains seismic gap.

Seismic Travel Times Across the Caldera

In our previous semi-annual report, we described observations of a pre-S phase seen at a single station SLK, northwest of Long Valley caldera, caused by earthquakes southeast of the caldera. The number of these observations has grown to 200, and is described more fully by Peppin and Delaplain (1986). These observations produce a single-station, multi-event travel-time curve which is unusual in that the "apparent velocity" is the same as S but the time intercept is *negative* (Peppin, 1986.)

At present we have found two models which more or less fit the travel times of these pre-S phases (RMS residual 0.1 to 0.2 second for all the observations).

References:

Crittenden, M. D., 1951, Geology of the San Jose and Mount Hamilton quadrangles California. California Division of Mines and Geology Bulletin 157.

Dibblee, T. W., 1972-1980, Various quadrangle maps and reports: San Jose East quadrangle, 1972a; Milpitas quadrangle, 1972b; Lick Observatory quadrangle, 1972c; Calveras Reservoir quadrangle, 1973a; Gilroy quadrangle, 1973b; Gilroy Hot Springs quadrangle, 1973c; Morgan Hill quadrangle, 1973d; Mount Sizer quadrangle, 1973e; Hollister quadrangle, 1975; Tres Pinos, 1979; niles quadrangle, 1980a; Hayward quadrangle, 1980b; Richmond quadrangle, 1980c; Brones Valley quadrangle, 1980d; Diablo quadrangle, 1980e; Las Trampas Ridge quadrangle, 1980f; Walnut Creek quadrangle, 1980g, and Tassara quadrangle, 1980h; U.S. Geological Survey Open-File Reports and Maps.

Herd, D. G., 1978, Map of Quaternary faulting along the northern Calaveras fault zone: U.S. Geological Survey Open-File Report OFR 78-308.

Herd, D. G., 1982, Map of the principal recently active faults in the southern San Francisco Bay region. California U.S. Geological Survey Miscellaneous Field Studies Map, Scale 1:125,000.

Pavlis, G. L. and N. B. Hokanson (1985). Separated earthquake location, J. Geophys. Res., 91, 6522-6534.

Thurber, C. H. (1983). Earthquake locations and three-dimensional crustal structure in the Coyote Lake area, central California, J. Geophys. Res., 88, 8226-8236.

One consists of an S to P conversion on a plane with a NE strike dipping about 45 ° SE fairly close to SLK (and not associable with the caldera ring fault). The other consists of an S to P to S conversion in an elliptical zone about 10 km across within the caldera, and possibly caused by conversion at the boundary of the magma bodies proposed by Sanders (1984) within the caldera (except that the conversion points must be quite shallow, less than 5 km in depth). While the second model appears more fanciful than the first, it is supported by the pattern of epicenters which produce the phase: an elongated zone whose long axis is aligned with the Sanders magma bodies in the caldera and station SLK (**Figure 4**). A measurement of the apparent velocity of the phase can discriminate between (or eliminate) these models. Zucca and Mills (1986) found a similar-appearing phase for cross-caldera earthquakes recorded in this vicinity and concluded, based on particle motion and apparent velocity, that the phase was a deep P-reflection; however, this model cannot fit the present observations because of the distribution of causative earthquakes with distance (Figure 4).

References Cited

Peppin, W.A., 1986. Exotic seismic phases recorded near Mammoth Lakes and their use in the delineation of shallow-crustal (magma?) anomalies, *Pure and App. Geophys.*, submitted.

Peppin, W.A. and Delaplain, T.W., 1986. A new constraint on lateral variations of crustal structure at Mammoth Lakes, California, abstract submitted for December meeting of the American Geophysical Union.

Ryall, A.S. and Ryall, F.D., 1983. Increased potential for a major earthquake in the White Mountains seismic gap, *Univ. Nevada Rpt., 23 p.*

Sanders, C.O., 1984. Location and configuration of magma bodies beneath Long Valley, California, determined from anomalous earthquake signals, *Jour. Geophys. Res.*, **89**, 8287-8302.

Strand, R.G., 1967. Geologic Map of California, Mariposa Sheet, *Calif. Div. Mines and Geology*, scale 1:250,000.

Vetter, U.R., 1986. Focal mechanisms and the boundary of the Great Basin tectonic province, *Earthquake Notes*, **57**, 21.

Wallace, R.E., 1978. Patterns of faulting and seismic gaps in the Basin province, *U.S.G.S. Geol. Survey Open-File Report 78-943*, 857-868.

Zucca, J.J. and Mills, J.M., 1986. Observation of a reflection from the base of a magma chamber in Long Valley caldera, California, *Bull. Seism. Soc. Am.*, accepted.

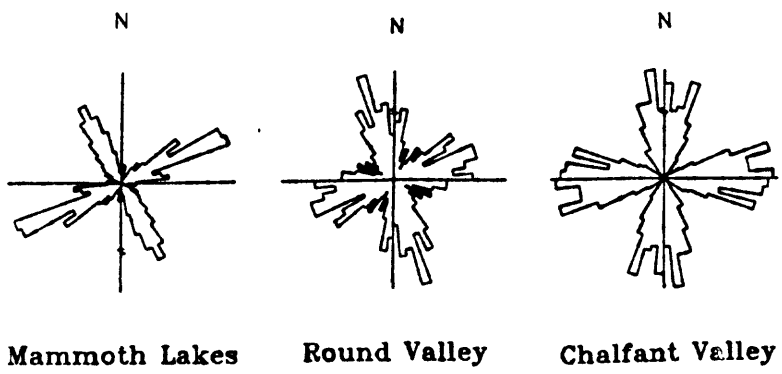

Figure 3. Rose diagrams showing P and T axes for earthquakes in the mountain block south of Long Valley caldera ("Mammoth Lakes"), for the Round Valley earthquake of 1954 and its aftershocks ("Round Valley") and for the 1986 Chalfant Valley sequence ("Chalfant Valley"). The T axes trend EW and the P axes trend NS. Notice the clockwise rotation from left to right, corresponding to a trend from west to east.

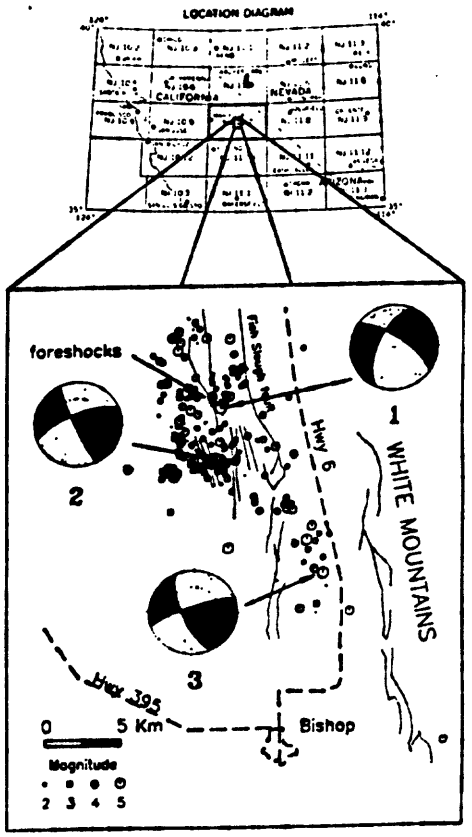

Figure 1. Epicenter Map of all earthquakes greater than magnitude 2, July 20-21, plus all all earthquakes greater than magnitude 4, July 22-31, 1986. Foreshocks are indicated by triangles. Light lines are Quaternary faults from Strand (1967). Shown are equal-area, lower-hemisphere projections of the earthquakes of 20 July 1986 at 1429 (M = 5.6), 21 July at 1442 (M = 6.2), and 21 July at 2207 (M = 5.6), labelled "1", "2", and "3", respectively.

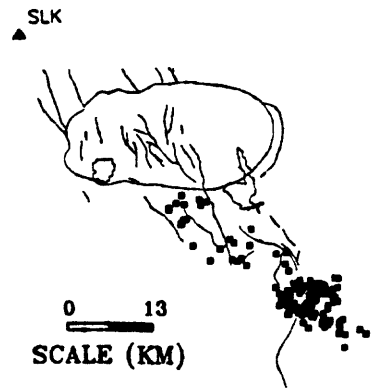

Figure 4. Map view showing the location of station SLK and the 166 epicenters producing a "better" pre-S observation at that station. The UNR catalog contains many earthquakes outside the NW trend of epicenters which do *not* show the pre-S phase at SLK.

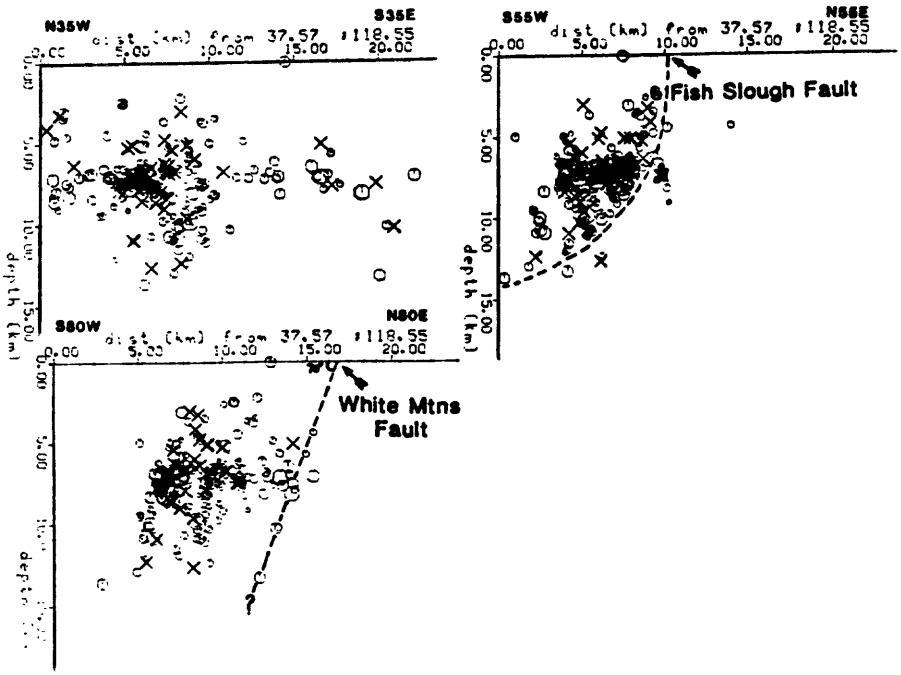

Figure 2. Vertical cross-sections through the hypocenters. The upper ones are parallel and transverse to the preferred focal plane for the mainshock. The lower left section is transverse to the front of the White Mountains.

Basement Tectonic Framework Studies
Southern Sierra Nevada, California

9910- 01291

Donald C. Ross
Branch of Engineering Seismology and Geology
345 Middlefield Road, MS 77
Menlo Park, CA 94025
(415) 323-8111, ext. 2341

Investigations

1. Compilation of photolineaments from aerial photographs of the southern Sierra Navada.

2. Revision, following technical review, of report on metamorphic framework rocks of the southern Sierra Nevada.

3. Compilation of a reconnaissance geologic map of the basement rocks of the southern Sierra Nevada.

Results

1. Photolineaments that are well-defined on aerial photographs of the southern Sierra Nevada are generally anomalously straight stream traces controlled by joints in the granitic basement rocks. This becomes more obvious in the higher elevations where exposure is much better. There families of northwest to northeastern joints (or microfaults) are developed.

2. Prominent photolineaments are well-developed in the Kern Plateau area of Tulare County north and east of Big Meadow. This area has also been the site of recent (1983 to 1984) seismicity. The location of individual seismic events indicates a north-trending zone and focal mechanism of these events indicate northwest to northeast striking, steeply dipping planes (Jones and Dollar, 1986). No throughgoing fault has yet been mapped in this area, but the coincidence of northwest to northeast-trending lineaments may identify microfaults such as Lockwood and Moore (1979) have described that may record the traces of surface movement related to these recent seismic events.

3. Some 90 map units (mostly granitic) have now been identified in the southern Sierra Nevada ranging from felsic plugs no more than a square kilometer in outcrop area to large plutons of several hundred square kilometers in extent. By far the greater number of the plutonic unit are Creteceous, but significant bodies of Jurassic and Triassic age are found along the east side of the Sierra Nevada between lat. 35°30' and 36°00 north. Most of the metamorphic framework rocks are Mesozoic (probably Triassic and Jurassic) but some on the east side of the Sierra Nevada may be Paleozoic.

Salton Trough Tectonics and Quaternary Faulting

9910-01292

Robert V. Sharp
Branch of Engineering Seismology and Geology
U.S. Geological Survey
345 Middlefield Road, MS 977
Menlo Park, CA 94025
415-323-8111, ext. 2596

Investigations

1. Cone penetrometer, augering, and trenching investiagtion of pre-1940 displacement on the Imperial fault at the International Boundary with Mexico.

2. Continuing search for northwest-trending strands of the San Jacinto fault zone in the northwestern Imperial Valley region.

3. Field search for surface faulting associated with the M_L 5.9 North Palm Springs earthquake of 8 July 1986.

4. Manuscript preparation of shallow postseismic displacement on the Lost River fault associated with the Borah Peak, Idaho earthquake of 1983.

Results

1. The stratigarphic section accessible by trenching is limited downward by the high water table near the All American Canal. To better define the configuration of a buried erosional irregularity offset by the western break of the fault, an array of cone penetrometer profiles were made on each side of the fault, and calibrated against augering profiles. Two candidate correlations across the fault trace are permitted by the new data: one implies a probable single event comparable in displacement to the 1940 event, about 3-4 meters, and the other implies at least several events whose cumulative offset exceeds 20 meters.

   The age of the earlier event(s) is constrained by a buried erosional surface that is overlain by nearly three meters of strata offset only once - in 1940. New trenches have revealed charcoal-bearing strata close to and both above and below this erosional surface. Accelerometer dating of this new material may change previous estimates of the duration of pre-1940 inactivity on this part of the Imperial fault.

2. Structural mapping in the San Felipe Hills has been extended into areas not previously investigated in detail, but so far only normal faults whose orientations lie in the northeast quadrant have been encountered. Additional thoroughgoing strands of the right-lateral San Jacinto fault zone between the Clark fault an the Coyote Creek have not been identified yet.

3. Surface fractures formed along the trace of the Banning strand of the San Andreas fault near San Gorgonic Pass in association with the 8 July earthquake. The term *fractures* rather than *ruptures* or *surface faulting* is

used to emphasize the incipiency of the right-lateral displacement on the breaks along this fault trace. Ground fractures caused by spreading, lurching, gravitational collapse of unsupported free faces and slopes, and shattering of ridge crests and hill tops during the strong shaking of this event were widespread phenomena near some parts of the Banning fault, as well as near the traces of the Garnet Hill fault in Whitewater Canyon and the Mission Creek strand of the San Andreas in northern Coachella Valley. Fractures considered to be tectonic in origin, however, are spatially associated only with the Banning trace, previously identified geologically and geomorphically in detail by Allen (1957), Proctor (1968), and Clark (1984), and Matti and others (1985).

Fracturing along the Banning fault was incipient, and the component of the right-lateral slip attributed to it was infinitesimal. Barring the complication of distributed slip not expressed as fractures in the poorly consolidated alluvial materials cut by the fault, tectonic displacement for this event was near the limit of resolution for non-geodetic field methods for determining tectonic offset. A single man-made feature, a curb at the edge of State Highway 62, gave some clue to the absence of significant right-lateral offset on the fault as well as the probable absence of distributed slip. However, definitive data on the role of distributed movement may depend on remeasurement of an alinement array monitored by Caltech at Devers Hill near the east end of the trace fracturing.

4. In progress.

Reports

Sharp, Robert V., Rymer, M.J., and Morton, D.M., 1986, Trace-fractures on the Banning fault associated with the 1986 North Palm Springs earthquake: *Bulletin of the Seismological Society of America*, in press.

Sharp, Robert V., 1986, Trace-fractures on the Banning fault, in Report on the North Palm Springs, California, earthquake - July 8, 1986 [abs.]: *EERI Newsletter*, Vol. 20, no. 9, p. 2.

Rymer, M.J., Sharp, R.V., and Morton, D.M., 1986, Surface fractures on the Banning fault associated with the North Palm Springs, California, earthquake of 8 July 1986 [abs.]: *Transactions American Geophysical Union*, in press.

Detailed Geologic Studies, Central San Andreas Fault Zone

9910-01294

John D. Sims
Branch of Engineering Seismology and Geology
U.S. Geological Survey
345 Middlefield Road, MS 977
Menlo Park, California 94025
(415) 323-8111, ext. 2252

Investigations

1. Field investigations of late Holocene and historic slip rates on the San Andreas-Paicines-Calaveras fault system in the San Benito County area.

2. Investigation of uncertainties in radiocarbon dates derived from detrital charcoal.

Results

1. An alluvial deposit of the San Benito River at Melendy Ranch, located along the northern creeping segment of the San Andreas fault in central California, records an 800-year-long average rate of slip of 22^{+6}_{-5} mm/yr. This long-term rate of slip is within the 20 to 23 mm/yr range in slip rates that are recorded by geodetic instruments at Melendy Ranch, and it is identical to the rate of slip of 22 mm/yr that is recorded by an offset corral fence, 0.9 km from our study site. The similarity between the long-term and historic rates of slip, suggests that movement along the San Andreas fault at Melendy Ranch has not deviated significantly from 22 mm/yr during the past 800 years. The long-term slip rate of 22 mm/yr for the San Andreas fault at the Melendy Ranch is significantly less than the 34 mm/yr rate found along the San Andreas fault south of the creeping segment, and significantly greater than the 12 mm/yr found along the fault north of the creeping segment. The northwestward decrease in long-term slip rate of about 20 mm/yr along the San Andreas fault is attributed to transfer of slip from the San Andreas fault to the Paicines fault. If about 20 mm/yr slip is found along the Paicines fault, a similar amount may be found across the Hayward and Calaveras faults, because the Paicines fault is the southernmost extension of the Hayward-Calaveras fault system. The 20 mm/yr rate of slip that may be occurring across the Calaveras-Hayward fault system is significantly greater than that suggested by short-term geodetic data. The discrepancy in long- and short-term slip rates along the Hayward and Calaveras faults may reflect undetected strain accumulation along faults in the eastern San Francisco Bay region.

2. The radiocarbon method is one of the most useful dating techniques available for slip-rate studies. The inherent uncertainty in radiocarbon dating, as in any other dating method, must be incorporated into slip-rate calculations for a reliable rate to result. Four sources of uncertainty must be accounted for in slip-rate age determination that are based on

radiocarbon dates, which result from: (1) the analytical assay of the radiocarbon sample (analytical undertainty), (2) calibration of the conventional radiocarbon age (calibration uncertainty), (3) relating the radiocarbon age to the age of the strata from which the dated sample was recovered (depositional uncertainty), and (4) relating the age of the strata to the age of the displaced feature (relational uncertainty).

Each of the four sources has the potential to introduce large amounts of uncertainty to the age determination. Analytical uncertainty ranges from a few decades to a few millenia and is dependent upon the calculated age of the sample, the nature and quantity of the sample, and the analytical method used. Analytical error typically is on the order of ±100 years for late Holocene ages, and it increases with sample age until the limit of the dating method is reached at 40-70 ka. Analytical uncertainty is most critical for radiocarbon ages younger than about 1000 yr B.P., because the assay error is large relative to the age. Calibration uncertainty results from conversion, or the lack of conversion, of a radiocarbon age to a calendric age, which is necessary to account for the variance between the radiocarbon time scale and the calendric time scale. Calibration data sets are available for radiocarbon ages younger than about 8000 yr B.P., and most calibrated ages contain little uncertainty. However, calibrated ages younger than about 1000 yr B.P. have a large relative uncertainty because the analytical uncertainty inherent in the conventional radiocarbon age is transferred to the calibrated age and often the calibration is inexact. Radiocarbon ages older than about 8000 yr B.P. cannot be calibrated, and they should be assigned estimated uncertainty as large as several thousand years. Depositional uncertainty reflects the uncertainty in the assumption that the dated sample is coeval with the strata from which it was recovered. Syndepositional and postdepositional processes can incorporate carbonaceous material into strata that may have a radiocarbon age much different fromt that of the deposit. In deposits associated with active faulting, it is often difficult to identify allochthonous carbonaceous material, and its effect may go undetected if few dates are available or if no high-quality samples are dated. Relational uncertainty may be large if the age estimation is based on (1) dated strata that predate and postdate the displaced feature whose ages are much different, or (2) the dated strata do not stratigraphically bracket the displaced feature. At present, the only constraint on relational uncertainty is comparison of the reconstructed depositional history of a study site to sedimentologic models of deposition in a similar environment. From such a comparison the time periods of deposition and nondeposition can be estimated, the sum of which places temporal constraints on relating the age of the dated strata to the displaced feature.

Reports

Perkins, J.A., Sims, J.D., and Sturgess, S.S., in press, Late Holocene movement along the San Andreas fault at Melendy Ranch: Implication for the distribution of fault movement in central California: *Journal of Geophysical Research*.

Seismotectonic Framework and Earthquake Source Characterization - Wasatch Front, Utah, and Adjacent Intermountain Seismic Belt

14-08-0001-G1163

R.B. Smith, W. J. Arabasz, and J.C. Pechmann*
Department of Geology and Geophysics
University of Utah
Salt Lake City, Utah 84112
(801) 581-6274

Investigations

1. Focal mechanisms for aftershocks of the 1983 Borah Peak, Idaho earthquake.

2. Contemporary tectonics of the Wasatch front region from earthquake focal mechanisms.

3. Synthetic seismogram modeling of ground motion in two-dimensional inhomogeneous media with application to the Wasatch front.

Results

1. We have completed a systematic study of focal mechanisms for aftershocks of the 1983 M_s 7.3 Borah Peak, Idaho, earthquake that were well recorded by a dense network of portable seismographs operated for 3 weeks following the mainshock. Use of a grid search computer algorithm provided objective nodal plane determinations together with estimates of uncertainty in the slip vectors and compression and tension axes. Mechanisms of 47 aftershocks ($2.3 \leq M_L \leq 5.8$) show predominantly normal faulting with varying amounts of strike-slip motion (Figure 1). Since hypocenters along the central and SE portions of the fault define a SW-dipping zone that appears to outline the main fault break, one might expect the focal mechanisms here to show slip along either the main fault or related antithetic faults. However, there is considerable diversity among the focal mechanisms, and less than half of them are compatible with this simple interpretation. Most of the aftershocks appear instead to represent complex fracturing on subsidiary structures adjacent to the main fault.

Orientations of tension axes are much more consistent from event to event than orientations of compression axes or slip vectors. The tension axes indicate an overall extension direction that is not perpendicular to the main fault but instead trends NNE-SSW, perpendicular to the strike of

*H.M. Benz, I. Bjarnason, and L.L. Leu also contributed significantly to this project during the report period.

the western splay observed in the surface faulting (Figure 1). Attempts to unravel the kinematics of aftershock slip suggest the important influence of (1) the bifurcation of the fault plane at its NW end, (2) possible edge effects of faulting at the SE end where the rupture began, and (3) variability of stress conditions with depth along the main central segment of the fault.

2. We have undertaken a comprehensive study of focal mechanisms of digitally recorded, small earthquakes ($2.5 \leq M_L \leq 4.4$) that occurred in the Wasatch front region in Utah during 1981-86. Single event solutions for 24 events were determined using recently revised crustal models and a computerized grid search technique.

Overall, the mechanisms show predominantly normal faulting on N-S striking nodal planes with moderate dip. Thus, on the average, the mechanisms indicate E-W crustal extension and vertical crustal shortening. T-axis orientations suggest a possible rotation of the extension direction from E-W in the northern part of the study area to ESE-WNW in the southern part. Oblique slip, when observed, is characterized by left-lateral motion on planes striking N to NE or right-lateral motion on planes striking N to NW. Most of the mechanisms with significant amounts of oblique-slip motion occur in the southern part of the study area, where P-axis orientations range from near vertical to near horizontal. Thus, the mechanisms suggest a change in stress regime from north to south along the Wasatch front. Despite geologic evidence for low-angle faults in the study area, shallowly-dipping nodal planes are relatively uncommon.

3. A robust finite element modeling technique is being used to compute synthetic seismograms for realistic, two-dimensional models of large, fault-bounded, alluvial basins such as the Salt Lake and Cache valleys in Utah. The primary goal is to quantify the effects of the valley fill on strong ground motion produced by slip on the normal faults which bound these valleys. Present modeling results show that for surface-breaking, normal-fault earthquakes, a large-amplitude Rayleigh wave is produced within the valley sediments. In addition, the sediment-filled basin causes resonance of large S-wave phases. This contrasts with modeling results for homogeneous velocity structures, which show relatively simple S-wave phases generated by the faulting. Interestingly, dip-slip normal-fault earthquakes that do not break the free surface also produce a large Rayleigh wave. This is a consequence of the sharp velocity boundary between the sedimentary basin and the mountain front, which acts as a significant scatterer of Rayleigh wave energy. This study indicates that valley sediments have a major amplifying effect on ground motion in comparison to uniform velocity models routinely used to investigate strong ground motion.

Reports and Publications

Arabasz, W.J. (1986). Seismotectonics of the Basin and Range–Colorado Plateau transition in Utah, Geol. Soc. Am. Abstracts with Programs, 18, 338.

Benz, H.M., and R.B. Smith (1986). Kinematic modeling of normal faulting earthquakes in heterogeneous media, Terra Cognita, 6, 436.

Benz, H.M., and R.B. Smith (1986). Kinematic modeling of normal faulting earthquakes using the finite element method, submitted to Geophys. J. R. Astron. Soc.

Leu, L.L. (1986). Three-dimensional velocity structure of the 1983 M7.3, Borah Peak, Idaho, earthquake area using tomographic inversion of aftershock travel times, M.S. thesis, University of Utah, Salt Lake City, Utah, 99 pp.

Loeb, D.T. (1986). The P-wave velocity structure of the crust-mantle boundary beneath Utah, M.S. thesis, University of Utah, Salt Lake City, Utah, 126 pp.

Peinado, J.F. (1986). Moment-magnitude relations in the Intermountain seismic belt from regional seismic data: Applications of an indirect network calibration scheme, M.S. thesis, University of Utah, Salt Lake City, Utah, 91 pp.

Richins, W.D., J.C. Pechmann, R.B. Smith, C.J. Langer, S.K. Goter, J.E. Zollweg, and J.J. King (1986). The 1983 Borah Peak, Idaho earthquake and its aftershocks, submitted to Bull. Seism. Soc. Am.

Smith, R.B., W.D. Richins, D.I. Doser, and L.L. Leu (1986). The 1983 Borah Peak, Idaho, earthquake: Regional seismicity, fault kinematics and extensional mechanism, submitted to Bull. Seism. Soc. Am.

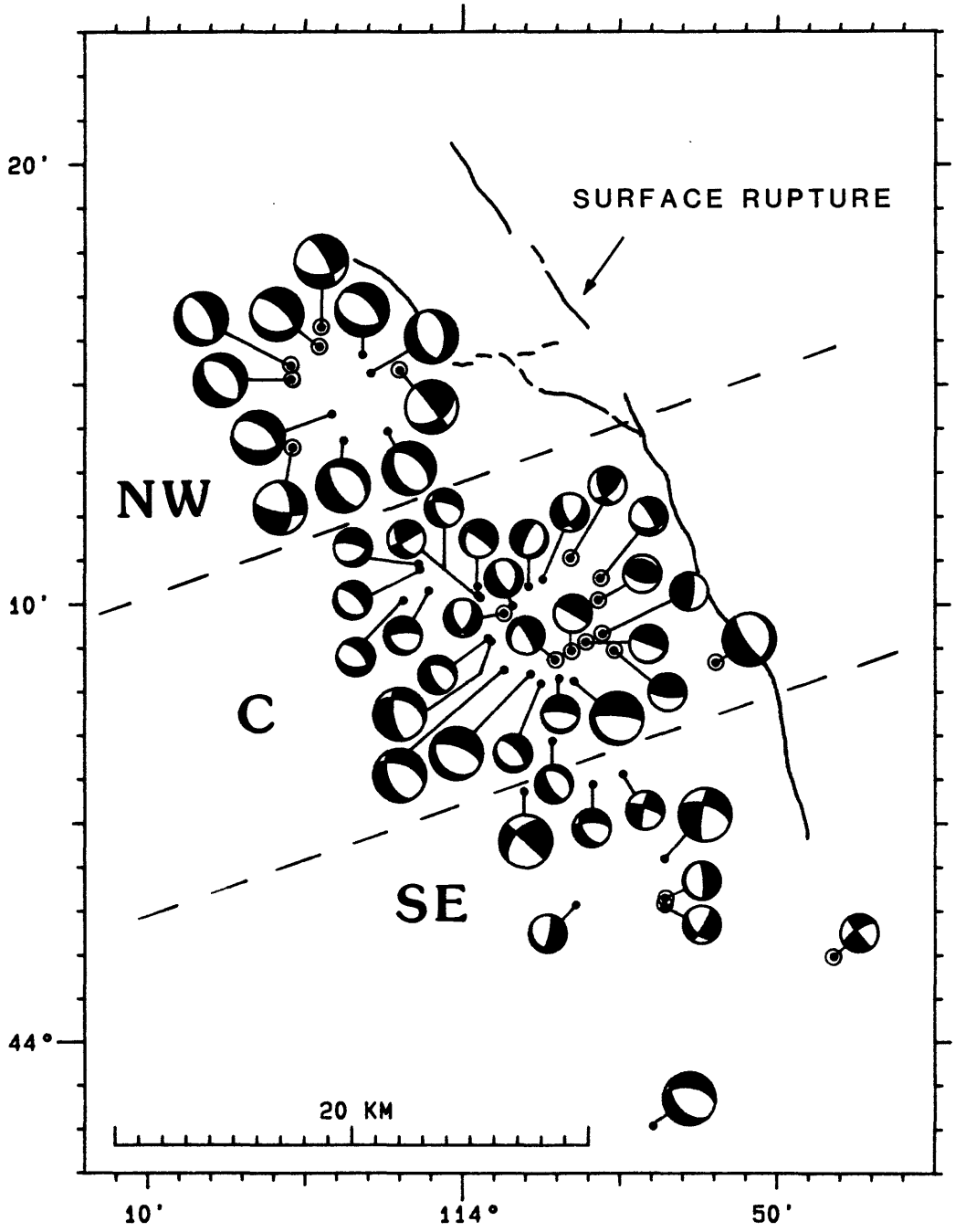

Figure 1. Summary map of focal mechanisms for aftershocks of the 1983 Borah Peak, Idaho, earthquake. These are lower hemisphere projections with compressional quadrants shaded. The larger focal spheres represent events of magnitude 3.5 and greater. Dots mark the epicenters of the earthquakes, and epicenters of events shallower than 9 km are circled. The southernmost mechanism is the short-period focal mechanism of Doser and Smith (1985) for the mainshock. Although most of the focal mechanisms show oblique normal faulting, the faulting during the aftershock sequence appears to be quite complex.

PREDICTION OF GROUND MOTION FROM THE GOODNOW, NEW YORK EARTHQUAKE OF 7 OCTOBER, 1983

Contract No. 14-08-0001-22047

George H. Sutton, Jerry A. Carter, and Noel Barstow
Rondout Associates, Incorporated, P.O. Box 224, Stone Ridge, NY 12484
(914) 687-9150

The purpose of this research is to generate seismograms similar to those of the main Goodnow earthquake using a small aftershock as an empirical Green's function and a realistic velocity structure for extrapolation to different distances and focal depths. Preliminary results from this research were reported in the previous semi-annual summary. The fact that the nearest digital station, RSNY, is near a nodal plane for the main shock and the aftershocks has complicated and reduced the reliability of the results of subsequent research, which will be reported in our final report. The Ardsley, N.Y. earthquake of October 19, 1985, however, is a much better candidate for the contemplated research and results of studies of this earthquake are summarized in this report.

Investigations

1. Deconvolve the Ardsley, N. Y. main shock with its largest aftershock, as recorded at SRNY, $\Delta = 100$ km.

2. Generate full-waveform synthetic seismograms (frequency range 0-5 Hz) for a simple source and compare with the data at station SRNY.

Analyses and Results

The method of using small aftershocks as empirical Green's functions to deconvolve larger events is based on the assumption that the smaller event is a simple source compared to the larger event and that the two events have the same hypocenter and focal mechanism (Mueller, 1985). The closer the small event source function is to an impulse, the closer the event approximates the true Green's function. By assuming that the aftershock is a point source Green's function, the effect of propagation path, recording site response, and instrument response are eliminated as sources of major error. In many ways this approximation is better than can be made with synthetic seismogram Green's functions for which the effects of the propagation path are estimated.

The Ardsley earthquake (M = 4.0) occurred in southern New York state at 40.98 ° N, 73.83 ° W at a depth of 5 km. It was felt in many areas of New York, New Jersey, and Connecticut, as well as Pennsylvania, Massachusetts, and Rhode Island. The largest aftershock (M = 3.0) occurred two days later, also at a depth of 5 km. Both the main shock and the aftershock were recorded by station SRNY, 100 km away at 41.85 ° N, 74.15 ° W. SRNY is a three-component broadband digital station with a sample rate of 60 samples/second.

The uncorrected corner frequencies of the main shock and aftershock are 7 and 12.5 Hz respectively. As the assumption that the aftershock is an impulse is invalid above its' corner frequency, the data were band pass filtered between 0.5 and 12 Hz with a phase-free filter. The horizontal components were then rotated to the theoretical radial and transverse directions for station SRNY before deconvolving (Figure 1).

There are three distinct peaks in the deconvolution result (Figure 2) separated by times of .57 and .15 seconds. The later two spikes of the deconvolution result are larger than the first as might be expected when the data in Figure 1 are examined. The first peak corresponds to the alignment of the first arrivals from both events and the third peak corresponds to the visual alignment of the traces. The second peak cannot be easily seen by aligning the traces visually.

A suite of synthetic seismograms has been generated for the Ardsley event at the distance and azimuth of station SRNY for comparison to the recorded data. Records were synthesized at source depths of 0, 2, 6, 8 and 10 km up to a frequency of 5 Hz (Figure 3). The New England velocity (Taylor et al., 1980) and Q structure (Mitchell, 1981) were used for the computation. Because the main shock appears to be the superposition of three asperity ruptures, separated in time, it is not appropriate to compare the main shock directly to the suite of synthetics which were generated assuming a simple Green's function. We therefore compare the aftershock data to the synthetics. To match the 5 Hz high frequency limit of the synthetics and eliminate microseismic noise, the data were band pass filtered between .5 and 5 Hz prior to the comparison.

The match of the arrival times of the synthetics to the first three arrivals of the data is quite good at a depth of 4.5 km although the relative amplitudes are not well matched. Differences between the true focal mechanism and the one used to compute the synthetics could account for the difference in amplitudes. The excellent quality of the deconvolution is evidence that the main shock asperities and aftershock occurred at nearly the same depth.

As shown above, the additional complexity introduced into the wavetrain by the asperity ruptures makes identification of the depth phases extremely difficult unless the data are deconvolved. In many cases of interest, there will be no aftershock recorded with which the main shock can be deconvolved and the depth phases may easily be misidentified.

The question of resolution is closely tied to the complexity of the event. For any event, if we look at frequencies low enough, the source will appear "point-like" or very simple. Unfortunately, this conflicts directly with the need to use higher frequencies for improved depth resolution.

At this point, we do not know how widespread the problems of source complexity are at low magnitudes or even to what lower magnitude limit the complexities extend. We strongly recommend that, if depth phases are to be used to determine depth, then further research into the complexities of small events should be undertaken.

References

Mitchell, B. J., "Regional variation and frequency dependence on Q_β in the crust of United States," *Bull. Seim. Soc. Am.*, vol. 71 No. 5, pp. 1531-1538, 1981.

Mueller, C. S., "Source pulse enhancement by deconvolution of an empirical Green's function," *Geophys Res. Lett.*, vol. 12, pp. 33-36, 1985.

Taylor, S. R., M. N. Toksoz, and M. P. Chaplin, "Crustal structure of the northeastern United States: contrasts between Grenville and Appalachian provinces," *Science*, vol. 208, pp. 595-597, 1980.

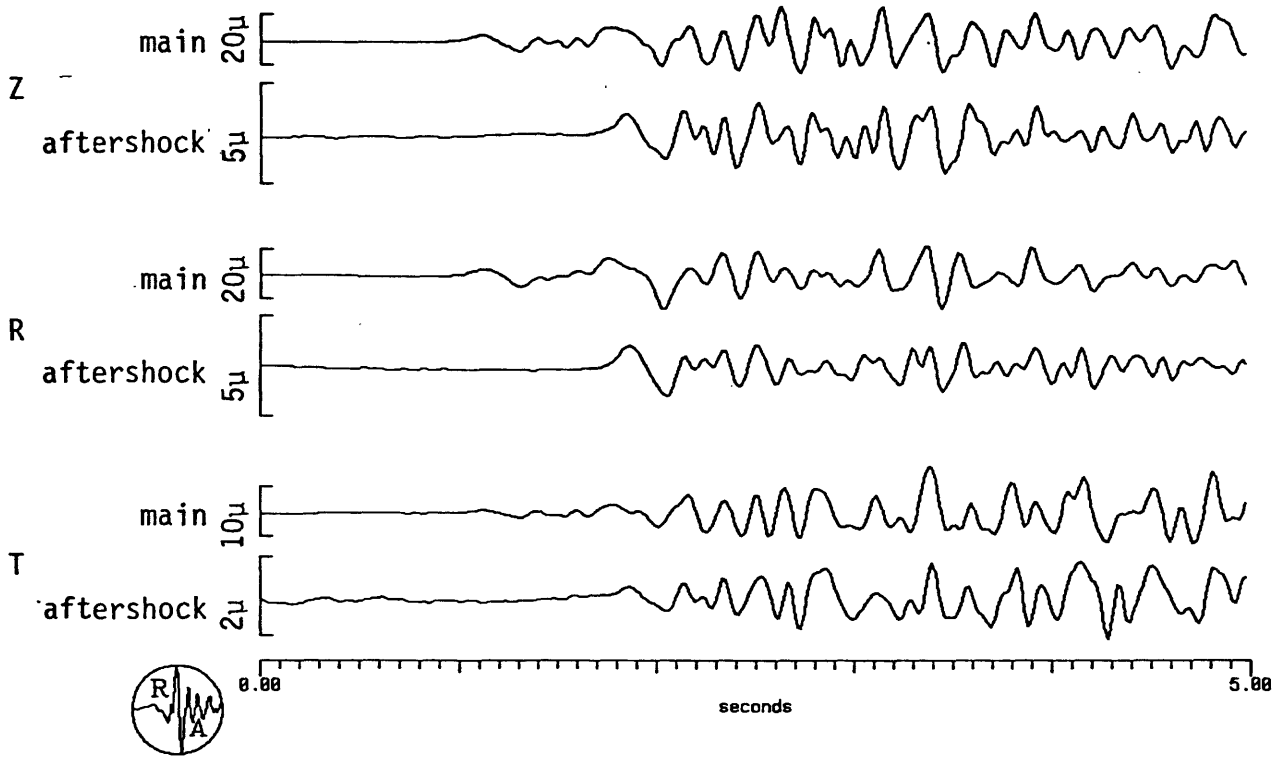

Figure 1. Ardsley, NY main shock and aftershock. Band-pass filtered 0.5 to 12 Hz and rotated to radial (R) and transverse (T) directions relative to station SRNY, $\Delta = 100$ km.

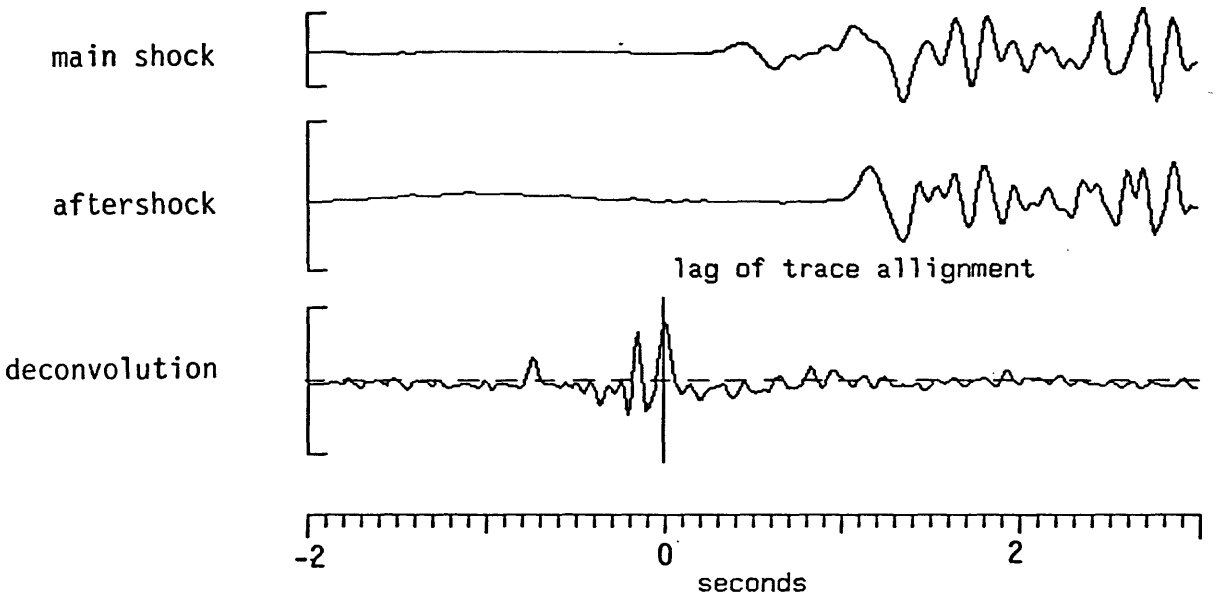

Figure 2. Deconvolution of the Ardsley main shock by its aftershock. SRNY data, $\Delta =$ 100 km.

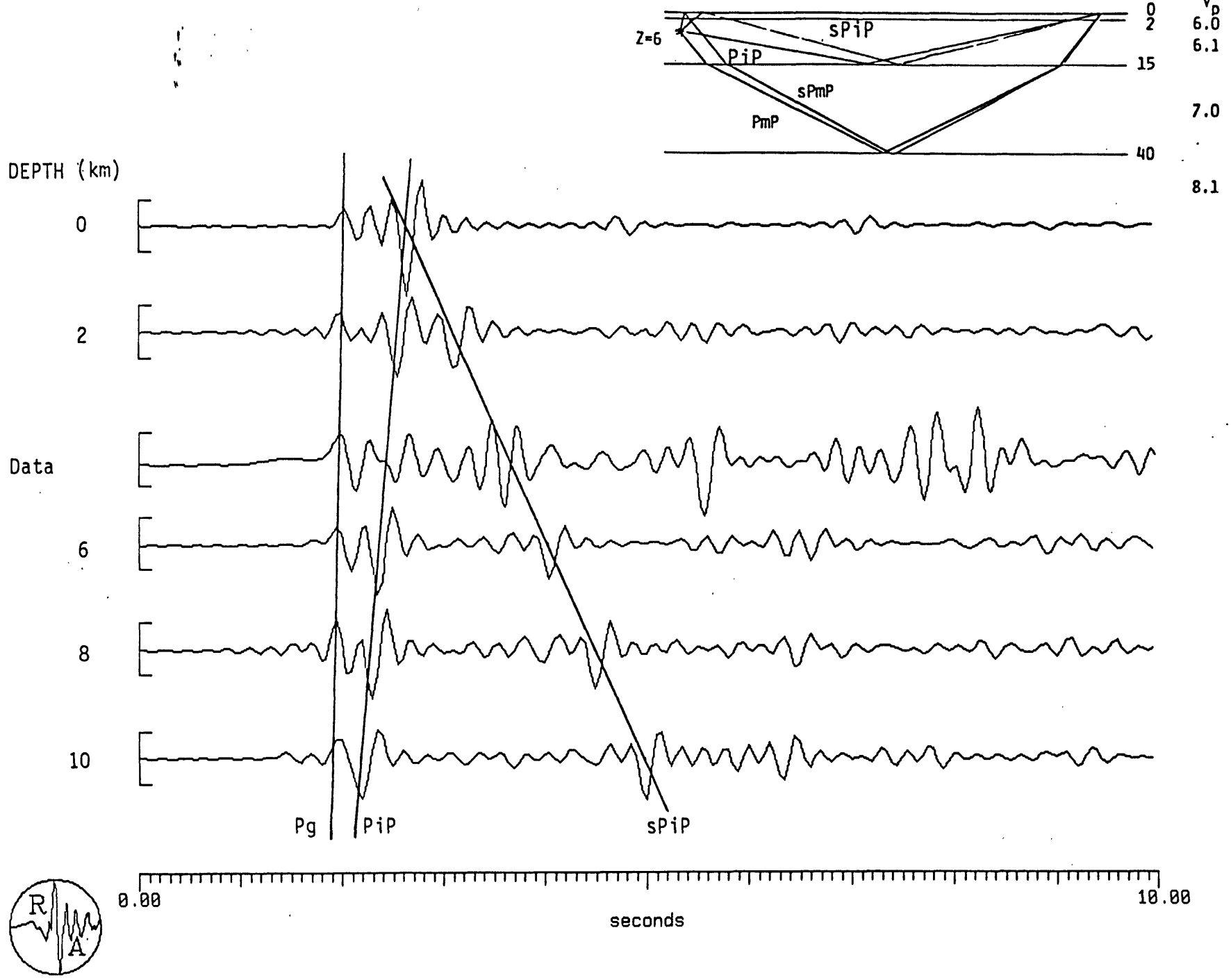

Figure 3. Vertical component synthetic seismograms for the Ardsley, NY aftershock and data at station SRNY, $\Delta = 100$ km.

Great Earthquakes and Great Asperities, Southern California: A Program of Data Anaysis

USGS 14-08-0001-G-1096

Lynn R. Sykes and Leonardo Seeber
Lamont-Doherty Geological Observatory of Columbia University
Palisades, New York 10964
(914-359-2900)

Investigations

During the period of this grant the principal investigators and their colleagues have carried out a number of major studies of earthquakes and tectonics of southern California. This work has resulted in three papers being published, one in press that will soon be published, one in preprint form that is nearly ready for journal submission and the final study "Fault mechanisms associated with the southern San Andreas fault: seismicity of the eastern Transverse Ranges" by Williams, Sykes, Nicholson and Seeber which should be completed by the end of 1986.

Results

The paper "Great earthquakes and great asperities, San Andreas fault, southern California" by Sykes and Seeber was published in *Geology* in December 1985. They find that the big bend region of the southern San Andreas fault consists of two great asperities that rupture infrequently in great earthquakes. The eastern knot near San Gorgonio Pass, which has not ruptured historically in a great event, is the main locus of plate motion, appears to break in great events every few hundred years and is more advanced in the cycle of strain accumulation than the western knot. The large size of these apserities results in the properties of these earthquakes being nearly invariant over many cycles of great shocks. An unusual sequence of moderate-size shocks within the eastern knot from 1940 to 1948 is an example of the type of precursory phenomena that might precede a great earthquake.

The paper "Seismicity and fault kinematics through the eastern Transverse Ranges, California: block rotation, strike-slip faulting and shallow-angle thrusts" by Nicholson, Seeber, Williams and Sykes, was published in the *Journal of Geophysical Research* in April 1986. This paper uses data from the southern California seismic network to study focal mechanisms and detailed distribution of earthquakes in the major tectonic knot in southern California near San Gorgonio Pass. Surprisingly, little seismic activity can be directly associated with major throughgoing faults. Seismicity is generally absent in the upper 5 km. This pattern of behavior appears to be typical of the inter-seismic period between great earthquakes. Great earthquakes in this area, which appear to have a repeat time of 300 to 500 years, are thought to mainly rupture the throughgoing faults. The predominant style of faulting above 10 to 12 km is oblique slip with a large reverse (thrust) component. The spatial distribution of relocated hypocenters and first-motion data suggest the presence of left-slip faults striking northeast. The pattern of faults in conjunction with an unusual set of normal and reverse focal mechanisms is interpreted as the clockwise rotation of the small set of crustal blocks subjected to regional right-lateral shear. At depths of greater than about 10 km seismicity defines a wedge-shaped volume undergoing pervasive internal deformation and a combination of

strike-slip and low-angle thrust faults. A low-velocity seismic zone beneath the San Bernadino Mountains and the transition between block rotation and the deeper style of deformation may correspond to a major detachment under much of the region and would imply that the overthrust San Bernadino Mountains are allochthonous. The present pattern of seismic deformation may change systematically as a region prepares to accommodate large right-lateral displacements in an eventual future great earthquake.

The paper "Seismic evidence for conjugate slip and block rotation within the San Andreas fault system, southern California" by Nicholson, Seeber, Williams and Sykes was published in *Tectonics* in August 1986. This paper expands a number of the ideas developed in the previous paper for the region near San Gorgonio Pass to other areas of southern California. Again, the pattern of seismicity for small to moderate size earthquakes of the past ten years indicates that much of that activity is presently occurring on secondary structures, several of which are oriented nearly orthogonal to the strikes of major throughgoing faults. Slip along these secondary transverse features is predominantly left-lateral and is consistent with the reactivation of conjugate faults by the current regional stress field. A number of small to moderate size crustal blocks are defined which are undergoing contemporary rotation in response to the regional stress field. A rotational block model accounts for a number of structural styles characteristic of strike-slip deformation in California including; variable slip rates and alternating transtensional and transpressional features observed along strike of major wrench faults; domains of evenly-spaced anthithetic faults that terminate against major fault boundaries; continued development of bends and faults with large lateral displacements; anomalous focal mechanisms; and differential uplift in areas otherwise expected to experience extension and subsidence. Low-angle structures like detachments may be involved in the contemporary tectonics of southern California. Changes in the translation of small crustal blocks and their relative rotation rates could represent important premonitory changes prior to large to great earthquakes along major throughgoing faults.

The paper "Block rotation along the San Andreas fault system in California: long-term structural signature and short-term effects in the earthquake cycle" by Seeber and Nicholson, which is in preprint form, describes the rotation of small crustal blocks located between closely spaced subparallel strike-slip faults. Block rotation can allow one of these strands to grow at the expense of the other. Not only structural and paleomagnetic data, but also recent small earthquakes provide evidence for block rotation of this type. Associated seismicity often occurs on left-lateral secondary faults that strike northeast and are symptomatic of block rotation. Examples of this phenomena are illustrated for Coyote ridge, which is located between branches of the San Jacinto fault zone of southern California and the complex rupture involved in the Coyote Lake earthquake of 1979 along the Calaveras fault of northern California.

Bogen and Seeber (preprint) in their paper "Late Quaternary block rotation within the San Jacinto fault zone, southern California" report abundant structural and seismological evidence for block rotation during the past 0.94 million years or less in the region between two major branches of the San Jacinto fault zone between Anza and Borrego in southern California.

Williams, Sykes, Nicholson and Seeber (in preparation) examined fault mechanisms and seismicity in the vicinity of the southernmost San Andreas fault and the eastern Transverse Ranges of southern California. Data from the southern California seismic network for the period 1977 to 1985 were used to study precise locations of small earthquakes, focal mechanisms and the state of stress. The southernmost San Andreas fault in the Coachella Valley is essentially quiescent at the microearthquake level. Relocation of earthquakes using only stations northeast of the San Andreas fault, proximal to the activity but outside the Salton trough does not seriously effect epicentral locations, suggesting the observed offset of epicenters from the San Andreas fault is not an artifact of the velocity models used. Many of

the earthquakes in the broad region to the northeast of the San Andreas fault occur along steeply dipping, left-lateral faults striking northeasterly. Focal mechanisms involve strike-slip, normal fault or a combination of the two mechanisms. In contrast, reverse and strike-slip faulting characterize San Gorgonio Pass and the region to the west within the big bend region of southern California. These observations imply that relatively high normal stresses of tectonic origin are present across the San Andreas fault in San Gorgonio Pass, while lower normal stresses are found across the southernmost San Andreas fault from Palm Springs to the Salton Sea. One stress regime appears to be associated with long repeat times for great earthquakes within the two major tectonic knots in southern California whereas shorter repeat times are indicated for the other stress regimes near the southernmost San Andreas fault.

Continuing Studies

Continuing work on earthquakes and tectonics of southern California includes the following studies: examination of regional time-space patterns of seismicity for the period 1932 to 1986 (Seeber, Armbruster, Williams and Sykes); analysis of teleseismic source mechanisms of July 1986 earthquakes (M_L>5) (Pacheco and Nabelek); documentation of triggered slip on the southern San Andreas after the July 8, 1986 North Palm Springs earthquake (Williams, Fagerson and Sieh).

Publications

Bogen, N. and L. Seeber, Late Quaternary block rotation within the San Jacinto fault zone, southern California, submitted for publication, 1986.

Nicholson, C., L. Seeber, P. Williams, and L. R. Sykes, Seismicity and fault kinematics through the eastern Transverse Ranges, California: Block rotation, strike-slip faulting and shallow-angle thrusts, *J. Geophys. Res., 91*, 4891-4908, 1986.

Nicholson, C., L. Seeber, P. L. Williams, and L. R. Sykes, Seismic deformation along the southern San Andreas fault, California: Implications for conjugate slip and rotational block tectonics, *Tectonics, 5*, 629-649.

Pacheco, J., and J. Nabelek, Source mechanisms of three moderate southern California earthquakes of July 1986, (abstract), *EOS, Trans. AGU,* in press, 1986.

Seeber, L., and C. Nicholson, Block rotation along the San Andreas fault system in California: Long term structural signature and short term effects in the earthquake cycle, preprint, 1986.

Seeber, L., J. G. Armbruster, P. Williams, and L. R. Sykes, Faults antithetic to the San Andreas delinated by seismicity in the San Gorgonio Pass of southern California (abstract), *EOS, Trans. AGU*, in press, 1986.

Sykes, L. R., and L. Seeber, Great earthquakes and great asperities, San Andreas fault, southern Caifornia, *Geology, 113,* 835-838, 1985.

Williams, P., S. Fagerson, and K. Sieh, Triggered slip of the San Andreas fault after the July 8, 1986 North Palm Springs earthquake (abstract), *EOS, Trans. AGU,* in press, 1986.

Williams, P. L., L. R. Sykes, C. Nicholson, and L. Seeber, Seismicity and state of stress in the eastern Transverse Ranges: Implications for seismic potential of the southern San Andreas fault, California, in preparation.

Tectonic Analysis of Active Faults

9900-01270

Robert E. Wallace

Office of Earthquakes, Volcanoes, and Engineering
345 Middlefield Road, MS 977
Menlo Park, California 94025
(415) 323-811, ext. 2751

Investigations

1. Tectonics of the central Nevada and eastern California seismic belts.

2. Tectonics of the San Andreas fault system.

3. International Geological Correlation Program (IGCP)--Project 206--Active Faults of the World.

Results

1. Organized a group of authors to prepare a professional paper on the San Andreas fault. Chapters are being written; some first drafts are completed.

2. As member of panel on Seismic Hazard Assessment for NRC/NAS, participated in several writing sessions and have in progress a chapter on "how probabilistic seismic hazard assessment techniques capture earth-science information."

3. Have in progress a joint paper comparing the San Andreas, Tan Lu, Alpine, and North Anatolia faults and the Median Tectonic Line under IGCP project 206.

Reports

1. Zhang, Buchun, Liao, Yuhua, Guo, Shunmin, Wallace, Robert E., Bucknam, Robert C., and Hanks, Thomas C., 1986, Fault Scarps related to the 1739 earthquake, and seismicity of the Yinchuan Graben, Ningxia, Huizu Zizhiqu, China: Seismological Society of America Bulletin, v. 76, no. 5, p. 1253-1287.

2. Wallace, Robert E., 1986, Geologists and Ideas: A History of North American Geology, Centennial Special Volume 1, a review: Science, v. 232, no. 4755, p. 1278-1279.

3. Wallace, Robert E., and Morris, Hal T., 1986, Characteristics of Faults and Shear Zones in Deep Mines: PAGEOPH, v. 124, no. ___, p. ____.

Geothermal Seismotectonic Studies

9930-02097

Craig S. Weaver
Branch of Seismology
U. S. Geological Survey
at Geophysics Program AK-50
University of Washington
Seattle, Washington 98195
(206) 442-0627

Investigations

1. Continued analysis of the seismicity and volcanism patterns of the Pacific Northwest in an effort to develop an improved tectonic model that will be useful in updating earthquake hazards in the region. (Weaver, Baker, Yelin,)

2. Continued acquisition of seismicity data along the Washington coast, directly above the interface between the North American plate and the subducting Juan de Fuca plate. (Weaver, UW contract)

3. Continued seismic monitoring of the Mount St. Helens area, including Spirit Lake (where the stability of the debris dam formed on May 18, 1980 is an issue) and Elk Lake, and the southern Washington-northern Oregon Cascade Range. The data from this monitoring is being used in the development of seismotectonic models for southwestern Washington. (Weaver, Grant, Shemeta, UW contract)

4. Study of Washington seismicity, 1960-1969. Efforts are underway to determine magnitudes based on a revised, empirical Wood-Anderson-coda duration relation. Earthquakes with magnitudes greater than 4.5 are being re-read from original records and will be re-located using master event techniques. Focal mechanism studies are being attempted for all events above magnitude 5.0. (Yelin, Weaver)

5. Detailed analysis of the seismicity sequence accompanying the May 18, 1980 eruption of Mount St. Helens. Earthquakes are being located in the ten hours immediately following the onset of the eruption, and the seismic sequence is being compared with the detailed geologic observations made on May 18. (Weaver, Shemeta, UW contract)

6. Review of crust and upper mantle structure of California, Oregon, and Washington for a chapter in a the GSA Memoir "Geophysical Framework of the Continental United States". (w/Walter Mooney, Weaver)

7. Analysis of a swarm of over 500 sub-edificial (depths 3 - 14 km) earthquakes that occurred at Mt. St. Helens prior to the 1980 eruption. The better-located events in this sequence define a structure presently interpreted as a zone of failure around a feeder conduit. Studies are aimed at better resolution of the structure and understanding of the process of earthquake generation around it in terms of temporal variations in the radial pressure field. (Zollweg, UW contract)

8. Analysis of the sequence of high frequency earthquakes that followed the eruption of Nevado del Ruiz in Colombia, South America. (Zollweg, with D. Harlow and Colombian and Costa Rican investigators)

9. Detailed study of a swarm of tectonic earthquakes near Darrington in the Washington North Cascades. Cross-correlation and cross-spectrum techniques are being used to resolve the spatial relationships of the swarm events. (Zollweg, UW contract)

10. Comparison of spatial features of aftershock seismic moment release with surface faulting for the 1983 Borah Peak, Idaho earthquake. (Zollweg)

Results

1. A catalog of earthquakes in Washington and northern Oregon, spanning the decade 1960-1969, has been compiled. It is based upon earthquakes recorded by the seismograph station at Longmire, Washington (LON, on the south flank of Mount Rainier). The catalog is complete to duration magnitude (M(D)) 3.9, with the magnitude based on signal duration at LON. Based on the number of events with M(D) $>$ 5, the early 1960's are of particular interest in the recent history of seismicity in the region. The numbers of earthquakes with M(D) $>$ 5.0, M(D) $>$ 4.5, and M(D) $>$ 3.9 are, respectively: 9, 12, 37 (1960-1964); 2, 7, 21 (1965-1969); 0, 1, 10 (1970-1974); 0, 3, 11 (1975-1979); 2, 4, 14 (1980-1984), and after 1 3/4 years 0, 0, 2 (1985-September 30, 1986).

2. The Spirit Lake area is situated near the center of the St. Helens seismic zone, and nearly all earthquakes in the area occur on this zone. Based on the distribution of earthquakes on the St. Helens zone, four likely fault lengths (5, 12, 19, and 30 km) and two fault widths (ie., the depth of the fault plane) of 7 and 12 km were chosen for a regression analysis of fault length against expected magnitude and fault area against expected magnitude. The result of this analysis indicates that the area could be subject to earthquakes from magnitude 5.5 to about 7.0. The Spirit Lake area is the first in Washington to have an estimate of an expected earthquake that has been derived for a given structure; elsewhere in the state design earthquakes are based on the historical record and such events are allowed to "float" throughout an area of study.

3. An interagency agreement has been signed and implemented between the U.S. Geological Survey and the Bonneville Power Administration to allow the transmission of seismic data over existing BPA microwave facilities. Six commercial phone lines were replaced by BPA microwave links during the last six months of FY86.

4. A small-diameter ($\sim$ 1 km), near-vertical seismogenic region beneath Mt. St. Helens was defined by sub-edificial earthquakes occurring before the 1980 eruption. The structure as presently known extends from 4 to 13 km in depth. It is interpreted as a zone of brittle failure which occurred in response to magmatic pressure variations in a narrow feeder conduit. Resolution of this structure is the first indication that has been found in the seismographic data that deep magma transport at Mt. St. Helens may be confined to small, well-defined structures.

5. High frequency earthquakes at Nevado del Ruiz, Colombia, were about as frequent as low-frequency earthquakes in the first six months following the catastrophic plinian eruption of 13 November, 1985. While eruptive activity was minimal during this time period, high frequency earthquakes did not show any clear relationship to surface activity. Instead, they have been interpreted as being in part due to intrusion of magma in dike-like sheets along faults. The spatial extent of the high frequency earthquakes implies that a significant volume of new magma may have intruded the volcanic edifice following the 13 November 1985 eruption.

6. A swarm of earthquakes having magnitudes as high as 3.6 occurred near Darrington in the Washington North Cascades in early 1986. This was the second-most intense

swarm to occur in northwest Washington since 1970. Cross-correlation and cross-spectral analysis of digital data from the UW net indicates that the source region was a 400 by 700 meter area at a depth of about 9 km. The earthquakes tended to occur in tight clusters within this area, probably at asperities along a fault. Reanalysis of regional seismicity with station corrections developed in the investigation of this sequence shows evidence for an east-west striking fault structure dipping to the south. The Darrington sequence would fall on this structure and the computed focal mechanisms agree well in both strike and dip.

7. Aftershock seismic moment release concentrations seem to correlate spatially with minima in the surface faulting throws for the Borah Peak, Idaho earthquake of 1983. This suggests that barriers extending down-dip along the fault plane were important features of the rupture process.

Reports

Shemeta, J. E. and Weaver, C.S., 1986, Seismicity accompanying the May 18, 1980 eruption of Mount St. Helens, Washington, *in, Proceedings, Mount St. Helens Five Years Later,* Eastern Washington University Press, Cheney, WA., (in press).

Grant, W. C. and Weaver, C. S., The 1958-1962 earthquake sequence near Swift Reservoir, Washington, *Bulletin of the Seismological Society of America,* (in press).

Grant, W. C. and Weaver, C. S., Seismicity of the Spirit Lake area: Estimates of possible earthquake magnitudes for engineering design, in *The formation and significance of major lakes impounded during the 1980 eruption of Mount St. Helens, Washington, U. S. Geological Survey Professional Paper,* edited by R. L Shuster and W. Meyer, (in press).

Weaver, C. S. and G. E. Baker, Geometry of the Juan de Fuca plate beneath Washington: Evidence from seismicity and the 1949 South Puget Sound earthquake, submitted to *Bulletin of the Seismological Society of America.*

Baker, G. E. and C. A. Langston, Source parameters of the magnitude 7.1, 1949, South Puget Sound, Washington, earthquake determined from long-period body waves, submitted to *Bulletin of the Seismolgical Society of America.*

Langston, C. A and G. E. Baker, Source parameter constraints from strong ground motions of the April 13, 1949, Puget Sound earthquake, submitted to *Bulletin of the Seismological Society of America.*

Weaver, C. S. and J. E. Shemeta, Seismicity of the May 18, 1980 eruption of Mount St. Helens, Washington: Reservoir geometry, magma transport, and volcanic earthquakes, submitted to *J. Geophys. Res.*

Weaver, C. S., Shemeta, J. E., and W. C. Grant, Crustal spreading at Mount St. Helens, Washington, submitted to *J. Geophys. Res.*

Zollweg, J. E., D. H. Harlow, R. D. Norris, and F. Guendel, Post-eruption seismicity at Nevado del Ruiz, Columbia: Implications for the reservoir system and continued activity, (abs), *EOS, Trans. Am. Geophys. Union, 67,* 406, 1986.

Guffanti, M. and C. S. Weaver, Distribution of late Cenozoic volcanic vents in the Cascade Range and northwestern Basin and Range province, (abs), *EOS, Trans. Am. Geophys. Union., 67,* (in press).

Ludwin, R. S., L.L. Noson, A. I. Qamar, R. S. Crosson, C. S. Weaver, S. D. Malone, W. C. Grant, and T. S. Yelin, Seismicity in the northwestern U.S., (abs), *EOS, Trans. Am. Geophys. Union., 67,* (in press).

Atwater, B. F. and W. C. Grant, Holocene subduction zone earthquakes in coastal Washington, (abs), *EOS, Trans. Am. Geophys. Union, 67,* (in press).

Browne, P. and J. Zollweg, The 1986 Darrington, Washington Earthquake Swarm: Evidence for Tightly Clustered Asperities?, (abs), *EOS, Trans. Am. Geophys. Union,*

in press.

Jonientz-Trisler, C. and J. Zollweg, Sub-edificial Seismicity at Mt. St. Helens Prior to the 1980 Eruption, (abs), *Proceedings, Hawaii Symposium on How Volcanoes Work,* in press.

Zollweg, J., F. Munoz, H. Meyer, D. Harlow, and F. Guendel, Post-eruptive High Frequency Seismicity at Nevado del Ruiz, Colombia, (abs), *Proceedings, Hawaii Symposium on How Volcanoes Work,* in press.

EVALUATION OF SEISMICITY ALONG THE COAST RANGES-SIERRAN BLOCK BOUNDARY ZONE, CALIFORNIA

U.S.G.S. Contract 14-08-0001-22019

Ivan G. Wong
Woodward-Clyde Consultants
1390 Market Street, Suite 250
San Francisco, California 94102
(415) 553-2000

INVESTIGATIONS

The faults within the boundary zone between the Coast Ranges tectonic province and the Sierran crustal block of California have probably been the source of several earthquakes greater then M_L 6 during historical times. However, this zone has generally not been recognized as a source of significant earthquakes and has received very little scientific attention because of (1) the lower level of seismicity and hence less apparent seismic hazard compared to the adjacent San Andreas fault system, and (2) the lack of association, until recently, with any significant earthquakes. The somewhat surprising occurrence of the damaging 2 May 1983 Coalinga earthquake has now focused greater attention on seismicity along the western margin of the Great Valley and the resulting seismic hazard. In this study, we have analyzed and interpreted all available seismographic data for selected events from 1969 to the present. The objectives were to characterize the contemporary seismicity, both spatially and temporally, and to define the style and orientation of faulting and tectonic stresses along the boundary from the town of Red Bluff southeast to San Luis Dam (Figure 1).

RESULTS

A total of 213 earthquakes in the study area of approximate M_L 1.5 and greater have been relocated using a two-velocity-model approach and station corrections determined from a set of 26 calibration earthquakes (Figure 1). Fault plane solutions for 24 of the largest events have been determined. The results are summarized in Figures 2 through 4. Preliminary observations are:

(1) Some of the seismicity appears to be associated with several known faults within the boundary zone, based upon locations and fault plane solutions. These include the Willows, Vaca, and Tesla-Ortigilita faults and a few unnamed faults.

(2) Reverse faulting on steeply dipping faults and strike-slip faulting on the NNW- to north-trending faults appear to be the dominant modes of seismic deformation along the boundary zone; this style is similar to that observed in the recent seismicity within the boundary zone along the southern Coast Ranges. This activity consisted of the 1975 Cantua Creek (M_L 4.9), 1976 Avenal (M_L 4.7), 1982 New Idria (M_L 5.4), 1983 Coalinga (M_L 6.7) and 1985 North Kettleman Hills (M_L 5.5) earthquakes.

(3) The stress field along the boundary zone appears to be characterized by northeast- to east-trending tectonic compression perpendicular to the boundary, in contrast to the generally north-south oriented compression and east-west extension and shear deformation observed along the San Andreas fault system to the west. The unusually frequent occurrence of reverse faulting and the change in the nature of the tectonic stress field probably reflect the influence of the boundary between the Coast Ranges and Sierran block and the kinematic interaction between the two crustal blocks. The recognition of the Coast Ranges - Sierran block boundary zone as a fundamental tectonic boundary along which seismic deformation can occur (albeit at a much lower level than along the plate boundary to the west) is consistent with the recent observations by Walter Mooney, Carl Wentworth, and others of the USGS, on the differing crustal structure and crustal history of the region.

PUBLICATIONS

Wong, I. G., 1984. "Re-evaluation of the 1892 Winters, California Earthquakes Based Upon a Comparison with the 1983 Coalinga Earthquake," EOS Transactions, American Geophysical Union, Vol. 65, pp. 996-997.

Wong, I. G. and R. W. Ely, 1983. "Historical Seismicity and Tectonics of the Coast Ranges - Sierran Block Boundary: Implications to the 1983 Coalinga, California Earthquakes," The 1983 Coalinga Earthquakes, California Division of Mines and Geology Special Publication 66, pp. 89-104.

Wong, I. G., A. Kollmann, and R. W. Ely, 1986. Contemporary Seismicity Along the Coast Ranges - Sierran Block Boundary Zone, California, Bulletin of the Seismological Society of America (in preparation).

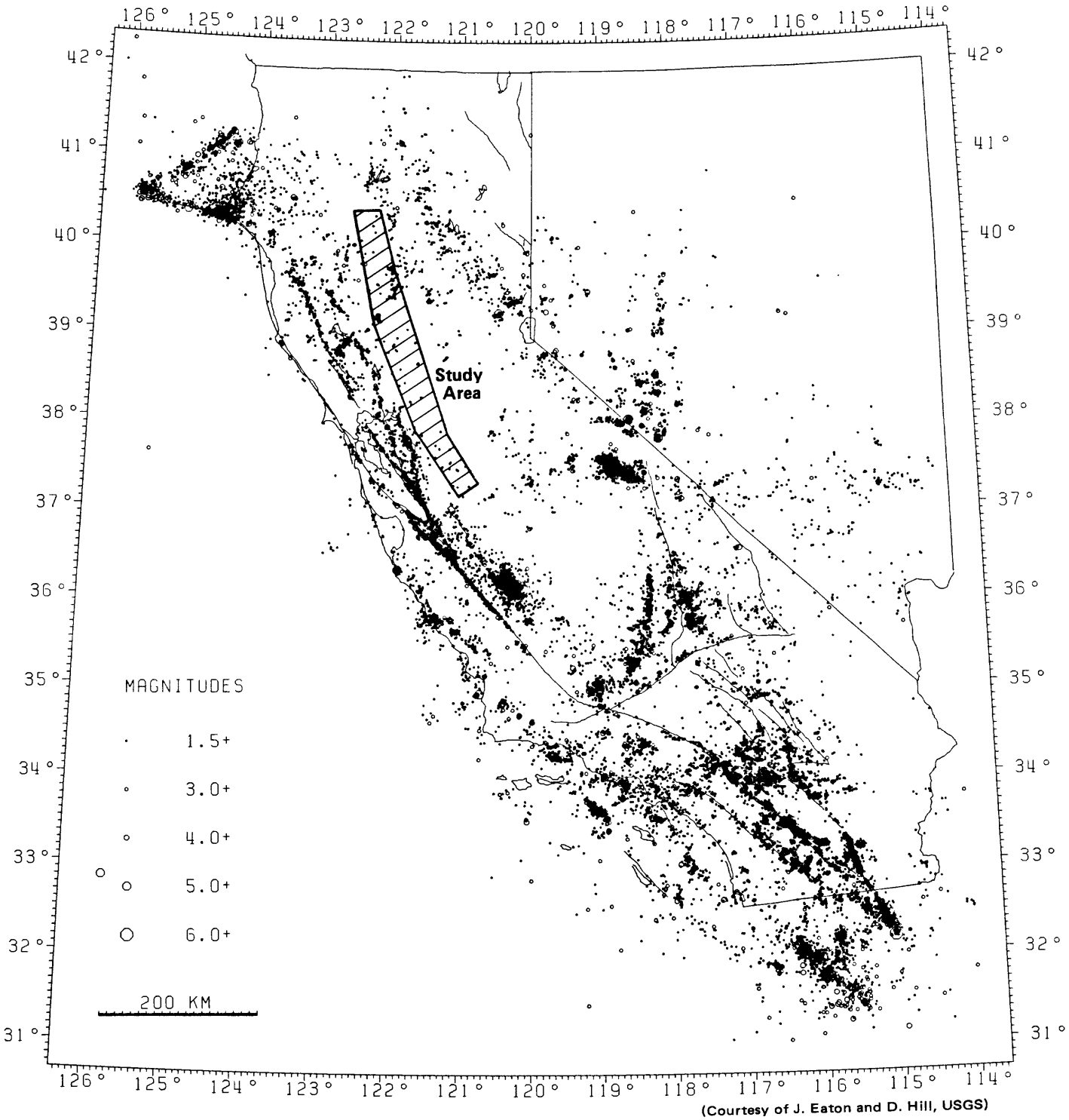
126° 125° 124° 123° 122° 121° 120° 119° 118° 117° 116° 115° 114°
42°
41°
40°
39°
38°
37°
36°
35°
34°
33°
32°
31°
Study Area
MAGNITUDES
1.5+
3.0+
4.0+
5.0+
6.0+
200 KM
(Courtesy of J. Eaton and D. Hill, USGS)

Figure 1

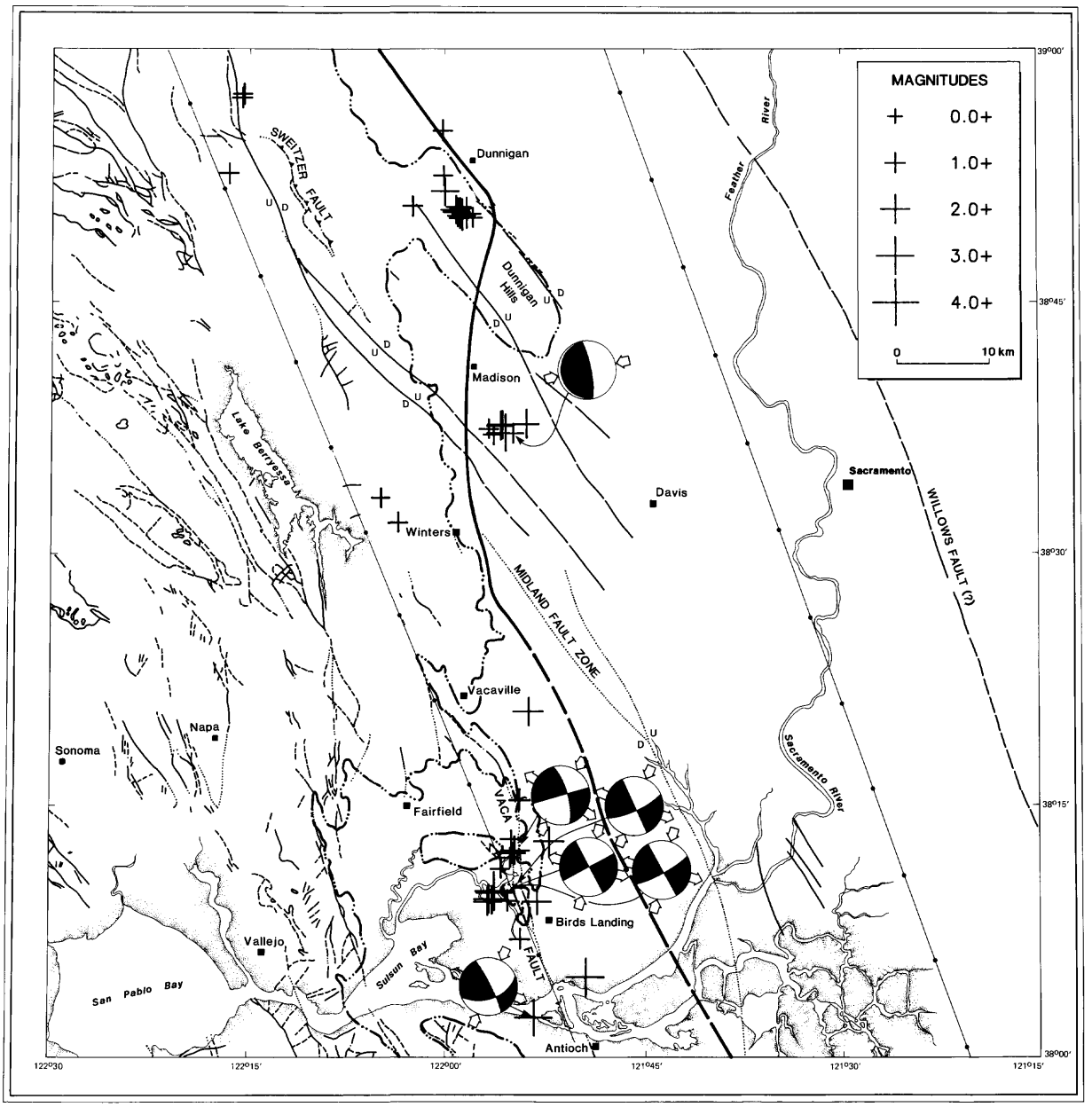
MAGNITUDES
0.0+
1.0+
2.0+
3.0+
4.0+
0
10 km
Dunnigan
Madison
Winters
Davis
Sacramento
Vacaville
Fairfield
Napa
Sonoma
Vallejo
Birds Landing
Antioch
SWEITZER FAULT
Dunnigan Hills
Feather River
Lake Berryessa
MIDLAND FAULT ZONE
WILLOWS FAULT (?)
Sacramento River
VACA
FAULT
San Pablo Bay
Suisun Bay
39°00'
38°45'
38°30'
38°15'
38°00'
122°30
122°15'
122°00'
121°45'
121°30'
121°15'

Figure 3

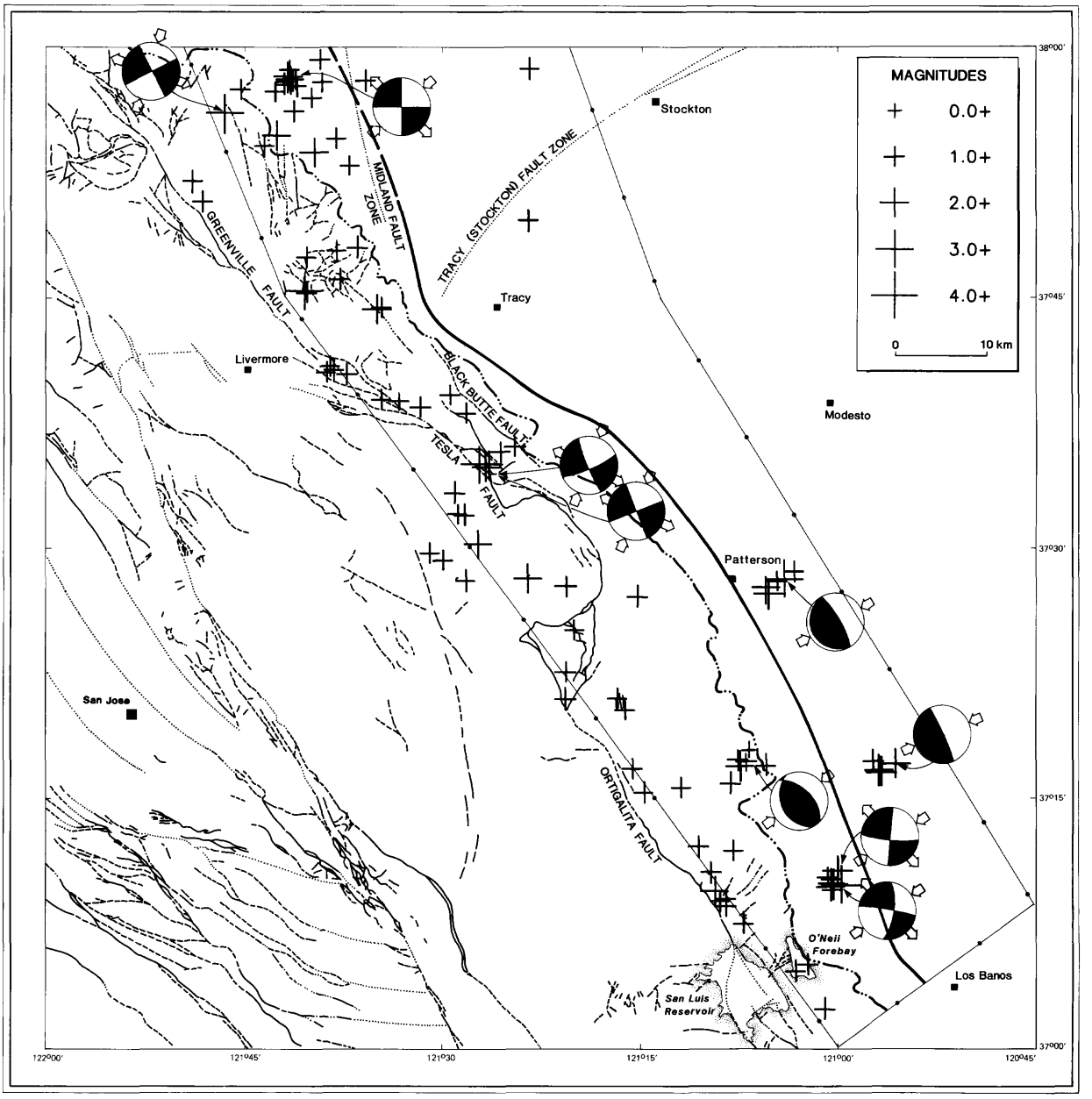
MAGNITUDES
0.0+
1.0+
2.0+
3.0+
4.0+
0
10 km
Stockton
Tracy
Livermore
Modesto
Patterson
San Jose
Los Banos
MIDLAND FAULT ZONE
TRACY (STOCKTON) FAULT ZONE
GREENVILLE FAULT
BLACK BUTTE FAULT
TESLA FAULT
ORTIGALITA FAULT
O'Neil Forebay
San Luis Reservoir
38°00'
37°45'
37°30'
37°15'
37°00'
122°00'
121°45'
121°30
121°15'
121°00'
120°45'

Figure 4

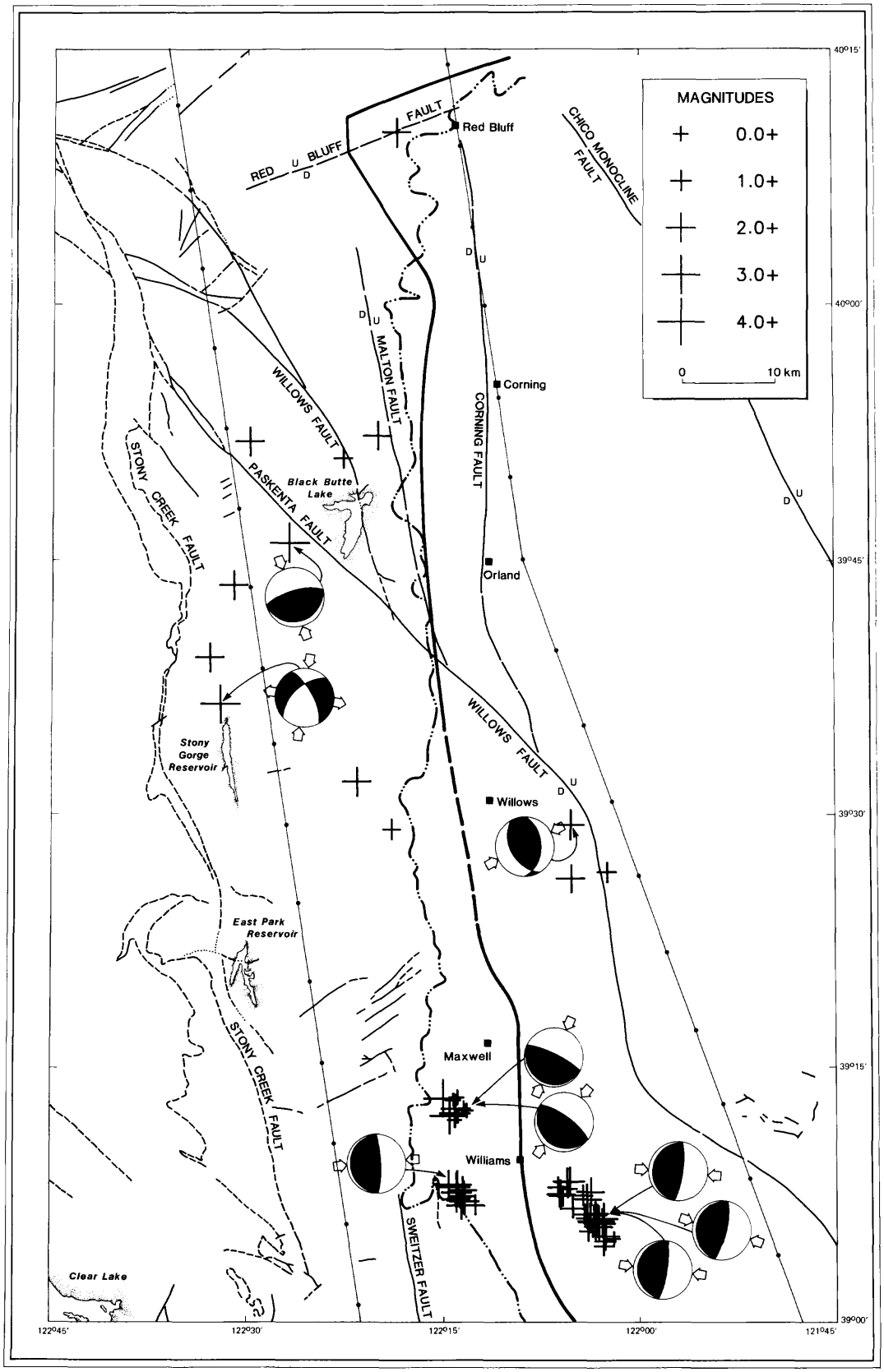
MAGNITUDES
0.0+
1.0+
2.0+
3.0+
4.0+
0
10 km
RED BLUFF FAULT
Red Bluff
CHICO MONOCLINE FAULT
MALTON FAULT
WILLOWS FAULT
CORNING FAULT
Corning
Orland
PASKENTA FAULT
STONY CREEK FAULT
Black Butte Lake
Stony Gorge Reservoir
East Park Reservoir
Willows
Maxwell
Williams
SWEITZER FAULT
Clear Lake
40°15'
40°00'
39°45'
39°30'
39°15'
39°00'
122°45'
122°30'
122°15'
122°00'
121°45'

Figure 2

Geologic Studies for Seismic Zonation of the Puget Lowland

9540-04004
Brian F. Atwater
Branch of Western Regional Geology
U. S. Geological Survey at Department of Geological Sciences
University of Washington AJ-20
Seattle, Washington 98195
(206) 543-0804 FTS 399-2927

INVESTIGATIONS

(1) Paleoseismic implications of buried tidal-marsh surfaces at Neah Bay, the Copalis River estuary, Grays Harbor, Willapa Bay, and the Columbia River estuary [Brian F. Atwater and Wendy C. Grant]

(2) Surficial geology of the Redmond 7.5-minute quadrangle [James P. Minard]

RESULTS

(1) Though lacking emergent terraces indicative of coseismic uplift, Washington's Pacific coast has many submerged terraces--tidal-marsh surfaces buried by tideflat deposits. Each tidal-marsh burial records rapid coastal submergence of about 0.3-1.0 m, the range for coseismic subsidence in coastal Shikoku (southwestern Japan) during Nankai-trough earthquakes of moment-magnitude >8.0. Sheets of sand probably deposited by tsunami immediately overlie some of the tidal-marsh surfaces at Willapa Bay (southwestern Washington). The sequence of buried tidal-marsh surfaces at Willapa Bay suggests that at least six great subduction earthquakes have struck the Pacific Northwest during the past 5000-7000 years.

(2) The Redmond quadrangle, an area of rapid residential and commercial development east of Seattle, is covered chiefly with glacial deposits formed about 15,000 years ago. The surficial distribution of these and other deposits has been determined at 1:24,000 scale, and the resulting geologic map has passed peer review. The map fills a void in the large-scale geologic mapping of the Puget Sound lowland. Such mapping will be needed for accurate delineation of ground-shaking hazards.

REPORTS

Atwater, B. F., and Grant, W. C., 1986, Holocene subduction earthquakes in coastal Washington [abs.]: EOS (in press).

Surface Faulting Studies

9910-02677

M. G. Bonilla
Branch of Engineering Seismology and Geology
U. S. Geological Survey
345 Middlefield Road, MS 977
Menlo Park, CA 94025
(415) 323-8111, Ext. 2245

Investigations

1. Appearance of active faults in exploratory trenches.
2. Preparation of reports.

Results

1. In collaboration with J.J. Lienkaemper, the number of trench exposures was increased by 37% in order to improve the statistical base of the study. All new data has been checked for accuracy at both the hand entry and computer entry stages. Older data has been revised as needed to conform to improved procedures. Preliminary results are that normal-slip faults have distinctly fewer occurrences of strands that die out upward or that have obscure segments on them than reverse- and strike-slip faults. Analysis of other aspects of the improved data base is not yet complete.

2. A draft report was prepared, for a Geological Society of America Centennial volume, on the increase in knowledge about the process of faulting and seismic activity that has resulted from the investigation of engineering projects and on the impact of the process on such projects. Investigations related to the projects have provided new information on the location, nature, and degree of activity of faults in many areas. Topical research stimulated by the projects has yielded a better understanding of the near-surface aspects of faulting and on the investigation of active faults. Background research for the report shows that, in addition to the many structures that have been directly damaged by the process, many engineering projects have been greatly modified or even abandoned because of anticipated future faulting and earthquakes; these projects include pipelines, dams, and several nuclear reactors. Clearly, the appraisals of the risks from faulting and earthquakes must be accurate in order to avoid costly overconservatism or underconservatism.

   In collaboration with various coauthors, open-file reports on faulting associated with the 1983 Guinea and 1983 Idaho earthquakes were revised for more formal publication.

Reports:

Bonilla, M.G., 1986, Minimum earthquake magnitude associated with coseismic surface faulting [abs.]: *Geological Society of America Abstracts with* Programs, vol. 18, no. 6, p. 546.

SOIL DEVELOPMENT AND DISPLACEMENT ALONG THE HAYWARD FAULT

14-08-0001-21929

Glenn Borchardt
California Department of Conservation
Division of Mines and Geology
380 Civic Drive
Pleasant Hill, CA 94523-1997

(415) 671-4926

Investigations

Its high rate of activity (>5 mm/yr) and urban location make the Hayward fault potentially the most destructive in the San Francisco Bay Area (Steinbrugge and others, 1986a, 1986b). The fault may be due for a major earthquake--the Fremont segment ruptured 118 years ago, while the Berkeley segment may have ruptured 150 years ago. The objective of this work is **to use soils and sediments to determine the long-term slip rate, the recurrence interval, and the amount of displacement to be expected for major earthquakes on the Hayward fault.**

The trench exploration phase of the investigation was begun on the Fremont segment in cooperation with Jim Lienkaemper and Dave Schwartz of the U.S. Geological Survey. The City of Fremont gave permission and kindly supplied occasional needed advice and materials. Student assistants Kim Seelig and Taryn Lindquist helped in preparing the trench logs. We excavated a series of trenches parallel to the fault at Fremont City Hall in an area in which previous work had shown a gravel unit offset against fine sandy overbank deposits (Cotton, Hays, and Hall, 1983; 1986; Levish, 1986). The site, on the Niles alluvial cone, occurs in an area in which the fault is confined to a single strand about 2 to 5 m wide.

Results

1. Fremont Study Site

Channel Offset

The offset gravel unit depicted in trench logs of previous workers is part of a fluvial system containing a buried channel fill that appears to have been right-laterally offset at least 28 m. Charcoal fragments from above the channel fill on the northeastern side of the fault and from below the channel fill on the southwestern side are being dated by using AMS (accelerator mass spectrometry).

Two parallel trenches (43 and 57 m long) were excavated 14-m apart on either side of the fault. Two additional short trenches were excavated further to the northeast and to the southwest to determine the orientation of the channel fill with respect to the fault. Projections from all four trenches indicate that the channel fill appears to intersect the fault plane at an angle between 36 and 66 degrees. The contact between the channel fill and adjacent pebbly sand deposits is gradational and highly variable in each exposure. Present data restricts the offset to a minimum of 28 m, but the determination of the true offset awaits further work, scheduled for spring of 1987. We will then include excavations to delineate the configuration of the channel, to locate its piercing point on the fault plane, and thus to determine the precise amount of offset.

Warp

The present topography contains a warp or sag on the northeast side of the fault. The channel fill is overlain by a thin gravel stringer that is easily identified, extends throughout both trenches, and provides a once-level marker bed that can be used to estimate tectonic deformation. The bed occurs at depths between 1.5 and 4 m and is overlain by fine sandy to silty clay overbank deposits. On the northeast side of the fault, the surface of the gravel descends to the northwest 320 cm in 35 m, but on the southeast side it descends only 80 cm in 35 m. Tectonic subsidence in the warped area was thus at least 240 cm since fluvial deposition.

Soils

The soils, which are formed in the overbank deposit, demonstrate minimal development and appear to be late Holocene in age. In general, they are Mollisols lacking evidence for clay illuviation or structural B horizon development. Perhaps because of their location near what was once Stiver's Lagoon, they contain pedogenic carbonate in an incipient Bk horizon at the 70-cm depth. Four soil profiles were sampled and described and will be analyzed in detail.

On the northeastern side of the fault the three profiles across the warped zone are part of a catena (topographically controlled drainage sequence) along the flanks of the warp. They have horizons designated: Ap/A/AB/Bk/Bj (horizon designation proposed here for Mn-oxide/Fe-oxide accumulation) /C/2C/3ACb1/3Cb1. A single well-drained soil exists in the trench exposures on the southwest side of the fault. This soil has horizons designated: Ap/A/(A/C)/C/2C/3ACb1/3Cb1. The buried paleosol consists of locally variable zones consisting of the bioturbated former surface of the fluvial deposit.

MRT dates are being obtained for representative samples of the organic carbon and of the pedogenic carbonate in the most poorly drained soil. The soils at the site, although quite variable in character, are at present estimated to be about 2,500 years old (range: 1,500 to 3,500 B.P.). This is based on comparisons with a soil dated at 1,000 B.P. about 1.4 km to the north (Shlemon, 1984) as well as a 2,400 B.P. organic horizon in Tyson's Lagoon, a sag pond near the Fremont BART station to the north (Woodward-Clyde and Associates, 1970).

Preliminary Slip Rate

Assuming that the channel deposits are indeed offset at least 28 m, and assuming that the 2,500 B.P. estimate for the soil is only slightly less than that of the channel, the preliminary slip rate is about 11 mm/yr for this segment of the fault. Given the present uncertainty in the age and amount of offset, however, the slip rate could range between 8 and 37 mm/yr. Subsidence in the warp or sag is about 1 mm/yr (range: 0.7 to 1.6 mm/yr). Precise values for the slip rate and the subsidence rate await the arrival of the carbon dates and the completion of more detailed excavations.

2. Point Pinole Study Site

Landslide at the Distal Portion of the Fault

Wood taken from the slide plane of a landslide at the projected northwest end of the fault gave a C-14 date of >40,000 years. A much younger date was expected in view of the minimal soil cover and the fact that the landslide obscuring the distal portion of the fault is mapped as not having been displaced by the fault (Herd, 1978). This locality is being studied in greater detail and a log of the bay cliff exposure is being prepared.

Bay Mud Site

A sedimentary peat deposit encountered beneath 36-cm of bay mud in the tidal marsh adjacent to the fault gave a C-14 date of 1360±80 B.P. This unit or its correlative may be offset by the fault within two embayments in the southwest facing linear scarp mapped as the solitary trace at Point Pinole. The date also gives an estimate of 0.26 mm/yr for sea level rise/tectonic subsidence during the last millennium. The trench exploration phase of the project will attempt to explore the amount of displacement of this unit.

References

Cotton, W. R., Hall, N. T., and Hay, E. A., 1983, Holocene behavior of the Hayward-Calaveras fault system, San Francisco Bay Area, California: U.S. Geological Survey Open-file Report 83-918, p. 103-106.

Cotton, W. R., Hall, N. T., and Hay, E. A., 1986, Holocene behavior of the Hayward-Calaveras fault system, San Francisco Bay Area, California: Final Technical Report to the U.S. Geological Survey (Contract No. 14-08-0001-20555), Foothill-De Anza Community College District, 12345 El Monte Road, Los Altos Hills, CA, 15 p.

Herd, Darrell, 1978, Map of Quaternary faulting along the northern Hayward fault zone: U.S. Geological Survey Open-file Report 78-308, scale 1:24,000.

Levish, Murray, 1986, Written communication.

Shlemon, R. J., 1984, Soil-stratigraphic assessment of fault activity, California School for the Blind, Fremont, California in Awtar Singh, ed., Geotechnical site investigation, fault and liquefaction study, California School for the Blind, Fremont, California: Newport Beach, CA, R. J. Shlemon & Assoc., Inc., Appendix A2 in unpublished consulting report prepared for the State of California, Office of the State Architect, Sacramento by Lockwood-Singh & Associates, Los Angeles, CA, Ref. No. 3126-42, 47 p.

Steinbrugge, K. V., Lagorio, H. J., Davis, J. F., Bennett, J. H., Borchardt, Glenn, and Toppozada, T. R., 1986a, Earthquake planning scenario for a magnitude 7.5 earthquake on the Hayward fault, San Francisco Bay area: California Geology, v. 39, p. 153-157.

Steinbrugge, K. V., Davis, J. F., Lagorio, H. J., Bennett, J. H., Borchardt, Glenn, and Toppozada, T. R., 1986b (forthcoming), Earthquake planning scenario for a magnitude 7.5 earthquake on the Hayward fault in the San Francisco Bay area: California Division of Mines and Geology Special Publication 78, 220 p.

Woodward-Clyde and Associates, 1970, Fremont Meadows active fault investigation and evaluation, Fremont, California: Unpublished report dated June 30, 62 p.

Northern San Andreas Fault System

9910-03831

Robert D. Brown
Branch of Engineering Seismology and Geology
U.S. Geological Survey
345 Middlefield Road, MS 977
Menlo Park, California 94025
(415) 323-8111, ext. 2461

Investigations

1. Continuing research on Quaternary deformation in the San Andreas fault system for a planned volume summarizing current geologic and geophysical knowledge of the fault system.

2. Research and review of work by others on the tectonic setting and earthquake potential at Diablo Canyon Power Plant (DCPP), near San Luis Obispo, California. Activities are in an advisory capacity to the Nuclear Regulatory Commission (NRC) and are chiefly to review and evaluate data and interpretations obtained by Pacific Gas and Electric (PG&E) through its long-term seismic program.

3. Serve (*ex-officio*) on Policy Advisory Board, Bay Area Earthquake Preparedness Project (BAREPP). A joint project of the State of California and the Federal Emergency Management Agency, BAREPP seeks to further public awareness of earthquake hazards and to improve mitigative and response measures used by local government, businesses, and private citizens.

Results

1. First draft of San Andreas Quaternary paper is about 60% complete; text, excluding introductory and concluding sections, is essentially complete, but most illustrations remain to be done.

2. Participated in several field and workshop reviews related to DCPP and provided oral and written review comments to NRC. Coordinated USGS efforts to gather reflection and refraction data during PG&E work near DCPP and obtained partial funding for acquisition of deep crustal data by investigators in Branch of Seismology and Branch of Atlantic Marine Geology.

3. Provided informal oral and written data, analysis, and recommendations to BAREPP and other Policy Advisory Board members on geologic, seismologic, and management issues relating to earthquake hazard mitigation in the San Francisco bay region.

Reports

Brown, Robert D. Jr., and Kockelman, William J., 1986, Editorial -- geologic principles for prudent land use: a decisionmaker's responsibility?: *Environmental Geology and Water Sciences*, v. 8, no. 4, p. 173-174.

LATE QUATERNARY SLIP RATES ON ACTIVE FAULTS OF CALIFORNIA

9910-03554

Malcolm M. Clark

Branch of Engineering Seismology and Geology
U.S. Geological Survey
345 Middlefield Road, MS 977
Menlo Park, CA 94025
(415) 323-8111, ext. 2591

Investigations

1. Late Quaternary activity along the Lone Pine fault, Owens Valley, California (L.K. Lubetkin, USFS, M.M. Clark, S. Beanland, K.K. Harms, and S.K. Pezzopane.

2. Recently active traces of the Calaveras fault at San Felipe Creek (J.W. Harden, Harms, Clark, Pezzopane, C.L. Terhune, Beanland).

3. Parkfield studies (J.L. Lienkaemper).

4. Holocene slip rates, Hayward fault (Lienkaemper).

5. Chalfant Valley earthquake of July 21, 1986 (Lienkaemper, Pezzopane, Clark).

6. Mt. Lewis earthquake of 31 March, 1986 (Pezzopane, Clark).

Results

1. Further investigation of the Lone Pine fault indicates that of the three events that offset the 10,000 to 21,000 year-old abandoned outwash fan of Lone Pine Creek, the oldest probably occurred slightly before abandonment. 1872 right-lateral component of displacement was apparently 4-6 m; dip slip component was 1-2 m. This additional information changes our previously reported average recurrence interval for the three earthquakes from 3,300-10,500 years to 5,000-10,500 years, and our average slip rate to 0.4-1.2 mm.yr for the Lone Pine fault.

   If we add the 1872 horizontal slip component for the Lone Pine fault of 4-6 m to the 1872 horizontal slip of 2.7-4.9 m reported for the adjacent main Owens Valley trace, the resulting total 1872 right-lateral slip component for the Owens Valley fault zone at Lone Pine is about 6-1/2 to 11 m, a very large value. If we assume 1872 was a characteristic earthquake, the associated average horizontal slip rate for the Owens Valley fault zone at Lone Pine is 0.6-2.2 mm/yr. Addition of the smaller dip slip component does not significantly increase these values.

2. Some fluvial deposits along San Felipe Creek have been displaced by the Calaveras fault near the northern end of Anderson Reservoir. Other deposits were deposited in response to lateral and/or vertical movement of the fault. We excavated thirteen backhoe pits to analyze the degree of soil development on each of six surfaces affected by faulting. We described twenty-four soils. We will use Harden's soil development index to assign ages to the surfaces. Two of these deposits yielded four ^{14}C samples that we will submit for radiocarbon dating. The resulting ages will be combined with displacements to yield late Quaternary slip rates for this section of the Calaveras fault.

3. In the preliminary analysis of the smallest stream channel offsets between Cholame Valley and Bitterwater Canyon, to the southeast, the highest quality sites with small offsets average about 6.1 m right-lateral slip. Given a deep crustal slip rate of 3.3 cm/yr, it would take 56 more years to accrue sufficient strain for 6.1 m of surface slip, assuming that a characteristic earthquake model is correct.

   Aerial photos have now been flown at 1:2400-scale for this entire section of the San Andreas fault zone and will serve as the basis for several methods of more detailed analyses of these channel offsets. One method is the compilation of digital topographic maps from these photos by USGS Astrogeology in Flagstaff. Permanent (benchmark) picture points to control these digital maps will also serve to monitor future slip.

4. Four trenches dug parallel to the Hayward fault at Fremont City Library exposed a buried gravel channel that correlates reasonably well across the fault. The current estimate of right-lateral slip, 28+/- 7 m, may change significantly after further trenching in Spring 1987 to map the piercing points in detail as they approach the fault. The age of the channel will be constrained by carbon-14 dates on charcoal lying stratigraphically above and below the channel. A preliminary minimum age, 1500-3500 yr BP, has been estimated for the soil formed on silty flood deposits that overlie the gravel channel, on the basis of similarity to dated soils nearby (Borchardt, this volume). From these preliminary data we compute a range of slip rate of 6 to 23 mm/yr since about 2500 yr BP. This range is grossly in accord with the 6 to 8 mm/yr creep rate for this segment of the Hayward fault. However, we may <u>not</u> yet conclude that the creep rate is likely to be lower than our late Holocene slip rate, because our age control postdates the time of channel formation; thus 6 mm/yr is not a strict minimum rate. We must wait for ^{14}C results before drawing even the most tentative conclusions about a Hayward fault earthquake cycle.

5. The M_S 6.2 Chalfant Valley earthquake occurred in the Volcanic Tableland north of Bishop. It was preceded by a large foreshock and several large aftershocks. This earthquake sequence was accompanied by surface rupture along more than 10 km of the White Mountains frontal fault zone with as much as 11 cm of right-lateral slip across the zone.

On the Volcanic Tableland, we found dominantly left-stepping surface ruptures along six fault zones that form a larger right-stepping system. These six major zones were 2 to 7 km long each and ranged in trend from 340 to 347°, roughly similar to the overall trend of the White Mountains frontal zone fractures, 350°. Because the dominant fracture trend in the tableland was about 355°, several degrees clockwise from the zone trends, we infer that the large openings of fissures in loose sand probably represented a few centimeters of right-lateral slip in the Volcanic Tableland fault system.

6. Our field investigation of the rugged epicentral area of the M 5.3 Mt. Lewis earthquake revealed no evidence of surface rupture. On one narrow ridge, intensified shaking moved boulders and cobbles horizontally to new positions. Geomorphic features that suggest Quaternary faulting, such as benches, hillside valleys, deflected channels, linear valleys, and notches are abundant in the epicentral area. Some of these features are alined N-S, parallel to fault strikes indicated by focal mechanisms and aftershocks of the earthquakes. Although these alined features could be the surface expression of Quaternary faulting, most could also result from landsliding, or differential weathering acting on lithologic boundaries, joints, faults, and shear zones in the chaotic Franciscan Formation that occupies the epicentral area and locally has N-S structural fabrics.

   Both the nature of the Franciscan Formation and the presence of rapid uplift and erosion in the epicentral area 1) make plausible either concentrated or diffuse tectonic displacement near the ground surface, and 2) make difficult the job of identifying small late Quaternary surface faulting, if it exists.

Reports

Harden, J.W., Harms, K.K., Mark, R.K., and Clark, M.M., 1986, Soil development as a tool for studying seismogenic faults, Soil Science Society of America Abstracts, Annual Meeting, Chicago, Illinois, December 4-9, 1986.

Lienkaemper, J.J., Pezzopane, S.K., Clark, M.M., and Rymer, M.J., 1986, Fault fractures associated with the M_S 6.2, Chalfant, California earthquake of 21 July 1986 [abs.]: Transactions, American Geophysical Union, December 1986 meetings.

Lienkaemper, J.J., Pezzopane, S.K., Clark, M.M., and Rymer, M.J., 1987, Fault fractures formed in association with the 1986 Chalfant, California earthquake sequence: preliminary report: Bulletin of the Seismological Society of America, in press.

Pampeyan, E. H., Holzer, T. L., Clark, M. M., 1986, Man-induced ground failure in the Garlock fault zone--Fremont Valley, California: submitted to Geological Society of America Bulletin.

Rymer, M.J., Harms, K.K., Lienkaemper, J.J., and Clark, M.M., in press, The Nunez fault and its surface rupture during the Coalinga earthquake sequence of 1983, in Rymer, M.J., and Ellsworth, W.L., eds., The May 2, 1983 Coalinga, California earthquake sequence: U.S. Geological Survey Professional Paper, 32 MS p.

Rymer, M.J., Lienkaemper, J.J., and Brown, B.D., in press, Distribution and timing of slip along the Nunez fault after June 11, 1983, in Rymer, M.J., and Ellsworth, W.L., eds., The May 2, 1983 Coalinga, California earthquake sequence: U.S. Geological Survey Professional Paper, 22 MS p.

Sharp, R.V., Rymer, M.J., and Lienkaemper, J.J., 1986, Surface displacement on the Imperial and Superstition Hills faults triggered by the Westmorland, California earthquake of 26 April 1981: Bulletin, Seismological Society of America, v. 76, p. 949-965.

Zoback, M.L., and Beanland, S., 1986, Stress and tectonism along the Walker Lake belt, Western Great Basin [abs.]: EOS, v. 67, p. 1225.

DETAILED GEOMORPHIC STUDIES TO DEFINE LATE QUATERNARY FAULT BEHAVIOR AND SEISMIC HAZARD, CENTRAL NEVADA SEISMIC BELT

14-08-0001-G-1205

**Karen Demsey, Philip Pearthree, William B. Bull,
Julia Fonseca, Suzanne Hecker, and Oliver Chadwick
Department of Geosciences
University of Arizona
Tucson, Arizona 85721
(602) 621-6024**

Project goals

Central Nevada is a region characterized by active seismicity and historical faulting. Our study includes detailed geomorphic investigations used to determine the timing, distribution, and behavior of late Quaternary faulting in this region. The geographic extent of the original study area has expanded to include more northerly and easterly portions of the central Nevada seismic province. Detailed studies of the faulting history in several subareas are being made in order to develop geophysical models to assess past, present, and future earthquake activity in this broad extensional tectonic regime.

Investigations

The most recent detailed study of late Quaternary fault history for the project has focused on the Wassuk mountains in west-central Nevada. The Wassuk Range, adjacent to Walker Lake, lies near the western margin of the Basin and Range province. Its eastern, fault-bounded flank is characterized by steep, linear mountain-piedmont junction and active fan deposition, suggesting a tectonically active mountain front. Although the range-bounding fault zone has not ruptured historically, evidence for recurring late Quaternary earthquake activity may have important implications for the safety of nearby communities such as Hawthorne, Schurz, and the Hawthorne Army Ammunition Plant.

Faulted late Quaternary alluvial surfaces provide data for fault-scarp morphology and soil studies, which are the principal geomorphic tools used to constrain ages of ruptured and unruptured surfaces. Wave-cut and depositional shoreline features formed during the latest Pleistocene highstand of Lake Lahontan (approx. 12 ka B.P.) are preserved in both bedrock and alluvium. The shoreline remnants serve as time lines for distinguishing Holocene (post-Lahontan) surfaces, and as topographic features for estimating amounts of Holocene faulting and associated tectonic uplift.

Fault scarps formed on several ages of piedmont surfaces document recurrent Holocene offset along the Wassuk mountain front. Scarps formed during the most recent event are relatively steep and sharp-crested, and cross-cut topographically low geomorphic surfaces that display little soil profile development. Older Holocene surfaces were additionally offset by an earlier faulting event, and composite scarps occur on some of these surfaces. At one locality in the northern portion of the range there is evidence for a third, earlier Holocene faulting event, which formed scarps only on the earliest of the Holocene surfaces.

Topographic profiles of the alluvial fault scarps along the Wassuk range are being analyzed using solutions to the diffusion equation, similar to the model of Hanks et al (1984), to obtain morphologic age estimates for the scarps. Recent studies indicate that the rate and processes of scarp degradation are dependent in part upon initial scarp height. Accordingly, the analysis of the fault scarps utilizes a degradation rate coefficient (c*) which is adjusted to account for scarp height (see Pierce and Colman, 1986).

Soil development on faulted and unfaulted alluvial surfaces was characterized in the field to establish a chronosequence for the Wassuk soils. The relative ages of the soils in the chronosequence can be quantified using the Maximum Horizon Index (MHI) of Harden (1982). This index has been applied successfully in other tectonic geomorphic studies in central Nevada (Hecker, in press; Fonseca, in press). Organic deposits and volcanic ashes were found in several of the Wassuk soils. These will provide absolute age control of the soil chronosequence, allowing ages of the surfaces to be estimated and timing of faulting events to be bracketed independently of age estimates provided by fault-scarp morphologic analyses.

The elevations of the latest Pleistocene Lahontan highstand shoreline remnants were surveyed along the length of the mountain front. Deformation of this initially horizontal datum will be used to estimate the total amount of Holocene uplift along the mountain front and to estimate fault offsets where the shoreline features cross fault zones. This analysis will complement estimates of Holocene uplift rates determined from the displacements of alluvial surfaces at the fault scarps.

The results of this geomorphic study of the Wassuk range-bounding fault will be used to evaluate the lengths of prehistoric surface ruptures, the timing of the events, and the potential seismic hazard associated with the fault zone.

References

Fonseca, Julia (in press). The Sou Hills -- a barrier to faulting in the Central Nevada Seismic Belt, Neotectonics.

Hanks, T.C., Bucknam, R.C., Lajoie, K.R., Wallace, R.E. (1984). Modification of wave-cut and faulting-controlled landforms, Jour. Geophys. Res. **89**, 5771-5790.

Harden, J.W. (1982). A quantitative index of soil development from field descriptions: Examples from a chronosequence in central California, Geoderma **28**, 1-28.

Hecker, Suzanne (in press). Timing of Holocene faulting in part of a seismic belt, west-central Nevada, Bull. Seism. Soc. Am.

Pierce, K.L., and Colman, S.M. (1986). Effect of height and orientation (microclimate) on geomorphic degradation rates and processes, late-glacial terrace scarps in central Idaho, Geol. Soc. Am. Bull. **97**, 869-885.

The Use of Radiocarbon in Paleoseismic Investigations on the San Andreas Fault

14-08-0001-22044

N. Timothy Hall, Edward A. Hay, William R. Cotton
Foothill-DeAnza Community College District
Los Altos Hills, California 94022
(408) 996-4774

Objective:

This research project is designed to evaluate and reduce uncertainties inherent in the use of radiocarbon dates for recurrence interval and slip rate determinations on active faults. Field investigations will focus upon Dogtown, a site on the San Andreas fault in Marin County, California, that has yielded evidence for three pre-1906 ground-rupturing events. Attempts to bracket their ages have been frustrated by wide-ranging radiocarbon dates for sedimentary layers cut by the fault.

Results:

Subsurface excavations at Dogtown indicate three pre-1906 ground rupturing earthquake events. In 1979 the youngest detrital charcoal age for a stratigraphic horizon dislocated by all ground ruptures resulted in an initial recurrence frequency estimate of 217 to 455 years. Assuming a maximum-value for ages used in these calculations, we concluded that each earthquake was probably of the 1906-type and that large magnitude earthquakes were probably characteristic of the northern segment of the San Andreas fault. We believed these large seismic events probably recurred about every 200 years (Cotton and others, 1982).

Later radiocarbon ages from detrital wood in a stratigraphic horizon also cut by the three pre-1906 ruptures require a significant modification of the 1979 view. The three pre-1906 earthquakes are now thought to have occurred during an interval of 186 ± 90 years, and therefore, probably were not 1906-type seismic events causing ground ruptures of four to five meters displacement. Our revised conclusion about paleoseismicity at Dogtown is that the three pre-1906 earthquakes were in the magnitude range of 6.5 to 7.0 and each may have produced ground ruptures of 2 meters or less, an amount consistent with the magnitude and rupture length record of strike-slip events in California (Wallace, 1970). The conclusion that three non-characteristic earthquakes (i.e., not like the 1906 earthquake) occurred at Dogtown prior to the large 1906 event is also

consistent with the historic record of ground rupturing earthquakes on the San Francisco Peninsula where temblors with estimated magnitudes of 6.5 to 7.0 were reported in 1838 and 1865.

Our most recent interpretation suggests that the recent regional rate of strain accumulation across the San Andreas fault at Dogtown is about 2.2cm/year. Such a rate would accumulate aproximately 2 meters of strain during the average maximum recurrence frequency interval as deduced from the Dogtown area trenches. Because this recurrence frequency is probably a maximum value, the actual ground displacements were likely less. Such displacements are consistent with the ground displacements expected from magnitude 6.5 to 7.0 earthquakes.

An important conclusion follows from the recognition that the San Andreas fault experienced several magnitude 6.5 to 7.0 earthquakes prior to the M_S=8.25 event of 1906. If this be a typical pattern of seismicity, then the recurrence frequency between 1906-type earthquakes is significantly longer than most researchers have previously concluded. Current estimates for strain rates in the Dogtown region of about 2.2cm/year imply that approximately 230 years is required to build up enough strain to trigger a 5-meter slip event such as occurred in 1906. Add to this the time necessary to accumulate sufficient strain to accommodate several magnitude 6.5 to 7.0 earthquakes, and the recurrence frequency for 1906-like earthquakes is extended to the 350 years range. As has been suggested by Ellsworth and others (1981), an interval of 50 years to 100 years or more of increased seismic activity with M_S=6.5 to 7.0 earthquakes might be the precursor to the next great earthquake on the San Andreas fault in northern California.

References cited:

Cotton, W.R., Hall, N.T., and Hay, E.A., 1982, Holocene Behavior of the San Andreas fault at Dogtown, Point Reyes National Seashore, California; Final Tech. Rept. for U.S.G.S. Contract No. 14-08-0001-19841, September, 1982.

Ellsworth, W.L., Lindh, A.G., Prescott, W.H., and Herd, D.G. 1981, The 1906 San Francisco earthquake and the seismic cycle, in proceedings, Third Maurice Ewing Symposium, Earthquake Prediction, May 12-16, 1980: American Geophysical Union.

Wallace, R.E., 1970, Earthquake Recurrence Intervals on the San Andreas Fault: Geol. Soc. America Bull., v. 81, p. 2875-2890.

Publication:

Hay, Edward A., and Hall, N.T., 1986. "Tectonic Creep Along the San Andreas Fault, Bitterwater Valley, California." The Geological Society of America, Cordilleran Section, Abstracts with Programs 18 (2): 115.

COASTAL TECTONICS, WESTERN U.S.

9910-01623

Kenneth R. Lajoie

Branch of Engineering Seismology and Geology
U.S. Geological Survey
345 Middlefield Road, MS 977
Menlo Park, CA 94025
(415) 323-8111, ext. 2642

Investigations

1. Age and deformation of Pleistocene marine strandlines and deposits in the San Pedro/Long Beach area, Los Angeles County, California.

2. Intra- and inter-shell reproducibility of amino-acid analyses in Saxidomous. This experiment is designed to refine correlations and age estimates of emergent marine strandlines using amino-acid analyses from fossil marine shells.

3. Coseismic uplift near the Mendocino triple junction.

4. Assisted G. Plafker in an investigation to determine the time interval between the 1964 earthquake and the previous large earthquake on Montague Island and at Cape Suckling in the Gulf of Alaska. We measured stratigraphic sections of emergent marine sediments and collected wood and shell samples for ^{14}C dating.

5. Amino-acid dating of fossil shells from marine sediments in east and west-central Japan. Near Tokyo the Jizodo, Semeta, Kamiizumi and Narita formations form a nearly continuous depositional sequence ranging in age from about 300 ka to 100 ka. Shells from the older Naganuma formation dated at about 600 ka extend the range of this study. Shells from various horizons in this independently dated (tephra) sequence provide a means of evaluating the amino-acid technique over a time period relatively devoid of fossils along the west coast of the United States. Uncertain stratigraphic correlations in this highly deformed sequence are also being checked.

Results

1. As a first approximation, it was assumed that the uppermost marine deposits (both surface and subsurface records) throughout the Los Angeles Basin correlated and were about 120 ka in age. Amino-acid data indicate this assumption is incorrect. The ages of the uppermost marine deposits vary from 120 ka to at least 300 ka. Also, the 120 ka sea-level highstand did not cover the entire basin, but was restricted to coastal areas near

the present shoreline and to narrow gaps presently occupied by the floodplains of major rivers. Consequently, the Palos Verdes sand as defined by Woodring does not occur northeast of the Newport-Inglewood fault (on the crest of Signal Hill, for example) as assumed by other workers. The youngest stratigraphic horizon that extends across the fault extensively and, therefore, forms a useful tectonic datum is probably about 300 ka in age.

2. Initial amino-acid data from well-preserved fossil Saxidomous in growth position indicated that the emergent marine platform at Isla Vista near Santa Barbara was cut during the 40 ka sea-level highstand. The tectonic implications of this relatively young age estimate were very important. If correct, this age estimate yielded an uplift rate of 1.3 m/ka (very high for the California coast) and a similar slip rate (vertical component) on the More Ranch fault, which offsets the platform. However, geologically this age estimate was problematical; it was much lower than age estimates on the same platform to the east and west. More detailed amino-acid analyses of the Saxidomous fossils show that ALO/I50 ratios vary significantly depending on which shell layer is sampled. The new amino-acid data indicate the age of the Isla Vista platform is 85 ka or 105 ka, which is consistent with geologic constraints in the area. A growing body of data indicates that individual shells of most genera can yield highly variable amino-acid ratios because each structural layer within the shell has a unique amino-acid composition. Consequently, serious systematic errors can be introduced in sampling and cleaning fossil shells for analysis. The problem is most acute in large shells because representative samples are difficult to obtain. The most consistent results are obtained from whole small shells or from uncleaned samples of large shells that include all structural layers. Surprisingly, systematic bias and scatter in the data are minimized by not cleaning samples.

3. Up to nineteen Holocene emergent marine strandlines record rapid tectonic uplift (maximum 4.0 m/ka) over the past 5 ka between Cape Mendocino and Big Flat south of the Mendocino triple junction. If all of these strandlines were of coseismic origin, the minimum average earthquake recurrence interval would be about 250 yr. However, many of these emergent strandlines are cobble berms that probably record major storm events, not tectonic uplift events. The six distinct strandline terraces in the area probably represent the minimum number of uplift events over the past 5 ka. Consequently, the maximum average recurrence would be about 830 yr. and the maximum average uplift would be about 3 m. Unfortunately, each strandline terrace cannot be dated independently, consequently, the pattern of uplift (time predictable or displacement predictable) cannot be determined.

4. At McCleod Harbor on southern Montague Island, Alaska, emergent bay sediments up to 7 m thick appear to record only the 1964 uplift event over the last 1.3 ka. At Cape Suckling emergent marine sediments are so thin or are so poorly exposed that no meaningful interpretation of earthquake interval can be made.

5. Preliminary amino-acid data from Saxidomous follow relative ages in the Jizado to Narita sequence in east-central Japan with only minor discrepancies; some of these discrepancies may indicate that accepted stratigraphic correlations are incorrect. Several genera including Glycymerous, Pecten and Callista yield internally consistent data that agree with the data from Saxidomous.

Reports

Lajoie, Kenneth R., 1986, Rapid tectonic uplift near the Mendocino triple junction recorded by emergent marine strandlines: EOS, v. 67, no. 44, p. 1224 (abs).

McCrory, P.A., and Ingle, J.C., Jr., 1986, Late Neogene history of the Humboldt Basin and its relationship to convergence of the Juan de Fuca plate: EOS, v. 67, no. 44, p. 1220.

Additional Work to Date Probable Earthquake Deformed Beds in Kern County, California
14-08-0001-22018

D. L. Lamar and P. M. Merifield
Lamar-Merifield Geologists, Inc.
1318 Second Street, Suite 25
Santa Monica, CA 90401
(213) 395-4528

W. E. Reed
Department of Earth and Space Sciences
University of California, Los Angeles
Los Angeles, CA 90024
(213) 825-2819

and

T. K. Rockwell
Geology Department
San Diego State University
San Diego, CA 92182
(619) 265-4441

Investigations

Load structures and intrusion structures in lucustrine sediments in Kern Lake at the southern end of the San Joaquin Valley were described under previous U. S. Geological Survey Contract 14-08-0001-16791 (Lamar and others, 1979ab). The structures are similar to earthquake-induced structures described by others. Truncation of the deformed structures by the base of the soil and a local unconformity indicate that deformation occurred in two distinct events. Figure 1 illustrates an intrusion structure truncated by the unconformity at 87 cm depth; a subsequent event caused the intrusion structure to be reactivated and penetrate the unconformity. Efforts to date the deformation events under the original contract yielded ambiguous results which prompted the current investigation.

Under the current contract the earthquake deformed structures were again exposed in a test trench and the sediments were sampled for organic material at six locations and the samples were sent to the University of Arizona for carbon 14 dating.

Results

The carbon 14 dates relative to the earthquake deformation structures are illustrated in Figure 1. One sample yielded insufficient carbon for dating and the 42,620 years B.P. age is believed to be from reworked carbon of unknown origin and not representative of the time of deposition of the lake sediments. The other four samples yielded fairly consistent results which indicate that the structures formed in lake sediments between about

1400 and 2500 years B.P. Kern Lake was active until 1891 when flow into the lake was intercepted and directed into Buena Vista Lake to the west, thus it was expected that the carbon 14 dates would yield younger ages for the earthquake deformed structures. The test pit was located south of the recent lake shorelines at an average elevation of 282 feet; the carbon 14 dates indicate that deposition in this area ceased about 1400 years ago.

The deformation structures clearly demonstrate two earthquake shaking events in the southern San Joaquin Valley between about 1400 and 2500 years ago. The most probable causitive faults are the San Andreas, White Wolf and Garlock faults. The dates of the events are too imprecise and old to allow correlation with earthquake sequences established along the San Andreas fault by Sieh (1984) and Sieh and Jahns (1984).

References

Lamar, D. L., S. G. Muir, P. M. Merifield and W. E. Reed, 1979a, Possible earthquake deformed sediments in Kern Lake, Kern County, California: Geol. Soc. of Amer., Abstracts with Programs, Vol. 11, No. 3, p.88.

Lamar, D. L., S. G. Muir, P. M. Merifield and W. E. Reed, 1979b, Description of earthquake deformed sediments in Kern Lake, Kern County, California: Lamar-Merifield Tech. Report 79-1, Final Tech. Report for U. S. Geological Survey Contract 14-08-0001-16791, 44 p.

Sieh, K. E., 1984, Lateral offsets and revised dates of large prehistoric earthquakes at Pallett Creek, southern California: Jour. Geophys. Res., Vol. 89, No. B9, p. 7641-7670.

Sieh, K. E. and Jahns, R. H., 1984, Holocene activity of the San Andreas fault at Wallace Creek, California: Geol. Soc. Amer. Bull., Vol. 95, p. 883-896.

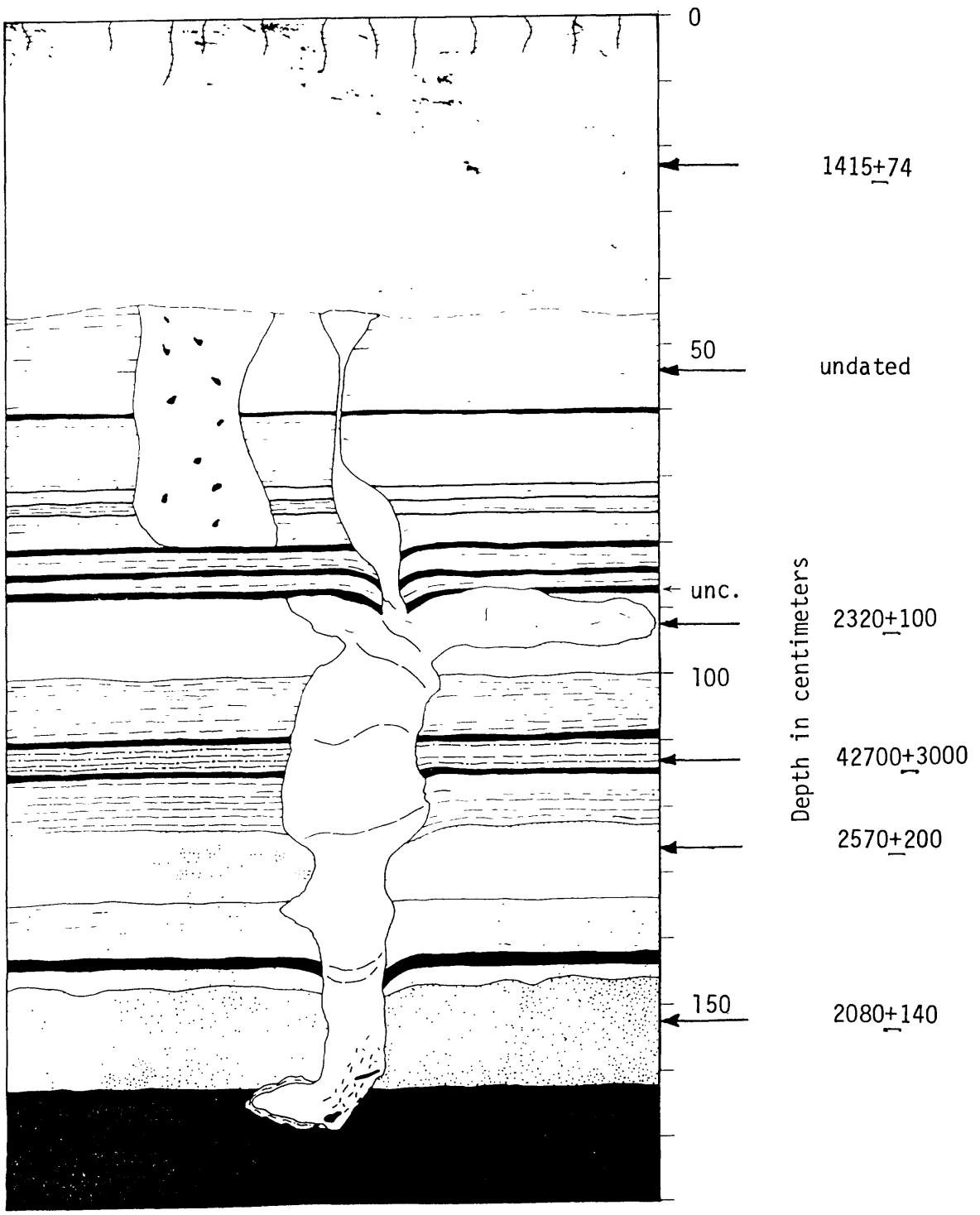

Fig. 1 - View of intrusion structure reactivated by shaking event which penetrated unconformity at 87 cm depth. Positions of carbon 14 dates related to earthquake deformation structures indicated on right.

STUDY OF SEISMIC ACTIVITY BY SELECTIVE TRENCHING ALONG THE SAN JACINTO FAULT ZONE, SOUTHERN CALIFORNIA

Contract 14-08-0001-22033

P.M. Merifield and D.L. Lamar
Lamar-Merifield Geologists, Inc.
1318 Second Street, Suite 25
Santa Monica, CA 90401
(213) 395-4528
and
T.K. Rockwell and C.C. Loughman
Geology Department
San Diego State University
San Diego, CA 92182
(619) 265-4441

Investigations: The objectives of this investigation include determination of the Holocene slip rate and timing of the most recent earthquakes on the Clark fault strand of the San Jacinto fault zone. This strand shows the most convincing geologic evidence of Holocene movement and the largest cumulative displacement of any on the San Jacinto fault zone; however, it has not experienced a ground-breaking earthquake in historic time.

Results: Four slip-rate determinations have been made during the current study. Charcoal from fine-grained alluvium interpreted to have ponded behind a shutter ridge was dated at 28,650±980 years B.P. This date and the offset from the shutter ridge yield an estimated slip rate of 6-18 mm/yr. Alluvial fan deposits are offset about 200 m, as indicated by the offset of an abandoned channel which incises the fan deposits. The age of the fan deposits has been estimated by soil profile development to be 16,500±3000 years old, yielding an estimated slip rate of 10-15 mm/yr. Charcoal from the upper part of the stream gravels in the abandoned channel was dated at 3860±110 years. This date and the minimum offset of the stream channel of 48 m yield a minimum slip rate of 12 mm/yr. Another previously reported date (Rockwell et al, 1986) from fine-grained alluvial deposits interpreted to be displaced ponded sediments yields a minimum slip rate for the last 9500 years of 9±1 mm/yr, but allows for a much larger slip rate. Collectively, these estimates bracket the slip rate on the Clark fault north of Anza at 12-17 mm/yr for the last 30,000 years. At least one ground-breaking event has occurred in the last 730±60 years, as indicated by a carbon 14 date from sediments displaced by one of several strands of the fault at Hog Lake.

Reports: Rockwell, T.K., P.M. Merifield, and C.C. Loughman, 1986, Holocene activity of the San Jacinto fault in the Anza seismic gap, southern California, Geol. Soc. Am., Abstracts with Programs, vol. 18, no. 2, p. 177.

MORPHOLOGIC DATING OF FAULT SCARPS

14-08-0001-21960

David B. Nash, Principal Investigator
James S. Beaujon, Research Assistant
Department of Geology
University of Cincinnati
Cincinnati, Ohio 45221-0013
(513) 475-3732

Investigation

A one dimensional diffusion model successfully predicts the pattern of degradation observed on some hillslopes. According to this model, the downslope flux of debris per unit width of contour at a point on a hillslope profile, q, is proportional to the profile's gradient at that point or

$$q = -c \frac{\partial y}{\partial x} \qquad (1)$$

where c is a constant of proportionality and x and y are the horizontal and vertical coordinates respectively. The rate of lowering at a point on the profile is equal to the downslope divergence of the volumetric debris flux:

$$\frac{\partial y}{\partial t} = c \frac{\partial^2 y}{\partial_x{}^2} \qquad (2)$$

where t is time. Numerous investigators have determined the morphologic age, tc, of hillslopes by matching the observed profiles with profiles predicted by the diffusion model (morphologic dating).

To determine the age of a hillslope, its morphologic age must be divided by c. Because c may be influenced by the character of the colluvial and vegetation covers, the local climate, and the direction in which the hillslope faces (aspect), an appropriate value of c should be determined for each hillslope to be dated from an analysis of a nearby hillslope of known age. Dated hillslopes are seldom available, limiting the applicability of morphologic dating.

This study investigates the effect climate, vegetation, underlying material, and aspect have on c by examining hillslopes of known ages that are underlain by a variety of different materials, in a variety of climatic regions, and having a variety of aspects. If the influence of these factors on c could be determined with sufficient accuracy, an appropriate value for c could be estimated directly by measurement of the factors, eliminating the need for a hillslope of known age.

Results

An extensive set of profiles taken from the same aged terrace scarps near Jenny Lake Junction in Grand Teton National Park (GTNP), Wyoming (Fig. 1) yields morphologic ages ranging over two orders of magnitude (Fig. 2). The morphologic ages for each terrace scarp are unrelated to their known relative ages but instead appear to be determined by the scarps' offset, a relationship first defined by Pierce and Colman (1986) for terrace scarps in central Idaho. Because t is the same or nearly the same for all of these scarps, the variance in morphologic age must result from variation in c. The observed relationship between scarp offset and morphologic age is nearly linear. This linear relationship may be used to normalize the morphologic age of each scarp to its morphologic age if it had an offset of two meters (Fig. 3). The decision to normalize to an offset of two meters is arbitrary but two meter high scarps are quite common. The same tendency for morphologic age to increase with scarp height was observed at another study site in GTNP but the linear relationship predicts negative morphologic ages for low scarps (Fig. 4). Because negative morphologic ages are not possible, the relationship between tc and offset can not be linearly at low offsets.

The small variation in vegetation density and the size and sorting of colluvial material within each study site has no observable effect on morphologic age. Contrary to the findings of Pierce and Colman (1986), scarp aspect also appears to have little or no effect on c (Fig. 3). The wide age limits for the studied scarps makes comparison of c values between the different study sites difficult. Using an age of 15,000 to 17,000 years for the terrace sequence at Jenny Lake Junction (GTNP) as suggested by Ken Pierce (USGS, Denver) yields $c = 0.37\text{-}0.42 \times 10^{-3}$ m^2/yr for a scarp with a two meter offset. Analysis of scarps carved by the Bonneville flood(s) near Pocatello, Idaho yields $c = 1.64\text{-}1.75 \times 10^{-3}$ m^2/yr for a scarp with a two meter offset if Scott *et al.*'s (1982) age of 14,000-15,000 years is assumed for the flood.

Despite the fact that the *rate* of scarp degradation probably can not be predicted with the diffusion model if a constant c is used, the model *does* accurately predict the *pattern* of morphologic change. Several other models were tested in which q was assumed to be proportional to the gradient raised to some power. None of the alternate models match the observed morphology of the scarps or the rate of degradation any closer than (2).

The apparent insensitivity of c to scarp aspect, underlying material, and vegetation cover is encouraging and supports Hanks and Wallaces's (*in press*) suggestion that a value of $c = 1.0 \times 10^{-3}$ m^2/yr may be applicable over wide areas in the southern Basin and Range province. The strong tendency for c to increase with scarp offset is distressing and should be investigated thoroughly. Although morphologic dating still holds considerable promise for determining the age of fault and terrace scarps, until the nature of c is better understood, such dating should be done with caution.

A PC program, SLOPEAGE, for morphologic dating was written for use with this contract and is available from the authors. The program is

less restrictive than other morphologic dating techniques.

References

Hanks, T.C., and Wallace, R.E. (in press). Morphological analysis of Lake Lahontan shoreline and beachfront fault scarps, Pershing County, Nevada.

Nash, D.B. (1984). Morphologic dating of fluvial terraces scarps and fault scarps near West Yellowstone, Montana, Geol. Soc. Am. Bull. 95, 1413-1424.

Pierce, K.L., and S.M. Colman. (1986). Effect of height and orientation (microclimate) on geomorphic degradation rates and processes, late-glacial terrace scarps in central Idaho, Geol. Soc. Am. Bull. 97, 869-885.

Scott, W.E, K.L. Pierce, J.P. Bradbury, and R.M. Forester. (1982). Revised Quaternary stratigraphy and chronology in the American Falls area, southwest Idaho, in Cenozoic Geology of Idaho, B. Bonnichsen and R.M. Breckenridge, eds., Idaho Bureau of Mines and Geology Bull. 26, 581-595.

Figure Captions

Figure 1. Map of the Jenny Lake Junction study site (GTNP).

Figure 2. A strong correlation between scarp offset and morphologic age is observed at the Jenny Lake Junction study site (GTNP). Differences in morphologic age are unrelated to the relative ages of the terraces.

Figure 3. Although there may be a slight tendency for aspect to affect the normalized morphologic age at the Jenny Lake Junction study site (GTNP), the tendency is not nearly as strong as that documented by Pierce and Colman (1986).

Figure 4. A fairly strong correlation between scarp offset and morphologic age is observed at the Teton Point Turnout study site (GTNP). Extrapolating the linear relationship to lower scarp offset yields negative morphologic ages (an impossibility).

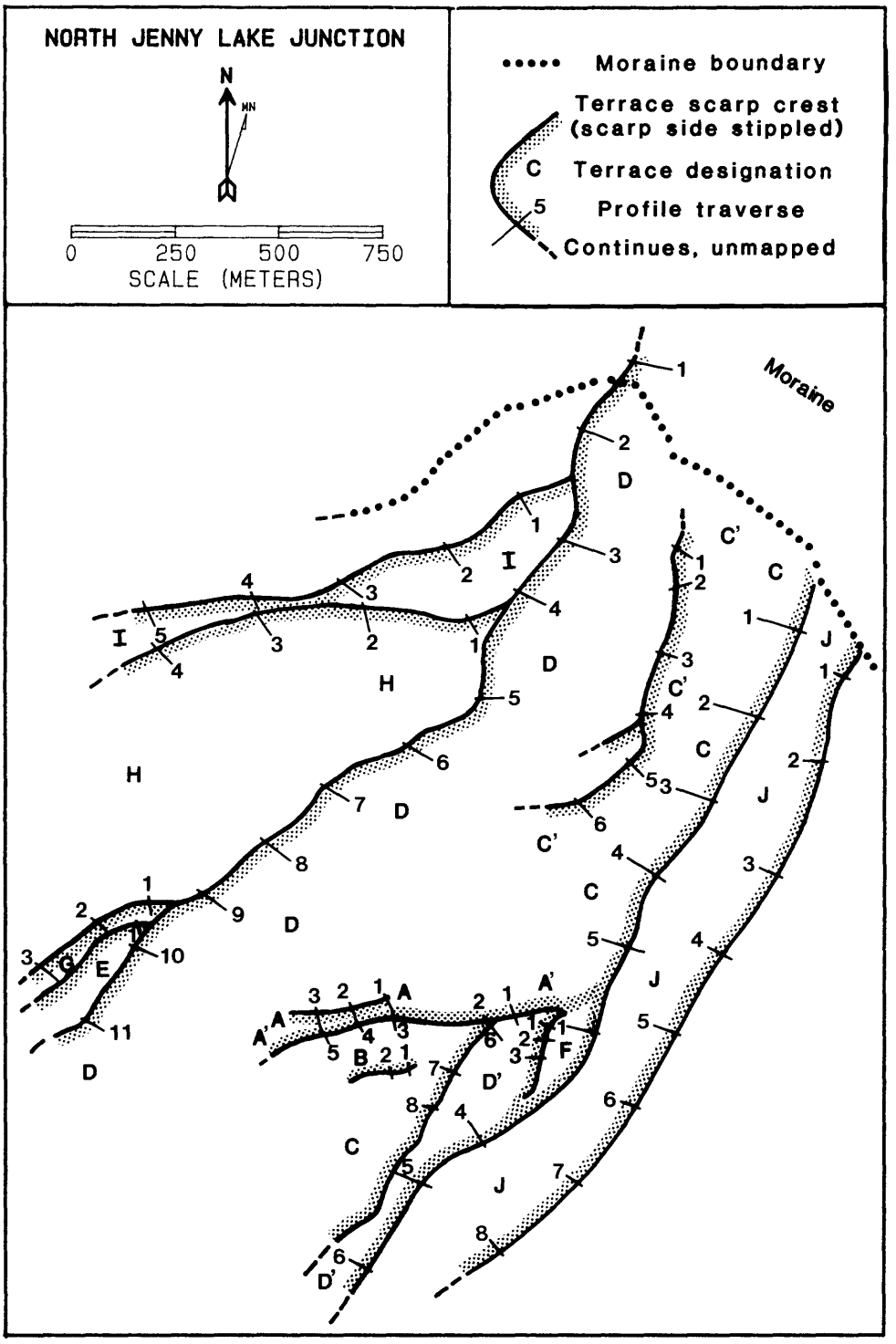
NORTH JENNY LAKE JUNCTION
N
MN
0 250 500 750
SCALE (METERS)
Moraine boundary
Terrace scarp crest (scarp side stippled)
C Terrace designation
5 Profile traverse
Continues, unmapped
Moraine

FIGURE 1

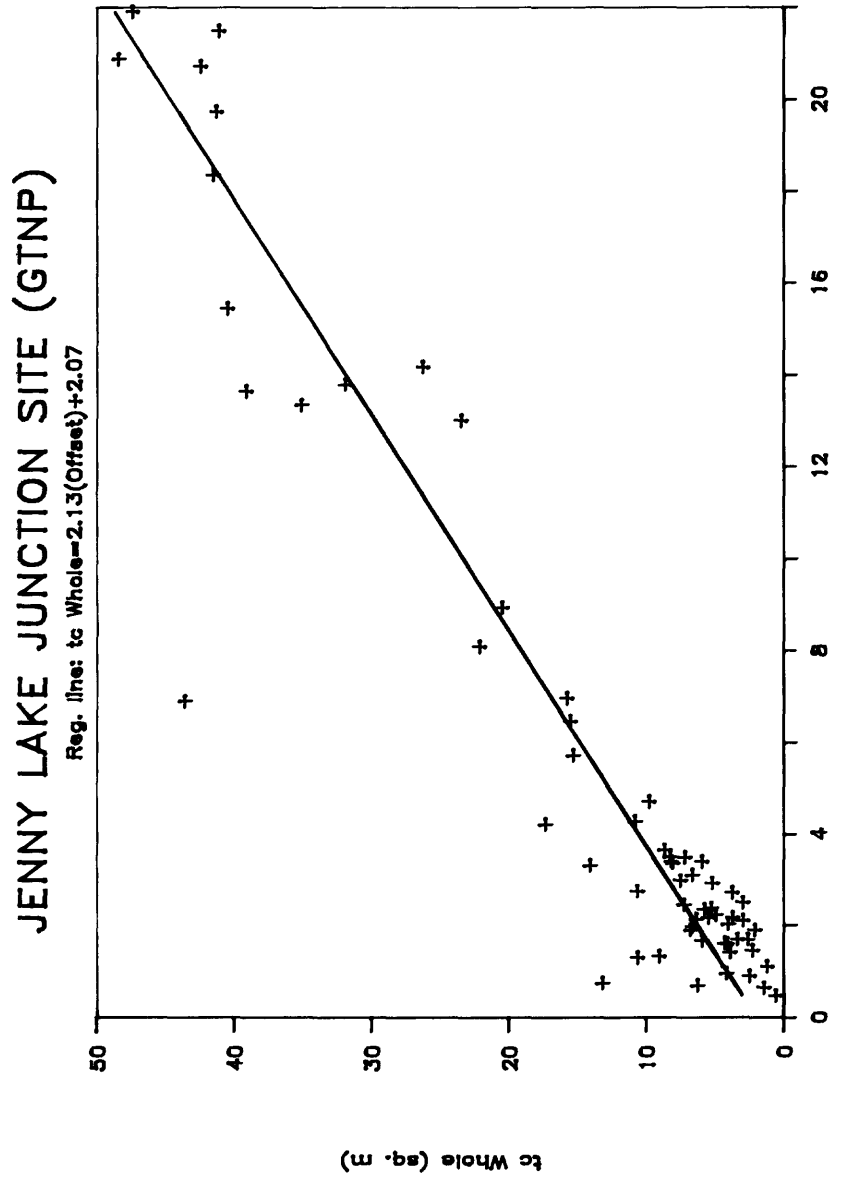
JENNY LAKE JUNCTION SITE (GTNP)
Reg. line: tc Whole=2.13(Offset)+2.07
tc Whole (sq. m)
Scarp Offset (m)
(r = .94)
0
10
20
30
40
50
0
4
8
12
16
20

FIGURE 2

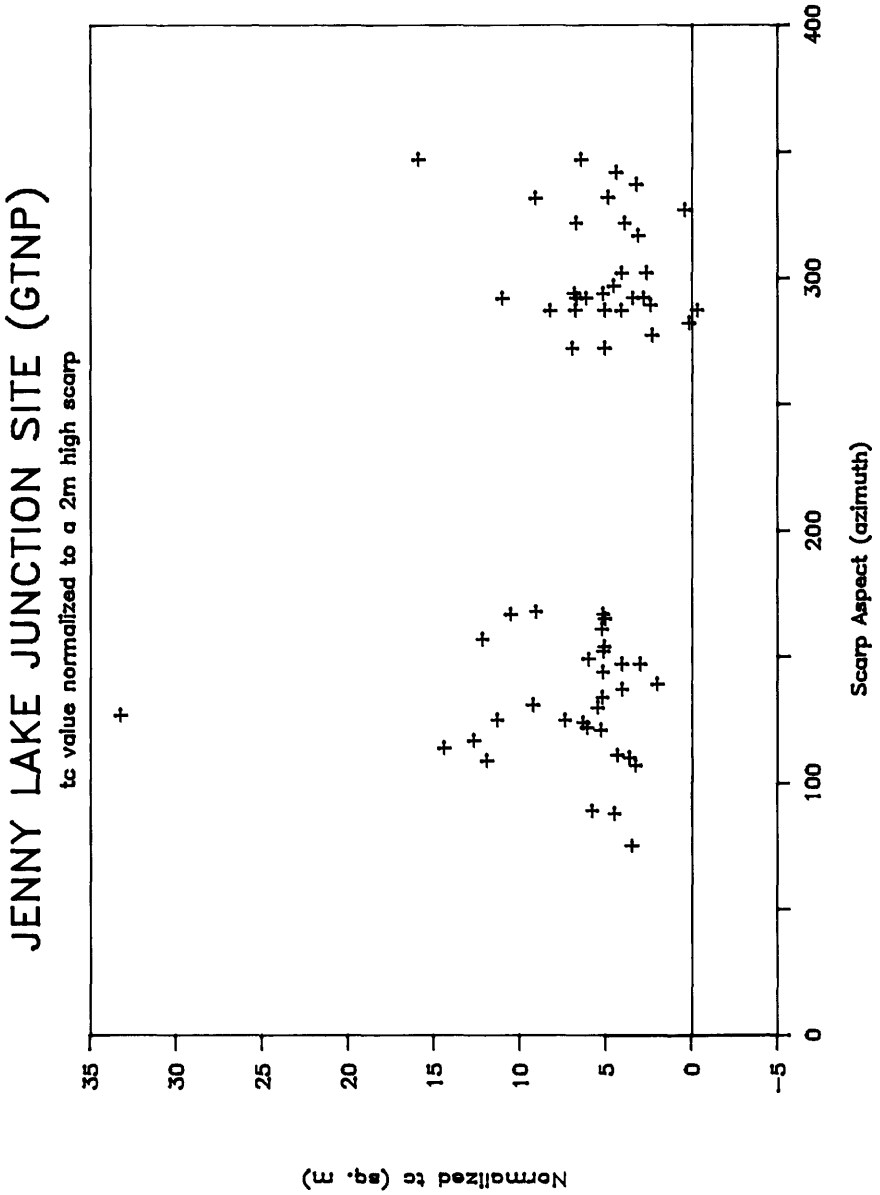
JENNY LAKE JUNCTION SITE (GTNP)
tc value normalized to a 2m high scarp
Normalized tc (sq. m)
35
30
25
20
15
10
5
0
-5
0
100
200
300
400
Scarp Aspect (azimuth)

FIGURE 3

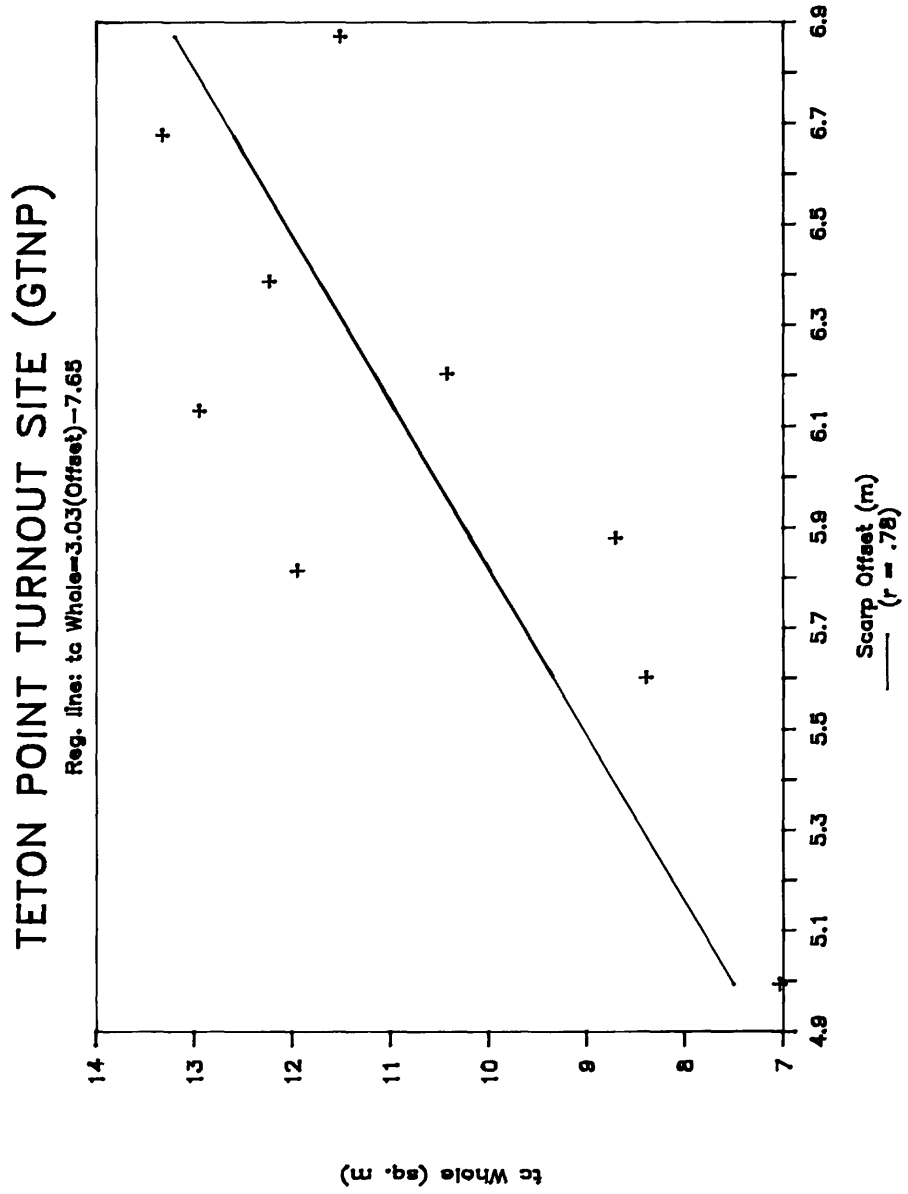
TETON POINT TURNOUT SITE (GTNP)
Reg. line: tc Whole=3.03(Offset)-7.65
tc Whole (sq. m)
14
13
12
11
10
9
8
7
4.9
5.1
5.3
5.5
5.7
5.9
6.1
6.3
6.5
6.7
6.9
Scarp Offset (m)
(r = .78)

FIGURE 4

EVALUATION OF ACTIVITY OF THE SAN GABRIEL FAULT ZONE, LOS ANGELES AND VENTURA COUNTIES, CALIFORNIA

14-08-0001-21928

F.H. Weber, Jr.
California Department of Conservation
Division of Mines and Geology
107 South Broadway, Room 1065
Los Angeles, CA 90012
(213) 620-3560

Investigations

The State of California only recently has approved expenditure of the funds for trenching and other excavation work planned. At this writing on October 7, 1986, a detailed budget is being prepared for final allocation of funds for carrying out the work. While awaiting approval of funds for the excavation work, the portion of the contracted work involving geologic field mapping has continued.

Results

Detailed mapping between Hardluck Canyon and Castaic continues to provide evidence that lateral slip along the San Gabriel fault is small, in contrast to findings of previous studies. For example, Crowell (1982, p. 28-29) calculates that only about 2.5 km of right slip occurs along a segment of the principal strand of the fault zone in the Hardluck-Beartrap canyons area, between 7 and 13 km southeast of its northwestern terminus. Crowell (1982, p. 29) concludes, however, that "much larger displacements" took place on the Piru fault, a branch of the San Gabriel fault zone that lies to the southwest of the principal strand. Mapping by the writer shows, in contrast, that the Piru fault appears to be at least partly a depositional contact along which relatively minor faulting has taken place. The segment of this fault about 7 km southeast of the northwestern terminus of the San Gabriel fault zone dips only about 30° northeast. Furthermore, clasts of gneiss in Violin Breccia in fault contact there with Precambrian gniess to the southwest appear to be derived from that gneiss. It appears unlikely, therefore, that large right slip has taken place along the Piru fault, and that total right slip along the San Gabriel fault zone in the Hardluck-Beartrap canyons area is no more than 2.5 km.

Just northwest of Castaic, near the mouth of Violin Canyon, mapping shows that the San Gabriel fault zone is a throughgoing structure, as exposed along the ground surface. It is not overridden from the west by rocks of the Towsley Formation along an eastward extension of the Santa Felicia fault mapped by Yeats and others (1985) and Stitt (1986). No such fault can be observed within 1.5 km west of the San Gabriel fault.

References Cited

Crowell, J.C, 1982, The tectonics of Ridge Basin, southern California, in Crowell, J.C., and Link, M.H., eds., 1982, Geologic history of Ridge Basin, Southern California: Pacific Section, Society of Economic Paleontologists and Mineralogists, Los Angeles, California, p. 25-41.

Stitt, L.T., 1986, Structural history of the San Gabriel fault and other Neogene structures of the central Transverse Ranges, in Neotectonics in the area between the central and western Transverse Ranges, Field Trip No. 10, in Ehlig, P.E., compiler, Guidebook and Volume, Neotectonics and faulting in southern California: Prepared for the 82nd Annual Meeting of the Cordilleran Section of the Geological Society of America, Los Angeles, California, March 25-28, 1986, p. 43-102.

Yeats, R.S., McDougall, J.W., and Stitt, L.T., 1985, Cenozoic structure of the Val Verde 7 1/2-minute quadrangle and south half of the Whitaker Peak 7 1/2-minute quadrangle, California: Final Technical Report to U.S. Geological Survey, Contract No. 14-08-21279, 32 p.

Reports

Weber, F.H., Jr., 1986 (in press), Geologic relationships along the San Gabriel fault between Hardluck Canyon and Castaic, Los Angeles and Ventura counties, California: California Geology.

Central California Deep Crustal Study

9540-02191

Carl M. Wentworth
Branch of Western Regional Geology
U.S. Geological Survey
345 Middlefield Road, MS 975
Menlo Park, California 94025
(415) 323-8111 ext. 2474

Investigations

Seismic reflection profiling, in concert with other geophysics and geology, is being used to examine crustal structure between the California Coast Ranges and the Sierran foothills (see map, p. 149, USGS Open-File Report 85-22 for location of profiles; line CC-2 extends 30 km further into the Sierra Nevada than shown).

1. Contrary to earlier assertions, processing of reflection lines CC-1 and CC-2 continued.

2. Interpretation of CC-1 and CC-2 continued, in concert with adjacent refraction profiles and coordinated gravity and magnetic modeling.

3. Work on basement configuration was extended in preliminary fashion to the Sacramento Valley (with Jachens and Griscom).

4. Revision of the Wentworth/Zoback chapter for the Coalinga professional paper was completed.

5. Tentative consideration of the tectonics of the Parkfield, CA region began (with Jachens and Simpson).

Results

1. It was discovered that the prominence and evident continuity of events in reflection lines CC-1 and CC-2 was highly sensitive to playback parameters, particulary gain (AGC). Greatly improved record sections have now been produced, after considerable experimentation, in which reflections are clearly evident beneath the basement surface in the Great Valley on CC-1 and at shallow depth in the Sierran foothills on CC-2.

2. Consideration of CC-1 and CC-2 together yield evidence of eastward-directed obduction, both in assembly of the Sierran foothills and in emplacement of the Franciscan assemblage farther west. East-dipping structure in the Foothills metamorphic belt seems to be expressed in the reflection record there, and seems to persist westward beneath the Great Valley where a first order boundary indicated by magnetic and gravity modeling also dips eastward. These upper crustal features are underlain by strong, west dipping (35^{o}) reflections that seem to represent a mid-crustal zone of thrusting that, in turn, obliquely truncates underlying layered structure. Beneath exposed Franciscan rock at the west end of CC-1, a

narrow band of reflections at the base of 5.8 km/s rock obliquely transects abundant horizontal events and rises gently eastward. In depth section, this band is aligned with the base of a 5.5-5.7 km/s layer that forms the uppermost basement in the Great Valley to the east. We suggest that this upper basement layer is an eroded remnant of Coast Range ophiolite that extends westward beneath the Franciscan, but because of its similar velocity is indistinguishable there from the overlying Franciscan. Exposed Coast Range ophiolite underlies a depositional base of the Great Valley sequence at several places in the eastern Coast Ranges and could have been variously overridden or peeled up with the Great Valley sequence by eastward thrusting of the Franciscan wedge.

3. The surface of crystalline basement beneath the San Joaquin Valley that is reached by the drill dips gently westward. About three-quarters of the way westward across the valley, according to refraction and reflection profiles, this surface steepens westward, and reaches a depth of 15 km beneath the easternmost Coast Ranges. This steepening is spatially associated with a west-facing gravity gradient that extends the length of the Great Valley. Computer location of the steepest part of this gradient (using Magspot) demonstrates this association and predicts the location of the breakover along the western side of the Sacramento Valley. The young Dunnigan Hills anticline near Woodland lies just west of the implied breakover and may, like Coalinga anticline, be a product of eastward-directed thrusting that abuts a shallowing basement.

4. The Stockton arch at the northern end of the San Joaquin Valley is defined by the northeastward-trending Stockton fault and, to the southeast, by erosional truncation of gently southeast-dipping strata beneath a mid-Tertiary unconformity. The implied structural arch or southeastward tilt is not, however, expressed in the surface of underlying crystalline basement. This fact seems to require either that the arching resulted from supra-basement thrusting -- perhaps northward-directed thrusting in the early Tertiary, to couple with the revised, up-to-the-south movement of the Stockton fault at that time -- or that the southern flank of the arch is simply the result of a major sedimentary thickening of Cretaceous strata beneath the apparent arch. Participation in the Parkfield Drilling Workshop at Asilomar, fall, 1986, demonstrates the need for a synthesis of the regional tectonic setting of the Parkfield reach of the San Andreas fault as part of the current studies of the impending Parkfield earthquake. Preparation for the workshop, using Dibblee's 1:62,500 geologic maps and available gravity and magnetic surveys, yielded exciting questions and a very stimulating cartoon of structure in the region. We find that large subsurface masses of serpentinite and high density rock can be inferred adjacent to the Parkfield reach of the San Andreas and that only the western boundary fault consistently truncates geophysical features along its length. Major cross-cutting structures trend toward both ends of the Parkfield fault reach from the east. Abundant evidence of compression perpendicular to the fault, including the Coalinga thrusts only 35 km to the northeast, complicates a simple strike-slip view. Deformational behavior of the blocks east and west of the San Andreas is strikingly different. Our attempt to draw a crustal cross section through the Coalinga and Parkfield hypocenters raises major anatomical and kinematic questions.

Reports

Wentworth, C.M., 1986, Testing an obduction model of Franciscan emplacement, Coast Range-Great Valley boundary, California (abs.): DOSECC, inc. (abstracts for) Continental Scientific Drilling Wrokshop, Rapid City, South Dakota, June 12-14, 1986, P. 69-70.

Wentworth, C.M., Colburn, R.H., Griscom, A., Jachens, R.O., Mooney, W.D., Walter, A.W., Whitman, D., Holbrook, W.S., and Zoback, M.D., 1986, A geophysical transect across central California (abs.): University of Cambridge, Department of Earth Sciences, Second International Symposium on Deep Seismic Reflection Profiling of the Continental Lithosphere, July 15-17, 1986, Abstracts of Lectures and Posters, p. 14.

Wentworth, C.M., and Zoback, M.D. 1986, An integrated faulting model for the Coalinga earthquake: a guide to thrust deformation along the Coast Range-Great Valley boundary in central California (abs.): American Geophysical Union, 1986 full meeting, accepted.

Wentworth, C.M., Zoback, M.D., Griscom, Andrew, Jachens, R.O. and Mooney, W.D., 1986, A transect across the Mesozoic accretionary margin of central California: Geophysical Journal, Royal Astronomical Society, special volume on Deep Seismic Reflection Profiling of the Continental Lithosphere, submitted.

Zigler, J.L., Frei, L.S., Wentworth, C.M., and Bartow, J.A., 1986, Structure contour map of the top of the Temblor Formation in the Kettleman Hills and Lost Hills areas, Fresno, Kings, and Kern Counties, California: U.S. Geological Survey Miscellaneous Field Studies Map MF-1896, scale 1:100,000, in press.

Zigler, J.L., Wentworth, C.M., and Bartow, J.A., 1986, Structure contour map of the tops of the Kreyenhagen Formation and Cretaceous strata in the Coalinga area, Fresno and Kings Counties, California: U.S. Geological Survey Miscellaneous Field Studies Map MF-1843, scale 1:100,000.

Comparative Study of the Neotectonics of the Xianshuihe Fault, China

Grant No. 14-08-0001-G1088

Clarence R. Allen
Seismological Laboratory, California Institute of Technology
Pasadena, California (818-356-6904)

Objectives

The purpose of this study is to investigate, together with Chinese colleagues from the Bureau of Seismology of Sichuan Province, the Xianshuihe fault of western Sichuan. This structure is among the world's most active faults, having producing 3 earthquakes during this century exceeding magnitude 7 along a 200-km length of the zone. At least 6 such events have occurred since 1725. In the more limited 60-km-long segment between Luhuo and Daofu, major earthquakes in 1923, 1973, and 1981 (M = 7½, 7.6, 6.9) were associated with overlapping surficial fault ruptures, and with individual left-lateral displacements as large as 3.6 m. Specific objectives of the study include the questions of (1) whether the current burst of activity is typical of late Quaternary activity, (2) whether the high degree of activity of the fault could be readily ascertained from physiographic features even in the absence of the historic record, and (3) a comparison of neotectonic features of the Xianshuihe fault with those of other active strike-slip faults in China and elsewhere.

Results

The Principal Investigator, together with Caltech graduate student Zhou Huawei, visited China from 8 May to 20 June 1986, and, with superb cooperation from the Sichuan Bureau of Seismology, we were able to spend about one month in the field along the Xianshuihe fault. The principal Chinese participants were Luo Zhuoli, Director of the Sichuan Bureau, and geologists Qian Hong and Wen Xueze. These scientists will visit the United States during November and December, at which time our final report will be put together. At the moment, we are still waiting for the results of Carbon 14 dating, which will be critical in establishing a slip rate for the fault.

The Xianshuihe fault is remarkably well exposed and is intermittently easily accessible throughout the 300-km-long segment from Moxi on the southeast to near Ganze on the northwest, and most of this segment was visited during this study. Physiographic features of recent faulting are even more obvious than along much of California's San Andreas fault, owing to (1) the recent ground-rupturing 1923 and 1973 earthquakes, (2) the fact that frequent magnitude 7-7½ events may give rise to fresher appearing geomorphic features than infrequent magnitude 8 events, even at comparable or lower slip rates, (3) the fact that several of the recent earthquakes have occurred in mid-winter, rupturing the frozen ground in a blocky, truly spectacular manner, and (4) the high altitude (to 4300 m) and relatively dry climate (av. precip. 600

mm/yr), which tend to preserve geomorphic features of late Quaternary faulting. En-echelon fractures associated with the 1973 Luhuo earthquake (M = 7.6), which was associated with lateral displacements of up to 3.6 m, still appear remarkably fresh. Moreover, individual en-echelon cracks of the 1923 earthquake (M = $7\frac{1}{2}$), centered farther southeast, are also still visible, as are, questionably, cracks associated with the 1893 event still farther southeast near Laoqianning (M = 6-3/4). Progressing even farther southeast, en-echelon fractures resulting from the 1955 "Kangding earthquake" on the Zheduotang fault are also still clearly visible. We were able to document overlapping ruptures from several of these events to a greater extent than previously thought. Much of the fault physiography is reminiscent of that of the San Andreas fault in California's Carrizo Plain, and the fault could, almost of first glance, be identified as having a high degree of activity as compared, e.g., to the Red River fault of Yunnan Province.

Various offset geologic features hold promise of yielding Carbon 14 dates and will hopefully permit assignment of an accurate slip rate to the Xianshuihe fault. Among these features are offset terrace risers, offset stream-channel fillings, and offset glacial moraines. The moraines, in particular, are cleanly displaced and represent the latest Pleistocene ice advance; four of these moraines were identified and three were visited and sampled during this study. The fact that some cultural features near Luhuo (e.g., terraced field edges) are offset at least twice as much as the displacement observed nearby during the 1923 earthquake suggests that the burst of seismicity during this century represents ongoing activity, probably characteristic of late Quaternary time. Identification of these various offset features would have been virtually impossible without the use in the field of excellent vertical aerial photographs.

The northwestern 180-km-long segment of the fault is relatively continuous and simple, with a single major active trace and without major step-overs. Almost all of this segment is easily accessible, because the main Chengdu-Lhasa road follows the fault-controlled rift valley. South of Laoqianning, the recent trace abruptly terminates, and its place is taken locally by a fault of different orientation with a large normal component of displacement. Still farther southeast, between Laoqianning and Kangding, several sub-parallel branches of the fault are present within the 12-km-wide fault zone, and one of these branches apparently broke throughout its entire 25-km length during the 1955 earthquake, of M = 7.5. Southeast of Kangding, the fault again is marked by a relatively simple single trace, at least as far as Moxi; this segment of the fault probably last broke in 1786 ($M \geq 7\frac{1}{2}$) and represents a particular dangerous segment of the fault at the present time.

One of the most intriguing aspects of the Xianshuihe fault is the fact that creep is currently occurring along parts of it, and this has been particularly well documented by Chinese investigators near Xialatuo and Luhuo. But it is still not clear whether this slip represents after-creep of the 1973 earthquake, which was centered in this area, or whether it represents continuing creep similar to that on parts of the San Andreas fault. The presence of creep along parts of the Xianshuihe fault, taken together with its high degree of historic seismic activity, overlapping ruptures, segmentation, excellent exposures, and relatively good accessibility, make it a particularly promising feature for earthquake-prediction and hazard-evaluation studies.

Investigations of late Pleistocene and Holocene Thrust Faulting in Coastal California north of Cape Mendocino.

14-08-0001-G1082
Gary A. Carver and Raymond M. Burke
Department of Geology
Humboldt State University
Arcata, CA 95521
(707) 826-3931

Investigations

1. Trenching and detailed analysis of selected sites on thrust faults in coastal northern California.
2. Field and laboratory analyses of catenas formed on scarps developed on terraces offset by thrust faults.

Results

Trenches were excavated across well defined scarps of the Mckinleyville, Mad River, and Little Salmon faults in coastal Humboldt Co., California. Each fault was investigated where it displaces a late Pleistocene or Holocene terrace and exhibits geomorphic, structural, and stratigraphic relationships pertinent to the faults paleoseismicity. Carbon samples obtained from key stratigraphic positions on the Mckinleyville and Little Salmon faults have been forwarded to a dating laboratory. Soils of the fault scarp related catenas exposed in the trenches were described and sampled. Laboratory analysis of the soil samples has been started.

Summary of trench sites

Mckinleyville Fault- Blue Lake site:
During this study the Mckinleyville fault was trenched where it displaces a fluvial terrace of the Mad River near the town of Blue Lake. The trenches, placed across a prominent 6 meter high scarp, exposed an 18-to-24 degree northeast dipping thrust fault displacing river terrace gravels and an overlying floodplain sequence. The overlying sequence consists of well stratified lacustrine silts, overbank floodplain silts and sandy gravels, and several scarp-derived colluviums. Wood, peat, and charcoal were obtained

from several of the lacustrine, floodplain and colluvial units for radiometric dating. Geomorphic position of the terrace and soil development on the terrace sediments suggest a latest Pleistocene or early Holocene age for the terrace gravels, lacustrine silts, and floodplain stratigraphy, and a late Holocene age for the colluviums.
The fault is traceable to within 0.8 meters of the ground surface, and displaces floodplain sediments of the hanging wall a minimum of 3.3 meters over a distinctive colluvium and zonal soil in the footwall. We interpret this displacement to represent the minimum slip resulting from the last faulting event. In addition to fault displacement, anticlinal folding of the hanging wall contributed to the development of the scarp. Beds above the fault plane dip as steeply as 45 degrees toward the footwall within 10 meters of the fault, and are overturned within 2 meters of the fault plane. Angular unconformities within the floodplain stratigraphy in the hanging wall and between older, more deeply buried scarp-derived colluviums in the footwall suggest at least 4 slip events of similar displacement (~3.5 meter per event) have occurred since the cutting of the terrace. Total dip slip displacement of the terrace gravels is ~12 meters.

Mad River fault- School road site:
During this study the northernmost imbricate strand of the Mad River fault was trenched where it displaces a late Pleistocene Marine terrace about 1 km inland from the coastline. The trench exposures show the near surface expression of the fault is a sharp overturned anticline. The terrace abrasion surface, cut into Franciscan complex lithologies, and the terrace cover deposits, including an abrasion lag of rounded and polished cobbles and boulders, and a well stratified sequence of marine terrace sands and gravels, provide datums traceable across the fold. The overturned limb of the fold contains the overturned terrace abrasion surface, abrasion lag, and terrace cover deposits with an overturned zonal soil preserved in the cover deposits.
Six well defined scarp-derived colluvial wedges, each with a basal stone line consisting of cobbles eroded from the abrasion lag, extend downslope from beneath the overturned limb of the fold. The anticline is interpretated to represent a fault propagation fold at the tip of a shallow blind thrust. A fault tip exposed below the lowest colluvial wedge in one trench dips to the northeast at 20 degrees. Each of the colluvial wedges is about 1.5 m thick at its upper end where it terminates against the overturned fold limb. These colluvial wedges are interpreted to represent colluvial sheets shed from the scarp crest after slip events and associated growth of the fold. Preliminary calculations of the amount of slip, on a 25 degree dipping

blind thrust, necessary to generate the fold growth represented by the colluvial wedges is about 3.5 m per event. Because only one of three principal imbricate thrusts of the Mad River Fault was investigated , the magnitude and number of slip episodes interpretated reflects a minimum for the paleoseismicity.

Little Salmon fault- Little Salmon Creek site:
During this study, a site in the lower Little Salmon Creek valley where the flat valley floor is vertically offset across a zone of scarps, troughs, and mole-track like ridges was investigated in detail. The site is located on the western of two traces of the Little Salmon Fault. The valley floor of Little Salmon Creek is composed of silty floodplain sediments graded to the present margin of Humboldt Bay; thus it is interpreted to be late Holocene.

The sediments exposed in the trenches are well stratified and include sequences of thinly laminated lacustrine silts. The scarps, swales, and ridges correspond to large open folds and small 10-to-30 degree northeast dipping thrusts developed in the valley fill sediments. The deformation encompasses a zone approximately 80 meters wide. The valley floor is 8 meters higher on the northeast side of the zone. A distinctive laminated lacustrine silt unit was traced in the trench exposures across the deformed zone and found to be at least 12 meters higher on the northeast side. Well stratified floodplain silts and sands overlay the lacustrine marker unit on the downdropped southwest side of the deformation zone and onlap the lacustrine unit in the flank of the folds. The folds and faults are interpreted to represent deformational structures resulting from slip at the tip of a shallow northeast dipping burried thrust, with most of the slip accommodated at the surface by folding. Preliminary analysis of the structures in the valley fill sediments suggests at least 25 meters of slip on a 25 degree dipping blind thrust is required to generate the structures found in the trenches. The amplitude of the folds is greater for lower stratigraphic levels exposed in the trenches and the higher units in the floodplain sequence show depositional onlapping on the uplifted structures, indicating growth of the structures during the depositional history of the valley.
The youngest floodplain sediments are elevated more than 2.6 meters across the deformation zone and cut by a single thrust fault which extends to within 0.6 meters of the surface, the depth of active bioturbation. This floodplain unit buries the base of existing redwood tree stumps, and has an extremely weak soil development. The evidence thus suggests the last slip event occured within the last few hundred years and involved as much as 6

meters of slip. Wood and charcoal collected from key stratigraphic positions have been submitted to a dating lab.

Soil Catenas. To date, 28 soil profiles have been descibed from backhoe pits and trenches across the three fault scarps in an effort to establish pedologic and geomorphic variations down scarps of various ages. Preliminary analysis of the field data has been completed and laboratory analyses have begun. Soils were described in five catenary positions along the slope from the crest to the toe of the scarp. In all cases, the crest and shoulder positions appear to be areas of erosion while toe and footslope positions appear to be areas of deposition. Soils formed on backslope positions appear to be formed in sites of erosion above the trace of the fault, but in sites of depositon below the trace of the fault. This complexity of soil development is increased with depostion off the scarp which is formed either by the fault or the associated fold in the upper plate.

Soils on the Mckinleyville fault are generally A/Bw/C profiles except in the toe position where only an A/C profile is expressed. The soils near the upper end of the slope are complicated by the colluvial units but there is a noticable lack of buried soils suggesting a fairly short time between colluviation events. Because the original stratigraphy of the surficial units can still be recognized and are not involved in bioturbation of the surface soil, the total time of soil development is suggested to be late Pleistocene to Holocene in age.
Soils formed on the Mad River fault scarp are like those of the catena formed on the Mckinleyville fault scarp. The similar catenary relationships and the similar degree of soil development suggest similar ages for the formation of the two scarps. The soils of the Mad River scarp appear to represent slightly more total weathering and thus slightly more total time. There are weak,but distinct, buried soils in the colluvial units associated with the stone lines giving support to the idea of a measurable amount of time between colluvial (and thus slip) events. As mentioned above, there does appear to be a partially preserved soil which is overturned in the fold of the upper plate.
Soils formed on the catena of the Little Salmon fault scarp are extremely weak profiles with only A/C development throughout the slope. There are some buried units in the lower backslope position which have retained an A/C profile similar to the surface soil development. These suggest there has been a similar amont of time between the depostion of these units.

Late Pleistocene and Holocene Paleoseismicity of the San Gabriel Fault

14-08-0001-G1196

William R. Cotton
William Cotton and Associates
318B North Santa Cruz Avenue
Los Gatos, California 95030
(408) 354-5542

Objectives:

Our goal is to establish a Holocene chronology of faulting along the Rye Canyon segment of the San Gabriel fault near Valencia, California. Radiocarbon ages for a number of post-Pleistocene alluvial horizons, in conjunction with fault-dislocation measurements for a variety of geologic piercing points, hold the potential for slip-rate determinations. In addition, the sense of slip on the fault during Holocene time can be established by subsurface exploration of buried paleogeomorphic features, as well as by excavations to expose fault-gouge slickensides and associated striae.

Results:

1. 28 24" bucket auger borings enabled us to contour the surface of a paleoridge that is buried beneath Holocene alluvium. The ridge is truncated by the active surface of the San Gabriel fault. Across the fault the paleoridge was exposed by a deep bulldozer cut during field work in prior years. The ridge axis has been offset between 15 feet and 21 feet in a right-lateral sense, with a dip-slip component such that the southwest side of the fault is up between 2 feet and 5 feet with respect to the northeast side.

2. A paleochannel located to the immediate south of the paleoridge is also offset in an oblique-slip manner. The right lateral component is 18.6 feet, with the southwest side up 5.5 feet.

3. Slickensides and associated striae exposed on fault-gouge surface were measured at plunge angles of between 14° and 30°, with the prominent and most frequently observed values in the $20° \pm 6°$ range. This describes the dip-slip component of what has been dominantly right-lateral movement during the Holocene Epoch on the near-vertical San Gabriel fault. Such a dip-slip component is consistent with the offsets observed on the paleoridge and the paleochannel described above.

4. A preliminary slip-rate determination of approximately .6 mm/yr. is suggested by the amount the paleoridge and the paleochannel have been displaced during Holocene time, assuming that alluvial burial of these paleogeomorphic features began at the close of the Pleistocene Epoch.

5. Additional field work remains. It will investigate dislocated stratigraphic horizons that are younger than the exhumed paleochannel, and collect from them charcoal to be used for slip-rate determinations.

Publications:

Cotton, W.R., 1986, "Holocene Activity of the San Gabriel Fault, Valencia, California", The Geological Society of America, Cordilleran Section, Abstracts with Programs, 18 (2):96.

Cotton, W.R., 1986, "Holocene Paleoseismology of the San Gabriel Fault, Sangus/Castaic Area, Los Angeles County, California", in Neotectonics and Faulting in Southern California (Guidebook and Volume), GSA, Cordilleran Section, 82nd ann. mtg., p. 31-41.

Source and Seismic Potential Associated with Reverse Faulting and Related Folding

14-08-0001-G1165

Edward A. Keller
Dept. of Geological Sciences
University of California
Santa Barbara, California 93106
(805) 961-4207

Objective: Investigate tectonic framework, geometry, and uplift rates associated with folding on upper plates of buried reverse faults. Study sites are Wheeler Ridge, San Emigdio Canyon, and the Los Lobos folds near Bakersfield, California.

Results: Active tectonics at the Southern end of the San Joaquin Valley is demonstrated near the piedmont area of the San Emigdio Mountains at Wheeler Ridge and San Emigdio Canyon. Rates of uplift derived from 14-C dates on deformed alluvial surfaces from the latest Pleistocene and Holocene to present along the piedmont are approximately 2 to 4 mm/yr.

Wheeler Ridge anticline is actively forming on the upper plate of a buried thrust fault system. The rate of uplift associated with folding, from latest Pleistocene and Holocene to present at Wheeler Ridge is about 1.4 mm/yr. Immediately south of Wheeler Ridge, the San Emigdio Mountains are being uplifted at the front by the active Pleito fault at a rate of about 0.5 mm/yr. (Hall, 1984). Therefore, the combined rate of uplift along the piedmont is about 2 mm/yr. A paleosol is offset vertically, approximately 26 m along the Pleito fault (Hall, 1984), and this soil is folded over the Wheeler Ridge anticline with a minimum of 90 m of vertical displacement. This soil at Wheeler Ridge is estimated to be 90 to 150 ka, suggesting that total uplift since late Pleistocene is close to 2 mm/yr.

At San Emigdio Canyon the mountain front has migrated several km northward since late Pleistocene time, as delineated from detailed geomorphic evaluation of the San Emigdio Canyon alluvial fan. Radial profiles of the oldest (buried) fan segment places the late Pleistocene position of the fan apex at an intramontane mountain front that coincides approximately with the location of the Pleito fault. Radial profiles of younger segments point to the present active mountain front. These relationships are shown on Figure 1. At San Emigdio Canyon, the Pleito fault is no longer active and active deformation is presently along the range bounding Wheeler Ridge and Los Lobos faults.

Their presence is indicated by active folding and subsurface data. Holocene rates of uplift due to folding above the concealed Wheeler Ridge and Los Lobos faults are respectively 2.0, 1.6 mm/yr., providing a combined rate of 3.6 mm/yr. for the front.

REFERENCES CITED:

Hall, N.T., 1984, Late Quaternary history of the eastern Pleito thrust fault, northern Transverse Ranges, California: unpublished Ph.D. thesis, Stanford University, California.

PUBLICATIONS:

Laduzinsky, Dennis, M., Seaver, Din B., and Keller, Edward A., 1986. "Tectonics of an active fold-thrust belt." The Geological Society of America, Abstracts with Programs 18 (2): 126.

Seaver, D. B., 1986, "Quaternary evolution and deformation of the San Emigdio Mountains and their alluvial fans, Transverse Ranges, California: unpublished M.A. thesis, Department of Geological Sciences, University of California, Santa Barbara.

Zepeda, Ricardo, L., Keller, Edward A., and Rockwell, Thomas K., 1986. "Rates of active tectonics at Wheeler Ridge, Southern San Joaquin Valley, Californa." The Geological Society of America, Abstracts with Programs 18 (2): 202.

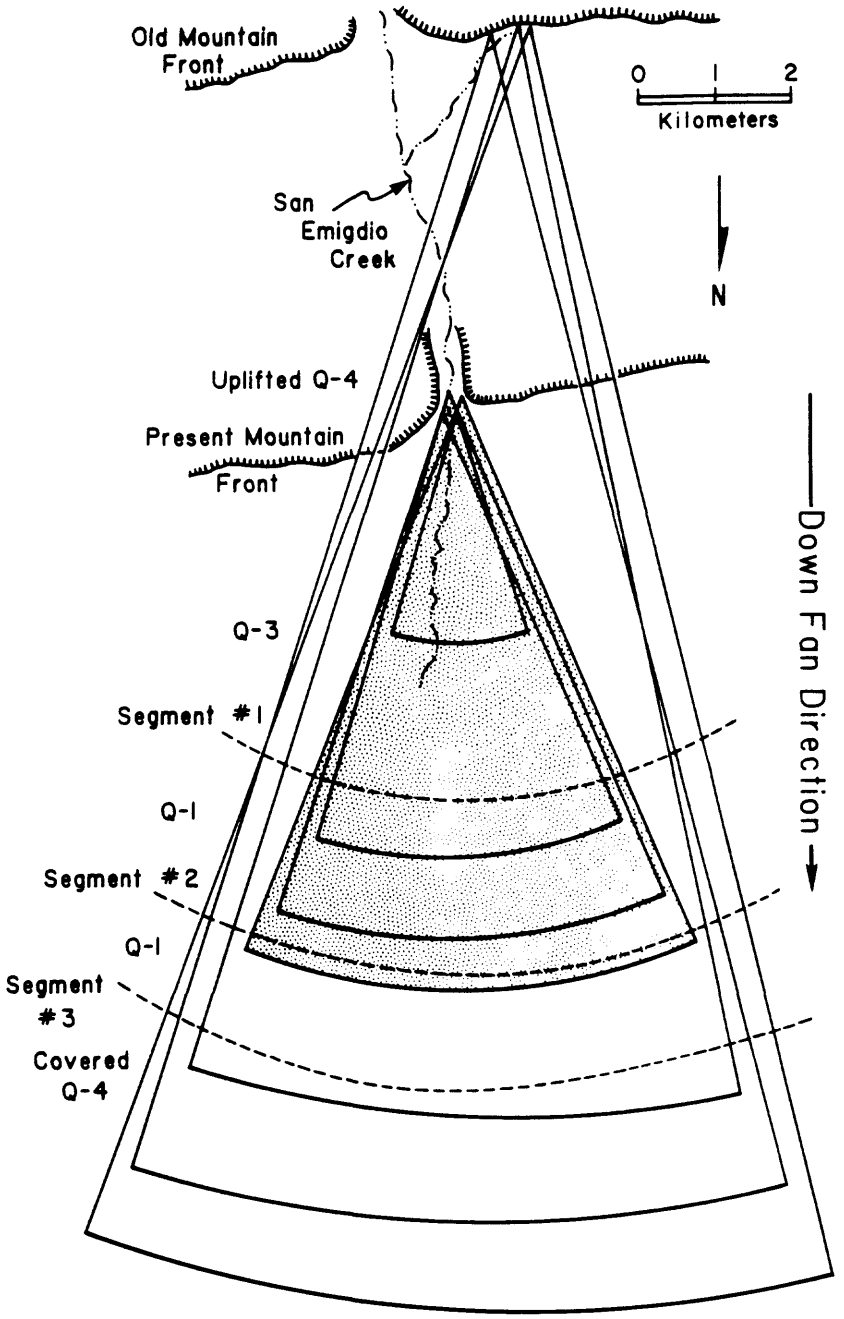

Figure 1: Radial profiles of the San Emigdio Canyon fan. The age of Q4, which is the older fan segment covered by Q1 deposits, is estimated to be 130,000 years. The Q3 surface is Holocene in age (Seaver, 1986).

Paleomagnetism of the Neogene Saugus Formation, Transverse Ranges, California: Timing and Deformation Rates of Potentially Active Faults

14-08-0001-G1155

Shaul Levi

Geophysics, College of Oceanography
Oregon State University
Corvallis, Oregon 97331
(503) 754-2912

Background:

We are continuing paleomagnetic investigations of the Saugus Formation in Los Angeles County, California to determine tectonic movements, timing and deformation rates associated with potentially active faults. Our previous studies have shown that the Saugus in this area was deposited during the Matuyama and Brunhes chrons (Levi, et al., 1986).

Results:

1) Initial paleomagnetic results were obtained from six Saugus sedimentary beds in the Horse Flats syncline, where the uppermost Saugus reflects coeval uplift of the Santa Susana Mountains (Saul, 1975) and initial movement of the Santa Susana Fault (Yeats, 1979). Our results to date indicate that three sites have normal polarity. The data from the remaining units is difficult to interpret, as their remanence may reflect overprinting. However, there are no indications of reversed remanence at any of these sites. At present we interpret these results to indicate that the uppermost Saugus sediments at the Horse Flats syncline were deposited during the Brunhes chron and therefore are younger than 0.73 Ma, implying that their uplift and folding has occurred since that time.

2) Additional Saugus sites (including the Sunshine Ranch Member) were sampled along the Van Norman Lakes, and the paleomagnetic measurements are currently in progress.

3) In the San Gabriel block we sampled the Saugus exposed in Soledad Canyon along the Southern Pacific railroad tracks adjacent to and northeast of the San Gabriel Fault to study the effect of the fault on tectonic rotations. Paleomagnetic measurements of these units are not yet completed.

References:

Levi, S., Schultz, D.L., Yeats, R.S., Stitt, L.T., and Sarna-Wojcicki, A.M., 1986, Magnetostratigraphy and paleomagnetism of the Saugus Formation near Castaic, Los Angeles County, California: in Neotectonics and Faulting in Southern California, Cordilleran Section Field Trip Guidebook and Volume, p. 103-108, Geological Society of America, Los Angeles, California.

Saul, R.B., 1975, Geology of the southeast slope of the Santa Susana Mountains and geologic effects of the San Fernando earthquake, California Div. Mines and Geology Bull., v. 196, p. 187-194.

Yeats, R.S., 1979, Stratigraphy and paleogeography of the Santa Susana fault zone, Transverse Ranges, California: Pac. Sec., Soc. Econ. Paleontologists and Mineralogists Cenozoic Paleography Symposium, p. 191-204.

ANALYSIS OF RECURRENT HOLOCENE FAULTING NORTHERN ELSINORE FAULT

Grant No. 14-08-0001-G1164

T.K. Rockwell
J.F. Brake
R.S. McElwain
Department of Geology
San Diego State University
San Diego, CA 92182

Objectives

The objectives of this investigation are to further constrain the timing of slip events, the displacement per event, and a slip rate on the Glen Ivy North strand of the Elsinore fault zone in Temescal Valley through a detailed study of the faulted late Holocene stratigraphy at Glen Ivy Marsh.

Results

Recent work has concentrated on determining lateral offset of specific channels and other features. Of particular note is the lateral offset, totalling about 50 cm, across two strands within the fault zone which moved only during the 1300 A.D. earthquake; some plastic deformation probably also occurred but the extent of this has not yet been determined. In addition, two historical features, a concrete flume and a terra cota pipe, are offset laterally by the fault. The flume, offset about 30 cm, is probably pre-1900 and may have experienced offset during the May 1910 earthquake. The pipe was emplaced circa 1914 and, inasmuch as there have been no earthquakes since then to account for the $\pm$20 cm of lateral slip, there appears to be a component of creep along this section of the fault. Studies are now focusing on the location and documentation of other displaced historical features.

Very Precise Dating of Earthquakes at Pallett Creek, and Their Interpretation

14-08-0001-G1086

Kerry Sieh
Division of Geological and Planetary Sciences
Caltech, Pasadena, CA 91125
(818) 356-6115

Recent improvements in radiocarbon dating afford the opportunity to date more precisely the 12 paleoearthquakes recorded along the San Andreas fault at Pallett Creek, California. With Minze Stuiver at the University of Washington and David Brillinger at the University of California at Berkeley, I am attempting to date more precisely these earthquakes. Two-sigma uncertainties for dates of individual earthquakes are on the order of 100 years at the present time. We hope to reduce the uncertainties for most of the earthquake dates to 30 years or less. This should enable us to recognize patterns of earthquake recurrence and to determine more precisely what variability exists in the actual recurrence intervals. From these more precise earthquake dates the probability of a great earthquake in the next couple decades can be determined with more confidence.

At the end of the first year of this grant (August, 1986), Minze Stuiver had completed analysis of the first suite of samples, and David Brillinger and I had begun statistical analysis of the sample dates. Our preliminary assessment of the data is that we will indeed be able to narrow the dating imprecision of several of the prehistoric earthquakes. For example, event "I" appears to be constrained to 1003 $\pm$ 27 A.D. The average value for the last 9 recurrence intervals is 131 $\pm$ 2 years. Of these 9 intervals, the two which follow the two smallest slip events (events I and N) appear to be no longer than a few decades.

Very Precise Dating of Earthquakes at Pallett Creek, and Their Interpretation

14-08-0001-C1083

Minze Stuiver

Department of Geological Sciences and Quaternary Research Center
University of Washington, Seattle, WA 98195, (206)545-1735

Objective: High precision radiocarbon dating, with age errors less than two decades for samples up to 5000 yrs old, is applied to the organic deposits of the stratigraphic section at Pallett Creek. This section contains the record of twelve large earthquakes. The radiocarbon dating project is part of the Kerry Sieh and David Brillinger project described elsewhere in this volume. The ultimate goal is to discern patterns of earthquake recurrence and to determine more precisely any variability in actual recurrence intervals and the probability of a great earthquake in the next couple of decades.

Data Acquisition and Analysis: Some thirty odd samples have been measured so far. For most samples, the radiocarbon age errors (one standard deviation) are between 12 and 18 yr. These errors are based on the reproducibility of the measurements, and thus represent the full uncertainty of the measuring process. Realistic error assignment is important because the prevalent use of counting statistics to calculate radiocarbon errors may underestimate the error by up to a factor of two. To determine recurrence intervals in calendar years, a radiocarbon age calibration curve is used for the conversion of the radiocarbon ages. A high precision calibration curve is needed (Stuiver and Pearson, Radiocarbon 28,805-838,1986). For our Pallett Creek samples, the maximum range of calendar years compatible with one standard deviation in the radiocarbon age averages 45 calendar years. Probability distributions within these ranges also play a role. A more detailed assessment of these distributions on earthquake prediction will be made by D. Brillinger and K. Sieh.

Oak Ridge Fault, Ventura Basin, California: Slip Rates and Late Quaternary History

14-08-0001-G1194

Robert S. Yeats
Department of Geology
Oregon State University
Corvallis, Oregon 97331-5506
(503) 754-2484

David A. Gardner
Staal, Gardner & Dunne, Inc.
121 N. Fir Street, Suite F
Ventura, California 93001
(805) 653-5556

Thomas K. Rockwell
Department of Geology
San Diego State University
San Diego, California 92182
(619) 265-4441

Investigations

Carbon samples from the Bardsdale trench and the Saticoy Country Club trench were collected and submitted for dating by T.K. Rockwell. The soils in these trenches were also collected and described in detail by Rockwell to assess the age of the deposits exposed in the trenches. Gary Huftile completed a study of the recently-discovered Chaffee Canyon oil field which has new well-control points on the Oak Ridge fault. Robert Yeats determined rates of vertical separation on the Oak Ridge fault from 4 Ma to the present day. Mapping of the western Montalvo mound was completed by Russ Van Dissen and John Powell, building on the earlier work of E. A. Hall, and the soils were described by T. K. Rockwell.

Results

Charcoal recovered from faulted alluvial-fan sediments in a trench at Bardsdale yielded a ^{14}C age of 2010 ± 145 years. The soils in this trench have an A/Cox profile and are similar to other late Holocene soils in the Ventura basin. Normal-fault separation of this deposit is 1.7 to 2.0 m and apparently occurred as a single event (see previous report in Summaries of Technical Reports v. XXII (O.F.R 86-383), p. 196-201).

Charcoal was also recovered from an *in situ* burn zone in the Saticoy Country Club trench, yielding a ^{14}C age of 30,300 ± 750 years. The soil developed in the overlying alluvium is consistent with this date and helps further constrain the age of undated fine-grained soils in the Ventura basin. The alluvium is not faulted and is apparently not warped. This is significant in that the trench was excavated across an air-photo lineament which is on the eastern extension of the Ventura fault.

Soils developed in fine-grained alluvium (Saugus Formation; fluvial facies) in the Montalvo mounds are stronger than the dated fine-grained soil at Saticoy, which suggests a greater age. These soils are folded and have dips as high as 20°; bedding in the Saugus dips as high as 40° (Hall, 1982). Lab data on the soils will help provide a relative age between the soils described in this project and other dated soils in Ventura basin, thereby providing an approximate age of the Montalvo mound alluvium.

Vertical separation rates have been calculated for the Oak Ridge fault from the coast east to Shiells Canyon from the time of beginning of Pico deposition to the present day. Rates are based upon the following age assumptions: Repetto-Sisquoc contact, 4 Ma; top of Repetto, 3 Ma; Microfaunal Horizon 5, 1 Ma; base of Saugus (San Pedro), 0.65 Ma; top of Saugus, 0.2 Ma. It can be demonstrated that the top of the Saugus dated by amino-acid age estimates (Lajoie and others, 1982) is close to the top of the section in the Santa Clara valley to the south (see Fig. 6 of Yeats, 1983 and Fig. 8, 10, and 11 of Yeats, 1982). In addition, the upper Saugus can be correlated by electric log across the trough to the Oxnard Plain on the hanging wall of the Oak Ridge fault and eastward in the trough to Saticoy. The age of youngest Saugus in the east Ventura basin is 0.4 Ma based on magnetostratigraphy calibrated by the Bishop tuff (Levi and others, 1986), suggesting that the top of the Saugus does not become much older eastward. The thickness of post-0.2 Ma gravels cannot be determined in the footwall block between Santa Paula and Piru because the Saugus there is flat-lying, and its lithology is similar to that of the overlying gravels. However, where Santa Clara River deposits locally overlie beds strongly deformed along the Oak Ridge fault or south-dipping strata on the north flank of the Santa Clara syncline, the river gravels rest with angular unconformity on these deformed strata, and their thickness can be determined: 40-50 m near the Bardsdale trench and 390 m in the Union-SPS 1 well in the city of Santa Paula. Separation rate curves now include these river gravels in the Saugus and are, accordingly, too high for the Saugus and too low for the last 0.2 Ma. If the top of the Saugus is considered to be at the base of the 390 m of flat-lying gravels in the Union-SPS 1 well, the vertical separation rate for the Saugus at South Mountain is 2.3 mm/y, and the post-Saugus rate is 11.1 mm/y. The post-Saugus rate is probably at least this high farther east, at Shiells Canyon.

Vertical separation rates are shown in Figure 1. Two trends are apparent: an increase in separation rates for the last 4 m.y., and an increase from west to east. Rates for the Repetto are 0.5 to 1.1 mm/y, for the remainder of the Pico, 0.6 to 2.3 mm/y, for the Saugus 1.4 to 7.5 mm/y, and for post-Saugus time, 0 (in the coastal plain west of Oak Ridge) to more than 11 mm/y from South Mountain eastward, taking into account the flat-lying gravels in Union SPS 1 as younger than Saugus. The post-Saugus rates show a sharp inflection west of Oak Ridge, whereas the older rates increase monotonically from west to east. What is the reason for this? One explanation may be that the post-Saugus slip vector trends northeast, as suggested by Yeats (1976), whereas older slip vectors trend more northerly. A northeast slip vector would be nearly parellel to Oak Ridge fault strike in the coastal plain and more normal to fault strike east of South Mountain. This would explain the Montalvo pressure riedges as formed by almost pure left-lateral strike slip.

References

Hall, E. A., 1982, Geological observations on the Montalvo mounds, in Cooper, J. D., compiler, Neotectonics in southern California; Guidebook prepared for the Cordilleran Section, GSA meeting, p. 53-57.

Lajoie, K. R., Sarna-Wojcicki, A. M., and Yerkes, R. F., 1982, Quaternary chronology and rates of crustal deformation in the Ventura area, California, in Cooper, J. D., compiler, Neotectonics in Southern California: Guidebook prepared for the Cordilleran Section, GSA meeting, p. 43-51.

Levi, S., Schultz, D. L., Yeats, R. S., Stitt, L. T., and Sarna-Wojcicki, A. M., 1986, Magnetostratigraphy and paleomagnetism of the Saugus Formation near Castaic, Los Angeles County, California, in Ehlig, P. L., compiler, Neotectonics and Faulting in Southern California: Guidebook prepared for the Cordilleran Section GSA meeting, p. 103-108.

Yeats, R. S., 1976, Neogene tectonics of the central Ventura basin, California: in Fritsche, A. E., and others, eds., The Neogene Symposium: Pacific Sec. SEPM, p. 19-32.

Yeats, R. S., 1982, Low-shake faults of the Ventura basin, California, in Cooper, J. D., compiler, Neotectonics in Southern California: Guidebook prepared for the Cordilleran Section, GSA meeting, p. 3-15.

Yeats, R. S., 1983, Large-scale Quaternary detachments in Ventura basin, southern California: Journal of Geophysical Research, v. 88, p. 569-583.

Reports

Yeats, R. S., 1986, Active faults related to folding, in Wallace, R. E., ed., Active Tectonics: Washington, D. C., National Academy Press, p. 63-79.

Yeats, R. S., 1986, Flake tectonics revisited: Crustal section through the central Transverse Ranges, in Ehlig, P. L., compiler, Neotectonics and Faulting in Southern California: Guidebook prepared for the Cordilleran Section GSA meeting, p. 5-6.

Yeats, R. S., 1986, The Santa Susana fault at Aliso Canyon oil field: ibid., p. 13-22.

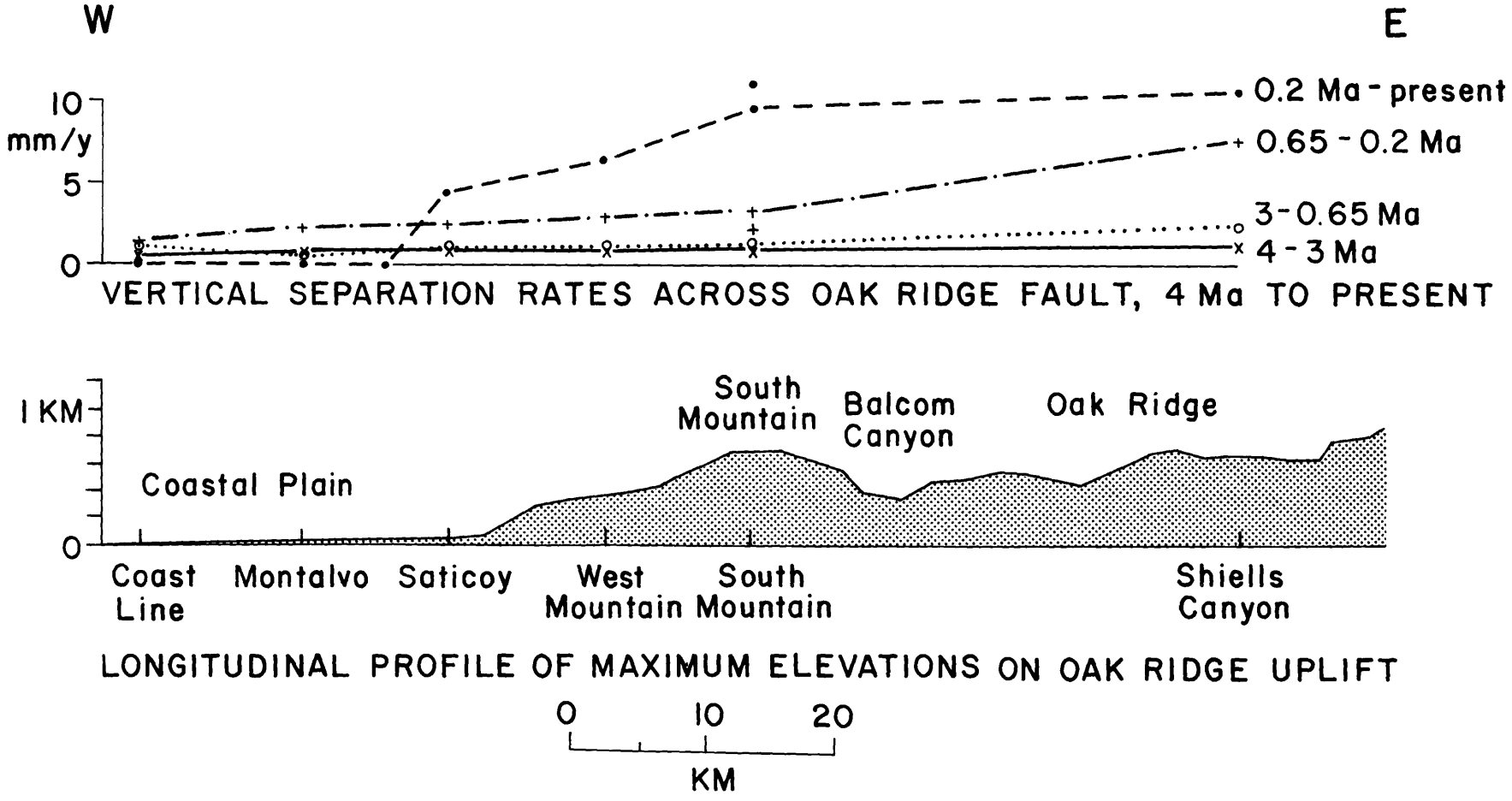

Figure 1. Longitudinal profile along Oak Ridge fault from coastline east to east end of Oak Ridge, where the fault is in contact with the Santa Susana fault. Top diagram shows vertical separation rates, assuming top of Saugus is 0.2 Ma in age and is near the surface in the Santa Clara River. Isolated symbols at South Mountain show rates based on 390 m of post-Saugus gravels in Union-SPS 1 well.

Analysis of USGS Local Seismic Network Data for Earthquake Prediction

14-08-0001-A-0036
Keiiti Aki
Center for Earth Science
Department of Geological Sciences
University of Southern California
Los Angeles, CA 90089-0741
(213) 743-3510

Objective. Seismicity quiescence preceding large earthquakes has attracted many investigators, because many examples have been identified and it could be a very important intermediate-term precursor for earthquake prediction. The purpose of this study is to clarify the magnitude threshold dependence of the observed seismicity patterns and propose a physical basis for such dependence. The same basis may be related to observed coda Q change before large earthquakes, which is the major topic under study in this project.

Data Analysis and Results. Different temporal variations of seismicity pattern preceding the same large earthquakes are sometimes reported by different investigators. For examples, both quiescence and increased activity are reported in the epicentral areas of the 1952 Kern County and 1971 San Fernando, California earthquakes (Kanamori, 1981; Ishida and Kanamori, 1978, 1980; Wesson and Ellsworth, 1973). In our study, we used the Caltech Catalog and Reasenberg's (1985) method to remove aftershocks. In this method, aftershocks are identified based on the earthquake interaction process which is modeled with one spatial and one temporal parameter. With the identified aftershocks removed, the cumulative number of events from the epicentral area of the coming large event vs. time curve is plotted. Figure 1 shows such a curve for the 1952 Kern County earthquake (M=7.7) with low cut-off magnitude threshold M=2.0. We see that the seismic rate is almost a constant for 20 years from 1932 to 1952. There is a slightly quiet time period from 1941 to 1946. In five years before the 1952 main shock, the seismic activity is increased compared with the normal trend before 1941. This is consistent with Wesson and Ellsworth's (1973) analysis. When we change the cut-off magnitude threshold to M=3.5, the curve appears very differently as shown in Figure 2. There is an eleven years quiescence starting from 1941 before the main shock. This is in general consistent with Ishida and Kanamori's (1980) and Kelleher and Savino's (1975) analysis, who identified quiet period before the 1952 Kern County earthquake to be 15 and 20 years respectively. A similar case was observed for the 1971 San Fernando earthquake (M=6.4). The seismic activity increased in the few years before the main shock when we choose the low cut-off magnitude to be M=2.0. However, when the cut-off magnitude is M=3.0, we found a 3 years quiet period starting from 1967. The most recent example is the Oceanside San Diego earthquake (July 13, 1986, M=5.3). Hutton et al. (1986, written communication) plotted the seismicity before this earthquake with cut-off magnitudes M=2.5 and 3.0. Their figures show that the seismic activity increased for M>2.5 and decreased for M>3.0 before the earthquake. This cut-off magnitude dependence was also found by other investigators such as Evison (1977) and Tsai et al. (1979) for the Inangahua earthquake (M=7.1) of 1968 and for several moderate earthquakes in the eastern Taiwan.

We propose to explain the threshold magnitude dependence of seismicity pattern before large earthquakes as a consequence of the slip-weakening

friction law. In our previous work simulating seismicity with a slip weakening frictin law, we (Cao and Aki, 1984) showed that quiescence of seismicity before large earthquakes can be simulated by specifying relatively large critical weakening slip. On the other hand, a recent study by Aki on the frequency-magnitude relation for small earthquakes suggests distinctly different parameters of the friction law between earthquakes with magnitude greater than 3 and those smaller than 3. The critical weakening slip may increase sharply with magnitude at around 3. Thus, our numerical simulation can explain why the quiescence shows up only for earthquakes with magnitude greater than about 3 and may indicate the physical basis for such cut-off magnitude dependence of the precursory seismicity pattern.

References

Cao, T., and K. Aki, Seismicity simulation using a mass-spring model characterized by the displacement hardening-softening friction law, PAGEOPH, 122, 10-24, 1984.

Evison, F. F., Precursory seismic sequences in New Zealand, N.Z.J. Geol. Geophys., 20, 129-141, 1977.

Ishida, M., and H. Kanamori, The foreshock activity of the 1971 San Fernando earthquake, California, Bull Seismol. Soc. Am., 68, 1265-1279, 1978.

Kanamori, H., The nature of seismicity patterns before large earthquakes. In Earthquake Prediction - An International Review, Maurice Ewing Series 4, Amer. Geophys. Union, 680pp, 1981.

Reasenberg, P., Second-order moment of central California seismicity, 1969-1982, J. Geophy. Res., 90, 5479-5495, 1985.

Tsai, Y. B., T. Q. Lee, and Z. S. Liaw, A study of microearthquake activity preceding sme moderate earthquakes in eastern Taiwan, EOS, Trans. Amer. Geophys. Union, 60, 884, 1979.

Wesson, R. L., and W. L. Ellsworth, Seismicity preceding moderate earthquakes in California, J. Geophys. Res., 78, 8527-8546, 1973.

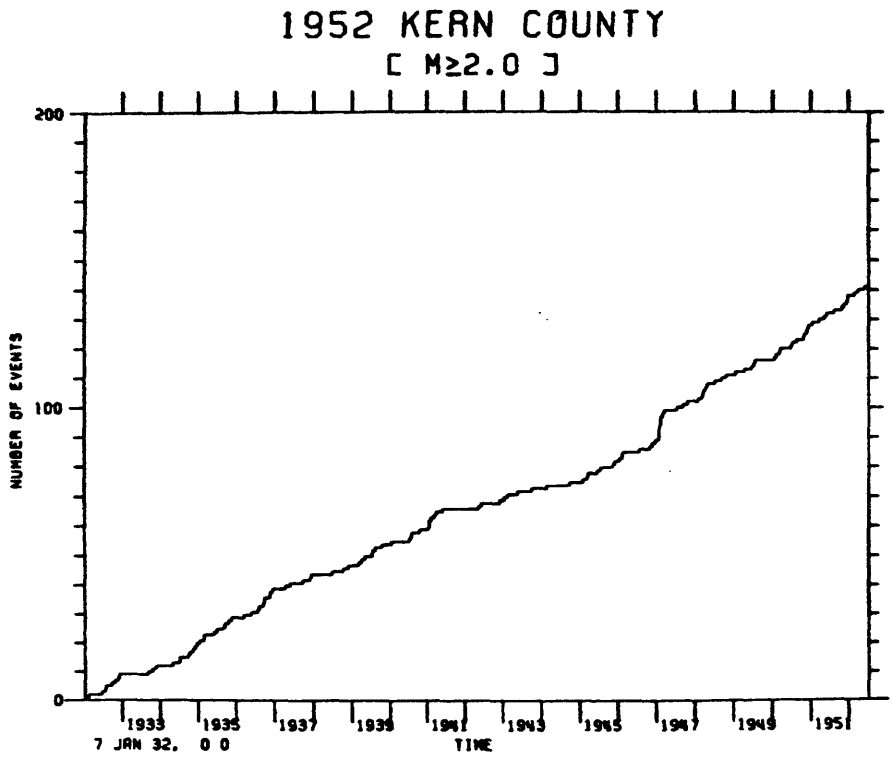

Figure 1

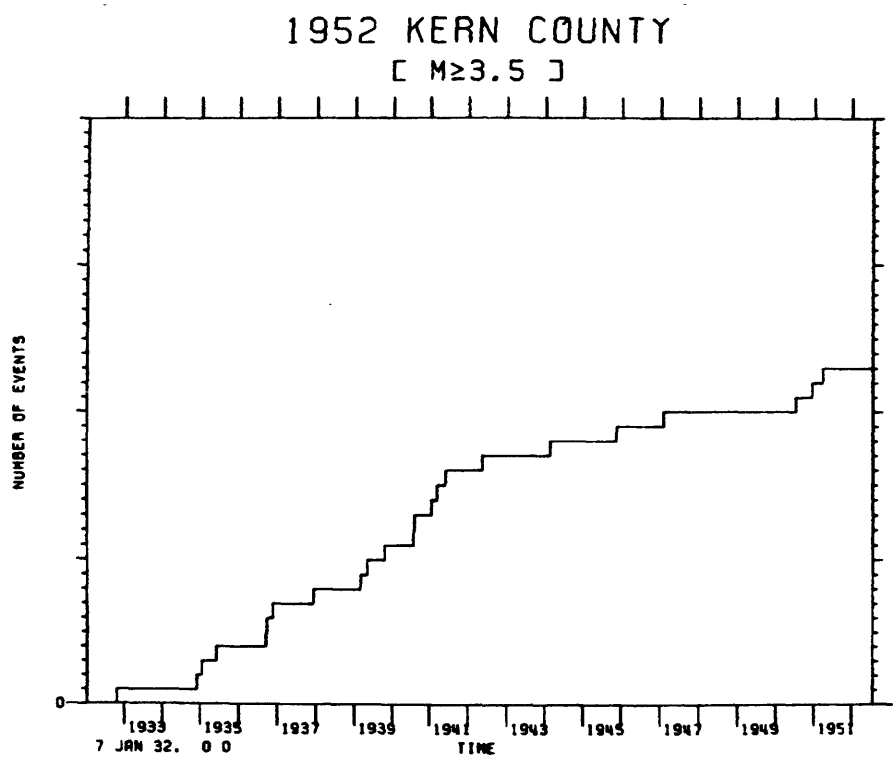

Figure 2

On-Line Seismic Processing

9930-02940

Rex Allen
Branch of Seismology
U.S. Geological Survey
345 Middlefield Road, MS 77
Menlo Park, California 94025
(415) 323-8111 ext 2240

Investigations and Results

During this period work was completed in adapting the Motorola VME/10 to offline processing of the analog tapes produced by the fiveday recorders used in aftershock studies. These tapes carry 6 seismic channels (3 components at high and low gain), and two timing channels. This system is capable of digitizing and saving the digital samples of all 8 channels at 100 samples per second, but processing only the high-gain vertical for event detection. The tapes are played back at a time compression of 20, requiring the system to deal with 16000 samples per second realtime, and pushing some of the system components well past their design limits. In particular, the Motorola A/D converters were found to be too slow and required extensive modification of their control firmware to get up to the required speed. Critical sections of the FORTRAN picker algorithm were also hand optimized for efficiency and the system now meets speed requirements.

After processing an analog tape the digital record of the traces is written out to a standard nine-track digital tape for further analysis on an offline system. The plan here at Menlo Park is for this to be done on the CUSP offline system, and Peter Johnson has written a program to deal with these tapes in the CUSP environment. The tape format involves no multiplexing of traces or other tricky shortcuts, so the tapes should be easily adapted to any other system with nine-track 1600-bpi tape drives.

We have taken delivery on a new 68020-based development system and are adapting the online Real-Time Processor to the new Hardware. When complete it is expected to do the job now done by the Mk I RTP and also to save the digital traces for offline analysis in the same way as the previously described 5-day system.

Jim Ellis has continued work on the multiproject effort to develop new digital field instruments.

Sam Rodriguez has continued the good fight in maintaining the Mk I RTP's here at Menlo Park and at the University of Washington and the University of Utah. He has steadily whittled away at problems as they have appeared, refining the original hardware where required, and has succeded in making them quite reliable, even though they are growing a bit long in the tooth by electronics equipment standards.

Crustal Deformation Observatory, Part F

USGS-14-08-0001-G-1152

Roger Bilham and John Beavan
Lamont-Doherty Geological Observatory of Columbia University
Palisades, New York 10964
914-3359-2900

Investigations

1. The two 532 m long Michelson Tiltmeters at PFO exhibit different noise levels and long term drifts. Since the signals are derived from two water level measurements and two deep reference measurements at each end of each instrument it was considered mutually of interest to introduce a short length of water pipe from the LDGO vault to the IGPP tiltmeter vault that would enable the two instruments to be compared.

2. A new detector for a manual water level monitor has been examined. The set point is determined by observing the null distortion of the water surface produced by a subsurface pointer. A long term repeatability ± 1 micron is sought.

3. A pair of float type water sensors from Wuhan, PRC has been lent to us by Chinese colleagues for installation on the PFO tiltmeter. In exchange we have offered the Wuhan group a pair of laser interferometer water level sensors.

4. A new $\lambda/4$ fringe counter is being developed for the laser interferometer detector. The new electronics will provide a digital precision of 0.5 nanoradians in the LDGO tiltmeter.

5. The possibility of installing a pair of Michelson tiltmeters at Mammoth Lakes to monitor subsurface magma chamber inflation and deflation has been investigated.

Results

1. Water pipes have been connected between PFO and LDGO tiltmeters. Micrometer sensors are being constructed to enable a precise hydrostatic transfer between the end piers of each instrument. The accuracy of this height transfer is anticipated to be better than ±2 μm at each end, corresponding to a tilt comparison accuracy of 7.5 nanoradians between the two tiltmeters.

2. Tests of the new detector show that it is possible to set the micrometer barrel repeatedly to an accuracy of 1 μm. The viewing assembly consists of a lens with a Ronchi ruling at its focus on which an image of the ruling is superimposed after reflection from the water surface. Fringes are absent when the micrometer tip is below the water surface but are dense when the tip is close or in contact. Two possible set points may be chosen with the pointer at the point of contact (with the water surface depressed by several microns) or with the pointer in contact such that water surface distortion is minimal. The latter appears preferable; experiments to

eliminate subjective setting of the set point continue.

3. New piers are being designed for the Wuhan instruments so that they may occupy the same vault as the existing LDGO sensors.

4. The $\lambda/4$ electronics are designed around a new (HP) processing chip that contains a built in up/down counter, and associated logic circuity that replaces much of our existing discrete circuity. The electronics for the interferometer have been tested and are now being laid out on a single board.

5. The groundwork for a two axis water pipe tiltmeter at Mammoth Lakes has been completed. To minimise ground disturbance in the area of the Inyo National Forest, authorities have requested that the 1 km long tiltmeter pipe be buried beneath existing roads. Subsurface radar and leveling surveys of a possible L-shaped route 800 m north of Mammoth Lakes airport indicate that a single horizontal water pipe can be installed at an average depth of 1.5 m without encountering in-situ rock. If this can be achieved it will be possible to monitor the surface tilt vector with three sensors. Contracting work on pipe installation is anticipated to start soon.

Remote Monitoring of Source Parameters for Seismic Precursors

9920-02383

George L. Choy
Branch of Global Seismology and Geomagnetism
U.S. Geological Survey
Denver Federal Center
Box 25046, Mail Stop 967
Denver, Colorado 80225
(303) 236-1506

Investigations

1. Teleseismic estimates of radiated energy and acceleration spectrum. We are developing a method of computing radiated energy and acceleration spectrum from direct measurements of teleseismically recorded broadband body waves.

2. Rupture process of moderate-sized earthquakes. We are using digitally recorded broadband waveforms to characterize the rupture process of selected moderate-sized earthquakes. Broadband data have sufficient frequency content to resolve complexities of rupture and to provide both dynamic and static properties of the source.

3. Improvement of NEIC reporting services. We have developed a procedure for routinely extracting some source parameters from broadband data and incorporating these parameters and data into the flow of NEIC reporting services.

Results

1. We have applied our algorithm for the computation of radiated energy to large, shallow-focus earthquakes. Generally, indirect estimates of energy (e.g., those using simplistic relations with moment) may overestimate energy if the rupture process involves a sizeable component of aseismic slip. In the frequency range 0.1-1.0 Hz, a teleseismically derived acceleration spectrum compares very well with spectra from near-field accelerograms. This implies that we can make routine estimates of strong ground motion from large earthquakes with teleseismic data. The variation in the spectra of P-wave acceleration from a suite of large, shallow-focus earthquakes ranging in size from M_S 6.2 to M_S 8.1 suggests that the high frequency spectral level is more strongly proportional to the asperity area than to the seismic moment of an earthquake.

2. A study of the Yemen earthquake of 13 December 1982, has been completed. This event was found to consist of two events that occurred 3 s apart on a steeply dipping fault that trended NNW. The analysis of a suite of Selected IASPEI events has been completed. This study showed that depth phases could be easily and routinely read from broadband data.

3. In contrast to conventional band-limited data, broadband data often show the source-time functions of body waves very clearly. We are now routinely reading depth phases from broadband data for all earthquakes with $m_b > 5.8$. Where data are sufficient an inversion for depth is made. The data and the results are now routinely entered into the flow of NEIS operations. Results are published in the monthly PDE as well as the EDR. We are in the process of implementing a computer package that will enable us to compute radiated energy as part of the routine NEIS operations.

Reports

Boatwright, J., and Choy, G.L., 1986, Teleseismic estimates of the energy radiated by shallow earthquakes: Journal of Geophysical Research, v. 91, p. 2095-2112.

_____1986, Acceleration spectra for subduction zone earthquakes [abs.]: EOS (Transactions, AGU), v. 67, p. 310.

Choy, G.L., and Engdahl, E.R., 1986, Analysis of broadband seismograms from selected IASPEI events: Physics of the Earth and Planetary Interiors, in press.

Choy, G.L., and Kind, R., 1986, Rupture complexity of a moderate-sized (m_b 6.0) earthquake: Broadband body-wave analysis of the North Yemen earthquake of 13 December 1982: Bulletin of the Seismological Society of America, in press.

Seismic Analysis of Large Earthquakes and Special Sequences in Northern California

9930-03972

Robert S. Cockerham
Jerry P. Eaton
A.M. Pitt
Branch of Seismology
U.S. Geological Survey
345 Middlefield Road, Mail Stop 977
Menlo Park, California 94025
(415) 323-8111, Ext 2963

1) Continued monitoring and analysis of the seismicity in the Mammoth Lakes to Bishop area of Eastern California (R.S. Cockerham).

2) Collection and analysis of data from large earthquakes recorded by the northern and southern California telemetered networks in support of (J. P. Eaton):
   a) development of better regional velocity models and associated station corrections,
   b) evaluation of magnitude calculations based on maximum amplitude and associated period,
   c) determination of regional variations in focal mechanisms of large California quakes.

3) Review of historical and recent instrumental seismicity to identify the probable source of 1892 Vacaville-Winters earthquakes (J. P. Eaton).

4) Review of the development of seismic and strain networks in Hawaii (J. P. Eaton).

5) Compilation of a USGS Yellowstone seismic catalog covering the years 1964 through 1981 (A. M. Pitt).

Results

1. The overall spatial distribution of epicenters within the Mammoth Lakes to Bishop area remained unchanged (Fig. 1) during this six month period except for the Chalfant Valley sequence of July 1986 (discussed below; see Fig. 1). This sequence occurred in an area that had had little seismic activity before July 1986 (Fig. 2a). A notable temporal change in activity (in addition to the Chalfant area) involved an increase in the occurrence rate of earthquakes in the Sierran block just south of the caldera beginning about mid-June (Fig. 2b). This increase began about one month prior to the Chalfant Valley mainshock (M_L = 6.4) on 21 July. Subsequent to this event the Sierran block occurrence rate decresed to a level about the same as prior mid-June (Fig. 2b). In contrast, within Long Valley caldera the occurrence rate appears to have increased slightly, beginning in early July and continuing through the Chalfant Valley sequence (Fig. 3).

Chalfant Valley sequence. At 1442 (UTC) on July 1986 a magnitude (ML) 6.4 earthquake shook the Bishop-Mammoth Lakes area of eastern California. The hypocentral coordinates of the main shock are 37° 32.3'N 118° 26.6'W at a depth of 11.2 km. This earthquake sequence was preceeded by a distinctive series of foreshocks that began on 3 July and culminated with a ML 5.9 event on 20 July at 1429 (UTC). These foreshocks occurred a few kilometers north of the main shock epicentral area. Following the mainshock, the rate of earthquake occurrence decreased from several hundred to about 50 events (M>1.0) per day as of 1 September. On 31 July at 0722 (UTC) an aftershock of M_L = 5.8 shook the area with an epicenter 12 km southeast of the mainshock. The foreshocks and aftershocks outline a boomerang shaped area (Fig. 1) about 24 km in length and in 6 to 8 km in width. The northern arm generally strikes N-S while the southern arm strikes N25°W subparallel to the strike, N20°W, of the White Mountain frontal fault zone (WMFFZ). Focal depths range from 4 km to 12 km and shallow to the northwest and the southeast from the ML 6.4. Focal mechanisms for the largest events on July 20, 21, and 31 exhibit strike-slip motion: left-lateral strike-slip on a nearly vertical plane striking N25°E, pure right-lateral strike-slip on a plane striking N25°W and dipping 60°SW, and pure right-lateral strike-slip on a vertical plane striking N25°W, respectively. A projection of the preferred nodal plane (N25°W) for the ML 6.4 event intersects the surface within 0.5 km of the WMFFZ surface trace that showed up to 11 cm of right-lateral slip with no net vertical offset observed.

2. The western edge of the Sacramento Valley north of Carquinez Straights is marked by scattered earthquakes and low hills (folds) in the sediments of the valley just east of the Coast Range/Great Valley (CR/GV) boundary. The largest earthquake (M 4.3) along this zone between Antoich and Williams during 1972-1985 appears to have occurred on a SW-dipping thrust at a depth of about 12 km. This earthquake, as well as the large shocks of the 1892 Vacaville-Winters sequence in the same region, occurred beneath the low hills east of the CR/GV boundary. The gross similarity of the geology and seismicity of the Winters-Vacaville region to that of the Coalinga-Kettleman region encourages us to speculate that the 1892 Vacaville-Winters earthquakes occurred on hidden reverse faults along or east of the CR/GV boundary like those that produced the 1983 Coalinga earthquake and the 1985 Kettleman earthquake.

3. A well-constrained focal mechanism has been obtained for another moderate earthquake off the central California coast. The earthquake occurred at 00h 40m 22.95s UTC on July 8, 1986 at 36°03.7'N 121°50.5'W and about 12 km depth. This location is 30 km south of Point Sur and about 20 km to the west of the coast. It has an M_L of 4.6, based on amplitudes measured on low-gain stations of the USGS Central California seismic network. One nodal plane is well constrained (strike N30°W, dip 34°NE) and the other (strike N30W, dip 56°SW) is well enough constrained to require that the faulting be primarily reverse slip. Thus, the preferred interpretation suggests that this earthquake occurred on a thrust fault striking N 30°W and dipping 34°NE, and the continental upper plate was driven southwestward over the oceanic lower plate in a direction approximately perpendicular ot the adjacent coastline.

4. A catalog of earthquakes in the Yellowstone Park-Hebgen Lake region from 1973 to 1981 was completed and submitted for review. In addition to hypocenters for approximately 6000 earthquakes, the catalog contains a history of the USGS Yellowstone network, epicenter maps, frequency-

magnitude plots, and a brief discription of the velocity model developed from the earthquake data by Edi Kissling (ETH, Zurich, Switzerland). Work is proceeding on a 1:250,000 scale map showing epicenters of the 1973-1981 events and of additional events occurring from 1964-1972. The older data are derived from ISC phase data from stations out to 1000 km from Yellowstone and from USGS nontelemetered seismograph stations operating before the network was upgraded in 1973. A few large events, well recorded by local Yellowstone stations, were used as master events to determine station corrections for the stations reported by the ISC. This map will show seismicity patterns for a 17 year period beginning in 1964. The map will also show topography and traces of Quaternary faults.

Reports

Cockerham, Robert S., The Chalfant earthquake sequence, eastern California, of July and August 1986: preliminary results, (abs.), Trans. Amer. Geophys. Union, 67, p. 1106, 1986.

Cockerham, Robert S., Seismotectonics of the northern California Coast Ranges from San Francisco to Eureka, (abs.), Trans. Amer. Geophys. Union, 67, p. 1214, 1986.

Eaton, Jerry P., Tectonic environment of the 1892 Vacaville/Winters earthquake, and the potential for large earthquakes along the western edge of the Sacramento Valley, U.S. Geological Survey Open-File Report 86-370, 9 pg., 1986.

Eaton, Jerry P., History of the development of the HVO seismograph and deformation networks, Adm. Rpt., Oct. 8, 1986.

Eaton, Jerry P., Narrative account of instrument developments at HVO from 1953 through 1961, and a summary of further developments from 1961 through 1978, Adm. Rpt., Oct. 8, 1986.

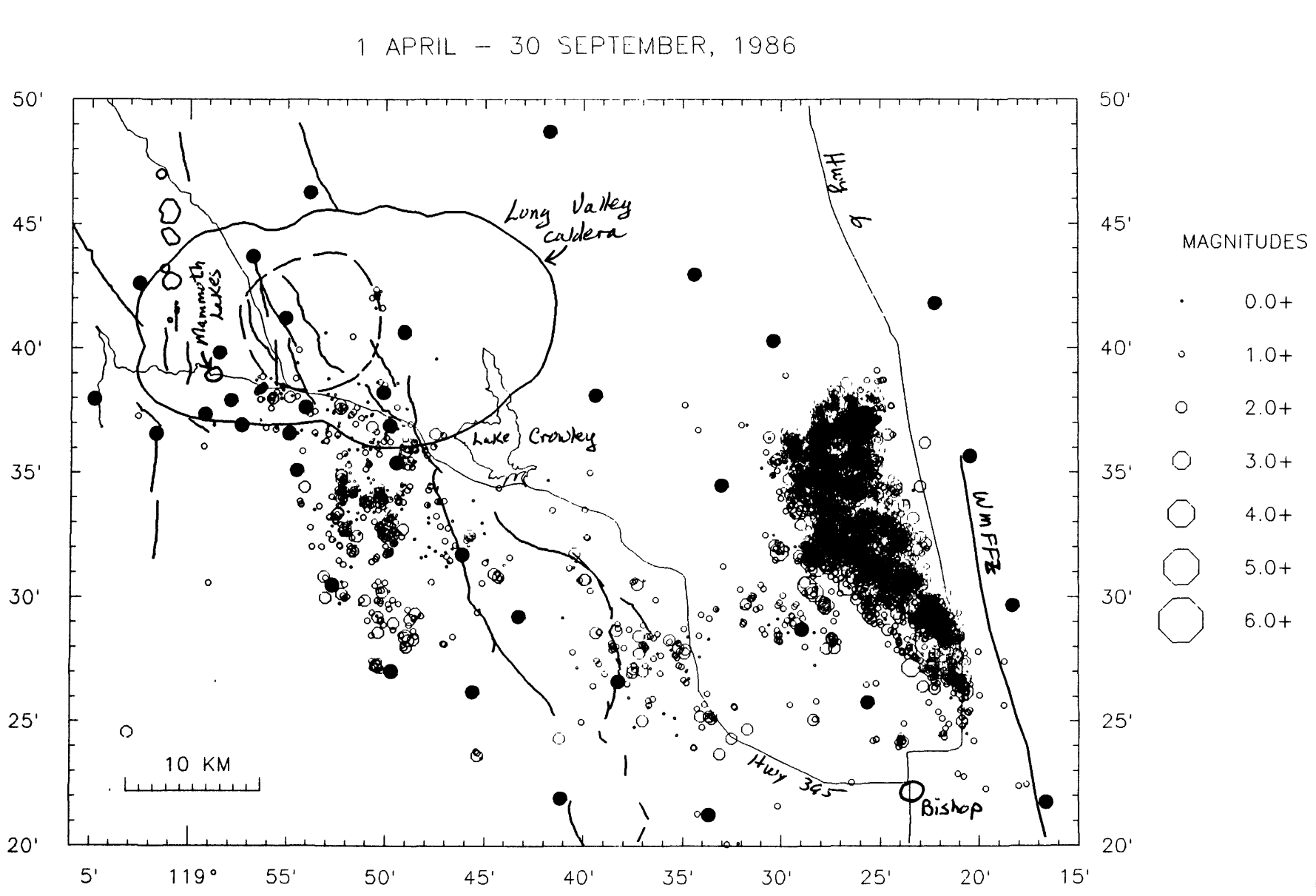

FIGURE 1. A map of the Mammoth Lakes to Bishop area of eastern California showing the epicentral locations of earthquakes (magnitude ≥ 1.0, RMS of the P-wave travel-time residuals ≤ 0.10s, and the number of stations used in the location ≥ 6) that occurred between April 1 and October 1, 1986. The heavy concentration of epicenters west of the White Mountain frontal fault zone (WMFFZ) is the Chalfant Valley sequence. The solid circles are seismic stations operated by the USGS, Univ. of Nevada at Reno, and Division of Mines and Geology, State of California.

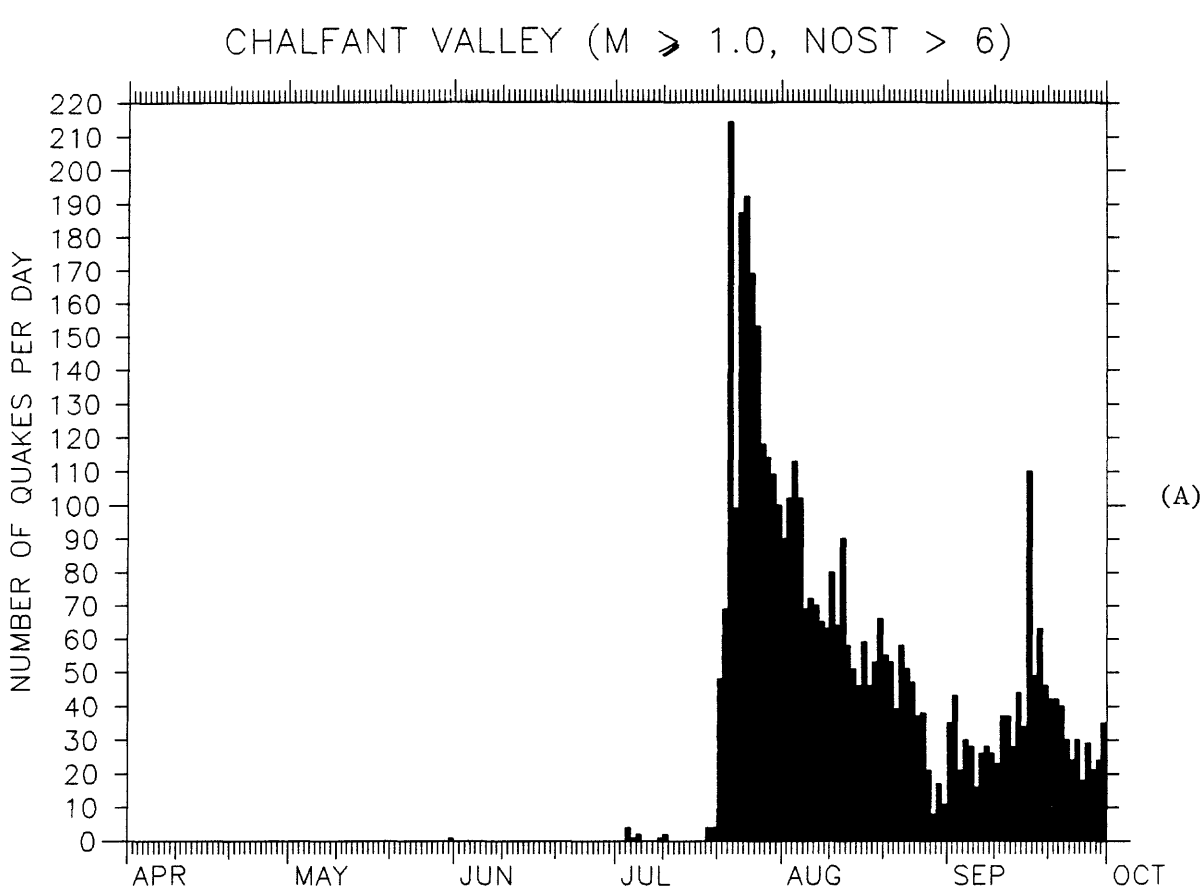
CHALFANT VALLEY (M ⩾ 1.0, NOST > 6)
NUMBER OF QUAKES PER DAY
220
210
200
190
180
170
160
150
140
130
120
110
100
90
80
70
60
50
40
30
20
10
0
APR
MAY
JUN
JUL
AUG
SEP
OCT

(A)

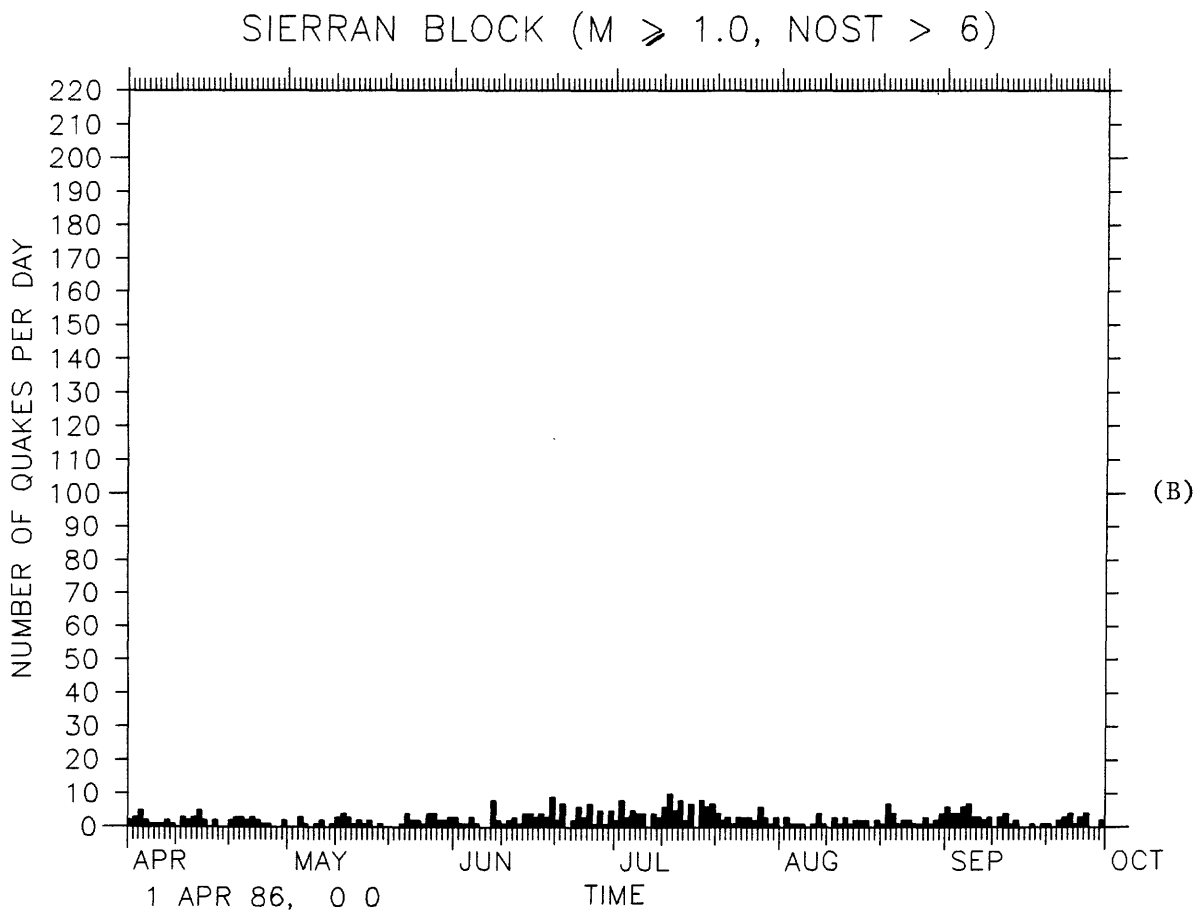
SIERRAN BLOCK (M ⩾ 1.0, NOST > 6)
NUMBER OF QUAKES PER DAY
220
210
200
190
180
170
160
150
140
130
120
110
100
90
80
70
60
50
40
30
20
10
0
APR
MAY
JUN
JUL
AUG
SEP
OCT
1 APR 86, 0 0
TIME

(B)

FIGURE 2

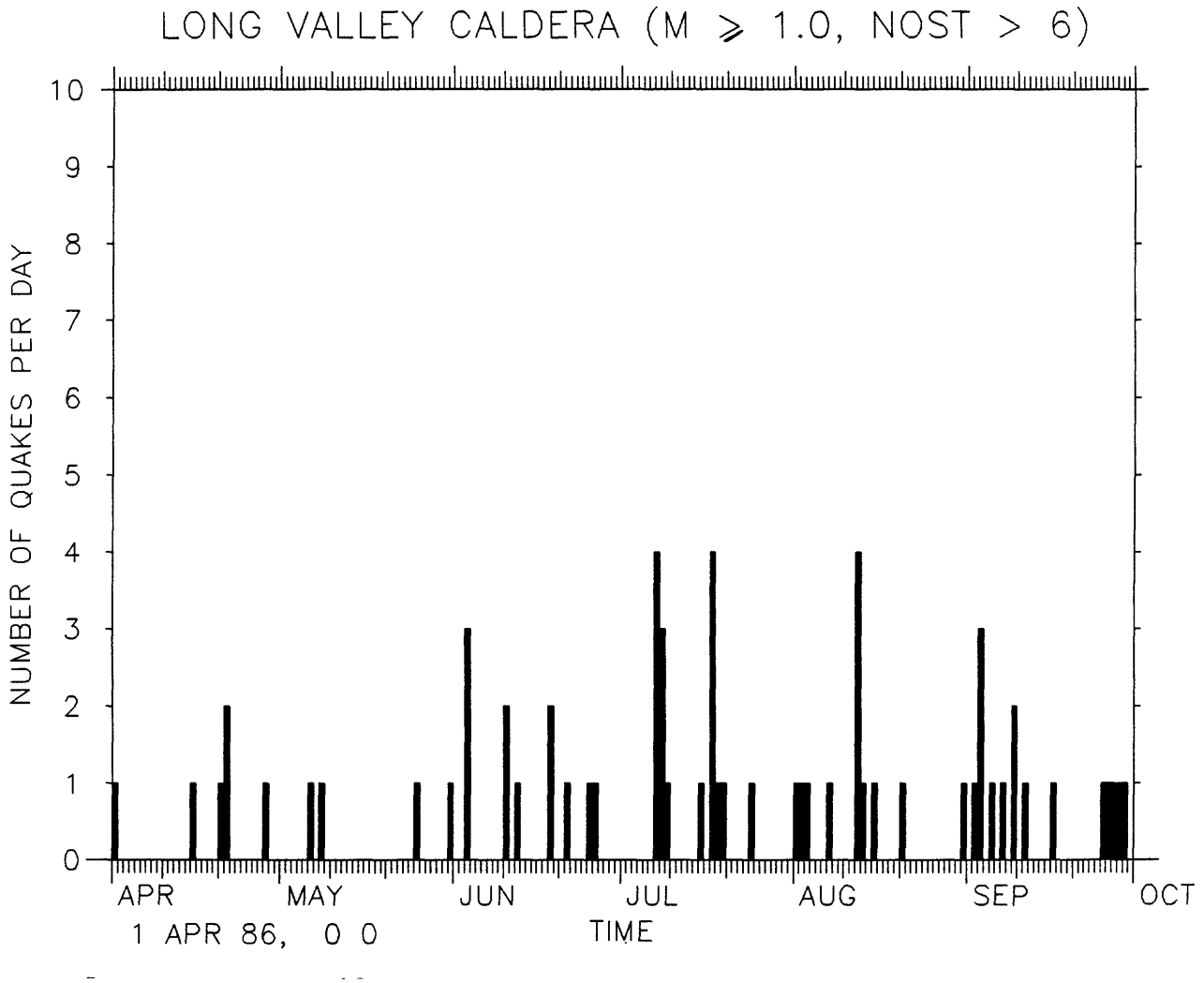
LONG VALLEY CALDERA (M ⩾ 1.0, NOST > 6)
NUMBER OF QUAKES PER DAY
0
1
2
3
4
5
6
7
8
9
10
APR
MAY
JUN
JUL
AUG
SEP
OCT
1 APR 86, 0 0
TIME

FIGURE 3

STUDIES OF EXTENSIVE-DILATANCY ANISOTROPY IN WESTERN USA

14-08-0001-G1169

Stuart Crampin
British Geological Survey, Murchison House,
West Mains Road, Edinburgh EH9 3LA, Scotland, UK
(031-667-1000)

Investigations

Shear-wave splitting diagnostic of some form of effective anisotropy has been recognized above small earthquakes in many different parts of the world (Crampin et al., 1980; Buchbinder, 1984; Crampin and Booth, 1985; Crampin et al., 1986; Kaneshima et al., 1986; etc.). The project sought shear-wave splitting on records from the UCSD/USGS seismic network in the Anza seismic gap. The characteristics of these observations of anisotropy are consistent with distributions of stress-aligned fluid-filled cracks or microcracks which are known from petrological evidence to exist in all sedimentary, metamorphic, and igneous rocks in the crust (Crampin, 1985; Crampin and Atkinson, 1985).

The critical observation we have been seeking is evidence of temporal changes in the behaviour of the splitting before earthquakes. This would confirm the cause of the splitting as aligned cracks or microcracks (the only possible cause of temporal variations in anisotropy), as well as allowing the effects of stress changes before earthquakes to be monitored remotely.

Results

Shear-wave splitting was identified in observations of small earthquakes beneath the Anza network. The polarizations of the leading shear-waves are parallel to the estimated regional stress field at all stations except KNW near the Hot Springs fault. The polarizations show no variation with time at any of the stations. Delays between split shear-waves are difficult to identify reliably and, as is usually the case, the observations at Anza show a large scatter. The scatter appears to be stable in time at all stations except KNW where, for a wide range of directions, the delays display an increase in time which is significant at the 99% level (Peacock et al., 1986). This increase could be interpreted as an increase in aspect ratio (elastic "bowing") of the aligned microcracks as the stress increases before an impending earthquake in the seismic gap. This earthquake would be expected to be sited near the Hot Springs fault.

To our knowledge all short period shear-waves propagating through the crust display evidence for the effective anisotropy of stress-aligned nearly vertical fluid-filled microcracks. The importance of this for earthquake prediction research is that observations of shear-wave splitting (preferably in VSPs which avoid the complicated interactions of the shear waves with the free surface and are easier to model) should allow stress changes before impending earthquakes to be monitored in detail.

Acknowledgements

The major part of this research was supported by the Natural Environment Research Council and is published with the approval of the Director of the British Geological Survey (NERC).

References

Buchbinder, G.G.R., Shear-wave splitting and anisotropy in the Charlevoix seismic zone, Quebec, *Geophys.Res.Lett., 12*, 425-428, 1985.

Crampin, S., Evidence for aligned cracks in the Earth's crust, *First Break, 3*, 12-15, 1985.

Crampin, S., and B.K. Atkinson, Microcracks in the Earth's crust, *First Break, 3*, 16-20, 1985.

Crampin, S., and D.C. Booth, Shear-wave polarizations near the North Anatolian Fault - II. Interpretation in terms of crack-induced anisotropy, *Geophys.J.R.Astr.Soc., 83*, 75-92, 1985.

Crampin, S., D.C. Booth, M.A. Krasnova, E.M. Chesnokov, A.B. Maximov, and N.T. Tarasov, Shear-wave polarizations in the Peter the First Range indicating crack-induced anisotropy in a thrust-fault regime, *Geophys.J.R.Astr.Soc., 84*, 401-412, 1986.

Crampin, S., R. Evans, B. Üçer, M. Doyle, J.P. Davis, G.V. Yegorkina, and A. Miller, Observations of dilatancy-induced polarization anomalies and earthquake prediction, *Nature, 286*, 874-877, 1980.

Kaneshima, S., S. Crampin, and M. Ando, Shear-wave splitting above small earthquakes in the Kinki District of Japan, *Phys.Earth.Planet. Inter.*, in press.

Peacock, S., and S. Crampin, Shear-wave vibrator signals in transversely-isotropic shale, *Geophysics, 50*, 1285-1293, 1985.

Peacock, S., S. Crampin, and J.B. Fletcher, Shear-wave polarizations in the Anza seismic gap, Southern California: temporal changes at one station - a possible precursor?, *J.Geophys.Res.*, submitted.

Reports

Booth, D.C., S. Crampin, E.M. Chesnokov, and M.A. Krasnova, The effects of near-vertical parallel cracks on shear-wave polarizations, *Geophys.J.R.Astr.Soc.*, in press, 1986.

Crampin, S., The geological and industrial implications of extensive-dilatancy anisotropy, *Nature*, submitted, 1986a.

Crampin, S., Water and stress in the Earth's crust and extensive-dilatancy anisotropy, *Nature*, submitted, 1986b.

Crampin, S., R. McGonigle, and M. Ando, Extensive-dilatancy anisotropy beneath Mount Hood, Oregon, and the effect of aspect ratio on seismic velocities through aligned cracks, *J.Geophys.Res.*, in press, 1986.

Peacock, S., S. Crampin, and J.B. Fletcher, Shear-wave polarizations in the Anza seismic gap, Southern California: temporal changes at one station - a possible precursor?, *J.Geophys.Res.*, submitted, 1986.

Stress Transfer, Nonlinear Stress Accumulation and Seismic Precursory Phenomena at a Subduction-Type Plate Boundary

14-08-0001-G1203

R. Dmowska and J. R. Rice (PI)
Division of Applied Sciences and
Department of Earth and Planetary Sciences
Harvard University
Cambridge, MA 02138
(617)495-3452, 3445

(For period Dec. 1, 1985 to May 31, 1986)

Investigations

1. Stress accumulation and transfer between a subducting slab and the thrust contact zone during the whole earthquake cycle is being modelled. The model describes the pulsating part of the stress field in the upper part of the descending slab, caused by steady pull of the descending slab and the presence of large thrust earthquakes in the uppermost part of the slab and, sometimes, large normal earthquakes in the lower part of the slab. Phenomena under discussion occur in short slabs (example: Mexico subduction zone) or in the upper parts (up to depths of the order of 300 km) of longer slabs. The study describes the interaction between stress build-up and relaxation in different parts of the slab, as revealed by lower-level seismicity. Comparison is made with whole earthquake cycle observations for the Middle American Trench, performed by K. McNally and her group.

Results

1. To gain insights into stress accumulation and transfer between a subducting slab and the thrust contact zone during the whole earthquake cycle we use a simple mechanical one-dimensional model of a semi-infinite elastic slab, driven by gravitational sinking and/or drag from steady mantle motions (Fig. 1). The slab is purely elastic with viscoelastic surroundings, and we approximate the interaction between the slab and surrounding mantle by the Elsasser shear coupling. The model ignores slab bending and thermal stresses; periodic stick-slip behavior is assumed for the thrust zone, and large, normal earthquakes down-dip in the slab are included. Some details of our analysis were presented in the previous report (USGS Open File Report 86-31, Oct 1985, pp. 430-434), and the full text is in preparation. Here we present some of our results.

Figure 2 shows the periodic non-dimensional stress versus non-dimensional distance along the slab, H being the slab thickness (for Mexico $H \simeq 30$ km, Valdes et al., 1986). The stress is given in dimensionless form and represents a thickness average extensional stress in the slab, considering only the time variable part

adjusted to zero average over the cycle. Time, expressed in parts of the whole earthquake cycle T, is marked on each stress-distance curve (again, for Mexico, the average cycle length is 36 yr). The figure clearly shows the stress build-up and relaxation during the cycle x = 0 is placed at the lower edge of the zone ruptured in large thrust earthquake. The stress disturbance caused by the thrust earthquake reaches distances on the order of 3 to 4 x/H, which for H = 30 km equals 90-120 km The effect slightly depends on the choice of relaxation time for mantle material, which for Fig. 1 is $t_r = 0.138\ T_{cycle}$.

In our analysis we include large normal earthquakes, occurring down-dip from thrust contact zone, which in our model have the form of extensional slips occurring at distance x_1 and time t_1. Fig. 3 presents combined effects of both, thrust and normal earthquakes, on stress-time distribution in the slab. The normal event here happens at $t_1 = 0.6T$ (for T=36 yr this is 14.5 yr before the next thrust event) and $x_1 = 1.4H$ (for H = 30 km x_1 = 42 km down the slab from the lower edge of large thrust rupture zone). We choose the slip component parallel to the slab for the normal event to be 0.6 of the slip in large thrust earthquake. It is obvious that the occurrence of normal earthquake relaxes the stresses in this area, but also disturbs the stress build-up in the zone of future thrust earthquake as well. The effect depends on the position of normal event in the slab and time in the cycle; Fig. 3 shows the same effect but for a normal event occurring deeper, at $x_1 = 4.3H$ (for H=30 km it is 130 km down-dip). It could be noticed that stress regime in the thrust zone is most affected by close-by events. Also, large normal event affects significantly the area of the order of 2 x/H along the slab.

The next two figures, Fig. 5 and 6, show the effects of progression of slip into locked thrust zone occurring in the second part of the cycle, in our model in steps happening at times $t_i/T = 0.72, 0.75, 0.78, 0.81$ and 0.83. In the simple model now under discussion, this is represented by small displacements (of the value of 0.05 of the slip displacement in thrust earthquake) of the semi-infinite slab end at the times indicated, which occur in addition to the large displacement at the start of each cycle. Fig. 5 presents dimensionless stress versus dimensionless time (T=1) for different positions x along the slab; Fig. 6 shows the same data in the previous stress-distance plot. It is clear here that up-dip progression of slip into locked thrust zone unloads temporarily region of slip, and, also, the area down-dip as well, possibly quietening normal minor seismicity down-dip the slab.

We compare our model predictions with seismicity observations on the whole earthquake cycle gathered recently by McNally and her group (Gonzalez et al., 1984, Bataille and McNally, 1986, Brown and McNally, 1986, Gonzalez-Ruiz and McNally, 1986, O'Mara and McNally, 1986); the full text is in preparation (Dmowska et al., 1986).

References

Bataille K. and K.C. McNally, Seismicity patterns in the Petatlan area, Mexico, submitted to Geophys. Res. Lett., 1986.

Brown E. and K.C. McNally, Seismicity patterns of the 1973 Colima and 1980 Playa Azul, Mexico, earthquakes, submitted to Geophys. Res. Lett., 1986.

Gonzalez J., K.C. McNally, E.D. Brown and K. Bataille, The whole earthquake cycle of the Middle American Trench, offshore Mexico, EOS, Trans. Am. Geophys. Union, 65, N.45, p. 998, 1984.

Gonzalez-Ruiz, J. and K.C. McNally, Seismicity patterns before and after 1982 Ometepec, Guerrero, Mexico, earthquakes, submitted to Geophys. Res. Lett. 1986.

O'Mara, M. and K.C. McNally, Seismicity patterns associated with the 1978 Oaxaca, Mexico, earthquake (M_w = 7.6): A reexamination, submitted to Geophys. Res. Lett., 1986.

Valdes, C.M., W.D. Mooney, S.K. Singh, R.P. Meyer, C. Lomnitz, Y.H. Luetgert, C.E. Helsley, B.T.R. Lewis and M. Mena, Crustal structure of Oaxaca, Mexico, from seismic refraction measurements, BSSA, 76, N.2, 547-563, 1986.

Publications

Dmowska, R., L. Lovison and J.R. Rice,
Stress accumulation and transfer between a subducting slab and the thrust contact zone during the whole earthquake cycle, EOS, Trans. Am. Geophys. Union, 67, N.16, p. 307, 1986.

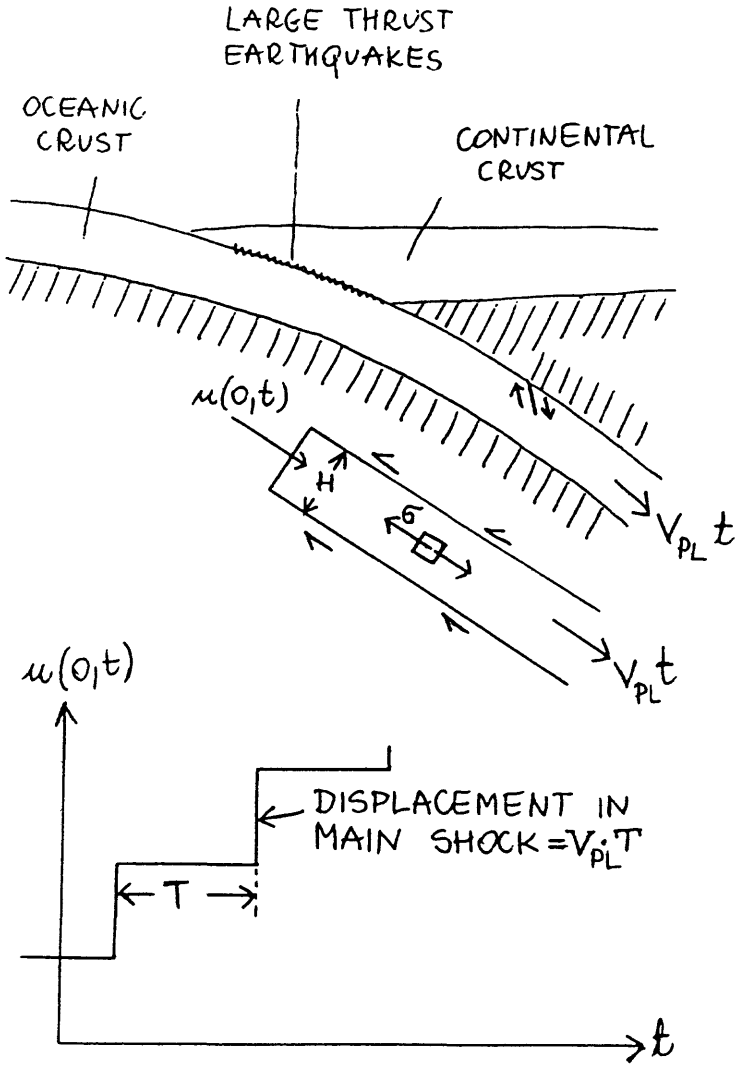

FIG. 1.

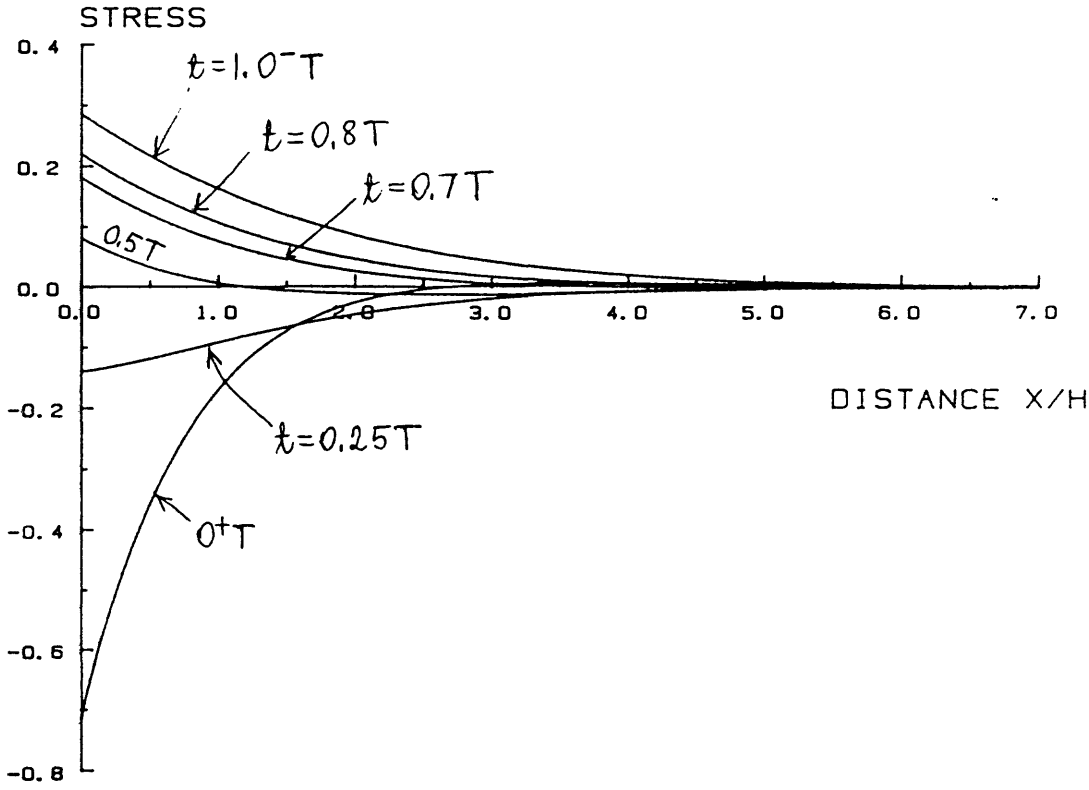
STRESS
0.4
0.2
0.0
-0.2
-0.4
-0.6
-0.8
t=1.0⁻T
t=0.8T
t=0.7T
0.5T
t=0.25T
0⁺T
0.0
1.0
2.0
3.0
4.0
5.0
6.0
7.0
DISTANCE X/H

FIG. 2.

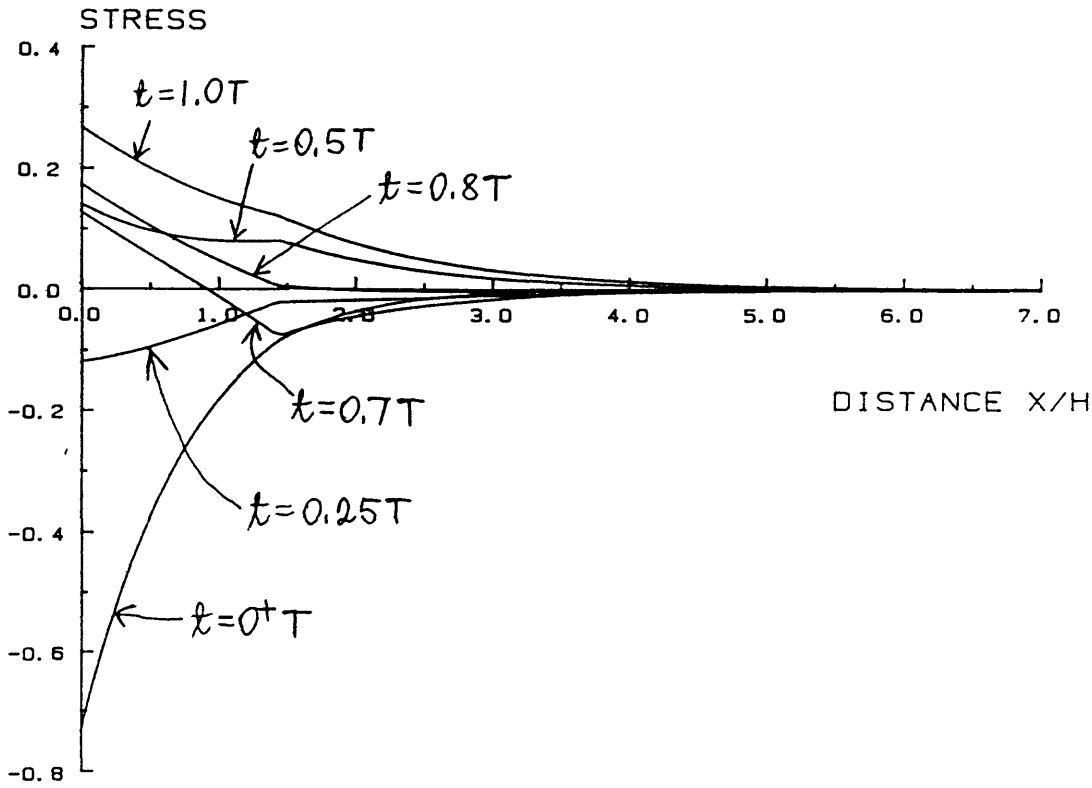
STRESS
0.4
0.2
0.0
-0.2
-0.4
-0.6
-0.8
t=1.0T
t=0.5T
t=0.8T
t=0.7T
t=0.25T
t=0⁺T
0.0
1.0
2.0
3.0
4.0
5.0
6.0
7.0
DISTANCE X/H

FIG. 3.

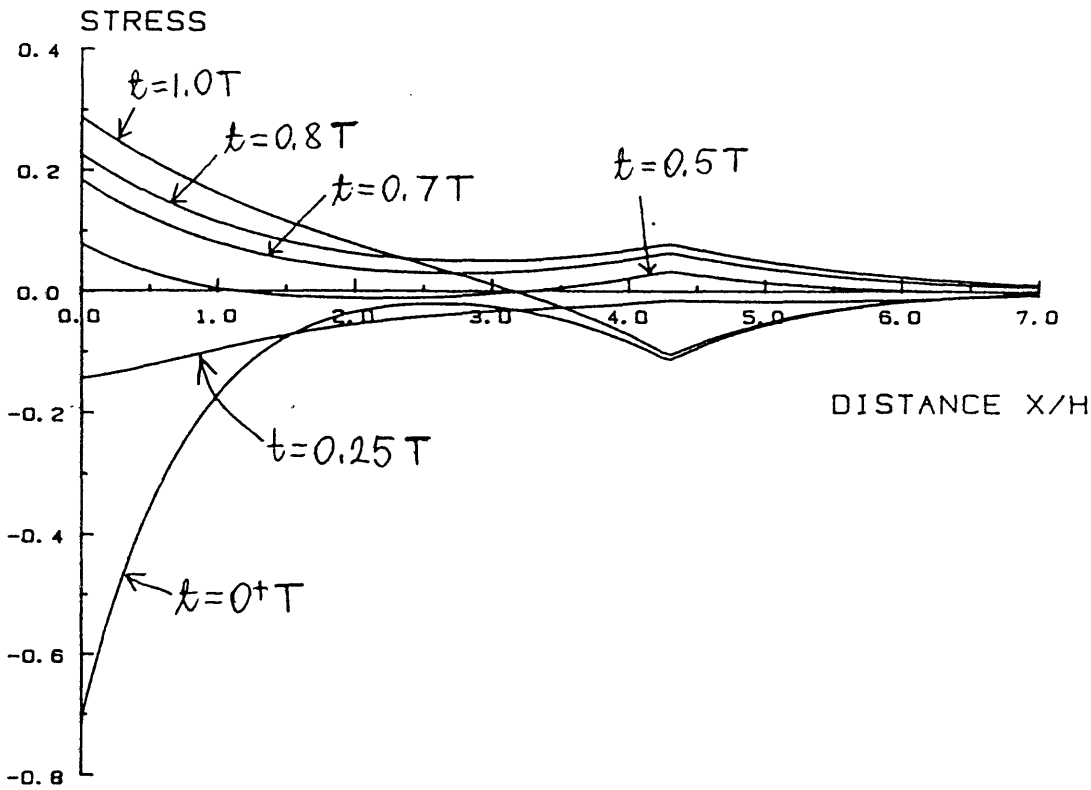
STRESS
0.4
0.2
0.0
-0.2
-0.4
-0.6
-0.8
0.0
1.0
2.0
3.0
4.0
5.0
6.0
7.0
t=1.0T
t=0.8T
t=0.7T
t=0.5T
t=0.25T
t=0+T
DISTANCE X/H

FIG.4.

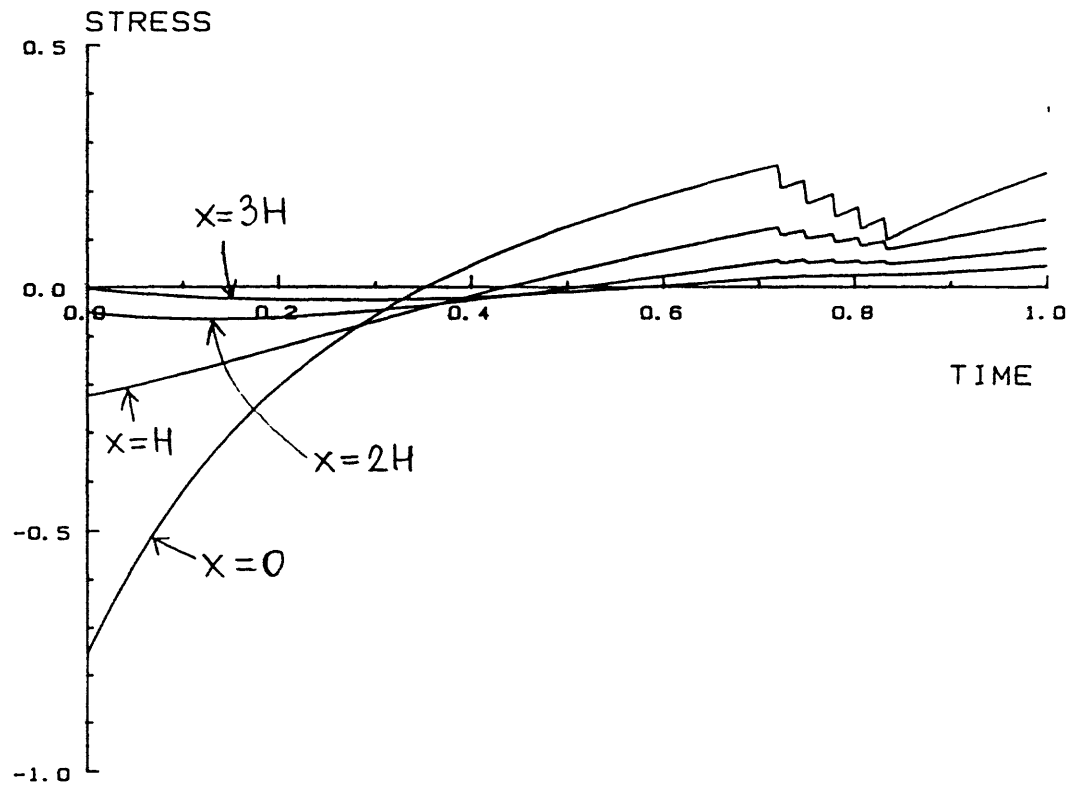
STRESS
0.5
0.0
-0.5
-1.0
0.0
0.2
0.4
0.6
0.8
1.0
x=3H
x=H
x=2H
x=0
TIME

FIG.5.

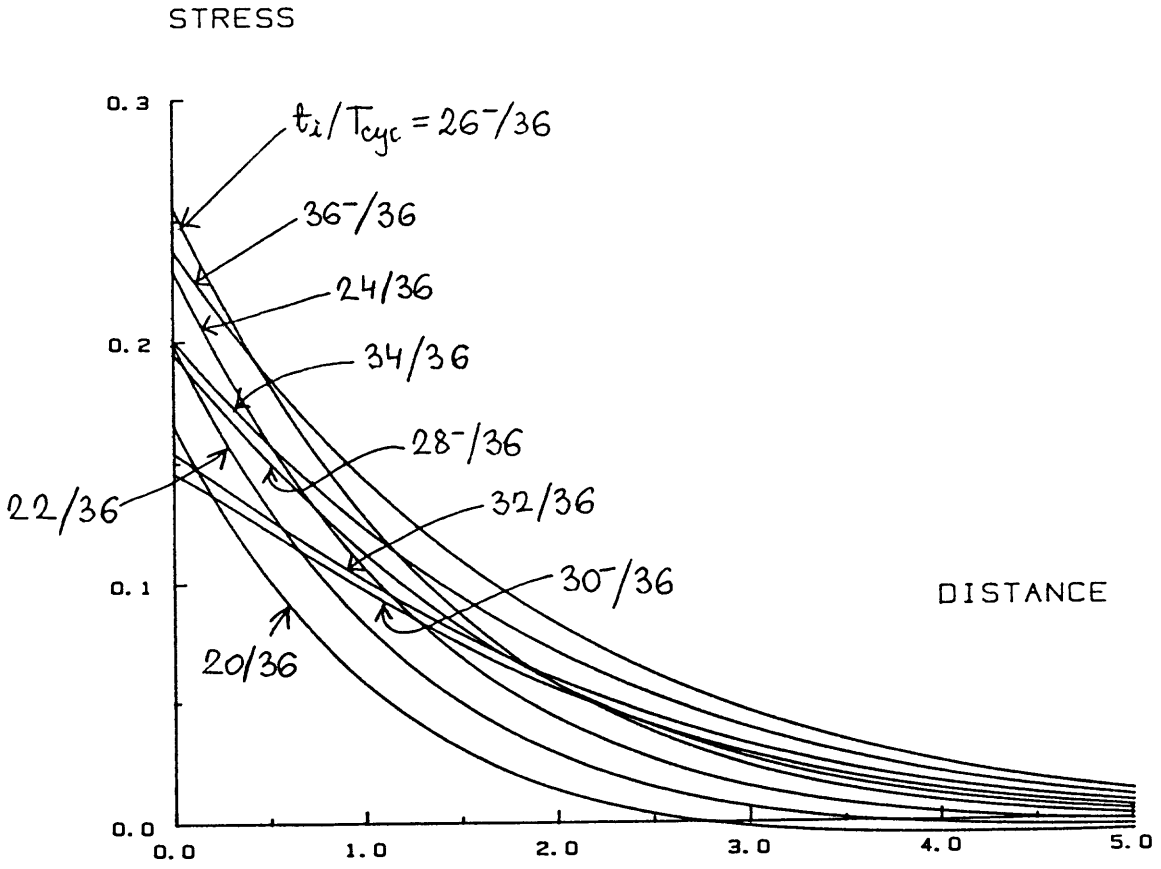
STRESS
0.3
0.2
0.1
0.0
$t_i/T_{cyc} = 26^-/36$
$36^-/36$
24/36
34/36
$28^-/36$
32/36
$30^-/36$
22/36
20/36
DISTANCE
0.0
1.0
2.0
3.0
4.0
5.0

FIG.6.

Stress Transfer, Nonlinear Stress Accumulation and Seismic Precursory Phenomena at a Subduction-Type Plate Boundary

14-08-0001-G1203

R. Dmowska and J.R. Rice (PI)
Division of Applied Sciences and
Department of Earth and Planetary Sciences
Harvard University
Cambridge, MA 02138
(617) 495-3452,3445

(For period June 1, 1986 to Oct. 1, 1986)

Investigations

1. Work has been completed on detailed analysis of seismicity patterns during the whole earthquake cycles for seven separate areas of the great earthquakes occurring between 1964 and 1982 along the Middle America Trench zone, Mexico. The analysis focused on general characteristic patterns, and, especially, on identifying episodes of down-dip-up-dip seismicity migrations, as indicators of stress transfer along the subducting slab. The results of this analysis are now being used as input data in our model of stress accumulation and transfer between a subducting slab and the thrust contact zone during the whole earthquake cycle.

2. Some progress has been made on the more complex model of stress accumulation and transfer between a subducting slab and the thrust contact zone.

Results

1. Our independent observations of earthquake patterns during the whole earthquake cycle for different regions of the Middle America Trench are generally similar to the unpublished observations of the McNally group at Santa Cruz (McNally, et. al., 1986; Gonzalez-Ruiz and McNally, 1986; McNally and Gonzalez-Ruiz, 1986; O'Mara and McNally, 1986; Brown and McNally, 1986; Bataille and McNally, 1986) for the same area. They have recognized essentially three loading stages in the whole earthquake cycle:

1) Extensional stress transfer progressing from downdip to updip between 5 and 15 years before the main shock;

2) Quiescence of the future rupture zone betweeen 1 and 5 years before the main shock;

3) Slab reextension both downdip and updip, resulting in failure of the locked zone and consequently a main earthquake.

We conducted our analysis with the use of the ISC catalog and, for the focal mechanism solutions, the data from Lefevre and McNally, 1985, integrated with the Harvard CMT solutions. The researched areas were of the following great earthquakes: Colima 30 Jan. 1973, Playa Azul 25 October 1981, Petatlan 14 March 1979, Ometepec 7 June 1982, Oaxaca 2 August 1968, Oaxaca 29 November 1978 and Oaxaca 23 August 1965. We observe the following general stages during the whole earthquake cycle:

1) In the area of the main earthquake, and in the immediately adjacent regions down-dip from that area, the seismicity is initially abundant (aftershocks, signifying the adjustment of the whole area to the new stress levels after the main earthquake), and then decreases to some 'background level', which lasts for approximately half of the earthquake cycle, sometimes even for three quarters of the cycle as in the Ometepec area.

2) After this period the seismic activity increases significantly in frequency and in magnitude. This period lasts about 5 years (from 1966 to 1971) for the Colima area; about 12 years, of which 7 in the downdip part of the slab and 5 years (from 1974 to 1979) updip the slab, for the Playa Azul area; 13 years of which 5 years of seismicity mostly on the downdip part of the slab and 8 years updip, on the thrust contact zone of the Petatlan area (from 1964 to 1977); 9 years (from 1966 to 1975) in the Ometepec area, as well as in the Oaxaca 1978 area (from 1965 to 1974).

The period in which the thrust contact zone seems to become active, with small and moderate events, starts from 15 years to at least 4 years (Oaxaca '68), but with an average of about 8 years before the main earthquake, and it lasts from 4 years to 13 years.

3) The period of higher activity ends some time before the main earthquake, and the zone at the future shock exhibits a well-defined quiescence. Of course, the length of the quiescent period depends on the cut-off magnitude (generally we used $m_b \geq 4.0$), the quality of the data catalogs, and the definition of quiescence used (eg., there would be difference in quiescence time depending on if we accept the presence of two earthquakes with $m_b \leq 5.0$, per year as still quiet time or not).

Our observations show the following quiescent periods: 39 months for the Colima area (from 1969 to 1973), 23 months for the Playa Azul zrea (from 1979 to 1981), 18 months for the Petatlan area (from 1977 to 1979), 6 months for the Oaxaca 1968 area, 11 months for the Oaxaca 1978 area (but 48 months if we consider earthquakes with $m_b \geq 4.7$), and at least 19 months for the Oaxaca 1965 area.

Generally, the quiescent period seems to begin from about 4 years to 6 months before the main earthquake.

4) Foreshock activity (where foreshocks are defined, according to Tajima and McNally, 1983, as events that occur within the aftershock zone and during the year prior to the main shock) has been observed in the Playa Azul and Petatlan areas for about 3 months, in the Oaxaca 1978 area for about 6 months, and in the Oaxaca 1965 area for about 9 months. No teleseismic activity was detected in the Colima area. One foreshock was recorded about 4 months prior to the main event in the Oaxaca 1968 area.

Generally, the foreshock activity can be associated with the incipient rupture of the strongest asperity in the area, as documented in the Petatlan case (Hsu et al., 1983, 1985; Valdes et al., 1982).

These observations of quiescence and foreshock activity seem to be in approximate agreement with the mechanical model of the last stages of an earthquake cycle as described by Dmowska and Li (1982). In this model, the seismically active zone is interpreted as a slipping front, approaching the thrust locked zone from

below (from the direction of the sinking, subducting slab) and being stopped by the strongest asperities, which ultimately break in the great earthquake. According to this model foreshocks (if they occur) represent the progression of the slipping front through the last smaller asperities, or perhaps the initial but not yet unstable penetration of the slipping front into the main asperity. The foreshocks are usually spatially close to the area of the future main shock.

5) An important part of our observations is the seismic behavior of areas downdip from the main quake rupture zone, in the direction of the sinking slab. Generally, these areas are comparatively quiet in the first half of the earthquake cycle and later show higher seismic activity, most of which is of extensional, normal type. This activity coincides with, but usually precedes, the activity described above, in the area of main shock and in the surrounding areas. The downdip activity culminates in quite strong normal-type events, which are present in all studied areas and also before significant historical earthquakes. For example, in the Oaxaca region, 5 years before the main Oaxaca event in 1978, a normal fault earthquake of m_b = 6.6 occured downdip the descending slab; in the Ometepec region, 2 years before the main shock, a normal fault earthquake of m_b = 6.3 occured downdip the descending slab; and in the Petatlan region, a normal fault event of m_b = 6.3 occured 15 years before the main event.

Apparently, this kind of activity, that is, strong normal earthquakes positioned at greater depths downdip from the area of the future main shock, is a sign that the subducting slab had accumulated large tensile stresses, being partially relieved by these normal earthquakes, which are transmitted as shear loading to the thrust contact zone. In one case, such as the Oaxaca 1978 sequence, the large normal earthquake has such a major effect that the seismicity updip virtually ceases for four years afterwards.

6) We believe that the seismicity and associated aseismic slippage in the lower thrust zone as discussed in point 2 above, may transiently relieve the extensional stresses of the slab somewhat downdip. This concept, to be tested by future modelling, (see: Dmowska et al., 1986), may account for the sometimes observed lapse in extensional faulting at intermediate depths during the years before the main shock (Playa Azul 1981, Oaxaca 1978).

7) Other important observations involve cases of lateral migration of seismicity, as observed in the Colima 1973 area, toward the northwest and southeast; in the Playa Azul 1981 area toward the northwest and southeast, on the Michoacan 1985 rupture area; in the Petatlan 1979 area toward the north, in the Playa Azul 1981 rupture area; in the Ometepec 1982 area, toward the Acapulco 1957 main rupture area; in the Oaxaca 1968 area toward the west, in the Ometepec 1982 rupture area, and in the Oaxaca 1978 area toward an unbroken segment, to the northwest.

The results have been summarized in an October 1986 M.A. thesis by L. Lovison, and are being prepared as a report by Lovison and Dmowska.

2. The formulation of the model was given in the previous reports. We are now using the model to test the possibility that stresses leading to extensional seismicity downdip interact with those leading to thrust zone activity. One particular possibility under study is that the seismic activity in the lower part of the thrust contact zone, presumed to be accompanied by aseismic slip there, acts to

transiently reduce the extensional stresses somewhat downdip in the slab. The work is in progress.

References

Bataille, K. and K.C. McNally, Seismicity Patterns in the Petatlan Area, Mexico, unpublished manuscript, 1986.

Brown, E. and K.C. McNally, Seismicity Patterns of the 1973 Colima and 1980 Playa Azul, Mexico, Earthquakes, unpublished manuscript, 1986.

Dmowska, R. and V.C. Li, A Mechanical Model of Precursory Source Processes for Some Large Earthquakes, Geophys. Res. Lett., vol. 9, n.4, 393-396, 1982.

Dmowska, R., L. Lovison and J.R. Rice, Stress Accumulation and Transfer between a Subducting Slab and the Thrust Contact Zone during the Whole Earthquake Cycle, (Abstract), EOS, Transactions of Am. Geophys. Union, vol. 67, n.16, p. 307, 1986.

Gonzalez-Ruiz, J. and K.C. McNally, Seismicity Patterns before and after the 1982 Ometepec, Guerrero, Mexico Earthquakes, unpublished manuscript, 1986.

Hsu, V., J. Gettrust, C. Helsley and E. Berg, Local Seismicity Preceding the March 14, 1979, Petatlan, Mexico Earthquake (M, 7.6), J.G.R., vol. 88, 4247-4262, 1983.

Hsu, V. C. Helsley, E. Berg and D. Novelo-Casanova, Correlation of Foreshocks and Asperities, Pure and Appl. Geophys., 122, n.6, 1985.

Lefevre, L.V. and K.C. McNally, Stress Distribution and Subduction of Aseismic Ridges in the Middle America Subduction Zone, J.G.R., vol 90, 4495-4510, 1985.

McNally, K., J. Gonzales-Ruiz and C. Stolte, Seismogenesis of the 1984 Great (M_s = 8.1) Michoacan, Mexico Earthquake, Geophys. Res. Lett., 13, N.6, 585-588, 1986.

McNally, K and J. Gonzalez-Ruiz, Predictability of the Whole Earthquake Cycle and Source Mechanics for Large ($7.0 \leq M_w \leq 8.1$) Earthquakes along the Middle America Trench Offshore Mexico, Abstract, Earthquake Notes, vol. 57, N.1, p.22, 1986.

O'Mara, M. and K.C. McNally, Seismicity Patterns Associated with the 1978, Oaxaca Mexico Earthquake (M_w = 7.6): a Reexamination, unpublished manuscript, 1986.

Tajima, F. and K.C. McNally, Seismic Rupture Patterns in Oaxaca, Mexico, J.G.R., vol. 88, 4263-4275, 1983.

Valdes, C., R.P. Meyer, R. Zuniga, J. Havskov and S.K. Singh, Analysis of the Petatlan Aftershocks: Numbers, Energy Release, and Asperities, J.G.R., vol 87, 8519-8527, 1982.

Analysis of Natural Seismicity Anza

9910-03982

Joe Fletcher, Art Frankel, Leif Wennerberg, and Linda Haar
Branch of Engineering Seismology and Geology
U.S. Geological Survey
345 Middlefield Road, MS 977
Menlo Park, California 94025
(415) 323-8111, ext. 2384

Investigations:

1. In this section, we describe the work we have done recently to evaluate path effects at Anza. We analyzed the coda of microearthquakes in the Anza array to determine the attenuative properties of the middle and lower crust. We examined the S-wave spectra of small earthquakes to estimate the apparent attenuation of the shallow crust benearth the sites (Frankel and Wennerberg).

2. Processing of digital seismic data for hypocenters and source parameters.

Results:

1. We have developed a new model of seismic coda based on the balance between the energy in the direct wave and the energy in the seismic coda (see Frankel and Wennerberg, 1986). This energy-flux model yields a simple formula for the amplitude and time decay of the seismic coda that explicitly separates the scattering and intrinsic Q values of the medium. This new model also incorporates the effects of multiple scattering. The energy-flux model successfully predicts the coda decay and amplitude of synthetic seismograms derived from finite difference simulations of seismic wave propagation through random media. In contrast, the single-scattering model typically used in the analysis of microearthquake coda does not account for the gradual coda decays observed in simulations for random media with moderate scattering attenuation ($Q_s \leq 200$).

   We used the energy-flux model of coda to constrain the intrinsic (anelastic) and scattering Q values for the middle to lower crust near the Anza seismic network. First, the intrinsic Q was determined from the time decay of microearthquake coda. For 30 HZ S-waves, the intrinsic Q (Q_I) was calculated to be about 1300, based on analysis of seismograms from two earthquakes. The results indicate that coda Q values found from the single-scattering model of coda are rough measures of the intrinsic Q and are unrelated to the scattering Q of the crust.

   The scattering Q in the crust near Anza was constrained from the ratio between the coda amplitude and the energy in direct arrival. Figure 1 shows the coda envelopes calculated from the energy-flux model for various values of scattering Q, superimposed on a filtered seismogram (25-35 Hz) from the Anza network. The absolute amplitudes of these theoretical envelopes are determined from the energy in the direct S-wave, which is cal-

culated by integrating the square of the seismogram amplitude over the time window indicated by the bracket below the seismogram. Figure 1 illustrates that a scattering Q of 500 or less would produce a coda envelope much larger than the observed coda amplitude. The envelopes for scattering Q's between 1000 and 5000 bracket the observed coda amplitude. This initial analysis indicates that the scattering of Q for shear waves in the mid-crust must be high (at 30 Hz), between 1000 and 5000. We should stress that analysis of coda decay and amplitude do not resolve the attenuation at shallow depth ($\leq$ 3 km) beneath the receiver, *i.e.*, the site response.

We have also made substantial progress in characterizing the site response for several stations of the Anza array. For each station, we stacked the displacement spectra for small earthquakes occurring in distinct source regions. Figure 2 depicts the stacked displacement spectra at station BZN (with one standard deviation) for several earthquakes in the Table Mountain and Anza source regions. Note that the stacked spectra are essentially identical despite the difference in source locations. Figure 3 shows the stacked spectra for station FRD for the same two source regions. Again, the stacked spectra are similar for the two source regions. However, the stacked spectra are clearly different between the two stations (BZN and FRD). At BZN, the spectra are flat from 2 Hz to about 9 Hz and then fall off at about ω^{-2} for frequencies above 10 Hz. At FRD, the spectra start to fall-off at 2 Hz, and have a gradual roll-off (ω^{-1}) from 2 Hz to about 15 Hz. These observations indicate that the site response, rather than the source dimension, is probably controlling the spectral shapes observed at these stations for small earthquakes, producing the observed corner frequencies.

To date we have applied this stacking procedure to spectra determined for stations FRD, BZN, SND, and LVA. For the source regions studied so far, the stacked spectra are very similar at any particular station, as long as the hypocentral depths are greater than about 7 km. This implies that there is strong attenuation at shallow depths ($\leq$ 3 km) beneath these stations of the network (FRD, BZN, SND, LVA). These stations have already been identified as having low f_{max} values, relative to stations RDM, KNW and PFO. We will shortly apply the stacking method to se if we can characterize the site response for the stations with higher f_{max}.

The one event with distinctly lower corner frequencies than the other events studied was located at a depth of 1.1 km near station WMC, adjacent to the surface trace of the San Jacinto fault. Preliminary analysis of P-wave pulse widths at stations SND and WMC for this event indicate that the Q for P-waves is about 10 to 20 for shallow-depth material ($\leq$ 3 km) within the fault zone.

2. Approximately 550 earthquakes have been processed for locations and source parameters such as moment and stress drop. The largest is about 10^{22} dyne-cm. Figure 4 shows the locations for all of the events since the array was turned on in October 1982. The size of the symbol is proportional to the logarithm of the moment. Most events continue to occur in the clusters identified during the first few years of operation, such as the HS (Hot Springs) and KN (Keenwild) clusters near station KNW.

Initially, energies were calculated with an attenuation scheme that just used a constant Q of 300. However, many events, particularly those that were just outside the array, had energies that were orders of magnitudes higher than seemed reasonable from using the Richter formula

(logE = 11.8 + 1.5M).

In order to solve this problem, a new attenuation algorithm, was installed about a year ago and enough data has been processed to suggest that the new algorithm is producing more stable energies. The new algorithm is composed of two parts: a site-dependent part that is based on that site's f_{max} and a distance correction that used a Q of 1990. The value of Q was arrived at by calculating the correction needed to bring accleration spectra to a curve that was constant above f_{max} and subtracting out 1(pi f_{max}). With this correction, the logarithm of the energies are greater than the Richter formula by about 0.8.

Reports:

None.

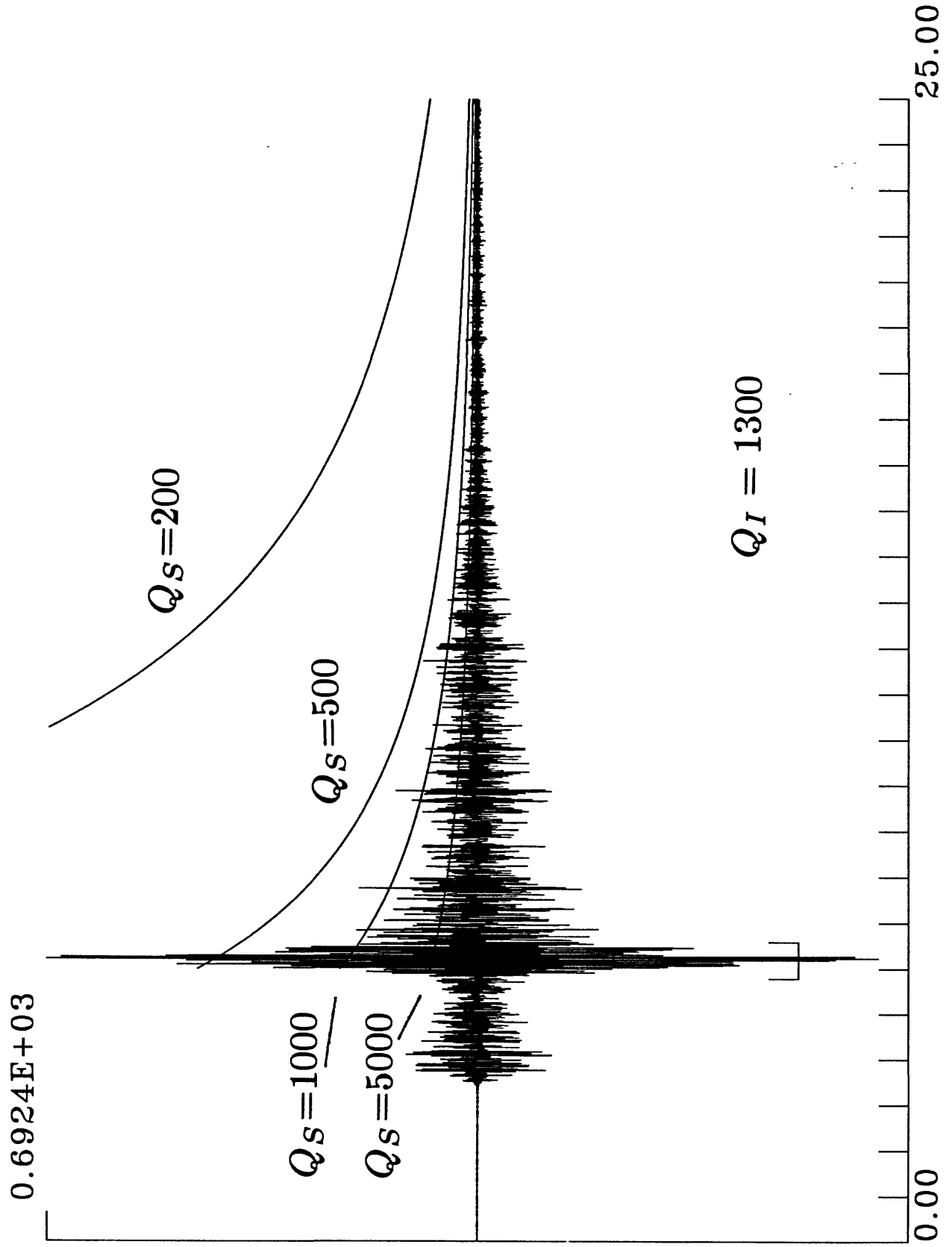
0.6924E+03
0.00
25.00
25.0 35.0
Q_S=200
Q_S=500
Q_S=1000
Q_S=5000
Q_I = 1300
02720025.RDM

Figure 1

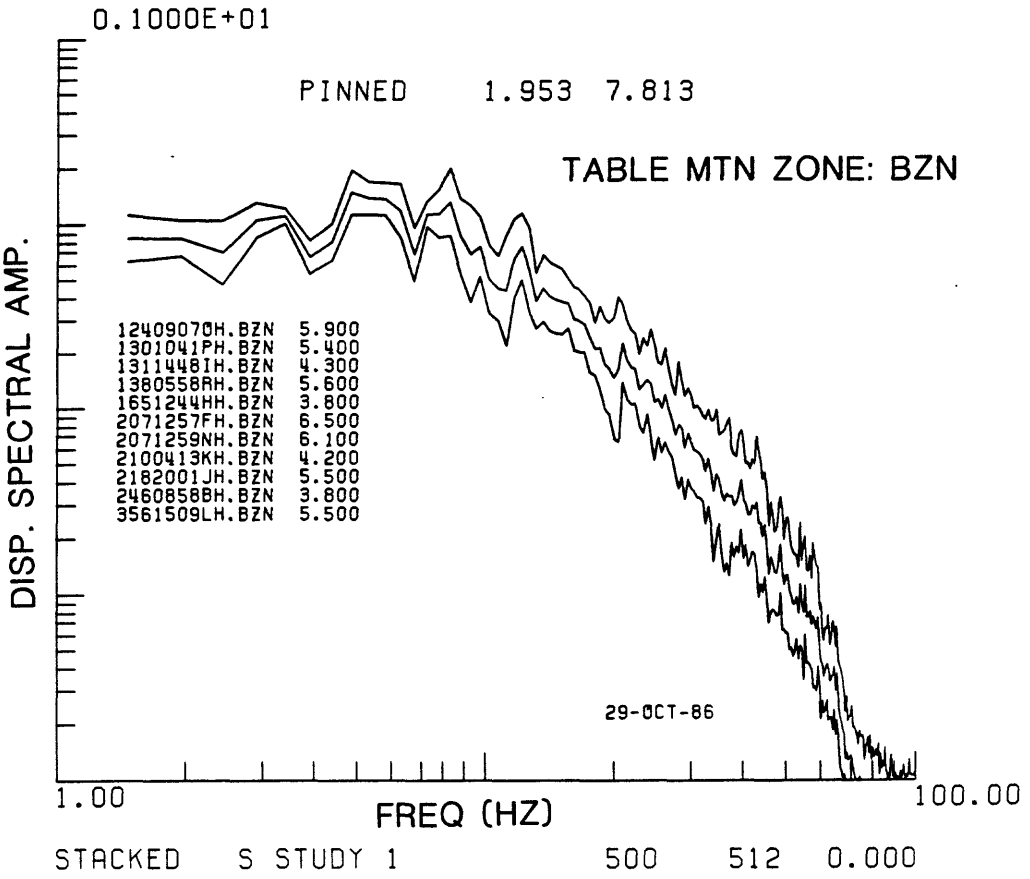
0.1000E+01
PINNED 1.953 7.813
TABLE MTN ZONE: BZN
DISP. SPECTRAL AMP.
12409070H.BZN 5.900
1301041PH.BZN 5.400
1311448IH.BZN 4.300
1380558RH.BZN 5.600
1651244HH.BZN 3.800
2071257FH.BZN 6.500
2071259NH.BZN 6.100
2100413KH.BZN 4.200
2182001JH.BZN 5.500
2460858BH.BZN 3.800
3561509LH.BZN 5.500
29-OCT-86
1.00
100.00
FREQ (HZ)
STACKED S STUDY 1 500 512 0.000

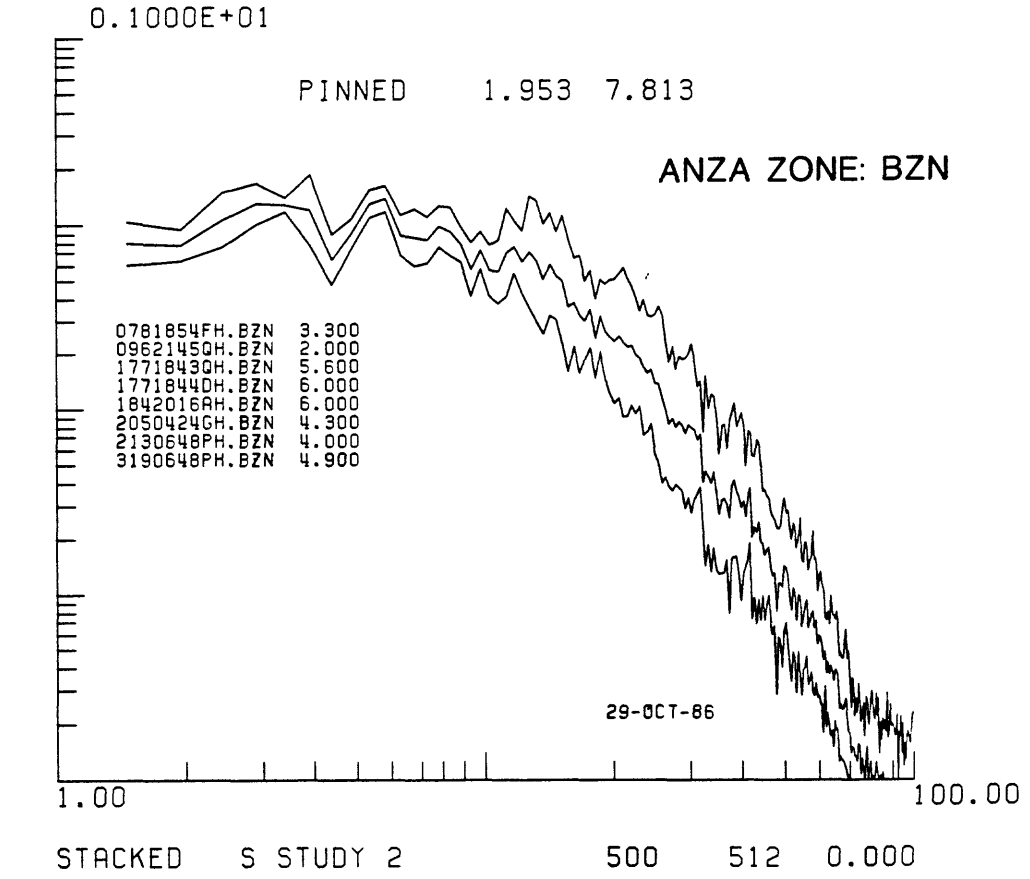
0.1000E+01
PINNED 1.953 7.813
ANZA ZONE: BZN
0781854FH.BZN 3.300
0962145QH.BZN 2.000
1771843QH.BZN 5.600
1771844DH.BZN 6.000
1842016AH.BZN 6.000
2050424GH.BZN 4.300
2130648PH.BZN 4.000
3190648PH.BZN 4.900
29-OCT-86
1.00
100.00
STACKED S STUDY 2 500 512 0.000

Figure 2

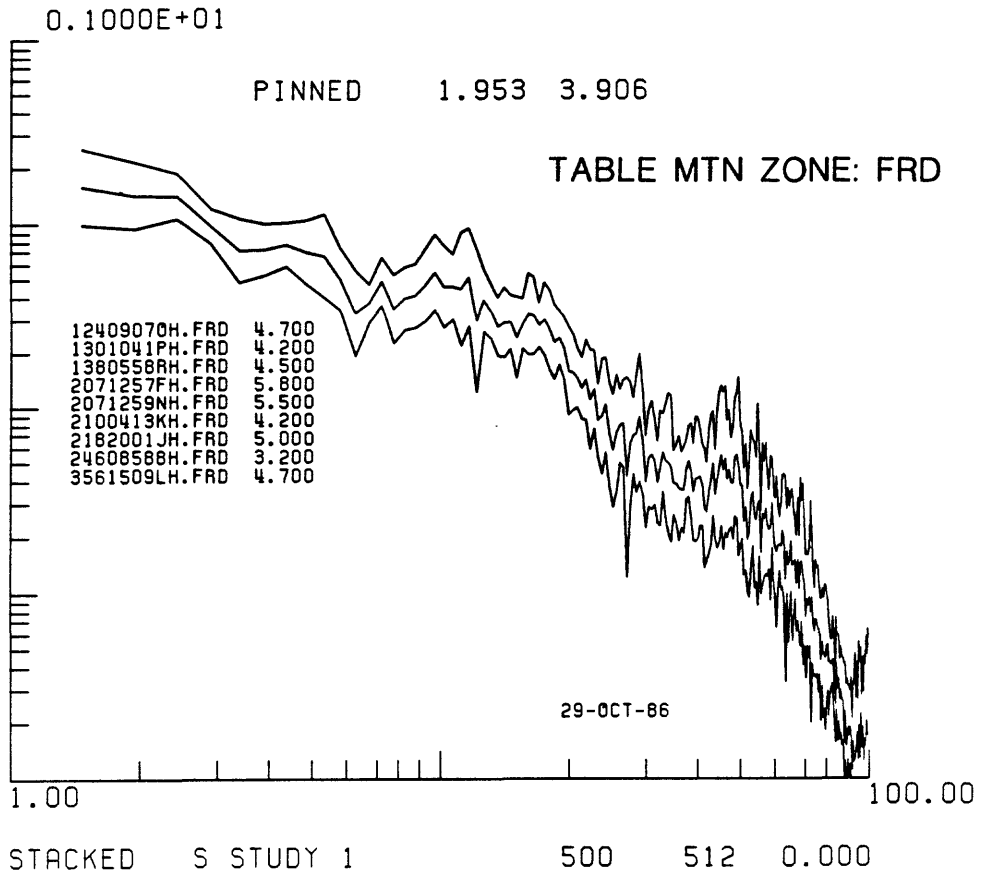
0.1000E+01
PINNED 1.953 3.906
TABLE MTN ZONE: FRD
12409070H.FRD 4.700
1301041PH.FRD 4.200
1380558RH.FRD 4.500
2071257FH.FRD 5.800
2071259NH.FRD 5.500
2100413KH.FRD 4.200
2182001JH.FRD 5.000
24608586H.FRD 3.200
3561509LH.FRD 4.700
29-OCT-86
1.00
100.00
STACKED S STUDY 1 500 512 0.000

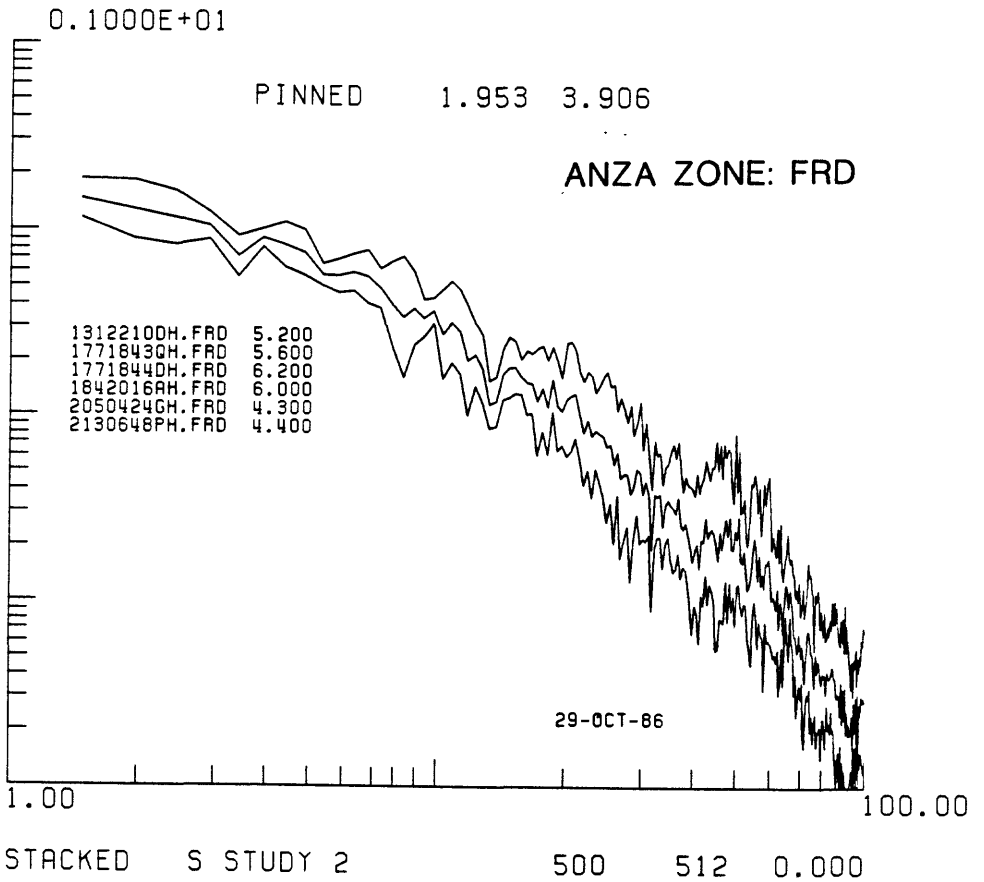
0.1000E+01
PINNED 1.953 3.906
ANZA ZONE: FRD
13122100H.FRD 5.200
17718430H.FRD 5.600
17718440H.FRD 6.200
1842016AH.FRD 6.000
2050424GH.FRD 4.300
2130648PH.FRD 4.400
29-OCT-86
1.00
100.00
STACKED S STUDY 2 500 512 0.000

Figure 3

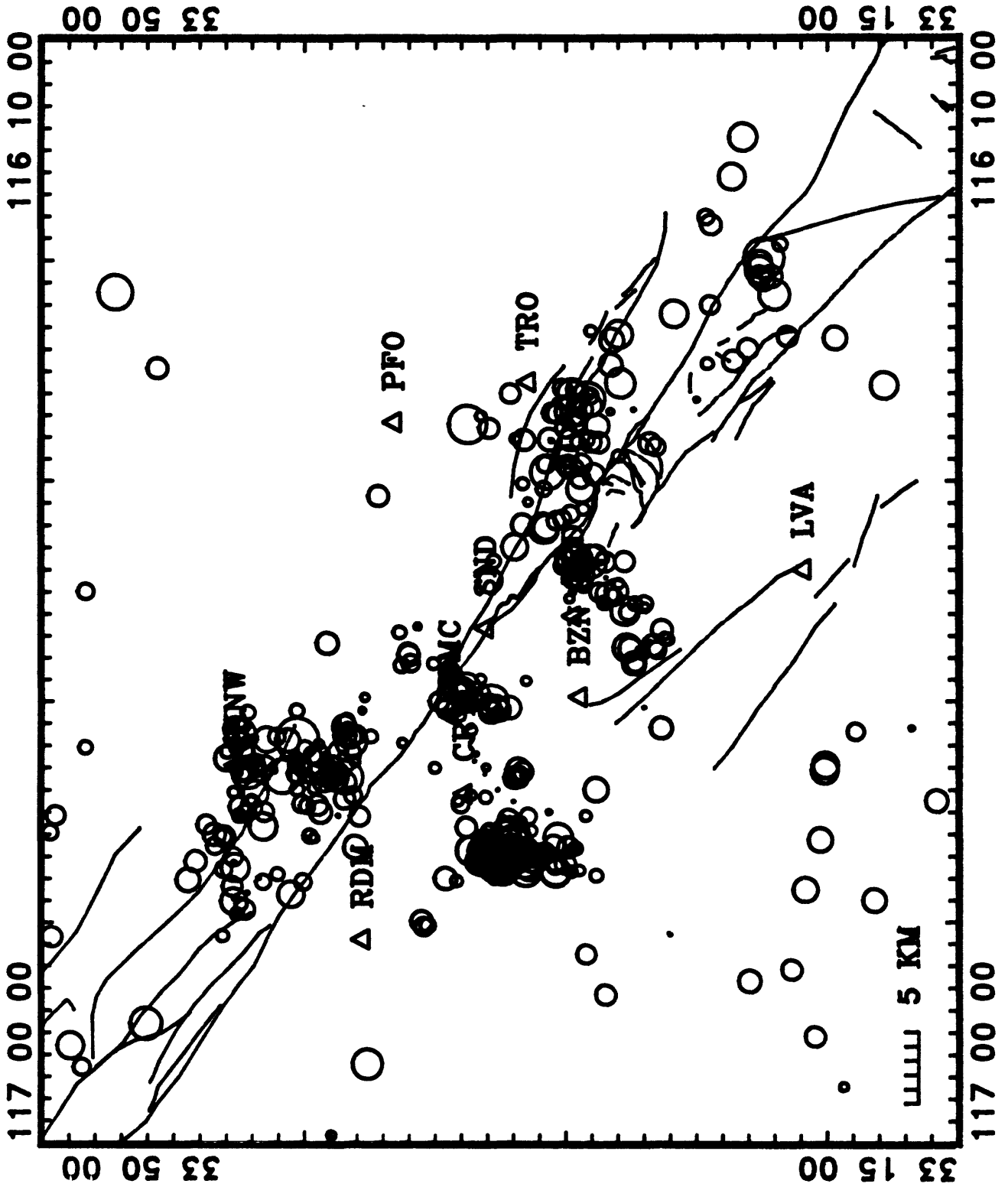

Figure 4

Quantitative Determination of the Detection History of the California Seismicity Catalog

14-08-0001-G-992

R.E. Habermann
School of Geophysical Sciences
Georgia Institute of Technology
Atlanta, Georgia 30332
(404) 894-2860

We have made progress on several aspects of this work during the last six months. We finished our analysis of the detection history in the Bear Valley segment of the San Andreas fault. We are also nearing completion of the Bitterwater segment of the San Andreas. The completion of these segments will bring our coverage to all of the San Andreas from Parkfield to San Juan Bautista as well as all of the Calaveras fault. Work which is currently in progress includes: broadening the statistical framework of our analysis by combining a number of statistical tests proposed by other authors into our programs, examination of the effects of sample duration on the results, synthesis of regional variations, comparisons of Berkeley and CALNET magnitudes for all of Central California since 1969, and integration of station histories into the analysis. Each of these tasks are described in more detail below.

The Bear Valley Segment of the San Andreas Fault

The segment of the San Andreas between 36.1 and 36.9oN was studied. We found that the northern and southern parts of this segment showed different behaviors, so a division was made at 36.63oN. The principle goal of this study was to determine magnitude corrections for this region. The following corrections were determined for the period from November, 1974 to June of 1980:

South of 36.63					North of 36.63				
		Mag					Mag		
Dates		Min	Max	Corr	Dates		Min	Max	Corr
211174	130875	0.0	10.0	-.15	211174	90476	0.0	10.0	-.11
140875	240578	0.0	10.0	-.30	100476	80278	0.0	10.0	-.23
250578	220680	0.0	10.0	-.35	90278	250680	0.0	10.0	-.10
230680	140983	0.0	10.0	-.10					
150983	290884	0.0	10.0	.10					

Addition of New Statistical Tests of Rate Differences

The statistical framework we have used to compare rates relies on a function termed AS(t) which is used to determine the times and significance of rate changes. Several U.S.G.S. scientists have recently

proposed that this function overestimates the significance of anomalies by between 4 and 10%. We examined the data that formed the basis of this proposition using statistical tests of rate differences which have been proposed by other authors in the earthquake prediction literature. We found our results to be consistent with the results of all of these tests. We concluded that the criticism was based on incorrect data which was insufficiently tested by the authors of the criticism.

During our examination of these data we incorporated other statistical frameworks into our analysis programs. These include two tests which assume that the seismicity is Poisson (one used by Ohtake et al. and McNally in Mexico and Central America and one described by Veniziano), as well as the Kolmogorov-Smirnov test which is non-parametric. We plan to add the ratios test and the Anderson-Darling statistic described by Frohlich in the near future. Our goal is to provide a general rate analysis program which allows the user to select the statistical test used for rate comparisons, thus making comparison of results of different statistical tests very easy. This goal will be reached by the end of the year.

Effect of Sample Duration on Statistical Tests.

U.S.G.S. scientists also criticized the use of an arbitrary sample duration in our rate calculations. They implied that this selection somehow invalidated our results. This claim was made without any support from actual data analysis. We tested this assertion by calculating the seismicity rates during two time periods using sample bin sizes varying from 42 to 336 hours. We then compared the rates during these two periods using the z test for a difference between two means and examined the resulting z-values. We did this test using data from the Parkfield region. The results of comparisons of rates between December 28, 1983 and November 27, 1984 to those between November 28, 1984 and June 4, 1985 in 52 different magnitude bands are shown in Figure 1. Four sets of comparisons using bin sizes which differ by a factor of eight are shown.

This example comes from a recent study of systematic changes in magnitudes in the Parkfield region (Habermann, 1986). We use it here because of the strong variations in rate changes as a function of magnitude band which should provide a good test of the effects of bin size on the comparisons. Some bands show strong increases in rates (e.g. 1.0 and below), some show strong decreases (e.g. 1.1 and above), and some show little change (e.g. 0.5 and above).

From this test we see that differences in evaluating rate changes which are introduced by varying bin size are extremely small in all magnitude bands. It is clear that the differences between the various sample sizes are not important. We agree that the selection of a bin size is arbitrary, but this example clearly demonstrates that the selection is not crucial to the results. The only practical limitation on bin size would seem to be that it must be small compared to the duration of the changes one is interested in examining.

Regional Variations in Effects of Man-made Changes.

Several man-made changes exist in the CALNET data which everyone involved expects might have an effect on the data. These include the gain change during 1977, the boundary between preliminary and final data during 1978, the installation of the RTP system during late 1980, and modifications to the RTP system since that time. We have recently been able to compare the effects of these changes in different regions.

The RTP system began to be used for coda determinations during the end of 1980 and the beginning of 1981 depending on location. The primary effect of this was a large increase in the number of small events reported, a detection increase. This increase is clear in the Southern Calaveras Fault, Bear Valley, and Bitterwater regions. It is not as strong and occurs later in the Northern Calaveras region. In the Parkfield region the installation of the RTP is mixed with a magnitude decrease caused by the inclusion of Lindh's events in the CALNET catalog so the effect is not as clear.

The second strong change which is almost certainly related to the RTP system occurs during July, 1981. This change is a complicated combination of a decrease in the number of small events reported and a strong decrease in the magnitudes for those events. This change is clear in the same regions where the detection of small events is strongly affected by the installation of the RTP system. The cause of the change during July, 1981 is presently unknown, but it likely to be an adjustment to the RTP system in these areas.

The fact that our analysis has included so much of the seismically active region of central California allows us to make regional comparisons of known man-made changes. This will add greatly to the understanding of these changes and to the prevention of them in the future.

Comparison of Berkeley and CALNET Magnitudes.

Some controversy resulted from our finding that the gain change during April, 1977 had little effect on the magnitudes in the Calaveras region. This result was in apparent conflict with preliminary results described in a memo by Bakun. His results were achieved by examining temporal variations in the differences between CALNET and Berkeley magnitudes. We are reexamining these differences to determine the cause of the conflict. We are including all Berkeley events (4000+) from 1969 to 1984. This will extend Bakun's results considerably in time and space.

REPORTS (Available on request)

The Detection History of the Calaveras Fault: A preliminary Assessment

The Detection History of the Parkfield Segment of the San Andreas fault:

A Preliminary Assessment

The Detection History of the Bitterwater Segment of the San Andreas fault: A Preliminary Assessment

Man-made Seismicity Changes

Constructing Synthetic Magnitude Signatures

ORAL PRESENTATIONS

July 26-27 NEPEC Meeting, Menlo Park (Written summaries included in USGS Open-file Report #85-754):

The Detection History of the Calaveras Fault: A preliminary Assessment

The Detection History of the Parkfield Segment of the San Andreas fault: A Preliminary Assessment

AGU meetings:

Recognition and Evaluation of Seismicity Anomalies in California, EOS, 66, 308.

The Central California Seismicity Catalog: Detection and Reporting History, EOS, 66, 971.

Seismic Quiescence at Parkfield: Real or Man-Made?, EOS, 66, 983.

Comparison of Berkeley and CALNET magnitudes for the period 1969-1984 (Fall, 1986)

A test of two techniques for identifying systematic errors in magnitudes using data from the Parkfield, California region (Fall, 1986)

PAPERS SUBMITTED

Man-Made Changes in Seismicity Rates (In Press, BSSA)

A test of two techniques for identifying systematic errors in magnitudes using data from the Parkfield, California region (In Press, BSSA)

Reply to Comment by Matthews and Reasenberg (to JGR, with M. Wyss)

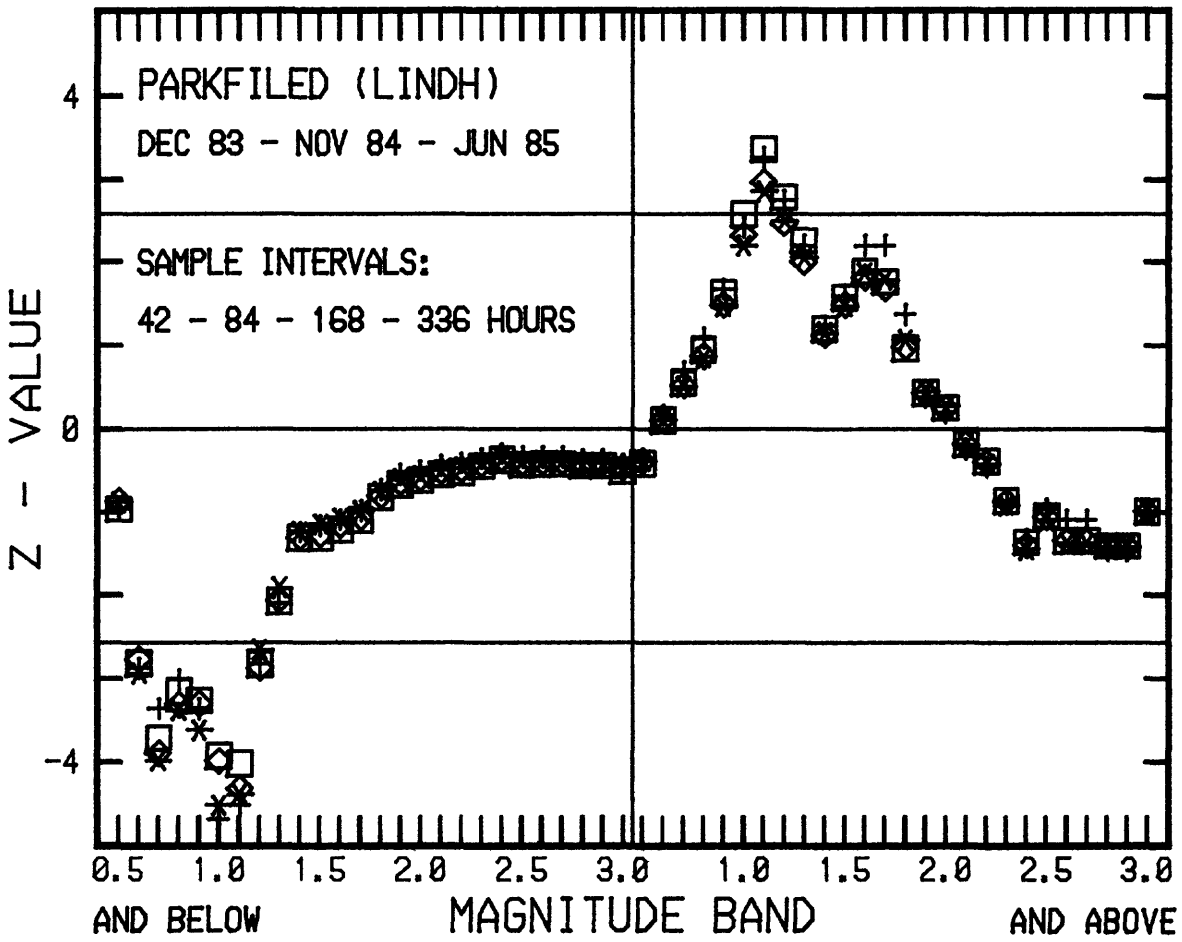

Figure 1. Z-values resulting from comparisons of the seismicity rates in the Parkfield, California region between December 28, 1983 and November 27, 1984 to those between November 28, 1984 and June 4, 1985 in 52 different magnitude bands. The bands on the left side of the plot are bounded by upper magnitude cutoffs and those on the right are bounded by lower cutoffs. Positive z-values indicate that the rate during the second period is lower than during the first, negative z-values indicate that is is higher. The two time periods were divided into samples with durations ranging from 42 to 336 hours (.25 to 2 weeks) and the rates during the two periods were compared. Using this range of sample durations the two time periods being compared contain between 12 and 192 samples each. The z-values which result from this series of comparisons are virtually independent of sample duration for sets with strong rate increases and decreases and for sets which show little change in rates (z-values near zero). The claim by Matthews and Reasenberg that the arbitrary choice of sample duration biases our results is without basis.

Instrument Development and Quality Control

9930-01726

E. Gray Jensen
Branch of Seismology
U.S. Geological Survey
345 Middlefield Road - Mail Stop 977
Menlo Park, California 94025
(415) 323-8111, Ext. 2050

Investigations

This project supports other projects in the Office of Earthquake, Volcanoes and Engineering by designing and developing new instrumentation and by evaluating and improving existing equipment in order to maintain high quality in the data acquired by the Office.

Results

Development of a small, digital, seismic refraction recorder with solid-state data storage is under way. Referred to as the J1000, a hardware prototype and necessary development tools have been assembled. When complete this unit will digitize one component at 100 or 200 samples per second with 120 dB. dynamic range at preprogrammed times. It will be capable of storing 500 KBytes or about 42 minutes of data at the lower sample rate. The units will have recording parameters set by and recorded data collected by a GRIDcase lap-top style (IBM PC equivalent) computer. Collected data will be stored on 800 KB, 3.5 in. floppy diskettes. Software development for this project is currently in progress. Planned enhancements include larger data storage memory, event detecting, additional components and direct telemetry of data.

During this period a geophysicist from this project returned with others from the USGS to Manizales, Colombia to repair and modify a seismic network installed earlier on Ruiz Volcano. This action comp]etes the USGS involvement in this operation. Approximately 500 J120 telemetry discriminators have been constructed and 80 have been tuned and are ready for service. A modified J502 preamp/VCO, known as the J502A, has been designed which has a power circuit that is cheaper, simpler to build and which shuts itself off when the input voltage is too low thereby avoiding interference with other stations. A board comprised of only the power circuit, the J601, has also been created. The identification and subsequent correction of problems in the CUSP/Tustin digitizing systems led to the elimination glitches and channel switching in the data.

Numerous CalNet sites were visited for maintenance, repair or upgrading. Sixteen staions in the Yellowstone network were upgraded with V02L boards during the yearly maintenance visit. A new 70 KW power generator with a 30 KW uninterruptible power supply has been purchased and will be installed soon. Development of an alarm system for the microwave telemetry system is nearly complete. In addition numerous telemetry radios and seismometers were repaired, adjusted or calibrated and support was provided for Seismic Cassette Recorder operations.

Southern California Earthquake Hazard Assessment

7-9930-04072

Lucile M. Jones and Douglas D. Given
Branch of Seismology
U.S. Geological Survey
Seismological Laboratory 252-21
California Institute of Technology
Pasadena, California 91125

INVESTIGATIONS

1. Routine Processing of Southern California Network Data.

Routine processing of seismic data from stations of the cooperative southern Califoria seismic data from stations of the cooperative southern California seismic network was continued for the period April through September 1986 in cooperation with scientists and staff from Caltech. Routine analysis includes interactive timing of phases, location of hypocenters, calculation of magnitudes and preparation of the final catalog using the CUSP analysis system. About 1300 events are detected in most months with a regional magnitude threshold of 1.8. The occurrence of three large earthquakes in southern California during July 1986, more than tripled this rate with 3000 events processed so far for the first three weeks of July. Because of this large increase in recorded events, six weeks in November and December 1985 and eight weeks from July to September 1986 are still unprocessed. However, as of October 1986, events are being processed about twice as fast as they are being recorded so these backlogs should be eliminated within the next two or three quarters.

2. Foreshocks in Southern California

Analysis of the characteristics of immediate foreshocks (those that occur within hours or days of their mainshocks) in southern California is continuing. The probability as a function of magnitude and time that any southern California earthquake will be a foreshock has been determined as well as a site-specific result for possible foreshocks to the characteristic Parkfield earthquake. The same technique, in which the increased probability of a large earthquake occurring after a possible foreshock is combined with the conditional probability of a large earthquake determined from recurrence intervals, is being applied to the whole San Andreas and the San Jacinto faults. These results are also applied to real time earthquake hazard assessment.

3. Focal Mechanisms and State of Stress in Southern California.

The state of stress in southern California is being analyzed from focal mechanisms of small and moderate earthquakes. Two projects are currently underway. First, the state of stress as a function of position along strike

of the southern San Andreas fault has been determined from earthquakes of M $\geq$ 2.6 with epicenters within 10 km of the surface trace of the fault. In addition, temporal changes in the state of stress on the San Andreas fault are being examined by comparing the aftershocks of the North Palm Springs earthquake to background seismicity in the same region recorded in the last 8 years. In both studies, focal mechanisms are determined from local network data and then inverted for information about the stress state.

4. The North Palm Springs Earthquake of July 1986.

The M = 5.9 North Palm Springs earthquake of July 08, 1986 and its aftershocks are being analyzed. Focal mechanisms are being determined for the M $\geq$ 3.0 aftershocks. All of the aftershocks are being relocated using a master event technique. The results are compared to the geologic structures to better understand the deformation occurring on the southern San Andreas fault.

5. Quaternary Faulting in the Los Angeles Region.

Active Quaternary faults in the Los Angeles region are compared to the pattern of present seismicity. A map has been prepared showing Quaternary faults with their slip rates, if known, with the M $\geq$ 2.0 earthquakes recorded between 1978 and 1984. The epicentral and depth distribution of the earthquakes are compared to the locations of the faults.

RESULTS

1. Foreshocks in Southern California.

Analysis of the earthquakes recorded in the Parkfield region since 1932 has shown that the most likely site of foreshocks to future Parkfield mainshocks is a small area of the San Andreas fault just north of the mainshock hypocenters under the Middle Mountain alarm box. An analytic expression has been derived for the probabiity that the characteristic Parkfield earthquake will occur within some time period after a smaller earthquake occurs in the Middle Mountain alarm box. This probability is:

$$P(t, T, M) = \left[1 + 0.307 \times 10^{-0.12T} \left(\frac{3135 \times 10^{-0.62M}}{1 - \exp(-\lambda t)} \right) - 1 \right]^{-1}$$

where t is the time after the possible foreshock in hours, T is time since 1986/1/1 in years, M is the magnitude of the possible foreshock and λ = 0.022. From this result, the probability that a M = 4.5 earthquake in the Middle Mountain alarm box in 1988 will be followed within 3 days by the characterstic Parkfield earthquake is 53%.

2. Focal Mechanisms and the State of Stress in Southern California.

Focal mechanisms have been determined for small and moderate earthquakes occurring within 10 km of the surface trace of the southern San Andreas Fault (SAF) between 1978 and 1985. On the basis of these mechanisms, the southern SAF has been divided into five stress regimes - Fort Tejon, Mojave, San

Bernardino, Banning and Indio - and the focal mechanisms data in each region has been inverted for information about the state of stress. Reverse faulting predominates in Fort Tejon and Mojave. An abrupt change occurs at the end of the 1857 rupture zone, where reverse faulting in Mojave changes to normal faulting in San Bernardino. Indio also shows oblique normal faulting with strike-slip and reverse mechanisms, with the type of mechanism depending on the depth of the earthquake. The inversion of these data shows that one of the principal stresses is vertical in each region, but it is the minimum principal stress at Fort Tejon and Mojave, the intermediate principal stress at Banning and Indio, and the maximum principal stress at San Bernardino. If the vertical stresses are lithostatic and thus relatively similar in the five regions, then the magnitudes of the stresses are higher in the 1857 rupture zone than elsewhere on the southern San Andreas. The strike of the maximum horizontal stress also varies between the regions, rotating 35° clockwise from north to south. In Fort Tejon and San Bernardino, the orientation of the horizontal stresses is parallel to that of the principal strains recorded by Savage and others over the last 13 years. In Mojave and Indio, the stress direction is rotated about 15° clockwise from the strain direction.

3. The North Palm Springs Earthquake.

The mainshock and aftershocks of the North Palm Springs earthquake sequence have been relocated using the master event technique. The aftershock distribution clearly delineates a planar structure that strikes N65°W and dips 45° northeast. This structure is most likely the down-dip extention of the Banning fault. The aftershocks are distributed symetrically about the mainshock but tend to cluster. They occur through a depth range of 2 to 18 km with a peak in activity at 11 km; the depth of the mainshock. The aftershock pattern northwest of the mainshock is markedly different from that to the south-east. Northwest of the mainshock most events lie on the dipping planar structure and gradually peter out with distance along strike. In contrast, the events to the southeast are diffuse, shallower on average, and cease abruptly at a distance of about 7 km along strike from the mainshock. The different pattern of aftershocks on either side of the mainshock coincides with the southern kink of the "big bend" in the San Andreas fault zone and a persistent boundary between high activity in San Gorgonio Pass and low activity in the Coachella Valley. This suggests that the earthquake occurred at a point where the fault zone undergoes a significant change in regime.

REPORTS

1. Jones, L.M., L.K. Hutton, D.D. Given, and C.A. Allen, The North Palm Springs earthquake sequence of July 1986, in press, Bull. Seismol. Soc. Amer., December 1986.

2. Jones, L.M., and A.G. Lindh, Foreshocks and earthquake prediction at Parkfield, California, in review, submitted to Bull. Seismol. Soc. Amer., 1987.

3. Ziony, J.I., and L.M. Jones, Map showing late Quaternary faults and 1978-1984 seismicity of the Los Angeles region, California, U.S. Geological Survey Miscellaneous Field Studies Map MF-xxx, 1987.

4. Norris, R., L.M. Jones, and L.K. Hutton, The Southern California Network Bulletin, II, July through December, 1985, U.S. Geol. Surv. Open-file Report 86-337, 1986.

5. Given, D.D., R. Norris, L.M. Jones, L.K. Hutton, C.E. Johnson, and S. Hartzell, The Southern California Network Bulletin, III, January through June, 1986, U.S. Geol. Surv. Open-File Report 86-??, 1986.

6. Jones, L.M., L.K. Hutton, D.D. Given, and C.A. Allen, The North Palm Springs earthquake sequence of July 1986, (abst.), in press, Trans Amer. Geophys. Union, November, 1986.

7. Given, D.D., Master event relocations of the North Palm Springs earthquake sequence of July 1986, in press, Trans. Amer. Geophys. Union, November, 1986.

8. Michael, A.J., and L.M. Jones, Stress fluctuations due to the North Palm Springs earthquake, in press, Trans. Amer. Geophys. Union, November, 1986.

9. Hutton, L.K., C.A. Allen, D.D. Given, C.E. Johnson, and L.M. Jones, DNAG Summary of southern California seismicity, in press, Trans. Amer. Geophys. Union, November, 1986.

10. Nicholson, C., R.L. Wesson, D.D. Given, J. Boatwright, and C.R. Allen, Aftershocks of the 1986 North Palm Springs earthquake and relocation of the 1948 Desert Hot Springs earthquake sequence, in press, Trans. Amer. Geophys. Union, November 1986.

State of Stress Near Seismic Gaps

Contract No. 14-08-0001-G1170

Hiroo Kanamori
Seismological Laboratory, California Institute of Technology
Pasadena, California 91125 (818-356-6914)

Investigations

1) Interplate Coupling and Temporal Variation of Mechanisms of Intermediate-depth Earthquakes in Chile.
Luciana Astiz and Hiroo Kanamori

2) Regional Variation of the Short-Period (1 to 10 sec) Source Spectrum
Yuru Zhuo and Hiroo Kanamori

Results

1) Interplate Coupling and Temporal Variation of Mechanisms of Intermediate-depth Earthquakes in Chile

We investigated the temporal variation of the mechanisms of large intraplate earthquakes at intermediate depths in relation to the occurrence of large underthrusting earthquakes in Chile. Focal mechanisms were determined for three large events (March 1, 1934: M = 7.1, d = 120 km, April 20, 1949: M = 7.3, d = 70 km and May 8, 1971: M_w = 7.2, d = 150 km) which occurred down-dip of the great 1960 Chilean earthquake (M_w = 9.5) rupture zone. The 1971 event is down-dip compressional: θ (strike) = 12° , δ (dip) = 80° , λ (rake) = 100°. The 1949 earthquake focal mechanism is θ = 350°, δ = 70° and λ = –130°. The data available for the 1934 event are consistent with a down-dip tensional mechanism. Thus, the two events which occurred prior to the great 1960 Chilean earthquake are down-dip tensional. Published fault plane solutions of large intermediate-depth earthquakes (March 28, 1965 and November 7, 1981) which occurred down-dip of the Valparaiso earthquakes of 1971 (M_w = 7.8) and 1985 (M_w=8.0) are also down-dip tensional. These results suggest that before a major thrust earthquake, the interplate boundary is strongly coupled and the subducted slab is under tension at intermediate depths; after the occurrence of an interplate thrust event, the displacement on the thrust boundary induces transient compressional stress at intermediate depth in the down-going slab. The interpretation is consistent with the hypothesis that temporal variations of focal mechanisms of outer-rise events are due to changes of interplate coupling.

2) Regional Variation of the Short-Period (1 to 10 sec) Source Spectrum

We determined $\hat{m}_b$, the body-wave magnitude calculated from the maximum amplitude of short-period P waves, of 38 large earthquakes in various tectonic provinces. The data are divided into three groups; Group 1 (subduction-zone thrust events), Group 2 (non-subduction zone dip-slip and oblique-slip events), and Group 3 (strike-slip events). Group 2 and Group 3 include intraplate earthquakes. Comparison of $\hat{m}_b$ values for these three groups of events suggests that the source spectral amplitudes of intraplate events at a period of about 1.4 sec is 2 to 5 times larger than those of subduction-zone events with the same M_w. We also determined the source spectra of 24 large earthquakes (M_w = 6.5 to 7.7) directly from the GDSN (Global Digital Seismographic Network) data, over a period range from 1 to 10 sec. At periods from 1 to 2 sec, the source spectral amplitudes of intraplate earthquakes are 2 to 4 times larger than those of subduction-zone events with the same M_w. The difference decreases as the period increases to 10 sec.

References

Eissler, Holly, Luciana Astiz, and Hiroo Kanamori, Tectonic setting and source parameters of the September 19, 1985 Michoacan, Mexico Earthquake, *Geophys. Res. Lett., 13*, No. 6, pp. 569-572, 1986.

Houston, Heidi and Hiroo Kanamori, Source characteristics of the 1985 Michoacan, Mexico earthquake at short periods, *Geophys. Res. Lett, 13*, No. 6, pp. 597-600, 1986.

Astiz, Luciana and Hiroo Kanamori, Interplate coupling and temporal variation of mechanisms of intermediate-depth earthquakes in Chile, Bulletin of the Seismological Society of America, in press, 1986.

Zhuo, Yuru and Hiroo Kanamori, Regional variation of the short-period (1 to 10 sec) source spectrum, Bulletin of the Seismological Society of America, in press, 1986.

FAULT MECHANICS AND CHEMISTRY

9960-01485

C.-Y. King
Branch of Tectonophysics
U.S. Geological Survey
345 Middlefield Road, MS/977
Menlo Park, California 94025
(415) 323-8111, ext. 2706

Investigations

1. Water temperature and radon content were continuously monitored at three water wells in San Juan Bautista and Parkfield, California.

2. Water level was continuously recorded at six other wells.

3. Water temperature and electric conductivity were periodically measured, and water samples were taken from most of these wells and two springs in San Jose for chemical analysis.

4. Radon content of ground gas was continuously monitored at Cienega Winery, California, and at Nevada Test Site.

5. Predictability of slip events along a laboratory fault was studied.

Results

1. Predictability of slip events along a laboratory fault

   A "long" sequence of stick-slip events generated along a laboratory fault, which consists of eight spring-connected masses that are elastically driven to slide on a frictional surface, has been examined to check whether the "large" events are predictable. The large events are found to recur at intervals of very different durations, although the elastic and frictional properties along the fault are quite uniform. The recurrence intervals are, however, approximately proportional to the displacements of the preceding events, but not of the following events. Thus the occurrence time of a large event is approximately predictable, whereas its displacement is not. The size (logarithmic energy release) distribution of all the events of different sizes can be fitted by a maximum-entropy model, which has an upper bound in size corresponding to the complete release of the maximum strain energy stored along the fault.

2. Observational and physical basis for gas-geochemical approaches to earthquake prediction: a review

Terrestrial gases in ground water and soil air have been extensively studied in recent years in seismically active areas, especially in USSR, China, Japan and USA, in search of premonitory changes that might be useful for earthquake prediction. Concentrations of radon, helium, hydrogen, mercury, carbon dioxide and several other volatiles have been found generally to be anomalously high along active faults, suggesting that the faults may be paths of least resistance for the terrestrial gases generated or stored in the earth to escape to the atmosphere. Temporal concentration changes with durations of a few hours to many months have been observed before many large earthquakes at a relatively few favorably situated stations at epicentral distances of up to several hundred kilometers. These "sensitive" stations are generally located along active faults, especially at intersections or bends of faults, or some other structurally weak zones, possibly because of relatively high porosity and permeability, and concentration of tectonic strain changes at such places. Gas changes have also been observed at times of underground explosions and in association with earth tides, and in rock-mechanics experiments. The results have been used to delineate the mechanisms of earthquake-related gas anomalies. However, gas concentrations, especially those measured at or near the ground surface, may also be significantly affected by meteorological, hydrological and other nontectonic changes in the environment. The nontectonically-induced variations must be carefully eliminated or recognized in the search of true earthquake-related anomalies.

Reports

Scarpa, R., and King, C.-Y., 1986, Modeling of volcanic processes: Preface: Earth Evolution Sciences, [in press].

King, C.-Y., 1986, Gas geochemistry applied to earthquake prediction: an overview: Journal of Geophysical Research, v. 91, [in press].

King, C.-Y., 1986, Preface to special section on gas geochemistry of volcanism, earthquakes, resource exploration, and earth's interior: Journal of Geophysical Research, v. 91, [in press].

King, C.-Y., 1986, Predictability of slip events along a laboratory fault: Geophysical Research Letters, [in press].

King, C.-Y., 1986, Predictability of slip events along a laboratory fault (abs.): EOS (Transactions of the American Geophysical Union), [in press].

Friedmann, H., Aric, K., King, C.-Y., and Cakmak, I. T., 1987, Radon measurements for earthquake prediction along the North Anatolian Fault Zone: a progress report: Tectonophysics, [in press].

King, C.-Y., 1986, Observational and physical basis for gas-geochemical approaches to earthquake prediction (abs.): U.S.G.S. Workshop on Physical and Observational Basis for Intermediate-Term Earthquake Prediction, Nov. 13-17, 1986, in Monterey, CA.

Southern California Cooperative Seismic Network

7-9930-01174

Charles Koesterer
U.S. Geological Survey
Branch of Seismology
525 S. Wilson Avenue
Pasadena, CA 91106

INVESTIGATIONS

1. Continued operation, maintenance, and recording of the southern California seismic network consisting of 189 U.S.G.S. short period seismograph stations and 66 other agency instruments. All stations being recorded onto the CUSP analysis system and 200 stations recorded on FM tape units for back-up of digital recording.

2. Provision of logistics, management, and computer support for three other U.S.G.S. projects within the Pasadena Field Office.

RESULTS

1. Continued testing and implementation of phone lines onto the microwave radio telemetry system. Due to telephone company restraints, the completion date of 14 channels of data onto the system is now projected to be early 1987.

2. Continued construction of and modification on AMP/VCO units for network upgrades.

3. Conducted a snapshot of system components on each seismic station for calculations of system responses.

4. Continued operation and maintenance of field stations and office recording systems with very little failures during this reporting period.

Microearthquake Data Analysis

9930-01173

W. H. K. Lee
U.S. Geological Survey
Branch of Seismology
345 Middlefield Road, Mail Stop 977
Menlo Park, California 94025
(415) 323-8111, Ext. 2630

Investigations

The primary focus of this project is the development of state-of-the-art computation methods for analysis of data from microearthquake networks. For the past six months I have been involved mainly in a project called "Investigation of signal characteristics of quarry blasts, nuclear explosions, and shallow earthquakes for regional discrimination purposes" for the Defense Advanced Research Projects Agency. The objective is to collect high-frequency seismic data generated by quarry blasts, controlled explosions, and shallow earthquakes, to study their signal characteristics, and to develop a method to discriminate between these three different sources.

Results

We have examined several hundred quarry blasts and shallow earthquakes at four quarry sites. We performed spectral analyses on both shorth (2.56 sec) and long (1.24 sec) windows, beginning shortly before the P-arrival time. We noted the differences between quarry and earthquake spectra, and quantified them by ratios of spectral amplitudes. Results indicated that quarry blasts and earthquakes could be separated into two distinct populations by spectral amplitude ratios. Quarry blasts were observed to be richer in lower frequency signals at short distances than earthquakes. This observation is opposite to the well established fact for explosion/earthquake at regional and teleseismic distances. Several explanations are possible: (1) signals from quarry blasts at short distances traveled through mostly the near surface rocks where fractures are common and thus effectively filter out the high-frequency signals, (2) the staggering of shots in a quarry blasts stretches out the source-time function and the high-frequency signals are more likely subjected to destructuve interferences, and (3) for small magnitude events, the source dimension for an earthquake is much smaller than that for a quarry blast.

Reports

Lee, W. H. K., and C. V. Valdes, HYP071PC: A personal computer version of the HYP071 earthquake location program, USGS Open-File Report, 85-749, 1985.

Lee, W. H. K., and others, A preliminary study of Coda Q in California and Nevada, Bull. Seism. Soc. Am., 76, 1143-1150, 1986.

Aviles, C. A., and W. H. K. Lee, Variations in signal characteristics of small quarry blasts and shallow earthquakes, Abstract submitted to EOS (Transaction AM. Geophys. Union), v. 67, p. 1093.

Phillips, W. S., W. H. K. Lee, and J. T. Newberry, Spatial variation of crustal coda Q in California, EOS, v. 67, p. 1093.

Peng, J. Y., K. Aki, and W. H. K. Lee, Scattering and attenuation of high-frequency (1-25 Hz) seismic waves in the lithosphere with application to earthquake prediction, EOS, v. 67, p. 1086.

Analysis of Large Tremors Associated with Gold Mining Operations in South Africa

9901-04100

Art McGarr
Branch of Engineering Seismology and Geology
U.S. Geological Survey
345 Middlefield Road, MS 977
Menlo Park, California 94025
(415) 323-8111, ext. 2708

Investigations:

Seven seismic stations were installed in and around the major gold mining districts of South Africa during March 1986 to study tremors in the magnitude range of 3 and greater at local and regional distances.

Results:

A vast number of tremors of $M \geq 3$ have been recorded and analyzed for source and ground motion parameters. In addition, studies have been initiated of the nature of high frequency wave propagation from the seismic source to distances of up to 400 km.

Reports:

Monthly status reports to AFTAC and DARPA since October 1985.

CRUSTAL STRAIN

9960-01187

W.H. Prescott, J.C. Savage, M. Lisowski, N. King
Branch of Tectonophysics
U.S. Geological Survey
345 Middlefield Road, MS/977
Menlo Park, California 94025
(415) 323-8111, ext. 2701

Investigations

The principal subject of investigation was the analysis of deformation in a number of tectonically active areas in the United States.

Results

1. Extremely High Shear Strain Rate Measured Across the Fairweather Fault Near Yakutat, Alaska

Trilateration surveys in 1983 and 1986 of two strain networks that extend across the Fairweather fault near Yakutat, Alaska, show shear strain accumulating at an average rate of 1.6 ± 0.2 ppm/yr within an 8-km-wide zone centered on the fault. The direction of maximum right-lateral shear in both networks is nearly parallel to the N36°W trend of the Fairweather fault. This same rate and direction of shear was reported for one of the networks during the epoch 1967 to 1983. A part of one of the networks extends from 10 to 20 km west of the fault, where the average shear strain rate is 0.8 ± 0.2 ppm/yr with maximum right-lateral shear across a vertical plane bearing N25°W ± 8°. The broad zone of strain accumulation is consistent with a simple elastic dislocation model of the Fairweather fault, in which the fault is locked from the surface to a depth of 9 km and slipping right-laterally at a rate of 5.4 ± 0.3 cm/yr below that depth. This rate is in good agreement with the 5.3 ± 0.2 cm/yr of plate motion parallel to the Fairweather fault predicted by global plate motion models. The strain accumulation rates observed across the Fairweather fault are from 3 to 5 times greater than contemporary strain rates measured across locked parts of the tectonically similar San Andreas fault in California.

2. Parkfield Area Short-Range Trilateration Networks

Repeated measurements of four short-range trilateration networks located in the Parkfield area were analyzed to determine shallow slip on the San Andreas fault between 1974-77 to 1986.

The computed average slip rate was 27 ± 1 mm/yr near Slack Canyon, to 10 ± 1 mm/yr at Parkfield, to 7 ± 1 mm/yr at Gold Hill, and to 4 ± 1 mm/yr at Cholame. The rate of slip at each network has remained fairly constant over the 1974 to 1986 interval, but there are gaps as long as 4 years between surveys in some networks.

3. Strain Accumulation in the Olympic Mountains, Washington, 1982-1986

Surveys in 1982, 1983, and 1986 of a 21-line, 30-km aperture strain network located in the Olympic Mountains of western Washington show average principal strain rates of 0.12 ± 0.06 ppm/yr at N31°W ± 10° and -0.03 ± 0.06 ppm/yr at N59°E ± 10° (extension positive). The maximum engineering shear strain rate of 0.15 ± 0.06 ppm/yr and the direction of maximum contraction is similar to that deduced from repeated triangulation surveys in this century that cross the nearby Strait of Juan de Fuca. A simple elastic model of the subduction of the Juan de Fuca plate beneath the North American plate, however, would predict primarily contraction in the N60°E direction of plate convergence instead of the extension parallel to the plate boundary observed in the Olympic network. It is possible that the compression has been masked by systematic error in dilatation, a type of error that is common in trilateration surveys. Scale error of perhaps 0.1 ppm/yr superimposed on a tectonic contraction could produce the observed strain field.

4. Deformation Associated with the 1986 Chalfant Valley Earthquake, Eastern California

The Chalfant Valley earthquake (July 21, 1986; epicenter about 25 km north of Bishop, California) occurred within a precise trilateration network that had last been surveyed in January 1985. The line-lengths in the network average about 20 km and changes in length of as much as 180 mm were observed. The observed changes would be consistent with 1.3 m right-slip and 0.7 m normal slip on a 15-km-long buried fault dipping 50° S55°W. The inferred seismic moment is equivalent to a magnitude (M_L or M_S) 6.4 earthquake.

5. Strain Accumulation in the Yakataga, Alaska Seismic Gap

The Yakataga seismic network was resurveyed in June 1986. The network continues to exhibit contraction in the N19°W direction, but the longer data base now available suggests that the shortening is concentrated near the Chugach-St Elias fault in an area completely covered by the Bering glacier. The block north of the Chugach-St Elias fault appears to be subject to right-lateral shear parallel to that fault, shear that is tentatively attributed to the Contact fault.

6. Deformation in the Long Valley Caldera, Eastern California, 1985-1986

The 40-line Long Valley caldera was resurveyed in late July 1986 following the nearby Chalfant Valley earthquake. The 1985-1986 deformation in the network appeared to the comparable to the 1984-1985 deformation. However, the annual deformation is now close to the precision of measurement and comparisons between annual deformations are quite uncertain. The southeastern part of the network was disturbed by the Chalfant Valley earthquake.

7. Deformation Along the San Andreas Fault 1982-1986 as Indicated by Frequent Geodolite Measurements

Frequent (4 to 12 times per year) measurements of six 3-line (lengths 10 to 40 km) strain networks located along the locked sections of the San Andreas fault in southern and central California provide a time history of deformation along the fault in the interval 1982 to 1986. The standard error in measurement ranges from 0.4 ppm in line-length for the shortest lines to 0.2 ppm for the longest lines. Except for one example of coseismic offset and postseismic relaxation, the observations are at least marginally consistent with uniform in time deformation. The records of deformation at the networks closest to the epicenters of two recent magnitude-6 California earthquakes (1984 Morgan Hill and 1986 North Palm Springs) were particularly stable in the year preceding the earthquakes. Thus, it is unlikely that these earthquakes were triggered by regional strain events. However, marginally significant anomalies were observed 12 to 18 months before both earthquakes.

8. Global Positioning Observations

The U.S. Geological Survey has begun a series of experiments designed to investigate the application of Global Positioning System (GPS) technology to the measurement of crustal deformation. Experiments in progress involve lines with lengths between 2 and 350 km. The results reported here have been obtained using a misture of "broadcast" orbits and postprocessed orbits obtained from the Naval Surface Weapons Station in Dahlgren, Virginia. Twenty measurements of line-lengths of a 43 km north-south line have an rms scatter of 1.7 cm (0.4 ppm). Twelve observations of a 32 km east-west line have an rms scatter of 3.5 cm (1.1 ppm). The observations span nearly a one year interval. Both baselines are located in central California and have also been observed with a Geodolite and aircraft, an electronic distance measuring system with a demonstrated precision of 0.2 ppm (0.9 cm at 43 km and 0.6 cm at 32 km). There is a significant difference between the two systems (Figure). Part of this offset may be due to errors in the ground survey

connecting the two different stations used by GPS and the Geodolite surveys. Observations of a smaller quadrilateral near Parkfield, California (side lengths: 6.7, 10.8, 11.9, 4.5, 6.7, and 2.7 km) yield an rms standard error of 2 to 9 mm. In parts per million the scatter on these shorter lines is again about 0.5 to 1.0 ppm. Thus, for these short lines, even with present orbits, the precision is comparable to careful single color laser distance measurements. We have also begun observations of a larger triangle in southern California with the specific objective of examining the improvement that water vapor radiometers can make to GPS measurements. We are just beginning to accumulate data for this evaluation. It is clear that presently available orbit sources are inadequate. Under a contract from the U.S. Geological Survey, the University of Texas at Austin is tracking the GPS satellites from stations in Westford, Massachusetts, Austin, Texas, and Mojave, California. We have begun to receive orbits calculated by Texas. This should produce a significant improvement in precision.

Reports

Gu, G.-H., and W.H. Prescott, Discussion on displacement analysis: detection of crustal deformation, J. Geophys. Res., 91(B7), 7439-7446, 1986.

Prescott, W.H. and S.-B. Yu, Geodetic measurement of horizontal deformation in the northern San Francisco Bay region, California, J. Geophys. Res., 91(B7), 7475-7484, 1986.

Savage, J.C., and M. Lisowski, Strain accumulation in the Shumagin seismic gap, Alaska, J. Geophys. Res., 91, 7447-7454, 1986.

Savage, J.C., and M. Lisowski, Strain accumulation in the Yakataga seismic gap, southern Alaska, J. Geophys. Res., 91, 9495-9506, 1986.

Savage, J.C., M. Lisowski, and W.H. Prescott, Reply, J. Geophys. Res., 91, 7559-7560, 1986.

Savage, J.C., W.H. Prescott, and G. Gu, Strain accumulation in southern California, 1973-1984, J. Geophys. Res., 91, 7455-7473, 1986.

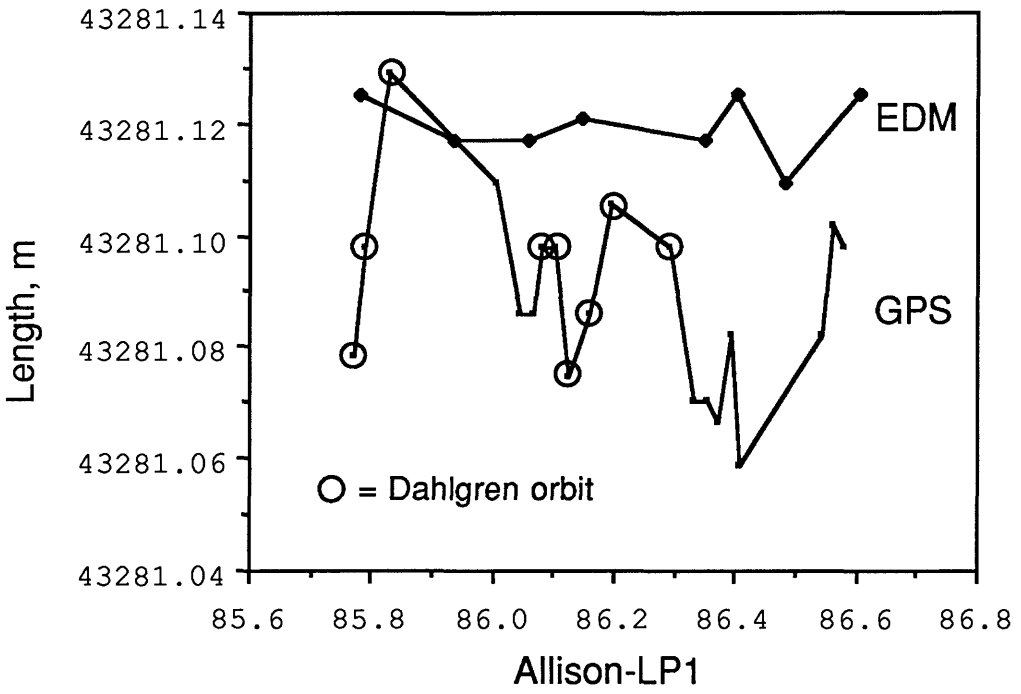

Figure. Length of the line Allison to LP1 as measured by Global Positioning System receivers (GPS) and by Geodolite (EDM). Circled points were reduced with orbits calculated at Dahlgren, VA. Other GPS points use broadcast orbits. The two systems use different stations at LP1 and an error in measuring the difference between these two stations may account for part of the offset between the two systems.

Seismic Studies of Fault Mechanics

9930-02103

Paul A. Reasenberg

Branch of Seismology
U.S. Geological Survey
345 Middlefield Road, Mail Stop 977
Menlo Park, California 94025
(415) 323-8111, ext. 2049

Investigations

Our activity in this reporting period focused on a problem in statistical seismology often referred to as the "precursory seismic quiescence hypothesis". The quiescence hypothesis states that decreases in the rate of seismicity in a surrounding earthquake source regions precede the mainshocks in a systematic, non-random way, such that an observation of a rate decrease provides information about the time and location (and possibly magnitude) of a future earthquake. Numerous cases of precursory seismic quiescence have been reported in recent years. Some investigators have interpreted these observations as evidence that seismic quiescence is a somewhat reliable precursor to moderate or large earthquakes. However, because failures of the pattern to predict earthquakes are generally not reported, and because numerous earthquakes are not preceded by quiescence, the validity and reliability of the quiescence precursor have not been established.

Results

We have analyzed the seismicity rate prior to, and in the source region of, 37 shallow earthquakes (M 5.3-7.0) in central California and Japan for patterns of rate fluctuation, especially precursory quiescence. Nonuniformity in rate for these pre-mainshock sequences was relatively high, and numerous intervals with significant ($p \leq 0.10$) extrema in rate were observed in some of the sequences. In other sequences, however, the rate remained within normal limits up to the time of the mainshock. Overall, in terms of an observational basis for intermediate-term earthquake prediction, no evidence was found in the cases studied for a systematic, widespread, or reliable pattern of quiescence prior to the mainshocks.

In earthquake sequences comprising full seismic cycles for 5 sets of repeat earthquakes on the San Andreas fault near Bear Valley, Ca., seismicity rate was found to be uniform. A composite of the estimated rate fluctuations for the sequences, normalized to the length of the seismic cycle, reveals a weak pattern of low rate in the first third of the cycle, and high rate in the last few months. While these observations are qualitative, they may represent weak expressions of physical processes occurring in the source region over the seismic cycle.

Re-examination of seismicity rate fluctuations in volumes along the creeping section of the San Andreas fault specified by Wyss and Burford

(1985) qualitatively confirm the existence of low-rate intervals in volumes 361, 386, 382, 372, and 401. However, only the quiescence in volume 386 was found by the present study to be statistically significant.

Reports

Reasenberg, P.A., and M.V. Matthews, Precursory seismic quiescence: a critical assessment of the hypothesis, U.S.G.S. Conference on the Physical and Observational Basis for Intermediate-Term Earthquake Prediction, Open-File Report (in preparation).

Matthews, M.V., and P.A. Reasenberg, Statistical Methods for investigating quiescence and other temporal seismicity patterns, U.S.G.S. Conference on the Physical and Observational Basis for Intermediate-Term Earthquake Prediction Open-File Report (in preparation).

COUPLED DEFORMATION - PORE FLUID DIFFUSION EFFECTS IN FAULT RUPTURE

14-08-0001-G-978

J.W. RUDNICKI
Dept. of Civil Engineering,
Northwestern University
Evanston, Illinois 60201
(312)491-3411

Investigations

1. Dilatant hardening effects due to uplift and near-fault microcracking accompanying fault slip.

2. Coupled deformation - pore fluid diffusion effects accompanying slip on an impermeable fault.

Results

1. Work on dilatant hardening effects accompanying frictional slip is described in the following recently completed manuscripts:

Rudnicki, J.W., Asymptotic analysis of stabilization of frictional slip by coupled deformation - fluid diffusion, submitted to Quarterly Journal of Mechanics and Applied Mathematics, Septmeber, 1986.

Rudnicki, J.W. and C.-H. Chen, Stabilization of rapid frictional slip on a weakening fault by dilatant hardening, in final preparation for submission to J. Geophys. Res.

This work is summarized in the following abstract (having the same title and authors as the second manuscript above) which has been submitted for presentation at the Fall AGU meeting:

"Frictional slip is often accompanied by dilatancy due to uplift in sliding over asperities and microcracking in the adjacent material. If dilatancy occurs more rapidly than pore fluid can flow into the newly created void space, the local pore pressure is reduced and the effective normal stress is increased in compression, tending to inhibit further slip. This dilatant hardening is analyzed for a simple model of a slab. One surface is loaded by compressive stress and shear displacement and connected to a reservoir of pore fluid held at constant pressure. The other boundary is a frictional surface, assumed to have formed at peak stress, on which the shear stress decreases from a peak value τ_p to a residual value τ_r as slip increases from zero to δ_0. In the absence of pore fluid effects, an instability corresponding

to an unbounded slip rate occurs when the slope of the shear stress versus slip relation is more negative than the unloading stiffness of the surrounding material. Dilatant hardening prevents this instability provided that the pore pressure in the reservoir is high enough. If the pressure in the reservoir is too low, the pressure at the fault surface can be reduced to the point at which the pore fluid bulk modulus decreases rapidly, eliminating the stabilizing effect. This result is consistent with observations of Martin [GRL, 1980] on pore pressure stabilization of failure in Westerly granite. The smallness of the ratio of the time scale of imposed deformation to the time scale of fluid mass exchange makes possible an asymptotic analysis. This analysis predicts that the maximum pressure reduction on the frictional surface is $(\tau_p - \tau_r)m_o^{-1}[1 - 2\delta_o G/3h(\tau_p - \tau_r)]$ where m_o is a friction coefficient, G is the elastic shear modulus, and h is the thickness of the slab."

2. Work in this area is described in the following two manuscripts:

Rudnicki, J.W., Slip on an Impermeable Fault in a Fluid-Saturated Rock Mass, in Earthquake Source Mechanics, Geophysical Monograph 37 (Maurice Ewing 6), pp. 81-89, 1986.

"Previous solutions for slip in elastic-fluid-saturated rock masses are appropriate for permeable faults because they assume no change in pore fluid pressure on the fault (slip) plane. Faults in situ are, however, often barriers to fluid flow, possibly because they contain much clay or very fine-grained gouge material. Here, the solution for a dislocation suddenly emplaced on an impermeable fault is used to analyze coupled deformation diffusion effects for impermeable faults. In contrast to predictions for the permeable fault, the shear stress induced by sudden slip on an impermeable fault does not decay monotonically in time from the undrained (instantaneous) value to the drained (long-time) value, but instead, first rises to a peak in excess of the undrained value by about 20% of the difference between the drained and undrained values. This rise in shear stress suggests that coupling between deformation and diffusion is initially destabilizing. Using two opposite signed dislocations to simulate a finite length fault suggests that the rise in shear stress occurs for 1.5 to 15 days for a fault 4 km in length and diffusivities of 0.1 m^2/s to 1.0 m^2/s. A characteristic time, defined as the time needed for the shear stress on the fault to decay to one-half of its long-time value, is $a^2/4c$ for the impermeable fault compared with $a^2/16c$ for the permeable fault where a is half the fault length and c is the diffusivity. Consequently, diffusive reloading of the fault, suggested as a contributor to aftershocks, does not begin immediately and occurs much more slowly for the impermeable fault. The pore pressure change on the impermeable fault is not zero as for the permeable fault, but is discontinuous and the values are opposite in sign on different sides of the fault. For the permeable fault, the position of the maximum pore pressure change moves away from the fault with time, but the maximum pore pressure change for the impermeable fault is always located at the dislocation."

Rudnicki, J.W., Plane Strain Dislocations in Linear Elastic Diffusion Solids, submitted to J. Appl. Mech., May, 1986

"Solutions are obtained for the stress and pore pressure due to sudden introduction of plane strain dislocations in a linear elastic, fluid-infiltrated, Biot, solid. Previous solutions have required that the pore fluid pressure and its gradient be continuous. Consequently, the antisymmetry (symmetry) of the pore pressure p about $y=0$ requires that this plane be permeable ($p=0$) for a shear dislocation and impermeable ($\partial p/\partial y = 0$) for an opening dislocation. Here Fourier and Laplace transforms are used to obtain the stress and pore pressure due to sudden introduction of a shear dislocation on an impermeable plane and an opening dislocation on a permeable plane. The pore pressure is discontinuous on $y=0$ for the shear dislocation and its gradient is discontinuous on $y=0$ for the opening dislocation. The time-dependence of the traction induced on $y=0$ is identical for shear and opening dislocations on an impermeable plane, but differs signficiantly from that for dislocations on a permeable plane. More specifically, the traction on an impermeable plane does not decay monotonically from its short-time (undrained) value as it does on a permeable plane; instead, it first increases to a peak in excess of the short-time value by about 20% of the difference between the short and long time values. Differences also occur in the distribution of stresses and pore pressure depending on whether the dislocations are emplaced on permeable or impermeable planes."

Hydrogen Monitoring (86-II)
9980-02773

Motoaki Sato and Susan Russell-Robinson
Branch of Igneous and Geothermal Processes
U.S. Geological Survey, MS/959, Reston, VA 22092
(FTS 959-6766)

INVESTIGATIONS

Hydrogen (H_2) in soil along the San Andreas and Calaveras faults are monitored at 10-min. intervals at eight sites by using fuel-cell sensors and data are telemetered to Menlo Park, CA. Efforts are directed toward accumulation of valid data, correlations with seismic data, understanding of tectonic and chemical mechanisms for H_2 emissions along active faults, and improvement of the monitoring method.

RESULTS

Instrumental

Main effort during this reporting period was focussed on the reduction of instrumental noise due to power supply instability. Stations operating on 12V alkaline batteries suffered from a gradual drift of the signal baseline due to voltage drop. Use of 12V air-zinc batteries was precluded by the size of our instrumental vaults. After a long search, we found a new miniature DC/DC converter which consumes less than 50 mA from 3-7V source to provide regulated 12V power. We installed this converter together with 5V air-zinc batteries at all non-solar powered stations. The result is very satisfactory.

At solar-powered stations, gradual aging (loss of capacity) of storage batteries resulted in increased daily fluctuations of the supply voltage. This caused major instrumental noise. We have doubled the battery capacity and also added an IC voltage regulator at these sites. Substantial improvement in data quality has been achieved.

Observational

General: No major (>1,000 ppm) H_2 anomalies have been recorded at any site during this reporting period. Minor changes were recorded in the Parkfield area starting in late June.

Calaveras Fault

Shore Road (H2SH): This site suffered from multiple instrumental problems that were caused by the flooding of the vault in the winter. The station finally became fully operational in mid-August. A barely perceptible peak was recorded on Sept. 24.

Wright Road (H2WR): Telemetry was down until mid-May. The problem was traced to the receiver card in Menlo Park. In addition, the telemetry transmitter seems to have a problem; the signal jumps up and down by 256 counts. A broad but small (150 ppm) peak began on July 21 and ended on Aug. 1.

San Juan Bautista (H2SJ): No notable event as usual, although the station seems to be working well.

Cienega Winery (H2CW): No recognizable anomaly. It is noteworthy that this site did not respond to the Stone Canyon quake cluster (main shock M4.5 on May 31) in spite of their proximity (18 km). These quakes, however, were generally very shallow (main shock 0.21 km). This site responded to the M>5 Coalinga earthquakes of 1982-83 that occurred 110 km away on a different fault (Sato et al., JGR, in press). The Coalinga quakes occurred near the base of the seismogenic crust, like many other damaging quakes in this region. The non-reponse of H_2 to nearby shallow quakes probably indicates the deep origin of H_2, perhaps generation in the greenschist facies environment within the ductile crust.

Melendy Ranch (H2MR): A barely recognizable peak may have occurred on June 24, but the validity of this peak is highly questionable because the telemetry transmitter battery went dead soon afterwards. The Stone Canyon quake cluster occurred only 6 to 10 km away, but there was no sign of H_2 response at this site, as at Cienega Winery.

Slack Canyon (H2SC): No event. The irregularity in mid-August was caused by recharging of new storage battery and resulting drift of the amplifier null voltage.

Middle Mountain (H2MM): Data prior to May 15 were of very poor quality due to power supply problem. There was a small H_2 peak on Aug. 13 and subsequent drop in H_2 level through the month of September. An oxygen return line was accidentally broken by a back hoe working for another project on Sept. 3, and the validity of the data after this date is in question until our next visit. This site is really jinxed.

Parkfield (H2PK): There was a marked decrease in H_2 right after the Mount Lewis earthquake of March 31, ending the 4-month long H_2 activities at this site. There was a barely recognizable peak and subsequent irregular decreases starting on May 3 and ending on May 17. A brief decrease occurred on June 23-24, and complex changes took place between July 10 and July 17. A sudden decrease occurred on Aug. 13 followed by small peaks (<50 ppm) on Aug. 24, Sept. 12 and Sept. 14.

Gold Hill (H2GH): A small increase was followed by a decrease between May 3 and May 17. Another peak occurred on June 24. These changes were concurrent with the changes at Parkfield (Fig. 3). A brief 700-ppm peak took place on Sept. 29.

Publication:

Sato, M., A. J. Sutton, K. A. McGee, S. Russell-Robinson (in press) Monitoring of hydrogen along the San Andreas and Calaveras faults in central California in 1980-1984: J. Geophys. Res., Gas Geochem. Spec. Volume.

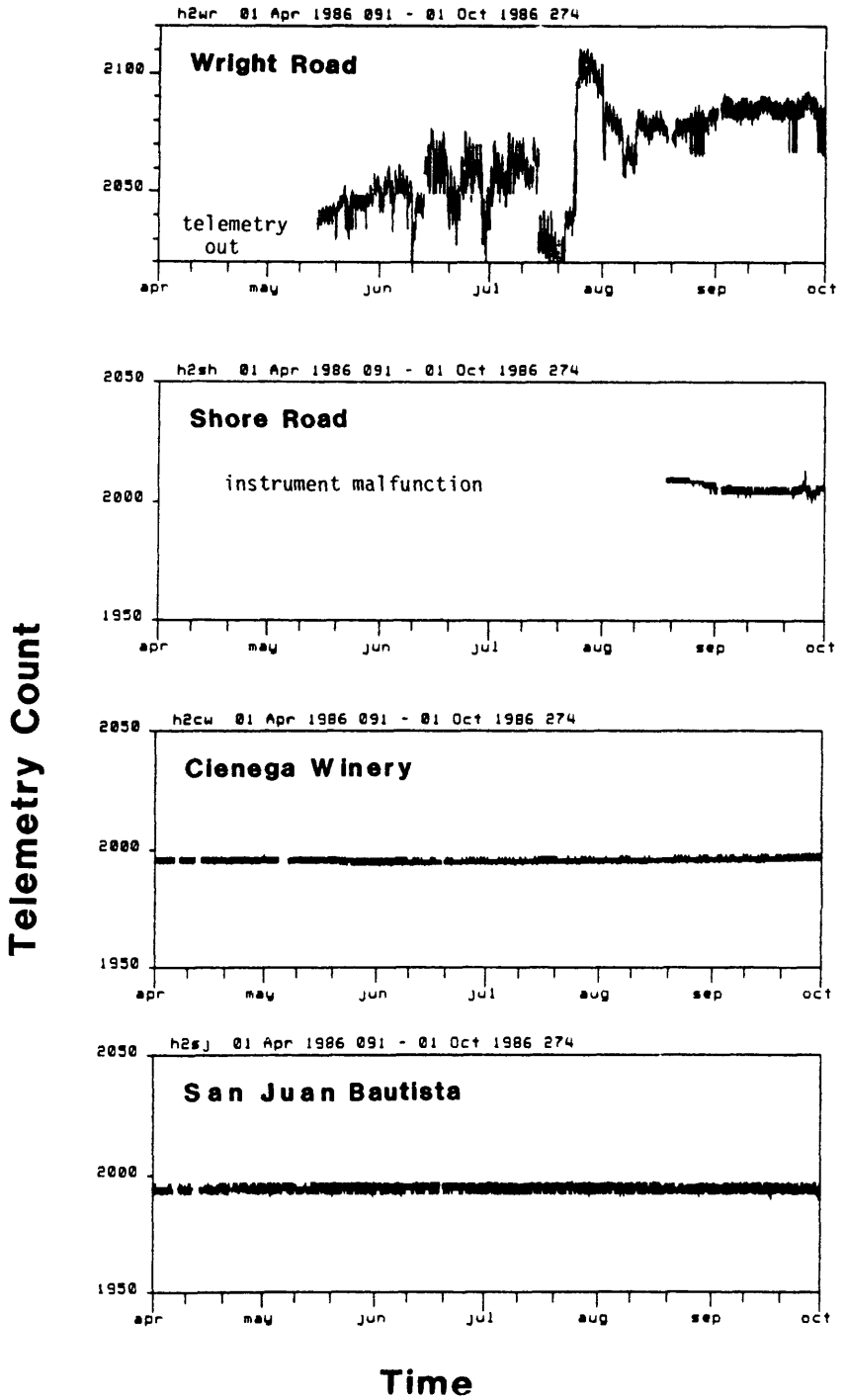

Figure 1. H_2 monitoring sites along the Calaveras Fault and the northern part of the San Andreas Fault network exhibited little change in hydrogen emission during the 6-month study period.

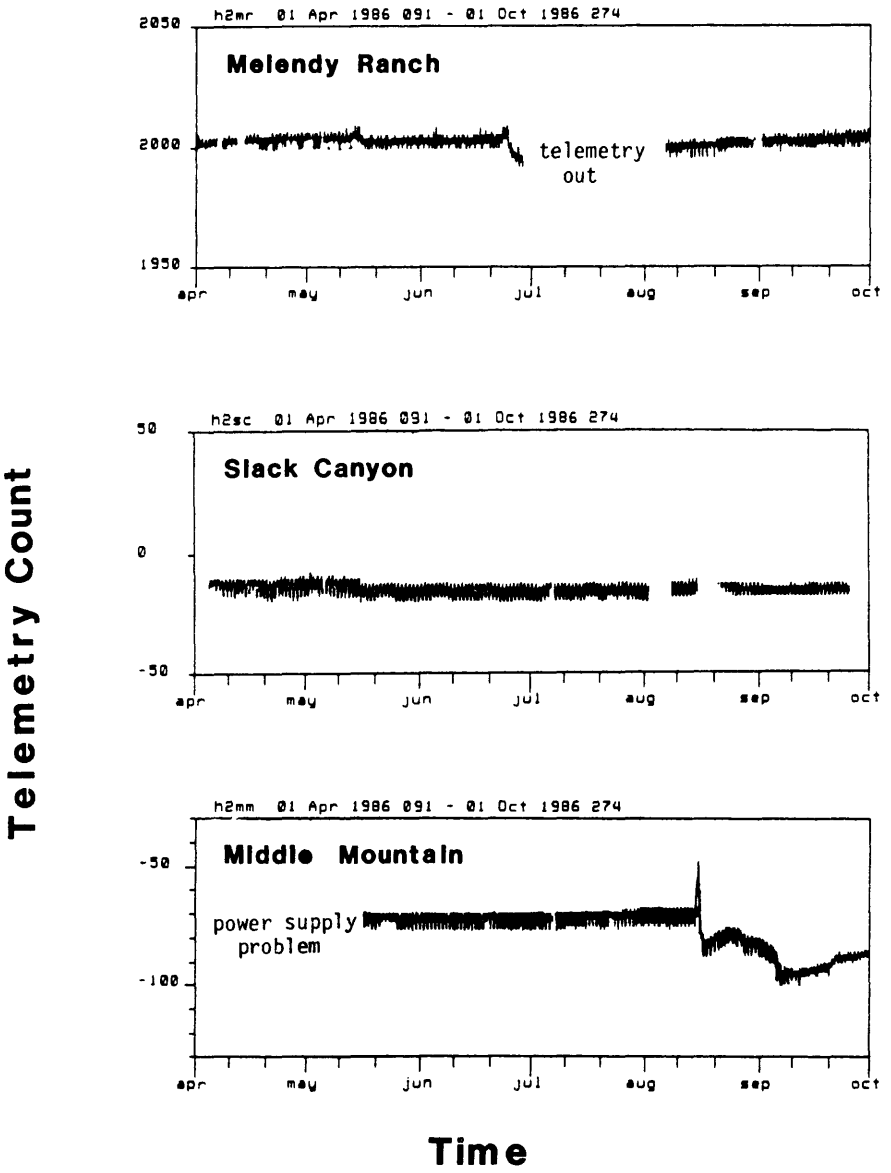

Figure 2. The middle region of the San Andreas Fault network exhibited little variation during the 6-month period.

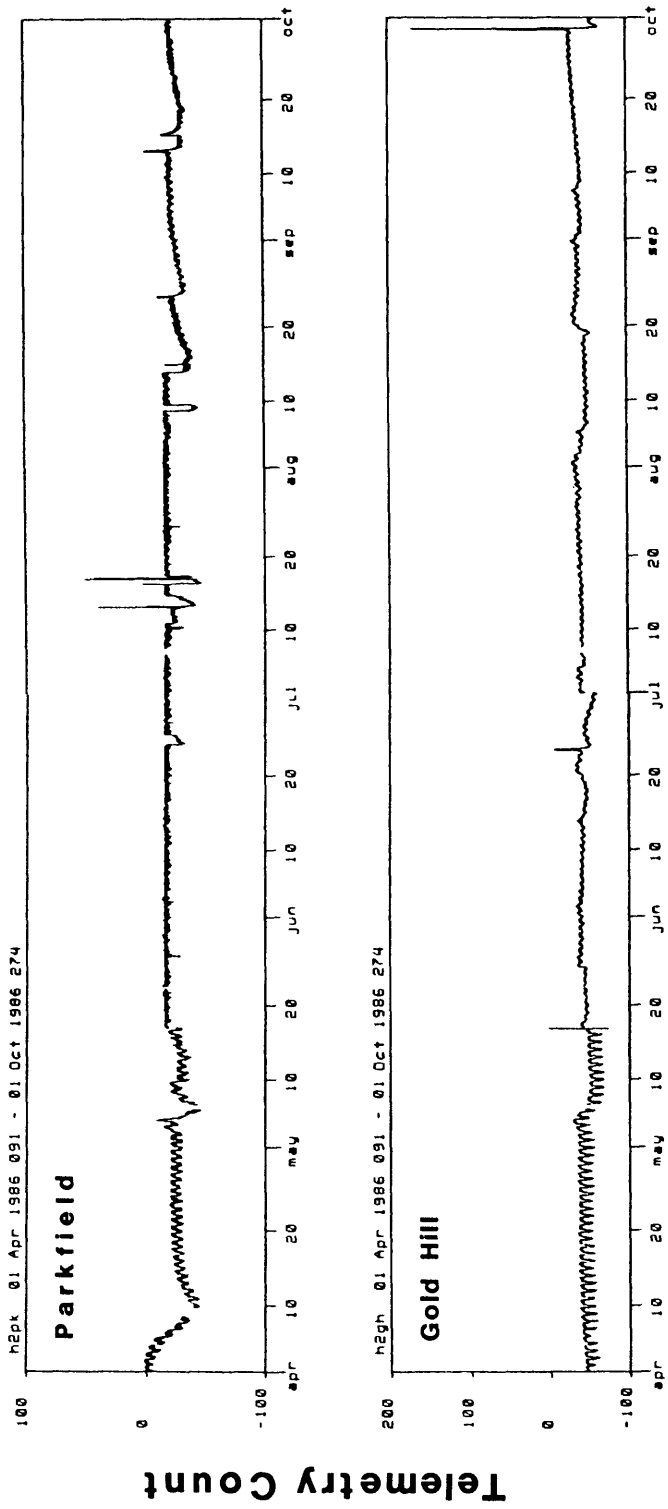

Figure 3. Several small hydrogen events occurred at the two southernmost hydrogen sites. The largest peak occurred in late September at Gold Hill. A change of 100 telemetry counts is equivalent to a change of 320 ppm in the hydrogen value.

FAULT ZONE TECTONICS

9960-01188

Sandra S. Schulz
Branch of Tectonophysics
U.S. Geological Survey
345 Middlefield Road, MS/977
Menlo Park, California 94025
(415) 323-8111 x 2763

Investigations

1. Directed maintenance of creepmeter network in California.

2. Updated archived creep data on PDP 11/44 computer.

3. Installed a replacement creepmeter for SHR1 on the Calaveras fault north of Hollister, and installed two new creepmeters in the Parkfield area.

4. Continued to establish and survey alinement array network on California faults.

6. Monitored creepmeter and alinement array data for retardations or other possible earthquake precursors, and for seismic effects on creep rates.

Results

1. Currently 31 extension creepmeters operate; 23 of the 31 have on-site strip chart recorders, and 21 of the 23 are telemetered to Menlo Park (Figure 1).

2. Fault creep data from USGS creepmeter sites along the San Andreas, Hayward and Calaveras faults have been updated through September, 1986, and stored in digital form (1 sample/day). Telemetry data covering the period after September are stored in digital form (1 sample/ten minutes), updated every ten minutes, and merged with the daily-sample data files to produce complete plots when needed.

3. Hollister

   SHR1 (Shore Road) creepmeter on the Calaveras fault 10 km north of Hollister was found pulled apart following the January 26, 1986, Tres Pinos earthquake. A new 14-meter wire creepmeter (XSH1) has been installed at the same site

and is now on telemetry (Figure 1).

Parkfield

During July, a 36-meter-long invar wire creepmeter and a stainless steel strong motion creepmeter (XMD1, XMDB) were installed in the same conduit near the Middle Ridge alinement array approximately 2.4 km southeast of XMM1 (Middle Mountain) creepmeter (Figure 1). In August, a similar set of creepmeters 26 meters along (X461, X46B) were installed near Quadrilateral QH (1966) (Figure 1), 2 km south of Highway 46, just beyond the southernmost surface fractures mapped after the 1966 earthquake. Both sets of instruments are transmitting on satellite telemetry.

4. Parkfield

A contract for quarterly surveying of five Parkfield alinement arrays was awarded to a private surveying firm. One set of surveys had been completed by the end of September.

A new alinement array (VAR4) was installed across the San Andreas main trace, halfway between MID and MID-E 2-color laser reflector sites. The new array is located approximately 3 km southeast of XMD1 (Middle Ridge) creepmeter and 2.9 km northwest of XPK1 (Parkfield) creepmeter (Figure 1). If a creepmeter can be sited at VAR4, there will be four instruments spaced approximately 3 km apart along Middle Mountain.

One year of surveys of the Ranchita Road line (RCW5) shows right-lateral creep appears to be occurring on the fault trace that broke in 1966 on the western side of Parkfield Valley (Figure 2). The movement appears to be substantial--at least 15.7 mm per year over the 278-meter length of the line. R. Burford reports that measurements of the 2-color laser line to Todd across the southwest trace support the interpretation of approximately 15 mm of right-lateral slip on this trace in the last year. It is interesting to note that the apparent right-lateral creep at RCW5 coincides with a similar amount (right-lateral) at XPK1 during the same time, and a notable lack of creep at both XTA1 and XDR2 creepmeters on the main trace opposite RCW5 (see Figure 1 for station locations). It would appear our picture of surface activity along the fault is as yet quite incomplete. To remedy this, we hope to install other alinement arrays on the southwest trace, seek out other moving traces in the valley, and begin regular measurements.

A computer program continues to check Parkfield telemetry data once each hour and alert Project personnel whenever unusual fault movement occurs.

Hollister

Last summer, in a study of seismic quiescence as a possible earthquake precursor, Max Wyss and Bob Burford used apparent creep retardations to target several sections along the San Andreas fault southeast of Hollister they found to be areas "... within which statistically significant seismic quiescences exist at present". (1) Wyss and Burford further stated that one or more of these targeted areas might experience earthquakes within the magnitude range $4.2 \leq M_L \leq 5.5$ before the end of May, 1986. On Saturday, May 31, 1986, a magnitude 4.4 (NEIC) (M_L 4.7, UCB) earthquake occurred at latitude 36° 36.8', longitude 121° 16.8' (CUSP locations), between Stone Canyon and Bear Valley southeast of Hollister (near XMR1) and within Wyss and Burford's "Polygon 386" area (1).

Creepmeters northwest of and near the epicenter recorded varying coseismic responses in the near-surface fault zone (Figure 3; see Figure 1 for station locations). It is interesting to note that the Cienega Winery (CWN1, CWC3), where a creep event had begun 20 hours before the earthquake, is located in "Polygon 372", one of the two other seismic gaps identified by Wyss and Burford. Station XMR1 (Melendy Ranch), presumably right next to the epicenter, did not show pre-, co-, or post-seismic response.

Parkfield

In August, after more than 3 years of inactivity since the Coalinga earthquake (5/2/83; mag. 6.7), XGH1 (Gold Hill) creepmeter resumed right-lateral movement with a 1.3 mm creep event (see Figure 1 for station location). The event was not recorded at nearby CRR1 (Carr Ranch) or WKR1 (Work Ranch) creepmeters, or on the Gold Hill tiltmeters or dilatometer. The event resembles "normal" creep events seen periodically at XGH1 between its installation in 1969 and the 1983 Coalinga earthquake. XGH1, near the southernmost end of the creeping trace, is the last Parkfield creepmeter to resume regular creep following the Coalinga earthquake.

On September 3, a 3.8 mm creep event was recorded at XMM1 (Middle Mountain) creepmeter coincident with excavation of drain trenches nearby. Figure 4 illustrates the physical layout of the site, with XMM4 alinement array located north of the creepmeter. Array monuments 2 and 3 are on opposite

sides of the fault near the instrument vault; the drain trench passes close to the anchor vault. Figure 5 shows cumulative movement over the entire array, between monuments 2 and 3, and between the creepmeter piers.

Greater detail of the 9/3 creep event appears on Figure 6, showing satellite telemetry values recorded at 10-minute intervals between 5 p.m. 9/2 and 5 p.m. 9/3. Due to data collection problems, telemetry dropped out between approximately 12:30 and 1:30 p.m. Times of various events during the trenching operation are estimated, and it is interesting to note actual right-lateral movement began before we reached the site. Onset of significant movement occurred around the time the backhoe crossed the first hard fault contact. Lunch break was taken after the backhoe had passed the anchor end, and most of the 3.5 mm of creep may be attributable to relaxation of the ground around the anchor pier toward the trench and away from the instrument pier. However, it is possible that some part of the event could have been highly localized release of stress previously released across the wider zone (compare rate of XMM4 between May 1985 and June 1986 with rate for XMM1, Figure 5). This could explain why movement between monuments 2 and 3 is greater between 6/24 and 9/16 than that over the entire array, but less than that recorded on the creepmeter. By 3:30 p.m., most shallow stored stress had been released, the ground had stopped relaxing and had reached equilibrium, further movement was halted by backfilling, or some combination of these had occurred.

It is our conclusion that although most of the 3.5 mm creep event recorded at XMM1 coincident with trenching on 9/3 may be attibutable to pier movement, some may represent release of accumulated shallow stress in the fault gouge adjacent to XMM1 and bracketed by array monuments 2 and 3.

(1) Wyss, M., and R.O. Burford, Current episodes of seismic quiescence along the San Andreas fault between San Juan Bautista and Stone Canyon, California: Possible precursors to local moderate mainshocks?, in Minutes of the National Earthquake Prediction Evaluation Council, July 26-27, 1985, Menlo Park, California, C.F. Shearer, editor; U.S. Geological Survey Open-File Report 85-754, Appendix A.23., p. 367-426, 1985.

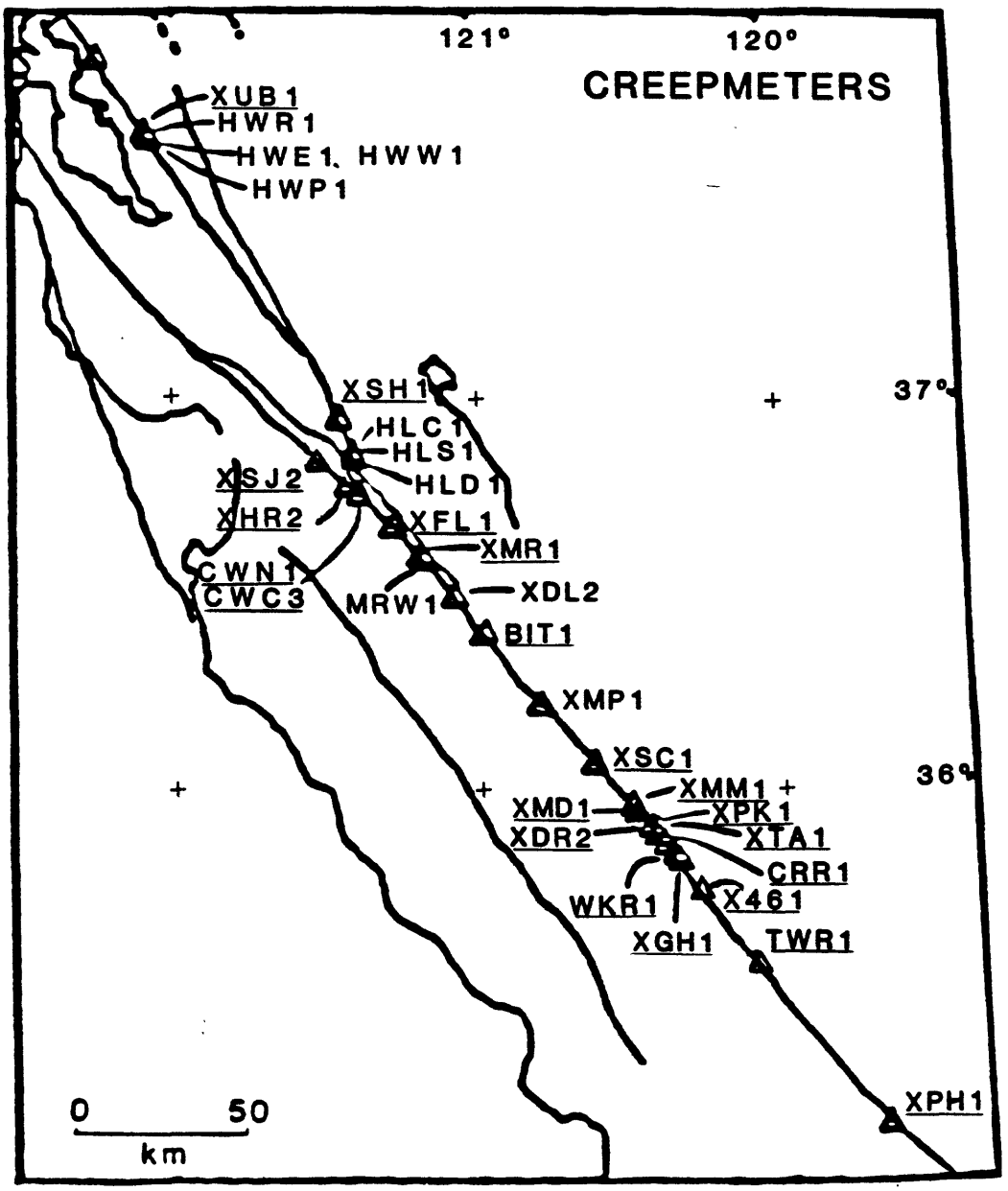

FIGURE 1. USGS creepmeter stations in Northern and Central California. Instruments with underlined names transmit on telemetry.

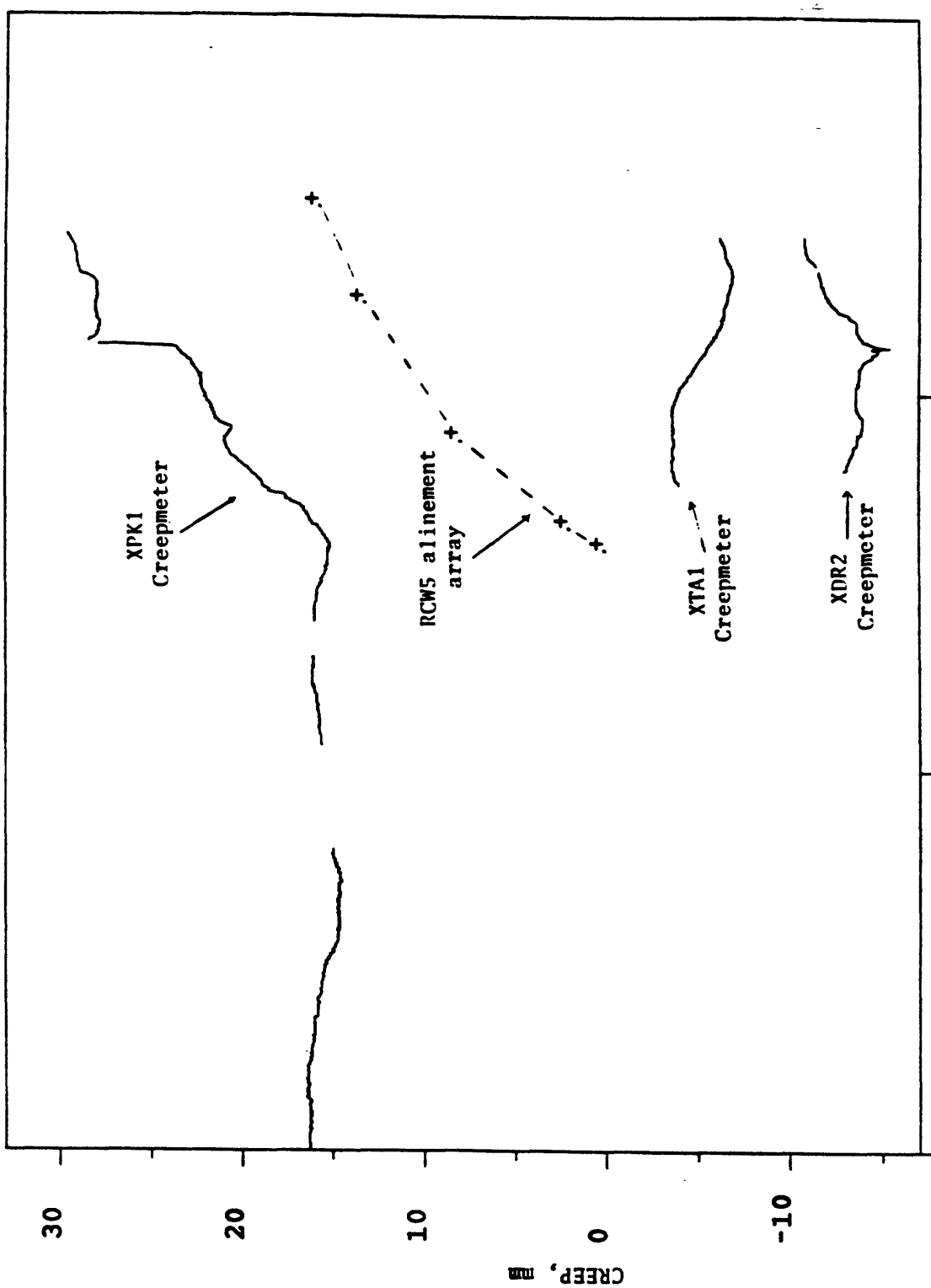

FIGURE 2. Cumulative creep (mm) measured at RCW5 alinement array on southwest trace compared to cumulative creep recorded at three creepmeters on main trace adjacent to RCW5 (See Figure 1 for creepmeter locations.)

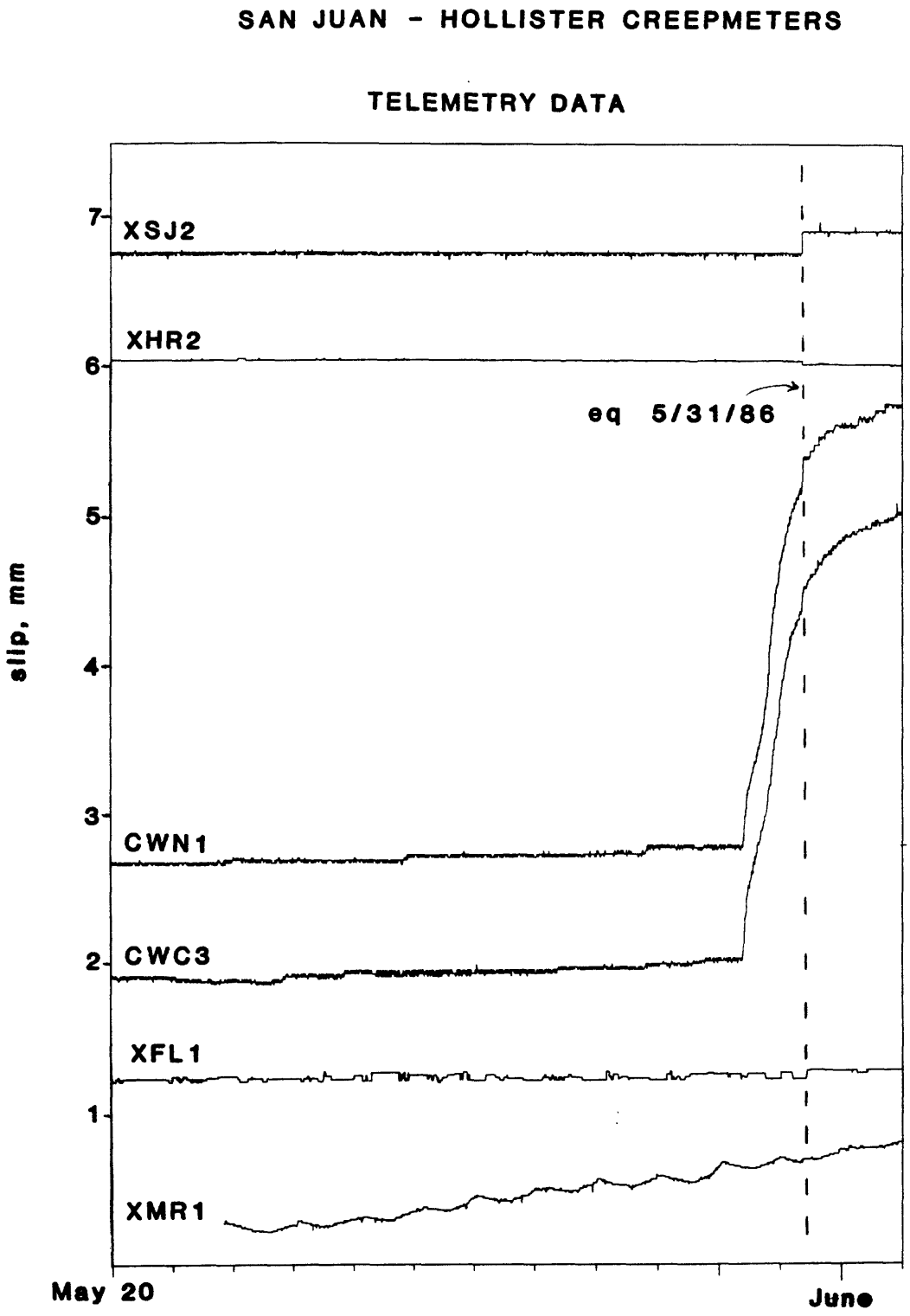

FIGURE 3. Coseismic responses on USGS creepmeters during earthquake 5/31/86 (mag. 4.4) on San Andreas fault south of Hollister. Creep event on the two Cienega Winery instruments (CWN1, CWC3) began 20 hours before earthquake.

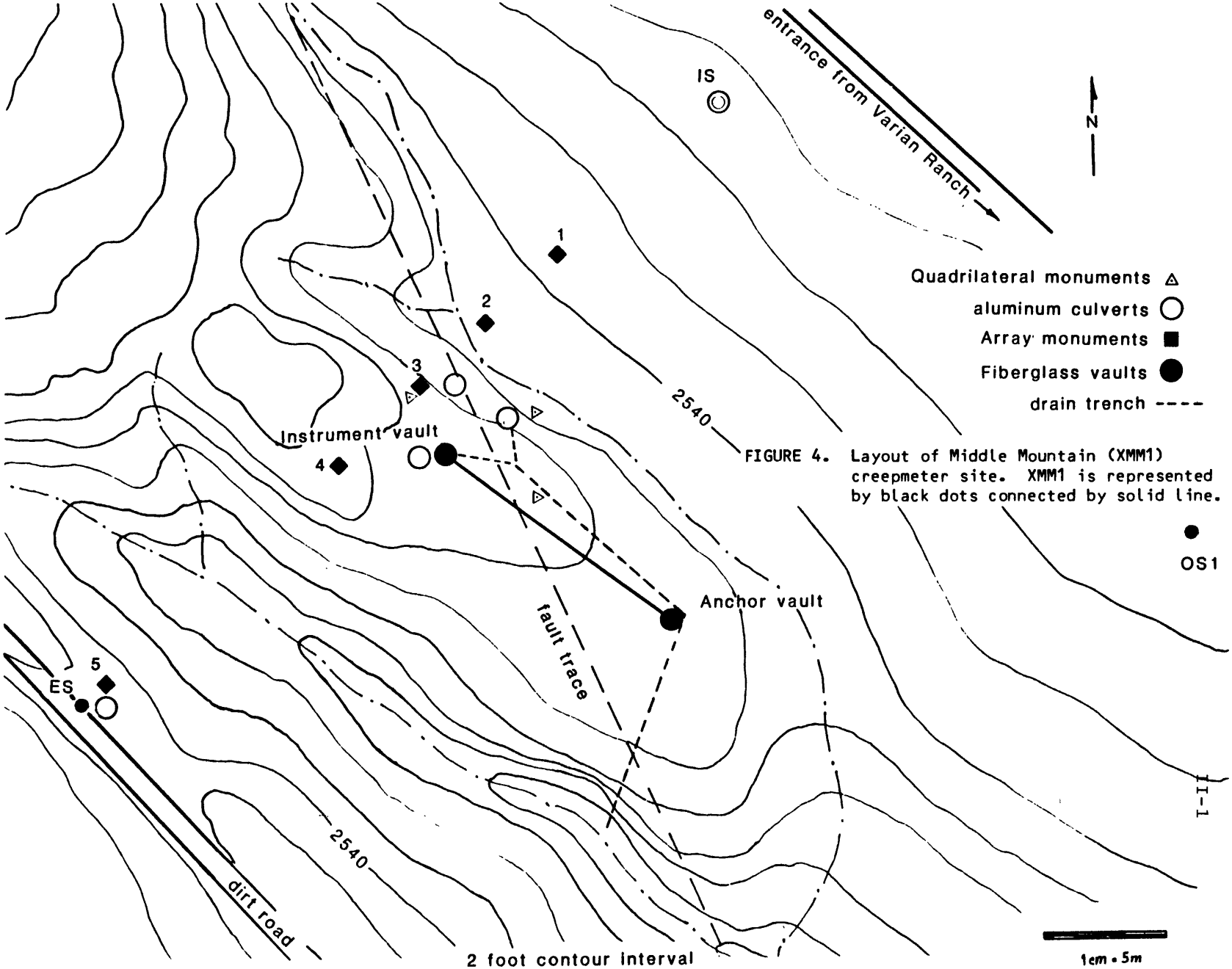

FIGURE 4. Layout of Middle Mountain (XMM1) creepmeter site. XMM1 is represented by black dots connected by solid line.

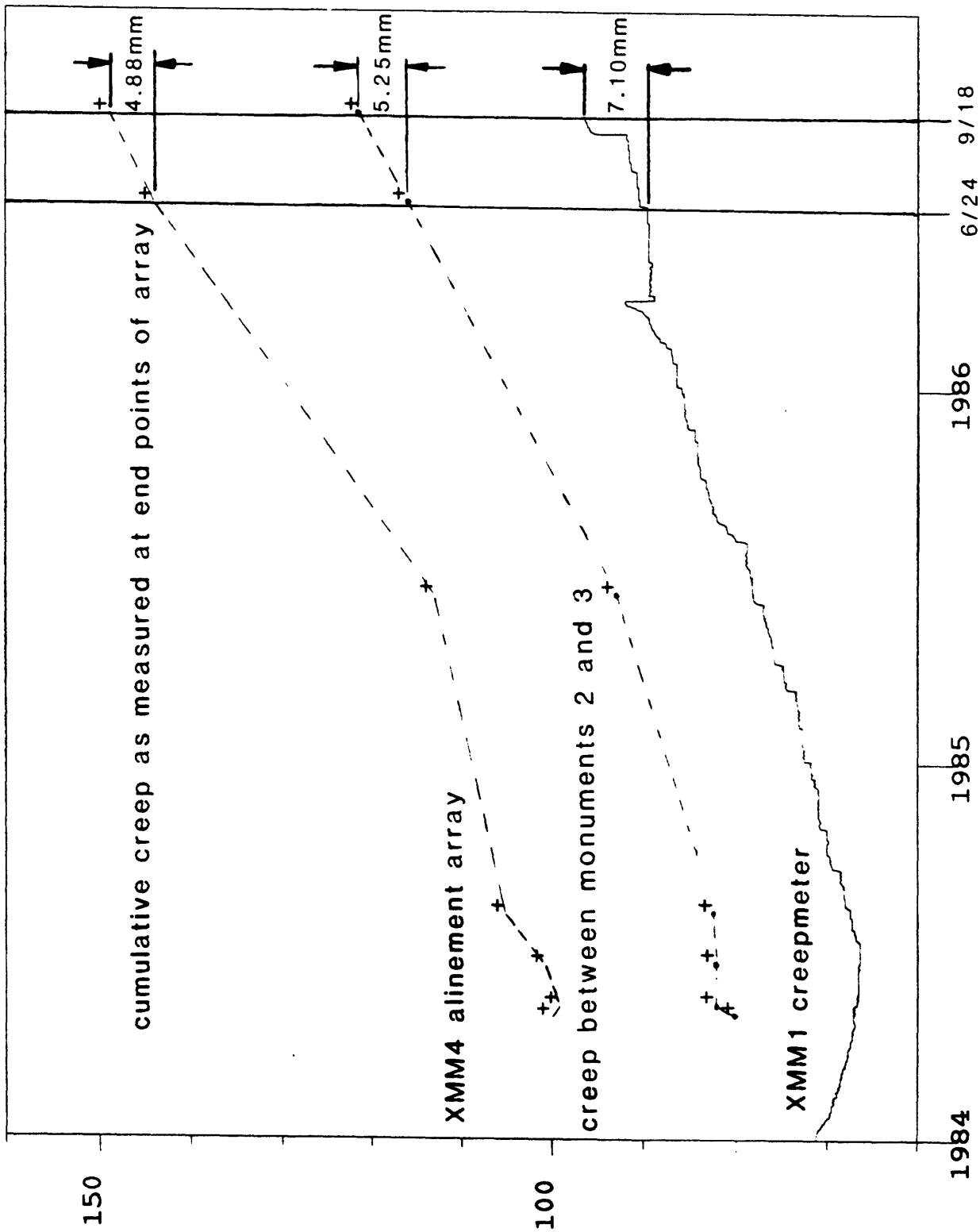

FIGURE 5. Cumulative creep (mm) over length of XMM4 alinement array, between array monuments 2 and 3, and between XMM1 creepmeter piers.

FIGURE 6. Satellite telemetry record of movement on XMM1 creepmeter during excavation of drains, 9/3/86, showing timing of various phases of trenching. Data collection problems caused drop-out of signal between 12:30 and 1:30 p.m., PDT.

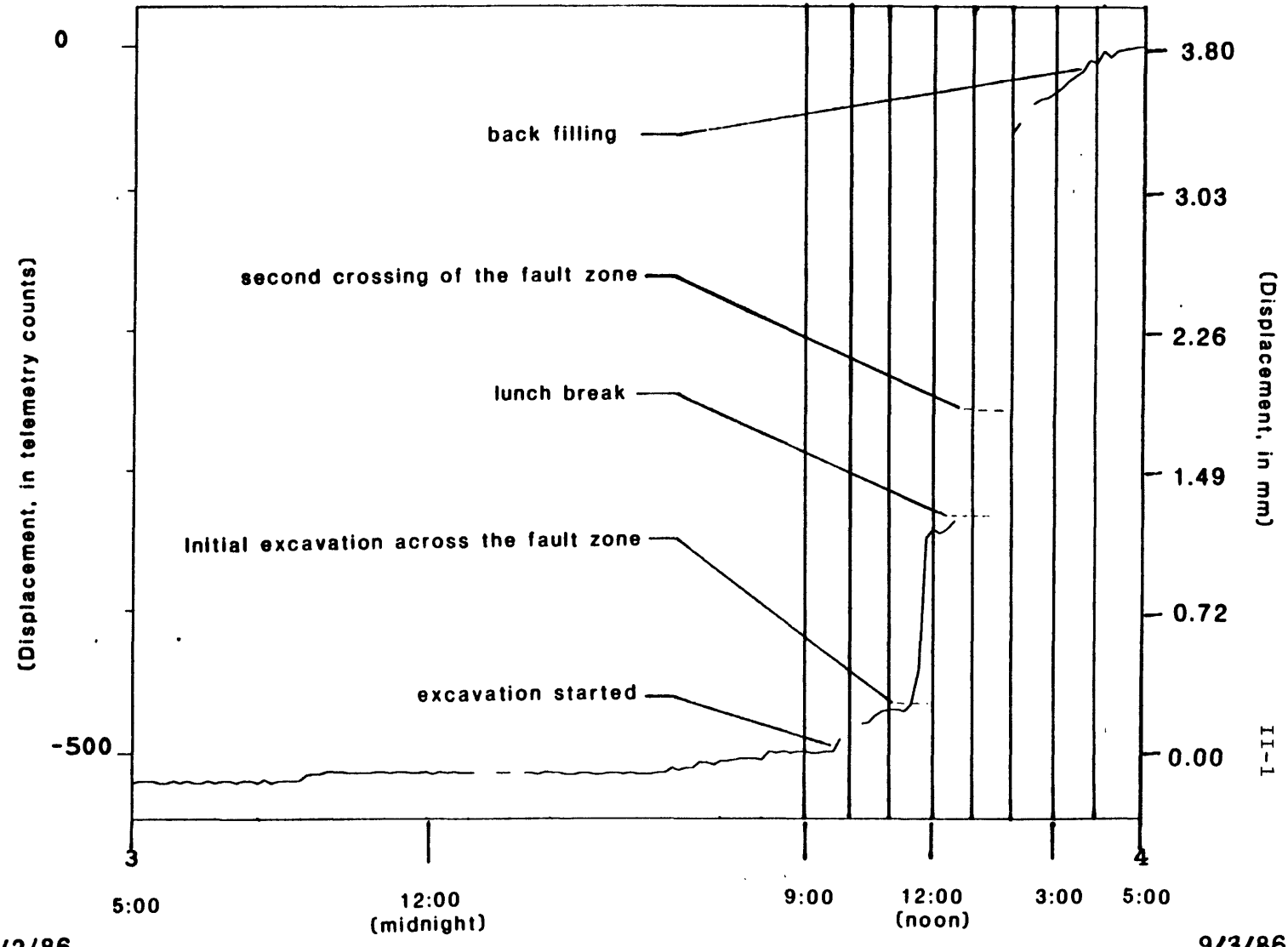

Analysis of Seismic Data from the Shumagin Seismic Gap, Alaska

14-08-0001-G-1094

John Taber and Klaus H. Jacob
Lamont-Doherty Geological Observatory of Columbia University
Palisades, New York 10964
(914) 359-2900

Investigations

Digitally recorded seismic data from the Shumagin seismic gap in eastern Aleutian arc, Alaska, are analyzed for detecting space-time variations in the seismicity, focal mechanisms, and dynamic faulting parameters that could be precursory to a major earthquake expected in this seismic gap. The seismic results obtained from the network data are being integrated with crustal deformation data that are independently collected, with volcanicity data of nearby Aleutian volcanoes, and with teleseismic information to identify basic tectonic processes which may be precursory to a great earthquake.

Results

Work is continuing on the determination of the details of the transition from a single to double Wadati-Benioff zone within the Shumagin seismic gap. The boundary is located near a change in seismic station distribution so it was necessary to check that the transition is not an artifact of our processing technique. Errors could arise either from an uneven station distribution or an inadequate velocity model. It is unlikely that we have missed events in the single plane region because the station coverage is best there. Since the station distribution changes greatly directly over the observed transition, it is possible that the lower plane events are mislocated. However, the deepest part of the plane extends under the southeast coast of the peninsula where the distribution of stations is fairly uniform, so the accuracy of relative locations there should be uniform across the transition.

To test the effects of station geometry and velocity model, we calculated travel times from artificial events in a simple subduction zone model using an approximate three-dimensional ray tracing algorithm (Thurber, 1984). The artificial events were placed in two planes that were separated in depth by 20 km. The location of the subducting slab and the surface stations were chosen to agree with the geometry of the Shumagin network. The artificial travel times were then used to calculate locations based on our standard one-dimensional velocity model. The resulting locations were only slightly different from the original artificial locations for both planes. We conclude that for actual data, the double zone region could not result from what really is a single plane. Also, the lack of a lower plane in the single zone region is not an artifact of station distribution bias.

The abrupt change in the seismicity distribution may help explain the discrepancy between Savage and Lisowski's (1986) suggestion of aseismic slip below the Shumagin Islands and the historic record of great earthquakes. Their calculated lack of strain accumulation is based on trilateration measurements over a 5 year period. If the change in seismicity is related to a change in stress then the aseismically slipping region may be limited to the narrow region under the Shumagin Islands where there is a single Wadati-Benioff zone.

To test this hypothesis, we have reproduced the dislocation model used by Savage and Lisowski (1986) to predict strain rates in the Shumagin network. The model was then

modified so that the plate interface is locked only to the west of the Shumagin Islands. The resulting model shows a rapid decrease in strain accumulation with distance away from the edge of the locked interface. Annual strain accumulation is reduced by a factor of 4 within 10 km from the boundary between the aseismically slipping and locked regions and drops to zero within about 30 km from the boundary. Most of the trilateration network benchmarks are at least 10 km from the boundary between single and double Wadati-Benioff zones. Therefore strain accumulation due to a locked plate interface to the west of the Shumagin Islands would probably not be observed in the Islands themselves.

References

Savage, J.C., and M. Lisowski, Strain accumulation in the Shumagin seismic gap, Alaska, *J. Geophys. Res. 91,* 7447-7454, 1986.

Thurber, C.H., Seismic detection of the summit magma complex of Kilauea volcano, Hawaii, *Science 223,* 165-167, 1984.

Reports

Hudnut, K.W. and J.J. Taber, Transition from double to single Wadati-Benioff seismic zone in the Shumagin Islands, Alaska, submitted to *Geophysical Research Letters*, 1986.

Seismic Reflection Investigations of Mesozoic Basins, Eastern U. S.

9950-03869

John D. Unger
Branch of Geologic Risk Assessment
U. S. Geological Survey
922 National Center
Reston, VA 22092
(703) 648-6790

ONGOING INVESTIGATIONS

1. Consolidation and synthesis of available seismic reflection information that pertains to the internal and external structure of Mesozoic basins, with special emphasis on the hypocentral area of the present seismicity at Charleston, South Carolina and the Ramapo fault zone in New Jersey and Pennsylvania.

2. Generation of 2-D synthetic seismic reflection models of the basement structure along selected seismic reflection traverses in the Charleston and Ramapo regions as an aid to processing and interpretation of the seismic reflection data and to allow the use of ray-tracing algorithms to be used for earthquake relocation.

3. Determination of optimal crustal velocity data from seismic reflection profiles within and surrounding eastern Mesozoic basins by using methods, such as p-t inversion, capable of greater interval velocity resolution than the standard normal-moveout techniques.

4. Investigation of the role of Mesozoic basins as seismogenic tectonic features in the Eastern U.S.

RESULTS

1. Reprocessing of proprietary seismic reflection data collected by NORPAC, Inc. across the Newark basin and the extension of the Ramapo seismic zone is almost completed. This reflection profile is one of the best in this type of tectonic setting. I began with the raw field data and have completed detailed velocity analyses. Preliminary stacks of the data at this stage using the new velocity structure show that the reprocessing has been successful in delineating additional features in the profile. Careful definition of the reconstruction line and selective trace editing as well as the careful determination of normal moveout velocity are responsible for these improvements. Both of these tasks were time consuming but have proved their value.

The stacking velocities found differ significantly in some areas along the line from those calculated by the contractor. In

general, the velocities I have used are higher than what one might expect in Mesozoic sedimentary rocks such as those found in the Newark basin. Some of these high velocities may be simply due to the geometric effect of dip, but even the flat-lying reflectors give high stacking velocities.

The results show improvement in the overall quality of the character of the reflectors in many parts of the line. A few coherent reflectors have been identified in the crust beneath Buckingham Hills structure, where Paleozoic - Precambrian rocks outcrop near the central part of the basin, but it is still difficult to identify any specific features in this area that might be traced to the Ramapo fault further north.

I have begun to migrate this data set to attempt to correct for the severely crossing reflections and diffractions present at the bottom of the basin structure and in preparation for converting the traces from time to true depth. Migration will also show the true attitude of the dipping reflectors in the section. Progress is slow in the migration processing because this operation is very computer intensive and some of the parameters have to be determined more or less by trial and error. But the first results are promising.

To speed-up the migration processing and to gain a better understanding of the effects of velocity on migration, a microcomputer program to migrate line drawings of unmigrated seismic reflection profiles has been developed. This program has been published as a U.S.G.S. Open-file Report.

REPORTS

1) Unger, J. D., 1986, A microcomputer program to migrate line drawings of seismic reflection sections, U.S.G.S. Open-file Report 86-296, 32 pages.

Seismic Evidence for Tectonic Process

9930-03353
Peter L. Ward
Branch of Seismology
U.S. Geological Survey
345 Middlefield Road, Mail Stop 977
Menlo Park, California 94025
(415) 323-8111, Ext. 2838

Investigations

Determine the relationship between volcanism on land and plate motions of oceanic plates.

Results

The distribution of 9,705 radiometric ages of volcanic rocks in the western United States and Mexico gives new insight into the relationship of volcanism to plate motions. Maps of locations of dated rocks for different age ranges in the Cenozoic agree closely with detailed maps of outcrop patterns and appear to give a reliable estimate of volcanic output during the Cenozoic and Upper Mesozoic. Most ages for extrusive rocks are less than 40 m.y. The number of ages of pyroclastic and felsic extrusives increases significantly at 40 m.y. and remains relatively constant until 1.5 m.y. when there is another sharp increase. The number of ages of mafic extrusives is low before 18 m.y. and peaks at 15 m.y., 3 m.y., and the present. The number of reported ages of intrusive rocks south of the Snake River Plain peaks at 70 to 75 m.y. and 35 to 40 m.y., but is 4 times lower between 40 and 60 m.y., the period when the Farallon plate was being subducted under the southwestern U.S. at rates of 15 cm/yr (Jurdy, 1984; Engebretson, 1984) or even 38 cm/yr (Alvarez et al., 1980). Thus the best documented period of very rapid subduction coincides with a distinct magmatic lull.

Plots of age vs. distance along the North American plate margin show a clear migration of volcanic activity beginning in West Texas at 38 m.y. and progressing in steps to northern California today, at the rate that the Mendocino Triple Junction is believed to have traveled. A similar trend in the reverse direction began at 90 m.y. and ended in Arizona at about 60 m.y., just before the period of rapid subduction. The Coney and Reynolds (1977) hypothesis for an inland sweep of the subduction zone results from plotting these trends on a cross-section that is highly oblique to the continental margin.

Great Basin volcanism from southern Washington to Arizona peaks between 10 and 17 m.y. Most other volcanic trends are nearly perpendicular to the plate margin including the Rio Grande trend most active from 0 to 5 m.y. and 20 to 25 m.y., the Great Basin trend active between 25 and 40 m.y., the Snake River trend active between 0 and 14 m.y., and the Idaho-Central Montana trend active at 50 m.y. and between 60 and 80 m.y. These trends are parallel to fracture zones in the ocean and appear to be related to continental rifting caused by different rates of subduction or strike-slip faulting at different places along the plate margin. Migration of activity along most of these trends is seen but is far more complex than the simple pattern predicted by the hotspot model.

The greatest volume of extrusive and intrusive volcanic rocks in the western U.S. appears to be related temporally to continental rifting and changes in plate configuration, rather than to arc volcanism above subduction zones.

A detailed paper is in review relating specific peaks in volcanism to periods of subduction and strike-slip faulting. Since the Jurassic, the oceanic plates west of North America have become coupled to North America in major triple junction complexes at least four times. The most recent began at 43 m.y. Since that time volcanism in the western U.S. has moved about in a stepwise manner remaining at any one location for about 6 m.y. These periods of major volcanism are separated by periods of very rapid strike-slip. For example, I provide evidence that opening of the Gulf of California and major motion on the San Andreas fault occured primarily between 1.5 and 3.3 m.y. at rates in excess of 10 cm per year. Motion is now slowing down. From 3.3 to 8 m.y. the Mendocino escarpment remained just north of San Francisco. At 8 m.y. rapid motion of about 40 km on the Hayward and 140 km on the Calavaras and similarly large motion on the San Gregorio and Hosgri faults allowed the Mendocino escarpment to jump northward from south of Hollister. Seven such jumps can be documented since 43 m.y. with varying levels of certainty. This strike-slip model of plate interactions appears to explain the detailed distribution of volcanism, major calderas, eras of faulting, metamorphic core complexes, changes in plate motion, paleomagnetic data on terrane motions, etc.

References

Alvarez, W., Kent, D. V., Silva, I. P., Schweickert, R. A., and Larson, R. A., 1980, Franciscan complex limestone deposited at 17° south paleolatitude: Geological Society of America Bulletin, v. 91, part I, p. 476-484.

Coney, P. J., and Reynolds, S. J., 1977, Cordilleran Benioff zones: Nature, v. 270, p. 403-406.

Engebretson, D. C., Cox, A., and Gordon, R. G., 1985, Relative motions between oceanic and continental plates in the Pacific Basin: Geological Society of America Special Paper 206, 59 p.

Jurdy, D. M., 1984, The subduction of the Farallon plate beneath North America as derived from relative plate motions: Tectonics, v. 3, no. 2, p. 107-113.

Reports

Ward, P. L., 1986, Volcanism and plate tectonics of the Western United States: EOS Trans. Amer. Geophys. Union, v. 67, in press.

Ward, P. L., 1986, Volcanism and plate tectonics of western north America: in press, Hawaii Symposium on How Volcanoes Work.

Two studies of Earthquake Fault Behavior

14-08-0001-G-1157

Steven N. Ward
and
Sergio E. Barrientos

C.F. Richter Laboratory
Earth Sciences Board
University of California
Santa Cruz, CA 95064
(408) 429-2480

INVESTIGATIONS

1. Hebgen Lake and Borah Peak. We deduce the fault geometry, coseismic slip and moment from geodetic observations for two of the largest historic earthquakes that have occurred in the Basin and Range of the western U.S: The **M** =7.3, 1959 Hebgen Lake, Montana, earthquake and the **M** = 6.9, 1983 Borah Peak, Idaho, event.

2. Central Chile. Central Chile has been the site of several large earthquakes in the last few centuries. The historical record starts in 1575 followed by large events in 1647, 1730, 1822, 1906, and temporarily concludes in March, 1985 with an M_S = 7.8 event. Leveling lines surveyed in 1981 and 1985 (before and after the 1985 earthquake) give us an excellent opportunity to compare the coastal uplift in the Algarrobo–San Antonio region, and to estimate the modes of slip distribution on the fault plane associated with the main event. Variable slip models have been successfully applied in extensional regimes where the fault intersects the Earth's surface [Ward and Barrientos, 1986]. Here we apply the variable positive slip model to estimate the rupture dimensions, slip distribution, and moment release associated with deeper thrust type events like the March 1985 central Chile earthquake.

RESULTS

1. Hebgen Lake. Newly augmented data sets of vertical deformation from geodetic leveling and from lake shoreline changes were modeled by simple dislocations in an elastic half–space. Figure 1 shows the distribution of observations. The new data are BM's 2, 3, 4, 5, 6, and 7 on Missouri Flats (between Madison Range and Cliff Lake). The r.m.s. signal to noise ratio is 12 for the Hebgen Lake data and 38 for the Borah Peak set. The residuals for both models are about twice as large as the noise. The Hebgen Lake earthquake struck on the 15 to 25 km long en echelon Hebgen and Red Canyon faults (Figure 2), dipping 45°–50° and extending to a vertical depth of 10 to 15 km. The 7.5 and 7.8 m of dip–slip on these faults produce a combined moment of of 1.2 x 10^{20} N m. The dip of the Red Canyon fault may decrease slightly with depth (in a listric manner), abutting the planar Hebgen fault at a a depth of 8 km. In addition, up to 1 m of deep slip occured on the Holocene segment of the adjacent Madison Range Fault, 10 km west of the Hebgen fault. The Borah Peak segment of the Lost River fault was found to dip 49°. Slip of 2.1 m occurred at the south fault end, extending to a depth of 14 km; 1.4 m of slip occured at the north end, where the fault reached only to 6 km depth. A listric fault shape is not permitted by the geodetic data at Borah Peak. Both the Hebgen-Red Canyon and the Lost River faults are high–angle and nearly planar, despite the much greater age and length of the Lost River fault in comparison to the en echelon Hebgen faults. The chief difference between the earthquakes is the 3-4-fold higher slip at Hebgen relative to Borah Peak and all other well–studied Basin and Range shocks, as revealed by surface rupture and the modeled slip at depth. Thrusts faults located close to these active normal faults must either dip steeply at depth, or were not reactivated.

2. Central Chile. Figure 3 shows Central Chile from 31°S to 34°S, the epicenter of the 1985 event (star), its foreshock (small dashed ellipse) and aftershock (large dashed) areas and the leveling line (small

triangles) that extends for nearly 130 km from the coastal city of San Antonio to Santiago. The plane containing the elemental point sources strikes $10°E$ and dips 25° to the west. The dashed rectangle contains the regular mesh of dots which represents the projection of the sources on the surface of the Earth. The application of the gradient technique with positivity contraints developed by Ward and Barrientos [1986] results in the slip distribution presented in Figure 4. Maximum values of $\sim$ 2.7 m are located along the coast from San Antonio to Quintero at a depth of 35 km. A second maximum (2.5 m) was detected just north of the largest aftershock (M_S=7.2) of the sequence at a depth of 45 km. The total moment estimated from the geodetic line is 1.5 x10^{28} dyne cm, 30% larger than the estimated from surface waves.

REFERENCES

Barrientos, S. E., R. S. Stein, and S. N. Ward, A comparison of the 1959 Hebgen Lake, Montana, and the 1983 Borah Peak, Idaho, earthquakes from geodetic observations. Submitted to *Bull. Seism. Soc. Am.*

Ward, S. N., S. E. Barrientos, An inversion for slip distribution and fault shape from geodetic observations of the 1983, Borah Peak, Idaho, earthquake, *J. Geophys. Res. 91*, 4909–4919, 1986.

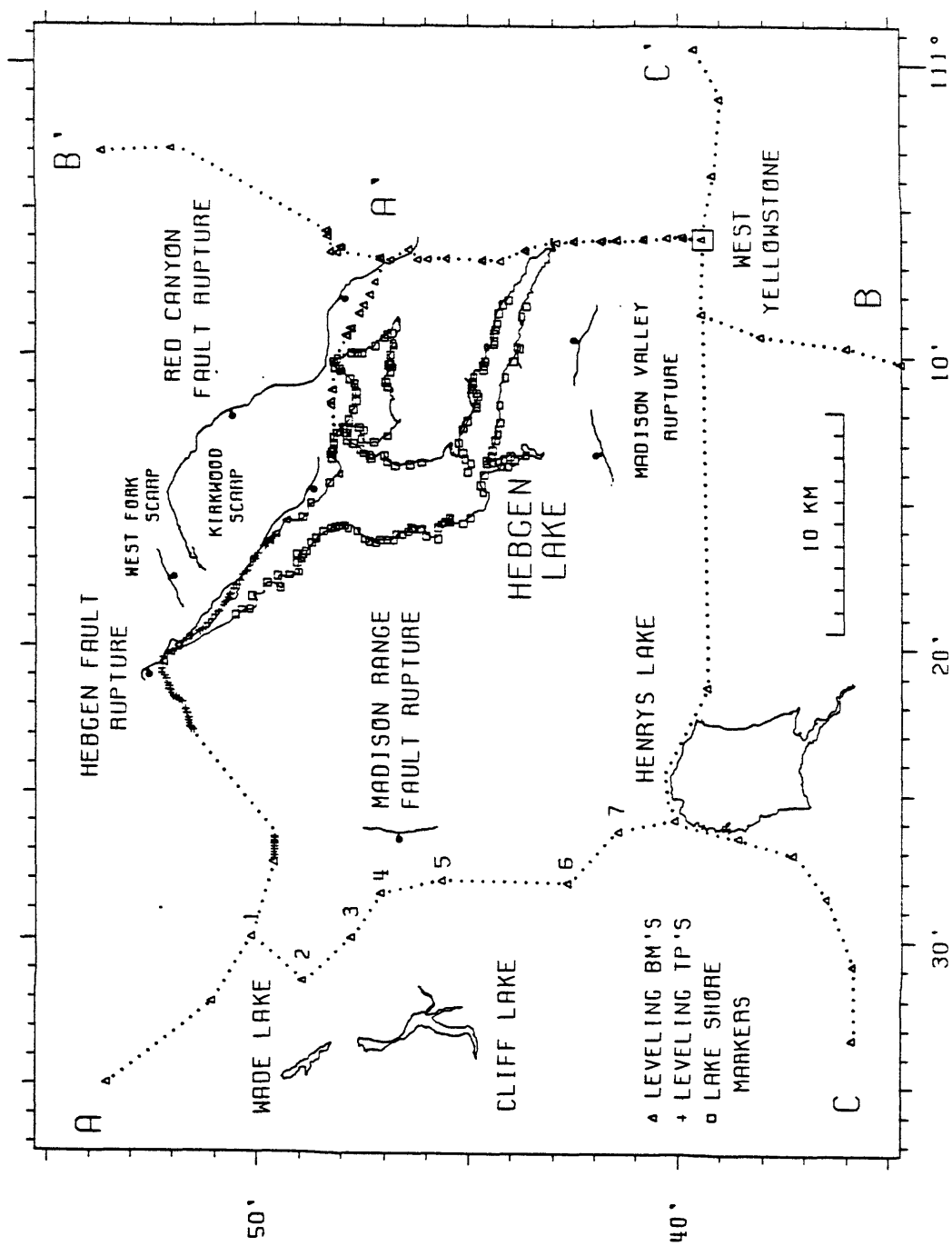

Figure 1. Main ruptures and data distribution at Hebgen Lake. Line A–A' is based on leveling benchmarks (triangles) and leveling turning points (crosses). Two other lines, B–B' and C–A consist of leveling benchmarks. Squares represent lake shore height changes.

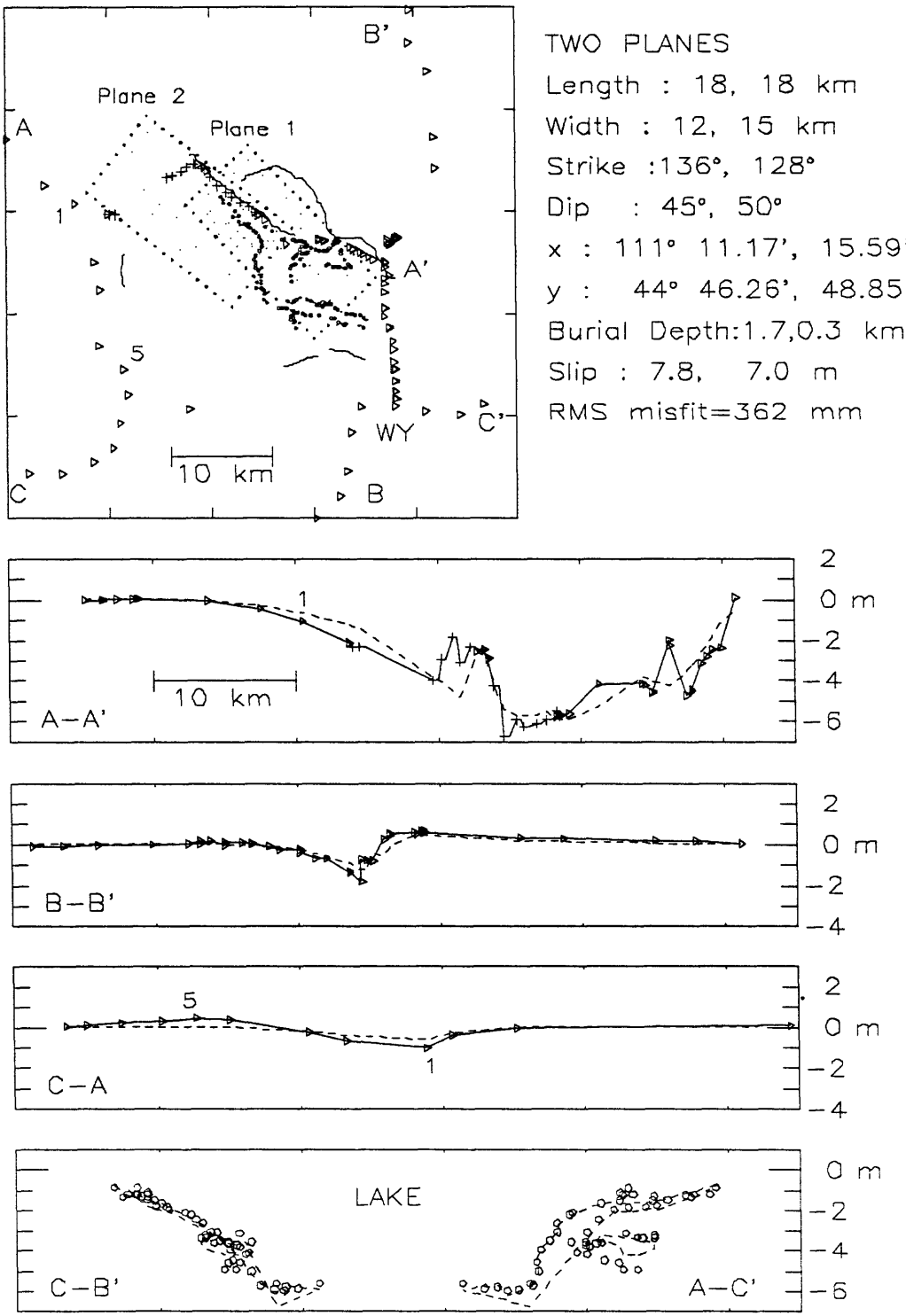

Figure 2. Best two–plane model for Hebgen Lake. The upper box shows the data distribution and the surface projection of the fault plane. Observations (solid) and predicted vertical elevation change (dashed) along the lines A–A', B–B', and C–A. Two projections of lake shore height changes (circles) are compared with the theoretical values in the lower box. Two overlapping fault planes that closely follow the rupture traces and dip 45° and 50° best satisfy the observations.

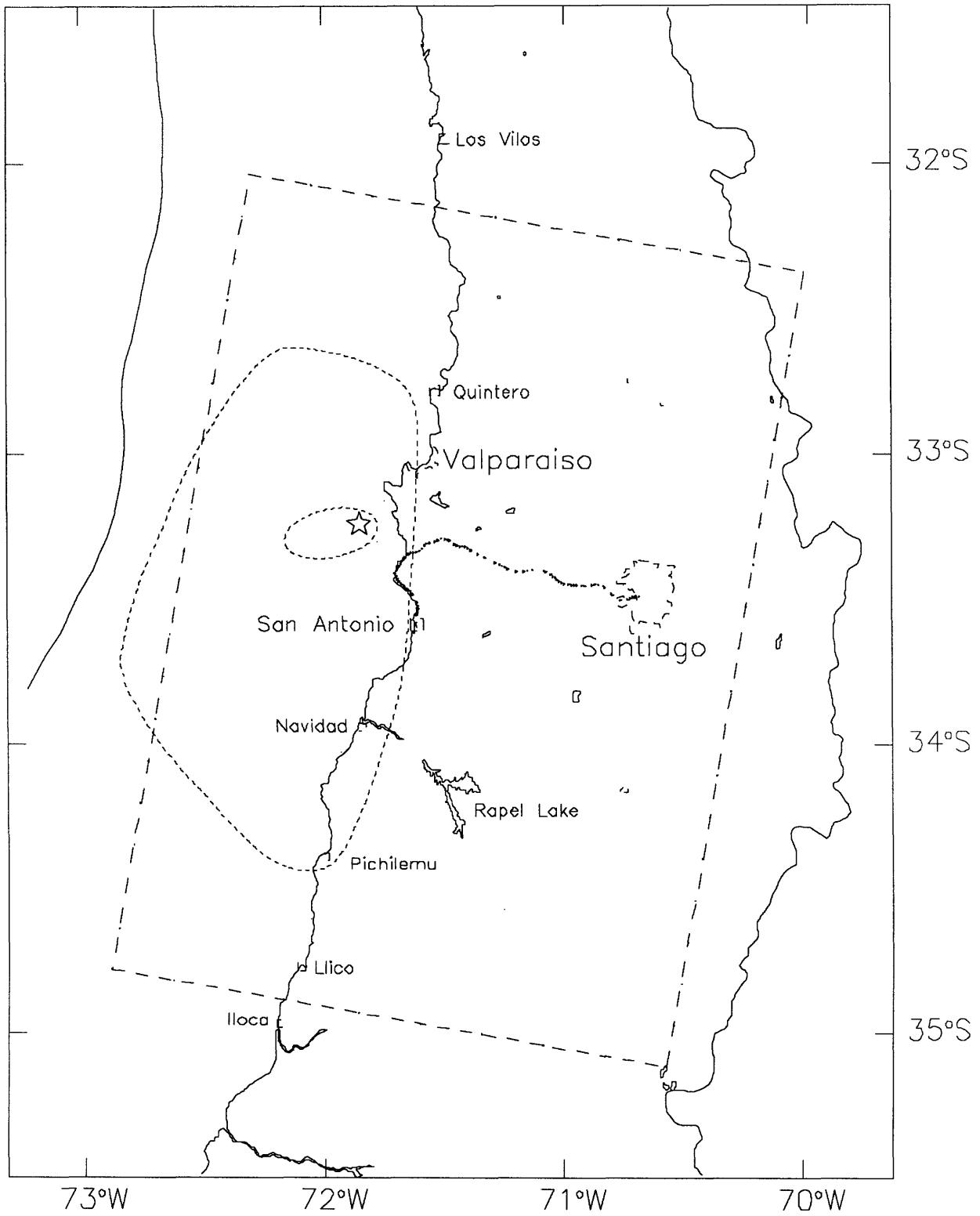

Figure 3. Central Chile, site of the 1985, March 3, earthquake (star). The small dashed ellipse encloses the foreshock area, the large dashed region is the aftershock zone. The leveling line (small triangles) connects the cities of San Antonio and Santiago. The regular mesh of dots inside the dashed rectangle represents the surface projection of the planar source.

LAS = 310
LDD = 230
BASE = 15
SSR = 0.304E-01
M = 1.44E+28
Φ = 10
δ = 20
λ = 105

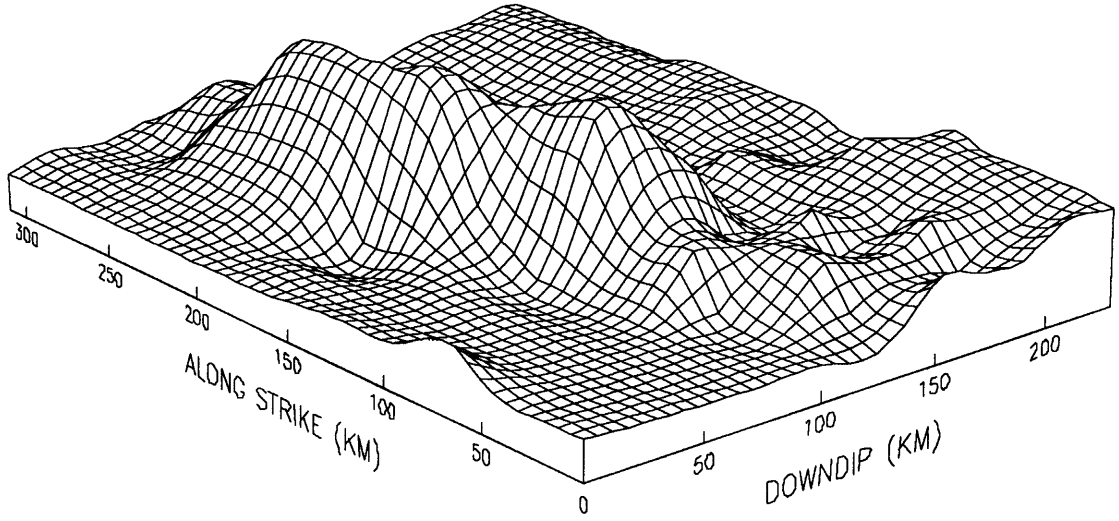

Figure 4. Variable slip model that best fits the coseismic observations.

XO = -100.0
YO = -120.0
ZO = 10.0

WATER VAPOR RADIOMETER CORRECTIONS AND GPS BASELINE ACCURACY

14-08-0001-G1179

Randolph H. Ware

Cooperative Institute for Research in Environmental Sciences
University of Colorado
Boulder, CO 80309-0449
(303) 492-1586

INVESTIGATIONS

Corrections for tropospheric delay in Global Positioning System (GPS) baseline determinations are commonly calculated from a tropospheric model that uses surface meteorological (met) data including pressure, temperature, and humidity. For GPS signals the several-meter radio path delays resulting from transmission through the troposphere and attributed to constituents other than water vapor can usually be modeled to an accuracy of about one centimeter using surface pressure data. Delays resulting from water vapor (wet path delays) can be several tens of centimeters in magnitude and are often poorly modeled using surface humidity and temperature measurements. This poor modeling can produce path delay errors as large as 20 cm, depending on geography, climate, season, and weather conditions. Estimation of wet path delays can usually be improved to about one centimeter accuracy using water vapor radiometer (WVR) observations of water vapor emission along a line-of-sight through the troposphere.

We are investigating GPS vector baseline errors that result for several geographical locations under a variety of weather conditions when surface met observations are used to compute wet path delays. We intend to generate synthetic GPS data which include delays computed from WVR observations at one end of a baseline. We will then proceed with baseline determination using delays computed from surface met data which were observed simultaneously with the WVR data. This will allow us to estimate the vector baseline errors that occur when surface met corrections are used.

RESULTS

The creation of the software necessary to compute GPS baselines using synthetic satellite phase data and tropospheric corrections based on WVR or surface met data is now in progress.

We have obtained simultaneous WVR and surface met data from desert areas in California, from a high plains site on the eastern margin of the Rocky Mountain Cordillera in Colorado, and from tropical seashore areas in Baja California, on the Pacific Coast of Mexico, and in the Caribbean.

Comparisons of WVR and surface met data are shown in Figures 1 and 2 for sites in California and Mexico. The dry conditions which often prevail in the east-central desert areas of California are evident in the observations from Owens Valley, which show zenith path delays of 11 cm or less. More humid conditions are evident at Cabo San Lucas, at the southern end of Baja California, where zenith path delays vary from 12 to 30 cm.

The zenith path delays estimated from WVR and surface met data are quite variable and differ by up to 4 cm at Owens Valley and 8 cm at Cabo San Lucas. For GPS viewing at elevation angles of 20 degrees, which is quite common, this represents phase errors of 10 to 20 cm. Such errors could prevent phase ambiguity resolution, which is necessary for optimum GPS accuracy. An estimation of GPS vector baseline errors that result for a variety of geographical, climatic, seasonal and weather conditions should be available soon from our analysis using synthetic phase data.

REPORTS

Ware, R. H., K. J. Hurst, and C. Rocken, GPS Baselines: Comparing Tropospheric Corrections Based on WVR Data to Those Based on Surface Met Data, **EOS**, abstract submitted for Fall AGU Meeting, December, 1986.

Ware, R. H., C. Rocken, and K. J. Hurst, A GPS Baseline Determination Including Bias Fixing and Water Vapor Radiometer Corrections, **Journal of Geophysical Research, 91**, 9183-9192, 1986.

Ware, R. H., C. Rocken, K. J. Hurst, and G. W. Rosborough, Determination of the OVRO-Mojave Baseline During the Spring 1985 GPS Test, **Proceedings of the Fourth International Symposium on Satellite Positioning**, Austin, Texas, April 28 - May 2, 1986.

Ware, R. H., C. Rocken, and J. B. Snider, Experimental Verification of Improved GPS-Measured Baseline Repeatability Using Water Vapor Radiometer Corrections, **IEEE Transactions on Geoscience and Remote Sensing, GE-23**, 467-473, 1985.

Ware, R. H., C. Rocken, and K. J. Hurst, Water Vapor Radiometer Corrections for Tropospheric Errors in a GPS Baseline Determination, **EOS, 46**, 844, 1985.

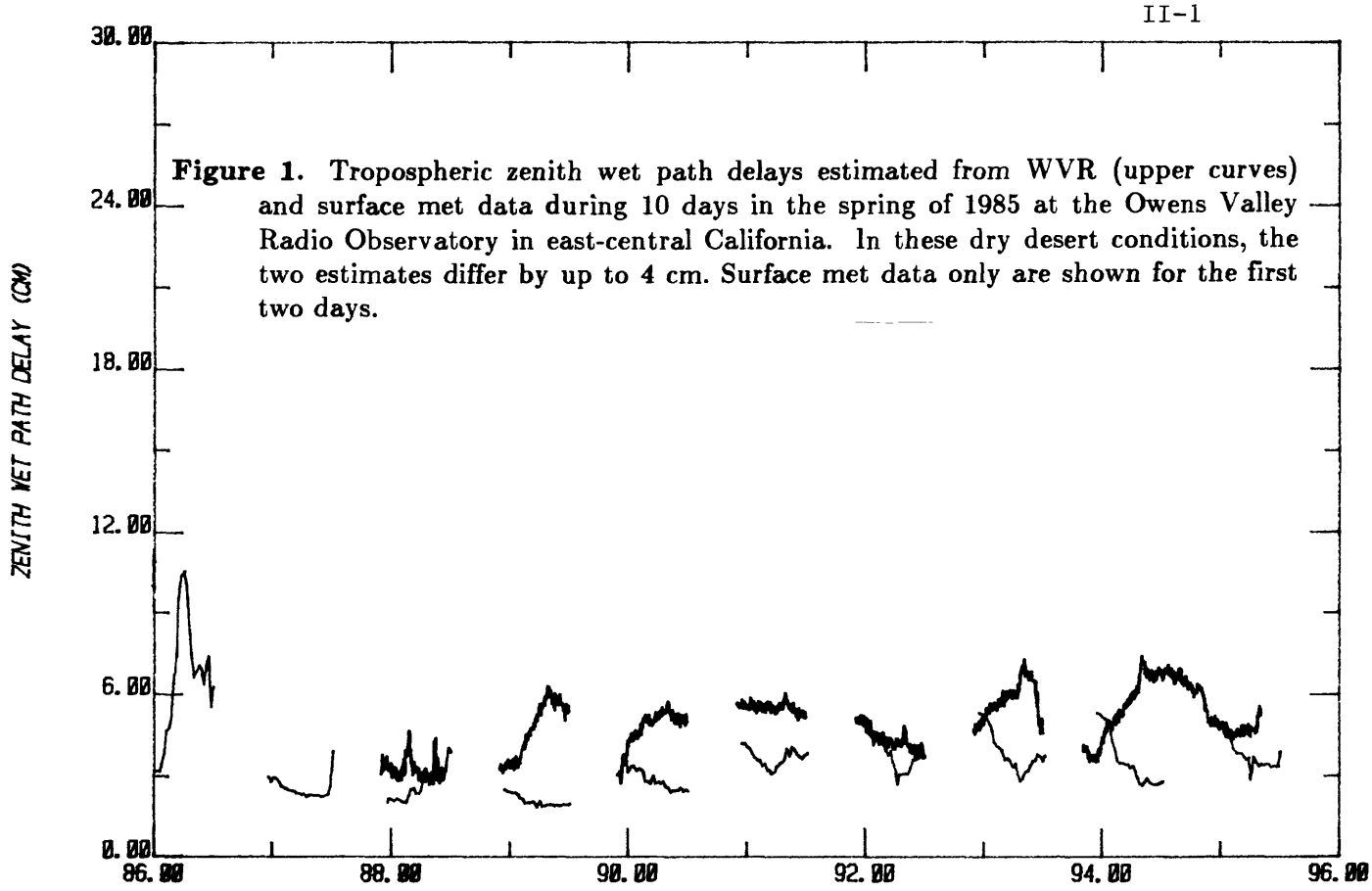

Figure 1. Tropospheric zenith wet path delays estimated from WVR (upper curves) and surface met data during 10 days in the spring of 1985 at the Owens Valley Radio Observatory in east-central California. In these dry desert conditions, the two estimates differ by up to 4 cm. Surface met data only are shown for the first two days.

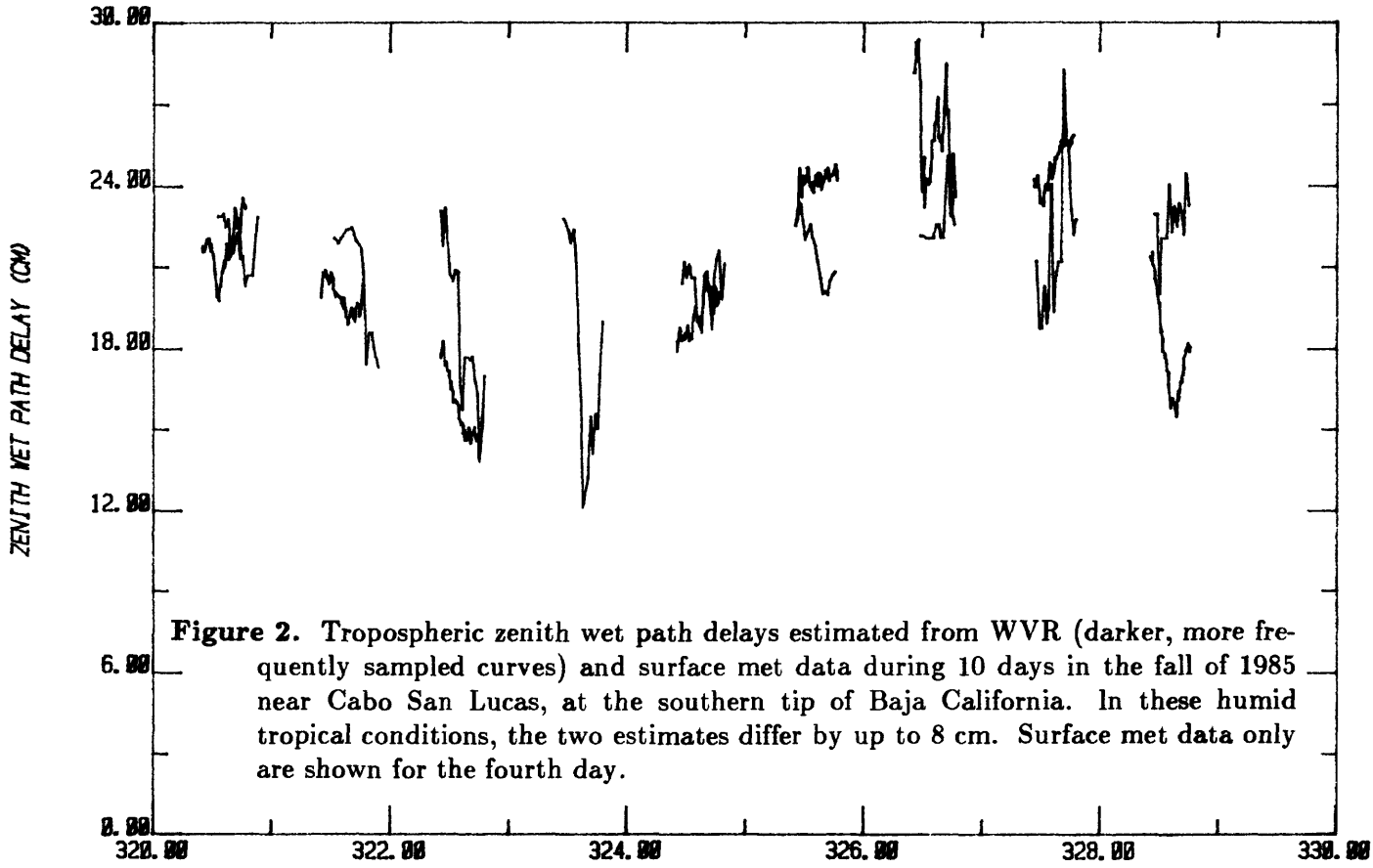

Figure 2. Tropospheric zenith wet path delays estimated from WVR (darker, more frequently sampled curves) and surface met data during 10 days in the fall of 1985 near Cabo San Lucas, at the southern tip of Baja California. In these humid tropical conditions, the two estimates differ by up to 8 cm. Surface met data only are shown for the fourth day.

Latin American Seismic Studies

9930-01163

Randall A. White, David H. Harlow
U.S. Geological Survey
Branch of Seismology
345 Middlefield Road, Mailstop 977
Menlo Park, California, 94025
(415) 323-8111. Ext. 2570

Investigations

1. Ruiz Volcano, Columbia. On November 13, 1985, Ruiz Volcano erupted, generating catastrophic mudflows that killed about 25,000 people. We left for Colombia immediately and installed 6 telemetered seismic stations to monitor and help predict future eruptions of the volcano. The objective was to help establish the Colombian National Volcanic Observatory (Observatorio Vulcanologicos Nacional de Colombia) to monitor the on-going volcanic activity and warn of any future large-scale eruptions. Detailed training was given in the monitoring and analysis of the daily seismic activity.

2. During visits to Colombia, data from the 3 1/2 months prior to the catastrophic eruption were examined and are reported below.

3. In the wake of the eruption of Volcano Ruiz disaster, the USGS/OFDA Volcano Early warning Disaster Assistance Program (VDAP) has been initiated. The team is still being organized, and is being designed for rapid deployment to any imminent volcanic eruptions in Latin America or the Caribbean that may pose a serious threat to populous areas.

Results

1. The most important result of the establishment of the Colombian observatory was the successful prediction of the largest eruption since the catastrophic eruption of 13 November 1985. This eruption occurred on January 4, 1986 and appropriate towns in threatened areas were evacuated.

2. The results of analysis of precursory avtivity is as follows. Felt earthquakes were first reported at Ruiz volcano in December 1984, and thereafter 15 to 30 events were felt each month through September 1985 though few were felt beyond the immediate vicinity of the volcano. We estimate that the largest did not exceed magnitude 4.5. Analysis of seismograms from July, 1985 on indicate that approximately 75 percent of the tectonic earthquakes occurred in small swarms with durations of one to several hours. Most of the hypocenters are located at depths of less than 8 km beneath the volcanic cone, while a few are located 5 to 10 km from the crater. Between July and early September, the rate of seismic energy release was constant. On September 5, however, a clear period of premonitory seismic activity began and continued until September 11 when strong phreatic eruptions began. During this premonitory period the rate of seismic energy release from local tectonic type earthquakes increased by a factor of 5. Also during this period, "periodic tremor", consisting of 5 to 20 minute episodes of harmonic tremor at average intervals of 65 to 85 minutes, was continuously recorded. Phreatic eruptions occurred intermittently until about September 27 and

during these eruptions harmonic tremor was recorded continously until October 2, but steadily decreased in amplitude. In contrast to the premonitory seismic activity in early September, the seismic energy release rate was very low during the month prior to the November 13 eruption. The only premonitory activity prior to this eruption was a small earthquake swarm November 9, and low level harmonic tremor beginning on November 10 and continuing to November 13. At 15:06 local time on November 13, a blast event of about 15 minutes duration was recorded and minor ash fall was reported about one hour later at towns 35 km NE of the crater. Harmonic tremor mixed with small eruption events followed this small eruption, but diminished rapidly in amplitude and frequency until 21:08 local time. At this time the Plinian eruption started, generating catastrophic mudflows.

3. Ecuador, Colombia and Costa Rica were visited in order to: introduce the USGS/OFDA VDAP program to relevant national and international agencies and institutions; form scientific and administrative liaisons necessary to assure the successful interaction of VDAP with these agencies and institutions; conduct an inventory of each country's volcano hazards and available resources in equipment, personnel, and institutions for the mitigation of volcanic hazards; to investigate and propose methods and avenues that might improve each countries posture toward volcanic hazards; to obtain baseline materials (publications, maps, photographs etc.) required to improve hazards evaluations and reports and to facilitate rapid and effective response in the event of future volcanic unrest.

Reports

Harlow, David H., Munoz C., Fernando, and Cuellar, Jairo, 1986, Seismic activity preceeding the 13 November 1985 eruption of Ruiz Volcano, Colombia: Trans. Am. Geophysical Union, v. 67, p. 403.

Harlow, David H., White, Randall A., and many others, 1987, The 13 November 1985 eruption of Volcano Ruiz, Colombia: Science (article submitted).

Herd, D. G., D. H. Harlow, R. A. White, and others, 1986, The 1985 Ruiz Volcano Disaster: EOS, Trans. Am. Geophys. Union, 67, 457-460.

Munoz C., Fernando, Hans-Juergen Meyer, and David H. Harlow, "Seismic activity preceeding the 13 November 1985 eruption of Ruiz Volcano, Colombia." (abs: Hawaii Symposium on How Volcanoes Work)

Zollweg, J. E., D. H. Harlow, R. A. White, R. D. Norris, F. Guendel, 1986, Post-eruption seismicity at Nevado del Ruiz, Colombia: implications for reservoir system and continued activity: Trans. Am. Geophysical Union, v. 67, p. 406.

Crustal Deformation Observatory Part J: Askania Borehole Tiltmeter

14-08-0001-G1153

Frank Wyatt, Duncan Carr Agnew, Hadley Johnson
Institute of Geophysics & Planetary Physics
Scripps Institution of Oceanography
University of California, San Diego
La Jolla, CA 92093
(619) 452-2019

Walter Zürn
Geowissenschaftliches Gemeinschaftsobservatorium Schiltach
Universitäten Karlsruhe
D-762 Wolfach, Heubach 206, FRG

This grant supports the installation and operation of an Askania borehole tiltmeter at Piñon Flat Observatory (PFO) and analysis of data from it. This work is part of the Crustal Deformation Observatory (CDO) program, as a cooperative enterprise with Dr. Walter Zürn of Karlsruhe University (West Germany), who has provided the instrument on loan. The goals of this project are to:

1. Establish techniques (and costs) for emplacing and orienting removable tiltmeters in boreholes of various depths. We have placed special emphasis on developing methods that may be applied at greater depth than has yet been customary; most installations of Askania instruments have been at depths from 10 to 30 m.
2. Compare these borehole tilt measurements with those from adjacent tiltmeters, including both long-base surface instruments and other borehole installations. Such comparisons should enable us to identify sources of instability and noise, and to establish the limitations of borehole tilt measurements using a high-quality instrument.
3. Use the borehole instrument to accurately monitor tilt in a tectonically active area. The existing long-base tiltmeters sense only east-west tilt.

The Askania tiltmeter arrived in La Jolla in early 1985, and was installed at PFO in December, in a 24 m-deep cased borehole. The installation was made 83 days after drilling and 21 days after cementing the casing in.

Figure 1 shows data from both components of the Askania beginning a few hours after installation and running through the day 110 of 1986. Offsets of order 0.1 μrad caused by nearby drilling (15 m away) and induced cable-motion have been removed, but no detrending has been done. Both components show a rapid transient adjustment over the first few days, probably caused by temperature changes as the instrument comes to equilibrium with its surroundings and by stress relaxation of the instrument support points. The NS component (actually at azimuth 170.5°) appears to have settled in very rapidly to an annual tilt rate of 0.85 μrad/a, while the EW is still equilibrating. We do not yet know the reason for this, or whether it reflects adjustment of the tiltmeter in its housing or creep in the cement that couples that housing to the earth. We are encouraged by the excellent behavior of the NS component to believe that this mode of installation is a good one.

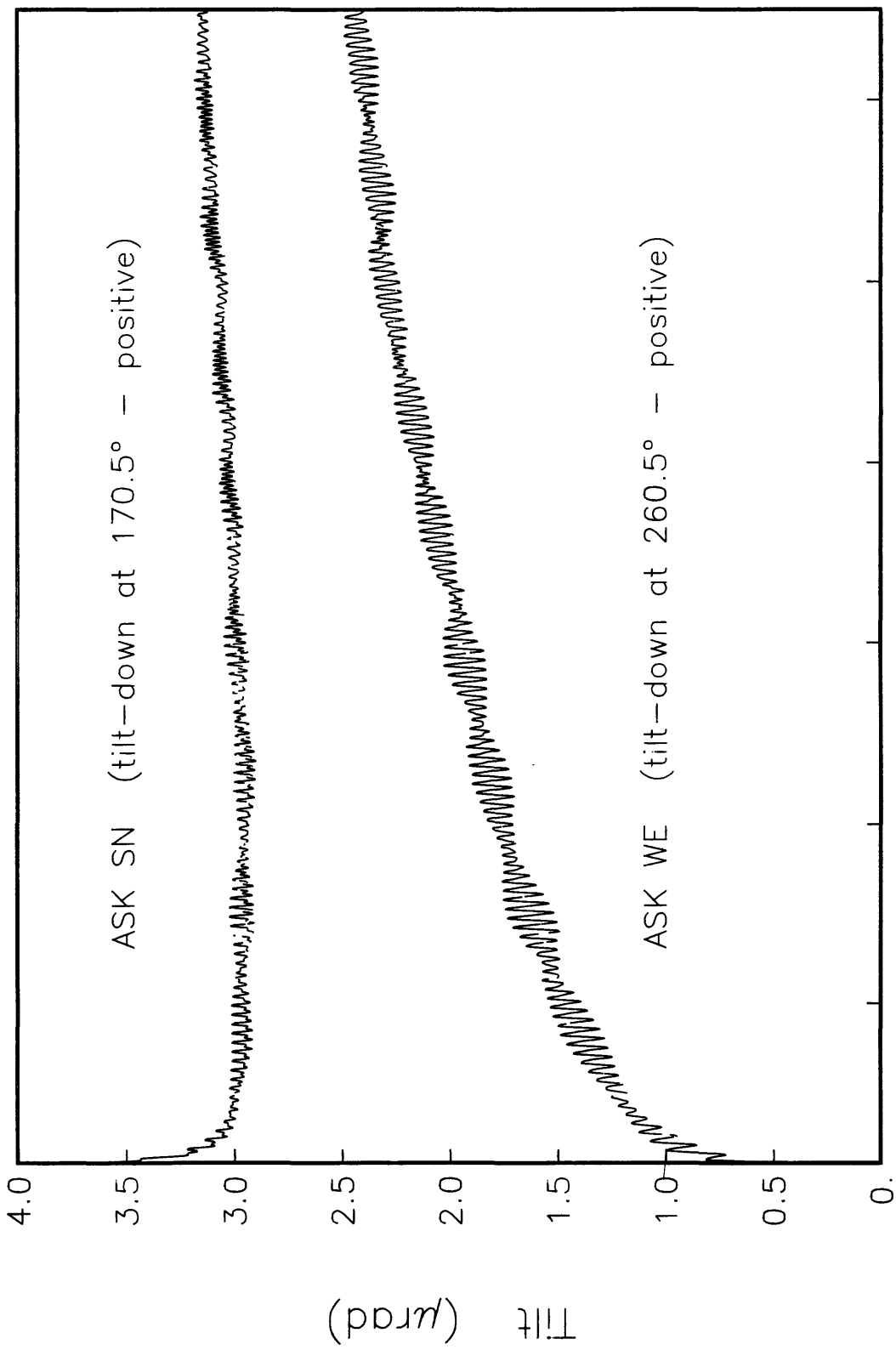
Askania Borehole Tiltmeter at PFO
ASK SN (tilt-down at 170.5° - positive)
ASK WE (tilt-down at 260.5° - positive)
Tilt (μrad)
Time (day numbers - 1986)
4.0
3.5
3.0
2.5
2.0
1.5
1.0
0.5
0.
0
20
40
60
80
100

Figure 1.

Piñon Flat Observatory: A Facility for Studies of Crustal Deformation

14-08-0001-G1178

Frank Wyatt, Duncan Carr Agnew,
Mark A. Zumberge, Jonathan Berger
Institute of Geophysics & Planetary Physics
Scripps Institution of Oceanography
University of California, San Diego
La Jolla, CA 92093
(619) 452-2019

This two-year grant supports the operation of Piñon Flat Observatory (PFO) by providing one-half the funds needed for running the shared facility. Matching funds are provided by the National Science Foundation. The work done at PFO includes establishing the accuracy of instruments designed for measuring various geophysical quantities by comparing results from them with data from reference standard instruments. This comparison also allows reliable monitoring of strain and tilt changes in the area near the observatory, between the active San Jacinto fault and dormant southern San Andreas fault systems. All of this effort is intended to foster development of precision geophysical instrumentation.

This report presents results from some of the instruments for the time around the most interesting earthquake occurring near PFO in the last few years: the "North Palm Springs" earthquake, a M_L 5.9 event which occurred on July 8, 1986, at 09:21 UTC. The earthquake was 45.5 km from PFO at an azimuth of -18°. Seismic data (pers. commun. from L. Jones, USGS) indicate right-lateral slip on a fault striking N60°W and dipping 50° to the north, probably on the Banning fault. Unfortunately, several coincidental power failures at our lab in La Jolla just prior to the earthquake had stopped the datalogger that records telemetered data at high speed (every 1 and 0.05 sec). The data from PFO indicate that the earthquake caused a brief power-dip at the observatory, thus hindering the interpretation of coseismic signals from many of the instruments.

Laser strainmeter data are shown in Figure 1 for the best of the three instruments (the Northwest-Southeast instrument). Because the laser strainmeters are not on uninterruptible power we do not expect that they will provide reliable data on the coseismic signals, and this was indeed the case. The offset shown in this figure (the vertical dashed line) is that expected theoretically, **not** that measured; it has been included to provide a scale for strain relative to slip at the source. Particularly intriguing in this figure is the postseismic response, whose amplitude is nearly equal to that accrued annually. A possible explanation for this is given below.

A large number of borehole tiltmeters are currently operating at PFO. The coseismic offsets on these were generally inconsistent with each other and much larger than theoretical models predict (~2 nrad). We believe this is a result of high accelerations causing small displacements of the ground around the sensors. Even the elaborately installed Askania tiltmeter showed tilts of about 300 nrad, probably induced by flopping of the 23 m-long signal cables.

The UCSD long fluid tiltmeter is equipped with uninterruptible power and did not indicate any coseismic tilt above a level of 3 nrad, nor did it show any postseismic signal.

Only one of the Carnegie Institution of Washington borehole dilatometers was operating at the time of the earthquake (instrument CIA). This instrument is troubled by short-period "glitches" every few hours, so that it is not as valuable as it might be in looking for preseismic events. Unfortunately, because of the high gain at which we are operating it, the instrument had to be reset by opening the internal valve, so we have no information on the size of the coseismic offset that was sensed.

Water level records are shown in Figure 2. The records in boreholes CIA and UQA come from compensated pressure sensors; the record for CIC comes from a float gauge operating a potentiometer. The CIA water level showed no clear coseismic change, but did show a rapid increase in water level in the hours following the event, though the total change was small. The largest coseismic offset was in borehole UQA, in which the water level dropped about 1.0 m. The level in this well showed a gradual recovery of about this amount over the next 25 days. The similarity in shape of this and the strain data (Figure 1) lead us to speculate that the change there may reflect local strains caused by hydrologic changes at PFO rather than further motion at the source (after-slip).

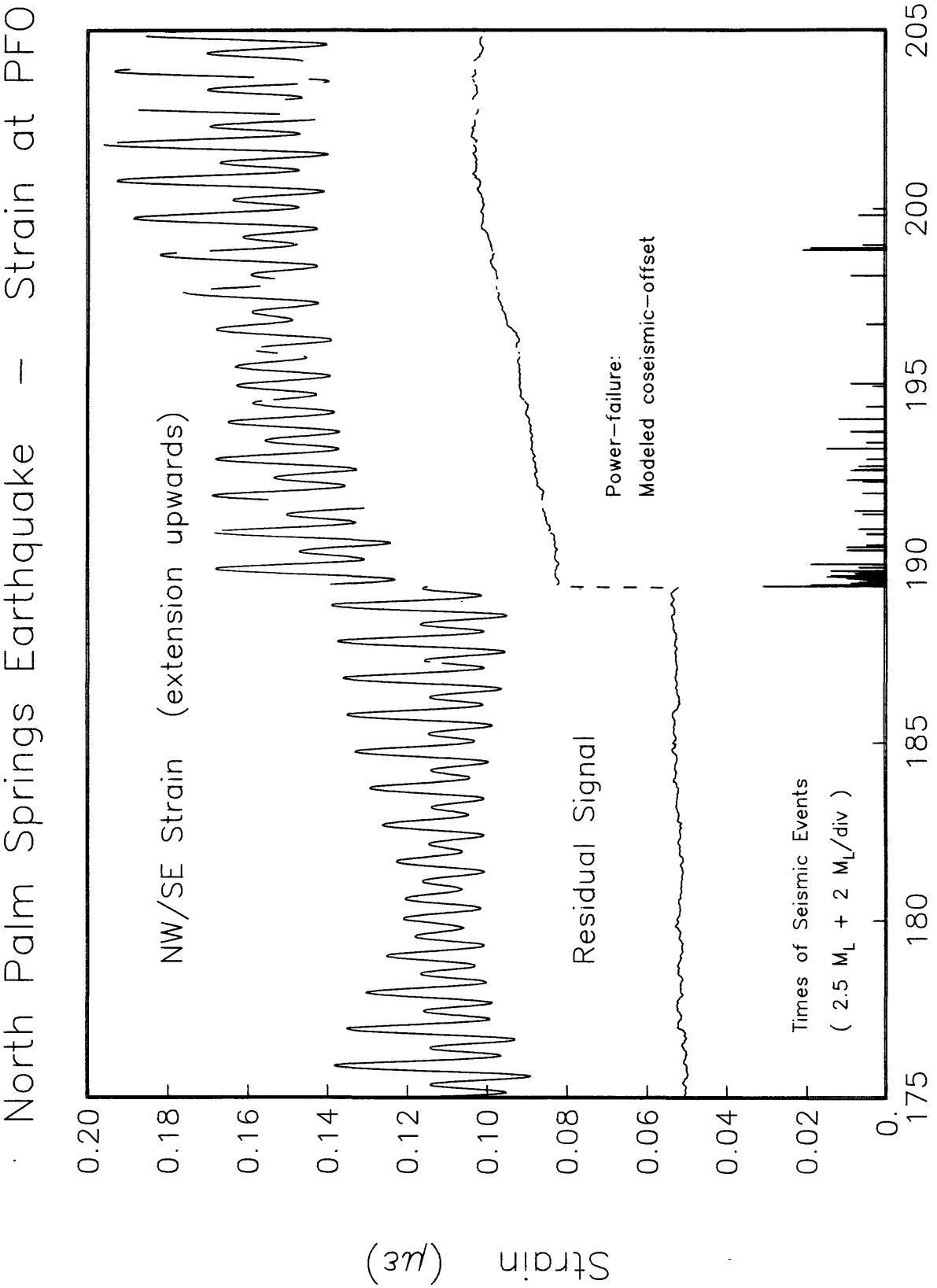
North Palm Springs Earthquake – Strain at PFO
NW/SE Strain (extension upwards)
Residual Signal
Power–failure:
Modeled coseismic–offset
Times of Seismic Events
(2.5 M_L + 2 M_L/div)
Strain (με)
Time (Days – 1986)
0.20
0.18
0.16
0.14
0.12
0.10
0.08
0.06
0.04
0.02
0.
175
180
185
190
195
200
205

Figure 1.

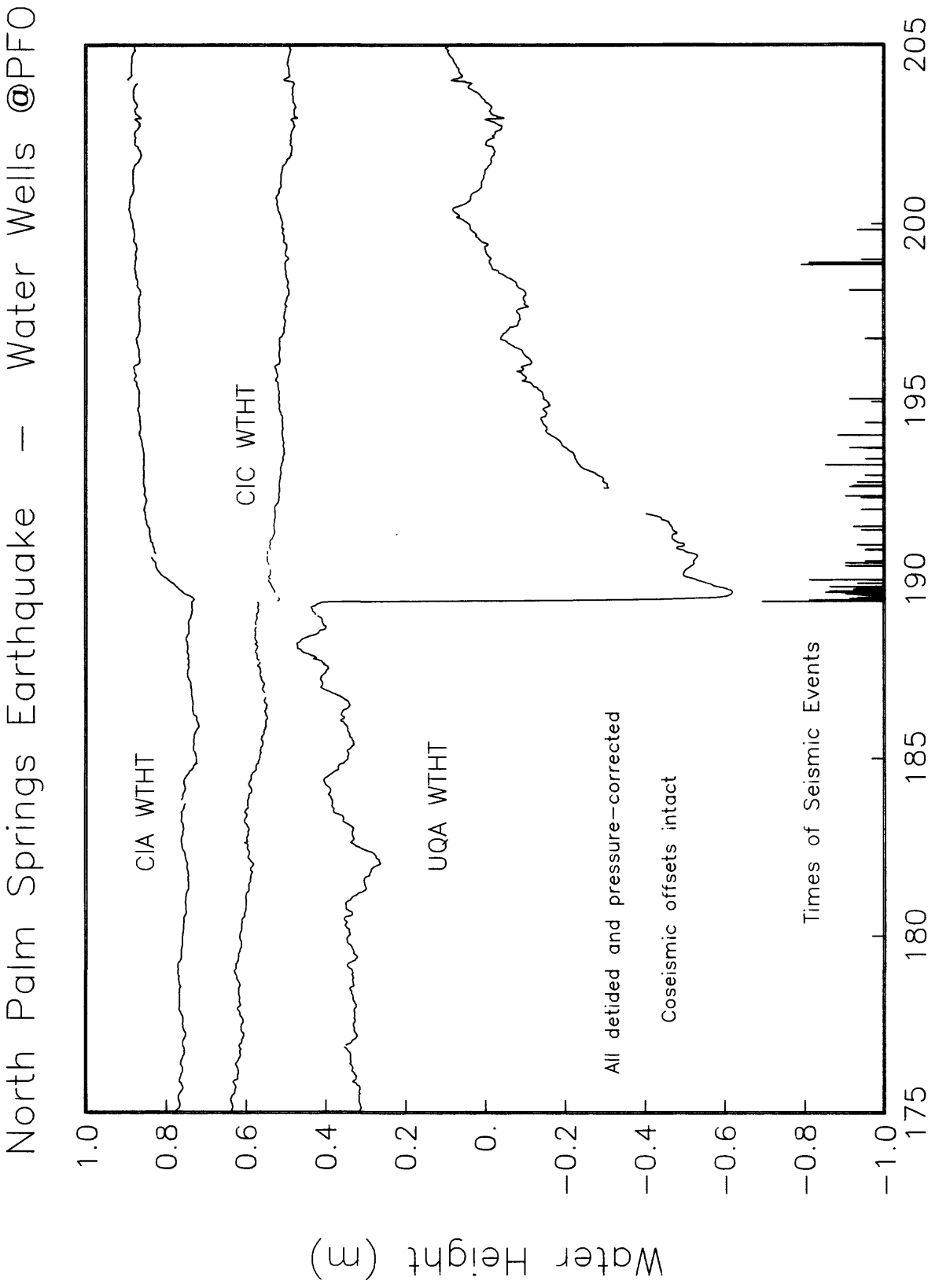
North Palm Springs Earthquake — Water Wells @PFO
CIA WTHT
CIC WTHT
UQA WTHT
All detided and pressure-corrected
Coseismic offsets intact
Times of Seismic Events
Water Height (m)
Time (Days — 1986)
1.0
0.8
0.6
0.4
0.2
0.
−0.2
−0.4
−0.6
−0.8
−1.0
175
180
185
190
195
200
205

Figure 2.

Piñon Flat Observatory: Cooperative Studies with Outside Investigators

14-08-0001-G1197

Frank Wyatt and Duncan Carr Agnew
Institute of Geophysics & Planetary Physics
Scripps Institution of Oceanography
University of California, San Diego
La Jolla, CA 92093
(619) 452-2019

This grant provides assistance for independent investigators working at Piñon Flat Observatory (PFO) under the auspices of the U.S. Geological Survey. This assistance includes research coordination, instrument operation and testing, data logging, preliminary data reduction, and collaborative data analysis. Part of this is a cooperative program (the Crustal Deformation Observatory Project) to evaluate instruments for measuring long-period ground deformation. Such evaluation involves understanding and reducing noise in the instruments and also developing improved methods to describe measurement error. Most of the studies currently underway are conducted independently, with investigators establishing their own associations to compare results; in the Crustal Deformation Project there is a more formal agreement to share observations.

Most of the sensors operated by outside investigators have continued to work well with only occasional attention, notably the various borehole tiltmeters, which include an Askania tiltmeter (24 m depth) run in cooperation with Walter Zürn of Karlsruhe University; two tiltmeters (24 and 36 m depths) designed by Judah Levine and Chuck Meertens of the University of Colorado; and three St. Louis University tiltmeters (depth 4.5 m) developed by Sean-Thomas Morrissey. There are also two long-base tiltmeters developed by outside groups; one of these, the LDGO instrument (installed by John Beavan and Roger Bilham) has been disturbed for much of this period by the installation of short tubes to make a hydraulic tie from this instrument to the UCSD long-base tiltmeter. This tie will make possible a direct comparison between these two high-quality instruments.

In June 1986 the National Geodetic Survey (NGS) set five closely-spaced class A bench marks at one end of the long fluid tiltmeters, with future surveys (by both NGS and the University of California Santa Barbara) being planned to study the stability of these monuments. Under the direction of Ross Stein (USGS) NGS also levelled a loop around the greater Pinyon Flat area, tying the observatory into the national vertical control net. Similar horizontal ties were provided in June by GPS surveys (also done by NGS), in which observations were made at the absolute gravity pier and VLBI pad, as well as at other marks nearby. Additional control on the broader-scale deformation should be forthcoming in the next few years from a 2-color geodimeter network set up by John Langbein (USGS); the first survey was done in March.

In August a USGS drill crew bored three holes in the area south of the instrument trailer, to depths of 150 m (2 holes) and 275 m. These will be used in a study of the effects of surface layers on high-frequency seismic measurements. From the standpoint of crustal deformation, the drilling of these holes caused large signals on many of the instruments; understanding these should help to elucidate how groundwater motions affect tilt and strain records.

Towards a Widely-Deployable Long-Base Tiltmeter: Sensors and Anchors

14-08-0001-G1200

Frank Wyatt, Mark Zumberge, Duncan Carr Agnew
Institute of Geophysics & Planetary Physics
Scripps Institution of Oceanography
University of California, San Diego
La Jolla, CA 92093
(619) 452-2019

This grant supports the construction and testing of improved systems needed for long-base tiltmeters to operate without skilled attention and to return good data from areas of relatively unstable surface materials. The systems to be developed are:

- A water-level sensor that will be an improved version of the existing white-light interferometer, with separate servo controls for platform leveling and water-surface tracking.
- Anchors that will use optical fiber interferometers to provide the integrated strain (displacement) from various depths to the surface, a technique that offers the possibility of a very robust and easily-maintained system.

Initial installations and tests are being made at Piñon Flat Observatory for comparison with existing instruments and for training of personnel. The goal of this program is to have both a proven design and the trained personnel necessary for the deployment of a field-worthy long baselength tiltmeter.

In August 1986, a borehole was drilled 125 m beyond the east end (TAU) of the original 535 m-long tiltmeter. This location near TAU is close enough to allow us to estimate reliably the ground deformation there and thus to evaluate our new techniques. Several fibers (from 5-50 m), short invar rods, and open pipes are cemented in the borehole. Our plan is to use a pair of fibers, one shallow, the other deep, in a Michelson interferometer to measure the displacement accumulating between their lower ends. An invar rod will monitor from the bottom of the shallow fiber to the surface. (Optical fiber is far too temperature-sensitive for accurate displacement measurements near the surface.) Vault construction around the borehole casing is presently underway.

With additional funds from NSF, we are conducting a program of testing optical fibers for crustal strain measurement, supplementary to the field program covered here. As part of this, we have constructed a vertical fiber test chamber in the basement shaft of IGPP. Figure 1 displays the first results of our fiber testing, in which we operated a 23 m equal-arm optical fiber interferometer in the test shaft. For about two months we monitored the difference in optical path lengths between two fibers fixed at the top and bottom of the shaft. In principle, all strain, temperature, and pressure signals were common to both arms, and any remaining signal indicates either unequal drift in the fibers or incomplete compensation of common-mode effects. The temperature in the shaft, which we also monitored, seems to correlate with the fiber data, suggesting such incomplete compensation. We find this data set encouraging because the slope, even with no attempt to subtract out the residual temperature signal, is only about 5×10^{-7} ϵ/a. This level of stability is adequate for many geophysical applications where strain measurements are made differentially.

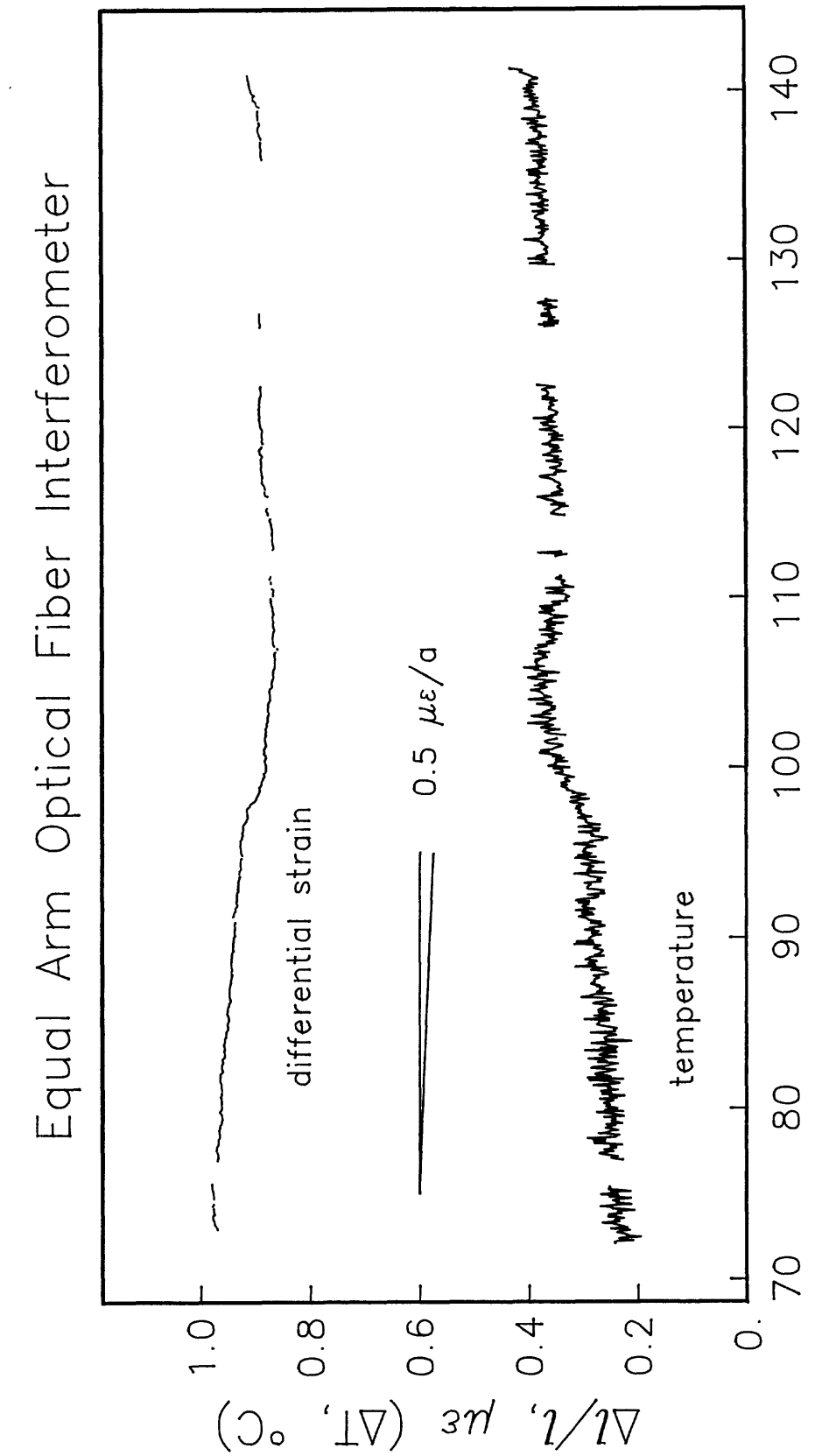
Equal Arm Optical Fiber Interferometer
differential strain
0.5 με/a
temperature
Day Number, 1986
Δl/l, με (ΔT, °C)
0.
0.2
0.4
0.6
0.8
1.0
70
80
90
100
110
120
130
140

Figure 1.

THE RELATIONSHIP BETWEEN CREEP AND SEISMICITY RATE ALONG THE CENTRAL SAN ANDREAS FAULT

14-08-0001-G1089

Max Wyss
CIRES
University of Colorado
Boulder, CO 80309

R. E. Habermann
School of Geophysics
Georgia Institute of Technology
Atlanta, GA 30332

An isolated segment of the San Andreas fault, approximately 10-km long, showed a period of seismic quiescence lasting from May 1985 through 22 June 1986, the end of the available data. This may be interpreted as a precursor to a moderate magnitude earthquake in that fault segment. Our initial analysis yields the following preliminary prediction: An earthquake of $M_L = 5 \pm .5$ is expected to rupture the San Andreas fault segment between latitude 36.39 ° and 36.45 ° N, between December 1986 and January 1988.

During the spring of 1985 an analysis of seismicity rates in a 100-km long segment of the San Andreas fault from San Juan Bautista to Stone Canyon by Wyss and Burford (1985) revealed three segments of the fault which were experiencing low seismicity rates. These authors proposed that these regions would be the sites of mainshocks in the near future. The size of the upcoming event could not be prescribed unambiguously because of the possibility that more than one of the quiet fault segments would be involved in the rupture, so two possible scenarios were proposed. On May 31, 1986 an event with $M_L = 4.6$ occurred near Stone Canyon. Its aftershocks filled one of the quiet regions recognized by Wyss and Burford (1985) (Figure 1). Thus one of the predictions was fulfilled. This success supports our contention that seismicity rate variations can be used for earthquake prediction in California. In work supported by this grant we discovered a segment of the fault, about 10-km long, which has been quiet since May, 1985. The quiescence in this zone is similar to that prior to the earthquake of 31 May, 1986. Therefore it may be hypothesized that this fault segment will be the site of the next moderate event in this area.

The magnitudes of the events in the region were corrected using the techniques developed by Habermann. Clustered events were removed from the catalog using the algorithm developed by Reasenberg (1985). We first corrected the magnitudes, then eliminated all events with magnitudes less than 1.5, and then applied the cluster identification algorithm of Reasenberg (1985). Using the magnitude signature technique we determined that detection and reporting of earthquakes with magnitudes larger than 1.7 were constant during most of the time since 1974.

Figure 2 shows the cumulative number of independent events with corrected magnitudes $M_L > 1.7$ in volume 618, defined in Figure 4. Note that this volume shows a 58-week long quiet period at the end of the data set, while the neighboring volumes 616 and 620 do not show this change (Figure 2). We evaluated the significance of this period of low activity by several statistical tests using three tests based on the Poisson assumption and the z-test for a difference between two means. The probabilities that this period are anomalous are: Poisson test (complete period as background): 0.9985; Poisson test (short background): 0.9993; Binomial test: 0.9990; z-test (z-value=5.9): 0.999+. On the basis of these tests we feel confident that this period of quiescence is unexpected using the assumption of a stationary process.

Man-made changes occur in the seismicity catalog and represent a potential error source for seismicity studies. The long-term stability of the seismicity rates in Figure 2 suggests, however, that we have successfully corrected for these changes. Nevertheless, it is possible that the anomaly could be due to some man-made effect that we failed to recognize and correct for. To guard against this possibility we examined seismicity rates in the two fault segments of the same size adjacent to the target volume 618 (Figure 2). The segment to the north of the anomaly (volume 616) shows remarkably stable seismicity rates throughout the period considered. The rate in the region to the south of the anomaly (volume 620) is not as constant as that to the north. This area shows an apparent activation of seismicity near the beginning of the quiescence to the north, and more recently the activity has decreased. These observations may be interpreted to suggest that this area may contain the future rupture initiation point.

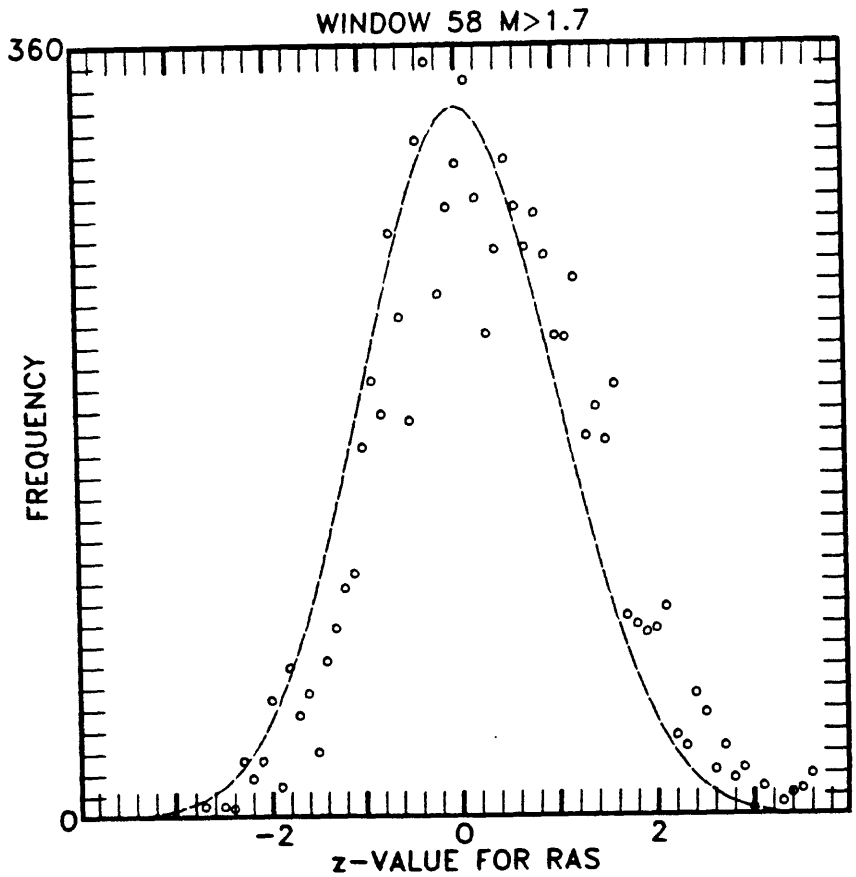

Figure 3: Histogram of z-values for comparisons of mean seismicity rates within 58-week intervals in 17 fault segments to the north and south of volume 618. The z-value for the target period is the largest for any of the 8313 comparison made, and plots outside of the figure's bounds at z=6.

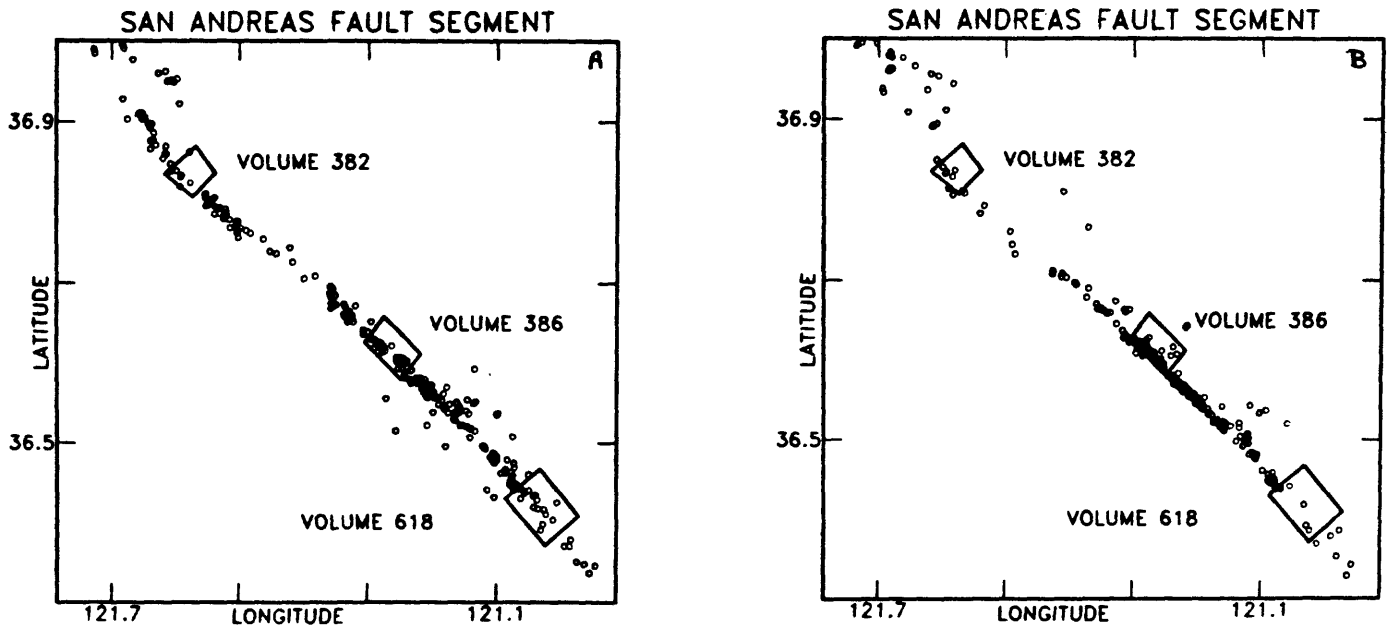

Figure 4: Epicenter maps of the San Andreas fault segment containing sub-segments with recently low seismicity rate. In the southernmost of these (618) we expect an earthquake of M_L =5± 0.5 before the end of 1987. The central segment (386) contained the predicted 31 May 1986 mainshock. The northernmost (382) is the location for which Wyss and Burford (1985) also expected a mainshock by may 1986 but none occurred as yet. Figure A shows the randomly chosen background period of 58 weeks between November 1979 and December 1980, figure B is for the 58 weeks between May 1985 and June 1986.

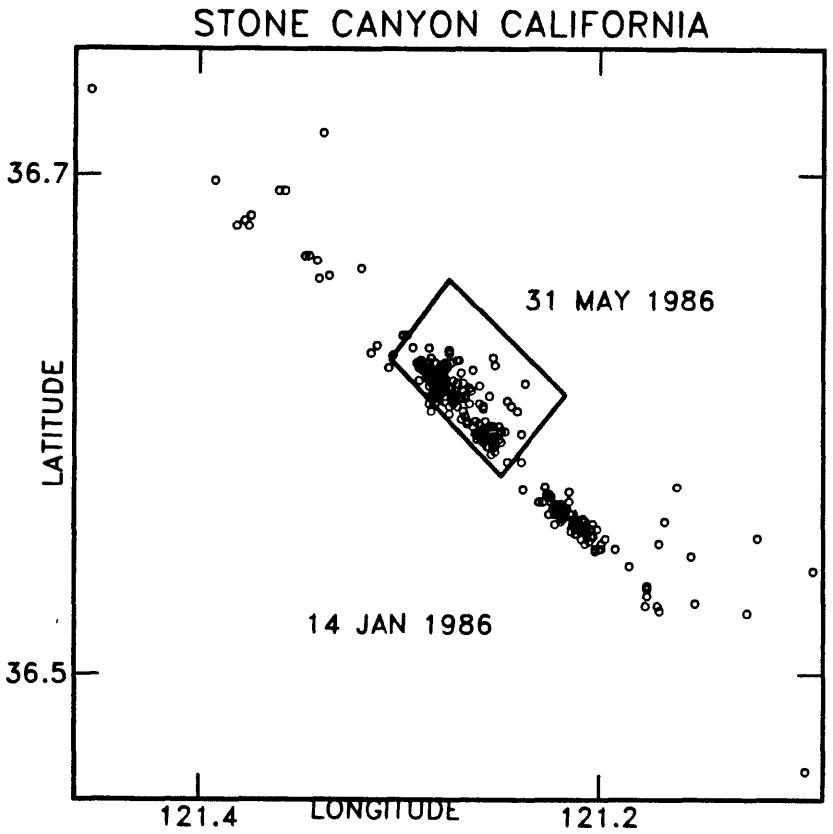

Figure 1: Map of the Stone Canyon segment of the San Andreas fault (the fault zone extends from the upper left to the lower right corner). The epicenters shown are for the earthquakes which occurred during the two-week periods following the mainshocks (M_L =4.6) of 14 January 1986 and 31 May 1986.

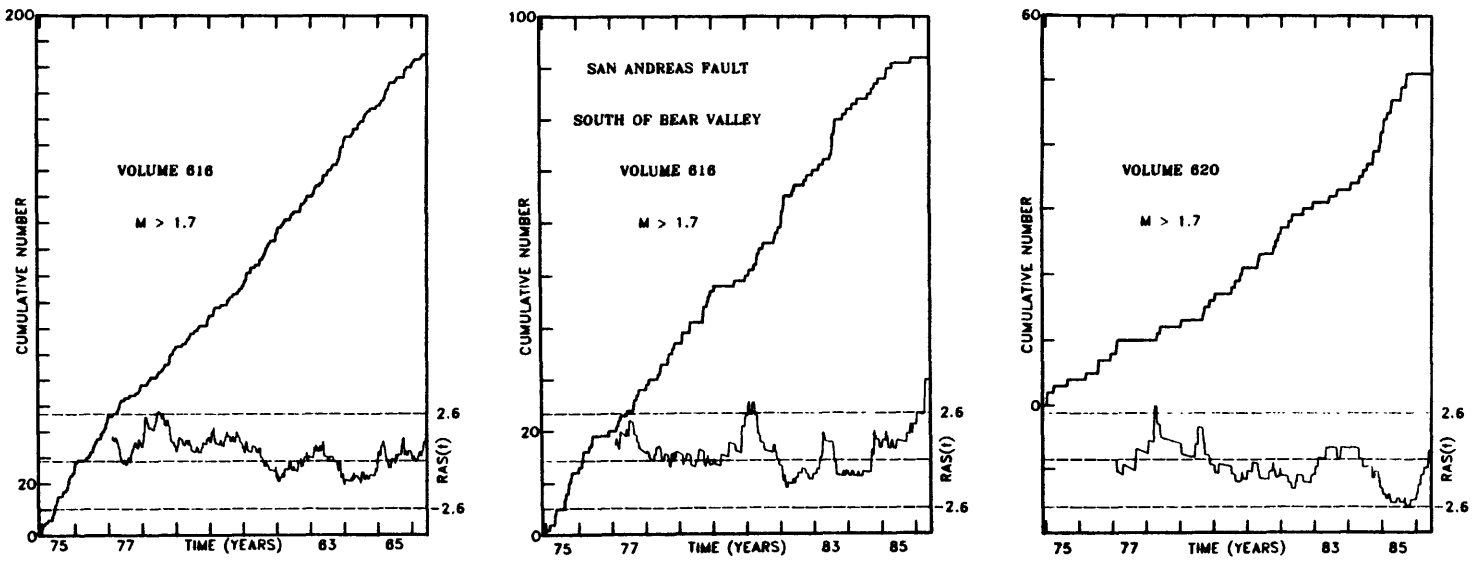

Figure 2: Cumulative numbers of earthquakes as a function of time for three adjacent segments of the San Andreas fault, each of length approximately 10 km. The central one of these segments (volume 618, for location see Figure 4) shows a seismic quiescence during the last 58 weeks of the data. The statistical function labeled RAS (near bottom of each plot) shows a large deviation from zero for this time period in volume 618.

At the time of the analysis the available data ended on June 22, 1986, and the anomaly had a duration of 58 weeks. To evaluate the uniqueness of the anomaly we slid a 58-week window through the data set one week at a time and compared the rate in that window with the rate during the period before the window, using the z-test for a difference between two means. The resulting functions are shown in Figure 2 for volumes 616, 618, and 620. The z-values are plotted at the end of the sliding window because in a real-time situation that is when the information becomes available.

We repeated this test in 17 segments of the fault with the same length as the segment with the anomaly. Even numbered volumes, 610 through 624, abut each other, odd ones overlap the even ones by 50%. No adjustments of the volume positions were made to optimize the anomaly. The uniqueness test yielded 8313 comparisons of potential anomalous periods to background periods (Figure 3). The highest z-value of all these comparisons (5.98) occurred in volume 618. In other words, for this window length this anomaly is the most significant to have occurred in an 85-km long section of the fault between early 1975 and the present. The second highest z-value (4.4) occurred in a region which experienced an event with M_L =4.9 during 1982. A detailed analysis of this precursor anomaly will be submitted soon for publication in a journal.

The size of the expected mainshock is estimated by assuming that its rupture length, L, will approximately equal that of the quiet volume 618. Thus we estimate that $5 < L < 15$ km, which corresponds approximately to a magnitude of $M_L = 5 \pm 0.5$.

The most poorly constrained parameter is the occurrence time, because we have few precedents with known duration of quiescence. The two mainshocks which occurred in the study area and the time period since 1974 both had quiescence precursors. Their magnitudes were M_L =4.9 (August 1982) and M_L =4.6 (May 1986) and their precursory quiescences lasted 84 and 137 weeks, respectively. We will assume that the average of these durations, 110 weeks, is the most likely value for the precursor time of the expected event. The uncertainty is at least 30 weeks.

In summary the parameters of the prediction are: Location: in the quiet volume 618 (Figure 4) with the initiation of rupture possibly located in the adjacent volumes; Size: 5 to 15-km long rupture, $M_L = 5 \pm 0.5$; Time: between December of 1986 and January 1988 inclusive of these dates; Probability: equivalent rate changes have not occurred without being followed by a mainshock. We recommend that the seismicity of the 85-km fault segment centered on volume 618 be studied and monitored in detail.

COORDINATES FOR VOLUMES DISCUSSED

Volume 616	Volume 618	Volume 620
36.531 - 121.100	36.467 - 121.032	36.408 - 120.974
36.491 - 121.149	36.430 - 121.086	36.371 - 121.026
36.429 - 121.084	36.371 - 121.024	36.299 - 120.942
36.467 - 121.032	36.408 - 120.972	36.341 - 120.897

REFERENCES

Reasenberg, P., Second-order moment of central California seismicity, 1969-1982, *J. Geophys. Res., 90*, 5479-5495, 1985.

Wyss, M. and R. Burford, Current episodes of seismic quiescence along the San Andreas Fault between San Juan Bautista and Stone Canyon, California: Possible precursors to local moderate mainshocks, U.S. Geol. Survey open-file report, 85-754, 367-426, 1985.

Creep and Strain Studies in Southern California

Grant No. 14-08-0001-G1177

Clarence R. Allen and Kerry E. Sieh
Seismological Laboratory, California Institute of Technology
Pasadena, California 91125 (818-356-6904)

Investigations

This semi-annual Technical Report Summary covers the six-month period from 1 April 1986 to 30 September 1986. The grant's purpose is to monitor creepmeters, displacement meters, and alignment arrays across various active faults in the southern California region. Primary emphasis focuses on faults in the Imperial and Coachella Valleys.

Results

During the reporting period, alignment arrays were resurveyed across the San Jacinto fault at COLTON, across the San Andreas fault at BERTRAM, NORTH SHORE, RED CANYON, DILLON ROAD (twice), and INDIO HILLS (twice), across the Mission Creek fault at THOUSAND PALMS CANYON and YERXA, across the Banning fault at DEVERS HILL (twice), and across the Imperial fault at HIGHWAY 80. Creepmeters were serviced at MECCA BEACH (twice), NORTH SHORE (twice), HEBER ROAD (twice), TUTTLE RANCH (twice), HARRIS ROAD, and SUPERSTITION HILLS. A new creepmeter, to be telemetered to Pasadena via SMS-GOES satellite, was installed on 4/21/86 at SALT CREEK. Slipmeters were serviced at JACK RANCH and TWISSELMAN RANCH.

The 8 July 1986 North Palm Springs earthquake, ML = 5.9, was followed by minor slip along portions of the southernmost 70 km of the San Andreas fault (Fig. 1)(Fagerson et al., in press). Across this segment of the fault, Caltech maintains 7 theodolite alignment arrays, a dial-gauge extensometer, and a telemetered extensometer and tiltmeter. While the alignment arrays are not well suited to measure episodic displacements of less than 1 cm, the records from their resurveys have yielded upper limits on the amount of coseismic displacement. Using 2σ errors on the sightings to different targets, limits on the amount of allowable coseismic displacement are <14 mm at DEVERS HILL, on the Banning fault 13.6 km from the hypocenter, <1.5 mm at INDIO HILLS and <5.6 mm at DILLON ROAD, both on the San Andreas fault near Indio. All three sites have shown ongoing slip at rates near 2 mm/yr over the last decade (Louie et al., 1985). There may well have been no coseismic displacements at these sites in connection with the 8 July earthquake. Better resurveys are available from the new alignment array across the Mission Creek fault at THOUSAND PALMS CANYON. Target measurements average about 1 mm of dextral slip between 12 December 1985 and 8 July 1986 (following the earthquake). This slip could be the result of either a 1 mm or smaller coseismic displacement, 7 months of ongoing slip at 2 mm/yr or less, or some combination of these two. Since ground breakage was not observed here following the earthquake, it is possible, again, that there was no coseismic displacement. A few more years of resurveys will be necessary to confirm the suggestion that the Mission Creek fault is actively creeping.

The most illuminating measurements of slip related to the North Palm Springs earthquake come from the combination extensometer and tiltmeter across the San Andreas fault at MECCA BEACH. This digitally-recording instrument produced a detailed record of aseismic slip on the fault segment triggered by the 86-km-distant earthquake. Sympathetic slip on this same segment of the southern San Andreas fault occurred previously in response to the 1968 Borrego Mountain earthquake (Allen et al., 1972) and the 1979 Imperial Valley earthquake (Sieh, 1982). In both instances, the extent and magnitude of the triggered slip were derived mainly from the mapping of small ground fractures, controlled by nearby alignment array measurements. The 1986 record from MECCA BEACH gives new information on the exact timing and rate of the displacement motions.

Episodes of slip and tilt have been recorded instrumentally at MECCA BEACH previously on two occasions, in April and July of 1984 (Allen and Sieh, 1985). The April displacement exceeded 1 cm, while the July displacement was smaller but was preceded by a tilting event a few hours earlier.

Over a period of 20 days following the 8 July earthquake, the MECCA BEACH instrument recorded 3 episodes of dextral slip totaling 3.8 ± 0.6 mm, and tilt in 2 directions of up to 31 μradians. (Note that the measurements of Fig. 2 have not been corrected for temperature.) The effects of ground shaking during this earthquake, as well as during the 13 July earthquake near Oceanside (ML = 5.4), can be seen on the tilt records, with instantaneous inclinations of up to 20 μradians captured by the 5-min sampling interval. The history of motions is summarized in the following table.

History of Triggered Slip at Mecca Beach, July 1986

Date, July	Time, PDT	Dextral Slip, mm	Tilt, μradian	Dip Direction	Comments
8	02:25	~-0.1	15±2	N54±10°W	Coseismic response.
9	11:30	1.4±0.1	31±2	S59±15°E	Tilt began ~12 hr before slip.
13	06:51	~0.05	<3	unresolved	At time of Oceanside M_L =5.4 event, 195 km to west.
13	16:34	2.0±0.3	17±2	S54±9°E	Slip and tilt begin simultaneously.
22	01:31	0.4±0.5	14±2	N83±70°W	Tilt began ~12 hr before slip. Temp. change adds error.

Probably the most significant phenomenon in the records is the variation in the timing of the slip and tilt events. Whereas the registration of a slip episode indicates that the fault ruptured at the surface at MECCA BEACH, a tilt signal indicates that the fault broke near the site, but that the rupture did not necessarily extend to the instrument. Thus tilt in the absence of slip suggests that a rupture of limited area has occurred within a few kilometers, either below or away from the site. During the 8 July event, the instantaneous coseismic tilt probably is the effect of a triggered coseismic rupture near but not at the site. After 21 hr, the trend of tilting

reversed, and fault slip then began after another 12 hr. This suggests the migration of coseismic rupture from another area, eventually reaching the surface at MECCA BEACH 33 hr after the earthquake. Inasmuch as the tilts from such millimeter-size displacements could not be recorded from a rupture front more than 2 or 3 km away, the migration velocity of these ruptures is probably 1 km/day or less.

The third slip episode, beginning 21 July (Fig. 2), is similar to the first in that tilting precedes rupture by about half a day. However, the second episode, which follows the 195-km-distant 13 July Oceanside earthquake by 9-1/2 hr, has a different character; both slip and tilt begin simultaneously, indicating that a rupture occurred at the surface at MECCA BEACH without migrating from elsewhere.

These observations bear on the question of the mechanism for the triggered sympathetic slip that is now known to occur systematically on the southern San Andreas fault in response to regional earthquakes. Four possible mechanisms have been proposed (Allen et al., 1972; Fuis, 1982): (1) a change in the regional static strain field resulting from the triggering earthquake; (2) dynamic strain caused by ground shaking; (3) migration of creep from the hypocentral area; and (4) a regional strain event at depth which is manifested as seismicity in one area and aseismic slip in another. Mechanism (1) has been found to produce very small strains at moderate epicentral distances--of an order of magnitude less than for mechanism (2). Mechanism (2) cannot explain the recent slip, which took more than a day to propagate to the instrument. Apparently only certain portions of the fault may be triggered by dynamic strain, perhaps related to the sawtooth fault geometry noted by Bilham and Williams (1985). Mechanism (3) seems to be ruled out for this event by the coseismic tilt associated with the 8 July earthquake, indicating nearby fault rupture. Thus mechanism (4) tentatively appears attractive. The propagation of slip to MECCA BEACH from a regional strain event below seismogenic depths would indicate velocities in the range of 1-10 km/day, similar to those found for the propagation of creep events along the San Andreas fault in central California (King et al., 1973). Such a model must, however, be tested by regional geodetic measurements.

References

Allen, C. R., and Sieh, K. E., 1985, Creep and strain studies in southern California: U.S. Geol. Survey Open-File Rept. 85-464, p. 219-222.

Allen, C. R., Wyss, M., Brune, J. N., Grantz, A., and Wallace, R. E., 1972, Displacements on the Imperial, Superstition Hills, and San Andreas faults triggered by the Borrego Mountain earthquake: U.S. Geol. Survey Prof. Paper 787, p. 87-104.

Bilham, R., and Williams, P., 1985, Sawtooth segmentation and deformation process on the southern San Andreas fault, California: Geophys. Res. Lett., v. 12, p. 557-560.

Fagerson, S. H., Louie, J. N., Allen, C. R., and Sieh, K. E., in press, Measurements of triggered slip on the southern San Andreas fault associated with the North Palm Springs earthquake [abstract]: Am. Geophys. Union fall meeting, San Francisco (1986).

Fuis, G. S., 1982, Displacement on the Superstition Hills fault triggered by the [1979 Imperial Valley] earthquake: U.S. Geol. Survey Prof. Paper 1254, p. 145-154.

King, C.-Y., Nason, R. D., and Tocher, D., 1973, Kinematics of fault creep: Royal Soc. London Phil. Trans. A, v. 274, p. 1655-1662.

Louie, J. N., Allen, C. R., Johnson, D. C., Haase, P. C., and Cohn, S. N., 1985, Fault slip in southern California: Seismol. Soc. America Bull., v. 75, p. 811-833.

Sieh, K. E., 1982, Slip along the San Andreas fault associated with the [1979 Imperial Valley] earthquake: U.S. Geol. Survey Prof. Paper 1254, p. 155-159.

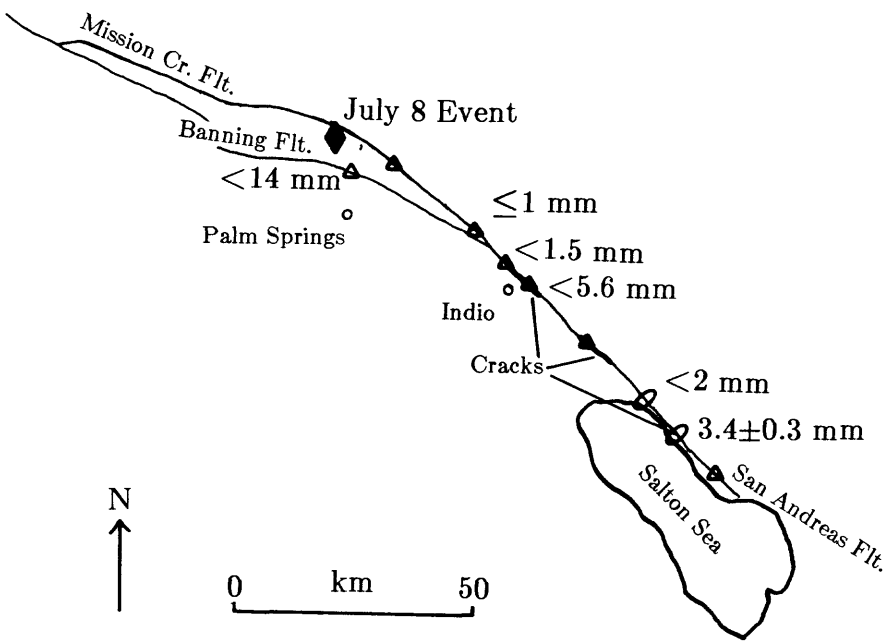

Fig. 1— Map of the Coachella Valley area with major faults and locations of geodetic measurements. Triangles are alignment arrays; ovals are creepmeters. The figures give the possible amount of dextral slip coseismic with the July 8, 1986 North Palm Springs earthquake at selected sites. Cracks are those mapped by Williams, Fagerson, and Sieh (in prep.).

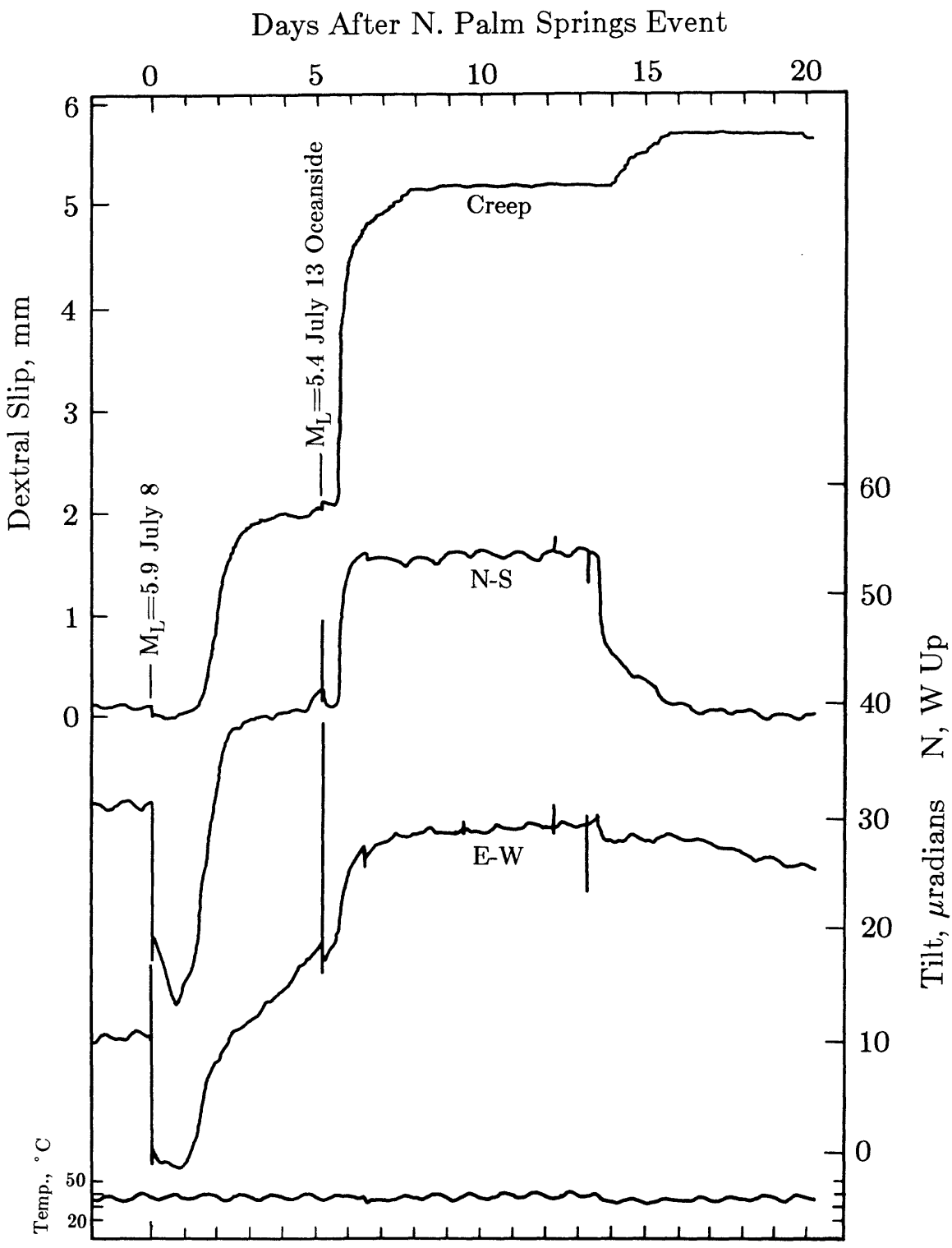

Fig. 2— Telemetered records from the extensometer and tiltmeter installed at Mecca Beach on the southern San Andreas fault, for the 20-day period following the July 8, 1986 North Palm Springs earthquake 86 km to the northwest.

Studies of Coalinga Aftershock Sequence

9910-03976

Mary Andrews
Branch of Engineering Seismology and Geology
U.S. Geological Survey
345 Middlefield Road, MS 977
Menlo Park, California 94025
(415) 323-8111, ext. 2752

Investigations:

1. Analysis of borehole recordings of Kettleman Hills aftershocks.

2. Analysis of geotechnical data from shallow boreholes at Coalinga.

3. Continued efforts to identify and model the source, path, and recording site chracteristics of the 1983 Coalinga, California earthquake sequence.

4. Compilation of USGS Bulletin on site studies at Coalinga.

Results:

1. Aftershocks of the Coalinga, California, earthquake showed large frequency-dependent amplitude variations along a linear array extending from a soil site in the city of Coalinga to a rock site in the nearby foothills. To investigate these variations in ground motion, three-component uphole and downhole seismometers were deployed in 100-meter-deep boreholes located at both ends of the array. The borehole seismographs recorded over 40 earthquakes at distances ranging from 10 to 50 km. Comparisons of uphole and downhole ground motion show that maximum P- and S-wave amplitudes are three to five times larger at the ground surface than at depths of 80 to 100 m. Uphole-downhole spectral ratios show: 1) pronounced maxima of 4 to 5 near 20 Hz for P-waves at each site; 2) no well-defined maxima exceeding about 3 for S waves at the sandstone site; and 3) pronounced maxima of about 5 in the band 10-30 Hz at the alluvium site. The average uphole-downhole spectral ratios computed for 40 events indicate that across the frequency band 0.1 to 30 Hz, P wave uphole-spectra are about three times larger than downhole spectra at both sites and S wave uphole-spectra are about 1.6 times greater at the sandstone site and about 3 times greater at the alluvium site. These observations lead to the following conclusions: 1) near-surface materials may significantly amplify the higher frequency (10-40 Hz) components of motion; 2) the response of near-surface deposits may have contributed to damage sustained by the older masonry structures in Coalinga; 3) the use of downhole sensors to improve seismic detection levels in the 0.1-40 Hz band requires that noise levels at depths of 100 m be less than those at the surface by factors of at least three to five.

2. We have logged a 150 m deep borehole in Pleasant Valley, California, using a repeating shear-wave source. The source consists of two horizontal hammers driven by compressed air; it produces shear-wave pulses that are reproducible in both shape and amplitude. The site is underlain by 38 m of clay on top of interbedded sand and gravel. First arrival times and first zero crossing times were picked to obtain the shear-wave velocity structure, which increases gradually from 200 m/s near the surface to 540 m/s at 55 m. There is a narrow zone from 105-120 m with a velocity of 900 m/s, below which the velocity decreases to about 600 m/s. The first half cycles of the pulses are used to estimate the attenuation from the relation $\Delta t^* = 2\ \Delta\tau_{\frac{1}{2}}$ giving cumulative attenuations of .012 and .022 secs for the upper 60 and 130 m, respectively.

   The shear-wave attenuation has also been estimated by the spectral ratio technique where the spectral ratios of the initial pulses are fit from 5 to 150 Hz. The relative amplification and attenuation can be resolved over 12 m intervals. The apparent Q is constant with frequency up to 70 Hz. The geometrical spreading from 15 to 150 m is fit to first-order by the integral over depth of the shear-wave velocity times the square root of the seismic impedance. The resulting estimates of Q range between 3 and 20, and vary markedly with depth. Scattering from small scale velocity variations appears to be a significant attenuation mechanism, even in this sedimentary structure.

3. Several techniques have been used to determine P- and S-wave attenuation in the vicinity of Coalinga, California. The broadening of explosion waveforms with distance indicates that Q_p=20 in the alluvium of Pleasant Valley, and that Q_p=30 in the interbedded sandstones and shales of Anticline Ridge. Spectral ratios of borehole recordings of a repeating shear-wave source show that Q_s ranges from 5 to 20 in the upper 150 m of alluvium. Analysis of Rayleigh wave amplitudes at frequencies of 1-4 Hz indicate that Q_s ranges from 20 to 40 in the upper 1 km of sedimentary rock. And the decay of the high-frequency spectral amplitudes of earthquakes suggests that Q_s is on the order of 70 in the upper 10 km of the crust. Earthquake spectra have been corrected for these low values of Q in order to improve the accuracy of source parameter determinations. The corrected spectra of small earthquakes generally yield higher stress drops which are more consistent with constant stress drop scaling.

4. The USGS Bulletin on site studies at Coalinga will include papers on the local geology, the near-surface P and S wave velocities, the direct, measurement of near-surface attenuation, and the site amplification inferred from linear array recordings and from borehole recordings of earthquakes. Efforts to compile and edit the contributions to the bulletin are still in progress.

Reports:

Andrews, M., Source and peak-motion parameters of the Coalinga, California, earthquake sequence: to be submitted to *Journal of Geophysical Research*.

Andrews, M., and Borcherdt, R., 1986, Response of near-surface geology from uphole-downhole arrays at Coalinga, California: *EOS (American Geophysical Union, Transactions)*, in press.

Boatwright, J., Porcella, R., Fumal, T., and Liu, H.-P., 1986, Direct estimates of shear wave amplifications and attenuation from a borehole near Coalinga, California: *Earthquake Notes*.

Boatwright, J., 1986, Seismic radiation from composite models of faulting: submitted to *Bulletin of the Seismological Society of America*.

Frankel, A., and Andrews, M., 1986, A note on path effects and the apparent scaling of small earthquakes: submitted to *Bulletin of the Seismological Society of America*.

Mueller, C., 1986, The influence of site conditions on near-source high-frequency ground motion: case studies from earthquakes in Imperial Valley, California, Coalinga, California, and New Brunswick, Canada: Ph.D. thesis, Department of Geophysics, Stanford University.

Digital Signal Processing of Seismic Data

9930-02101

William H. Bakun
Branch of Seismlogy
U.S. Geological Survey
345 Middlefield Road - Mail Stop 977
Menlo Park, California 94025
(415) 323-8111 x2777

Investigations

Coordination of activities in the Parkfield prediction experiment. Analysis of USGS coda-duration measurements for magnitude determination.

Results

A real-time earthquake prediction experiment is underway at Parkfield.

Reports

Bakun, W.H., J. Bredehoeft, R. O. Burford, W.L. Ellsworth, W.J.S. Johnston, L. Jones, A.G. Lindh, C. Mortensen, E. Roeloffs, S. Schulz, P. Segall, and W. Thatcher, 1986, Parkfield earthquake prediction scenarios and response plans, U.S. Geological Survey Open-File Report 86-365, 30 pp.

Bakun, W.H., G.C.P. King, and R.S. Cockerham, 1986, Seismic slip, aseismic slip, and the mechanics of repeating earthquake on the Calaveras fault. California, in Maurice Ewing Ser. vol. 6, edited by S. Das, J. Boatwright, and C.H.S. Scholz, pp. 195-207, AGU, Washington, D.C.

Tectonic Tilt Measurement: Salton Sea

14-08-0001-G1097

John Beavan and Roger Bilham

Lamont-Doherty Geological Observatory of Columbia University
Palisades, New York 10964
(914) 359-2900

Investigations

1. Historical water level measurements at three sites on the Salton Sea are being investigated to determine tectonic tilting, taking account of as many noise and error sources as possible.

2. The tectonic tilt derived from Salton Sea records is being carefully compared with leveling data from the area.

3. LDGO-designed pressure sensor gauges are being installed at several sites around the Sea to measure water level continuously, to investigate noise sources, and to determine the level of detectability of tectonic tilt signals in the data.

Results

Our analysis of the historical data is almost complete; a paper is about to be submitted to JGR. Despite our improved analysis methods, we have not significantly reduced the noise level in the data reported earlier by Wilson and Wood (1980). We have, however, greatly improved our understanding of the noise in the data, have reproduced the 1950-78 results reported by Wilson and Wood, and have brought their analysis up to date (Figs. 1 and 2). The early 1970's data in Figure 2 differs somewhat from a similar plot presented earlier (Open File Rept. 86-31, p. 273); this is due to an incorrect treatment of gaps in the earlier plot.

The Salton Basin tilted steadily downwards towards the SE at ~0.1 μrad/yr between 1950 and the early 1970's. The exact direction of tilt is not known as only one component of the vector was measured; the tilt magnitude could therefore be greater than 0.1 μrad/yr. The tilt direction changed in the early to mid 1970's, and since the late 1970's has been down towards the WSW at ~0.2 μrad/yr. The direction is given by the 6 mm/yr subsidence of FTJS relative to SSSP, and the almost zero subsidence of SB relative to SSSP. The NW-SE component of tilt derived from sea level agrees fairly well (Fig. 3) with 1956, 69 and 78 raw leveling data taken on the west side of the sea using Wild N-3 (non-magnetic) instruments. The reasons for the lack of agreement in 1974 are unknown. Agreement between sea level and leveling from the east side of the sea is poor, but most of these lines were measured using the Zeiss Ni-1 which has significant magnetic errors. Also, these lines are considerably further from the sea level sites, and local tectonic effects may have occured on the east side of the Sea (Bilham and Williams, 1985; Reilinger, 1985). It is possible that the sea level data contain errors of a few cm due to local settling of gauges or tide-staffs. However, even allowing for this possibility, the sea level data do not support interpretations of the leveling data that require large and rapid changes in vertical crustal motion (Castle et al., 1984; Gilmore, 1986).

The first LDGO-designed pressure gauge was installed at SSSP (Fig. 1) in May 1985. Following good results, a second was added at SB in January 1986. Three more will be installed in November or December 1986. Initially we experienced a number of data gaps due to the behaviour of the IBM-PC power supply during short (< 5 sec) power outages. This problem has now been solved and we have recently obtained more than 3 months of uninterrupted data. Some of these data are shown in Fig. 4a. In Fig. 4b we show low-pass filtered differences of the 9 months data collected since both gauges have been operating. The rms noise level at periods longer than 4 days is < 8 mm. The data show a trend of ground tilt down towards the south at 0.08 μrad/yr. This is not significantly different from zero and does not

contradict the data obtained from the staff and float gauges at SSSP and SB (we presently have these only through April 14 1986). No corrections have been made for temperature, air pressure or salinity in the data presented in Figure 4b, so it is possible that the data contain part of an annual cycle. We are currently investigating the best way to make such corrections. Salinity and temperature measurements in the Sea indicate that the maximum temperature-induced error in the difference signal at periods between a few days and a few weeks is ~5 mm; errors due to salinity variations may be as much as 2 cm under worst-case conditions. At longer periods (months to years), both error sources are attenuated, and we estimate their combined effect to be less than ~1 cm. The 8 mm rms suggests that tectonic signals of greater than 2.5 cm amplitude at periods longer than 4 days should be detectable; it may be possible to improve this with further processing.

No anomalous signals were observed prior to the July 8, 1986 Palm Springs earthquake.

References

Bilham, R. and P. Williams, 1985. Sawtooth segmentation and deformation processes on the southern San Andreas fault, California, *Geophys. Res. Lett.,* **12;9,** *557-560.*

Castle, R., M. Elliot, J. Church, and S. Wood, 1984. The evolution of the southern California uplift, 1955 through 1976, *U.S.G.S. Prof. Paper,* **1342.**

Gilmore, T., 1986. Historic vertical displacements in the Salton Trough and adjacent parts of southeastern California, *U.S.G.S. Open-File Report,* **86-380.**

Reilinger, R., 1985. A strain anomaly near the southern end of the San Andreas fault, Imperial Valley, California, *Geophys. Res. Lett.,* **12;9,** *561-564.*

Wilson, M.E. and S.H. Wood, 1980. Tectonic tilt rates derived from lake-level measurements, Salton Sea, California, *Science,* **207;** (11 Jan), *183-185.*

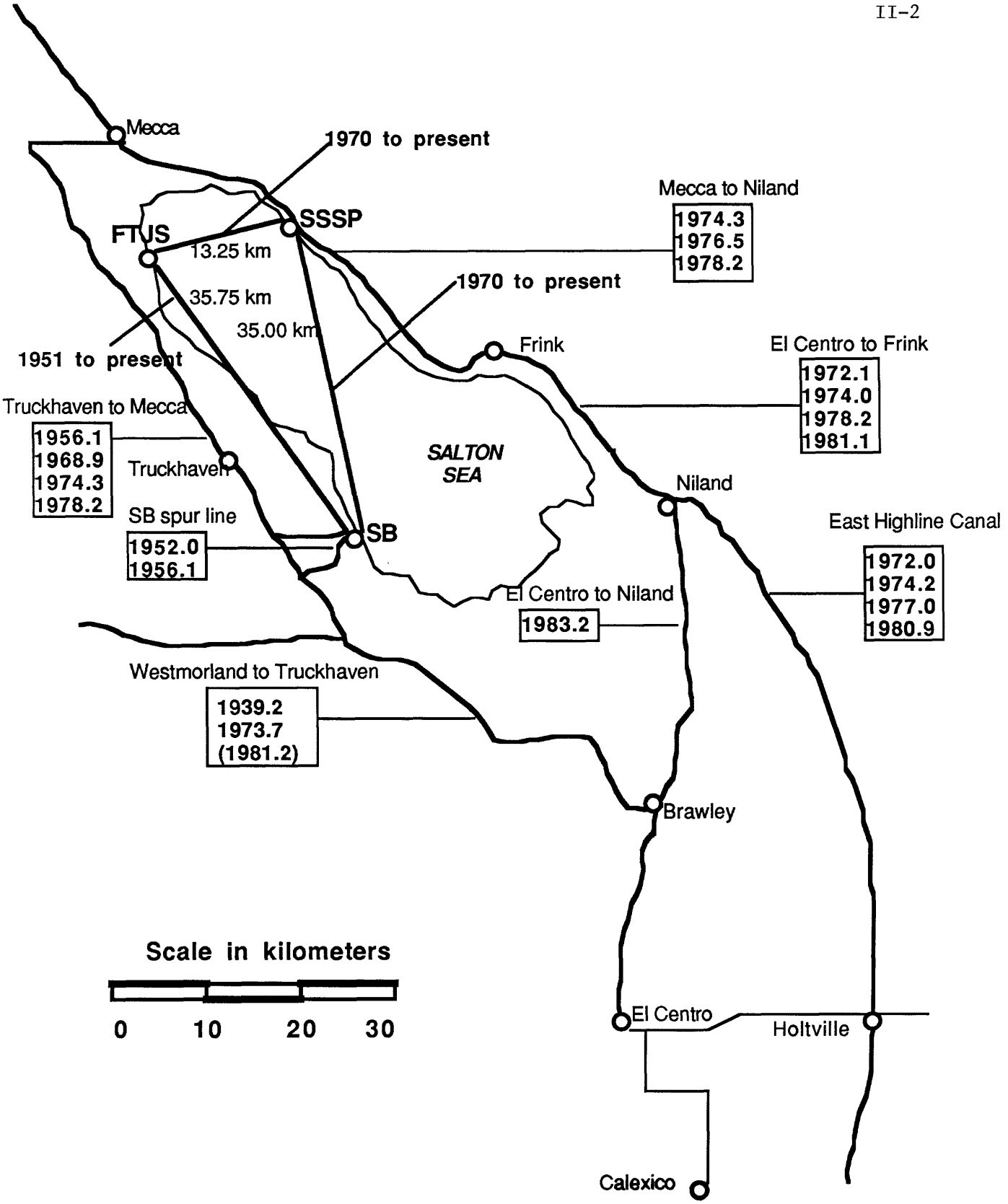

Figure 1. Map of the study region, showing the sea-level gauge network (with distances between gauges given), and the leveling routes (with dates of surveys given). Continuously recording pressure gauges have operated at SSSP since May 1985, and at SB since January 1986.

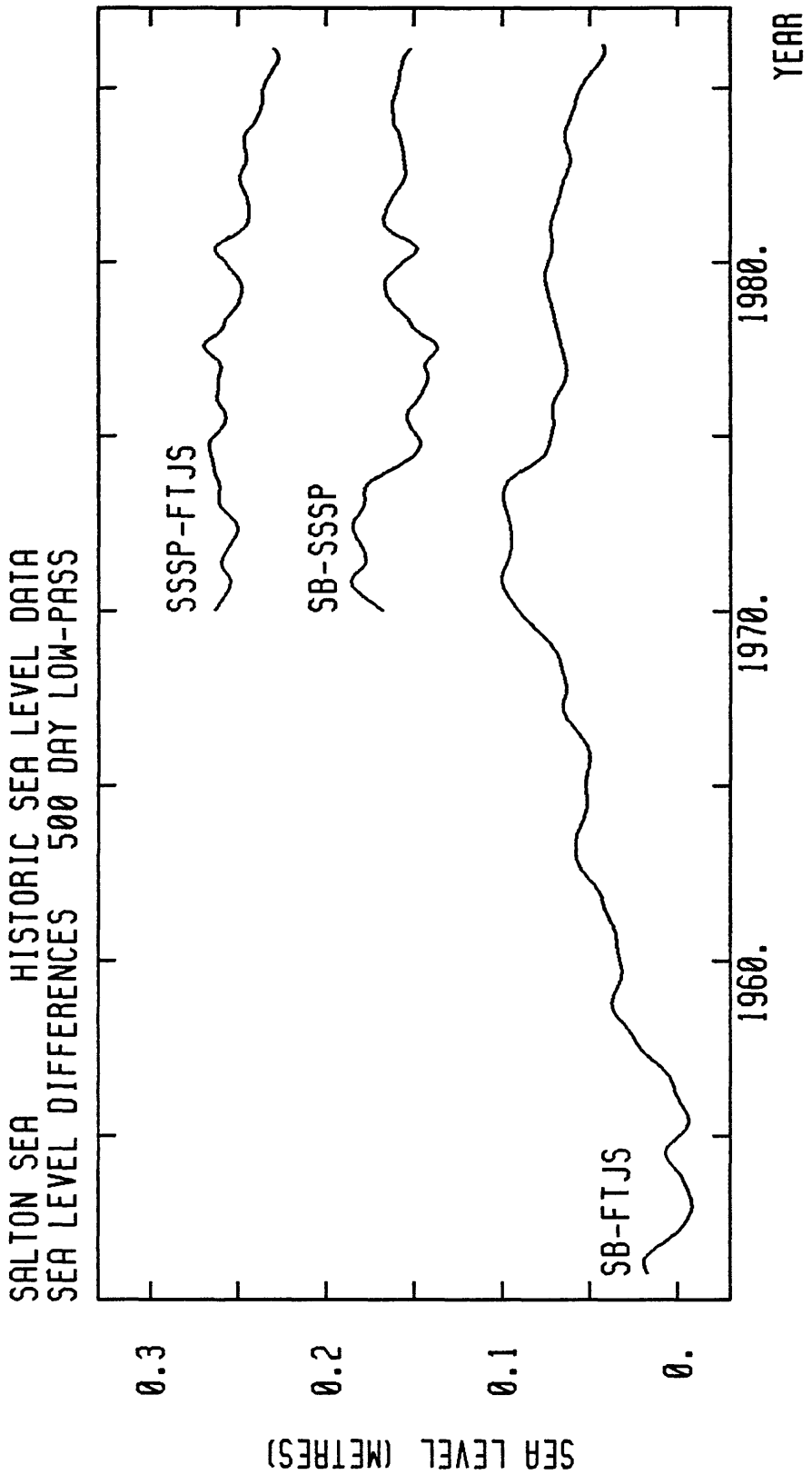

Figure 2. Differences between historical sea-level records. These are obtained by fitting smoothing splines to the unevenly sampled, low resolution raw data; differencing the resulting evenly sampled series; then low-pass filtering the differences. The clearest results are the ~0.1 μrad/yr ground tilt down to the SE prior to about 1970, the tilt reversal in the early 1970's, and the ~0.2 μrad/yr tilt down to the WSW since the late 1970's.

The curves are offset vertically for clarity. Tick marks on the time axis are at the start of the labelled year.

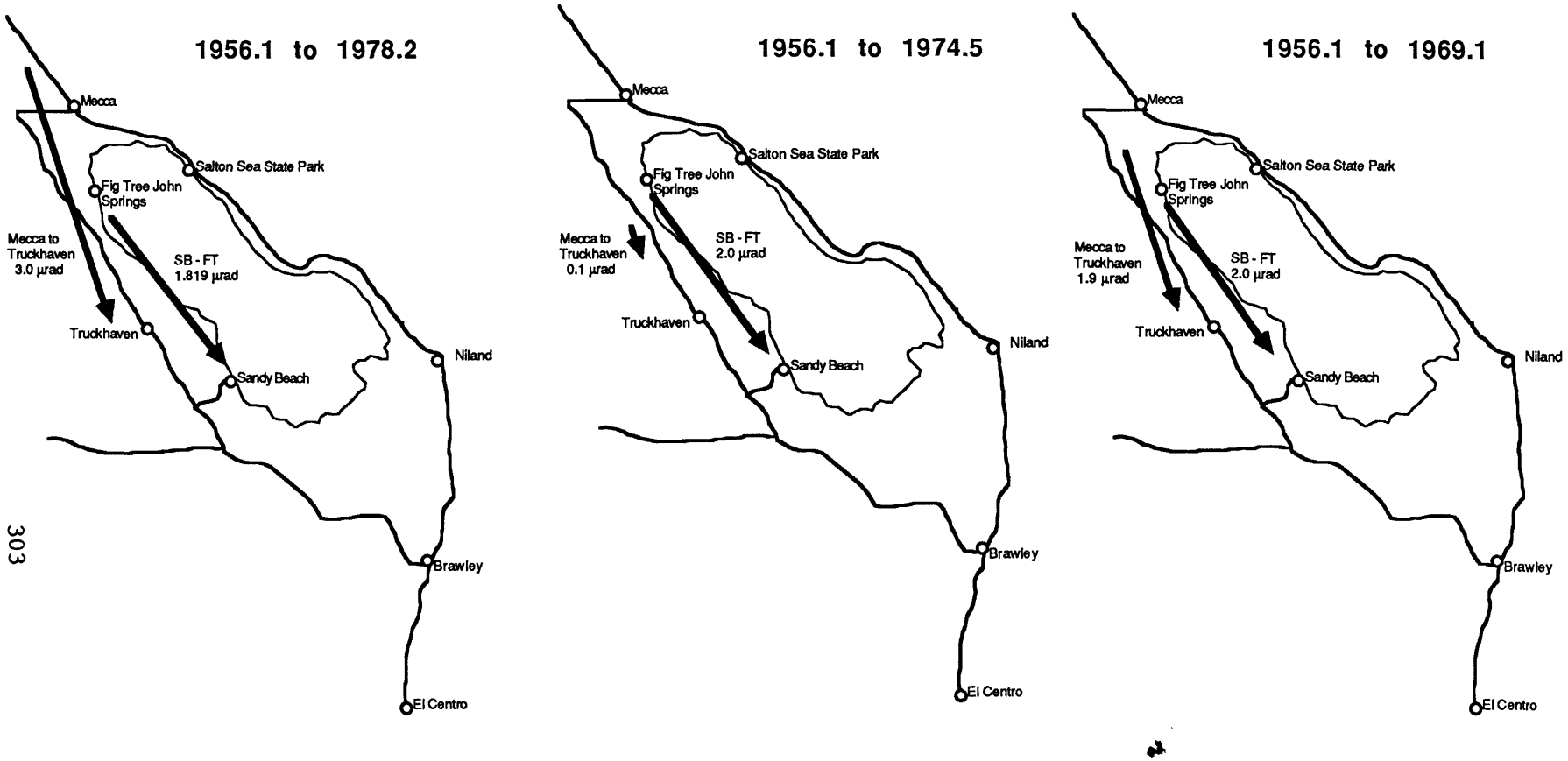

Figure 3. Map view showing tilt components derived from sea-level differencing (SB-SSSP) and from west side levelings (Mecca to Truckhaven) for the time periods indicated. The 1956, 69 and 78 levelings show fairly good agreement with sea level.

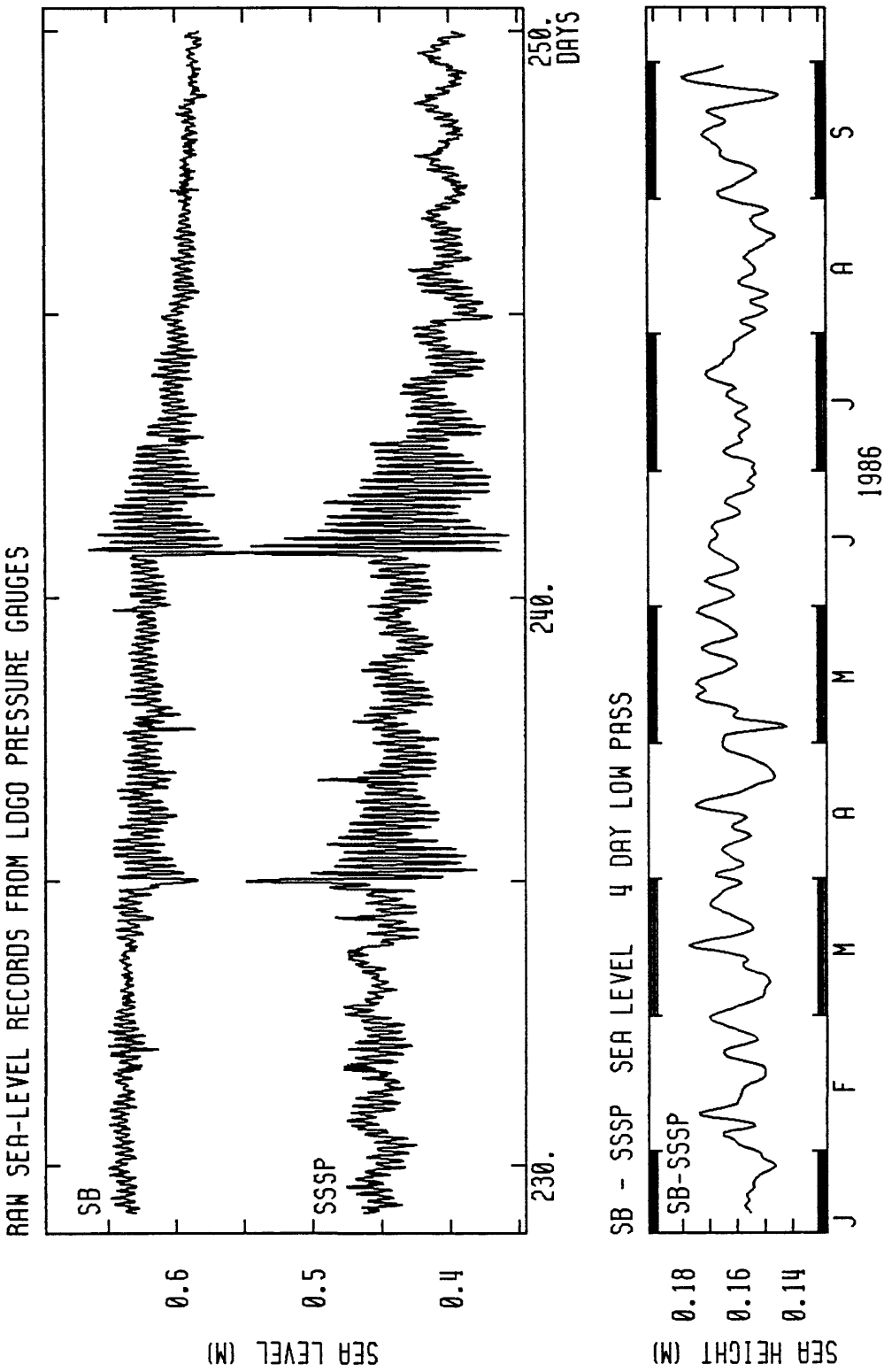

Figure 4. (a) A 3 week sample of recent data from the LDGO-designed pressure sensors. The 3 hour seiche is clearly visible, as is its modulation by wind storms. The origin of the ~2 cm daily variation on the SSSP record has not yet been positively identified.

(b) Low-pass filtered water level difference between SB and SSSP since both gauges became operational in January 1986. The rms noise level is ~8 mm, and the trend of < 3 mm/yr is not significantly different from zero.

PARKFIELD TWO-COLOR LASER STRAIN MEASUREMENTS

9960-02943

Robert Burford
Branch of Tectonophysics
U.S. Geological Survey
345 Middlefield Road, MS/977
Menlo Park, California 94025
(415) 323-8111, ext. 2574

and

Larry Slater
CIRES
University of Colorado
Boulder, Colorado 80309
(303) 492-8028

Investigations

The CIRES two-color laser ranging system has been operated at the Parkfield CAR HILL site to obtain frequent distance readings to reflector sites shown in Figure 1. Additional measurements were made occasionally to sites without permanent reflectors as well as to reference marks at the permanent sites.

Results

Plots of detrended length changes obtained since late June, 1984 are shown in Figure 2. Details of these changes from April 1, 1986 through September 30, 1986 are shown in Figure 3. The record for station MID (Figure 2) is composed of 2 separate parts owing to loss of the original reflector during late December 1984, with resulting loss of zero. The reflector pier at PITT has shown continuing instability and the line has been dropped, except for infrequent length measurements for comparison with on-site pier-tilt readings. A new station has been established as a replacement (station POMO, Figure 1).

Results of a model, consisting of shallow slip plus uniform strain, indicate that dextral shear (tensor) accumulated at a rate of 1.2 ± 0.2 ppm/yr through March 1986. Subsequently, the shear rate decreased to about 0.8 ± 0.3 ppm/yr. Dextral shear, presumably caused by deep slip buried beneath a shallow locked zone, was accompanied by 10.6 ± 1.8 mm/yr slip within the upper 1.5 km on the main fault. The model also indicates significant fluctuations in areal dilatation within the network. However, the dilatational component is

subject to systematic error due to possible drift in instrument scale. Occasional comparisons between the observatory instrument and a portable 2-color geodimeter indicate that drift between the two instruments is about +0.4 ± 0.1 ppm/yr (observatory-portable). It now appears that a substantial part of the apparent drift between these instruments is due to instability of the surface monument occupied by the portable instrument.

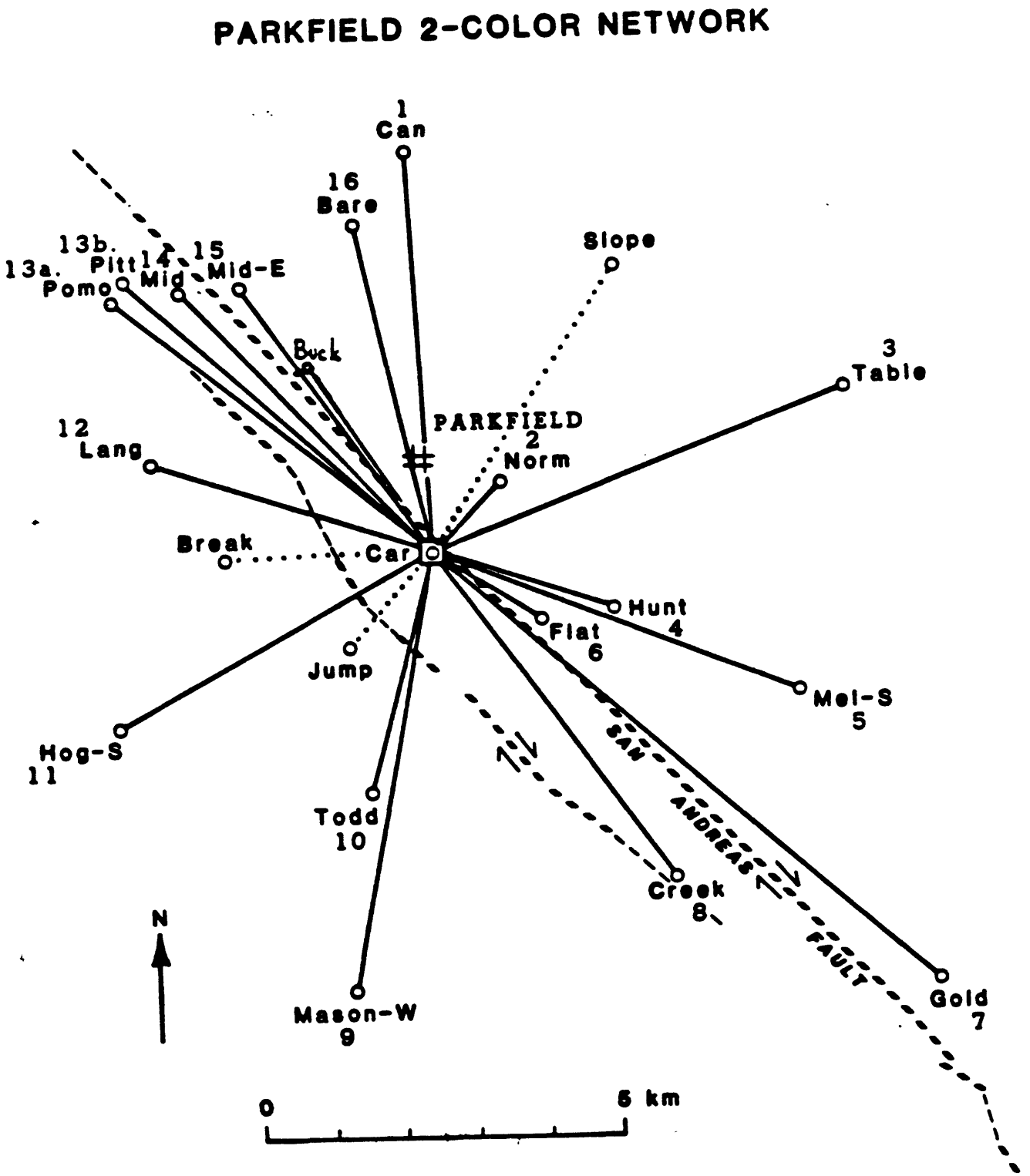

Figure 1. Map of the Parkfield 2-color laser network showing traces of the 1966 surface breaks within the San Andreas fault zone. Solid rays designate frequently monitored lines to permanent reflector points. Dotted rays represent lines to monuments occasionally occupied with a portable reflector for supplemental distance readings.

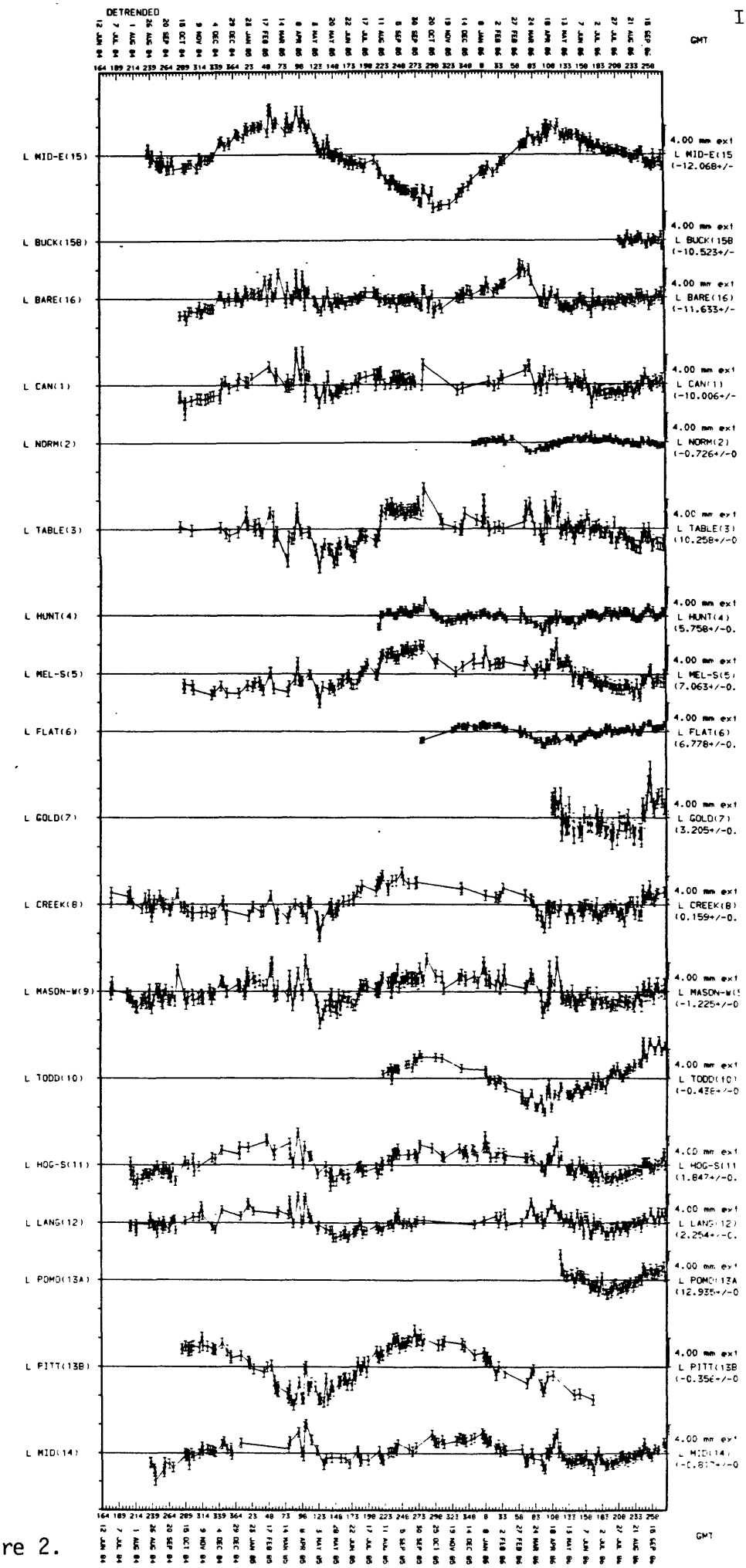
DETRENDED
GMT
L MID-E(15)
L BUCK(158)
L BARE(16)
L CAN(1)
L NORM(2)
L TABLE(3)
L HUNT(4)
L MEL-S(5)
L FLAT(6)
L GOLD(7)
L CREEK(8)
L MASON-W(9)
L TODD(10)
L HOG-S(11)
L LANG(12)
L POMO(13A)
L PITT(13B)
L MID(14)
4.00 mm ext
L MID-E(15
(-12.068+/-
L BUCK(158
(-10.523+/-
L BARE(16)
(-11.633+/-
L CAN(1)
(-10.006+/-
L NORM(2)
(-0.726+/-0
L TABLE(3)
(10.258+/-0
L HUNT(4)
(5.758+/-0.
L MEL-S(5)
(7.063+/-0.
L FLAT(6)
(6.778+/-0.
L GOLD(7)
(3.205+/-0.
L CREEK(8)
(0.159+/-0.
L TODD(10)
L HOG-S(11)
(1.847+/-0.
L LANG(12)
(2.254+/-0.
L POMO(13A)
(12.935+/-0
L PITT(13B)
(-0.356+/-0
L MID(14)

Figure 2.

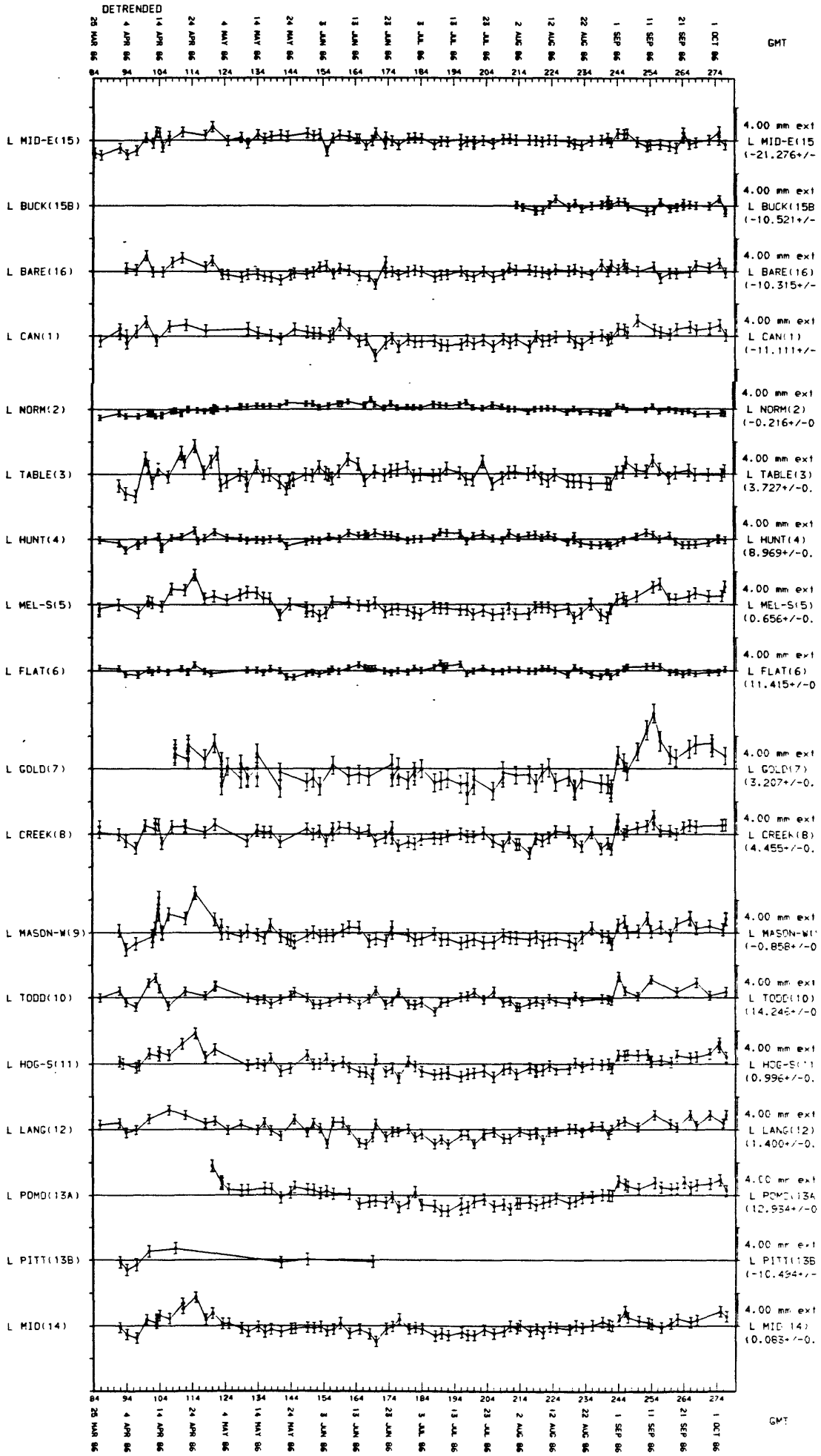

Figure 3.
Detrended 2-color data, Car Hill Observatory

SEARCH FOR ELECTROMAGNETIC PRECURSORS TO EARTHQUAKES (A5126)

William Daily
Lawrence Livermore National Laboratory
P.O. Box 808, L-156
Livermore, California 94550
(415) 422-8623

Observations of electromagnetic (EM) precursors have been reported for large earthquakes in Greece, Japan, Iran, Chile, and the Soviet Union (e.g., by Gokhberg, et al., 1980). In fact, Varotsos et al. have been predicting earthquakes in Greece for the past few years with about an 80% success rate. They use telluric-type voltage measurements from an array of stations in that country (Varotsos and Alexopoulos, 1984). In addition, recent observations of very low frequency (VLF) precursors measured by GEOS satellites have been reported by Parrot and Lefeuvre (1984). Mechanisms and semiquantitative models advanced to explain the observations have been discussed by Gokhberg, Gufeld and Dobrovolsky (1979) and Warwick, Stoker, and Mezer (1982). Laboratory demonstration of radio frequency emission from cracking rocks has also been reported (Nitsan, 1977; Vorobev, 1977). Reported herein are the results of a study to search for EM earthquake precursors along the San Andreas Fault system in California, using ground based, broadband electromagnetic monitors.

Several very low frequency radio receivers have been built to monitor broadband EM noise near a fault zone. These receivers have been placed into operation near the San Andreas Fault in 1983 and 1984. It is unlikely that one such monitoring station will be capable of monitoring events along more than a few hundred kilometers of the fault. Therefore, we have emplaced receivers along the San Andreas Fault. The exact location of each site was determined by: 1) the estimated probability of an earthquake of Richter magnitude greater than about 5 (precursors are typically seen only with larger magnitude events); 2) accessibility of site to facilitate deployment and periodic equipment checks; 3) isolation from cultural sources of wide band EM noise; 4) availability of power source and reasonable security. To allow some discrimination of source location, monitoring stations were spaced far enough apart that signals from an event will not be seen equally well by all sensors. If the source region for these signals is deep (a few kilometers), signals at the surface should be confined near the epicenter--attenuation will be high due to propagation long distances through high loss crust from the source. If the source region is near the surface, signals will be measurable at larger distances. From these considerations and published measurements of precursors, we estimate that the locations monitored should be a few hundred kilometers apart, but also chosen for their high potential as an epicenter for a large earthquake. The five locations originally chosen for placement of monitors are: 1) Coyote Lake, near Morgan Hill; 2) Bear Valley, near Hollister; 3) Turkey Flat, near Parkfield; 4) Adobe Mountain, near Palmdale; and 5) Pinon Flat U.S.G.S. observatory near Palm Springs. During the last year, only the stations at Turkey Flat and Pinon Flat were deployed.

Cultural noise, both narrow band and broadband is the main source of low frequency signal. Narrow band signals are mostly from marine related VLF

transmissions above about 20 kHz. In addition, there are harmonics of 60 Hz from the electric power grid. Broadband signals result from several sources, but especially from automobile ignition systems and telluric currents. Of course, there is a continual lightning-induced low frequency background. Any EM emission associated with a seismically active area will most likely be broadband. Laboratory measurements from cracking rocks are of broadband EM emission. All proposed mechanisms for EM earthquake precursors would result in broadband emissions. Finally, all reported EM precursors were presumed to be broadband emissions. Therefore, for maximum signal to noise ratio, we designed the receivers to be broadband with three bands recorded: 1) 200 Hz to 1 kHz, 2) 1 kHz to 10 kHz, 3) 10 kHz to 100 kHz. Each system uses a three-meter-long vertical monopole antenna referenced to a ground plane. Data was recorded continuously on a strip chart recorder and each station was battery powered.

The broadband capability helps to reduce variation in cultural noise, especially the narrow band (radio station) sources. Reported measurements of events indicate that a high sensitivity system is not required. Each channel has a 60 dB dynamic range (logarithmic amplifiers) recorded on the strip chart recorder. This is used because of its effectiveness, simplicity, reliability, and low cost.

The signal received by each station is very site specific. At some sites, the signal in all frequency bands is continuously highly variable on a time scale of a few hours. At other sites, the measured signal levels are nearly constant for periods of weeks at a time. The reason for this difference is unknown, but some sites may have high levels of cultural noise which would be variable in amplitude.

The monitoring network described above has recorded EM anomalies for a series of earthquakes between 1983 and 1986. These anomalies appear to be of two types which are presumably caused by separate effects, both ralated to stress induced changes in the crust just prior to fault rupture. The first of these anomalies consists of radio emissions believed to originate in fracturing rocks. These emissions normally occur several hours to a few days before fault rupture. The other anomaly appears to result from an interruption in the intensity of received background radio frequency signals for many hours, several days before an earthquake. Comparisons between dipole and monopole antennas indicates that these depressions may be caused by fluctuations in the ground electrical properties rather than a reduction in background EM flux density.

It is tempting to make a connection between the anomalous EM signals we have recorded and the earthquakes with which they seem to be associated. This is especially true given the success Varotsos and coworkers have reported in predicting earthquakes from spontaneous potential fluctuations. We believe that the results to date are encouraging enough to warrant continued monitoring of EM emissions along the San Andreas until a more complete data set is collected. This work should also include monitoring spontaneous potential to see if the results reported by Varotsos can be duplicated along the San Andreas fault system.

Bibliography

Gokhberg, M. B., V. A. Morgounov, T. Yoshino, and I. Tomizawa, "Experimental Measurement of Electromagnetic Emissions Possibly Related to Earthquakes in Japan," J. Geophys. Res., 87, 7824, 1982.

Gokhberg, M. B., I. L. Gufeld, I. P. Dobrovolsky, and G. I. Shevtsov, "Studies of Mechanoelectric Effects under Laboratory Conditions," Preprint N 9, Acad. of Sci. of the U.S.S.R., Moscow, 1980.

Gokhberg, M. B., I. L. Gufeld, and I. P. Dobrovolsky, "On the Sources of Electromagnetic Earthquake Precursors," Preprint N 10, Acad. of Sci. of the U.S.S.R., Moscow, 1980.

Gokhberg, M. B., V. A. Morgounov, and T. Yoshino, "The Experimental Results of Appearance of Electromagnetic Emissions Related with Earthquake at Sugadaira Observatory in Japan," University of Electro-Communications, I - 5 - I.

Nitsan, U., "Electromagnetic Emission Accompanying Fracture of Quartz-Bearing Rocks," Geophys. Res. Letters, 4, 333, 1977.

Parrot, M. and F. Lefeuvre, "Study of VLF Emissions Apparently Associated with Earthquakes from Ground-Based and GEOS Satellite Data, Results of the ARCAD 3 Project and of the Recent Programmers in Magnetospheric and Ionospheric Physics," 2-25 Mai 1984, Toulouse, France, 1984.

Varotsos, P. and K. Alexopoulos, "Physical Properties of the Variations of the Electric Field of the Earth Preceding Earthquakes. II. Determination of Epicenter and Magnitude," Techtonophysics, 110, 99-125, 1984.

Vorob'ev, A. A., "Electromagnetic Radiation in the Process of Crack Formation in Dielectrics," Difektoskopiya, No. 3, 128, 1977.

Theodolite Measurements of Creep Rates on San Francisco Bay Region Faults

14-08-0001-G1186

Jon S. Galehouse
San Francisco State University
San Francisco, CA 94132
(415) 469-1204

We began measuring creep rates on San Francisco Bay region faults in September 1979. Amount of slip is determined by noting changes in angles between sets of measurements taken across a fault at different times. This triangulation method uses a theodolite set up over a fixed point used as an instrument station on one side of a fault, a traverse target set up over another fixed point used as an orientation station on the same side of the fault as the theodolite, and a second traverse target set up over a fixed point on the opposite side of the fault. The theodolite is used to measure the angle formed by the three fixed points to the nearest tenth of a second. Each day that a measurement set is done, the angle is measured 12 times and the average determined. The amount of slip between measurements can be calculated trigonometrically using the change in average angle.

We presently have theodolite measurement sites at 20 localities on faults in the Bay region (see location map). Most of the distances between our fixed points on opposite sides of the various faults range from 75-215 meters; consequently, we can monitor a much wider slip zone than can be done using standard creepmeters. The precision of our measurement method is such that we can detect with confidence any movement more than a millimeter or two between successive measurement days. We remeasure most of our sites about once every two months.

The following is a brief summary of our results thus far:

Seal Cove-San Gregorio fault - We began our measurements on the Seal Cove fault (Site 7) in Princeton, San Mateo County, in November 1979. For the next 6.6 years, the Seal Cove fault showed net movement of only 4.1 millimeters in a right-lateral sense. Any small amount of tectonic slip that may be occurring is difficult to ascertain because of seasonal effects, often involving apparent left-lateral slip that tends to occur toward the end of a calendar year.

Various logistic problems have occurred at our Site 8 across the San Gregorio fault near Pescadero in San Mateo County. The width of fault zone we are monitoring (452 meters) is the widest of all our 20 sites and measuring it is difficult. We have had considerable variations in the amounts and directions of movement from one measurement day to another. The presently-calculated average is 1.4 millimeters per year of right-lateral slip for the past 4.1 years.

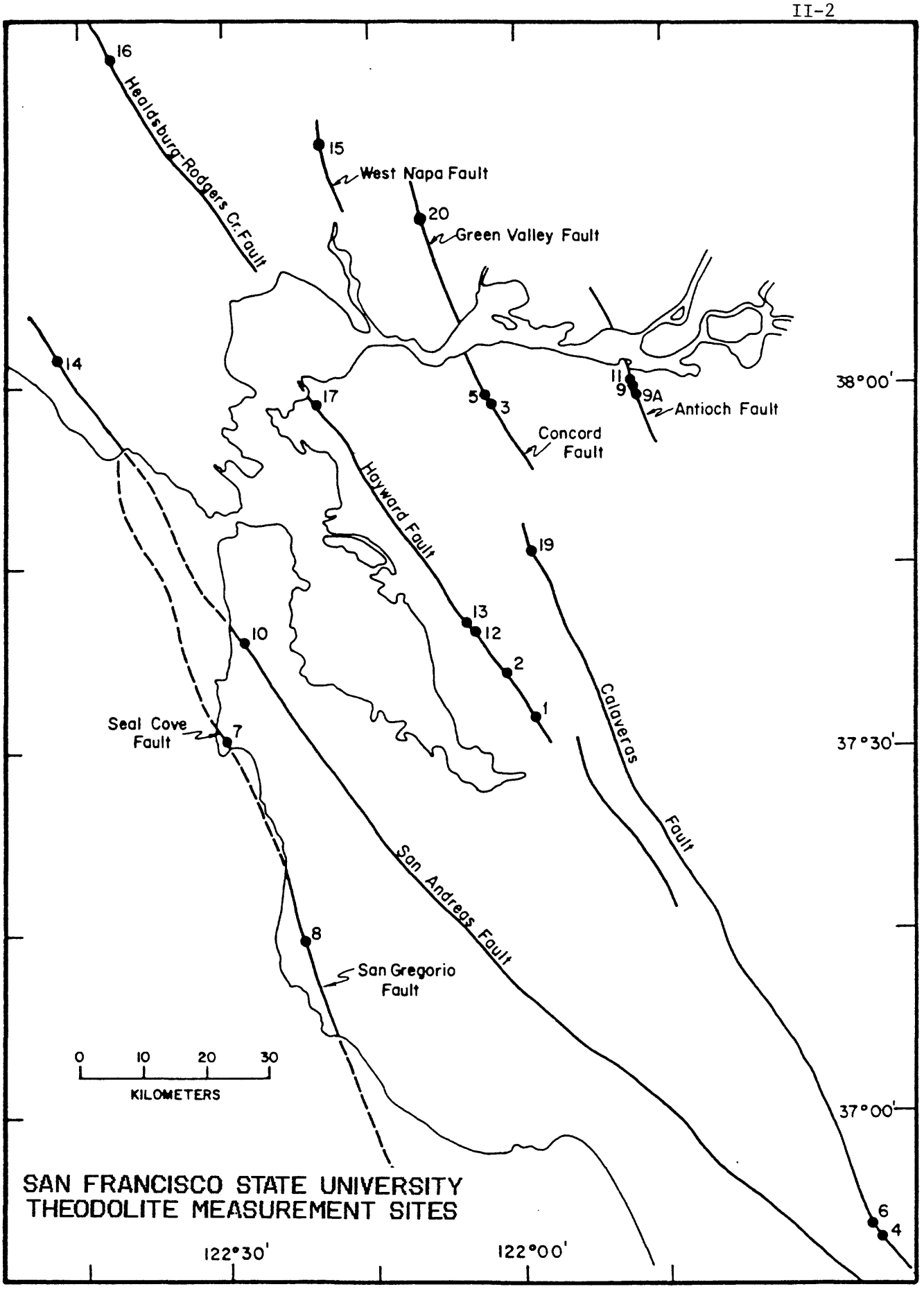

SAN FRANCISCO STATE UNIVERSITY
THEODOLITE MEASUREMENT SITES

San Andreas fault - In the 6.3 years since March 1980 when we began our measurements across the San Andreas fault in South San Francisco (Site 10), virtually no net slip has occurred. We reestablished our Site 14 in Marin County, this time at the Point Reyes National Seashore Headquarters in February 1985. Results after 1.5 years of measurements indicate right-lateral slip of about 1.1 millimeters. Our Site 18 (not shown on the location map) in the Point Arena area has averaged 1.3 millimeters per year of right-lateral slip in the five years from January 1981 to January 1986. These results indicate that the northern segment of the San Andreas fault is virtually locked, with very little, if any, creep occurring.

Rodgers Creek fault - In the 5.4 years from August 1980 to January 1986, our Site 16 on the Rodgers Creek fault in Santa Rosa has had an average of less than a millimeter per year of left-lateral slip. However, our results show large variations in the amounts and directions of movement from one measurement day to another. These are probably due to seasonal and/or gravity-controlled mass movement effects, not tectonic slip. Recently, our line of sight at this locality became obscured and we abandoned the site. We then established a new site on the Rodgers Creek fault east of Penngrove and made our first measurement in September 1986.

West Napa fault - In the 6.2 years since July 1980, our Site 15 on the West Napa fault in the City of Napa has shown virtually no net slip. Similarly to our results for the Rodgers Creek fault, however, large variations up to nearly a centimeter have occurred in both a right-lateral and a left-lateral sense between measurements days. The magnitude of these nontectonic effects is obscuring the small amount of any tectonic slip that may be occurring.

Green Valley fault - We established Site 20 on the Green Valley fault north of Suisun Bay in June 1984. After 2.3 years, measurements show right-lateral slip at a rate of 8.8 millimeters per year. Large variations occur between measurement days. Continued monitoring over a longer period of time will confirm whether or not this apparently high rate of slip is real.

Hayward fault - We began our measurements on the Hayward fault in late September 1979 in Fremont (Site 1) and Union City (Site 2). During the next 7 years, the average rate of right-lateral slip was 5.0 millimeters per year in Fremont and 4.0 millimeters per year in Union City. We began measuring two sites within the City of Hayward in June 1980. During the next 6.2 years, the average annual rate of right-lateral movement was 4.7 millimeters at D Street (Site 12) and 4.8 millimeters at Rose Street (Site 13). During the three month interval from December 1985 to March 1986, the Hayward Fault in Fremont and at D Street in Hayward moved about a centimeter (much more rapidly than usual). However, since then the fault at these sites has slowed down and the overall average rate of movement is about the same as that at nearby sites.

We began measurements in San Pablo (Site 17) near the northwestern end of the Hayward fault in August 1980. For the past 6.1 years, the average rate of movement has been about 4.6 millimeters per year in a right-lateral sense. However, superposed on this overall slip rate are changes between some measurement days of up to nearly a centimeter in either a right-lateral or a left-lateral sense. Right-lateral slip tends to be measured during the first half of a calendar year and left-lateral during the second half.

In summary, the average rate of right-lateral movement on the Hayward fault is about 4 to 5 millimeters per year over the past 6 to 7 years.

Calaveras fault - We have three measurement sites across the Calaveras fault and the nature and amount of movement are different at all three. We began monitoring our Site 4 within the City of Hollister in September 1979. Slip along this segment of the Calaveras fault is quite episodic, with times of relatively rapid right-lateral movement alternating with times of little net movement. For the past 6.9 years, the fault moved at a rate of 7.2 millimeters per year in a right-lateral sense.

At our Site 6 across the Calaveras fault on Wright Road just 2.3 kilometers northwest of our site within the City of Hollister, the slip is much more steady than episodic. In the 6.8 years since October 1979, the Calaveras fault at this site has been moving at a rate of 12.8 millimeters per year in a right-lateral sense, the fastest rate of movement of any of our sites in the San Francisco Bay region.

U.S.G.S. creepmeter results in the Hollister area are quite similar to our theodolite results. Creepmeters also show a faster rate of movement at sites on the Calaveras fault just north of Hollister than at sites within the City of Hollister itself.

The rate of movement is much lower at our Site 19 in San Ramon, near the northwesterly terminus of the Calaveras fault. Only about one-half millimeter per year of right-lateral slip has occurred during the past 5.4 years.

The epicenter of the 24 April 1984 Morgan Hill earthquake occurred on the Calaveras fault between our Hollister area sites which are southeast of the epicenter and our San Ramon site which is northwest of it. Two papers that we published regarding our theodolite measurements and observations of surface displacement related to the earthquake are listed at the end of this summary. No unusual movement appears to have occurred prior to the Morgan Hill earthquake.

The epicenter of the 26 January 1986 Tres Pinos earthquake occurred on the Quien Sabe fault south of Hollister. It appears that the earthquake may have triggered a few millimeters of right-lateral slip at our site on the Calaveras fault in Hollister. However, no unusual movement occurred either before or after the earthquake at our Wright Road site north of Hollister.

Concord fault - We began our measurements at Site 3 and Site 5 on the Concord fault in the City of Concord in September 1979. Both sites showed about a centimeter of right-lateral slip during October and November 1979, perhaps the greatest amount of movement in a short period of time on this fault in the past two decades. Following this rapid phase of movement by about two months were the late January 1980 Livermore area moderate earthquakes on the nearby Grenville fault.

After the relatively rapid slip on the Concord fault in late 1979, both sites showed relatively slow slip for the next four and one-half years at a rate of about one millimeter per year right-lateral. However, in late Spring-early Summer 1984, both sites again moved relatively rapidly, slipping about seven millimeters in a right-lateral sense in a few months. The rate has again slowed since late August 1984 (through August 1986).

The overall rate of movement on the Concord fault (combining the two periods of relatively rapid movement with those of slower movement) is about 4.1 millimeters per year (Site 3) and 3.2 millimeters per year (Site 5) of right-lateral slip in the past 6.9 years.

Antioch fault - We began our measurements at the more southeasterly of two original sites on the Antioch fault (Site 9) in the City of Antioch in January 1980. During the next 27 months, we measured a net right-lateral displacement of nearly two centimeters. However, large changes in both a right-lateral and a left-lateral sense occurred between measurement days. Three times left-lateral displacement occurred toward the end of one calendar year and/or beginning of the next. We abandoned this site in April 1982 because of logistic problems and relocated it (Site 9A) just southeast of the City of Antioch in November 1982. The fault at this newer site has shown virtually no net movement for the past 3.6 years.

The more northwesterly of our original sites on the Antioch fault (Site 11) is located where the fault zone appears to be less specifically delineated. In the 6.1 years since May 1980, we have measured a slight amount of left-lateral slip. Much subsidence and mass movement creep appear to be occurring both inside and outside the Antioch fault zone and it is probable that these nontectonic movements are obscuring any tectonic slip that may be occurring.

Publications

Galehouse, J.S., 1986, Theodolite Measurements: in Geodetic Observations section of "The Morgan Hill, California Earthquake of April 24, 1984"; U.S. Geol. Survey Bull. 1639, pp. 121-123.

Galehouse, J.S. and Brown, B.D., 1986, Surface Displacement Near Hollister, California: in Geological Observations section of "The Morgan Hill, California Earthquake of April 24, 1984"; U.S. Geol. Survey Bull. 1639, pp. 69-72.

DEEP BOREHOLE PLANE STRAIN MONITORING
14-08-0001-G1190

Michael T Gladwin,

Department of Physics
University of Queensland
St.Lucia, 4067
AUSTRALIA.

ACTIVITIES

1. Processing of the data from the two borehole tensor strainmeters installed in California in 1983 has been continued. Both instruments have provided data of excellent quality. The instrument is most useful in simple shear environments where volume strain is minimal, where diagnostic shear strain data are required soon after installation of an instrument, or where large volumetric noise sources such as migration of water tables dominate the strain field.

2. Fabrication of three new instruments for installation in the Parkfield region during this summer field season was completed on schedule, and the instruments are on site for installation October/November. In the new instruments, electronic noise has been reduced by more than 30 dB compared with the instruments presently in operation in San Juan Bautista and Pinon Flat.

3. Comparison of the data from the Pinon Flat installation with the laser strain meter data set has been begun in collaboration with D.Agnew and F.Wyatt (I.G.P.P., U.C.S.D.). This has permitted evaluation of the coupling coefficients previously estimated only from instrument geometry and estimates of rock parameters.

4. Co-seismic strain steps associated with the Palm Springs earthquake were observed at the Pinon Flat site. As previously, amplitude and inferred orientation agreed well with far field strain estimates from seismically determined source parameters.

5. Disturbances of strain associated with the drilling of a deep hole a few humdred meters from the Pinon Flat instrument have been recorded and will be compared with other data taken at the site.

RESULTS

1. The coseismic step observed at the Pinon Flat site for the July 8 north Palm Springs earthquake agreed well with that expected from strain step estimates at the site using the seismically determined moment and source parameters. The strain step is shown in figure 1. Implied moment is approximately $1.6 * 10^{25}$ dyne cm. The sampling interval in each case is 18 minutes (limited by the total data throughput in the satellite retrieval system). The time history of the shear strain response for the event differed significantly from the volumetric strain response.

2. Preliminary results for the calibration of the instrument against both the theoretical ocean loaded tide for the Pinon site and the long baseline laser strainmeter indicate that for the three major tidal components, the hydrostatic coupling factor is 1.71 with a scatter of 0.01. This parameter measures the amplification of the solid earth strain caused by the presence of the hole and its inclusion. Phases agreed to within 1 degree for the three harmonics. To obtain consistent amplitude and phase calibration for the shear it was necessary to assume instrument orientation was approximately 6 degrees different from that indicated by the internal compass. With this adjustment, amplification factor was 2.7 with a scatter of 0.2, while the phases agreed to within 5 degrees. The expected value of the shear coupling constant was between 3 and 3.6 on estimates of rock parameters.

3. Significant disturbance of the site strain field occurred during drilling of a new hole to 1000 feet approximately 250m to the south-west of the instrument. Figure 2 shows the perturbation to the dilatation and shear strain fields.

PUBLICATIONS

Gladwin, M. T., High Precision multi component borehole deformation monitoring. *Rev.Sci.Instrum., 55,* 2011-2016, 1984.

Gladwin, M.T., Gwyther, R., Hart, R., Francis, M., and Johnston, M.J.S., Borehole Tensor Strain Monitoring in California. *J. Geophys. Res.* In review.

Gladwin, M. T. and Hart, R. Design Parameters for Borehole Strain Instrumentation. *Pageoph.,123,* 59-88, 1985.

Gladwin, M. T., Hart, R., and Gwyther, R. L. Tidal Calibration of Borehole Vector Strain Instruments.*EOS, (Trans. Am. G. Un.) 66,* 1057, 1985.

Gladwin, M. T. and Johnston, M.J.S. Strain Episodes on the San Andreas Fault following the April 24 Morgan Hill, California Earthquake. *EOS,(Trans. Am.G.Un.), 65,* 852, 1984.

Gladwin, M.T., and Johnston, M.J.S. Coseismic moment and total moment of the April 24, 1984, Morgan Hill and the January 26, 1986, Quiensabe earthquakes. *EOS,(Trans.Am.G.Un.), 67, R 308, 1986.*

Gladwin, M. T. and Wolfe, J. Linearity of Capacitance Displacement Transducers. *J.Sc.Instr. 46,* 1099-1100, 1975.

Johnston, M.J.S., Gladwin, M.T., and Linde, A.T. Preseismic Failure and Moderate Earthquakes. *I.A.S.P.E.I.* , Tokyo, August 19-30, S7-65, 35 , 1985.

Johnston, M. J. S., Linde, A.T., Gladwin, M.T., and Borcherdt, R.D. Fault Failure with Moderate Earthquakes. Tectonophys., In Press.

Johnston, M.J.S., Borcherdt, R.D., Glassmoyer, G., Gladwin, M.T., and Linde, A.T. Static and Dynamic Strain during and following January 26, 1986, Quiensabe, California, Earthquake. *EOS,(Trans., Am. G. Un.), 67,* 16, 308, 1986.

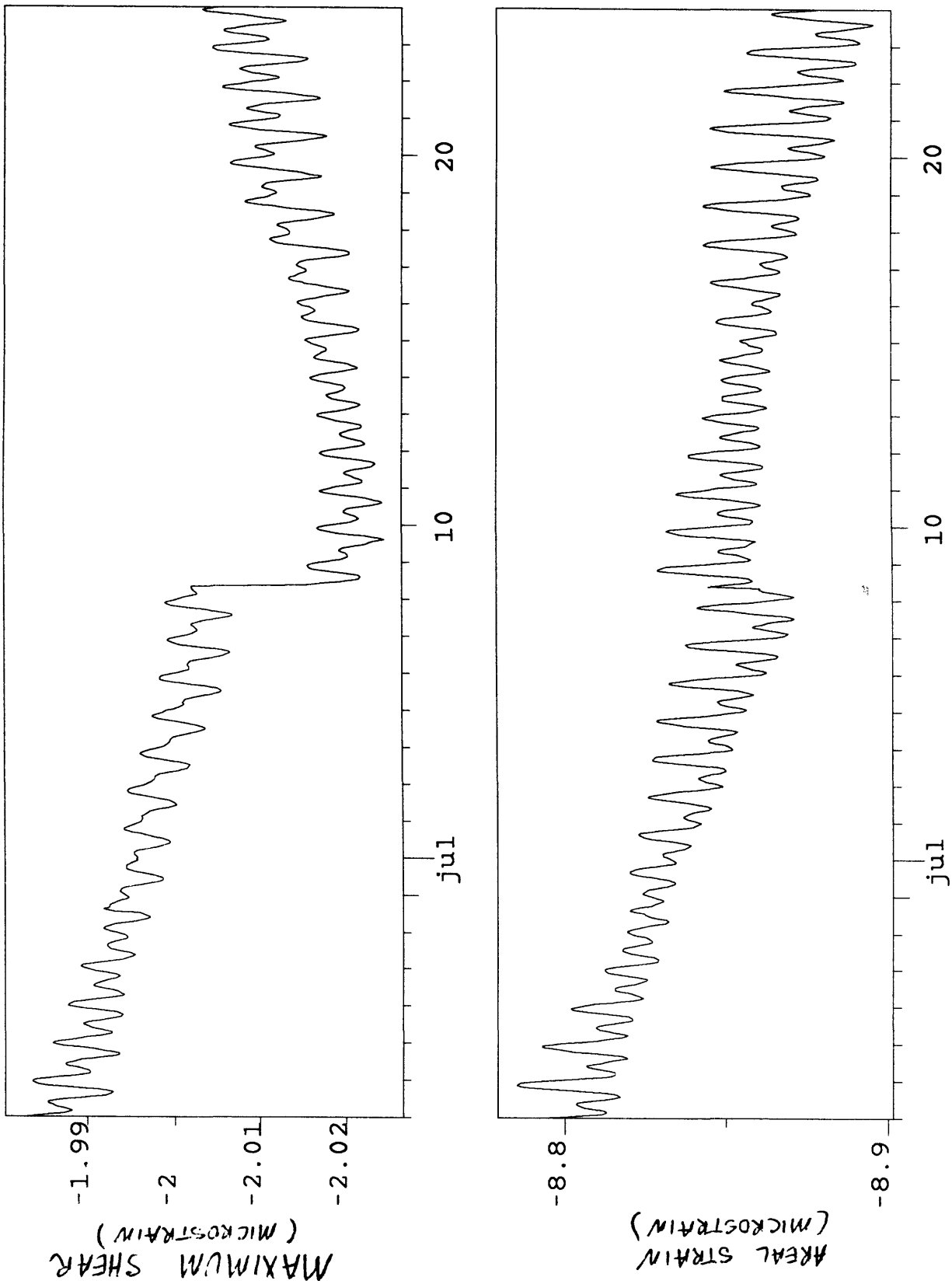

1. Co-seismic steps obtained for the Palm Springs earthquake.

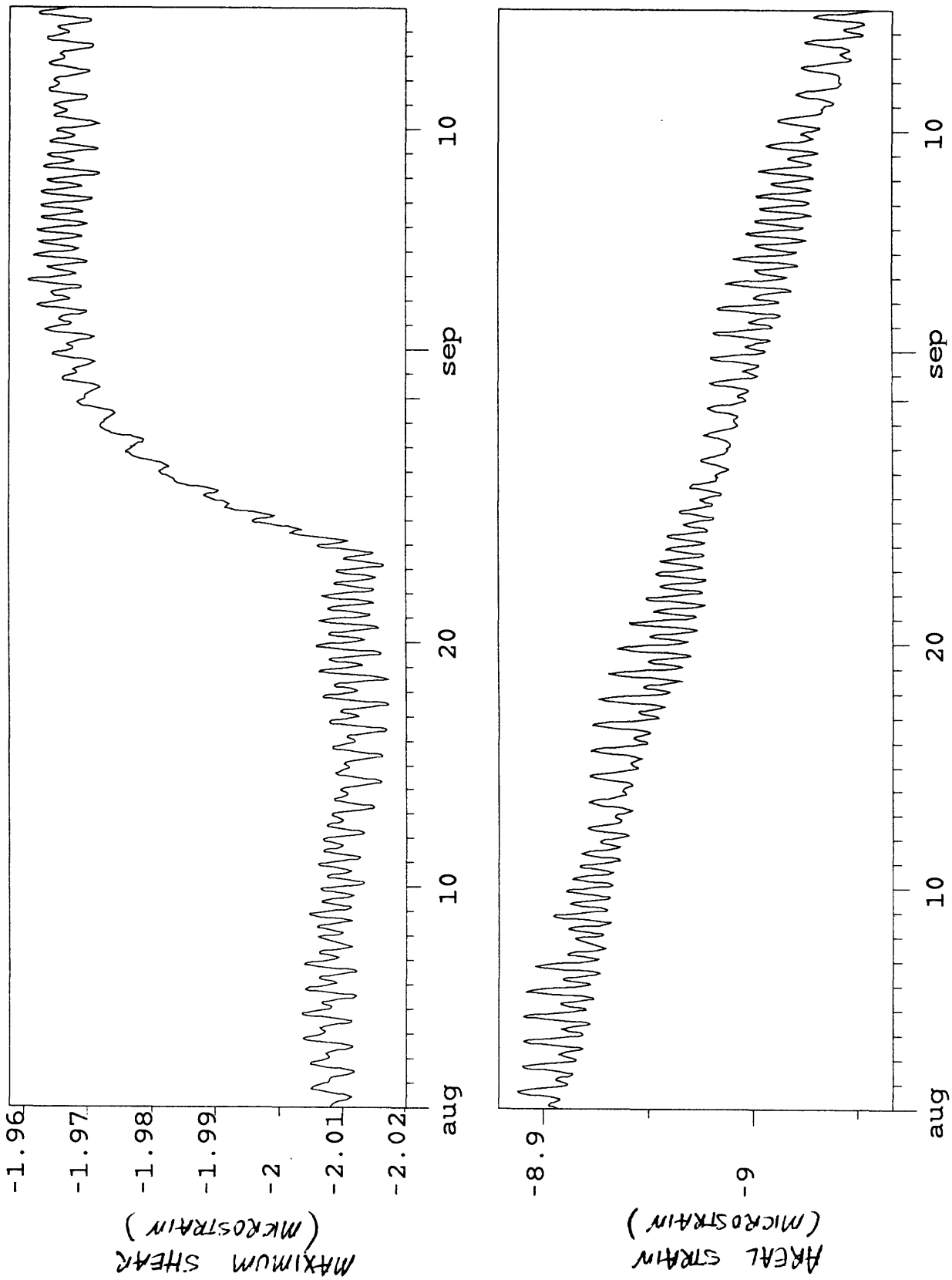

2. Observed strain changes during drilling of deep borehole. approximately 250 m from the instrument.

San Andreas Earthquake/Parkfield Geophysics

9380-03074

Robert C. Jachens, Carter W. Roberts, and Robert W. Simpson
U.S. Geological Survey, MS's 989 and 977
345 Middlefield Rd., Menlo Park CA 94025
(415) 323-8111, x4248 or 4256

Investigations

1) Repeat precision gravity surveys were conducted in May and covered:

   a) the high precision base station network
   b) a 100-km-long profile perpendicular to the San Andreas fault and passing through Cajon Pass
   c) the two-color laser site at Holcomb Ridge. During this survey, we were accompanied by Mr. Li Jia-Zheng of the Seismological Bureau of Hebei Province who has had extensive precision gravity experience and wanted to learn how we conduct our surveys.

2) A new gravity map of the Parkfield area and surrounding regions was compiled from a number of sources including an excellent new data set from the Department of Defense.

3) A new aeromagnetic map of the Parkfield area, based on data taken along flightlines spaced at 0.8 km at a height of 300 m above average terrain, was received and merged with a survey to the south flown earlier at a constant barometric elevation of 2 km. A derivative map of magnetic boundaries was generated from the merged aeromagnetic map.

4) A preliminary qualitative interpretation of the combined gravity, magnetic, topographic, and geologic data was begun in cooperation with Carl Wentworth of the Western Regional Geology Branch.

Results

1) The latest precision gravity surveys show continuing patterns of low amplitude, long period gravity fluctuations that, at Holcomb Ridge, correlate with measured areal strain changes.

2) The preliminary interpretation of the geophysical and geologic data surrounding Parkfield revealed a wealth of new information about the structure and lithology in this area.

   a) Southwest of the fault, the data suggest a relatively coherent, little deformed region. Contained within this region is a large dense, magnetic block, including the Red Hills basement outcrop, that appears to be bounded on the northeast by the San Andreas fault and on the southwest by a northeast-dipping reverse fault.
   b) Both the gravity and magnetic data suggest a major interface that corresponds to the southwest strand of the San Andreas fault north of Gold Hill. In contrast, the northeast, presumably active strand of San Andreas fault is not reflected in the gravity and magnetic

data. In fact, at least one strong gravity anomaly appears to cross the northeast strand uninterrupted, suggesting that this strand may be quite recent.

c) The magnitude data indicate a large, magnetic body (probably serpentinite) in the region northeast of the San Andreas fault. The body appears to be in contact with the fault surface in the creeping region northwest of the preparation zone and shows evidence of having been smeared out along the fault zone. To the southeast, the body swings eastward away from the fault until it eventually surfaces as extruded serpentinite at Table Mountain. The obvious mobility of the serpentinite at Table Mountain and the spatial correlation of the concealed body with the creeping part of the fault lends support to the earlier suggestion that serpentinites might substantially influence fault behavior.

d) In contrast to the relatively undeformed region southwest of the fault, the region to the northeast shows evidence of significant and pervasive deformation. The gravity and magnetic data indicate southwestward directed thrusting of Franciscan rocks over rocks in the Parkfield syncline and of Great Valley sequence rocks over Tertiary deposits north of Middle Mountain. Carl Wentworth's synthesis of the structural geologic data indicates numerous synclines and anticlines with axes parallel to the San Andreas fault. Taken together, the geologic and geophysical data indicate a pervasive set of structures suggesting a significant component of compression normal to the San Andreas fault.

e) The gravity map shows a broad low roughly centered over the preparation zone and extending roughly 10 km to the northwest, northeast and southwest. The low lies over both exposed Franciscan rocks with presumed densities of about 2.67 g/cm^3 and Tertiary deposits which should be significantly less dense. The source of this low is not known but its presence over the preparation zone is intriguing.

TILT, STRAIN, AND MAGNETIC FIELD MEASUREMENTS

9960-2114
M. J. S. Johnston
Branch of Tectonophysics
U. S. Geological Survey
Menlo Park, California 94025
415/323-8111, ext. 2132

Investigations

[1] To investigate the mechanics of failure of crustal materials using data from both deep borehole tensor and dilational strainmeters and near surface strainmeters, tiltmeters, and arrays of absolute magnetometers.

[2] To develop physical models of incipient failure of the earth's crust by analysis of real-time records from these instruments and other available data.

Results

[1] **Borehole Strain Observations during the July 8, 1986, M_L 5.9 North Palm Springs, California, Earthquake.**

Crustal strain during the July 8, 1986, North Palm Springs earthquake (M 5.9) was recorded on several Sacks-Evertson dilatometers (PUBS at 125 km, AMSS at 127.2 km, BBSS at 121 km and others at greater distances), a 3-component (tensor) strainmeter (MPFS - 24.3 km distant), all installed at depths of about 200 m, and 3-component surface seismic velocity transducers at the PUBS and more distant dilatometer sites. Dynamic strain and velocity for the foreshock, mainshock, and aftershocks were recorded at a 300 Hz sampling rate and high gain on digital recorders (GEOS). The moment of the earthquake was estimated from displacement spectra generated using the dynamic strain and velocity seismograms and also from the static strain offsets recorded on the strainmeters. The seismic moments determined from the surface velocity tranducers at the dilatometer locations are between 0.6-$1.4*10^{25}$ dyne-cm. The static moments are larger (between 2-$3*10^{25}$ dyne-cm). Post-seismic strain, consistent with continued failure on the rupture plane, continued for about 30 minutes. This was followed by apparent rebound for several days after the earthquake. The post-seismic moment was less than 10% of that of the earthquake. Precursive strains during the period days to 10 minutes before the event are not apparent in the data from the closest instrument, MPFS. The coseismic shear strain decrease and normal strain increase at this 3-component strainmeter site was 0.06 and 0.02 μ strain, respectively. The North Palm Springs earthquake decreased the effective strength ($\sigma_p - 0.6\sigma_n$) for right-lateral failure in nearby sections of the San Jacinto fault and, therefore, increases the probability of earthquakes in sections of this fault.

[2] **Seismomagnetic Observation during the July 8, 1986, M_L 5.9 North Palm Springs, California, Earthquake.**

A differentially connected array of 24 proton magnetometers has been operated along the San Andreas fault since 1976. On July 8, 1986, a M_L 5.9 earthquake occurred at epicentral distances of 3 km and 9 km from stations OCH and LSB, respectively. Seismomagnetic offsets of 1.2 nT and 0.3 nT were observed at these stations and represent the first such observations in over a decade of records. The observations are consistent with a seismomagnetic model of the earthquake in which right-lateral rupture is assumed on a 10 km segment of the Banning fault at a depth between 6 km and 12 km. The rupture segment is assumed have 15 cm of displacement in a direction N70° W and dip at 45° down to the north in a region with average magnetization of 1 A/m. Observations of surface magnetization at the two sites range between 1.0 A/m and 0.1 A/m. An alternate explanation in terms of electokinetic effects seems unlikely since the changes are complete within a 10 minute period.

[3] **Static and Dynamic Strain During the July 21, 1986, Chalfant Earthquake near the Long Valley Caldera, California.**

Crustal strain preceding, during and following the July 21, 1986, Chalfant earthquake (M 6.0) was recorded on a Sacks-Evertson dilatometers (POPS at 40.1 km) installed at a depth of about 200 m in granite on the western edge of the Long Valley caldera. Dynamic strain and velocity for the foreshock, main shock and aftershocks were also recorded at a 300 Hz sampling rate and high gain at other borehole strain sites throughout California on digital recorders (GEOS). The moments of the main earthquake and the foreshock, and many aftershocks were estimated from displacement spectra generated using the dynamic strain and velocity seismograms and from the static strain offsets recorded on the strainmeter. The seismic moments determined from the surface velocity tranducers at the dilatometer locations are between 1.7-2*10^{25} dyne-cm. The static moment required to match the observed strain step of 0.3 μ strain by modelling the earthquake with 1.28 m of right-lateral strike slip in a N25° direction and 0.82 m of dip slip at 55° SW on a 10*10 km fault segment at the earthquake hypocenter, is 5*10^{25} dyne-cm. This is in good agreement with other independent moment determinations from geodetic displacements and a 2-color network within the Caldera. Post-seismic strain, consistent with continued failure on the rupture plane, occurred for several hours after the earthquake. The post-seismic moment is at about 10% of that of the earthquake.

[4] **Deep and Near-surface Fault Creep Near Parkfield, California.**

Surface observations of aseismic fault displacement (fault creep) exhibit episodic behavior (creep events) whose sources are typically limited in extent and complex in character. Strain, tilt and displacement data obtained near and across the fault segments where these events are occurring indicate that they are triggered by deeper slip of longer duration. On August 18, 1986, fault displacement of 1.5 mm was observed on a creep meter XGH1 at Gold Hill near Parkfield, California. At this location, two borehole dilational strainmeters are installed at distances of 1.0 km and 1.35 km from the fault. Strain changes preceding and during the creep event have similar form but maximum amplitudes of 22 and 5 nanostrain, respectively. These data are consistent with a slip moment for the creep event of 2*10^{19} dyne-cm. If centered on the creepmeter, the patch that slipped could be several hundred meters square. During the previous two weeks, and at other times, strain transients of several hundred nanostrain occurred. The apparent rupture velocities obtained by replicating the strain data with simple quasistatic models of the deep creep are about 1 km/day or less. These apparent deeper

slip episodes could explain the general correspondence over periods of months between higher than normal average creep and higher rates of occurrence of moderate seismicity reported previously and should be easily detected with a small 2-dimensional arrays of low-noise borehole strainmeters planned for this area. Routine detection of these episodes may allow prediction of related moderate magnitude earthquakes in this creeping/locked transition zone

[5] **Fault Failure with Moderate Earthquakes in California**

High resolution strain and tilt recordings were made prior to, and during, the May, 1983, Coalinga (M_L 6.7, Δ 51 km) earthquake, the August 4, 1985, Kettleman Hills (M_L 5.5, Δ 34 km) earthquake, the April, 1984, Morgan Hill (M_L 6.1, Δ 55 km) earthquake, the November, 1984, Round Valley (M_L 5.8, Δ 58 km) earthquake, the July 8, 1986, North Palm Springs (M_L 5.9, Δ 44 km) earthquake, the July 21, 1986, Chalfant (M_L 6.0, Δ 40 km) earthquake, the January 14, 1978, Izu, Japan, earthquake (M_L 7.0, Δ 28 km), and several other smaller magnitude earthquakes. These recordings were made with near surface instruments (resolution 10^{-8}), with borehole dilatometers (resolution 10^{-10}) and a 3-component borehole strainmeter (resolution 10^{-9}). While observed co-seismic offsets are generally in good agreement with expectations from elastic dislocation theory, and while post-seismic deformation continued, in some cases, with a moment comparable to that of the main shock, pre-seismic strain or tilt perturbations from hours to seconds (or less) before the main shock are not apparent above the present resolution. Precursory slip for these events, if any occurred, must have had a moment less than a few % of that of the main event. To the extent that these records reflect general fault behavior, the strong constraint on the size and amount of slip triggering major rupture makes prediction of the onset times and final magnitudes of the rupture zones a difficult task unless the instruments are fortuitously installed near the rupture initiation point. These data are best explained by an inhomogeneous failure model for which various areas of the fault plane have either different stress-slip constitutive laws or spatially varying constitutive parameters. Other work on seismic waveform analysis and synthetic waveforms indicates the rupturing process is inhomogeneous and controlled by points of higher strength. These models indicate rupture initiation occurs at smaller regions of higher strength which, when broken, allow runaway catastrophic failure.

[6] **Crowley Lake Level Monitoring**

Four water level monitoring sites have been installed on Lake Crowley in the Long Valley/ Mammoth Lakes region (Fig 1). These stills will provide differential water level measurements (tilt) equivalent to 6 independent tiltmeters with baselines of up to 8 kilometers at varying angles to the center of the resurgent dome. Each site has been surveyed into the existing level line routes around the lake by John Estrum and NGS. The time constants of the stills are approximately 40 minutes to minimize effects from the primary sieche periods at 18 minutes and 13 minutes, respectively. The water level data, together with water temperature, wind speed, and other parameters, are being transmitted by the low frequency satellite data collection system to Menlo Park at a sample period of 2 minutes.

[7] **Parkfield Strainmeter Installations**

Sites for six dilatometers and 4 tensor strainmeters to be installed in boreholes at depths between 500 and 1000 feet in the Parkfield region have been selected (Fig 2) and are presently being drilled. Installation will be started in a early November.

Reports

Bakun, W. H., R. O. Burford, M. J. S. Johnston, A. G. Lindh, P. Olds, E. Roeloffs, S. Schulz, P. Segall, and R. Simson, 1986, Parkfield, Ca. Earthquake Prediction Experiment - A Status Report, Trans A.G.U., 67, 904.

Bakun, W. H., Bredehoeft, J., Burford, R. O., Ellsworth, W. L., Johnston, M. J. S., Jones, L., Lindh, A. G., Mortensen, C. E., Roeloffs, E., Schulz, S., Segall, P., and Thatcher, W., 1986, Parkfield Earthquake Prediction Scenarios and Response Plans, U.S.G.S. Open-file Rep. 86-365.

Borcherdt, R. D., G. Glassmoyer, and M. J. S. Johnston, 1986, On the Simultaneous Detection of Anelastic Volumetric Strain and Seismic Displacement Fields near the San Andreas Fault, Trans. A.G.U., 67, 1092.

Gladwin, M. T., and M. J. S. Johnston, 1986, Tectonomagnetism and Intermediate Term Stress Monitoring, Proceedings of Workshop on Intermediate-Term Earthquake Precursors, U.S.G.S. Open- file Report 86- .

Gladwin, M. T., Gwyther, R. L., Hart, R., Francis, M., and Johnston, M. J. S., 1986, Borehole Vector Strain Measurements in California, J. Geophys. Res. (in press).

Johnston, M. J. S., 1986, Local Magnetic Fields, Uplift, Gravity, and Dilational Strain Changes in Southern California, J. Geomag. Geoelec., (in press).

Johnston, M. J. S., Tectonomagnetism and Tectonoelectricity, 1986, Reviews of Geophysics, (in press).

Johnston, M. J. S., A.T. Linde, M. T. Gladwin, R. D. Borcherdt, 1986, Fault Failure with Moderate Earthquakes, Tectonophysics, (in press).

Johnston, M. J. S., A.T. Linde, M. T. Gladwin, R. D. Borcherdt, 1986, Fault Failure with Moderate Earthquakes, Trans. A.G.U., 67, 1106.

Linde, A. T., and Johnston, M. J. S., 1986, Parkfield Prediction Scenario, A.A.A.S. Meeting, (in press).

Linde, A.T., Takagi, A., Johnston, M. J. S., Stefansson, R., 1986, Some Results from the Carnegie Borehole Strainmeter Program, Abs. Seis. Soc. Japan, Tokyo, Japan, October, 1986.

Mueller, R.J., and M. J. S. Johnston, 1986, Seismomagnetic Effect during the July 8, 1986, M_L 5.9 North Palm Springs, California, Earthquake, Trans A. G. U., 67, 1090.

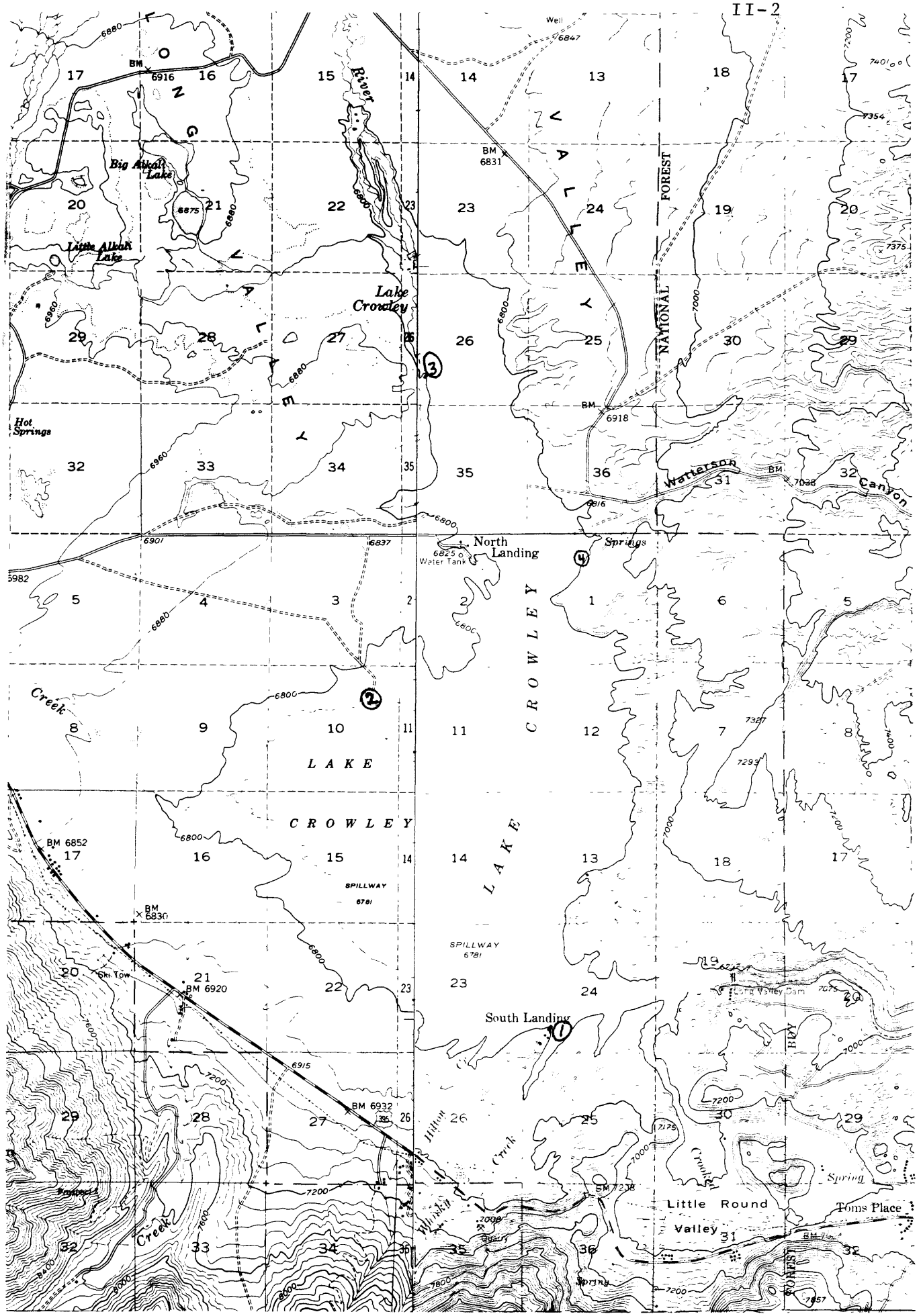

Figure 1. Sites of level monitoring stills round Crowley lake

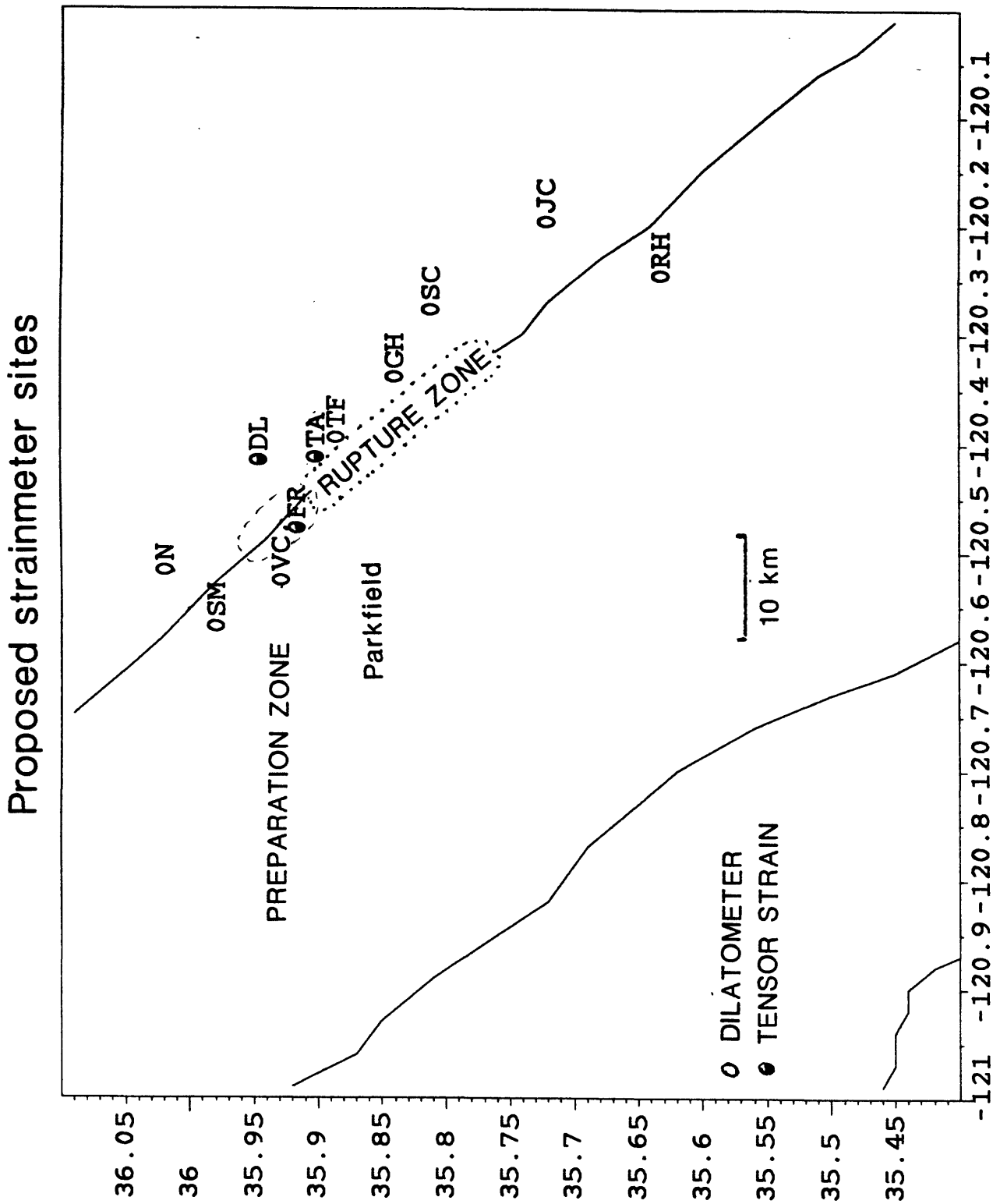

Figure 2. Location of proposed new dilational and tensor strainmeter sites in relation to the expected rupture zone of the hypothetical 1986-1987 "Parkfield Earthquake"

Earthquake and Seismicity Research Using SCARLET and CEDAR

Contract No. 14-08-0001-G1171

Hiroo Kanamori, Clarence R. Allen, Robert W. Clayton
Seismological Laboratory, California Institute of Technology
Pasadena, California 91125 (818-356-6914)

Investigations

1. Anomalous Shear-Wave Attenuation in the Shallow Crust Beneath the Coso Region, California
   Sanders, C., D. Rinn, P. Ho-liu, and H. Kanamori

2. Changes in NTS Seismograms Recorded in the Source Region of the North Palm Springs Earthquake of 7/8/86
   Magistrale, H., and H. Kanamori

Results

1. Anomalous Shear-Wave Attenuation in the Shallow Crust Beneath the Coso Region, California

Shear-wave seismograms are used to image anomalous attenuation regions in the shallow crust beneath the Coso volcanic/geothermal region of eastern California. Vertical component seismograms archived by CUSP (Caltech-USGS Seismic Processor) for earthquakes which occurred in the Indian Wells Valley-Coso-southern Sierra Nevada region from October 1983 to February 1984 were analyzed to determine if attenuated S_v wave signals were present along some raypaths. Signals of this type have previously been documented in the Long Valley magmatic area and elsewhere. We have analyzed sixteen small earthquakes with S_v signals which change considerably with azimuth and take-off angle. 360° ray coverage used in forward modelling and a tomographic inversion illuminates several small regions within a 20 by 30 km area of the shallow crust (some shallower than 5 km) which attenuate S-waves passing through them. This area is beneath the Indian Wells Valley south of the Coso Range and is coincident with the epicentral location of intense earthquake swarms which occurred in 1982-1983. This swarm sequence began in a centralized cluster which with time became two clusters that migrated several kilometers north and south. No attenuating effects were seen for rays passing beneath the Coso geothermal area above about 5 km depth.

2. Changes in NTS Seismograms Recorded in the Source Region of the North Palm Springs Earthquake of 7/8/86.

The North Palm Springs earthquake of 7/8/86 occurred near station WWR of the Caltech-USGS southern California seismograph array. Seismic waves from blasts at the Nevada test site (NTS) recorded at WWR travel through the volume of crust occupied by aftershocks of the North Palm Springs earthquake. We examined seismograms and spectra of four NTS blasts recorded at stations WWR and EWC. EWC is 25 km east of WWR, out of the aftershock zone. Three blasts occurred before the earthquake and one after. All blasts occurred at the same location within NTS. The seismograms and spectra from EWC are similar for all four blasts. The seismograms and spectra from WWR are shown in Figure 1. Spectra are plotted from .5 to 10 Hz. Seismograms are 8 secs long. The records of the two 1984 blasts are similar. The records of the 1985 blast, one year before the earthquake, show relatively more high frequencies. The records of the 1985 blast, 9 days after the earthquake, show relatively less high frequencies.

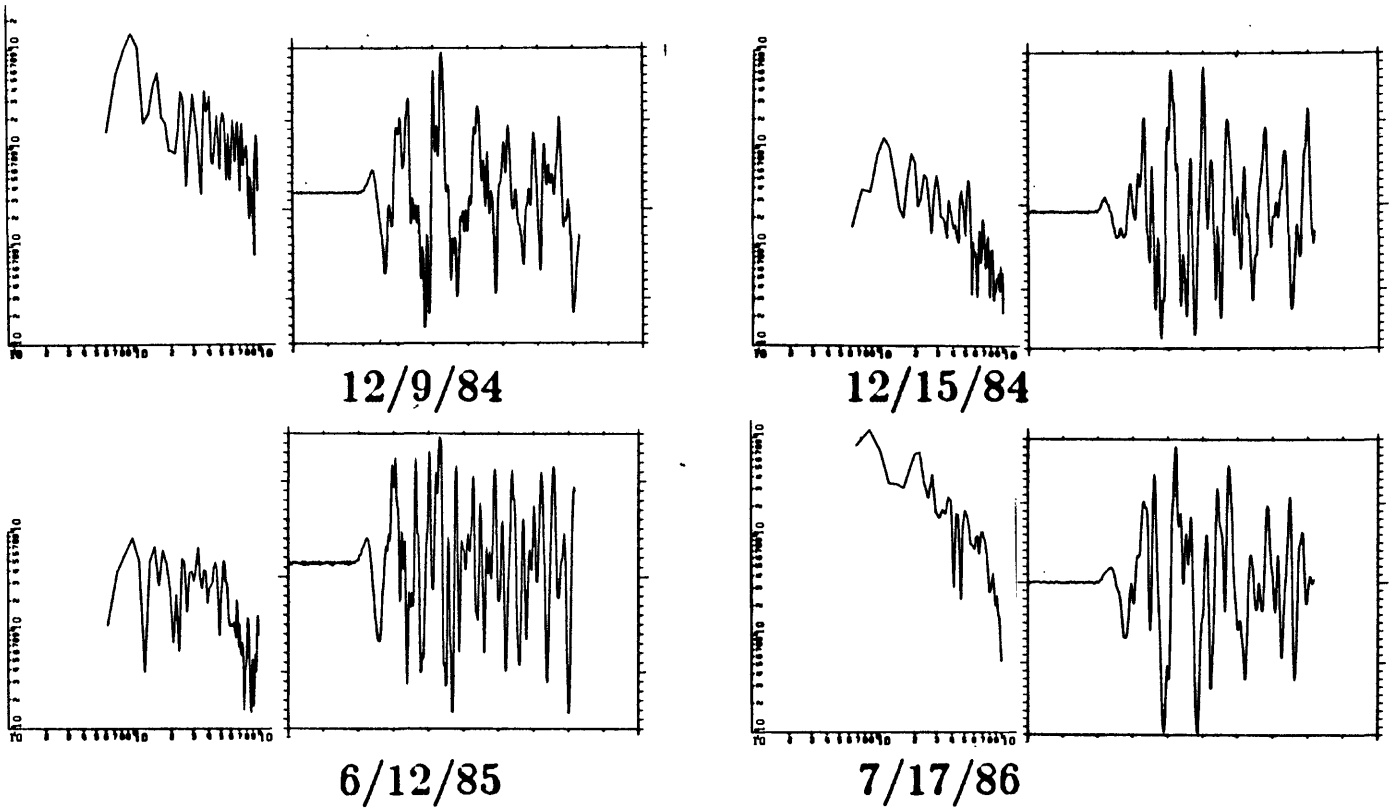

References

Sanders, Chris, Harold Magistrale, and Hiroo Kanamori, Rupture patterns and preshocks of large earthquakes in the Southern San Jacinto Fault Zone, *Seismo. Soc. Amer., Bull., 76,* No. 5, pp. 1187-1206.

Sanders, Chris, David Rinn, Phyllis Ho-Liu, and Hiroo Kanamori, Anomalous shear-wave attenuation in the shallow crust beneath the Coso Region, California, Journal of Geophysical Research, in press, 1986.

GEODETIC STRAIN MONITORING

9960-02156

John Langbein
Branch of Tectonophysics
U.S. Geological Survey
345 Middlefield Road, MS/977
Menlo Park, California 94025
(415-323-8111, ext. 2038

Investigations

Two-color geodimeters are used to survey, repeatedly, geodetic networks within selected regions of California that are tectonically active. This distance measuring instrument has a precision of 0.1 to 0.2 ppm of the baseline length. Currently, the crustal deformation is being monitored within the south moat of the Long Valley Caldera in eastern, California, and near Pearblossom, California on a section of the San Andreas fault that is within its Big Bend section. Periodic comparisons with the proto-type, 2-color geodimeter are also conducted near Parkfield, California. These inter-comparison measurements serve as a calibration experiment to monitor the relative stabilities of the portable and proto-type geodimeters.

Results

1) Long Valley

Data from the expanded 2-color geodimeter network, Figure 1, within the Long Valley caldera is shown in Figure 2. The most notable deformation during the interval 1986.25-1986.75 is compressional strain change oriented in an east-west direction coincident with the time of the 21 July 1986 Chalfant Valley earthquake. The epicenter of this earthquake is located roughly 45 km ESE of the station Casa. The average coseismic strain change measured using Casa as a common station is -.60 ± 0.08 ppm oriented N69°W ± 4° and +0.13 ± 0.07 ppm oriented N21°E ± 4°. For the baselines in common with station Whitmore, the average strain change is -1.42 ± 0.15 ppm oriented N74°W ± 4° and 0.24 ± 0.18 ppm oriented N16°E ± 4°. The observed line-length changes can be adequately modeled with slip on a plane which is defined by the locus of aftershocks in Chalfant Valley. The moment determined from the two-color data is $4.9 \pm 0.2 \times 10^{25}$ dyne-cm or an equivalent earthquake of magnitude 6.4. The estimate for the moment is a formal standard deviation and does not incorporate bias due to location of the fault plane

and slip mechanism. Variations of modeled focal mechanism changes the computed moment by 10-20%.

The baseline Casa-Miner (Figure 2) show substantial fluctuation in rate during 1986.0 through 1986.5. The rapid compression during late May and June, 1986 may be due to downhill creep of Miner in response to snow melt. To verify the stability of Miner, we installed a new station, Wall, which is located in Sierra Bedrock rather than in glacial morraine.

The continued secular extension of a number of baselines including Casa-Krakatau, Knolls, and Shark indicate that inflation beneath the resurgent dome is still occurring, but at a substantially lower rate than in mid-1983.

2. Pearblossom

Due to the high rate of deformation in Long Valley and our limitation of only one operating two-color geodimeter that is currently reliable and portable, the frequency of observations at Pearblossom has been significantly reduced. This network was resurveyed in June 1986, and is consistent with previous measurements.

3. Instrument Inter-Comparison

Since January 1986, we have completed 3 intercomparison experiments at Parkfield, California using both the portable and prototype two-color geodimeter. Each instrument is set up over an adjacent monument on Carr Hill and length measurements are made on 14 baselines which uniformly cover a 360° range in azimuth. Using the differences in observed baseline lengths, we have deduced both the stability of the geodimeters and the monuments to within 0.05 ppm and 0.4 mm respectively. During this 9 month interval, peak to peak variation of the relative instrument length scale is 0.15 ppm and 0.6 mm relative monument displacement.

Previous to January 1986, we conducted this experiment on a reduced set of baselines using only 150° range in azimuths. Data from these experiments, which go back to June 1984, indicate that both the geodimeters and monuments have changed relative to each other. For instance, the inferred instrument length scale have fluctuated as much as 0.4 ppm and fluctuations in monument displacements were on the order of 2 mm. However, the limited range in azimuthal control precluded us from resolving the ambiguity of change in instrument length scale and monument displacement.

5. Parkfield

In July 1986, we installed an 18 baseline network on Middle Mountain north of Parkfield. This network uses two instrument set-up stations; one on Middle Mountain located within 1 km of the epicenter of the 1966 mainshock, and the second monument located 3 km to the east. Initial measurement of the network was made in August, 1986.

4. Pinon Flat

No measurements of this network were made during the interval 1986.25-1986.75 due to the increase of activity in Long Valley.

Reports

Langbein, J.O., M.F. Linker, and D.L. Tupper, Coseismic strain changes observed within the Long Valley caldera due to 21 July 1985 Chalfant Valley earthquake (Abs.), EOS, December 1986.

Langbein, J.O., M.F. Linker, A.F. McGarr, and L.E. Slater, Precision of two-color geodimeter measurements: Results from 15 months of observations, submitted to Jour. Geophys. Res., 1986.

Linker, M.F., J.O. Langbein, A. McGarr, Decrease in deformation rate observed by two-color ranging in Long Valley caldera, Science, v. 232, p. 213-216, 1986.

Figure Captions

Fig. 1. Map showing the location of the baselines that comprise the two-color geodimeter network within the Long Valley caldera.

Fig. 2. Line-length changes observed for the baselines in Figure 1. The length changes have been normalized to the nominal length of each baseline; hence the displacements are plotted as strain changes. The error bars represent one standard deviation. Time of the 21 July, 1986 Chalfant earthquake is indicated with a vertical line.

mammoth net

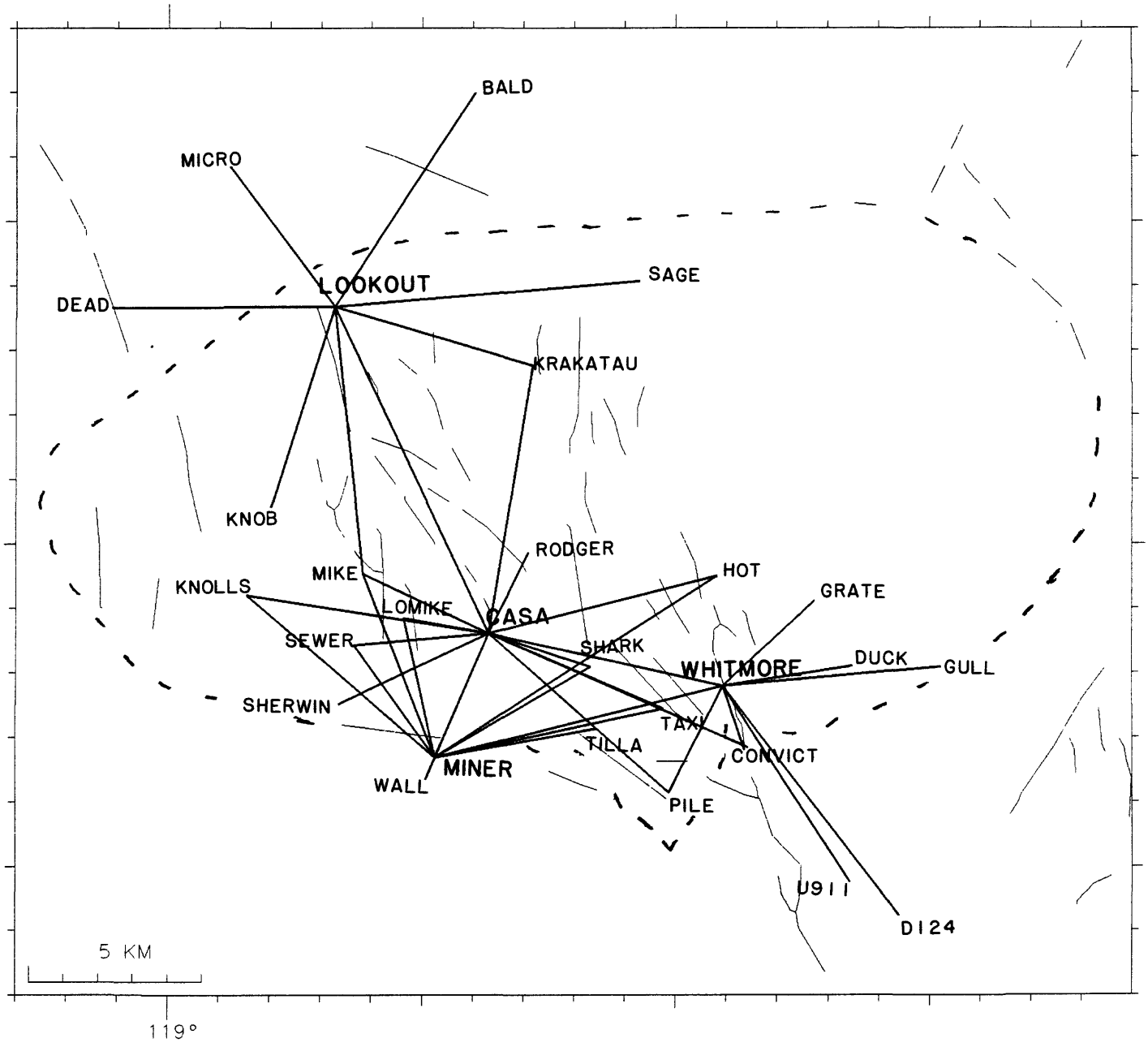
BALD
MICRO
LOOKOUT
SAGE
DEAD
KRAKATAU
KNOB
RODGER
MIKE
HOT
KNOLLS
GRATE
LOMIKE
CASA
SEWER
SHARK
WHITMORE
DUCK
GULL
SHERWIN
TAXI
TILLA
CONVICT
MINER
WALL
PILE
U911
D124
5 KM
119°

STRAIN CHANGE (L - Lo)/Lo in PPM
30
25
20
15
10
5
0
1983
1984
1985
1986
LOOKOUT-BALD
LOOKOUT-DEAD
LOOKOUT-KNOB
LOOKOUT-KRAKATAU
LOOKOUT-MICRO
LOOKOUT-MIKE
LOOKOUT-SAGE

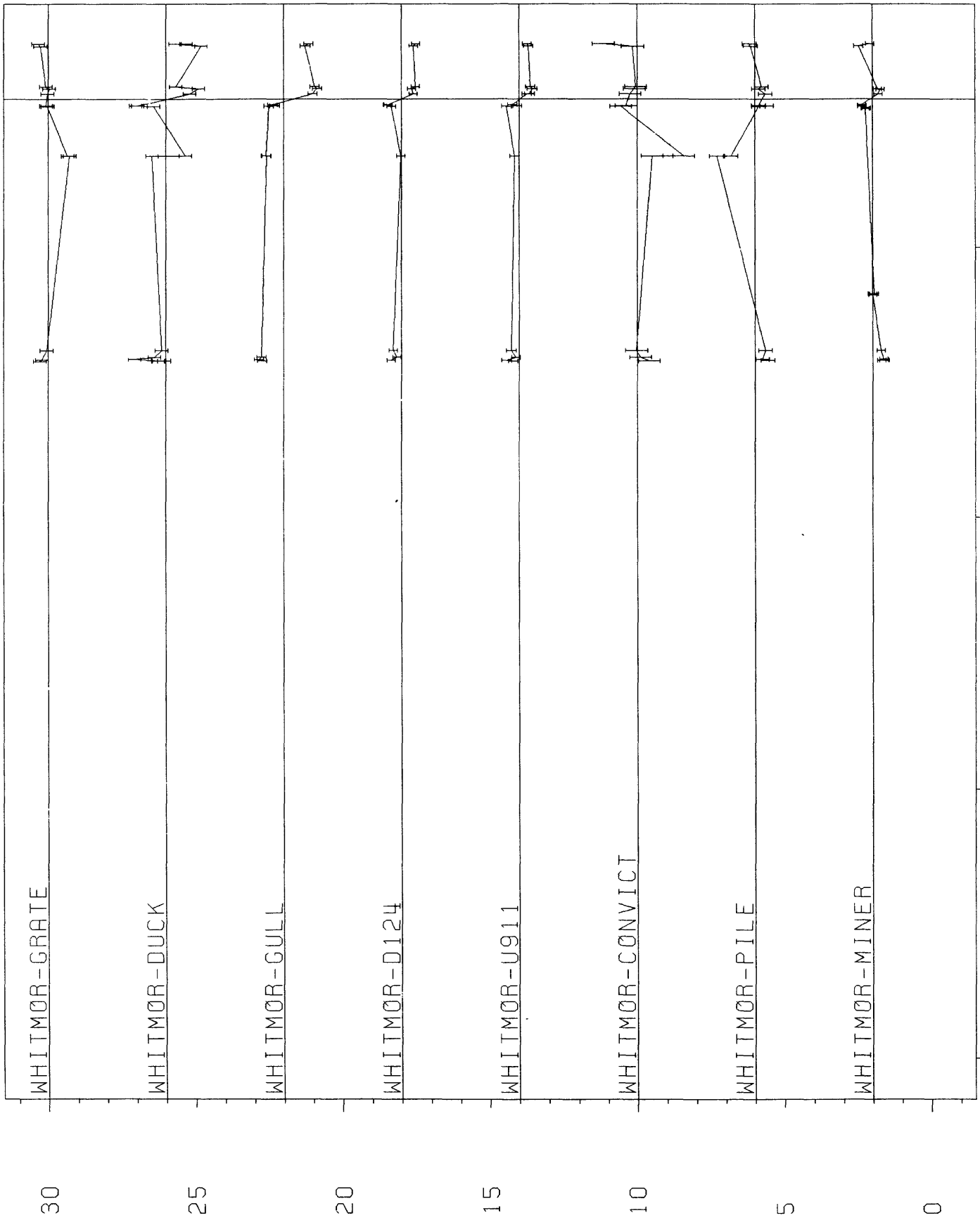
WHITMOR-GRATE
WHITMOR-DUCK
WHITMOR-GULL
WHITMOR-D124
WHITMOR-U911
WHITMOR-CONVICT
WHITMOR-PILE
WHITMOR-MINER
1983
1984
1985
1986
30
25
20
15
10
5
0
STRAIN CHANGE (L - Lo)/Lo in PPM

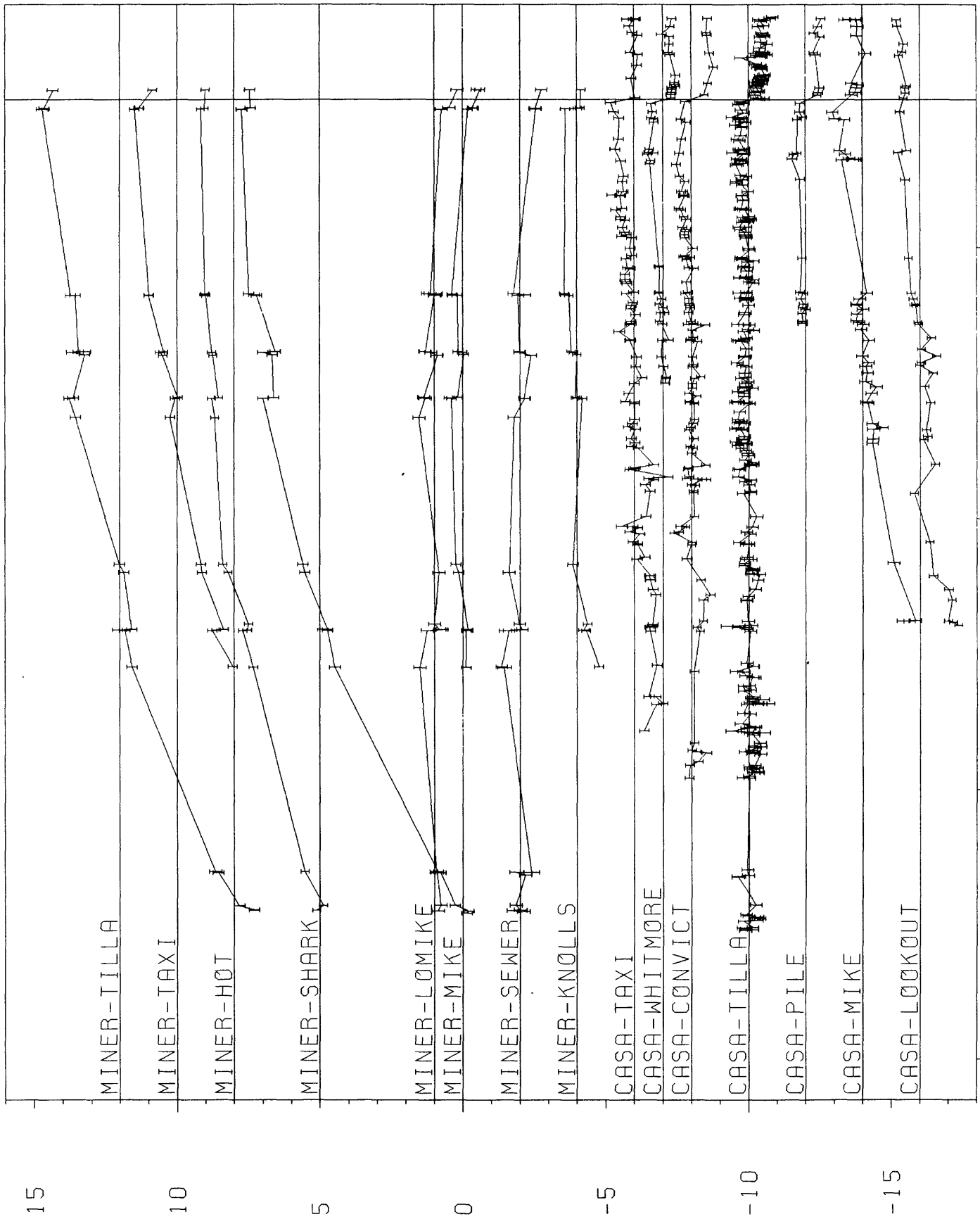
STRAIN CHANGE (L - Lo)/Lo in PPM
15
10
5
0
-5
-10
-15
1983
1984
1985
1986
MINER-TILLA
MINER-TAXI
MINER-HØT
MINER-SHARK
MINER-LØMIKE
MINER-MIKE
MINER-SEWER
MINER-KNØLLS
CASA-TAXI
CASA-WHITMØRE
CASA-CØNVICT
CASA-TILLA
CASA-PILE
CASA-MIKE
CASA-LØØKØUT

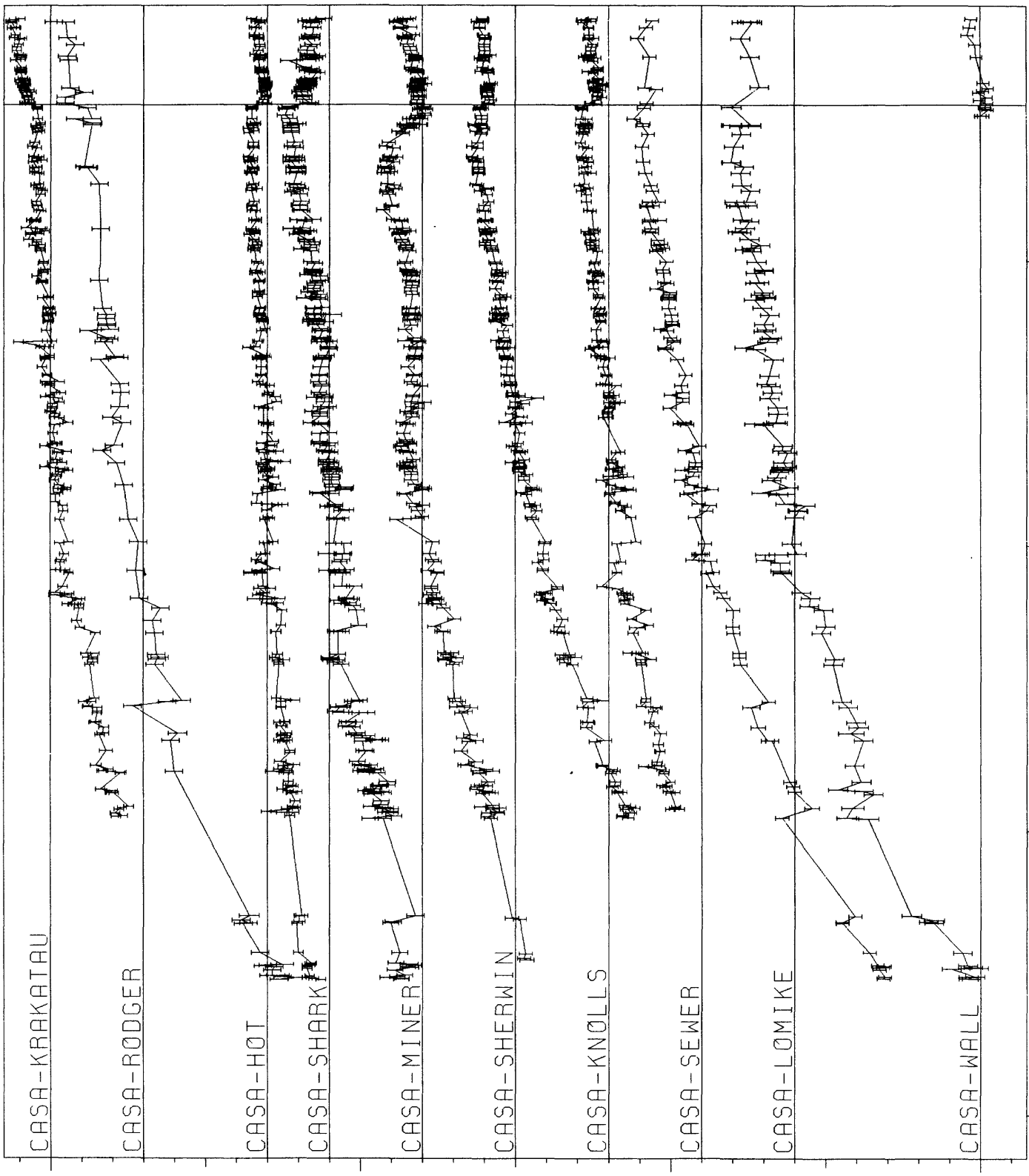
CASA-KRAKATAU
CASA-RODGER
CASA-HOT
CASA-SHARKI
CASA-MINER
CASA-SHERWIN
CASA-KNOLLS
CASA-SEWER
CASA-LOMIKE
CASA-WALL
1983
1984
1985
1986
30
25
20
15
10
5
0
STRAIN CHANGE (L - Lo)/Lo in PPM

Parkfield Prediction Experiment

9930-02098

Allan G. Lindh
Catherine M. Poley and Barry Hirshorn
Branch of Seismology
U.S. Geological Survey
345 Middlefield Road, MS-977
Menlo Park, California 94025
(415) 323-8111, Ext. 2042

Investigations

1. Real-time monitoring and analysis of Parkfield seismicity, as part of the Parkfield Prediction Experiment, with special attention given to seismicity near Middle Mtn.
2. Continued work on long term earthquake probabilities along the San Andreas system.
3. Relocation and spatio-temporal analysis of central California coastal seismicity.
4. Coda-magnitude and "envelope magnitude" study.
5. Daily reprocessing and maintenance of RTP data, with an eye to seismicity changes. Bi-weekly review of station and network performance.
6. Continued work on incorporation of RTP and CUSP data into one database.

Results

1. The level of seismic activity at Parkfield averaged 16 events per month from May 1, 1986 thru October 31, 1986 (92 total). There were an average of 3-4 events per month near Middle Mtn (22 total), with a spurt of activity in June (8 events) (see Fig 1). Of these events, 4 qualified as level D alerts and 1 as level C alert (see Bakun, this volume). This is just slightly above the anticipated rate for these alert levels.

   Events of interest include: (1) a magnitude 2 on August 22nd near Simmler, the furthest south of of any events in this area to date; (2) a magnitude 3.8 on August 29th at the town of Parkfield, similar to a magnitude 3.2 event which occurred on January 4th, 1985; (3) a magnitude 2.8 on September 1st near Gold Hill; (4) several events larger than magnitude 2.0 in the creeping section of the fault, unusual for this region of the fault. (See Fig. 2)

   Catherine Poley, with Al Lindh and Bill Bakun, has completed analysis of the last 15 years of seismicity near Middle Mtn. and a short paper has been submitted to Nature. Work on short term recurrence patterns within the Parkfield region has resulted in the identification of at least two patterns; one in the

Parkfield preparation zone (M=3 per 39-40 months) and another in the creeping section of the fault (M=3 per 5 yrs.). A paper dealing with these recurrence patterns is in preparation for Nature.

2. Al Lindh, using the different approaches used to calculate foreshock probability gains for Parkfield, has extended his study to determine the likelihood that the next characteristic Parkfield earthquake will be a foreshock to a larger earthquake on the southern section of the San Andreas. A paper concerning this question is in preparation.

3. Catherine Poley, with Al Lindh and Jerry Eaton, has started gathering all the phase data for the coastal region of central California in order to begin relocating and analysing the data. This study is in its early stages. The results will be presented at a special GSA symposium in May 1987.

4. Barry Hirshorn, with Al Lindh, is developing techniques for determining coda magnitudes from low-gain, short-period, vertical seismometers added to CALNET in 1985. Current coda magnitudes from high-gain seismometers underestimate local Richter magnitudes above M_L=3.5. A clear linear relationship between M_{τ}, from the low-gain instruments, and M_L based on Wood-Anderson seismographs in the $3.5 \lesssim M_L \gtrsim 5.7$ range exists. Implementation on the the RTP is imminent.

   He is also developing an "envelope magnitude", M_e, based on earlier work done with surface waves by Brune (1963) and adopted to body-waves by Al Lindh in the early 1980's. The method is based on fitting a power equation, of the form At^{-a}, in log amplitude-log time space, to the envelope of the s-wave coda decay. Integration yields the area under the envelope which forms the basis of the magnitude estimation. This is also potentially related to more fundamental parameters of the EQ source (ie. seismic moment and/or radiated energy around the corner frequency of the event). M_e is also providing an accurate estimation of M_L in the $3.5 \lesssim M_L \gtrsim 5.7$ range and provides an additional, independent measurement of magnitude, in real-time within 5-10 minutes of the occurrence of the event.

   An open-file report is in preparation concerning these results.

5. Barry Hirshorn, in conjunction with reprocessing of RTP data, runs the weekly station quality meetings. Al Lindh meets with John Van Schaack twice a week to review station performance. Progress is being made in holding the net together in the face of reduced funding for station maintenance.

6. Successful efforts continue to incorporate RTP data into the CUSP database.

Reports

Poley, C. M., Lindh, A. G., Bakun, W. H., and Schulz, S. S., 1986, Temporal Changes in Microseismicity and Creep near Parkfield, California, Nature, in press.

Jones, L. M. and Lindh, A. G., 1986, Foreshocks and Earthquake Prediction at Parkfield, California, in branch review.

Bakun, et al., 1986, Parkfield Earthquake Prediction Scenarios and Response Plans, U. S. Geological Survey Open-File Report 86-365.

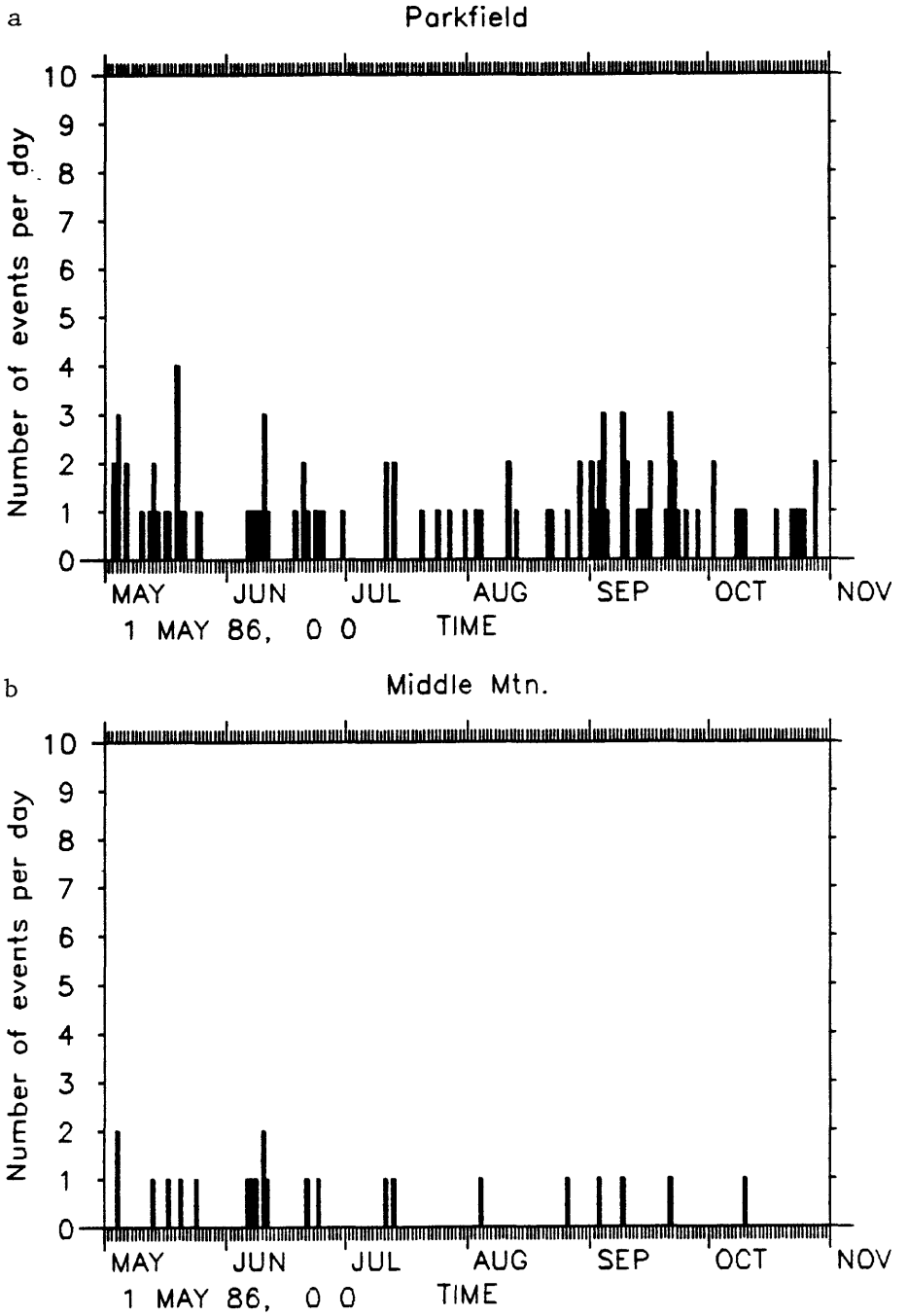

Fig. 1 Histograms of seismicity, M ≥ 0, from May 1, 1986 thru October 31, 1986. a) Parkfield seismicity. b) Middle Mtn. seismicity (quadrilateral in Fig. 2).

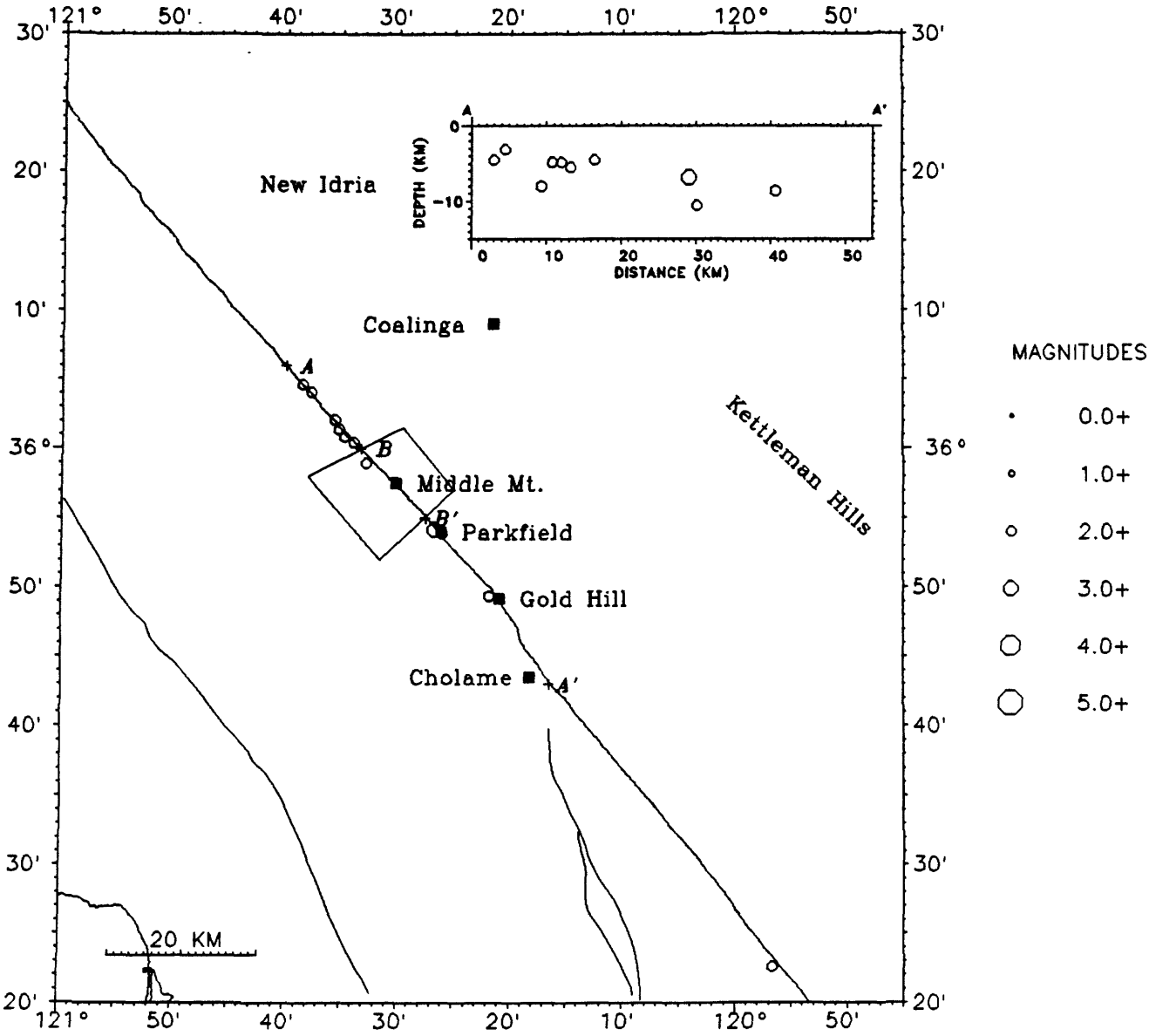

Fig. 2 Map of epicentral locations, M ≥ 2.0, from May 1, 1986 thru October 31, 1986. Inset is cross-section along A-A'. The Middle Mtn. region is indicated by the quadrilateral.

SEISMIC WAVE MONITORING IN CENTRAL CALIFORNIA

14-08-0001-G1149

T.V. McEvilly
R. Clymer
Seismographic Station
University of California
Berkeley, California 94720
415/642-3977

Program Objectives

Our primary goal is to establish a routine (four times per year) program of seismic wave measurements at Parkfield to detect changes in wave velocity and shear wave anisotropy using an array of downhole seismometers and a shear-wave vibrator. Secondarily, we are attempting to maintain the long-standing P-wave monitoring program at Hollister.

Specific Goals and Investigations

1. Cooperation with the University of California at Santa Barbara (UCSB) and the USGS for installation of 3-component borehole seismometers at Parkfield and instrumentation of these sites with UCB telemetry equipment.
2. Development and testing of a telemetered multi-channel recording system suitable for efficient acquisition of both VIBROSEIS and earthquake data from eight 3-component sites at Parkfield. This system replaces the single-channel system used at Hollister.
3. Preliminary field work:
   a) To study local crustal reflectivity with short profiles to establish target events for monitoring and to attempt to detect anisotropy. Results are being compared to the COCORP Parkfield line.
   b) To determine signal-to-noise ratios for various source and receiver locations.
   c) To establish procedures and vibrator sites for the monitoring program.
4. To continue to make periodic measurements at Hollister.

Results

1. In FY85, five borehole seismometers were installed (Figure 1), three by UCSB and two by UCB at depths of about 60-225m. Presently, the USGS and UCSB are drilling and instrumenting several more sites, to be completed this calendar year. During this same time frame, the USGS will install the UCB telemetry equipment permanently at each site, to a total of eight.
2. Field work at Parkfield in FY85 established conclusively that the Hollister single-channel recording system was too inefficient for the planned Parkfield data set. During four field trips in the summer of 1986, we tested a new multi-channel acquisition system, featuring 16-bit digital telemetry by Refraction Technology, interfaced to a centrally-located computer-based recording system made by Weston Geophysical Company (Figure 2). Numerous problems have been gradually overcome, primarily involving bugs in the new equipment, RF interference at the seismometer sites, and interference with and by USGS equipment at the same sites. Most recently, data collection at the seismically active Geysers geothermal area north of San Francisco established that the event detection algorithm works well, and the system produces high-quality recordings of

earthquakes.

3. In addition to trouble-shooting, some preliminary data have been obtained.
   a) One short profile was obtained with two receiver sites and a number of vibrator sites lying on the COCORP line. The COCORP data have been regathered at the Lawrence Berkeley Laboratory for direct comparison once the new data have been processed.
   b) Useful data have been acquired using the two established receiver sites north-east of the San Andreas fault in Joaquin Canyon with the vibrator in the fault zone up to 10 km distant. The northern of the two Vineyard Canyon sites south-west of the fault zone receives weaker signals; it appears that a vibrator site must be within a few kilometers of this receiver. The southern Vineyard Canyon site has not been used due to telemetry difficulties caused by terrain. The Gold Hill site has been extremely noisy during our recording attempts, but the noise source has subsequently been discovered and eliminated.
   c) Specific sites for the monitoring program have not been chosen. It seems that three to five vibrator locations will be necessary to obtain a high signal-to-noise ratio at all receiver sites.
4. Several measurements have been made at the Stone Canyon array, including measurements before and after the magnitude 4.8 Stone Canyon earthquake on May 31, 1986. No significant variations of first arrival travel times were observed. Monitoring attempts at the Winery area have been plagued by vibrator truck break-downs.

Future Plans

The final installations of telemetry equipment at eight Parkfield seismometer sites should be completed and the final problems with the acquisition system should be solved by December, 1986. Preliminary data collection and choice of permanent vibrator sites will be finished soon thereafter, and monitoring should begin in the winter or spring of '87, depending on the weather.

Attempting to carry on with the Hollister program has diluted our efforts at Parkfield; we feel the latter are more important. The Hollister monitoring will probably be limited in the future to the Winery area, this being the only segment of that part of the San Andreas fault which has not recently experienced a moderate earthquake.

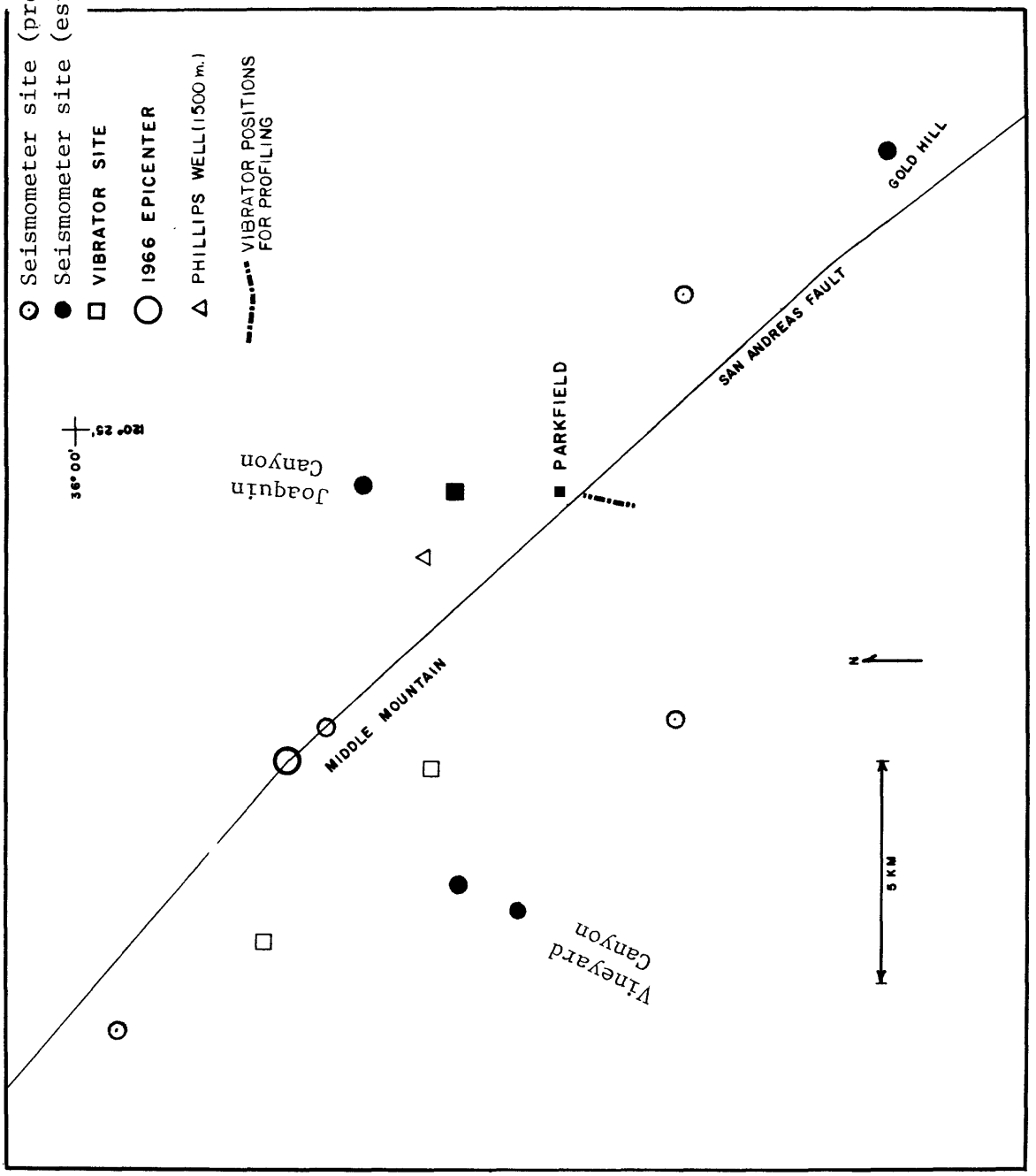

Figure 1. Parkfield area location map, showing 3-component, borehole seismometer sites and preliminary vibrator locations.

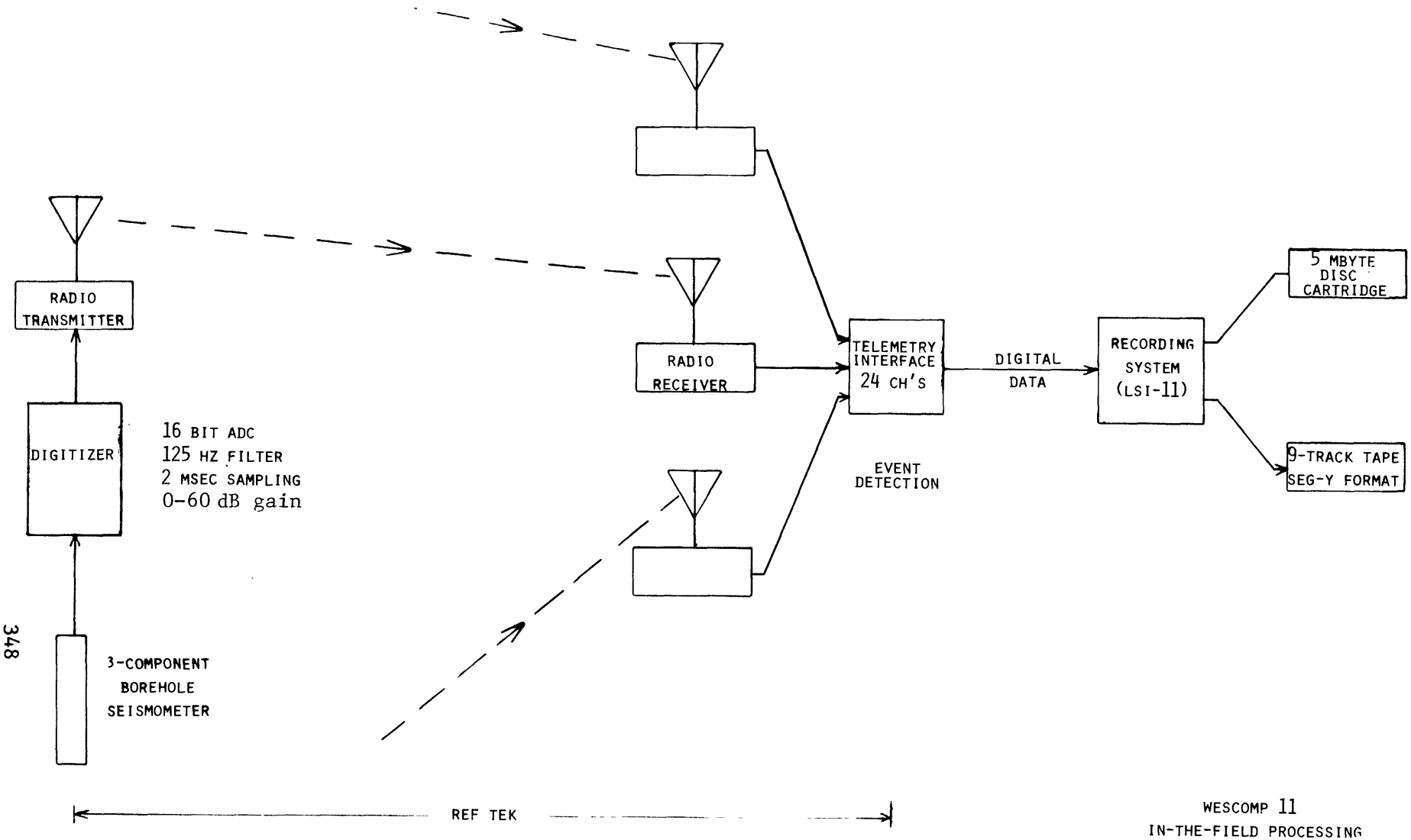

Figure 2. Schematic diagram of the UCB/LBL seismic data acquisition system, featuring digital telemetry, computer-based recording, and in-field processing. The system is expandable to more channels than shown, and is capable of recording both VIBROSEIS and earthquake data, the latter with triggered event recording. Recording on SEG-Y, 9-track tapes allows processing with DISCO software at the Center for Computational Seismology at Lawrence Berkeley Laboratory.

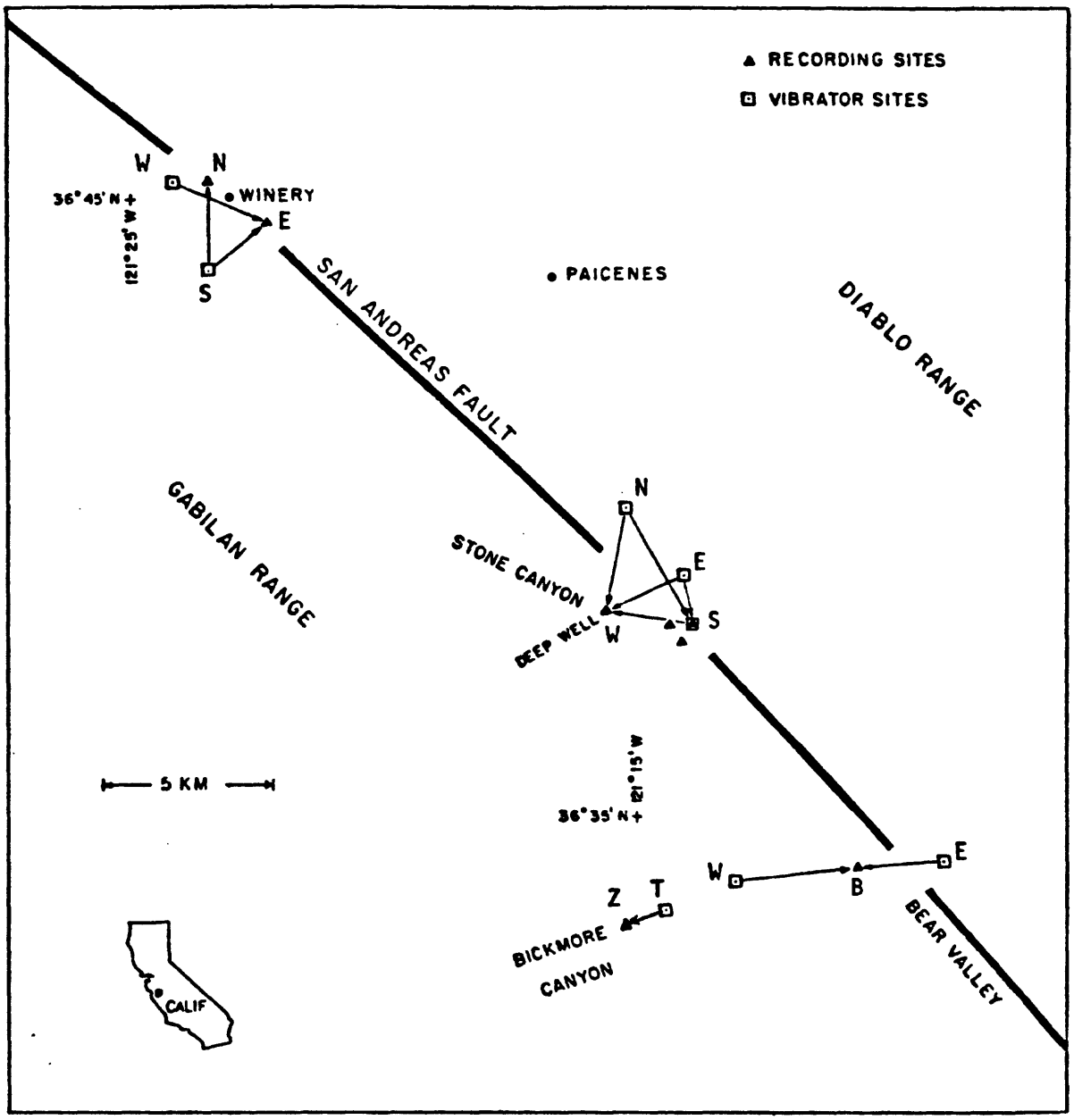

FIGURE 3 . Source and receiver sites, Winery, Stone Canyon and Bickmore Canyon areas.

Crustal Studies

9930-02102

Walter D. Mooney
Gary S. Fuis
Branch of Seismology
United States Geological Survey
345 Middlefield Road - MS 977
Menlo Park, California 94025
415-323-8111 X2476/2569

Investigations

1. Continued analysis of seismic-refraction data from southern Alaska. This is part of the Trans-Alaska Crustal Transect (TACT) (Fuis, Ambos, Mooney, Page).

2. Analysis of seismic-refraction data from western Arizona - southeastern California. This part of the Pacific to Arizona Crustal Experiment (PACE) from seismic refraction data. (Fuis, McCarthy, Wilson).

3. Revision and re-submission of manuscript on deep crustal structure of Yunnan Province, PRC (Mooney).

4. Continued analysis of seismic refraction data from Maine and Quebec (Luetgert, Klemperer, Mann).

5. Completion of a manuscript on the seismic properties of the continental lithosphere (Mooney and Brocher).

6. Field work in central California (Walter and Ambos).

7. Seismicity investigation in Jordan (Kohler).

8. Lithospheric studies in Nevada (Catchings, Mooney, Whitman).

Results

1. In 1984, the U.S. Geological Survey initiated the Trans-Alaska crustal Transect (TACT) program-- a coordinated geological and geophysical study of the structure, composition, and evolution of the Alaskan crust along a corridor parallel to the Trans-Alaska oil pipeline, from Valdez to Prudhoe Bay and across the adjacent Pacific and Arctic continental margins. TACT is a major element of the multi-institutional Trans-Alaska Lithosphere Investigation (TALI). The TACT project was launched in southern Alaska: in succeeding years the investigations will shift northward with the goal of completing the transect by the end of the decade.

A summary of the results from TACT are given in Page et al. (1986). Geologic, seismic, gravity, and magnetic data from the northern Chugach Mountains and southern Copper River Basin, Alaska indicate that the Chugach terrane (CGT) and the composite Peninsular/Wrangellia terrane (PET/WRT) are thin (<10 km), rootless sheets bounded on the south in both cases by north-dipping thrust faults that sole into a shallow, horizontal, low-velocity zone. The CGT has been thrust at least 40 km beneath the PET/WRT along the Border Ranges fault system (BRFS). Adjacent to the BRFS, uplift and erosion of 30-40 km since Jurassic time have exposed blueschist-facies rocks in the CGT and mafic and ultramafic cumulate rocks in the PET/WRT. Four paired north-dippping layers of low and high seismic velocities extend beneath the northern CGT and southern PET/WRT and may be slices of subducted oceanic crust and upper mantle; the upper two pairs may now be joined to the continental plate.

2. PACE

During 1985, the U.S. Geological Survey initiated the Pacific to Arizona Crustal Experiment (PACE), a multidisciplinary transect across western Arizona, southern California, and the offshore Pacific continental margin. Two hundred and sixty km of reversed seismic-refraction/wide-angle reflection data were recorded as a part of PACE across the Whipple Mountain metamorphic core complex in southeastern California (Fig. 1). The data were acquired along two perpendicular profiles consisting of 30 shots, 20 shotpoints, and station spacing of 500 m on one profile and 1000 m on the other. Collectively, these data represent one of the most detailed geophysical studies to date across a metamorphic core complex and provide an understanding of the crustal and geologic history of these isolated regions of unusually large extension.

Although analysis of the PACE seismic-refraction data is still underway, several significant results are already evident. First, on the NE-oriented profile a sharp velocity discontinuity is present throughout the survey at a depth of 16-18 km. This discontinuity separates a 6.0-km/s upper crust from a 6.5- to 7.2-km/s middle crust. In addition to this high-velocity layer, laterally discontinuous 6-8-km-thick low-velocity zones (LVZs) are evident both above and below it. The upper crustal LVZ is analogous to those previously identified in the northern Basin and Range province, but the lower-crustal LVZ has no counterpart in the Basin and Range. The data recorded on the perpendicular profile indicate a markedly different structure: a fairly monotonous 6-km/s crust with no high- or low-velocity layers that are continuous over large distances (more than 10 km). It is interesting to speculate that the absence of a high-velocity mid-crustal refractor on the NW-oriented line may be influenced, at least in part, by velocity anisotropy. Jones and Nur (1982) have shown that velocity anisotropy of as much as 20Δ can occur in many phyllosilicate-rich mylonitic rocks and that velocities are typically fastest in the direction of elongation in the core complexes, as is found in the midcrustal layer of Whipple Mountains. Another possible explanation for the midcrustal layer is intermediate to mafic sills. The

crust must have been thickened by magma injection or some as-yet-unknown process of crustal convection beneath the Whipple Mountains, because, in spite of extreme extension in this mountain range compared to adjacent ones, the crust is of uniform thickness throughout the region.

3. A manuscript entitled "Crustal Structure of Yunnan Province, Peoples Republic of China, from seismic refraction profiles" by Kan et al. was revised and published in Science.

4. In recent years, the northern Appalachians have been recognized as being composed of several distinct terranes, having distinguishably separate orogenic histories prior to coalescence in their present form. Recently, active seismic experiments (both reflection and refraction) have been undertaken crossing the Appalachians in Maine and Quebec to characterize the crustal velocity structure. Preliminary results show upper crustal velocities that range from 5.7-6.3 km/sec with localized regions of low velocity within the upper crust. Secondary arrivals provide evidence for a higher velocity lower crust (6.8-7.2 km/sec) below 22 km. Crustal thickness varies from 38-40 km in NW Maine to 32-55 km in the coastal volcanic belt.

   A particularly fruitful approach to the analysis of the refraction data has been the examination of wide-angle reflections from the Moho and from horizons in the lower crust through the use of normal moveout corrected record sections. This examination has provided (1) regional measures of crustal thickness; (2) a measure of variation from region to region of the reflective character of the crust; and (3) evidence for local abrupt changes in depth to the Moho. The latter may be, in some instances, related to the boundaries between recognized terranes.

   Six shots were recorded along a 145-km profile parallel to the northeastern coastline of Maine within the Avalon terrane. An upper crustal model for the first 10 km has been determined using 2-D modelling programs which accounts for all first arrivals on the travel-time curves for each of the shots. To determine the lower crustal structure, deeper reflections were analyzed by applying normal moveout (NMO) corrections routinely used in reflection processing. The NMO record sections contain easily distinguishable major reflective boundaries at approximately 4, 7, and 10 to 10.5 sec. The latter, deeper reflection corresponds to the crust-mantle boundary. Preliminary results show a correspondence between the crustal thickness in the Avalon terrane and its counterparts in Europe.

5. Nearly fifty coincident seismic reflection/refraction studies provide an improved understanding of the continental lithosphere. Some conclusions include: 1) A transparent upper crust, a common observation on vertical reflection profiles, cannot be generally correlated with velocity gradients or low velocity zones. Rather, a transparent upper crust may be explained by short wave-length, steeply dipping features in the brittle upper crust, and to a lesser degree by signal contamination from source generated noise. 2) The reflective lower crust in extensional terranes

appears to be characterized by a high average seismic (6.6-7.3 km/s), and to consist of laminated high- and low-velocity layers with typical thicknesses of 100-200 m. 3) Landward-dipping reflectors observed in he middle to lower crusts of convergent zones have been identified as paired high- and low-velocity slabs which represent oceanic crust and mantle accreted via underplating to the continental margin. 4) The crust-mantle boundary may differ sufficiently when imaged with vertical-incidence and wide-angle data to justify the retention, for the present, of the concept of separate reflection and refraction Mohos. While there is good evidence that these features are coincident within measurement uncertainties in most regions, in two high-quality data sets they may differ by as much as 2 s two-way time (TWT), or 6 km in depth. 5) Upper-mantle reflections which cannot be migrated into the lower crust remain rare, despite isolated unequivocal examples. The wide-angle method appears likely to provide the most reliable information on the velocity structure and physical state of this portion of the lithosphere for some years to come. 6) There appear to be clear and consistent basic differences between convergent and extensional terranes which have been identified from coincident experiments; these differences may be sufficiently universal to infer the tectonic history of poorly exposed terranes. 7) No three-dimensional coincident experiment has been conducted, but some 3-D data have been collected using both methods. Measurements of attenuation, Poisson's ratio, and anisotropy within the crust using coincident data sets remain frontiers in seismology.

6. New data were collected in field programs in 1) the Morro Bay-San Luis Obispo region, and 2) across the Tehachapi Mtns. The first consisted of a strike profile entirely within Franciscan rocks of the Sur-Nacimiento block, near the coast. The second profile was recorded in cooperation with CALCRUST between Bakersfield and Lancaster, CA. Both of these profiles fill important data gaps and will provide new constraints on the crustal structure in areas of geologic interest.

7. The USGS, in cooperation with the US Agency for International Development and the Jordanian Nataural Resources Authority is currently operating an eight-station seismic network in Jordan, which is being upgraded to a 32-station network. Over the past three years, approximately 2000 events have been recorded and located, which are supplying critical data about the crustal structure and the state of tectonic stress in the vicinity of the Dead Sea Rift Zone. In October, 1986, Will Kohler traveled to Jordan to install and test new computer programs for real-time detection of earthquakes using a PDP 11/23 computer. The new programs are currently operating in Jordan and are expected to supply more accurate and timely information about events detected by the Jordanian network.

8. PASSCAL Northern Nevada Lithospheric Experiment

   With funding from the USGS, the Air Force Geophysical Lab, and PASSCAL (Program for Array Seismic Studies of the Continental Lithosphere - NSF funded), the USGS participated in a major seismic investigation in northern Nevada.

Northwestern Nevada has long been identified as an area of unusually thin crust (Eaton, 1963), but recent COCORP data (Klemperer et al., 1986) suggest that this may not be the case. A re-evaluation of the older USGS refraction data (Fallon-Eureka profile) suggests that the area may has a velocity structure much like that observed in many continental rifts. This interpretaion is supported by a second refraction data set (Stauber, 1980), which crosses the older USGS (Fallon-Eureka) profile. In a new study, H. Patton and K. Priestley have located an area of high LG-wave attenuation associated with the Carson Sink. In addition, they note an increase in P-wave velocity and a decrease in S-wave velocity over the Carson Sink. Northwestern Nevada has also experienced large historic earthquakes and a relatively greater amount of Quaternary normal faulting (Smith, 1978) than most of the rest of the Basin and Range. Our primary objective is to better determine the lithospheric velocity structure of the area in order to better understand many of the anomalous geological and geophysical characteristics of the Basin and Range Province.

Other objectives of this experiment include an evaluation of: (1) the effectiveness of combining refraction and reflection recording and processing, (2) the effectiveness of sources (e.g. vibroseis vs explosives) in conducting crustal studies, (3) explosive shot sizes vs frequency content of the signal, (4) how efficiently explosive sources yield S-wave energy in the Basin and Range, and (5) strong ground motion from explosive sources.

Participating institutions: Stanford University; U. C. Santa Barbara; University of Utah; University of Nevada, Reno; United States Geological Survey; Air Force Geophysical Lab.; Air Force Weapons Lab.; Princeton University; University of Wisconsin - Oshkosh; M. I. T.; Boston College; SUNY-Binghamton; Werdlinger Assoc., University of Texas, El Paso; Texas A and M; BLM.

REPORTS

Colburn, R., and Mooney, W.D., 1985, Crustal structure of the Great Valley, California: Axial profile Bull. Seis. Soc. Am. 76, 1305-1322, 1986.

Daley, M.A., Ambos, E.L., and Fuis, G., 1985, Seismic refraction data collected in the Chugach Mountains and along the Glenn Highway in southern Alaska in 1984: U.S. Geological Survey Open-File Report 85-531, 32 pp., 12 plates.

Fuis, G.S., Ambos, E.L., Mooney, W.D., and Page, R.A., 1985, Velocity structure of accreted terranes of southern Alaska, EOS, Transactions Am. Geophys. Union 66, p. 1074.

Hwang, L., and Mooney, W.D., 1985, Qp and velocity modeling of seismic refraction data: Central Valley, Ca., Bull. Seis. Soc. Am. 76, 1053-1067.

Ackerman, H.D., Mooney, W.D., Snyder, D.B., and Sutton, V.D., Preliminary interpretaton of seismic refraction and gravity studies west of Yucca Mountain, Nevada and California U.S.G.S. Circular "Studies of the Southern Great Basin", M. Carr (edit) (in press; 21 pp., 10 fig.).

Meltzer, A.S., Levander, A.R., and Mooney, W.D., 1985, Interpretation of seismic refraction profiles east of Livermore, Ca., submitted to Bull. Seis. Soc. Am. 8/82.

Whitmann, D., Walter, A.W., and Mooney, W.D., 1985, Crustal structure of the Great Valley, California: Cross Profile, EOS, Transactions Am. Geophys. Union 66, p. 973.

Fuis, G.S., and Ambos, E.L., 1986, Deep structure of the Contact fault and Prince William terrane: preliminary results of 1985 TACT seismic-refraction survey, in U.S. Geological Survey in Alaska, Accomplishments during 1985: U.S. Geological Survey Circular.

Fuis, G.S., McCarthy, J., and Howard, K., 1986, A seismic-refraction survey of the Whipple Mountains metamorphic core complex, southeastern Calif.: A progress report from PACE: Geological Society of America Abstract with Program, Rock Mountain Section Meeting, Spring 1986.

Fuis, G.S., Walter, A.W., Mooney W.D., and McCarthy, J., Crustal velocity structure of the Salton Trough, western Mojave Desert, and Colorado Desert, from seismic refraction (abs.): Geological Society of America Abstracts with Programs, Cordilleran Section Meeting, Spring 1986.

Gettings, M.E., Blank, H.R., Mooney, W.D., and Healy, J.H., 1986, Crustal Structure of Saudi Arabia, Jour. Geophy. Res. 91, 6491-6512.

Kan, R.J., Hu, H.X., Zeng, R.S., Mooney, W.D., and McEvilly, T.V., 1986, Crustal structure and tectonics of Yunnan Province, Southwest China, from seismic refraction profiles, SCIENCE 234, 433-437.

Kohler, W.M. and Fuis, G.S., 1986, Travel-time, time-term, and basement depth maps for the Imperial Valley region, California, from explosions, Bull. Seis. Soc. Am., 76, 1289-1303.

McCarthy, J., Fuis, G.S., and Howard, K., Seismic-refraction studies across the Whipple Mountains, Calif.: A progress report from the Pacific-Arizona Crustal Experiment (PACE) (abs.): Geological Society of America Abstracts with programs, Cordilleran Section Meeting, Spring 1986.

Mooney, W.D. and Brocher, T.M., Coincident seismic reflection/refraction studies of the continental lithosphere: A Global Review, submitted to Reviews of Geophysics (extended abstract also submitted to Geophy. J. Royal Astro Soc.).

Mooney, W.D., and Ginzburg, A., 1986, Seismic measurements of the internal properties of fault zones, in, The Internal Properties of Fault Zones, C.Y. Wang (edit.) PAGEOP (in press); 24 pp. 6 fig.

McCarthy, J., Fuis, G.S., Wilson, J., Crustal structure of the Whipple Mountain metorphic core complex, submitted to Geophys. J. Royal Astro. Soc.

Page, R.A., Plafker, George, Fuis, G.S., Nokleberg, W.J., Ambos, E.L., Mooney W.D., and Campbell, D.L., 1986, Accretion and subduction tectonics in the Chugach Mountains and Copper River Basin, Alaska: Initial results of the Trans-Alaska Crustal Transect: Geology, v. 14, 501-505.

Plafker, George, Ambos, E.L., Fuis, G.S., Mooney, W.D., Nokleberg, W.J., Page, R.A., and Campbell, D.L., Late Mesozoic and early Tertiary accretion and subduction along the southern Alaska continental margin (abs.): Geological Society of America Abstracts with programs, Cordilleran Section Meeting, Spring 1986.

Valdez, C.M., Mooney, W.D., Singh, S.K., Meyer, R.P., Lomnitz, C., Luetgert, J.H., Helsley, C. and Lewis, B.T.R., 1986, Crustal structure of Oxaca, Mexico, from seismic refraction measurements, Bull. Seis. Soc. America, 76, p. 547-563.

Fisher, M.A., Brocher, T.M., Page, R.A., Plafker, G., Fuis, G.S., Nokleberg, W.J., and Campbell, D.L., 1986, Seismic Reflection images of deep-crustal features of south-central Alaska: preliminary results of a survey for TACT (abs.): EOS Transactions America Geophysical Union (in press).

Taber, J.J., Fuis, G.S., Ambos, E.L., Mooney, W.D., Page, R.A., 1986, Seismic velocity structure of the Prince William terrane, Alaska (abs): EOS Transactions American Geophysical Union (in press).

Goodwin, E.B., Ambos, E.L., Fuis, G.S., Mooney, W.D., Page R.A., and Campbell, D.L., 1986, The crustal structure of Wrangellia, southern Alaska, from seismic refraction measurements (abs.): EOS Transactions American Geophysical Union (in press).

Colburn, R.H., and Fuis, G.S., 1986, Velocity structure across the northern boundary of the Peninsular terrane, Copper River Basin, Alaska (abs.): EOS Transactions American Geophysical Union (in press).

Page, R.A., Fuis, G.S., Ambos, E.L., and Stephens, C.D., 1986, Relocated earthquakes along the TALI corridor in the Chugach Mountains, southern Alaska (abs.): EOS Transactions American Geophysical Union (in press).

Wolf, L.W., Levander, A.R., and Fuis, G.S., 1986, Upper crustal velocity structure of the accreted Chugach terrane, Alaska (abs.): EOS Transactions American Geophysical Union (in press).

Fuis, G.S., Ambos, E.L., Mooney, W.D., Page, R.A., Fisher, M.A., Brocher, T.M., and Taber, J.J., Velocity structure of accreted terranes of southern Alaska: (submitted to the Geophysical Journal of the Royal Astronomical Society).

Meador, P.J., Ambos, E.L., and Fuis, G.S., 1986, Data report for the North and South Richardson Highway profiles, TACT, seismic-refraction survey, southern Alaska: U.S.G.S. Open-File Report 86-274, 51 p.

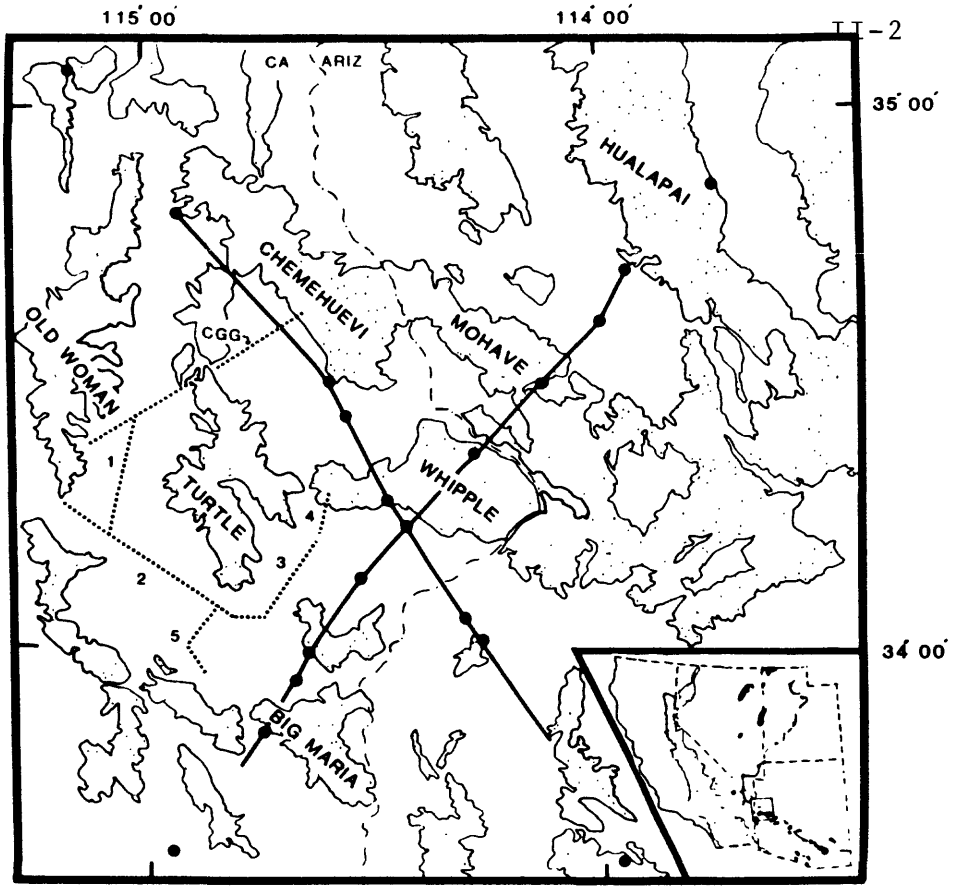

Fig. 1) Location of PACE refraction and CALCRUST reflection profiles. Reflection profiles are dashed, refraction profiles are solid. Blackened circles mark shotpoint locations. CALCRUST profiles are labeled by line number. Location of Whipple study area is marked by the box in the bottom right index figure. Sierra Nevada batholith is stippled, metamorphic core complexes are blackened, and the Cordilleran fold and thrust belt is barbed.

Fig. 1) Location of PACE refraction and CALCRUST reflection profiles. Reflection profiles are dashed, refraction profiles are solid. Blackened circles mark shotpoint locations. CALCRUST profiles are labeled by line number. Location of Whipple study area is marked by the box in the bottom right index figure. Sierra Nevada batholith is stippled, metamorphic core complexes are blackened, and the Cordilleran fold and thrust belt is barbed.

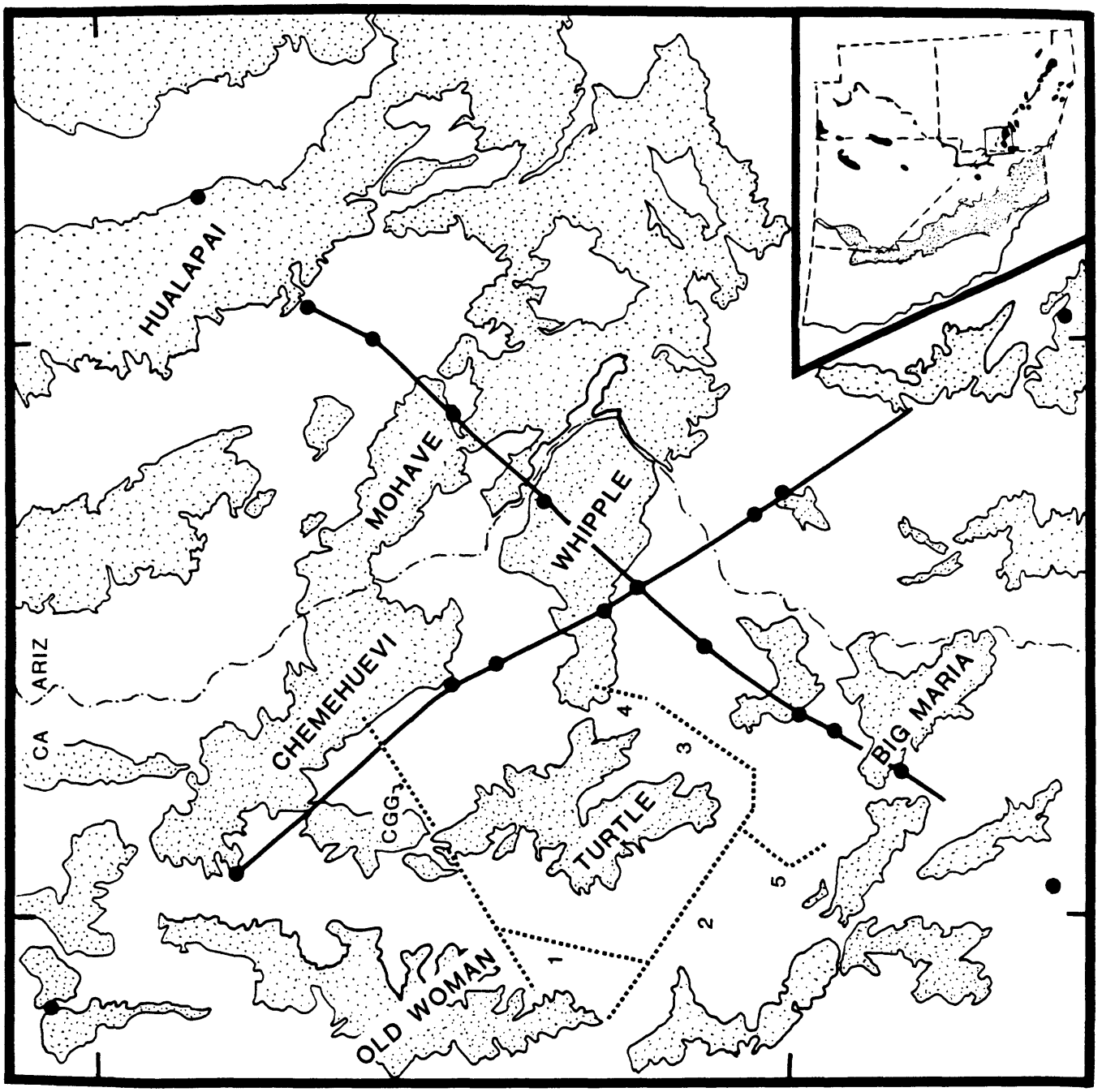
35° 00'
34° 00'
114° 00'
115° 00'
HUALAPAI
MOHAVE
WHIPPLE
CHEMEHUEVI
BIG MARIA
TURTLE
OLD WOMAN
CGG
CA
ARIZ
1
2
3
4
5

Tiltmeter and Earthquake Prediction Program in S. California and at Adak, AK

14-08-0001-21244

Sean-Thomas Morrissey
Saint Louis University
Department of Earth and Atmospheric Sciences
P.O. Box 8099 - Laclede Station
St. Louis, MO 63156
(314) 658-3129

I: Task 1: The Tiltmeter System

Objective: To continue to improve the performance of bubble sensor tiltmeter systems and to investigate other sensor systems for use in moderate depth boreholes, seeking relatively low-cost, readily deployed instrumentation.

Accomplishments: In conjunction with the major maintenance trip for the Adak seismic network, the batteries of the eight Adak tiltmeters were replaced in August and the on-site backup Rustrak recorder charts were replaced. While the noise level of these instruments is rather high because they are quite shallow (1-2 meters) and have serious siting quality problems according to current standards, the continued consistent operation of the electronics, etc., is a valuable experiment in long-term remote operation of such complex systems. Although the instruments had not been visited for over a year, there were no failures among the eight tiltmeters, although we still have problems with rats chewing exposed micro-thermometer cables.

II: Task 2: The Installation Method

Objective: To improve the installation methods for borehole instruments with a goal of installing them as deep as 100 meters.

Accomplishments: Little work has been done on the new remote preleveling installation system since the technician resigned in May. No new installations or installation changes were done at Adak. There are no technical problems anticipated in completing the new installation system, with modifications to work at the 25 meter depth.

III: Task 3: The Digital Data Systems

Objective: To continue to develop and operate a digital data acquisition system to acquire geodetic data and to thoroughly monitor the environment of the instrument installations.

Accomplishments: The digital systems at the test site near St. Louis and at Adak continue to operate well. Since 1980, 54,000 hours of continuous data have been recorded from each of five remote 14-channel digitizers operating from batteries in the tundra at Adak. Less than 40 hours of data is missing; the total file of raw data amounts to over 128 megabytes. A special effort is underway to reprocess all the digital data with the latest techniques for assuring quality and absolute continuity

of the time series in preparation for submitting the entire data set to the USGS as part of the final technical report.

IV: Task 4: Data Interpretation

Objectives: To process the digital data and make efforts to remove the environmental noise from the data, so as to establish the intrinsic long-term stability of the tiltmeters. Various analysis techniques are then utilized to present the data in meaningful formats such that any precursory tilt events would become evident.

Accomplishments: In order to assure continuous data quality, routine data analysis is always done on each 8-day floppy disk as they arrive in St. Louis. Of particular interest is the data relating to the M_S 7.7 earthquake that occurred at 22:47 z on 7 May 1986, approximately 2 degrees southeast of the tiltmeter array. Aftershocks have defined a rupture zone that spans about 3°, ending south of Adak. All the tiltmeters showed similar co-seismic tilts, but the most consistent data is from the three-instrument West site, which shows a net tilt of 2.46 $\pm$ 0.64 micro-radians down to the east-southeast, the direction of the epicenter. This data is shown in Figure 1. Any evidence of precursory tilting will have to wait until linear thermal corrections are made on the data, a task which is in progress.

Also of interest is the tide gauge data from our self-contained differential pressure unit as well as from the NOAA nitrogen bubbler. Figure 2 shows the original water tide data, and the detail of the tsunami waves that showed up within minutes of the earthquake. An attempt was made to detect any net change of elevation of the pier, as independent evidence of co-seismic tilting, and statistical analysis of the month of data before and after the event shows a subsidence of 32.5 $\pm$ 2.1 mm after the tides and barometric pressure are removed, a process shown in Figure 3. This, of course, could be entirely a seasonal effect, so work is in progress to analyze longer data sets about the event.

V: Problems and Plans

No further funding for this program has been provided, and the present contract ends October 31. As long as this Principal Investigator has to go to Adak to maintain the CIRES seismic network, we will probably continue to run the tiltmeter array, since the cost is minimal, unless, of course, someone comes up with a more urgent need for the units.

VI: Reports

A preliminary report, "Near-Field Tilt and Water-Tide Gauge Data from Adak, Alaska, Associated with the M = 7.7 Western Aleutian Earthquake of May 7, 1986," was prepared prior to the Adak maintenance trip. The data are currently being refined for presentation at the fall AGU meeting.

Sean-Thomas Morrissey
Senior Research Scientist
24 October 1986

figure 1

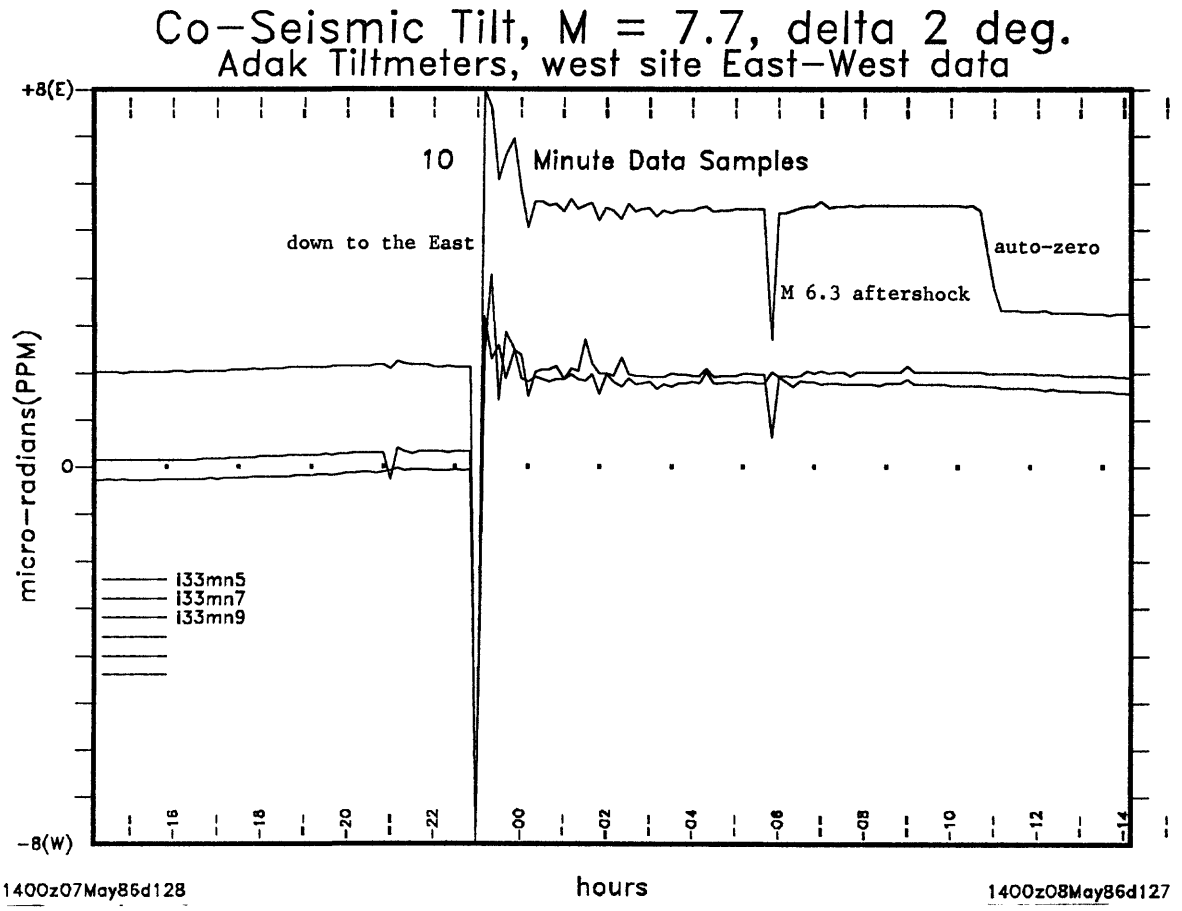
Co-Seismic Tilt, M = 7.7, delta 2 deg.
Adak Tiltmeters, west site East-West data
+8(E)
10 Minute Data Samples
down to the East
auto-zero
M 6.3 aftershock
micro-radians(PPM)
0
i33mn5
i33mn7
i33mn9
-8(W)
-16
-18
-20
-22
-00
-02
-04
-06
-08
-10
-12
-14
1400z07May86d128
hours
1400z08May86d127

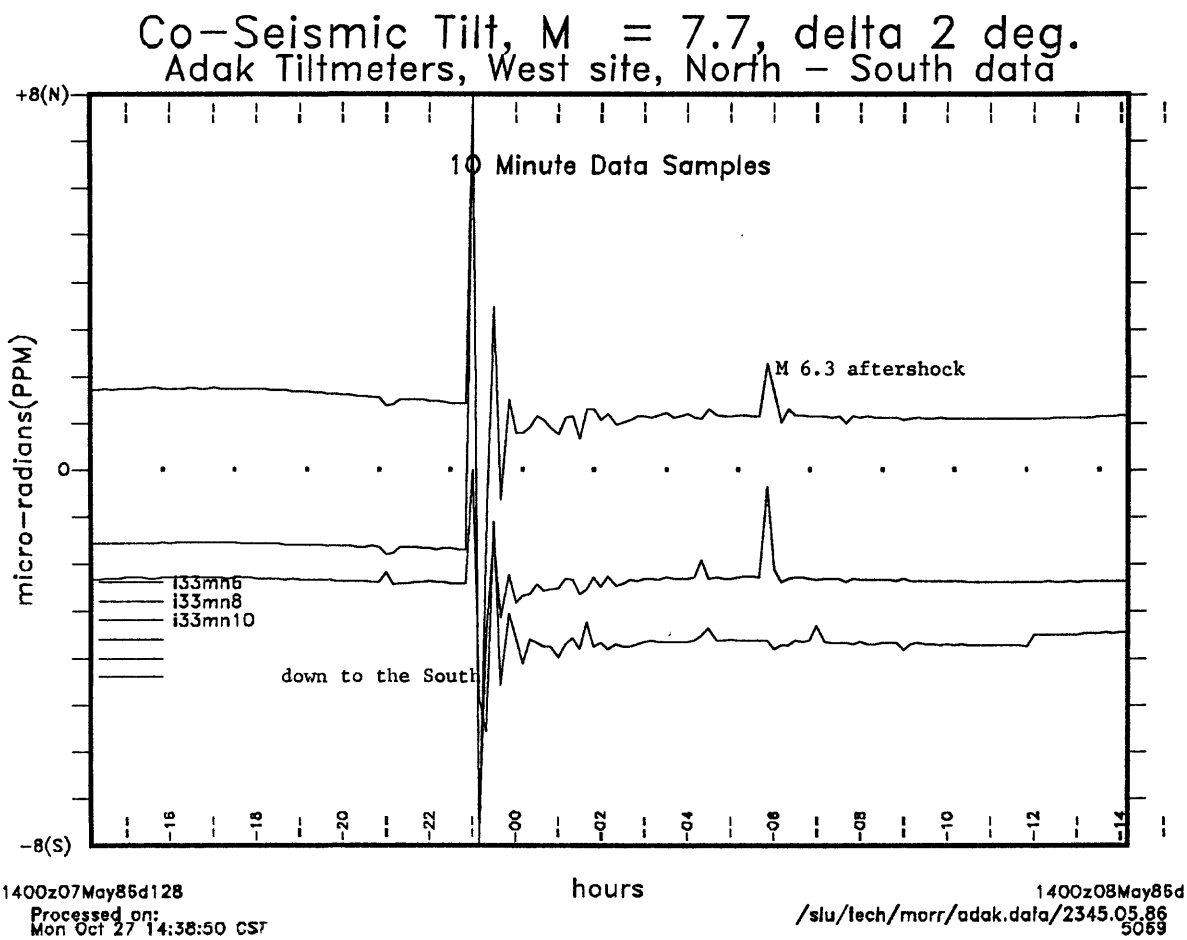
Co-Seismic Tilt, M = 7.7, delta 2 deg.
Adak Tiltmeters, West site, North - South data
+8(N)
10 Minute Data Samples
M 6.3 aftershock
micro-radians(PPM)
0
i33mn6
i33mn8
i33mn10
down to the South
-8(S)
-16
-18
-20
-22
-00
-02
-04
-06
-08
-10
-12
-14
1400z07May86d128
hours
1400z08May86d11
Processed on:
Mon Oct 27 14:38:50 CST
/slu/tech/morr/adak.data/2345.05.86
5069

figure 2

Adak Tide Gauge Data
SLU/CIRES differential pressure gauge

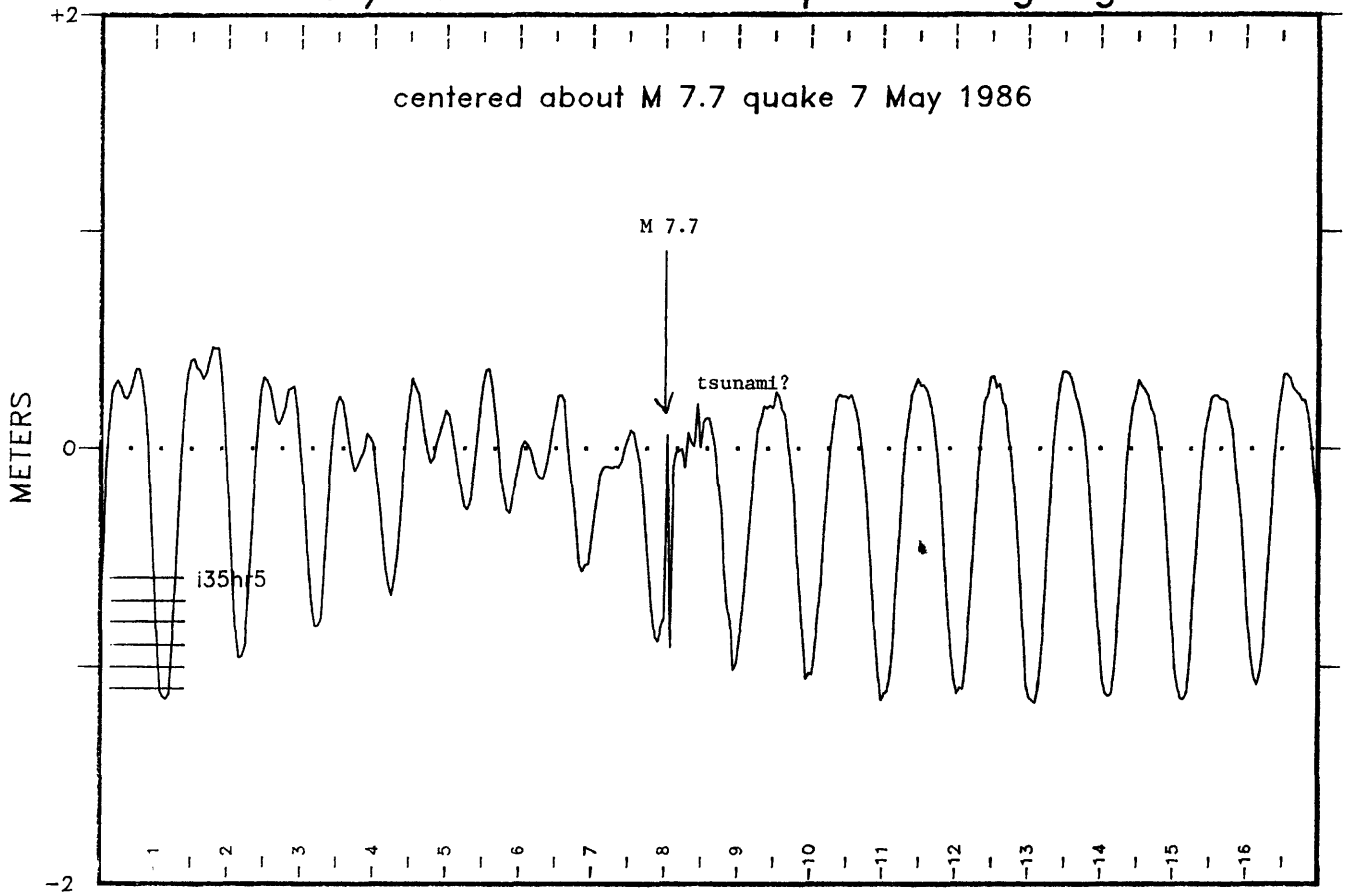

0440z30Apr86d120
Processed on:
Fri Jul 18 13:04:53 CDT 1986

days
(hourly samples)

2200z16May86d13
/slu/tilt/nadk.data/w236.7
26787

Adak Tide Gauge Data
SLU/CIRES differential pressure gauge

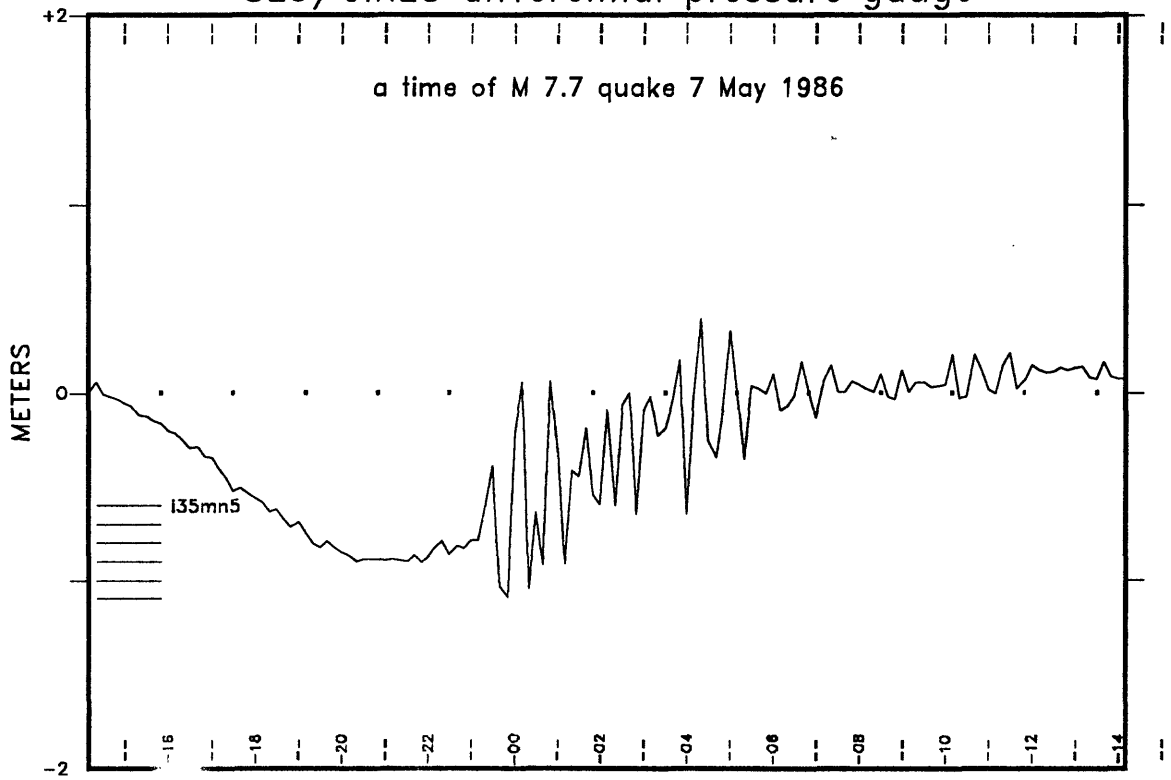

1400z07May86d11

hours

1400z08May86d11

Crustal Deformation Observatory, Part (i)
Shallow Borehole Tiltmeters

14-08-0001-21939

Sean-Thomas Morrissey
Saint Louis University
Department of Earth and Atmospheric Sciences
P.O. Box 8099 - Laclede Station
St. Louis, MO 63156
(314) 658-3129

Objective: To apply the latest innovations and technology of instrumentation and installation methods to the shallow borehole tiltmeters at Pinon Flat such that their performance, particularly with regard to longterm stability, will compare more favorably with the data from the long baseline tiltmeters. Remotely pre-leveled installations in 10 and 20 meter deep holes are planned.

Accomplishments and Problems: Since the last report in May, the technician for these programs resigned and cannot be replaced. So the installations in the 10 and 20 meter holes at Pinon Flat that were planned for June had to be delayed since the Principal Investigator then had full responsibility for the major maintenance trip of the Adak seismic network, a joint program with CIRES of the University of Colorado. With the required preparations in June, and the effort at Adak, Alaska, running from mid-July to mid-October, little work has been done on this project.

Sean-Thomas Morrissey
Senior Research Scientist
24 October 1986

Cooperative Tiltmeter Program at Parkfield, California

14-08-0001-G1204

Sean-Thomas Morrissey
Saint Louis University
Department of Earth and Atmospheric Sciences
P.O. Box 8099 - Laclede Station
St. Louis, MO 63156
(314) 658-3129

Objective: To apply the latest state-of-the-art technology to shallow borehole tiltmeter installations and data acquisition in the Parkfield area, which is forecast to be the locale of a moderate earthquake in the near (3-8 years) future. Considerations of the current failure model, based on known creep data and fault-constituitive models, allows locating the tiltmeters such that the probability of acquiring large coherent signals during the precursory stages is enhanced. The cooperative aspect involves the assistance of the U.S. Geological Survey in site selection, preparation, maintenance, and data acquisition.

Accomplishments: A proposal to continue this work was submitted in response to Announcement 1721, but was not funded because this program has been delayed. The panel has recommended that installations at the Turkey Flat site await completion of the 10 and 20 meter installations at Pinon Flat, but these have been delayed because the irreplaceable technician resigned, and the Principal Investigator had to devote most of his effort to a major maintenance trip for the Adak seismic network, a cooperative program with CIRES at the University of Colorado, an effort which ran from June to mid-October. A no-cost extension of the program will be requested in order to complete these installations.

Sean-Thomas Morrissey
Senior Research Scientist
24 October 1986

EXPERIMENTAL TILT AND STRAIN INSTRUMENTATION

9960-01801

C.E. Mortensen
Branch of Tectonophysics
U.S. Geological Survey
345 Middlefield Road, MS/977
Menlo Park, California 94025
(415) 323-8111, ext. 2583

Investigations

1. The major focus of effort during the period 1 April through 30 September was, again, the installation, operation and maintenance of the satellite telemetry system. A major setback occurred on May 4th with the destruction of GOES 7 shortly after launch. The GOES WEST satellite, which should have been replaced more than one year ago, is still serving as the primary relay for western Data Collection System (DCS) operations. Its badly inclined orbit causes periodic dropouts in reception of several hours each day. These gaps in the data are generally filled in by the expedient of transmitting each data value two or three times, several hours apart. Every ten minutes the Data Collection Platform (DCP) transmits the current value, a value that is three hours old, and in some cases, also a six-hour old value. This works well for the DCPs that transmit data at 10-minute intervals, but there is insufficient memory in the DCP for this to be effective for the DCPs that collect data at 10-minute intervals but transmit at 3-hour intervals. All DCPs that relay data from critical instruments operated by this Branch in the Parkfield and Mammoth areas transmit at 10-minute intervals.

   The Direct Readout Ground Station (DRGS) portion of the DCS has been relatively reliable during the period of this report. Nevertheless, additional equipment has been procurred as backup/spares for key elements of the DRGS. A variety of bugs and failures have been experienced with the DCPs, which collect data from sensors and transmit to the GOES spacecraft. Among the various hardware and software problems, the most debilitating has proven to be one wherein the antenna manifests an unsatisfactorily high reflected power (standing wave ratio). This results from a mismanufacture of the antennas, which hopefully is being rectified by the manufacturer. This problem has caused some transmitters to fail, and is partially responsible for a high return rate (up to ~10% at any given time) of the DCPs.

There has been only one loss of a DCP to environmental causes.

2. An important accomplishment has been the development, under contract to Reese Cutler of Cutler Digital Design, of an interface to the DCPs that will greatly enhance their capabilities. Known as the "Companion", the device has an NCI 65A02 CPU, 128K of non-volatile CMOS RAM, four RS-232C serial ports, several parallel ports and an operating system and programming capability in the FORTH language. The Companion interfaces through its serial ports to either a 12- or 16-bit DCP and to other devices such as radio timecode receivers, PCs, and modems. The prototype has been tested as an on-all-the-time telemetry system independent of the GOES spacecraft, and is capable of serving as an interrogatable telemetry system. It can also be used to synchronize the DCP to a precise time standard, to process raw data, and to feed processed data to the DCP for transmission to the GOES or transmit over landline via a modem. It is a powerful system that permits modifications and extensions to be made by implementing programs in FORTH. For example, it will be used to test the feasibility of using an adaptive algorithm to adjust the DCP transmission rate interactively.

3. Two years ago a collimating reflector was designed for the 2-color laser project and 14 reflectors were produced. That design has been modified to facilitate mounting on a standard tripod. Also the focusing mechanism for the secondary mirror has been completely redesigned. Parts for 7 reflectors of the new design are on hand.

4. A system that will enable rapid and reliable radio communications to and from the field has been conceptualized in consultation with Bob McClearn and others. Equipment is either on hand or on order that will implement the system for key personnel involved in monitoring the earthquake hazard at Parkfield.

5. Networks of tiltmeters, creepmeters and shallow strainmeters have been maintained in various regions of interest in California. A network of 14 tiltmeters located at seven sites monitor crustal deformation within the Long Valley caldera. Other tiltmeters are located in the San Juan Bautista and Parkfield regions. Creepmeters are located along the Hayward, Calaveras and San Andreas faults from Berkeley to Parkfield, and shallow strainmeters are located in the Parkfield region. Observatory type tiltmeters and strainmeters are located at the Presidio Vault in San Francisco and a tiltmeter is sited in the Byerley Seismographic

Vault at Berkeley. Data from all of these instruments are telemetered to Menlo Park via the GOES satellite, by phonelines and radio links, or both.

Results

1. Data spanning 12-1/2 years, since 1974, have been compiled from the mercury-tube tiltmeter in the Byerley Seismographic Vault at UC Berkeley. These data show a remarkably steady tilting downward in a direction N39E at a rate of 17.3 microradians per year. This direction of tilting is exactly perpendicular to the axis of folding of the severely folded and overturned, bedded chert of the Claremont formation that surrounds the tunnel. This rate is higher than the regional strain rate measured geodetically, and may reflect a shearing of the tunnel resulting from relaxation of strain within the folded formation after the adit was constructed. Such a signal may be superimposed on a rotation caused from strain of relaxation of the folding or from slip on the nearby Wildcat fault (~180m away). If slip on the Wildcat fault provides a substantial portion of the tilt signal, a significant reverse component would seem to be required.

MAGNETIC FIELD OBSERVATIONS

9960-03814

R. J. Mueller
Branch of Tectonophysics
U.S. Geological Survey
345 Middlefield Road, MS/977
Menlo Park, CA 94025
(415) 323-8111 ext. 2533

INVESTIGATIONS

1) Investigation of total field magnetic intensity measurements and their relation to seismicity and strain observations along active faults in central and southern California.

2) Recording and processing of synchronous 10 minute magnetic field data and maintenance of the 12 station telemetered magnetometer network.

RESULTS

1. Due to reductions in funding for FY86, operation of 12 of the 24 telemetered magnetometer stations was discontinued. This leaves 2 stations operating in southern California, 7 stations in the Parkfield region of central California, and 3 stations in the Mammoth Lakes region. The 2 stations in southern California and the 3 stations in the Mammoth Lakes region are also going to be discontinued in the near future, which will leave only the station in the Parkfield region operational.

2. The epicenter of the North Palm Springs earthquake (M_L=5.9) on July 8, 1986, is located at distances of 3 km and 9 km from telemetered magnetometer stations OCH and LSB, respectively. Seismomagnetic offsets of 1.2 nT and 0.3 nT were observed at these stations and represent the first near-field coseismic observations from the magnetometer array in over a decade of records. The observations are consistent with a seismomagnetic model of the earthquake in which right-lateral rupture is assumed on a 10 km segment of the Banning fault at a depth between 6 km and 12 km. The rupture segment is assumed to have 15 cm of displacement in a direction N70W and dip at 45 degrees to the north, in a region with average magnetization of 1 A/m. Observations of surface magnetization at the two sites range between 0.1 A/m and 1.0 A/m.

3. Planning of logistics for the installation of 3 component borehole strainmeters in the Parkfield region of California. Installations are scheduled for the fall of 1986.

4. Conversion of one magnetometer station in the Parkfield region of central California from telephone line telemetry to satellite telemetry. All stations in the network are now using satellite telemetry and solar power.

5. Testing of electronics and pressure transducers to be used in a lake level monitoring experiment at Crowley Lake near Mammoth Lakes, California. After testing, the electronics were installed into silling wells located around Lake Crowley and some data are presently being recorded. More work is required to make this network operational.

REPORTS

Mueller, R.J., and M.J.S. Johnston, 1986, Seismomagnetic Observations During the July 8, 1986, M=5.9, North Palm Springs Earthquake in Southern California, Trans. Am. Geophy. Un., (in press).

Dilatometer Operations

9960-03815

G. Douglas Myren
Branch of Tectonophysics
U.S. Geological Survey
345 Middlefield Road, MS/977
Menlo Park, California 94025
415-323-8111, ext. 2705

Investigations and Results

Since April of 1986 most of the time has been spent on instrument maintenance. However, we completed the installation of the automatic valve opener at all dilatometer locations. It has now been incorporated in the electronics for the next eight dilatometers and one spare.

GEOS data recorders installed at Searle Road, Gold Hill, Punchbowl, and Devils Postpile are now recording signals from the dilatometer at the 0 and 36 db levels.

All dilatometer installations are now telemetering data to Menlo Park via 16 bit satellite data collection platforms. Telephone line telemetry still operates as a backup telemetry system at all sites.

Thirteen core holes were drilled in the Parkfield area to determine potential sites for strainmeter installation. Of these thirteen, seven were chosen as suitable for dilatometer strainmeter installation. Drilling has been completed at two of these locations and instruments will hopefully be installed in November. Tensor (3-comp) strainmeters and 3-component seismometers will be colocated with the dilatometer at some of these seven locations.

Existing previously drilled holes at Vineyard Canyon and Frolich will be reconditioned and have dilatometer and tensor strainmeters installed.

In order to facilitate ease of installation a commercially available hydraulic hoist and crane was ordered and installed on a 2 ton flat bed truck (from Tom Moses' drilling operation).

The next year will be spent finishing the installation of strainmeters.

Helium Monitoring for Earthquake Prediction

9570-01376
G. M. Reimer
U.S. Geological Survey, MS 963
Denver Federal Center
Denver, CO 80225
(303) 236-7886

Investigations

The variations of helium in soil-gas from sample collecting stations along the San Andreas Fault near San Benito, California continue to be observed and related to nearby seismic activity. Data to determine if soil moisture can be a primary cause for the seasonal variations continue to be collected and will be evaluated after a full data cycle has obtained. Several of the sampling stations had been vandalized this year and were repaired or replaced.

Results

The observations show that helium decreases precede seismic activity by a period of 1 to 7 weeks. The accumulating data set over a 7 year period also indicates that there may be a relationship between distance to the epicenter and magnitude of an earthquake or degree of strain released. The relationship was looked for during the course of the study but only first discernable in 1985. An earthquake M=3.1 near Hollister, CA on September 14, 1986 was preceded by a helium soil-gas decrease beginning 3 weeks before. The May 31, 1986 earthquake of M=4.8 was preceded by a decrease in late April. This decrease of helium concentration remained low or had a second reduction after a slight recovery and corresponds to a precursor of the several M>3 <3.6 earthquakes from May 31 to June 11 near Hollister. However, a distance to magnitude relationship is not clear from the other correlations involving helium decreases and earthquake epicenters up to 160 km distant from the sample collecting stations. This relationship will continue to be evaluated as data are accumulated. From the present evaluation criteria, the Parkfield area is only marginally within the zone for which we feel the present monitoring system is capable of being responsive.

Reports

None this semi-annual period.

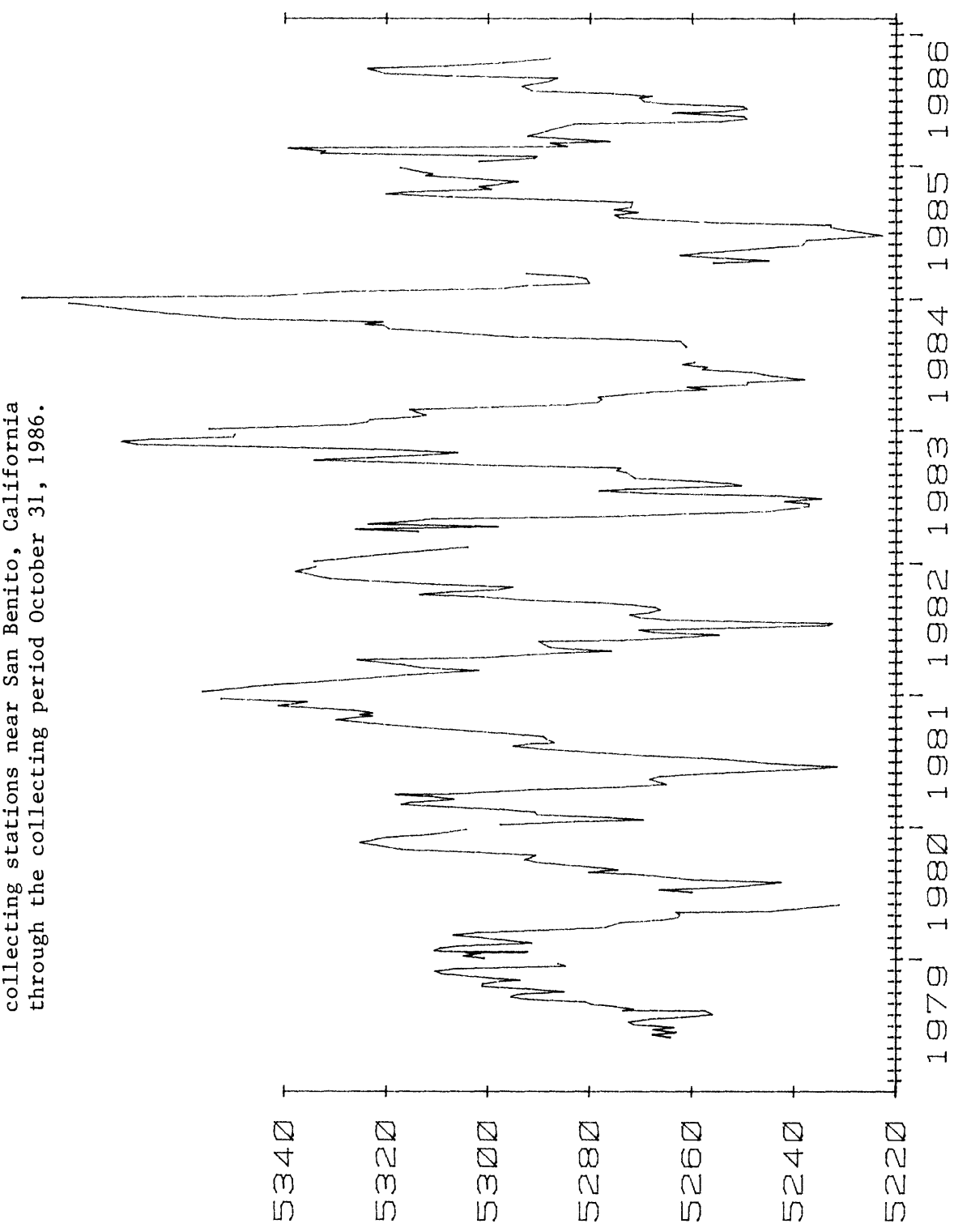

Helium soil-gas concentrations for sample collecting stations near San Benito, California through the collecting period October 31, 1986.

Late Quaternary Faulting, Southern San Andreas Fault Zone

9910-04098

Michael J. Rymer
Branch of Engineering Seismology and Geology
U.S. Geological Survey
345 Middlefield Road, MS 977
Menlo Park, California 94025
(415) 323-8111, ext. 2081

Investigations:

1. Late Quaternary history of the Banning and Mission Creek segments of the San Andreas fault zone in the Indio Hills, Riverside County.

2. Continued investigation of structure of the San Andreas fault zone in the middle of the creeping section, Monterey and San Benito Counties.

3. Post-earthquake investigations of the July 8 North Palm Springs and July 21 Chalfant earthquakes.

Results:

1. This is a new project and so is starting with basic information about the late Quaternary setting of the San Andreas fault zone in the Coachella Valley. To date, about half of the Indio Hills have been geologically mapped at a scale of 1:24,000. This mapping is a more detailed and improved version of earlier thesis mapping in the area. Features found that are of use in constraining the age of the deposits, and therefore offsets along the faults that cut the deposits, include: a fossil horse skull, fossil horse(?) vertabrae, a volcanic ash in Pushawalla Canyon, and a volcanic ash at Garnet Hill. Also of use in constraining the age of the deposits are a paleomagnetic study of the Ocatillo Formation, a soils chronology study, and the search for fossil microtine teeth. The volcanic tuff at Garnet Hill (first reported by Proctor, 1958, as being in the Imperial Formation) appears to be in a lacustrine or fluvial deposit below the Imperial. Andrea Sarna-Wojcicki is currently using trace-element chemistry for tephrachronologic correlations of this tuff. The tuff in Pushawalla Canyon is degraded to predominantly clay minerals and therefore cannot be used for tephrachronologic analyses, but the tuff is useful as a time horizon in mapping. The preliminary paleomagnetic study of fluvial deposits in the Ocatillo Formation (conducted with Ray Weldon) shows that the coarse sandy material has a paleomagnetic signal and that the Brunhes/Matuyama chron boundary is represented in the Indio Hills. A more extensive effort is planned for this coming year. Initiation of the soils chronologic work (with Tom Rockwell) is aimed at constraining the age of the initial uplift of the Indio Hills, when sediment from alluvial fans to the north was no longer deposited at this site. The time of uplift therefore is the total time allowed for development of geomorphic features in Indio Hills, including offset streams. Offset streams in the hills show as much as 1 km of right-lateral displacement across the Mission Creek

fault. The search for fossil microtine teeth (with Robert Reynolds) is still underway; three samples of 450 to 950 kg were collected, washed, and separated--they are now being picked.

2. Field mapping of the San Andreas fault zone in the middle of the creeping section is now complete. Last summer's mapping was in the Priest Valley 7-1/2 quadrangle. A composite strip geologic map of the Mustang Ridge area, approximately 22 km long, is now being drafted for review.

3. In July and August local faults were checked for surface displacements after the July 8 North Palm Springs and 21 July Chalfant earthquakes. (See reports listed under R.V. Sharp and J.J. Lienkaemper (M.M. Clark, project chief) for details of these respective investigations.)

Reports:

Rymer, M.J., Harms, K.K., Lienkaemper, J.J., and Clark, M.M., in press, The Nunez fault and its surface rupture during the Coalinga earthquake sequence of 1983, in Rymer, M.J., and Ellsworth, W.L., eds., The May 2, 1983 Coalinga, California earthquake sequence: *U.S. Geological Survey Professional Paper,* 32 ms p.

Rymer, M.J., Lienkaemper, J.J., and Brown, B.D., in press, Distribution and timing of slip along the Nunez fault after June 11, 1983, in Rymer, M.J., and Ellsworth, W.L., eds., The May 2, 1983 Coalinga, California earthquake sequence: *U.S. Geological Survey Professional Paper,* 22 ms p.

Eaton, J.P., and Rymer, M.J., in press, Regional seismotectonic model for the southern Coast Ranges, and the May 2, 1983 Coalinga, California earthquake sequence, in Rymer, M.J., and Ellsworth, W.L., eds., The May 2, 1983 Coalinga, California earthquake sequence: *U.S. Geological Survey Professional Paper,* 18 ms p.

Sharp, R.V., Rymer, M.J., and Morton, D.M., in press, Trace-fractures on the Banning fault created in association with the 1986 North Palm Springs earthquake: *Bulletin of the Seismological Society of America.*

Sharp, R.V., Rymer, M.J., and Morton, D.M., in press, Surface fractures on the Banning fault created in association with the 1986 North Palm Springs earthquake [abs.]: *Transactions American Geophysical Union.*

Lienkaemper, J.J., Pezzopane, S.K., Clark, M.M., and Rymer, M.J., in press, Fault fractures associated with the M_s 6.2 Chalfant, California earthquake of 21 July 1986 [abs.]: *Transactions American Geophysical Union.*

Lienkaemper, J.J., Pezzopane, S.K., Clark, M.M., and Rymer, M.J., in press, Fault fractures associated with the M_s 6.2 Chalfant, California earthquake sequence: Preliminary report: *Bulletin of the Seismological Society of America.*

Mechanics of Faulting and Fracturing

9960-02112

Paul Segall and Ruth Harris
Branch of Tectonophysics
U.S. Geological Survey
345 Middlefield Road, MS/977
Menlo Park, California 94025
415-323-8111, ext. 2635

Investigations

1. Determination of average interseismic slip distribution on San Andreas fault near Parkfield from analysis of geodetic data.

2. Determination of coseismic slip during the 1966 Parkfield, California, earthquake and comparison with accumulated slip deficit since 1966.

3. Examination of temporal fluctuations in deformation from analysis of Carr Hill 2-color geodimeter measurements.

Results

1. Trilateration measurements along the Parkfield-Cholame segment of the San Andreas fault have helped elucidate the distribution of coseismic slip accompanying the 1966 M6 Parkfield earthquake as well as the rate of interseismic slip between 1966 and the present. Inversions of the long-term fault creep and geodetic data reveal that the 1966 rupture zone has been essentially locked since 1966 (Figure 1). Analysis of model resolution demonstrates that short wavelength characteristics of the slip distribution are not resolvable, while longer wavelength features are fairly well resolved. The data require that the locked zone extend nearly as far northwest as the 1966 hypocenter. The vertical extent of the locked zone is poorly resolved. We have found that in order to satisfactorily fit the trilateration measurements it is necessary to include a component of contraction normal to the trend of the San Andreas. The inversion results suggest a spatially uniform normal strain of -0.06 μstrain/yr. The orientation of the contraction is compatible with geologic and seismic evidence of active folding and reverse faulting in the region. The magnitude of the contraction is consistent with convergence rates inferred from global plate motion models. The fit to the geodetic data, including normal strain as a

parameter in the inversions, is shown in Figure 3.

2. Inversions of the coseismic line-length changes and surface offsets in 1966 indicate that fault slip at depth was significantly greater than measured at the earth's surface (Figure 2). Given the rate of which slip since 1966 (Figure 1) has lagged the deep slip rate, it is possible to estimate when the average slip deficit on the Parkfield rupture surface equals the average coseismic slip. Our models suggest it takes 14 to 25 years for this to occur. By adopting extreme prior assumptions we are able to find acceptable models that extend this range to between less than 10 years and greater than 29 years. The slip models can be used to estimate both the coseismic stress drop and the average rate of stress accumulation during the interseismic epoch (Figure 4).

3. We have tested the interseismic slip model, by comparing rates of line-length change predicted by the model with repeated distances measured with the Carr Hill 2-color geodimeter operated by L. Slater and R. Burford. The comparison is shown in Figure 5. The observed secular trends for 6 of the 10 baselines in the 2-color network are within 1 or 2 mm/yr of the rates predicted by the long-term model, although significant short-period fluctuations in the data are not addressed by this comparison. The largest misfit, 6.6 mm/yr on the line to Table, may be dominated by an offset at the time of the Kettleman Hills earthquake. The line to Mide shows large amplitude fluctuations about the secular trend not predicted by the model. The trend for this baseline is 3.8 mm/yr less than predicted by the model, which may reflect a slowdown in shallow fault creep at Middle Mountain following the 1983 Coalinga earthquake. The rates of change on 10 two-color lines have been inverted using the long-term slip model as the prior expectation. Preliminary analysis suggests that the post Coalinga creep slowdown along the central Parkfield segment may be limited to shallow depths. Inverting the more frequent 2-color measurements with a long-term slip model may be a powerful way to search for temporal changes in aseismic fault slip that might be premonitory to the expected earthquake.

Reports

Harris, R. and P. Segall, Detection of a locked zone at depth on the Parkfield, California segment of the San Andreas fault, Jour. Geophys. Res. (in review), 1986.

King, N. E., P. Segall, and W. Prescott, 1986, Geodetic Measurements Near Parkfield, 1959-1984, Jour. Geophys. Res. (in review), 1986.

Martel, S.J., P. Segall and D.D. Pollard, Cataclastic overprinting of ductile deformation textures associated with the development of strike-slip fault zones in granite, Trans. Amer. Geophys. Union (EOS), Fall 1986.

Segall, P. and R. Harris, Deformation in the Transition Between the Central Creeping and Southern Locked Zones of the San Andreas Fault, Trans. Amer. Geophys. Union (EOS), v. 67, p. 359, 1986.

Segall, P. and R. Harris, Slip deficit on the San Andreas fault at Parkfield, California, as revealed by inversion of geodetic data, Science, 233, 1409-1413, 1986.

Segall, P. and R. Harris, Slip Deficit at Parkfield Revealed by Inversion of Geodetic Data (Abs.) Amer. Assoc. Adv. Science Abstracts of Programs, 1986 National Meeting, p. 24, 1986.

Segall, P., R.O. Burford, and R. Harris, The earthquake cycle at Parkfield: Comparing recent strain measurements with a long-term interseismic slip model, Trans. Amer. Geophys. Union (EOS) Fall 1986.

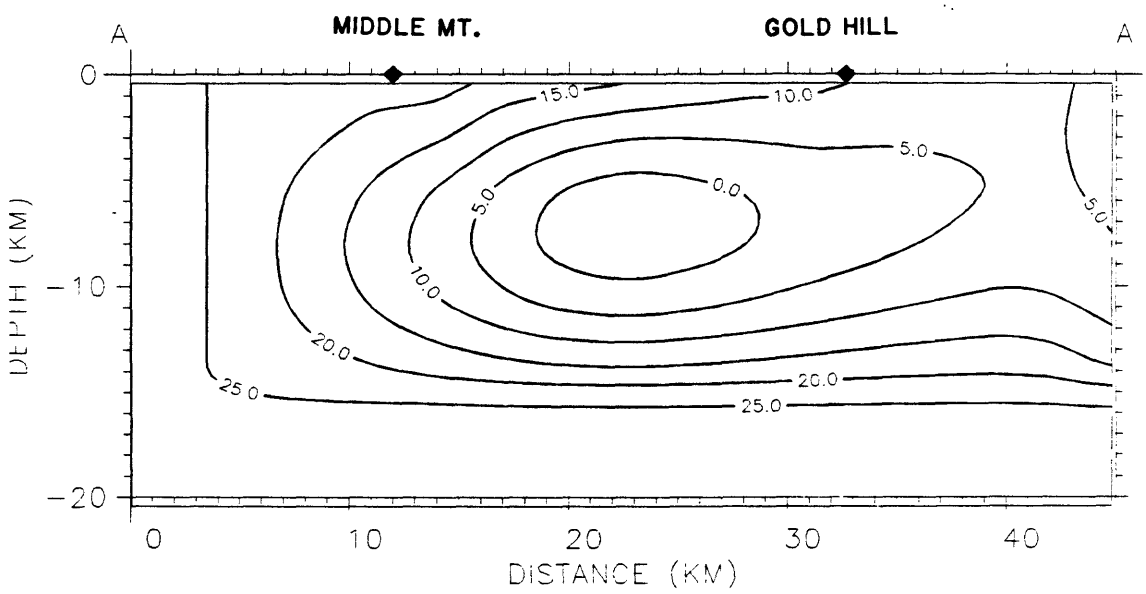

Figure 1. Preferred interseismic slip model. Contours indicate average aseismic slip-rate in mm/yr.

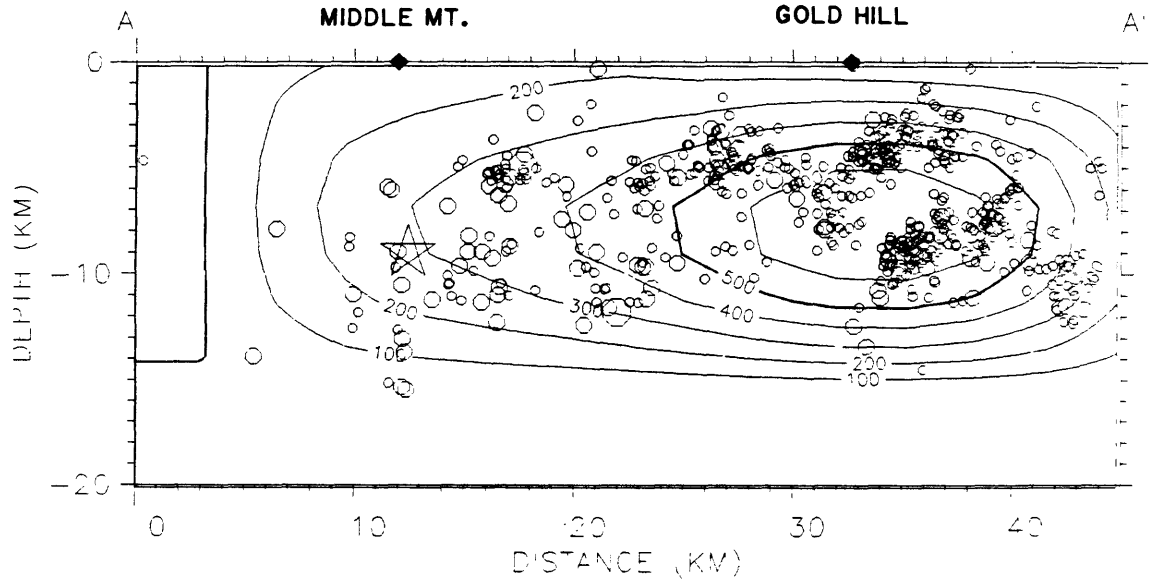

Figure 2. Preferred co- and postseismic slip model with aftershocks (circles) of the 1966 earthquake. Mainshock hypocenter indicated by star. Contours indicate slip in mm.

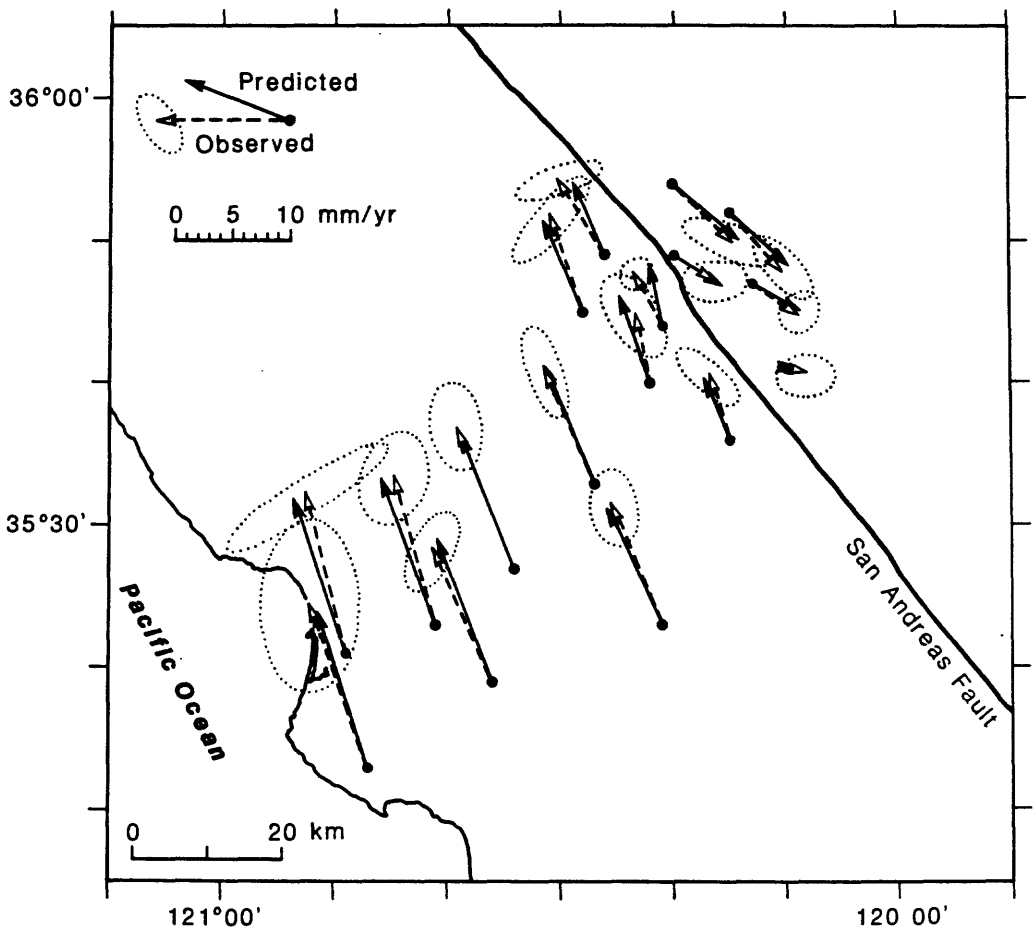

Figure 3. Comparison of observed station velocities (dashed vectors) with velocities predicted by inverse model (solid vectors) including both fault slip and uniform contraction normal to the fault. Ellipses indicate two-standard deviation confidence intervals in the observed motions.

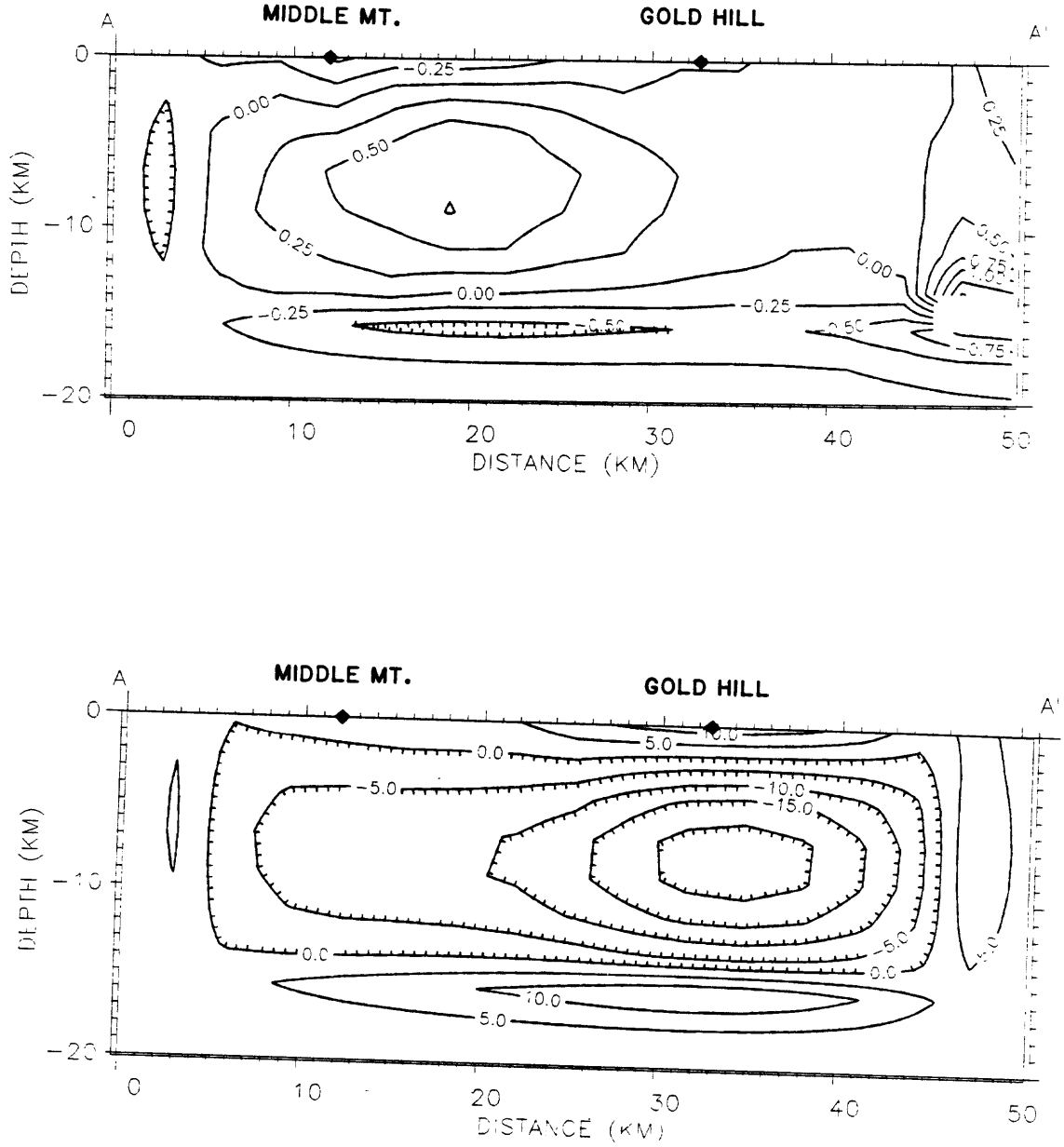

Figure 4. (a) Interseismic stressing rate calculated from the slip model shown in Figure 1 contour interval 0.25 bar/yr. (b) Coseismic stress change corresponding to slip model in Figure 2. Contour interval 5.0 bars.

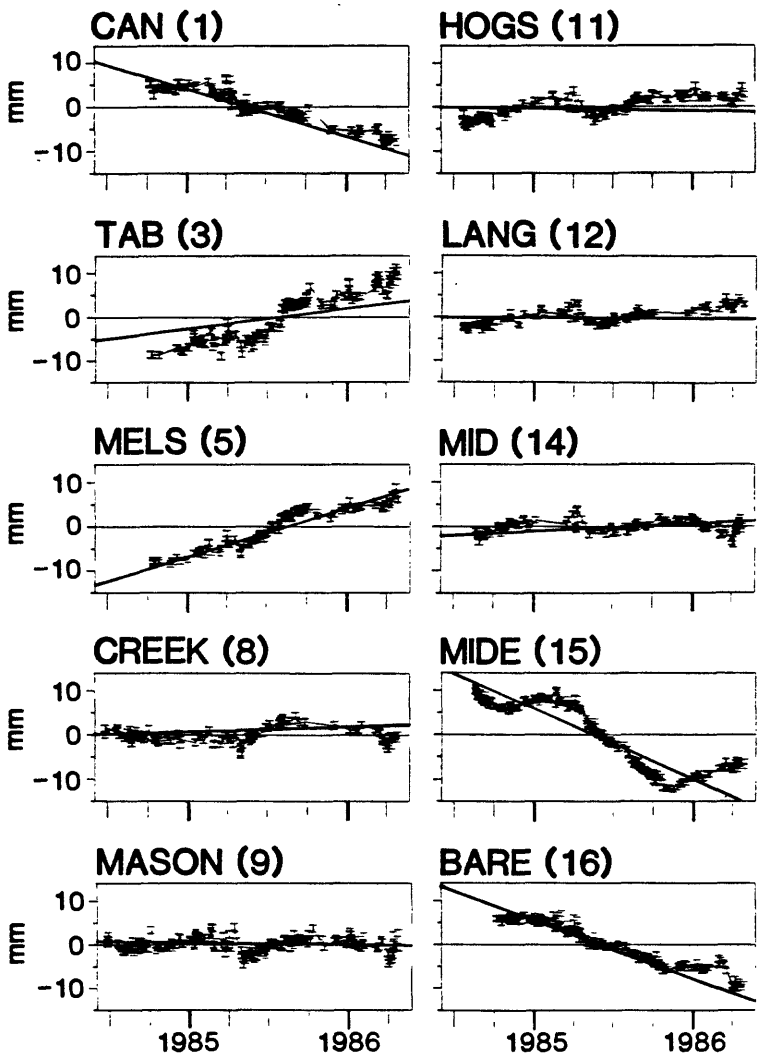

Figure 5. Comparisons of observed length changes of baselines in the Parkfield 2-color geodimeter network with extension rates predicted from the slip model shown in Figure 1. The model is based on inversion of long-term geodetic and fault creep data for the Parkfield region.

LOW FREQUENCY DATA NETWORK

9960-01189

S. Silverman, K. Breckenridge, J. Herriot,
U.S. Geological Survey
Branch of Tectonophysics
345 Middlefield Road, MS/977
Menlo Park, California 94025
415-323-8111, ext. 2933

Investigations

1. Real-time monitoring, analysis, and interpretation of tilt, strain, creep, magnetic, and other data within the San Andreas fault system and other areas for the purpose of understanding and anticipating crustal deformation and failure.

2. Enhancements to satellite-based telemetry system for reliable real-time reporting and archiving of crustal deformation data.

3. Compilation and maintenance of long-term data sets free of telemetry-induced errors for each of the low frequency instruments in the network.

4. Development and implementation of backup capabilities for low frequency data collection systems.

5. Specialized monitoring and display of data relevant to the Parkfield region.

Results

1. Data from low frequency instruments in southern and central California have been collected and archived using the Low Frequency Data System. In the six months over four million measurements from 160 channels have been received via telephone telemetry and subsequently transmitted to the Low Frequency 11/44 UNIX computer for archival and analysis. In the same period, more than 50 satellite platforms have been monitored, accounting for an additional four million measurements on the 11/44 system.

2. The project continues to operate a configuration of one PDP 11/44 computer running the UNIX operating system and two PDP 11/03 computers running real-time data collection software. Two AT&T PC 7300 computers are used as backup

machines for collection of satellite and telephone telemetered data. The 11/44 has been operational with less than 1% down-time. Data from the Network are made available to investigators in real-time and software for data display and analysis has been enhanced. Tectonic events, such as creep along the fault, can be monitored while still in progress.

3. The project continues to use a five meter satellite receiver dish installed in Menlo Park for retrieval of real-time surface deformation data from California, and South Pacific islands. The GOES geostationary satellite together with transmit and receive stations makes possible a greatly improved telemetry system. Due to orbital problems with the current satellite however, modifications to platforms in the field and software in the system have increased the use of redundant data to provide more complete data sets. Additional reporting platforms containing waterwell and climate data are being added to the collection end of the system. Further expansion of the number of platforms monitored is anticipated.

4. Software has been developed to operate two AT&T PC 7300 computers as backup systems for collection and storage of data from satellite and telephone data collection systems. The 7300 computers have been linked to the 11/44 system so that data may be transferred between systems and users may access the AT&T machines via the 11/44 computer.

5. The project continues to take an active part in the Parkfield Prediction activities. Programs automatically plot strain and creep records and record the status of the satellite telemetry system for the Parkfield region. These plots are routinely available on a daily basis and have been improved for readability. Additional displays have been produced to show the alert level status at Parkfield for a given time period and to relate the alerts to field instrumentation. Kate Breckenridge continues as the alternate monitor for Parkfield creep events, which includes contact via paging system during periods of increased activity. Processing which monitors creep events has been expanded with the addition of several new creepmeters. The system has signalled alerts for creep events on several occasions and has also notified researchers of malfunctioning field equipment.

6. New computer equipment has been purchased to provide adequate facilities for low frequency data work involved with the Parkfield experiment. Most of the system has been delivered and work will begin shortly on the initial stages of bringing the system into use. When operational, the new

equipment will replace the 11/44 as the primary data collection and analysis system for the Low Frequency Data Network.

7. The project has continued to provide real-time monitoring of designated suites of instruments in particular geographical areas. Terminals are dedicated to real-time color graphics displays of seismic data plotted in map view or low frequency data plotted as a time series. During periods of high seismicity these displays are particularly helpful in watching seismic trends. The system is used in an ongoing basis to monitor seismicity and crustal deformation in central California and in special areas of interest such as Mammoth Lakes.

Parkfield Area Tectonic Framework

9910-04101

John D. Sims
Branch of Engineering Seismology and Geology
U.S. Geological Survey
345 Middlefield Road, MS 977
Menlo Park, California 94025
(415) 323-8111, ext. 2252

Investigations:

1. Field investigations of structural and stratigraphic relationships between late Cenozoic sedimentary units and underlying Franciscan and Late Cretaceous units in the Parkfield-Cholame area.

2. Field investigations of late Holocene and historic slip rates in the Parkfield-Cholame area.

3. Geologic consultation and field examination of borehole instrumentation sites in the Parkfield prototype earthquake prediction experiment.

Results:

1. An alluvial fan deposit on the west side of Cholame Valley is located on the Parkfield reach of the San Andreas fault in central California. The site records an 1800-year-long average rate of slip of $27.1^{+2.9}_{-2.4}$ mm/yr. This long-term rate of slip is lower than long-term slip-rates recorded at Wallace Creek, 33.2 ± 2.9 mm/yr for the past 3,700 years (Sieh and Jahns, 1984). The long-term rate in Cholame Valley is within the range of values for the long-term slip rate at Melendy Ranch in the creeping section, 32^{+6}_{-5} mm/yr for the past 800 years (Perkins, Sims, and Jahns, *in press*). Near-field geodetic measurements near this site show that fault creep occurs at a rate of 4±1 mm/yr. A fence about 100 m to the NW of this site was built in 1908 and records a slip rate of 9±0.4 mm/yr. These data suggest an accumulation of stress at this site of about 23 mm/yr since the 1966 earthquake, and an average stress accumulation of 18 mm/yr since 1908. Both figures for stress accumulation are maximum values because of the likelihood that short-term surface displacement, including coseismic slip, is less than deep slip on the fault (Segal and Harris, 1986).

Reports:

None.

Dense Seismograph Array at Parkfield, California

9910-03974

Paul Spudich
Branch of Engineering Seismology and Geology
U.S. Geological Survey
345 Middlefield Road, MS 977
Menlo Park, California 94025
(415) 323-8111, ext. 2395

Investigations

1. Design and installation of a dense seismograph array at Parkfield.

Results

The array will be co-sited with strong-motion arrays operated by the Electric Power Research Institute (EPRI) and the California Strong Motion Instrumentation Program. The array will consist of about 15 surface three-component geophones. All elements will be connected to a local central computer facility by underground wires, and all data will be digitized using a 16-bit digitizer at 200 samples/s. The use of geophones and 16-bit digitization will guarantee both unclipped recording of all seismic events exceeding ground noise, and good resolution of small events when our array data is combined with that from the others. We expect to make nearly complete recordings of the foreshock and aftershock sequence.

The site of the array will be on the Scobie Ranch (35° 15.5'N, 120° 16.6'W), where hard Temblor sandstone outcrops. This region is about 7 km off the San Andreas fault near the *en echelon* offset of the San Andreas in the Cholame Valley. The landowners have already given us verbal permission to install the array described herein.

The instrumental system we have chosen is rather like the ANZA seismic network (Berger and others, 1984) with wires replacing radio links between the seismographs and central recorder. For recording the sensor outputs we have chosen a distributed-intelligence system that maximizes data capacity and reliability. Six channels of analog sensor output go into a commercially available electronics package made by Refraction Technology (Ref-tek) containing a 16-bit analog-to-digital converter (A/D), 512 Kbytes of memory for data, and an 80C86 microprocessor. These Ref-tek packages will be located at the array elements when space permits and when digital signal transmission is required to achieve acceptable signal-to-noise ratios. Otherwise, they will be located in the central computer structure. Each package does independent trigger calculations, sends trigger information to the front-end MicroVax via a local-area-network (LAN), and performs other status checking. Data recovery by the MicroVax will be initiated when it detects a pre-defined number of triggers within a specified time window. Digital ground velocity and acceleration data packets are then transmitted to the Micro Vax via the LAN.

The front-end MicroVax receives digital data blocks and trigger information from the field units via the Computrol interface. It stores data locally in the 500 Mbyte Megatape tape drive and forms disk files of the data (trigger times, time series) on the backend MicroVax II. The MicroVax boots from a hard disk, floppies, or ROM but then runs using memory only. Consequently, a disk failure will not cause a loss of data.

References

Baker, J., Baker, L., Brune, J., Fletcher, J., Hanks, T., and Vernon, F., 1984, The Anza array: A high dynamic range, broadband, digitally radio-telemetered seismic array: *Bulletin, Seismological Society of America*, **74**, 1469-1481.

Reports

Spudich, P., and Oppenheimer, D., 1986, Dense seismograph array observations of earthquake rupture dynamics, in *Earthquake Source Dynamics*, Geophysical Monograph 37 of the American Geophysical Union, Das, S., Boatwright, J., and Scholz, C., eds., p. 285-296.

MODELING AND MONITORING CRUSTAL DEFORMATION

9960-01488

Ross S. Stein, Wayne Thatcher
Branch of Tectonophysics
U.S. Geological Survey
345 Middlefield Road, MS/977
Menlo Park, California 94025
(415) 323-8111, ext. 2120

Investigations

1. Comparative study of extensional faulting in the Basin and Range province of the western United States from geodetic leveling and geologic data (1959 M = 2.3 Hebgen Lake, MT, and 1983 M = 7.0 Borah Peak, ID, earthquakes).

2. Examination of the potential of the Peninsular San Andreas fault for $M \simeq 7$ earthquakes, from geodetic strain and geologic data.

Results

1. Fault geometry and slip for large Basin and Range Earthquakes

We deduce the fault geometry, coseismic slip and moment for two of the largest historic earthquakes that have occurred in the Basin and Range of the western United States: The M = 7.3 1959 Hebgen Lake, Montana, earthquake and the M = 6.9 1983 Borah Peak, Idaho, event. Newly augmented data sets of vertical deformation from geodetic leveling and from lake shoreline changes were modeled by simple dislocations in an elastic half-space. The r.m.s. signal to noise ratio is 12 for the Hebgen Lake data and 38 for the Borah Peak set. The residuals for both models are about twice as large as the noise. The Hebgen Lake earthquake struck on the 15 to 25 km long en echelon Hebgen and Red Canyon faults, dipping 45°-50° and extending to a depth of 10 to 15 km. The 7.0 and 7.8 m of dip-slip on these faults produced a combined moment of 1.2×10^{20} N m. The dip of the Red Canyon fault may decrease slightly with depth (in a listric manner), abutting the planar Hebgen fault at a depth of 8 km. In addition, up to 1 m of deep slip occurred on the Holocene segment of the adjacent Madison Range fault, 10 km west of the Hebgen fault. The Borah Peak segment of the Lost River fault was found to dip 49°.

Slip of 2.1 m occurred at the south fault end, extending to a depth of 14 km; 1.4 m of slip occurred at the north end, where the fault reached only to 6 km depth. A listric fault shape is not permitted by the geodetic data at Borah Peak. Both the Hebgen-Red Canyon and the Lost River faults are high-angle and nearly planar, despite the much greater age and length of the Lost River fault in comparison to the en echelon Hebgen faults. The chief difference between the earthquakes is the 3 to 4-fold higher slip at Hebgen relative to Borah Peak and all other well-studied Basin and Range shocks. Thrust faults located close to these active normal faults must either dip steeply at depth, or were not reactivated (Barrientos, Stein Ward).

2. Seismic Potential of the San Andreas Fault

The long-term (decade or longer) seismic potential of the Peninsular San Andreas fault (PSAF), the 125-km-long segment SE of San Francisco, has been assessed by comparing the slip accompanying the 1906 M = 8.3 earthquake with the amount of this slip deficit made up since 1906. Of particular importance is the longstanding factor-of-two inconsistency between 1906 surface offsets ($\leq$1.5 m) and geodetically-determined coseismic slip (2.7 $\pm$ 0.3 m) on the southern 90 km of the PSAF [Thatcher, 1975]. In re-examining this issue we find the discrepancy cannot be attributed to either large observational uncertainties in the geodetic data or shortcomings in fault modeling. Rather, the problem lies in the complexity of this 90-km-long fault reach, where the PSAF trend changes by 6°, the zone of recent deformation is 0.5 to 2 km wide, and much of the fault is heavily-vegetated and inaccessible. Farther NW on the 1906 rupture, where the fault geometry is much simpler, evidence from deformed fences shows that right-lateral coseismic slip was commonly distributed across a zone $\sim$20 to 600 m wide, with only about 70% of the total slip occurring at the main fault trace. The general importance of distributed coseismic deformation and the evidence for fault complexity indicate the best estimate of 1906 slip on this 90 km fault segment is the geodetically-constrained value of 2.6 $\pm$ 0.2 m. Following previous work, we have assessed the risk posed to the southern PSAF by two broad classes of earthquakes. The possibility of an M 6 to 6-1/2 event on the 30-km-long segment NW of San Juan Bautista cannot be completely precluded but the evidence bearing on its likelihood is contradictory. In contrast with previous appraisals we find that the risk of an event M $\simeq$ 7 rupturing the southern $\sim$90 km of the PSAF during the next several decades is quite low (Thatcher, Lisowski).

Reports (excluding abstracts)

Barrientos, S. E., R. S. Stein, and S. N. Ward, A comparison of the 1959 Hebgen Lake, Montana, and the 1983 Borah Peak, Idaho, earthquakes from geodetic observations, submitted to Bull. Seismol. Soc. Am., special issue on the Borah Peak earthquake, 1986.

Stein, R. S., Contemporary plate motion and crustal deformation, U.S. Nat'l Report on Geodesy, I.U.G.G. 1983-86 Quadrennium, submitted to Reviews of Geophysics, 1986.

Stein, R. S., Evidence for surface folding and subsurface fault slip from geodetic elevation changes associated with the 1983 Coalinga, California, Earthquake, submitted to the U.S.G.S. Professional Paper on the Coalinga Earthquake, in press, 1986.

Stein, R. S., C. T. Whalen, S. R. Holdahl, W. E. Strange, and W. Thatcher, Saugus-Palmdale, California, field test for refraction error in historical leveling surveys, Journ. of Geophys. Res., 91, 9031-9044, 1986.

Stein, R. S., and R. C. Bucknam, Quake replay in the Great Basin, Natural History, v. 95(6), 28-35, 1986.

Thatcher, W., Cyclic deformation related to great earthquakes at plate boundaries: Models and observations, Proc. Int'l Symp. on Recent Crustal Movements, Wellington, New Zealand, in press, 1986.

Thatcher, W. and M. Lisowski, Long-term seismic potential of the San Andreas fault southeast of San Francisco, California, submitted to J. Geophys. Res., 1986.

TECHNICAL REPORT, SEMI-ANNUAL, 1986

NEARFIELD GEODETIC INVESTIGATIONS OF CRUSTAL MOVEMENTS, SOUTHERN CALIFORNIA

Contract No. USDI-USGS 14-08-0001-G1081

Arthur G. Sylvester
Department of Geological Sciences, and
Marine Science Institute
University of California
Santa Barbara, California 93106
(805) 961-3156

REPORT SUMMARY

INVESTIGATIONS

Repeated surveys of 27 of 45 existing precise leveling arrays across active faults have been done during the first half of the contract period. The leveling array at Pinyon Flat Geophysical Observatory was resurveyed once.

The purpose of these surveys is to search for and monitor the spatial and temporal nature of vertical displacement across active and potentially active faults. Thus, we document pre-, co- and post-seismic displacement and creep, if any, especially where seismographic, paleoseismic and geomorphic data indicate current or recent fault activity. The investigations are intermediate in scale between the infrequent, regional geodetic surveys traditionally done by the National Geodetic Survey, and point measurements by continually recording instruments such as creepmeters, tiltmeters, and strainmeters. All surveying is done according to First Order, Class II standards.

RESULTS

Precise leveling arrays in Coachella Valley (Fig. 1) were releveled in the period 14-16 July after the North Palm Springs earthquake of 8 July 1986. Each array is comprised of from 22 to 53 permanent bench marks in a line oriented nearly perpendicular to the fault it straddles. Array lengths, numbers of bench marks, and distances from the epicentral area are as follows: Miracle Hill (726 m; 22; 5 km), Painted Canyon (1505 m; 44; 60 km), North Shore (871 m; 28; 75 km), and Bat Caves (1537 m; 44; 92 km). No height changes greater than 0.5 mm were detected in any of the arrays relative to surveys done in September, 1985, which is not surprising given the relative small magnitude of the earthquake (M 5.9) and how far three of the arrays are from the epicentral area. Our measurements also show that vertical movement was *not* triggered on the Mission Creek strand of the San Andreas fault by the

earthquake on the nearby Banning fault.

Arrays on the San Jacinto fault at similar epicentral distances (Anza - 43 km; SBVC - 78 km) also showed no changes relative to surveys done from 5 days (Anza) to 7 months (SBVC) previously.

Resurveys were done across the Hilton Creek fault in McGee Creek and the Furnace Creek fault in Fish Lake Valley (Fig. 1) following the Chalfant Valley earthquake of 21 July 1986. A resurvey at McGee Creek on 22 July 1986 shows that the earthquake triggered no vertical movement on the fault greater than 0.5 mm relative to a survey in July 1985. Relevelings were also done on 24 July and on 3-5 September, 1986, at McGee Creek to bracket a swarm of earthquakes which occurred in Chalfant Valley in the period 22-24 July. The surveys failed to detect any changes whatsoever here or in Fish Lake Valley where a 250 m-long array was surveyed in September 1986 and compared to a survey in July 1985. These results shouldn't be surprising either given the relatively small magnitude of the earthquake (M 6) and the fact that our arrays across the Hilton Creek fault and across the Furnace Creek fault are 35 km and 50 km, respectively, from the epicentral area in Chalfant Valley.

Two relevelings across the San Andreas fault in Parkfield in 1986 show that the northeast fault block ceased its 3 mm/yr rise between 1980 and 1985 relative to the southwest block. The cumulative vertical separation across the fault is nearly 15 mm since 1980, and nearly all of that uplift took place at the surface trace of the fault. Relevelings of tilt arrays in summer 1986 at Pitt Ranch and Flenge Flat also showed no changes since 1985.

Three relevelings across the Sierra Madre fault in Arroyo Seco, Pasadena, showed that the mountain side of the fault *subsided* 6 mm relative to the valley side between January and August 1986 after having *risen* 9 mm between June 1984 and August 1985 without accompanying detectable earthquake activity. As shown in Figure 2, the array is 1900 m long with 43 permanent bench marks. The rise and fall occurs over a zone about 500 m wide, and the height changes observed in each survey are not related to the prevailing air temperature at the time of surveys.

Resurveys of all other arrays during the first half of the 1986 contract period, notably those across the San Jacinto fault, *failed* to reveal noteworthy height or tilt changes.

We acquired a Wild TC2000 total station distance meter and tested it at Pinyon Flat Observatory. Much of our future efforts will focus on resurveying all of our leveling arrays with the distance meter to specify the relative positions of all bench marks horizontally and well as vertically.

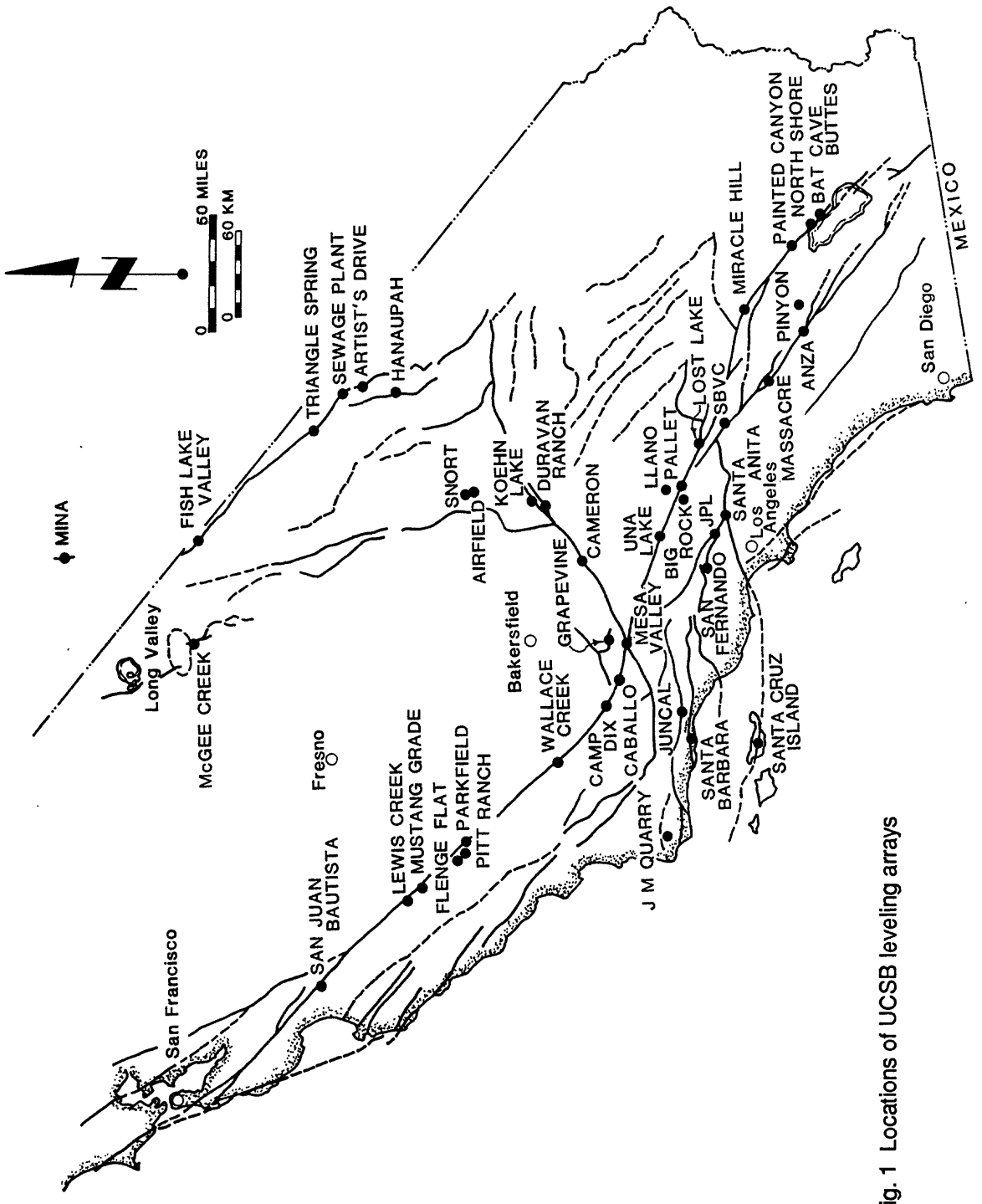

Fig. 1 Locations of UCSB leveling arrays

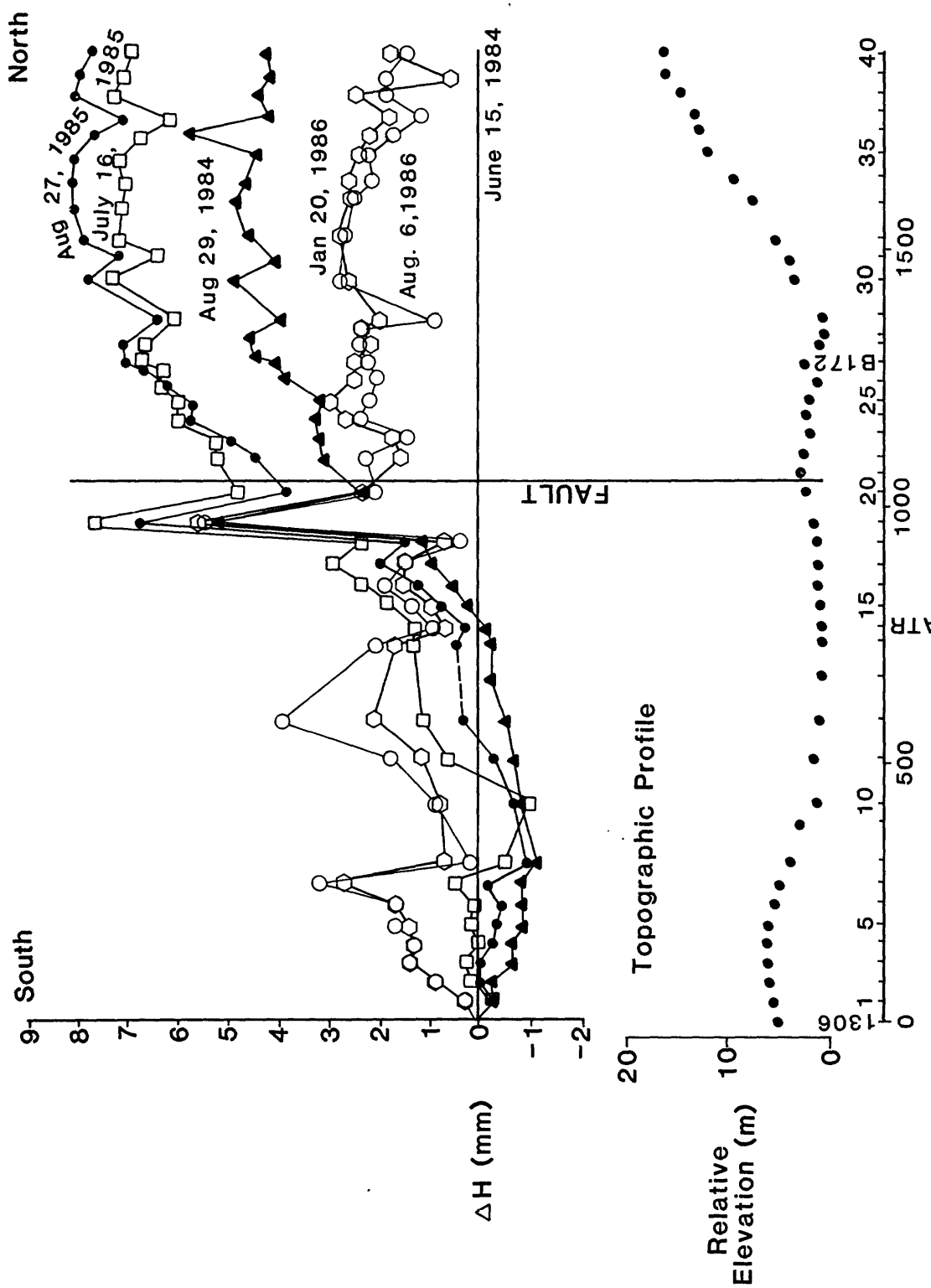

Fig. 2. Height changes of bench marks in leveling arrays across the Sierra Madre fault in Arroyo Seco, Pasadena. Bench mark 1306 is arbitrarily held fixed. Bench mark 19 was damaged by vandals between the first and second survey. Most of the uplift of the north half of the line occurred between June and August, 1985, whereas its fall occurred between August 1985 and August 1986.

Earthquake Process

9930-03483

Robert L. Wesson
Branch of Seismology
U.S. Geological Survey
922 National Center
Reston, Virginia 22092
(703) 648-6785

INVESTIGATIONS

1. Analysis of theoretical and numerical models of the processes active in fault zones leading to large earthquakes.

2. Analysis of seismological and other geophysical data pertinent to understanding of the processes leading to large earthquakes.

3. Analysis of the potential for earthquakes induced by deep well injection.

RESULTS

Fault creep can be viewed as arising from the interplay of three factors: stress applied to the fault from external sources, stress caused by the geometry and distribution of displacement on the fault-arising from the elastic response of the surrounding medium to the displacements within the anelastic fault zone itself, and the constitutive relations characterizing the resistance to slip on the fault. Analytic solutions have been developed for a simple, one dislocation element, quasi-static model of non-propagation fault creep assuming viscous and quasi-plastic (power law creep) characterizations of fault zone rheology, and for a multi-element, quasi-static model assuming a viscous rheology. Viscous rheology implies solutions based on decaying exponentials. The simple, one-element, quasi-plastic model is in excellent agreement with the form of creep events observed at Melendy Ranch California. A matrix formulation has been developed for the calculation of dislocation stresses on a fault zone in a halfspace or plate, involving the division of the dislocation surface into strips of rectangles and the use of published solutions to calculate the stress resulting from displacements on those elements. Results from the matrix method show excellent agreement with analytic results for equilibrium displacements on "stress free" cracks. The matrtix formulation can be used as the basis for a numerical method to simulate one- and two-dimensional propagation creep assuming a quasi-plastic rheology. Excellent agreement is obtained between calculations and observations of afterslip from the 1975 Oroville, California, earthquake, and of a propagating creep event observed along the southern Calaveras fault, central California, during July, 1977. These calculations indicate that the characteristics of fault creep phenomena-including the secular and episodic nature of fault creep, the simple shape of some individual events and the multiple, composite shape of

others, and the propagation of creep events-can be explained by this method of analysis and the assumption of a rheological model for creeping fault zones that assumes a quasi-plastic, power law creep-after the attainment of a yield stress that varies with position on the fault zone. On the southern Calaveras fault, the observations of propagating creep seem to require that the yield stress be near zero at the surface and throughout must of the fault zone, but they also require a zone with a yield stress on the order of 12 bars at a depth of about 0.5 km, about 5 km long. The methods of calculation presented should be applicable to the simulation of many problems in the dynamics of faulting.

REPORTS

Harding, S.T., Wesson, R.L., Nicholson, C., and Morton, D., Shallow seismic reflection profiling across the trace of the southern San Andreas fault, EOS, Trans. Am., Geophys. Un., 67, 1200, 1986.

Nicholson, C., Wesson, R.L., Given, D., Boatwright, J., and Allen, C.R., Aftershocks of the 1986 Palm Springs earthquake and relocation of the 1948 Desert Hot springs earthquake sequence, EOS, Trans. Am. Geophys. Un. 76, 1089, 1986.

Wesson, R.L., Gibson, R.W., Morton, D., Campbell, R.H., and Nicholson, C., Interpretation of surface cracks and other fault-line surface deformation associated with the North Palm Springs earthquake of July 8, 1986. EOS Trans. Am. Geophys. Un., 67, 1090, 1986.

Wesson, R.L., Modelling aftershock migration and afterslip of the San Juan Bautista earthquake of October 3, 1972, Tectonophysics, in press.

Wesson, R.L., and Nicholson, C., (editors): Studies of the January 31, 1986, northeastern Ohio earthquake, U.S. Geological Survey Open-File Report 86-331, 1986.

PERMEABILITY OF FAULT ZONES

9960-02733

James Byerlee
Branch of Tectonophysics
U.S. Geological Survey
345 Middlefield Road, MS/977
Menlo Park, California 94025
(415) 323-8111, ext. 2453

Investigations

Laboratory studies of the permeability of rocks and gouge are carried out to provide information that will assist us in evaluating whether in a given region fluid can migrate to a sufficient depth during the lifetime of a reservoir to trigger a destructive earthquake. The results of the studies also have application in the solution of problems that arise in nuclear waste disposal.

Results

Our current research on 'crystalline' rock types represents a continuation of our permeability and fluid-rock interaction studies at elevated temperatures. The ultimate goals of this work are (a) to identify the paths that fluids follow through the crystalline rock samples for which we have performed high-temperature permeability experiments (Moore et al., 1983; Morrow et al., 1985) and (b) to determine any changes in the flow paths (e.g., mineral deposition in microfractures, fracture enlargement through mineral dissolution) that can be correlated with the observed permeability changes. The rocks included in this study are an anorthosite, a gabbro, a quartzite, and two granodiorites.

The work conducted this past year was centered around two topics:

(1) Comparison of the compositions of the fluids that had been collected during the permeability experiments with the mineral chemistries of the rock types that were tested. This work will yield information on the types of mineral dissolution and precipitation reactions that took place during the experiments. Such comparisons have been made between the two granodiorites (Moore et al., 1983). The present study extends these comparisons to include the other three rock types.

(2) Petrographic examination of the starting material and run products of the permeability experiments, to identify

probable fluid paths in the different rock types. This work is a preliminary step to future SEM and crack section examinations of crack formation in these rocks. The information gained from the petrographic studies, along with the knowledge of what mineral reactions occurred during the experiments, will help to optimize the SEM and crack section studies. Some preliminary SEM work has been conducted on Westerly granite (Vaughan et al., 1986); this work dealt principally with crack formation and sealing processes in quartz.

Reports

Vaughan, P., Moore, D., Morrow, C., and Byerlee J., 1986, Role of cracks in progressive permeability reduction during flow of heated aqueous fluids through granite: Journal of Geophysical Research, v. 91, p. 7517-7550.

Vaughan, P., Moore, D.E., Morrow, C.A., and Byerlee, J.D., 1985, The mechanism of permeability reduction during flow of hydrothermal fluids through Westerly granite: U.S. Geological Survey Open-File Report 85-262.

ROCK MECHANICS

9960-01179

James Byerlee
U.S. Geological Survey
Branch of Tectonophysics
345 Middlefield Road, MS/977
Menlo Park, California 94025
(415) 323-8111, ext. 2453

Investigations

Laboratory experiments are being carried out to study the physical properties of rocks at elevated confining pressure, pore pressure and temperature. The goal is to obtain data that will help us to determine what causes earthquakes and whether we can predict or control them.

Results

During the frictional sliding of fault gouge, differences in the displacement dependence of friction have been observed when the strain rate is varied. A slower sliding velocity will generally produce a steeper slope of the stress-strain curve than a faster velocity. This has a number of consequences, including differences in the amount of sliding necessary to reach the maximum shear stress level, as well as a change from displacement strengthening to displacement weakening under some conditions. To understand the cause of this effect, frictional sliding experiments were performed on sawcut samples of granite filled with a layer of simulated gouge. Ottawa sand was used to study the behavior of round grains, crushed Westerly granite and crushed quartzite was used to test angular grains. Shear stress and pore volume were measured as the strain rate was alternated between 10^{-5} and 10^{-7}/sec at normal stresses from 12.5 to 100 MPa. The results showed that the velocity effects were tied to changes in the pore volume of the gouge layer. These pore volume changes were in turn found to be linked to the rate-dependent consolidation state of the gouge particles. During sliding, the gouge layer will dilate or compact until the critical void ratio has been reached for a particular velocity. This process involves either grains riding over one another or grain cracking. At low normal stresses with round grains, the former process is important. At high normal stresses and/or with angular grains, where the degree of interlocking is greater, grain cracking predominates, resulting in higher shear stresses. Hence, the velocity-dependent consolidation state of the gouge is also a function of normal stress and grain angularity. These friction experiments corroborate

this point, since the observed velocity-dependent strain hardening effects become more pronounced at higher normal streses, and with more angular grains.

Reports

Jin, Ma, Moore, D., and Byerlee, J., 1985, The effect of temperature on the frictional behavior of illite gouge and muscovitization: Earthquake Research in China, v. 1, no. 1, p. 41-47.

Jin, Ma, Moore, D.E., Summers, R., and Byerlee, J.D., 1985, The effect of temperature, pressure and pore pressure on the strength and sliding behavior of the gouges: Seismology and Geology, v. 7, no. 1, p. 15-24.

Lockner, D., and Byerlee, J., 1986, Laboratory measurements of velocity-dependent frictional strength: U.S. Geological Survey Open-File Report 86-417, pp. 26.

Lockner, D., and Byerlee, J., 1986, Velocity dependent gouge dilatancy and shear strength (abs.): Earthquake Notes, Seismological Society of America, v. 57, p. 24.

Moore, D., and Byerlee, J., 1986, Correlation between sliding motion and deformation features developed in fault gouge during friction experiments (abs.): Geological Society of America, v. 18.

Moore, D., Summers, R., and Byerlee, J., 1986, Slip surfaces and sliding modes of heated illite gouge (abs.): Earthquake Notes, Seismological Society of America, v. 57, p. 24.

Mechanics of Earthquake Faulting

9960-01182

James H. Dieterich
U.S. Geological Survey
Branch of Tectonophysics
345 Middlefield Road, MS/977
Menlo Park, California 94025
415-323-8111, ext. 2573

Investigations

Constitutive Properties of Faults with Variable Normal Stress

Work continued on the experimental measurement of fault constitutive properties under conditions in which normal stress is independently varied during slip. The goal of this study is to develop a more general formulation for rate- and state-variable fault constitutive laws which currently assume constant normal stress.

Nucleation and Triggering of Earthquake Slip

Analysis and modeling of the processes associated with the nucleation and triggering of earthquake slip was continued. Emphasis was given to comparisons of analytic solutions that permit simple calculations for earthquake potential under time varying stress conditions with results of detailed 20 numerical calculations.

Deformation Mechanics of Active Volcanoes

Models for the stability of the south flank of Kilauea volcano and the relationships between intrusions and earthquake processes continued to be worked upon.

Results

Constitutive Properties of Faults with Variable Normal Stress

Mark Linker and Jim Dieterich completed a series of experiments at 50 bars normal stress with continuous high speed servo-control of normal stress and slip rates. The experiments are with 5 x 5 cm blocks of Westerly granite in a double-direct shear apparatus under servo control. The observations from three types of programmed sliding histories have been examined. Normal stress change range from 1% to 40% of 50 bars. All of the experiments are performed from an initial steady state.

1) A step change in normal stress results in an instantaneous change in the frictional strength followed by an evolution over a characteristic displacement which restores friction to steady state. This evolution with displacement appears to have the same form and characteristic displacement as that observed for velocity steps.

2) Similarly, a pulse in normal stress of short duration results in a jump in friction followed again by an evolution over displacement to steady state. Although not conclusive, the occurrence of this jump indicates significant hysteresis in the normal stress effect.

3) Experiments following the sequence of steps consisting of: slide at constant normal stress and slip velocity, hold slip velocity at zero, pulse the normal stress, continued hold and finally resumption of slip at constant slip velocity have been compared with similar slide-hold-slide tests without a pulse in normal stress. The results demonstrate that the effect of the pulse is to further increase the frictional resistance beyond that for a simple hold by an amount that varies with hold time. This last observation indicates that only part of the variation in friction due to normal stress changes may be accounted for by a dependence of the state variable θ, the apparent contact time, on normal stress σ.

We propose the following constitutive expressions to model these observations:

$$\mu = \mu_o + A \ln V + B \ln\theta + C \ln(\psi/\sigma)$$

Where ψ is a newly introduced state variable that is independent of V and t. At steady state $\theta = d_c/V$ and $\psi = \sigma$. Under varying normal stress θ and ψ evolve as:

$$d\theta = (1/V + \theta/d_c)dx + (S\theta/B\sigma)d\sigma$$

for $\sigma \geq \psi$	$\psi = \sigma$
for $\sigma < \psi$	$d\psi/dx = (\sigma - \psi)/d_c$

where x is displacement across the sliding surface. The value of S may depend on the sign of $d\sigma$.

These results demonstrate significant normal stress effects that are not accounted for in earlier state- or rate-dependent fault constitutive formulations. We anticipate application of these results to problems where shear and normal stress acting on fault surfaces vary simultaneously. One such area of application is the triaxial configuration for fault friction measurement.

Nucleation and Triggering of Earthquake Slip

An efficient numerical method for calculation of two-dimensional problems for the nucleation of unstable slip on faults with state- and rate-dependent fault friction was developed. Results of computations with the models are in very close agreement with earlier, single degree of freedom fault models for both the time to instability from an initial stress state and for the accelerating displacement as a function of time of the point of initiation of the instability. Independent of a wide range of initial conditions, the instability nucleates on a patch with dimensions well predicted by the simpler single degree of freedom models. A complete report on these results is in preparation.

Deformation Mechanics of Active Volcanoes

Hawaiian volcanic rifts have been modeled as long ridges with the geometry of flattened triangular prisms. Stress in the prism arises from faulting, dike injection along the ridge axis, and gravitational sagging of the topography. Of particular interest are the possible mechanisms affecting long-term persistence of rifts, mechanisms of accommodation to repeated dike injection with cumulative spreading of perhaps a kilometer or more, and interactions between faulting and rift intrusions.

In extreme models with very steep slopes and high Poisson's ratio, corresponding to the gelatin models of rifts by Fiske and Jackson (1972, Proc. R. Soc. London A.), finite element calculations indicate that gravity induced stresses are sufficient to trap a dike to propagate parallel to the rift as proposed by Fiske and Jackson. However, these trapping stresses will not persist after a few dike injection episodes and the mechanism does not work for low flank dips or more acceptable Poisson's ratio of about 0.25. For mature Hawaiian rifts with possibly thousands of dikes and low flank dips it appears therefore that additional processes must act to control the stresses that permit continued dike intrusion and rift persistence.

Finite element models and fault stability calculations indicate that accommodation to dike emplacement by deep faulting on roughly horizontal faults of the type proposed for the 1975 Kalapana earthquake is compatible with gravity and intrusion stresses. Additionally, such faulting, originating near the base of rift dikes, results in stress patterns along the rift axis that favor trapping of dikes within the rift. Consequently, such faulting not only pro-

vides a means for the flanks to continuously adjust to rift dikes, it also generates the stress patterns needed to constrain future dikes to propagate along the rift axis. Other possible faulting mechanisms such as shallow gravity slides and normal faulting of the flanks, do not appear to be favored by the intrusion stresses and do not result in stress patterns that would favor rift persistence.

A model for rift growth is proposed in which slip on a deep, roughly horizontal fault acts to relieve the stresses from rift intrusions. As suggested by others for the 1975 Kalapana earthquake, the fault could coincide with the contact of the volcano with the seafloor within the weak seafloor sediments. At all times the stress state in the volcano is near that required for faulting. In this model the horizontal stress generated by a standing column of magma at the time of dike emplacement, the stresses in the ridges, and fault strength are coupled. This results in a feedback between the maximum height magma can rise along the rift, fault friction and fault width. Through the feedback, the slope of the volcano flank is controlled by the fault friction. Applied to Kilauea the model yields an estimate for the coefficient of fault friction as high as 0.4 assuming normal hydrostatic pore fluid pressure. An implication of this model, supported by other studies, is that rift intrusion and lateral speading could be a significant contributor to volcano growth.

Reports

Dieterich, J. H., 1986, A Model for the Nucleation of Earthquake Slip: Earthquake Source Mechanics, Geophysical Monograph 37 (Maurice Ewing 6) p. 37-47.

Dieterich, J. H., 1986, Nucleation and Triggering of Earthquake Slip: Effect on Periodic Stresses, Tectonophysics, 21 p., in press.

Dieterich, J.H., 1986, Growth and Persistence of Hawaiian Volcanic Rifts (abstract) accepted for the Hawaiian Symposium on How Volcanoes Work.

Linker, M.F. and J.H. Dieterich, 1986, Effects of Variable Normal Stress on Rock Friction: Observations at 50 bars Normal Stress: (abstract), EOS, p. 1186.

Okubo, P. G., and Dieterich, J. H., 1986, State Variable Constitutive Relations for Dynamic Fault Slip: Earthquake Source Mechanics, Geophysical Monograph 37 (Maurice Ewing 6) p. 25-35.

In Situ Stress Measurements

9960-01184

John Healy
Branch of Tectonophysics
U.S. Geological Survey
345 Middlefield Road, MS/977
Menlo Park, California 94025
415-323-8111, ext. 2535

Investigations and Results

All of our effort during this period has been devoted to preparing for stress measurements in the deep drill hole at Cajon Pass. This hole will be the first deep hole drilled under the National Program to Deep Observations and Sampling of the Continental Crust. We believe that stress measurements at 16,000 feet in this hole will be the first measurements of stress in the Earth's crust at seismogenic depths.

There are no available systems to measure stress under the conditions that we expect to encounter in this hole, and we have undertaken an extensive program of development and testing with TAM International to develop systems for these measurements. This development has proceeded on schedule and we expect to be ready to begin measurements in January, 1987, the anticipated date when the hole will be drilled to 6,000'.

Constitutive Relations for Frictional Rock Sliding and Computer Modelling of the Elastic-Sliding Interactive System

14-08-001-G1191

Bruce E. Hobbs
CSIRO Division of Geomechanics
Box 54, Mt. Waverley, 3149
Australia
(03) 235-1355

Objective: This project is aimed at (i) generalizing the constitutive relations for frictional sliding already developed by Dieterich (1979, 1981) and Ruina (1980, 1983) by including a dependence upon normal stress and at (ii) modelling the interaction between constitutive behavior of the fault and the elastic response of the surrounding rocks using hybrid distinct element-boundary element codes.

Experimental Studies: A new HP 3852A data acquisition system has been installed with a HP 320 computer to monitor and control experiments in a large capacity direct shear frame. The apparatus is being used to examine the response of shear stress to changes in normal stress at constant and at constantly changing load point sliding velocity. Some results are shown in Figures 1a,b,c and d. Figure 1a shows the history of horizontal displacement measured by an LVDT which is housed in the actuator responsible for applying the horizontal (shear) force; this plot gives the imposed load point displacement history. Figure 1b shows the history of normal force across the sliding interface measured by a load cell near the specimen. Figure 1c shows the history of shear force measured by another load cell near the specimen and Figure 1d shows the history of displacement of one of the sliding blocks measured by a DCDT attached to the block. Between A and B the block is sliding (with about 100 μm of accumulated gouge at the interface) at a constant imposed load point velocity of 1.42 $\mu m\ s^{-1}$ as shown in Figure 1a and with a constant normal force of 125 KN (the area of the block interface is $6.25 \times 10^{-2} m^2$) as shown in Figure 1b. The shear force is oscillatory as shown in Figure 1c with small jumps in displacement (Figure 1d). At B the normal force is suddenly increased from 125 KN to 248 KN (Figure 1b) whilst the imposed load point velocity remains constant (Figure 1a). There follows a slow increase in shear force (Figure 1c) to a coefficient of friction similar to that at the lower normal force; this is accompanied by a complicated velocity response of the block itself (Figure 1d). At C the block is sliding again with the same average velocity as at A except that oscillatory and stick-slip events are now better developed; these tend to be chaotic. At D the velocity is decreased to 0.16 $\mu m\ s^{-1}$ resulting in slower oscillations in shear stress. This behavior is typical of the response to changes in normal stress. A systematic study of this behavior is now commencing.

Modelling Studies: A hybrid distinct element-boundary element code (HYDEBE) described in detail by Lorig, Brady and Cundall (1986) has been used to model a single fault embedded in a jointed medium (Figure 2). In this model the far field (outside the circular boundary element array) is elastic and under compression in a NE-SW direction. Inside the circle the material is elastic and the joints and fault have Mohr-Coulomb behavior. After the fault starts to move, the constitutive law for sliding is a single state variable Dieterich-Ruina law with no upper velocity cut-off. Figure 3 shows the history of shear stress at various places on the fault. At each end of the fault the shear stress is low and there is no sliding motion at these points. The shear stress rises to a maximum at the center of the fault and the history of shear stress here is oscillatory with no sharp stress drops. However between each end of the fault and the center of

the fault the stress history is oscillatory with sharp stress drops late in the sliding history. This behavior is similar to that reported by Horowitz and Ruina (1986). The work is being extended to other fault geometries. In this example, the normal stiffness of the fault is set very low so that there is no change in normal stress across the fault. Future developments involve incorporation of the constitutive description of frictional normal stress dependence determined from the experimental work.

References:

Horowitz, F.G., and Ruina, A., 1986. Frictional slip patterns generated in a spatially homogeneous elastic fault model. Submitted to J.G.R.

Lorig, L.J., Brady, B.H.G., and Cundall, P.A., 1986. Hybrid distinct element-boundary element analysis of jointed rock. Int. J. Rock Mech. Min. Sci. and Geomech. Abst., 23, 303-312.

Figure Captions

Figure 1(a) Displacement history of sliding block system measured by an LVDT housed in the actuator driving the shear displacement.

Figure 1(b) Normal (vertical) force history measured by a load cell close to the specimen.

Figure 1(c) Shear (horizontal) force history measured by a second load cell to the specimen.

Figure 1(d) Horizontal displacement of the block measured by a DCDT close to one of the sliding blocks.

Figure 2. Fault model: an isolated fault is embedded in a jointed medium.

Figure 3. Stress history at various places on the fault in Figure 2.

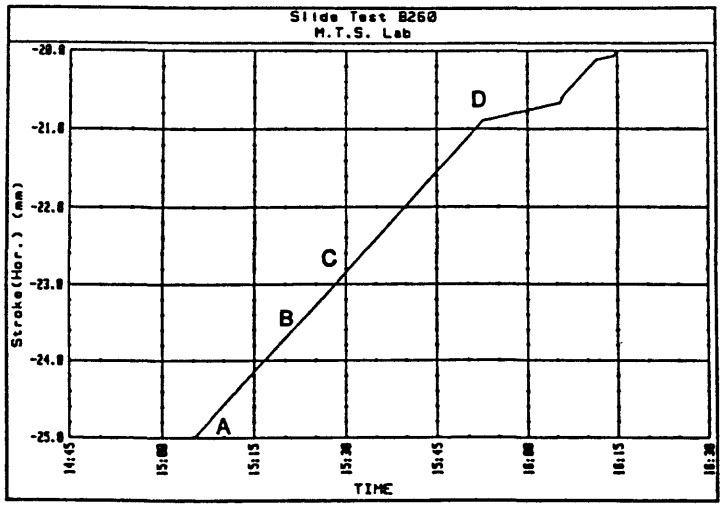

a

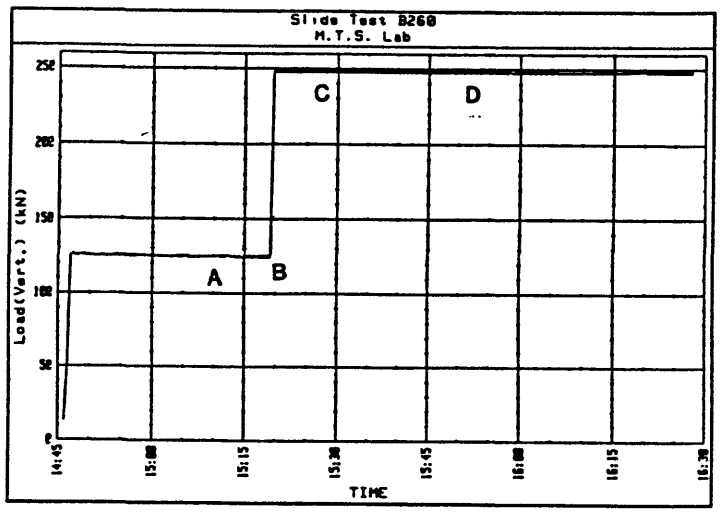

b

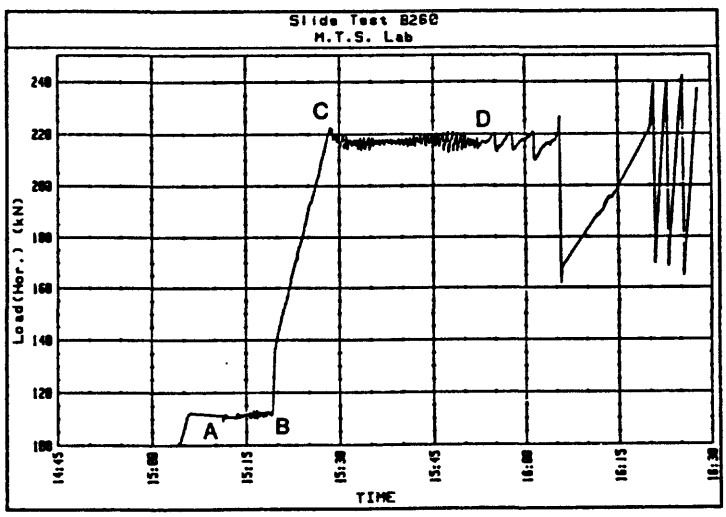

c

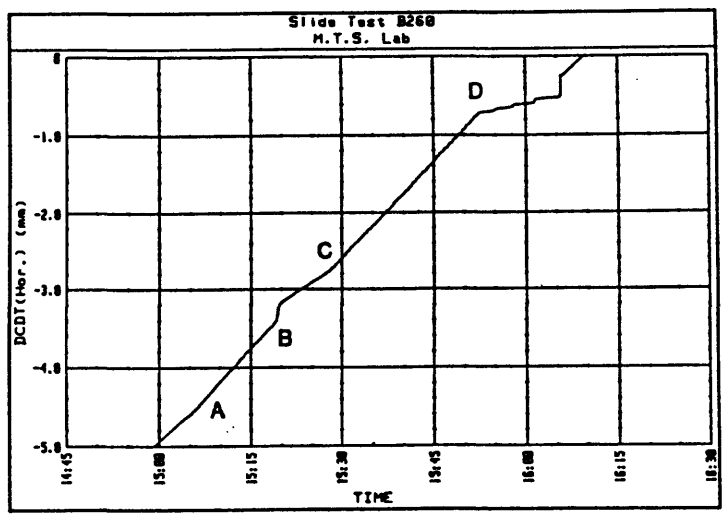

d

Proposed layout for fig 1.

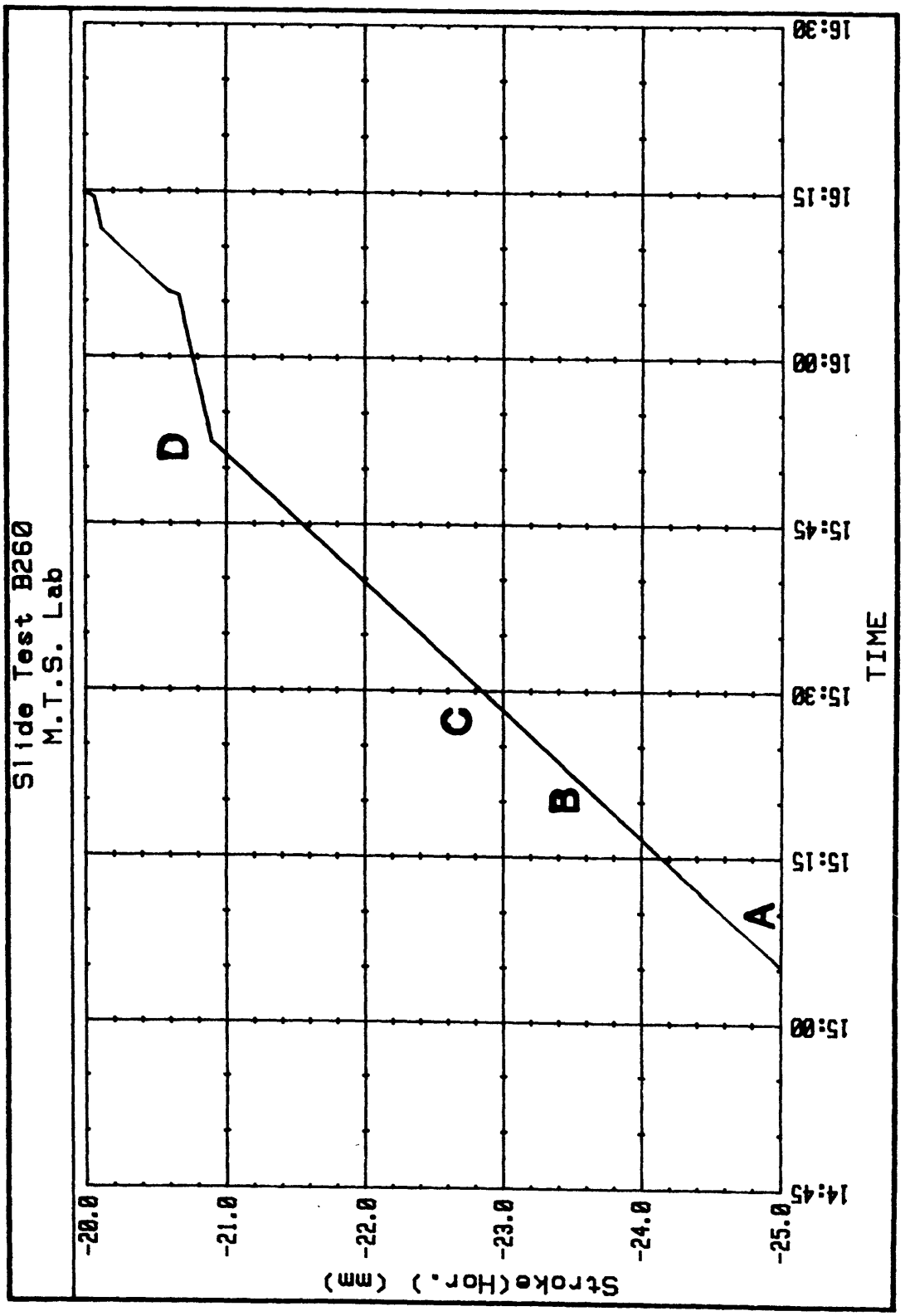
Slide Test B260
M.T.S. Lab
Stroke(Hor.) (mm)
-20.0
-21.0
-22.0
-23.0
-24.0
-25.0
14:45
15:00
15:15
15:30
15:45
16:00
16:15
16:30
TIME
A
B
C
D

a

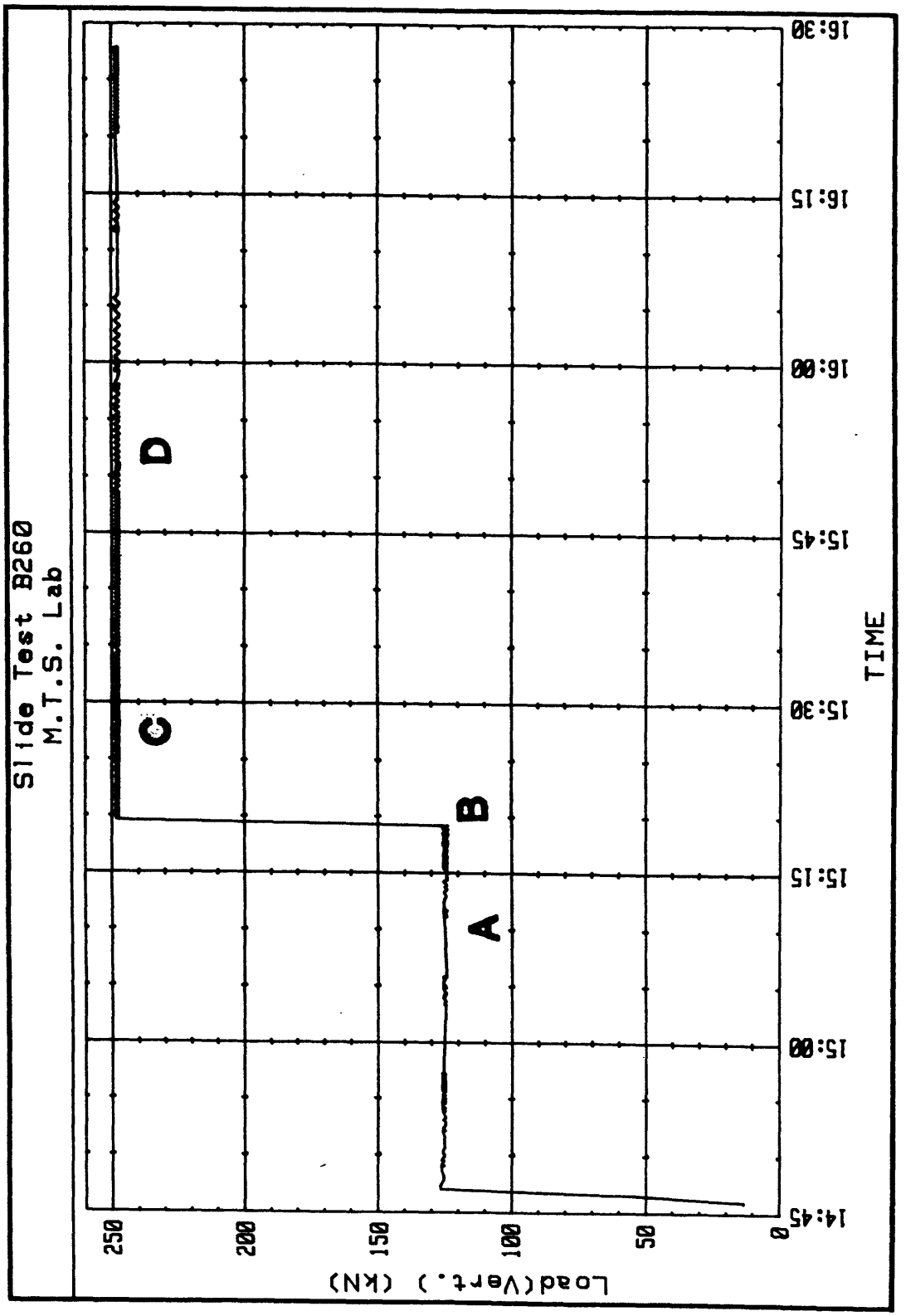
Slide Test B260
M.T.S. Lab
Load(Vert.) (KN)
250
200
150
100
50
0
14:45
15:00
15:15
15:30
15:45
16:00
16:15
16:30
TIME
A
B
C
D

b

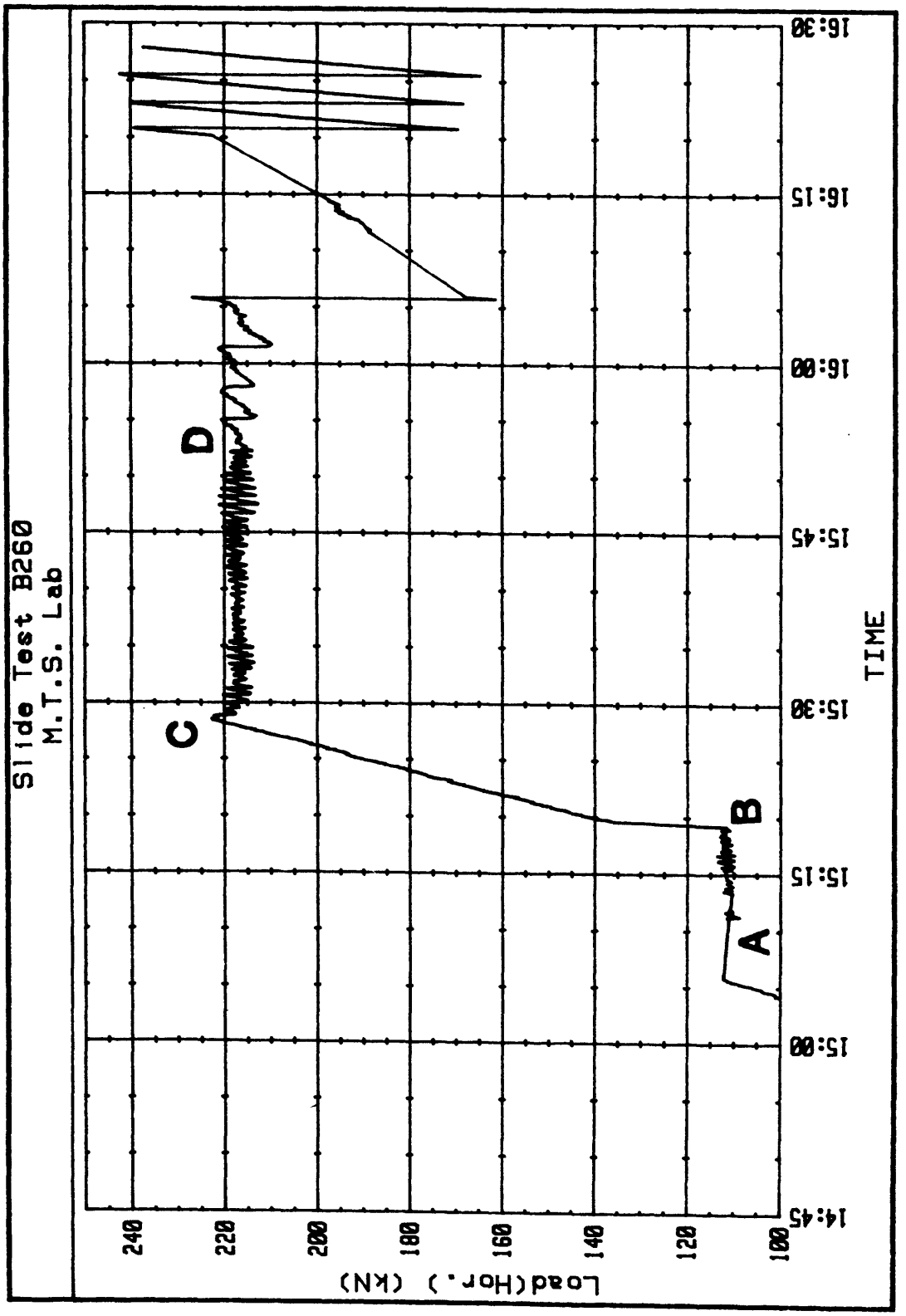
Slide Test B260
M.T.S. Lab
Load(Hor.) (KN)
240
220
200
180
160
140
120
100
14:45
15:00
15:15
15:30
15:45
16:00
16:15
16:30
TIME
A
B
C
D

C

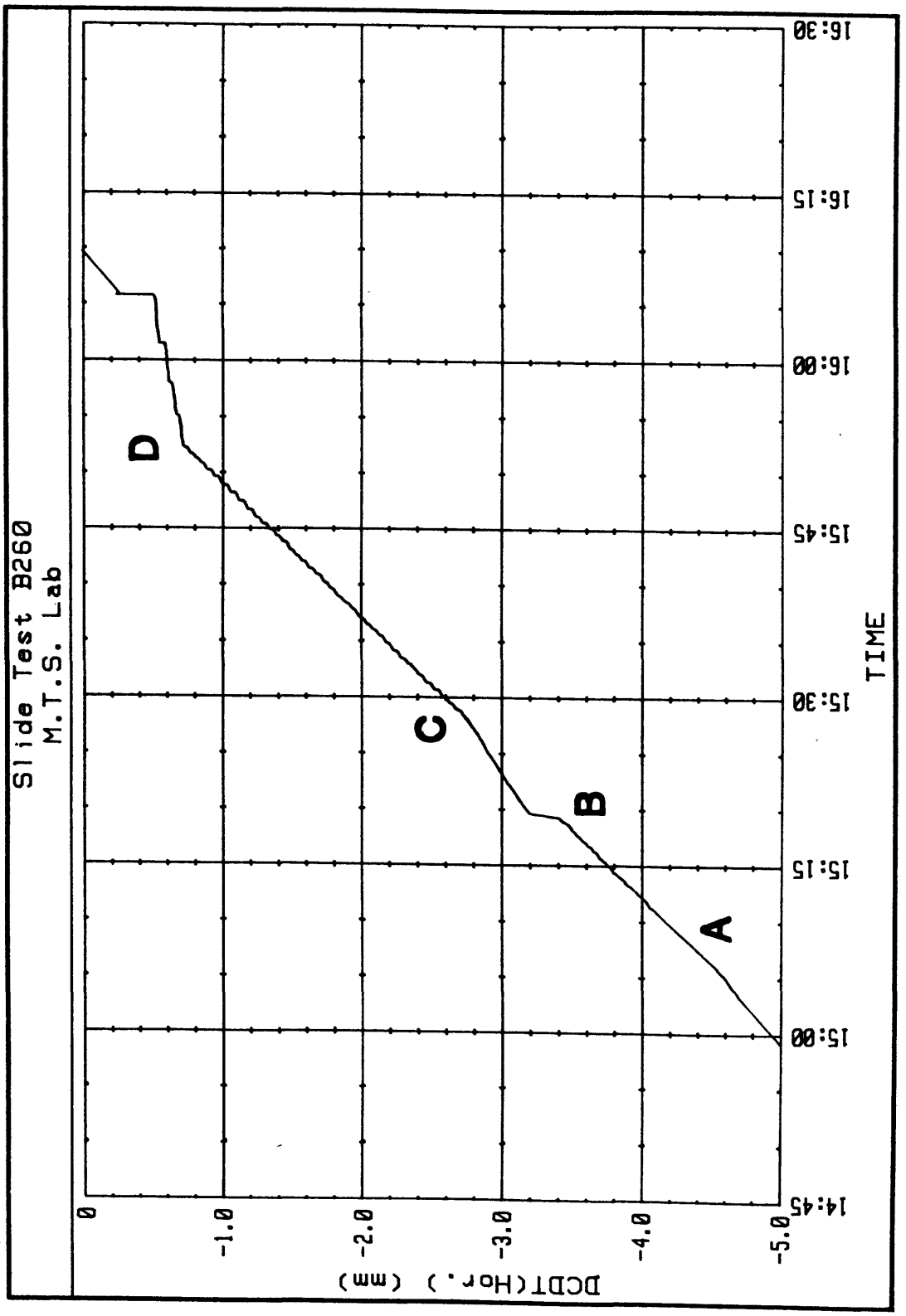
Slide Test B260
M.T.S. Lab
DCDT(Hor.) (mm)
0
-1.0
-2.0
-3.0
-4.0
-5.0
14:45
15:00
15:15
15:30
15:45
16:00
16:15
16:30
TIME
A
B
C
D

d

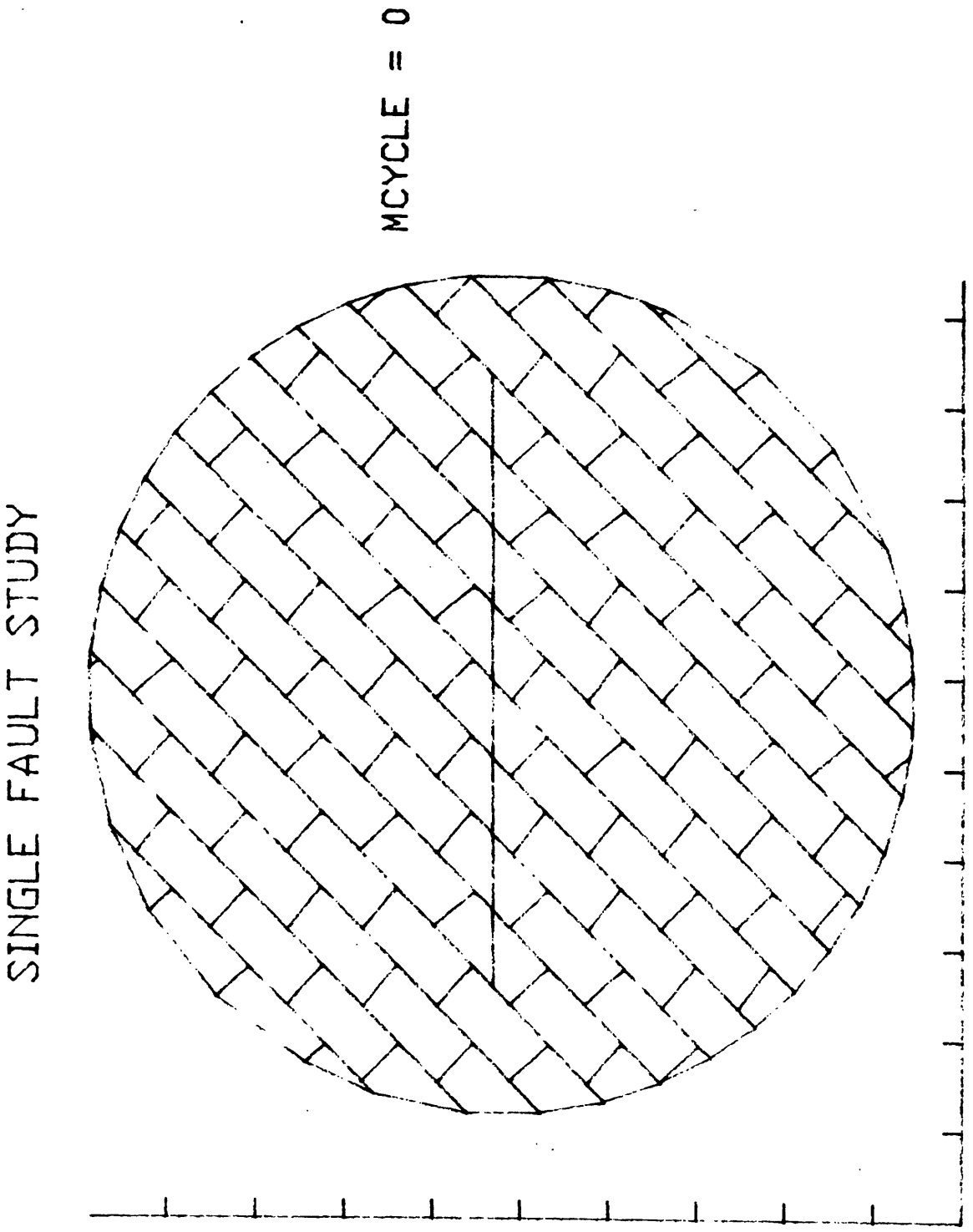
SINGLE FAULT STUDY
MCYCLE = 0

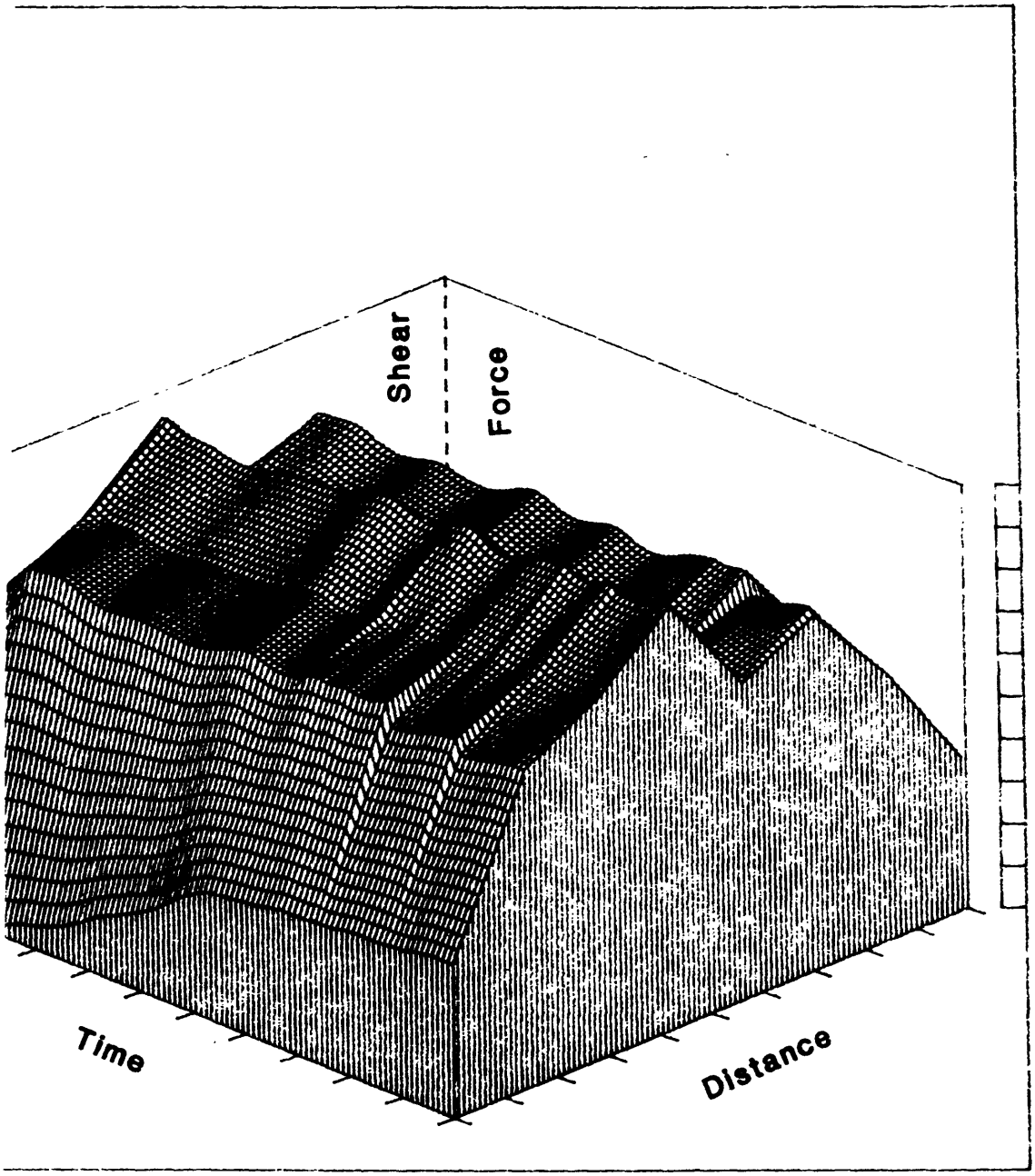
Shear
Force
Time
Distance

Earthquakes and the Statistics of Crustal Heterogeneity

9930-03008

Bruce R. Julian

Branch of Seismology
U.S. Geological Survey
345 Middlefield Road - MS77
Menlo Park, California 94025
(415) 323-8111 ext. 2931

Investigations

Both the initiation and the stopping of earthquake ruptures are controlled by spatial heterogeneity of the mechanical properties and stress within the earth. Ruptures begin at points where the stress exceeds the strength of the rocks, and propagate until an extended region ("asperity") where the strength exceeds the pre-stress is able to stop rupture growth. The rupture termination process has the greater potential for earthquake prediction, because it controls earthquake size and because it involves a larger, and thus more easily studied, volume within the earth. Knowledge of the distribution of mechanical properties and the stress orientation and magnitude may enable one to anticipate conditions favoring extended rupture propagation. For instance, changes in the slope of the earthquake frequency-magnitude curve ("b-slope"), which have been suggested to be earthquake precursors and which often occur at the time of large earthquakes, are probably caused by an interaction between the stress field and the distribution of heterogeneities within the earth.

The purpose of this project is to develop techniques for determining the small-scale distributions of stress and mechanical properties in the earth. The distributions of elastic moduli and density are the easiest things to determine, using scattered seismic waves. Earthquake mechanisms can be used to infer stress orientation, but with a larger degree of non-uniqueness. Some important questions to be answered are:

** How strong are the heterogeneities as functions of length scale?

** How do the length scales vary with direction?

** What statistical correlations exist between heterogeneities of different parameters?

** How do the heterogeneities vary with depth and from region to region?

Scattered seismic waves provide the best data bearing on these questions. They can be used to determine the three-dimensional spatial power spectra and cross-spectra of heterogeneities in elastic moduli and density in regions from which scattering can be observed. The observations must, however, be made with seismometer arrays to enable propagation direction to be determined. Three-component observations would also be helpful for identifying and separating different wave types and modes of propagation.

The stress within the crust is more difficult to study. Direct observations require deep boreholes and are much too expensive to be practical for mapping small-scale variations. Earthquake mechanisms, on the other hand, are easily studied and reflect the stress orientation and, less directly, its magnitude, but are often not uniquely determined by available data.

This investigation uses earthquake mechanisms and the scattering of seismic waves as tools for studying crustal heterogeneity.

Results

Automatic real-time earthquake monitoring

Over the last several years, the USGS has developed a system for monitoring central and northern California earthquakes automatically in real time, using phase arrival information generated by the Real-Time Processor (RTP). The arrival data are processed by a separate computer system, which automatically computes earthquake hypocenters locations and magnitudes, maintains a data base of this information, and displays maps showing current activity on interactive graphics terminals. In addition, the system also detects large earthquakes and swarms and automatically notifies seismologists by means of a radio paging system.

A disadvantage of this system is that detailed alarm criteria must be specified ahead of time, so it is useful primarily for regions that are already under scrutiny. We have now extended the system to automatically detect and report significant changes in seismic activity. To do this, we divide central California into regions, using a scheme recently developed by Fred Klein. Every day, we count the number of earthquakes in each region, compare it with a one-year record of past history, and report activity levels that are unusual at the 99% level (either high or low).

Already, this simple process has scored one success. As soon as it began operating in early July, it began detecting and reporting unusually high seismicity levels in the Chalfant Valley region of east-central California. This activity, which increased for about three weeks, turned out to be a foreshock sequence to the magnitude 6.4 Chalfant Valley earthquake of July 21.

Work is continuing to refine and extend this automatic processing. In particular, we are developing more sophisticated statistical methods for deciding when activity is "unusual", and we are planning to make use of information about earthquake magnitudes.

Observations of Chalfant Valley aftershocks

In late July and early August, a large cooperative crustal structure experiment took place in west-central Nevada. Following this experiment, the USGS seismic refraction instruments were moved to the area of the magnitude 6.4 Chalfant Valley earthquake of 21 July 1986, where they were used to record aftershocks at short distances. About one hundred instruments were deployed in two dense 1 km arrays at the north and south ends of the aftershock region and in a 10 km linear spread connecting them. We hope that data from such dense arrays, which have heretofore been lacking, will answer several questions about seismic coda waves. In particular, we hope to learn about the mode of propagation of coda waves, and about the spatial distribution in the crust of the scatterers that produce them.

Revised estimate of maximum size of tensile earthquakes

In a previous semiannual report, we described theoretical studies of fluid-driven tensile cracks, undertaken jointly with Prof. Charles Sammis of the University of Southern California. These studies showed that the propagation of such cracks is not necessarily limited, as had been thought, by the speed at which the driving fluid can flow in the crack; in many realistic situations the crack can propagate catastrophically, even if the fluid does not flow at all. However, the predicted sizes of earthquakes generated by tensile cracks turned out to be somewhat smaller than the largest of the anomalous earthquakes at Long Valley caldera, which had originally motivated the investigations. It was clear that using more realistic models of the stress field around a magma chamber would increase the predicted size, and might predict earthquakes as large as those observed, but the quantitative analysis of this problem presents formidable difficulties.

Recently, Dr. Paul Delaney called our attention to estimates of the fracture toughness of rocks based on field observations of the shapes of dikes near Shiprock, New Mexico. These estimates are roughly 100 times larger than values obtained in the laboratory, and lead to larger predicted sizes for tensile earthquakes. For conditions appropriate to Long Valley caldera, dimensions comparable to the radius of the magma chamber (about 7 km) are expected for tensile faults starting from flaws a meter or so in size.

Thus fluid-flow and crack stability arguments do not rule out the possibility that some of the Long Valley earthquakes may have been cause by tensile failure at high fluid pressure. The most serious difficulty still facing this hypothesis is to explain why some of the observed first motions are dilatational. More realistic dynamic modeling of the radiation from fluid-driven tensile cracks may help answer this question.

Mechanism of volcanic tremor

We have continued investigations on modeling volcanic tremor as a flow-induced nonlinear vibration of the walls of cracks transporting magmatic fluids. In particular, we are extending the theory to include the effects of interaction of the vibrating section of the crack with the acoustic waves radiated into the fluid. By analogy with musical wind instruments, we expect the vibrations to become synchronized with the modes of oscillation of the fluid-filled cracks or chambers to which the vibrator is connected. This effect will cause tremor to be sensitive both to the geometry of the network of magma chambers and passages and to the rate of magma flow, and will complicate the problem of estimating flow rates from tremor observations.

Reports

Sammis, Charles G., and Julian, Bruce R., 1985, Fracture instabilities accompanying dike intrusion: J. Geophys. Res. (accepted).

Experimental Rock Mechanics

9960-01180

Stephen H. Kirby
Branch of Tectonophysics
U.S. Geological Survey, MS/977
345 Middlefield Road
Menlo Park, California 94025
(415) 323-8111, Ext. 2872

Investigations

1. Phase changes and shear zones in the crust and upper mantle.
2. Physical mechanisms of deep earthquakes.
3. Aseismic fault zones in the mantle.
4. Structure and rheology of the lithosphere.

Results

1. Phase changes and shear zones in the upper lithosphere

Our previous discovery of a marked weakening of polycrystalline olivine by light hydrothermal alteration in friction experiments at 400°C and 500 MPa confining pressure has been followed up by SEM investigation of the sliding surfaces of altered and heat-treated samples by John Pinkston and Laura Stern. The samples heat-treated at 600°C show deep microfracturing damage and no particular role of grain boundaries that were previously altered but partially dehydrated by the heat treatment. The sliding surfaces of the altered samples have excavated grain boundaries with significant mineral growth on the sliding surfaces. The presence of serpentine and a chlorite on the sliding surface apparently plays some role in reducing the resistance to frictional sliding, which is dramatically lower than the frictional resistance of pure olivine or serpentine samples themselves. For our Fall AGU presentation, we will speculate on the possible role of retrograde hydrothermal alteration of fault surfaces in reducing shear stresses along mid-crustal faults. Also, we are starting a collaboration with Howard Wilshire in the study of frictional processes on sliding surfaces in naturally deformed mantle peridotites brought up by basalts as xenoliths. These shear fractures may have produced microearthquakes.

2. The discovery paper on localized phase transformations, high-pressure faulting and their implications for deep earthquakes was completed and submitted for publication in the special issue of JGR on deep earthquakes (Kirby, 1986). This work proposes an entirely new source mechanism for earthquakes in relatively cold deeply-subducted lithosphere where sluggish polymorphic phase changes are thought to occur. A USGS Postdoctoral Fellowship was awarded to Lisa DellAngelo of Brown University to follow up on this work by exploring a variety of polymorphic phase changes under non-hydrostatic stress.

3. Aseismic fault zones in the mantle

Along with our Chinese colleagues at the State Seismological Bureau in Beijing, we continue to study the mylonitic peridotite xenoliths that have been brought up from the mantle by basalts that issue from the Tangchen-Lujiang fault zone, a major plate-scale fault zone in eastern China. Recent work includes the study of olivine preferred orientations, which are remarkably weak considering the large strains that these rocks have sustained. This weak fabric development is consistent with superplastic deformation connected with grain boundary sliding and may explain why strains may be localized in mantle fault zones. We have also had the opportunity to examine peridotite samples dredge-hauled from fracture zones near the SW Indian Ridge by H.B. Dick of Woods Hole Oceanographic Institute. At these localities, the mantle outcrop on the ocean floor and many of them are remarkably fresh and show even more extreme mylonitic textures than the China peridotite xenoliths. We are exploring the possibility of participating in Leg 115 of the Ocean Drilling Project in which it is proposed to recover long drill core from the oceanic mantle near the SW Indian Ridge. This offers the exciting possibility of studying the structures acquired by the oceanic lithosphere near where it is created and modified by transform-fault deformation.

4. Structure and rheology of the lithosphere

A review of the U.S.G.S.-sponsored Workshop on the Geophysics and Petrology of the Deep Crust and Upper Mantle was completed (Kirby et al., 1986) and the short papers were edited and were sent off for publication as a U.S.G.S. circular. Also, work commenced on the IUGG report on the rheology of the lithosphere, co-authored by Andreas Kronenberg of Texas A & M. Topics to be reviewed included seismic anistropy and flow in the upper mantle, strain localization and the Moho as a rheological discontinuity.

Reports

Kirby, S. H., 1986, Localized polymorphic phase transformations in high-pressure faults and applications to the physical mechanism of deep earthquakes, Journal of Geophysical Research (in press).

Kirby, S. H., Hearn, B. C., Jr., He, Yongnian, and Lin, Chuanong, 1986, Geophysical evidence of mantle xenoliths: evidence for fault zones in the deep lithosphere of eastern China: U.S. Geological Survey Circular, Kirby, S. H., Nielson, Jane, and Noller, J., eds. (in press).

Kirby, S. H., Nielson, J., and Noller, J., eds., 1986, Geophysics and petrology of the deep crust and upper mantle: Introduction to the Workshop Proceedings, U.S. Geological Survey Circular (in press).

Kronenberg, A. K., and Kirby, S. H., 1986, Ionic conductivity of quartz: DC time dependence and transition in charge carriers: American Mineralogist (in press).

Kronenberg, A. K., Kirby, S. H., Aines, R. D., and Rossman, G. R., 1985, Solubility and diffusional uptake of hydrogen in quartz at high pressures: implications for hydrolytic weakening: Journal of Geophysical Research (accepted, in press).

Pinkston, J., Stern, L. and Kirby, S., 1986, Sliding resistance at elevated temperatures of polycrystalline olivine with trace hydrothermal alteration and implications for fault-zone rheology, Trans. A.G.U. (EOS), 67 (in press).

Rupture Mechanics of Slip-Deficient Fault Zones

14-08-0001-G1167

J. R. Rice (PI) and R. Dmowska
Division of Applied Sciences and
Department of Earth and Planetary Sciences
Harvard University
Cambridge, MA 02138
(617)495-3445, 3452

(For period Dec. 1, 1985 to May 31, 1986)

Investigations

1. Work has been completed on formulating a depth variable model of rate and state dependent frictional constitutive properties at a transform margin and on analyzing slip accumulation as a function of depth and time over the earthquake cycle.

2. Studies are underway on possible nonuniformities in the fault loading rate at Parkfield due to interactions between the Central California creeping zone and the presently locked zones of the 1857 and 1906 earthquakes. This may be important to interpreting the times of past Parkfield earthquakes for purposes of predicting future ones. We also consider effects of Parkfield ruptures on stress transfer to the southeast.

3. Some progress has been made on modelling crack growth through a medium of variable fracture resistance.

Results

1. Many of the results from this study were presented in the October 1985 progress summary (USGS Open-File Report 86-31, p.430-434) for the predecessor grant 14-08-0001-G-823. A full report in the form of a 25 page paper, 'Crustal earthquake instability in relation to the depth variation of frictional slip properties' by S.T. Tse and J.R. Rice, is now in press in JGR. A shortened abstract follows.

Stability studies using constitutive relations of the type found to describe frictional slip in the laboratory have provided a new explanation for the depth cut-off of shallow crustal earthquakes. For sliding at a fixed slip rate V, and fixed normal stress and temperature, shear strength τ evolves towards a steady state value $\tau^{ss}(V)$. A surface with $d\tau^{ss}/dV<0$ has been shown to be potentially unstable but one

with $d\tau^{ss}/dV>0$ has stable steady state sliding, at least for a broad class of constitutive laws described in the paper. Experiments by Dieterich and Tullis and Weeks on Westerly granite with mature sliding surfaces indicate $d\tau^{ss}/dV$ is negative at room temperature, whereas higher temperature experiments by Stesky show that $d\tau^{ss}/dV$ becomes positive above about 300°C. These observations suggest that the depth cut-off can be understood as a variation with increasing depth from a regime with $d\tau^{ss}/dV<0$ to one with $d\tau^{ss}/dV>0$. This is not inconsistent with, but rather refines, suggestions that the cut-off is due to a transition from brittle friction to ductile flow. Following Mavko, a two dimensional quasistatic strike-slip fault model is analyzed numerically, but the model is based on laboratory constrained depth variations of constitutive properties as described above. Resulting predictions of slip distributions versus depth throughout the earthquake cycle show confinement of earthquakes to shallow depths and development of locked patches in the crust, and give recurrence times and seismic stress drops and displacements that seem generally compatible with large scale strike slip earthquakes along the San Andreas fault.

2. The issues being addressed are the following. First, how do Parkfield earthquakes affect stress accumulation to the southeast, along the presently locked portion of the San Andreas fault beyond Cholame? For example, studies by K.E. Sieh and co-workers suggest that the portion of fault between Cholame and Bitterwater Valley to the southeast may have a recurrence time on the order of 100 years and thus could rupture again following the coseismic, or short term post-seismic, stress perturbations from a rupture initiating at Parkfield. Second, how uniform in time is the loading rate at Parkfield? To the extent that the lithosphere is essentially elastic on the earthquake timescale, it must be assumed that motion accumulates with some non uniformity in time along the creeping zone due to the episodic nature of slip in the bordering great 1857 and 1906 rupture zones. We are attempting to quantify this non-uniformity since it may be important for interpreting the times of occurrence of prior Parkfield earthquakes for purposes of predicting future ones.

The first question has been studied to some extent by modelling techniques for the stressing of locked patches as developed in some of our previous work (Tse, Dmowska and Rice, BSSA, 75, p. 709, 1985). Here we describe briefly the manner by which the second question is being addressed. We assume that an elastic, transform-faulted surface plate, thickness H, must accommodate a steady velocity V(y) of flow at the base of a Maxwell viscoelastic asthenosphere foundation for the plate. Here x, y are coordinates in the plane of the plate, x is along strike of the transform fault. In terms of thickness averaged stresses σ in the plate, equilibrium equations of type

$$H(\partial\sigma_{xx}/\partial x + \partial\sigma_{yx}/\partial y) = \tau_x$$

must be satisfied, where τ is the shear traction on the base of the plate due to coupling to the asthenosphere. Stresses σ are related to gradients of thickness average in-plane displacements u by the usual relations of plane stress elasticity. Asthenospheric coupling is approximated in the Elsasser form

$$\partial\tau_x/\partial t + \tau_x/t_r = c[\partial u_x/\partial t - V(y)]$$

where t_r is the relaxation time and c is an elastic stiffness. The imposed deep flow rate V(y) varies from $-(1/2)\ V_{pl}$ to $+(1/2)\ V_{pl}$ as y increases from large negative to large positive values; V_{pl} = plate velocity.

Assuming for simplicity that a semi-infinite creep zone (x>0, y=0) slips at

constant stress σ_{xy} while the semi-infinite adjacent fault zone ($x<0$, $y=0$), while normally locked, stick-slips periodically with displacement $V_{pl}T_{cyc}$ at end of each earthquake cycle of time T_{cyc}, the displacement and stress fields may be shown to have the form

$$u_x = V_{pl}\, t/2 + u_x^{(o)}(x,y) + \tilde{u}_x(x,y,t) \qquad (y>0)$$

$$\sigma_{xy} = \sigma_{xy}^{(o)}(x,y) + \tilde{\sigma}_{xy}(x,y,t)$$

Here the fields $\tilde{u}_x$, $\tilde{\sigma}_{xy}$ are strictly periodic in time and are adjusted to zero average over the cycle. The time-independent parts, $u^{(o)}$ and $\sigma^{(o)}$, depend on the detailed form of $V(y)$, but $\tilde{u}$ and $\tilde{\sigma}$ do not. Boundary conditions are that $\tilde{\sigma}_{xy} = 0$ on the creep segment and that u_x is a prescribed function of time, with saw-tooth variation in time, on the stick-slipping segment. Following the modelling procedures of Lehner, Li and Rice (J. Geophys. Res., 86, p. 6155, 1981), we calculate u_x as the solution to

$$\frac{\pi H}{4}\,2\,\frac{\partial}{\partial t} + \frac{1}{t_r}\,\frac{\partial^2}{\partial y^2} + (1+\nu)^2\,\frac{\partial^2}{\partial x^2}\,\tilde{u}_x = \frac{\partial}{\partial t}\,\tilde{u}_x$$

where $\tilde{u}_x$ is prescribed on $y=0$, $x<0$ and $\partial\tilde{u}_x/\partial y = 0$ on $y=0$, $x>0$.

Fig. 1 shows results for the slip rate $\dot{\delta}$ ($= V_{pl} + 2\,\partial\tilde{u}_x/\partial t$) along the creep zone at various times during the cycle for $t_r/T_{cyc} = 1/15$ (e.g., 10 yr. relaxation time, 150 yr. cycle time). Evidently, slip rates near the junction are expected to be very strongly non uniform over the first quarter of a cycle, with significant changes continuing up to about half the cycle.

To interpret these results for Parkfield (the episodic nature of slip there is neglected in the model just discussed), we should focus on the predicted slip rates in the vicinity of $x = H$ to $2H$ (Parkfield earthquakes seem to nucleate around 35 km from the end of the locked 1857 rupture zone). Assuming a 150 year cycle time, strong non uniformities of loading occur in the quarter cycle up to about 1895 and significant non uniformities continue in to the half-cycle time around 1930. These factors should be considered in forming average recurrence times based on past Parkfield earthquakes.

3. Recent theoretical elasticity solutions that we have derived allow the analysis of stresses along the fronts of planar cracks in certain three-dimensional solids when the crack front lies along an arc that is perturbed slightly from a simple (e.g., straight line, circle) shape. These solutions are now being used to as the starting point for determining successive crack front locations as remote loading drives the crack through a region of locally variable fracture resistance. Our interest in such work is to better understand the mechanism by which a slipping fault zone may penetrate locally into a locked, slip-resistant asperity on the fault plane prior to instability. As a more distant application, we hope to understand the statistics of small-scale instabilities, and time variations in their occurrence and distribution, as local asperities fail prior to overall instability of a locked region of the crust which is being attacked by slip, and hence stress concentration, from below.

Presentation of results on crack front position in relation to specific local variations of fracture toughness is deferred since these are fragmentary at present. Here we present a result of the basic elasticity solution (Gao and Rice, J. Appl.

Mech., in press) which provides the starting point. Consider a half plane crack on y=0 in an infinite elastic solid. Suppose that the applied loadings are such that, if the crack front is straight and lies along the line x=a, parallel to the z axis on y=0, a uniform set of stress intensity factors is induced along the crack front. Denote these factors by

$$K_1^o[a] \quad , \quad K_2^o[a] \quad , \quad K_3^o[a]$$

(1: tensile mode; 2: in-plane shear; 3: anti-plane shear mode). Then when the crack front is not straight but instead lies along the general arc x=a(z) in the plane y=0, and da(z)/dz is small, one has the following set of stress intensity factors at place z along the crack front:

$$K_1(z) = K_1^o[a(z)]\{1 + f(z)\}$$

$$K_2(z) = K_2^o[a(z)]\{1 + (2-3\nu)f(z)/(2-\nu)\} - 2K_3^o[a(z)][da(z)/dz]/(2-\nu)$$

$$K_3(z) = K_3^o[a(z)]\{1 + (2+\nu)f(z)/2-\nu) + 2(1-\nu)K_2^o[a(z)][da(z)/dz]/(2-\nu)$$

Here ν = Poisson ratio, f(z) is the principal value integral

$$f(z) = \frac{1}{2\pi} \int_{-\infty}^{+\infty} (z'-z)^{-1}[da(z')/dz']dz' \ ,$$

and the results are exact to first order in da(z)/dz. Similar results have been derived when the loadings are such that a non-uniform stress intensity factor distribution is induced along a straight crack. Also, the analogous solution has been derived for tensile-loaded cracks that are perturbed from a circular reference shape.

Publications/presentations

Dmowska, R., V.C. Li and J.R. Rice, 'Nonuniform stressing in the Parkfield region from interactions between adjacent creeping and locked fault zones', presentation at AGU Fall Meeting, San Francisco, Dec 1985 (abstract: EOS, Trans. A.G.U., 66, N. 46, p. 985, 1985)

Gao, H. and J.R. Rice, 'Shear stress intensity factors for a planar crack with a slightly curved front', J. Appl. Mech., in press, 1986.

Rice, J.R. and R. Dmowska, 'Fault stressing near Parkfield', presentation at Symposium on the Parkfield Prediction Experiment, AAAS Annual Meeting, Philadelphia, May 1986.

Rice, J.R. and S.T. Tse, 'Dynamic motion of a single degree of freedom elastic system with rate and state dependent friction', J. Geophys. Res., 91 (B1), 521-530, 1986.

Tse, S.T. and J.R. Rice, 'Crustal earthquake instability in relation to the depth variation of frictional slip properties', J. Geophys. Res., in press, 1986.

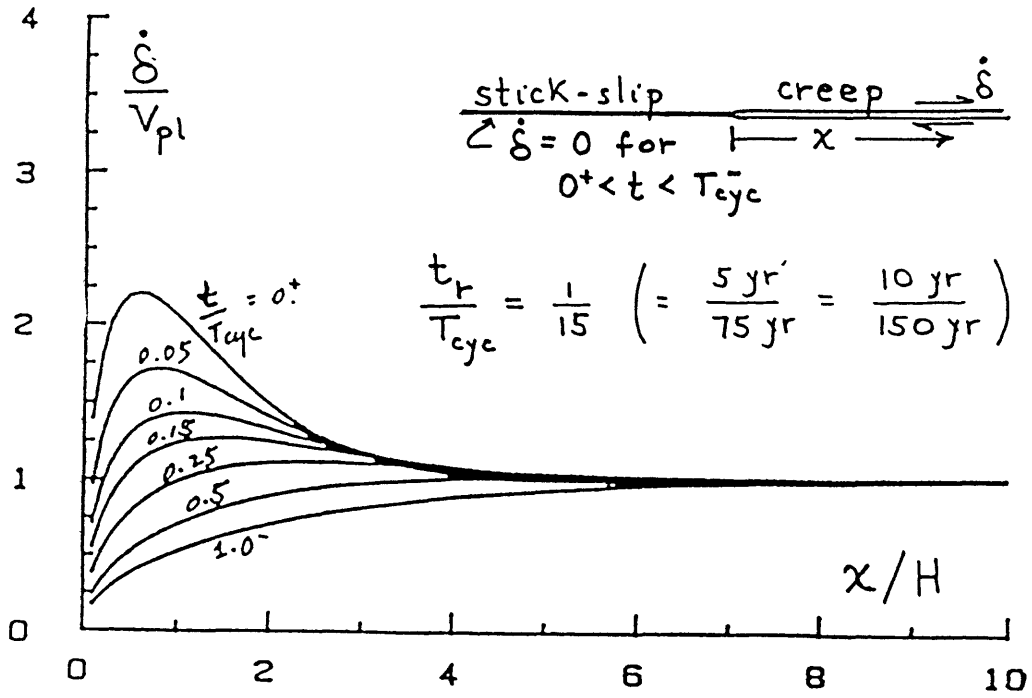
4
3
2
1
0
$\frac{\dot{\delta}}{V_{pl}}$
stick-slip
creep
$\dot{\delta}$
$\dot{\delta} = 0$ for
$0^+ < t < T_{cyc}^-$
x
$\frac{t_r}{T_{cyc}} = \frac{1}{15}$ (= $\frac{5\ yr}{75\ yr}$ = $\frac{10\ yr}{150\ yr}$)
$\frac{t}{T_{cyc}} = 0^+$
0.05
0.1
0.15
0.25
0.5
1.0⁻
x/H
0
2
4
6
8
10

FIG. 1.

Rupture Mechanics of Slip-Deficient Fault Zones

14-08-0001-G1167

J.R. Rice (P.I.) and R. Dmowska
Division of Applied Sciences and
Department of Earth and Planetary Sciences
Harvard University
Cambridge, MA 02138
(617)495-3445, 3452

(for period June 1, 1986 to Oct. 1, 1986).

Investigations

1. Seismic, geologic and geodetic data are used to constrain parameters of a model of stress accumulation along the presently locked great earthquake segments of the San Andreas fault. The basic concept is that adjoining elastic plates are loaded through a viscoelastic asthenosphere, owing to steady mantle motions below that are compatible with average plate velocity, and that the fault zone within the elastic plates is locked over a shallow depth interval but deforms at constant stress at greater depths.

2. Non-uniformities in the long term fault loading rate at Parkfield, due to transient interactions between the central California creeping zone and the adjacent zones of the great 1857 and 1906 earthquakes, are under study.

3. Crack growth modelling is underway for the penetration of a slipping zone into a locked fault zone, assuming spatially non-uniform resistance to initiation of slip (i.e., local asperities).

Results

1. This study has led to a manuscript to be submitted to JGR in Oct. 1986 by V.C. Li (M.I.T.) and Rice, as an expansion and reconsideration of their March 1985 report on a similar topic. The abstract is given as the next paragraph.

Periodic crustal deformation associated with repeated strike slip earthquakes is computed for the following model: A depth L ($\leq$H) extending downward from the Earth's surface at a transform boundary between uniform elastic lithospheric plates of thickness H is locked between earthquakes. It slips an amount consistent with remote plate velocity V_{pl} after each lapse of earthquake cycle time T_{cy}. Lower portions of the fault zone at the boundary slip continuously so as to maintain constant resistive shear stress. The plates are coupled at their base to a Maxwellian viscoelastic asthenosphere through which steady deep-seated mantle motions, compatible with plate velocity, are transmitted to the surface plates. The coupling is described approximately through a generalized Elsasser model. We argue that the model gives a more realistic physical description of tectonic loading, including the time dependence of deep slip and crustal stress build-up throughout the earthquake cycle, than do simpler kinematic models in which loading is represented as imposed uniform dislocation slip on the fault below the locked zone. Parameters of

the model are chosen in accordance with seismic and geologic constraints and to fit the apparent time-dependence, throughout the earthquake cycle, of surface strain rates along presently locked traces of the 1857 and 1906 San Andreas ruptures. We find that prediction based on the resulting parameters compare reasonably to data on variations of contemporary surface strain and displacement rates as a function of distance from the 1857 and 1906 rupture traces, although the data is generally affected by asymmetry relative to the fault and by adjacent fault strands. Specifically, we fix V_{pl} = 35 mm/yr, T_{cy} = 160 yr and L = 9 to 11 km as a representative earthquake nucleation depth with a 2 km allowance for possible upward motion of the locked zone border during the earthquake cycle. We then find that the geodetic data is described reasonably, within the context of a model that is locally uniform along strike and symmetric about a single San Andreas fault strand, by lithosphere thickness H = 17 to 25 km and Elsasser relaxation time t_r = 10 to 16 yr. We conclude that the asthenosphere appropriate to describe crustal deformation on the earthquake cycle time scale lies in the lower crust and perhaps crust-mantle transition zone, and has an effective viscosity between about 2 x 10^{18} and 10^{19} Pa-s, depending on the thickness assigned to the asthenospheric layer.

The data on the time dependence of surface strain rates along the fault trace assembled by Thatcher (1983, JGR, 88, p. 5893) is shown in Figure 1, together with a series of model predictions. These led to our conclusion that the elastic plate thickness and relaxation times are in the ranges cited above, given our separate seismic and geologic constraints on locked zone depth and plate velocity. The results were used to predict contemporary fault-parallel surface displacement and strain rates as a function of distance from the fault and compared to data from King and Savage (1984; JGR, 89, p. 2471) for the Palmdale region of the 1857 rupture zone, and from Prescott and Yu (1986; JGR, 91, p. 7475) for the 1906 rupture zone north of San Francisco Bay around Point Reyes. The predictions agree reasonably well with the data from the Palmdale area and from the northeast side of the fault from the Point Reyes area. The Prescott-Yu displacement data shows pronounced departures from asymmetry relative to the fault at Point Reyes, with much smaller strain rates to the southwest. We noted that this may be due to a rapid rate of crustal thining near Point Reyes: According to Moho depths inferred by Oppenheimer and Eaton (1981; JGR, 86, p. 6067), the depth beneath the fault there is 23 km and reduces at an abnormally large rate of 1.2 km per 10 km motion towards the fault from the northeast. Thus the base of the crust to the southwest of the fault may be too shallow, and hence to cool, to allow to exist there the type of lower crustal asthenosphere that we have inferred elsewhere along the fault.

2. Modelling continues on this topic with the following improvements. First, we are accounting approximately for the finite length of the central California creeping zone. Our model as explained in the previous summary report assumed an infinite elastic plate, sitting on a viscoelastic asthenosphere below which steady deep mantle motions were imposed. The plate had a semi-infinite locked fault zone, that periodically slips, adjoining its extension as a semi-infinite fault zone that creep-slips at constant resistive stress. An approximate treatment of the finite length creeping zone is given by combining two such semi-infinite fault solutions, in a manner suggested by the form of the exact solution for a finite length slipping shear crack in an elastic plate that is decoupled from its foundation. Second, we are making use of the study outlined above to narrow the range of parametric

values for plate thickness and relaxation time needed in our numerical evaluations of the predicted time dependence.

3. The background in three dimensional elastic crack theory is given in the previous progress report. Our mathematical solution (Gao and Rice, 1986; J. Appl. Mech., in press) for the half-plane shear crack with slightly non-straight crack front in an infinite solid is used to study locally non-uniform or wavy advance of the crack front. The non-uniformity of resistance to slip initiation along a fault, i.e., an asperity distribution, is represented in this work as a non-uniform spatial distribution of the critical fracture toughness of elastic crack mechanics. The mathematical solution derived enables us to express the local stress intensity factors along the crack front in terms of the applied loadings and a linear integral operator on $d\alpha(z)/dz$ where $\alpha(z)$ gives the crack depth at some distance z along the reference straight crack front. Thus we obtain an integral equation for crack depth which is now being solved numerically.

Figure 2 shows some preliminary results for anti-plane shear loading, as representative of a strike slip zone. The crack front is initially straight and coincides with the z axis. The fault surface ahead of the crack front alternates from regions of high (z=0 to 0.5L) to low (z=0.5L to 1.0L) to high (z=1.5L to 2.0L) toughness, in a pattern that repeats periodically with period 2L. The ratio of critical stress intensity factors for the high and low toughness zones is 2 in the case shown. As the applied shear loading is increased the crack front begins to bow-out between the high toughness regions, and to gradually penetrate them. Successive crack front locations are shown. The last corresponds to break-through, after which the crack is no longer stable and will propagate until stopped by the next asperity or a barrier. The same calculations have been carried out for in-plane shear loading, representing the thrust fault situation. In that case the thumbnail-like penetration of the slipping zone into the locked zone at break-through is found to be 1.8 times what is shown in figure 2.

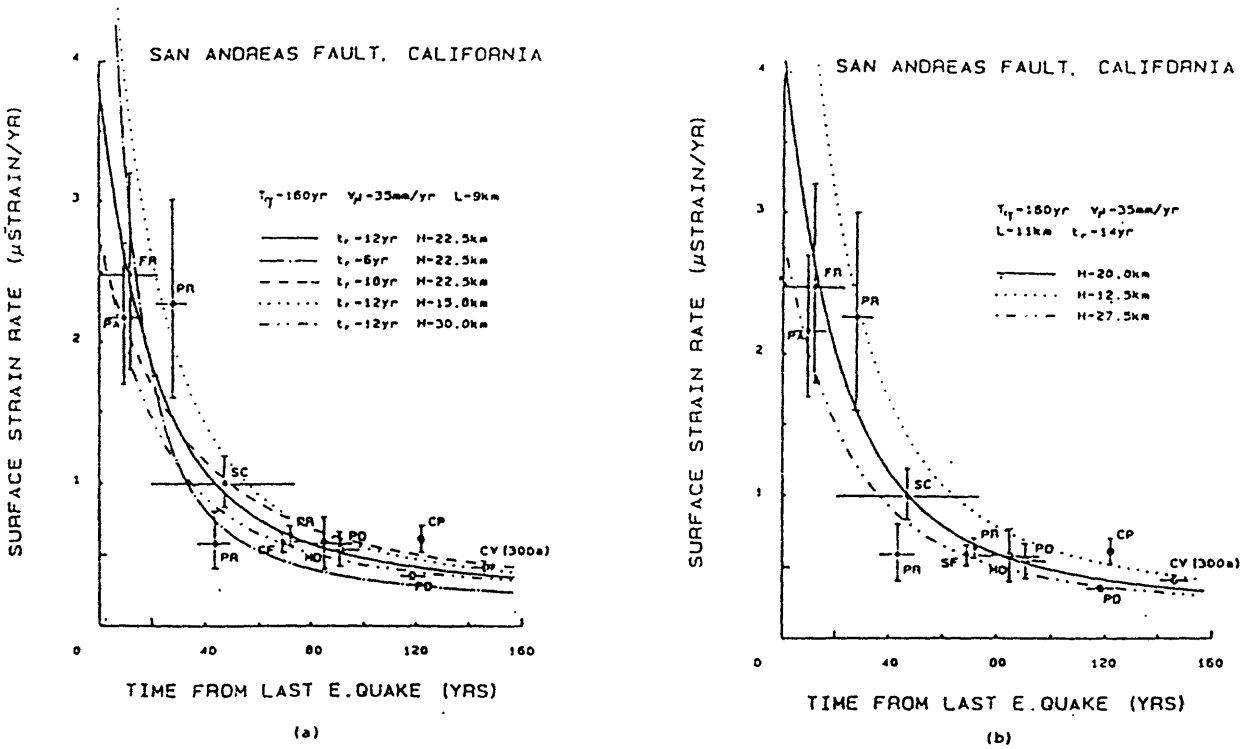
SAN ANDREAS FAULT, CALIFORNIA
SURFACE STRAIN RATE (μSTRAIN/YR)
TIME FROM LAST E.QUAKE (YRS)
(a)
SAN ANDREAS FAULT, CALIFORNIA
SURFACE STRAIN RATE (μSTRAIN/YR)
TIME FROM LAST E.QUAKE (YRS)
(b)

Fig. 1

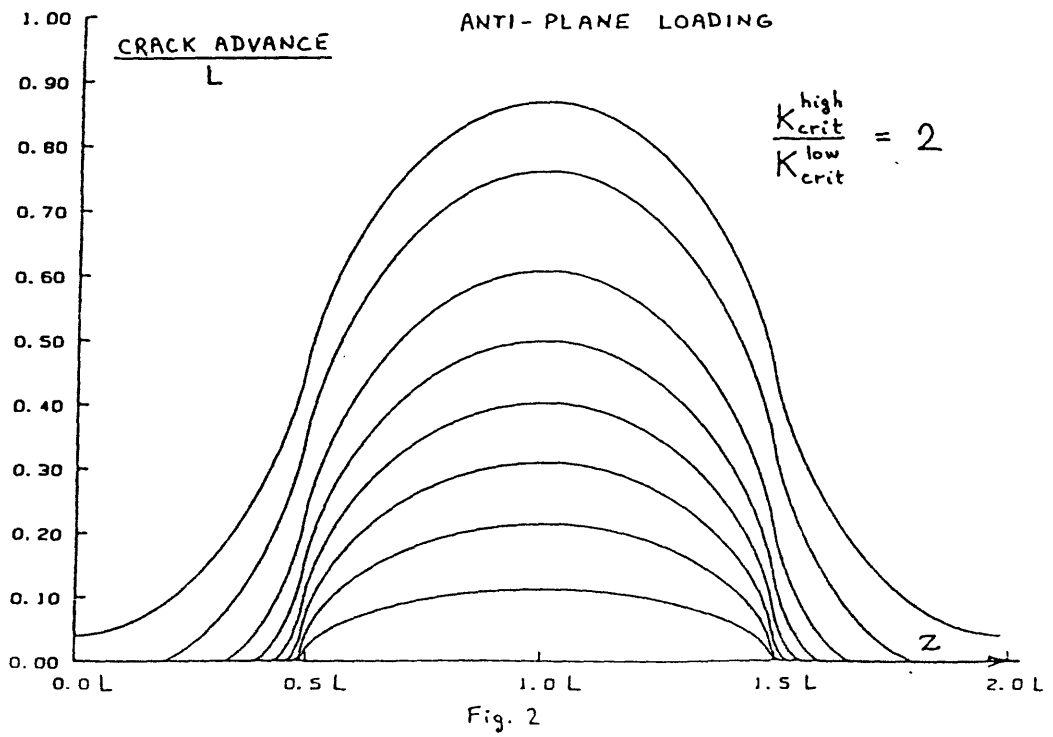
ANTI-PLANE LOADING
CRACK ADVANCE / L
K high crit / K low crit = 2
z
0.0 L
0.5 L
1.0 L
1.5 L
2.0 L

Fig. 2

An explanation of weakening of rock by water under low pressure is that in dilatant cracks in and around the minerals the broken Si-O bonds in the silica tetrahedra and other crystal structures can be replaced by hydrogen bonds of the water molecules. The high surface tension and capillarity of water explains why it would invade microcracks in dilatant rock. A diagram of how water in a crack in quartz might satisfy the broken bonds is shown in Figure 3. The theoretical surface energy of the Si-O bonds in quartz is 93 J/m^2; the experimental value is 0.7 J/m^2; and the hydrogen bond strength H-O is about 0.05 J/m^2. Pores and microcracks interrupt the mineral crystal bonding and apparently reduce the theoretical bond strength by 100 times, and water in dilatant cracks could reduce the rock strength by another factor of 10. Stress corrosion by alkali ions to extend crack tips may be important in weakening certain rocks, but hydrogen bonded water can explain weakening of all rocks with dilatant cracks. Under reservoirs water under only gravity head can flow through the permeable joints and breccia of a fault to 15 km, and by its strong capillarity the water will move into available cracks and pores, form hydrogen bonds with exposed oxygen atoms in silica, carbonate, and other mineral crystal structures, and weaken the rock. An increase in the amount of water in a fault zone can be precursory to movement by creep or as an earthquake; such change can be detected by resistivity methods; Fuye and others (1983) have correlated resistivity anomalies with a number of earthquakes in China. Water in a fault can of course originate as rain, and a possible correlation of rainfall with creep on the San Andreas and Calaveras faults is shown in the report of Shulz and others (1983).

References

Brace, W. F., 1972, Pore pressure in geophysics, in Flow and fracture of rocks, Amer. Geophys. Union Monograph 16, p. 265-273.

Byerlee, J. D., 1967, Frictional characteristics of granite under high confining pressure, Jour. Geophys. Res., v. 72, p. 3639-3648.

Colback, P. S. B., and Wiid, B. L., 1965, The influence of moisture content on the compressive strength of rock, Rock. Mech. Sympos., Dept. Mines Tech. Surveys, Mines Branch, Ottawa, p. 65-83.

Fuye, Q., Yulin, Z., Mouming, Y., Zhixian, W., Xiaowei, L., and Simin, C., 1983, Geoelectric resistivity anomalies before earthquakes, Scientific Simica, v. 26, p. 135-145.

Ismail, I. A. H., and Murrell, S. A. F., 1976, Dilatancy and the strength of rocks containing pore water under undrained conditions, Royal. Astron. Soc. Geophys. Jour., v. 44, p. 107-134.

Handin, J., Hager, R. V. Jr., Friedman, M., and Feather, J. N., 1963, Experimental deformation of sedimentary rocks under confining pressure: Pore pressure tests, Amer. Assoc. Petrol. Geol. Bull., v. 47, p. 717-755.

Raleigh, C. B., Healy, J. H., and Bredehoeft, J. O., 1976, An experiment in earthquake control at Rangely, Colorado, Amer. Assoc. Adv. Sci. Science, v. 191, no. 4233, p. 1230-1237.

Robertson, E. C., 1972, Strength of metamorphosed graywacke and other rocks, in The nature of the solid earth, ed. E. C. Robertson, McGraw-Hill, New York, p. 631-659.

Schulz, S., Burford, R. O., and Mavko, B., 1983, Influence of seismicity and rainfall on episodic creep on the San Andreas fault system in Central California, Jour. Geoph. Res. v. 188, p. 7475-7484.

Simpson, D. W. 1986, Triggered earthquakes, Ann. Rev. Earth Planet. Sci, v. 14, p. 21-42.

ROCK DEFORMATION

9950-00409

Eugene C. Robertson
Branch of Geologic Risk Assessment
U.S. Geological Survey
MS 922, National Center
Reston, Virginia 22092
(703) 648-6792

Investigations

Studies of earthquakes induced by filling of reservoirs and of fractures developed in rock samples containing only small amounts of water indicate that high pore pressure of the water may not be necessary to weaken the rock, and a chemical weakening may explain the reduction in rock strength.

Results

The classic experimental study of Handin and others (1963) on the reduction of effective stress and of shear stress required for failure by application of pore water pressure up to 200 MPa in rocks was followed by numerous similar studies (Brace, 1972). The field pumping tests at Rangely, Colorado, done by Raleigh and others (1976) demonstrated earthquake control by applying and relieving 30 MPa water pressure. Reservoir induced seismicity (RIS) has occurred at many dams due to the water under a head of about 100 m (1 MPa). However, earthquakes at 5 - 15 km focal depths were induced under Flathead Lake (Fig. 1) by raising its level 3 m, thus adding water head of only 0.03 MPa. No earthquakes were induced by the filling of the adjacent Hungry Horse reservoir (Fig. 1), which is not surprising, as only 10 percent of reservoirs show RIS; the rock under Flathead Lake must be under some moderate principal stress difference say, half the strength. (Triggering of RIS was reviewed by Simpson, 1986).

As shown in Figure 2, sandstone samples (15 percent porosity) were weakened merely by subjecting them to humidity, i. e., water under very low pore pressure (Colback and Wiid, 1963). In triaxial compression experiments by Ismail and Murrell (1976) on sandstone (12 percent porosity) and by Robertson (1972) on graywacke (3 percent porosity), water in dilatant cracks was found to weaken the rocks to about half their dry strength, and with excess pore water at confining pressure, the rocks were weakened even more. Water just wetting a sliding surface reduces friction strength (Byerlee, 1967). The conditions for RIS and in such laboratory experiments show that water under very low pressure does weaken dilatant rocks, either by reducing cohesive strength, the friction coefficient, or both. Apparently, high pore pressure is a sufficient but not a necessary condition for weakening of rock under stress.

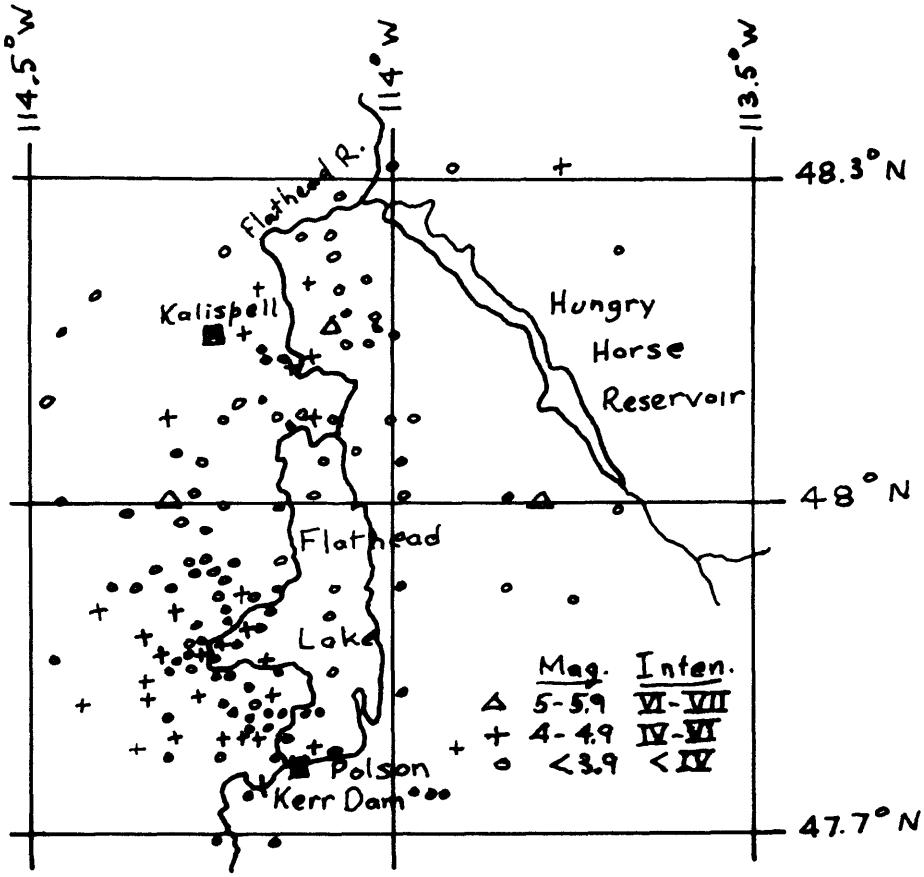

Figure 1. Earthquakes in Flathead Lake area, Montana, 1938 - 1986.

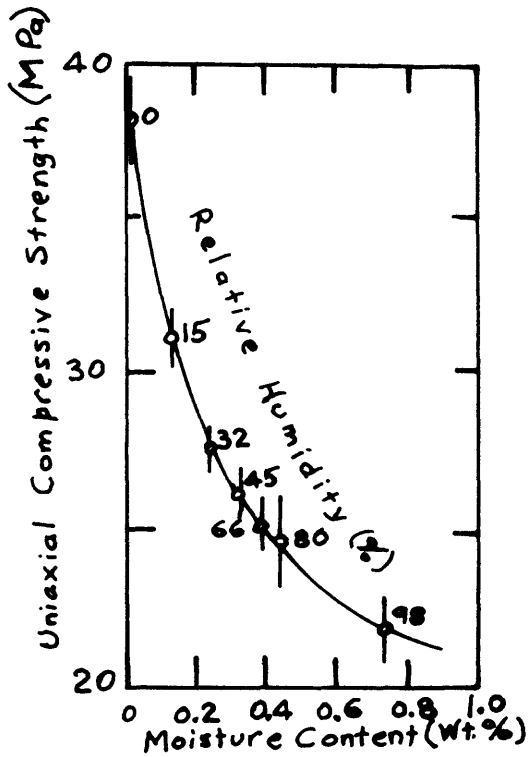

Figure 2. Effect of water on strength of sandstone.

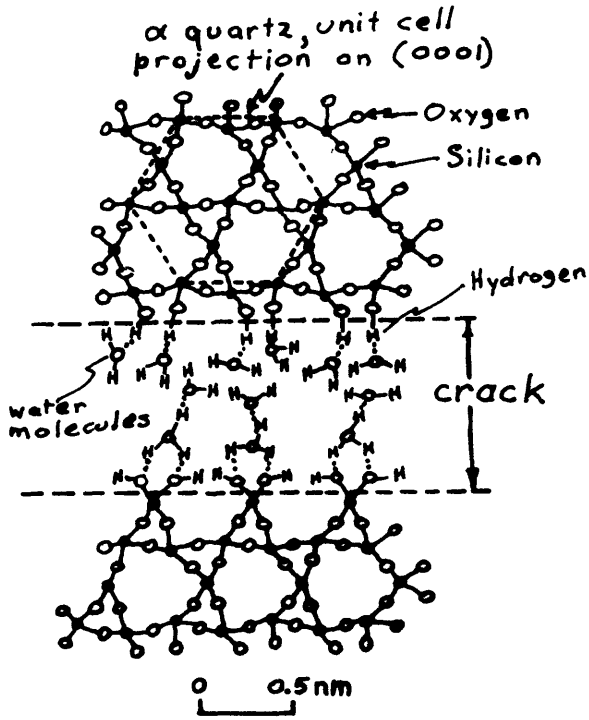

Figure 3. Hydrogen bonding of water to silicon and oxygen in a crack in quartz.

Heat Flow and Tectonic Studies

9960-01177

John H. Sass
Branch of Tectonophysics
U.S. Geological Survey
2255 North Gemini Drive
Flagstaff, AZ 86001
(602) 527-7226
FTS: 765-7226

Arthur H. Lachenbruch
Branch of Tectonophysics
U.S. Geological Survey
345 Middlefield Road
Menlo Park, CA 94025
(415) 323-8111, ext. 2272
FTS: 467-2272

Investigations:

Preliminary interpretation of heat flow from the 1975 PACE studies was completed.

Post-drilling temperature-measurements continued at the Salton Sea drillsite.

Heat-flow data at and near Cajon Pass were analyzed and interpreted.

Methods for rapidly estimating frictional heating on strike-slip faults were reviewed.

A preliminary interpretation of heat-flow data near Parkfield was completed.

A long-term (~6 month) stability test of the precise downhole temperature monitor was carried out.

Results:

PACE Studies. New control in the NE corner of the southern California study area (Figure 1) will change the size and shape of the 100+ mWm^{-2} anomalous zone associated with the southern extension of the Death Valley fault zone. A new value at Ogilley provides badly needed control for the 80 mWm^{-2} contour in southeasternmost California (Figure 1).

Salton Sea. The time series of temperature logs relative to the April 1, 1986, baseline (Figure 2) resulted in a smoothing out of the temperature profile and a predictable increase in temperature. The advantage of continuous downhole recording in a dewared "slickline tool" over conventional spot measurements using electromechanical devices has been clearly demonstrated. The transfer of this technology to other ultrahot and/or ultradeep wells should be very straightforward.

Cajon Pass. Twenty-two heat-flow determinations and eight estimates (from thermal gradients) in the region near Cajon Pass indicate a somewhat more complex thermal regime than was heretofore apparent. At the Cajon Pass site, a combination of Pleistocene-Holocene uplift and erosion, topography, and a steeply dipping but poorly characterized contact between

rocks of differing thermal conductivity introduce large uncertainties into the value for regional heat flow to 1.8 km. Heat flow near the San Andreas fault and within the Mojave Block averages about 70 mWm^{-2} but may be underestimated by 10% or so owing to systematic effects of climatic changes and downward water flow in the upper 150 to 200 meters.

Friction. A review of the simplest models of frictional heating provides a useful order-of-magnitude perspective on coseismic and post-seismic thermal effects and their relation to earthquake parameters. In addition to fault slip and friction, which determine the energy dissipation, coseismic temperatures are sensitive to event duration, slip velocity, and width of the shear zone. Although coseismic heating may differ by several hundred degrees for events with the same slip and friction, the associated post-seismic temperature anomalies will generally be indistinguishable a few days after faulting. As suggested by McKenzie and Brune, the product of slip and friction might be recovered by thermal observations in a well drilled into the slip zone of moderate to large earthquakes. Precision temperature logs obtained within a few months of the event should help identify the slip zone, and subsequent disturbances caused by faulting, drilling, and the possible occurrence of water movements sometimes invoked in faulting models.

Parkfield. Preliminary temperature profiles from six wells near Parkfield when combined with measurements of thermal conductivity on the few available core samples give an estimate of regional flux of about 75 mWm^{-2} which is consistent with other estimates of heat flow near the San Andreas fault in the southeastern Coast Ranges. Because of the lateral variation in thermal properties near the fault, it may not be possible to refine these estimates much, even with additional thermal conductivities and temperature profiles that are nearer to thermal equilibrium.

Downhole monitor. The precision downhole temperature monitor was tested over a six-month period at the 116-foot depth in the borehole at our laboratory in Menlo Park. The resolution was better than 10^{-4} °C and the total temperature excursion recorded over the period was less than 10^{-3} °C. This performance should allow us to look for the effects of shear-strain heating in an appropriate configuration near an active fault.

Reports:

DeRito, R. F., 1986, The effects of weak crust upon the strength of the continental lithosphere (extended abstract): U.S. Geological Survey Circular, in press.

DeRito, R. F., Cozzarelli, F. A., and Hodge, D. S., 1986, A forward approach to the problem of temperature and the long-term thickness of the mechanical lithosphere: Journal of Geophysical Research, v. 91, p. 8295-8313.

Lachenbruch, A. H., 1986, Reply to Comment by J. C. Mareschal: Journal of Geophysical Research, v. 91, p. 7565-7569.

Lachenbruch, A. H., 1986, Simple models for the estimation and measurement of frictional heating by an earthquake: U.S. Geological Survey Open-File Report 86-508.

Lachenbruch, A. H., and Marshall, B. V., Climatic warming: Geothermal evidence from permafrost in the Alaskan Arctic (Branch approval, March 1986).

Lachenbruch, A. H., Sass, J. H., Lawver, L. A., Brewer, M. C., Marshall B. V., Munroe, R. J., Kennelly, J. P., Jr., Galanis, S. P., Jr., and Moses, T. H., Jr., Temperature and depth of permafrost on the Alaskan Arctic Slope: Pacific Section - SEPM Special Publication and U.S. Geological Survey Professional Paper 1399 (Branch approval, March 1986).

Lachenbruch, A. H., Sass, J. H., Moses, T. H., Jr., and Galanis, S. P., Jr., 1986, Thermal considerations and the Cajon Pass borehole: U.S. Geological Survey Open-File Report 86-469.

Pollack, H. N., and Sass, J. H., 1986, Thermal regime of the lithosphere, in Haenel, R., Rybach, L., and Stegena, L., eds., Handbook of Terrestrial Heat-Flow Density Determination (Guidelines and Recommendations of the International Heat Flow Commission), in press.

Sass, J. H., Salton Sea Scientific Drilling Program: U.S. Geological Survey Yearbook, in press.

Sass, J. H., and Elders, W. A., 1986, Salton Sea Scientific Drilling Project--Scientific Program: Geothermal Resources Council Bulletin, v. 15, p. 21-26.

Sass, J. H., Lachenbruch, A. H., Galanis, S. P., Jr., Munroe, R. J., and Moses, T. H., Jr., 1986, An analysis of thermal data from the vicinity of Cajon Pass, California: U.S. Geological Survey Open-File Report 86-468.

Sass, J. H., Priest, S. S., Robison, L. C., and Hendricks, J. D., 1986, Salton Sea Scientific Drilling Project on-site science management: U.S. Geological Survey Open-File Report 86-397.

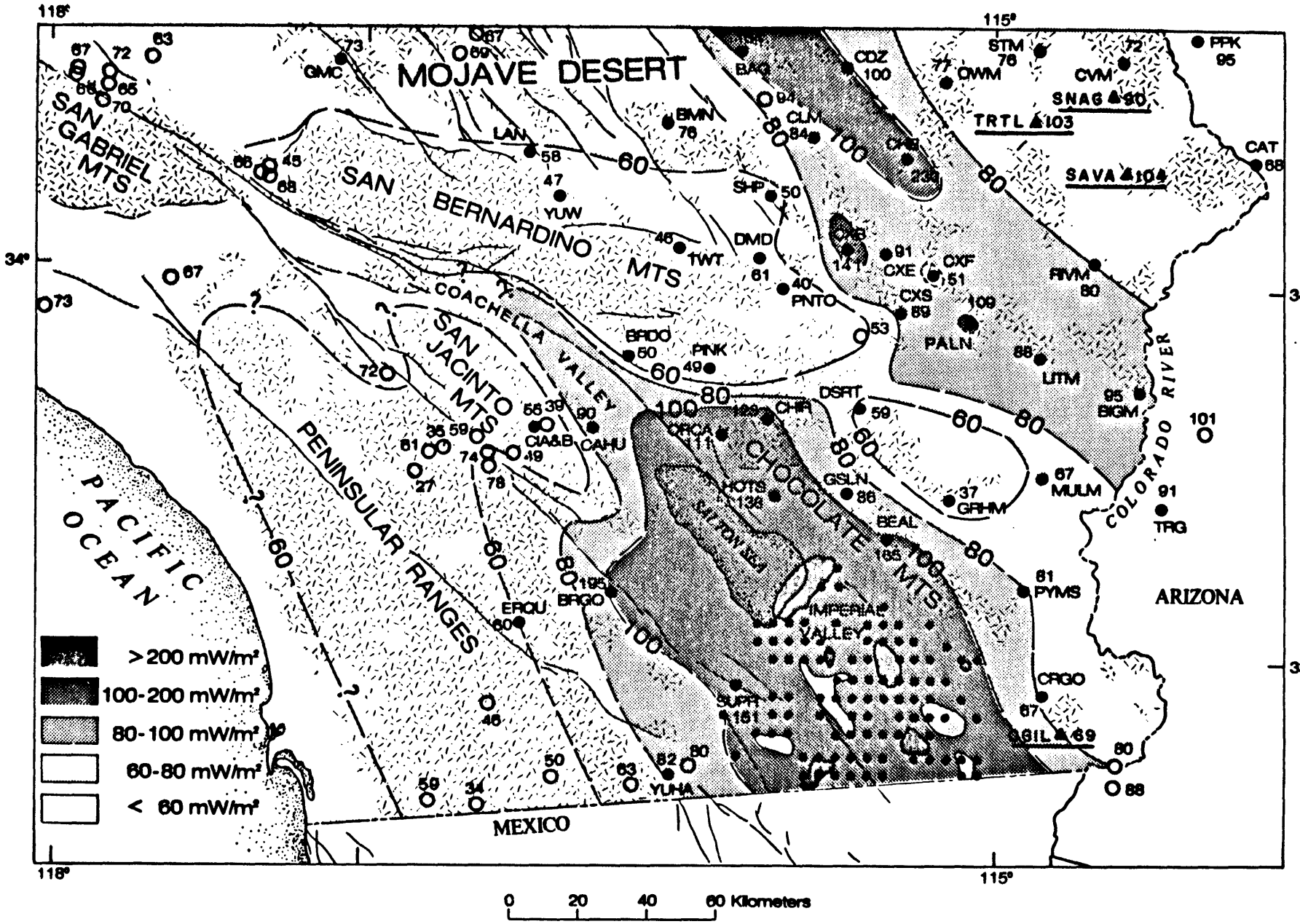

Figure 1. Heat-flow map of southernmost California (from Lachenbruch et al., 1985). Solid circles represent new data (as of 1985); open circles represent previously published values. Small dots show midpoints of rectangles (3 arc min latitude by 3 arc min longitude) for which average heat flows were calculated. Triangles represent new PACE data.

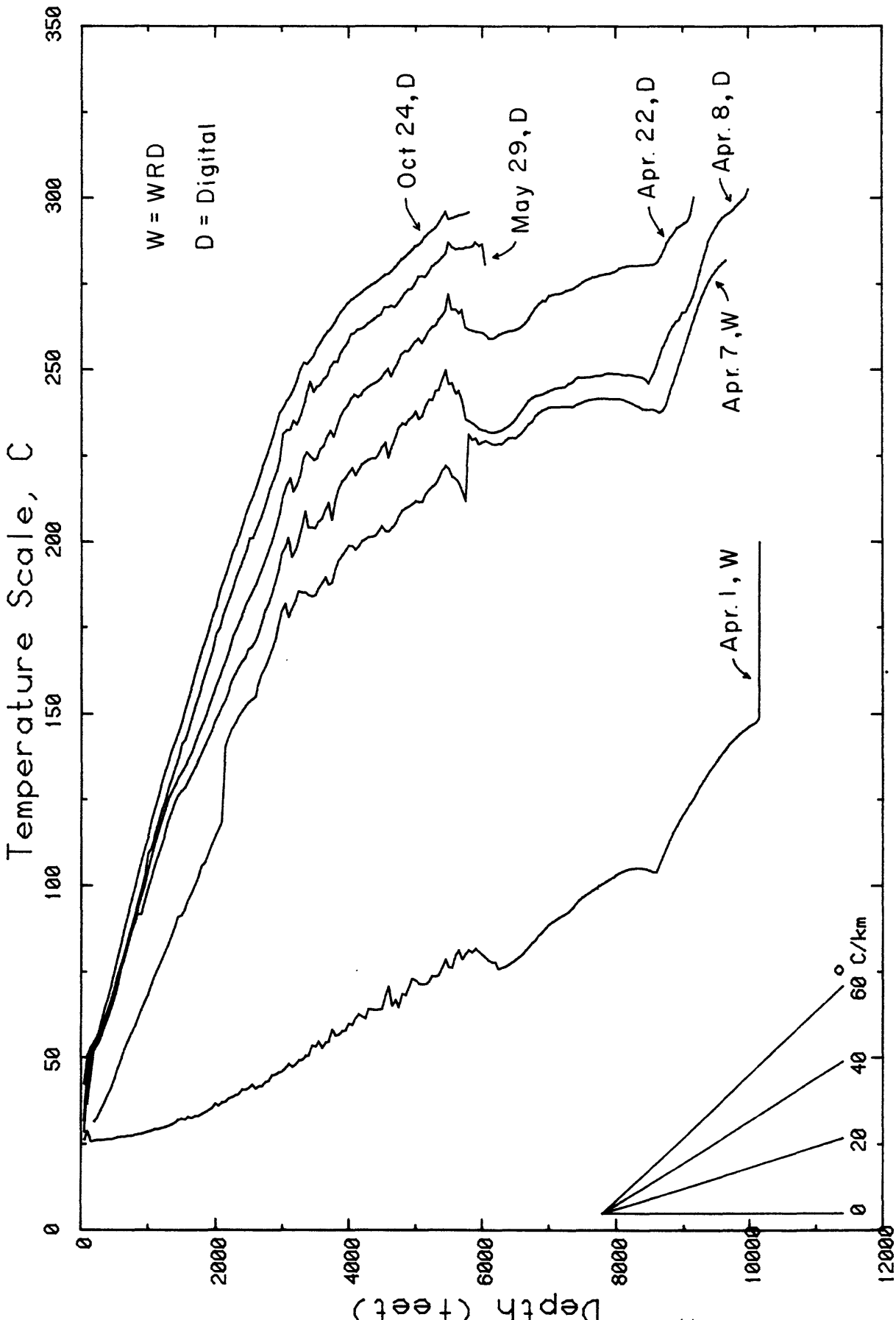

Figure 2. Time series of temperature logs from the Salton Sea well. Profiles labeled "W" were obtained using USGS Water Resources wireline with conventional surface readout; profiles labeled "D" using a dewared slickline device with downhole digital recording.

Fractal Heterogeneity of Faults

14-08-0001-G-1161

C. H. Scholz
Lamont-Doherty Geological Observatory
and Dept. Geological Science, Columbia Univ.
Palisades, NY 10964
(914)359-2900

Investigations:

Studies have been made or are underway of the geometry of active faults, using fractal analysis. Two scale ranges have been studied, the micro and macro scale, 10^{-5}-1 M, which can be measured with profilometers, and the mega scale, 10^{3}-10^{6} M, by the analysis of maps.

Results:

1. Fractal Geometry of Faults and Faulting
   (Scholz, Aviles)

The Alquist-Priolo (I:24,000) fault hazard maps of the San Andreas fault system were digitized and analysed using the spectral technique. These results were compared with our earlier work, using profilometers, of the topography of joints and other natural rock surfaces. It was found that these surfaces were fractal, or nearly fractal, over the entire 10 decade spectral band studied, but
that the fractal dimension is itself a function of scale.

These results have consequences in terms of the size distribution of asperities and earthquakes, and with regard to scaling of frictional constitutive relations that may apply to real faults.

2. Fractal Analysis of Characteristic Segments of the San Andreas fault
   (Aviles, Scholz, Boatwright)

A thorough study of variations in fractal dimension along the San Andreas fault was carried out. Because the segmentation of the fault into strands was found to create problems with the spectral technique, this study employed the ruler method. It was found that all sections of the San Andreas fault were fractal at the megascale, with considerable variation of fractal dimension
along strike. No obvious correlation was found between the seismic behavior of different fault segments and the fractal dimension.

3. Profilometry Studies of Active Fault Surfaces
   (Scholz, Brown, Boitnott)

A joint investigation with Power and Tullis of Brown Univ. is underway of the topography of slickensided fault surfaces using profilometers. They made measurements in the field of a number of slickensided fault surfaces in Nevada and Utah, using our field profilometer, which was modified for remote field use. Measurements on a smaller scale were made from samples from the
same outcrops using our lab profilometer.

Results so far show that these surfaces are fractal out to a length scale of 10M, but that they are strongly anisotropic. They tend to be much less jagged, when measured parallel to the slip direction, than other rock surfaces we have measured, and about as jagged when measured

perpendicular to slip.

4. Study of Mechanisms for Seismic Quiescences (Scholz)

The different types of seismic quiescences that have been reported were reviewed. Three distinct types of quiescence were recognized: post-seismic quiescence, that occurs for 50-70% of the recurrence time following a major earthquake; intermediate-term quiescence, that occurs for months
or years preceeding a major earthquake in the region surrounding the source; and short-term quiscence, that follow premonitory swarms in the rupture initiation zone and have durations of hours to days. Various mechanisms for these are discussed and analyzed.

Reports

Scholz, C. H. and C. A. Aviles, Fractal geometry of faults and faulting, in 5th Ewing Symposium, Earthquake Source Mechanics (ed. S. Das, J. Boatwright, C. Scholz) Ewing V. 6, AGU, p. 147-155, 1986.

Aviles, C. A., C. H. Scholz, and J. Boatwright, Fractal Analysis of Characteristic segments of the San Andreas fault, J. Geophys. Res., in press, 1986.

Power, W. L., T. E. Tullis, S. R. Brown, G. N. Boitnott, and C. H. Scholz, Roughness of natural fault surfaces, subm. Geophys Res Lett, 1986.

Scholz, C. H., Mechanisms of Seismic quiescences, subm. USGS redbook conf., "Intermediate-term Precursors, Monterey, Cal., Nov., 1986.

Systems Analysis of Geologic Rate Processes

9980-02798

Herbert R. Shaw and Anne E Gartner
Branch of Igneous and Geothermal Processes, U. S. Geological Survey
MS-910, 345 Middlefield Road, Menlo Park, CA 94025
(415) 323-8111, X4169, X4170

Objective: The work on this project has the objective of dynamic interpretation of paleoseismic data compiled by Shaw and others (1981). An aspect is the interpretation of self-similarity and fractal geometry of fault sets.

Results: The geometric variability of faulting and inferred seismicity previously reported is being explored from the viewpoint of multifractal analyses. One approach being taken is to generate sets of apparent fault lengths based on an assumed length-magnitude relation using earthquake occurrences within a specified spatial domain to define the data set. The length-set is then plotted logarithmically in terms of frequencies of occurrences at different lengths. In these plots the set as a whole defines an aggregate length as a function of length scale; this permits an estimate of the apparent fractal dimension of the overall set (the fractal dimension is obtained from the slopes of cumulative length vs. length scale as discussed in Shaw and Gartner, 1986). Within the aggregate set, however, there are length-frequency trends that also locally satisfy criteria of fractal self-similarity. On this basis it is found that a given frequency-magnitude pattern, usually characterized by a single coefficient (b-value), often displays fractal dimensions that vary in an alternating fashion with increasing magnitude among fractal subsets in the range $0 \leq D \leq 3$ (a given frequency-magnitude data point simultaneously "lives" on trends of more than one fractal dimension). In other words, b-values as usually determined by some form of statistical regression mask retrievable geometric information. The maximum entropy method of Main and Burton (1984) helps but does not resolve this problem; their approach and Aki's (1981) fractal interpretation of b-values are useful for insights into the possible geometric meanings of multifractal sets.

Multifractal analyses based on the above constructions have been applied to historic seismicity in California and environs, using the earthquake catalogs of Real and others (1978) and Toppozada and others (1979). Data sets have been constructed for earthquakes of magnitude 5 and above for fourteen subregions within and immediately surrounding the state; subregions were defined arbitrarily for purposes of this study. Patterns differ in detail from sub-region to subregion, but several have similar subtrends with conspicuous subsets at about $D = 0$ and $D = 2.4$ (others have maximum observed D-values of 1.8, 2.3, and 2.9). The value $D = 2.4$ is reduced by about one dimensional unit to roughly $D = 1.4$ for the data referred to a maximum topologic dimension of two (map plane). This value is close to the estimated fractal dimension of young faults at the statewide scale reported by Shaw and Gartner (1986), and the range $D = 0.8$ to $D = 1.9$ is similar to the range inferred from fault data for the contiguous U.S. (see Figure 5a in that report). Geographic resolution is at present inadequate to draw specific inferences concerning relationships to tectonic patterns.

A goal of this work is to build parallel sets of multifractal data, one based on seismically defined fractal dimensions, the other on fault-

defined fractal dimensions. If a one-to-one mapping of comparative sets is achievable, then there is a concrete basis for geographic interpretations of complex seismic distributions. In other words, this represents an alternative approach to the impossible goal of identifying every seismic event at every magnitude with a geologically defined actual and(or) potential slip event. At the present regional scale of analysis, the general range of seismically defined fractal variability fits the discussion of fault fractal variability in Shaw and Gartner (1986). To go farther in this direction will require automating the method for events at low magnitudes.

A second approach is being taken based on experimental studies (numerical and physical) reported in the literature of nonlinear dynamics. Researches on spatial structures found in fluid motion near the onset of turbulence represent a useful guide to the interpretation of multifractal structures and behaviors in systems having a complexity analogous to that generated by processes of crustal deformation. There are strong geometric analogies between the data of fluid turbulence and the above seismic fractal structures in that the former also display fractal subsets that have specific ranges of characteristic dimensions. Because most of the work to date in fractal nonlinear dynamics refers to analysis of a single output variable, the data are not directly comparable to the seismic data (rescaling of the seismic data, however, reveals some numerical resemblances to the data of fluid turbulence). Multifractal fabrics in these studies have been termed singularity spectra; a comprehensive description is given by Halsey and others (1986). Shaw and Chouet (1987) have found that a one-dimensional analysis of seismic tremor defines sets of singularity spectra with similar functional form to the sets studied by Halsey and others (1986). It is tentatively concluded that the earthquake history of California may also be describable in terms of characteristic singularity spectra qualitatively like those found in fluid dynamics.

References Cited:

Aki, K., 1981, A probabilistic synthesis of precursory phenomena, in Simpson, D.W., and Richards, P.G. (eds.) Earthquake Prediction, Washington, DC, American Geophysical Union, p. 566-574.

Halsey, T.C., Jensen, M.H., Kadanoff, L.P., Procaccia, I., and Shraiman, B.I., 1986, Fractal measures and their singularities: The characterization of strange sets: Phys. Rev. A, v. 33, p. 1141-1151.

Main, I.G., and Burton, P.W., 1984, Information theory and the earthquake frequency-magnitude distribution: Seis. Soc. Am., Bull., v. 74, p. 1409-1426.

Real, C.R., Toppozada, T.R., and Parke, D.L., 1978, Earthquake epicenter map of California: California Div. Mines and Geol., Map Sheet 39.

Toppozada, T.R., Real, C.R., Bezore, S.P., and Parke, D.L., 1979, Compilation of pre-1900 California earthquake history: California Div. Mines and Geol., Open-file Report OFR 79-6 SAC.

Reports:

Shaw, H.R. and Gartner, A.E., 1986, On the graphical interpretation of paleoseismic data: U.S. Geol. Survey, Open-file Report 86-394.

Shaw, H.R. and Chouet, B., 1987, Kilauean volcanic tremor as a case study of multifractal attractor dynamics: Abstracts, Symposium on How Volcanoes Work, Hilo, HI, January 19-25, 1987.

Fault Patterns and Strain Budgets

9960-02178

Robert W. Simpson
U.S. Geological Survey
Branch of Tectonophysics
345 Middlefield Road, MS/977
Menlo Park, California 94025
415-323-8111, ext. 4256

Investigations

Purpose is to understand the interactions of faults and fault segments through time using very simple elastic dislocation models. Believable results must be robust and largely independent of second-order twiddling with model geometry and model parameters. This approach is based on the assumptions that there are still some first-order things to be learned about fault behavior and that, given our ignorance of many important Earth properties, simplicity is a great virtue.

Results

A simple dislocation model of the San Andreas fault near Parkfield, California has raised some interesting questions about the geometry of the fault in that region (fig. 1). Numerous investigators have pointed out the presence of a right-stepping offset of the active fault trace in Cholame Valley (e.g. Brown, 1970). Rick Sibson has recently focused attention on this area as a possible deep-drilling target. The right offset is thought to be approximately at the north end of a locked zone that last broke in a magnitude 8+ earthquake in 1857 (Stuart and others, 1985; Segall and Harris, 1986). Farther to the north along the fault, near the epicenter of the 1966 Parkfield earthquake, Lindh and Boore (1981) have pointed out the existence of a 5° bend in the fault trace that may overlie a discontinuity at depth responsible for the location of recurring Parkfield earthquakes (Bakun and Lindh, 1985). Several investigators have mentioned this offset and bend in broader discussions of the effects of fault geometry upon the concentration of stress and the location of earthquakes (e.g. King and Nabelek, 1985; Segall and Pollard, 1980).

The simple dislocation model described below and geologic considerations suggest (1) that the bend and offset in the fault trace near Parkfield may be more fruitfully regarded as parts of an asymmetric three-dimensional ***bulge*** or ***warp*** in the fault plane, (2) that the warp may be a predictable consequence of the locked patches that exist at Parkfield and to the south of Cholame Valley, and (3) that the warp may grow with time until a new straighter trace eventually breaks through. The bulge is shown greatly simplified in figure 1. It can be viewed in a broader perspective with the help of a straight-edge and a map showing faults such as Jennings (1977). The southeastern end of the bulge in Cholame Valley is more abruptly curved than the northwestern end. The bulge extends from approximately 15 km southeast of Gold Hill, to approximately 40 km northwest. Beyond its ends to southeast and northwest, two rather straight, 70-km-long segments of the San Andreas fault system line up remarkably well with each other. (Distortions caused by map projections have not yet been confronted, but should be small compared to the size of the bulge.)

Chinnery (1966), Bridwell (1975), and other researchers have remarked upon the tendency for the ends of slipping dislocations in an elastic medium to rotate. (Ends of an isolated RL slipping patch will tend to rotate counter-clockwise when viewed from above.) Bridwell (1975) pointed out that behavior of this sort could, over the long term, produce the sinuous pattern of fault traces observed on geologic maps. He described a finite-element model simulating the coseismic distortion

of the fault plane during Parkfield earthquakes. The coseismic deformation is a bulge of the fault trace toward the southwest. The interseismic deformation turns out to be a bulge to the northeast.

The simple dislocation model consists of a set of 5-km-square vertical dislocations just below the Earth's surface that can slip in a linear viscous fashion in response to shear stresses, a set of 10-km-square dislocations extending from 5 km to 10 km depth, and a single long driving dislocation below 15 km that is forced to slip at 35 mm/yr. Most of the 10-km-square dislocations are free to slip viscously, except that three in the vicinity of Parkfield are assigned finite breaking strengths that causes them to break every 22 years. The region to the south of these three is completely fixed over the time spans considered (except for the driving segment below 15 km) to simulate the locked area that last broke in 1857.

During the 22 year interval leading up to a Parkfield-like earthquake, the model fault is warped to the northeast in the vicinity of Middle Mountain. When a Parkfield-like earthquake occurs in the model, the fault plane returns almost to vertical near Parkfield (the model's viscous response slows the process somewhat), and the bulge is transferred southward to Cholame Valley where the north end of the second locked zone is located. Figure 2a shows in plan view the horizontal displacements calculated from the elastic model after one Parkfield cycle. The maximum horizontal deformation perpendicular to the fault occurs at a rate of approximately 4 mm/yr. Figure 2b shows that the horizontal displacements perpendicular to the fault decrease with depth, so that the shape of the warped fault trace in three-dimensions approximates the contours of a sail boat hull. In a perfectly elastic Earth, the entire warp would disappear after a repeat of the 1857 shock if both locked patches broke and the stresses momentarily relaxed over a large section of the fault.

However, the Earth is not a perfect elastic half-space (R. Wallace, oral commun., 1986), especially in it upper reaches, so that it seems unlikely that the horizontal warp in the fault will disappear entirely, even after a repeat of 1857. By way of simple analogy, if one stretched a rubber band by an additional increment every year for many years and suddenly then released it, one would hardly expect it to return to its original length.

Geologic and regional geophysical investigations ought to offer a longer term perspective on possible effects of the warping process (C.Wentworth, R.Jachens, oral commun., 1986). The area to the northeast of the Parkfield-Cholame reach of the San Andreas fault forms an unusual embayment of low topographic relief. This embayment is flanked at least on its northeast side by a probable reverse fault. The low-lying Cholame Valley lies at the southeast end of the embayment, where the warp in the fault combined with right-lateral slip ought to be removing material. The high topography of Middle Mountain, the Parkfield syncline, and the overpressured Varian well lie along the northwest end of the warp where the fault geometry and RL slip together with the anelastic behavior of the materials that have been forced to travel around the warp ought to combine to produce a compressional regime.

Mafic igneous rocks exposed at Gold Hill offer another interesting constraint. On the basis of lithologic similarities with igneous rocks at Eagle Rest Peak in the San Emigdio Mountains about 150 km to the southeast, the rocks at Gold Hill are believed to have been transported to the north as part of the Pacific plate (J.Sims, oral commun., 1986). Similar rocks at Logan Quarry near Hollister about 180 km to the northwest may have been adjacent to Gold Hill about 5 m.y. ago given a rate of travel of 30 mm/yr. The presence of exotic, far-travelled rocks at Gold Hill, which presently lies on the east side of the San Andreas fault, suggests that a former now abondoned trace of the San Andreas system must now lie to the east of Gold Hill. (An alternative explanation is that Gold Hill materials were somehow transported across the San Andreas fault.) There are indeed both mapped faults and geophysically inferred faults that lie to the northeast of Gold Hill, and these could be older traces of the San Andreas that have been bulged eastward with time. Given

the present distance to the Gold Hill-like rocks near Hollister, Gold Hill was probably dropped off at Parkfield about 5 m.y.b.p. The fault to the east of Gold Hill is presently about 5 km off the unwarped trend of the San Andreas, suggesting horizontal offset rates for Gold Hill over the last 5 m.y. on the order of 1 mm/yr. Given the calculated model warping rates of 4 mm/yr, Gold Hill's location could be explained if approximately 25 percent of the interseismic warping, at least in the near-surface materials, were anelastic and was not recovered at the times of earthquakes. A smaller anelastic component (less than 10 percent) is required if the active trace 5 m.y.b.p. were already warped just as the presently active trace is.

It will be noted that this discussion assumes that the warp has been in the same place relative to Gold Hill and the embayment for at least 5 m.y. If the explanation for the warp advanced here is correct, it would imply that the locked patch to the South of Cholame Valley has remained stationary relative to Gold Hill and to the northeast side of the fault for this same period. If the locked patch and its accompanying warp had been moving northward with time, the effects of warping on the northeast side of the fault might be expected to have left a longer wake.

A second piece of evidence bearing on the proposed warp comes from the detailed aftershock study of the 1966 Parkfield earthquake by Eaton and others (1970, fig. 9). Eaton's best fitting plane to all of the aftershocks dips slightly (86°) to the southwest, but deeper shocks south of Gold Hill seem to lie even farther to the southwest of the shallower ones than the dip of this plane would predict. In particular, the subparallel clusters of earthquakes near the offset in Cholame Valley (that have on occasion been presented as evidence for two overlapping but offset faults) are consistent with most of the seismic activity occurring on a single warped fault plane dipping to the southwest (see Lindh and Boore, 1981, fig. 3c), because the two apparently subparallel clusters seen in plane view occur at very different depths. The Southwest Fracture, which lies about 1.5 km to the southwest of the present San Andreas fault near Parkfield, may be a potential successor to the presently active trace, because it offers a straighter, less warped alternative for slip. Ground breakage was observed along the Southwest Fracture after the 1966 shock, and alinement arrays have recently detected up to 1 cm of motion along the Southwest Fracture during a period when creep on the adjacent segment of the San Andreas fault had stopped (S. Shulz, oral commun., 1986).

Conclusions and (Mostly) Speculations

(1) The 50 km long bulge in the San Andreas fault, from roughly Cholame on the southeast to north of Middle Mountain on the northwest, may be a direct consequence of the presence of locked patches at depth under Parkfield and south of Cholame Valley. The bulge may persist and even grow with time because of the long-term anelastic behavior of Earth materials in the region.

(2) The bulge, when viewed at depth may actually be a three-dimensional warp with decreasing amounts of horizontal offset at deeper levels.

(3) The geology to the northeast of the warp, including the exotic lithologies exposed at Gold Hill, suggests that warping of San Andreas traces to the northeast has been occurring in this vicinity for some time (5 m.y.?). This implies that the locked patch south of Cholame Valley may have remained fixed relative to the northeast side of the fault for some time, and that periodically, when the active trace of the fault becomes too warped, slip is gradually transferred to a new straighter plane to southwest, and the former active trace is abandoned.

(4) The possibility that the Parkfield locked patch has resulted from geometric complications associated with the warping needs to be explored. Perhaps large locked patches may be able to spawn smaller locked patches out in front of themselves by distorting a section of the adjacent fault that otherwise might be inclined to creep.

(5) The potential role of the Southwest Fracture as a new straighter trace and the possible role of older traces still capable of slipping both underscore the importance of monitoring not just the presently most active trace for premonitory signs of the next Parkfield earthquake. There are indications in both creep data and two-color laser data that various strands are trading slip back and forth over time, and that several stable patterns of slip may be alternating in a quasi-periodic pattern (R. Buford, oral commun., 1986). A truly integrated picture of the tectonics of the Parkfield region will require that we understand how all of the various faults and other structures in the vicinity are interacting both in the shorter term and the longer term. To achieve this goal we need to do a better job of monitoring slip on other faults than we are doing at present, and we need to know which of the many faults in the area are active players.

References Cited

Bakun, W.H., and Lindh, A.G., 1985, The Parkfield, California, earthquake prediction experiment: Science, v. 229, p. 619-624.

Bridwell, R.J., 1975, Sinuosity of strike-slip fault traces: Geology, v. 3, p. 630-632.

Brown, R.D., Jr., and others, 1967, The Parkfield-Cholame, California, Earthquakes of June-August 1966—Surface geologic effects, water-resources aspects, and preliminary seismic data: U.S. Geological Survey Professional Paper 579, 66 p.

Brown, R.D., Jr., 1970, Map showing recently active breaks along the San Andreas and related faults between the northern Gabilan Range and Cholame Valley, California: U.S. Geological Survey Miscellaneous Investigations Map I-575, scale 1:62,500.

Chinnery, M.A., 1966, Secondary faulting—I. Theoretical aspects: Canadian Journal of Earth Sciences, v. 3, p.163-190.

Eaton, J.P., O'Neill, M.E., and Murdock, J.N., 1970, Aftershocks of the 1966 Parkfield-Cholame, California, earthquake: a detailed study: Bulletin of the Seismological Society of America, v. 60, p. 1151-1197.

Jennings, C.W., 1977, Geologic map of California: California Division of Mines and Geology, California Geologic Data Map Series, scale 1:750,000.

King, Geoffrey, and Nabelek, John, 1985, Role of fault bends in the initiation and termination of earthquake rupture: Science, v. 228, p. 984-987.

Lindh, A.G., and Boore, D.M., 1981, Control of rupture by fault geometry during the 1966 Parkfield earthquake: Bull. of the Seismological Society of America, v. 71, p. 95-116.

Segall, P. and Harris, R., 1986, Slip deficit on the San Andreas fault at Parkfield, California, as revealed by inversion of geodetic data: Science, v. 233, p. 1409-1413.

Segall, P. and Pollard, D.D., 1980, Mechanics of discontinuous faulting: Journal of Geophysical Research, v. 85, p. 4337-4350.

Stuart, W.D., Archuleta, R.J., and Lindh, A.G., 1985, Forecast model for moderate earthquakes near Parkfield, California: Journal of Geophysical Research, v. 90, p. 592-604.

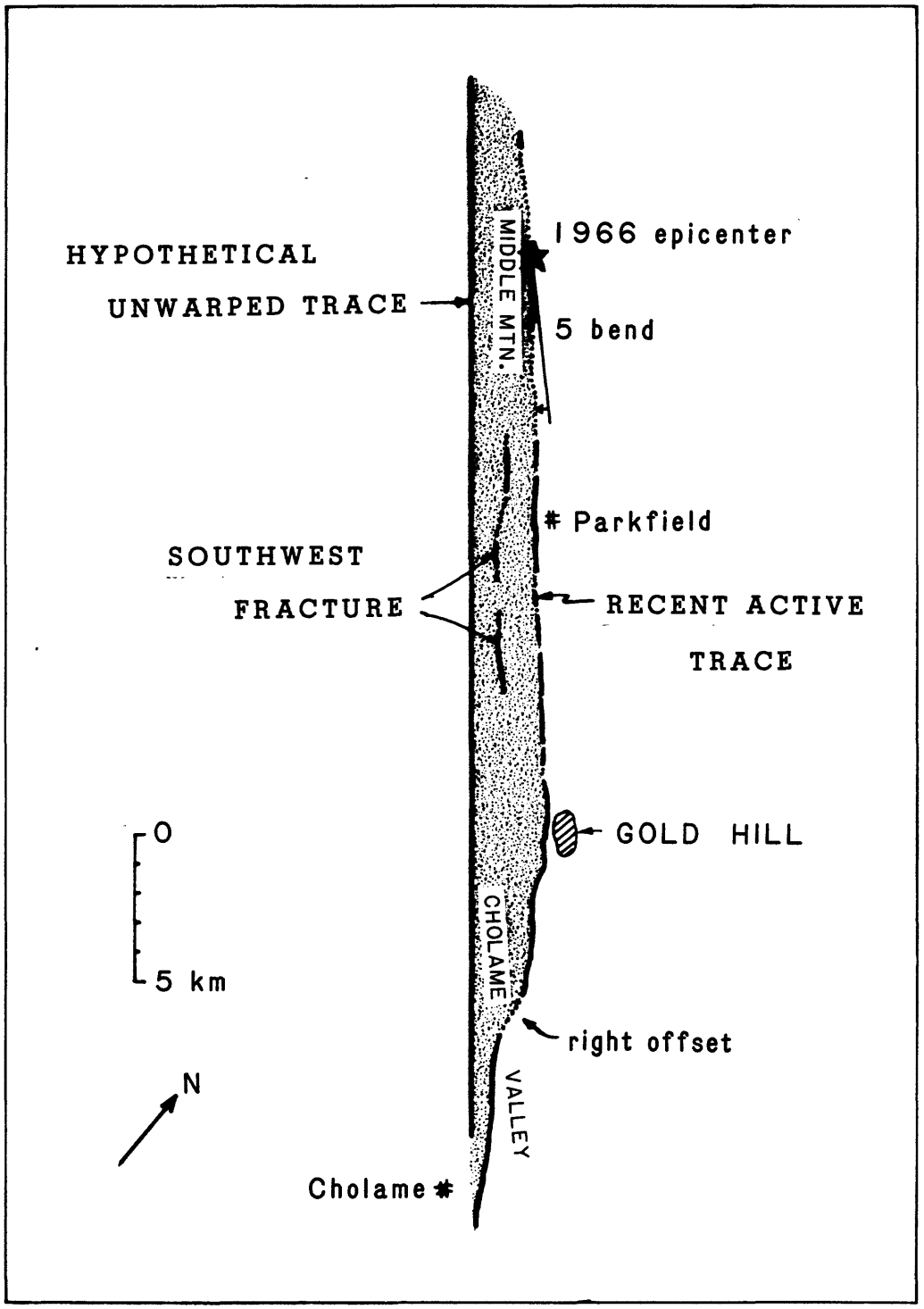

Figure 1. Bulge defined by fracture zone of June-July 1966 (Brown and others, 1967) and by approximate position of unwarped trace inferred by connecting straight segments of the San Andreas to NW and SE of area shown here (see Jennings, 1977).

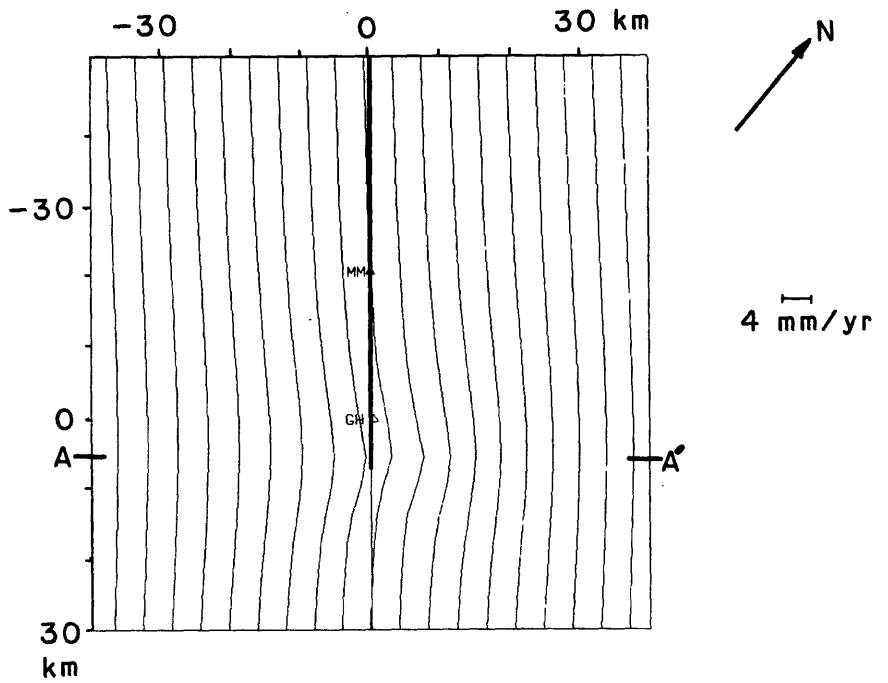

Figure 2a. Map view showing average horizontal displacement rates perpendicular to the model fault trace after one Parkfield cycle. Amplitude of warping of the vertical lines shows displacement rate relative to scale bar on the right side of the figure. Displacement rates are calculated for elastic deformation. Letters show approximate locations of real features relative to the model: GH = Gold Hill, MM = Middle Mountain creepmeter and 1966 epicenter. Fault trace marked by light line south of Gold Hill simulates the locked patch that last broke in 1857.

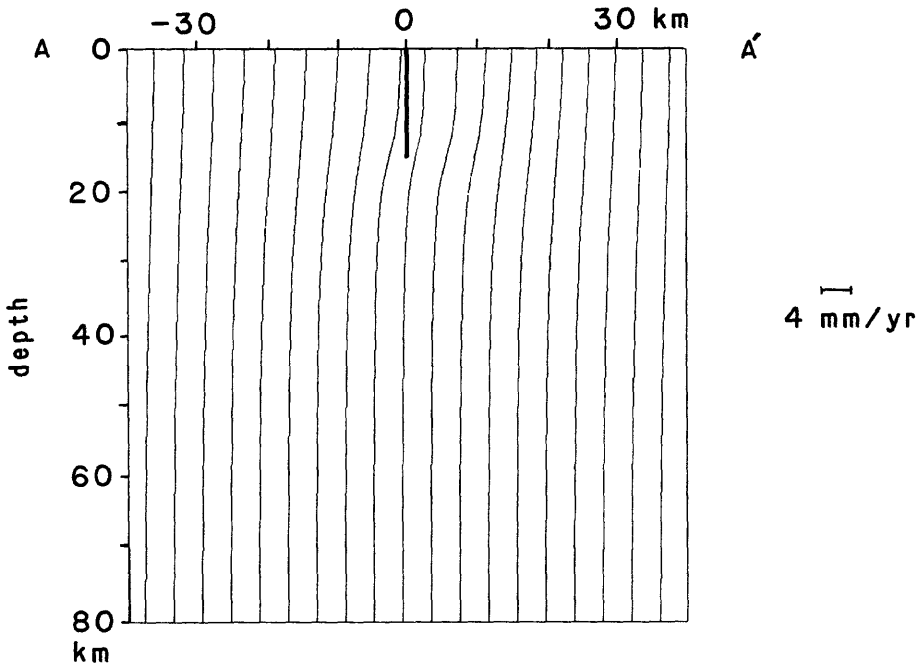

Figure 2b. Vertical section (from A to A' in figure 2a) showing average horizontal displacement rates as in figure 2a.

EARTHQUAKE FORECAST MODELS

9960-03419

William D. Stuart
U.S. Geological Survey
Branch of Tectonophysics
Pasadena, California 91106
(818) 405-7816

Investigations

1. An earthquake instability model for the Nankai Trough subduction zone has been formulated and is now being tested with geodetic data associated with the 1944 Tonankai and 1946 Nankaido earthquakes. The model is two-dimensional and represents fault zone constitutive behavior by a slip and velocity dependent fault law. Forcing is by a constant rate of relative plate motion applied at depth. This work is another test of the validity of instability models and their possible application to earthquake forecasting. Two specific models for the San Andreas fault have been analyzed previously, one for moderate earthquakes near Parkfield, the other for large and great earthquakes in southern California. The two models for the San Andreas fault are three-dimensional and allow for variation of fault properties along strike.

Results

As with earlier related models by Mavko (unpubl. ms., 1983) and Tse and Rice (J. Geophys. Res., 1986), the model simulates repeated earthquake cycles including post-, inter-, pre-, and coseismic stages of each cycle. For plausible values of constitutive and geometric parameters the model is able to reproduce most of the main features of observed uplift profiles reported by Thatcher (J. Geophys. Res., 1984). In the model accelerating fault slip on the brittle section of the fault starts several years before unstable (earthquake) faulting. The accelerating slippage produces uplift anomalies that may be large enough to detect by leveling surveys. Within about 30 km of the fault trace over the fault plane, the free surface rises about 10 cm in the last 3 days before instability. A corresponding but smaller subsidence occurs between about 30 and 60 km from the fault trace.

The apparent consistency of the model with levelling observations would seem to justify construction of a three-dimensional instability model for the Nankai Trough. Such

a model might account for the times and sizes of historical great earthquakes and might also help clarify if and when the Tokai gap will have a great earthquake.

Reports

Stuart, W. D., Forecast model for large and great earthquakes in southern California, J. Geophys. Res., 91 (in press), 1986.

An Experimental and TEM Study of Cataclastic Flow in Quartzo-Feldspathic Rocks

14-08-0001-G-1180

Jan Tullis and Richard Yund

Department of Geological Sciences
Brown University
Providence, RI 02912
(401) 863-1921

Investigations

In order to understand the factors governing whether fault slip is stable or unstable, and how this fits within the macroscopic brittle-ductile transition, it is important to determine the operative grain scale deformation mechanisms and relate these to the empirical constitutive laws. One of the important deformation mechanisms within fault zones is cataclastic flow, which involves distributed, intragranular cracking and rotation and frictional sliding of the resulting fragments. We have undertaken an experimental study, over a wide range of T and P, of the conditions and mechanisms of cataclastic flow in feldspar and in quartz aggregates. Because the deformation products include extremely fine-grained material, transmission electron microscopy (TEM) is an important part of the study.

In the first year of our study we have been studying (1) the locations in P,T space of the transitions from brittle faulting to ductile cataclastic flow, and from cataclastic flow to dislocation creep, for dry non-porous monomineralic aggregates of albite, intermediate plagioclase (An_{78}), and quartz; and (2) the micromechanical processes operating within the cataclastic flow regimes as revealed by optical microscopy and TEM.

Results

1. Cataclastic flow field: One of the major results of the study to date has been the demonstration that increased pressure alone at room temperature is insufficient to induce a transition from brittle faulting to ductile cataclastic flow in albitite, anorthosite, or quartzite which are initially non-porous (Hadizadeh and Tullis, 1986). Samples undergo (seismic) faulting and stick-slip, with gouge development, at pressures up to 1500 MPa. This is consistent with previous results on granite, although it stands in contrast to the early results of Heard on Solnhofen limestone. Our results also are different from those on initially porous aggregates (sandstones, basalts); these materials do show a transition to ductile cataclastic flow with increasing pressure at room temperature. These results indicate that (a) high pressure alone is insufficient to stabilize cracking and produce cataclastic flow in silicates, at least in a dry environment; and (2) the collapse of initial porosity during pressurization apparently causes distributed cracking and crushing which allows continued cataclastic flow during deformation at modest pressures even at room temperature.

A second major result concerns the difference in behavior of quartz and feldspar. At pressures of 1000-1500 MPa and a strain rate of 10^{-5}/sec,

anorthosite shows a transition with increasing temperature from (seismic) faulting with gouge at 20°C, to ductile shear zones of increasing width (and increasing degree of distributed deformation away from the shear zones), until at 600-700°C the sample deformation is homogeneous. It is obvious from optical examination that grain scale faulting on the two cleavages acts almost like slip to allow this ductility. Quartzites, in contrast, exhibit brittle faulting with gouge development up through 600°C, uniform flow with some non-crystallographic grain scale faults in orientations of high resolved shear stress at 700°C, and steady state dislocation creep with dynamic recrystallization at 800°C and above. The lack of good cleavage planes in the quartzites appears to make a major difference.

A third preliminary result is the observation that cataclastic flow in feldspar aggregates (with no dislocations present; see below) can occur at a steady state flow stress; no strain hardening is observed at 400, 500, or 600°C for total strains up to 40%.

2. Micromechanical processes: One of the major results of our TEM investigations to date has been to begin to outline the contributions of dislocations, microcracks, microfaults, and microcrush zones to the macroscopic process of cataclastic flow (Tullis and Yund, 1986, and In Preparation). For anorthosite we have found that no dislocations are observed in samples deformed at <600°C (at 10^{-5}/sec). Thus cataclastic flow can occur solely by grain-scale brittle processes, in the absence of plastic flow, but seem to require moderate temperatures (at least at laboratory strain rates, and in the absence of water). In these samples we see microcracks, often along cleavage planes, with very strong strain contrast; microshears with glass along them; and microcrush zones containing grains so small they are not resolvable in the TEM ($d < .01$ μm). It should be noted that on the optical scale these samples exhibit many of the "criteria" for crystal plastic deformation, such as flattened original grains, undulatory extinction (sometimes extreme), and deformation bands (discussed in Tullis and Yund, 1986).

Observations on higher temperature samples show that the definition of cataclastic flow is somewhat problematic and scale-dependent. At 700, 800, and 900°C deformation of anorthosites continues to involve some grain-scale faulting, especially earlier in the strain history, but high dislocation densities are present and obviously have contributed a substantial proportion of the total strain. It remains to determine whether dislocation glide and microcracking continue to be associated at higher strain (> 40%), or whether the production of very fine grain size gradually allows the onset of a new steady state process. In any event, there is no major discernable difference in the optical microstructures between 600°C samples (with no dislocations) and 700°C samples (with high dislocation densities).

TEM observations of the experimentally deformed quartzite samples show a rather different behavior (Hirth and Tullis, 1986). At 500 and 600°C, extremely high dislocation densities are present but the samples develop brittle faults; at 700°C, there is still a very high dislocation density with little evidence of recovery, together with microcracks and microcrush zones; at 800°, the dislocation density is lower, there is some evidence of recovery, and no cracks or microcrush zones are observed. Apparently the mere presence of an extremely high dislocation density is not sufficient to stabilize cracking, but a degree of mobility and recovery insufficient for steady state dislocation creep does suffice to stabilize cracking.

Reports

Tullis, J., and Yund, R.A., 1985, Cataclastic flow of feldspar: an experimental study: Geol. Soc. Amer. Abstr. Prog., 17, 737-738.

Hadizadeh, J., and Tullis, J., 1986, Transition from brittle faulting to cataclastic flow for anorthosite: both P and T are required: Trans. Amer. Geophys. Union, 67, 372-373.

Hirth, G., and Tullis, J., 1986, Cataclastic flow in dry, non-porous quartzites: Trans. Amer. Geophys. Union.

Tullis, J., and Yund, R.A., 1986, Transition from cataclastic flow to dislocation creep of feldspar: mechanisms and microstructures: submitted to Geology.

Hadizadeh, J., and Tullis, J., Transition from brittle faulting to ductile cataclastic flow in anorthosite: effect of pressure and temperature, and optical microstructures: to be submitted to Tectonophysics.

Tullis, J., and Yund, R.A., Transition from brittle faulting to ductile cataclastic flow in anorthosite: TEM observations of micromechanical processes: to be submitted to Tectonophysics.

EXPERIMENTS ON ROCK FRICTION CONSTITUTIVE LAWS APPLIED TO EARTHQUAKE INSTABILITY ANALYSIS

USGS Contract 14-08-0001-G-1185

Terry E. Tullis
John D. Weeks
Department of Geological Sciences
Brown University
Providence, Rhode Island 02912
(401) 863-3829

Investigations

1. We have continued work on determining the detailed constitutive behavior for frictional sliding of several rock types, including granite at high sliding velocity. We are now preparing samples of pure quartz rock.

2. We have continued our numerical investigation of unstable sliding by modelling different types of high velocity constitutive behavior and by including inertial effects.

3. We have concluded our numerical investigation of the behavior and stability of sliding governed by a two state variable constitutive law.

Results

1. In order to increase our understanding of the micromechanical processes involved in frictional sliding, and to apply constitutive equations to unstable sliding and earthquakes, we have investigated the frictional behavior of granite over a 6.5 order of magnitude range in velocity. Most workers have assumed that above 10 μm/s the steady state frictional resistance becomes independent of slip velocity. However, our previous work on dolomite, calcite and halite and that of others on shows that the velocity dependence switches from negative (velocity weakening) at low velocity to positive (velocity strengthening) at high velocity, and we now have found this behavior for granite. We slid initially bare, roughened, moistened samples of Westerly granite at 50 MPa normal stress in our rotary shear high pressure apparatus at slip velocities from 0.001 to 3162 μm/s. With this unique apparatus we achieved a total slip displacement in excess of 370 millimeters, which is by far greater than has been achieved previously for rock samples under confining pressure. The coefficient of friction and loading velocities for the entire experiment are plotted versus displacement in Figure 1. Much of the small-scale variability in the friction record is caused by the imposed changes in loading velocity. During the experiment a 30-200 μm thick layer of gouge formed. The gouge is optically isotropic and contains a well-defined centralized sliding surface. The velocity dependence of steady state friction is found to vary with slip velocity such that it changes from velocity weakening at slip rates below 10 μm/s to velocity strengthening above 30 μm/s. Figure 2 shows **a** - **b**, the magnitude of the change in steady state coefficient of friction per factor of e change in slip rate, plotted versus load point velocity for most of the velocity steps shown in Figure 1. Values of **a** - **b** range from -0.004 at < 0.1 μm/s to $+0.008$ at > 1000 μm/s. Numerical simulations of the granite data using a one state variable constitutive law shows that the magnitude of **a**, the term measuring the instantaneous direct dependence of friction on velocity, remains nearly constant at 0.012 to 0.014 at all rates up to at least 100 μm/s. This suggests that the increase of **a** - **b** with velocity is due to reduction of the term **b** which measures the contribution to the resistance from a state variable that evolves with slip; that evolution may cease at velocities higher than our maximum 3162 μm/s. Decay distances for the state evolution

measured by **b** are on the order of 10 microns, but at high velocity additional evolution occurs with a decay distance on the order of mm to cm; while this is too long-term to affect the stability of sliding, it causes large reductions in the frictional resistance and may reflect processes of delocalization of slip in the gouge resulting from the short-term velocity strengthening.

2. We have continued our efforts to develop constitutive laws that accurately reflect frictional behavior, concentrating particularly on the behavior at high velocity. We have corrected an error in the simulation code that was used for Figures 2 and 3 in the previous Technical Summary (volume XXII). This changes the shapes of trajectories on the phase-plane, but does not alter the conclusions we reached previously: a transition from velocity weakening at low velocity to velocity strengthening at high velocity causes arrest of unstable events and allows us to match many of the characteristics of unstable events observed in experiments on granite. We have expanded this study to include two different forms of constitutive laws. Both display steady state velocity weakening at low velocity and at high velocity either no steady state velocity effect ("zero slope") or velocity strengthening ("positive slope"). The former model has been assumed by various workers, but experimental observations of the behavior of several rock types suggests that the second model is more accurate (see section 1 above). In the positive slope model we assume that the steady state coefficient of friction is proportional to ln(V) with the slope at high velocity equal to the magnitude of the "direct effect" ("**a**" in Ruina's (1983) law) while at low velocity the slope in both cases is **a** - **b** as in the simple log-linear Ruina law. Both of these models will arrest an unstable event even in the absence of inertia, as opposed to the simple constant slope velocity weakening model often used which results in infinite velocities. The details of unstable events are, however, different depending on the model chosen. On a log(V) vs. stress plot, the zero slope model yields a trajectory that passes through and recovers below the steady state line, while the positive slope model causes the unstable event to arrest and recover along the steady state line. In consequence, during unstable events with the zero slope model, the stress drops to a minimum value that depends on the size of perturbation and on load point velocity, while the positive slope model yields minimum stresses that are nearly constant (see Figure 4). The latter situation more nearly reproduces unstable events we observe in our experimental study of granite, as can be seen in Figure 3 in which data for several unstable events on granite are shown along with simulations done with both the zero slope (light lines) and constant slope (heavy lines) models. In addition to these modifications of the constitutive laws, we have started some numerical modelling in which inertial effects are included. Using the simple log-linear steady state function (no transition at high velocity) and inertial parameters estimated from the known torsional stiffness and calculated moment of inertia of our sample assembly, we find very similar results to those found for the modified constitutive laws in that inertia arrests the instability and at higher load point velocity the unstable stress drops are smaller. However, the stress drops predicted are too large by 50 to 100 per cent. Consequently, we conclude that the particular unstable events we observed (shown in Figure 3) were limited more by a transition in the steady state velocity dependence than by inertia. However, our results indicate that this may depend on the stiffness and the frictional and inertial parameters of a given system; the relative position of the inertial cut-off and the change in slope of the frictional model will determine which causes arrest in an earthquake.

3. We have concluded our numerical study of the behavior and stability of sliding governed by the Ruina constitutive law using two state variables to describe the frictional response of the sliding surface. Modeling of experimental data has shown that two state variables are often needed to satisfactorily describe the frictional behavior of several rock types. Since the values of the constitutive parameters have been found to vary widely with rock type and fault roughness, we investigated the way in which different values of the parameters affected the frictional behavior. In addition to the results reported in volume XXII of this report, we have found that interesting behavior can result if $\mathbf{b}_1$, the magnitude of the shorter term state evolution, is positive for a system which exhibits steady state velocity strengthening. Although in this case the long-term frictional response to perturbations of stress or loading velocity is necessarily stable sliding at constant velocity, short-term acceleration can result in arbitrarily high slip velocities before steady state is achieved.

Reports

Blanpied, Michael L. and Terry E. Tullis, The stability and behavior of a frictional system with a two state variable constitutive law, in press: *Pure Appl. Geophys., 124*, 1986.

Tullis, Terry E., and Weeks, John D., Constitutive behavior and stability of frictional sliding of granite, in press: *Pure Appl. Geophys., 124*, 1986.

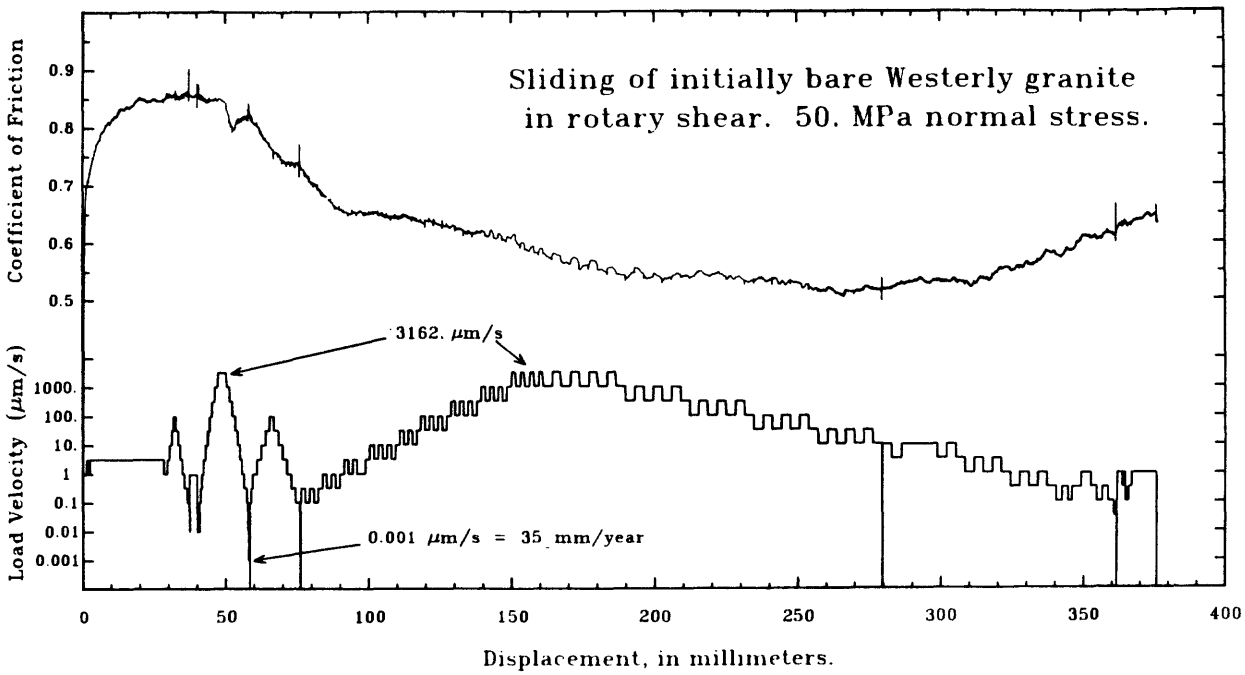

Figure 1. Coefficient of friction and load velocity plotted vs. load point displacement for an entire sliding experiment on granite. This experiment achieved a total displacement of over 370 mm. Load point velocity was varied stepwise over a range from 0.001 μm/s (31.5 mm/yr) to 3162 μm/s. The short-scale variability in the friction data is due mostly to these step changes in load point velocity. The longer-scale evolution is probably due both to the development of a gouge layer and to changes in the gouge structure between regimes of velocity weakening (strain localization) and velocity strengthening (strain delocalization).

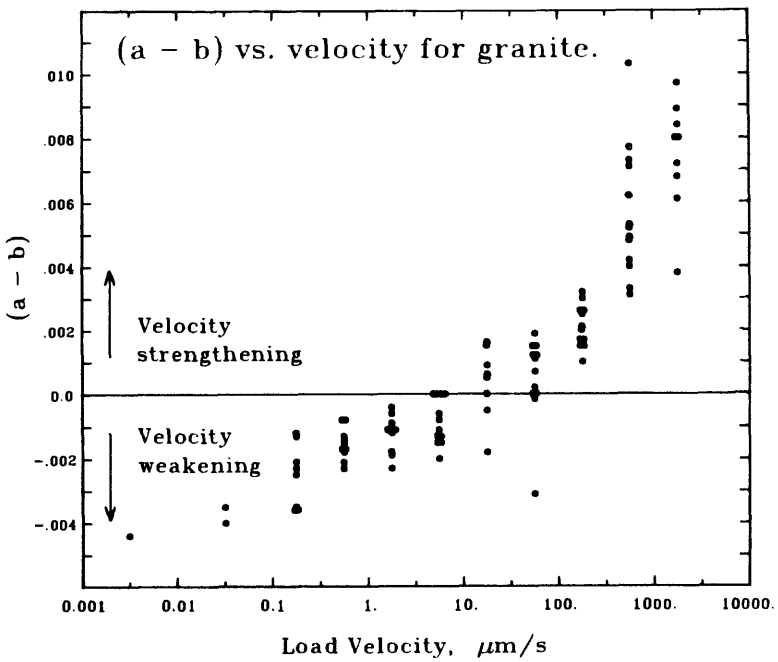

Figure 2. **a - b** plotted vs. velocity for most of the velocity steps illustrated in Figure 1. The points are plotted half way between the velocities before and after the step; identical points are shifted horizontally for clarity. The data illustrate the strong variation of the steady state velocity dependence of friction (**a - b**) with velocity, and show that the dependence switches from velocity weakening at low velocity to velocity strengthening at high velocity.

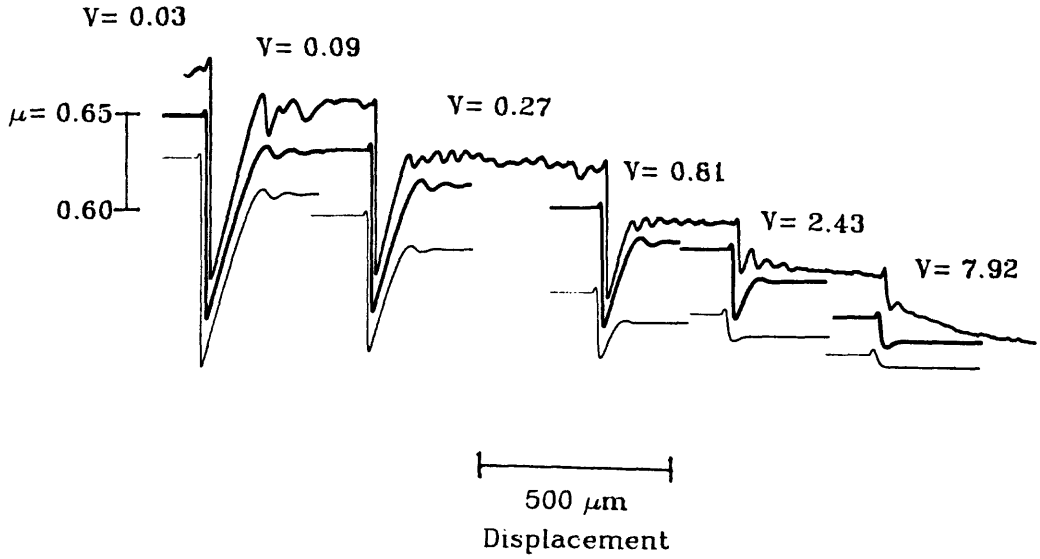

Figure 3. Comparison of data (top trace) and simulations done with the positive slope model (heavy curves) and zero slope model (light curves). The data consists of the reponses to a series of load point velocity jumps, each velocity being a factor of 3 higher than the last. The equation for the steady state function that resulted in the heavy curves was $\mu - \mu_0 = \mathbf{a} \ln(V/V_0) - \mathbf{b} \ln(V/V_0 + V/V_t)$ with $\mathbf{a} = 0.004$, $\mathbf{b} = 0.022$, and $V_t = 10.0$ μm/s. The steady state function for the light lines was $\mu - \mu_0 = (\mathbf{a} - \mathbf{b}) \ln(V/V_0 + V/V_t)$ with $\mathbf{a} = 0.004$, $\mathbf{b} = 0.022$, and $V_t = 2.0$ μm/s. V_t was changed in order to match the stress drop for the first velocity change.

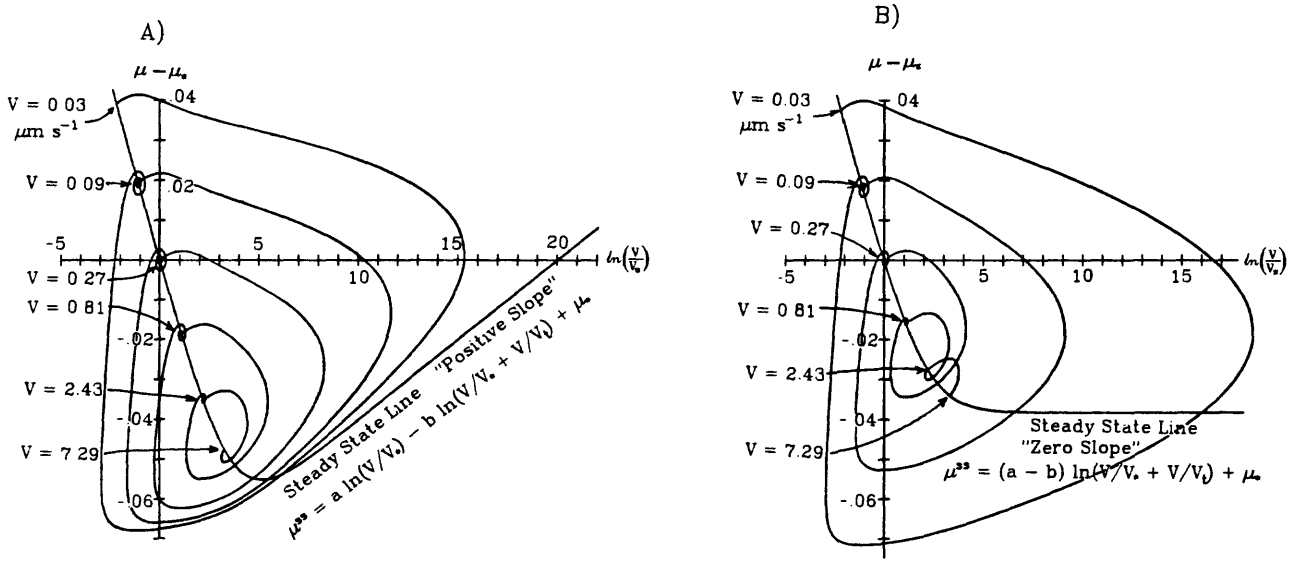

Figure 4. Plots of $\mu - \mu_*$ versus $\ln(V/V_*)$ for the same simulations shown in Figure 3; A) positive slope model, B) zero slope model. Note in A) that at lower initial velocities (to the upper left) the positive slope trajectories recover along the steady state curve. This tends to channel the trajectories for different load point velocities to nearly the same minimum point on this plot with the result that the stress drops to nearly the same level regardless of load point velocity. In contrast, the zero slope model (B) results in trajectories that cut through the zero slope portion of the steady state curve such that the minimum stress rises with increasing load point velocity.

Stress and Pore Pressure Change Due to Annual Water Level Cycles in Seismic Reservoirs

Contract 14-08-0001-22022

Evelyn A. Roeloffs, Taechin F. Cho and Bezalel C. Haimson
University of Wisconsin-Madison
1509 University Avenue
Madison, WI 53706
608-262-2563

INVESTIGATION

Reservoir-induced seismicity appears to be related to water level changes. We are investigating reservoir impoundment effects by calculating stress, pore pressure, and strength changes on a pre-existing fault plane resulting from fluctuations in the reservoir water level. The water level cyclic variation at Lake Oroville was selected for the model calculation.

RESULTS

The stresses and pore pressures in a porous elastic medium have been calculated by using a two dimensional finite element program. This program can solve the coupled (Biot) equations of elastic deformation and pore fluid flow. As the reservoir water level changes, coupling of deformation with pore fluid diffusion results in a phase lag between the achieved peak compressive stress and the peak pore pressure. This creates a temporary excess of pore pressure changes vis-a-vis the total compressive stress change, thus reducing the magnitude of the effective stress. Model calculation of pore pressure at five different locations (A - E in Figure 1) reveals that, for a diffusivity of $1.0 m^2/s$, the phase lag becomes larger as the distance from the reservoir increases (see Figure 2). This phenomenon can be identified by comparing the time of the peak pore pressure at each location following a rapid water level drop at 79 months after initial impoundment. Owing to the phase lag, the time when the largest effective stress change occurs during water level fluctuation is different for each location. This suggests that reservoir-triggered seismic activity can be induced during reservoir loading or unloading depending on the hypocenter location and the frequency of lake level fluctuation.

To account for the effects of both pore pressure and stress changes induced by the reservoir loading, the strength changes (as defined by Bell and Nur, 1978) prevailing when the main seismic activity near Lake Oroville occurred (94 months after initial impoundment) have been calculated on an imaginary plane which simulates a normal fault striking north-south and dipping 60° to the west. As shown in Figure 1, strength weakening prevails below the reservoir. However, the region outside the reservoir is strengthened, albeit by a small amount. The distribution of strength changes constrains the location of a potential reservoir-induced seismic source. The source may have

a wide range of depths, but its lateral position is confined to or in the vicinity of the reservoir boundary.

The strength changes at points A - E (see Figure 1), along planes parallel to the normal fault defined above, resulting from reservoir water level fluctuation have also been calculated, and are shown in Figure 3. At location A the magnitude of weakening varies almost in phase with the reservoir water level fluctuation. This is to be expected since location A is so close to the reservoir that the pore fluid readily diffuses to this zone. At locations B, C, D, and E the magnitudes of weakening continuously increase since the initial impoundment, and are only slightly affected by the water level fluctuation. This implies that at these locations the strength changes, for a diffusivity of 1.0 m^2/s, are caused mainly by the pore pressure build-up due to fluid diffusion, and the effect of water level fluctuation on strength change is not significant.

Reports

Roeloffs E.A., 1985, Stress and Pore Pressure change Due to Annual Water Level Cycles in Seismic Reservoir, (abstract), EOS, Trans. Am. Geophys. Union, Vol. 66, No. 18.

Roeloffs E.A., Cho T. F., and Haimson B. C., 1986, Reservoir-Induced Seismicity: The Effects of Short-Term Variations in Reservoir Water Level on Fault Stability, (abstract), EOS, Trans. Am. Geophys. Union, Vol. 67 (in press).

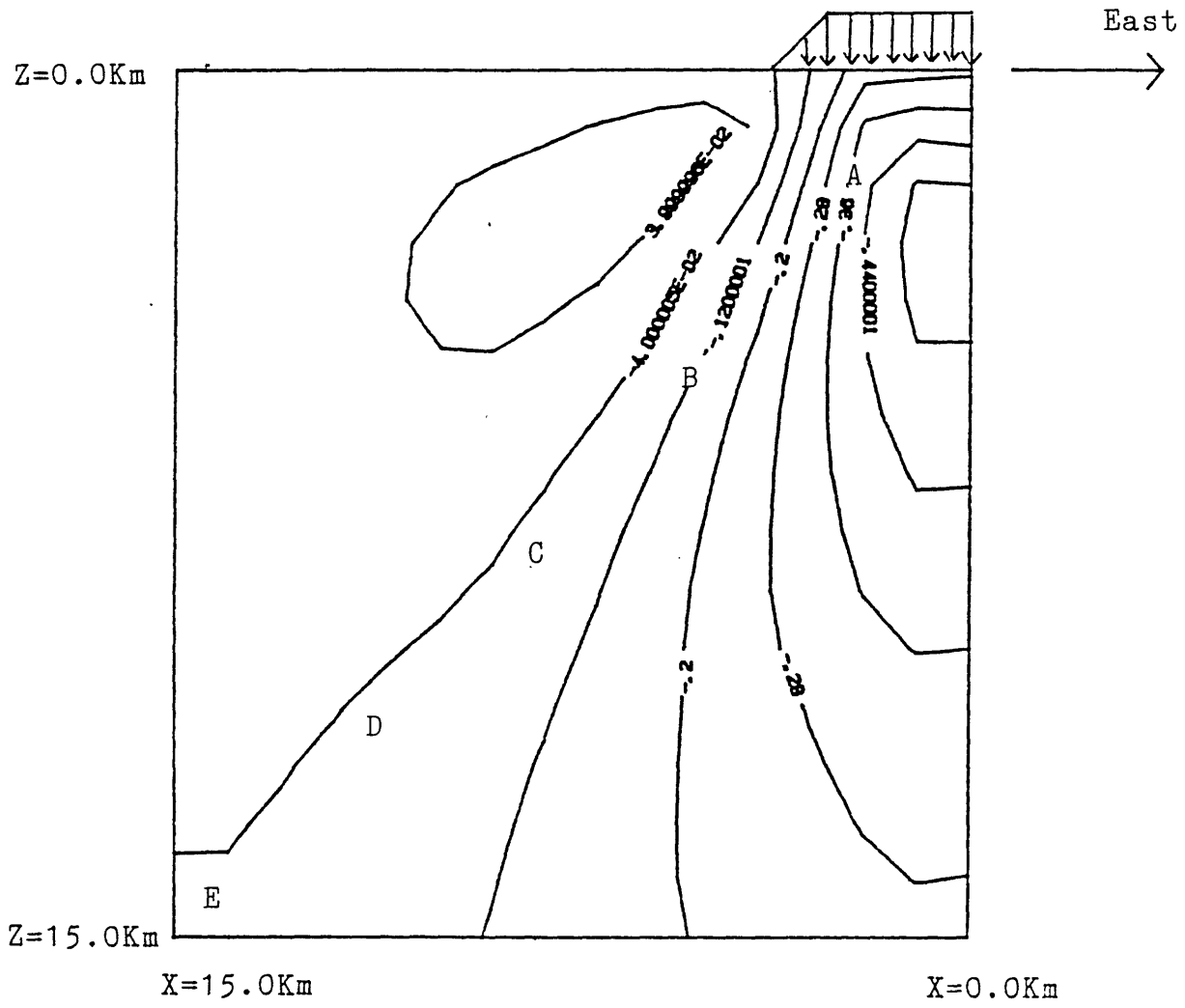

Location A: X, Z = 2.25Km
B: X, Z = 5.25Km
C: X, Z = 8.25Km
D: X, Z = 11.5Km
E: X, Z = 14.5Km

Figure 1 Strength Change (MPa) due to Reservoir Loading at 94 Months after Initial Impoundment along Planes Parallel to a Normal Fault Striking N-S and Dipping 60° to West. Negative Sign Indicates Weakening.

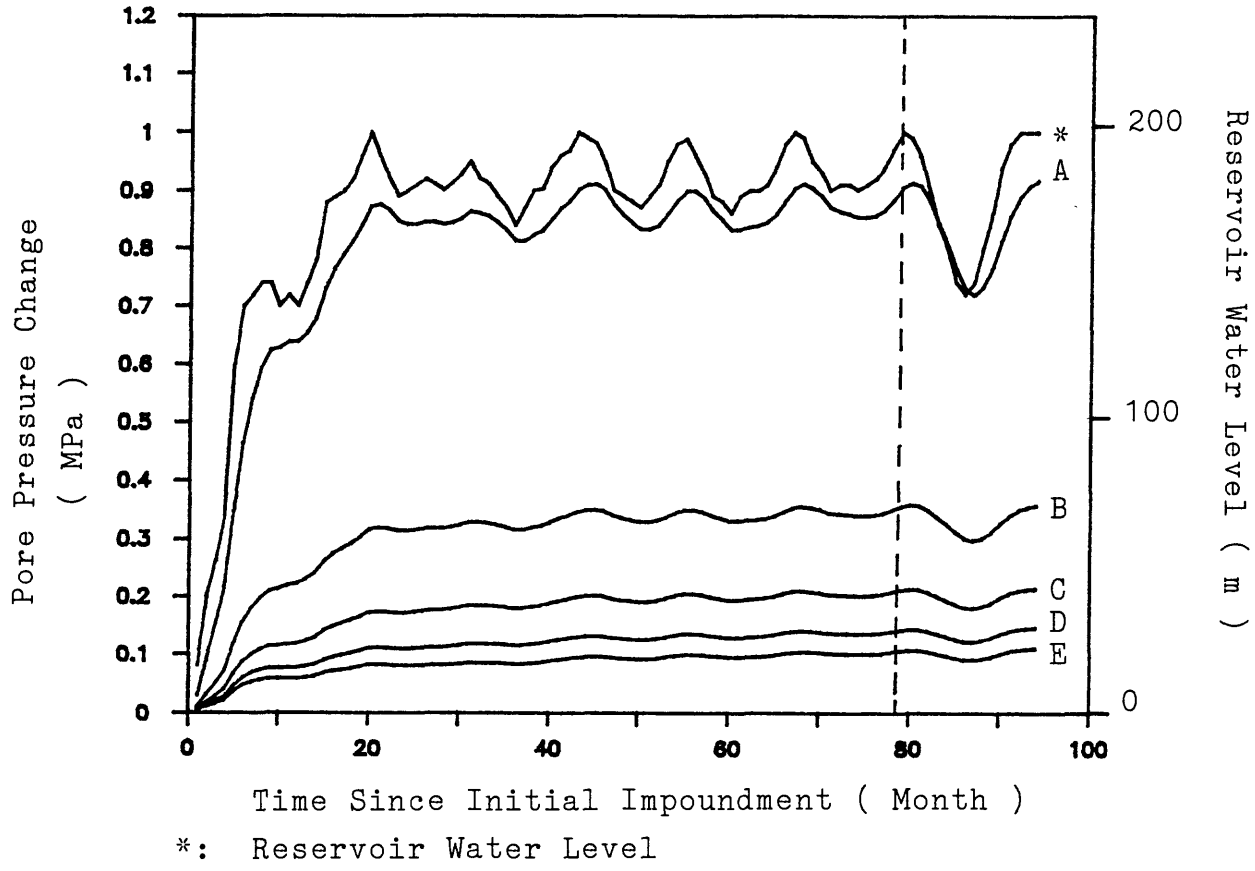

Figure 2 Variation of Reservoir Water Level and the Pore Pressure Changes at Points A - E (see Figure 1)

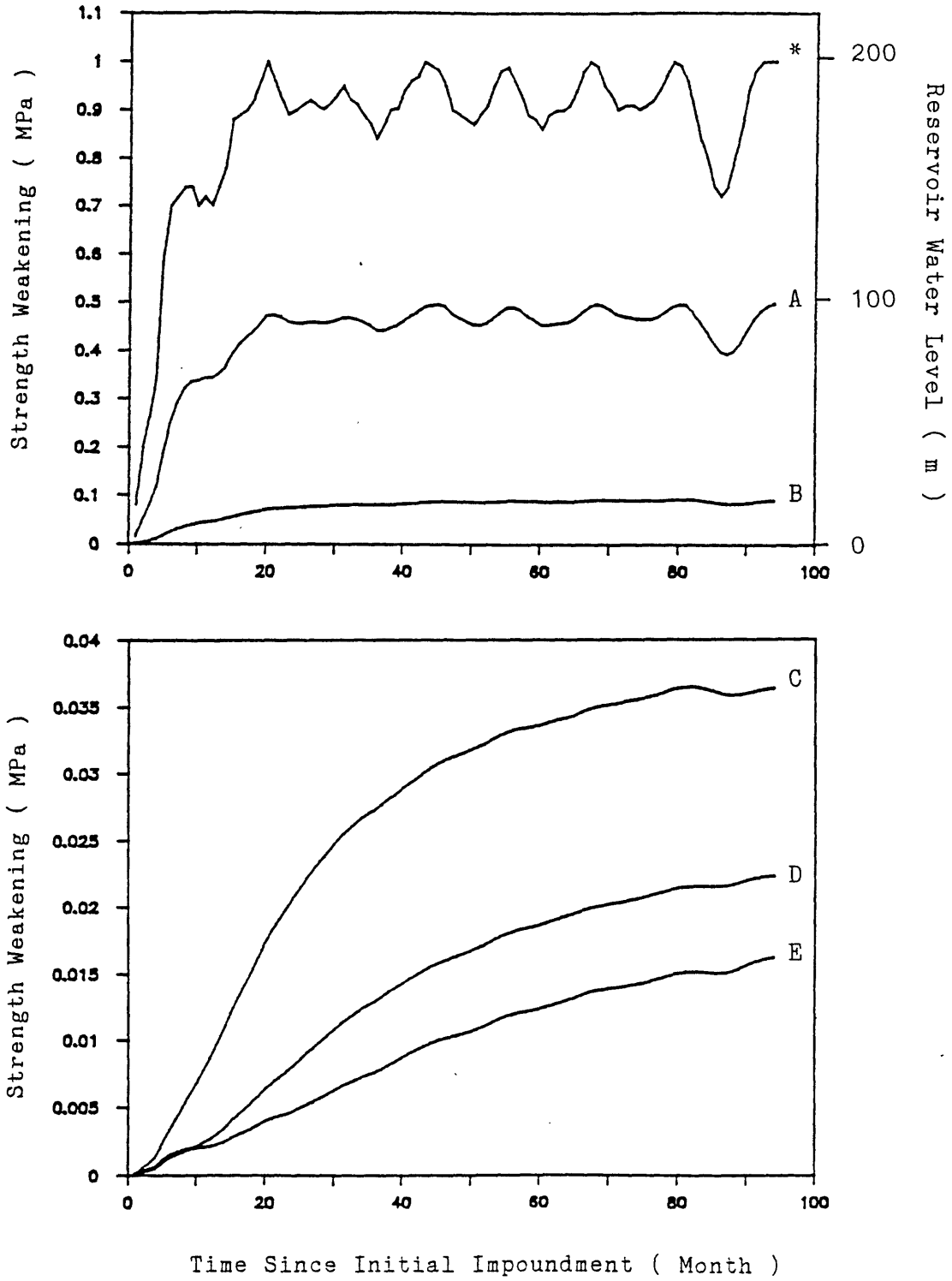

Figure 3 Fluctuation of Reservoir Water Level and the Resulting Strength Weakening at Points A - E along Planes Parallel to a Normal Fault (as Defined in Figure 1).

Deep Hole Desalinization of the Dolores River

9920-03464

William Spence
National Earthquake Information Center
U.S. Geological Survey
Denver Federal Center
Box 25046, Mail Stop 967
Denver, Colorado 80225
(303) 236-1506

Investigations

This project relates to monitoring the seismicity of the region of the intersection of the Delores River and Paradox Valley, southwest Colorado. The project is a component of the Paradox Valley Unit of the Colorado River Basin Salinity Control Project and is being performed for the U.S. Bureau of Reclamation with support from the Induced Seismicity Program of the U.S. Geological Survey. In this desalinization project, it is proposed to pump approximately 30,000 barrels/day from brine-saturated rocks beneath the Dolores River through a borehole to the Madison-Leadville limestone formation of Mississippian age, some 15,000 feet below the surface. There is a possibility of seismicity being induced by this desalinization procedure, especially in the long term. The project objectives are to establish a pre-pumping seismicity baseline and, during the pumping phase, to closely monitor the discharge zone for possible induced seismicity. If induced seismicity does occur, it should be possible to relate it to formation characteristics and to the pumping pressure and discharge rates.

Results

A 10-station seismograph network is centered at the location of the proposed injection well. This high-gain network has a diameter of about 80 kilometers, and has been in operation since September 1983. Seismic data are brought to Golden, Colorado, via microwave and phone line transmission. These data are fed through an A/D converter and then through an event detection algorithm. The network has operated at high quality, except for two periods when it was decommissioned by lighting strikes. Analysis procedures have been considerably complicated by a high rate of blasting activity in the region, but means have been developed to distinguish the occurrence of natural earthquakes to good reliability.

Notable regional earthquake activity are a swarm of shallow events (maximum magnitude 3.2) near Carbondale, Colorado, a similar swarm near Crested Butte, Colorado, a magnitude 3.4 shallow earthquake near Blue Mesa Reservoir, Colorado, and a magnitude 2.8 earthquake that was preceded by three events and followed by four events all located about 25 km SE of Grand Junction, Colorado. In the vicinity of the network, the earthquake catalog is complete to about magnitude 2.0, but very few earthquakes have occurred in the immediate vicinity of the proposed injection well. Most of the seismicity in the area of the network is in the shallow crust. However

about 20 earthquakes have focal depths greater than 20 km, with several events at the depth intervals 30-35 km and 50-55 km. These results indicate that microearthquakes are distributed throughout the crust of the Colorado Plateau, with an occasional event in the upper mantle. The shallow and deeper earthquakes follow a diffuse north-south trend, parallel to the eastern boundary of the Colorado Plateau. These early results, combined with a lack of historical seismicity at the zone of the Paradox Valley seismic network, indicate that any seismicity induced by deep-well injection near Paradox Valley should be identifiable as such.

Report

Spence, W., and Chang, P-S., 1986, Seismic monitoring in the region of the Paradox Valley, Colorado--Annual Report, July 1985-June 1986: U.S. Bureau of Reclamation, Deep Well Injection Site, Paradox Valley Unit, Colorado River Basin Salinity Control Project, 11 p.

Regional and National Seismic Hazard and Risk Assessment

9950-01207

S. T. Algermissen
Branch of Engineering Geology and Tectonics
U.S. Geological Survey
Denver Federal Center, MS 966
Denver, CO 80225
(303) 236-1611

Investigations

1. Investigation of the consequences of alternative seismic source zone configurations on the estimated ground motion hazard along the eastern seaboard of the United States has been completed and the results summarized in a paper that is currently under revision following journal review.

2. A field intensity survey was undertaken following the July 8, 1986, earthquake near Palm Springs, California, $m_b=M_s=6.0$.

3. Revised computer programs are being developed to process digitally recorded seismic waveform data, for spectral analysis and to analyze spectral ratios of seismic data from different sites.

4. Data for a hypocenter and intensity catalog of seismicity data for Peru were reviewed and edited.

5. An investigation is underway to determine the usefulness of extreme value techniques in estimation of maximum magnitude regionally.

6. Investigations continue for development of strong ground motion attenuation relationships.

7. A program has been initiated to develop a method for estimating strong ground motion for large, extended rupture earthquakes from simple stochastic and kinematic models of the source.

8. Investigation of how to limit variability in seismic hazard estimates at long return periods has been underway.

9. Efficacy of alternative pattern recognition algorithms for tectonic investigations in the eastern U.S. has been examined.

10. Correlation of seismicity and hot springs in Southern California has been reviewed.

Results

1. Six configurations of regional seismic source zones were used to estimate the ground motion hazard (annual exceedance probability of 1 in 500) along the eastern seaboard of the United States. The source zones range from being strongly influenced by the regional spatial distribution of earthquakes in the historic record to complete independence of historic seismicity, that is,

source zones based solely upon tectonic provinces and basement structure as well as geodetic vertical movement data and geomorphological considerations. Maintaining the same maximum magnitude among all zones and for all source zone models, the results indicate (1) a factor of 3 difference among source zone models for calculated acceleration levels in eastern Massachusetts and coastal Maine; (2) a factor of 2 difference for much of New Jersey, Delaware, and extreme eastern Maryland as well as a broad area of the southeastern seaboard including the Charleston, South Carolina region; (3) a factor of about 1.4 for much of the interior Appalachian region extending from New Brunswick to the Gulf Coast. A primary conclusion to be drawn from this work is that, lacking certain knowledge of earthquake causal structures, ground motion hazard estimates can be significantly lowered in subregional areas from that which the historical record of seismicity would indicate if seismic source zones are based solely on speculative tectonic hypotheses without regard for the historical record of events.

2. The most severe damage was found to be in the Painted Hill subdivision northwest of Palm Springs. A careful survey was made of this area by car in order to test a new damage assessment questionnaire presently under development. A number of revisions are being incorporated into the computer-read questionnaire form as a result of this trial.

The area surveyed is 1 km from the epicenter and 6, 7, and 9 km, respectively, from recorded high accelerations: North Palm Springs .78g v and .68g h, Whitewater Trout Farm .38g v and .61g h, and Desert Hot Springs .59g v and .33g h.

Within the subdivision, damage was concentrated along the trace of the Banning Fault, which is evinced by shattered ridges and cracked ground.

3. The programs developed to analyze digitally recorded seismic data are being applied to recordings of aftershocks of the March 3, 1985 (M_s=7.8) earthquake in central Chile. These data are being used to analyze site response at a number of sites in central Chile having widely varying geotechnical properties.

4. A paper describing the catalogs of South American hypocenter and intensity data developed over the past 4 years was completed and has been reviewed. The paper is being published (along with the catalogs) by the Centro Regional de Seismología para América del Sur (CERESIS) in Lima, Perú.

5. The results of the study applying extreme value techniques to the estimation of regional maximum magnitudes are being incorporated into a paper on the estimation of maximum magnitudes using historical magnitude data (seismicity).

6. Previous analyses of strong-motion data from moderate-to-large earthquakes were augmented with peak accelerations from M_L=2.5-5.0 earthquakes. Preliminary attenuation relationships relating peak acceleration to magnitude and distance were developed from approximately 1,000 strong-motion recordings.

An analysis of residuals revealed significant soil-structure interaction and site-geology effects in the data. When compared to the standard recording located in a ground-level, one-story building on Quaternary alluvial and

Terrace deposits, peak accelerations associated with embedded buildings and those associated with rock sites were found to have smaller amplitudes, and those associated with shallow deposits over rock were found to have larger amplitudes. The lowest accelerations were associated with crystalline rock sites and the highest with shallow-soil sites underlain by crystalline rock.

There were sufficient data from two regions--Oroville and Imperial Valley, Calif.--with which to develop individual attenuation relationships. These analyses led to two significant findings. First, the two regions demonstrated different rates of attenuation. These differences may be due to systematic differences in focal mechanism rather than an intrinsic difference in anelastic attenuation. Second, individual recording sites exhibited significant systematic differences in peak accelerations within each region. These differences, as much as a factor of 10, could not be explained by differences in surface geology or soil-structure interaction effects.

7. We began adapting D. M. Boore's stochastic simulation method of predicting strong ground motion to large, extended rupture events. Computer codes implementing Boore's techniques were written and tested. The development of computer codes implementing the kinematics of the rupture progation process was begun, but as yet has not been tested.

8. A review of probabilistic seismic hazard analysis techniques used by the Electric Power Research Institute (EPRI) project show that differences among various EPRI-team hazard estimates for nuclear power plants are sensitive to (1) differences in maximum magnitude, (2) differences in distance to boundaries of active source zones, and (3) determination of seismic rates for zones in the vicinity of sites. Our work has shown that:

A. Magnitude sensitivity is important only when low maximum magnitudes are chosen for source zones. If one chooses maximum magnitudes as high as those given by maximum regional earthquakes whose source structures are unknown, probabilistic peak acceleration estimates become relatively insensitive to choices of maximum magnitude.

B. Producing a probabilistic "fuzz" in the location of source-zone boundaries greatly decreases the extreme sensitivity of site long-return-period ground motions to boundary location, for sites in the vicinity of source-zone boundaries. Accordingly, we have revised our seismic hazard mapping computer program to produce a version, SEISRISK III, which provides for uncertainty in source-zone boundary location.

C. Determination of seismicity parameters in the vicinity of a site may be highly variable because of the small sample sizes present. The variability has to be constrained in some manner. In our work, parametric fits to data are performed over a large area in order to reduce the spatial variability of seismicity. These regional fits are allocated to zones according to a maximum likelihood process.

Alternatively, hazard estimates are possible using, instead of source zones, the historical seismicity in the vicinity of a site. This local seismicity may be generalized by spatial smoothing and by magnitude spreading. The project investigations illustrated that these kinds of smoothing at scales of 40 km or more produce much reduced variability in

long-return period ground-motion hazard estimates between sites for a number of nuclear sites in the northeastern U.S.

All these studies suggest that long-return-period ground motion at nuclear sites in the eastern U.S. may be considerably less varied, on a regional basis, than the results of the EPRI methodology suggest.

9. A paper has been submitted to the BSSA, comparing a maximum likelihood formulation with an additive-scoring formulation of pattern recognition between earthquakes and geological and geophysical variables. Because of the complexity and unknown structure of the real data, no definitive results were obtained for comparing the methods in application to an eastern-U.S. data set. However in studies with simulated data having several different kinds of structural relationships in the independent variables, the maximum likelihood algorithm performed at least as well as the additive-scoring method, the method usually encountered in the seismological literature.

10. In review of an article appearing in Geology (v. 14, no. 11, p. 287-290), it was demonstrated, in a comment accepted by that journal, that the alleged correlation (which was not high), and its statistical significance, could not be accurately assessed given the spatial dependence of the respective data sets.

Reports

Algermissen, S.T., 1986, Some problems in seismic hazard assessment, in Hays, W.W., ed., Proceedings of Conference XXXIV, A workshop on probabilistic earthquake hazards assessments: U.S. Geological Survey Open-File Report 86-185, p. 35-52.

Askew, B.L., and Algermissen, S.T., 1986, South American hypocenter and intensity catalogs, Volumes 1-9: Centro Regional de Sismología para América del Sur, Lima, Peru.

Bender, B.K., Jones-Cecil, M., and Perkins, D.M., Limitations of pattern recognition techniques for identifying earthquake prone areas: Submitted to Seismological Society of America Bulletin.

Bender, B.K., and Perkins, D.M., SEISRISK III, a computer program for seismic hazard analysis: U.S. Geological Survey Bulletin 1772 (in press).

Bender, B., and Perkins, D.M., 1986, Comment on "Correlation between seismicity and the distribution of thermal and carbonate water in southern and Baja, California, United States and Mexico": Geology, November, v. 14, no. 11, p. 969-970.

Campbell, K.W., 1986, Engineering seismology, in Meyers, R.A., ed., The encyclopedia of physical science and technology: San Diego, Academic Press, 35 p., in press.

_____1986, Empirical prediction of free-field ground motion using statistical regression models, in Proceedings, Soil-structure interaction workshop, Bethesda, 1986: Brookhaven National Laboratory, 30 p., in press.

_____1986, The integration of geological and historical data in the probabilistic estimation of extreme earthquake occurrences, in Hays, W.W., ed., Probabilistic earthquake hazard assessments, proceedings, national earthquake hazards reduction program workshop, 34th, San Francisco, 1985: U.S. Geological Survey Open-File Report 86-185, p. 72-115.

_____1986, Strong-motion attenuation relationships, in Hays, W.W., ed., Probabilistic earthquake hazards assessments, proceedings, national earthquake hazards reduction program workshop, 34th, San Francisco, 1985: U.S. Geological Survey Open-File Report 86-185, p. 197-248.

Thenhaus, P.C., 1986, Seismic source zones in probabilistic estimation of the earthquake ground motion hazard: A classification with key issues, in Hays, W.W., ed., Proceedings of Conference XXXIV, A workshop on probabilistic earthquake hazards assessments: U.S. Geological Survey Open-File Report 86-185, p. 53-71.

Regional and Local Hazards Mapping in the Eastern Great Basin

9950-01738

R.Ernest Anderson
Branch of Geologic Risk Assessment
U.S. Geological Survey
Box 25046, MS 966, Denver Federal Center
Denver, CO 80225
(303) 236-1684

Investigations

1. Continued field mapping and analysis of data pertaining to earthquake hazards along the Wasatch fault zone. (Machette, Nelson, and Personius)

   a. Identified sites for potential trenching across the Wasatch fault zone and secured permission for such a study (item 1b, Machette, Nelson, and Personius)

   b. In September 1986, the USGS and Utah Geological and Mineral Survey (UGMS) undertook a cooperative trenching program on the Wasatch fault zone. Twelve trenches were dug in three areas (Brigham City, Ogden, and American Fork Canyon) to better understand the recency and history of Holocene movement along discrete segments of the fault zone. This intense trenching operation is the final phase of our data collection. (Machette, Nelson, and Personius). In addition, cooperative research on thermoluminescene dating of fault materials, mainly colluvial wedges, is being conducted with Steve Forman (University of Colorado) and James McCalpin (Utah State University).

   c. Conducted a 2-day field review of geologic mapping and earthquake hazards analysis along the Wasatch fault zone, including a review of our trenching operations. The 40-50 participants included members of the USGS, UGMS, University of Utah, Utah State University, University of Colorado, Bureau of Reclamation, Utah State County geologists program, and landowners. (Machette, Nelson, and Personius)

   d. Prepared draft of research results on "The tectonic and earthquake potential of the Wasatch Front area and other parts of Utah" for the 1986 Earthquake Hazards Conference held July 14-18 at Salt Lake City, Utah. Chaired two half-day sessions of the conference and prepared final summary and comments for subsequent Earthquake Hazards planning session. (Machette)

2. Completed analysis and interpretation of data bases that might reflect segmentation of the Wasatch fault zone, and completed and submitted for internal review a 267-page draft of a Professional Paper chapter. (Wheeler)

3. Continued studies to evaluate the segmentation and history of Quaternary faulting along the Lost River fault, Idaho. (Crone)

4. Consultation by T. Barnhard with J. Angelier and his colleagues, University of Paris, on the use and application of a new generation of software developed by Angelier for use on Personal Computers.

Results

1. Field mapping and analysis of data:

   a. Four trenches were opened by Steve Personius and Hal Gill (UGMS) along the Wasatch fault zone in the Brigham City area; however, only a single 30-m-long trench across a 7-m-high fault scarp near Bowden Canyon, on the eastern limits of the city, proved to be productive. This trench is the first to be excavated across the main trace of the Brigham City segment of the Wasatch fault zone (fig. 1; also see our previous reports on fault segmentation), and it has the potential for vastly expanding our knowledge of the paleoseismic history for this part of the Wasatch fault zone. The trench is in early and middle Holocene alluvial-fan sediments, which consist primarily of silty, poorly sorted debris-flow deposits. Preliminary interpretation of relations exposed in the trench walls indicates a total vertical offset of approximately 6 m across a complex, 3-m-wide zone of normal faults. Analysis of the colluvial-wedge stratigraphy suggests movement on three different faults, with a total of three and possibly four surface-faulting events.

   b. Five trenches were opened by Alan Nelson, Bob Klauk (UGMS), Mike Lowe (Weber and Davis County geologist), and John Garr (Utah State University) along the Weber segment of the Wasatch fault zone on the east edge of the city of Ogden. These trenches are in lower to upper Holocene alluvial-fan deposits.

      Double scarps, 5 and 7 m high, cut the lower to middle fan deposits. These scarps are 1 to 3 m high in adjacent upper Holocene fan deposits. Stratigraphic displacements in all trenches are similar to displacement values obtained from topographic profiles across the scarps. The two deepest trenches exposed deltaic deposits of probable Provo age (14 ka) beneath the fan deposits in the hanging-wall block of each scarp. Preliminary interpretation of the colluvial stratigraphy in the trenches suggests a large displacement event of 3 to 4 m during the lower or middle Holocene on the 5 m scarp followed by a much smaller 1 m event in the late Holocene. Carbon-14 analysis on concentrated organic material from buried A horizons and TL analysis by Jim McCalpin (Utah State University) and Steve Forman (University of Colorado-Boulder) may provide maximum and minimum ages for these events. On the 7-m scarp there is clear evidence of a 2.5- to 4-m event during the middle or late Holocene and a 1.5- to 2.5-m event during the late Holocene; there may also have been an early Holocene event. A small trench across an antithetic fault exposes sediments displaced about 1 m during the latest event. Charcoal as well as A-horizon samples may constrain the ages of these events.

Radiocarbon analysis of buried A-horizon samples (collected in FY85) from an exposure at Garner Canyon near the north end of the Weber segment suggests a pre-2-ka-displacement event on the main fault of 1.3 m, a 1.5-m event shortly after 1.9 ka, and a most-recent event of 1.3 m shortly after 1.1 ka. This displacement history agrees well with that proposed for the Kaysville site 30 km farther south along the segment.

c. Three trenches were dug across the American Fork segment of the Wasatch fault zone by Michael Machette and Bill Lund (UGSM). These trenches penetrated middle to lower Holocene alluvial=fan and debris-flow deposits that lie unconformably on lacustrine sediments of the highest stand of Lake Bonneville (ca. 15,000-17,000 yrs old). The longest of the three trenches (AF-1; 55 m) crosses two fault scarps: the upper one is about 1 m high and the lower one is nearly 7 m high. Relations between colluvial wedges derived from fault scarps and the faulted Holocene sediments show three discrete surface-faulting events on the main strand of the fault zone. The net vertical offset is about 6.8 m, which compares favorably with the 7-m fault scarp. Charcoal was collected from the basal part of the youngest colluvial wedge and organic rich A horizons were sampled from the two other (older) wedges. Two shorter trenches were excavated across the same age alluvial-fan complex; AF-2 across an east-facing fault scarp the forms a graben adjacent to the main strand of the fault zone and AF-3 across a small normal (west-dipping) fault that is part of a basinward left-stepping zone of en echelon faults. Charcoal and organic-rich A horizons were collected from both of these trenches. Three fault movements were recognized in AF-2, but evidence for only two movements was found in AF-3. Results from radiocarbon and TL dating should allow us to correlate fault movements between trenches and to tell whether the American Fork and Provo segments proposed by Machette (fig. 1) really have different histories of movement.

d. As a result of the trenching effort we now have at least 15 samples of organic carbon from buried soils developed on colluvial wedges and 4 samples of charcoal from colluvial wedges and alluvium. Concentration of the organic carbon will be preformed this winter, and the concentrates will be submitted for conventational and accelerator radiocarbon dating in FY87. The results from the dating should help establish a firm chronology of Holocene faulting on the Brigham City, northern part of the Weber, and American Fork segments of the Wasatch fault zone.

2. The preceding Semi-Annual Technical Report (OFP 86-383, v. 22, July 1986, p. 481-482) summarized evidence for four places where the Wasatch fault has been segmented throughout most of all of its evolution. These persistent segment boundaries occur at, and only at, the Pleasant View, Salt Lake, Traverse Mountains, and Payson salients, and are named after them. The boundaries are expressed as places along the fault where transverse anomalies in six kinds of geological and geophysical data tend to coincide. During the reporting period statistical analyses of simulations showed that this coinciding should not be attributed to chance. Of the processes that are consistent with the geological history

of north-central Utah, only segmentation of the Wasatch fault can reasonably explain this coincidence of transverse anomalies. Mapping by M.N. Machette, A.R. Nelson, and S.F. Personius shows that scarps of the last few large seismic ruptures that occurred at or near the salients have started or stopped at these persistent segment boundaries. By inference, such ruptures have also tended to start or stop at the salients through most or all of the evolution of the Wasatch fault. Segmented seismic rupturing is the mechanism by which the fault became geometrically segmented by the salients. Persistence of these four segment boundaries allows the suggestion that the next few large seismic ruptures on the fault near the salients are also likely to start or stop at the salients.

The mapping of scarps and related features shows the existence of five more boundaries between rupture segments (fig. 1). Two of these boundaries lie between the Traverse Mountains and Payson salients, and three lie in the sparsely populated north and south ends of the fault. These five bondaries might be nonpersistent because they were not recognized in the pre-Quaternary geological and geophysical records that revealed the persistent boundaries. Most of these nonpersistent boundaries are inferred from scarps of only the last one to several large surface ruptures. Accordingly, it is not clear whether these nonpersistent boundaries should be expected to continue to influence the next few large seismic ruptures.

Mapped Bouguer gravity data show large along-strike steps in depths of hanging-wall basins along the Wasatch fault. In 1983 M. L. Zoback identified 10 of these transverse gravity zones (TGZ's). Six TGZ's occur at the four persistent segment boundaries (two of these boundaries are wide enough to include two TGZ's each). At the mouth of the Provo River and near Sevier Bridge Reservoir between Levan and Gunnison, two other TGZ's coincide with two of the nonpersistent segment boundaries. The large structural relief implied by the TGZ's suggests that their formation occupied much but not necessarily all of the history of the Wasatch fault. These two segment boundaries might be of intermittent persistence, affecting several successive seismic ruptures, then not affecting the next few ruptures. As mapping and trenching shows that a particular intermittently persistent boundary has affected more and more of the most recent surface ruptures, it becomes more and more likely that the boundary will similary affect the next rupture on that part of the fault.

At the Utah-Idaho border and near Plymouth about 15 km south of the border, two more TGZ's occur without nonpersistent boundaries. These TGZ's might represent intermittently persistent boundaries that were active in the past, but are presently in an inactive state and so have not affected the last few ruptures. An intermittently persistent boundary will be either in an active state or in an inactive state at any specified time. The idea of segmentation implies that a segment boundary will tend to persist through more than one rupture, and probably through more than two successive ruptures. Otherwise, the boundary would be merely the end of one rupture among many that are scattered helter-skelter along an unsegmented fault. If we know where the boundaries of segments are, we also know where the interiors of segments are. If boundaries tend to persist, so do interiors. Intermittent boundaries that are in active and which thus lie in segment interiors will tend to remain so for more than

one rupture and probably for more than two successive ruptures. An intermittently persistent boundary will tend to remain in its present state for the next rupture, whether that state is active or inactive. Therefore, intermittently persistent boundaries that are presently active, and which have affected the Holocene or late Quaternary record, are more likely to affect the next one or several large seismic ruptures than are intermittently persistent boundaries that are presently inactive, and which have not affected the young geologic record. A TGZ with an associated nonpersistent boundary is more likely to affect the next one or few ruptures than is a TGZ that does not coincide with a nonpersistent boundary.

3. Evaluation of the segmentation and history of Quaternary faulting along the Lost River fault, Idaho.

   a. The completed detailed mapping of the 1983 Borah Peak earthquake scarps shows that the earthquake generated 36.4±3.1 km of surface faulting along the Lost River fault. The main 20.8-km-long section of surface faulting was along the Thousand Springs segment of the fault with minor surface faulting along the Warm Spring segment to the northwest. Geologic, seismologic, and geodetic data suggest that barriers on the fault confined the primary coseismic rupture to the Thousand Springs segment. The primary rupture propagated from the southeast end of the segment unilaterally to the northwest where, at the Willow Creek hills, it was either halted or was deflected away from the Lost River fault andon to subsidiary faults. The primary rupture triggered comparatively minor surface faulting on the Warm Spring segment to the northwest. Fault-scarp morphology and bedrock geology suggest that the Lost River fault at the Warm Spring-Thousand Springs segment boundary has probably ruptured less frequently and had less net slip during much of the late Cenozoic than the interior of the adjacent segments.

   b. Seven trenches were excavated at four sites along the Warm Spring and Mackay segments of the Lost River fault to help characterize the sequence of faulting on the segments adjacent to the main section of 1983 surface faulting. Cursory examinations of the trenches at two sites on the Warm Spring segment (northwest of main 1983 surface faulting) suggest more than one late Quaternary surface-faulting event. Charcoal recovered from deposits related to the fault may help constrain the age of faulting on this segment.

      Three trenches at two sites on the Mackay segment (southeast of main 1983 surface faulting) exposed discontinuous horizons of volcanic ash believed to be related to the eruption of Mt. Mazama about 6,800 years ago. Cursory examination of stratigraphic relations in these trenches suggests that the last movement on this part of the fault is younger than the ash. Studies at all four sites will continue into 1987.

4. Assisted J. Angelier in development, debuging, and documentation of Fortran programs developed for resolving single and multiphase paleostress determinations. Fortran programs include data input, paleostress computation, separation of polyphase data sets into appropriate single-phase data subsets and simultaneously calculating the paleostress

orientation for each subset. Graphics programs to display multiple aspects of data attributes and resloved paleostress orientations are also available.

T. Barnhard acquired the programs from Angelier and will provide them to and assist other Survey scientists in their application and usage.

Publications

Anderson, R.E., 1986, Coeval mixed-mode dip-slip and strike-slip faulting in and adjacent to the Basin and Range, Utah-Nevada: Geological Society of America Abstracts with Program, v. 18, no. 5, p. 338.

Crone, A.J., Machette, M.N. Bonilla, M.G., Lienkaemper, J.J., Pierce, K.L., Scott, W.E., and Bucknam, R.C., 1987, Surface faulting accompanying the Borah Peak earthquake and segmentation of the Lost River fault, central Idaho: Seismological Society of America Bulletin, v. 77, 42 p., 3 oversized plates. [in press].

Machette, M.N., Lund, W.R., and Arabasz, W.J., 1986, Overview and comments on research progess--Tectonic and earthquake potential of the Wasatch Front area and other parts of Utah: U.S. Geological Survey Administrative Report, prepared for 1986 Earthquake Hazards Conference, Salt Lake City, Utah, 13 p.

Machette, M.N, Personius, S.F., Scott, W.E., and Nelson, A.R., 1986, Quaternary geology along the Wasatch Front--Evidence for ten fault segments and large-scale changes in slip rate on the Wasatch fault zone: U.S. Geological Survey Administrative Report, prepared for 1986 Earthquake Hazards Conference, Salt Lake City, Utah, 7 p.

Machette, M.N., Personius, S.F., and Nelson, A.R., 1986, Late Quaternary segmentation and slip-rate history of the Wasatch fault zone, Utah: EOS (Transactions, American Geophysical Union), v. 67, no. 44 [in press].

Machette, M.N., Personius, S.F., Menges, C.M., and Pearthree, P.A., Map showing Quaternary and Pliocene faults in the Silver City 1^{o} x 2^{o} quadrangle and Douglas 1^{o} x 2^{o} quadrangle, southeastern Arizona and southwestern New Mexico: U.S. Geological Survey Miscellaneous Field Studies Map 1465-C, scale 1:250,000 [in press]. (Directors approval June, 1986).

Machette, M.N., Documentation of benchmark photographs that show the effects of the 1983 Borah Peak earthquake with some considerations for studies of scarp degradation: Accepted by Bulletin of the Seismological Society of America, 15 ms. p., 3 figs., 4 tables [in press].

Sullivan, J.T., and Nelson, A.R., Quaternary displacement on the Morgan fault--A backvalley fault in the Wasatch Range of north-central Utah, in Hays, W.W., and Gori, Paula, eds., Assessment of regional earthquake hazards and risk along the Wasatch Front, Utah: U.S. Geological Survey Professional Paper. (Branch approval).

Wheeler, R.L., 1986, Stratigraphic evidence for Devonian tectonism on lineaments at Allegheny Front, West Virginia, in McDowell, R.C., and Glover, Lynn, III, eds., The Lowry Volume: Studies in Appalachian geology: Virginia Polytechnic Institute and State University Department of Geological Sciences Memoir No. 3, Blacksburg, Virginia, p. 47-66.

Wheeler, R.L., 1986, Comment on "Correlation between seismicity and the distribution of thermal and carbonate water in southern and Baja California, United States and Mexico": Geology, v.14, p. 969-970.

Wheeler, R.L., 1986, Reply to Comment on "Evaluating point concentrations on a map: Earthquakes in the Colorado Lineament": Geology, v. 14, p. 972-973.

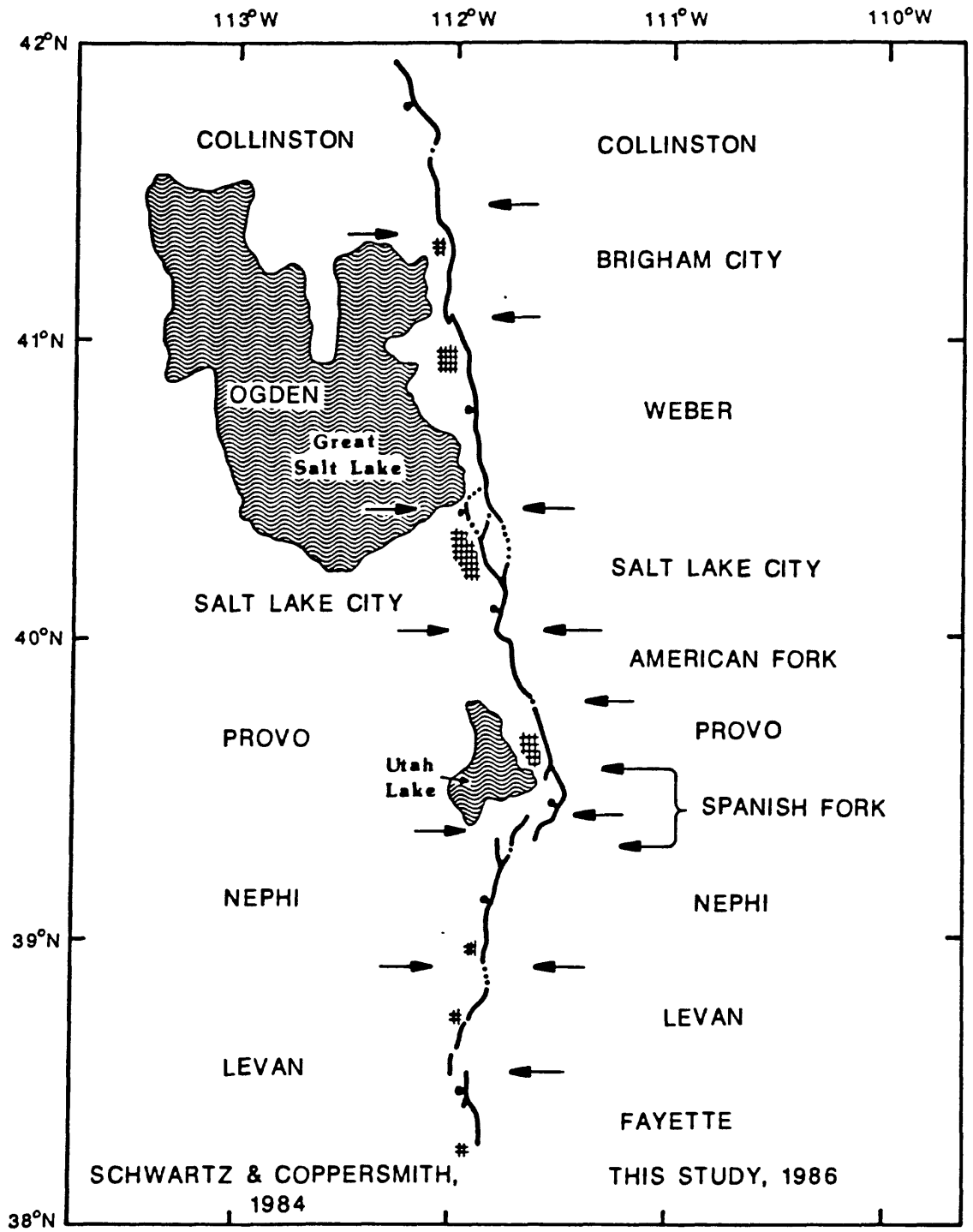

Figure 1. Segmentation of the Wasatch fault zone as proposed by Schwartz and Coppersmith (1984) and by this study. Large arrows indicate ends of segments.

Table 1. Lengths of segments proposed for the Wasatch fault zone.

Segment	Length of surface trace (km)	Length from end to end (km)	Comments
Collinston	15+	15+	Minimum length. No latest Quaternary movement.
Brigham City	45.4	39.5	1 km left step to north end of Weber segment. Holocene movement.
Weber	57.2	52.0	Fault enters bedrock south of Bountiful, may join East Bench fault 10 km to south.
Salt Lake City	44.1	36.9	Includes Warm Springs fault in northern Salt Lake City.
American Fork	18.5	15.4	From middle of Traverse Range south to Provo River.
Provo	19.0	17.2	Cuts across north end of Spanish Fork segment just north of Springville.
Spanish Fork	32.3	17.7	4 km right step and 5 km N-S overlap with Nephi segment.
Nephi	38.8	35.0	Includes uncertain fault connection between Juab Valley and Santaquin Canyon.
Levan	25.1	23.6	12.6 km gap between Nephi and Levan segments. Has 3 2-km-long gaps in segment; Holocene movement.
Fayette	14.1	13.0	Steps 4 km left at south end of Levan segment. No Holocene movement.

Note: Schwartz and Coppersmith proposed six segments. Their Odgen segment is divided here into the Brigham City (northern) and Weber (southern) segments (the Brigham City includes about 5 km of the original Collinston segment. Their Provo segment has been divided into the American Fork (northern), Provo (middle), and Spanish Fork (southern) segments. Their Levan segment has been divided into the Levan (northern) and Fayette (southern) segments.

Implementation of Research Results and Information Systems for Regional and Urban Earthquake Hazards Evaluation, Southern California

9950-03836

William M. Brown III
Branch of Geologic Risk Assessment
345 Middlefield Road, MS-998
Menlo Park, California 94025
(415) 856-7112/7119

Investigations:

This project is part of a long-range regional earthquake hazards evaluation for Southern California, directed by the U.S. Geological Survey. This phase of the project is oriented towards (1) Summarizing results of recent earth-science research on evaluating earthquake hazards; (2) Presenting examples of ongoing earthquake-hazard reduction efforts; and (3) Determining what additional scientific and technical information is needed and which hazard-reduction techniques are most effective. This phase draws upon research results published in U.S. Geological Survey Professional Paper 1360 (1985), and is intended to direct future research efforts based upon evaluation of those results.

The evaluation began during April-September 1985 with distribution of materials from Professional Paper 1360 and selective invitations for written statements on earthquake hazards evaluation. The distribution was directed to a multidisciplinary group of about 80 people from a variety of professions involved with the earthquake hazard for Southern California. These people were requested to prepare formal responses to those materials, and to present their analyses and recommendations at a major multidisciplinary workshop convened during November 12-13, 1985, at the University of Southern California, Los Angeles, California.

The workshop, "Future Directions in Evaluating Earthquake Hazards of Southern California" focused on (1) Evaluating earthquake and surface-faulting potential; (2) Predicting seismic intensities for response planning and loss estimation; (3) Predicting ground motion for earthquake-resistant design; (4) Predicting major earthquakes for preparedness planning; (5) Evaluating earthquake ground-failure potential for development decisions; and (6) Evaluating the shaking hazard for redevelopment decisions. Each of these elements was introduced from a scientific perspective, and was then evaluated by those who apply the scientific information.

Results:

The workshop consisted of a formal program of 80 presenters, moderators, panelists, and commentators during an intensive two-day session involving a plenary session and three working groups each day. Total participation, including speakers and audience, was 350. Those on the program represented a significant aggregation of the most prominent workers in earthquake hazards evaluation, reduction, and response for Southern California. The audience included scientists, engineers, attorneys, insurance actuaries, emergency

response officials, government officials, educators, geotechnical consultants, and representatives of many other professions. The workshop program and a roster of attendees are contained in the workshop proceedings volume cited below.

All presenters, moderators, panelists and commentators submitted written papers and statements for the workshop proceedings. All proceedings were recorded on audiotapes, and transcribed, condensed, and edited for publication. The bulk of work during April - September, 1986 was directed toward compiling, editing, and publishing the workshop proceedings. The proceedings were published by the U.S.G.S. in the NEHRP "Knowledge Utilization Series" of Open-File Reports.

Reports:

Brown, W.M., III, Kockelman, W.J., and Ziony, J.I., editors, 1986, Workshop on future directions in evaluating earthquake hazards of southern California -- Proceedings of Conference XXXII, November 12-13, 1985, Los Angeles, California: U.S. Geological Survey Open-File Report 86-401, 421 p.

Ziony, J. I., editor, 1985, Evaluating earthquake hazards in the Los Angeles Region -- An earth-science perspective: U.S. Geological Survey Professional Paper 1360, 505p.

Seismic Hazards of the Hilo 7 1/2' Quadrangle, Hawaii

9950-02430

Jane M. Buchanan-Banks
Branch of Geologic Risk Assessment
U.S. Geological Survey
David A. Johnston Cascades Volcano Observatory
5400 MacArthur Boulevard
Vancouver, Washington 98661
(206) 696-7810

Investigations

Preparation of research papers, and a geologic map and text of the Hilo 7 1/2' quadrangle continues.

Results

Maps of parts of the Pi'ihonua and Mountain View quadrangles showing chemical sample, radiocarbon, and paleomagnetic collection sites were prepared for publication. These quadrangles are adjacent to the Hilo quadrangle and the collection sites provided geologic data pertinent to the Hilo quadrangle. Examination of thin sections to provide more detailed information on the lithology of the lava flows, and to resolve mapping questions, is underway.

Two research papers are also in progress. One paper on the location and significance of the radiocarbon dates obtained within the Hilo quadrangle and the aforementioned adjacent quadrangles awaits input from one of the three coauthors. A second paper describing the chemistry of the lava flows and showing plots of the major elements versus SiO2 and MgO for lavas of all volcanoes has been prepared in first draft. The paper now awaits development of author expertise in the use of the Lotus 123 program in order to produce tables of the chemical data for publication.

SITE-RESPONSE AND LIQUEFACTION STUDIES INVOLVING THE CENTRIFUGE

Grant No. 14-08-0001-G1192

C. B. Crouse and Behnam Hushmand
Earth Technology Corporation
3777 Long Beach Blvd.
Long Beach, CA 90807
213-595-6611

Ronald F. Scott
California Institute of Technology
Pasadena, CA 91125
818-356-6811

Investigations

A new laminar box apparatus was constructed for use in the centrifuge at the California Institute of Technology. The box was filled with dry and saturated sand samples, which were subjected to earthquake-like excitations while the centrifuge was in flight. Lateral accelerations and displacements, pore-water pressures, and settlements were recorded as a function of time and are currently being analyzed.

Description of Box Apparatus

The laminar box consisted of rectangular aluminum rings stacked on top of one another. In plan view, the outside dimensions of each ring were 20.3 cm wide by 38.1 cm long. The corresponding inside dimensions were 2.54 cm shorter. Each ring was 1.27 cm thick, and a total of 19 rings comprised the box which was 24.9 cm high. Adjacent rings were separated by ball bearings. The top and bottom surfaces along the length of each ring were grooved to provide tracks for these bearings. The radius of each bearing was slightly larger than the depth of the grooves to prevent adjacent rings from rubbing together. This construction technique reduced the frictional forces between the rings and allowed the box of stacked rings to easily deform during lateral loading. Static lateral load tests on each ring of the assembled box during centrifugal accelerations of 50g and 75g confirmed that the friction between the rings was minimal. Further details of the apparatus are described in a paper by Hushmand et al. (1986 - in preparation).

Experimental Results

Shaking tests on dry, partially saturated and fully saturated sand samples were completed in September, 1986. Currently, the data are being reduced, and only a few results are available. A sample of the results from one test conducted at 50g on fully saturated sand is shown in Figures 1 and 2. Differences in the input (base) acceleration and the accelerations recorded at

various heights within the soil column are readily apparent in Figure 1. An obvious difference is the reduction of acceleration with height in the sand column. This reduction is directly the result of liquefaction, which can be inferred from the pore-water pressure plots in Figure 2. The pore-water pressures increased rapidly shortly after the shaking began and induced liquefaction over the entire depth of the sand column. The sand remained in a liquefied state during the shaking, after which the pore-water pressures gradually dissipated to their pre-shaking, static levels. Also shown in Figure 2 are the dynamic lateral displacements, which were recorded by LVDT transducers. These displacements clearly show a progressively increasing lateral drift. The settlement of the soil surface (not shown) also progressively increased during, and for a short time after, the shaking.

During the testing, no attempt was made to slow the dissipation of pore-water pressures by adding silicon oil or glycerin to the water as other researchers have done. Although this might have produced a more realistic prototype condition for pore-water pressure dissipation, a decision was made to concentrate more on the phenomenon leading to the onset of liquefaction. Nonetheless, the tests did capture all important features of the liquefaction phenomenon and did provide a good data base for evaluating and further understanding the occurrence of liquefaction in saturated sands.

Future Research

Most of the remaining research will be devoted to developing and calibrating analytical models which will approximately duplicate the experiment results, such as those in Figures 1 and 2.

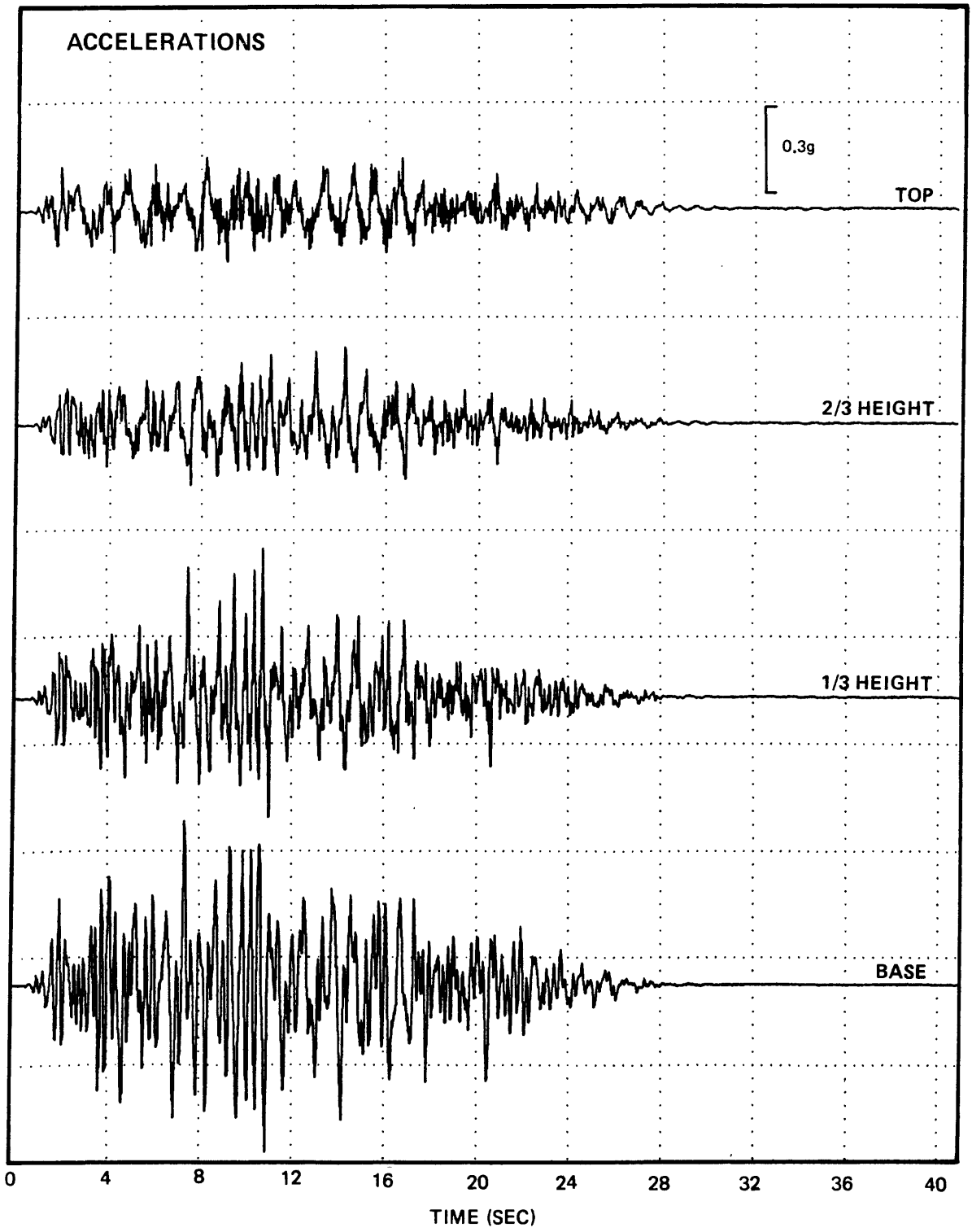

FIGURE 1. ACCELERATIONS RECORDED DURING 50g TEST (PROTOTYPE SCALE).

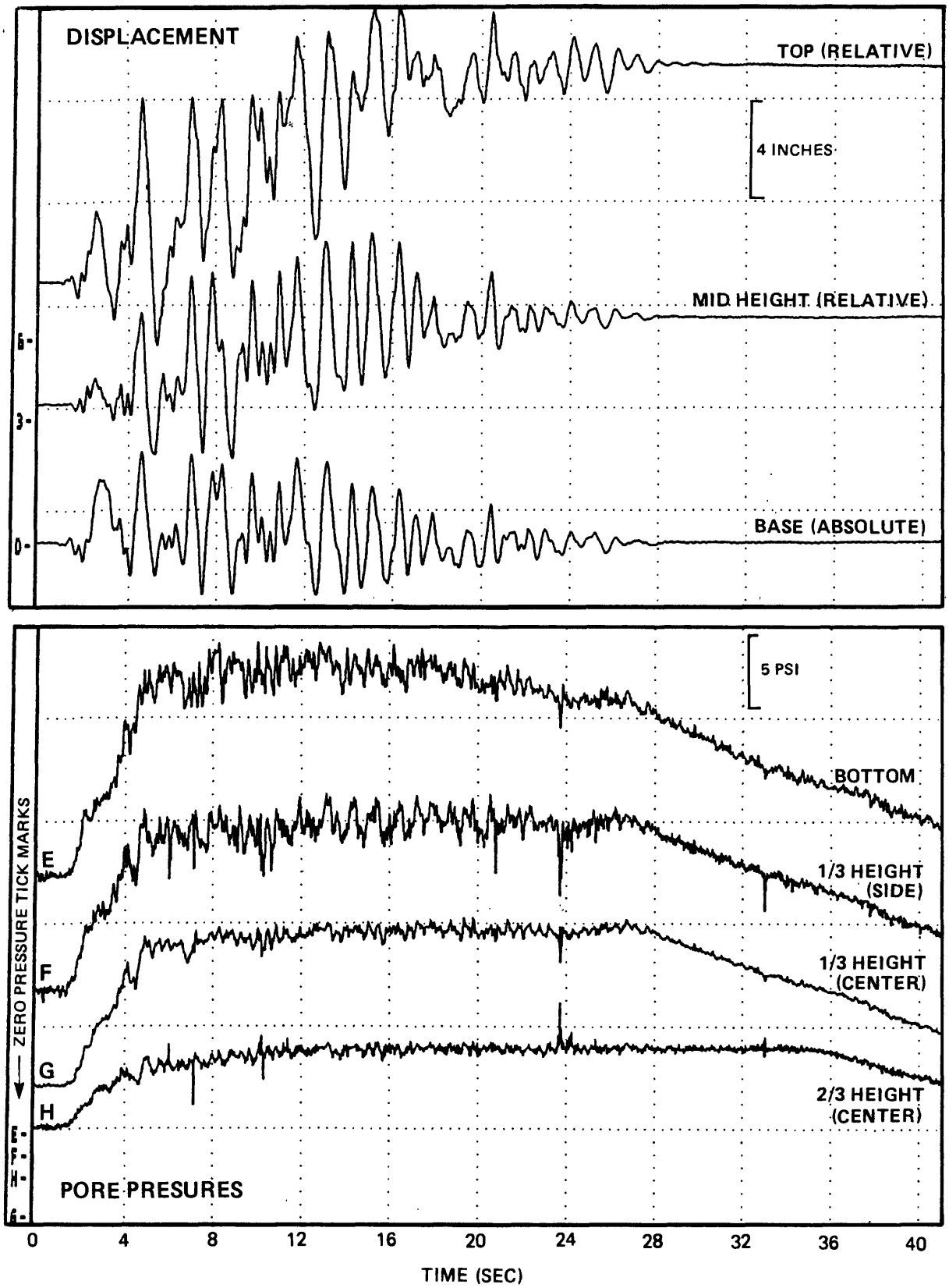

FIGURE 2. LATERAL DISPLACEMENTS AND PORE-WATER PRESSURES RECORDED DURING 50g TEST (PROTOTYPE SCALE).

Seismic Hazard Studies, Anchorage, Alaska

9950-03643

A. F. Espinosa
Branch of Geologic Risk Assessment
U.S. Geological Survey, MS 966
Denver Federal Center, Box 25046
Denver, CO 80225
(303) 236-1597

Investigations

1. Fifteen earthquakes recorded in the field seismological experiment conducted in Anchorage, Alaska have been edited. On the average six of the digital portable systems recorded the local events. The data is being used to relocate some of the events and the spectra analysis is being evaluated. This topic on "Ground amplification studies in areas damaged by the Alaskan earthquake" will be jointly used in the site response study obtained on different geologic environments with the damage evaluation along 15th Avenue and DeBarr Avenue.

2. A suite of seismicity maps and depth cross sections for the Anchorage and vicinity region in Alaska are being prepared. A technique has been developed to map the subducting plate on a three-dimensional finite-difference display for Anchorage and vicinity. ISC, USGS, and Menlo Park's local seismicity data files are used to perform the geometrical mapping of the lithosphere in this region. A paper was presented at the spring AGU meeting which discusses the technique and application of 3-D mapping of convergence zone-Alaska and the Aleutian Islands region.

3. The intensity catalogue covering the period 1899 through 1981 for the State of Alaska is being released as a USGS Bulletin.

4. The geologic map of the northwestern quarter of the Tyonek A-4 quadrangle at 1:31,680 scale has been revised and completed. Also, the geologic map of the Tyonek B-4 quadrangle has been reviewed. These two maps are in the process of being edited and will be released shortly.

5. The first draft of a USGS Bulletin interpreting results from geotechnical testing of cores from four drill holes in the Tyonek Formation has been completed.

6. The northeastern sheet of the three-sheet geologic materials map of the Municipality of Anchorage has been checked and further editing is being done.

7. A set of modified Mercalli intensity distribution maps of the most significant earthquakes which have occured in Alaska in the 1899-1981 time period has been released.

8. Contributions consisting of surficial geology input to the geologic map of the Gulkana B-1 quadrangle, covering about half of the map (which is being prepared as an adjunct to the Trans-Alaska Crustal Transect Project), has been completed. Work on the adjacent Nashesna B-6 map is in progress.

9. The intensity and earthquake parameters catalogue for the state of Alaska is being prepared for release on digital tape as an Open File Report.

10. Ten drill-hole resistivity logs are being processed digitally. The holes have a depth penetration from 6,000 to 14,000 ft and are located in the Anchorage and vicinity region, Alaska

11. A paper was presented at the Fifth International Congress of the International Association of Engineering Geology, Buenos Aires, Argentina, describing the application of the seismotechnistratigraphic cell concept to subsurface mapping in Anchorage, Alaska.

Reports

Bartsch-Winkler, Susan, and Schmoll, H.R., 1986, Earthquake couplets in Upper Cook Inlet: Alaskan Accomplishments Circular, 7p.

Brockman, S.R., Espinosa, A.F., and Michael, J.A., 1986, Catalog of Intensities I_0's and their corresponding magnitudes for earthquakes in Alaska and the Aleutian Islands, U.S. Geological Survey Bulletin, 250 p.

Espinosa, A.F., 1986, Directory of Earthquake Hazards Research and other related activites in Alaska; Seismic hazard studies, Anchorage, Alaska in Hays, W.W., and Gori, P. eds., Evaluation of Regional and Urban earthquake hazards and risk in Alaska: U.S. Geological Survey Open-File Report 86-79, C23-C30.

Espinosa, A.F., Brockman, S.R., and Michael, J.A., 1986, Modified Mercalli intensity distribution for the most significant earthquakes in Alaska, 1899-1981: U.S. Geological Survey Map 86-203.

Espinosa, A.F., Schmoll, H.R., Brockman,S.R., Yehle, L.A., Odum, J.K., Michael, J.A., and Rukstales, K.S., 1986, Seismic hazard studies, Anchorage, Alaska in Hays, W.W., and Gori, P., eds., Evaluation of regional and urban earthquake hazards and risk in Alaska: U.S. Geological Survey Open-File Report 86-79, p. 161-177.

Herraiz, M., and Espinosa, A.F., 1986, Scattering and Attenuation of High-Frequency Seismic Waves--Development of the theory of Coda Waves: U.S. Geological Survey Open-File Report 86-455, 91 p.

Odum, J.K., Compilation of field and laboratory geotechnical test data for U.S. Geological Survey drill holes 1C-79, 2C-80, CW81-2, and CE82-1, Beluga resource area, upper Cook Inlet region Alaska: U.S. Geological Survey Open-File Report 86-382, 8 p.

Odum, J.K., Yehle, L.A., Schmoll, H.R., and Gilbert, Chuck, 1986, Generalized interpretation of geologic materials from shot holes drilled for the Trans-Alaska Crustal Transect Project, Copper River Basin, Alaska, May 1985: U.S. Geological Survey Open-File Report 86-408, 18 p.

Odum, J.K., 1986, Point-load index and laboratory unconfined compressive strengths of the coal-bearing Tyonek formation, Beluga coal resource area, Upper Cook Inlet Region, Alaska: Focus on Coal 1986, Proceedings, Fairbanks, University of Alaska, School of Mineral Industry, MIRL Report. (In review.)

Schmoll, H.R., 1986, U.S.G.S. Engineering Geology projects in the Anchorage area, Alaska--A review--in Hays, W.W., and Gori, P., eds., Evaluation of regional and urban earthqauke hazards and risk in Alaska: U.S. Geological Survey Open-File Report 86-79, p. 134-147.

Schmoll, H.R., Espinosa, A.F., and Odum, J.K., 1986, Subsurface mapping at Anchorage, Alaska--A tool for the delineation of seismotechnistratigraphic (STS) cells: Proceedings, 5th International Congress, International Association of Engineering Geology, Buenos Aires, Argentina, October 20-15, 1986, v.6, p. 1829-1840.

Yehle, L.A., Odum, J.K., Schmoll, H.R., and Dearborn, L.L., Overview of the geology and geophysics of the Tikishla Park drill hole, USGS A-84-1, Anchorage, Alaska: U.S. Geological Survey Open-File Report 86-293, 10 p.

Yehle, L.A., and Schmoll, H.R., 1986, Surficial geologic map of the Anchorage (B-7)NW quadrangle, Alaska: U.S. Geological Survey Map, scale 1:25,000. [In press]

Soil Development as a Time-Stratigraphic Tool

9540-03852

Jennifer W. Harden
Branch of Western Regional Geology
U.S. Geological Survey
345 Middlefield Road, MS 975
Menlo Park, California 94025
(415) 323-8111 ext. 2039

Investigations

1. Slip-rate studies along the Calaveras Fault near San Felipe Creek: Jennifer Harden, Kathy Harms, Malcolm Clark.

2. Geochronology-soil chronology-remote sensing study of outwash fans near Independence, California.

Results

1. A slip-rate study was begun near San Felipe Creek along the Calaveras Fault. Four fluvial terraces were excavated on the SW side and two terraces were excavated on the NE side of the fault. Using gravel sources and soil development, terraces on either side of the fault will be matched for reconstruction of pre-fault geomorphology. Using soil development to estimate ages of the fluvial terraces, timing of offset will be used to determine slip rates, averaged over time since terrace formation. Four soil profiles were described and sampled on each terrace. Samples are being analyzed by Univ. of California, Berkeley contract for particle size, bulk density and iron oxides. Four charcoal sample were found and will be dated by accelerator mass spectroscopy.

2. Eight outwash fans along the eastern front of the Sierra Nevada were identified by A. Gillespie using multi-spectral imaging. At least 5 of those fans can be dated by their stratigraphic relationship to basalt flows dated by Ar 39-40 and K-Ar methods. Backhoe pits were excavated on each of the 8 fans, and 2-3 replicate soils were described and sampled. Soil data will provide calibration for deposits 10 to 1800 ka in age. Soils will then be used to correlate and date deposits in the region where basalts are absent. Soils are being analyzed by Humboldt State University in a cooperative effort.

Reports

Harms, K.K., Harden, J.W., Hoose, S.N., and Clark, M.M., 1984, Estimating slip rates along the Calaveras Fault, California, Using soils chronology and geometry of stream terraces: Earthquake Notes, v. 55, no. 1, p. 9.

Harden, J.W., Harms, K.K., Mark, R.K., and Clark, M.M., 1986, Soil development as a tool for studying seismogenic faults, Soil Science Society of America Abstracts, Annual Meeting, Chicago, Illinois, December 4-9, 1986.

Harden, J.W., Matti, J.C., and Terhune, C.L., 1986, Quaternary slip rates along the San Andreas fault near Yucaipa, California, derived from soil development on fluival terraces: Geological Society of America Abstracts with Program, v. 18, no. 2, p. 113. Cordilleran Meeting, Los Angeles, California, Programs with Abstracts.

Harden, J.W., Sarna-Wojcicki, A.M., and Dembroff, G., 1986, Soils developed on coastal and fluvial terraces near Ventura, California, in Harden, J.W., (ed): A series of soil chronosequences in the western United States, U.S. Geological Survey Bulletin 1590-B (in press). Director's approval, November 1985.

Terhune, C.L., Harden, J.W., and Matti, J.C., 1986, Application of a quantified field index of soil development to distinguish relative ages of geomorphic surfaces for regional geologic mapping: Geological Society of America Cordilleran Meeting, Los Angeles, California, Programs with Abstracts.

Seismic Slope Stability

9950-03391

Ed Harp
Geologic Risk Assessment
345 Middlefield Road MS 998
Menlo Park, California 94025
(415) 856-7124

Investigations

1. Completed field work measuring fracture characteristics of rock slopes along the Wasatch Front near Salt Lake City, Utah for evaluation of seismic slope stability.

Results

1. Measurement of fracture characteristics of rock slopes along the Wasatch Front near Salt Lake City from Mill Creek south to Little Cottonwood Creek has provided the necessary data to classify and quantify their seismic slope stability using a modified form of the rock-mass-quality-index. The field-gathered fracture data has made it possible to assign average index values of slope susceptibility to the various formations or lithologic units along the above-mentioned portion of the Wasatch Front. As a by-product of the modification of the rock-mass-quality-index for use in describing seismic slope stability, the index as used for this study also has the capability for the rapid empirical assessment of seismic slope stability on a site specific basis. It has become evident that the index can quickly and effectively give a good comparative estimate of the susceptibility of a given rock slope or slopes. The index therefore gives the engineer or geologist a way to rapidly and inexpensively determine whether a slope is unstable under seismic conditions (low Q values), stable under seismic conditions (highest Q values), or whether further analysis is required (intermediate values).

DEVELOPMENT OF A SEISMIC SLOPE STABILITY MAP FOR THE URBAN CORRIDOR OF UTAH, WEBER, EASTERN BOX ELDER, AND CACHE COUNTIES, UTAH

14-08-0001-G1173

Jeffrey R. Keaton
Department of Civil Engineering
Utah State University, Logan, Utah 84322-4100
Present Address: Center for Engineering Geosciences
Department of Geology, Texas A&M University
College Station, Texas 77843-3115

INVESTIGATIONS

1. Information on the distribution of landslides resulting from earthquakes in Utah from 1850 to 1985 was compiled and compared to magnitude-distance and magnitude-areal extent relationships published by Wilson and Keefer (1985) and Keefer (1984).

2. Limiting equilibrium analysis techniques used to compute values of critical acceleration required to reduce factors of safety to unity were compared to "Newmark" style slope displacement techniques based on Arias Intensity values published by Wilson and Keefer (1985).

3. Potential area affected by landslides due to a "characteristic" Wasatch earthquake was estimated on the basis of Arias Intensity and applied to 5 segments of the Wasatch fault from Nephi to Brigham City.

4. Manipulation of digital terrain data and geotechnical parameters continued; digital terrain data are not available for parts of the area and cannot be acquired within budget and/or time constraints.

RESULTS

1. References to slope failures were found in the reports of twelve earthquakes in Utah from 1850 to 1985 (Table 1). One of these refers to liquefaction (?) only and one refers to snow avalanches only. Estimates of the maximum distances from the slope failures to the epicentral areas and general areal extent of slope failures were compiled (Table 2) and compared to relationships published by Wilson and Keefer (1985) and Keefer (1984) (Figures 1 and 2). Substantial uncertainty exists in the seismological data for Utah; however, it appears that, in general, earthquakes in Utah follow the world-wide trend.

2. The technique used to evaluate seismic slope failure potential in Utah is the conventional pseudostatic limiting equilibrium analysis in which the horizontal component of earthquake acceleration required to reduce the factor of safety of an infinite slope is calculated and used as an index of seismic slope stability. This acceleration is considered to be the "critical" acceleration and it is compared to previously published probabilistic accelerations for the purpose of assigning qualitative hazard descriptions of high, moderate, low, or very low. This method is based on the same reasoning as liquefaction potential evaluations in northern Utah (Anderson et al., 1982, 1986) which have been received well by local decision makers.

Seismic slope stability has been evaluated on the basis of the estimated displacement of the slope material due to seismic shaking (Wieczorek et al., 1985, Wilson and Keefer, 1985). Failure criteria were established by Wilson and Keefer (1985) as 2 cm of displacement for

falls and disrupted slides and 10 cm of displacement for coherent slides. Empirical relationships between Arias Intensity and critical acceleration were developed by Wilson and Keefer (1985) for 10 earthquakes, so that seismic slope failure potential could be expressed in terms of Arias Intensity rather than critical acceleration. This approach is appealing because Arias Intensity incorporates both peak acceleration and duration of shaking. We viewed the applicability of this approach to seismic slope stability in Utah as marginal because of Utah's extensional tectonics whereas the relationship was developed using compressional earthquakes. However, following discussions with R.C. Wilson (written communication, 1986), we became convinced that the scatter in the seismological data combined with the general parallel trend of Utah's seismic slope failures to world-wide failures (Figures 1 and 2) was sufficient to use the relationships developed for compressional tectonics in the extensional stress regime in Utah.

The threshold acceleration values used to identify seismic slope failure potential in Utah were based on the probability that the accelerations would be exceeded in a 100-year time period combined with estimated geotechnical strength parameters and a range of ground water conditions (Table 3). The exceedance probability-peak acceleration relationship used for northern Utah (Figure 3) was developed during liquefaction potential studies (Anderson et al., 1982,1986). Displacement values as a function of critical acceleration (Figure 4) were computed by Wilson (written communication, 1986) for a "characteristic" Wasatch earthquake (rupture length = 32 km, slip = 2.5 m, M_0 = 4.57 E+26 dyne-cm, **M** = 7.1), for an earthquake with a 10 percent exceedance in 250 years, and for an earthquake with a 10 percent exceedance in 50 years. It can be seen that a displacement of 10 cm corresponds to a critical acceleration of 0.125 g for the Wasatch earthquake and that a displacement of 2 cm corresponds to 0.25 g. These values also correspond to exceedance probabilities of 50 percent and 10 percent for the 100-year time period in northern Utah (Figure 3). Consequently, it appears that the limiting equilibrium analysis yields results similar to those expected from a displacement analysis.

3. The size of the area potentially affected by seismically induced landslides was evaluated in the manner described by Wilson and Keefer (1985) on the basis of Arias Intensity and type of landlside. They found that the threshold of failure for coherent slides corresponded to an Arias Intensity of about 0.5 m/s and disrupted slides and falls corresponded to an Arias Intensity of about 0.15 m/s. A relationship among Arias Intensity (Ia), distance (r), and moment magnitude (**M**) was developed by Wilson and Keefer (1985). They further developed a corrected Arias Intensity (Ia*) to permit assessment of the attenuation of Ia for specific earthquake magnitudes.

The expected "characteristic" Wasatch earthquake is anticipated to be **M** = 7.1. So the relationships for corrected Arias Intensity published by Wilson and Keefer (1985) were adjusted to **M** = 7.1 as follows to yield mean values of Ia*:

$$\log(Ia^*) = -3.8 + \mathbf{M} - 2 \log r^*$$

where $r^* = (r^2 + \Delta^2)^{1/2}$, r = surface distance in km from the epicenter to the site, and Δ = focal depth in km. For strike -slip faults, r can be taken as the surface distance from the fault rupture trace. This relationship for **M** = 7.1 and Δ = 15 km is shown on Figure 5. The mean value of distance from the seismic source for Ia* = 0.5 m/s is about 60 km. The mean value of distance for Ia* = 0.15 m/s is about 110 km.

Using these results and the historic limit of seismically induced landslides published by Wilson and Keefer (1985), maps were prepared for northern Utah showing the potential area that might be affected by 1) coherent slides, and 2) disrupted slides and falls. For coherent slides generated by **M** = 7.1 earthquakes, the mean distance from the seismic source is about 60 km and the historic limit is about 140 km (Wilson and Keefer, 1985). For disrupted slides and falls generated by **M** = 7.1 earthquakes, the mean distance from the seismic source is about 110 km and the historic limit is about 175 km. These distances were applied to five segments of the Wasatch fault from Brigham City to Nephi and indicate that most of the populated area of Utah is exposed to substantial risk of damage due to seismically induced landslides.

4. Digital terrain data are not available for significant parts of the study area, particularly in the north. Consequently, we are manually evaluating the topography for evaluation of the critical acceleration. Geotechnical parameters are being evaluated on the basis of available subsurface data collected during liquefaction potential evaluations in northern Utah (Anderson et al., 1982, 1986).

During the initial attempts to use digital data, a technique was devised to flag those areas of slope where "infinite slope" geometry was not appropriate. The down-slope curvature (ß) was examined for concavity or convexity exceeding 15°, that is for slope geometry conditions other than$165° < ß < 195°$ (Figure 6). Areas flagged by this technique are examined for conditions that might make circular or irregular failure surfaces more appropriate.

REFERENCES

Anderson, L.R., Keaton, J.R., Aubry, Keven, and Ellis, S.J., 1982, Liquefaction potential map for Davis County, Utah: Utah State University and Dames & Moore, final report to the U.S. Geological Survey, Earthquake Hazards Reduction Program, Contract 14-08-0001-19127, 49 p.

Anderson, L.R., Keaton, J.R., Spitzley, J.E., and Allen, A.C., 1986, Liquefaction potential map for Salt Lake County, Utah: Utah State University and Dames & Moore, final report to the U.S. Geological Survey, Earthquake Hazards Reduction Program, Contract 14-08-0001-19910, 48 p.

Anderson, L.R., Keaton, J.R., and Bischoff, J.E., 1986, Liquefaction potential map for Utah County, Utah: Utah State University and Dames & Moore, final report to the U.S. Geological Survey, Earthquake Hazards Reduction Program, Contract 14-08-0001-21359, 48 p.

Keefer, D.K., 1984, Landslides caused by earthquakes: Geological Society of America Bulletin, Vol. 95, p.406 - 421.

Wieczorek, G.F., Wilson, R.C., and Harp, E.L., 1985, Map showing slope stability during earthquakes in San Mateo County, California: U.S. Geological Survey Map I-1257-E.

Wilson, R.C., and Keefer, D.K., 1985, Predicting areal limits of earthquake-induced landsliding: *in* Ziony, J.I., (editor), Evaluating earthquake hazards in the Los Angeles Region - An earth-science perspective: U.S. Geological Survey Professional Paper 1360, p. 317 -345.

Wilson, R.C., 1986, Geologist, U.S. Geological Survey, Geologic Risk Assessment Branch, Menlo Park, California, written communication July 31, 1986.

Table 1. Earthquake-induced ground failure in Utah, 1850 - 1985. Magnitude values for early earthquakes were computed from Modified Mercalli Intensity values using the conventional relationship from Gutenberg and Richter (M = 2 I/3 + 1); in some cases, magnitude values were reported by Arabasz, Smith, and Richins (1979) or U.S. Earthquakes through 1980.

EARTHQUAKE	DATE	INTENSITY/ MAGNITUDE	FELT AREA (SQ. MI)	REPORTED GROUND FAILURE (a)
Kelton	27 Dec1880	III 4.3	1000	Mud flats on the lake bear marks of a tidal wave. (Ref. 1).
Richfield	13 Nov1901	IX 7	50,000	In the mountains between Beaver and Marysvale, extensive rockslides occurred and nearly blocked the roads in Bullion and Cottonwood Canyons. Water and white sand were ejected from the Sevier River bottom near Richfield. (Ref. 1).
Elsinore	1 Oct1921	VIII 6.3	1000	Large rockfalls were caused on both sides of the valley. (Ref. 1)
Kosmo	12 Mar 1934	VIII 6.6	170,000	Several hundred tons of rock slid down hills at Monument Rock. Rock slide near Snowville. Rock fall in quarry at Aragonite. Several hundred cubic yards of rock and earth fell in quarry at Lakeside. (Ref. 2)
Southwest Utah	1 Nov 1949	VI 4.7	700	Small landslide from cliffs on east side of Tuweep Valley, Arizona. (Ref. 3).
Kanab	21 July 1959	5.5 VI	8000	Rockslide at Mather Point in Grand Canyon, Arizona. (Ref. 3).
Logan	30 Aug 1962 VII	5.7	65,000	West of Lewiston on Bear River, several mudslides covering several acres. At Cornish, a mudslide cut through an irrigation canal and water flooded low lands. Fallen rock observed from mouth of Logan Canyon to Curd Canyon. Falling rock at mouth of Logan Canyon broke water flume causing mudslide which blocked Highway 89. At Fairview, Idaho, two large areas of land broke loose to depths of 5 feet and slide 300 yards down a hill. (Ref. 3).

Table 1 (Continued). Earthquake-induced ground failure in Utah1850 - 1985.

EARTHQUAKE	DATE	INTENSITY/ MAGNITUDE	FELT AREA (SQ. MI)	REPORTED GROUND FAILURE
Magna	5 Sept 1962	5.1 VI	9000	At Bingham Canyon, practically all terraces on and in pit area showed small slides of unstable material. (Ref. 3).
Central Utah	4 Oct 1967	5.2 VII	15,000	At Junction City, large boulders fell from many mountains, some boulders rolled onto highways. At Anabella, people could hear rocks sliding in mountains. At Joseph, rock slides occurred in canyons. Rockslide 5 miles south of Sevier. (Ref. 3).
Pocatello Valley, ID	28 Mar 1975	6.1 VIII	61,760	Snow avalanches northeast of Pocatello Valley. (Ref. 3).
Moon Lake	30 Sept 1977	5.1 VI	7,700	Ground cracks interpreted to be landslide on alluvial fan and rock falls within 1 mile of epicenter. (Ref. 4).
Duchesne	11 Oct 1977	4.8 V	?	Small rock falls noted by USGS personnel at mouth of water diversion tunnel east of Grandaddy Mountain. (Ref. 3).

(a) References listed are as follows:
Ref. 1: Williams and Tapper, 1953
Ref. 2: U.S. Earthquakes, 1934
Ref. 3: Earthquake History of the United States through 1980
Ref. 4: Arabasz, Smith and Richins, 1979

Table 2. Magnitude- area and magnitude-distance relationships for reported earthquake-induced ground failure in Utah, 1850 - 1985.

EARTHQUAKE	DATE	MAGNITUDE	MAXIMUM DISTANCE (km)	ESTIMATED AREA AFFECTED BY FAILURES (square km)
Kelton	17 July 1880	4.3 [a]	5(?)	5(?)
Richfield	14 Nov 1901	7 [a]	10	115
Elsinore	1 Oct 1921	6.3 [a]	5	60
Kosmo	12 Mar 1934	6.6 [b]	110	1430
SW Utah	2 Nov 1949	4.7 [b]	10	90
Kanab	21 July 1959	5.5 [b]	100	100 (?) [e]
Logan	30 Aug 1962	5.7 [c]	20	380
Magna	5 Sept 1962	5.1 [c]	25	160
Central Utah	4 Oct 1967	5.2 [c]	30	400
Pocatello Val.	28 Mar 1975	6.1 [c]	10	25
Moon Lake	30 Sept 1977	5.1 [c]	6.4	25
Duchesne	11 Oct 1977	4.8 [d]	14.5	60

---

[a] Magnitude values from Arabasz and others (1979) based on maximum Intensity.

[b] Magnitude values from Arabasz and others (1979) based on Pasadena determinations.

[c] Magnitude values from Arabasz and others (1979) based on original Wood-Anderson seismograms.

[d] Magnitude value from Earthquake History of the United States through 1980.

[e] A single rockfall occurrence was reported at Mather Point in the Grand Canyon, about 100 km away from the epicenter and on a very susceptible slope.

Table 3. Criteria for assigning seismic slope failure potential based on comparison of the critical acceleration to the 100-year 50 percent and 10 percent probability accelerations and ground water conditions.

SEISMIC SLOPE FAILURE POTENTIAL	CRITICAL ACCELERATION CONDITIONS FOR A 100-YEAR PERIOD		
	DRY SLOPE CONDITIONS		WET SLOPE CONDITIONS
High Potential	$A_{c(dry)} \leq A_{50\%}$		-----
Moderate Potential	$A_{50\%} < A_{c(dry)} < A_{10\%}$	or	$A_{c(wet)} \leq A_{50\%}$
Low Potential	$A_{10\%} < A_{c(dry)}$	or	$A_{50\%} < A_{c(wet)} < A_{10\%}$
Very Low Potential	-----		$A_{10\%} \leq A_{c(wet)}$

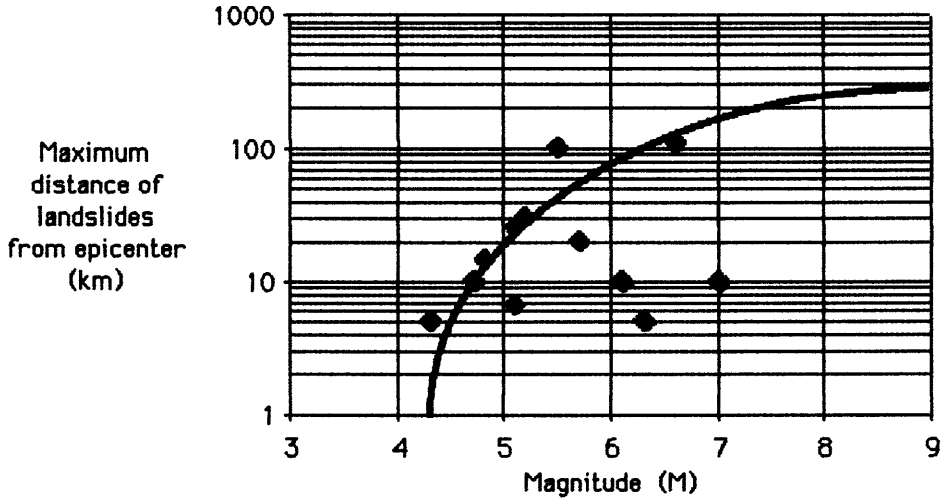

Figure 1. Maximum distance from earthquake epicentral area to landslides of any type due to earthquakes in Utah, 1850 - 1985. Curve represents the historical limit of disrupted slides and falls from Wilson and Keefer (1985).

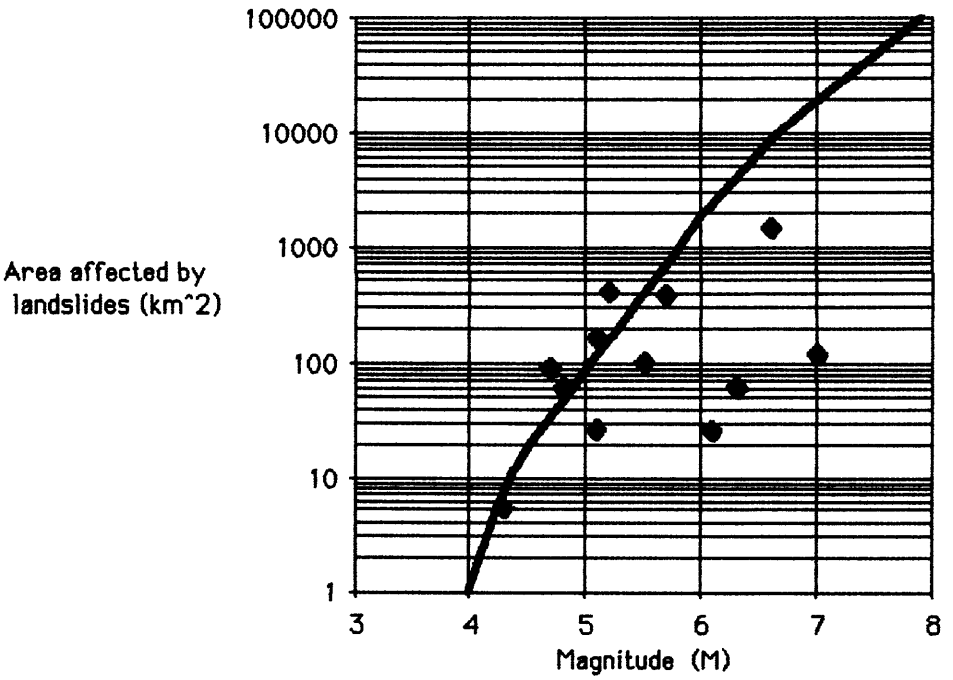

Figure 2. Approximate maximum areal extent of seismically induced landslides in Utah, 1850 - 1985. Curve represents historic limit of area affected by seismic landslides from Keefer (1984).

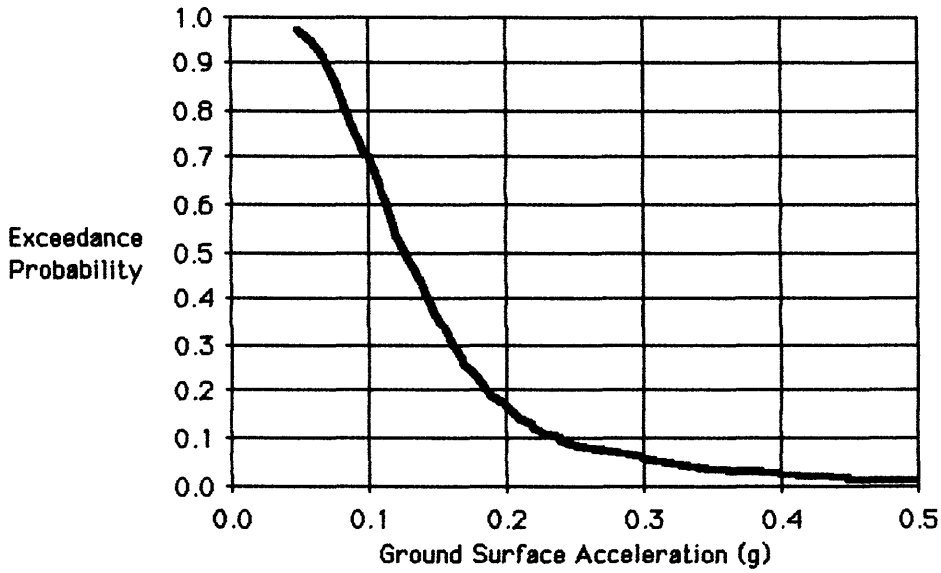

Figure 3. Exceedance probabilities of peak ground acceleration for a 100-year time period representative for the northern Utah area (from Anderson et al., 1982, 1986).

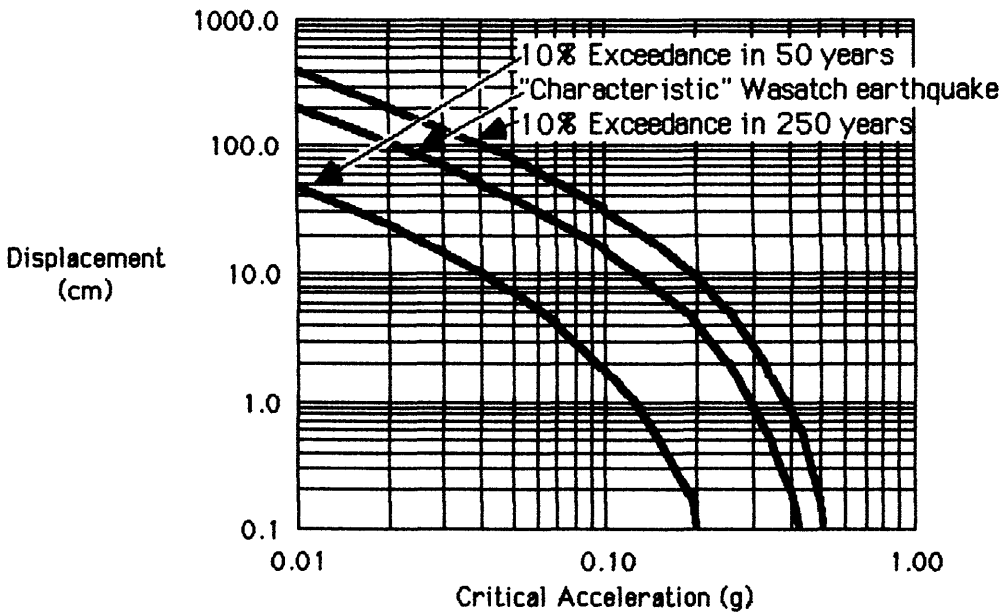

Figure 4. Computed displacement versus critical acceleration for earthquake with 10 percent exceedance probabilites during 50- and 250-year time periods and for the "characteristic" Wasatch earthquake. Unpublished data provided by R.C. Wilson (written communication, 1986).

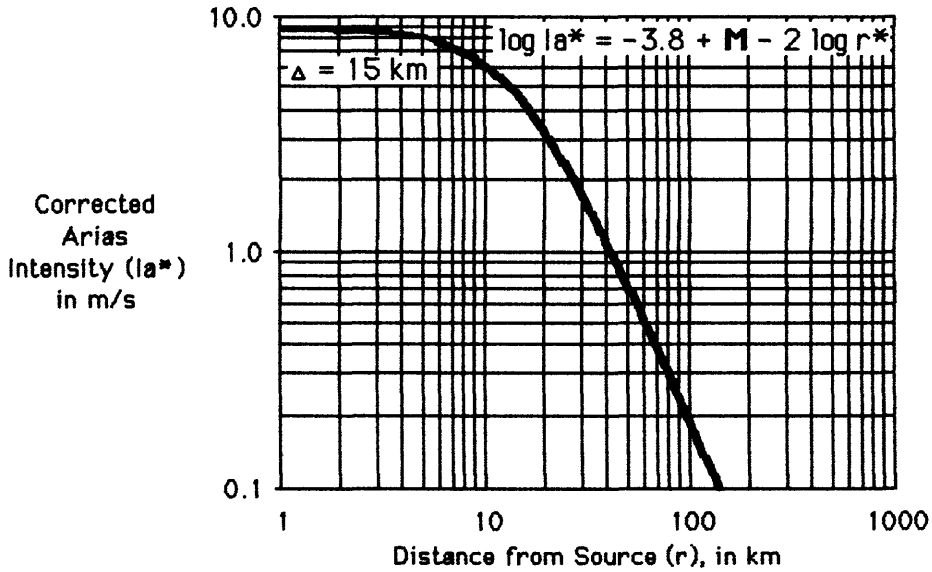

Figure 5. Corrected Arias Intensity versus distance from the seismic source area. The values of Arias Intensity were taken from Wilson and Keefer (1985, Table 47) and adjusted to be equivalent to a M = 7.1 event at the same source distance on the basis of an assumed log-linear relationship between magnitude and Arias Intensity for a given distance. Δ = focal depth; $r^* = (r^2 + \Delta^2)^{1/2}$.

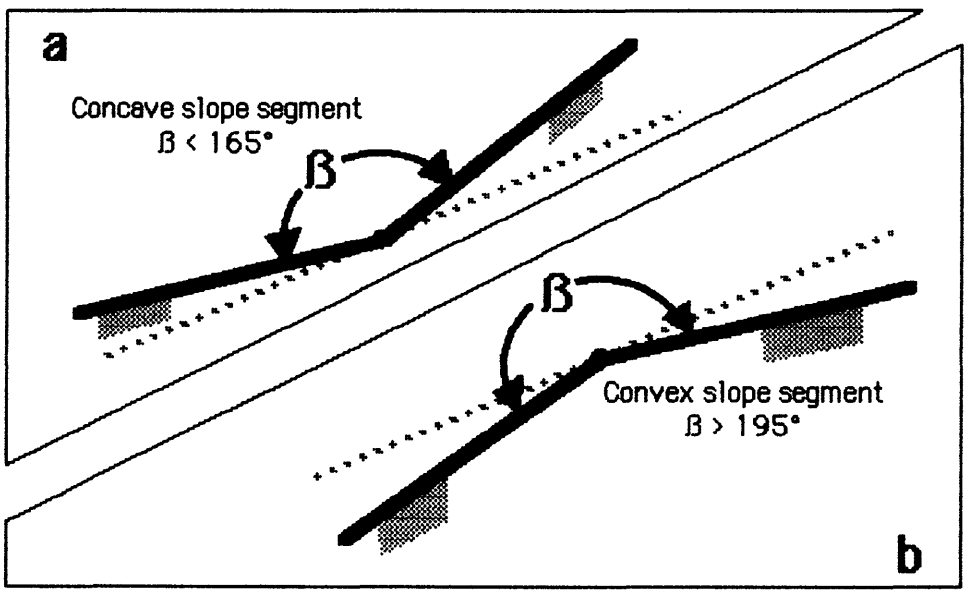

Figure 6. Limiting slope configurations for applicability of infinite slope geometry for pseudostatic stability analyses. Infinite slope geometry was considered to be appropriate for slopes within 15° of planar. **a** shows the concave condition and **b** shows the convex condition.

POTENTIAL CONSEQUENCES OF EARTHQUAKE-INDUCED TECTONIC DEFORMATION ALONG THE WASATCH FAULT, NORTH-CENTRAL UTAH

14-08-0001-G1174

Jeffrey R. Keaton
Department of Civil Engineering
Utah State University, Logan, Utah 84322-4100
Present address: Center for Engineering Geosciences
Department of Geology, Texas A&M University
College Station, Texas 77843-3115

INVESTIGATIONS

Regional tectonic deformation is an earthquake hazard known to accompany earthquakes on normal slip faults (Bonilla, 1982). Subsidence was observed at Hebgen Lake, MT due to an earthquake in 1959 (Myers and Hamilton, 1964) and subsidence and uplift were observed at Borah Peak, ID due to an earthquake in 1983 (Stein and Barrientos, 1985). Attention was drawn to possible lake-margin flooding along the Wasatch Front by Dr. Robert B. Smith of the University of Utah in an Earthquake Workshop sponsored by the U.S. Geological Survey and held in Salt Lake City in August, 1984.

The Wasatch fault has long been considered capable of generating major earthquakes. Recent studies suggest that typical surface offsets are on the order of 2 m and that the Wasatch fault consists of 10 independent segments, each about 35 km long. The objective of this research was to apply the profile of subsidence observed following the 1959 Hebgen Lake earthquake to the Wasatch fault from Brigham City to Nephi (virtually the entire populated length) and assess 1) potential lake margin inundation due to differing lake elevations at the time of the earthquake, 2) potential ponding of shallow ground water, and 3) potential damage to waste-water treatment plants due to tilting of the ground surface.

During the initial phases of investigation, it became clear that the ±6.6 m of observed fault offset that accompanied the 1959 earthquake greatly exceeded the ±2 m expected along the Wasatch fault. Consequently, an additional research objective was added to estimate the profile of subsidence using elastic deformation theory and the source parameters appropriate for an anticipated major earthquake on the Wasatch fault. Potential lake margin flooding, ponding of shallow ground water, and ground surface tilting were then assessed in the same manner as for the 1959 earthquake effects.

RESULTS

1. The profile of maximum subsidence observed in 1959 at Hebgen Lake (Figure 1) can be described mathematically by a fifth-order polynomial approximation:

$$S = - 0.0008\ D^5 + 0.03\ D^4 - 0.42\ D^3 + 2.50\ D^2 - 3.10\ D - 19.00$$

where S is tectonic subsidence in feet and D is distance from the fault trace in miles. This expression of $S = f(D)$ is valid for $0 \leq D \leq 10$ miles. The slope of the subsidence profile (Figure 2) is described by the first derivative:

$$dS/dD = - 0.004\ D^4 + 0.12\ D^3 - 1.26\ D^2 + 5.00\ D - 3.10.$$

The maximum slope of the subsidence profile occurs at a distance of 3.3 miles from the fault and has a magnitude of 3.5 feet/mile (0.07 percent).

This model of tectonic deformation was applied to the Brigham City, the Ogden, the Salt Lake, the Provo, and the Nephi segments of the Wasatch fault. Contours of subsidence (5-foot contour interval) were drawn on large format maps at scales of 1:125,000 north of 40° 30' North Latitude (about the southern boundary of Salt Lake County) and scales of 1:100,000 south of 40° 30'. Lake margin flooding was evaluated for the Great Salt Lake at potential altitudes of 4200, 4205, 4210, and 4215 feet. Utah Lake was evaluated for altitudes of 4485, 4490, and 4495 feet. Mona Reservoir was evaluated for its normal operating altitude of 4877 feet.

Potential ponding of shallow ground water was evaluated for those areas where the depth to ground water was considered to be less than 10 feet and the potential subsidence was considered to be greater than 10 feet. The depth to ground water was taken from liquefaction studies by Anderson and Keaton (1982, 1986). Tilt of the ground surface was evaluated at locations of waste water treatment plants and shown with an arrow indicating direction of tilt and a number representing magnitude of tilt in feet/mile. This model suggests that virtually all of the waste water treatment plants from Brigham City to Nephi will be adversely affected by lake margin flooding, shallow ground water ponding, tilting, or a combination of tectonic deformation effects.

2. Surface offset along segments of the Wasatch fault are not expected to exceed ± 2 m. Therefore, to evaluate potential consequences of tectonic deformation along the Wasatch Front, appropriate source parameters were used in a model of elastic dislocation theory developed by Okada (1985). The geometry of the source model is shown on Figure 3. The mathematical model consists of a surface integral evaluated over the rupture area of a planar fault. This elastic model was tested using source parameters for the Borah Peak earthquake summarized by Doser (1985) and conventional elastic constants (shear modulus = Lamé's constant = 3.3 E+11 dyne/cm^2). The profile of deformation (subsidence and uplift) predicted by this model closely approximated the observed deformation reported by Stein and Barrientos (1985).

The source parameters selected to represent an expected earthquake on a segment of the Wasatch fault consisted of a focal depth of 15 km (9.3 mi), a rupture length of 35 km (22 mi), a dip of 60°, and an average slip on the fault of 2.6 m (8.5 ft). These source parameters correspond to a seismic moment of 5.2 E+26 dyne-cm and an earthquake magnitude of $\mathbf{M_W}$ = 7.1 ($M_S \approx$ 7.5) which appears appropriate for segments of the Wasatch fault. The profile of maximum deformation (Figure 4) is similar in shape to the 1959 profile for the region extending out about 10 miles from the surface fault rupture. Tilt of the ground surface (Figure 5) was calculated using a finite difference approximation of the deformation profile evaluated at 0.5-mile intervals.

The results of the numerical model of tectonic deformation were applied to segments of the Wasatch fault in the same manner as described above for the 1959 earthquake. Lake margin flooding was evaluated for the same water surface altitudes indicated above. Shallow ground water ponding was considered possible in those areas where the depth to ground water was less than 10 feet and potential subsidence was greater than 3 feet. This model also suggests that many of the waste water treatment plants from Brigham City to Nephi may be adversely affected by lake margin flooding, shallow ground water ponding, tilting, or a combination of these effects.

Potential tectonic deformation appears to be an extremely difficult hazard with which to deal because it is regional. The probability that tectonic deformation will occur is directly related to the probability of slip on specific fault segments. Many existing facilities appear to be located in positions of relatively high risk of damage. Land use decisions for proposed facilities within areas of potential lake margin flooding or shallow ground water ponding are likely to be politically unpopular. Some sensitive facilities may be able to accomodate tilt if they can be releveled.

REFERENCES

Anderson, L.R., Keaton, J.R., Aubry, Keven, and Ellis, S.J., 1982, Liquefaction potential map for Davis County, Utah: Utah State University and Dames & Moore, final report to the U.S. Geological Survey, Earthquake Hazards Reduction Program, Contract 14-08-0001-19127, 49 p.

Anderson, L.R., Keaton, J.R., Spitzley, J.E., and Allen, A.C., 1986, Liquefaction potential map for Salt Lake County, Utah: Utah State University and Dames & Moore, final report to the U.S. Geological Survey, Earthquake Hazards Reduction Program, Contract 14-08-0001-19910, 48 p.

Anderson, L.R., Keaton, J.R., and Bischoff, J.E., 1986, Liquefaction potential map for Utah County, Utah: Utah State University and Dames & Moore, final report to the U.S. Geological Survey, Earthquake Hazards Reduction Program, Contract 14-08-0001-21359, 48 p.

Bonilla, M.G., 1982, Evaluation of potential surface faulting and other tectonic deformation: U.S. Geological Survey Open-file Report 82-732, 88 p.

Doser, D.I., 1985, The 1983 Borah Peak, Idaho and 1959 Hebgen Lake, Montana earthquakes: Models for normal fault earthquakes in the Intermountain Seismic Belt: U.S. Geological Survey Open-file Report 85-290, p. 368 - 384.

Myers, W.B., and Hamilton, Warren, 1964, Deformation accompanying the Hebgen Lake earthquake of August 17, 1959: U.S. Geological Survey Professional Paper 435-I, p. 55 - 98.

Okada, Yoshimitsu, 1985, Surface deformation due to shear and tensile faults in a half-space: Seismological Society of America Bulletin, Vol. 75, No. 4, p. 1135-1154.

Stein, R.S., and Barrientos, S.E., 1985, The 1983 Borah Peak, Idaho, earthquake: Geodetic evidence for deep rupture on a planar fault: U.S. Geological Survey Open-file Report 85-290, p. 459 - 484.

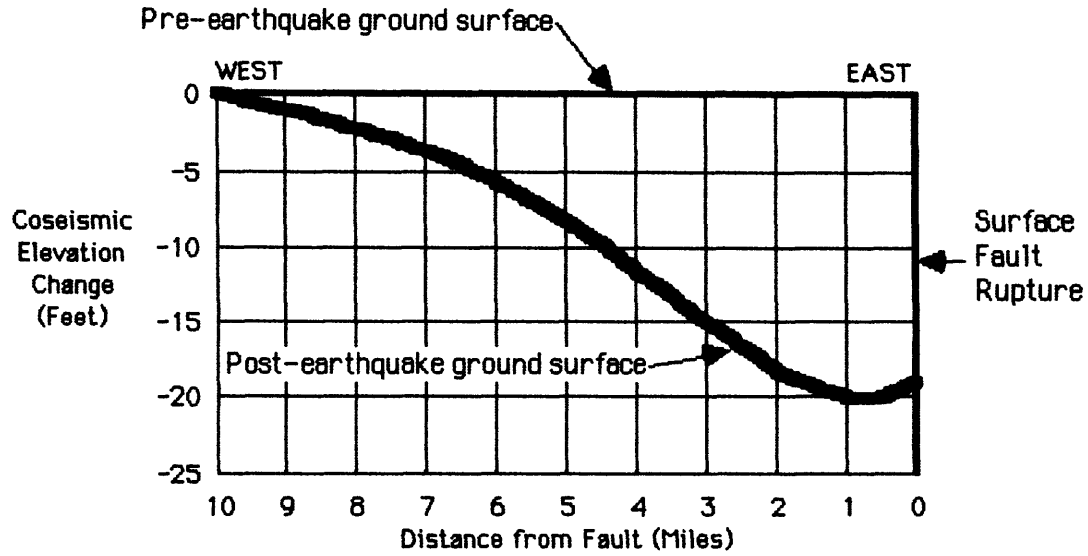

Figure 1. Profile of maximum coseismic elevation change observed at Hebgen Lake, MT in1959 (after Myers and Hamilton, 1964).

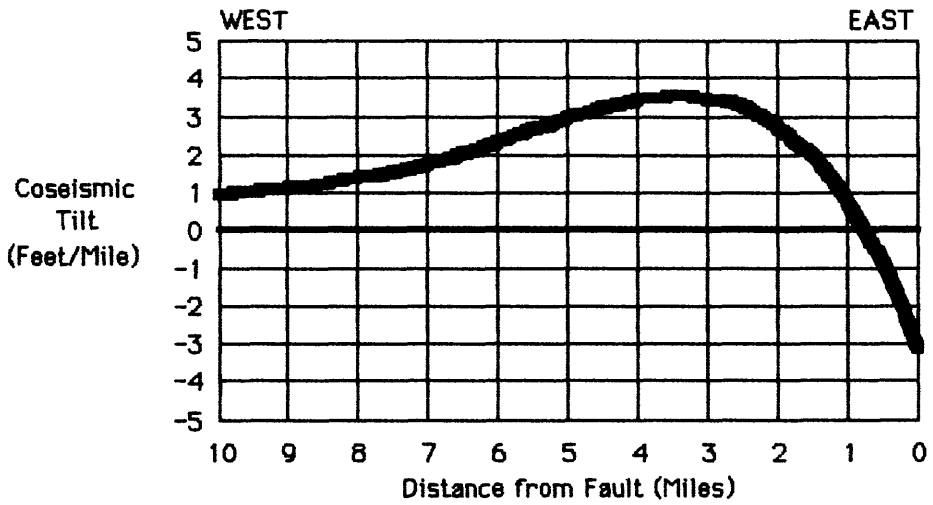

Figure 2. Coseismic tilt calculated from the profile of maximum elevation change observed by Myers and Hamilton (1964) at Hebgen Lake, MT due to the 1959 earthquake.

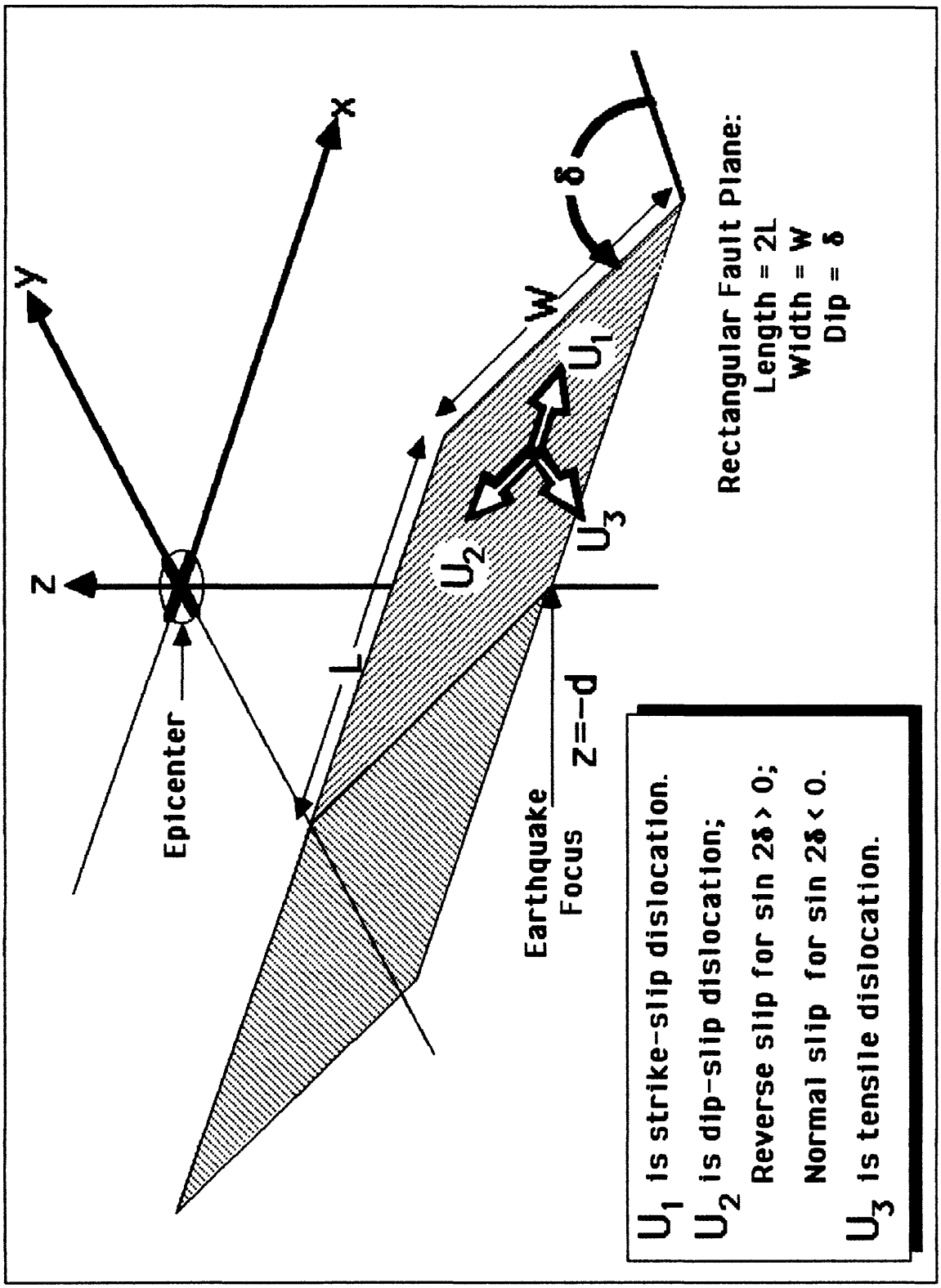

Figure 3. Geometry of the source model for Okada's (1985) elastic dislocation theory used to calculate surface deformation due to fault slip in a half-space.

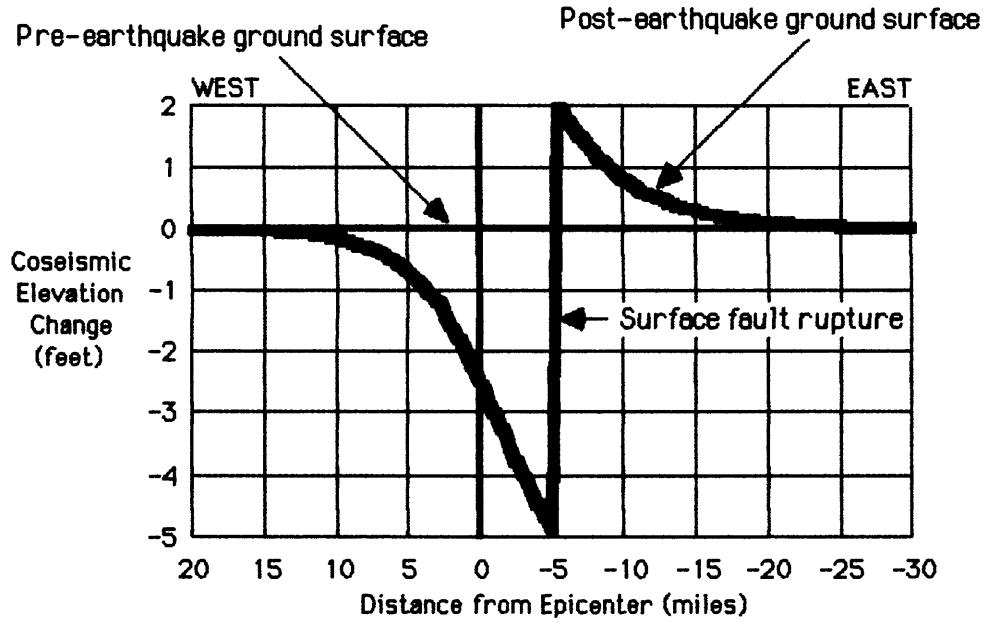

Figure 4. Profile of maximum coseismic elevation change predicted from elastic dislocation theory due to an expected major earthquake on a segment of the Wasatch fault in north-central Utah. The coordinate system for the dislocation model is shown in Figure 3 and has its origin at the epicenter.

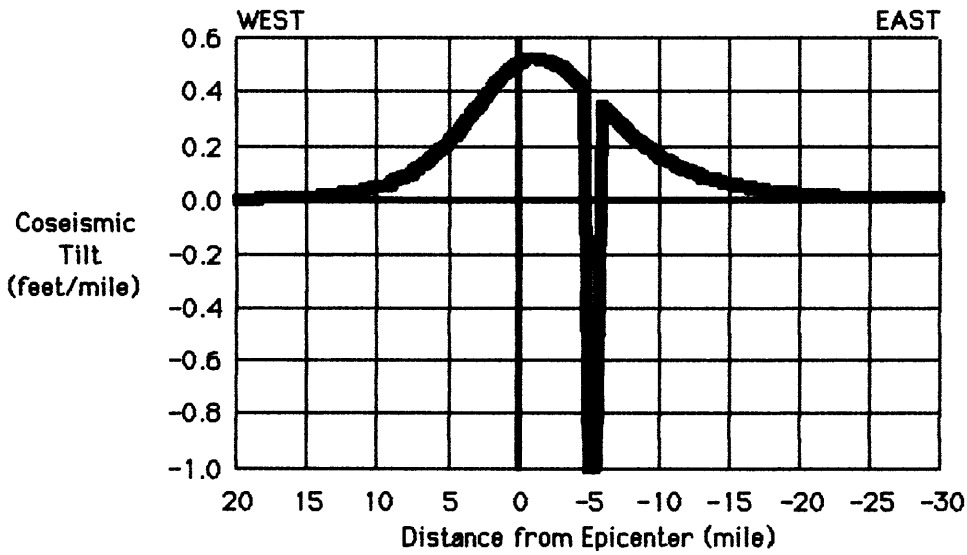

Figure 5. Coseismic tilt calculated from elevation change curve developed from elastic dislocation model using source parameters appropriate for an expected earthquake on one of the segments of the Wasatch fault in north-central Utah.

Urban Hazards Seismic Field Investigations and the Study of the Effects of Site Geology on Ground Shaking

9950-01919

Kenneth W. King and Arthur C. Tarr
Branch of Engineering Geology and Tectonics
U.S. Geological Survey
Denver Federal Center, MS 966
Denver, CO 80225
(303) 236-1591

Investigations

The general objectives of this project are: (1) to improve the understanding of how the shallow underlying geology affects ground shaking, and (2) to develop an integrated system from seismic field data to final report for hazards investigations. The specific objectives of this reporting period are: (1) to complete this project's chapter of a USGS Professional Paper on the urban hazards of the Wasatch area, (2) to examine the feasibility of correlating site response data with the geotechnical data derived from high-resolution shallow seismic reflection profiles, (3) to complete the seismic hazards report on the village of Paguate, N.M., and (4) to begin the urban hazards field investigation of the Puget Sound area.

Ground motions induced by an NTS nuclear test which were recorded at eight sites in Salt Lake City and five sites in the Provo area were analyzed. Detailed high-resolution shallow-reflection profiles were made at ten of the site-response sites. The results of the data analyzed are included in the USGS Wasatch Professional Paper.

The seismic field investigation at the Laguna Indian Reservation is complete. The program investigated the cause of damage to the structures in the village of Paguate, N.M. The project called for a damage investigation of 240 structures, design of a damage scale for adobe-type structures, study of attenuation and ground response by using down-hole blasts (outside the village) as the energy source, and establishing the periods and dampings of approximately 50 of the structures. An administrative report has been submitted to the Bureau of Indian Affairs. A USGS report will be published at a future date.

An urban hazards seismic field investigation was begun in the Puget Sound area. Induced seismic motions from quarry blasts and ambient background noise were recorded at eight sites in west Seattle and four sites in Olympia, Washington. Refraction profiles were made at all of the west Seattle sites.

Results

1. The new site response data and analysis methods on the Salt Lake-Provo data agree very closely with the report of Hays and King (1982). A chapter on the site response, shallow reflections, and other geotechnical data was submitted to the USGS Wasatch Professional Paper.

2. The high-resolution reflection profiling using shear waves has shown some success. However, more research will be needed before the method will be used on routine investigations. Several improvements have been made on the shallow high-resolution reflection field methods and equipment. New high pass (120-240 Hz) filters have been installed and the energy source (shotgun) has been improved. A successful method has been developed for analyzing the shallow reflection data. An abstract was submitted to GSA entitled, "Detection of Mined Coal Cavities Near Boulder, Colorado, Using High-Resolution Seismic Reflection Methods", from the reflection program.

3. The site response to shallow reflection correlation program is on hold until the geotechnical data from several new boreholes in the Wasatch area are available.

4. The Wasatch strong-motion network continued in stand-by ready mode. The equipment was inspected by Menlo Park personnel. The underlaying unconsolidated sediments were profiled using the reflection methods.

5. The DR-200 portable seismic system was recalibrated at the Sandia Laboratory. The system proved an adequate system for general and engineering seismic studies characterized by low internal noise.

6. The DR-200 software to the VAX is operating smoothly. Improvements are being incorporated as the methods evolve. The portable field computer hardware is installed. Software and methods are being developed for field applications. The reflection/refraction calculations are running but the graphics will need more development. A report is in progress.

7. Base or standard "rock" sites were located and defined by refraction methods in the urban areas of west Seattle and Olympia. The sonic velocity of the "rock" exceeds 7,500 ft/sec and were, therefore, considered adequate for response comparisons to other urban sites in the area. Preliminary analysis of the ground motions recorded at Seattle and Olympia indicate that the quarry blasts input energy source will give a 2 to 1 signal-to-noise ratio when the events are shot in the mid-afternoon. The data showed good energy in the 0.5 to 10 Hz bandwidth. Analysis of the ambient seismic background indicate that reflection energy in the 80 to 250 Hz bandwidth should give good results as the large amplitude ambient background and the surface waves from an impact source is generally in the 15-70-Hz bandwidth.

Reports

Carver, David, Cunningham, David, and King, K.W., 1986, Calibration and acceptance testing of the DR-200 digital seismograph with S-6000 and L-4C seismometers: U.S. Geological Survey Open-File Report 86-340.

King, K.W., and Algermissen, S.T., 1986, Engineering seismic investigation of the village of Paguate, New Mexico: U.S. Geological Survey Administrative Report to Bureau of Indian Affairs.

King, K.W., Williams, R.A., and Carver, David, A relative ground response study in east Salt Lake City and areas of Springville-Spanish Fork, Utah: U.S. Geological Survey Professional Paper (in press).

Williams, R.A., and King, K.W., 1986, Detection of mined coal cavities near Boulder, Colorado, using high-resolution seismic reflection methods [abs.]: Geological Society of America (in press).

Williams, R.A., and King, K.W., 1986, Application of spiking and predictive deconvolution to short record length reflection data: U.S. Geological Survey Open-File Report 86-299.

Determining Landslide Ages and Recurrence Intervals

9950-03789

Richard F. Madole
Branch of Geologic Risk Assessment
U.S. Geological Survey
P. O. Box 25046, MS 966
Denver, Colorado 80225
(303) 236-1617

Investigations

Fieldwork during 1984 identified three processes that provide a basis for determining landslide recurrence intervals. The processes are the translocation of pond deposits, the formation of lateral ridges, and landslide damming of lakes. All three processes record slope movements geomorphically and stratigraphically and produce deposits that commonly contain or bury ^{14}C-datable materials. Fieldwork during 1985 concentrated on lateral ridges and the deposits of landslide-dammed lakes. Fieldwork during 1986 focused on translocated pond deposits.

Results

Translocated pond deposits make it possible to identify and date discrete landslide events within landslide or flow deposits that have complex histories involving several episodes of movement. These pond deposits have been moved downslope from the topographic depressions where they accumulated by flow or slide to sites where they are exposed to subaerial weathering and soil formation. Translocated pond deposits generally can be easily distinguished from slope-movement deposits. Pond deposits tend to be fine grained and lack abundant clasts larger than 2 mm, and are commonly stratified and fossiliferous. Slope-movement deposits contain a large range of sediment sizes, including abundant clasts of cobble and boulder size, and generally lack stratification.

Soil development is widely used as a relative-dating technique for a variety of surficial deposits. However, soil studies tend to be least useful for dating landslide deposits, because most kinds of slope movements do not completely destroy pre-existing soils. Soils that are formed in translocated pond deposits are a special case. They are perhaps the only soils on landslide deposits that can safely be assumed to have formed after a landslide. Moreover, translocated pond deposits commonly contain ^{14}C-datable material that make it possible to determine the beginning and duration of soil formation. Knowing the numerical age of soils of two or more different ages allows relative soil development to be used to estimate the numerical age for deposits that do not contain ^{14}C-datable material.

In June 1974, a large slope failure was initiated on the Manti landslide in Sanpete County, Utah. By June 1975, deposits that had accumulated in a small pond located a little more than half-way up the slide path had been translocated about 150 m downslide. Since then, a new pond has formed, approximately in the same location as before, and the deposits of the former pond are draped over a topographically high area. Older pond deposits extend from near the edge of the recently displaced pond sediments downslide for a few hundred meters. Differences in soil profile development indicate that the older pond deposits are of three different ages (referred to below as deposits 1, 2, and 3, from oldest to youngest), the middle one of which is correlated with a major slope movement that occurred about 2000 B.P. (reported in previous semiannual report).

The translocated pond deposit of the 1974 landslide shows no evidence of soil formation. The next older pond deposit (deposit 3), which extends for at least 80-90 m in a downslide direction, has a weakly developed soil profile consisting of A/2A/2C horizons. A thin (2-5 cm) surface unit of eolian sediment is widespread in the area and is the reason that two parent materials are denoted by arabic numerals in this and other profiles described here. The two A horizons have a combined thickness that ranges from 3 to 10 cm, but is typically 6-7 cm. Because the cover of eolian sediment is uneven in distribution and thickness and the soil is thin and weakly developed, disturbance by tree roots causes much variation in profile thickness. The next older pond deposit (deposit 2), which extends at least 50-75 m downslide from deposit 3 and is thought to have been exposed to subaerial weathering for about 2000 years, has a soil profile consisting of A/2A/2AC/2C horizons. The combined thickness of the two A horizons is generally 9-11 cm and and they are underlain by a well-developed AC horizon that is about 10 cm thick. The oldest translocated pond deposit (deposit 1) extends for at least 75 m downslide from pond deposit 2 and differs from it in having an A horizon that is as much as 18-22 cm thick.

Relicts of late Pleistocene soils were not observed in deposits of the Manti slide, although they are present on other deposits in the area. Late Pleistocene soils are characterized by having weakly to moderately developed B horizons. All soils in deposits within the slide path, on lateral ridges, and in alluvial and lacustrine deposits produced by landslide damming lack B horizons and are believed to be Holocene, chiefly late Holocene. Observations of soils on the Manti slide lead to the following conclusions: (1) slope movement was so extensive at some time during the Holocene, probably the early part, that pre-existing soils were destroyed, (2) at some time during the Holocene, probably the middle part, a lengthy interval of stability allowed a thick (commonly 30 cm) A/C or A/AC/C profile to develop over most of the slide area, and (3) several large slope movements have occurred during the past 3000-4000 years (as many as six according to the ^{14}C chronology discussed in a previous semiannual report), but none obliterated the 30-cm-thick soil, except locally.

The most complete record of slope movements is obtained by combining the data compiled from studies of translocated pond deposits, lateral ridges, and deposits caused by landslide damming. Differences in soil development can be used to correlate the deposits and landforms recorded by these different processes. Soils developed on the pond deposits serve as standards because soil formation began on them at or very soon after the time of slope movement, and these soils can be assumed not to include relict profiles. Translocated pond deposits form a type of soil chronosequence (a series of soils for which all soil-forming factors other than time--climate, fauna and flora, topography, and parent material--are more or less the same) not previously described in the literature.

LATE QUATERNARY TECTONICS AND EARTHQUAKE HAZARD IN CACHE VALLEY, UTAH

14-08-001-G1091

James McCalpin
Department of Geology
Utah State University
Logan, UT 84322-0705

INVESTIGATIONS

Cache Valley is a major intermontane graben east of the Wasatch Fault which contains evidence of late Quaternary faulting. The valley population of 60,000 is clustered along the eastern valley margin close to the East Cache Fault which has experienced two $M_L>7$ paleo-earthquakes (Swan et al, 1983) since the occupation of the Bonneville Shoreline (roughly 15.5 - 17 ka). The objectives of this study are: 1) To map Quaternary geology and fault features along the fault zone at 1:50,000 from Avon, UT to Franklin, ID; 2) To determine if the Bonneville Shoreline in the area of the East Cache Fault is tectonically deformed and 3) To see if late Quaternary displacement patterns are similar to longer term patterns as deduced from tectonic geomorphology of the range front.

RESULTS

1. Quaternary geologic mapping on 1:20,000 - scale aerial photographs was transferred to 1:24,000 topographic bases for portions of the Paradise, Logan, Smithfield, and Richmond 7 1/2' quadrangles which straddle the East Cache Fault Zone. Subdivision of Quaternary units follows the scheme adopted by U.S.G.S. personnel who are mapping the Quaternary geology of the Wasatch Fault (Machette, personal communication.) Transfer of this mapping to a 1:50,000 base map and field checking are 90% complete.

   The East Cache Fault Zone appears to be composed of three segements (Figure 1). In Segment A (the northernmost, from North Logan, UT to Franklin, ID), no scarps offset Bonneville-age deposits. The fault zone consists of two parallel strands 3.5 km apart. In segment B (central, from North Logan to Hyrum, UT) there is a single fault at the range-front and range-front relief is steepest. Fault scarps record two post-Bonneville-shoreline events, the latter of which offsets a post-Provo-shoreline terrace (age 13-11 ka?); net vertical displacement is 1.4 - 1.6m for the later event, and up to 2.7m for the earlier event. Refined measurements of displacement and fault timing will be acquired in trenching operations to commence in October, 1986. Segment C (southernmost, from Hyrum to Avon, UT) is similar to segment A in that it contains two parallel normal faults roughly 2.5 km apart. Surface faulting is restricted to pre-Bonneville colluvium and pediment gravels; no Bonneville-age or younger

deposits are faulted. Surface offsets of pre-Bonneville pediments (150 ka?) measure up to 1.35m, indicating a long-term slip rate of 0.009m/ka. This rate is considerably lower than the slip rate of the central segment in the last 15 ka (0.28 m/ka).

2. The elevation of the Bonneville Shoreline was surveyed at 85 points along the eastern margin of Cache Valley to detect isostatic and tectonic deformation. Control traverses to create base stations were surveyed by trigonometric levelling between bench marks. From base stations near the shoreline, spot elevations of 4 - 5 shoreline sites were measured by radial shots from each base station. An early check revealed that shoreline elevations from radial shots deviated an average of only 0.5 ft from elevations measured from continuous shoreline traverses. At most of the 85 shoreline elevation points, the elevation of the original shoreline angle was reconstructed from topographic profiles across the shoreline platform, colluvial wedge, and wave cut cliff. Resulting accuracy for surveyed shoreline angle elevations on Figure 2 is thought to be $\pm$ 0.5m.

   The resulting shoreline elevation profile along the range front (Figure 2) shows that isostatic northward tilt, presumably from regional-scale unloading, is the dominant trend. However, the 19m of elevation decline does not occur uniformly; 58% of it occurs in two short reaches totalling only 10% of the length of the traverse. At each of these locations (the High/Cherry Creek site in segment A, and the Hyrum site in segment C) large delta complexes (2.5km by 3.2km by 100m thick) occur graded to the Bonneville or Provo shorelines.

   At the other large delta complex (Logan site, in segment B) no tilting is observed; however, this site is coincident with the only known post-Bonneville surface faulting. It is tenta-tively proposed that large deltaic loading has induced ductile bending of the range-front in segments A and C, where the range-front fault is developed in weak rocks of the Tertiary Salt Lake Formation. In contrast, depositional loading in the central segment has resulted in brittle failure of Paleozoic rocks and two surface-faulting events. This hypotheses will be tested by rheologic modeling in the next few months.

3. Detailed measurements of range front tectonic geomorphology are in progress. Qualitative field observations suggest that range front morphology is dominated by effects of fault splaying and variable range-front lithology rather than by uplift rates.

REFERENCES

Swan, F. H. III, Hanson, K. L., Schwartz, D. P. and Black, J. H., 1983, Study of earthquake recurrence intervals on the Wasatch Fault, Utah: Eighth Semi-Annual Technical Report, May 1983, U.S. Geological Survey Contract 14-08-0001-19842, 20 p.

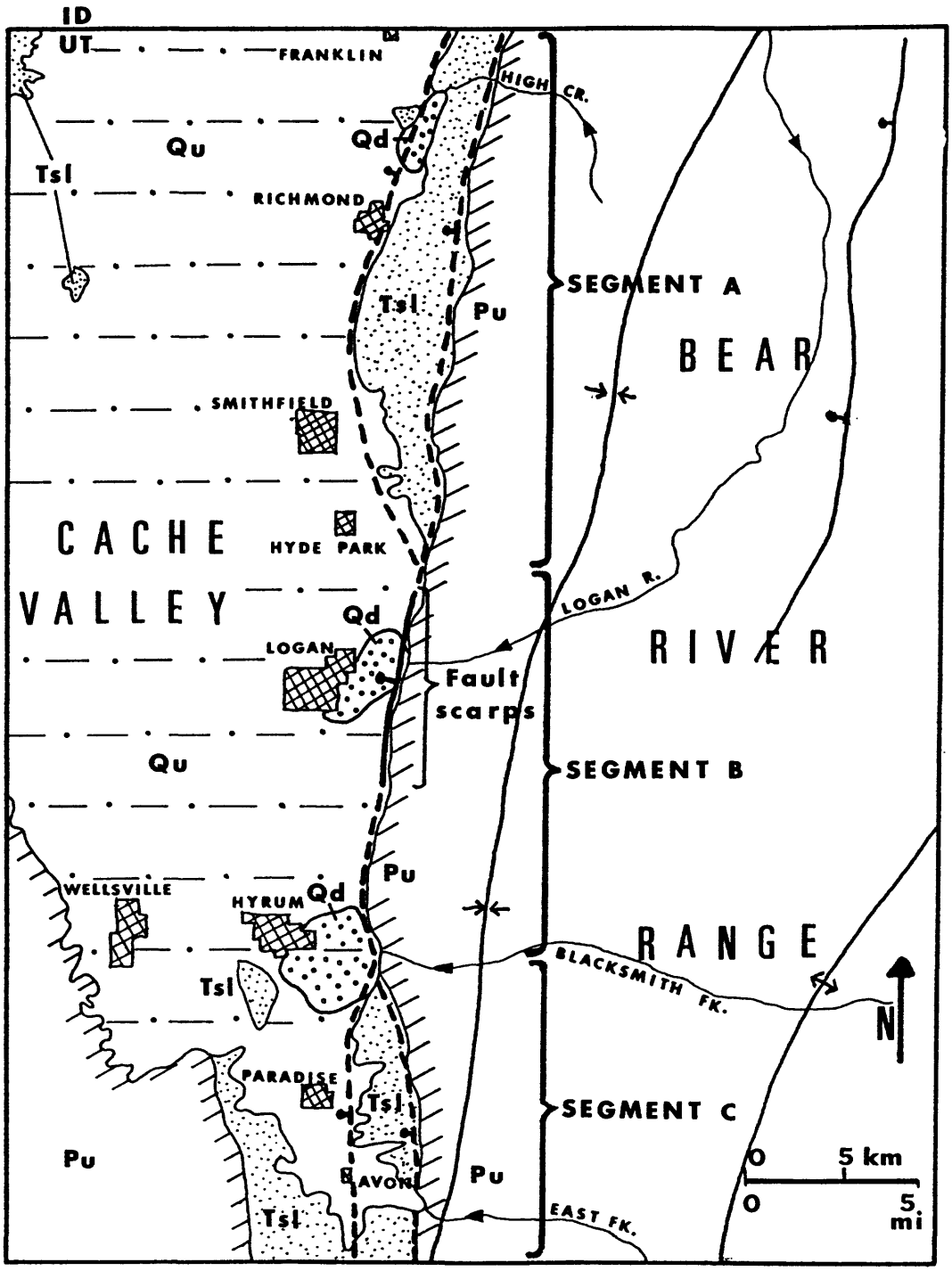

Fig. 1. Sketch map showing the overall pattern of the East Cache Fault Zone (heavy line in center, solid where Bonneville deposits are offset, dashed elsewhere). Qu - Quaternary deposits, undifferentiated; Qd - Quaternary deltaic deposits; Tsl - Tertiary Salt Lake Formation; Pu - Paleozoic rocks, undifferentiated.

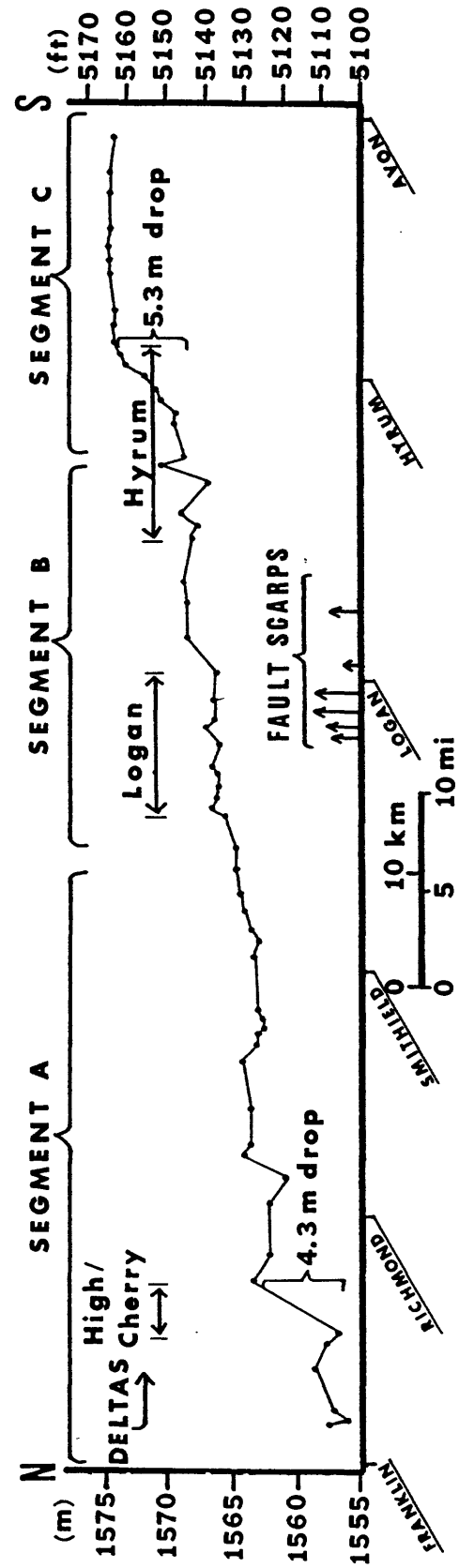

Fig. 2. Elevation profile of the Bonneville Shoreline along the eastern side of Cache Valley, from Franklin, ID (N) to Avon, UT (S). Elevation measurements (shown by dots) have an uncertainty of ± 0.5m, which is not shown on this plot. Locations of deltas, segment boundaries and towns are the same as on Fig. 1. Height of arrows under "FAULT SCARPS" indicates net surface offset (up to 4.1m) measured from scarp profiles.

Numerical Modeling of Rupture Mechanics and Ground Motion of the 1886 South Carolina Earthquake

14-08-0001-G1273

Otto W. Nuttli and Robert B. Herrmann
Department of Earth and Atmospheric Sciences
Saint Louis University
P.O. Box 8099 - Laclede Station
St. Louis, Missouri 63156
(314)-658-3124 and 3120

For numerically modeling the ground motion of the 1886 South Carolina earthquake we have so far considered three alternate values of the strike and dip of the fault plane and of the slip motion on it, and two distributions of high stress drop on the fault plane. Acceleration, velocity, and displacement time histories, as well as pseudo-velocity response spectra for frequencies of 5 to 0.05 Hz, have been calculated for six epicentral distances, ranging from 100 km to 600 km, and for sixteen azimuths.

The synthetic seismograms and response spectra will be compared with the contemporary description of the ground motion and its effects on people and structures. The synthetic time histories also can be simulated to pass through a short-period WWSSN seismograph, and body-wave magnitude calculated from them. Tentatively such calculations indicate that the preferred fault model is one that strikes north-south and has strike-slip motion.

Analysis of Earthquake Ground-Shaking Hazard For the Logan-Brigham City Region, Utah

G1189

M.S. Power, R.R. Youngs, and F.H. Swan
Geomatrix Consultants
One Market Plaza
Spear St. Tower, Suite 717
San Francisco, California 94105
(415) 957-9557

Objectives: We have completed a probabilistic assessment of the ground motion hazard for the Logan-Brigham City region of Utah. This has been combined with a previous study for the Salt Lake City-Provo-Ogden region to arrive at a probabilistic assessment of the ground motion hazard for the central urban corridor along the Wasatch Front, Utah from Nephi to the Idaho border. The hazard is expressed as levels of a ground motion parameter, such as peak acceleration, having certain probabilities of being exceeded during a specified time period. The results of this are to be reported in the form of regional maps showing contours of peak ground acceleration for selected probabilities of exceedance. Also, acceleration response spectra corresponding to selected probabilities of exceedance will be presented for representative locations in the study region for use in further evaluation of the damage potential of ground motions to buildings.

Probabilistic seismic hazard analysis incorporates the inherent uncertainty in the location, time of occurrence and size of future earthquakes and the uncertainty in the resulting levels of ground motion produced at a site in evaluating the probability of exceeding a specified ground motion level in a specified time period. These factors are incorporated into probabilistic models that utilize as inputs fault location, fault geometry, maximum earthquake magnitude, earthquake recurrence rate, and ground motion attenuation characteristics. There is usually uncertainty in selecting the appropriate probability models and evaluating the model parameters, arising from less than complete knowledge of the seismogenic processes. In the present study, the uncertainty in characterizing the potential sources of future seismicity and ground motion attenuation are explicitly incorporated in the analysis through the use of the logic tree formulation. The results of the analysis provide both the expected level of hazard and an assessment of the uncertainty in the hazard estimate.

Results: Geologic studies by numerous investigators have identified a number of active or potentially active faults in the region. Figure 1 shows the locations of known faults significant to the study. These faults are believed capable of generating moderate-to-large earthquakes. The maximum earthquake magnitudes and recurrence rates for large magnitude events on these faults were characterized based on geologic and paleoseismic data.

Evaluation of the historical and instrumental seismicity data for Utah (for the years 1850 to 1986 has been used to characterize the recurrence rates for smaller magnitude events. These evaluations, together with the results of other published studies indicate that much of the small-to-moderate magnitude seismicity cannot be directly associated with mapped faults. Consequently, a distributed area source of small-to-moderate magnitude earthquakes was included in the model of the regional seismicity.

There is uncertainty as to the appropriate attenuation characteristics for the study region. Examination of the various published studies indicates there are arguments for both a higher rate of attenuation and a lower rate of attenuation than that observed in California. There are very few recordings of earthquake strong ground motions in the study region to use in evaluating attenuation relationships. For the basic analysis, we used several California-type attenuation relationships that have been developed based on mainly California strong motion data. We also conducted additional sensitivity analyses using attenuation relationships having a lesser rate of attenuation. The results of the analysis indicate that the computed hazard levels are not greatly sensitive to variations in the rate of attenuation within a reasonable range.

Figure 2 shows the results of basic hazard computations for peak ground acceleration at selected locations throughout the study region. On the left are mean hazard curves for locations close to the Wasatch fault from Nephi to Brigham City. As can be seen, nearly identical hazard is obtained for points along the most active portion of the fault (Provo to Ogden). The hazard is lower at points along less active portions of the fault zone (Nephi and Brigham City). On the right are mean hazard curves for locations near less active fault traces. As can be seen, the hazard is significantly lower at these locations (Tooele, Colliston, Logan).

The results shown in Figure 2 represent the computed hazard at soil sites. For rock sites, the corresponding peak ground accelerations may be somewhat higher, depending on the probability level and the attenuation relationships used.

Related Report:
Youngs, R.R., Swan, F.H. III, Power, M.P., Schwartz, D.P. and Green, R.K., Analysis of earthquake ground-shaking hazard along the Wasatch Front, Utah: in Evaluation of Urban and Regional Earthquake Hazard and Risk in Utah, U.S. Geological Survey Professional Paper (in preparation).

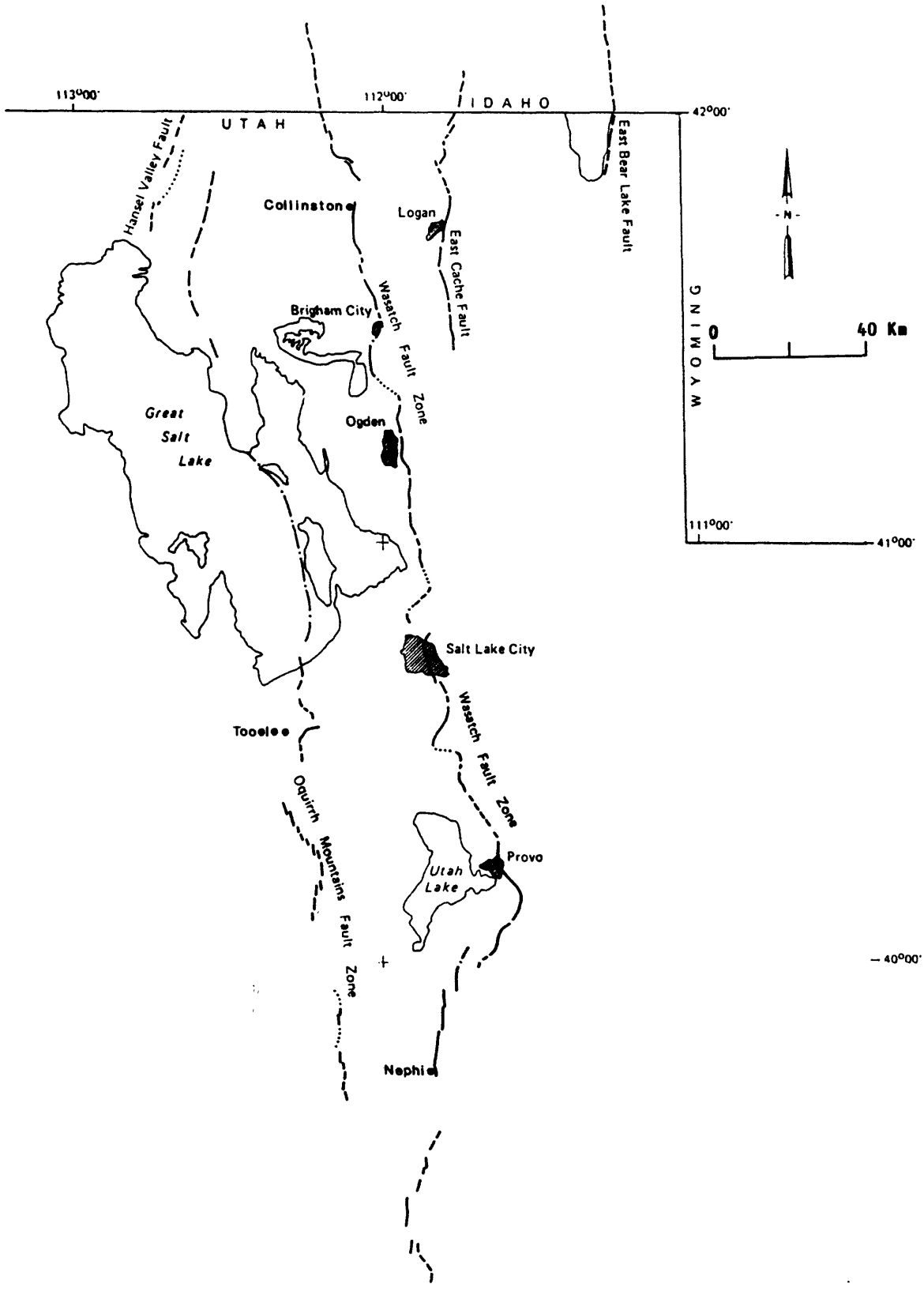

Figure 1. Map of faults used as seismic sources in seismic hazard analysis along the Wasatch Front, Utah.

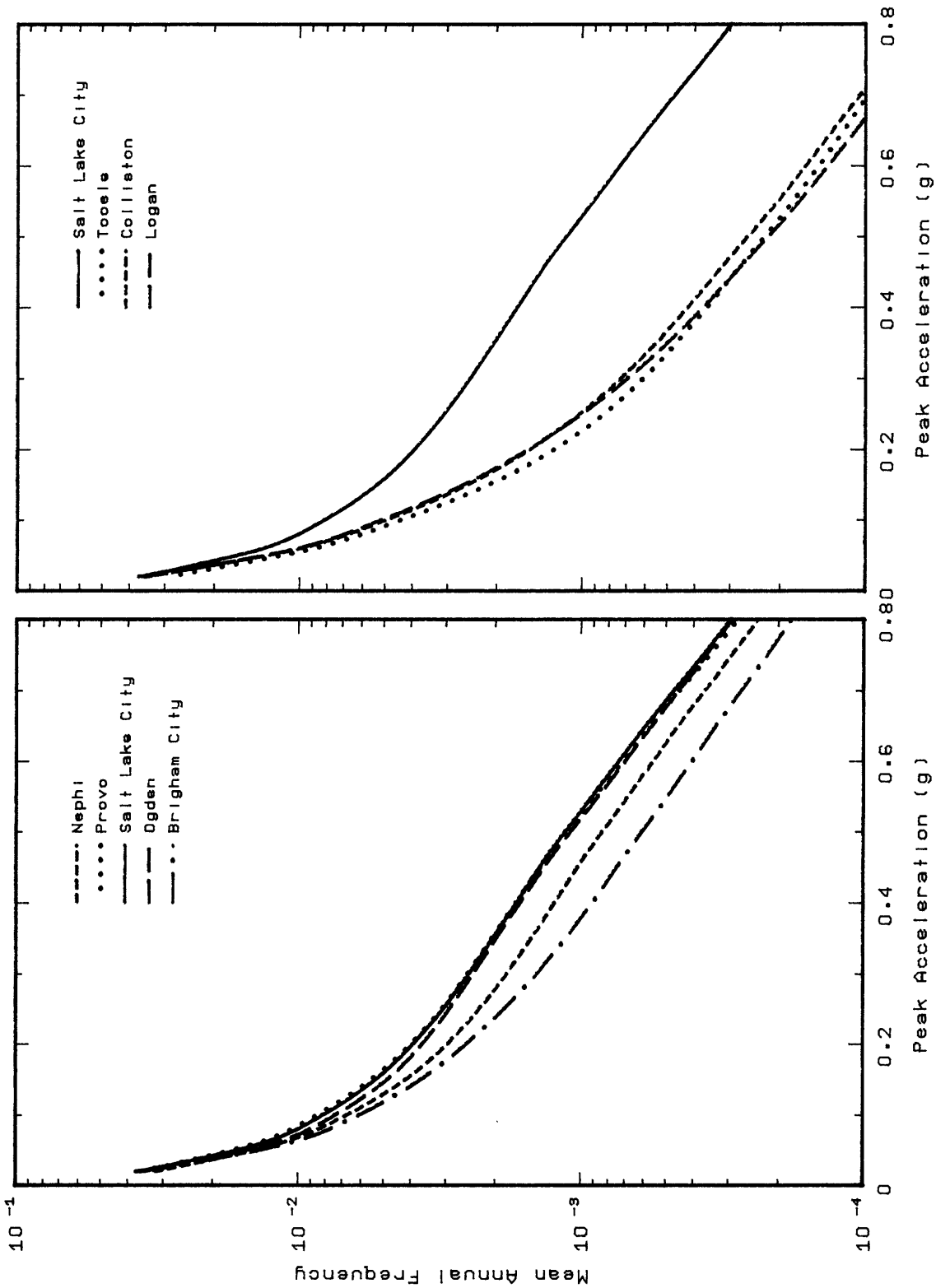

Figure 2. Computed hazard at selected locations in study area.

Source Properties of Great Basin Earthquakes

9950-03835

Arthur C. Tarr
Branch of Geologic Risk Assessment
U.S. Geological Survey
Box 25046, MS 966, Denver Federal Center
Denver, CO 80225
(303) 236-1605; (FTS) 776-1605

Investigations

Three investigations were pursued during the reporting period:

1. Analysis of digital data recorded at the Nevada Test Site.

2. Development of field computer system for urban hazards seismic studies.

3. Site Characterization Plan chapter for the proposed Yucca Mountain high-level nuclear waste repository.

The objective of the first investigation was to analyze digital seismic data that had been recorded in 1981 by DR-100 portable seismic systems and in subsequent years by the permanent Southern Great Basin Seismic Network (SGBSN). This investigation was in support of the Southern Great Basin Seismic Studies project (9950-02151).

The objective of the second investigation was to design a microcomputer system that could be used in the field to support the activities of the Urban Hazards Seismic Field Investigations project (9950-01919). Some of these activities include multi-channel reflection, refraction, and borehole profiles of the upper 100 m to determine basement depth and seismic parameters of Quaternary deposits. Analysis of seismic data in the field is expected to improve the productivity of seismic field experiments by reducing guesswork in laying out spreads and in selective filtering of data channels.

The objective of the third investigation was to prepare the seismology section of the geology chapter of the Site Characterization Plan (SCP) the USGS is preparing for the Department of Energy. The SCP is for the proposed Yucca Mountain repository near the Nevada Test Site. The goal for each section of the SCP was to synthesize existing information about the proposed site and to summarize the state of knowledge of the geology of the surrounding southern Great Basin.

Results

The results of the Jackass Flats study were published during the reporting period in Open-File Report 86-420.

Hardware for the field computer was purchased and installed during the reporting period. The field system was a standard IBM PC/XT modified with an accelerator board (9.54 MHz 8087 numerical processor and 8086 CPU), extended memory (2 Mbytes supplementing a maximum of 640 Kbytes of RAM on the system board), 30 Mbytes hard

disk storage, high-resolution monitor and graphics board, dot matrix printer for graphics output, and a mouse for phase picks and other waveform processing operations.

Completion of the seismology section of SCP Chapter 1 (Geology of the southern Great Basin and Yucca Mountain) required approximately three months, following extensive revision as a consequence of review of the first draft. The conclusions cited in the last Summaries of Technical Reports volume (XXII) essentially remained the same. The section was in second technical review at the end of the reporting period.

Reports

Tarr, Arthur C. and Rogers, A. M., 1986, Analysis of earthquake data recorded by digital field seismic systems, Jackass Flats, Nevada: U.S. Geological Survey Open-File Report 86-420, 72 p.

Quaternary Framework for Earthquake Studies
Los Angeles, California

9540-01611

John C. Tinsley
Branch of Western Regional Geology
U.S. Geological Survey
345 Middlefield Road, MS 975
Menlo Park, California 94025
(415) 323-8111, x 2037

Investigations

1. Completed drilling and sampling studies to depths of 200 ft subsurface at 20 instrument stations in the Salt Lake City area at which low-strain ground motion recordings have been made during the past decade. (J. Tinsley, D. Trumm, D. Carver, K. King).

2. Completed initial phase of trenching and soil stratigraphic studies in the San Gorgonio Pass region, with emphasis on determining the history of fault displacement along reverse faults that bound the south margin of the San Bernardino Mountains. (J. C. Tinsley, J. C. Matti, D. Trumm, S. Goldfinger, R. Versical).

3. Completed field studies of fluvial stratigraphy and Holocene fold deformation to determine rates of fold-related uplift across the Coalinga anticline along Los Gatos Creek west of Coalinga, CA. (D. Trumm, R. Versical, R.S. Stein, J.C. Tinsley).

Results

1. Lithologic logs, 3-inch Shelby-tube samples, down-hole shear-wave and compressional wave velocity logs, and soil parameters including bulk density, dry density, consolidation tests, particle size analyses, and unconfined compressive strength determinations comprise a suite of geologic and geotechnical data that will be used to characterize ground response at ground motion instrument sites in the Wasatch area. Engineering properties of the soils are being measured in the soils engineering laboratory at Brigham Young University by Mr. Kevin Misken, under the supervision of Dr. T. L. Youd. Geologic analysis of well cuttings and logs is in progress at the U.S. Geological Survey, Menlo Park, California. These data will be reported subsequently with the objective of improving predictions of site-dependent earthquake-generated ground motion in the Wastach region. The sites are listed in the accompanying table (table 1). These data also provide control for several of the high-resolution seismic reflection profiles recorded by Kenneth W. King (USGS, Golden, CO). (J. C. Tinsley, D. Trumm, D. Carver).

2. Four soil pits, three trenches, and one creek bank were excavated using a backhoe in order to examine and sample soils, paleosols, Quaternary stratigraphic relations and Holocene faulting within the San Gorgonio Pass fault zone, a zone of E-W trending reverse faults that offset the surface of alluvial fans 1.5 miles north of the town of Cabezon, CA (Cabezon 7.5' quadrangle). The deposits studied all lie within the Millard Canyon drainage, specifically section 32, T. 2 S, R. 2 E. and section 5, T. 3 S, R. 2 E. Soils sampled were apparently middle Holocene and younger, on the basis of soil profile characteristics. Four radiocarbon samples have been submitted for analysis to Beta Analytic, using the accelerator mass spectrometer facility at Zurich, Switzerland. We do not yet have results. Soils were described, sampled and submitted for analysis at the Quaternary Studies Laboratory, University of New Mexico, under the supervision of Dr. Leslie D. McFadden. Results of these soil analyses are not yet available.

Trench exposures showed conclusive evidence of faulting with remarkably continuous stratigraphic relations characterizing the coarse, bouldery alluvial fan deposits. The alluvial deposits often caved and raveled severely, and shoring of the excavations proved to be sporting. The Millard Canyon wash is intersected by a 1.5 to 2 m high scarp (section 5). Excavation of the side of the arroyo to a depth of about 2 m below the grade of the present channel of Millard Canyon created a sloping exposure about 7 m high. Strata were remarkably continuous here, and two shears were mapped extending from the base of the exposure to about 1/2 m below ground level, where burrowing animals had homogenized the stratigraphy. The measurable dip-slip offsets amounted to 173 cm plus warping of beds. Nothing in the exposure requires more than one episode of faulting deformation to produce. Radiocarbon samples were obtained (detrital charcoal) from two levels, above and below a disconformity.

A segmented, 20 m high scarp was trenched to a depth of 4 m at a point about 150 m north of Millard Canyon wash. The logs show four zones of displacement localized across the 32 m length of the trench exposure. The deformation is an outstanding example of reverse faulting in aluvial deposits, where the faulting occurs in a series of episodes across a wide zone of deformation.

A 4 m scarp was trenched in two places in section 32. The first trench intersected a gully fill and was unremarkable as a record of faulting. The second trench was distinguished by crudely bedded cobble gravels and only minimum measurements of fault displacement were obtained. To obtain recurrence estimates will require additional trenching, to greater depths than were explored using conventional backhoe excavations. Further analyses and limited rate of slip calculations await the results of the radiocarbon dating and the soil analyses.

3. Numerous hand-auger borings were obtained to locate additional fine-grained overbank facies beneath the bed of Los Gatos Creek between the town of Coalinga, CA and the axis of the Coalinga anticline. At promising sites, backhoe excavations were completed in order to deepen existing exposures in an effort to expose and date deposits that would enable a 5000 year old isochron to be extended from the axial plane of the anticline westward into the Pleasant Valley syncline. Few overbank deposits were encountered within reach of the backhoe, and detailed mapping of a 1 km long exposure (C84-24) of the floodplain sediments indicated that at least 4 episodes of cutting and filling have characterized the reach during the past 3000 to 5000 years. In two localities, additional charcoal samples were procured; results of the radiocarbon analyses are pending.

Publications

Tinsley, J. C., and Rogers, A. M., 1986, Suggested directions in earthquake ground-shaking microzonation research, in Proceedings of Workshop XXXII, Future directions in evaluating earthquake hazards of southern California, Nov. 12-13, 1985, Los Angeles: U.S. Geological Survey Open Report 86-401, p. 345-354.

Tinsley, J. C., Youd, T. L., Perkins, D. M., and Chen, A. T. F., 1986, Improving predictions of liquefaction potential in Brown, William M. (ed.) Proceedings of Conference XXXII, (Workshop on) future directions in evaluating earthquake hazards of southern California: U.S. Geological Survey Open-File Report 86-401,. p. 293-297.

Table 1

Station Number	Station Name	Address
4	Liberty Park	9th S. 6th E., SLC
6	Utah Geological & Mineral Survey	606 Blackhawk Way, SLC
15	Alta View Hospital (Alternate to Sandy City Fire Station)	9660 S. 13th E., SLC
17	S.L.C. International Airport	470 N. 2200 W., SLC
18	Salt Air (Morton Salt Co.)	Int. 80 - West
19	SLC Airport - Fire Station	Caterers Row, SLC
22	Bateman Dairy Farm	6985 S. 1300 W., SLC
24	N. Jordan Park	920 W. 800 S., SLC
29	4060 S. 725 W.	4070 S. 725 W., Murray
42	Sunnyside Training Center	2675 Michigan Ave, SLC
43	Bonneville Golf Course	Salt Lake City
44	Laird Park	Laird Ave + 1800 E., SLC
45	Westminster College	
46	Roosevelt Elem. School	3225 S. 800 E., SLC
47	Rosecrest Elem. School	3225 S. 800 E., SLC
49	Temple Sq. West	40 N. 2nd W., SLC
50	East Bench	11th E. 24th S., SLC
51	Magna Water District (Haynes Field)	2700 S. 6000 W., SLC

Liquefaction Risk Map for Boston

14-08-0001-G1188

Robert V. Whitman
Herbert H. Einstein
Daniele Veneziano

Department of Civil Engineering
Massachusetts Institute of Technology
Cambridge, Massachusetts 021139
(617) 253-7127

This study was formally established 1 December 1985, with work commencing 1 February 1986. The study has three major components: 1) the determination of liquefaction susceptibility of different soils by combining geological characterization with information from soil borings.; 2) estimation of earthquake intensities, recurrence intervals and based thereupon the shaking hazard at different locations; 3) combining of 1 and 2, taking into account in a rational manner uncertainties within both of these parts.

Geologic-Geotechnical Characterization

Ground conditions are used in two basic ways to establish liquefaction susceptibilities:

1. Natural sediments and artificial fill which have been loosely deposited and remained in this condition are potentially liquefiable. Ground conditions can thus be subjectively categorized based on geological and man-influenced history.

2. Geotechnical properties, notably SPT values, are established from boring records. Correlations among SPT, other geotechnical properties and natural geologic characterization are used to interpolate among widely-spaced groups of borings.

Geologic characterization can thus be used directly to establish liquefaction potential and indirectly to correlate with geotechnical properties indicating liquefaction potential. Geologic characterization as used in this context involves both natural ground and artificial fill. This is particularly important in Boston where the greater part of the city is located on fill.

Ample, although to some extent controversial, information is available concerning the natural geology. Literature searches have been conducted in the files of the USGS, Boston office, and in the geology libraries of M.I.T. and Harvard. The results obtained so far were discussed with Dr. B. Stone, USGS. The basic stratigraphy underlying the Boston Peninsula and surrounding areas in Cambridge and Brookline, was determined. Controversies are mainly related to the age and association of different deposits with particular periods (4 major ice advances versus 2 with a limited readvance). The information is, however, sufficient to start correlating it with the boring log information.

Originally, it was thought that fills would not be very problematic in the context of earthquake liquefaction in the Boston area. However, in addition to revealing a very complex history geographically, temporally and technically, initial review of available information also showed that many fill deposition procedures potentially produced loose soils in this area. In Back Bay, for instance, in addition to the well-known dumping of Needham sand-gravel from railroad cars, dredging and deposition with a suction dredge of material from the Charles River bottom, and also dumping from scows of material dredged from the river, were used. The latter two procedures can lead to loose deposits. This part of the work was therefore intensified. The work has consisted of archival studies in the Boston Public Library, Boston Athenaeum, the M.I.T. libraries and a number of public authorities. Detailed geotechnical information both on fill and natural deposits was obtained from the series of boring log collections produced by the Boston Society of Civil Engineers. Information from the 1941, 1956 and 1969 series was used but not from the 1914 series (the information is in a completely different format and is also duplicated by later borings). Data from about 50% of all boring logs has been completely digitized and represented in vertical cross sections through Boston and Cambridge. This work will continue toward complete digitizing of all logs.

Ground Motion Models for the Eastern United States

During this reporting period, we have addressed the problem of earthquake attenuation in the Eastern United States (EUS), under joint sponsorship of USGS and EPRI. In the past, attenuation models in the EUS have been obtained mainly by an indirect method which combines MM intensity attenuation relationships appropriate to the EUS with "intensity-to-ground-motion" conversions from the Western United States (WUS). Recently, instrumental data from a few moderate-size earthquakes has become available in the EUS, from which direct estimation of ground motion is possible. We have obtained direct estimates of attenuation from this data, using a regression model that recognizes variations of attenuation from earthquake to earthquake.

The main focus of our work has been however the development of a new statistical technique to compare and combine direct and indirect estimates of ground motion. The proposed method utilizes information on macroseismic and instrumental measures of ground motion from several geographical regions. Differences in attenuation among the regions are permitted and means are given to describe these differences either deterministically or probabilistically. Diagnostic quantities are calculated to verify the compatibility of assumptions about the similarity of attenuation in different regions with available data. The method has been used to estimate how peak ground acceleration (PGA) and spectral velocities at 1 and 10 herz for 5% damping ($S_V(1)$ and $S_V(10)$) attenuate in the EUS. These estimates are based on instrumental and MM intensity information from that region and instrumental data from the WUS. The proposed regressions for horizontal motion on rock are

$$\ell n PGA = 2.53 + 1.10\, m_{Lg} - 1.17 \ell nR - 0.003\, R$$

$$\ell n S_V(10) = -1.54 + 1.11\, m_{Lg} - 1.04\, \ell nR - 0.003\, R$$

$$\ell n S_V(1) = -6.96 + 2.10\, m_{Lg} - 1.10\, \ell nR - 0.003\, R$$

where PGA is in cm/sec^2, S_V is in cm/sec, and R is hypocentral distance in km. These relationships are consistent with results from the method of attenuated spectra and random vibration analysis.

A paper based on the above work has been submitted for publication to the BSSA.

Seismicity of the Northeastern United States

In most of the Eastern and Central United States, the mechanism of tectonic stress accumulation and the location of seismogenic features are not precisely known. This lack of physical knowledge has two important consequences on the modeling of earthquake activity: (1) recurrence relationships must be based primarily on historical earthquake data (as opposed to geological and geophysical measurements) and (2) such relationships can be meaningfully defined only for extended geographical regions (as opposed to individual faults). Models of seismicity in the Eastern U.S. are therefore rather crude and probably biased on a small geographical scale. In an attempt to reduce this bias and make more effective use of historical data, a method was developed in the EPRI (1986) study to fit earthquake recurrence relationships with spatially-varying parameters. The analyst can control the degree of smoothness of this spatial variability by selecting approximate "smoothness parameters." The choice of smoothness parameters was in the EPRI study based largely on subjective criteria.

As part of the present liquefaction risk study, we have looked at methods for the automatic selection of the smoothness parameters, based on earthquake catalog data. The main idea of the method is to use the maximum degree of smoothness that is statistically compatible with the historical data. Statistical compatibility is decided on the basis of various goodness-of-fit criteria. In many cases, results are very different from those under the assumption of homogeneous earthquake sources, with important consequences on seismic risk.

Conditional Liquefaction Probability Analysis

In order to estimate liquefaction risk by the method that we propose, it is necessary to quantify the probability of liquefaction, given certain earthquake and soil deposit characteristics, for example given peak ground acceleration and the blowcount number at same critical depth. The probability of liquefaction of a site in a given period of time is then obtained by combining this conditional probability of liquefaction with a probabilistic description of seismicity at the site (which is given through a regional seismicity model and a ground motion model) and a probabilistic description of local soil conditions.

Conditional liquefaction probability models have been obtained during the past year under a parallel project on liquefaction susceptibility, funded by the National Science Foundation. Extensive documentation of this work is in a doctoral thesis by Liao (1986).

References

Liao. S.S.C. (1986), "Statistical Modelling of Earthquake-Induced Liquefaction," Ph.D. Thesis, Dept. of Civil Engineering, MIT, Cambridge, Massachusetts.

Veneziano, D. and Heidari, M. (1986), "Statistical Analysis of Attenuation in the Eastern United States" Submitted for publication to the BSSA.

Worldwide Standardized Seismograph Network (WWSSN)

9920-01201

Russ Wilson
WWSSN Project Chief
Branch of Global Seismology and Geomagnetism
U.S. Geological Survey
Albuquerque Seismological Laboratory
Building 10002, Kirtland AFB-East
Albuquerque, New Mexico 87115-5000
(505) 844-4637

Investigations

1. Technical and operational support was provided to each station in the Worldwide Standardized Seismograph Network (WWSSN) as needed and required.

2. Two hundred one (201) modules and components were repaired, and two hundred ten (210) separate items were shipped to one hundred fifteen (115) separate locations to support the WWSSN network during this period.

Results

1. A continuous flow of high-quality seismic data from the cooperating WWSSN stations within the network was provided to the users in the seismological community.

WWSSN Maintenance and Calibration Visits:

1. During April 1986, Field Engineer, Mr. Juan Nieto, visited the WWSSN station at Ponta Delgada, Azors (PDA) for maintenance and calibration. This station (PDA) had been down for several months but is now fully operational.

2. During August 1986, Field Engineer, Mr. Gary S. Gyure, visited the following WWSSN stations for routine maintenance.

    1. Chiang Mai, Thailand (CHG)
    2. Lembang, Indonesia (LEM)
    3. Afiamalu, Samoa (AFI)

3. During September 1986, Field Engineer, Mr. Gary S. Gyure, visited the WWSSN station (RAB) at Rabul, New Britain for maintenance and calibration. The LP at RAB station had been down since May 1986, but is now fully operational.

4. During September 1986, Field Engineer, Mr. Gary S. Gyure, visited the WWSSN station (HNR) at Honiara, Guada Canal for maintenance and calibration. The HNR station has had problems with the LP CAL, but is now fully operational.

5. All WWSSN stations were informed that as of October 1, 1985, to record only four channels. The following stations have not responded: ARE, GSC, KOD, NDI, NNA, NUR, POO.

Hot Pen Conversion:

1. During April 1986, technical proposals to convert WWSSN photographic recording to hot pen recording were received from the following companies:

1. Kinemetrics, Inc.
   San Gabriel, California
2. Teledyne Geotech
   Garland, Texas
3. Springnether Instrument Company
   St. Louis, Missouri

2. A technical review committee, for the purpose of making a technical evaluation of RFP No. 6-4247 (Heated Pen Kits), was formed May 7, 1986, with the following members: Chairman--Mr. Bob Hutt, Geophysicist; Mr. Harold Clark, Electronics Engineer; and Mr. E. Russ Wilson, Electronics Technician. The proposals were from the companies listed above in item 1. A narrative of the technical evaluation was written to support the numerical score and forwarded to Contracting Officer, Lynda Carlson, Central Region.

3. A technical review committee to evaluate the cost proposals of RFP No. 6-4247 (Heated Pen Kits) was formed May 21, 1986, with the following members: Chairman--Mr. Bob Hutt, Geophysicist; Mr. Hal Butler, Geophysicist; and Mr. E. Russ Wilson, Electronics Technician. The proposals were from the companies listed above in item 1. A narrative of the cost proposals was written and forwarded to Contracting Officer, Lynda Carlson, Central Region.

4. As a result of the committee's evaluation of RFP No. 6-4247 and Cost Proposals No. 6-4247 from the companies listed above in item 1, the contract for producing the heated pen conversion kits was awarded to Kinemetrics, Inc., San Gabriel, California, in September 1986.

National Map of Liquefaction Hazard

14-08-0001G1187

T. Leslie Youd
Dept. of Civil Engineering
Brigham Young University
Provo, Utah 84602
(801) 378-6327

Objective: One of the key tools for evaluating earthquake hazards is a map showing liquefaction hazard. The purpose of this project is to prepare a national liquefaction hazard map for the 48 contiguous U.S. states. This map will show contours of a parameter termed liquefaction severity index (LSI) which is indexed to the anticipated severity of damage as a consequence of liquefaction of susceptible sediments. LSI will be contoured to provide an estimate of severity of expected liquefaction effects with a high degree of probability of not being exceeded in a given period of time. This LSI value, however, applies only to areas underlain by liquefiable sediment. The actual locations of liquefiable sediments will not and indeed cannot be effectively mapped at a national scale.

Data acquisitions and Analysis: The first six months of work on this project have involved modifications and verification of a computer program and revision of attenuation relationships required for the analysis.

1. A copy of a usable computer program and seismic input files was obtained from Dave Perkins and his colleagues at USGS in Golden Colorado. This program was modified as necessary to run on Brigham Young University computers and to perform the required analyses and to accept our LSI input data files.

2. An LSI attenuation correlation developed for the western U.S. was adapted to the eastern U.S. by adjusting the correlation on the basis of intensity attenuation with distance from large earthquakes and then verifying the adjusted correlations with the few LSI datum points available for the eastern U.S.

Map Compilation: The second six months of the project have been devoted to map compilation. A set of maps was prepared that show contours of LSI with 90% probability of not being exceeded in 10, 50, and 250 years, respectively. A draft of a report for the project was also written. Revisions to the maps and report are now being made.

Geophysical and Tectonic Investigations of the Intermountain Seismic Belt

9930-02669

Mary Lou Zoback
U. S. Geological Survey
Branch of Seismology
345 Middlefield Road, Mail Stop 977
Menlo Park, California 94025
(415) 323-8111, Ext 2367

Investigations

1) Subsurface fault geometry of the Wasatch fault zone interpreted from seismic reflection, gravity, and well data.

2) Analysis of fault slip data from Hampel Wash area, Nevada Test Site (with Virgil Frizzell, Branch of Western Regional Geology).

3) Update of North American tectonic stress database and initiation of activity on the World Stress Map project.

4) Analysis of the state of stress in the south-central United States (Oklahoma, northern Texas, and Arkansas-with special emphasis on the vicinity of the Meers fault in Oklahoma) using well-bore elongations.

Results

1) Seismic-reflection and gravity data suggest that the overall structure of Juab Valley, a basin in central Utah bounded on the east by the Wasatch fault zone, is an asymmetric sag, with beds on both sides of the valley tilting toeards the axis of the valley. Anderson and others (1983, GSA Bulletin) have identified this type of basin as commonly being bounded by one or more major, planar, steep normal faults. The maximum valley fill thickness is about 1.60 km based on interpretation of both the reflection and gravity data (assuming a density contrast for basin sediments of -0.4 g/cm^3). Possible displacement of a buried thrust, truncation of deep reflectors, and absence of reverse drag in basin sediments all are interpreted as evidence that the Wasatch fault zone has a planar, high-angle geometry (as opposed to a listric or low-angle geometry).

   On a more regional note, structural data suggest the presence of major ramps in the Mesozoic thrust system near the trace of the modern Wasatch fault at several localities along its length. One possible source for this ramping may be a major basement displacement on a normal fault zone formed along the north-trending, west-facing passive margin that developed through the region in late Proterozoic time (Stewart, 1972). Thus the Wasatch fault zone may be localized by a zone of pre-existing extensional faulting in Precambrian crystalline rocks.

2) Fault-slip data were collected from an area of relatively young faulting in a seismically active part of the Nevada Test Site 123 km NW of Mercury,

Nevada. The data come primarily from intensely faulted Miocene tuffaceous sedimentary rocks in Hampel Wash, which is bounded on the north by the Quaternary ENE-trending Rock Valley fault and on the south by a parallel unnamed fault.

Data from faults with known sense of displacement exhibit a bimodal distribution of slip angles (rakes). Faults exhibiting steep rakes (typically 70° to 90°) cluster about a N30°-35°E strike: most dip 65° to 80°. Faults have shallow rakes (generally less than 20°) exhibit a wide range of strikes (from N6°W to N80°E) and mostly dip between 80° and 90°. The predominant N30°-35°E strike of the steep-rake faults suggest a maximum horizontal stress orientation of about N30°-35°E and a least horizontal principal stress direction N55°-60°W.

Analysis of the data using a least-squares iterative inversion to determine a mean deviatoric principal stress tensor indicates a normal-faulting stress regime (S_1 vertical) with principal stress axes in approximately horizontal and vertical directions (S_1 trend = N19°E and plunge = 82°N; S_2, N30°E and 8°S; and S_3, N60°W and 2°E). The maximum horizontal stress, S_2, was found to be nearly intermediate in magnitude between S_1 and S_3. The N60°W least horizontal prinicpal stress orientation obtained from the fault-slip inversion agrees with our geometric analysis of the data and is consistent with a modern least horizontal principal stress orientation of N50°-70°W inferred from earthquake focal mechanisms, well-bore breakouts, and hydraulic fracturing measurements in the vicinity of the Nevada Test Site.

This solution fits all the data well, except for a subset of strike-slip faults that strike N30°-45°E, subparallel to the normal faults of the data set. Nearly pure dip-slip and pure strike-slip movement on similarly oriented faults, however, cannot be accommodated in a single stress regime. Superposed sets of striae observed on some faults suggest temporal rotations of the regional stress field or local rotations within the region of the fault zone.

3) An almost two-fold increase in the number of data points and adoption of a quality ranking system has enabled us to modify and somewhat simplify stress provinces in the continental United States previously defined by Zoback and Zoback (1980, JGR). The most important differences between the present data compilation and interpreted stress provinces and those reported previously are as follows:

   a) General ENE compression associated with the mid-plate stress field now appears to extend all the way to the Atlantic continental margin and possibly well into the western Atlantic basin. A distinct Atlantic Coastal Plain stress province (characterized by NW compression) is not supported or justified by the available data.

   b) Data defining NE compression associated with subduction of the Juan de Fuca plate is observed in western Washington and Oregon and comprise the Cascade convergence zone stress province.

   c) The extensional stress field associated with the Basin and Range and Rio Grande Rift is now observed in central Colorado and western

Wyoming. Thus, an approximately east-west oriented extensional stress field is generally associated with nearly the entire broad uplifted region of the western Cordillera and appears to completely surround the Colorado Plateau interior compressional province.

d) Young deformation, earthquake focal mechanisms, and wellbore breakout data within the Coast Ranges on either side of the San Andreas fault suggest compression in a more northeasterly direction than the generally N-S compression inferred from right-lateral strike-slip focal mechanisms along the fault itself. This component of compression across the fault may be linked to changes in Pacific absolute plate motion in the past 5 m.y.

In many regions the substantially enlarged data set confirms the generally broad-scale, tectonic origins of the stress field in the various provinces defined. The expanded data also defines numberous localized, relatively small-scale variations in the stress field within individual provinces.

As head of Study Team G of Working Group 3 (Intraplate Phenomena) of the International Lithosphere Program my primary responsibility is compilation of a World Stress Map. Our primary objective is a global stress database that can be compared with global plate kinematics in an attempt to evaluate the relative importance of the various plate-driving forces. Numerous international workers have been contacted and have agreed to contribute to the map. Our current stress database at the USGS is shown on Figures 1 and 2, maximum horizontal stress orientations are plotted. The data come from earthquake focal mechanisms, in-situ stress measurements, well-bore elongations (breakouts), young fault slip data, and volcanic vent alignments.

4) During the second half of FY86 Richard Dart continued to acquire and analyze dipmeter and fracture-identification well logs from oil and gas wells drilled in the south-central United States (Oklahoma, northern Texas and Arkansas) in order to determine orientations of well-bore elongation and infer tectonic stress orientations in the vicinity of the Meers fault. Telephone and mail canvassing of a number of large and small petroleum companies resulted in acquisition of 233 logs from wells located in all parts of the study area. The majority of the data received are concentrated primrialy in four areas: The Palo Duro basin in the Texas Panhandle, the Anadarko basin in west-central Oklahoma, and the Arkoma basin in west-central Arkansas. The 233 logs received to data have been evaluated for their data content; 165 yielded usable breakout data, 17 had no usable data, and 51 could not be evaluated because they were of the wrong type or very poor quality.

A preliminary analysis of the logs with usable data indicate good-quality breakout data and yield a consistent NNW-to N-trending mean breakout orientation implying a regional maximum horizontal compressive stress (S_{Hmax}) direction of ENE to E. However, there does appear to be some local variation or deviation from this regional trend. Our preliminary analysis of the data shows this apparent local variation to be centered in the area of the Ardmore and Marietta Basins south and west of the Wichita Mountains in southern Oklahoma aulacogen, a fault-bounded basement trough that has undergone rifting, sedimentary accumulation, deformation, and uplifting since early Paleozoic time. This local variation in the

regional stress field may be related to the area's complex tectonic and structural history and also to an extensive program of petroleum recovery and secondary pumping during this century.

Reports

Zoback, M. L., Subsurface geometry and structural style of the Wasatch fault zone in central Utah: contribution to a USGS Professional Paper on "Evaluation of Urban and Regional Earthquake Hazards and Risk in Utah", (through internal review).

Frizzell, V.A., and Zoback, M.L., (in press), Stress orientation determined from fault slip data in Hampel Wash area, Nevada, and its relation to contemporary regional stress field: Tectonics.

Zoback, M.L., and Zoback, M.D., (in press), Tectonic stress field of the continental United States: GSA Memoir "Geophysical Framework of the Continental United States, ed. by L.C. Pakiser and W. Mooney.

Lambert Azimuthal projection

Approximate Scale: 1:110,000,000

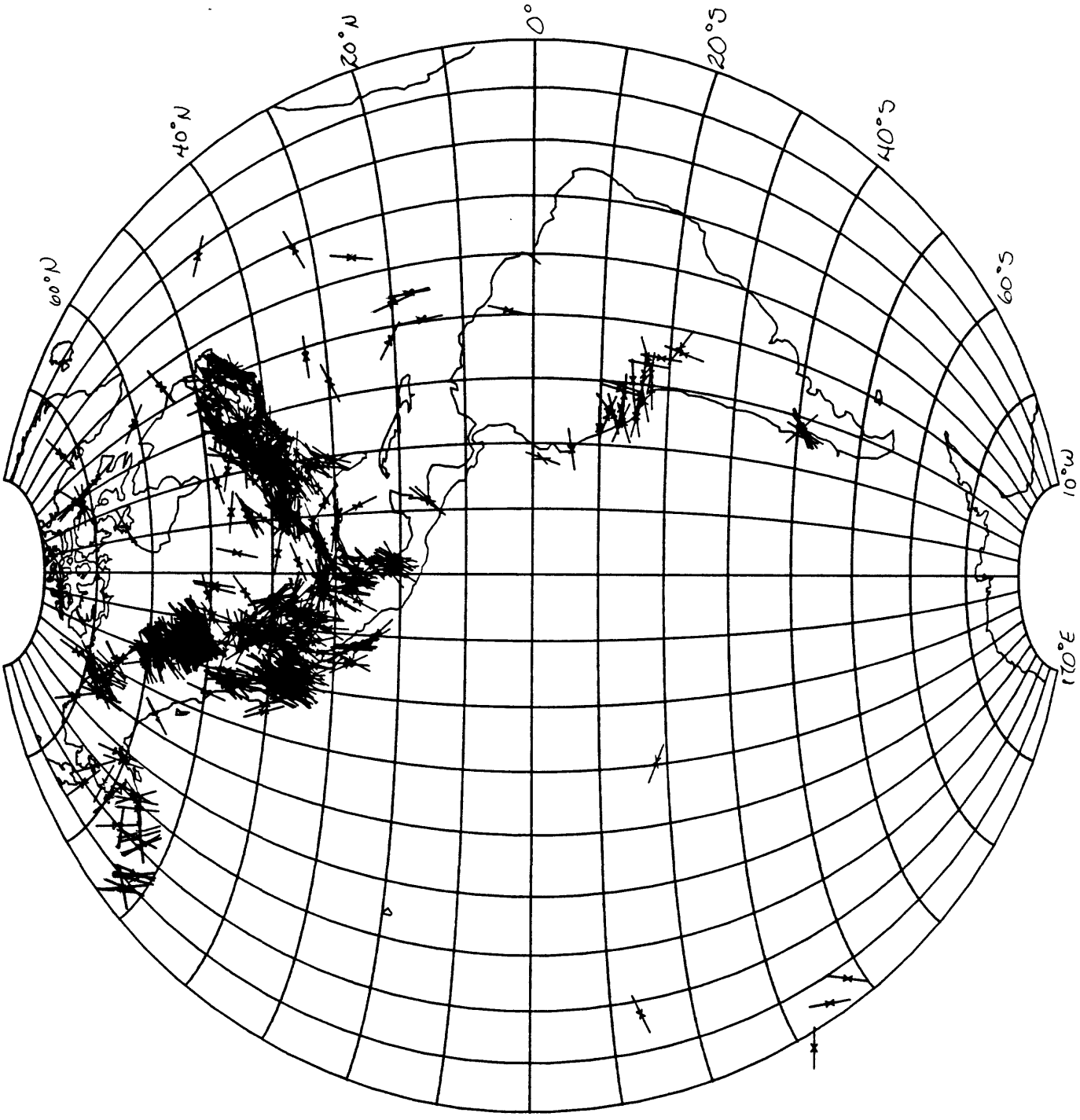

Figure 1. Maximum horizontal compressive stress orientations inferred from earthquake focal mechanisms, in-situ stress measurements, and geologic data. Western hemisphere, data compilation as of Nov. 6, 1986.

Lambert Azimuthal Projection

Approximate scale: 1:110,000,000

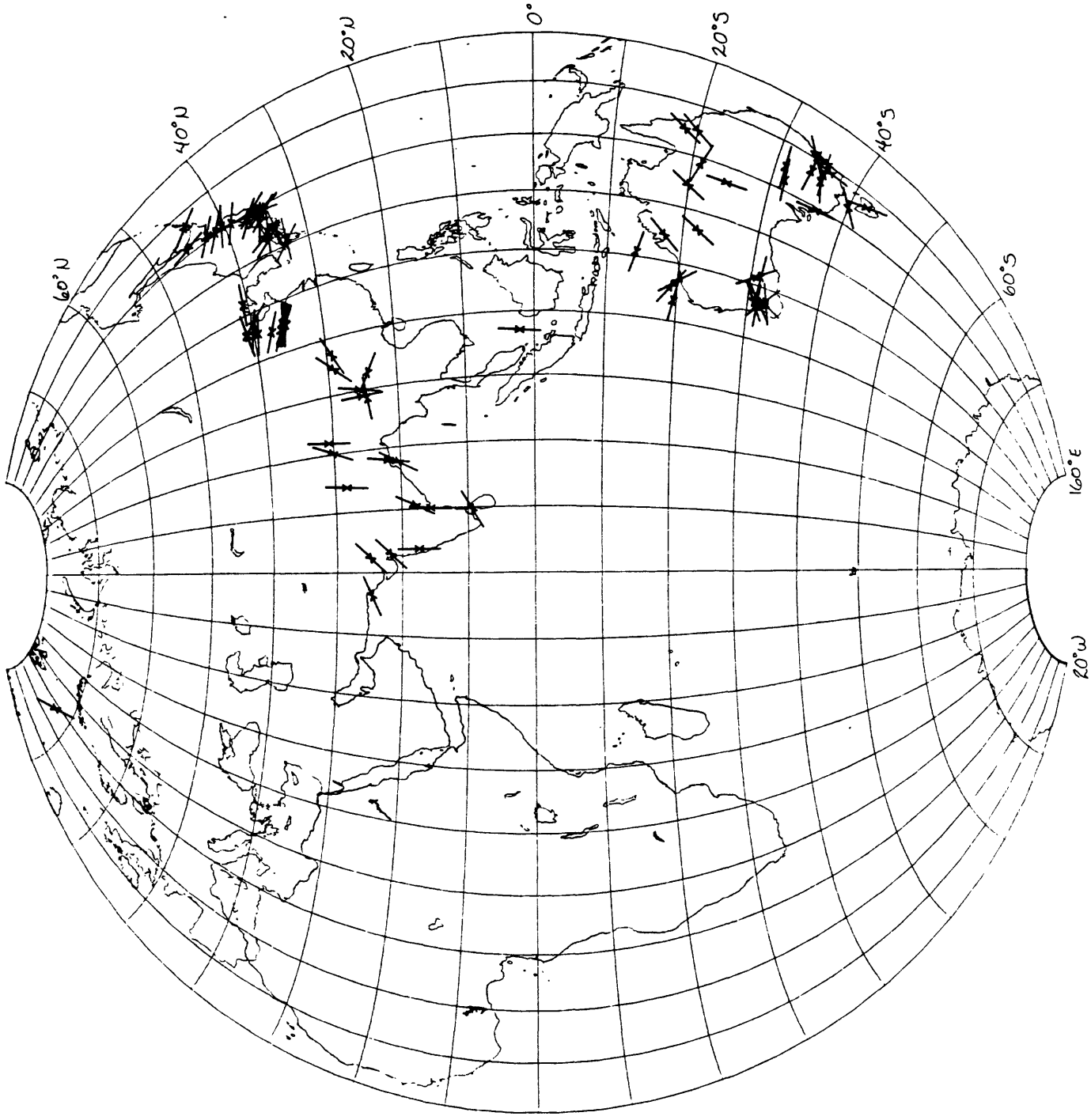

Figure 2. Maximum horizontal compressive stress orientations inferred from earthquake focal mechanisms, in-situ stress measurements, and geologic data. Eastern hemisphere, compilation as of Nov. 6, 1986.

EARTHQUAKE HAZARD EVALUATION
WEST VALLEY FAULT ZONE
SALT LAKE CITY URBAN AREA, UTAH

14-08-0001-22048

Jeffrey R. Keaton
Dames & Moore
250 E. Broadway, Suite 200, Salt Lake City, Utah 84111
Present Address: Center for Engineering Geosciences
Department of Geology, Texas A&M University
College Station, Texas 77843-3115

INVESTIGATIONS

1. Field investigations of previously known and newly discovered scarps in the urban area of Salt Lake County consisted of reconnaissance mapping, trenching, and borings.

2. Stratigraphic and geomorphic interpretations were made on sediments exposed in trenches and sampled in borings and relationships observed on stereoscopic aerial photographs.

3. Slip rates and recurrence intervals were estimated.

4. Consideration was given to the relationship between the West Valley fault zone and the Wasatch fault zone with respect to independent or sympathetic surface fault rupture potential.

RESULTS

1. The West Valley fault zone (initially called the Jordan Valley fault zone by Marine and Price, 1964) comprises two principal traces: the Granger fault on the west and the Taylorsville fault on the east. Both principal traces exhibit normal displacement with the east side down with respect to the west side. The area over which fault scarps are present in the urban area of Salt Lake County (Figure 1) is on the order of 105 square km, substantially larger than indicated on the basis of the early representations of the West Valley fault zone. All scarps indicated north of Utah Highway 201 (2100 South Street) on Figure 1 were discovered during this investigation. Urban development has thoroughly disguised the details of most surface evidence of the most recent few surface rupture events. The character of the faults in the subsurface suggests that they continue south-southeast from the points on Figure 1 where they are shown to terminate.

Convincing evidence of faulting was found at the ground surface in the form of discrete scarps which cut across topography and terrain. Early Holocene (?) distributary channels of the Jordan River below the elevation of the Gilbert shoreline of Lake Bonneville are cut by at least four fault traces over a zone about 4 km wide. Trenches were excavated across the Granger fault at one location and across the Taylorsville fault at two locations. Borings were drilled in the vicinity of the trenches across the Granger fault and at another location on opposite sides of the Granger fault about 3 km to the north.

Two contrasting styles of deformation were observed in the trenches. The Granger fault is characterized by discrete normal separation with Lake Bonneville sediments (Bonneville Alloformation) in contact with pre-Lake Bonneville sediments (Cutler Dam Alloformation). Borings across the Granger fault also penetrated sediments interpreted to

represent the Little Valley Alloformation. Tectonic quiescence during the high stand of Lake Bonneville is suggested by absence of colluvial wedge equivalent stratigraphy intercalated within Lake Bonneville sediments. At least two separate faulting events produced 5.2 to 6.7 m of down-to-the-east separation within the past 12 ka.

The near-surface expression of the Taylorsville fault is characterized by monoclinal flexures that warp Lake Bonneville and younger sediments about 1.5 m down-to-the-east. Minor step faults displace a soil developed on playa and deltaic deposits exposed in the northern of the two trench sites across the Taylorsville fault.

2. Sediments exposed in the trenches on the west (up) side of the Granger fault were interpreted as deposited in relatively deep still water. These sediments consisted of fine to medium sand with interbeds of clay. Samples were taken for dating by thermoluminescence (TL) techniques; the TL dates are summarized in Table 1.

On the east (down) side of the Granger fault, sediments interpreted to be transgressive lake deposits were found overlying a geosol formed in coarse alluvial sediments. The geosol consisted of a weak argillic Bk horizon (7.5YR) with clay films on gravel pieces. The lower part of the lake deposits consisted of well rounded cobbles interpreted to represent a beach environment. Ostracodes were found in deeper water deposits exposed in the trench and encountered in samples extracted from borings; Dr. R.M. Forester (USGS Denver) examined the ostracodes and identified them as *Limnocythere staplini, L. ceriotuberosa, Candona caudata,* and *Cyprideis* sp. Dr. Forester's interpretation of ostracode paleoecology is compatible with stratigraphic interpretations that suggest that these deposits represent the last three deep water lakes in the Bonneville basin separated by subaerial deposits with soil development. Ostracode samples were also submitted to Dr. W.D. McCoy for amino acid dating but the ostracodes apparently were diagenetically modified by ground water and/or pedogenic processes to such an extent that they were not datable. Samples were collected from borings for TL dating; the dates are summarized in Table 1.

Evaluation of morphostratigraphic features of post-Bonneville age proved to be relatively successful despite extensive surface modification due to urbanization. Distributary channels of the Jordan River below the Gilbert shoreline, hence Holocene in age (Currey and Oviatt, 1985), are clearly represented in aerial photographs taken in 1937 and 1946. These channels show at least two episodes of fault displacement: one on the Granger fault and a later one on the Taylorsville fault. The segment of the Taylorsville fault cutting the channel is itself cut by yet another later faulting event. Deposits associated with the most recent lakes are the Bonneville Alloformation, the Cutler Dam Alloformation, and the Little Valley Alloformation which are considered to be approximately 12 to 26 ka, 40 to 76 ka, and 130 ka, respectively (Currey and Oviatt, 1985, McCalpin, 1986, Oviatt et al., 1985).

3. Slip rates and recurrence intervals for surface faulting events on the Granger fault are summarized on Figure 2 for both cumulative and incremental offsets. Remarkable temporal variations are indicated. The slip rates and recurrence intervals are maximum vertical tectonic values because effects of local warping are not known well enough to provide a means for adjustment. The slip rate for the 2 to 4 ka immediately following the rapid decline of the last cycle of Lake Bonneville appears to be fully an order of magnitude greater than for the earlier 100 ka or the subsequent 8 to 10 ka. The hydrostatic loading of the earth's crust by Lake Bonneville appears to have had a significant influence on strain release in the West Valley fault zone region. It appears that strain release was supressed while Lake Bonneville was present because no evidence of fault displacement was observed in the Bonneville Alloformation exposed in the trenches across the Granger fault. Further, it appears that strain release was greatly enhanced as a result of the removal of the hydrostatic loading.

4. The West Valley fault zone clearly represents a surface rupture hazard in the urban area of Salt Lake County. At least three surface faulting events have occurred since Lake Bonneville retreated below the elevation of the Gilbert shoreline (about 11 ka) and they are suspected to be Holocene. The amount of offset of the post-Gilbert ground surface on the Granger fault and on the Taylorsville fault is about 1.5 m on what appears to single-event scarps. Thus, future surface rupture events are also expected to be accompanied by about 1.5 m of offset. The style of deformation on the Granger fault appears to be normal displacement on a discrete fault plane. The style of deformation on the Taylorsville fault consists of monoclinal flexuring accompanied by minor step faulting distributed over a horizontal distance of about 7 m.

Substantial uncertainty exists regarding the relationship of the West Valley fault zone to the Wasatch fault zone. The West Valley fault zone is situated directly west of the only location on the Wasatch fault zone where it deviates substantially from the base of the Wasatch Range. The chronology of surface offsets on the Wasatch fault zone in the immediate vicinity ot Salt Lake City is poorly known and cannot be used to assess possible independent or sympathetic activity on the West Valley fault zone. The Wasatch fault zone is considered to be a west-dipping listric normal fault. The West Valley fault zone is a normal fault zone that dips to the east at about 60° at the surface but its deeper subsurface character is unknown. Fault plane solutions for historic earthquakes in the region of the West Valley fault zone are equivocal, supporting either a shallow west-dipping normal fault or a steep east-dipping normal fault (Pechmann and Thorbjarnardottir, 1985).

A conservative approach based on current understanding is to consider the West Valley fault zone capable of generating earthquakes which are accompanied by surface offsets on the order of 1.5 m. Normal fault offsets on the order of 1.5 m on a world-wide mean basis are accompanied by earthquakes of M_S = 6.9 to 7.3 (Bonilla et al., 1984). The presently understood length of the West Valley fault zone appears to be too short to support magnitudes this large but the total extent of the fault zone has not yet been discovered.

REFERENCES

Bonilla, M.G., Mark, R.K., and Lienkaemper, J.J., 1984, Statistical relations among earthquake magnitude, surface rupture length, and surface fault displacement: Seismological Society of America Bulletin, V. 74, No. 6, p. 2379 - 2411.

Currey, D.R., and Oviatt, C.G., 1985, Durations, average rates, and probable causes of Lake Bonneville expansions, stillstands, and contractions during the last deep-lake cycle, 32,000 to 10,000 years ago: *in* Kay, P.A., and Diaz, H.F., (editors), Problems of and prospects for predicting Great Salt Lake levels: University of Utah Center for Public Affairs and Administration Special Publication, p. 9 - 24.

Marine, I.W., and Price, Don, 1964, Geology and ground-water resources of the Jordan Valley, Utah: Utah Geological and Mineral Survey Water-Resources Bulletin 7, 63 p.

McCalpin, J.P., 1986, Thermoluminescence dating in seismic hazard evaluations: an example from the Bonneville Basin, Utah: 22nd Idaho Symposium on Engineering Geology and Soils Engineering, Boise, ID, February 25-26, 1986.

Oviatt, C.G., McCoy, W.D., and Reider, R.G., 1985, Quaternary lalcustrine stratigraphy along the lower Bear River, Utah: evidence for a shallow early Wisconsin lake in the Bonneville Basin: Geological Society of America, Rocky Mountain Section, Abstracts with Program, V. 17, No. 4.

Pechmann, J.C., and Thorbjarnardottir, Bergthora, 1985, Investigations of an M_L 4.3 earthquake in the western Salt Lake Valley using digital seismic data: U.S. Geological Survey Open-file Report 84-763, p. 340 - 365.

Table 1. Summary of thermoluminescence dates from sediments across the Granger fault in Salt Lake County. Dating was performed by Alpha Analytic Inc of Coral Gables, Florida.

Lab No.	Age ± s.d. (y)	Material	Stratigraphic context
Alpha-2849	90,000±5,000 134,000±8,000	Lacustrine silty sand	Footwall of Granger fault in Cutler Dam Alloformation
Alpha-2850	36,800±6,000	Lacustrine silty sand	Hanging wall of Granger fault in Cutler Dam Alloformation
Alpha-2851	85,000±5,000 198,000±15,000	Lacustrine silty sand	Footwall of Granger fault in Little Valley Alloformation
Alpha-2852	49,000±3,500 88,000±8,000	Colluvial silty sand	Hanging wall of Granger fault in deposits below the Cutler Dam Alloformation

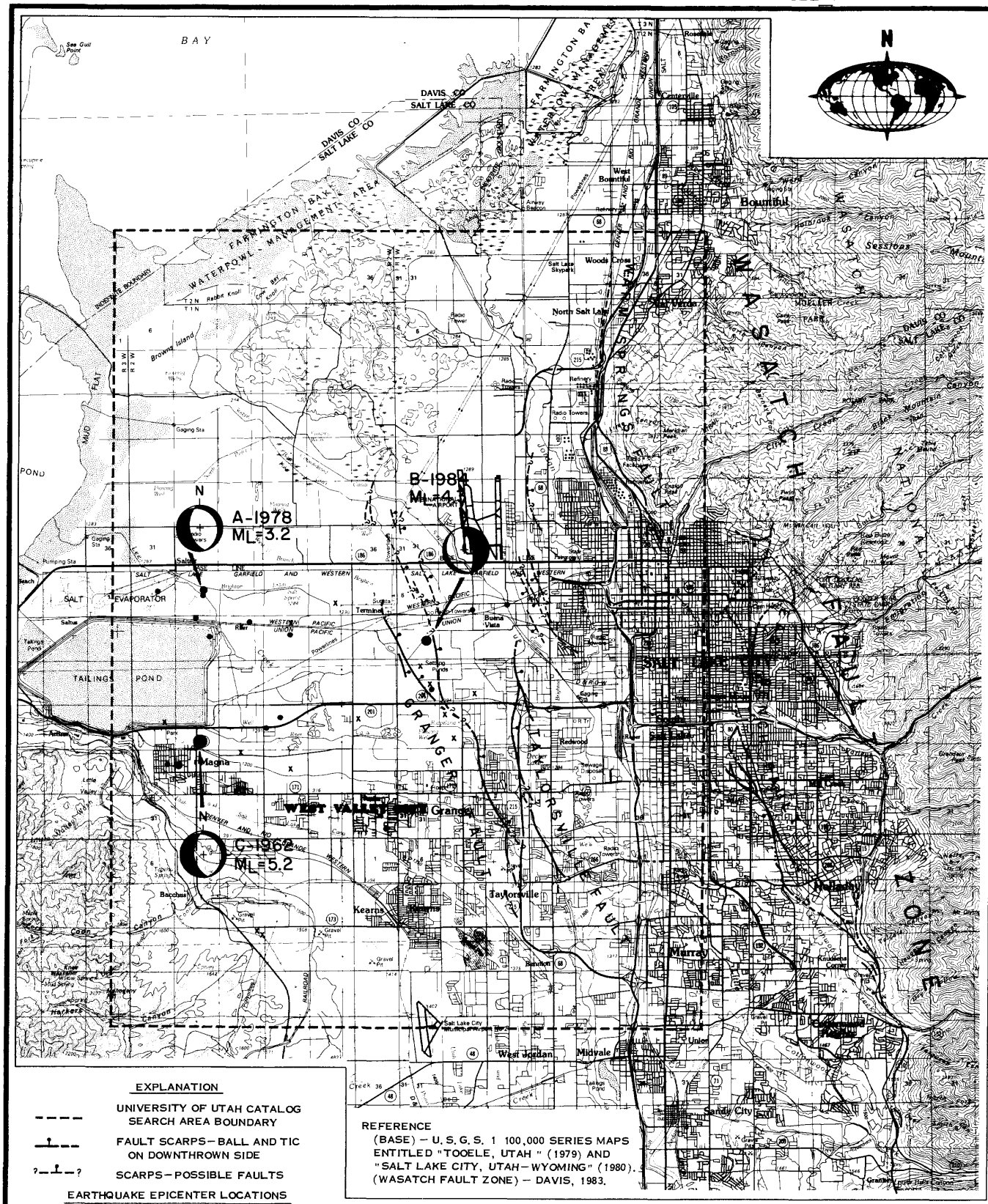

EARTHQUAKE EPICENTER PLOT FOR WEST VALLEY FAULT ZONE
(ALL EVENTS JULY 1962 - DEC. 1985)

Dames & Moore

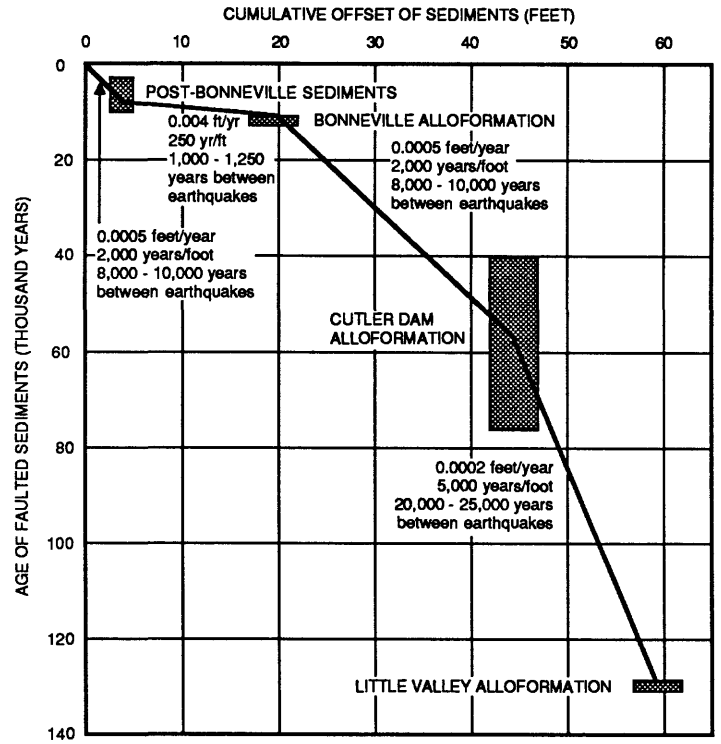

Summary of displacement history along the Granger trace of the West Valley fault zone. Offset of sediments estimated from 1) trench exposures and borings along the major southern part of the fault and 2) aerial photograph interpretation of two separate, sequentially-formed scarps along the northern part of the fault.

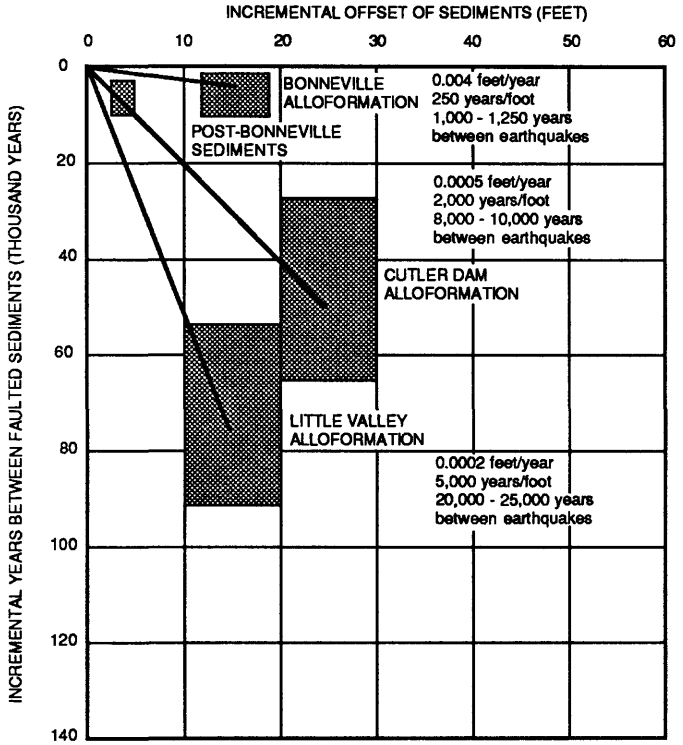

Summary of displacement history along the Granger trace of the West Valley fault zone. Offset of sediments estimated from 1) trench exposures and borings along the major southern part of the fault and 2) aerial photograph interpretation of two separate, sequentially-formed scarps along the northern part of the fault.

Figure 2. Summary of maximum slip rates and recurrence intervals for displacements within the past 140 ka on the Granger trace of the West Valley fault zone in the urban part of Salt Lake County.

Earthquake Hazards Studies, Metropolitan Los Angeles-Western Transverse Ranges Region

9540-02907

R. F. Yerkes
Branch of Western Regional Geology
345 Middlefield Road, MS 975
Menlo Park, California 94025
(415) 323-8111 x 2350

Investigations and results

1. Historic earthquakes. Phase data for 1974 through 1980 earthquakes now accessed, merged, and debugged for routine processing. Several velocity models were reviewed and tested via Hypo 71 against several sample earthquakes located in various geologic settings for efficiency, reproducibility, etc. Data processing programs organized and completed for routine processing by IBM PC-AT. Several hundred events have been processed and fault-plane solutions produced for those events along the Malibu Coast-Santa Monica-Raymond-Sierra Madre-Cucamonga zone. Processing and interpretation continue.

2. Quaternary stratigraphy, chronology, and tectonics, Ventura area (Sarna-Wojcicki, BWRG). This investigation is presently concentrating on: improvement of age control for Quaternary marine deposits in onshore sections such as those of the Ventura basin, developing more detailed oxygen-isotope records, and correlation of marine and continental sequences.

a. Field work in the Ventura area: during late summer, Sarna-Wojcicki, Bob Fehr (BWRG) and Kris McDougall (BPAS) continued sampling and measuring the Balcom Canyon section east of Ventura for tephrochronologic, oxygen-isotopic, and paleoenvironmental analyses. We extended the sampled interval from the base of the previously-sampled section, at the Bailey ash bed (1.2 Ma), down section to the base of the Pico Formation, below the Huckleberry Ridge ash bed (2.0 Ma), into transitional beds of the Repettian stage (ca. 2.5 to 3.4 Ma), and farther down section into the underlying Modelo Formation. A suite of 21 tephra layers was collected from the Modelo Formation. The age range of these beds is about 7.6 to 8.4 Ma, based on diatom biostratigraphy determined by John Barron (BPAS; written commun., 1986). Preliminary analysis of the volcanic glass shards of these tephra layers indicates that several correlate with tephra layers at other sites in the western region: (1) with beds of the marine Monterey Formation at the type section near Monterey, Ca.; (2) with continental beds of Clarendonian age west of Walker Lake in west-central Nevada; and (3) with upper Miocene siliceous and nannofossil muds in DSDP Hole 173 in the northeastern Pacific Ocean, west of Cape Mendocino, Ca.

b. Document displacement of a ca. 6 Ma tephra layer across the San Andreas Fault system, northern California: a tephra layer, dated about 6 Ma by K-Ar analysis and marine biostratigraphy, has been identified by chemical analysis of its volcanic glass at three localities that span the San Andreas Fault system in northern California. The localities are: (1) at the distal margin of the Delgada submarine fan, WSW of the San Andreas Fault (DSDP Hole 34), (2) in the Wilson Grove Formation north of San Francisco, east of the San Andreas Fault and west of the Hayward-Rodgers Creek Fault, and (3) in the

Green Valley Formation east of San Francisco, east of the Hayward-Rodgers Creek and Calaveras Faults. Geology of the first two sites suggests that tephra was transported by streams and marine currents from a source in the Sonoma Volcanics in the central Coast Ranges, across the continental shelf that now forms part of the western Coast Ranges, and down the Delgada sumbmarine canyon to the distal end of the fan. Moreover, facies relations between sediments in which this tephra layer was found suggest that sediments of the latter two sites were once much closer or juxtaposed. Assuming that the transport was generally normal to the San Andreas Fault system, rates of motion calculated from the displacement and the ca. 6 Ma age of this tuff are 3.75 cm/yr for the northern San Andreas Fault, 0.75 cm/yr for the Hayward-Rodgers Creek Fault, and 0.30 cm/yr for the Calaveras-Sunol Fault.

Reports:

Sarna-Wojcicki, A. M., Morrison, S. D., Meyer, C. E., and Hillhouse, J. W., Correlation of upper Cenozoic ash beds in sediments of the western United States and northeastern Pacific Ocean, and comparison with biostratigraphic and magnetostratigraphic data. Accepted by G.S.A. for the Bulletic, 57 MS p. Director approved.

Sarna-Wojcicki, A. M., Meyer, C. E., and Slate, J. L., Displacement of a ca. 6 Ma tuff across the San Andreas Fault system, northern California. Abs. in EOS for AGU Meeting, Dec., 1986, San Francisco.

Adam, D. P., Sarna-Wojcicki, A. M. , and Rieck, H. J., Thick upper Neogene lacustrine sequence in the Tulelake Basin, California and Oregon, U.S.A. Abs. for the G.S.A. Annual Meeting, March, 1986, San Antonio, Texas.

Adam, D. P., Sarna-Wojcicki, A. M., Bradbury, J. P., Dean, W. E., Forester, R. M., and Rieck, H. J., 1986, Tulelake, California: a 3.0-M.Y. core record from the Modoc Plateau. Abs. in American Quaternary Association, Program and Abstracts of the ninth biennial meeting, June, 1986, Champaign-Urbana, Ill., p. 112.

A Demonstration Project with Salt Lake City and Salt Lake County on Risk Analysis, Land Use Planning and Earthquake Hazards Reduction

14-08-0001-G1202

Philip C. Emmi
Department of Geography
University of Utah
Salt Lake City, Utah 84112
(801) 581-5562

Introduction

This demonstration project focuses on the urbanizable area of Salt Lake County. It addresses problems in the utilization of geotechnical information and its assimilation in the local public policy decision making process.

Substantial advances have been made recently in our knowledge of seismologic and related geologic hazards along Utah's Wasatch Front. USGS Open File Reports 84-763 and 86-383 summarize recent progess in understanding these hazards and associated risks. Further studies are currently under development with funding from the Earthquake Hazards Reduction Program. With improved understanding of seismic hazards, we are rapidly approaching a position from which informed action can be taken.

Risk to persons and property can be reduced through effective local governmental action, particularly through land use planning, amendments to zoning and subdivision ordinances, modification of building codes and adjustments in capital improvement programs. Such actions would affect a wide variety of publics and have important political implications. Local legislative bodies are reluctant to endorse such actions without full consideration of commensurate benefits and burdens. In particular, representatives of the Salt Lake City Corporation and the County of Salt Lake have indicated an interest in reducing exposure to geologic hazards, but they first want a clearer sense of the distribution and magnitude of risks and the likely effects of various mitigation options. The objectives of the demonstration project are to assess risk, evaluate mitigation options and assist local public bodies in assimilating advances in regional seismology and translating this knowledge into a coherent program of public action.

In order to assimilate seismologic research into local policy formulation, five core activities have been proposed. These activities are listed below and the relationship among activities is protrayed graphically in Figure 1.

A. Create a policy-relevant framework for the compilation of information on seismologic and related geologic hazards,
B. Integrate that information into an expandable, computer-based, geographic information system (GIS) with digital mapping capabilities,
C. Use GIS and computer mapping capabilities to assess risk and to model and map the effects of alternative mitigation policies on the

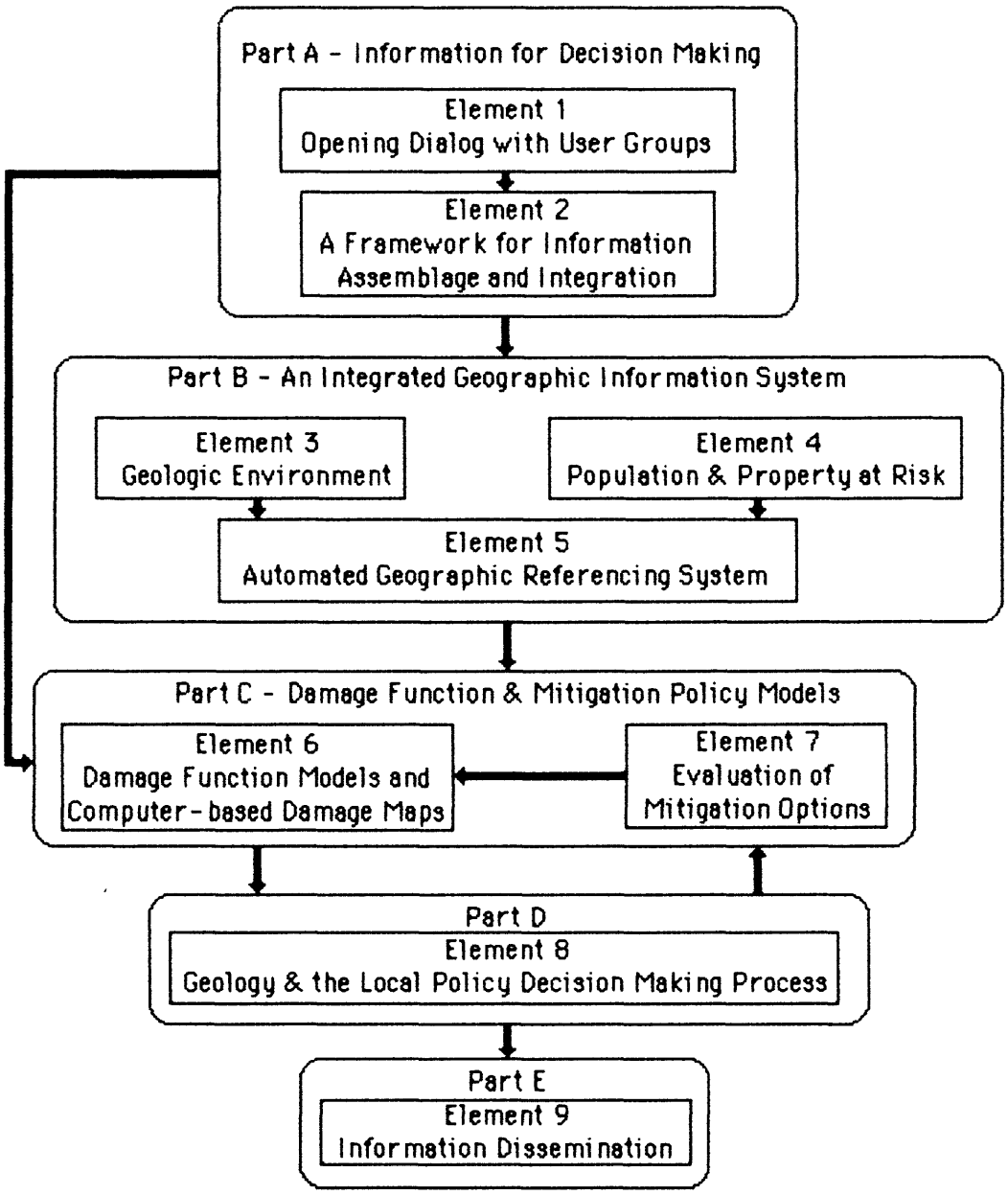

Figure 1. Schematic Representation of the Conceptual Framework

extent and spatial distribution of risk,

D. Initiate, with staff to the City and County Planning Commissions, a public policy decision process to consider local seismic hazard mitigation policy options, and
E. Produce an educational package for use by other communities within the Wasatch Front Region.

The first two parts of this project (i.e., items A and B above) have been funded. Efforts to date are detailed below.

Part A-Information For Decision Making

Activies under Part A were designed to orient both team members and information users to the problems and possibilities of assimilating technical perspectives into a politically charged public policy decision process. Meetings were held with professional staff of the Salt Lake City and Salt Lake County Planning Comissions. Geo-hazard reduction goals, mitigation policy options, and information needs were discussed. Preliminary arrangements for information exchange and technical assistance were made.

Part B-An Integrated Geographic Information System

After the information needs were determined, the following mapped data sets for the study area were acquired over from over a dozen different sources. This mapped data set was registered to a common projection and scale in preparation for digitizing:

Population, property at risk, critical facilites, and boundaries

1) Study area boundary
2) Public land survey system
3) School location and enrollment
4) Major water lines
5) Traffic zones & census tracts
6) Hospitals and nursing homes
7) Projected land use in 2005
8) Major natural gas pipelines
9) Electrical transmission network
10) Sewage/storm sewer network
11) Fire and police stations/jails
12) Major hotels and occupancy

The geologic environment

1) Critical acceleration for liquifaction
2) Ground slope failure mode
3) Ground shaking
4) Tectonic deformation
5) Depth to groundwater (in production)
6) Faults in quaternary deposits

Tabular data sets were also collected. These data sets and their geographic references are listed below:

Population and property at risk

1) Population (1985) by traffic zone
2) Population projections for 2005 by traffic zone

3) Total acreage used for transportation, utilities, residential, and commercial structures referenced by traffic zone
4) Total number of dwelling units (1985) by traffic zone
5) Individual residential structure attributes referenced by census block and township/range on:

   a. Type of construction
   b. Year of construction
   c. Effective age
   d. Number of stories
   e. Replacement cost
   f. Fair market value

6) A stratified uniform sample of individual commercial structure attributes referenced by township/range and Sidwell number:

   a. Type of construction
   b. Type of framing
   c. Quality of construction
   d. Year of construction
   e. Number of stories
   f. Building use
   g. Replacement cost
   h. Market value

Three tasks remain. First, the commercial structure data must be entered into the database. Secondly, the mapped data must be digitized and linked to the appropriate digitized reference systems. Third, the digital data sets must be delivered to USGS in digital format as stated in the grant contract. It is anticipated that these tasks will be completed by December 19, 1986.

Experimental Investigation of Liquefaction Potential

9910-01629

Thomas L. Holzer
Branch of Engineering Seismology and Geology
U.S. Geological Survey
345 Middlefield Road, MS 977
(415) 323-8111, Ext. 2760

Investigations

1. Design and installation of an instrumented site in Parkfield, California, to monitor pore pressures in sands and strong ground motion during the predicted Parkfield earthquake.

2. Evaluation of magnitudes of ground settlement during liquefaction and the effect of the densification on the liquefaction resistance to future earthquakes.

Results

1. Drilling, sampling, and installation of casing and pore-pressure transducers were completed at the Parkfield liquefaction array site. In addition, a network of bench marks was installed and surveyed at the site. The site when completed will consist of four downhole accelerometers at depths ranging from 3 to 30 m, a surface accelerometer, eight pore-pressure transducers at depths ranging from 5.2 to 15.2 m, an inclinometer casing, and a network of eight shallow bench marks referenced to two deep bench marks set below the liquefiable sand layer. The following components are presently operational: two downhole acclerometers, five pore-pressure transducers, the inclinomter casing, and the bench mark array.

2. Computer programs have been prepared for estimating ground settlement from compaction of sand layers during earthquakes. Compaction of both dry and saturated sand deposits is computed and the occurrence of liquefaction is taken into account.

Reports

Holzer, T.L., Bennett, M.J., Youd, T.L., Chen, A.T.F., 1986, Identification of a site to monitor liquefaction during the predicted 1988 Parkfield earthquake, Cholame Valley, California (abs.): *Association of Engineering Geologists Abstracts with Program*, Annual Meeting, 29th, San Francisco, p. 51.

Tinsley, J.C., Youd, T.L., Perkins, D.M., and Chen, A.T.F., 1986, Improving predictions of liquefaction potential, in Proceedings, Conference XXXII on Future directions in evaluating earthquake hazards of southern California: *U.S. Geological Survey Open-File Report, 86-401*, p. 293-297.

Near-Surface Lithologic and Seismic Properties

9910-01168

W.B. Joyner
J.F. Gibbs

Branch of Engineering Seismology and Geology
U.S. Geological Survey
345 Middlefield Road, MS 977
Menlo Park, California 94025
(415) 323-8111, ext. 2754, 2910

Investigations

Measurement of seismic velocity and attenuation to determine the effect of local geology on strong ground motion and to aid in the interpretation of seismic source parameters.

Results

We have survey a 195-meter, steel-cased drill hole near Parkfield for P- and S-wave velocity. Preliminary analysis shows no indication that the steel casing interfers with velocity determination.

We have also cooperated with H.-S. Liu and R.E. Warrick in measuring attenuation in San Francisco Bay mud at a site in Foster City, California.

Reports

Joyner, W.B., 1986, Strong-motion sesimology: *Reviews of Geophysics and Space Physics*, manuscript in review.

West Valley City Earthquake Hazards Reduction Program

West Valley City, Utah

14-08-0001-G1079

April 1, 1986 through March 31, 1987

Joseph L. Moore, Community Development Director
West Valley City
2470 South Redwood Road
West Valley City, Utah 84119
(801) 974-5501

Investigations:

I. The first objective is to research information about the geophysical and seismological features in the Jordan Valley, the Wasatch Range and the Oquirrh Range which are the most pertinent to the West Valley City area. The intention is to locate the potential geological hazards in and around our study area so that these can be considered in building policy decisions.

II. The second objective is to map these potential geologic hazards over our city basemap, using our computer mapping system, so that this information is as accurate as possible. This will be developed into a series of map overlays which will eventually reveal zones of potential geologic hazards within the city.

III. The third objective is to research zoning and building codes and ordinances which address and regulate geological hazards. The intention is to study case law which will guide the writing of such ordinances, as needed, for the city.

IV. When the above objectives are completed the information will be analyzed in light of the goal of forming reasonable policy proposals. This analysis will include delineating potential single and multiple geological hazard zones within the city and mapping them as such.

V. The final objective is to develop a "Hazards Mitigation Plan" for growth strategies and construction regulation in the study area within West Valley City. This goal will be to incorporate the findings from the geological studies into the long range plans for the areas analyzed in the city.

Results:

1. The research phase of the geological/seismological studies is completed. We have relied on the local experts in these fields for guidance in the research phase of the project. These experts include Walter Arabaz, University of Utah Seismological Station; Donald Currey, University of Utah Geography Department; Genevieve Atwood and Doug Sprinkle at the Utah Geological and Mineral Survey; Jeffery Keaton, Dames and Moore Engineering; and Loren R. Anderson, Utah State University. A large number of monographs and maps have been assembled, which specifically relate to our study area. Many of the studies are unpublished drafts being done as part of this same U. S. G. S. Wasatch Front cycle of studies. These have proven invaluable to the research, as they tend to be very specific to our study area. Much of this knowledge would have been unavailable two years ago, and this is the first time it has been aggregated for this type of site specific study. In this aspect the study can serve as a model for other local governments along the Wasatch Front that wish to get involved in geological hazards mitigation planning.

2. The computer mapping is proceeding at a pace that will see it done in a timely fashion for the final geological hazards analysis phase of the project. Some interesting scaling effects have been encountered due to widely divergent scales in the original source materials.

3. The research is continuing in the area of zoning and building codes which address the regulation of geological hazards. This is a small body of work compared to that of the geological related research. There is not a great deal of case law about these kinds of problems which would pertain to Utah State Statute. The most enlightened examples we have reviewed come from local governments in California. Our goal is to begin to compose model ordinance(s) which will eventually be proposed to the West Valley City Council for adoption.

4. The analysis phase of the project is a on-going process as the research is done. The mapping portion of the analysis is nearing completion. There are many overlay scenarios yet to do which will be crucial to interpolating and defining potential geological hazard areas. This phase will be the most crucial when it evolves to the format of corroborative evidence for an ordinance proposal.

5. The development of the "Hazards Mitigation Plan" will take the remainder of the grant funding period. The plan only addresses a part of the city. It is anticipated that Phase II of the study will allow us to complete the study for the entire city.

October 3, 1986

SEISMIC BIBLIOGRAPHY

Books:

Arabasz, Walter J., et al. Earthquake Studies in Utah 1850 to 1978. University of Utah: July, 1979.

Arabasz, Dr. Walter J. Seismic Environment of the Intermountain Region. The University of Utah.

Atwood, Genevieve. Governor's Conference on Geologic Hazards. December, 1983.

Cluff, Lloyd S., Brogan, George E., Glass, Carl E. Wasatch Fault, Earthquake Fault Investigation & Evaluation, A Guide to Land Use Planning. Woodward Clyde & Associated for Salt Lake City Utah, (1970).

County of San Diego. Seismic Safety Element Part V. Environment Development Agency, Jan., 1975.

TITLE? City of San Diego. Engineering and Development Department. July 1982.

Gauchat, Urs P., Schodek, Daniel L., Luft, Rene. Patterns of Housing Type and Density: A Basis for Analyzing Earthquake Resistance. N. S. F. Grant No. PFR-7800-258. Boston, Mass: Dept. of Architecture, Harvard University, 1984.

Goode, Harry D. Field-Trip Guide Environment Geology of the Middle Wasatch Front, Utah Salt Lake City to Ogden. DATE? PUBLISHER?

Hays, Walter W., Complied by Costello, Joce A. TITLE? Department of the Interior U.S. Geolocical Survey. DATE?

Hays, Walter W. and Gori, Paula L. complied by Kitzmiller and Downer, Lynne. Open file Report 84-763 Salt Lake City, Utah. U. S. Geologial Survey. DATE? LOCATION?

Hilpert, Lowell S., et al. Environmental Geology of the Wastatch Front. Utah Geological Association, Publication 1. 1971. LOCATION?

Keaton, Jeffrey R., Currey, Donald R., and Olig, Susan J. Paleoseismicity and Earthquake Hazards Evaluation Salt Lake City, Utah. Salt Lake City, Utah: Department of Geography and Department of Geology and Geophysics, 1985.

Menard, H. William. Progress Seismic Zonation in the San Fancisco Bay Region. 1979. PUBLISHER?

Richins, William D., et al. Earthquake Data for the Utah Region Jan. 1, 1981 to Dec. 31, 1983. Salt Lake City Utah: University of Utah, August, 1984.

Schnell, Mary L. and Hero, Darrell G. National Earthquake Hazards Reduction Program: Report to the United States Congress. U. S. Geological Survey Circular 918. Alexandra, Va.

Steinbrugge, Karl U. Earthquakes, Volcanoes, and Tsunamis. New York, N. Y., 1982.

U. S. Geological Survey. National Earthquake Hazards Reduction Program. Anchorage, Alaska, March 27, 1964.

U. S. Geological Survey. TITLE?. Open-file Report 76-89, 1976.

U. S. Geological Survey (1976). A Study of Earthquake Losses in Salt Lake City, Utah, Open file report 76-89. U. S. G. S.

U. S. Geological Survey. National Earthquake Hazards Reduction Program. California, May, 1983.

U. S. Geological Survey. Reducing Losses from Earthquakes Through Personal Preparedness. Open-File Report 84-765, 1984.

U. S. Geological Survey. Model Recovery Program, Open-file report 85-371 from ICSSC TR-6 Committee members. July, 1984.

U. S. Geological Survey. Evaluation of Regional and Urban Earthquake Hazards and Risk in Alaska. Open-File Report 86-79, September 5-7, 1985.

U. S. Geological Survey. National Earthquake Hazards Reduction Program, Open-File Report 86-383, 1986.

Utah Seismic Safety Advisory Council. Earthquake Safety in Utah and Recommendations for Risk Reduction, Salt Lake City, Utah, 1981.

Wallace, Gwynn J. Great Salt Lake Field Trip. March 19, 1978.

Woodward, Clyde and Associates. Wasatch Fault Earthquake Fault Investigation and Evaluation. Oakland, California. DATE?

Wyner, Alan J., Mann, Dean E. Preparing for California's Earthquakes: Local Government and Seismic Safety. Berkeley, California: University of California, Berkeley, 1986.

Articles:

Anderson, Ernest R., and Barnhard, Theodore R. Neotectonic Framework of the Central Sevier Valley Area, Utah. 1986. PUBLISHER?

Arnold, Christopher,and Reitherman, Robert. Building Configurations Seismic Design. Salt Lake City, Utah.

Atwood, Genevieve and Mabey, Don R. Earthquake Hazard Reduction In Utah. 1986.

Bapis, Jim. Geography Means a World of Difference. University of Utah, Salt Lake City, Utah: August/September, 1985.

Currey, Donald R. Paleolake History in Reconstructing Neotechtonic History and Assessing Earthquake Hazards. March, 1986. PUBLISHER?

Downick, D. J. Earthquake Resistant Design.

Machette, Michael N., Personius, Stephen F. Quaternary Geology Along the Wasatch Front. 1986.

French, Steven P., and Isaacson, Mark S. "Applying Earthquake Risk Analysis Techniques to Land." Journal of the American Planning Association, 1984. VOL.?

Gill, Harold. Utah Geological and Mineral Survey Excavation Inspection Program. 1986.

Guffirida, Louis O. FEMA Newsletter. Washington: July/August 1985. ARTICLE?

Hays, Walter. Making the Implementation Process of the National Earthquake Hazards Reduction Program Work In Utah. U. S. Geological Survey, 1986.

Hays, Walter W. Evaluation of Local Site Amplification of Earthquake Ground Motion. U. S. Geological Survey, 1986. LOCATION?

Highland, Lynn M. Earthquake Hazards to Domestic Water Distribution Systems. U. S. Geological Survey, 1986.

Kaliser, Bruce N. Thematic Mapping Applied to Earthquake Hazard Reduction. U. S. Geological Survey, 1986.

Keaton, Jeffrey R., and Reaveley, Lawrence D. Utah Earthquake Hazards Workshop. Salt Lake City, Utah, July 18, 1986.

King, Kenneth W., Effects on Site Geology on the Level of Ground Shaking Along the Wasatch Front. U.S. Geological Survey, 1986.

Kockelman, William J., Five Critical Elements for Reducing Earthquake Hazards. U.S. Geological Survey, 1986.

Kockelman, William J., Some Techniques for Reducing Landslide Hazards. 1986.

Lund, William and Schwartz, David. Evaluation of Fault Behavior and Earthquake Recurrence at the Dry Creek Site. 1986.

McCalpin, James, Robison, Robert M., and Garr, John D., Neotechtonics of the Hansel Valley-Pocatello Valley Corridor, Northern Utah and Southern Idaho. 1986.

Machette, Michael, Lung, William, and Arabasz, Walter. Triad for Tectonic Framework and Earthquake Potential of the Wasatch Front Area and Other Parts of Utah. July 14, 1986.

Machette, Michael, Personius, Stephen and Scott, William. Quaternary Geology Along The Wasatch Front. 1986

Miller, Richard D., Steeples, Don W., King, Kenneth W. and Knapp, Ralph W., In Situ Poisson's Ratio Measurements near Provo, Utah. October 1985. U.S. Geological Survey, 1986.

Nelson, Alan R. and Sullivan Timothy J., Late Quaternary History of the James Peak Fault, Southermost Cache Valley. 1986. U.S. Geological Survey, 1986.

Oaks, Sherry D., 1934 Hansel Valley, Utah Earthquakes. U.S. Geological Survey, 1986.

Perkins, David M. and Bender, Bernice K., Mathematical Modelling of Potential Large Earthquake Occurrences and Implications for Wasatch Hazard. U.S. Geological Survey, 1986.

Ringholz, Raye C. the Inevitability of Earthquake. Utah Holiday 1 Jan. 1981.

Rogers, Albert, Smith, Robert and Ward, Delbert. The Ground Shaking Hazard & Various Aspects of Loss Estimation in the Wasatch Front Area of Utah. July 1986.

Seismic Safety Advisory Council State of Utah. Earthquake Safety in Utah and Recommendations for Risk Reduction Salt Lake City Public Library, May 19, 1981.

Smith, Robert B. and Richins, William D. (1984). Seismicity and Earthquake Hazards of Utah and the Wasatch Front: Paradigm and Paradox. U. S. G. S. Workshop" Evaluation of Regional and Urban Earthquake Hazards and Risk in Utah, Salt Lake City, Utah.

Slosson, James E., Legal Issues Related To Hazard Mitigation Policies. 1986.

Taylor, Craig E., Ward, D.B., and Haber, J.M., Earthquake Loss Estimates for Utility Systems and State-Owned Buildings in Salt Lake and Davis Counties. 1986.

Thompson, Duane. Hazards, Vol. 20, No. 30. Vail, Colorado - S/25/85. Pg. 16.

Periodicals:

Arabasz, Walter J., Smith, R. B., and Richins, W.D. Earthquake Studies Along the Wasatch front, Utah. Vol. 70. No. 3. p.p. 1479-1499, October 1980.

Gori, P.L. Wasatch Front Forum. "Earthquake Hazards program." Vol.1 No. 4. Spring 1985.

Hays, Walter. Wasatch Front Forum. "Earthquake Hazards Program." Vol. 1. No. 3. March 1984.

Hays, Walter. Wasatch Front Forum. "Earthquake Hazards Program." Vol. 1. No. 2. September 1984, published by the Utah Geological and Mineral Survey.

Hays, Walter, and Gori, Paula. Wasatch Front Forum. "Earthquake Hazards Program." Vol. 11, No. 2 Winter 85.

Jarva, Jamine. Wasatch Front Forum. "Earthquake Hazards Program/" Vol. 11 No. 1. Fall 1985.

Kockelman, William J., Wasatch Front Forum. "Earthquake Hazards Program." Vol. 11, No. 3. Spring 1986.

Marine, Wendell and Price, Don . Geology and Ground-Water Resources of the Jordan Valley, Utah, Water Resources bulletin, Utah Geological and Mineral Survey, Salt Lake City, Utah: (Dec. 1964).

Wallace, Gwynn, J. Survey Notes Vol. 18, No. 1. Utah Geological and Mineral Survey, Spring 1984.

Utah Geological Mineralogical Survey Staff. Survey Notes Vol. 18, No. 4. Utah Geological and Mineral Survey, Winter 1985.

Tingey, James L. and Findlay, Ralph F., Emergency Management in Utah for Earthquakes. 1986.

U. S. Geological Survey Committee Members Triad IV. Collecting, Compiling, Translating, and Disseminating Earthquake-Hazards Information for Urban and Regional Planning and Development in the Wasatch Front Area. July 17, 1986.

Wheeler, Russell L., A Statistical analysis of segmentation of the Wasatch Fault. U.S. Geological Survey, 1986.

Zoback, Mary Lou, Interpretation of a 30km Seismic Reflection Profile. 1986. U.S. Geological Survey, 1986.

Maps:

Anderson Larry W., and Miller, Darryl G. "Quaternary Fault Map of Utah. Fungro, Inc. Long Beach, CA U.S.A. 1979.

Anderson, Loren R. Keaton, Jeffery R., Aubry, Kevin, Ellis, Stanley J. "Liquefaction Potential Map, Salt Lake County, Utah." Utah State University and Dames & Moore Consulting Engineers, Salt Lake City, Utah 1982.

Davis, Fitzhuch D. "Geologic Map of the Central Wasatch Front, Utah," Map 54-A. Utah Geologial and Mineral Survey, Utah Department of Natural Resources, May 1983.

Miller, Rovert D. "Surficial Geologic Map Along Part of the Wasatch Front, Salt Lake Valley, Utah;" Map MF1198. U. S. Geological Survey, Department of Interior, 1983.

Tooker, E. W., and Roberts, Ralph J. "Geologic Map of the Magna Quadrangle, Salt Lake County, Utah," Map 6Q-923. U. S. Geologic Survey, Department of Interior, 1979.

Hintze, Lehi F. "Geologic Map of Utah", Utah Geological and Mineral Survey, Utah Department of Natural Resources, 1980.

Van Horn, Richard. "Surficial Geologic Map of the Salt Lake City South Quadrangle, Salt lake County, Utah," Map 1-1173. U. S. Geological Survey, Department of Interior, 1979.

Reports:

Anderson, Loren R., et al. Liquefaction Potential Map for Davis County, Utah. Utah State University, Logan, Utah Feb. 1982.

Committee Members. Intergovernmental Hazard Mitigation Report. The State of Utah Aug. 1, 1983.

Seismic Safety Advisory Council State of Utah. Seismic Zones for Construction in Utah. Sept. 1979.

Ziony, J.I. et al. Evaluating Earthquake Hazards in the Los Angeles Region An Earth-Science Perspective. United States Government Printing Office. 1985

Techniques for Applying Earthquake Hazard Map Data--San Francisco Bay Area, California

14-08-0001-G1166

Jeanne B. Perkins
Association of Bay Area Governments
MetroCenter
Eighth and Oak Streets
[P.O. Box 2050--Oakland, CA 94604]
(415) 464-7934

INTRODUCTION

For the past several years, ABAG has been developing computer-based maps and map files of the San Francisco Bay Area depicting earthquake hazards. The information currently is underutilized. ABAG is working to correct this situation. As a first step, ABAG staff has conducted a comprehensive survey of local government staff in the Bay Area to identify past applications of ABAG research products and potential needs of this user community. This report summarizes the results of the survey.

SURVEY PROCEDURE

These conclusions were gathered by mailing an eight-page questionnaire in early July 1986 to local government staffs--all city and county managers and administrators, building officials, planning directors, and public works directors, and many fire chiefs. The offices of emergency services for the nine counties, San Jose and Oakland, as well as the five staff geologists were also mailed questionnaires. After three months, 185, or 35%, of the 518 questionnaires had been returned. At least one questionnaire was returned by 84% (89/106) of the jurisdictions. Follow-up telephone interviews were conducted with 66 of the respondents, focusing on existing use of ABAG work and on clarifying future needs. Approximately 18% had been personally living in their current jurisdiction when it was hit by a damaging earthquake.

PERCEPTIONS OF EARTHQUAKE HAZARDS BY LOCAL GOVERNMENT STAFF IN THE BAY AREA

Local government staff members described the level of *public awareness* of earthquake hazards in their jurisdictions as *moderate to moderately high.* They rated seismic safety slightly higher--a *moderately high priority*--as a *policy issue* within their own local government. Most believed that there *probably will be an earthquake* that causes moderate to severe property damage within their jurisdiction within the next fifty years.

Those surveyed were asked to rank a series of earthquake-related hazards based on how great they perceived this problem to be *within their own city or county.* (Note: 4=extremely serious problem, 3=somewhat serious problem, 2=not a very serious problem, and 1=not at all a problem.) As the graph below indicates, based on average (weighted mean) responses, proximity to faults ranks first, followed by disruption of surface transportation, disruption of power, curtailment of water supply and resultant fire hazard, and weak soils under building foundations. It is interesting to note, however, that the ranking of hazards based on responses for a question on the **one** item perceived to present the greatest problem yields different results. Here old brick/masonry buildings

ranks first, followed by the possibility of major damage to "critical" facilities, floods due to dam or dike failure, and proximity to faults.

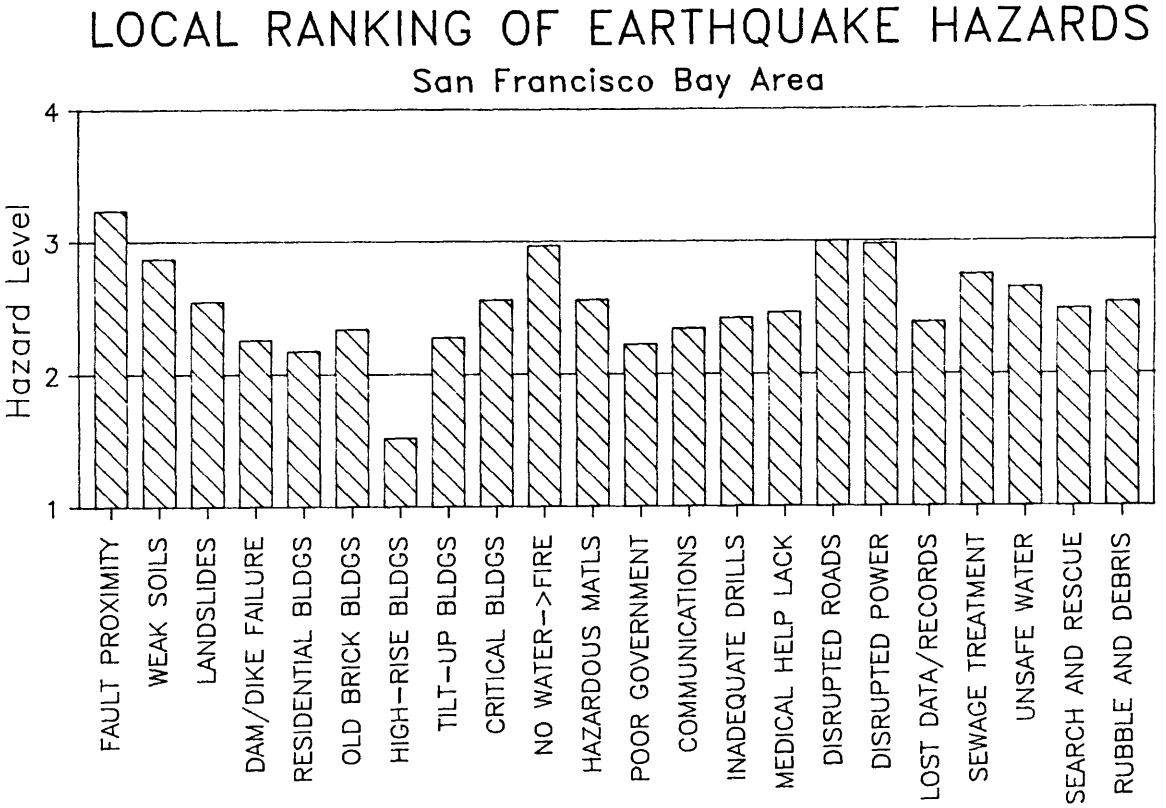

EXISTING AND POTENTIAL POLICIES AND PROGRAMS

Local governments have the ability to institute a number of policies and practices to help deal with the earthquakes. The most common uses include:

- o a disaster response plan;
- o the safety (including seismic safety) element of the General Plan;
- o soil studies for new construction;
- o geotechnical studies for new construction;
- o public information and education; and
- o procedures for reviewing proposed new developments.

Moderate use has been made of:

- o land use or zoning restrictions;
- o building inspection programs;
- o reconstruction/redevelopment plans;
- o special building design requirements;
- o disclosure requirements about earthquake hazards; and
- o back-up data or record storage/processing techniques.

Least common are:

- o hazardous building retrofit/abatement programs;
- o posting of signs on dangerous private or public structures; and
- o special requirements for non-structural components.

During the last five years, the most work has occurred in revising disaster response plans and public information and education programs. Least work has occurred on the three least common programs listed above. Two-fifths of those surveyed indicated they had additional programs other than those listed.

The three strategies not being used by cities that were listed as most important were:
#1--hazardous building retrofit/abatement programs;
#2--public information and education; and
#3--building inspection.

It is interesting to note that several respondents (21) indicated that public education programs exist in their jurisdictions, yet they perceived this as an important lack. The reason appears to be the perception that existing education programs are inadequate. However, most described their jurisdiction's "state of preparedness" as *reasonable*.

USE OF ABAG HAZARD MAPPING BY LOCAL GOVERNMENTS

Local government staff provided the following examples of use of ABAG research.
1. The Alameda County General Plan's seismic safety section refers to ABAG earthquake hazard maps as useful in defining earthquake hazards in the County.
2. Pleasant Hill reviewed ABAG's hazard maps in the process of updating its General Plan and developing requirements for soil and geotechnical studies for new construction.
3. Marin County used ABAG's hazard maps in developing the seismic safety portion of its General Plan. These maps have become source material for geotechnical studies, disclosure requirements, land use/zoning decisions, disaster response planning, and public information/ education programs.
4. The City of Napa references ABAG hazard maps in the seismic safety section of its General Plan.
5. San Francisco's building staff is working with ABAG to obtain data from four of the hazard maps on computer tape for each of their unreinforced masonry buildings as part of their hazardous building inspection program. San Francisco's planning staff used the hazard maps as background data for public information and education.
6. San Mateo County has used ABAG hazard maps as background information and for planning their public information and disclosure programs.
7. Daly City will be using ABAG hazard maps in the update of the seismic safety element of its General Plan. Staff will be ordering the maps at a more detailed scale from Geogroup Corp., ABAG's computer consultants.
8. Santa Clara County used the early land capability data in the preparation of the County's seismic safety element. Later hazard maps were used in reviewing geotechnical studies and public information programs.
9. In Campbell, ABAG maps are among the several sources of hazard maps used by consultants in implementing the General Plan policies for individual projects.
10. Gilroy has merely examined the hazard maps and used them as background reference information for soil and geotechnical studies for new construction, its disaster response plan, and public information and education.
11. Mountain View used ABAG hazard maps in public and staff meetings to help describe earthquake problems and gain support for mitigation programs such as building inspection, soil and geotechnical studies, and review of land use and zoning policies.
12. San Jose has referred consultants to ABAG hazard maps when they prepare geotechnical reports for new construction.
13. Santa Clara used the hazard maps as background information when revising its disaster plan and public information program, as well as for implementing its geotechnical study

requirement and the seismic safety portion of its General Plan.
14. Sunnyvale used the ABAG hazard maps as one source of map data in preparing the seismic safety portion of its General Plan. Therefore, these maps have been used indirectly in their land use and zoning programs, disaster response plans, and public information and education programs.
15. Dixon used these maps as background information as the City reviewed its land use and zoning programs, as well as its procedures for reviewing proposed new developments.
16. Vallejo is examining the hazard maps and is considering ordering the maps at a more detailed scale for use in their revised General Plan.
17. Sonoma County is using ABAG hazard maps in describing the earthquake threat as part of its public information program. These maps are also referenced in the safety element of the General Plan, a policy document that summarizes the disaster response plan. ABAG staff worked with the planning department to provide one map at a more detailed scale.
18. Petaluma ordered four of the ABAG hazard maps at a more detailed scale from ABAG's consultants. These maps were provided to the City's consultants in their current revisions of the General Plan.

FUTURE RESEARCH PRIORITIES

In an effort to design future research products to more effectively respond to the needs of local governments, the staff members were asked to rank the usefulness of various research and training topics. As shown below, *professional training* was considered to have the potential for the most direct impact on local earthquake programs. These needs were followed by a desire for *written-materials* on ABAG's hazard mapping *focused toward non-technical decision-makers*. Follow-up phone calls asking the reason for this work pointed out the need to convince local elected officials and planning commissioners of the extent of earthquake hazards in their community.

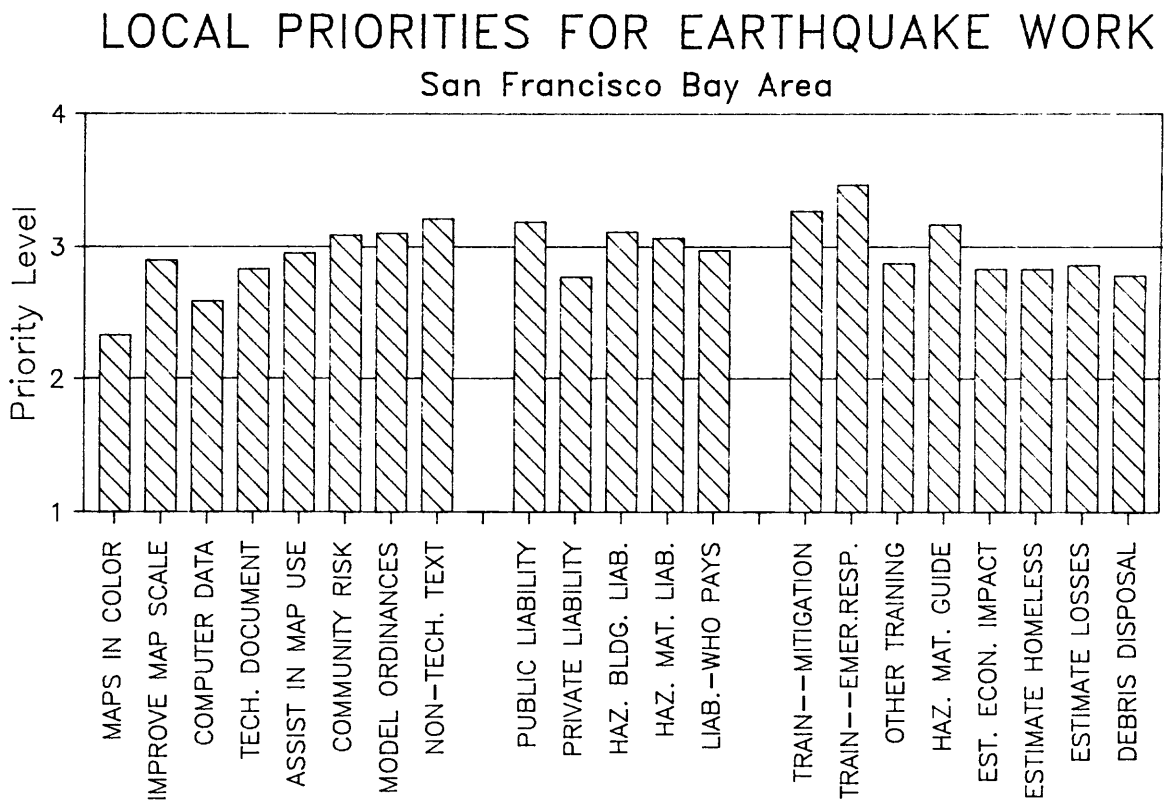

Historical Normal Fault Scarps -- Wasatch Front and Vicinity

9910-04102

David P. Schwartz
Branch of Engineering Seismology and Geology
U.S. Geological Survey
345 Middlefield Road, MS 977
Menlo Park, California 94025
(415) 323-8111, ext. 2689

Anthony J. Crone
Branch of Geologic Risk Assessment
MS 966, Box 25046
Denver Federal Center
Denver, Colorado 80225
(303) 236-1595

Investigations:

The project goal is to study historical normal fault scarps in the Great Basin in order to calibrate geological techniques used to identify individual past earthquakes and the amount of displacement during each, quantify earthquake recurrence intervals, and evaluate earthquake recurrence models and fault segmentation models. To date, investigations have concentrated on recurrence and segmentation along the 1983 Borah Peak, Idaho surface rupture and associated scarps of the Lost River Range.

Results:

1. During FY 86 Schwartz and Crone excavated trenches at four sites along the Lost River Range. These included a) Rattlesnake Canyon and 25 km Canyon, both located north of Willow Creek Summit along the 1983 surface rupture on the Warm Springs segment and b) Lone Cedar and Lower Cedar Creeks on the Mackay segment. Charcoal was found at Rattlesnake Canyon in a burn layer in an alluvial fan displaced by one pre-1983 event. Charcoal was also found in a burn layer on scarp colluvium derived from a single-event pre-1983 scarp at 25 km Canyon. Trenches across a single-event scarp at Lone Cedar Creek and a multiple event scarp at Lower Cedar Creek exposed a volcanic ash (Mazama ash?) that was displaced during the most recent event on the Mackay segment. The occurrence of datable material at each site is extremely encouraging with regard to dating and defining the lateral extent of past earthquakes on this fault zone.

   The existing trenches will be logged during Spring/Summer 1987. Radiocarbon dates and identification of the volcanic ash should be completed prior to the fieldwork. Encouraged by the finding of charcoal and ash, additional trenches at two sites along the Thousand Springs segment will be excavated to look for datable material that can be used to better constrain the timing of the pre-1983 earthquake on this reach of the 1983 surface rupture.

2. Mapping variability in morphology of the 1983 scarp continued. The type and extent of scarp morphology associated with the 1983 surface rupture (vertical free face, colluvium covered scarp, scarp with rotated blocks, folding instead of brittle failure, etc.) is being documented and cataloged. Information on variability in morphology and complexity of a scarp along its length can be used to better interpret trench exposures across other normal faults.

3. Schwartz and Hanks profiled the Thousand Springs segment at six locations at and just north of the trench site near Doublesprings Pass Road to reconstruct the pre-1983 scarp profile for diffusion modeling of its age.

Reports:

None.

San Andreas Segmentation: Cajon Pass to Wallace Creek

9910-03983

David P. Schwartz, Robert V. Sharp, and Ray J. Weldon
Branch of Engineering Seismology and Geology
U.S. Geological Survey
345 Middlefield Road, MS 977
Menlo Park, California 94025
(415) 323-8111, ext. 2689

Investigations

The project goal is to refine existing and/or develop new segmentation and fault behavior models for the San Andreas fault between Wallace Creek and Cajon Pass.

1. Develop new slip rate and recurrence data from Wallace Creek to south of Cajon Creek.

2. Critically review published and unpublished data and, where possible, existing field relationships to define and quantify uncertainties in: a) timing, displacement, and lateral extent of individual past earthquakes; and b) location-specific slip rate estimates.

3. Map and characterize the style of secondary faulting along the San Andreas, particularly near the junction with the San Jacinto fault on the south and near Liebre Mountain on the north.

Results

1. Investigations were begun at two sites on the San Andreas Fault, named 96 St. and Wrightwood, during FY 1986.

   a. The 96 St. site (Schwartz and Weldon)
   The 96 St. site near Littlerock, California, is 8-1/2 km northwest of Pallett Creek and 45 km northwest of the junction of the San Andreas and San Jacinto faults. Here, the fault is a well-defined zone 3 to 7 m wide that contains a vertical and a southwest-dipping trace. It offsets an alluvial fill sequence and post-fill pond and colluvial deposits. Charcoal from burn layers date the top of the fill at 1000 to 1200 years B.P. A stream offset of 19 m that post-dates the fill sequence yields a minimum slip rate of 16 to 19 mm/yr. The main fill-bearing channel is offset a maximum of 130 m. Charcoal from within the fill yielded an age of 3510 $\pm$ 220 ^{14}C yr B.P. This gives a maximum slip rate on the offset channel of 38 mm/yr. Tentative correlation of offset facies boundaries within the fill sequence suggests the latest Holocene slip rate is in the lower end of the of the 16 to 38 mm/yr range. A precise slip rate at this location on the Mojave segment is important for evaluating proposed rupture models for the San Andreas fault zone. Trenching and mapping will continue through Spring 1987 to better constrain the rate.

b. Wrightwood Site (Weldon, Schwartz, Fumal)
The Wrightwood site is located near the mouth of Government Canyon, approximately 4 km northwest of Wrightwood, California. A natural stream cut observed during initial exploration of the site exposed a sequence of layered peats displaced by minor faults immediately west of the main fault trace. A radiocarbon age of 3520, +60, -50 ^{14}C yr B.P. was obtained from the highest peat in the section (1.5 m below ground surface), and an age of 4990 ± 90 ^{14}C B.P. was obtained on a peat 0.5 m lower in the section. In September, two trenches were excavated. Trench WW1 (200 m long) exposed a broad zone of deformation (150 m wide) containing the main fault, subsidiary traces (strike-slip and normal faults), large and small wavelength folds, and liquefaction features. In this trench the main fault trace extends to to the surface and displaces layered peats that appear to be correlative with the section dated in the natural exposure. An additional 3 m-thick sequence of younger peats west of the main trace contains seven to eight minor fault traces that terminate at different levels and most likely represent the most recent events at the site. In trench WW2, located approximately 200 m to the north, the amount of deformation decreases upsection and faulting does not appear to extend to the surface. The abundance of peat, wood, and charcoal for radiocarbon dating, and the occurrence of faults that terminate at different levels, liquefaction features, and folds that are truncated by unfolded units indicate a high potential for dating individual earthquakes. Some of the events will be older than the Pallett Creek chronology. Others may overlap and therefore provide independent evaluation of timing of events interpreted at Pallett Creek. Radiocarbon analyses of trench samples will be obtained during Winter and Spring 1987. Result of the age-dating will guide the extensive trenching planned for Summer and Fall 1987.

2. Topographic features offset by the San Andreas fault at Cajon Creek near San Bernardino, southern California, were reexamined to evaluate the late Quaternary slip rate based on these features (Sharp).

An approximately 5900 year-old terrace riser on the northwest side of Cajon Creek is right-laterally offset by the fault. The discrepency between the offset stated for this feature by Weldon and Sieh (1985) and that shown on the USGS 1:24,000 topographic map prompted a detailed examination of the topography from large-scale aerial photographs taken before alteration of the feature by construction of a railroad line. A 1:5,000-scale topographic map made by PG2 plotter confirms the generalized correctness of the quadrangle map. Restoration of this terrace riser to its most probable original configuration, as judged on the basis of smoothness across the fault trace, requires 108 ± 5 m of slip. This is in contrast to the offset of 145 m measured by Weldon and Sieh for the break in slope between the riser and upper terrace tread. Weldon and Sieh (personal communication) acknowledge that the 108 m offset is possible and, perhaps, is the best alignment of this terrace riser. However, they also feel that the 145 m reconstruction cannot be eliminated and must be included in the uncertainty. The 108 m offset yields an average slip rate on the fault of $18.9\ ^{+5.0}_{-3.6}$ mm/yr for the past 5900 years.

Reports

Schwartz, D.P., and Weldon, R.D., (1986), Late Holocene slip rate on the Mojave segment of the San Andreas fault zone, Littlerock, California: preliminary results [abs.]: EOS, *Transactions American Geophysical Union*, v. 67, p. 906.

Weldon, R.D., and Matti, J., (1986), Geologic evidence for segmentation of the southern San Andreas fault [abs.]: EOS, *Transactions American Geophysical Union*, v. 67, p. 905.

Regional Syntheses of Earthquake Hazards in Southern California

9910-03012

Joseph I. Ziony
Branch of Engineering Seismology and Geology
U.S. Geological Survey
345 Middlefield Road, MS 977
Menlo Park, California 94025
(415) 323-8111, ext. 2944

Investigations

During this reporting period, our efforts were directed toward:

1. Compiling, editing, and producing the proceedings of a multidisciplinary workshop on southern California earthquake hazards that reviewed recent scientific results and to identify priorities for future research.

2. Efforts to initiate detailed geologic field studies along the Elsinore fault zone between Corona and Lake Elsinore in order to document late Quaternary offsets, estimate fault slip rates, and evaluate segmentation of the zone.

Results

1. The proceedings of the workshop, "Future Directions in Evaluating Earthquake Hazards of Southern California" (Los Angeles, at the University of Southern California on November 12 and 13, 1985). The USGS, FEMA, NSF, California Office of Emergency Services, California Division of Mines and Geology, California Seismic Safety Commission, Southern California Earthquake Preparedness Project, and Southern California Association of Governments jointly sponsored this workshop. About 330 people participated, including geologists, seismologists, engineers, planners, and emergency management experts. Numerous private firms, universities, and governmental units were represented.

   The workshop proceedings summarized key results of recent earth-science research on evaluating earthquake hazards; examined current activities where hazard information is being used in southern California to reduce potential earthquake losses; and discussed what additional scientific information is needed and which hazard-reduction techniques are most effective. Separate chapters of the proceedings contained papers addressing the following topics in depth:

   - o Evaluating earthquake and surface-faulting potential for hazard reduction actions.
   - o Predicting seismic intensities for response planning and loss estimation.
   - o Predicting ground motion for earthquake-resistant design.
   - o Predicting major earthquakes for preparedness planning.

- o Evaluating earthquake ground-failure potential for development decisions.
- o Evaluating the shaking hazard for redevelopment decisions.

The workshop proceedings, including papers of the speakers and panelists and summaries of individual working group discussions, will aid in transferring southern California's successful hazard-reduction efforts to other earthquake-prone regions.

2. No field work was undertaken on the Elsinore fault zone (per to the best knowledge of T. Fumal).

Reports

Brown, William M., III, Kockelman, W.J., and Ziony, J.I., (eds.,) 1986, Future Directions in evaluating earthquake hazards of southern California, *U.S. Geological Survey Open-File Report 86-401*, 421 p.

Jones, Lucile, and Ziony, J.I., (1987), Map showing late Quaternary faults and recent seismicity for the onshore and offshore Los Angeles region: 1:250,000-scale (in review).

Depth to bedrock map in the greater Tacoma area, Washington

9950-04073

Jane M. Buchanan-Banks
Branch of Geologic Risk Assessment
U.S. Geological Survey
David A. Johnston Cascades Volcano Observatory
5400 MacArthur Boulevard
Vancouver, Washington 98661
(206) 696-7810

Investigations

Research on the areal extent and depth of thick sediments, which could produce strong seismic-related ground shaking and slope failures in the greater Tacoma region, continues.

Results

1. A bibliographic reference file containing several hundred entries related to the geology and seismology of the area has been compiled. Copies of many of the pertinent papers have been obtained and work is proceeding on reading and synthesizing the information.

2. Oil well and water well data from various sources are being gathered, compiled, and analyzed to determine depth to bedrock.

3. Preliminary maps showing locations of deep water and oil wells, areas of bedrock geology, and geologic data sources are being compiled of the greater Tacoma area.

Earthquake Planning Scenario for the Newport-Inglewood Fault

14-08-0001-22037

K. Steinbrugge, C. Johnson,
T. Toppozada, H. Lagorio, J. Bennett, R. Saul, and J. Davis
California Department of Conservation
Division of Mines and Geology
1416 Ninth Street
Sacramento, CA 95814
(916) 455-1923

Introduction: This project involves the development of an earthquake planning scenario based upon the occurrence of a maximum credible earthquake on the Newport-Inglewood fault zone (NIFZ). The scenario characterizes plausible effects of the earthquake on principal lifelines and critical structures. These are hypothetical consequences for use in regional emergency planning, but do not portray the fate of individual facilities.

The evaluations that comprise the planning scenario for a specific earthquake are developed in three phases: (a) an isoseismal map is produced that portrays the predicted seismic intensity and areas of potential ground failure, i.e., surface rupture, liquefaction, landsliding, (b) inventories of lifelines and critical structures are compiled, and (c) the planning scenario is developed based on postulated damage to various lifeline components.

The Scenario Earthquake: The scenario earthquake results from rupture along 77 kilometers of the NIFZ from its northern end near Beverly Hills to offshore from Laguna Beach. The 77 km rupture length corresponds to a magnitude of about 7. For planning purposes, a corresponding maximum surface displacement of 6 feet is assumed, the displacement being oblique with equivalent horizontal and vertical components of about 4 feet. The earthquake generates potentially damaging ground shaking that continues for about 25 seconds within 25 miles of the fault zone. Aftershocks continue for about a month with a few events in the magnitude 5.5 to 6.5 range.

Predicted Seismic Intensity Distribution: The seismic intensity distribution map developed for this scenario earthquake indicates intensity IX (Modified Mercalli) shaking effects throughout much of the area within 8 kilometers of the NIFZ. Intensity VIII shaking effects extend throughout the alluvial sections of the Los Angeles basin east to the vicinity of Monrovia and West Covina, including the San Fernando Valley and virtually all of the populated alluvial areas of coastal Orange County south to San Juan Capistrano. The vast area subjected to intensity VIII (MM) effects is subdivided into high VIII and low VIII intensities to reflect differences in relative consolidation between younger (Holocene) and older Pleistocene alluvial deposits. Intensity VII and lesser intensities are postulated in the generally consolidated hill and mountain areas, including the Santa Monicas, Verdugos, Puente Hills, and the mountainous areas of Orange County.

Within the urban areas subjected to intensity VIII-IX shaking, there are significant areas where ground failures could produce intensities greater than IX. These include: (a) the areas within the NIFZ where surface rupture could occur; (b) significant areas where ground conditions are favorable to liquefaction effects, e.g., the Los Angeles and Long Beach harbors, Marina Del Rey, Newport Bay and Balboa, and significant areas of urban Orange County; (c) areas of potential landsliding, such as, the Palos Verdes Hills, Santa Monica bluffs, and some potentially unstable slopes in eastern Orange County.

Lifeline Inventory and Damage Assessments: Inventories of critical lifelines and structures are currently being compiled, certain major facilities are being inspected, and discussions are in progress with various transportation and utility lifeline operators.

Reducing Urban and Regional Earthquake Hazards

9900-90022

William J. Kockelman, Walter W. Hays, and Paula L. Gori
Office of Earthquakes, Volcanoes, and Engineering
U. S. Geological Survey
345 Middlefield Road, Mailstop 922
Menlo Park, California 94025
(415) 323-8111, ext. 2312

905 National Center
Reston, Virginia 22092
(703) 648-6711

Investigations

The National Earthquake Hazards Reduction Program represents a concerted effort by the Nation to reduce future losses of life and property from earthquakes and to prevent the severe socio-economic disruption that a catastrophic earthquake would cause. Achievement of these goals depends on the combined and coordinated actions of all governmental units--Federal, State, and local--as well as the private sector.

The Federal government leads, coordinates, and participates in earthquake hazard reduction efforts of the public and private sectors. Congress has designated four principal Federal agencies--Federal Emergency Management Agency (FEMA), United States Geological Survey (USGS), National Science Foundation (NSF), and National Bureau of Standards. FEMA has been designated by Congress to be the focal point at the Federal level for emergency preparedness, response, recovery, and hazard mitigation activities.

Hazard reduction, however, depends on the effectiveness of State and local programs that utilize the results of Federal studies and initiatives. Any Federal, State, local, or private program that has earthquake-hazard reduction as a goal needs five distinct and separate components, each a prerequisite for its successor:

- Conducting scientific and engineering studies of earthquake processes
- Translating such studies for nontechnical users
- Disseminating this translated information to users and assisting them
- Selecting and using appropriate hazard-reduction techniques
- Evaluating the effectiveness of the selected hazard-reduction techniques

Beginning October 1, 1983, the USGS initiated the "Regional Earthquake Hazards Assessments" program to develop the basic information and partnerships needed for evaluating earthquake hazards and assessing the risk in broad geographic regions containing important urban areas. The goal is to provide an integrated program having comprehensive research goals and producing generic information that can be used to reduce potential earthquake losses in urban areas. This program element requires a high degree of team work to accomplish the goals of each task. Users of the information produced by this program cannot find such an integrated synthesis and evaluation of earthquake hazards in the scientific literature.

Although the USGS is primarily a scientific research agency, it frequently takes the initiative to translate, disseminate, and foster the use of its work by State and local governments. An important aspect of this effort is ensuring a dialog between producers and users of scientific studies by cosponsoring and coordinating various types of workshops throughout the United States and its territories. This effort is led by the USGS Office of Earthquakes, Volcanoes, and Engineering (OEVE).

Results

Thirty-six workshops on earthquake issues have been convened by the USGS. A list of the 34 workshops for which proceedings are available is appended. Twenty-two of these workshops were specifically directed at the use of scientific information for reducing hazards. These workshops have been initiated and coordinated by the Deputy for Research Applications, OEVE. Because of the necessity for a multidisciplinary and intergovernmental team effort, he is assisted and supported by various USGS personnel as well as local, State, and other Federal agency officials and staffs.

These workshops have increased the state-of-knowledge about earthquake hazards throughout the Nation, increased the level-of-awareness and concern, and improved the state-of-practice in earthquake-resistant design. They have brought together more than 1,000 producers and users of hazards information in almost every earthquake-prone part of the United States. They have fostered local-state-Federal partnerships and enhanced the use of existing information networks as well as the creation of new networks. Seismic safety organizations have been created as a result of the workshops. Proceedings of past workshops have been disseminated to the participants for use in their program development and to over 5,000 others who have requested them for the information they contained.

Other activities to foster the use of scientific information for reducing earthquake hazards include: assisting and participating in conferences sponsored by State agencies and professional societies; designing and conducting training sessions for preparedness and response agencies; and providing other educational, advisory, and review services to various local, State, and Federal government agencies.

The seven most recent workshops are reported here:

- **San Juan, Puerto Rico, May 14-16, 1986**

Sixty-five individuals participated in a 3-day workshop on the "Assessment of geologic hazards and risk in Puerto Rico." It was cosponsored with FEMA, Puerto Rico Department of Natural Resources, Puerto Rico Planning Board, and Puerto Rico College of Engineers.

The workshop addressed the current earthquake vulnerability study of San Juan, the Mameyes landslides, and the new Puerto Rico building code, as well as the recent Mexico and Chile earthquakes in terms applicable to Puerto Rico. The participants formulated a multidisciplinary task force to upgrade the level of geologic, engineering, and seismological information needed for geologic hazards reduction programs in Puerto Rico. The Secretary of the Puerto Rico Department of Natural Resources, Alejandro Santiago Nieves, urged the establishment of a non-partisan commission to recommend to the Governor and Legislature Assembly of Puerto Rico a program to: establish an advisory council to consider all aspects of natural hazard mitigation; develop studies designed to fill existing gaps in knowledge; design and implement a program of public awareness, involving all levels of society and all economic sectors; and estimate the resources required and obtain a legislative commitment for funding.

- **Alaska, September 5-7, 1985**

Seventy-five earth scientists, social scientists, engineers, planners, and emergency management specialists participated in a 3-day workshop on "Evaluation of Urban and

Regional Earthquake Hazards and Risk in Alaska." The workshop, held in Anchorage, was cosponsored with FEMA, Alaska Division of Geological and Geophysical Surveys, and Alaska Office of Emergency Services.

The specific goal was to evaluate the advances made in the state-of-knowledge and the state-of-practice since the 1964 Prince William Sound earthquake and to identify the range of actions that can be undertaken in the next 3-5 years to accelerate progress, in terms of both research and implementation. Three discussion groups identified ten concerns and made recommendations about seismic safety policy in Alaska, the need for additional education pertaining to earthquake hazards, and the opportunities for and constraints to reducing earthquake losses. An evaluation elicited several suggested actions: increasing local awareness, improving building codes, developing seismic maps and seismic safety plans, and lobbying for a State commission for earthquake hazard research.

- **Puget Sound, Washington Area, October 29-31, 1985**

Over 100 geologists, seismologists, engineers, social scientists, emergency planners, and public officials participated in a 3-day workshop on earthquake hazards held in Seattle. The first two days, attended by 85 people, used an interactive problem-solving format. This part of the meeting was cosponsored with FEMA, the Washington Department of Natural Resources, and the Washington Department of Emergency Management.

The third day of the meeting was a special extension of the workshop which was organized as a meeting of a "working group" of experts on subduction zone earthquakes and earthquake preparedness. This meeting was cosponsored with the U.S. Nuclear Regulatory Commission. The goal of the "working group" was to discuss the potential for a large subduction-zone earthquake in the Puget Sound area and to define a research agenda for the next 3 to 5 years.

Several conclusions emerged from the workshop, for example: although a reasonable body of knowledge on earthquake hazards in the Puget Sound area has been accumulated, additional knowledge is needed to resolve important technical issues and to elimate or reduce controversy; high priority should be given to research concerning historical seismicity, seismogenic sources, earthquake recurrence rates, tsunamigenic sources, and local ground response; and high priority should be given to translation and dissemination, including maps of seismogenic zones, ground shaking, and regional liquefaction susceptibility, to education programs for the decisionmaker and the public, and to preparation of model codes and land-use plans.

- **Southern California, November 12-13, 1985**

About 330 people participated in the workshop; the attendees represented diverse backgrounds including earth science, social science, land-use planning, engineering, emergency management, public administration, law, public health, insurance, and real estate. Numerous private firms, universities, public utilities, and Federal, State, and local units of government were represented. The workshop was cosponsored with FEMA, NSF, three state agencies, and two regional agencies. The workshop had three objectives: to summarize results of recent earth-science research on evaluating earthquake hazards, to present examples of ongoing earthquake hazards reduction efforts, and to discuss what additional scientific and technical information is needed and which hazard-reduction techniques are most effective. The program was multidisciplinary and was intended for the presentation both of the key results of recent scientific research and of examples of earthquake hazard reduction efforts.

The current status and future directions and needs for not only earth science and technical information but for hazard reduction techniques were discussed and summarized in the workshop's proceedings for six major topics:

1. evaluating earthquake and surface-faulting potential for hazard reduction
2. predicting seismic intensities for response planning and loss estimation
3. predicting ground motion for earthquake-resistant design
4. predicting major earthquakes for preparedness planning
5. evaluating earthquake ground-failure potential for development decisions
6. evaluating the shaking hazard for redevelopment decisions

o **Central United States, November 25-27, 1985**

Sixty-six earth scientists, engineers, planners, and emergency management specialists participated in a 2-day workshop on "Earth science considerations for earthquake hazards reduction in the Central United States." The workshop held in Nashville, Tennessee, was sponsored with FEMA, Tennessee Emergency Management Agency, and the Central United States Earthquake Preparedness Consortium.

The workshop sought to identify the most up-to-date technical information available for hazard reduction and the kind of information and research needed to improve the capability of emergency planners to protect lives and property in the Central United States. The major focus was to assess availability of technical information needed for adoption of mitigation and response measures by public and private institutions, as well as recommend activities to increase the availability and type of information needed. The participants also recommended increasing the use of existing technical information, although they concluded that sufficient scientific and technical information was available to implement loss-reduction measures.

o **San Francisco, California, November 25-27, 1985**

Forty-five scientists and engineers participated in a 3-day workshop on "Probabilistic earthquake hazards assessments." It was cosponsored with the Nuclear Regulatory Commission. The workshop reviewed the methods currently used to assess earthquake hazards probablisitically, identified the issues, and suggested practical and innovative ways to improve the state-of-knowledge necessary to implement the assessments for the siting of nuclear power reactors. The participants concluded that although significant progress has been made in the past decade, great care must be taken to ensure: concentrated effort to resolve the controversy associated with the ground-shaking hazard; wise use of probabilistic models; cross-education of geologists, geophysicists, seismologists, and engineers; increased understanding of the physics of the earthquake generation process; and incorporation of more phsyics and mechanics into the analytical models.

o **Wasatch Front, Utah, 1983-1986**

The USGS program in Utah is unique in that a series of four workshops of various sponsorships, formats, and procedures were used over the past three years; these were:

-- Governor's Conference on Geologic Hazards, August 11-12, 1983

Its purpose was to bring together scientists and engineers, elected and appointed officials, leaders of business and private organizations, and private citizens to discuss

geologic hazards and to recommend appropriate actions to all levels of government. Thirty-six working groups recommended 171 actions that they felt should be taken to reduce the impacts of geologic hazards on the lives of Utah's citizens. They concluded that although much of the information needed to make site-specific decisions has not yet been developed or is not accessible, sufficient information does exist on which to base public policy and implement certain actions now.

The working groups also determined that the primary support for research on geologic hazards should come from the Federal government and that the State should take a major role in identifying research priorities and in making use of the knowledge gained. The working groups concluded that information collection and dissemination is the role of State agencies and that local governments should take a more active role in identifying their information needs and providing matching assistance.

The working groups recognized that the major funding and responsibility for basic research on geologic hazards is with Federal agencies, and that geologic hazard-reduction programs in Utah are heavily dependent upon this research. Also, because the Federal government manages most of the land in Utah, it should make a major contribution to programs concerned with defining geologic hazards and minimizing their impact. Coordination between State and Federal agencies concerned with geologic hazards is essential in identifying critical problems, avoiding undesirable duplication, and assuring a two-way flow of information.

-- Evaluation of Regional and Urban Hazards and Risk, August 14-16, 1984

One hundred fifteen participants having varied backgrounds in earth science, social science, planning, architecture, engineering, and emergency management participated in this workshop. The participants represented industry, volunteer agencies, and academic institutions from Utah, as well as representatives of local and State governments of Utah, other states, the private sector, and the Federal government. The participants represented a major part of the resources available to conduct research, to prepare for, to mitigate, and to respond to earthquake hazards in Utah.

The goal of the Wasatch Front studies is the reduction of loss of life and property from the earthquake hazards of ground shaking, surface-fault rupture, earthquake-induced ground failure, and tectonic deformation. Specific recommendations such as the following were made: earthquake potential of the entire Wasatch Front should be assessed carefully; improved deterministic and probabilistic estimates of the ground-shaking and ground-failure hazards are needed; vulnerability studies for buildings, other facilities, and lifeline systems are needed; user-friendly information systems are needed; and an extraordinary effort is needed to devise practical loss-reduction measures and to foster their use. In addition, special evening sessions were conducted on technical issues and on the needs of planners and decisionmakers for earthquake hazard information.

-- Earthquake and Landslide Hazards, July 10-11 and July 30-August 1, 1985

This workshop was cosponsored with the Utah Geological and Mineral Survey (UGMS), Utah Division of Comprehensive Emergency Management (CEM), and the University of Utah. The goal was to increase the capability of UGMS and CEM to meet the needs of government officials, private industry, universitites, engineers, and architects in Utah to incorporate earthquake and landslide hazard information into their programs. The first of the two workshops was attended by 25 scientists, emergency planners, architects and engineers. In this workshop, UGMS with the assistance of the

workshop participants identified viable goals and responsibilities of the State Survey. Several agencies and groups were identified who could assist or who could share these responsibilities.

The second workshop was designed to assist CEM and local governments to increase their use of hazard information and to devise and implement loss-reduction measures. For two days, 60 emergency managers, urban planners, and county geologists participated in discussions of earthquakes hazards identification and risk analysis and the use of hazard and risk information for land-use and emergency-response planning. Communication was greatly improved by spirited interaction between geologists, seismologists, social scientists, urban planners, emergency managers, architects, and engineers. On the third day of the workshop, participants took a field trip to see landslides, fault scarps, and examples of appropriate land use in earthquake- and landslide-prone areas. Two weeks later UGMS and USGS collaborated in a training exercise on fault identification and excavated a trench across the Wasatch Front zone in a dynamic laboratory exercise, and an hoc working group was created to evaluate the seismic zoning map for Utah.

-- Workplan for the Wasatch Front, July 14-18, 1986

This workshop was cosponsored with FEMA, UGMS, and CEM marked the end of the three-year effort to accelerate the research to foster the implementation process. Six triads prepared summary reports which included the status of the research and implementation in Utah after three years of concentrated effort and made suggestions for priority actions for the second phase. Specific tasks were identified for the following objectives: providing user groups with explicit information on the nature, extent, and severity of the earthquake hazards; institutionalizing the proceedures that make the information available for use; providing training and continuing education for professionals transferring relevant information on reduction techniques prepared in other parts of the United States to users in Utah; preparing for the scientific and emergency response requirements that a damaging earthquake in Utah will trigger; conducting a feasability study to determine how to use the professional communities to upgrade earthquake-resistant design provisions of the Uniform Building Code; and adopting policies and enacting legislation and ordinances that improve design, construction, and land-use practices.

Reports

Brown, Jr., R.D., and Kockelman, W.J., 1985, Geology for decisionmakers--protecting life, property and resources: Regents of the University of California Bulletin of the Institute of Governmental Studes, Public Affairs Report, Vol. 16, no. 1, 11 p.

Brown, W.M., III, Kockelman, W.J., and Ziony, J.I., editors, 1986, Future directions in evaluating earthquake hazards of southern California, Conference XXXII, Los Angeles, Proceedings: U.S. Geological Survey Open-File Report 86-401, 421 p.

Hays, W.W., 1986, Regional earthquake hazard assessments; draft workplan for phase II of research and implementation along the Wasatch Front, Utah; FY 87-88: Memorandum dated August 5, 1986, Reston, Triad Reports, 38 p.

Hays, W.W., editor, 1986, Probabilistic earthquake-hazards assessments, Conference XXXIV, San Francisco, Proceedings: U.S. Geological Survey Open-File Report 86-185, 380 p.

Hays, W.W., and Gori, P.L., editors, 1984, Evaluation of regional and urban earthquake hazards and risk in Utah, Conference XXVI, Salt Lake City, Proceedings: U.S. Geological Survey Open-File Report 84-763, 687 p.

_____, 1986, Evaluation of regional and urban earthquake hazards and risk in Alaska, Conference XXXI, Anchorage, Proceedings: U.S. Geological Survey Open File Report 86-79, 449 p.

_____, 1986, Earthquake hazards in the Puget Sound, Washington area, Conference XXXIII, Seattle, Proceedings: U.S. Geological Survey Open-File Report 86-253, 258 p.

Kockelman, W.J., 1986, Some techniques for reducing landslide hazards: Bulletin of the Association of Engineering Geologists, College Station, Tex., Vol. 23, no. 1, p. 29-52; also excerpted in Wasatch Front Forum, Utah Geological and Mineral Survey, Salt Lake City, Vol. 2, no. 3, p. 2.

Utah Geological and Mineral Survey, 1983, Governor's Conference on Geologic Hazards: Utah Geological and Mineral Survey Circular 74, Salt Lake City, 99 p.

APPENDIX -- CONFERENCES AND WORKSHOPS TO DATE

Conference I Abnormal Animal Behavior Prior to Earthquakes, I
Not Open-Filed
Conference II Experimental Studies of Rock Friction with Application to Earthquake Prediction
Not Open-Filed
Conference III Fault Mechanics and Its Relation to Earthquake Prediction
Open-File No. 78-380
Conference IV The Use of Volunteers in the Earthquake Hazards Reduction Program
Open-File No. 78-336
Conference V Communicating Earthquake Hazard Reduction Information
Open-File No. 78-933
Conference VI Methodology for Identifying Seismic Gaps and Soon-to-Break Gaps
Open-File No. 78-943
Conference VII Stress and Strain Measurements Related to Earthquake Prediction
Open-File No. 79-370
Conference VIII Analysis of Actual Fault Zones in Bedrock
Open-File No. 79-1239
Conference IX Magnitude of Deviatoric Stresses in the Earth's Crust and Upper Mantle
Open-File No. 80-625
Conference X Earthquake Hazards Along the Wasatch and Sierra-Nevada Frontal Fault Zones
Open-File No. 80-801
Conference XI Abnormal Animal Behavior Prior to Earthquakes, II
Open-File No. 80-453
Conference XII Earthquake Prediction Information
Open-File No. 80-843
Conference XIII Evaluation of Regional Seismic Hazards and Risk
Open-File No. 81-437
Workshop XIV Earthquake Hazards of the Puget Sound Region, Washington
Open-File No. 83-19
Workshop XV A Workshop on "Preparing for and Responding to a Damaging Earthquake in the Eastern United States"
Open-File No. 82-220
Workshop XVI The Dynamic Characteristics of Faulting Inferred from Recording of Strong Ground Motion
Open-File No. 82-591
Workshop XVII Workshop on Hydraulic Fracturing Stress Measurements
Open-File No. 82-1075
Workshop XVIII A Workshop on "Continuing Actions to Reduce Losses from Earthquakes in the Mississippi Valley Area"
Open-File No. 83-157
Workshop XIX Active Tectonic and Magmatic Processes Beneath Long Valley Caldera, Eastern California
Open-File No. 84-939
Workshop XX The 1886 Charleston, South Carolina Earthquake and Its Implications for Today
Open-File No. 83-843

Workshop XXI A Workshop on "Continuing Actions to Reduce Potential Losses from Future Earthquakes in the Northeastern United States"
Open-File No. 83-844

Workshop XXII A Workshop on "Site-Specific Effects of Soil and Rock on Ground Motion and the Implications for Earthquake-Resistant Design"
Open-File No. 83-845

Workshop XXIII A Workshop on "Continuing Actions to Reduce Potential Losses from Future Earthquakes in Arkansas and Nearby States"
Open-File No. 83-846

Workshop XXIV A Workshop on "Geologic Hazards in Puerto Rico"
Open-File No. 84-761

Workshop XXV A Workshop on "Earthquakes Hazards in the Virgin Island Region"
Open-File No. 84-762

Workshop XXVI A Workshop on "Evaluation of Regional and Urban Earthquakes Hazards and Risk in Utah"
Open-File No. 84-763

Workshop XXVII Mechanics of the May 1, 1983 Coalinga Earthquake
Open-File No. 85-44

Workshop XXVIII On the Borah Peak, Idaho, Earthquake
Open-File No. 85-290

Workshop XXIX A Continuing Action to Reduce Losses from Earthquakes in New York and Nearby States
Open-File No. 85-386

Workshop XXX Reducing Potential Losses from Earthquake Hazards in Puerto Rico
Open-File No. 85-731

Workshop XXXI A Workshop on "Evaluation of Regional Urban Earthquake Hazards and Risk in Alaska"
Open-File No. 86-79

Workshop XXXII Future Directions in Evaluating Earthquake Hazards of Southern California
Open-File No. 86-401

Workshop XXXIII A Workshop on "Earthquake Hazards in the Puget Sound, Washington Area"
Open-File No. 86-253

Workshop XXXIV Probabilistic Earthquake Hazards Assessment
Open-File No. 86-185

Ordering information for conference and workshop reports may be obtained from:

Open-File Services Section
Branch of Distribution
U.S. Geological Survey
Box 25425, Federal Center
Denver, Colorado 80225
Telephone: (303) 236-7476

Global Digital Network Operations

9920-02398

Howell M. Butler
Branch of Global Seismology and Geomagnetism
U.S. Geological Survey
Albuquerque Seismological Laboratory
Building 10002, Kirtland AFB-East
Albuquerque, New Mexico 87115-5000
(505) 844-4637

Investigations

The Global Digital Network Operations presently consists of 16 SRO/ASRO and 14 DWWSSN stations. The primary objective of the project is to provide technical and operational support to keep these stations operating at the highest percentage of recording time possible to provide high-quality digital seismic data to the seismic research community. This support includes operational supplies, replacement parts, repair service, modification of existing equipment, training, installation of systems and on-site maintenance and calibration. A service contract provides technicians to perform on-site maintenance and installations, as well as to perform repair-and-test of seismometers and all replaceable units that comprise the various network systems. Contract technicians are also provided for special projects such as on-site noise surveys, special telemetered system installations, system renovations, and evaluation and testing of seismological and related instrumentation.

The following station maintenance activity was accomplished:

AFI - Afiamalu, Samona - DWWSSN - One maintenance visit
ANMO - Albuquerque, New Mexico - SRO - Five maintenance visits
BDF - Brasilia, Brazil - DWWSSN - One maintenance visit
BOCO - Bogota, Columbia - SRO - One maintenance visit
CHTO - Chiang Mai, Thailand - SRO - One maintenance visit
LEM - Lembang, Indonesia - DWWSSN - One maintenance visit
SHIO - Shillong, India - SRO - One maintenance visit
ZOBO - Zongo Valley, Bolivia - ASRO - One maintenance visit

System Installation:

The Bar-Giygora, Israel (BGIO) SRO installation was completed in April.

Special Activity:

Seismic noise surveys were conducted in the countries of Argentina and Paraguay.

Nine China systems were checked out, shipped and installed during this period.

Results

The Global Digital Network continues with a combined total of 30 SRO/ASRO/ DWWSSN stations. The main effort of this project is to furnish the types of support at a level needed to keep the GSN at the highest percentage of operational time in order to provide the highest quality digital data for the worldwide digital data base.

U.S. Seismic Network

9920-01899

Marvin A. Carlson
Branch of Global Seismology and Geomagnetism
U.S. Geological Survey
Denver Federal Center
Box 25046, Mail Stop 967
Denver, Colorado 80225
(303) 236-1506

Investigations

U.S. Seismicity. Data from the U.S. Seismic Network are used to obtain preliminary locations and magnitudes of significant earthquakes throughout the United States and the world.

Results

As an operational program, the U.S. Seismic Network operated normally throughout the report period. Data were recorded continuously in real time at the NEIS main office in Golden, Colorado. At the present time, 100 channels of SPZ data are being recorded at Golden on develocorder film. This includes data telemetered to Golden via satellite from both the Alaska Tsunami Warning Center, Palmer, Alaska, and the Pacific Tsunami Warning Center, Ewa Beach, Hawaii. A representative number of SPZ channels are also recorded on Helicorders to give NEIS real-time monitoring capability of the more active seismic areas of the United States. In addition, 15 channels of LPZ data are recorded in real time on multiple pen Helicorders.

Data from the U.S. Seismic Network are interpreted by record analysts and the seismic readings are entered into the NEIS data base. The data are also used by NEIS standby personnel to monitor seismic activity in the United States and worldwide on a real time basis. Additionally, the data are used to support the Alaska Tsunami Warning Center and the Pacific Tsunami Warning Service. At the present time, all earthquakes large enough to be recorded on several stations are worked up using the "Quick Quake" program to obtain a provisional solution as rapidly as possible. Finally, the data are used in such NEIS publications as the "Preliminary Determination of Epicenters" and the "Earthquake Data Report."

Development is continuing on an Event Detect and Earthquake Location System to process data generated by the U.S. Seismic Network. We expect the new system to be ready for routine operational use by spring of 1987. At that time, the use of develocorders for data storage will be discontinued. Ray Buland and David Ketchum have been doing most of the developmental programming for the new system. A Micro Vax II will be used as the primary computer of the Event Detect and Earthquake Location System. PDP 11/23's and PDP 11/73's are being used as front ends to off load the real-time data collection from the Micro Vax II. A second Micro Vax II has been procured to serve as a backup to the primary system. The two Micro Vaxs share 1.3 gigabytes of disk storage.

Earth Structure and its Effects upon Seismic Wave Propagation

9920-01736

George L. Choy
Branch of Global Seismology and Geomagnetism
U.S. Geological Survey
Denver Federal Center
Box 25046, Mail Stop 967
Denver, Colorado 80225
(303) 236-1506

Investigations

1. Use of body wave pulse shapes to infer attenuation in the Earth. We have developed a method of generating synthetic waveforms that can simultaneously model the frequency-dependent effects of source finiteness and of propagation in the Earth. We applied this method to modeling P- and SH-type body waves in order to obtain frequency- and depth-dependent constraints on Q_α and Q_β of the Earth's mantle. Resolution of frequency-dependence requires analysis of a continuous frequency band from several Hz to tens of seconds.

2. Source parameters from broadband data. We are developing methods to extract source parameters from digitally recorded data by applying propagation corrections to waveforms. These corrections are most important for the midband frequencies (0.1-1.0 Hz) in which is located the corner frequency of most well-recorded teleseismic events ($m_b > 5.5$).

3. Use of differential travel-time anomalies to infer lateral heterogeneity. We are investigating lateral heterogeneity in the Earth by analyzing differential travel times of phases that differ in ray path only in very narrow regions of the Earth. Because such phases often are associated with complications near a cusp or caustic, their arrival times can not be accurately read without special consideration of the affects of propagation in the Earth as well as additional processing to enhance arrivals.

Results

1. The source parameters of a deep earthquake were derived using broadband P waveforms. Using the derived rupture process the t^*_β operators for SH-type body waves could be obtained. Differences between S and ScS body waves provided strong constraints on differential attenuation in the Earth. The mid-mantle between depths of 400 and 1600 km contributes primarily to attenuation of low frequencies (0.01 to 0.1 Hz). Below the mantle depth of 2000 km, the P and SH waveforms suggest little or no attenuation exists in the band of 0.01 to 5.0 Hz for the propagation paths investigated.

2. The attenuation correction is crucial to examination of midband and high frequency data. We have incorporated our depth- and frequency-dependent attenuation model into an algorithm for computing radiated energy, and velocity and acceleration spectra. In the frequency range 0.1-1.0 Hz, a teleseismically derived acceleration spectrum compares very well with spectra from near-field accelerograms. This implies that we can make routine estimates of strong ground motion from large earthquakes with teleseismic data.

3. We have analyzed differential travel times between PKP-DF, PKP-CD and PKP-C(diff). These body waves are particularly sensitive to the inner core-outer core boundary. However, in the distance range of about 134°-160° triplications and non-ray theoretical effects have made routine reports of body wave arrivals unreliable. By combining a source-deconvolution technique with synthetic seismograms we are able to resolve differential travel times. From the data, it is concluded that heterogeneity in and near the inner core is small. The anomalous residuals are due to variations in structure at the top of the outer core and lowermost mantle.

Reports

Boatwright, J., and Choy, G.L., 1986, Teleseismic estimates of the energy radiated by shallow earthquakes: Journal of Geophysical Research, v. 91, p. 2095-2112.

_____1986, Acceleration spectra for subduction zone earthquakes [abs.]: EOS (AGU, Transactions), v. 67, p. 310.

Choy, G.L., and Cormier, V.F., 1986, Direct measurement of the mantle attenuation operator from broadband P and S waveforms: Journal of Geophysical Research, v. 91, p. 7326-7342.

Cormier, V.F., and Choy, G.L., 1986, Seismic velocities and attenuation at the inner core boundary [abs.]: EOS (AGU, Transactions), v. 67, p. 311.

_____1986, A search for lateral heterogeneity in the inner core from differential travel times near PKP-D and PKP-C: Geophysical Research Letters, submitted.

Reanalysis of Instrumentally-Recorded United States Earthquakes

9920-01901

J. W. Dewey
Branch of Global Seismology and Geomagnetism
U.S. Geological Survey
Denver Federal Center
Box 25046, Mail Stop 967
Denver, Colorado 80225
(303) 236-1506

Investigations

1. Relocate instrumentally recorded United States earthquakes using the method of joint hypocenter determination (JHD) or the master event method, using subsidiary phases (P_g, S, L_g) in addition to first arriving P-waves, using regional travel-time tables, and expressing the uncertainty of the computed hypocenter in terms of confidence ellipsoids on the hypocentral coordinates.

2. Evaluate the implications of the revised hypocenters on regional tectonics and seismic risk.

Results

1. David Gordon continued his study of earthquakes in eastern and central Wyoming and revised his professional paper on the seismotectonics of the central United States.

2. Jim Dewey has spent most of his time writing a review paper on the seismicity and tectonics of the United States and a journal article on the seismicity of central Idaho. Revision of the review paper continues in the first half of FY87. Many of the conclusions of the central Idaho paper are similar to those reported for this project in Summaries of Technical Reports Volume XX (July 1985). However, in order to examine the evolution of the aftershock sequence of the Borah Peak earthquake of October 1983 (M_S = 7.3), the set of earthquakes relocated was extended to include events occurring from April 1984, through October 1985. Earthquakes occurring in the week following the Borah Peak main shock were concentrated in the immediate vicinity of the main shock rupture surface that was inferred from surface fault scarps and geodetic measurements. Later earthquakes, though they occurred on trend with the main shock rupture surface, were heavily concentrated to the north. This observation contradicts the assumption, commonly made in modern microearthquake studies, that loci of high microseismicity identified some time after an earthquake are concentrated on or very near the main shock rupture. The overall zone of seismicity during the entire two years following the Borah Peak main shock, though elongated parallel to the main shock fault plane, was twice as long.

Reports

Dewey, James W. (in press), Instrumental seismicity of central Idaho: Bulletin of the Seismological Society of America, 28 typed pages, 9 figures, 1 table.

Gordon, David W. (in press), Hypocenters and correlation of earthquake locations and tectonics in the central United States: U.S. Geological Survey Professional Paper 1364.

Global Seismology

9920-03684

E. R. Engdahl
and
J. W. Dewey

Branch of Global Seismology and Geomagnetism
U.S. Geological Survey
Denver Federal Center
Box 25046, Mail Stop 967
Denver, Colorado 80225
(303) 236-1506

Investigations

1. Depth Phases. Develop procedure for the global analyses of earthquake depth phases and source characteristics using broadband seismograms of body waves.

2. Earthquake Location in Island Arcs. Develop practical methods to accurately locate earthquakes in island arcs.

3. Subduction Zone Structure. Develop techniques to invert seismic travel times simultaneously for earthquake locations and subduction zone structure.

4. Global Synthesis. Synthesize recent observational results on the seismicity of the earth and analyze this seismicity in light of current models of global tectonic processes.

Results

1. Depth Phases. Displacement and velocity records of body waves with frequency content from 0.01 to 5 Hz can now be routinely obtained for most earthquakes with magnitude greater than about 5.5. These records are obtained either directly or by multichannel deconvolution of waveforms from digitally recording seismograph stations such as those of the GDSN (Global Digital Seismograph Network), RSTN (Regional Seismic Test Network), and GRF-array (Gräfenberg Seismological Observatory). Once the distortion of the seismograph filter is removed, the seismograms often show the source-time functions of the direct and surface-reflected phases, even for shallow events where depth phases may overlap the direct wave. A systematic procedure has been developed for analyzing broadband seismograms that identifies depth phases and subevents (for complex earthquakes). A natural benefit of the procedure is that better resolution of the focal mechanism can be obtained from the polarities of depth phases. In particular, the phase sP, which is also more clearly defined, provides additional valuable constraints on focal mechanism determinations. Because most large earthquakes are complex events, depth phases recorded on conventional seismograms are often incorrectly read and reported. The National Earthquake Information Center

is now utilizing digital waveforms routinely to obtain better estimates of focal depth, to identify subevents in complex earthquakes, and to improve focal mechanism determinations.

2. Earthquake Location in Island Arcs. A plate model determined by the simultaneous travel-time inversion for earthquake location and subduction zone structure (see section 3) is used to relocate teleseismically recorded earthquakes in the region of the May 7, 1986, Andreanof Islands earthquake. Digitally recorded short-period and broadband depth phases are used with a detailed model of arc crustal structure to accurately determine focal depths. The relocated earthquakes provide a complete description of the space-time history of earthquakes in the region, as well as an accurate portrayal of their relationship to regional tectonics. The rupture zone of the 1986 mainshock is clearly delineated, fine details of faulting along the plate interface are revealed, barriers and asperities are identified, and pre- and post-mainshock patterns of earthquake occurrence in the region are compared.

3. Subduction Zone Structure. A combined location and velocity inversion technique is applied to travel-time data from 151 well-recorded central Aleutian earthquakes. The data include P- and S-wave arrivals at stations of a local network and P-, pP-, and sP-wave arrivals at teleseismic stations. After correction for upper crustal structure at the reflection points, the depth phases pP and sP provide important constraints on subduction zone structure not ordinarily resolved by other data types. The structure is assumed to vary only across the arc and in depth; it is parameterized with cubic splines that provide a specification of velocity at each point of a gridded arc cross section. To avoid ray tracing, it is assumed that the velocity part of the problem is linear. Preliminary results show that deep earthquakes apparently occur within a narrow downdip zone near the upper surface of the descending slab, in contrast with previous studies which have located them within the presumably stronger and colder inner core of the slab. A slab thickness of 80-100 km and a downdip length of about 400 km, well below the deepest seismic activity, is indicated. The slab is characterized by seismic velocities as much as 11 percent higher than the surrounding mantle in its upper portions and 4-6 percent higher at depth. A sharp velocity gradient and lower velocities occur directly beneath the volcanic arc near the top of the slab. The slab anomaly appears to spread out and fall off very slowly with depth; these are probably not real effects but consequences of the omission of three-dimensional ray tracing.

4. Global Synthesis. The synthesis study is currently in outline form. Approximately half the synthesis is outlined in full sentences or paragraphs that are intended to be included directly into the final publication. The other half is outlined with a skeleton listing of topics that will be covered. Related work continues on a review of the seismicity of the United States and on a project to produce a map of the seismicity of North America.

A highlight of the Decade of North American Geology program is four new continent-scale tectonic maps (geothermal, stress, seismicity, and geologic) on a common base. The maps are in color, at a scale of 1:5,000,000, and use

a Transverse Mercator projection. Construction of the seismicity map has required the rationalization of more than one-half million earthquake epicenters from global, national, regional, and local catalogs. Duplicate entries were removed regionally based on a comparison of reported origin times, epicentral locations, and magnitudes. The reduced data base spans an interval from A.D. 1500 to 1985. Only those data that exceed the magnitude-completeness threshold for each region and time period were plotted. In all parts of the map, earthquakes of magnitudes less than 4 are represented by small dots, larger earthquakes by filled circles of various sizes in proportion to magnitude, and great earthquakes ($M \geq 7$) by large rings. Different colors are used to distinguish modern from historic data and to show deep ($h \geq 50$ km), intraplate earthquakes in subduction zones. The modern data are more useful than historic data for resolving seismotectonic features, as they have more accurate locations and lower magnitude-completeness thresholds. This scheme of symbols and colors reveals details of the seismotectonic fabric of North America yet preserves a perspective of historical earthquake occurrence.

Reports

Choy, G., and Engdahl, E.R., 1987, Analysis of broadband seismograms from selected IASPEI events: Physics fo the Earth and Planetary Interiors, in press.

Engdahl, E.R., and Billington, S., 1986, Focal depth determination of central Aleutian earthquakes: Bulletin of the Seismological Society of America, v. 76, p. 77-93.

Engdahl, E.R., and Kind, R., 1986, Interpretation of broadband seismograms from central Aleutian earthquakes: Ann. Geophysicae, v. 4, p. 233-240.

Engdahl, E.R., and Gubbins, D., 1987, Simultaneous travel-time inversion for earthquake location and subduction zone structure in the central Aleutian Islands: Journal of Geophysical Research, submitted.

Seismic Observatories

9920-01193

Leonard Kerry
Branch of Global Seismology and Geomagnetism
U.S. Geological Survey
Denver Federal Center
Box 25046, Mail Stop 967
Denver, Colorado 80225
(303) 236-1500

Investigations

Recorded and provisionally interpreted seismological and geomagnetic data at observatories operated at Newport, Washington; Cayey, Puerto Rico; and Agana, Guam. Continued operation of the Puerto Rican Seismic Telemetry Network from the main base located in Cayey, Puerto Rico. Operated advanced equipment for gathering research data for universities and other agencies at Cayey, Puerto Rico, and Agna, Guam. At Agana, Guam, a 24-hour standby duty was maintained to provide input to the Tsunami Warning Service operated at Honolulu Observatory by NOAA and to support the Early Earthquake Reporting function of the National Earthquake Information Service. Continued to telemeter long- and short-period seismic data on a real-time basis from Newport Observatory, Newport, Washington, to NEIC, Golden, Colorado; Pacific Tsunami Warning Center, Honolulu, Hawaii, and Alaska Tsunami Warning Center, Palmer, Alaska, to give support in the operation of their disciplines.

Results

Provided data on an immediate basis to the National Earthquake Information Service and the Tsunami Warning Service. Continued to send seismograms obtained from the WWSSN Systems operated at Agana, Guam, and Cayoy, Puerto Rico, to NEIS for use in the ongoing U.S. Geological Survey (USGS) programs. Analog seismic records and digital seismic tape records were obtained from the Agana, Guam SRO system and forwarded to ASL for use in ongoing USGS and other users' programs. Data from advanced research equipment was forwarded to universities or other agencies working in conjunction with USGS. Seismic data from the Puerto Rican net was provided on a continuing basis to the University of Puerto Rico for their use in studying and research of the seismicity of the Puerto Rican area.

Responded to requests from the public, interested scientists, universities, state, and Federal agencies regarding geophysical data and phenomena.

Global Seismograph Network Evaluation and Development

9920-02384

Jon Peterson
Branch of Global Seismology and Geomagnetism
U.S. Geological Survey
Albuquerque Seismological Laboratory
Building 10002, Kirtland AFB-East
Albuquerque, New Mexico 87115-5000
(505) 844-4637

Investigations

Work continued on the cooperative program to establish a digital seismograph network in China.

Results

All of the major facilities of the China Digital Seismograph Network (CDSN) were installed and operational by August 1986. These include nine stations, a data management center, and a depot maintenance center. Some work remains to get all network components in full operation and to stock and organize the maintenance depot. Data from some of the stations will be distributed on the GDSN network-day and event tapes beginning with the October 1, 1986, recording day. According to the cooperative agreement, data from the stations at Baijatuan (Beijing), Kuming, Lanzhou, Mudanjiang, and Urumqi will be sent to the Albuquerque Seismological Laboratory for distribution on the day tapes.

Digital Data Analysis

9920-01788

Stuart A. Sipkin
Branch of Global Seismology and Geomagnetism
U.S. Geological Survey
Denver Federal Center
Box 25046, Mail Stop 967
Denver, Colorado 80225
(303) 236-1506

Investigations

1. Moment Tensor Inversion. Apply methods for inverting body phase waveforms for the best point-source description to research problems.

2. Broadband Body-Wave Studies. Use broadband body phases to study lateral heterogeneity, attenuation, and scattering in the crust and mantle.

3. Computation of Free Oscillations. Study the effects of anelasticity on free oscillation eigenfrequencies and eigenfunctions.

4. Earthquake Recurrence Statistics. Use earthquake recurrence statistics and related parameters to better understand the earthquake cycle and study how they can be used for prediction and forecasting purposes.

5. Earthquake Location Technology. Study techniques for improving the robustness, honesty, and portability of earthquake location algorithms.

6. Real-Time Earthquake Location. Experiment with real-time signal detection, arrival-time estimation, and event location for regional earthquakes.

7. Data Collection Center. Develop a state-of-the-art data collection center to handle digital waveform data collection for the next decade.

8. NEIC Monthly Listing. Contribute both fault-plane solutions (using first-motion polarity) and moment tensors (using long-period body-phase waveforms) for all events of magnitude 5.8 or greater when sufficient data exists. Contribute waveform/focal-sphere figures of selected events.

Results

1. Moment Tensor Inversion. A catalog of moment tensors for all sufficiently large events during 1981-1983, including comparisons with the first-motion fault-plane solutions and the Harvard CMT solutions, is in press. The strengths and weaknesses of all three methods are assessed. A paper assessing the large number of non-double-couple earthquakes occurring in the Nazca plate subduction zone has been submitted for publication. We find that these earthquakes are caused by slip on non-planar fault surfaces which is, in turn, due to the extreme structural complexity in this region.

2. Broadband Body-Wave Studies. High-quality digitally recorded broadband data sets from the Gräfenberg Array in West Germany and the Regional Seismic Test Network in North America are being collected. New software is continuing to be developed.

3. Computation of Free Oscillations. An article on the use of variational methods in geophysics has been completed and will appear as a chapter in an IASPEI sponsored book on seismological algorithms.

4. Earthquake Recurrence Statistics. A journal article has been submitted in which recurrence time measurements are used to estimate a generic probability distribution. A key result is that all characteristic event earthquake recurrence times fit the same log-normal distribution if the recurrence intervals are normalized by the average recurrence time.

5. Earthquake Location Technology. An article reviewing state-of-the-art earthquake location technology has been completed and will appear as a chapter in the Encyclopedia of Geophysics.

6. Real-Time Earthquake Location. The real-time system developed in cooperation with the Instituto Nazionale di Geofisica (Italian Government) is being implemented in Golden, Colorado, for the United States Seismic Network. The system is being generalized to handle both digital and analog telemetry, different sample rates, and asynchronous channel timing. Dedicated microcomputer hardware has been procured for the near-real-time back-end system. Software for regional and teleseismic on-line event location is being tested. The current prototype is processing 128 analog channels. A color graphics workstation for doing the analysis has arrived and is being integrated into the system.

7. Data Collection Center. A new data collection system for the Albuquerque Seismological Laboratory is being implemented. By basing the hardware on 32-bit microcomputer and local area network technologies, it appears to be possible to achieve low cost, high reliability, and the flexibility to economically expand the capacity of the system from today's modest requirements to the full output of the proposed IRIS network a decade hence. The initial equipment will soon be delivered. Preparation for software conversion is progressing. The equipment needed to complete the initial system configuration is being studied.

8. NEIC Monthly Listing. Since January 1981, fault-plane solutions for large events have been contributed to the Monthly Listings. Since July 1982, moment tensor solutions and waveform/focal-sphere plots have also been contributed. Fault-plane solutions for the period 1981-1985, and moment tensor solution for the period 1981-1983, have recently been compiled and published. In the last six months solutions for approximately 64 events have been published.

Reports

Buland, R.P., 1987, Variational methods, in Doornbos, D.J., ed., Seismological Algorithms: Academic Press, in press.

_____1987, Earthquake location techniques, in James, D.E., ed., Encyclopedia of Geophysics: Van Nostrand, in press.

Buland, R.P., and Nishenko, S.P., 1986, A generic interval distribution for earthquake forecasting [abs.]: EOS (American Geophysical Union, Transactions), v. 67, in press.

Kubas, A., and Sipkin, S.A., 1987, Non-double-couple earthquake mechanisms in the Nazca plate subduction zone: Geophysical Research Letters, submitted.

Needham, R.E., 1986, Catalog of first motion focal mechanisms, 1981-1983, v. 1-3: U.S. Geological Survey Open-File Report 86-285A-C.

_____1986, Catalog of first motion focal mechanisms, 1984-1985, v. 1-3: U.S. Geological Survey Open-File Report 86-520A-C.

Nishenko, S.P., and Buland, R.P., 1987, A generic interval distribution for earthquake forecasting: Bulletin Seismological Society of America, submitted.

Nishenko, S.P., Perkins, D., and Buland, R.P., 1987, Normalized time and precursor reliability, in Proceedings of U.S. Geological Survey Red Book Conference, submitted.

Sipkin, S.A., 1986, Estimation of earthquake source parameters by the inversion of waveform data: Global seismicity, 1981-1983: Bulletin Seismological Society of America, v. 76, no. 6, in press.

_____1987, Moment tensor solutions estimated using optimal filter theory for 51 selected earthquakes, 1980-1984: Physics of the Earth and Planetary Interiors, in press.

Seismicity and Tectonics

9920-01206

William Spence
Branch of Global Seismology and Geomagnetism
U.S. Geological Survey
Denver Federal Center
Box 25046, Mail Stop 967
Denver, Colorado 80225
(303) 236-1506

Investigations

Studies carried out under this project focus on detailed investigations of large earthquakes, aftershock series, tectonic problems, and earth structure. Studies in progress have the following objectives:

1. Use earthquake focal mechanisms to infer the origins of present-day stresses acting at the proposed Cascadia subduction zone (W. Spence).

2. Provide tectonic setting for and analysis of the 1974 Peru gap-filling earthquake (W. Spence and C.J. Langer).

3. Examine the source properties (focal mechanism and depth) of aftershocks following large thrust earthquakes in subduction regions by using digital surface-wave data (C. Mendoza).

4. Determine the maximum depth and degree of velocity anomaly beneath the Rio Grande Rift and Jemez Lineament by use of a 3-D, seismic ray-tracing methodology (W. Spence and R.S. Gross).

Results

1. The seismicity of the Cascadia subduction zone is highly anomalous when compared to other subduction zones. A synthesis of nineteen focal mechanisms for the zone from Cape Mendocino to the Queen Charlotte fault shows that most of the offshore earthquakes are associated with maximum compressive stress axes that trend about N-S. The locations of these earthquakes indicate that much of the offshore plate system is being compressed by the northwestward motion of the Pacific plate. Similarly, there is considerable evidence for N-S compression in the shallow crust of the overriding North American plate. The fact that the South Gorda block is not subducting but is being driven northward (along with the northward movement of the Mendocino triple junction) suggests that a N-S shear traction can be transmitted into the overriding plate, consistent with the observed landward focal mechanism data. Earthquakes with downdip tension axes occur in the subducted Juan de Fuca plate, from southern Vancouver to just south of Puget Sound, indicating that the slab pull force is resisted at shallow depths there. Seismicity at the St. Helens seismic zone suggests that shallow resistance to the sinking of subducted Juan de Fuca plate exists that far south. However, the lack of seismicity at location of a

possible interface thrust zone for the entire Cascadia zone, the lack of seismicity in the subducted Juan de Fuca plate outside the indicated zone, and the cited predominant seismicity with N-S compression axes suggests that if subduction is occurring at the Cascadia zone, it is of very limited extent.

2. The great 1974 Peru thrust earthquake (M_S 7.8, M_W 8.1) occurred in a documented seismic gap, between two earthquakes each with magnitude of about 8, occurring in 1940 and 1942. Additional major earthquakes occurred in this region in 1966 and in 1970; all but the 1970 shock represent thrust faulting. The stress release of the October 3, 1974, main shock and aftershocks occurred in a spatially and temporally irregular pattern. The multiple-rupture main shock produced a tsunami with wave heights of 0.6 ft at Hawaii and which was observed, for example, at Truk Island and at Crescent City. The aftershock series essentially was ended with the occurrence of a M_S 7.1 aftershock on November 9, 1974. The several years of preseismicity data to this earthquake include an unusually clear example of the "Mogi donut" pattern.

3. Love and Rayleigh-wave signals recorded by the Global Digital Seismograph Network provide source-parameter information for moderate-magnitude aftershocks that followed the large (M_S 7.7) Colombia earthquake of 12 December 1979. Love/Rayleigh amplitude ratios observed in a 30-80 second passband are compared against theoretical values calculated for a suite of source models fixed at independently determined depths. In addition, a reference earthquake with known focal mechanism and depth is used to calibrate the procedure and to minimize the path and size effects. Source mechanisms compatible with the amplitude data and observed P-wave first motions are obtained. These mechanisms serve to identify subsidiary faulting not associated with the main shock rupture.

Similar surface-wave techniques are being implemented in the analysis of the aftershock sequence that followed the large (M_S 7.8) Chile earthquake of 3 March 1985. The earthquake ruptured about 1/3 of the rupture length inferred for the great (M_S 8.2-8.4) Valparaiso earthquake of 1906. By comparing the spectra observed in a 20-50 second period range, focal depths can be estimated and source mechanisms can be computed for the aftershocks. The aftershock properties should provide additional constraints on the faulting geometry produced by the main shock of 3 March 1985.

4. To a depth of about 160 km, the upper mantle P-wave velocity beneath the Rio Grande rift and Jemez lineament is 4-6 percent lower than beneath the High Plains Province. A 3-D, P-wave velocity inversion shows scant evidence for pronounced low P-wave velocity beneath the 240-km-long section of the Rio Grande rift covered by our array. However, the inversion shows a primary trend of 1-2 percent lower P-wave velocity underlying the northeast-trending Jemez lineament, down to a depth of about 160 km. The Jemez lineament is defined by extensive Pliocene-Pleistocene volcanics and late Quaternary faults. The upper mantle low-velocity segment beneath the Jemez lineament is at most 100 km wide and at least 150-200 km long, extending in

our inversion from Mt. Taylor through the Jemez volcanic center and through the Rio Grande rift. A Backus-Gilbert resolution calculation indicates that these results are well-resolved.

Reports

Mendoza, C., in press, Aftershock source properties using digital surface-wave data: The 1979 Colombia sequence: Bulletin of the Seismological Society of America.

Spence, William, 1986, The 1977 Sumba earthquake series: evidence for slab pull force acting at a subduction zone: Journal of Geophysical Research, 91, 7225-7239.

_____1986, Origins of stresses at the Cascadia subduction zone [abs.]: EOS (American Geophysical Union, Transactions), v. 67, p. 1115.

_____ in press, Slab pull and the seismotectonics of subducting lithosphere: Reviews of Geophysics.

United States Earthquakes

9920-01222

Carl W. Stover
Branch of Global Seismology and Geomagnetism
U.S. Geological Survey
Denver Federal Center
Box 25046, Mail Stop 967
Denver, Colorado 80225
(303) 236-1500

Investigations

1. One hundred and sixty-two earthquakes in 22 states were canvassed by a mail questionnaire for felt and damage data. Sixty-five of these occurred in Alaska and 37 in California. The largest magnitude event occurred on May 7 in the Andreanof Islands, Aleutian Islands, Alaska, at 51.41° N., 174.83° W., normal depth, magnitudes 6.5 m_b and 7.7 M_s, causing damage on Atka Island. A magnitude 6.5 M_s aftershock occurred on May 17. Four earthquakes in California (March 31 near San Jose, July 8 near Palm Springs, July 13 near San Diego, and July 21 near Bishop) and one on July 12 near Lima, Ohio, caused minor damage. The most damage was in the Palm Springs area where the preliminary estimate of damage was $4.5 million.

2. Hypocenters for earthquakes in the United States for the period April 1986, through September 30, 1986, have been computed and published in the Preliminary Determination of Epicenters (PDE) Weekly and Monthly Listings.

Results

A preliminary maximum intensity of VII was assigned to both the May 7, Aleutian Islands, Alaska, and the July 8, Palm Springs, California, earthquakes. The damage from the Aleutian Islands quake was on Atka Island where the air strip was badly cracked, some landsliding, and strong shaking of buildings. Most of the damage from the July 8 earthquake was in the Coachella Valley area from Palm Springs and areas to the north. The quake injured 19 people and caused minor damage to many homes and businesses but only seriously damaged 4 homes and 16 businesses. The July 12 Ohio earthquake, while only a magnitude 4.5 m_b was felt over most of Ohio and parts of Indiana, Kentucky, and Michigan.

Seismicity maps for the conterminous United States, Alaska, and the world showing earthquakes located during the month of the publication were included in each Monthly Listing of the PDE.

United States Earthquakes, 1983 (Bulletin 1698) has received director's approval and has been submitted for printing. A seismicity map of the conterminous United States and adjacent areas, 1975-1984 (GP-984) at a scale of 1:5,000,000 has received director's approval and is being printed.

Reports

Stover, C.W., 1985, Preliminary isoseismal map for the northeastern Ohio earthquake of January 31, 1986: U.S. Geological Survey Open-File Report 86-356, 7 p.

Data Processing Section

9920-02217

John Hoffman
Branch of Global Seismology and Geomagnetism
U.S. Geological Survey
Albuquerque Seismological Laboratory
Building 10002, Kirtland AFB-East
Albuquerque, New Mexico 87115-5000
(505) 844-4637

Investigations

1. Data Management Center for the China Digital Seismograph Network. The data processing system for the China Digital Seismograph Network has been installed in Beijing, China. Other than a few operational problems, some future modifications and a little more training this system is complete.

2. Data Processing for the Global Digital Seismograph Network. All of the data received from the Global Network and other contributing stations are reviewed and checked for quality.

3. Network-Day Tape Program. Data from the Global Network stations are assembled into network-day tapes which are distributed to regional data centers and other government agencies.

Results

1. Data Management Center for the China Digital Seismograph Network. The PDP 11/44 computer system for the Data Management Center was installed during February-March 1986. In June 1986, we returned to Beijing to install the system software for processing the station tapes and to assemble this data into network-day tapes which would include all of the data from this network for a specific day recorded on one digital tape. At the same time the Chinese computer operators were thoroughly trained in all operational aspects of the various programs. The primary problem in Beijing is maintenance of the computer system. We have contracted with the Digital Equipment Corporation, Hong Kong Office to maintain the equipment, which appears to be working satisfactorily, although at times there are considerable delays between the request for service and the arrival of the service technician. The field data is recorded on small 1/4-inch cartridge magnetic tapes which are forwarded by the stations to Beijing where they are copied and forwarded to Albuquerque. We are providing extra hardware to be installed in February 1987 for additional backup in copying these cartridge tapes. The Albuquerque Seismological Laboratory will continue to support the Data Management Center with supplies, spare parts and software assistance over the next several years.

2. Data Processing for the Global Digital Seismograph Network. During the past six months, 639 digital tapes (223 SRO/ASRO, 260 DWWSSN, and 156 RSTN) from the Global Network and other contributing stations were edited, checked for quality, corrected when feasible, and archived at the Albuquerque Seismological Laboratory (ASL). The Global Network is presently comprised of 12 SRO stations, 4 ASRO stations, and 14 DWWSSN stations. In addition, there are six contributing stations which include Glen Almond, Canada, plus the five RSTN stations which are supported by Sandia National Laboratories. Nine digitally recording stations have been installed in the People's Republic of China, and copies of their tapes have started to arrive on a regular basis at the ASL during the past four weeks.

3. Network-Day Tape Program. The network-day tape program is a continuing program which assembles all of the data recorded by the Global Digital Seismograph Network plus the contributing stations for a specific calendar day onto one magnetic tape. This tape includes all the necessary station parameters, calibration data, frequency response, and time correction information for each station in the network. Five stations from the China Digital Seismograph Network will be added to this network-day tape starting in October 1986.

Data Processing, Golden

9950-02088

Robert B. Park
Branch of Engineering Geology and Tectonics
U.S. Geological Survey
Box 25046, MS 966, Denver Federal Center
Denver, CO 80225
(303) 236-1638

Investigations

The purpose of this project is to provide the day-to-day management and systems maintenance and development for the Golden Data Processing Center. The center supports Golden-based Office of Earthquakes, Volcanoes, and Engineering investigators with a variety of computer services. The systems include a PDP 11/70, several PDP 11/03's and PDP 11/23's, a VAX/750, a VAX/780, a MicroVAX, and two PDP 11/34's. Total memory is 14 mbytes and disk space will be approximately 6 G bytes. Peripherals include five plotters, ten mag-tape units, an analog tape unit, five line printers, 5 CRT terminals with graphics, a Summagraphic digitizing table, and a laser disk. Dial-up is available on all the major systems and hardwire lines are available for user terminals on the upper floors of the building. Users may access any of the systems through a Gandalf terminal switch. Operating systems used are RSX11 (11/34's), Unix (11/70), RT11 (LSI's) and VMS (VAX's).

The three major systems are shared by the Branch of Global Seismicity and Geomagnetism and the Branch of Engineering Geology and Tectonics.

Results

Computation performed is primarily related to the Global Seismology and Hazards programs; however, work is also done for the Induced Seismicity and Prediction programs as well as for DARPA, ACDA, MMS, U.S. Bureau of Reclamation and AFTAC, among others.

In Global Seismology and Geomagnetism, the data center is central to nearly every project. The monitoring and reporting of seismic events by the National Earthquake Information Service is 100 percent supported by the center. Their products are, of course, a primary data source for international seismic research and have implications for hazard assessment and prediction research as well as nuclear test ban treaties. Digital time series analysis of Global Digital Seismograph Network data is also 100 percent supported by the data center. These data are used to augment NEIS activities as well as for research into routine estimation of earthquake source parameters. The data center is also intimately related to the automatic detection of events recorded by telemetered U.S. stations and the cataloging of U.S. seismicity, both under development.

In Engineering Geology and Tectonics, the data center supports research in assessing seismic risk and the construction of national risk maps. It also provides capability for digitizing analog chart recordings and maps as well as analog tape. Also, most, if not all, of the research computing related to the hazards program are supported by the data center.

The data center also supports equipment for online digital monitoring of Nevada seismicity. Also, it provides capability for processing seismic data recorded on field analog and digital cassette tape in various formats. Under development is a portable microprocessor-based system to be used by the field investigations group to do preliminary analysis and editing of temporary local networks and the GOES Satellite Event Detect System. Recent acquisitions include the VAX/750, laser plotter, three additional tape drives, two HP plotters, DECNET/ETHERNET, and 400 MB of disk storage. A VAX-based accounting system has been developed for an up-to-date reporting capability on branch projects.

National Earthquake Information Center

9920-01194

Waverly J. Person
Branch of Global Seismology and Geomagnetism
U.S. Geological Survey
Denver Federal Center
Box 25046, Mail Stop 967
Denver, Colorado 80225
(303) 236-1500

Investigations and Results

The Quick Epicenter Determinations (QED) continues to be available to individuals and groups having access to a 300-baud terminal with dial-up capabilities to a toll-free watts number or a commercial telephone number in Golden, Colorado. The time period of data available in the QED is approximately three weeks (from about two days behind real time to the current PDE in production). The QED program is available on a 24-hour basis, 7 days a week. From April 1, 1986 through September 30, 1986, we have had approximately 1264 log-ins.

The weekly publication, Preliminary Determination of Epicenters (PDE) continues to be published, averaging about 100 earthquakes per issue. The QED, PDE Monthly Listing and Earthquake Data Report (EDR) continue to be prepared on the VAX/1180 with very little down time encountered.

Telegraphic data are not being received from the USSR on magnitude 6.5 or greater earthquakes at this time. We are attempting to find out what the problems may be.

Data from the People's Republic of China via the American Embassy are being received in a very timely manner and in time for the PDE publication. We continue to receive four stations on a weekly basis from the State Seismological Bureau of the People's Republic of China. The Bulletins with additional data are not being received in time for the Monthly. We have rapid data exchange (alarm quakes) with Centre Seismologique European-Mediterranean (CSEM), Strasbourg, France, and Instituto Nazionale de Geofisica, Rome, Italy, and data by telephone from Mundaring Geophysical Observatory, Mundaring, Western Australia and Japan Meteorological Agency (JMA).

The Monthly Listing of Earthquakes is up to date. As of September 30, 1986, the Monthly Listing and Earthquake Data Report (EDR) were completed through May 1986. A total of 6,780 events were published for the 6-month period. Solutions continue to be determined when possible and published in the Monthly Listing and EDR for any earthquake having an m_b magnitude $\geq$ 5.8. Centroid moment tensor solutions from Harvard University continue to be published in the Monthly Listing and EDR. Moment tensor solutions are being computed by the U.S. Geological Survey and are also published in the above publications. Waveform plots are being published for selected events having

m_b magnitudes $\geq$ 5.8. Beginning with the month of October 1985, depths for selected events were obtained from broadband displacement seismograms and waveform plots published in the Monthly.

The Earthquake Early Alerting Service (EEAS) continues to provide information on recent earthquakes on a 24-hour basis to the Office of Earthquakes, Volcanoes, and Engineering scientists, news media, other government agencies, foreign countries, and the general public. Sixty releases were made from April 1, 1986 through September 30, 1986. The most significant earthquake released during the period in the United States: a magnitude 7.7 on May 7 in the Andreanof Islands, Aleutian Islands, a magnitude 6.0 in southern California on July 8, and a magnitude 5.8 in the same area on July 13. Foreign earthquakes: magnitude 6.9 in Romania on August 30, and a magnitude 5.9 in southern Greece on September 13.

Reports

Earthquake Information Bulletin, "Earthquakes," v. 17, no. 4, January-February 1985; "Earthquakes," v. 17, no. 5, March-April 1985; "Earthquakes," v. 17, no. 6, May-June 1985.

Monthly Listing of Earthquakes and Earthquake Data Reports (EDR); six publications from December 1985 through May 1986. Compilers: W. Jacobs, L. Kerry, J. Minsch, R. Needham, W. Person, B. Presgrave, W. Schmieder.

Person, Waverly J., Seismological Notes: Bulletin of the Seismological Society of America, v. 76, no. 2, May-June 1985; v. 76, no. 3, July-August 1985; v. 76, no. 4, September-October 1985, v. 76, no. 5, November-December 1985.

Preliminary Determination of Epicenters (PDE); 26 weekly publications from April 4, 1986 to September 26, 1986, numbers 10-86 through 10-86. Compilers: W. Jacobs, L. Kerry, J. Minsch, W. Person, B. Presgrave, W. Schmieder.

Quick Epicenter Determination (QED) (daily): Distributed only by electronic media.

National Earthquake Catalog

9920-02648

James N. Taggart
Branch of Global Seismology and Geomagnetism
U.S. Geological Survey
Denver Federal Center
Box 25046, Mail Stop 967
Denver, Colorado 80225
(303) 236-1506

Investigations

1. Answered inquiries concerning filmed historical seismograms, evaluated many of the seismograms, and supplied a limited number of the seismograms to requestors.

2. Edited and supplied a file of 163,000 global hypocenters for a new map of volcanoes, earthquakes, and tectonic plates.

3. Participated in the planning for a new national digital seismograph network.

Results

1. The distribution of copies of historical seismograms at cost continued to be a problem because of the poor quality of many of the films. Filmed 16mm and 35mm archival copies of original smoked paper seismograms commonly were too faint to be reproduced, and should be refilmed with different cameras and special illumination techniques. Many other seismograms lacked calibration or timing identification. Enlarged paper copies of the films were supplied to a few requestors, but generally the traces on these copies were too dim to permit digitization.

The filming of Worldwide Standardized Seismograph Network (WWSSN) records and the distribution at cost of standing and special orders of the films continued to be free of problems. Supervision of this work was transferred to this project on August 1, 1986. One contract employee and one part-time U.S. Geological Survey (USGS) employee checked and labeled the original paper seismograms, which were then sent to a photographic contractor. Another contract employee and three part-time USGS employees filed and inventoried the master archival film copies, pulled the masters for duplication, and refiled the masters when they were returned by the photographic contractor.

The contract for seismogram filming for the next fiscal year was considerably revised to overcome unanticipated problems that occurred during the first 15 months of operation under Geological Survey auspices. The future contract can run up to three years, permitting much more stability in the

cost to users of the various filming services. In addition, single seismograms can be obtained, rather than restricting purchases to complete reels of film.

2. Magnitude data for over 1600 earthquakes with M_s or $m_b \geq 6.8$, covering the years 1897-1980, was collected and edited from various papers by K. Abe and coauthors. This listing is the most complete file available of large earthquakes with uniformly determined instrumental magnitudes. This file was then merged into a file of 163,000 global earthquakes that will be used to prepare a map of volcanoes, earthquakes, and tectonic plates.

3. Maps of low noise level seismograph sites were prepared as part of a plan to develop a national digital seismograph network which would utilize transmission of data via commercial satellite. The distribution of the network stations is intended to provide location capability for all earthquakes with magnitudes > 2.5 in the conterminous states and with magnitudes > 3.5 in Alaska.

4. Plans were developed for a major change in the use of space by the National Earthquake Information Center (NEIC). A large operations area, equipped with interactive work stations, will permit the entire staff of Early Alerting Service analysts to locate and report the occurrence of significant or disastrous earthquakes without interruption from non-participants. In addition, the archival filmed seismograms will be moved into new quarters as part of World Data Center A for Seismology.

Seismic Review and Data Services

9920-01204

James N. Taggart
Branch of Global Seismology and Geomagnetism
U.S. Geological Survey
Denver Federal Center
Box 25046, Mail Stop 969
Denver, Colorado 80225
(303) 236-1506

Investigations and Results

R.P. McCarthy, former leader of this project, retired on August 1, 1986. J.N. Taggart is temporarily managing the project until a new leader is appointed.

Technical review and quality control were carried out on 410 station months of seismograms from the Worldwide Standardized Seismograph Network (WWSSN). Eleven to thirteen station months of Seismic Research Observatory (SRO and ASRO) seismograms were supplied to the National Earthquake Information Service each month to provide data for the PDE hypocenters. The WWSSN seismograms were also checked for first-motions of earthquakes with magnitudes $\geq$ 5.8.

Annual WWSSN Performance Reports have been postponed until a new project leader is appointed. The overall quality of the WWSSN seismograms remains high. Identified instrumentation problems were reported to the Albuquerque Seismological Laboratory (ASL), but in all cases the station operator already had advised ASL of the problem.

Monthly reports covering the analog and digital records received from the WWSSN, DWSSN, SRO, and ASRO networks have been discontinued, but the history and current status of the WWSSN seismograms are incorporated into a new inventory database. Advice and information about the WWSSN records were provided to the public via telephone or response to mail inquiries. The status of the digital networks is published elsewhere in a quarterly report.

Over 9,500 microfiche WWSSN seismogram copies and 37 reels of other microfilmed seismograms were supplied at cost to 19 researchers on special orders. Ten standing orders for all WWSSN seismograms received and filmed during the fiscal year and one standing order for Canadian National Network filmed seismograms were sent monthly to institutions and U.S. Geological Survey (USGS) repositories. Altogether 519,000 copies of seismograms were supplied to the public during this reporting period. About 90 percent of the original seismograms were mailed back to the stations at their request. The remaining seismograms, including those from USGS observatories, will be archived at the National Records Center in Denver.

Digital Data Acquisition for Strong Motion Seismology

9910-02089

Roger D. Borcherdt
James F. Gibbs

Branch of Engineering Seismology and Geology
345 Middlefield Road, MS 977
Menlo Park, CA 94025
(415) 323-8111, ext. 2910

Investigations

Cooperative seismological and engineering studies to extend bandwidth and detection thresholds for a variety of active and passive experiments including: near-source strong motion, source mechanisms for aftershock sequences, velocity and Q^{-1} structure for crust and upper mantle, short-period earth strain, high-frequency wave propagation from downhole arrays, local-site amplification studies and earthquake engineering. This project, during the report period, has been responsible for the maintenance, operation, and deployment of wide dynamic range, broad band digital recorders (General Earthquake Observation System, GEOS) to acquire data sets for the cooperative studies indicated. This project has been conducted in conjunction with project 9910-03009 (see Maxwell and Borcherdt) with contributions from G. Sembera, J. Sena, C. Dietel, R. Warrick, G. Jensen, D. Myren, D. Hopkins.

Results:

1. Maintenance laboratory; several improvements in laboratory maintenance procedures have been implemented by J. Sena, and C. Dietel, including: hardware modifications and tests to restrict least count noise levels to least significant bit at 60 dB gain, improved field check-out and instrument operation procedures, sensor maintenance and calibration procedures. The first phase of construction of GEOS units has been completed with 45 operational systems.

2. High frequency downhole array studies with emphasis on earthquake prediction - In cooperation with P. Malin at UCSB, six-component downhole arrays have been recorded on three GEOS since installation in July 1985. This project is focusing on extending bandwidth and signal resolution thresholds for seismic detection near Parkfield, California. Each sensor component has been calibrated and adjusted to 0.5 v/cm/s sensitivity with the installation of appropriate S and T resistors by R.E. Warrick and R. Frye. Since installation, several hundred event files have been processed by G. Glassmoyer. Preliminary analyses show that downhole background noise levels are about 15 dB less in power spectral density than those at the surface in the band 5-20 Hz. A larger improvement in signal to noise ratios is apparent for frequencies in the 20-100 Hz interval. Significant near-surface amplification (up to 20 dB in amplitude) is apparent for signals (5-15 Hz) recorded at each of the sites. Utilization of low-noise 16 bit digital recorders together with the 2 Hz downhole arrays has permitted

extensions of the bandwidth for detection of seismic signals both uphole and downhole. Amplitude spectra computed for a signal-to-noise ratio of greater than 2 (in power) suggest that signal detection bandwidths can be routinely extended to 70-75 Hz uphole and 80-85 Hz downhole for local events with magnitudes about 1.

3. Seismic Refraction Studies in support of Northern Nevada Lithospheric Experiment (PASSCAL) - In cooperation with investigators from 16 institutions, W. Mooney, G. Sembera and C. Dietel the Basin and Range experiment was conducted from 17 July to 2 August, 1986 in northwestern Nevada. Coincident with the controlled source experiments, which were executed on July 22, 25, and 28, experiments were conducted to record aftershocks from the M 6.1 earthquake, which occurred near Bishop, California at a distance of approximately 220 km on July 21, 1986. This report provides a preliminary summary of the data recorded using twenty 6-channel digital data acquisitions (GEOS) deployed in support of the acitve and passive experiments. For the active experiments the instrumentation was deployed to augment the measurements by 16 other institutions to infer 1) lithosperic structures of a region of active extension, 2) anomolous upper-mantle velocity structure, 3) characteristics of deep impedence boundaries as inferred from vertical and wide angle reflection data. For the passive experiments, the instrumentation was programmed to record earthquakes along profiles up to 60 km in length to provide information on upper mantle structures as inferred from 3 component recordings.

Profile locations for the GEOS were selected at distances to emphasize information on the transition from pre- to post-critical reflection for the mantle (Deployments 1 and 2) and lateral structure variations as inferrable from fan profiles at pre- and post-critical distances (Deployment 2). Experiments to record earthquakes were conducted during 24-48 hour periods prior to and after each of the controlled source experiments.

DATA SUMMARY

DEPLOYMENT LOCATIONS: Locations of sites occupied by GEOS and shotpoints are shown on figure 1. Eleven sites were occupied along the north-south line within 6-8 hours following the M 6.1 earthquake on July 21, 1986. An additional nine sites were occupied 24 hours later with two of these sites being at shotpoints on the ends of the N-S line. The profile was extended to record a fan profile for the east-west line for deployment 2. Sites along the east-west line were occupied for deployment 3.

EARTHQUAKE DATA: Forty earthquakes in the Bishop area were recorded at three or more sites during the experiment (see table 1 for listing derived from Calnet). Of this number 1,3 and 36 events occurred respectively in the magnitude ranges 5.5-6, 4-5, and 3-4. Even though the events did not always occur when the majority of instruments were programmed to record earthquakes, eight of the events were recorded simultaneously at eight or more sites. Five stations were deployed and recorded at the time of the largest aftershock (M 5.5). An example of the three-component recordings (z, r, t) obtained along the north-south line for one of the aftershocks ($M \sim 3.8$) is illustrated (figs. 2a, 2b, 2c.)

CONTROLLED SOURCE DATA: All twenty eight shots were recorded (see previous discussion for locations occupied for each deployment). Instruments were programmed to record as 6-channel systems to provide, in addition to 3-component velocity time histories, on scale acceleration recordings at locations G-69 and the two shotpoints at the end of the north-south line. The remaining systems were programmed to record as three-channel systems. A typical record section for the transverse component of motion recorded from one of the shotpoints on the east-west line is illustrated (fig. 3).

DATA PROCESSING: C. Dietel has transferred data from the computer compatible cartridge tapes recovered in the field to nine-track tapes for final merging and processing to be distributed in SEG-Y format via IRIS-DMC. He hopes to have data available for digital distribution by December 1, 1986.

4. Short Period Earth-Strain - In cooperation with M. Johnston and D. Myren of USGS, short period (10^{5} - 10^{-1}s) earth strain has been observed at four sites for which Sacks'-Evertson dilatometers have been installed in a cooperative project with A. Linde and S. Sacks of Carnegie Institution of Washington. The GEOS have been deployed in a long-term deployment configuration to simultaneously record the output of the downhole dilatometer and three component colocated seismometers. Operating the GEOS systems in event trigger mode, several hundred event files have been processed. Earth strain noise levels have been measured over the period band 10^{-7}-10^{2} Hz at 9 dilatometer sites. Utilization of 16 bit recorders has permitted extensions of both the resolution and bandwidth of signals detected by the Sacks'-Evertson dilatometers, as illustrated in the following figures.

   Figure 4 shows the present telemetry bandwidths for detection of volumetric strain and the short-period seismic networks superimposed on earth strain noise as determined at a dilatometer site near Hollister, California. Use of 16 bit on-site recording with selectable sample rates has extended the detection bandwidth for volumetric strain at earth noise levels into the passband of the short period seismic networks. Recordings of the recent North Palm Springs earthquake. Figures (5,6,7 and 8) serve to illustrate the improved detection capabilities. The original recordings (Figure 5) obtained at the Punchbowl site at a distance of 134 km when filtered between 1 and 10 Hz (Figure 6) show signals in the passband of short period seismic networks and when low-pass filtered (7) signals not previously observable in either of the telemetry passbands. The 16 bit resolution of the recorder permits more than a 2 order of magnitude improvement in detection thresholds down to levels of about 2×10^{-12} as illustrated in Figure 8.

5. Aftershock Sequence for Earthquake of January 31, 1986 near Painseville, Ohio - This project, conducted with contributions from G. Sembera and C. Dietel, in the field and J. Serran and G. Maxwell in the lab, resulted in the acquisition of aftershock data from a ten-station array of GEOS systems deployed during the time period of February 1, 1986-March 23, 1986. Analysis of the recordings are reported in a project entitled "Anelastic Wave Propagations" (Borcherdt; 9910-02689).

6. Aftershock Sequence for Chalfant earthquake near Bishop - In cooperation with D. Hill and B. Julian 20 GEOS were deployed in support of a dense array study together with 120 analog cassette recorders for source inversion studies following the Northern Nevada Lithospheric Experiment. Preliminary evaluations of the data indicate more than 100 events were recorded during the 48 hour period for which the GEOS were deployed. Interpretation of these data is being pursued by B. Julian and R. Cockerham.

Reports

Andrews, M., and Borcherdt, R.D., 1986, Response of near-surface geology from uphole-downhole asrrays at Coalinga, California [abs.]: *American Geophysical Union* Fall Meeting, December 1986, San Francisco.

Borcherdt, R.D., (ed.), 1986, Preliminary report on aftershock sequence for the earthquake of January 31, 1986 near Painesville, Ohio (time Period: 2/1/86-2/10/86): *U.S. Geological Survey Open-File Report 86-181.*

Johnston, M.J.S., Borcherdt, R.D., and Linde, A.T., 1986, Short period strain ($0.1\text{-}10^5{}_s$): near source strainfield for an earthquake (M_L 3.2) near San Juan Bautista, California: *Journal of Geophysical Research*, v. 91, p. 11,497-11,502.

Wesson, R.L., and Nicholson, C., (eds.), 1986, Studies of the January 31, 1986 northeastern Ohio earthquake: *U.S. Geological Survey Open-File Report 86-331*, 131 p.

Table 1

EARTHQUAKES RECORDED DURING NORTHERN NEVADA PASSCAL EXPERIMENT
(GEOS:CALNET LISTING)

DATE	HR/MN	SEC	LAT	LONG	DEPTH	MAG	RMS
860722	351	4.34	37-28.93	118-22.90	11.53	3.00	0.16
860721	2239	17.63	37-37.80	118-33.19	0.17	3.08	1.05
860722	221	32.15	37-39.39	118-33.91	2.88	3.11	0.76
860725	610	30.49	37-31.31	118-29.58	4.52	3.12	0.70
860724	922	30.19	37-34.02	118-25.62	6.18	3.13	0.70
860722	1215	47.17	37-36.89	118-28.65	10.81	3.14	0.43
860724	1134	51.00	37-33.13	118-26.29	12.41	3.16	0.05
860725	1011	3.97	37-35.10	118-29.00	9.40	3.18	0.40
860721	2151	44.45	37-36.58	118-26.39	5.04	3.19	0.10
860722	1712	0.62	37-30.49	118-28.58	6.40	3.21	0.10
860722	643	26.51	37-32.43	118-26.28	12.48	3.22	0.09
860722	1357	34.41	37-32.31	118-29.08	10.28	3.25	0.07
860722	633	38.63	37-32.39	118-25.65	13.31	3.26	0.50
860724	1458	44.53	37-29.94	118-23.25	8.04	3.28	0.10
860722	524	4.77	37-33.08	118-18.32	0.76	3.30	1.52
860722	318	47.66	37-32.20	118-26.27	10.58	3.32	0.09
860724	117	9.19	37-35.16	118-28.14	10.69	3.32	0.25
860724	1644	40.02	37-33.91	118-25.93	11.05	3.34	0.31
860722	934	15.57	37-27.27	118-22.45	12.00	3.37	0.08
860721	21 8	41.31	37-35.41	118-27.83	7.93	3.40	0.06
860722	829	15.28	37-32.10	118-24.91	5.88	3.45	0.25
860729	711	58.24	37-33.24	118-26.48	10.23	3.48	0.04
860721	2343	8.95	37-40.30	118-40.74	9.18	3.49	0.27
860724	610	4.84	37-28.21	118-22.14	9.12	3.51	0.12
860722	0 9	53.55	37-37.59	118-28.77	0.60	3.55	0.11
860722	3 2	10.30	37-35.43	118-28.58	8.33	3.56	0.25
860722	1334	5.34	37-39.17	118-52.09	4.45	3.58	0.57
860722	540	42.02	37-28.28	118-21.70	3.01	3.58	1.36
860724	243	10.41	37-36.52	118-28.26	4.06	3.58	0.08
860722	1224	49.65	37-32.00	118-28.57	11.65	3.62	0.26
860722	1717	21.00	37-31.29	118-26.26	11.34	3.64	0.06
860722	658	0.05	37-29.76	118-22.44	6.27	3.69	0.11
860722	621	52.24	37-27.13	118-22.97	15.01	3.81	0.09
860721	2036	4.67	37-32.02	118-26.96	10.97	3.81	0.05
860724	15 4	58.39	37-32.71	118-24.29	0.42	3.90	0.08
860722	1348	44.36	37-26.58	118-25.05	9.53	3.98	0.14
860724	19 3	25.43	37-28.81	118-22.43	9.99	4.2	0.09
860729	957	56.61	37-36.08	118-28.10	11.22	4.2	0.05
860722	1829	50.23	37-40.01	118-50.23	4.38	4.5	0.47
860721	22 7	0.99	37-29.76	118-23.60	10.26	5.50	0.08

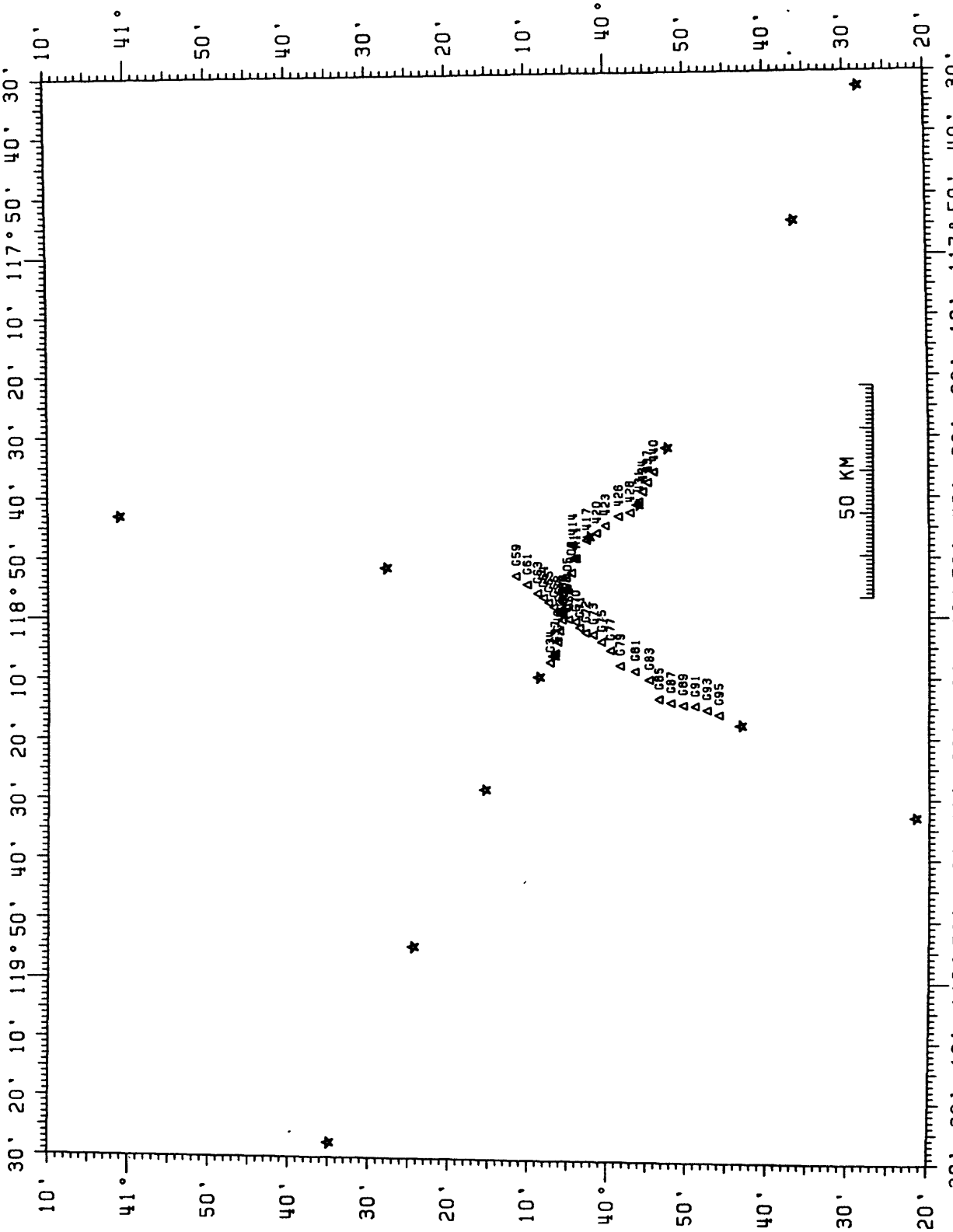

Figure 1

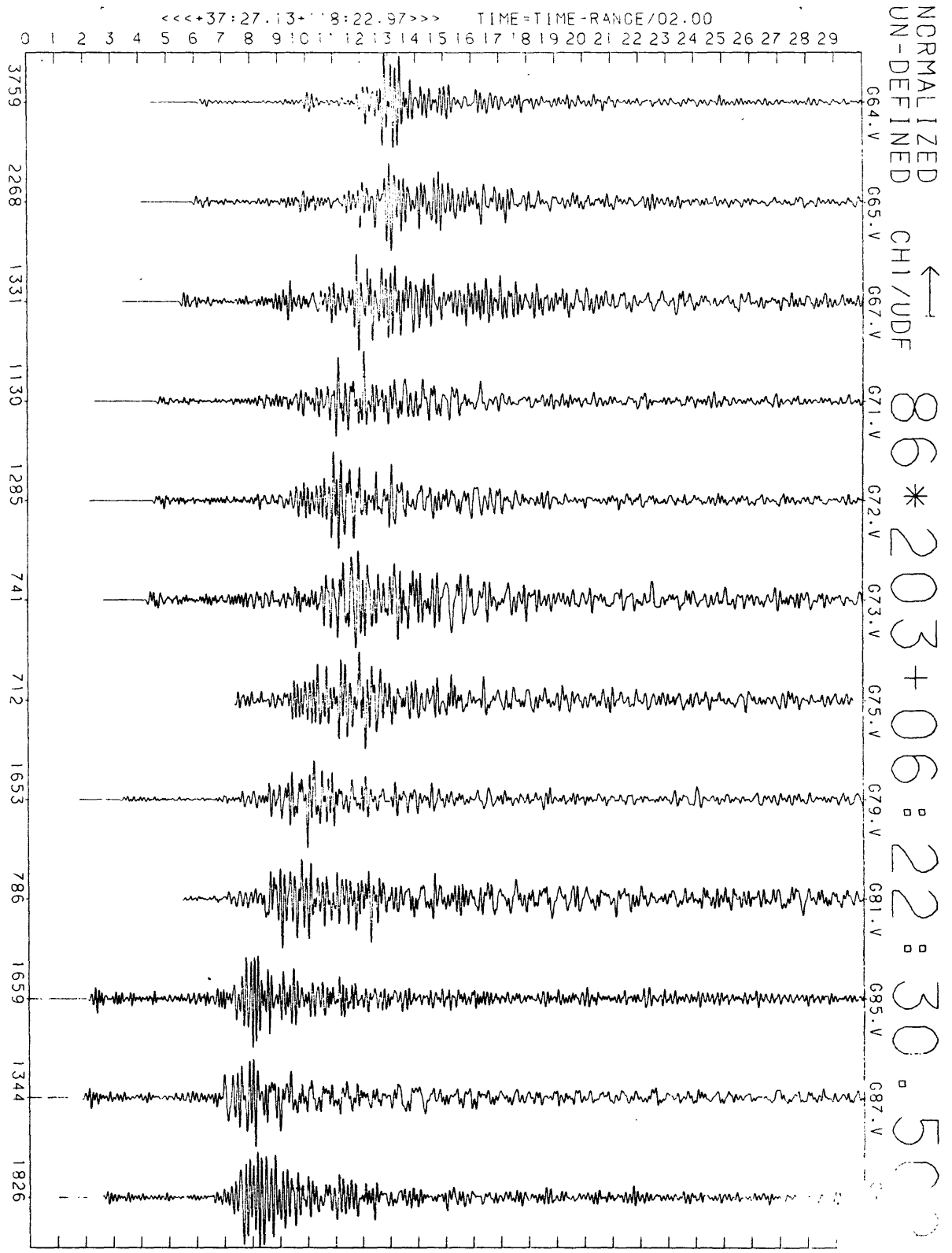
NORMALIZED
UN-DEFINED
CH1/UDF
86*203+06:22:30.50
<<<+37:27.13+ 8:22.97>>>
TIME=TIME-RANGE/02.00
0 1 2 3 4 5 6 7 8 9 10 11 12 13 14 15 16 17 18 19 20 21 22 23 24 25 26 27 28 29
3759
2268
1331
1130
1285
741
712
1653
786
1659
1344
1826
G64.V
G65.V
G67.V
G71.V
G72.V
G73.V
G75.V
G79.V
G81.V
G85.V
G87.V

Figure 2a

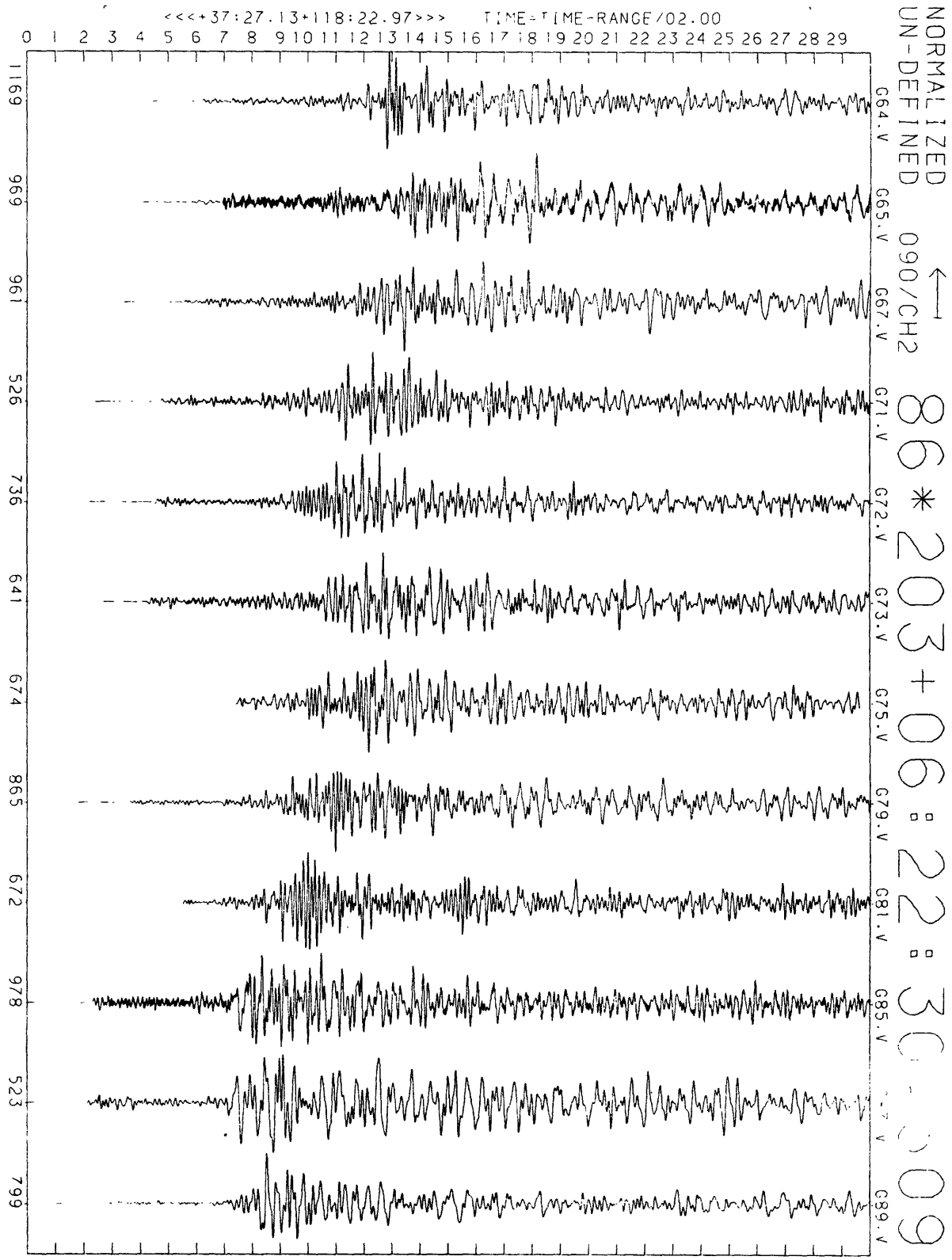
<<<+37:27.13+118:22.97>>> TIME=TIME-RANGE/02.00
0 1 2 3 4 5 6 7 8 9 10 11 12 13 14 15 16 17 18 19 20 21 22 23 24 25 26 27 28 29
NORMALIZED
UN-DEFINED
090/CH2
86*203+06:22:30.09
1169
969
961
526
736
641
674
865
672
978
523
799
G64.V
G65.V
G67.V
G71.V
G72.V
G73.V
G75.V
G79.V
G81.V
G85.V
G89.V

Figure 2b

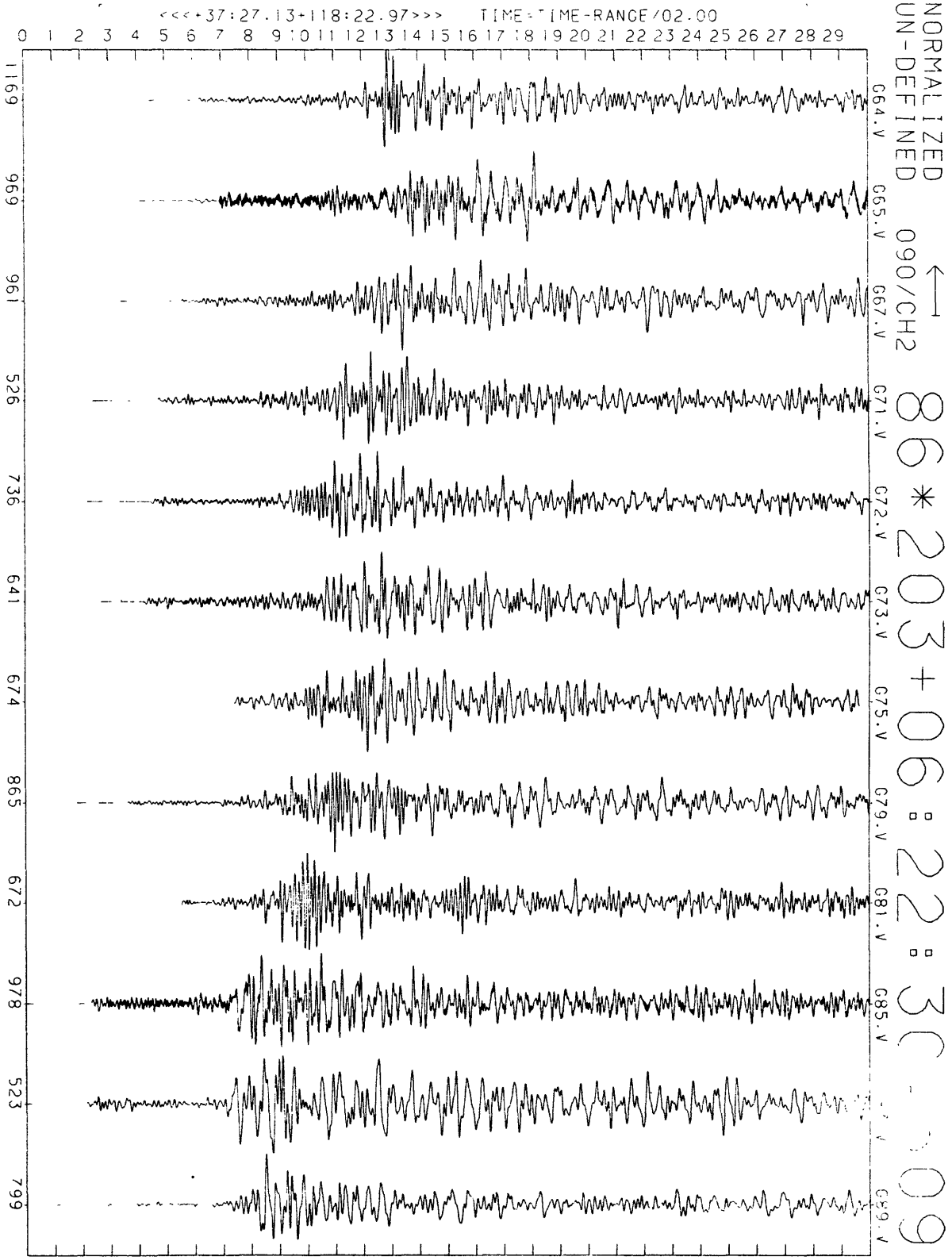
<<<+37:27.13+118:22.97>>> TIME=TIME-RANGE/02.00
0 1 2 3 4 5 6 7 8 9 10 11 12 13 14 15 16 17 18 19 20 21 22 23 24 25 26 27 28 29
NORMALIZED
UN-DEFINED
090/CH2
86*203+06:22:30.09
1169
969
961
526
736
641
674
865
672
978
523
799
G64.V
G65.V
G67.V
G71.V
G72.V
G73.V
G75.V
G79.V
G81.V
G85.V
G89.V

Figure 2c

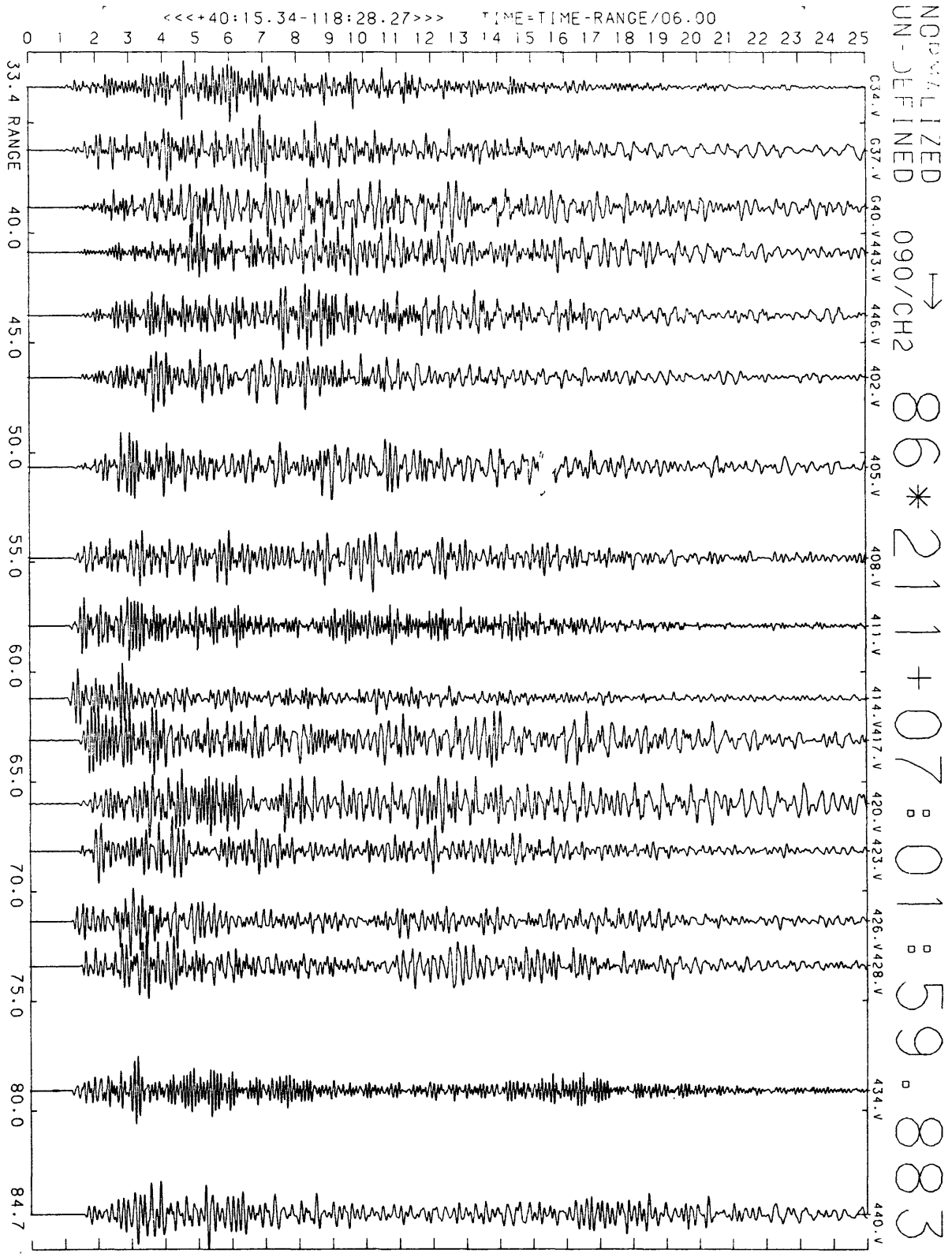
<<<+40:15.34-118:28.27>>>
TIME=TIME-RANGE/06.00
0 1 2 3 4 5 6 7 8 9 10 11 12 13 14 15 16 17 18 19 20 21 22 23 24 25
33.4 RANGE
40.0
45.0
50.0
55.0
60.0
65.0
70.0
75.0
80.0
84.7
C34.V G37.V G40.V443.V 446.V 402.V 405.V 408.V 411.V 414.V417.V 420.V 423.V 426.V428.V 434.V 440.V
NORMALIZED
UN-DEFINED
090/CH2
86*211+07:01:59.883

Figure 3

AMBIENT NOISE (EARTH STRAIN and GROUND VELOCITY)
POWER SPECTRAL DENSITY ((ΔV/V)^2/Hz in dB)
-300
-250
-200
-150
-100
SATELLITE TELEMETRY
(1 s/10 min.)
M2
SHORT PERIOD
SEISMIC NETWORK
10 SPS-GEOS-DC
50 SPS-GEOS-AC
1200 SPS-GEOS-AC
DOWNHOLE
UPHOLE
L-22E
100 Days
10 Days
1 Day
0.1Day
10^7
10^6
10^5
10^4
10^3
10^2
10
1
0.1
0.01
0.001
PERIOD (Seconds)
-190
-150
-100
-50
0
50
POWER SPECTRAL DENSITY ((cm/s)^2/Hz in dB ref. 1 m^2/s^2
(V = 3.16 km/s)

figure 4

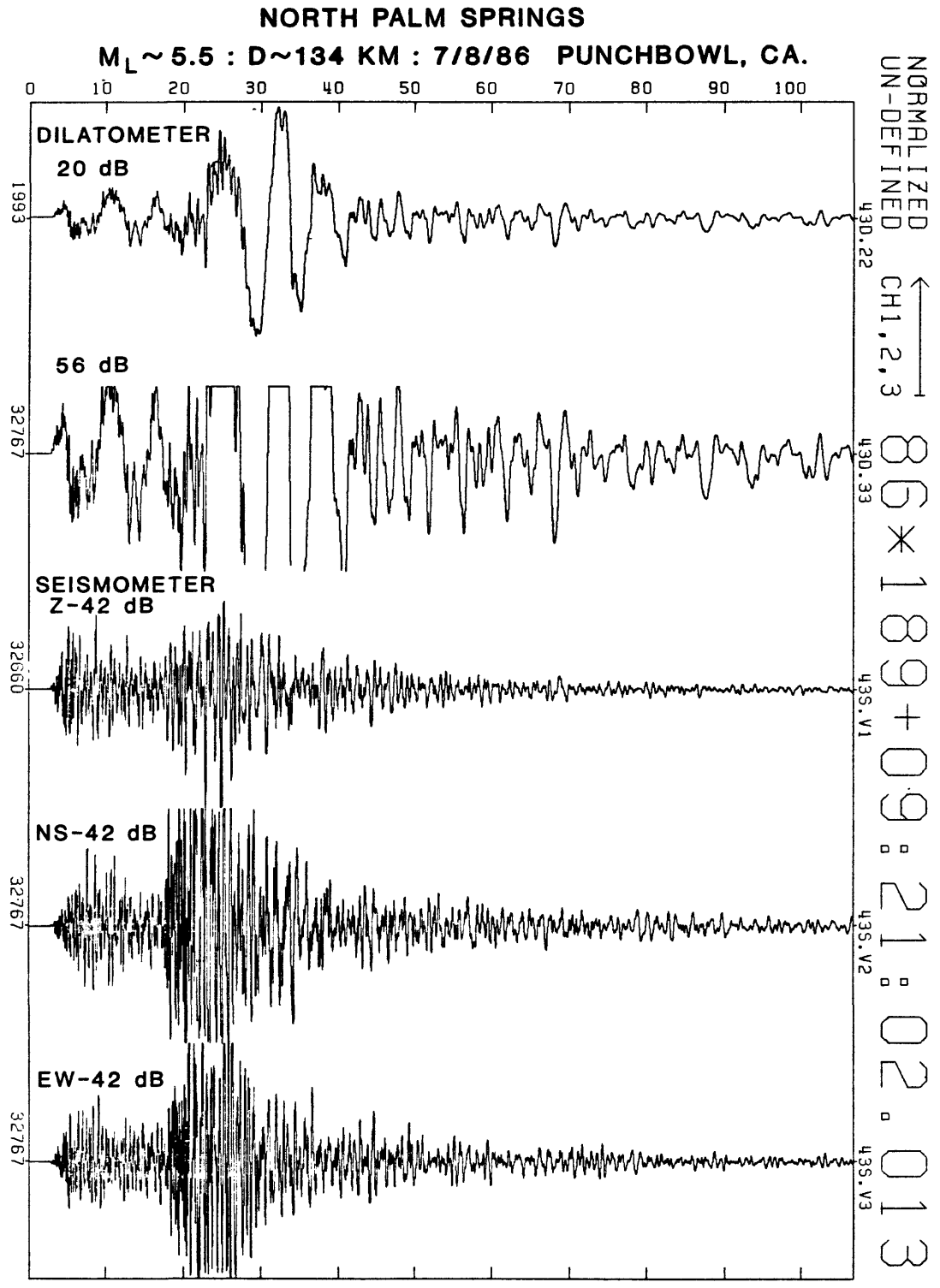
NORTH PALM SPRINGS
M_L ~ 5.5 : D~134 KM : 7/8/86 PUNCHBOWL, CA.
0 10 20 30 40 50 60 70 80 90 100
DILATOMETER
20 dB
1993
430.22
56 dB
32767
430.33
SEISMOMETER
Z-42 dB
32660
435.V1
NS-42 dB
32767
435.V2
EW-42 dB
32767
435.V3
NORMALIZED
UN-DEFINED
CH1,2,3
86*189+09:21:02:013

figure 5

NORTH PALM SPRINGS

M_L~5.5 : D~134 KM : 7/8/86 PUNCHBOWL, CA.

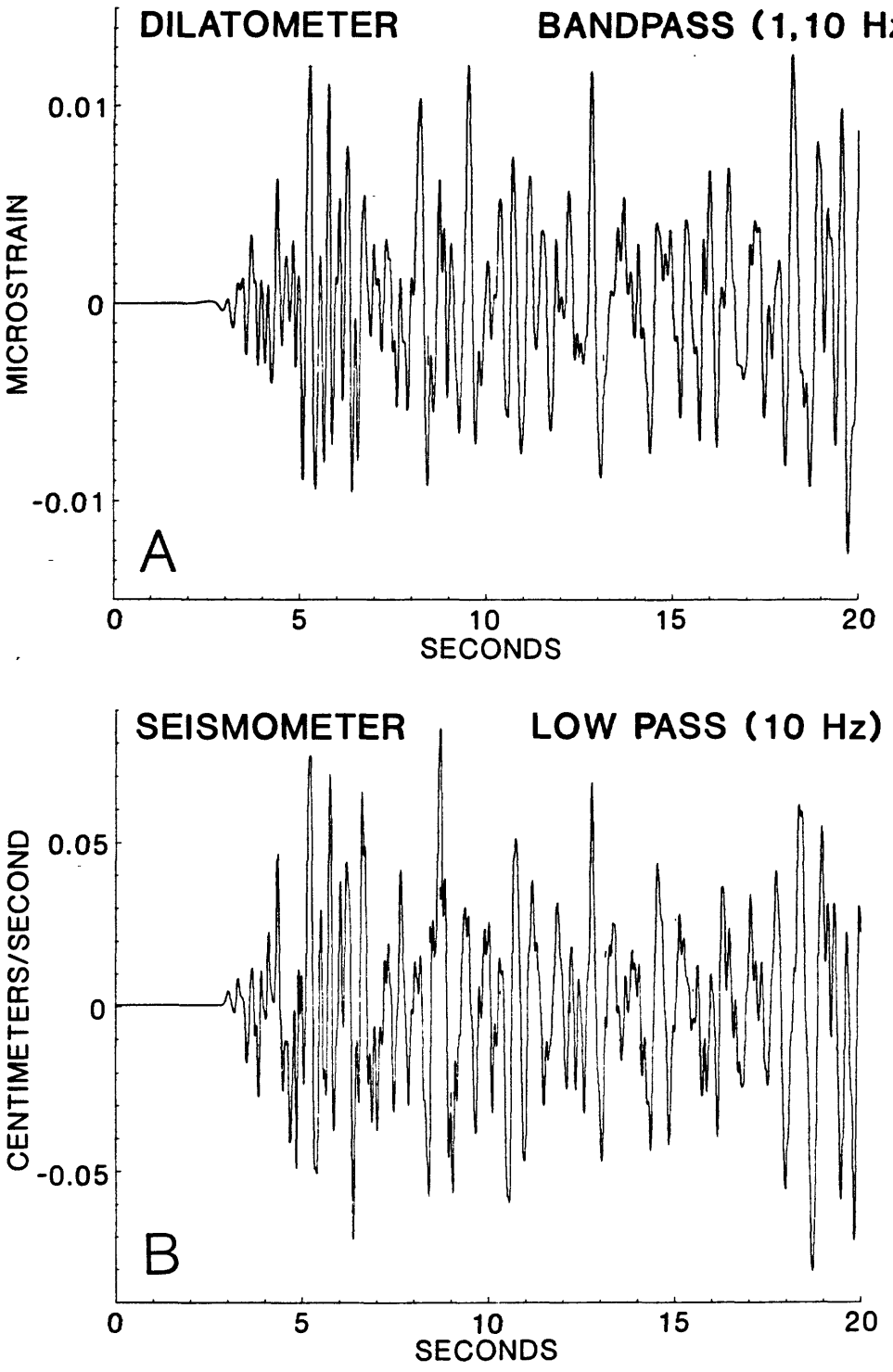

figure 6

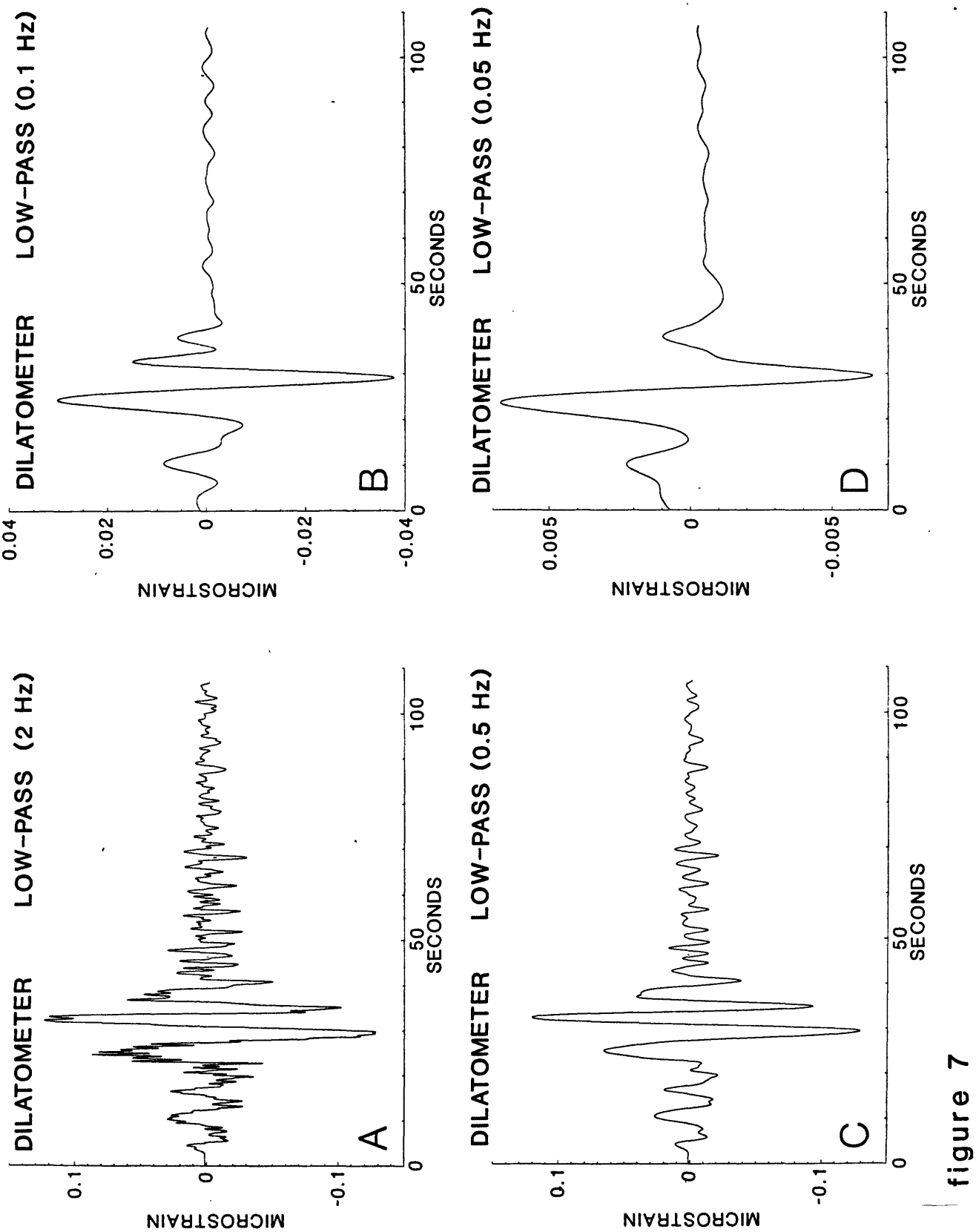
NORTH PALM SPRINGS
M_L~5.5 : D~134 KM : 7/8/86 PUNCHBOWL, CA.
DILATOMETER LOW-PASS (2 Hz)
A
DILATOMETER LOW-PASS (0.1 Hz)
B
DILATOMETER LOW-PASS (0.5 Hz)
C
DILATOMETER LOW-PASS (0.05 Hz)
D
MICROSTRAIN
SECONDS
0.1
0
-0.1
0.04
0.02
-0.02
-0.04
0.005
-0.005
50
100

figure 7

NORTH PALM SPRINGS

M_L~5.5 : D~134 KM : 7/8/86 PUNCHBOWL, CA.

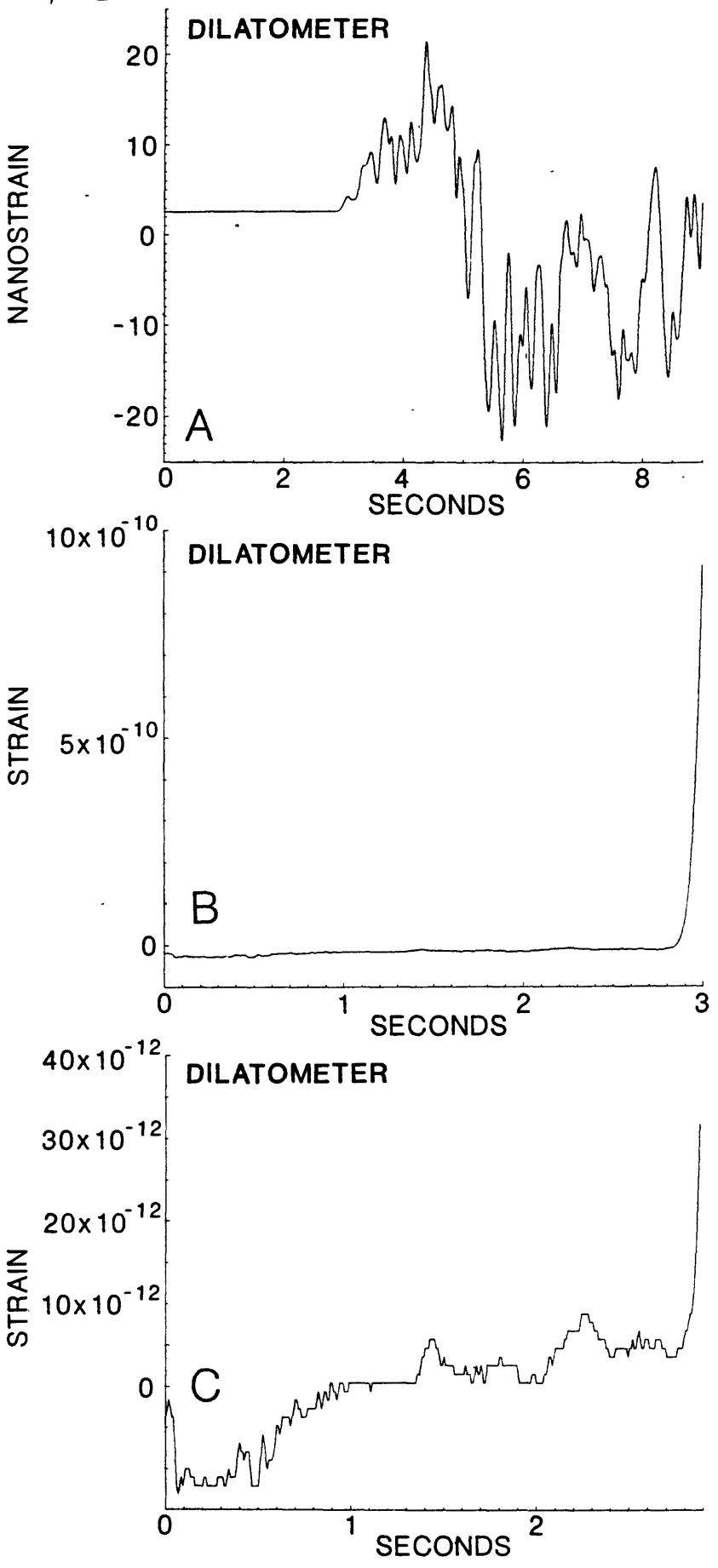

figure 8

National Strong-Motion Network: Data Processing

9910-02757

A.G. Brady
Branch of Engineering Seismology and Geology
U.S. Geological Survey
345 Middlefield Road, MS 977
Menlo Park, California 94025
(415) 323-8111, ext. 2881

Investigations

1. Routine Processing. In cooperation with strong-motion network personnel at the University of Chile, Civil Engineering Department, some of the more distant records of the Chilean earthquake have been digitized and processed. One significant record from Adak, Alaska, during the 5/8/86 Alaska earthquake has been processed for the U.S. Navy. Two earthquakes in California during July 1986 have produced records -- North Palm Springs July 8 (M5.9) and Chalfant Valley, near Bishop July 21 (M6.4). A set of 17 records from the North Palm Springs event are being processed.

2. Database. Work continues for the INGRES database on the DEC VAX. The incorporation of the strong motion permanent network data into the same database as the much more voluminous aftershock database (from temporary station locations) has allowed the main database design to be moved out of this project.

Results

1. Routing processing, including digitizing (D), computer processing (P), and report preparation (R) of strong-motion accelerograms continues: 11 records (D, P, R), Chile mainshock of March 3, 1985 and two aftershocks; 1 record (D), Alaska 5/8/86; 17 records (D) North Palm Springs, July 8, 1986, 18 records (R) from the aftershocks within the first two minutes of the Imperial Valley earthquake main shock, 15 October 1979.

Reports

Brady, A.G., Mork, P.N., and Silverstein, B.L., 1986, Processed strong-motion records from the 2317:41, 2318:20 and 2318:40 aftershocks of the October 15, 1979, 2613:53 GMT earthquake, Imperial Valley, California: *U.S. Geological Survey Open-File Report 86-441.*

Saragoni, R., Fresard, M., Brady, A.G., Celebi, M. (principal investigator), and Mork, P.N., 1986, Processed Chile earthquake records of 3 March 1985 and aftershocks: *U.S. Geological Survey Open-File Report* (in preparation).

National Strong-Motion Network: Engineering Data Analysis

9910-02760

A.G. Brady and G.N. Bycroft
Branch of Engineering Seismology and Geology
U.S. Geological Survey
345 Middlefield Road, MS 977
Menlo Park, California 94025
(415) 323-8111, ext. 2881

Investigations

1. Differential Ground Motions: Differential displacements and spectra have been calculated for the 1981 Westmorland and the 1986 Hollister earthquakes. The results are presented in an open-file report. A method of calculating multi-degree-of-freedom differential spectra is being developed.

2. Soil Structure Interaction: The problem of the impact of a column on an elastic halfspace has been solved and a computer program written for the numerical evaluation of the infinite integral occurring in the closed-form solution. The non-dimensionalized numerical results show the stress caused by the impact as a decaying series of reflected waves. A paper is being prepared.

3. The 17 digitized records from the North Palm Springs earthquake of 8 July 1986 will be used in several investigations planned at other institutions. Filtering decisions, specifically the long period limit, will depend on calculated ground displacements from several of the near-field stations.

Reports

Bycroft, G.N., and Mork, P.N., 1986, Differential displacements and spectra for 4 April 1981 Westmorland and 16 January 1986 Hollister earthquakes: *U.S. Geological Survey Open-File Report* (in preparation).

Bycroft, G.N., and Mork, P.N., 1986, Differential ground motion and their spectra: to be submitted to the *American Society of Civil Engineers*.

National Strong Motion Data Center

9910-02085

Howard Bundock
Branch of Engineering Seismology and Geology
U.S. Geological Survey
345 Middlefield Road, MS 977
Menlo Park, California 94025
(415) 323-8111, ext. 2982

Investigations:

The objectives of the National Strong Motion Data Center are to:

Maintain a strong capability for the processing, analysis, and dissemination of all strong motion data collected on the National Strong Motion Network and data collected on portable arrays;

Support research projects in the Branch of Engineering Seismology and Geology by providing programming and computer support including digitizing, graphics, processing and plotting capabilities as an aid to earthquake investigations;

Manage and maintain computer hardware and software so that it is ready to process data rapidly in the event of an earthquake.

The Center's facilities include a VAX 11/750 computer operating under VMS Version 4.4, a PDP 11/70 running RSX-11M+ and two PDP 11/73 computers. The Center's computers are part of a local area network woth other branch, OEVE, Geologic Division, and ISD computers, and we have access to computers Survey-wide over Geonet. Project personnel joined other office branches and ISD in support of the OEVE VAX 11/785.

Investigations during the last six months of FY86 included research into VAX/VMS compatible laser optical disk technology. Project personnel studied better methods of data access from our VAX 11/750 and PDP 11/70 and have looked at ways to read and use elevation data taken from Digital Elevation Model tapes. The project has joined with other Survey representatives in planning the forthcoming move to temporary quarters while asbestos fire-proofing is removed from buildings at 275 Middlefield Road. The project has agreed to increase its support of the OEVE VAX 11/785 by accepting full responsibility for management of that machine. As an ongoing policy, the project has kept its hardware up to current revision levels, and operating system, network, and other software at the most recent versions.

Results:

As a result of these and previous investigations, the project has:

Installed a demonstration "write once, read many" laser optical disk drive and VAX/VMS compatible software on the ES&G 11/750 and planned for further investigations of this technology;

Installed two 456MB Winchester type disks on the ES&G PDP 11/70 for better data access and storage capability;

Written a series of programs that read Digital Elevation Model data and use that data to plot surface contours, fault systems, and earthquake hypocenters for definition of fault planes;

Joined other Survey representatives in planning to keep Menlo computers up and running during the entire asbestos removal process at 275 Middlefield Road;

Met with OEVE VAX 11/785 project chiefs and ISD to begin the changeover to self-management of that computer system;

Managed and maintained all computer system hardware and software.

Reports:

None.

High Frequency Seismic and Intensity Data

9910-03973

Jack Evernden
Branch of Engineering Seismology and Geology
U.S. Geological Survey
345 Middlefield Road, MS 977
Menlo Park, California 94025
(415) 323-8111, ext. 2243

Investigations:

Investigated the correlation of seismic intensity and various other measured ground motion parameters (maximum and RMS acceleration and velocity, pseudo-velocity as a function of frequency, ground failure of various sorts, and per cent damage to California wood-frame and concrete structures).

Results:

Found detailed correlation of all above factors, indicating the potential for building a predictive model based on predicting seismic intensity and then using charts and tables (or computer programs) to predict all the other parameters.

Reports:

Have submitted a manuscript to "Earthquake Spectra" documenting the results given above and presenting the full set of figures and tables required for modeling seismic intensities, ground failure potential, ground motion characteristics, and expected loss to wood-frame and concrete buildings in any region of the U.S.A. (or other parts of the world, when augmented by data on building response to Modified Mercalli or Rossi-Forel intensities in these areas).

Strong-Motion Instrumentation Network Design, Development, and Operations

9910-02763, 02764, 02765

R.P. Maley
E.C. Etheredge

Branch of Engineering Seismology and Geology
U.S. Geological Survey
345 Middlefield Road, MS 977
Menlo Park, California 94025
(415) 323-8111, ext. 2881

Investigations

The Strong-Motion laboratory, in cooperation with several federal, state, and local agencies and advisory engineering committees, designs, develops, and operates an instrumentation program in 41 states and Puerto Rico. Program goals include: (1) recording of potentially damaging ground motion in regional networks and in closely spaced sensor arrays; and (2) monitoring the structural response of buildings, bridges and dams with sensors placed in critical locations. The present coordinated network consists of approximately 1,000 recording units installed at 600 ground sites, 27 buildings, 5 bridges, 56 dams, and 2 pumping plants.

New Instrumentation

Six ground motion stations were established in the Western United States: three at rock sites in San Francisco including the Golden Gate Bridge abutment, one on the Calaveras fault east of San Jose, and two in western Nevada, at Yerington and Montgomery Pass.

Two four-instrument structural arrays were installed at the Corps of Engineers John Day and the Dalles concrete dams located on the Columbia River between Oregon and Washington. At each structure the instrumentation configuration consists of two accelerographs in the lower gallery, one in the upper gallery, and one on abutment rock.

A 21 channel instrumentation system was completed at a 33-story steel frame building in Los Angeles. The structure is rectangular for the first 12 stories then topped by a 21-story triangular tower. Transducers are located at the basement level, and on the ground, 12th, 13th, and 33rd floors (fig. 1). This project was jointly funded by the USGS and the owner of the building.

A 15 channel structural monitoring system was installed for the Metropolitan Water District of Southern California on a truss bridge that was retrofitted with seismic isolation elastometric bearings. The bridge has three 180-foot long spans that carry a 10-foot diameter California Aqueduct water pipe across the Santa Ana River near Riverside. Transducers have been located in the middle of one truss section, at a pier above and below the elastometric bearing, on the bridge abutment and in a nearby recorder housing resting on rock (fig. 2).

Recent Earthquake Records

Several hundred earthquake records were recovered during the past six months from instrumentation located in California and Alaska. The following summarizes some of the more important results.

Earthquake Date	Magnitude	Location	Records	Peak Acceleration
30 December 1985	5.2	Anchorage, AK	11	Ground .08 g Structure .05 g (Humana Hospital 7th floor)
8 July 1986	5.9	N.Palm Springs, CA	68*	Ground .78 g Structure .12 g (Skinner dam crest)
13 July 1986	5.3	Offshore of Oceanside, CA	3	Ground .11 g
21 July 1986	6.0	Chalfant Valley, CA	16*	Ground .36 g Structure <.05 g (Several dams)

*More than 100 aftershock records were obtained from permanent and temporary accelerograph stations following the North Palm Springs and Chalfant Valley earthquakes.

Figure 3 shows the location of near-field recordings and peak accelerations from the July 8 North Palm Springs earthquake. Selected records from this event are shown in figure 4.

Figure 5 shows the location of near-field recordings and peak accelerations from the July 21 Chalfant Valley earthquake.

Reports

Ellis, F., 1986, Preliminary summary of strong-motion operations: earthquake of December 30, 1985, *Technical Report SM-1-86*,, 3 p.

Maley, R.P., Etheredge, E.C., and Acosta, A., 1986, Strong-motion records from the Chalfant Valley, California earthquake of July 21, 1986: *U.S. Geological Survey Open-File Report 86-568*, 15 p. and appendix.

Nielson, J., Risavich, F., Salsman, M., Acosta, A., Johnson, D., Etheredge, E., Forshee, R., Switzer, J., and Maley, R., 1986, Strong-motion accelerograms of the southern California earthquake of July 8, 1986, a quick look: *U.S. Geological Survey Open-File Report 86-386*, 6 p.

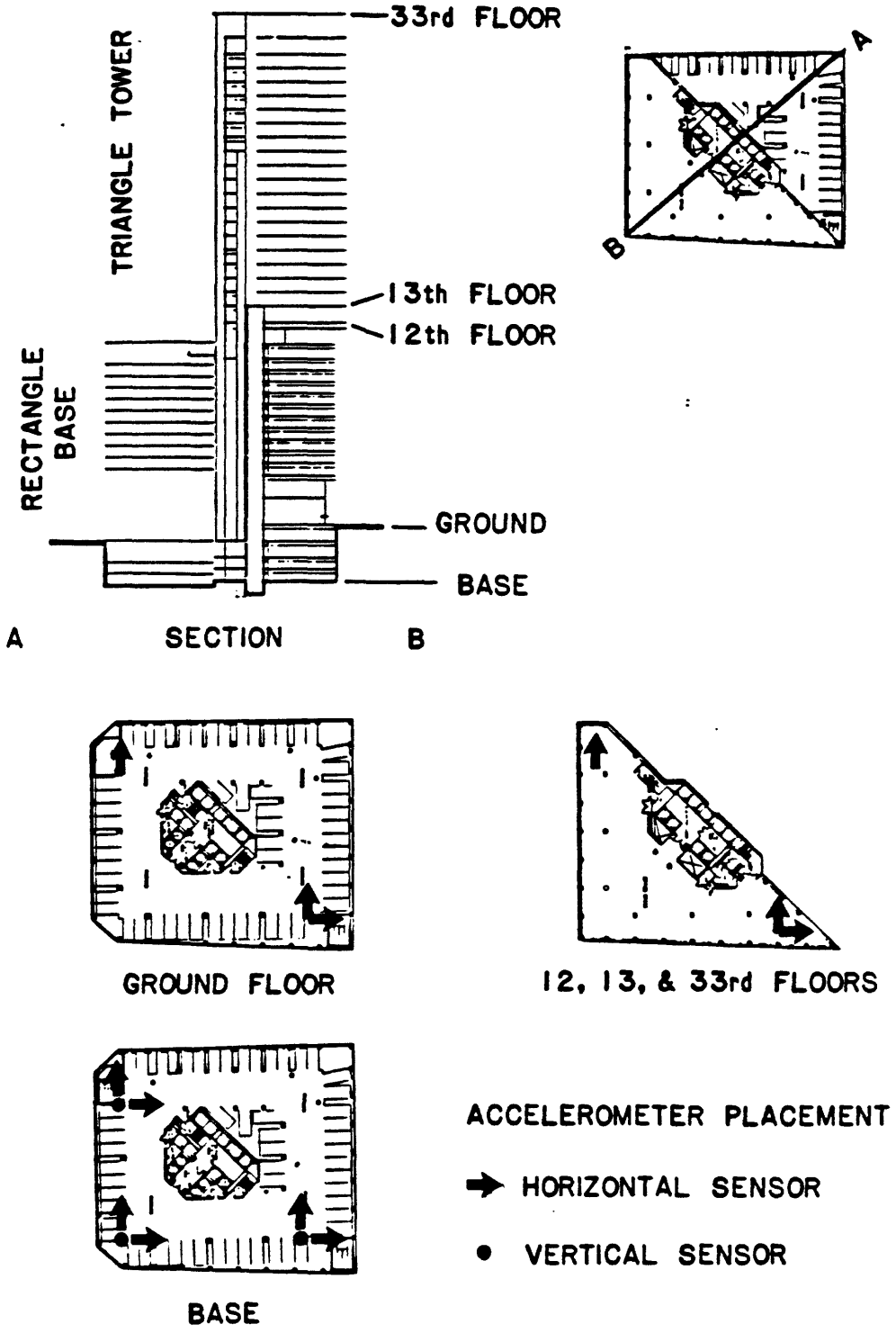

Figure 1.-Configuration of the strong-motion instrumentation system installed in a 33 story steel frame building in Los Angeles.

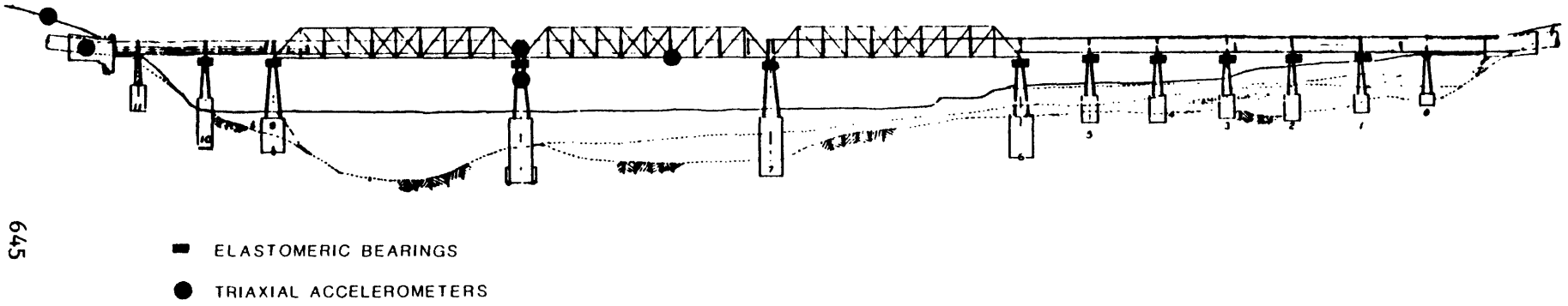

Figure 2.-Strong-motion instrumentation located on the Metropolitan Water District of Southern California Santa Ana river crossing for the California Aqueduct. This bridge carries a 10-foot diameter water pipe to bring Colorado river water to the Los Angeles area. Seismic isolation elastomeric bearings have been retrofitted between the concrete piers and the steel bridge frame.

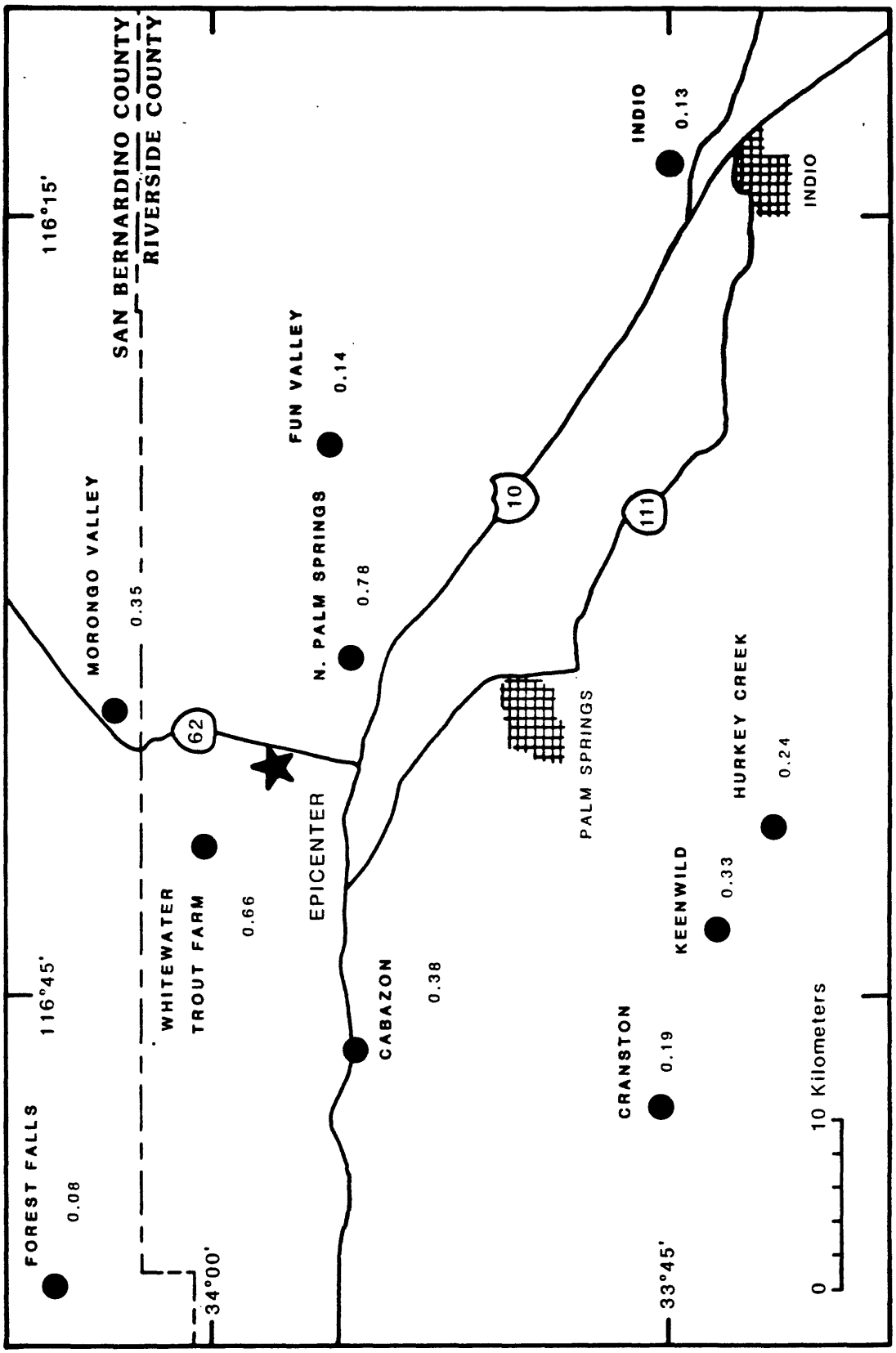

Figure 3.-Location of the USGS near-field strong-motion stations during the July 8, 1986 North Palm Springs earthquake. Maximum accelerations recorded during the event are shown in fractions of g at each site.

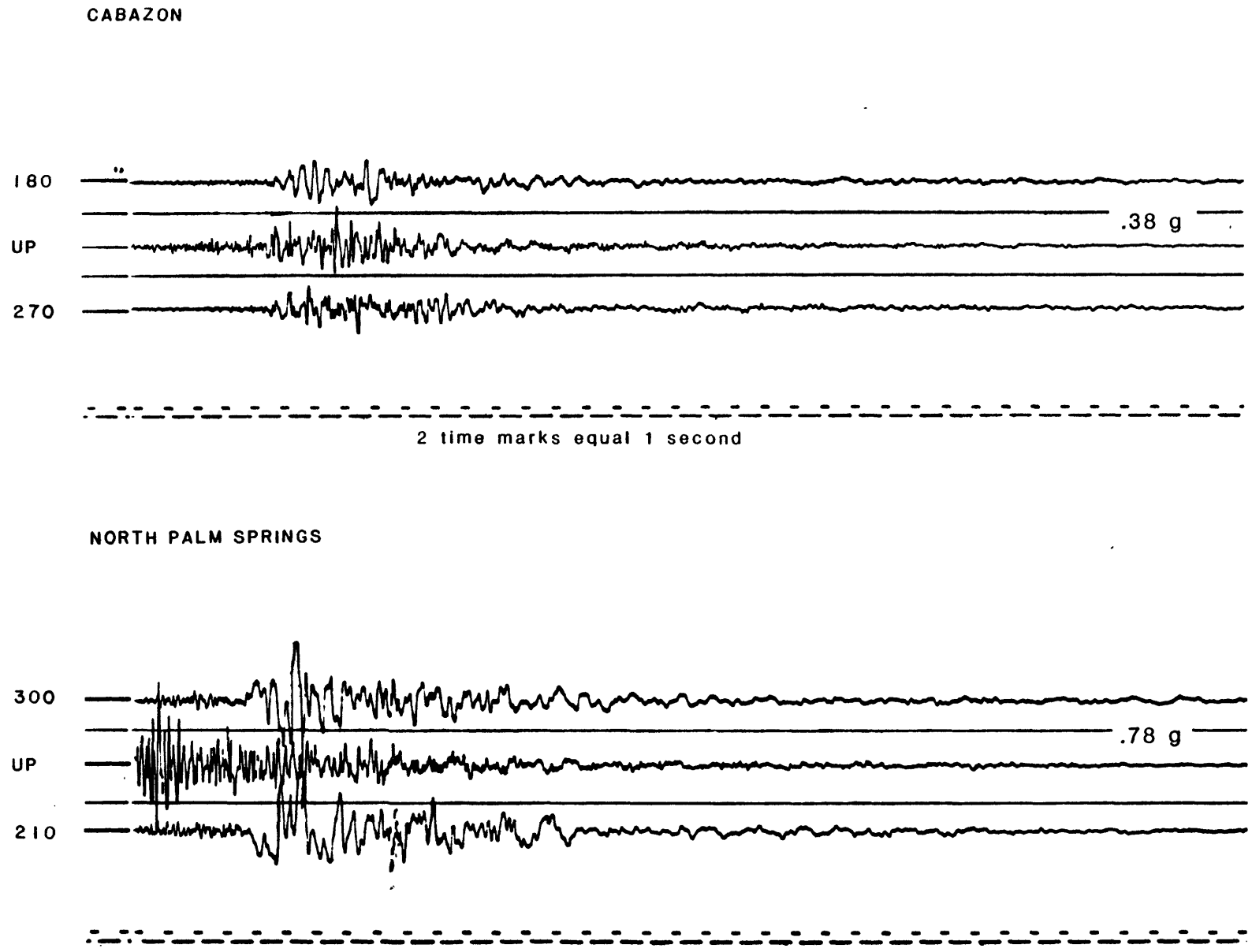

Figure 4a.-North Palm Springs earthquake records from Cabazon and North Palm Springs at respective epicentral distances of 16 and 9 km.

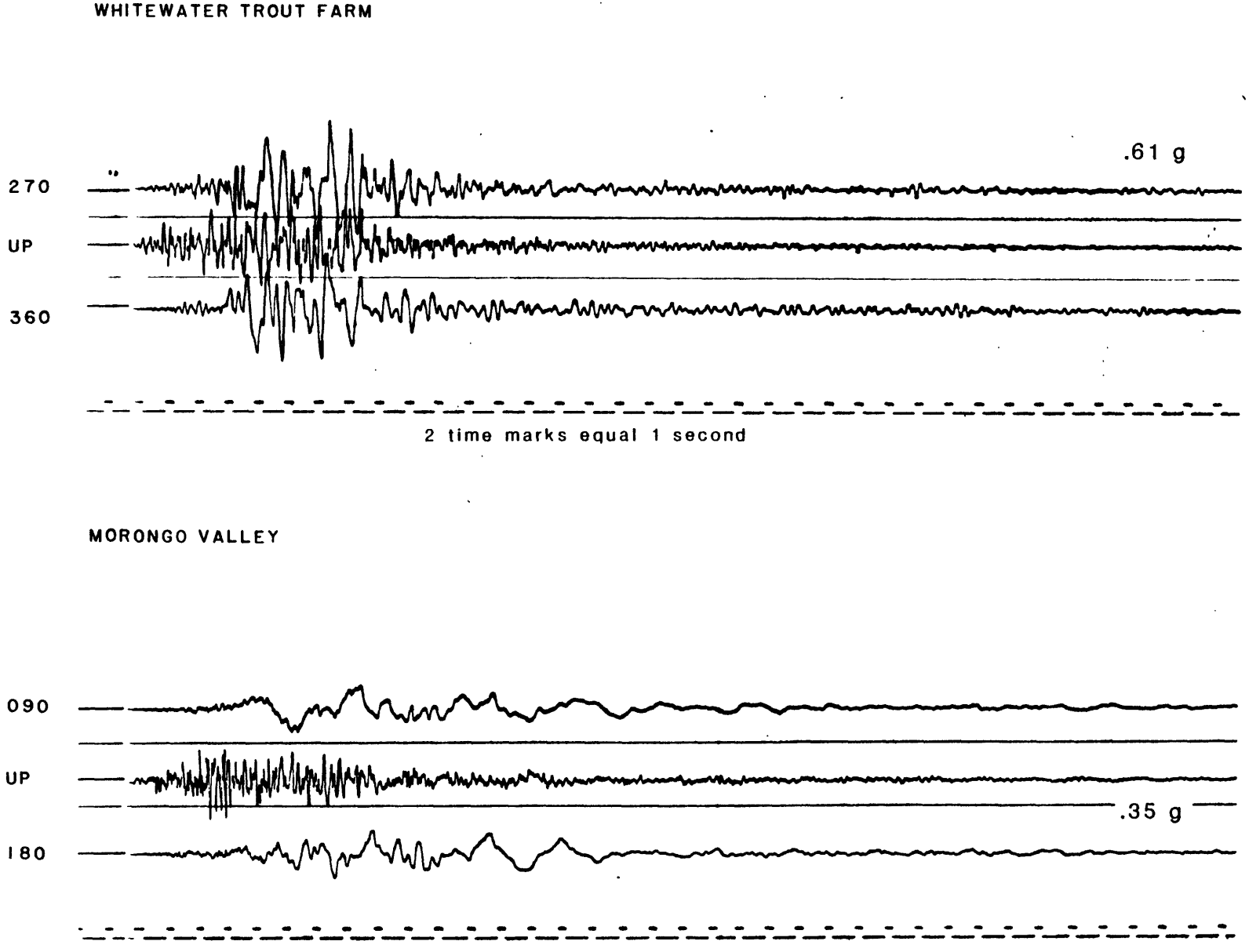

Figure 4b.-North Palm Springs earthquake records from Whitewater Trout Farm and Morongo Valley at respective epicentral distances of 5 and 10 km.

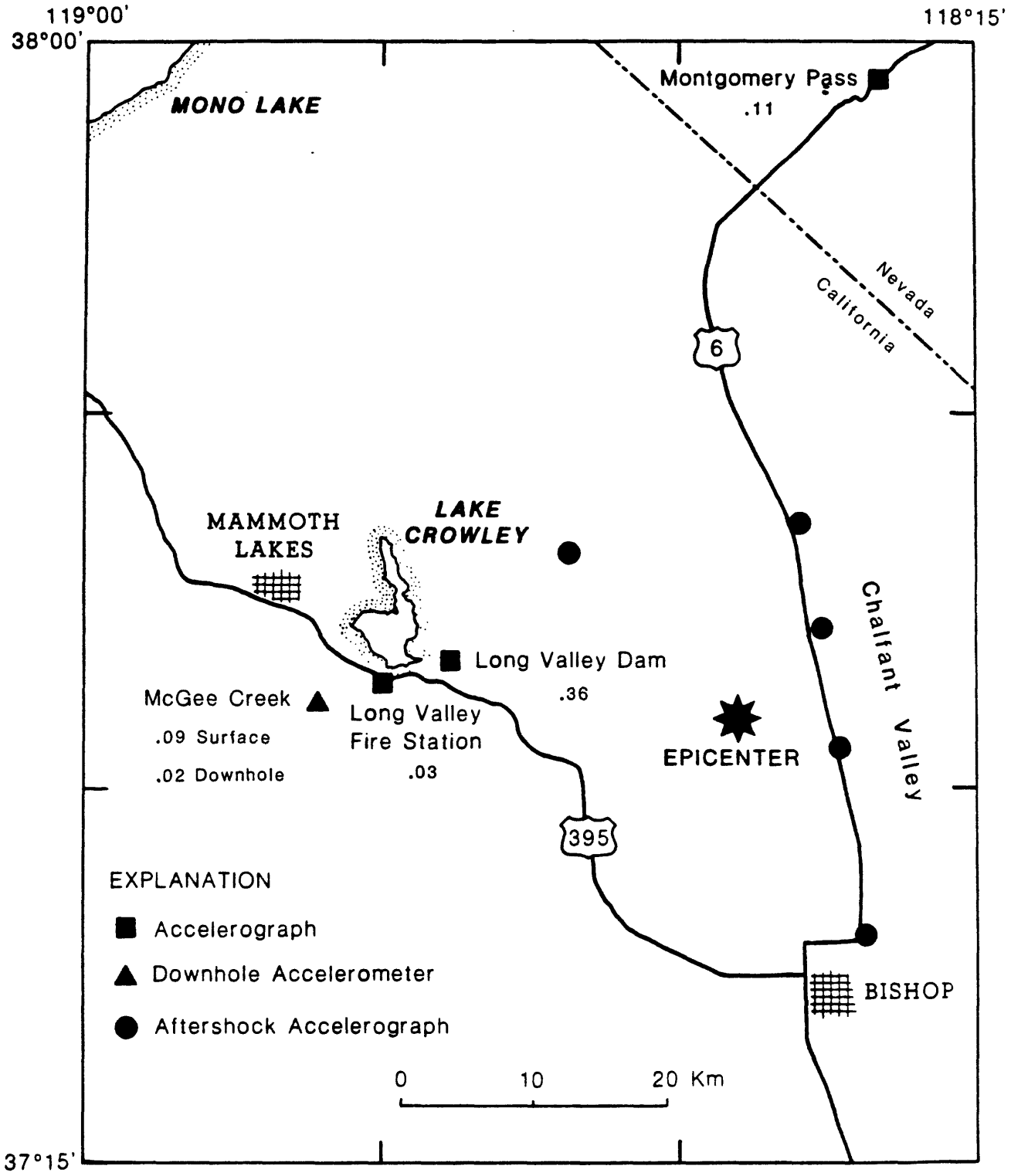

Figure 5.-Location of the USGS near-field permanent and aftershock strong-motion stations for the Chalfant Valley earthquake of July 21, 1986. Maximum accelerations recorded during the main shock are shown in fractions of g at each site.

General Earthquake Observation System (GEOS)
GEOS Analysis and Playback Systems (GAPS)

9910-03009

Gary L. Maxwell and Roger D. Borcherdt
Branch of Engineering Seismology and Geology
U.S. Geological Survey
345 Middlefield Road, MS 977
Menlo Park, California 94025
(415) 323-8111 ext. 2318 and 2910

Investigations

1. Development and construction of a portable, broad band, high-resolution digital data acquisition capability for seismology and engineering (GEOS).

2. Development of mini- and micro-computer systems (hardware and software) for retrieval, processing, and archival of large volumes of digital data (GAPS).

3. Development of hardware and software components to improve functionality, versatility, and reliability of digital data acquisition and retrieval systems.

Results

Design features and modifications to the General Earthquake Observation System (GEOS) incorporated or being investigated during this report period with assistance from J. Sena, M. Kennedy, C. Dietel, E.G. Jensen, and J. VanSchaack include:

1. Fine analysis of power utilization by GEOS instrumentation at the indivdual module level, with emphasis on reducing overall power consumption to increase battery life.

2. Procurement of one hundred small, versatile AC/DC inverters for use in trickle-charging individual units. These small chargers are desirable in that they monitor the condition of the GEOS internal battery packs for evidence of load loss, and keep the batteries in a continuous charged state, while exhibiting a satisfactory resilience to generating electronic noise.

3. Modifications to the engineering drawings and artwork in anticipation of building additional systems. Minor changes to system modules are being investiagted for the purpose of improving system functionality and reliability.

4. Completion of final construction of 270 channel high resolution (16 bit, 96 db), broad band (DC-500 Hz.) data acquisition capability. Forty-five operational recording units are now available for a variety of scientific investigations.

5. Final integration of software enhancements and hardware components (including expanded 28,000 word program memory and 16-by-16-bit arithmetic multiplication module) to provide a Finite-Impulse-Response filtering alogrithm to allow bandpass event-triggering detection.

Enhancements initiated or completed on the GEOS analysis and playback systems (GAPS) include:

1. Completion of hardware enhancements to the LSI-11/73 Analysis system, including installation of a Floating Point Arithmetic Accelerator and a diagnostic bootstrap module.

2. Upgrading of system software on both PDP-11/70 and LSI-11/73 machines to Digital Equipment Corporation's RSX-11M-Plus Operating System, Version 3.0. This version of the operating system includes many enhanced features, including disk data catching, increased network functionality, and support for Local Area Terminals over Ethernet Network Hardware. This upgrade operation improved the performance of these systems and provides better utilization by projects which analyze datasets gathered by GEOS instrumentation.

Longer term development efforts that were initiated during this report period include:

1. Engineering design efforts into increasing capacity of semiconductor memory to hold seismic data. Improvements in this area would allow recording of seismic data in hostile environments that prohibit the use of mechanical electromagnetic recording techniques.

2. Implementation of software to allow remote interrogation of instrumentation by means of a remote RS232-compatible interface. This improvement would allow technicians to monitor and modify recorder status and parameters from a central location, improving efficiency of operations and reducing costs for travel to remote sites.

3. Initiation of Request For Proposal contracting process to construct an additionafifty-five recording units has begun. Award of a contract for this RFP is anticipated by the end of the next report period.

Reports (utilizing data recorded by GEOS and processed by GAPS)

Johnson, M.J.S., Borcherdt, R.D., Linde, A.T., 1986, Short-period strain (0.1-10^5 s): near-source strain field for an earthquake (M_L 3.2) near San Juan Bautista, California: *Journal of Geophysical Research*, Vol. 91, no. B11, pp. 11,497-11,502.

Wesson, R.L., Nicholson, C. (eds.), 1986, Studies of the January 31, 1986 northeastern Ohio earthquake: a report to the U.S. Nuclear Regulatory Commission: *U.S. Geological Survey Open-File Report 86-331.*

Database Management

9910-03975

Charles S. Mueller
Branch of Engineering Seismology and Geology
U.S. Geological Survey
345 Middlefield Road, MS 977
Menlo Park, California 94025
(415) 323-8111, ext. 2989

Investigations

1. Development of techniques for data playback, processing and management, with emphasis on large datasets collected with portable digital event-recording seismographs.

2. Design and implement a prototype relational database for aftershock and special-experiment data. The goal of the database is to enhance researcher access to diverse Branch datasets.

Results

1a. The following new datasets were played back, processed, and archived:
Mexico City, Mexico: 1986 aftershock and structural response experiment.
Painesville, Ohio: 1986 aftershock experiment.
North Palm Springs, California: 1986 aftershock experiment.

1b. The following old dataset was organized and archived:
Imperial Valley, California: 1979 aftershock experiment.

1c. FORTRAN software developed to enhance data processing and archival procedures: FLIST, CLIPR.

2a. The first priority was to conceptually design database tables based primarily on seismological considerations - these table designs have been completed.

2b. Based on the tables designed in 2a, prototype applications to update and retrieve data have been implemented using INGRES software.

Reports

Borcherdt, R.D., (ed.), 1986, Preliminary report on aftershock sequences for earthquake of January 31, 1986 near Painesville, Ohio (Time period: 2/1/86 - 2/10/86): *U.S. Geological Survey Open-File Report 86-181.*

Structural Response in Support of National Strong Motion Program

9910-02759

Erdal Safak, Mehmet Celebi, A. Gerald Brady, and Richard Maley
Branch of Engineering Seismology and Geology
U.S. Geological Survey
345 Middlefield Road, MS 977
Menlo Park, California 94025
(415) 323-8111, ext. 2133

Investigations

1. Implementation of structural instrumentation and design of instrumentation schemes for structures selected by instrumentation advisory committees.

2. Develop methodologies and computer software to analyze structural vibration recordings.

3. Continue on site response studies and structural damage correlation during the 3 March 1985 Chile earthquake.

4. Continue on structural characteristic evaluation during the 19 September 1985 Mexico earthquake.

Results

1. As part of structural response study efforts through strong-motion instrumentation, and in accordance with recommendations of committees, two new structures are now instrumented. These are the 1100 Wilshire Building (33 stories) in Los Angeles and the Charleston Place Building (8 stories) in Charleston, South Carolina. Instrumentation schemes for these two buildings were designed.

2. A computer program is being developed to identify frequency, damping, and mode shapes of buildings from the ambient and earthquake vibration recordings.

3. After the 3 March 1985 Chile earthquake (M_s=7.8), and as a result of observation of damages on ridges, as well as alluvial and sandy sites, site response studies were conducted. The results showed that there were topographical and geological amplification and these two factors contributed to the patterns of responses observed during post-earthquake surveys. In addition, data obtained from structures are being studied.

4. Approximately 15 structures in Mexico City were tested in January 1986. Some of these structures were tested in 1962 also. Studies are being finalized on the changes of dynamic characteristics of these structures.

Reports

Safak, E., Celebi, M., Brady, G., and Converse, A., 1986, Recorded seismic response of three structures: ASCE Structures Congress, New Orleans, Louisianna, September 1986.

Scawthorn, C., Celebi, M., and Prince, J., 1986, Performance characteristics of structures, 1985 Mexico City earthquake: ASCE Mexico City Conference, September 19-21, Mexico City, Mexico.

Brady, G. and Celebi, M., 1986, Fundamental modal behavior of an earthquake excited bridge: III U.S. Conference on Earthquake Engineering, Charleston, South Carolina, August 1986.

Celebi, M., and Maley, R., 1986, Strong motion instrumentation of structures in Charleston, South Carolina and elsewhere: III U.S. Conference on Earthquake Engineering, Charleston, South Carolina, August 1986.

Physical Constraints on Source of Ground Motion

9910-01915

D.J. Andrews
Branch of Engineering Seismology and Geology
U.S. Geological Survey
345 Middlefield Road, MS 977
Menlo Park, California 94025
(415) 323-8111, ext. 2752

Investigations

Application of the diffusion equation to scarp degradation.

Implications of fault geometry for earthquake mechanics.

Results

Scarp profiles from Lakes Bonneville and Lahontan were reanlayzed using the cubic diffusion model, taking care to use appropriate ambient slopes. A manuscript was completed.

If a slip occurs at a triple junction of slip surfaces in a solid, a void must open. At a newly formed junction (a crack branch) the ratio of energy required to open the void to the elastic strain energy released by the crack, aside from geometrical factors, is P/G. Here P is mean compression stress, G is the shear modulus, and it is assumed that slip at the junction is comparable to the maximum slip on the crack. The ratio P/G is 0.01 or less for shallow faulting and ranges up to 0.16 for the deepest focus earthquakes. There is little impediment to rupture branching at shallow depths, but the larger value of P/G for deep focus earthquakes enforces less branching, which may explain fewer aftershocks. After an event, voids will fill with fluid or remineralize, and because of the previous displacement, the three slip surfaces at a junction will no longer have a common intersection. A new slip increment will produce a larger increment of void opening; the ration of energy to open the void to energy released is (2n-1)P/G, where n is the number of repeated events. As more events occur, the triple junction becomes more of a barrier to slip, and slip will transfer to fresh fractures. A shallow characteristic earthquake may repeat tens of times, but after a hundred events the controlling barriers will be entirely changed.

Reports

Andrews, D.J., and Bucknam, R.C., 1986, Fitting scarp degradation by a model with nonlinear diffusion (to be submitted to the *Journal for Geophysical Research*).

Andrews, D.J., 1986, Energy of crack branching: implications for characteristic earthquakes and fractal fault geometry varying with depth (abs.): EOS *Transactions of the American Geophysical Union*.

than the Ardsley event, which exhibited some strike-slip motion, the mechanism for for these events are thrust mechanisms. For the events where the fault plane can be discerned, the faulting appears to be high-angle reverse. Figure 1 shows the stress drops of these events plotted against the seismic moments. The seismic moments of the events range from 10^{17} to $2x10^{26}$ dyne-cm; the stress drops range from 20 to 200 bars, with an average of around 85 bars.

The Nahanni events appear to extend the range of constant dynamic stress drops to earthquakes with seismic moments greater than 10^{26} dyne cm. We note, however, that the Nahanni events exhibit "asperity" characteristics, suggesting that the stress release is markedly heterogeneous. The spectral shape determined for the October 5 events, exhibiting a pronounced intermediate spectral slope, is significantly different than the w^2 shapes generally used to predict peak ground motions.

Reports

Boatwright, J., 1987, The seismic radiation from composite models of faulting, submitted to *Bull. Seis. Soc. Am., 77.*

Boatwright, J., and G.L. Choy, 1987a, The acceleration spectra of large, shallow, subduction zone, earthquakes, submitted to *Jour. Geophys. Res., 92.*

Boatwrigth, J., and G.L. Choy, 1987b, Teleseismic analysis of the Nahanni earthquakes in Northwest Territories, Canada, submitted to *Bull. Seis. Soc. Am., 77.*

Characteristics of Seismic Fracture and Wave Propagation in Northeastern North America

9910-03589

John Boatwright
Branch of Engineering Seismology and Geology
U.S. Geological Survey
345 Middlefield Road, MS 977
Menlo Park, California 94025
(415) 323-8111, ext. 2485

Investigations

On October 5 and December 23, 1985, two large thrust earthquakes, M_s = 6.6 and 6.8, respectively, occurred near the South Nahanni River in the Canadian Northwest Territories. Following the first earthquake, the Earth Physics Branch of the Geological Survey of Canada deployed a set of MEQ-800 recorders and strong motion accelerographs in the epicentral area. The MEQ-800 recorders were maintained for a week and then removed, while the accelerographs recorded the December were left for the winter. All three of the accelerographs recorded the December 23 event, making this event the largest intra-plate earthquake to be recorded in the near-field in North America.

We have analyzed the teleseismic P-waves radiated by the two earthquakes in both the time and frequency domains. The method of spectral analysis used to analyze these events is derived in detail by Boatwright and Choy (1987a). The acceleration spectra of the recorded P-wave groups are averaged logarithmically and corrected for geometrical spreading and attenuation using the standard J-B earth model and a frequency-dependent **Q**. Using the focal mechanism determined from the time-domain analysis, the interference of the depth phases is modeled by generating "free surface operators" where the pP and sP depth phases have the appropriate amplitude and polarity and are delayed relative to the direct P wave by the appropriate time for the centroid depth. The P-wave is modeled as a single impulse, while the depth phases are modeled as clusters of impulses.

Results

The seismic moment of the October 5 event is $1.2x10^{26}$ dyne-cm. The dynamic stress drop can be estimated from the high frequency source spectral level of $|R\dot{u}|$ = $6.0x10^{6}$ cm^2/sec and the asperity radius of 7 km (see Boatwright, 1987) to be 90 bars. In contrast, the seismic moment of the December 23 event is $1.9x10^{26}$ dyne-cm, while the asperity radius is 11.0 km; this asperity radius is poorly determined, owing to the complexity of the stress release in the event. The high-frequency spectral level of $.40x10^{6}$ cm^2/sec and the asperity radius yield a dynamic stress drop of 41 bars.

Overall, these two shallow thrust earthquakes provide a possible example of the maximum credible earthquake in Northeast North America (NENA). The recent moderate seismicity in NENA has predominately occurred on shallow, high-angle reverse faults. The depths of faulting in the 1983 Miramichi and Gaza events, the 1984 Goodnow event, and the 1985 Ardsley event range from 3 to 8 km; other

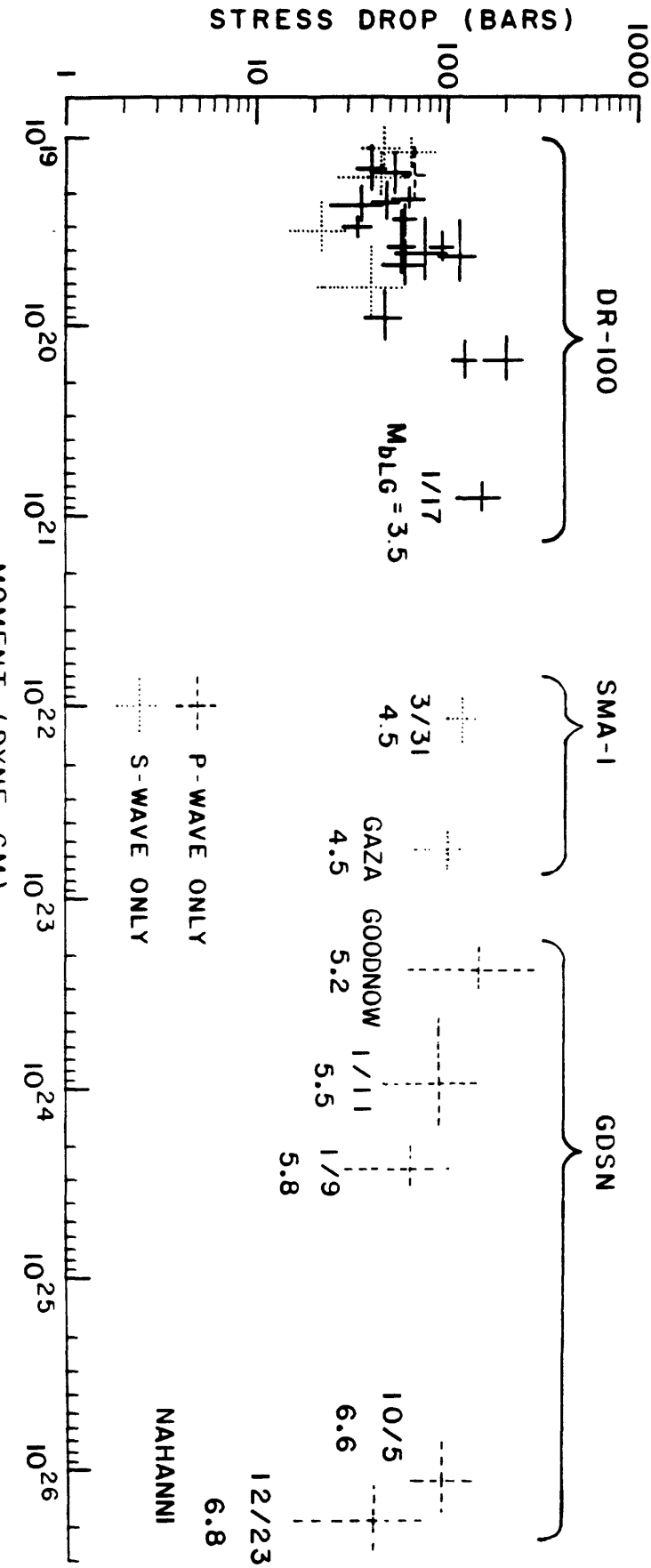

Figure 1. Dynamic stress drops of Northeastern North America earthquakes plotted against seismic moment. The events which are not identified by name occurred in the New Brunswick or Miramichi sequence. The brackets signify the data analyzed: Sprengnether DR-100, Kinemetrics SMA-1, or Global Digital Seismic Network.

Ground Motion Prediction for Critical Structures

9910-03833

David M. Boore
Branch of Engineering Seismology and Geology
U.S. Geological Survey
345 Middlefield Road, MS 977
Menlo Park, California 94025
(415) 323-8111, ext. 2698, 2154

Investigations:

Work continued on the theoretical prediction of ground motions in eastern North America and on the empirical analysis of data from the Eastern Canadian Telemetered Network.

Results:

The progress during the last half of FY 86 has been documented in the two quarterly reports submitted to the Nuclear Regulatory Commission, the agency funding the work. Copies of the reports are attached.

Reports:

Refer to the attached quarterly reports for a listing of reports.

Third Quarter Progress Report - FY 86
to
Nuclear Regulatory Commission

Project: Estimation of High-Frequency Ground Motion in the Central and Eastern United States

Investigator: David M. Boore

Progress Third Quarter: A paper describing some of the research accomplished with funding in this project was returned from the *Bulletin of the Seismological Society of America*, with a request for revisions. I took this opportunity to investigate several items not considered in the original paper. Several of the findings are described below. As part of the revision process, I visited with my coauthor, Gail Atkinson, in Buffalo, New York, on my return from a panel meeting of experts on ground motion attenuation in the eastern United States (of which I am a member) convened by the Lawrence Livermore Lab. This travel was done at no expense to the NRC.

The new studies included:

1. Effect of type of high-frequency filter:

It is generally acknowledged that an additional filter to eliminate high-frequency motions must be applied in addition to the standard Q-attenuation. I have accomplished this in two ways: 1) use a Butterworth filter that is down by a factor of 0.7 at the frequency f_m, with a rapid decay (24 db/octave) at higher frequencies, and 2) use a filter of the form exp(-pi*k*f). The latter filter is favored by some (Anderson and Hough) as being more realistic. It starts to eliminate energy at much lower frequencies than the Butterworth filter. In lieu of observational evidence in the eastern U.S., the question is which filter is appropriate, and does it really matter. The answer to this question is "no", if motions on hard-rock sites are of concern, as long as the characteristic frequency of the filter is higher than the predominant frequency of the ground motion parameter of interest. For example, figure 1 shows predicted and observed pseudo-response spectra as a function of distance for 2 and 10 Hz oscillators. An f_m of 50 Hz was used, and the parameter k in the exponential filter was chosen as $1/\pi f_m$ and $1/2\pi f_m$ (the latter comes from the requirement that the rms acceleration is the same for both filters). As can be seen in the figure, the choice of filter function makes little difference, as long as the parameters are suitably chosen.

2. Effect of source scaling law:

The most commonly used source scaling law and spectral shape are due to Brune, in which constant stress is combined with a spectral shape for which spectral acceleration grows as omega-squared at frequencies below a single corner frequency, and is flat above. An extension of this was proposed by Joyner in 1984, in which the single corner is replaced by two corners. In Joyner's model, similarity can exist if the two corners are proportional to one another. For earthquakes greater than a specified magnitude, however, one corner becomes fixed, thus allowing a breakdown in similarity and a divergence from the scaling expected from the Brune scaling. The sensitivity

of predicted ground motions in the eastern United States was investigated. Figure 2 shows a plot similar to figure 1, except that f_m was fixed at 50 Hz and the Brune and Joyner models were considered (the critical magnitude in the Joyner model was 7.0). Figure 3 shows the scaling with magnitude predicted at a distance of 30 km for the Brune model and the Joyner model with critical magnitudes of 6.0, 6.5, 7.0, and 7.5. Clearly, as long as the magnitude of the earthquake for which motions are being predicted is less than the critical magnitude, the particular scaling law makes little difference to the predictions. We have no information concerning the critical magnitude for eastern earthquakes; for strikeslip earthquakes in the western U.S. the critical magnitude may be around 7.0, but even here the quantity is not well determined.

RPT,OBS RDUCD TO M=4.5,DUR=1/FA+0.05*R,Q4
DS=100 BARS,BRUNE,FM=50 & FK, FK2=50 HZ
DATA.QPL Q4R1S4BKM45.OUT 8-JUL-86 18:32:08

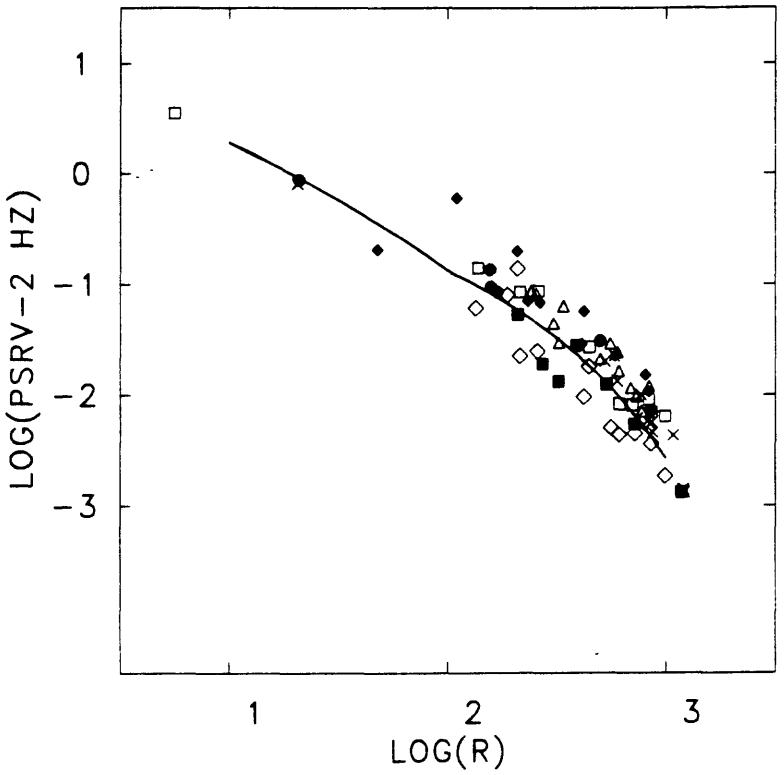

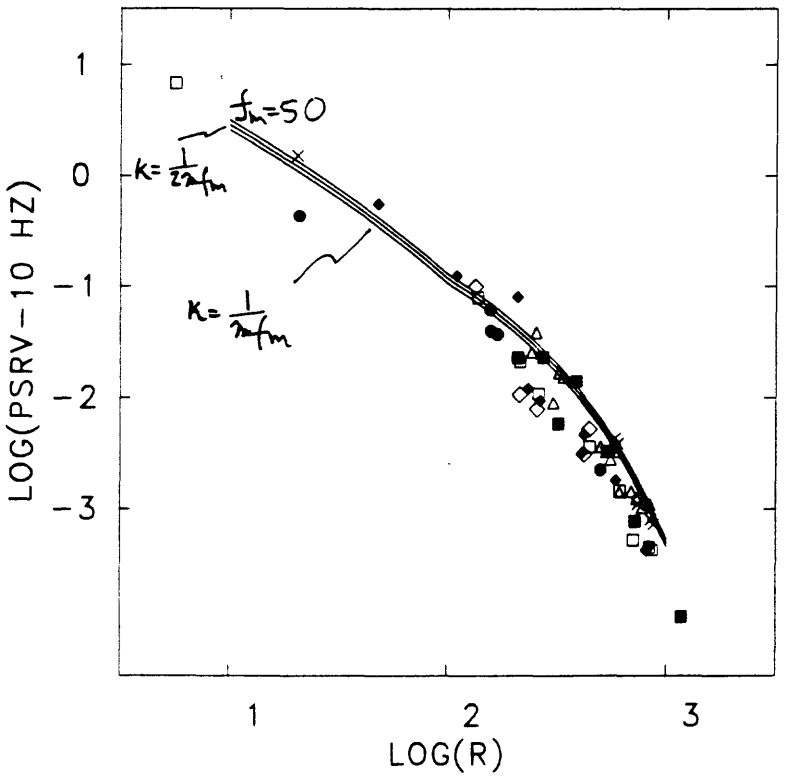

Figure 1

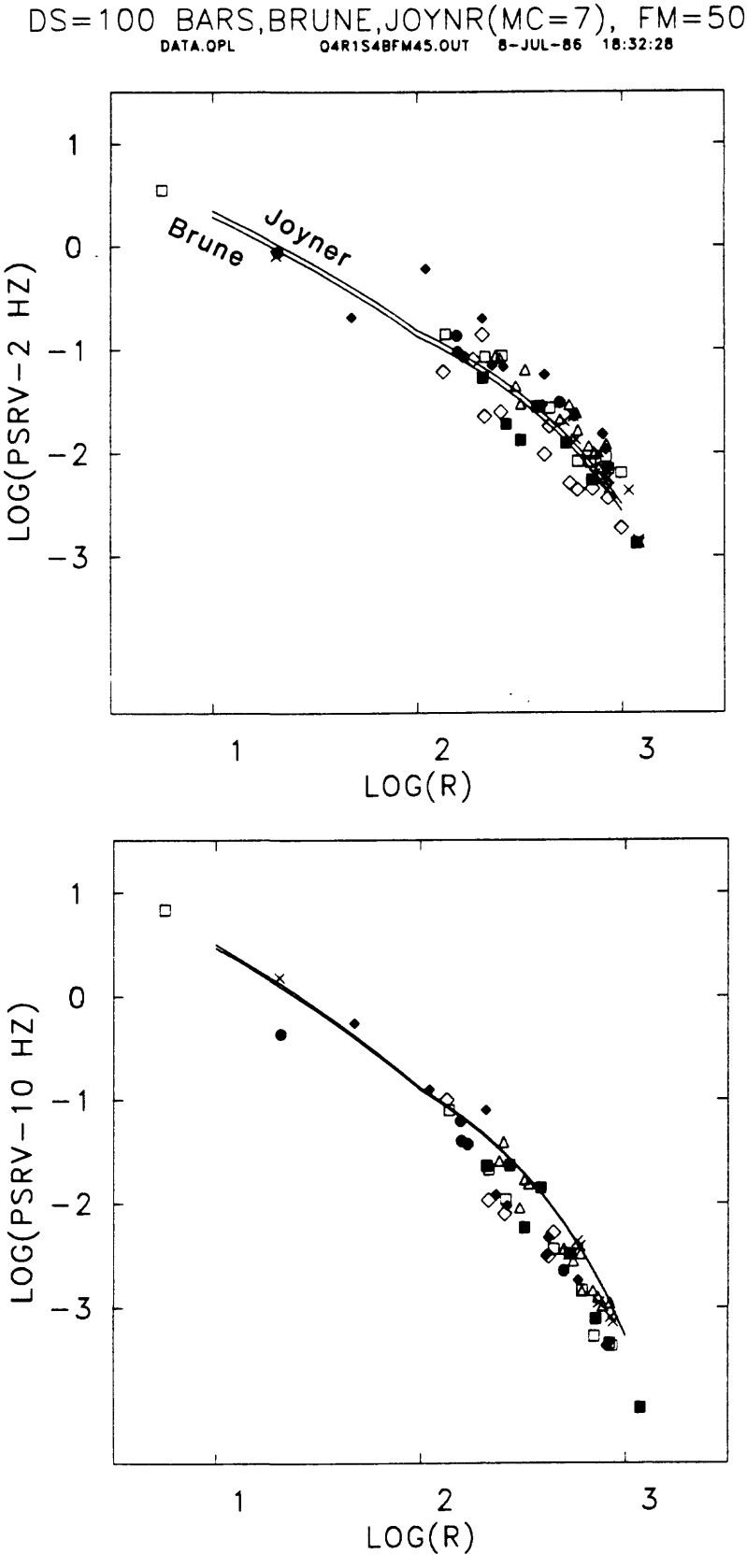
RPT,OBS RDUCD TO M=4.5,DUR=1/FA+0.05*R,Q4
DS=100 BARS,BRUNE,JOYNR(MC=7), FM=50 HZ
DATA.OPL Q4R1S4BFM45.OUT 8-JUL-86 18:32:28
Joyner
Brune
LOG(PSRV-2 HZ)
LOG(R)
LOG(PSRV-10 HZ)
LOG(R)

Figure 2

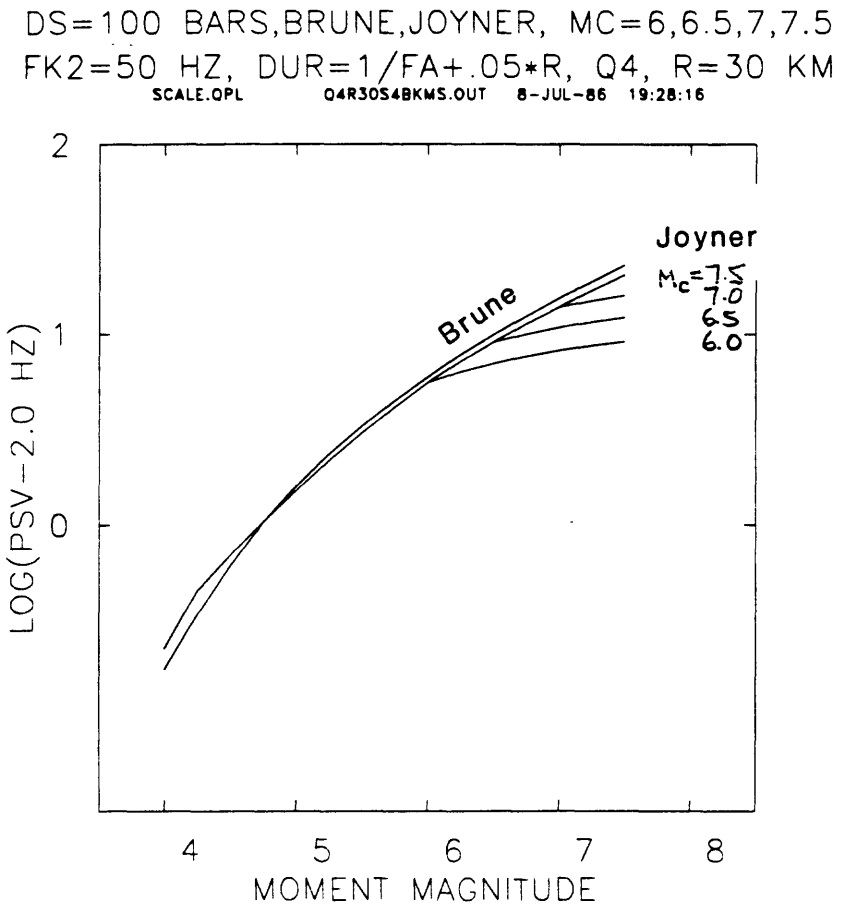
DS=100 BARS,BRUNE,JOYNER, MC=6,6.5,7,7.5
FK2=50 HZ, DUR=1/FA+.05*R, Q4, R=30 KM
SCALE.OPL Q4R30S4BKMS.OUT 8-JUL-86 19:28:16
2
1
0
LOG(PSV-2.0 HZ)
Joyner
Mc=7.5
7.0
6.5
6.0
Brune
4
5
6
7
8
MOMENT MAGNITUDE

Figure 3

FOURTH QUARTER PROGRESS REPORT - FY 86
TO
NUCLEAR REGULATORY COMMISSION

PROJECT: Estimation of High-Frequency Ground Motion in the Central and Eastern United States

INVESTIGATOR: David M. Boore

PROGRESS DURING THE FOURTH QUARTER: Work continued on the theoretical model and on the empirical analysis of data from the Eastern Canadian Telemetered Network.

BSSA paper. A paper describing the prediction of ground motions in eastern North America (ENA) is slated for publication in the April, 1987, issue of the Bulletin of the Seismological Society of America. It will be one of about 6 papers dealing with ground motions in ENA. Final revisions of the paper necessitated several investigations, including a study of the effect of the high-frequency filter used in the predictions. It was found that both the Butterworth and the exponential filters gave essentially equivalent answers for the motions on hard-rock sites. Also studied were the prediction equations, derived from regression fits of a functional form to theoretical ground motions at a set of magnitude, distance points. Because the predicted magnitude scaling is nonlinear and is a function of distance, the functional form needed is somewhat cumbersome. Attempts were made to fit simpler forms to the predictions, but the resulting misfit of the form to the computed points was intolerable. The final prediction equations are given as a simple able of coefficients that are easy to include in computer programs. Also studied during the fourth quarter was a scheme to smooth out the transition from $1/r$ to $1/\sqrt{r}$ geometrical spreading. Previously, the transition between the two was made at a fixed crossover distance r_x. The new scheme uses a Monte Carlo scheme to smooth out the transition: the results from a number of runs, each using a value of r_x chosen randomly from a specified distribution, are averaged to obtain the final answers. In our application we used 30 runs with r_x distributed uniformly between 60 and 170 km. Surprisingly, the overall results were very similar to those obtained using r_x = 100 km, although some smoothing was evident. The new curves and new prediction equations based on these curves are in the final version of the BSSA paper, which will be included in the next quarterly report.

Comparison with western United States predictions. For our information, we compared predictions of *PSV* at 4 oscillator periods for our ENA model and the WUS model in Boore, BSSA 76, 43–64. The results are shown in Figure 1. The two models differ in several ways: in ENA the crustal velocity is slightly higher, f_m is much higher (50 Hz vrs. 15 Hz), little amplification is expected at hard-rock sites, and a higher stress parameter is required to fit the meager data (100 bars vrs 50 bars). These differences are reflected in a complicated way in the comparison shown in Figure 1. For example, compared to the WUS, for the 20 Hz *PSV* the ENA motions are considerably higher because of the higher f_m, and for the 5 Hz *PSV* the ENA motions are lower because of the higher crustal velocity and lack of an amplification effect. This amplification effect is

frequency dependent, being near unity for frequencies less than about 1 HZ, and therefore the 1 Hz *PSV* again shows that ENA motions are higher (because of the higher stress parameter). Finally, the 0.2 Hz *PSV* is not very sensitive to the stress parameter, since the corner frequencies of all but the M7 event are higher than the oscillator frequency, and therefore the ENA and WUS motions are similar.

Low frequency errors in estimations of design motions. The usual procedure used by engineers to produce time series for use in dynamic analysis is to window filtered white noise. Safak and Boore (1987) show that such a procedure leads to large errors for the response of oscillators whose periods are longer than the corner period of the earthquake (Figure 2) . The procedure used by Boore (1983) in his implementation of the stochastic model avoids the problem. The difference is in the order of the filtering and the windowing; windowing of the white noise should come before the filtering.

Analysis of ECTN data: Multiple step-wise linear regression analyses were performed on the Fourier acceleration amplitude spectra of Eastern Canada Telemetered Network (ECTN) data for 7 moderate earthquakes (M3.6 to M5.2). This work has not been reported on in previous quarterly reports; the bulk of the work was done by Gail Atkinson, with some advice from David Boore.

70 observations (vertical component only) of the L_g phase for frequencies between 0.6 and 10 Hz were used, with the primary emphasis on determination of anelastic attenuation and local site response. Most of the sites are hard-rock, two (OTT and MNT) are soft-rock sites, and one (WEO) has soil beneath the station. The following conclusions were reached:

1. Q increases with frequency. Allowing the geometric attenuation to be determined by the regression, instead of being fixed at some constant value ($r^{-0.83}$, $r^{-0.50}$, or $r^{-1.00}$), increases the scatter in the linear trend of Q vrs. log f, but does not change this conclusion. If fixed before the regression, however, the rate assumed for geometric spreading does influence the derived Q value. For example, with a spreading of $r^{-1.0}$ for $r < 100$ km and $r^{-0.5}$ for $r > 100$ km, and a group velocity of 3.5 km/s, we obtain

$$Q = (539 \pm 30) f^{(0.414 \pm 0.026)} .$$

   If we assume a geometric spreading of $r^{-0.83}$, then

$$Q = (870 \pm 70) f^{(0.240 \pm 0.040)} .$$

2. The data set cannot help us in determining which geometric attenuation is more appropriate. The goodness-of-fit is slightly better for the first Q model shown above. The coefficients of geometric spreading determined from the regression analyses vary between 0.5 and 1 (depending on the frequency), with a value near 0.8 appearing to be best. The coefficients, however, are not well-constrained by the data. We have only two observations at distances within 100 km, and if these values are removed, then the geometric spreading factors are not well determined.

3. Site response at WEO, the only soil site, is very pronounced at high frequencies (a factor of 10), but it is negligible for frequencies near 1 or 2 Hz (Figure 3).
4. The two soft-rock sites (OTT and MNT) do not show any site amplification relative to the hard-rock sites (Figure 3).

These findings, which are subject to further analysis, are of importance in predicting high-frequency motions in eastern North America.

PUBLICATIONS: A report on the work being done on this project was presented at the International Workshop on Seismicity and Earthquake Risk in Erice, Sicily in August (at no expense to the NRC). A paper on the low frequency errors was submitted for publication to the ASCE Journal of Engineering Mechanics.

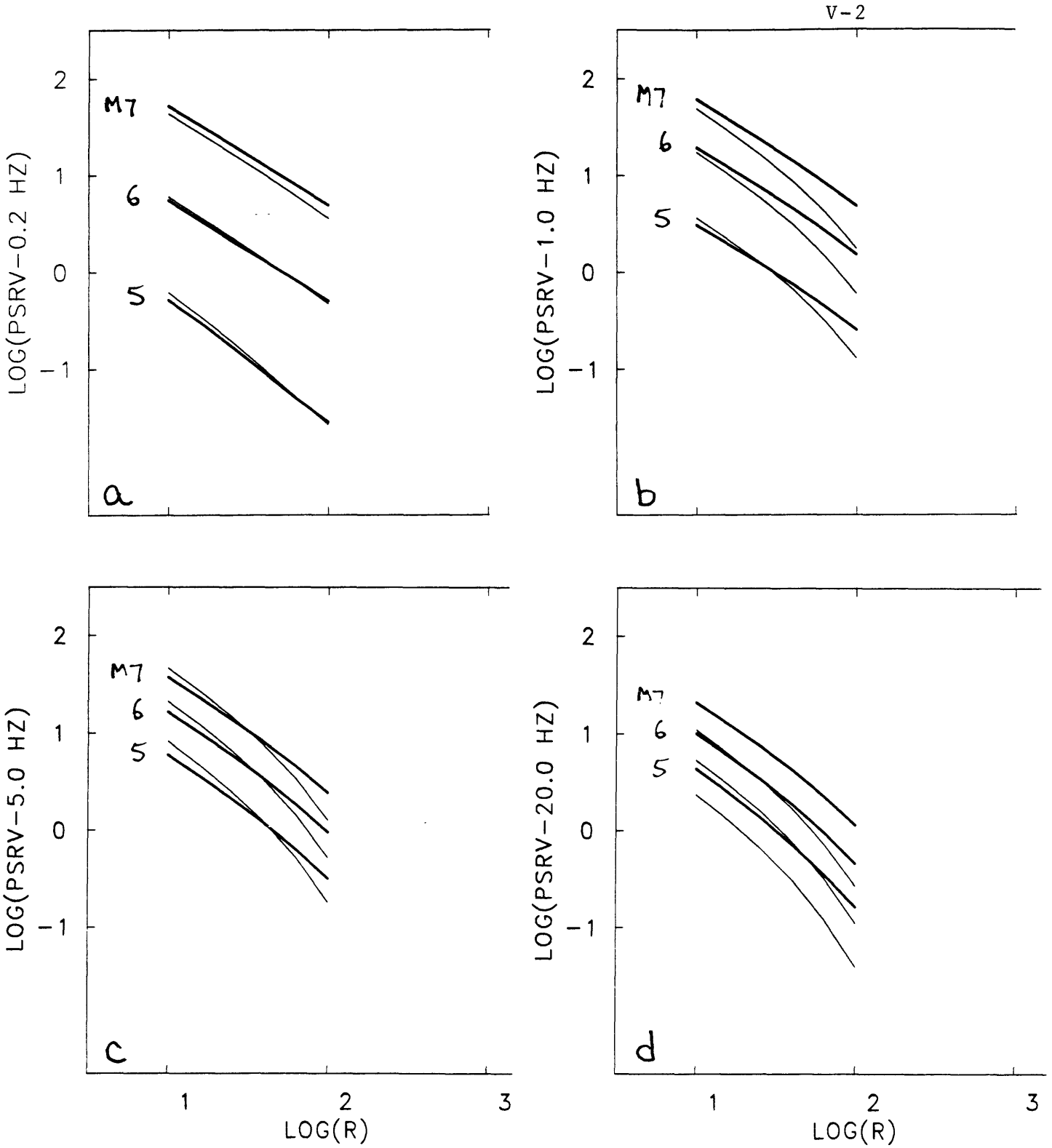

Figure 1. log *PSV* versus log *r* for 5-percent damped oscillators at 4 frequencies (parts a,b,c,d). In each figure, results are shown for moment magnitudes 5, 6, and 7. The ENA and WUS predictions are given by heavy and light lines, respectively.

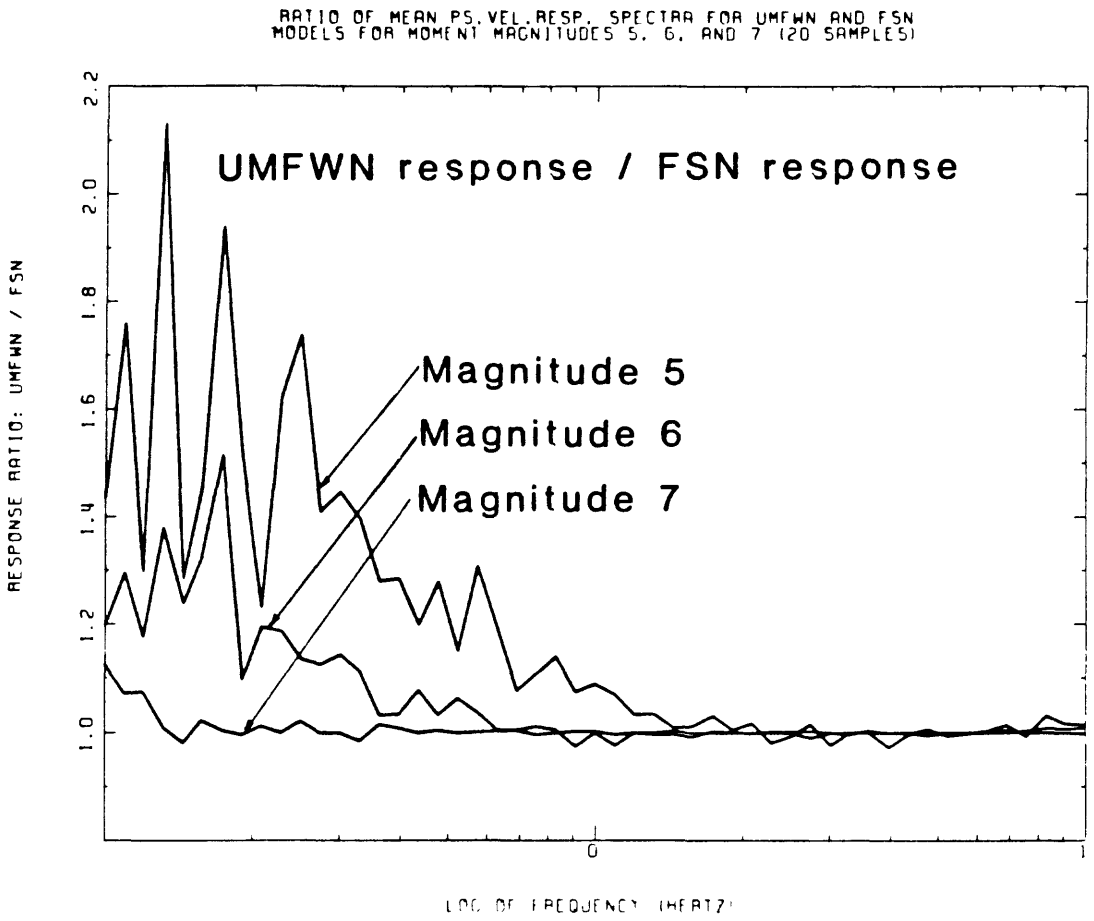

Figure 2. Ratio of pseudo-velocity response spectra due to the incorrect model usually used by engineers (UMFWN) and that due to the correct model in which windowing of the random time series occurs before filtering (from Safak and Boore, 1987).

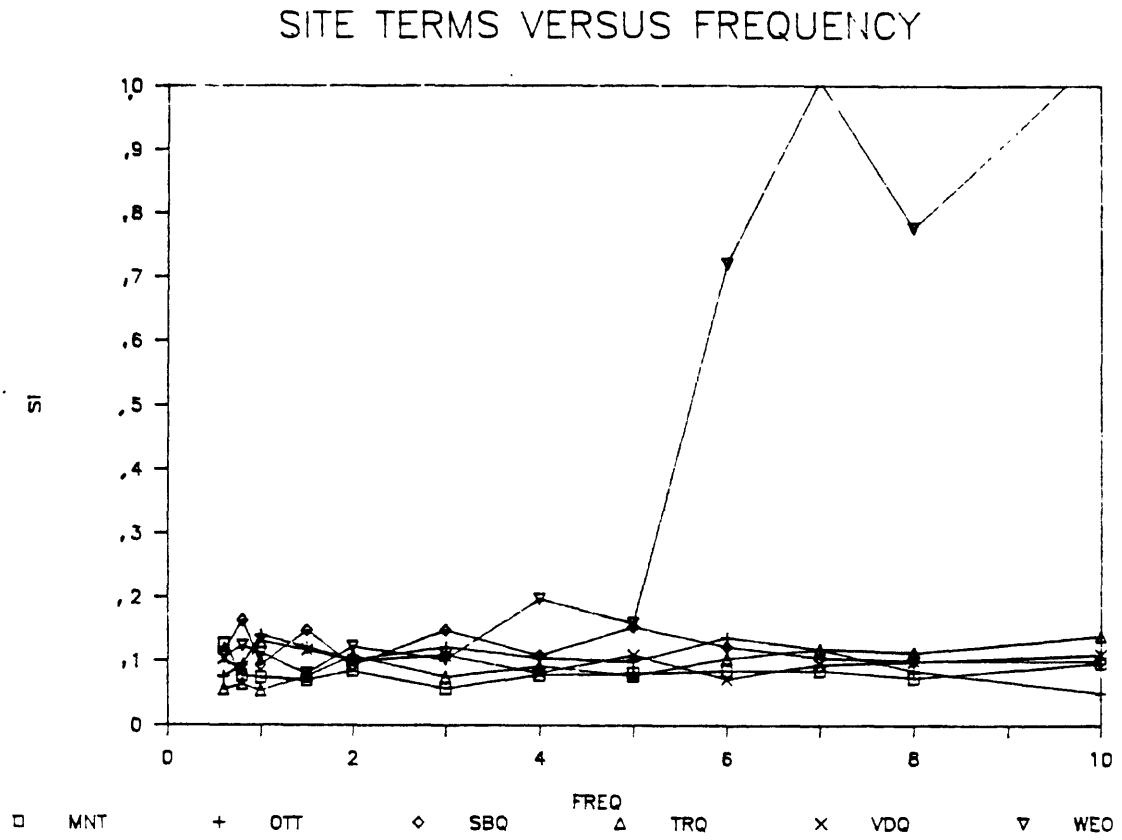

Figure 3. Site terms, in terms of the log of the motion, vrs. frequency , for sites indictaed by symbols. Note large amplification at WEO at high frequencies. Site terms were determined as the average residual after accounting for distance attenuation, considering all events and stations as a whole; they are equivalent to the station corrections used in magnitude studies.

Ground Motion Prediction for Critical Structures

9910-01913

David M. Boore and William B. Joyner
Branch of Engineering Seismology and Geology
U.S. Geological Survey
345 Middlefield Road, MS 977
Menlo Park, California 94025
(415) 323-8111, ext. 2698 or 2754

Investigations:

1. Predict ground motions and response spectra.

Results:

1. We are developing a revised set of predictive equations for earthquake ground-motion response spectra. The equation are derived by regression analysis of a dataset which includes data not available when we did our preliminary work four years ago. The two-stage regression technique used previously has been modified to treat more correctly the case where there may be random variability from earthquake to earthquake in addition to the random variability from station to station for the same earthquake. Earthquake-to-earthquake variability might be caused, for example, by variations in average stress drop. Prediction errors are estimated by Monte Carlo techniques, which are necessary because of the strong nonlinearity of the regression. Monte Carlo methods are also used to assess the magnitude-dependence of the cure of response as a function of distance.

Reports

Joyner. W.B. and Boore, D.M., Predictive equations for response spectra [abs.]: *Earthquake Notes 57*, p. 15.

Measurement and Analysis of Aftershock Sequences for the Moderate Earthquake on January 31, 1986 near Painesville, Ohio

9910-04111

Roger D. Borcherdt
Branch of Engineering Seismology and Geology
U.S. Geological Survey
345 Middlefield Road, MS 977
Menlo Park, California 94025
(415) 323-8111, ext. 2755

Investigations:

Reported under Projects 9910-02089 and 9910-02689.

Results:

Reported under Projects 9910-02089 and 9910-02689.

Reports:

Reported under Projects 9910-02089 and 9910-02689.

Anelastic Wave Propagation

9910-02689

Roger D. Borcherdt
Branch of Engineering Seismology and Geology
U.S. Geological Survey
345 Middlefield Road, MS 977
Menlo Park, California 94025
(415) 323-8111, ext. 2755

Investigations:

1. Effects of anelastic boundaries on the physical characteritsics of inhomogeneous P, elliptical S, and linear S waves.

2. Short period volumetric strain (10^5 - 10^{-1}s).

3. High frequency (20 - 130 Hz) radiation near seismic sources.

Results:

1. Working in conjunction with G. Glassmoyer a general computer code (WAVES) was utilized to calculate anelastic reflection-refraction coefficients, energy flow, and the physical characteristics of plane waves reflected and refracted by general P, type-I S, and type-II S waves incident on anelastic boundaries. The exact anelastic formulation with no low-loss approximations predicts the existence of an anelastic Rayleigh window, which accounts for the discrepancy noted by Brekovskikh (1960) between measured reflection data and predictions based on classical elasticity theory. Characteristics of the anelastic Rayleigh window are expected to be evident in certain sets of wide-angle ocean-bottom reflection data and to be useful in estimating Q^{-1} for some ocean-bottom reflectors. Reflection data from the East Pacific Rise provided by J. Mutter and P. Buhl (LDGO), is being examined for evidence of this "Rayleigh window".

2. Short-period strain - In conjunction with M. Johnston and others (see Borcherdt and Gibbs; 9910-02089) dilatational earth strain, associated with the radiation fields for several hundred local, regional, and teleseismic earthquakes, has been recorded over and extended bandwidth and dynamic range at four borehole sites near the San Andreas fault, California. The general theory of linear viscoelasticity is applied to account for anelasticity of the near-surface materials and to provide a mathematical basis for interpretation of seismic radiation fields as detected simultaneously by co-located volumetric strain meters and seismometers. The general theory is applied to describe volumetric strain and displacement for general (homogeneous or inhomogeneous) P and S-I waves in an anelastic whole space. Solutions to the free-surface reflection problems for incident general P and S-I waves are used to evaluate the effect of the free surface on observations from co-located sensors. Corresponding expressions are derived for a Rayleigh-type surface wave on a linear viscoelastic half-space. The theory predicts a number of anelastic wave

field characteristics that can be inferred from observation of volumetric strains and displacement fields as detected by co-located sensors that cannot be inferred from either sensor alone. Volumetric strain meters respond to P waves but not S waves, with simultaneous observations permitting resolution of superimposed P and S wave fields into their respective components. The amplitude and phase for components of the displacement fields depend on angle of incidence, azimuth and inhomogeneity of the wave field. As volumetric strain shows no similar dependencies, simultaneous measurement permits inference of these characteristics as well as *in situ* material parameters. Conversion of S energy to dilatational strain energy by the free surface is largest at angles of incidence for which inhomogeneity of this reflected P wave is near its physical limit (that is, amplitudes vary rapidly along surfaces of constant phase). For such angles of incidence in a low-loss anelastic half-space, the particle motions for the reflected P waves are elliptical, amplitudes increase near the surface with depth and phase propagation is not parallel to the free surface. Volumetric strain for a Rayleigh-type surface wave shows an exponentially damped sinusoidal dependence on depth not evident for a Rayleigh wave on an elastic half-space.

3. High-frequency seismic radiation - In cooperation with G. Glassmoyer high resolution, a ten-station array of portable digital instrumentation (GEOS) was deployed to record the aftershock sequence of the moderate ($m_b \sim 4.9$) earthquake that occurred on January 31, 1986 near Painesville, Ohio. High-resolution (16-bit; 96 dB), broadband (400 sps; 200 Hz) recordings of two of the larger aftershocks (m_b 2.2; 2.5) show that seismic signals as high as 130 Hz were resolvable above background noise levels at hypocentral distances up to 18 km. Spectral ratios computed with respect to "rock" site to estimate the amplitude response of local soil deposits at a site near Perry, Ohio suggest strong site resonances near 20 Hz and other resonances at frequencies exceeding 60 Hz. Strong-motion records from the Perry nuclear plant with bandwidth extending up to 30 Hz, also show exaggerated ground shaking near 20 Hz. Modeling of the soil response based on two-dimensional anelastic wave propagation suggests that the exaggerated levels of shaking near 20 Hz could be due in part to response of near-surface soil layers to S energy incident at angles of incidence near 30 degrees and due in part to the response of the nuclear containment structure. Accurate prediction of peak acceleration values at the site is shown to require characterization of the local site response at frequencies higher than those conventionally considered for site evaluation.

Reports

Borcherdt, R.D., Glassmoyer, G., and Wennerberg, L., 1986, Influence of welded boundaries in anelastic media on energy flow and characteristics of general P, S-I, and S-II waves. Observational evidence for inhomogeneous body waves in low-loss solids, *Journal of Geophysical Research*, v. 91, p. 11,503-11,518.

Borcherdt, R.D., Glassmoyer, G., and Wennerberg, L., 1985, On physical phenomena associated with the reflection and refraction of anelastic waves: *EOS*, v. 66, p. 984.

Borcherdt, R.D., Glassmoyer, G., and Johnston, M., 1986, On the simultaneous detection of anelastic volumetric strain and seismic displacement fields near the San Andreas Fault [abs.]: American Geophysical Union Fall Meeting, December 1986, San Francisco.

Borcherdt, R.D., 1986, Volumetric strain and particle displacements for body and surface waves in a general viscoelastic half-space: submitted to *Journal of Geophysical Research*.

Borcherdt, R.D., and Wennerberg, L., 1985, General P, type-I S, and type-II S waves in anelastic solids: Inhomogeneous wave fields in low-loss solids: *Bulletin, Seismological Society of America*, v. 75.

Glassmoyer, G. and Borcherdt, R., King, J., Dietel, C., Sembera, E., Roeloffs, E., Valdes, C., and Nicholson, C., 1986, Source and propagation characteristics for aftershock sequence near Painseville, Ohio [abs]: American Geophysical Union Spring Meeting, 1986, Baltimore.

Glassmoyer, G. and Borcherdt, R., 1986, Effects of local geology on high-frequency ground motions observed near Painesville, Ohio [abs.]: American Geophysical Union Fall Meeting, December 1986, San Francisco.

Wennerberg, L., and Glassmoyer, G., 1986, Absorption effects on plane waves in layered media: *Bulletin of the Seismological Society of America*, v. 76, p. 1407-1432.

Strong Motion Accelerograms of the 3 March 1985 Central Chile Earthquake

9910-04103

Mehmet Celebi
Branch of Engineering Seismology and Geology
U.S. Geological Survey
345 Middlefield Road, MS 977
Menlo Park, California 94025
(415) 323-8111, ext. 2394

Investigations:

1. Strong motion records of 3 March 1985 Central Chile earthquake and its important aftershocks were obtained through Chilean counterparts of this project. These records were visually examined and later digitized.

2. During the early process of digitization, a research staff from University of Chile spent approximately two months in Menlo Park and was trained in digitization and processing of records.

3. All digitized records will be part of the USGS Strong Motion Data Bank and will be forwarded to Distribution Center for Strong Motion Records in Denver, CO (NOAA).

4. The strong-motion records of 3 March 1985 main event digitized in Chile were obtained from Chilean counterparts.

Results:

1. The digitized acceleration records for 3 March 1985 Central Chile Earthquake are processed to obtain time histories of velocities and displacements, velocity and acceleration spectra, and Fourier amplitude spectra.

2. The records are used in various other projects of the USGS.

Reports:

1. A single (open-file) report will be issued and it is now being finalized. The draft title of the report is "Processed Chile Earthquake Records of 3 March 1985 and Aftershocks" coauthored by USGS and Chilean counterparts. The report will contain the records digitized by USGS and those digitized by the Chilean counterparts.

Instrumentation of Structures

9910-04099

Mehmet Celebi
Branch of Engineering Seismology and Geology
U.S. Geological Survey
345 Middlefield Road, MS 977
Menlo Park, California 94025
(415) 323-8111, ext. 2394

Investigations:

1. The process of selection of structures to be recommended for strong-motion instrumentation has continued in Los Angeles, Orange County, New Madrid area, southeastern United States (Charleston), northeastern United States (Boston), Alaska, and Hawaii.

2. The process of designing instrumentation schemes for selected structures has continued. During this period, instrumentation schemes for two structures, one for Los Angeles and the other in Charleston, SC, have been completed.

3. The process of actual instrumentation of structures has continued in Los Angeles (1100 Wilshire Finance Building) and in Charleston, SC (the Charleston Place).

4. New committees are being formed. Immediate committee being formed for Puget Sound Region (Seattle area).

Results:

1. The advisory committee in Charleston, SC, has reached its recommendations and an open-file report has been issued. Along with this report preparation effort, the structure ranked top for instrumentation (the Charleston Place) was being instrumented while the construction process was going on. By the time of the III U.S. National Conference on Earthquake Engineering held in Charleston between August 24-28, 1986, the instrumentation of this selected building was completed. A technical paper describing the instrumentation of this building and others was presented at the referenced conference.

2. The advisory committee in the Los Angeles area, while deliberating on the list of structures to be recommended for instrumentation in Los Angeles, advised to instrument the 1100 Wilshire Finance Building which was under construction. USGS in cooperation with the structural engineering firm and the owner of the building carried out the implementation of strong-motion instrumentation of this building.

3. The New Madrid Area committee has concluded its deliberations and a draft report has been prepared and will be issued shortly.

4. The Alaska committee has concluded its deliberations and a draft report is being prepared. Implementation of instrumentation of a structure in Anchorage, Alaska will start immediately after the report has been issued.

5. The Boston Area committee is nearing completion of its deliberations.

Reports:

Celebi, M. (Coordinator) and Lindbergh, C. (Chairman), et. al., 1986, Report on recommended list of structures for seismic instrumentation in southeastern United States: *U.S. Geological Survey Open-File Report 86-398* (July 1986).

Celebi, M. (Coordinator) and Durbin, W. (Chairman), et. al., 1986, Report on recommended list of structures for seismic instrumentation in New Madrid (St. Louis) area: *U.S. Geological Survey Open-File Report* (in draft preparation).

Celebi, M., and Maley, R., 1986, Strong-motion instrumentation of structures in Charleston, South Carolina and elsewhere: *Proceedings, III U.S. National Conference on Earthquake Engineering,* Charleston, South Carolina, vol. II, pp. 1273-1283.

Strong Ground Motion Data Analysis

9910-02676

J. Fletcher, A. McGarr, and J. Boatwright
Branch of Engineering Seismology and Geology
U. S. Geological Survey
345 Middlefield Road, MS 977
Menlo Park, California 94025
(415) 323-8111, exts. 2881, 2708, 2485

Investigations

1.) Analysis of 30 HZ. amplitudes of P waves to test the appropriateness of the ω^{-2} and ω^{-3} source models and in particular the ω^{-3} stress relaxation model of Archambeau. Recently, Evernden *et. al.* (1986) suggested that explosions could be discriminated from earthquakes on the basis of a ω^{-3} spectral scaling for earthquakes but a ω^{-2} scaling for explosions for P waves. This investigation is being led by J. Brune of the University of California, San Diego, IGPP, and co-authored by W. Walters, K. Priestley, F. Vernon, J. Berger, S. Hough, J. Fletcher, and T. Hanks.

2.) The failure of an asperity, that is, the rupture of a small fault area surrounded by a broken or weak fault area which slips after the asperity fails, is proposed as the appropriate model for the rupture processs of a sub-event within a larger earthquake. If the fault area surrounding the asperity equals the fault area of the composite earthquake, then the boundary conditions allow a set of asperities to be superposed together to make up the composite event. The scaling of the high and low frequency radiation from composite events composed of asperities is commensurate with generally observed spectral scaling laws, in contrast to composite events composed of cracks, or smaller events.

Results

1.) Figure 1 shows the Fourier component at 30 Hz. for P waves from earthquakes that span a wide range in moment. These data are compared with the predictions of the ω^{-2} and ω^{-3} source models as well as the Sharpe model of explosions. The 30 Hz. amplitudes increase with moment throughout the moments plotted in figure 1 in contrast to the prediction of the ω^{-3} model which predicts a levelling off at between 10^{19} to 10^{20} dyne-cm. Apparently, the increase comes from the continued arrival of high frequency energy throughout the source duration of the earthquakes rather than from a higher initial amplitude. Thus scaling proposed by the stress relaxation model of Archembeau does not appear to be consistent with observation. Usually, the data appear to be less than the Sharpe curve and this may be used to discriminate from explosions, but enough scatter exists in the data that the reliability of this method may not be high enough to be used in practice.

2.) A simple filtering strategy is derived to filter the waveforms radiated by cracks to simulate the waveforms radiated by asperities. Although the simulation of asperity waveforms by filtering crack waveforms represents a weak spatial approximation of the asperity faulting process, the resulting waveforms are minimally affected. To obtain the radiation for a composite event, the radiation from the asperity sub-events must be delayed and summed appropriately. The summation for a single wave-type c is simply

$$u_c(t) = \sum_{i=1}^{n} \left(\frac{\Delta\sigma_i}{\Delta\sigma} \right) z_c\left(t - T_r(\xi_i) - T_c(\xi_i, \boldsymbol{x})\right)$$

where $\Delta\sigma_i$ is the stress drop of the ith sub-event, $\Delta\sigma$ is the stress drop of the Green's function event, and $T_c(\xi_i, \boldsymbol{x})$ is the travel time from ξ_i to the receiver at $\boldsymbol{x}$. $z_c(t)$ is the asperity waveform obtained by filtering the waveform of the Green's function event.

To test this analysis, the P and S-waves radiated by by a M_L = 5.2 which occurred on May 9, 1983, at Coalinga, California, are modelled using the P and S-waves radiated by a M_L = 3.6 aftershock of the event. An abbreviated trail and error search yielded a faulting geometry which fits both P and S waveforms, using the high angle, east-dipping, nodal plane as the fault plane.

Reports

Boatwright, J., 1987, The seismic radiation from composite models of faulting: submitted to *Bulletin of the Seismological Society of America*, v. 77.

Brune,J.N., Walters, W.R., Priestly, K., Fletcher, J., Vernon, F., Berger, J., Hough, S., and Hanks, T.C., (1985), Preliminary observations of 30 Hz P-wave spectra compared with w^{-2} and w^{-3} source models: submitted to *Proceedings of Workshop on Research in High-Frequency Seismology*, Dallas, Texas, January 1986.

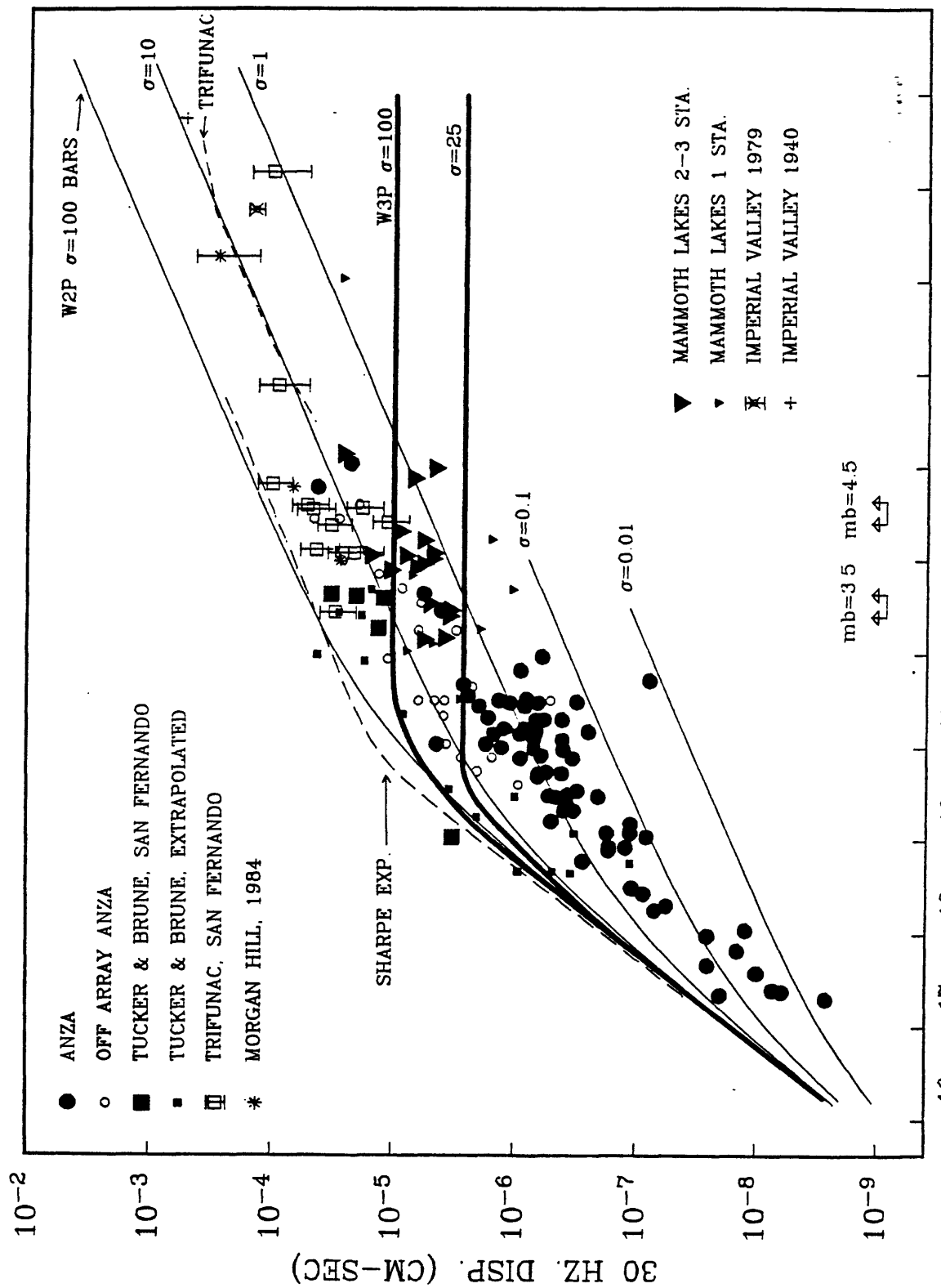

FIGURE 1. 30 Hz P-wave displacement spectral observations plotted as a function of moment, and compared with various theoretical surves. All symbols and curves normalized to a central distance of 10 km. σ respresents stress drop. Approximate m_b values corresponding to given moments are above the abissa, with the distance between the arrows indicating the uncertainty.

FIGURE 1.

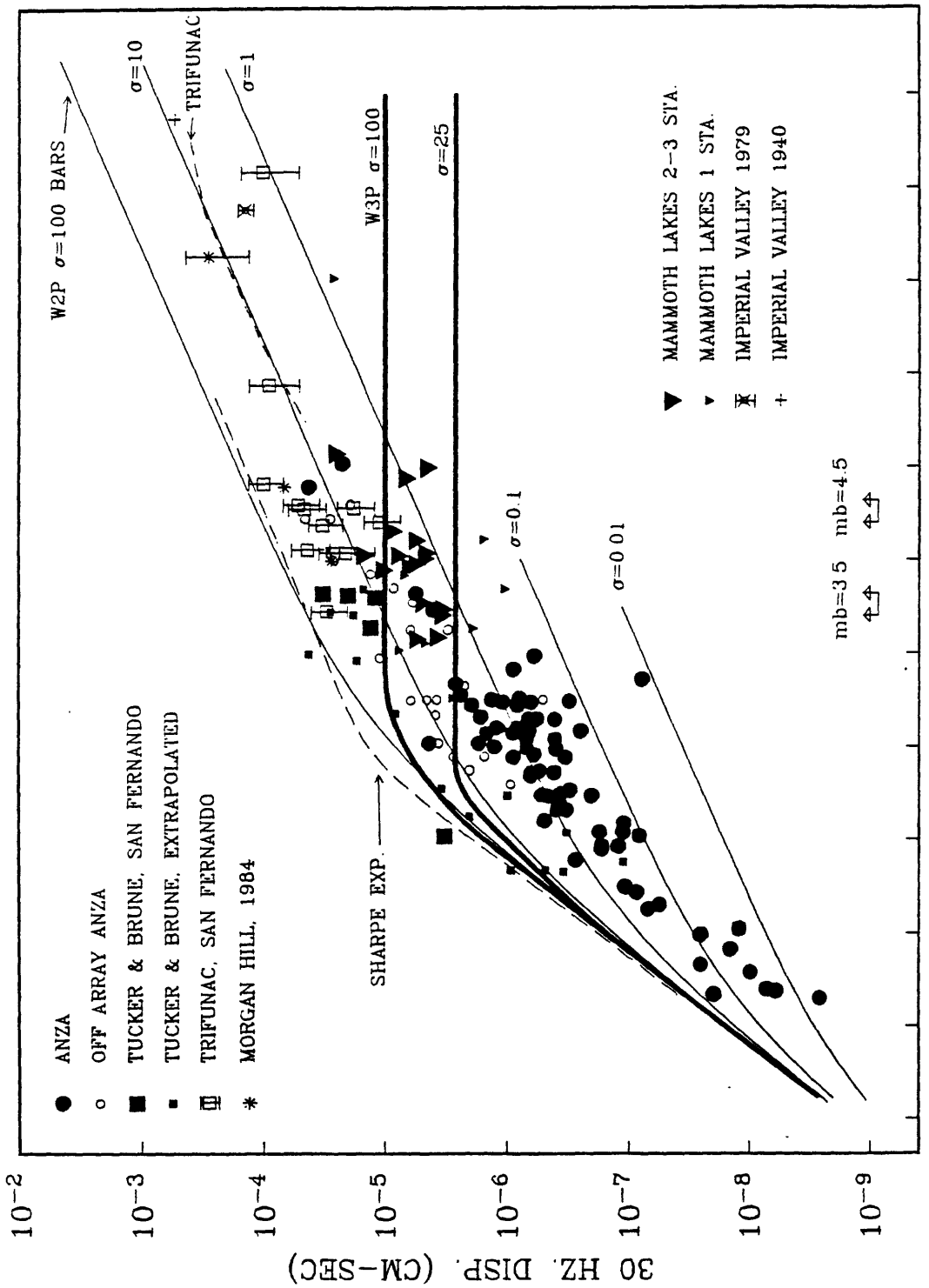

FIGURE 1. 30 Hz P-wave displacement spectral observations plotted as a function of moment, and compared with various theoretical curves. All symbols and curves normalized to a central distance of 10 km. σ respresents stress drop. Approximate % values corresponding to given moments are above the abissa, with the distance between the arrows indicating the uncertainty.

FIGURE 1.

RESULTS

1. There is strong evidence that there is active convergence at about 4 cm/yr on the 1200 km-long Cascadia subduction zone. Furthermore, there are many similarities between the physical characteristics of the Cascadia subduction zone and other subduction zones that have experienced large earthquakes. Even though there have not been large historic subduction earthquakes in the Pacific Northwest (at least 140 year), there is the possibility that the Cascadia subduction zone is storing energy to be released in future great earthquakes. If the Cascadia subduction zone is locked, then a sequence of several great earthquakes (M_w 8) or a giant earthquake would be necessary to fill this gap. If great subduction earthquakes occur, then relatively strong shaking can be expected over a large area of the Pacific Northwest, including the Puget Sound and Willamette Valley regions. Large and potentially very destructive tsunamis would be expected if large subduction events do occur.

2. Peak amplitudes from the long- and short-period Benioff records are given in Figure 1 for earthquakes in the magnitude range of 7.4 to 9.5. The synthetic values in Figure 1 are for a self-similar, ω-squared source model. The amplitudes for the self-similar model diverge from the observations for $M_w > 8.2$. The data points saturate at about this magnitude. This saturation means that for larger earthquakes the self-similar, ω-squared model overestimates the amplitude of 15 sec and 1.5 sec energy (predominant periods in the Benioff 1-90 and short-period records). The absolute level of the synthetic points is tied to the assumed value of the stress drop. We have used 30 bars. The correct value of stress drop to be used is arguable and smaller values will bring the synthetic points down by a uniform amount. However, the curve defined by the synthetic points would still not have the saturation characteristics seen in the data.

These results are consistent with the observation that the ω-squared model overestimates the amplitude of 20 sec surface waves and the value of M_s (Boore, 1986). The findings of this study are also consistent with the Benioff 1-90 spectra computed by Hartzell and Heaton (1985) for earthquakes with M_w 7.0. Their spectra tend to coalesce at high frequencies indicating the same saturation.

One factor which may affect the spectral shape of the large earthquakes ($M_w > 8.0$) is the possibility of rupture extending into the uppermost mantle. Signifcant rheological differences would then exist from the top to the bottom of the fault. Under these conditions the lower portion of the fault may not radiate as much high frequency energy as the brittle near-surface portion of the fault. However, the deep sections of the fault could still be regions of large moment release.

3. In order to investigate local site responses and regional structural effects at the U.S.G.S. network stations, recordings of deep events with simple source time functions are studied. Figure 2 shows records of three impulsive sources from Fiji at five of the network stations. Station KYP (34.102°N, 118.879°W) in the Transverse Ranges shows a clear phase 14 sec after the P-wave. This phase is not seen at most of the other network stations and its amplitude depends on the back azimuth to the source. We tentatively associated this phase with a reflection off

NORTHWEST U.S. SUBDUCTION ZONE

RISK ASSESSMENT

9930-03790

Thomas H. Heaton
Branch of Seismology
U.S. Geological Survey
525 S. Wilson Avenue
Pasadena, CA 91106
(818) 405-7814

The purpose of this project is to assess the potential seismic hazards due to large shallow thrust earthquakes along the Cascadia subduction zone of the northwestern United States. This project is currently in its final phase and the major problems that are now being considered are studies of southern California earthquakes, particularly as they relate to the southern California short-period telemetered array. A paper summarizing our major conclusions about the hazards associated with subduction in the northwestern United States has been prepared and we are finalizing some additional work on the nature of energy release associated with very large subduction earthquakes. Several new projects are now beginning; we are analyzing waveforms from teleseismic and regional earthquakes recorded on the southern California short-period network, and we are modeling the strong ground motions and teleseismic body waves from the 8 July 1986 M_L 5.9 North Palm Springs earthquake. As a final note, many of the administrative and monitoring responsibilities of the Pasadena Field Office are covered under this project.

INVESTIGATIONS

1. Provide an overview on the potential for large earthquakes on the Cascadia subduction zone and to provide an assessment of the ground motions that might result from such earthquakes.

2. For earthquakes larger than magnitude 8, limited data has made estimation of the seismic source specturm difficult. Long and short-period Benioff records from southern California stations are studied to investigate the seismic radiation from these large earthquakes. Comparison of the teleseismic Benioff records with synthetics for a self-similar, ω-squared source model is used to test the self-similarity hypothesis.

3. As part of an ongoing effort to utilize the waveform data from the southern California short-period network of telemetered stations, the station responses are being calibrated. Initial uses of this data include the study of waveforms and spectra for simple, deep earthquakes in the western Pacific to assess site responses.

a deep local structure.

Using the technique discussed in Stewart and O'Neill (1980), the response of the seismometer and other electronics is removed from the seismogram. Spectral ratios of ground displacement are then computed where transparent hard rock sites are compared with sites in other geologic settings. Analysis of these spectral ratios should reveal information on local site effects that will be important for future waveform studies.

REFERENCES

Boore, D. (1986). Short-period P- and S-wave radiation from large earthquakes: implications for spectral scaling relations, Bull. Seism. Soc. Am. 76, 43-64.

Hartzell, S. and T. Heaton (1985). Teleseismic time functions for large shallow subduction zone earthquakes, Bull. Seism. Soc. Am. 75, 965-1004.

Stewart, S. and M. O'Neill (1980). Calculation of the frequency response of the USGS telemetered short-period seismic system, USGS open-file report 80-143, 83.

REPORTS

Heaton, T. and S. Hartzell (1986). Earthquake hazards on the Cascadia subduction zone, submitted to Science, 27p.

Heaton, T. and S. Hartzell (1986). Estimation of strong ground motions from hypothetical earthquakes on the Cascadia subduction zone, Pacific Northwest, submitted to Pure and Applied Geophysics, 120p.

Heaton, T. and S. Hartzell (1986). Failure of self-similarity for large shallow subduction earthquakes, EOS, vol. 66.

Heaton, T. and S. Hartzell (1986). Estimation of strong ground motions from hypothetical earthquakes on the Cascadia subduction zone, Pacific Northwest, U.S. Geol. Surv. Open-file Rep. 86-328.

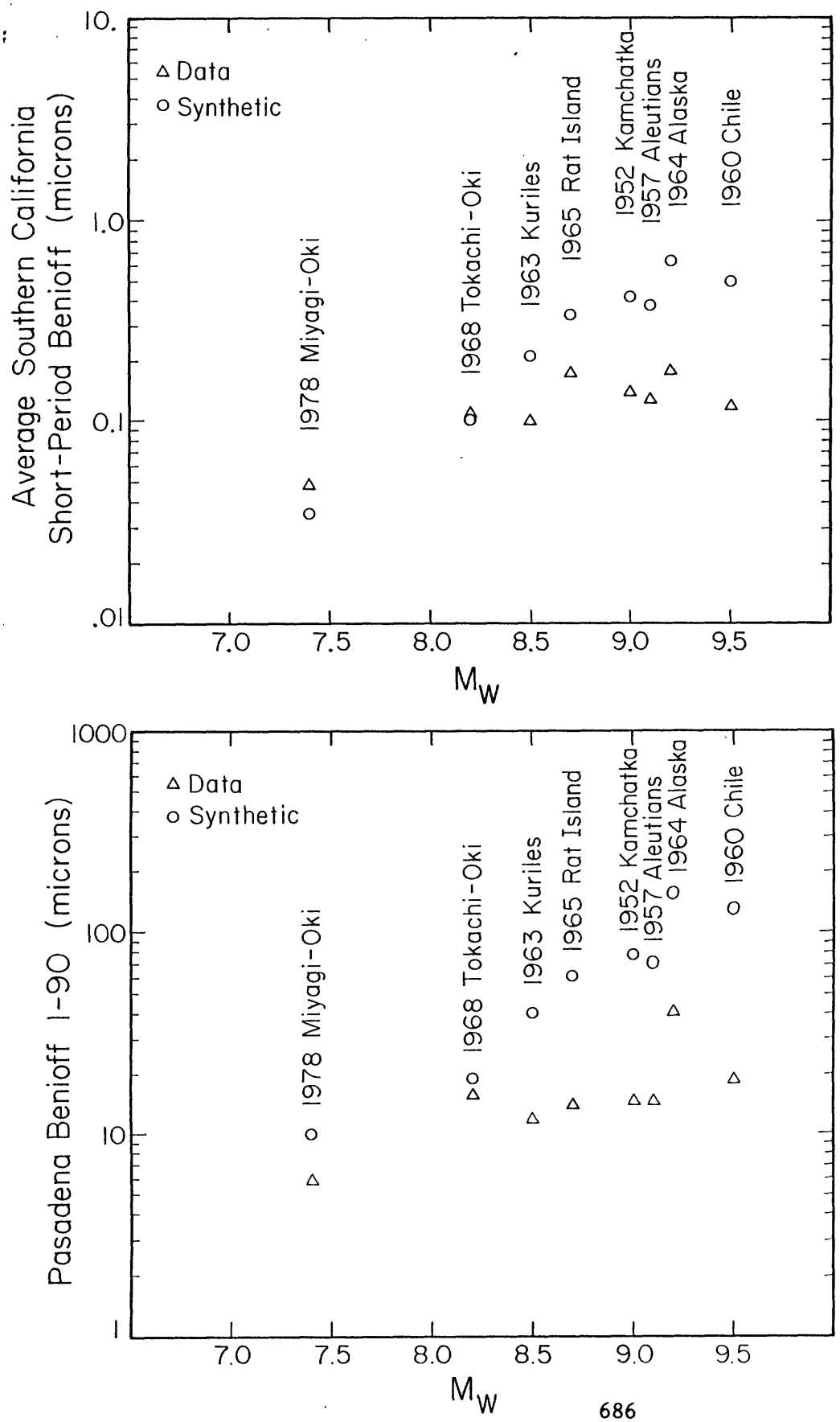
Average Southern California
Short-Period Benioff (microns)
10.
1.0
0.1
.01
Data
Synthetic
1978 Miyagi-Oki
1968 Tokachi-Oki
1963 Kuriles
1965 Rat Island
1952 Kamchatka
1957 Aleutians
1964 Alaska
1960 Chile
7.0
7.5
8.0
8.5
9.0
9.5
M_W
Pasadena Benioff 1-90 (microns)
1000
100
10
1
Data
Synthetic
1978 Miyagi-Oki
1968 Tokachi-Oki
1963 Kuriles
1965 Rat Island
1952 Kamchatka
1957 Aleutians
1964 Alaska
1960 Chile
7.0
7.5
8.0
8.5
9.0
9.5
M_W

Fig. 1

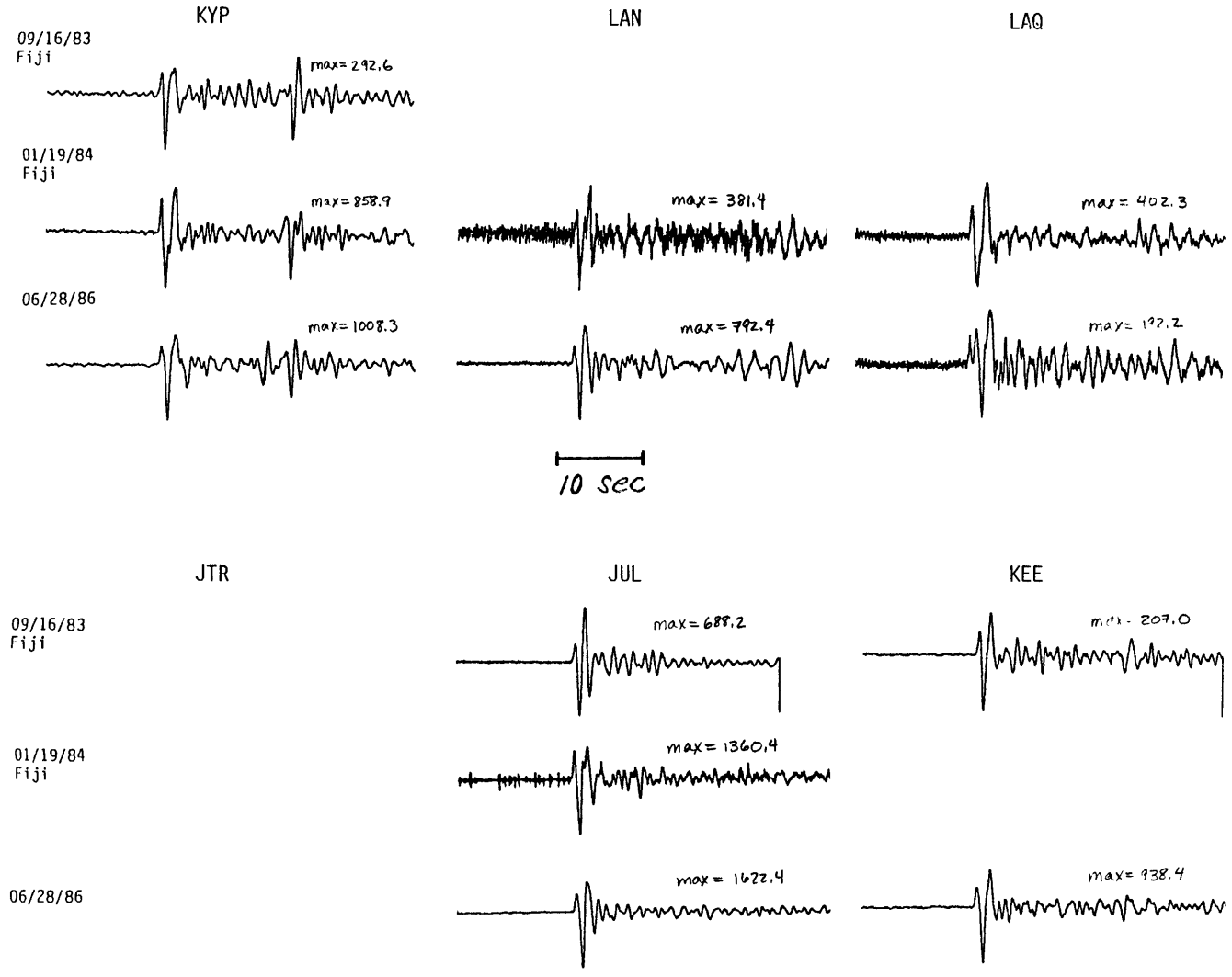
KYP
LAN
LAQ
09/16/83
Fiji
max= 292.6
01/19/84
Fiji
max= 858.9
max= 381.4
max= 402.3
06/28/86
max= 1008.3
max= 792.4
max= 197.2
10 sec
JTR
JUL
KEE
09/16/83
Fiji
max= 688.2
max= 207.0
01/19/84
Fiji
max= 1360.4
06/28/86
max= 1622.4
max= 938.4

Fig. 2

Spirit Lake Hazard Evaluation

9910-03590

Thomas L. Holzer
Branch of Engineering Seismology and Geology
U.S. Geological Survey
345 Middlefield Road, MS 977
Menlo Park, California 94025
(415) 323-8111, ext. 2760

Investigations:

1. Evaluation of liquefaction resistance of debris in blockages impounding Spirit, Castle Creek, and Cold Water lakes north of Mount St. Helens, Washington.

Results:

1. Instrumentation array consisting of accelerometers and pore-pressure transducers is being maintained to measure response of debris material to strong ground motion.

Reports:

None.

Precise Velocity and Attenuation Measurements in Engineering Seismology

9910-02413

Hsi-Ping Liu
Branch of Engineering Seismology and Geology
U.S. Geological Survey
345 Middlefield Road, MS 977
Menlo Park, California 94025
(415) 323-8111, ext. 2731

Investigations

1. *In situ* measurement of seismic shear-wave velocity and attenuation in the San Francisco Bay mud. Seismic properties of near-surface earth materials have a significant effect on the earthquake ground motions. The September 19, 1985 Mexican earthqauke provides a striking example. Because of the amplification of ground motions caused by shallow lake deposits, considerable damages were sustained in Mexico City, more than 400 km away from the epicenter. In order to properly characterize the earthquake site response, seismic velocity and attentuation measurements are needed. It is straight forward to measure the compressional- and shear-wave velocities using first arrivals excited by appropriate compressional- or shear-wave sources. Seismic attenuation determination, on the other hand, involves amplitude measurements which can be influenced by many factors. Systematic errors must be evaluated in order to obtain meaningful results. Sections of San Francisco bay mud having thickness greater than 20 m can be found on the west San Francisco bay shore from Redwood City to San Francisco. These sections of young bay mud lack horizontal stratification; they are suitable for development of methodology for *in situ* seismic attenuation measurements. Moreover, the San Francisco bay mud is an important earthquake engineering material whose *in situ* physical properties need to be determined. We are using a highly repeatable shear-wave generator (Liu, *et al.*, 1986a) and digital recorders (Borcherdt *et al.*, 1985) in investigations aimed to answer the following questions: How does the San Francisco bay mud attenuate shear waves? and can PVC-cased holes be used in seismic attenuation measurements in geologically young sediments?

2. Design and construction of a 2-Hz, 3-component velocity borehole geophone which can be leveled to 0.1 degrees from an initial maximum tilt of 10.5 degrees. These units can be operated continuously under a maximum confining pressure of 80 bars and a maximum temperature of 105° C.

3. Measurement of the effect of tidal stress on seismic shear-wave travel times in glaciated and jointed granite at Silver Lake, California.

Results

1. An undeveloped site at the Lutheran Church in Foster City, CA, has been selected for *in situ* measurement of seismic attenuation in the San Francisco bay mud. As determined from drilling, the top sediments consist of 23.2 m of young bay mud overlain by 1.8 m of hydraulically filled sand and underlain by

another section of clayey sand. Two Mark products L-28LT-3DS geophones, each clamped in a hollow annulus in order to make the overall geophone-package density equal to that of the bay mud, were emplaced at depths of 10.4 m and 16.6 m respectively in an uncased hole on September 11, 1986. The borehole was then allowed to close in upon the geophones. The first of a series of shear-wave velocity and amplitude measurements was made on September 22, 1986. For reliable measurements of the ground motions, the geophones were calibrated *in situ*. Additional measurements and data reduction and analysis are currently underway.

2. Horizontal electromagnetic geophones of natural period greater than 0.5 s need to be leveled to better than 1.5 degrees. Using the leveling device described by Liu *et al.* (1986b), a gimballed 3-component borehole geophone package has been designed, constructed, and tested. The first two units will be installed in the ANZA seismic gap in southern California in boreholes of 300 m and 150 m depths, respectively.

3. A continuous stretch of data lasting 40 hours which measure the shear-wave travel time through glaciated and jointed granite has been collected at Silver Lake, California from 231d 00h to 232d 16h (U. T.). The purpose is to study the effect of tidal stress on the shear-wave travel times. Data reduction and analysis are being undertaken at the present.

References Cited

Liu, H.-P., R.E. Warrick, R.E. Westerlund, J.B. Fletcher, and G.L. Maxwell, 1986a, An air-powered impulsive shear-wave source with repeatable signals, submitted to *Bulletin of the Seismological Socoiety of America*.

Liu, H.-P., R.E. Westerlund, J.B. Fletcher, and R.E. Warrick, 1986b, A borehole geophone leveling device, U.S. Geological Survey Open-File Report 86-351.

Borcherdt, R.D., J.B. Fletcher, E..G Jensen, G.L. Maxwell, J.R. Van Schaack, R.E. Warrick, E. Cranswick, M.J.S. Johnston, and R. McClearn, 1985, A general earthquake observation system (GEOS), *Bulletin of the Seismological Society of America*, v. 75, p. 1783-1825.

Reports

Liu, H.-P., J.J. Fedock, and J.B. Fletcher, 1986, Mode identification of an arch dam by a dynamic air-gun test, Proceedings of the Third National Conference on Earthquake Engineering, vol. 1, p. 753-764.

Liu, H.-P., R.E. Westerlund, J.B. Fletcher, and R.E. Warrick, 1986, A borehole geophone leveling device, U.S. Geological Survey Open-File Report 86-351.

Liu, H.-P., R.E. Warrick, R.E. Westerlund, J.B. Fletcher, and G.L. Maxwell, 1986, An air-powered impulsive shear-wave source with repeatable signals, submitted to *Bulletin of the Seismological Society of America*.

Strong Ground Motion Prediction in Realistic Earth Structures

9910-03010

P. Spudich
Branch of Engineering Seismology and Geology
U.S. Geological Survey
345 Middlefield Road, MS 977
Menlo Park, California 94025
(415) 323-8111, ext. 2395

Investigations

1. Development of an automated iterative procedure for determining earthquake rupture behavior based on near-source ground motion records.

2. Studies of the S wave coda of aftershocks of the 1984 Morgan Hill earthquake.

Results

1. In collaboration with G. Beroza of MIT, we have developed an iterative procedure for modeling strong motion records and finding rupture mechanisms. Ground motions are linearly related to the amount of slip on the fault but are nonlinearly related to rupture time. Consequently, to invert for rupture time, an iterative procedure is employed. Using the isochrone formalism, it is computationally rapid to calculate the partial derivatives of seismograms with respect to rupture time and slip amplitude on the fault. The inverse of this partial derivative matrix is multiplied by 'residual' seismograms to obtain a perturbation to the current slip and rupture time model. We usually obtain convergence in 5-10 iterations. The inversion is stabilized by applying smoothness and positivity restraints to the slip perturbation. The positivity constraint is implemented using the primal method. Preliminary results for the 1984 Morgan Hill earthquake indicate that there was significant deceleration of the rupture under Anderson Dam.

2. Using an array analysis technique reported on previously, T. Bostwick and I have examined the composition of waves comprising the S wave coda in aftershocks of the 1984 Morgan Hill earthquakes. At some stations a significant proportion of the coda energy appears to consist of waves that reverberate in a shallow region beneath the station, whereas this reverberation is largely absent at others. Coda-Q, however, is unaffected by these large station-to-station variations, further substantiating the hypothesized deep lithospheric origin for codas waves.

Reports

None.

INDEX 1

INDEX ALPHABETIZED BY PRINCIPAL INVESTIGATOR

INDEX 2

INDEX ALPHABETIZED BY INSTITUTION

San Francisco State University	Galehouse, J. S.	313
Southern California, University of	Aki, K.	183
Southern California, University of	Hauksson, E.	71
Southern California, University of	Teng, T.	41
U.S. Geological Survey	Algermissen, S. T.	468
U.S. Geological Survey	Allen, R. V.	186
U.S. Geological Survey	Anderson, R. E.	473
U.S. Geological Survey	Andrews, D. J.	655
U.S. Geological Survey	Andrews, M.	295
U.S. Geological Survey	Atwater, B. F.	129
U.S. Geological Survey	Bakun, W. H.	298
U.S. Geological Survey	Bekins, B.	8
U.S. Geological Survey	Boatwright, J.	656
U.S. Geological Survey	Bonilla, M. G.	130
U.S. Geological Survey	Boore, D. M.	659
U.S. Geological Survey	Boore, D. M.	671
U.S. Geological Survey	Borcherdt, R. D.	622
U.S. Geological Survey	Borcherdt, R. D.	672
U.S. Geological Survey	Borcherdt, R. D.	673
U.S. Geological Survey	Brady, A. G.	637
U.S. Geological Survey	Brady, A. G.	638
U.S. Geological Survey	Brown, R. D.	135
U.S. Geological Survey	Brown, W. M., III	483
U.S. Geological Survey	Buchanan-Banks, J. M.	485
U.S. Geological Survey	Buchanan-Banks, J. M.	581
U.S. Geological Survey	Bucknam, R. C.	49
U.S. Geological Survey	Bundock, H.	639
U.S. Geological Survey	Burford, R.	305
U.S. Geological Survey	Butler, H. M.	593
U.S. Geological Survey	Byerlee, J. D.	399
U.S. Geological Survey	Byerlee, J. D.	401
U.S. Geological Survey	Carlson, M. A.	595
U.S. Geological Survey	Celebi, M.	676
U.S. Geological Survey	Celebi, M.	677
U.S. Geological Survey	Choy, G. L.	51
U.S. Geological Survey	Choy, G. L.	189
U.S. Geological Survey	Choy, G. L.	596
U.S. Geological Survey	Clark, M. M.	136
U.S. Geological Survey	Cockerham, R. S.	191
U.S. Geological Survey	Dewey, J. W.	598
U.S. Geological Survey	Dieterich, J. H.	403
U.S. Geological Survey	Diment, W. H.	56
U.S. Geological Survey	Engdahl, E. R.	600
U.S. Geological Survey	Espinosa, A. F.	490
U.S. Geological Survey	Evernden, J.	641
U.S. Geological Survey	Fletcher, J. B.	209
U.S. Geological Survey	Fletcher, J. B.	679
U.S. Geological Survey	Hall, W.	19
U.S. Geological Survey	Harden, J. W.	493
U.S. Geological Survey	Harding, S. T.	67
U.S. Geological Survey	Harp. E. L.	495